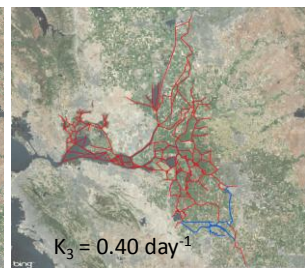
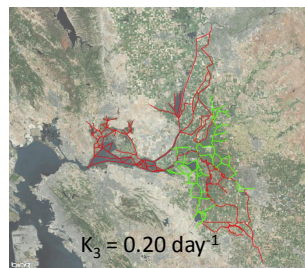
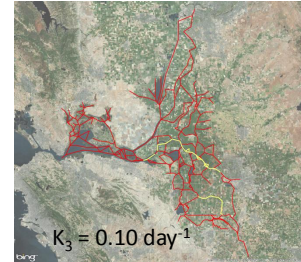
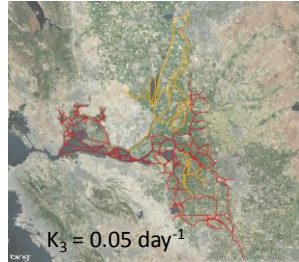


Turbidity Modeling with DSM2-QUAL: QUAL Recalibration and Historical Models



The plots in this figure illustrate the five decay values and associated regions in the recalibrated QUAL turbidity model!

Prepared For:
Metropolitan Water District of Southern California
March, 2013

Contact:
Dr. Paul Hutton
Authorized Technical Representative
916 – 650 – 2620

Prepared By:
Resource Management Associates
4171 Suisun Valley Road, Suite J
Fairfield, CA 94534

Contact:
Dr. Marianne Guerin
707 – 864 – 2950

Table of Contents

1	Executive Summary	1
2	Introduction.....	5
2.1	Objectives.....	5
2.2	Background	5
2.3	Challenges in modeling turbidity	6
3	Turbidity Model Calibration - Background and Methodology.....	7
3.1	Definition of calibration	7
3.2	QUAL turbidity calibration background and data.....	7
3.3	Methodology for turbidity calibration.....	11
3.4	Residual analysis	16
3.5	Linear regression analysis	17
3.6	Documentation of statistics	17
3.7	Model output and calibration calculations	17
4	Model set-up	19
4.1	High flow period Historical simulations: WY2010, WY2011, WY2012.....	19
4.2	Long term (1975 – 2011) Historical Simulations.....	19
5	Calibration Results.....	31
5.1	Calibration priorities	31
5.2	Calibration metrics	31
5.2.1	Location-specific calibration metric	31
5.2.2	Model Skill: Three Delta-wide calibration metrics	32
5.3	Calibration results for WY2010 and WY2011, comparing revised and original DMS calibration simulations	32
6	Evaluation of USGS-SSC data and WARMF Model Output as Boundary Conditions at Freeport and Vernalis.....	39
6.1	Background	39
6.2	WY2010 and WY2011 Model Results	39
7	Results of the Long Term QUAL Historical Turbidity Simulation – Water Years 1975 - 2011.....	55
7.1	EMP data.....	55

7.2	Simulation results – Model residuals and regressions comparing long-term simulations with EMP data.....	55
7.3	Summary of results.....	56
8	Formation of South Delta Turbidity Bridge.....	71
8.1	Analysis methodology.....	71
8.2	Results	71
8.3	Summary of turbidity bridge analysis	72
9	Summary and Conclusions	93
10	References.....	96
11	Appendix I	98
11.1	Model Skill	98
11.1.1	Background.....	98
11.1.2	Decisions on model skill assessment for this project.....	99
11.2	Spatial Animation.....	100
11.2.1	Background.....	100
11.2.2	Interpolation methodology.....	100
11.2.3	Grid development.....	101
12	Appendix II – Updated QUAL Turbidity calibration statistics	104
12.1	Daily-averaged CDEC data and model output – WY2011.....	104
12.2	Daily-averaged CDEC data and model output – WY2010.....	134
13	Appendix III – Initial QUAL turbidity calibration by DMS.....	159
13.1	Daily-averaged CDEC data and model output – WY2011.....	159
13.2	Daily-averaged CDEC data and model output- WY2010	189
14	Appendix IV – Updated QUAL Turbidity calibration statistics, 15-min	214
14.1	Fifteen Minute CDEC data and model output – WY2011	214
14.2	Fifteen minute CDEC data and model output – WY2010.....	244
14	Appendix V – Figures and Statistics Documenting WY2010 and WY2011 with Mixed-SSC-WARMF and WARMF-Only Model Boundary Conditions	268
15.1	WY2010 Mixed-SSC-WARMF results.....	268
15.2	WY2011 Mixed-SSC-WARMF results.....	294
15.3	WY2010 WARMF-Only results.....	323

15.4	WY2011 WARMF-Only results.....	348
15	Appendix VI – Figures and Statistics Documenting DSM2 QUAL Historical 1975 – 2011 Turbidity Model Application with Mixed SSC-WARMF Boundary Conditions.....	377
31.1	Early years: 1975 -1990.....	377
31.2	Recent years: 1991 – 2011.....	404
16	Appendix VII – Figures and Statistics Documenting DSM2 QUAL Historical 1975 – Turbidity Model Application with WARMF Model Boundary Conditions	429
48.1	Early years: 1975 -1990.....	429
48.2	Recent years: 1991 – 2011.....	456

Figures

Figure 3-1 CDEC turbidity measurement locations.....	9
Figure 3-2 Location of the three turbidity compliance locations.....	10
Figure 3-3 The colored lines define the DSM2 grid channels – the segments that aren't red define channels where the K_3 parameter was set to the indicated value. These figures show the lowest two values used for the settling parameter.....	13
Figure 3-4 The colored lines define the DSM2 grid channels – the segments that aren't red define channels where the K_3 parameter was set to the indicated value. These figures show two middle values used for the settling parameter.....	14
Figure 3-5 The colored lines define the DSM2 grid channels – the segments that aren't red define channels where the K_3 parameter was set to the indicated value. This figure shows the highest value used for the settling parameter.	15
Figure 3-4 An illustration of the calculations made at each data location in order to calculate location-specific calibration statistics for each water year. This location is the compliance site at Prisoner's Point. Peaks in the data (upper plot) not captured in the model in February are due to wind/rain events.....	18
Figure 4-1 WY2010 flow BC at Freeport, Vernalis, the Yolo Bypass and Cosumnes River locations.....	21
Figure 4-2 WY2010 flow BC at the Calaveras and Mokelumne locations and export BC at the CVP and SWP locations.	22
Figure 4-3 WY2010 Freeport and Vernalis turbidity BC showing all three available sets of data – CDEC (15-min), WARMF (daily) and USGS-SSC (daily). USGS-SSC values were transformed to turbidity using a linear translation.	23
Figure 4-4 WY2011 flow BC at Freeport, Vernalis, the Yolo Bypass and Cosumnes River locations.....	24
Figure 4-5 WY2011 flow BC at the Calaveras and Mokelumne locations and export BC at the CVP and SWP locations.	25
Figure 4-6 WY2011 Freeport and Vernalis turbidity BC showing all three available sets of data – CDEC (15-min), WARMF (daily) and USGS-SSC (daily). USGS-SSC values were transformed to turbidity using a linear translation.	26
Figure 4-7 WY2012 flow BC at Freeport, Vernalis, the Yolo Bypass and Cosumnes River locations.....	27
Figure 4-8 WY2012 flow BC at the Calaveras and Mokelumne locations and export BC at the CVP and SWP locations.	28
Figure 4-9 WY2012 turbidity BC at Freeport and Vernalis – only CDEC data was available for this time frame.	29
Figure 4-10 Long-term simulation options for the Freeport and Vernalis turbidity boundary conditions. USGS-SSC values were transformed to turbidity using a linear translation. Both data sets are composed of daily data.	30

Figure 6-1 WY2010 contour plot comparison of the Mixed-SSC-WARMF and WARMF-Only simulations during a peak inflow period before turbidity reached the central Delta.....	47
Figure 6-2 WY2010 contour plot comparison of the Mixed-SSC-WARMF and WARMF-Only simulations, with values shown for modeled 15-min compliance location turbidity on Jan. 24, 2010.....	48
Figure 6-3 WY2010 contour plot comparison of the Mixed-SSC-WARMF and WARMF-Only simulations, with values shown for modeled 15-min compliance location turbidity on Jan. 25, 2010.....	49
Figure 6-4 WY2010 contour plot comparison of the Mixed-SSC-WARMF and WARMF-Only simulations – date chosen for modeled daily peak Victoria Canal compliance location turbidity on Jan. 24, 2010. In comparison with Figure 6-2, these daily average values are much lower than 15-minute results, particularly in Victoria Canal. Neither model exceeded the compliance value at all three locations.	50
Figure 6-5 WY2011 contour plot comparison of the Mixed-SSC-WARMF and WARMF-Only simulations during a peak inflow period. Turbidity has intruded into the Central Delta.	51
Figure 6-6 WY2011 contour plot comparison of the Mixed-SSC-WARMF and WARMF-Only simulations, with values shown for modeled 15-min compliance location turbidity on Mar. 22, 2011. This is the peak time for compliance location values for the WARMF-Only simulation. .	52
Figure 6-7 WY2011 contour plot comparison of the Mixed-SSC-WARMF and WARMF-Only simulations, with values shown for modeled 15-min compliance location turbidity on Mar. 22, 2011. This is the peak time for compliance location values for the Mixed-SSC-WARMF simulation.....	53
Figure 6-8 WY2011 contour plot comparison of the Mixed-SSC-WARMF and WARMF-Only simulations, The time was chosen for modeled daily peak Victoria Canal compliance location turbidity on Mar. 28, 2011. Both simulations exceeded the compliance maximum of 12 NTU at all three locations.	54
Figure 7-1 The figure shows the location of EMP stations (green triangles), DSM2 channels (red) and nodes (black) in the western Delta.	58
Figure 7-2 The figure shows the location of EMP stations (green triangles), DSM2 channels (red), and nodes (black) in the northern Delta.	59
Figure 7-3 The figure shows the location of EMP stations (green triangles), DSM2 channels (red) and nodes (black) in the eastern Delta.	60
Figure 7-4 The figure shows the location of EMP stations (green triangles), DSM2 channels (red) and nodes (black) in the southern Delta.	61
Figure 7-5 WARMF-Only results at D26 in the recent years time frame.	62
Figure 7-6 Mixed-SSC-WARMF results at D26 in the recent years time frame.....	63
Figure 7-7 Comparison of 15-minute model results on Dec. 27, 1983 at 08:00 with the Mixed-SSC-WARMF and WARMF-Only boundary conditions during a high inflow period.	68

Figure 7-8 Comparison of 15-minute model results on Dec. 28, 1983 at 10:00 at the time of maximum turbidity values at the three compliance locations with the Mixed-SSC-WARMF and WARMF-Only boundary conditions. Note change in scale from previous contour plot. 69

Figure 7-9 Comparison of daily-averaged model results on Dec. 28, 1983 at 10:00 at the time of maximum turbidity values at the three compliance locations with the Mixed-SSC-WARMF and WARMF-Only boundary conditions. Only two of three compliance stations had turbidity values over the maximum of 12 NTU. This day gives the daily maximum at the Victoria Canal location. 70

Figure 8-1 Locations used to investigate the formation of a turbidity bridge in the south Delta illustrated in the DSM2 grid. 73

Figure 8-2 Turbidity initially intrudes from Sacramento inflow down Old and Middle Rivers - San Joaquin turbidity later influences the south Delta in WY1991..... 75

Figure 8-3 Daily-averaged turbidity time series during the formation of the turbidity bridge in WY1991. The blue dashed line is the 12 NTU compliance value..... 76

Figure 8-4 Turbidity initially intrudes from Sacramento inflow down Old River along intrusion in the south from San Joaquin turbidity – Middle River turbidity later increases above 12 NTU in February of WY1992. 77

Figure 8-5 Turbidity intrudes from Sacramento inflow down Old and Middle Rivers along with some San Joaquin turbidity in the south, but a turbidity bridge never forms in March/April of WY1992..... 78

Figure 8-6 Daily-averaged turbidity time series during the formation of the turbidity bridge in WY1992. The blue dashed line is the 12 NTU compliance value..... 79

Figure 8-7 Turbidity initially intrudes from Sacramento inflow down Old River along intrusion in the south from San Joaquin turbidity – Middle River turbidity later increases above 12 NTU in January of WY1993. 80

Figure 8-8 Daily-averaged turbidity time series during the formation of the turbidity bridge in WY1993. The blue dashed line is the 12 NTU compliance value..... 81

Figure 8-9 A turbidity bridge never forms in WY1994..... 82

Figure 8-10 Turbidity initially intrudes from Sacramento inflow down Old River along intrusion in the south from San Joaquin turbidity – Middle River turbidity later increases above 12 NTU in January of WY1995. 83

Figure 8-11 A second turbidity bridge forms in March of WY1995 primarily due to intrusion in the south from San Joaquin turbidity – turbidity increased primarily along Middle River as it flows out of the Delta..... 84

Figure 8-12 Daily-averaged turbidity time series during the formation of the turbidity bridge in WY1995. The blue dashed line is the 12 NTU compliance value..... 85

Figure 8-13 Turbidity initially intrudes from Sacramento inflow down Old River along intrusion in the south from San Joaquin turbidity – Middle River turbidity much later increases above 12 NTU in February of WY1996..... 86

Figure 8-14 Turbidity increases above the 12 NTU level in the south Delta and along Middle River in May of WY1996.	87
Figure 8-15 Daily-averaged turbidity time series during the formation of the turbidity bridge in WY1996. The blue dashed line is the 12 NTU compliance value.....	87
Figure 8-16 Turbidity initially intrudes from the south Delta northward due to high turbidity from San Joaquin inflow - in this case the bridge forms up Middle river in the lower San Joaquin in January of WY1997.....	88
Figure 8-17 Daily-averaged turbidity time series during the formation of the turbidity bridge in WY1997. The blue dashed line is the 12 NTU compliance value.....	89
Figure 8-18 Turbidity initially intrudes from San Joaquin inflow northward in January, with the turbidity bridge forming as Sacramento turbidity flows into the central Delta in February of WY1998.....	90
Figure 8-19 Daily-averaged turbidity time series during the formation of the turbidity bridge in WY1998. The blue dashed line is the 12 NTU compliance value.....	91
Figure 8-20 Turbidity initially intrudes from both Sacramento and San Joaquin River inflows forming a turbidity bridge initially along Old River in February of WY2000.	92
Figure 8-21 Daily-averaged turbidity time series during the formation of the turbidity bridge in WY2000. The blue dashed line is the 12 NTU compliance value.....	92
Figure 11-1 This figure illustrates the grid developed to visualize DSM2 one-dimensional model output. Note the Franks Tract area was developed in 2-D.....	102
Figure 11-2 The pink stars indicate the locations where DSM2 output is used to create the interpolated contours. Green triangles are EMP data locations. Black lines denote the channels in the DSM2 model grid. Note the interpolation grid (Figure 11-1) is different from the DSM2 grid.	103
Figure 12-1 WY2011 revised calibration results at Antioch.	105
Figure 12-2 WY2011 revised calibration results at Cache-Ryer.....	106
Figure 12-3 WY2011 revised calibration results at Decker Island.....	107
Figure 12-4 WY2011 revised calibration results at False River.....	108
Figure 12-5 WY2011 revised calibration results at Freeport.....	109
Figure 12-6 WY2011 revised calibration results at Georgiana-Below-Sac.....	110
Figure 12-7 WY2011 revised calibration results at Georgiana-at-Sac.	111
Figure 12-8 WY2011 revised calibration results at Grant Line.....	112
Figure 12-9 WY2011 revised calibration results at Grant-Line Tracy.....	113
Figure 12-10 WY2011 revised calibration results at Holland Cut.	114
Figure 12-11 WY2011 revised calibration results at Hood.	115
Figure 12-12 WY2011 revised calibration results at Little Potato Slough-at-Terminus.	116
Figure 12-13 WY2011 revised calibration results at Mallard Slough.	117
Figure 12-14 WY2011 revised calibration results at Middle River-at-Howard Rd.....	118
Figure 12-15 WY2011 revised calibration results at Middle River-at-Holt.	119
Figure 12-16 WY2011 revised calibration results at Miner Slough.	120

Figure 12-17 WY2011 revised calibration results at Mokelumne-at-San Joaquin.....	121
Figure 12-18 WY2011 revised calibration results at Mossdale.....	122
Figure 12-19 WY2011 revised calibration results at North Mokelumne.	123
Figure 12-20 WY2011 revised calibration results at Prisoner Point.	124
Figure 12-21 WY2011 revised calibration results at Prisoner Point-at-Terminus.	125
Figure 12-22 WY2011 revised calibration results at Rio Vista.....	126
Figure 12-23 WY2011 revised calibration results at Rough-N-Ready Island.....	127
Figure 12-24 WY2011 revised calibration results at San Joaquin-at-Garwood.	128
Figure 12-25 WY2011 revised calibration results at San Joaquin-at-McCune (Vernalis).	129
Figure 12-26 WY2011 revised calibration results at South Mokelumne.	130
Figure 12-27 WY2011 revised calibration results at Threemile-Slough-at-San Joaquin.	131
Figure 12-28 WY2011 revised calibration results at Turner Cut-at-Holt.....	132
Figure 12-29 WY2011 revised calibration results at Victoria Canal-at-Byron.	133
Figure 12-30 WY2010 revised calibration results at Antioch.	134
Figure 12-31 WY2010 revised calibration results at Cache-at-Ryer Island.	135
Figure 12-32 WY2010 revised calibration results at Decker Island.....	136
Figure 12-33 WY2010 revised calibration results at False River.	137
Figure 12-34 WY2010 revised calibration results at Freeport.....	138
Figure 12-35 WY2010 revised calibration results at Georgiana-Below-Sac.....	139
Figure 12-36 WY2010 revised calibration results at Georgiana-Sac.	140
Figure 12-37 WY2010 revised calibration results at Grant Line.....	141
Figure 12-38 WY2010 revised calibration results at Holland Cut.	142
Figure 12-39 WY2010 revised calibration results at Hood.	143
Figure 12-40 WY2010 revised calibration results at Little Potato Slough-at-Terminus.	144
Figure 12-41 WY2010 revised calibration results at Mallard Slough.	145
Figure 12-42 WY2010 revised calibration results at Middle River-at-Holt.	146
Figure 12-43 WY2010 revised calibration results at Miner Slough.	147
Figure 12-44 WY2010 revised calibration results at Mokelumne-at-San Joaquin.....	148
Figure 12-45 WY2010 revised calibration results at Mossdale.....	149
Figure 12-46 WY2010 revised calibration results at Prisoner Point.	150
Figure 12-47 WY2010 revised calibration results at Prisoner Point-at-Terminus.	151
Figure 12-48 WY2010 revised calibration results at Rio Vista.....	152
Figure 12-49 WY2010 revised calibration results at Rough-N-Ready Island.....	153
Figure 12-50 WY2010 revised calibration results at San Joaquin-at-Garwood.	154
Figure 12-51 WY2010 revised calibration results at San Joaquin-at-McCune (Vernalis).	155
Figure 12-52 WY2010 revised calibration results at Threemile-Slough-at-San Joaquin.	156
Figure 12-53 WY2010 revised calibration results at Turner Cut-at-Holt.....	157
Figure 12-54 WY2010 revised calibration results at Victoria Canal-at-Byron.	158
Figure 13-1 WY2011 original calibration results at Antioch.	160
Figure 13-2 WY2011 original calibration results at Cache-at-Ryer Island.	161

Figure 13-3 WY2011 original calibration results at Decker Island.	162
Figure 13-4 WY2011 original calibration results at False River.	163
Figure 13-5 WY2011 original calibration results at Freeport.	164
Figure 13-6 WY2011 original calibration results at Georgiana-Below-Sac.	165
Figure 13-7 WY2011 original calibration results at Georgiana-Sac.	166
Figure 13-8 WY2011 original calibration results at Grant Line.	167
Figure 13-9 WY2011 original calibration results at Grant Line-Tracy.	168
Figure 13-10 WY2011 original calibration results at Holland Cut.	169
Figure 13-11 WY2011 original calibration results at Hood.	170
Figure 13-12 WY2011 original calibration results at Little Potato Slough-at-Terminous.	171
Figure 13-13 WY2011 original calibration results at Mallard Slough.	172
Figure 13-14 WY2011 original calibration results at Middle River-at-Howard.	173
Figure 13-15 WY2011 original calibration results at Middle River-at-Holt.	174
Figure 13-16 WY2011 original calibration results at Miner Slough.	175
Figure 13-17 WY2011 original calibration results at Mokelumne-at-San Joaquin.	176
Figure 13-18 WY2011 original calibration results at Mossdale.	177
Figure 13-19 WY2011 original calibration results at North Mokelumne.	178
Figure 13-20 WY2011 original calibration results at Prisoner Point.	179
Figure 13-21 WY2011 original calibration results at Prisoner Point-at-Terminous.	180
Figure 13-22 WY2011 original calibration results at Rio Vista.	181
Figure 13-23 WY2011 original calibration results at Rough-N-Ready Island.	182
Figure 13-24 WY2011 original calibration results at San Joaquin-at-Garwood.	183
Figure 13-25 WY2011 original calibration results at San Joaquin-at-McCune (Vernalis).	184
Figure 13-26 WY2011 original calibration results at South Mokelumne.	185
Figure 13-27 WY2011 original calibration results at Threemile-Slough-at San Joaquin.	186
Figure 13-28 WY2011 original calibration results at Turner Cut-at-Holt.	187
Figure 13-29 WY2011 original calibration results at Victoria Canal-at-Byron.	188
Figure 13-30 WY2010 original calibration results at Antioch.	189
Figure 13-31 WY2010 original calibration results at Cache-at-Ryer Island.	190
Figure 13-32 WY2010 original calibration results at Decker Island.	191
Figure 13-33 WY2010 original calibration results at False River.	192
Figure 13-34 WY2010 original calibration results at Freeport.	193
Figure 13-35 WY2010 original calibration results at Georgiana-Below-Sac.	194
Figure 13-36 WY2010 original calibration results at Georgiana-Sac.	195
Figure 13-37 WY2010 original calibration results at Grant Line.	196
Figure 13-38 WY2010 original calibration results at Holland Cut.	197
Figure 13-39 WY2010 original calibration results at Hood.	198
Figure 13-40 WY2010 original calibration results at Little Potato Slough-at-Terminous.	199
Figure 13-41 WY2010 original calibration results at Mallard Slough.	200
Figure 13-42 WY2010 original calibration results at Middle River-at-Holt.	201

Figure 13-43 WY2010 original calibration results at Miner Slough.	202
Figure 13-44 WY2010 original calibration results at Mokelumne-at-San Joaquin.	203
Figure 13-45 WY2010 original calibration results at Mossdale.	204
Figure 13-46 WY2010 original calibration results at Prisoner Point.	205
Figure 13-47 WY2010 original calibration results at Prisoner Point-at-Terminus.	206
Figure 13-48 WY2010 original calibration results at Rio Vista.	207
Figure 13-49 WY2010 original calibration results at Rough-N-Ready Island.	208
Figure 13-50 WY2010 original calibration results at San Joaquin-at-Garwood.	209
Figure 13-51 WY2010 original calibration results at San Joaquin-at-McCune (Vernalis).	210
Figure 13-52 WY2010 original calibration results at Threemile-Slough-at-San Joaquin.	211
Figure 13-53 WY2010 original calibration results at Turner Cut-at-Holt.	212
Figure 13-54 WY2010 original calibration results at Victoria Canal-at-Byron.	213
Figure 14-1 WY2011 15-min revised calibration results at Antioch.	215
Figure 14-2 WY2011 15-min revised calibration results at Cache-Ryer.	216
Figure 14-3 WY2011 15-min revised calibration results at Decker Island.	217
Figure 14-4 WY2011 15-min revised calibration results at False River.	218
Figure 14-5 WY2011 15-min revised calibration results at Freeport.	219
Figure 14-6 WY2011 15-min revised calibration results at Georgiana-Below-Sac.	220
Figure 14-7 WY2011 15-min revised calibration results at Georgiana-at-Sac.	221
Figure 14-8 WY2011 15-min revised calibration results at Grant Line.	222
Figure 14-9 WY2011 15-min revised calibration results at Grant-Line Tracy.	223
Figure 14-10 WY2011 15-min revised calibration results at Holland Cut.	224
Figure 14-11 WY2011 15-min revised calibration results at Hood.	225
Figure 14-12 WY2011 15-min revised calibration results at Little Potato Slough-at-Terminus.	226
Figure 14-13 WY2011 15-min revised calibration results at Mallard Slough.	227
Figure 14-14 WY2011 15-min revised calibration results at Middle River-at-Howard Rd.	228
Figure 14-15 WY2011 15-min revised calibration results at Middle River-at-Holt.	229
Figure 14-16 WY2011 15-min revised calibration results at Miner Slough.	230
Figure 14-17 WY2011 15-min revised calibration results at Mokelumne-at-San Joaquin.	231
Figure 14-18 WY2011 15-min revised calibration results at Mossdale.	232
Figure 14-19 WY2011 15-min revised calibration results at North Mokelumne.	233
Figure 14-20 WY2011 15-min revised calibration results at Prisoner Point.	234
Figure 14-21 WY2011 15-min revised calibration results at Prisoner Point-at-Terminus.	235
Figure 14-22 WY2011 15-min revised calibration results at Rio Vista.	236
Figure 14-23 WY2011 15-min revised calibration results at Rough-N-Ready Island.	237
Figure 14-24 WY2011 15-min revised calibration results at San Joaquin-at-Garwood.	238
Figure 14-25 WY2011 15-min revised calibration results at San Joaquin-at-McCune (Vernalis).	239
Figure 14-26 WY2011 15-min revised calibration results at South Mokelumne.	240

Figure 14-27 WY2011 15-min revised calibration results at Threemile-Slough-at-San Joaquin.	241
Figure 14-28 WY2011 15-min revised calibration results at Turner Cut-at-Holt.	242
Figure 14-29 WY2011 15-min revised calibration results at Victoria Canal-at-Byron.	243
Figure 14-30 WY2010 15-min revised calibration results at Antioch.	244
Figure 14-31 WY2010 15-min revised calibration results at Cache-at-Ryer Island.	245
Figure 14-32 WY2010 15-min revised calibration results at Decker Island.	246
Figure 14-33 WY2010 15-min revised calibration results at False River.	247
Figure 14-34 WY2010 15-min revised calibration results at Freeport.	248
Figure 14-35 WY2010 15-min revised calibration results at Georgiana-Below-Sac.	249
Figure 14-36 WY2010 15-min revised calibration results at Grant Line.	250
Figure 14-37 WY2010 15-min revised calibration results at Holland Cut.	251
Figure 14-38 WY2010 15-min revised calibration results at Hood.	252
Figure 14-39 WY2010 15-min revised calibration results at Little Potato Slough-at-Terminus.	253
Figure 14-40 WY2010 15-min revised calibration results at Mallard Slough.	254
Figure 14-41 WY2010 15-min revised calibration results at Middle River-at-Holt.	255
Figure 14-42 WY2010 15-min revised calibration results at Miner Slough.	256
Figure 14-43 WY2010 15-min revised calibration results at Mokelumne-at-San Joaquin.	257
Figure 14-44 WY2010 15-min revised calibration results at Mossdale.	258
Figure 14-45 WY2010 15-min revised calibration results at Prisoner Point.	259
Figure 14-46 WY2010 15-min revised calibration results at Prisoner Point-at-Terminus.	260
Figure 14-47 WY2010 15-min revised calibration results at Rio Vista.	261
Figure 14-48 WY2010 15-min revised calibration results at Rough-N-Ready Island.	262
Figure 14-49 WY2010 15-min revised calibration results at San Joaquin-at-Garwood.	263
Figure 14-50 WY2010 15-min revised calibration results at San Joaquin-at-McCune (Vernalis).	264
Figure 14-51 WY2010 15-min revised calibration results at Threemile-Slough-at-San Joaquin.	265
Figure 14-52 WY2010 15-min revised calibration results at Turner Cut-at-Holt.	266
Figure 14-53 WY2010 15-min revised calibration results at Victoria Canal-at-Byron.	267
Figure 15-1 WY2010: WY2010: DSM2 daily-averaged turbidity model results using Mixed-SSC-WARMF turbidity at the inflow boundaries– location is Antioch.	269
Figure 15-2 WY2010: WY2010: DSM2 daily-averaged turbidity model results using Mixed-SSC-WARMF turbidity at the inflow boundaries– location is Cache-at-Ryer.	270
Figure 15-3 WY2010: WY2010: DSM2 daily-averaged turbidity model results using Mixed-SSC-WARMF turbidity at the inflow boundaries– location is Decker-Island.	271
Figure 15-4 WY2010: DSM2 daily-averaged turbidity model results using Mixed-SSC-WARMF turbidity at the inflow boundaries– location is False-River.	272

Figure 15-5WY2010: DSM2 daily-averaged turbidity model results using Mixed-SSC-WARMF turbidity at the inflow boundaries– location is Freeport.....	273
Figure 15-6WY2010: DSM2 daily-averaged turbidity model results using Mixed-SSC-WARMF turbidity at the inflow boundaries– location is Georgiana-Below-Sac.....	274
Figure 15-7WY2010: DSM2 daily-averaged turbidity model results using Mixed-SSC-WARMF turbidity at the inflow boundaries– location is Georgiana-Sac.....	275
Figure 15-8WY2010: DSM2 daily-averaged turbidity model results using Mixed-SSC-WARMF turbidity at the inflow boundaries– location is Grant-Line.....	276
Figure 15-9WY2010: DSM2 daily-averaged turbidity model results using Mixed-SSC-WARMF turbidity at the inflow boundaries– location is Holland-Cut.....	277
Figure 15-10WY2010: DSM2 daily-averaged turbidity model results using Mixed-SSC-WARMF turbidity at the inflow boundaries– location is Hood.....	278
Figure 15-11WY2010: DSM2 daily-averaged turbidity model results using Mixed-SSC-WARMF turbidity at the inflow boundaries– location is Little-Potato-Slough-at-Terminus...	279
Figure 15-12WY2010: DSM2 daily-averaged turbidity model results using Mixed-SSC-WARMF turbidity at the inflow boundaries– location is Mallard Slough.....	280
Figure 15-13WY2010: DSM2 daily-averaged turbidity model results using Mixed-SSC-WARMF turbidity at the inflow boundaries– location is Middle-River-at-Holt.....	281
Figure 15-14WY2010: DSM2 daily-averaged turbidity model results using Mixed-SSC-WARMF turbidity at the inflow boundaries– location is Miner Slough.....	282
Figure 15-15WY2010: DSM2 daily-averaged turbidity model results using Mixed-SSC-WARMF turbidity at the inflow boundaries– location is Mokelumne-at-San Joaquin.....	283
Figure 15-16WY2010: DSM2 daily-averaged turbidity model results using Mixed-SSC-WARMF turbidity at the inflow boundaries– location is Mossdale.....	284
Figure 15-17WY2010: DSM2 daily-averaged turbidity model results using Mixed-SSC-WARMF turbidity at the inflow boundaries– location is Prisoner-Point.....	285
Figure 15-18WY2010: DSM2 daily-averaged turbidity model results using Mixed-SSC-WARMF turbidity at the inflow boundaries– location is Prisoner-Point-at-Terminus.....	286
Figure 15-19WY2010: DSM2 daily-averaged turbidity model results using Mixed-SSC-WARMF turbidity at the inflow boundaries– location is Rio Vista.....	287
Figure 15-20 WY2010: DSM2 daily-averaged turbidity model results using Mixed-SSC-WARMF turbidity at the inflow boundaries– location is Rough-N-Ready Island.....	288
Figure 15-21 WY2010: DSM2 daily-averaged turbidity model results using Mixed-SSC-WARMF turbidity at the inflow boundaries– location is San Joaquin-at-Garwood.....	289
Figure 15-22 WY2010: DSM2 daily-averaged turbidity model results using Mixed-SSC-WARMF turbidity at the inflow boundaries– location is San Joaquin-at-McCune.....	290
Figure 15-23 WY2010: DSM2 daily-averaged turbidity model results using Mixed-SSC-WARMF turbidity at the inflow boundaries– location is Threemile-Slough-at-San Joaquin....	291
Figure 15-24 WY2010: DSM2 daily-averaged turbidity model results using Mixed-SSC-WARMF turbidity at the inflow boundaries– location is Turner-Cut-at-Holt.....	292

Figure 15-25 WY2010: DSM2 daily-averaged turbidity model results using Mixed-SSC-WARMF turbidity at the inflow boundaries– location is Victoria-Canal-at-Byron.	293
Figure 15-26 WY2011: DSM2 daily-averaged turbidity model results using Mixed-SSC-WARMF turbidity at the inflow boundaries– location is Antioch.	294
Figure 15-27 WY2011: DSM2 daily-averaged turbidity model results using Mixed-SSC-WARMF turbidity at the inflow boundaries– location is Cache-at-Ryer.	295
Figure 15-28 WY2011: DSM2 daily-averaged turbidity model results using Mixed-SSC-WARMF turbidity at the inflow boundaries– location is Decker-Island.....	296
Figure 15-29 WY2011: DSM2 daily-averaged turbidity model results using Mixed-SSC-WARMF turbidity at the inflow boundaries– location is False-River.....	297
Figure 15-30 WY2011: DSM2 daily-averaged turbidity model results using Mixed-SSC-WARMF turbidity at the inflow boundaries– location is Freeport.....	298
Figure 15-31 WY2011: DSM2 daily-averaged turbidity model results using Mixed-SSC-WARMF turbidity at the inflow boundaries– location is Georgiana- Below-Sac.....	299
Figure 15-32 WY2011: DSM2 daily-averaged turbidity model results using Mixed-SSC-WARMF turbidity at the inflow boundaries– location is Georgiana at Sac.	300
Figure 15-33 WY2011: DSM2 daily-averaged turbidity model results using Mixed-SSC-WARMF turbidity at the inflow boundaries– location is Grant Line.	301
Figure 15-34 WY2011: DSM2 daily-averaged turbidity model results using Mixed-SSC-WARMF turbidity at the inflow boundaries– location is Grant-Line-at-Tracy.....	302
Figure 15-35 WY2011: DSM2 daily-averaged turbidity model results using Mixed-SSC-WARMF turbidity at the inflow boundaries– location is Holland Cut.....	303
Figure 15-36 WY2011: DSM2 daily-averaged turbidity model results using Mixed-SSC-WARMF turbidity at the inflow boundaries– location is Hood.	304
Figure 15-37 WY2011: DSM2 daily-averaged turbidity model results using Mixed-SSC-WARMF turbidity at the inflow boundaries– location is Little-Potato-Slough-at-Terminus...	305
Figure 15-38 WY2011: DSM2 daily-averaged turbidity model results using Mixed-SSC-WARMF turbidity at the inflow boundaries– location is Mallard Slough.	306
Figure 15-39 WY2011: DSM2 daily-averaged turbidity model results using Mixed-SSC-WARMF turbidity at the inflow boundaries– location is Middle River at Howard.	307
Figure 15-40 WY2011: DSM2 daily-averaged turbidity model results using Mixed-SSC-WARMF turbidity at the inflow boundaries– location is Middle River at Holt.	308
Figure 15-41 WY2011: DSM2 daily-averaged turbidity model results using Mixed-SSC-WARMF turbidity at the inflow boundaries– location is Miner Slough.	309
Figure 15-42 WY2011: DSM2 daily-averaged turbidity model results using Mixed-SSC-WARMF turbidity at the inflow boundaries– location is Mokelumne at San Joaquin River.....	310
Figure 15-43 WY2011: DSM2 daily-averaged turbidity model results using Mixed-SSC-WARMF turbidity at the inflow boundaries– location is Mossdale.	311
Figure 15-44 WY2011: DSM2 daily-averaged turbidity model results using Mixed-SSC-WARMF turbidity at the inflow boundaries– location is North Mokelumne.....	312

Figure 15-45 WY2011: DSM2 daily-averaged turbidity model results using Mixed-SSC-WARMF turbidity at the inflow boundaries– location is Prisoner Point.....	313
Figure 15-46 WY2011: DSM2 daily-averaged turbidity model results using Mixed-SSC-WARMF turbidity at the inflow boundaries– location is Prisoner Point at Terminous.	314
Figure 15-47 WY2011: DSM2 daily-averaged turbidity model results using Mixed-SSC-WARMF turbidity at the inflow boundaries– location is Rio Vista.	315
Figure 15-48 WY2011: DSM2 daily-averaged turbidity model results using Mixed-SSC-WARMF turbidity at the inflow boundaries– location is Rough-N-Ready Island.	316
Figure 15-49 WY2011: DSM2 daily-averaged turbidity model results using Mixed-SSC-WARMF turbidity at the inflow boundaries– location is San Joaquin at Garwood.	317
Figure 15-50 WY2011: DSM2 daily-averaged turbidity model results using Mixed-SSC-WARMF turbidity at the inflow boundaries– location is San Joaquin at McCune.	318
Figure 15-51 WY2011: DSM2 daily-averaged turbidity model results using Mixed-SSC-WARMF turbidity at the inflow boundaries– location is South Mokelumne.....	319
Figure 15-52 WY2011: DSM2 daily-averaged turbidity model results using Mixed-SSC-WARMF turbidity at the inflow boundaries– location is Threemile at San Joaquin.....	320
Figure 15-53 WY2011: DSM2 daily-averaged turbidity model results using Mixed-SSC-WARMF turbidity at the inflow boundaries– location is Turner Cut at Holt.....	321
Figure 15-54 WY2011: DSM2 daily-averaged turbidity model results using Mixed-SSC-WARMF turbidity at the inflow boundaries– location is Victoria Canal at Byron.	322
Figure 15-55 WY2010: WY2010: DSM2 daily-averaged turbidity model results using WARMF-Only turbidity at the inflow boundaries– location is Antioch.....	323
Figure 15-56 WY2010: WY2010: DSM2 daily-averaged turbidity model results using WARMF-Only turbidity at the inflow boundaries– location is Cache-at-Ryer.	324
Figure 15-57 WY2010: WY2010: DSM2 daily-averaged turbidity model results using WARMF-Only turbidity at the inflow boundaries– location is Decker-Island.....	325
Figure 15-58 WY2010: DSM2 daily-averaged turbidity model results using WARMF-Only turbidity at the inflow boundaries– location is False-River.....	326
Figure 15-59 WY2010: DSM2 daily-averaged turbidity model results using WARMF-Only turbidity at the inflow boundaries– location is Freeport.....	327
Figure 15-60 WY2010: DSM2 daily-averaged turbidity model results using WARMF-Only turbidity at the inflow boundaries– location is Georgiana-Below-Sac.....	328
Figure 15-61 WY2010: DSM2 daily-averaged turbidity model results using WARMF-Only turbidity at the inflow boundaries– location is Georgiana-Sac.....	329
Figure 15-62 WY2010: DSM2 daily-averaged turbidity model results using WARMF-Only turbidity at the inflow boundaries– location is Grant-Line.....	330
Figure 15-63 WY2010: DSM2 daily-averaged turbidity model results using WARMF-Only turbidity at the inflow boundaries– location is Holland-Cut.	331
Figure 15-64 WY2010: DSM2 daily-averaged turbidity model results using WARMF-Only turbidity at the inflow boundaries– location is Hood.....	332

Figure 15-65WY2010: DSM2 daily-averaged turbidity model results using WARMF-Only turbidity at the inflow boundaries– location is Little-Potato-Slough-at-Terminus.....	333
Figure 15-66WY2010: DSM2 daily-averaged turbidity model results using WARMF-Only turbidity at the inflow boundaries– location is Mallard Slough.	334
Figure 15-67WY2010: DSM2 daily-averaged turbidity model results using WARMF-Only turbidity at the inflow boundaries– location is Middle-River-at-Holt.	335
Figure 15-68WY2010: DSM2 daily-averaged turbidity model results using WARMF-Only turbidity at the inflow boundaries– location is Miner Slough.	336
Figure 15-69WY2010: DSM2 daily-averaged turbidity model results using WARMF-Only turbidity at the inflow boundaries– location is Mokelumne-at-San Joaquin.	337
Figure 15-70WY2010: DSM2 daily-averaged turbidity model results using WARMF-Only turbidity at the inflow boundaries– location is Mossdale.	338
Figure 15-71WY2010: DSM2 daily-averaged turbidity model results using WARMF-Only turbidity at the inflow boundaries– location is Prisoner-Point.	339
Figure 15-72WY2010: DSM2 daily-averaged turbidity model results using WARMF-Only turbidity at the inflow boundaries– location is Prisoner-Point-at-Terminus.	340
Figure 15-73WY2010: DSM2 daily-averaged turbidity model results using WARMF-Only turbidity at the inflow boundaries– location is Rio Vista.	341
Figure 15-74 WY2010: DSM2 daily-averaged turbidity model results using WARMF-Only turbidity at the inflow boundaries– location is Rough-N-Ready Island.	342
Figure 15-75 WY2010: DSM2 daily-averaged turbidity model results using WARMF-Only turbidity at the inflow boundaries– location is San Joaquin-at-Garwood.....	343
Figure 15-76 WY2010: DSM2 daily-averaged turbidity model results using WARMF-Only turbidity at the inflow boundaries– location is San Joaquin-at-McCune.....	344
Figure 15-77 WY2010: DSM2 daily-averaged turbidity model results using WARMF-Only turbidity at the inflow boundaries– location is Threemile-Slough-at-San Joaquin.	345
Figure 15-78 WY2010: DSM2 daily-averaged turbidity model results using WARMF-Only turbidity at the inflow boundaries– location is Turner-Cut-at-Holt.....	346
Figure 15-79 WY2010: DSM2 daily-averaged turbidity model results using WARMF-Only turbidity at the inflow boundaries– location is Victoria-Canal-at-Byron.	347
Figure 15-80 WY2011: DSM2 daily-averaged turbidity model results using WARMF-Only turbidity at the inflow boundaries– location is Antioch.....	348
Figure 15-81 WY2011: DSM2 daily-averaged turbidity model results using WARMF-Only turbidity at the inflow boundaries– location is Cache-at-Ryer.	349
Figure 15-82 WY2011: DSM2 daily-averaged turbidity model results using WARMF-Only turbidity at the inflow boundaries– location is Decker-Island.....	350
Figure 15-83 WY2011: DSM2 daily-averaged turbidity model results using WARMF-Only turbidity at the inflow boundaries– location is False-River.....	351
Figure 15-84 WY2011: DSM2 daily-averaged turbidity model results using WARMF-Only turbidity at the inflow boundaries– location is Freeport.	352

Figure 15-85 WY2011: DSM2 daily-averaged turbidity model results using WARMF-Only turbidity at the inflow boundaries– location is Georgiana- Below-Sac.....	353
Figure 15-86 WY2011: DSM2 daily-averaged turbidity model results using WARMF-Only turbidity at the inflow boundaries– location is Georgiana at Sac.	354
Figure 15-87 WY2011: DSM2 daily-averaged turbidity model results using WARMF-Only turbidity at the inflow boundaries– location is Grant Line.	355
Figure 15-88 WY2011: DSM2 daily-averaged turbidity model results using WARMF-Only turbidity at the inflow boundaries– location is Grant-Line-at-Tracy.....	356
Figure 15-89 WY2011: DSM2 daily-averaged turbidity model results using WARMF-Only turbidity at the inflow boundaries– location is Holland Cut.....	357
Figure 15-90 WY2011: DSM2 daily-averaged turbidity model results using WARMF-Only turbidity at the inflow boundaries– location is Hood.....	358
Figure 15-91 WY2011: DSM2 daily-averaged turbidity model results using WARMF-Only turbidity at the inflow boundaries– location is Little-Potato-Slough-at-Terminous.....	359
Figure 15-92 WY2011: DSM2 daily-averaged turbidity model results using WARMF-Only turbidity at the inflow boundaries– location is Mallard Slough.	360
Figure 15-93 WY2011: DSM2 daily-averaged turbidity model results using WARMF-Only turbidity at the inflow boundaries– location is Middle River at Howard.	361
Figure 15-94 WY2011: DSM2 daily-averaged turbidity model results using WARMF-Only turbidity at the inflow boundaries– location is Middle River at Holt.	362
Figure 15-95 WY2011: DSM2 daily-averaged turbidity model results using WARMF-Only turbidity at the inflow boundaries– location is Miner Slough.	363
Figure 15-96 WY2011: DSM2 daily-averaged turbidity model results using WARMF-Only turbidity at the inflow boundaries– location is Mokelumne at San Joaquin River.....	364
Figure 15-97 WY2011: DSM2 daily-averaged turbidity model results using WARMF-Only turbidity at the inflow boundaries– location is Mossdale.	365
Figure 15-98 WY2011: DSM2 daily-averaged turbidity model results using WARMF-Only turbidity at the inflow boundaries– location is North Mokelumne.....	366
Figure 15-99 WY2011: DSM2 daily-averaged turbidity model results using WARMF-Only turbidity at the inflow boundaries– location is Prisoner Point.....	367
Figure 15-100 WY2011: DSM2 daily-averaged turbidity model results using WARMF-Only turbidity at the inflow boundaries– location is Prisoner Point at Terminous.	368
Figure 15-101 WY2011: DSM2 daily-averaged turbidity model results using WARMF-Only turbidity at the inflow boundaries– location is Rio Vista.	369
Figure 15-102 WY2011: DSM2 daily-averaged turbidity model results using WARMF-Only turbidity at the inflow boundaries– location is Rough-N-Ready Island.	370
Figure 15-103 WY2011: DSM2 daily-averaged turbidity model results using WARMF-Only turbidity at the inflow boundaries– location is San Joaquin at Garwood.	371
Figure 15-104 WY2011: DSM2 daily-averaged turbidity model results using WARMF-Only turbidity at the inflow boundaries– location is San Joaquin at McCune.	372

Figure 15-105 WY2011: DSM2 daily-averaged turbidity model results using WARMF-Only turbidity at the inflow boundaries– location is South Mokelumne.....	373
Figure 15-106 WY2011: DSM2 daily-averaged turbidity model results using WARMF-Only turbidity at the inflow boundaries– location is Threemile at San Joaquin.....	374
Figure 15-107 WY2011: DSM2 daily-averaged turbidity model results using WARMF-Only turbidity at the inflow boundaries– location is Turner Cut at Holt.....	375
Figure 15-108 WY2011: DSM2 daily-averaged turbidity model results using WARMF-Only turbidity at the inflow boundaries– location is Victoria Canal at Byron.....	376
Figure 16-1 DSM2 daily-averaged turbidity model results using USGS-SSC at Freeport and Vernalis, and WARMF turbidity at other inflow boundaries compared to EMP grab-sample data, early years– location is EMP C3.....	378
Figure 16-2 DSM2 daily-averaged turbidity model results using USGS-SSC at Freeport and Vernalis, and WARMF turbidity at other inflow boundaries compared to EMP grab-sample data, early years– location is EMP C7.....	379
Figure 16-3 DSM2 daily-averaged turbidity model results using USGS-SSC at Freeport and Vernalis, and WARMF turbidity at other inflow boundaries compared to EMP grab-sample data, early years– location is EMP C9.....	380
Figure 16-4 DSM2 daily-averaged turbidity model results using USGS-SSC at Freeport and Vernalis, and WARMF turbidity at other inflow boundaries compared to EMP grab-sample data, early years– location is EMP C10.....	381
Figure 16-5 DSM2 daily-averaged turbidity model results using USGS-SSC at Freeport and Vernalis, and WARMF turbidity at other inflow boundaries compared to EMP grab-sample data, early years– location is EMP D4.....	382
Figure 16-6 DSM2 daily-averaged turbidity model results using USGS-SSC at Freeport and Vernalis, and WARMF turbidity at other inflow boundaries compared to EMP grab-sample data, early years– location is EMP D6.....	383
Figure 16-7 DSM2 daily-averaged turbidity model results using USGS-SSC at Freeport and Vernalis, and WARMF turbidity at other inflow boundaries compared to EMP grab-sample data, early years– location is EMP D7.....	384
Figure 16-8 DSM2 daily-averaged turbidity model results using USGS-SSC at Freeport and Vernalis, and WARMF turbidity at other inflow boundaries compared to EMP grab-sample data, early years– location is EMP D8.....	385
Figure 16-9 DSM2 daily-averaged turbidity model results using USGS-SSC at Freeport and Vernalis, and WARMF turbidity at other inflow boundaries compared to EMP grab-sample data, early years– location is EMP D9.....	386
Figure 16-10 DSM2 daily-averaged turbidity model results using USGS-SSC at Freeport and Vernalis, and WARMF turbidity at other inflow boundaries compared to EMP grab-sample data, early years– location is EMP D10.....	387

Figure 16-11 DSM2 daily-averaged turbidity model results using USGS-SSC at Freeport and Vernalis, and WARMF turbidity at other inflow boundaries compared to EMP grab-sample data, early years– location is EMP D11. 388

Figure 16-12 DSM2 daily-averaged turbidity model results using USGS-SSC at Freeport and Vernalis, and WARMF turbidity at other inflow boundaries compared to EMP grab-sample data, early years– location is EMP D12. 389

Figure 16-13 DSM2 daily-averaged turbidity model results using USGS-SSC at Freeport and Vernalis, and WARMF turbidity at other inflow boundaries compared to EMP grab-sample data, early years– location is EMP D14A..... 390

Figure 16-14 DSM2 daily-averaged turbidity model results using USGS-SSC at Freeport and Vernalis, and WARMF turbidity at other inflow boundaries compared to EMP grab-sample data, early years– location is EMP D15. 391

Figure 16-15 DSM2 daily-averaged turbidity model results using USGS-SSC at Freeport and Vernalis, and WARMF turbidity at other inflow boundaries compared to EMP grab-sample data, early years– location is EMP D16. 392

Figure 16-16 DSM2 daily-averaged turbidity model results using USGS-SSC at Freeport and Vernalis, and WARMF turbidity at other inflow boundaries compared to EMP grab-sample data, early years– location is EMP D19. 393

Figure 16-17 DSM2 daily-averaged turbidity model results using USGS-SSC at Freeport and Vernalis, and WARMF turbidity at other inflow boundaries compared to EMP grab-sample data, early years– location is EMP D22. 394

Figure 16-18 DSM2 daily-averaged turbidity model results using USGS-SSC at Freeport and Vernalis, and WARMF turbidity at other inflow boundaries compared to EMP grab-sample data, early years– location is EMP D24. 395

Figure 16-19 DSM2 daily-averaged turbidity model results using USGS-SSC at Freeport and Vernalis, and WARMF turbidity at other inflow boundaries compared to EMP grab-sample data, early years– location is EMP D26. 396

Figure 16-20 DSM2 daily-averaged turbidity model results using USGS-SSC at Freeport and Vernalis, and WARMF turbidity at other inflow boundaries compared to EMP grab-sample data, early years– location is EMP D28A..... 397

Figure 16-21 DSM2 daily-averaged turbidity model results using USGS-SSC at Freeport and Vernalis, and WARMF turbidity at other inflow boundaries compared to EMP grab-sample data, early years– location is EMP MD7A. 398

Figure 16-22 DSM2 daily-averaged turbidity model results using USGS-SSC at Freeport and Vernalis, and WARMF turbidity at other inflow boundaries compared to EMP grab-sample data, early years– location is EMP MD10..... 399

Figure 16-23 DSM2 daily-averaged turbidity model results using USGS-SSC at Freeport and Vernalis, and WARMF turbidity at other inflow boundaries compared to EMP grab-sample data, early years– location is EMP P8. 400

Figure 16-24 DSM2 daily-averaged turbidity model results using USGS-SSC at Freeport and Vernalis, and WARMF turbidity at other inflow boundaries compared to EMP grab-sample data, early years– location is EMP P10A.	401
Figure 16-25 DSM2 daily-averaged turbidity model results using USGS-SSC at Freeport and Vernalis, and WARMF turbidity at other inflow boundaries compared to EMP grab-sample data, early years– location is EMP P12.	402
Figure 16-26 DSM2 daily-averaged turbidity model results using USGS-SSC at Freeport and Vernalis, and WARMF turbidity at other inflow boundaries compared to EMP grab-sample data, early years– location is EMP S42.	403
Figure 16-27 DSM2 daily-averaged turbidity model results using USGS-SSC at Freeport and Vernalis, and WARMF turbidity at other inflow boundaries compared to EMP grab-sample data, recent years– location is EMP C3.	405
Figure 16-28 DSM2 daily-averaged turbidity model results using USGS-SSC at Freeport and Vernalis, and WARMF turbidity at other inflow boundaries compared to EMP grab-sample data, recent years– location is EMP C7.	406
Figure 16-29 DSM2 daily-averaged turbidity model results using USGS-SSC at Freeport and Vernalis, and WARMF turbidity at other inflow boundaries compared to EMP grab-sample data, recent years– location is EMP C9.	407
Figure 16-30 DSM2 daily-averaged turbidity model results using USGS-SSC at Freeport and Vernalis, and WARMF turbidity at other inflow boundaries compared to EMP grab-sample data, recent years– location is EMP C10.	408
Figure 16-31 DSM2 daily-averaged turbidity model results using USGS-SSC at Freeport and Vernalis, and WARMF turbidity at other inflow boundaries compared to EMP grab-sample data, recent years– location is EMP D4.	409
Figure 16-32 DSM2 daily-averaged turbidity model results using USGS-SSC at Freeport and Vernalis, and WARMF turbidity at other inflow boundaries compared to EMP grab-sample data, recent years– location is EMP D6.	410
Figure 16-33 DSM2 daily-averaged turbidity model results using USGS-SSC at Freeport and Vernalis, and WARMF turbidity at other inflow boundaries compared to EMP grab-sample data, recent years– location is EMP D7.	411
Figure 16-34 DSM2 daily-averaged turbidity model results using USGS-SSC at Freeport and Vernalis, and WARMF turbidity at other inflow boundaries compared to EMP grab-sample data, recent years– location is EMP D8.	412
Figure 16-35 DSM2 daily-averaged turbidity model results using USGS-SSC at Freeport and Vernalis, and WARMF turbidity at other inflow boundaries compared to EMP grab-sample data, recent years– location is EMP D9.	413
Figure 16-36 DSM2 daily-averaged turbidity model results using USGS-SSC at Freeport and Vernalis, and WARMF turbidity at other inflow boundaries compared to EMP grab-sample data, recent years– location is EMP D10.	414

Figure 16-37 DSM2 daily-averaged turbidity model results using USGS-SSC at Freeport and Vernalis, and WARMF turbidity at other inflow boundaries compared to EMP grab-sample data, recent years– location is EMP D11..... 415

Figure 16-38 DSM2 daily-averaged turbidity model results using USGS-SSC at Freeport and Vernalis, and WARMF turbidity at other inflow boundaries compared to EMP grab-sample data, recent years– location is EMP D12..... 416

Figure 16-39 DSM2 daily-averaged turbidity model results using USGS-SSC at Freeport and Vernalis, and WARMF turbidity at other inflow boundaries compared to EMP grab-sample data, recent years– location is EMP D14A..... 417

Figure 16-40 DSM2 daily-averaged turbidity model results using USGS-SSC at Freeport and Vernalis, and WARMF turbidity at other inflow boundaries compared to EMP grab-sample data, recent years– location is EMP D15..... 418

Figure 16-41 DSM2 daily-averaged turbidity model results using USGS-SSC at Freeport and Vernalis, and WARMF turbidity at other inflow boundaries compared to EMP grab-sample data, recent years– location is EMP D16..... 419

Figure 16-42 DSM2 daily-averaged turbidity model results using USGS-SSC at Freeport and Vernalis, and WARMF turbidity at other inflow boundaries compared to EMP grab-sample data, recent years– location is EMP D22..... 420

Figure 16-43 DSM2 daily-averaged turbidity model results using USGS-SSC at Freeport and Vernalis, and WARMF turbidity at other inflow boundaries compared to EMP grab-sample data, recent years– location is EMP D24..... 421

Figure 16-44 DSM2 daily-averaged turbidity model results using USGS-SSC at Freeport and Vernalis, and WARMF turbidity at other inflow boundaries compared to EMP grab-sample data, recent years– location is EMP D26..... 422

Figure 16-45 DSM2 daily-averaged turbidity model results using USGS-SSC at Freeport and Vernalis, and WARMF turbidity at other inflow boundaries compared to EMP grab-sample data, recent years– location is EMP D28A..... 423

Figure 16-46 DSM2 daily-averaged turbidity model results using USGS-SSC at Freeport and Vernalis, and WARMF turbidity at other inflow boundaries compared to EMP grab-sample data, recent years– location is EMP MD7A. 424

Figure 16-47 DSM2 daily-averaged turbidity model results using USGS-SSC at Freeport and Vernalis, and WARMF turbidity at other inflow boundaries compared to EMP grab-sample data, recent years– location is EMP MD10. 425

Figure 16-48 DSM2 daily-averaged turbidity model results using USGS-SSC at Freeport and Vernalis, and WARMF turbidity at other inflow boundaries compared to EMP grab-sample data, recent years– location is EMP P8. 426

Figure 16-49 DSM2 daily-averaged turbidity model results using USGS-SSC at Freeport and Vernalis, and WARMF turbidity at other inflow boundaries compared to EMP grab-sample data, recent years– location is EMP P10A. 427

Figure 16-50 DSM2 daily-averaged turbidity model results using USGS-SSC at Freeport and Vernalis, and WARMF turbidity at other inflow boundaries compared to EMP grab-sample data, recent years– location is EMP P12. 428

Figure 17-1 DSM2 daily-averaged turbidity model results using and WARMF model turbidity at all inflow boundaries compared to EMP grab-sample data, early years– location is EMP C3. . 430

Figure 17-2 DSM2 daily-averaged turbidity model results using and WARMF model turbidity at all inflow boundaries compared to EMP grab-sample data, early years– location is EMP C7. . 431

Figure 17-3 DSM2 daily-averaged turbidity model results using and WARMF model turbidity at all inflow boundaries compared to EMP grab-sample data, early years– location is EMP C9. . 432

Figure 17-4 DSM2 daily-averaged turbidity model results using and WARMF model turbidity at all inflow boundaries compared to EMP grab-sample data, early years– location is EMP C10. 433

Figure 17-5 DSM2 daily-averaged turbidity model results using and WARMF model turbidity at all inflow boundaries compared to EMP grab-sample data, early years– location is EMP D4. 434

Figure 17-6 DSM2 daily-averaged turbidity model results using and WARMF model turbidity at all inflow boundaries compared to EMP grab-sample data, early years– location is EMP D6. . 435

Figure 17-7 DSM2 daily-averaged turbidity model results using and WARMF model turbidity at all inflow boundaries compared to EMP grab-sample data, early years– location is EMP D7. . 436

Figure 17-8 DSM2 daily-averaged turbidity model results using and WARMF model turbidity at all inflow boundaries compared to EMP grab-sample data, early years– location is EMP D8. . 437

Figure 17-9 DSM2 daily-averaged turbidity model results using and WARMF model turbidity at all inflow boundaries compared to EMP grab-sample data, early years– location is EMP D9. . 438

Figure 17-10 DSM2 daily-averaged turbidity model results using and WARMF model turbidity at all inflow boundaries compared to EMP grab-sample data, early years– location is EMP D10. 439

Figure 17-11 DSM2 daily-averaged turbidity model results using and WARMF model turbidity at all inflow boundaries compared to EMP grab-sample data, early years– location is EMP D11. 440

Figure 17-12 DSM2 daily-averaged turbidity model results using and WARMF model turbidity at all inflow boundaries compared to EMP grab-sample data, early years– location is EMP D12. 441

Figure 17-13 DSM2 daily-averaged turbidity model results using and WARMF model turbidity at all inflow boundaries compared to EMP grab-sample data, early years– location is EMP D14A. 442

Figure 17-14 DSM2 daily-averaged turbidity model results using and WARMF model turbidity at all inflow boundaries compared to EMP grab-sample data, early years– location is EMP D15. 443

Figure 17-15 DSM2 daily-averaged turbidity model results using and WARMF model turbidity at all inflow boundaries compared to EMP grab-sample data, early years– location is EMP D16. 444

Figure 17-16 DSM2 daily-averaged turbidity model results using and WARMF model turbidity at all inflow boundaries compared to EMP grab-sample data, early years– location is EMP D19. 445

Figure 17-17 DSM2 daily-averaged turbidity model results using and WARMF model turbidity at all inflow boundaries compared to EMP grab-sample data, early years– location is EMP D22. 446

Figure 17-18 DSM2 daily-averaged turbidity model results using and WARMF model turbidity at all inflow boundaries compared to EMP grab-sample data, early years– location is EMP D24. 447

Figure 17-19 DSM2 daily-averaged turbidity model results using and WARMF model turbidity at all inflow boundaries compared to EMP grab-sample data, early years– location is EMP D26. 448

Figure 17-20 DSM2 daily-averaged turbidity model results using and WARMF model turbidity at all inflow boundaries compared to EMP grab-sample data, early years– location is EMP D28A. 449

Figure 17-21 DSM2 daily-averaged turbidity model results using and WARMF model turbidity at all inflow boundaries compared to EMP grab-sample data, early years– location is EMP MD7A. 450

Figure 17-22 DSM2 daily-averaged turbidity model results using and WARMF model turbidity at all inflow boundaries compared to EMP grab-sample data, early years– location is MD10.. 451

Figure 17-23 DSM2 daily-averaged turbidity model results using and WARMF model turbidity at all inflow boundaries compared to EMP grab-sample data, early years– location is P8. 452

Figure 17-24 DSM2 daily-averaged turbidity model results using and WARMF model turbidity at all inflow boundaries compared to EMP grab-sample data, early years– location is P10A. ... 453

Figure 17-25 DSM2 daily-averaged turbidity model results using and WARMF model turbidity at all inflow boundaries compared to EMP grab-sample data, early years– location is P12. 454

Figure 17-26 DSM2 daily-averaged turbidity model results using and WARMF model turbidity at all inflow boundaries compared to EMP grab-sample data, early years– location is S42. 455

Figure 17-27 DSM2 daily-averaged turbidity model results using and WARMF model turbidity at all inflow boundaries compared to EMP grab-sample data, recent years– location is EMP C3. 456

Figure 17-28 DSM2 daily-averaged turbidity model results using and WARMF model turbidity at all inflow boundaries compared to EMP grab-sample data, recent years– location is EMP C7. 457

Figure 17-29 DSM2 daily-averaged turbidity model results using and WARMF model turbidity at all inflow boundaries compared to EMP grab-sample data, recent years– location is EMP C9. 458

Figure 17-30 DSM2 daily-averaged turbidity model results using and WARMF model turbidity at all inflow boundaries compared to EMP grab-sample data, recent years– location is EMP C10. 459

Figure 17-31 DSM2 daily-averaged turbidity model results using and WARMF model turbidity at all inflow boundaries compared to EMP grab-sample data, recent years– location is EMP D4. 460

Figure 17-32 DSM2 daily-averaged turbidity model results using and WARMF model turbidity at all inflow boundaries compared to EMP grab-sample data, recent years– location is EMP D6. 461

Figure 17-33 DSM2 daily-averaged turbidity model results using and WARMF model turbidity at all inflow boundaries compared to EMP grab-sample data, recent years– location is EMP D7. 462

Figure 17-34 DSM2 daily-averaged turbidity model results using and WARMF model turbidity at all inflow boundaries compared to EMP grab-sample data, recent years– location is EMP D8. 463

Figure 17-35 DSM2 daily-averaged turbidity model results using and WARMF model turbidity at all inflow boundaries compared to EMP grab-sample data, recent years– location is EMP D9. 464

Figure 17-36 DSM2 daily-averaged turbidity model results using and WARMF model turbidity at all inflow boundaries compared to EMP grab-sample data, recent years– location is EMP D10. 465

Figure 17-37 DSM2 daily-averaged turbidity model results using and WARMF model turbidity at all inflow boundaries compared to EMP grab-sample data, recent years– location is EMP D11. 466

Figure 17-38 DSM2 daily-averaged turbidity model results using and WARMF model turbidity at all inflow boundaries compared to EMP grab-sample data, recent years– location is EMP D12. 467

Figure 17-39 DSM2 daily-averaged turbidity model results using and WARMF model turbidity at all inflow boundaries compared to EMP grab-sample data, recent years– location is EMP D14A. 468

Figure 17-40 DSM2 daily-averaged turbidity model results using and WARMF model turbidity at all inflow boundaries compared to EMP grab-sample data, recent years– location is EMP D15. 469

Figure 17-41 DSM2 daily-averaged turbidity model results using and WARMF model turbidity at all inflow boundaries compared to EMP grab-sample data, recent years– location is EMP D16. 470

Figure 17-42 DSM2 daily-averaged turbidity model results using and WARMF model turbidity at all inflow boundaries compared to EMP grab-sample data, recent years– location is EMP D22. 471

Figure 17-43 DSM2 daily-averaged turbidity model results using and WARMF model turbidity at all inflow boundaries compared to EMP grab-sample data, recent years– location is EMP D24. 472

Figure 17-44 DSM2 daily-averaged turbidity model results using and WARMF model turbidity at all inflow boundaries compared to EMP grab-sample data, recent years– location is EMP D26. 473

Figure 17-45 DSM2 daily-averaged turbidity model results using and WARMF model turbidity at all inflow boundaries compared to EMP grab-sample data, recent years– location is EMP D28A. 474

Figure 17-46 DSM2 daily-averaged turbidity model results using and WARMF model turbidity at all inflow boundaries compared to EMP grab-sample data, recent years– location is EMP MD7A. 475

Figure 17-47 DSM2 daily-averaged turbidity model results using and WARMF model turbidity at all inflow boundaries compared to EMP grab-sample data, recent years– location is EMP MD10. 476

Figure 17-48 DSM2 daily-averaged turbidity model results using and WARMF model turbidity at all inflow boundaries compared to EMP grab-sample data, recent years– location is EMP P8. 477

Figure 17-49 DSM2 daily-averaged turbidity model results using and WARMF model turbidity at all inflow boundaries compared to EMP grab-sample data, recent years– location is EMP P10A. 478

Figure 17-50 DSM2 daily-averaged turbidity model results using and WARMF model turbidity at all inflow boundaries compared to EMP grab-sample data, recent years– location is EMP P12. 479

Tables

Table 5-1 WY2010 revised calibration of QUAL turbidity – final calibration run. Bold font in the name indicates compliance locations; blue font in the statistics denotes an improved result in comparison with Table 5-2.	34
Table 5-2 WY2010 DMS calibration of QUAL turbidity. Bold font in the name indicates compliance locations; blue font in the statistics denotes an improved result in comparison with Table 5-1.	35
Table 5-3 WY2011 revised calibration of QUAL turbidity – final calibration run. Bold font in the name indicates compliance locations; blue font in the statistics denotes an improved result in comparison with Table 5-4.	36
Table 5-4 WY2011 DMS calibration of QUAL turbidity. Bold font in the name indicates compliance locations; blue font in the statistics denotes an improved result in comparison with Table 5-3.	37
Table 5-5 Overall calibration metrics for the revised final calibration run and the initial DMS section calibration run. Blue font indicates a superior calibration result.	38
Table 6-1 WY2010 Mixed-SSC-WARMF residual results. Bold font in the name indicates compliance locations; blue font in the statistics denotes an improved result in comparison with Table 6-2.	41
Table 6-2 WY2010 WARMF-Only residual results. Bold font in the name indicates compliance locations; blue font in the statistics denotes an improved result in comparison with Table 6-1. .	42
Table 6-3 WY2011 Mixed-SSC-WARMF residual results. Bold font in the name indicates compliance locations; blue font in the statistics denotes an improved result in comparison with Table 6-4.	43
Table 6-4 WY2011 WARMF-Only residual results. Bold font in the name indicates compliance locations; blue font in the statistics denotes an improved result in comparison with Table 6-3. .	44
Table 6-5 Overall metrics for the two sets of boundary conditions – Mixed SSC-WARMF and WARMF-Only.	44
Table 6-6 Cross-comparison WY2010 results for Location Metrics. Note that the Recalibration results in this Table are NOT directly comparable to the other two columns, as the Location Metrics were calculated in comparison to the DMS model.	45
Table 6-7 Cross-comparison WY2011 results for Location Metrics Note that the Recalibration results in this Table are NOT directly comparable to the other two columns, as the Location Metrics were calculated in comparison to the DMS model.	46
Table 7-1 WARMF-Only boundary conditions simulation for early years (1975 – 1990). Blue font in the statistics denotes an improved result in comparison with Table 7-2.	64
Table 7-2 Mixed-SSC-WARMF boundary conditions simulation for early years (1975 – 1990). Blue font in the statistics denotes an improved result in comparison with Table 7-1.	65
Table 7-3 WARMF-Only boundary conditions simulation for recent- years (1991 – 2011). Blue font in the statistics denotes an improved result in comparison with Table 7-4.	66

Table 7-4 Mixed-SSC-WARMF boundary conditions simulation for recent years (1991 – 2011). Blue font in the statistics denotes an improved result in comparison with Table 7-3. 67

Table 8-1 Approximate values for important flow and turbidity locations in the DSM2 model during the high flow/high turbidity periods WY1991 to WY2000. Shaded lines indicate high flow period when a turbidity bridge did not form..... 73

1 Executive Summary

For several years, the Metropolitan Water District of Southern California (MWD) has funded Resource Management Associates (RMA) for the development of a turbidity transport model in the Sacramento San Joaquin Delta (RMA 2008, 2009a, 2009b, 2010a, 2010b, 2011a, 2011b, 2012a, 2012b) in an ongoing effort to model the hydrodynamic transport of turbidity as a proxy for the transport of suspended sediment. The motivation behind these developments is that turbidity has long been associated with the movement and habitat preferences of the endangered delta smelt, although the exact nature of the links between delta smelt and turbidity is subject to differing interpretations. The initial turbidity modeling effort was undertaken in RMA two-dimensional models along with particle tracking models simulating hypothetical turbidity-seeking behaviors of adult delta smelt. Recently, the Delta Modeling Section (DMS) of the Department of Water Resources (DWR) implemented a similar turbidity model approach in the one-dimensional QUAL transport module of the DSM2 suite of models, as discussed in (DWR 2011).

For the work discussed in this report, RMA used the DMS's initial QUAL turbidity modeling effort in support of two main project objectives, to:

1. Refine the DMS QUAL turbidity model calibration
2. Develop a historical simulation of turbidity in QUAL covering the period 1975–2011 to support development of a Turbidity ANN (Artificial Neural Network, work undertaken by Tetra Tech) using DSM2 QUAL model output.

A secondary objective was to use the long-term model simulations to investigate the conditions under which a turbidity bridge forms linking the south and central Delta. A brief analysis was performed using the historical turbidity simulations to accomplish this objective.

To document the accomplishment of the two objectives, statistical measures were employed to quantify the success of the modeling efforts. Although the two objectives of the project were clear at the outset, the criteria for determining the sufficiency of the QUAL turbidity calibration or the “best” set of synthetic boundary conditions for the long term turbidity model were not specified. Metrics were thus defined to quantify the success of the modeling effort at individual data locations and also to quantify Delta-wide “model skill”. The intent of these metrics was to supply information to aid in appropriate model application with a focus on decision support - the objective was to maximize model skill by minimizing model error. Some measure of subjectivity in the metrics chosen for model skill assessment was inevitable. For example, although a model should be able to simulate both the amplitude and the pattern of measurement variability, the decision of which of these factors is more important is dependent on the application and a subjective assessment of importance (Taylor 2000).

Work refining the QUAL turbidity calibration, covered in Objective One, focused on improving QUAL's accuracy in modeling turbidity in the winter when high tributary inflows carrying sediment load

substantially increase turbidity in the Delta. Increases in Delta turbidity are associated with increases in delta smelt entrainment in south Delta export locations, particularly when conditions, including export pumping, increase central Delta turbidity and the potential of forming a “turbidity bridge” to the south Delta. High inflow pulses of turbidity primarily originate in the Sacramento and San Joaquin Rivers, and to a lesser extent in the eastern Delta tributaries. Given the establishment of three turbidity measurement compliance locations in the central and south Delta – at Holland Cut, Prisoner Point and Victoria Canal at Byron – and the importance of delta smelt to restrictions on current Delta operations, the QUAL turbidity model calibration discussed herein placed a high priority on improving the QUAL turbidity calibration at these three locations. Three water years (WYs) were investigated in the calibration effort, WY2010, WY2011 and WY2012 as the quantity and quality of turbidity data has improved substantially in recent years.

A series of calibration statistics were calculated for the wet seasons of WY2010 and WY2011 quantifying the results of the recalibration effort (in comparison with the initial DMS turbidity model) at individual data locations with a focus on the compliance locations. Although the wet season of WY2012 was modeled, it was not included in the calibration assessment and the results are not included in this report, as inflow and turbidity concentrations were low and at the boundary of the suggested application of the QUAL turbidity model.

The calibration statistics document that the recalibration improved the representation of Delta turbidity, with the model recalibration showing significant improvement in WY2011, and also improvement in WY2010. As has been mentioned in previous documentation (RMA 2010b, 2011a, 2011b, 2012b), the compromise of using a turbidity model instead of a physically-based suspended sediment model means that the accuracy of model results can vary widely from year-to-year as variations in the character of the suspended sediment at inflow locations are not captured in turbidity measurements.

Objective Two focused on supporting the development of a Turbidity ANN interfacing with the DSM2 QUAL turbidity model output (from the recalibrated model). The work for this task entailed developing a set of QUAL turbidity boundary conditions for Historical model years 1975 – 2011, a time period comprised mainly of years when turbidity data needed for boundary conditions was not available. Two sets of alternative data were available for the Freeport and Vernalis turbidity boundary conditions: WARMF model output for turbidity was calculated by Systech from WARMF sediment output; and, USGS suspended sediment concentration (SSC) data. WARMF model output was used for the other tributary inflow boundaries –Yolo Bypass, Cosumnes, Mokelumne and Calaveras Rivers. Documentation on the development of improved WARMF results at these four locations is available in (RMA 2012a).

The DMS supplied the historical hydrodynamic model input for the HYDRO runs for the water years 1975 – 2010 and separately for recent years through December 2011. From previous turbidity forecasting results (RMA 2010b, 2011a, 2011b, 2012b), RMA supplied additional information mainly for historical turbidity data used for developing boundary conditions and for calibration.

Work for Objective Two had three major steps – the first step entailed assessing two sets of QUAL turbidity model simulation results prepared using USGS-SSC or WARMF data to develop boundary

conditions at Freeport and Vernalis. One set of simulations used a refined USGS Vernalis SSC concentration (*i.e.*, Vernalis SSC*0.3) and an unaltered USGS Freeport SSC for boundary conditions – these are denoted the “Mixed-SSC-WARMF” simulations. A second set of simulations – the “WARMF-Only” simulations – used WARMF model calculations supplied by Systech specifically for this project for turbidity boundary conditions at Vernalis and Freeport. Both sets of simulations used WARMF model outputs at the other tributaries, and a constant 20 NTU at the Martinez boundary. Modeling results for this step were assessed by comparing residual statistics for WY2010 and WY2011 simulations using these two set of boundary conditions in the recalibrated QUAL model. These statistics were calculated in the same manner as the calibration statistics, with a focus on comparing the results at the three compliance locations for each of the two sets of boundary conditions. The end result was that the Mixed-SSC-WARMF model statistics were better than the WARMF-Only statistics at the three compliance locations for both the WY2010 and WY2011 time frames.

The second step in Objective 2 concerned the development of long-term QUAL turbidity simulations for the ANN. The Mixed-SSC-WARMF boundary conditions were used in the newly calibrated turbidity model for the years 1975 – 1990, the “early years” and separately for the “recent years” 1991 – 2011. The “early years” simulations used the DSM2 model set-up supplied with the long-term (1975 – 2010) Historical model, while the “recent years” simulations used the most up-to-date DSM2 Historical model set-up which ran through 2011. These results, including both DSM2 model set-ups for HYDRO and the recalibrated QUAL turbidity model using the Mixed-SSC-WARMF boundary conditions, were supplied to Tetra Tech for further use in ANN development.

Subsequently, the third step used “early years” and “recent years” model set-ups with both the Mixed-SSC-WARMF and WARMF-Only boundary conditions to calculate model residual statistics in comparison with Environmental Monitoring Program (EMP) grab sample data available during these years. The objective was to further assess these two sets of boundary conditions. Statistics were computed at each available data location in each time frame (recent years and early years) by comparison of EMP data with daily averaged model results – note that EMP data did not include the three compliance locations. In these statistics, the entire time frame was used, not just the high flow portion of the water years, although it should be noted that the intent is to use the turbidity only during high flow and turbidity periods. These statistics show that the WARMF-Only simulation has a regular bias resulting in an under-prediction of the EMP data, and mixed overall results for both the Mixed-SSC-WARMF and WARMF-only simulations when viewed in aggregate over the Delta.

Subsequent to the turbidity model recalibration and development of the 1975-2011 historical turbidity model, the individual statistical measures were aggregated in several ways to provide a measure of “model skill” in the model domain as a whole¹ to enable comparison for WY2010 and WY2011 of the DMS calibration with the recalibration of QUAL turbidity and comparison of the two sets of alternative boundary conditions. Given time constraints for the delivery of the results of Objective 2 to Tetra Tech,

¹ The “Location Metrics” and the model skill metrics calculated in this report were improved for the current document to supply a better normalized value. These calculations have not changed previous conclusions.

these additional statistical measures were not available for distribution initially. However, they are important to a comprehensive understanding of the capabilities of the turbidity model.

In the “model skill” statistical assessment for WY2010 and WY2011, the statistics verified better model skill at the three compliance locations for the Mixed-SSC-WARMF simulations. However, two other Delta-wide statistics showed somewhat better results for the WARMF-Only simulations when viewed over all of the Delta data locations in WY2010. Not surprisingly, WY2010 and WY2011 simulations using actual turbidity data had significantly superior results at the individual data locations in comparison with the two alternative boundary condition applications.

The model skill results for the “early years” and the “recent years” simulations do not give a compelling advantage to either the Mixed-SSC-WARMF or the WARMF-only boundary conditions for use in the long term historical simulation, as comparison of the residual statistics shows that each of these models had significant difficulties in reproducing available EMP turbidity data.

In order to better interpret the DSM2 Model results, a spatial interpolation tool was created to visualize the one-dimensional model output as spatial contours (see Section 11.2.2 for technical details). A selected set of figures illustrate that there are substantial differences in the resulting turbidity fields using the Mixed-SSC-WARMF or the WARMF-only boundary conditions. Although the Mixed-SSC-WARMF matched the real daily-averaged turbidity values better in the both the WY2010 and WY2011 statistical results, two examples showed the result in terms of exceeding the compliance value (12 NTU) at the three locations was the same. Although data at the three compliance locations was not available to use in comparison for the model results in the example illustrating the “early years” simulation results, the turbidity magnitudes show the predictions would have led to the same operational decision.

It is suggested that for scenario-testing type of turbidity model applications, for example where CALSIM is used to determine Delta operations, the WARMF model should be considered to supply both inflow and turbidity boundary conditions particularly if some improvements can be made in WARMF calculations for turbidity at Freeport and Vernalis. The reasons are two-fold: first, in these model applications, the WARMF model flow differs somewhat from the inflows developed in CALSIM, while the WARMF turbidity calculation is conceptually consistent with WARMF model flow calculations; and, second, with some additional effort (and funding), it is quite likely that the WARMF turbidity calculations at Vernalis and Freeport can be improved to more closely match available turbidity data. Results from WY2012 improvements in the WARMF model calculations (RMA 2012a) of turbidity boundary conditions at Yolo Bypass, Cosumnes, Mokelumne and Calaveras Rivers were very encouraging, and supply confidence that with additional effort, further improvements can be made in the more complicated SSC sources at Vernalis and Freeport.

As suggested in previous RMA documentation (RMA 2010b, 2011a, 2011b, 2012b) and in Section 2.3 following, development of a true suspended sediment model should be considered. The capability in a suspended sediment model to include wind-driven re-suspension of sediments, tidally-influenced suspension of sediments, variations in the character of suspended sediment composition at model

boundaries, and other factors that are not considered in these turbidity model calculations, have the potential to improve the quality of model results.

The Mixed-SSC-WARMF simulation was used to analyze the modeled conditions under which a turbidity bridge linking the central and south Delta was likely to form. Animations using the spatial interpolation tool were utilized along with time series of daily-averaged model output. The high flow/high turbidity periods of water years 1991 – 2000 were selected as they represent a wide range of conditions. The results suggest further analyses could be made to see if the modeled results indicating that there are preferred routes for a turbidity bridge to form through Old River or Middle River - depending on the dominant source of turbidity - hold true for similar conditions in model scenarios. In general, the analysis shows that there is more than one mode under which a turbidity bridge is likely to form. It should be noted that this analysis is based on a turbidity model developed with synthetic or externally calculated (i.e., from WARMF results) boundary conditions, so results analyzing the flow and turbidity conditions under which a turbidity bridge may form should be interpreted with caution.

2 Introduction

2.1 Objectives

In this report, RMA utilized DWR-DMS's early turbidity modeling effort in DSM2-QUAL in support of two main project objectives, to:

1. Refine the initial DMS QUAL turbidity model calibration
2. Develop a historical model of turbidity in QUAL covering the period 1975 – 2011 to support development of a Turbidity ANN (Artificial Neural Network, work undertaken by Tetra Tech) using DSM2 QUAL model output.

The work refining QUAL turbidity calibration, covered in Objective One, focused on improving QUAL's accuracy in modeling turbidity in the winter when high tributary inflows substantially increase turbidity in the Delta. The initial QUAL turbidity calibration undertaken by the Delta Modeling Section (DMS) of the Department of Water Resources (DWR) in California using Water Year 2010 (WY2010) data is discussed in (DWR 2011). Work on the second objective compared the use of USGS daily suspended sediment measurements and WARMF model calculated turbidity as boundary conditions for the Sacramento and San Joaquin Rivers in the revised calibration of the turbidity model, with the overall objective of developing a long term simulation of turbidity (1975 – 2011) in QUAL to use in training an ANN to model turbidity in the Delta.

2.2 Background

Turbidity has long been associated with the movement and habitat preferences of delta smelt (RMA 2008, 2009a, 2009b, 2010a, 2010b). Although the exact nature of the links between delta smelt and turbidity are subject to differing interpretations, common hypotheses include: facilitating feeding through visual contrast of delta smelt prey against the background; as a form of cover from predators; and, as a cue for winter migration upstream to fresher waters to spawn. Increases in Delta turbidity

have also been associated with increases in entrainment in south Delta export locations, particularly when export pumping increases central Delta turbidity by forming a “turbidity bridge” linking the south Delta with high inflow pulses of turbidity from Delta tributaries, primarily the Sacramento River and the San Joaquin River.

These factors have prompted the development of turbidity transport models, through funding from MWD for RMA (RMA 2008, 2009a, 2009b, 2010a, 2010b, 2012a, 2012b) and subsequently in work undertaken by DWR-DMS (DWR 2011). As turbidity measurement locations have become more numerous in the Delta, the additional data has prompted the recalibration of the QUAL turbidity model to use in forecasting turbidity during the wet season when turbidity increases during periods of high inflow may prompt the movement of delta smelt into the central Delta, possibly subjecting them to the influence of the export pumps.

Given the establishment of three turbidity measurement compliance locations – at Holland Cut, Prisoner Point and Victoria Canal at Byron – and the importance of delta smelt to current Delta operations, the QUAL turbidity model calibration discussed herein placed a high priority on calibration at these locations. These three turbidity compliance locations in the Central Delta are used by the Delta Smelt Working Group for setting constraints on Delta operations.

This document describes the calibration process, presents calibration results along with several metrics designed to establish the quality of the refined QUAL turbidity model calibration in comparison with the calibration originally performed by the DMS. Three Delta-wide calibration metrics were developed to supply a method of determining model skill. In addition, this document describes the development and assessment of a long-term simulation of Historical turbidity in the Delta. As turbidity data was not available to set boundary conditions, available USGS-SSC data and WARMF model output were used to supply a set of boundary conditions that estimate historical conditions.

2.3 Challenges in modeling turbidity

As discussed in previous documentation (RMA 2008, 2009a, 2009b, 2010a, 2010b, 2011a, 2011b, 2012b), there are conceptual challenges to modeling turbidity in a transport model such as DSM2-QUAL, or RMA11 (King 1995), as turbidity is an optical property of water not a physical property. The more appropriate quantity to model is suspended sediment concentration (SSC), as the transport of sediment has a known physical interpretation. That said, there is frequently a linear relationship between measured turbidity and SSC, and reasonable success has been obtained by using simple one parameter decay rates in the RMA11 transport model or settling rates for a non-conservative constituent in the QUAL model.

A turbidity model based on settling coefficients or decay rates is not capable of capturing all of the processes in sediment transport, so some mismatch between the model and turbidity data is not unexpected as turbidity measurements are used as a proxy for suspended sediment concentration. The model calibration results presented herein illustrate the difficulties in several aspects of the turbidity/suspended sediment relationship: the relationship can vary by location, by the characteristics of upstream suspended sediment load, by the characteristics of the underlying sediment, and by effects

driven by local meteorology such as wind, rain and run-off. As a consequence, it can be expected that any turbidity model calibration will work better in some years than others, and since coefficients are not related to changes in the bed or in other sediment characteristics that change in time, the model will perform better at some locations and times than at others.

3 Turbidity Model Calibration - Background and Methodology

3.1 Definition of calibration

Although there are many different ways to define model calibration, in this document we assume the simple definition that calibration is the process of adjusting a set of model parameters so that model agreement with respect to a set of experimental data is maximized (Trucano et al., 2006). Similarly, validation is the quantification of the predictive ability of the model through comparison with a set of experimental data (Trucano et al., 2006). For both calibration and validation, these definitions assume that a set of criteria for assessing the goodness-of-fit of the model to the data have been selected. For the purposes of this project, the general calibration methodology discussed in Moriasi (2007) was modified for the turbidity model assessment.

3.2 QUAL turbidity calibration background and data

As discussed in (DWR 2011), the QUAL nutrient model equation for CBOD was used to simulate the transport of turbidity in the DSM2 model domain. Water temperature and the other nutrients in the QUAL nutrient model were not simulated.

The CBOD function in QUAL is expressed as:

$$\frac{dL}{dt} = -K_1L - K_3L$$

where:

- L = concentration of CBOD (mg/L)
- K_1 = deoxygenation rate coefficient (day^{-1})
- K_3 = settling rate of CBOD (day^{-1}).

For our purpose, K_1 was set to zero, as were all other coefficient in the QUAL nutrient model except K_3 which was used to represent the settling of sediment as an approximation to the transport of turbidity.

Turbidity data needed for the calibration and to set Freeport and Vernalis boundary conditions was downloaded from the CDEC database – locations used in the calibration process are shown in Figure 3-1. Turbidity compliance locations are shown in Figure 3-2. Statistics were calculated for all available data of sufficient quality – the turbidity data was “cleaned”, i.e., questionable values were deleted using professional judgment based on familiarity with the data. For example, significant increases in turbidity are generally reflected in downstream locations, so when downstream locations did not reflect

upstream changes, local increases could frequently be ascribed to instrument fouling or to short term trends in magnitude. However, increases in turbidity due to wind and rain events were not screened out, nor were changes in turbidity that were deemed reasonable. For example, changes in magnitude that did not appear to be due to instrument fouling or wind but were not necessarily reflected downstream (i.e., that might be due to localized events) were not screened out of the data set. Missing or deleted data values were filled using linear interpolation in HEC DSSVue software.

Calibration of the settling rate coefficient (K_3) to turbidity data began by using the wet season data of three water years - 2010, 2011 and 2012. These years were chosen as they have the best (least noisy) data and most numerous turbidity measurement stations, as well as the having data available for setting boundary conditions at Martinez, Freeport and Vernalis. The other boundary locations for WY2010 and WY2011 were set using WARMF model output - the Yolo Bypass, and the Calaveras, Cosumnes and Mokelumne Rivers. WARMF model output at these locations was improved in the recent calibration of WARMF (2012) for sediment and turbidity done in collaboration with RMA in WY2011 (RMA 2012a). WARMF model output was not available for WY2012 from Systech, and the WARMF model output used in forecasting for WY2012 was frequently of poor quality, so data at the nearest downstream location to a boundary was used instead.

A validation step was not performed using a separate dataset; given the challenging nature of turbidity calibration as discussed above in Section 2.3, at least one additional year of data during a relatively high flow could be used for validation at some future time. Although the wet season of three water years (2010, 2011, 2012) were developed for calibration statistics, in the end only two years - 2010 and 2011 - are used for presenting the final results as the boundary condition inflow and turbidity were deemed to be at the boundary of the useful range for turbidity model application in Water Year 2012, and not suitable for use in model calibration or validation.

Turbidity data was also obtained from Environmental Monitoring Program data base². These are discrete water samples (*aka* "grab samples") generally collected from land-based collection locations or from DWR or USBR research vessels. Field methods are available at the following website:

<http://www.water.ca.gov/bdma/meta/discrete.cfm>

These data were used in comparison with QUAL long term turbidity simulation output, 1975 – 2011, to assess the performance of the model run with the Mixed-SSC-WARMF and the WARMF-Only boundary conditions. Figures showing the locations used and the results are discussed in Section 7.1.

²<http://www.water.ca.gov/bdma/meta/index.cfm>

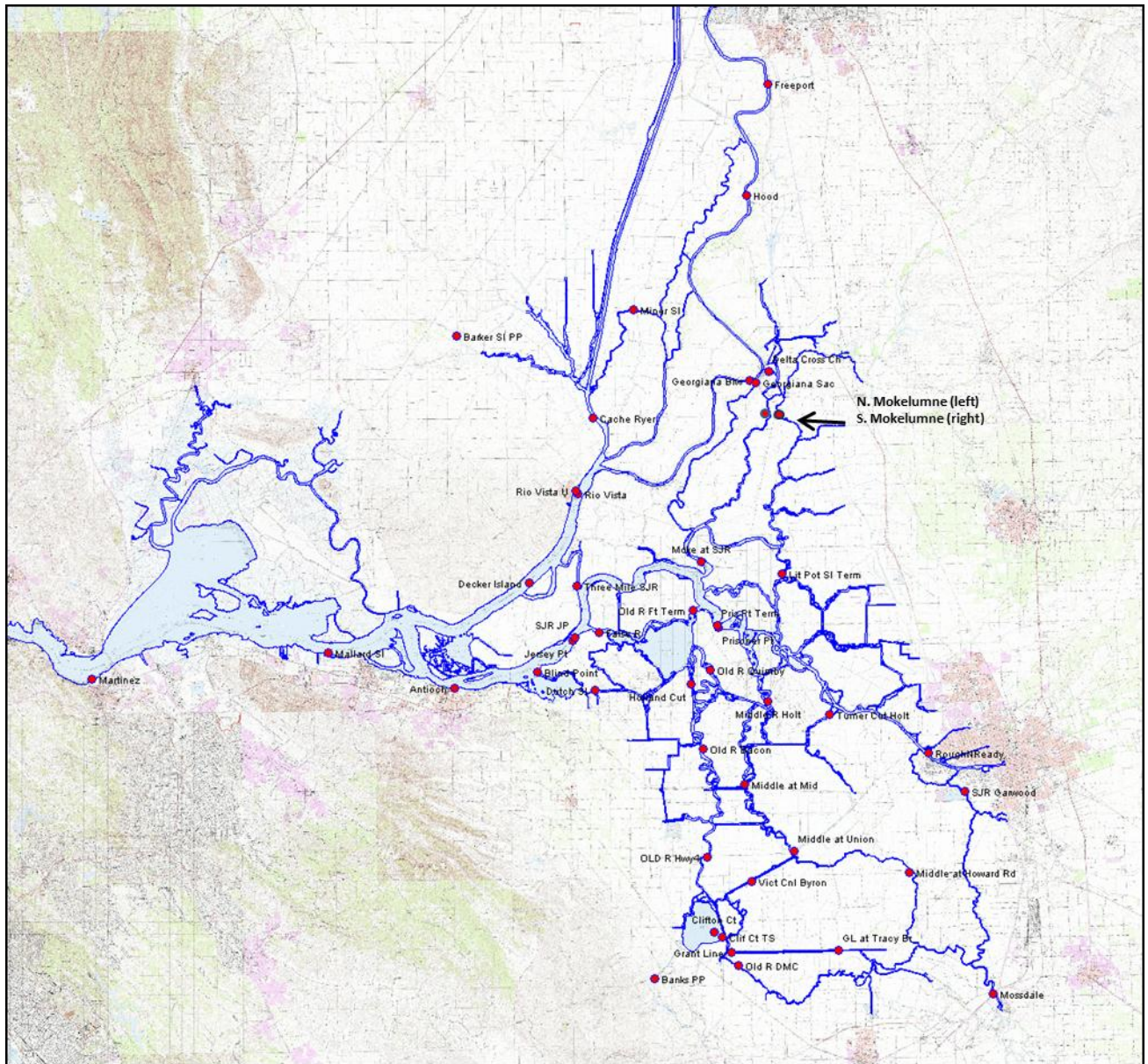


Figure 3-1 CDEC turbidity measurement locations.

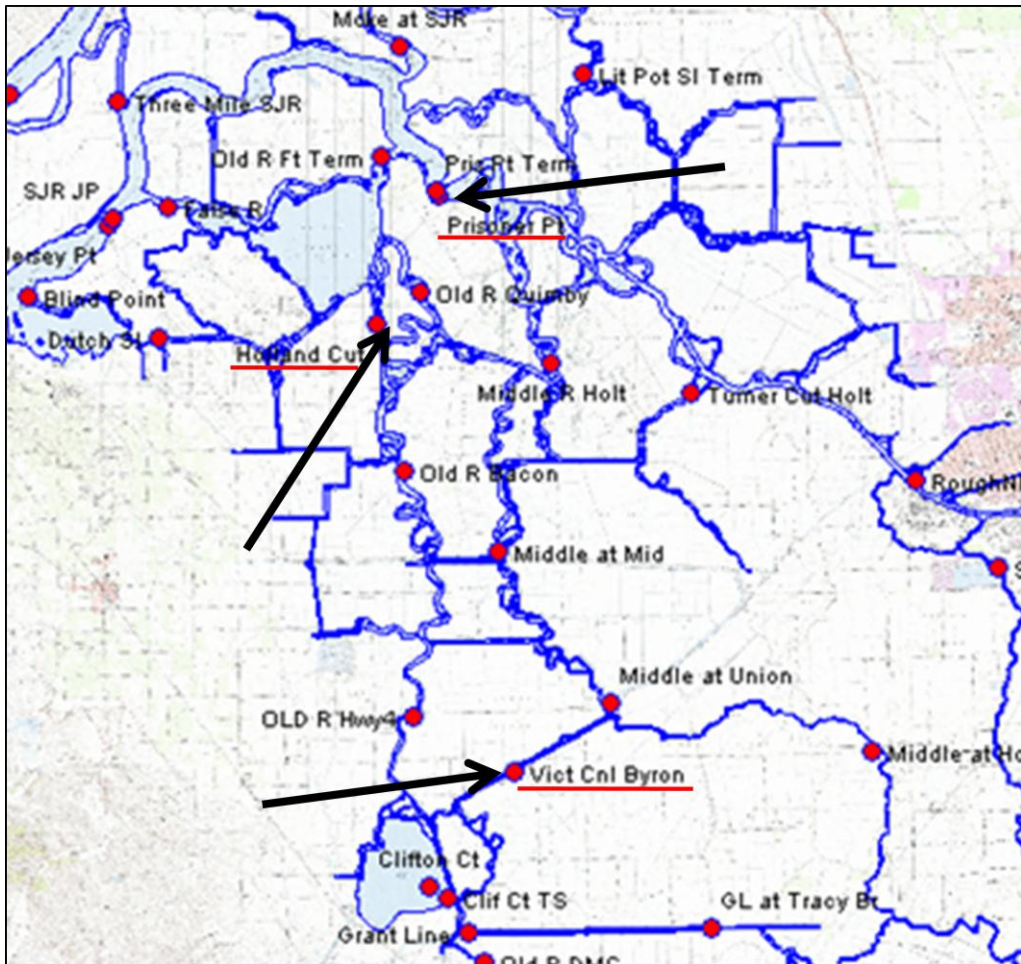


Figure 3-2 Location of the three turbidity compliance locations.

3.3 Methodology for turbidity calibration

The majority of the statistics used to assess model calibration at each Delta data location were calculated from model residuals. A residual is defined herein as the difference between a data value and the corresponding calculated model value (*i.e.*, data - model). Residuals were calculated at each location with available data. Three widely used statistics discussed in Moriasi (2007) were used to assess the goodness-of-fit of the model to the data using the residuals – the Nash-Sutcliffe efficiency (NSE), Percent Bias (PBIAS) and root mean square error (RMSE).

In addition, linear regressions were calculated along with the R^2 goodness of fit statistic between the data and the calibrated model at each available data location. Both daily-averaged and 15-minute CDEC data and model output were calculated, but the daily-averaged data were used to assess the quality of the calibration³. After daily averaging the model output and data, model residual statistics and linear regression statistics were calculated and recorded at each available data location.

The final interpretation of the calibration statistics was driven by the need to develop a methodology consistent with possible future uses of the calibrated turbidity model, in part to be used for wet season turbidity forecasting simulations and in part for applications where measurement data may not exist to inform the boundary conditions. In addition to presenting statistics at each measurement location, several metrics were developed to assess the overall quality of the calibration – *i.e.*, a “model skill” assessment.

Model calibration proceeded until the final set of rate constants represented a condition in which the calibration statistics for any year did not improve significantly or degrade at the compliance locations, in comparison with previous simulations and the original DMS calibration. In what follows, calibration metrics are presented in comparison with the previous QUAL turbidity calibration undertaken by DWR (DWR 2011).

The final set of values for the K_3 parameter are documented in Figure 3-3 through Figure 3-5. An ancillary objective for the calibration was to keep the number of regions and parameter values to a minimum, so only five parameter values were used. In two regions of the model, near the western model boundary and downstream of Vernalis to the Head of Old River, K_3 was set to zero (Black channels in the figure). Near Martinez, tidal influences tend to resuspend bed sediments, so no decay was needed particularly in periods of low inflow. Near Vernalis, data indicated that little settling occurs downstream to Mossdale. On the other hand, downstream of the Head of Old River to the export locations on Old River and down the San Joaquin River past Stockton, previous observation (RMA 2010b, 2011a, 2011b, 2012b) indicated that sediment settles out quickly, very likely due to substantial decreases in velocity. For this region (blue channels), K_3 was set to highest value of 0.4 day^{-1} . The settling parameter K_3 was set at three additional values: 0.05 day^{-1} (orange channels), 0.1 day^{-1} (yellow channels), and 0.2 day^{-1} (green channels).

Statistics were also calculated to assess the “model skill” with respect to the two sets of boundary conditions used in the “early years” simulations. In this case, Environmental Monitoring Program (EMP)

³ Statistical results using the 15-minute data and model output are presented in the Appendices.

grab sample data was compared with daily-averaged model output on the collection day. This information is covered in Section 7, while model skill is discussed in Appendix I, Section 11.1.

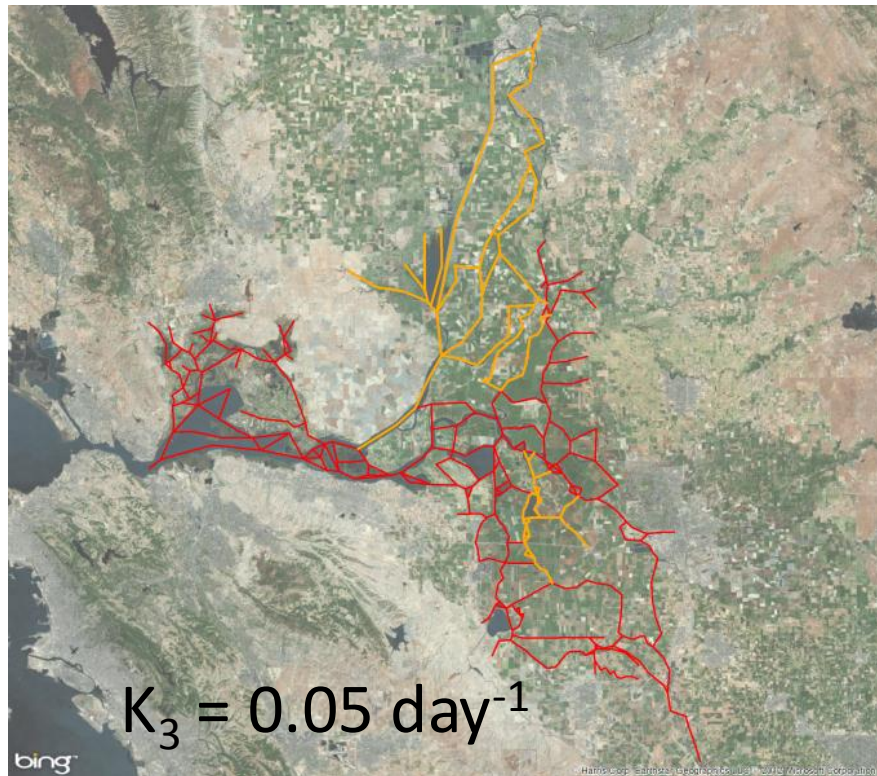
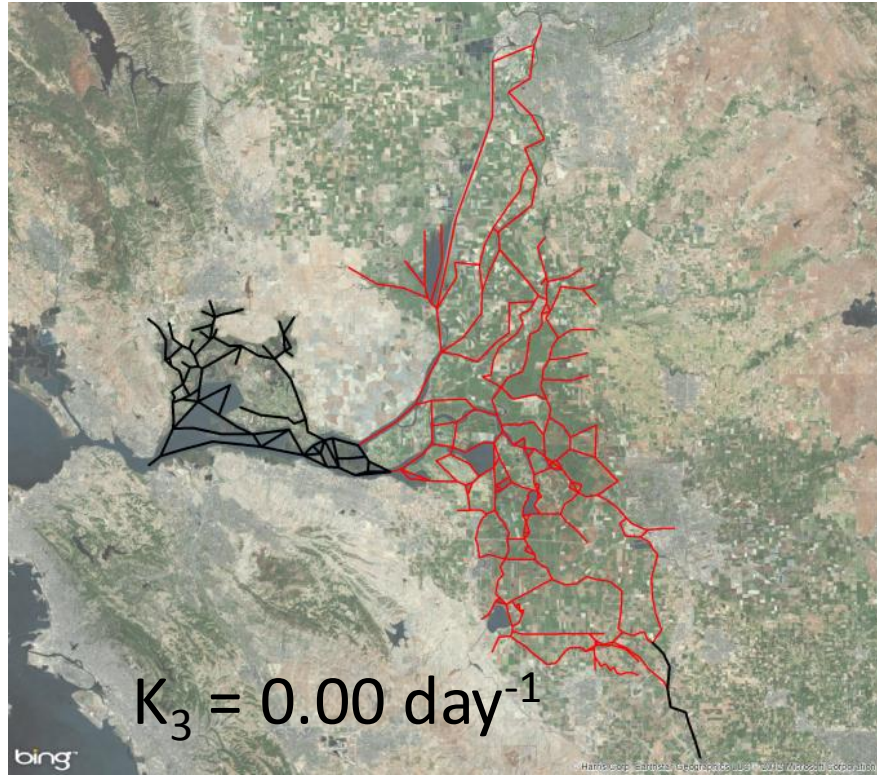


Figure 3-3 The colored lines define the DSM2 grid channels – the segments that aren't red define channels where the K_3 parameter was set to the indicated value. These figures show the lowest two values used for the settling parameter.

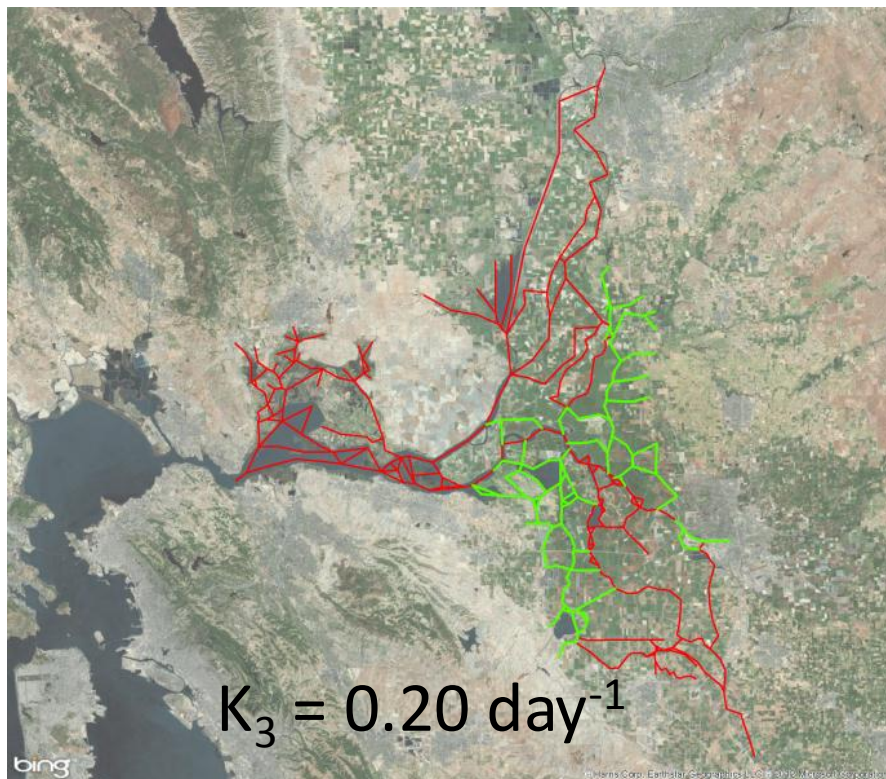
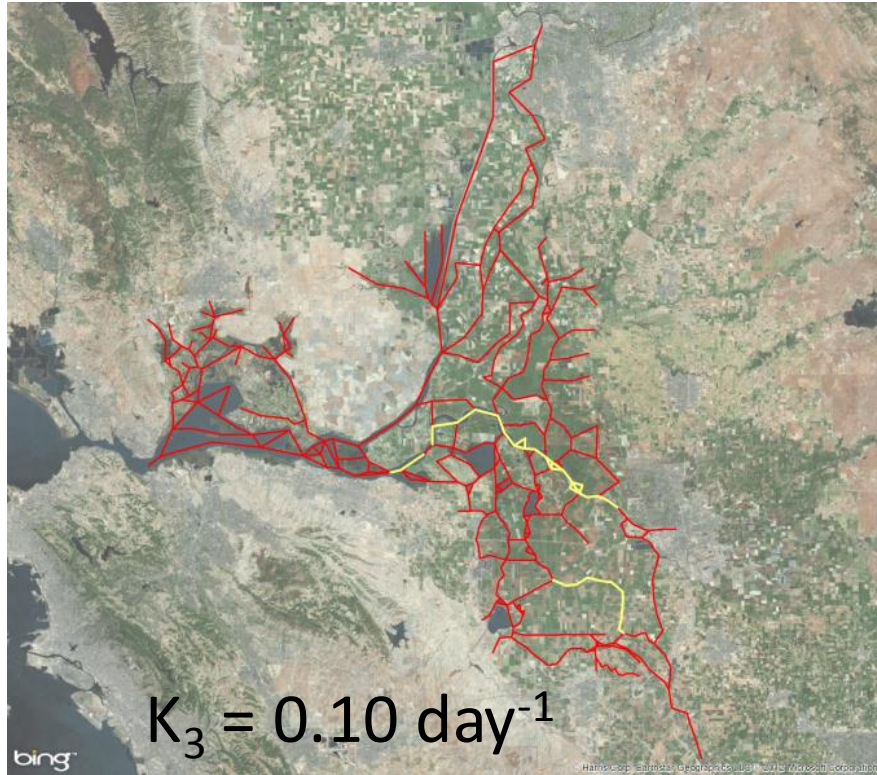


Figure 3-4 The colored lines define the DSM2 grid channels – the segments that aren't red define channels where the K_3 parameter was set to the indicated value. These figures show two middle values used for the settling parameter.

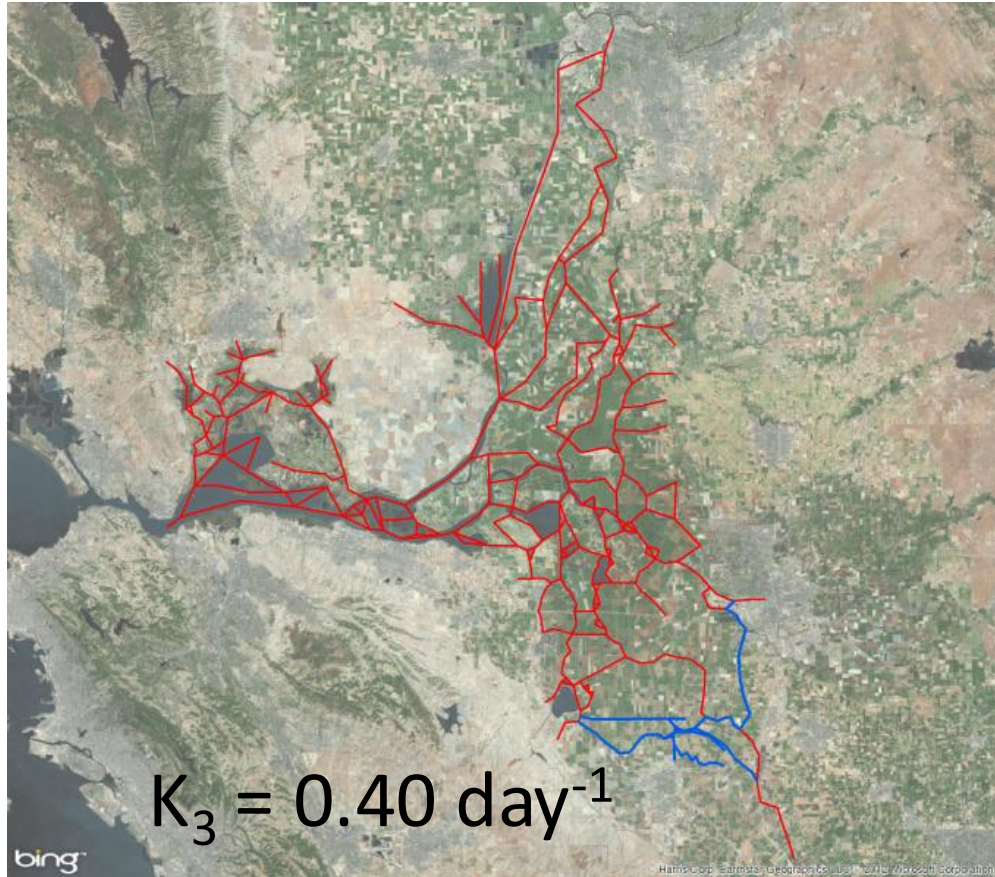


Figure 3-5 The colored lines define the DSM2 grid channels – the segments that aren't red define channels where the K_3 parameter was set to the indicated value. This figure shows the highest value used for the settling parameter.

3.4 Residual analysis

Residuals are defined as the difference (data – model) between the measured data and the modeled result. The following definitions (Moriassi et al., 2007) were used for calculating residual statistics:

Mean Residual – The mean of the residual values gives an indication of the magnitude of model under-prediction (positive residuals) or over-prediction in a region. The optimal value is zero, which occurs in the unlikely situation that the model is a perfect fit for the data.

Standard Deviation of Residual – The standard deviation of the residual values gives an indication of the variability in model under-prediction and over-prediction in a region.

Residual Histogram – The histogram documents the shape of the residual distribution. Along with the mean and standard deviation, this gives a first-order view of the goodness of model fit. The ideal histogram would have an approximately normal shape centered at zero with a small spread. Histograms were prepared using daily averaged calculations at each data location.

MSE – The Mean Squared Error is a standard statistic that measures the quality of the prediction. The optimal value is zero:

$$MSE = \left[\frac{\sum_{i=1}^n (Y_i^{Obs} - Y_i^{Sim})^2}{n} \right] \quad (A3)$$

RMSE – The Root Mean Squared Error is a standard statistic used to indicate the accuracy of the simulation. It is the square root of the MSE. The optimal value is zero.

NSE – The Nash-Sutcliffe Efficiency is a normalized statistic that measures the relative magnitude of the residual variance compared to the data variance. NSE indicates how well the measured vs. modeled data fit the 1:1 line (Moriassi et al., 2007). A value of 1 is optimal, values between 0 and 1 are acceptable, and negative values indicate that the data mean is a better predictor of the data than the model:

$$NSE = 1 - \left[\frac{\sum_{i=1}^n (Y_i^{Obs} - Y_i^{Sim})^2}{\sum_{i=1}^n (Y_i^{Obs} - Y_i^{Mean})^2} \right] \quad (A4)$$

PBIAS – Percent bias measures the average tendency of the simulated data to be larger or smaller than the measured data. A value of 0 is optimal – a positive value indicates underestimation bias and a negative value indicates overestimation bias:

$$PBIAS = \left[\frac{\sum_{i=1}^n (Y_i^{Obs} - Y_i^{Sim}) * 100}{\sum_{i=1}^n (Y_i^{Obs})} \right] \quad (A5)$$

RSR– The RMSE-observation standard deviation ratio is a statistic that normalizes the RMSE using the standard deviation of the observations. Because it is normalized, it can be used to compare errors among various constituents (Moriassi et al., 2007). A value of 0 is optimal:

$$RSR = \frac{\left[\sqrt{\sum_{i=1}^n (Y_i^{Obs} - Y_i^{Sim})^2} \right]}{\left[\sqrt{\sum_{i=1}^n (Y_i^{Obs} - Y_i^{Mean})^2} \right]} \quad (A6)$$

3.5 Linear regression analysis

Linear regressions were calculated and recorded in plots, along with the R² goodness of fit statistic and the regression equation, comparing the data to the model output at each available location for the newly calibrated model and for the original QUAL turbidity model developed by the DMS. Note that the intercept was NOT forced through zero in the linear regressions. For many locations, the NSE statistic and the R² values are the same within two decimal places – this indicates that the linear regression nearly fits the 1-1 line (*i.e.*, with an intercept at zero).

3.6 Documentation of statistics

Documentation of the statistical analyses is accomplished using tabular information and figure plots. The tables in Section 5.3 document all regression statistics as well as the overall “model skill” statistics. Figures (for example, Figure 3-6) show a comparison between the data and model output, the residual plot, a linear regression analysis with associated statistics (slope, intercept and R²), and a histogram of the residual along with the numerical values of the regression statistics.

3.7 Model output and calibration calculations

At each data location and for each water year, daily-averaged data and model output and residuals were plotted, linear regressions were calculated and plotted, and residual statistics were calculated and plotted along with a residual histogram. Figure 3-6 is an illustration of the output provided at each location – Prisoner’s Point in WY2011 is shown for the revised turbidity calibration. Appendix II, Section 12.1 and Section 12.2 present the complete set of these figures. For comparison, Section 14 in Appendix IV presents figures and associated statistics using 15-minute data and model output. However, these results were not used in the final analyses as daily-averaged data is used in the calculation of compliance location turbidity values.

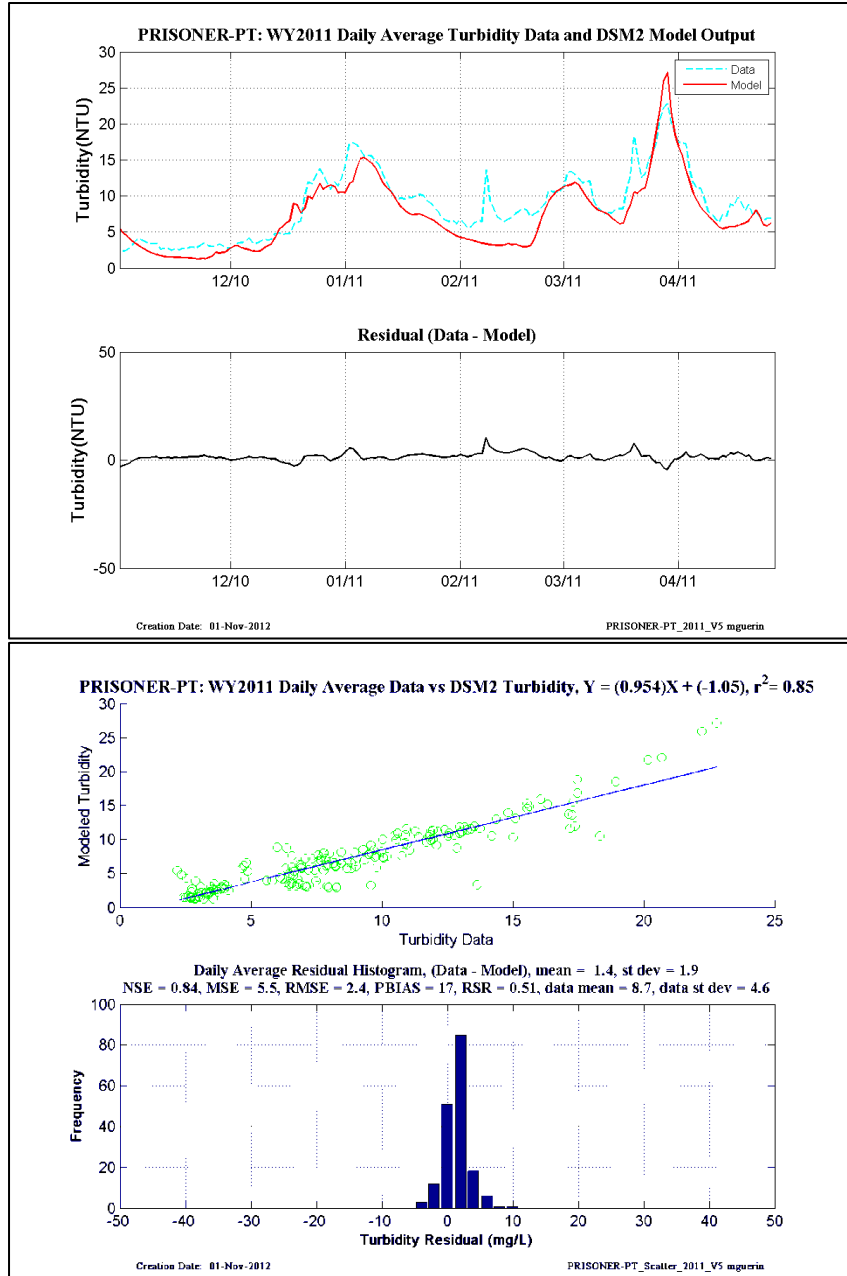


Figure 3-6 An illustration of the calculations made at each data location in order to calculate location-specific calibration statistics for each water year. This location is the compliance site at Prisoner’s Point. Peaks in the data (upper plot) not captured in the model in February are due to wind/rain events.

4 Model set-up

4.1 High flow period Historical simulations: WY2010, WY2011, WY2012

DSM2 was run with the Mini-calibration set-up and V8.0.6 of HYDRO and QUAL⁴. Gate operations and export flows for HYDRO for the calibration time frames were obtained from the DMS and implemented as received – only winter high flow periods were simulated for use in calibration. Inflow boundary conditions for turbidity were developed at RMA. Details can be found in the input files for each model run. DICU values were used as developed by the DMS, with DICU turbidity return flow concentrations set at a constant 10 NTU.

Turbidity boundary conditions at the inflow boundaries and at Martinez were set as follows, after a QA/QC step to clean, refine and possibly time shift the data:

- Sacramento River turbidity was set using the refined values from CDEC data at Freeport with a time shift to match downstream peaks where indicated.
- San Joaquin River turbidity was set using the refined values from CDEC data near Vernalis (SJR-McCune)
- Martinez stage boundary was set using refined values from CDEC data at Martinez
- All other inflow boundaries:
 - For WY2010 and WY2011 (Yolo Bypass, Calaveras R., Mokelumne R. and Cosumnes R.) were set using WARMF model BC.
 - For WY2012, BC were set using the nearest downstream data location applied at the model boundary (WARMF output was not available).

For WYs 2010, 2011 and 2012, the model was run both with the refined set of calibration parameters for turbidity and with the original DMS set of parameters (i.e., the CBOD settling coefficient). The results were then compared using the residual and regression analyses discussed in Sections 3.4 and 3.5.

In addition, as part of the second objective of developing the long term simulation (1975 – 2012), the WY2010 and WY2012 were run with both Mixed-SSC-WARMF and with WARMF-Only turbidity boundary conditions using the refined calibration. The only differences between these two sets of simulations were the Freeport and Vernalis turbidity boundary time series.

Plots illustrating the inflow and main export boundary conditions for WY2010 through WY2012 high flow periods as well as the available Freeport and Vernalis turbidity boundary conditions for these three water years are shown in Figure 4-1 through Figure 4-9.

4.2 Long term (1975 – 2011) Historical Simulations

DSM2 was run with the Mini-calibration set-up and V8.0.6 of HYDRO and QUAL. The DMS supplied the historical hydrodynamic model input for the HYDRO runs (gate operations, exports and inflows, and

⁴<http://baydeltaoffice.water.ca.gov/modeling/deltamodeling/models/dsm2/dsm2.cfm>

stage at Martinez) for the water years 1975 – 2010 and separately for the recent years through December 2011. The simulations for the water years 1975 – 2011 were run in two steps: the “early years” 1975 – 1990, and separately for the “recent years” 1991 – 2011. The “early years” simulations used the DSM2 model set-up supplied with the long-term (1975 – 2010) Historical model (e.g., without Liberty Island), while the “recent years” simulations used the most up-to-date DSM2 Historical model set-up which ran through 2011.

Two sets of QUAL turbidity model simulation results were prepared using either USGS-SSC data or WARMF model calculations to develop boundary conditions at Freeport and Vernalis. One set of simulations used a reduced USGS Vernalis SSC concentration (*i.e.*, Vernalis SSC*0.3) and an unaltered USGS Freeport SSC concentration for boundary conditions – these are denoted the “Mixed-SSC-WARMF” simulations. A second set of simulations – the “WARMF-Only” simulations – used WARMF model calculations supplied by Systech for this project for turbidity boundary conditions at Vernalis and Freeport. Both sets of simulations used WARMF model outputs at the other tributaries, and a constant 20 NTU at the Martinez boundary. Figure 4-10 illustrates the turbidity boundary conditions used for these simulations at Freeport and Vernalis.

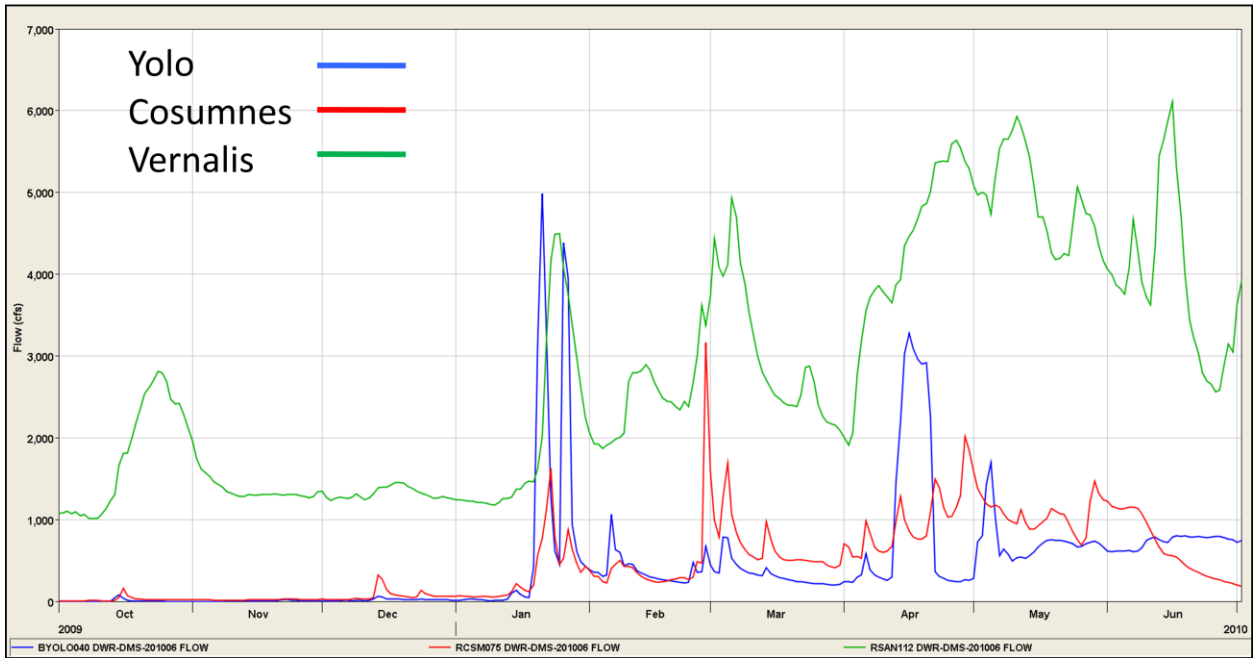
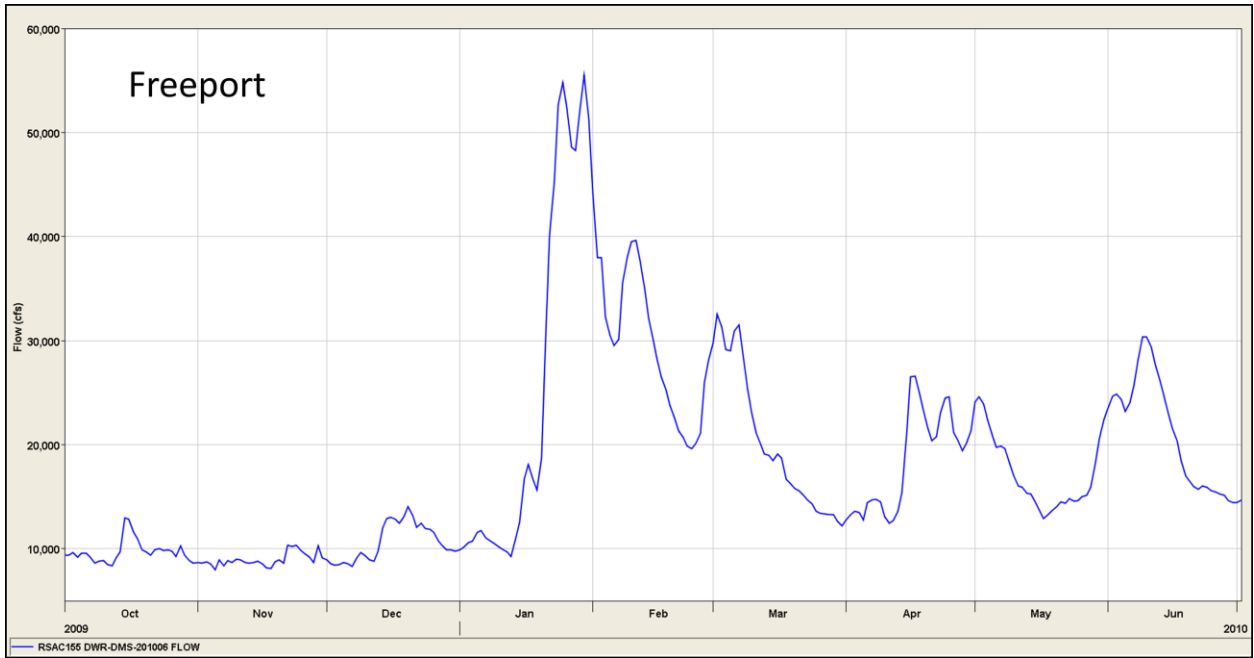


Figure 4-1 WY2010 flow BC at Freeport, Vernalis, the Yolo Bypass and Cosumnes River locations.

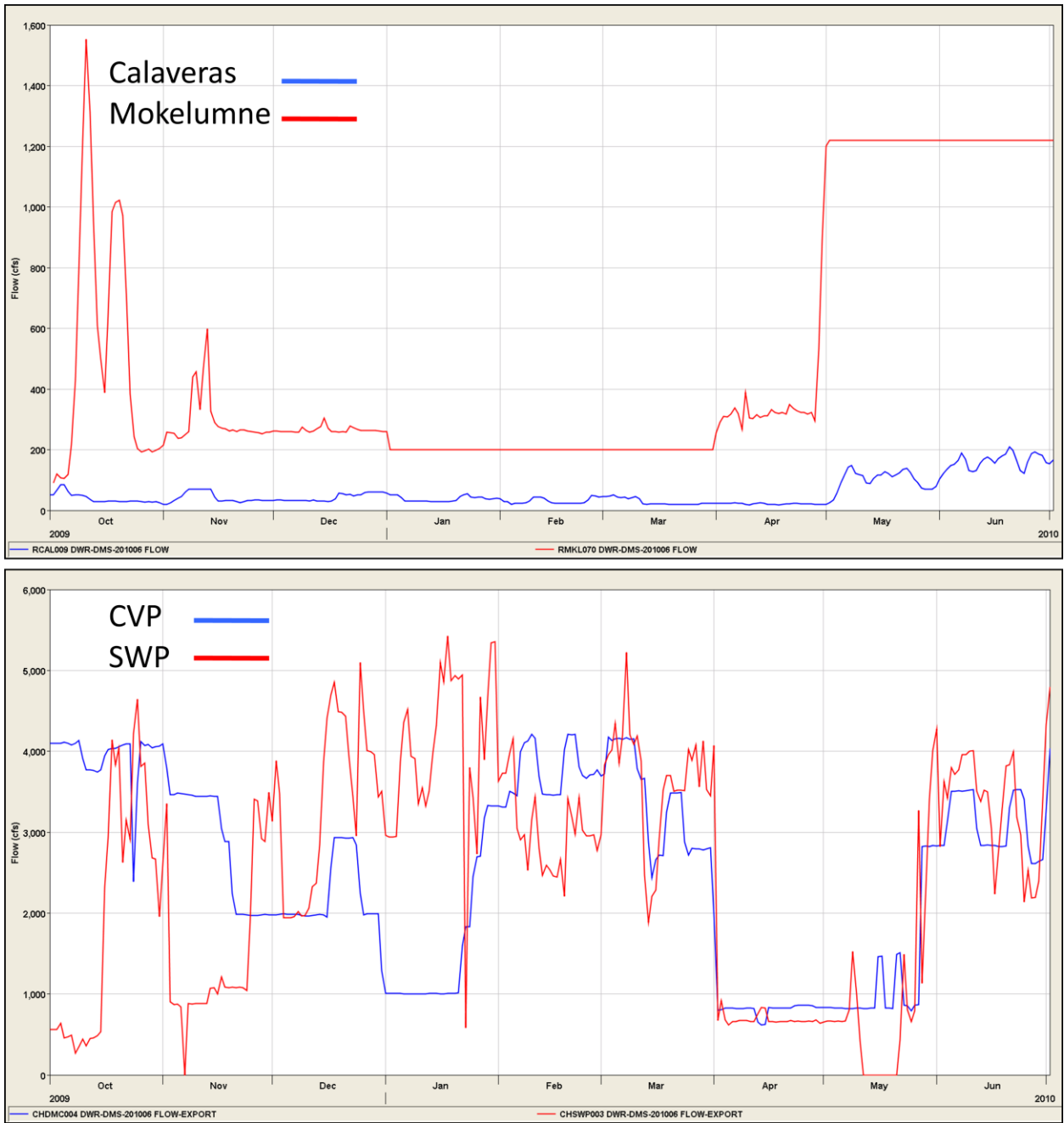


Figure 4-2 WY2010 flow BC at the Calaveras and Mokelumne locations and export BC at the CVP and SWP locations.

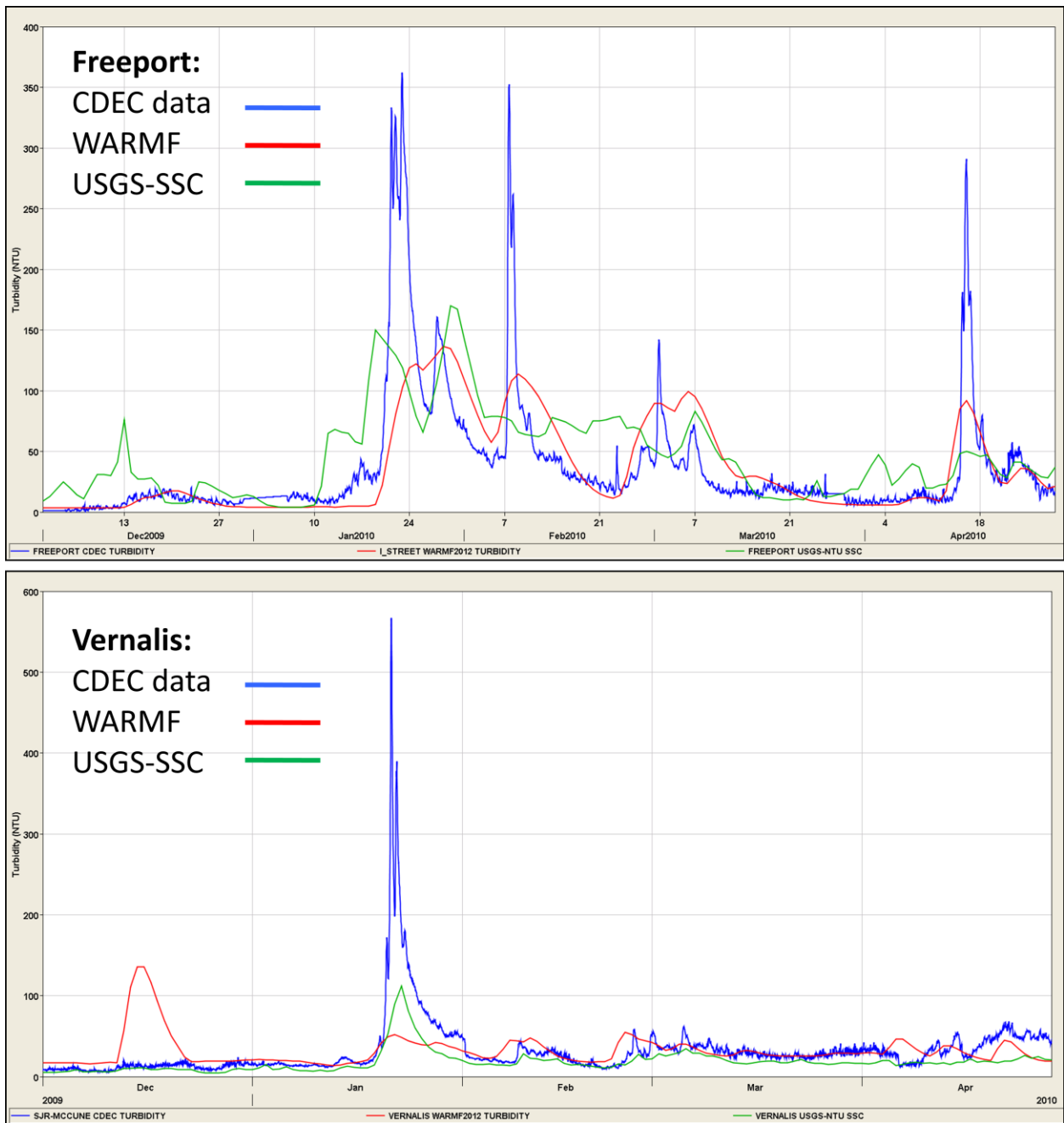


Figure 4-3 WY2010 Freeport and Vernalis turbidity BC showing all three available sets of data – CDEC (15-min), WARMF (daily) and USGS-SSC (daily). USGS-SSC values were transformed to turbidity using a linear translation.

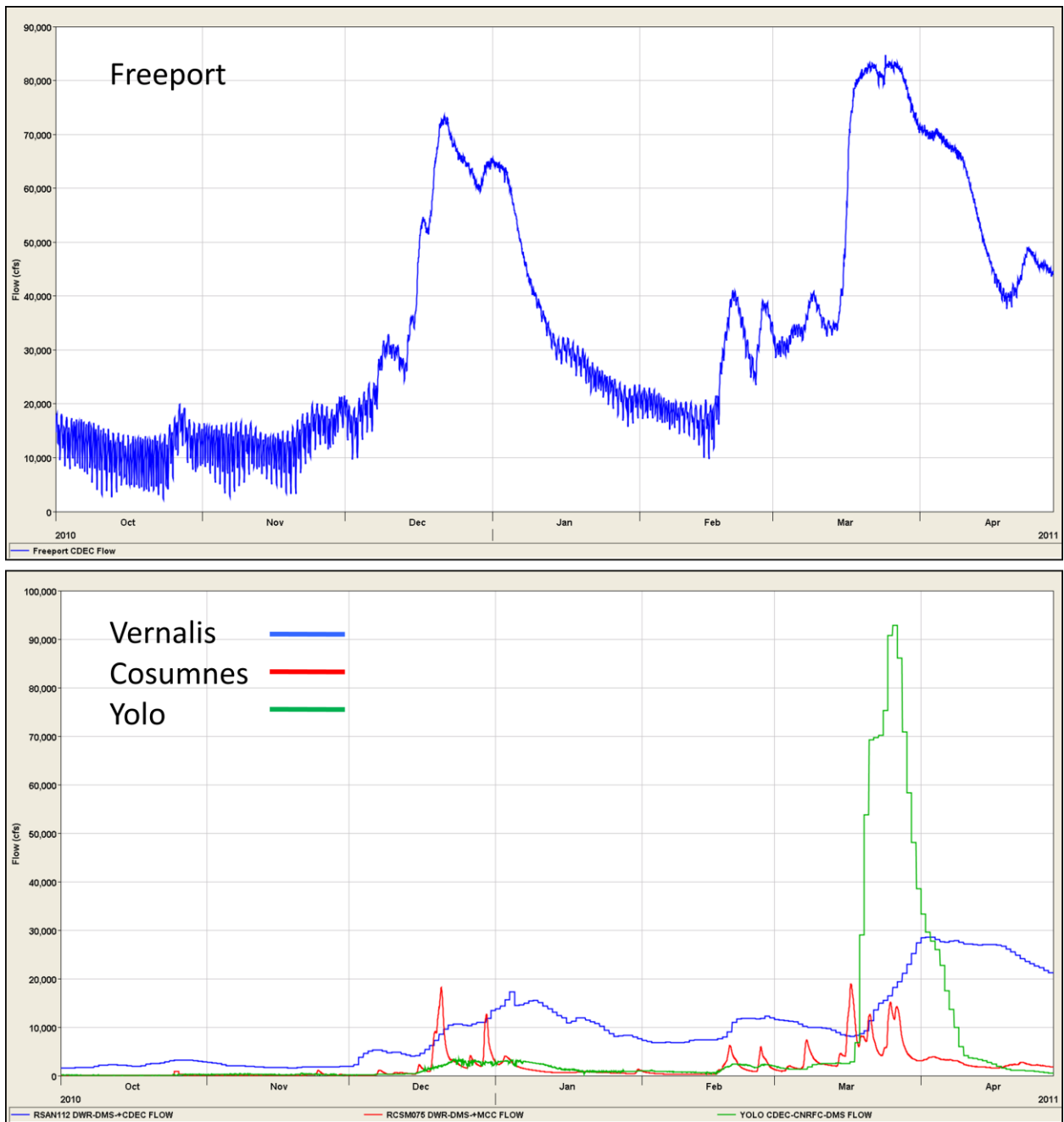


Figure 4-4 WY2011 flow BC at Freeport, Vernalis, the Yolo Bypass and Cosumnes River locations.

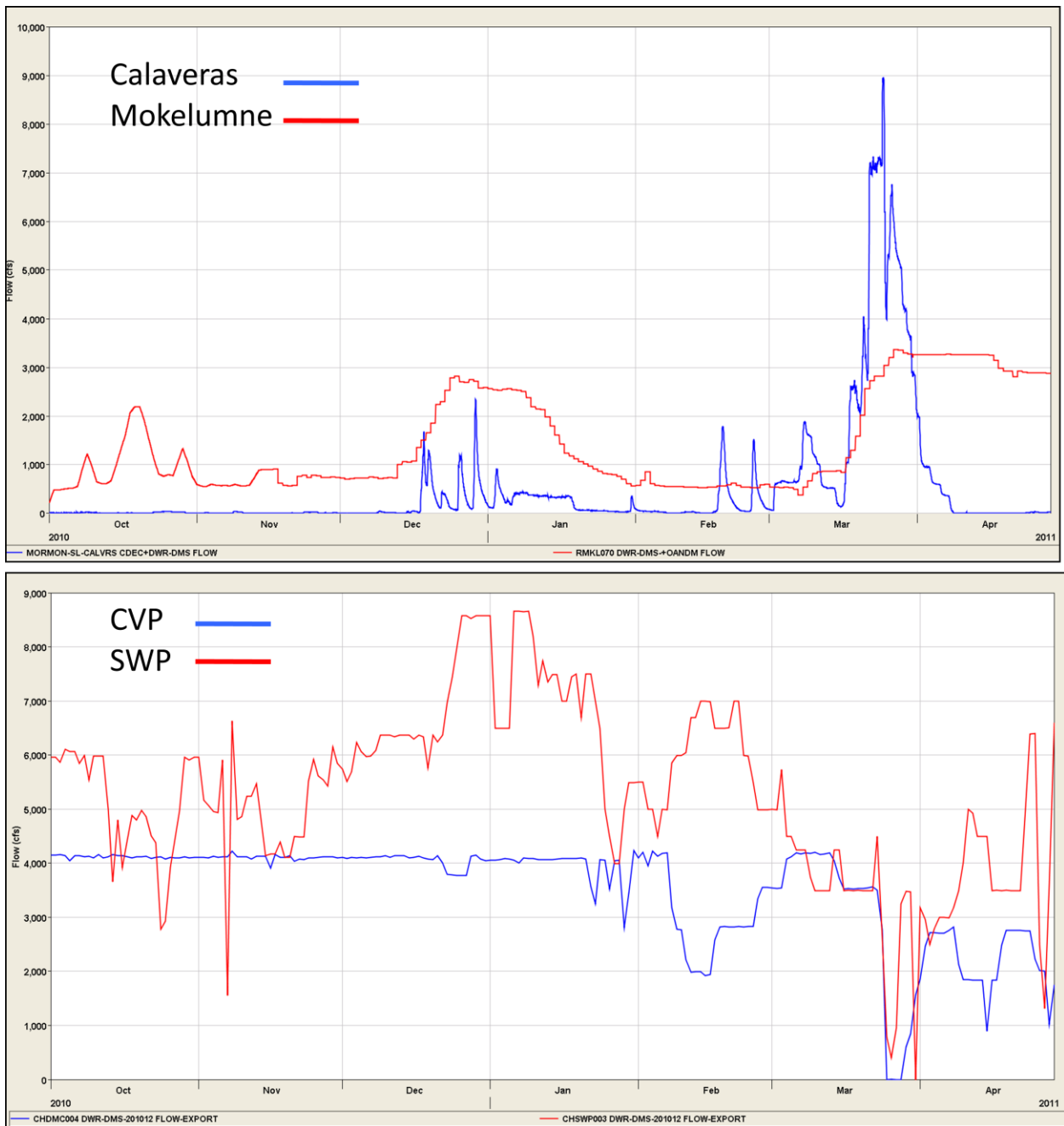


Figure 4-5 WY2011 flow BC at the Calaveras and Mokelumne locations and export BC at the CVP and SWP locations.

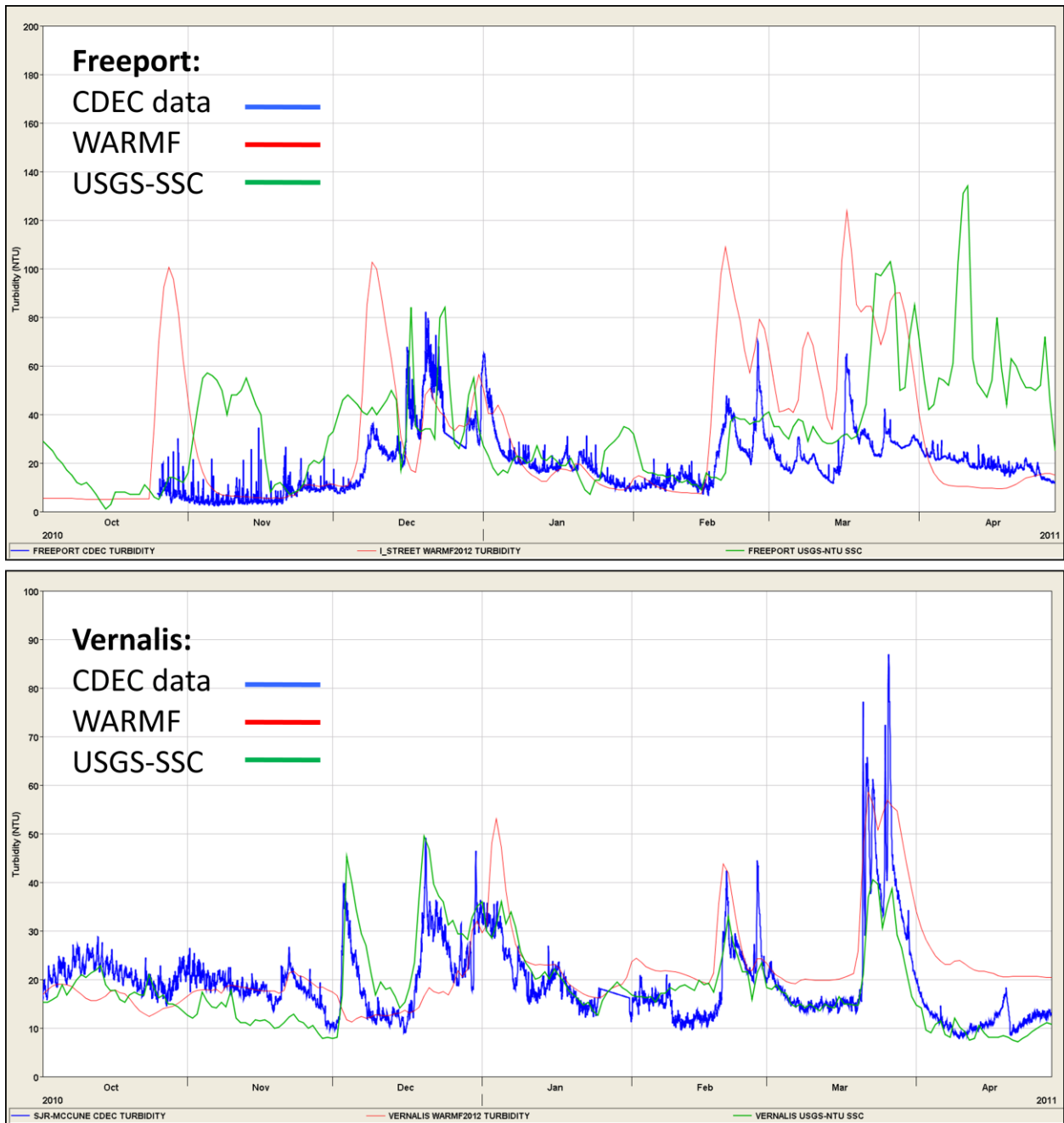


Figure 4-6 WY2011 Freeport and Vernalis turbidity BC showing all three available sets of data – CDEC (15-min), WARMF (daily) and USGS-SSC (daily). USGS-SSC values were transformed to turbidity using a linear translation.

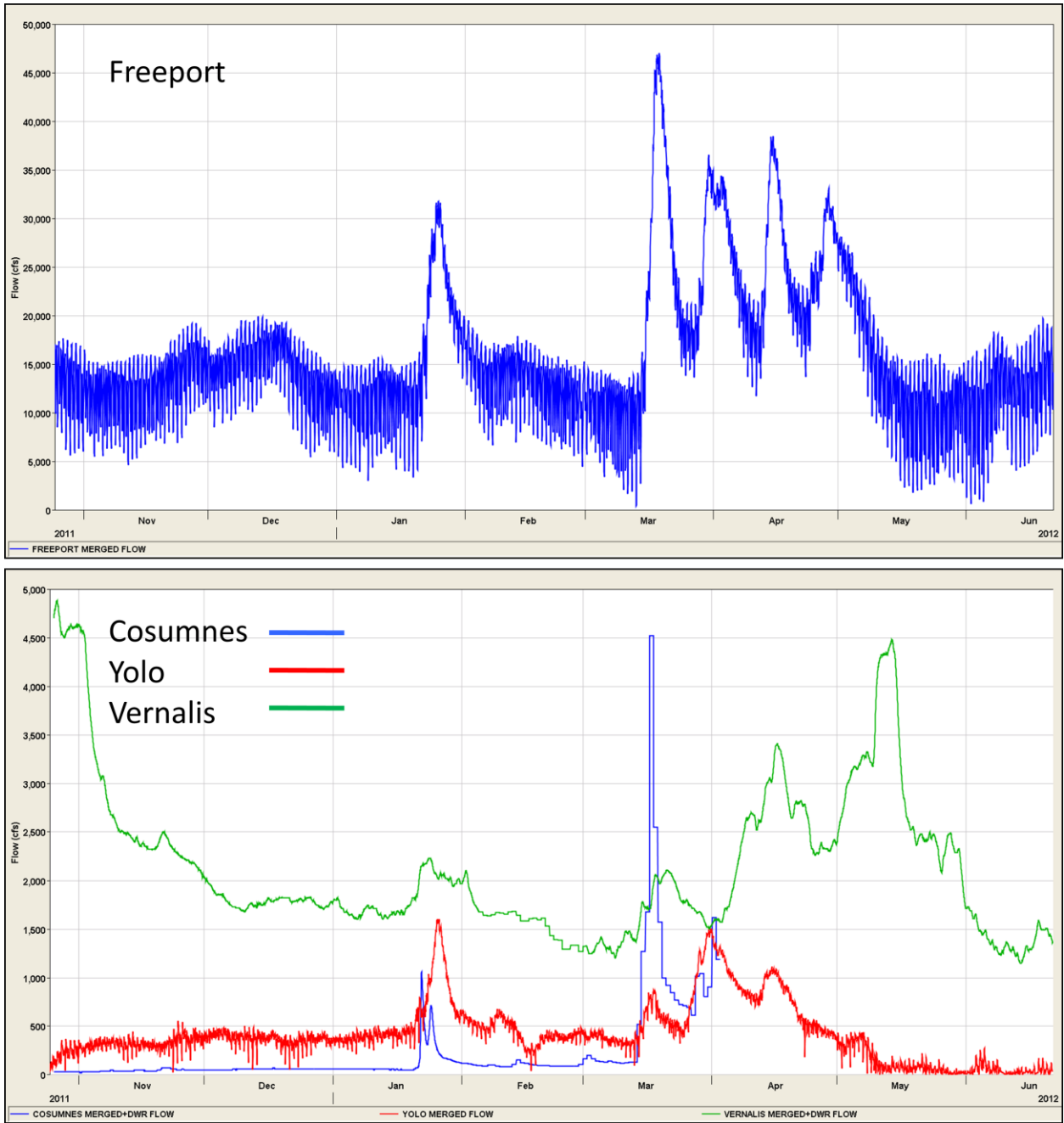


Figure 4-7 WY2012 flow BC at Freeport, Vernalis, the Yolo Bypass and Cosumnes River locations.

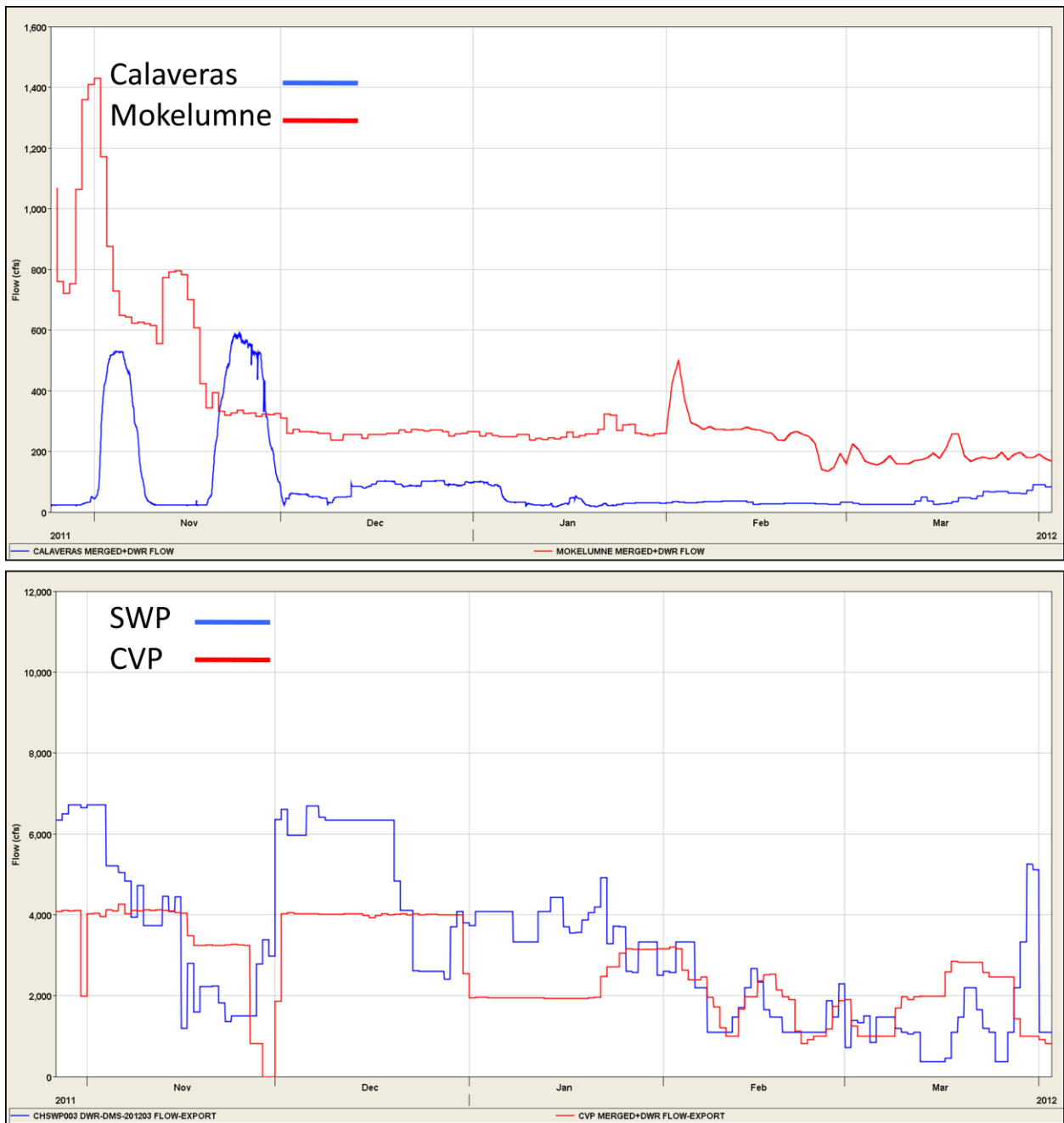


Figure 4-8 WY2012 flow BC at the Calaveras and Mokelumne locations and export BC at the CVP and SWP locations.

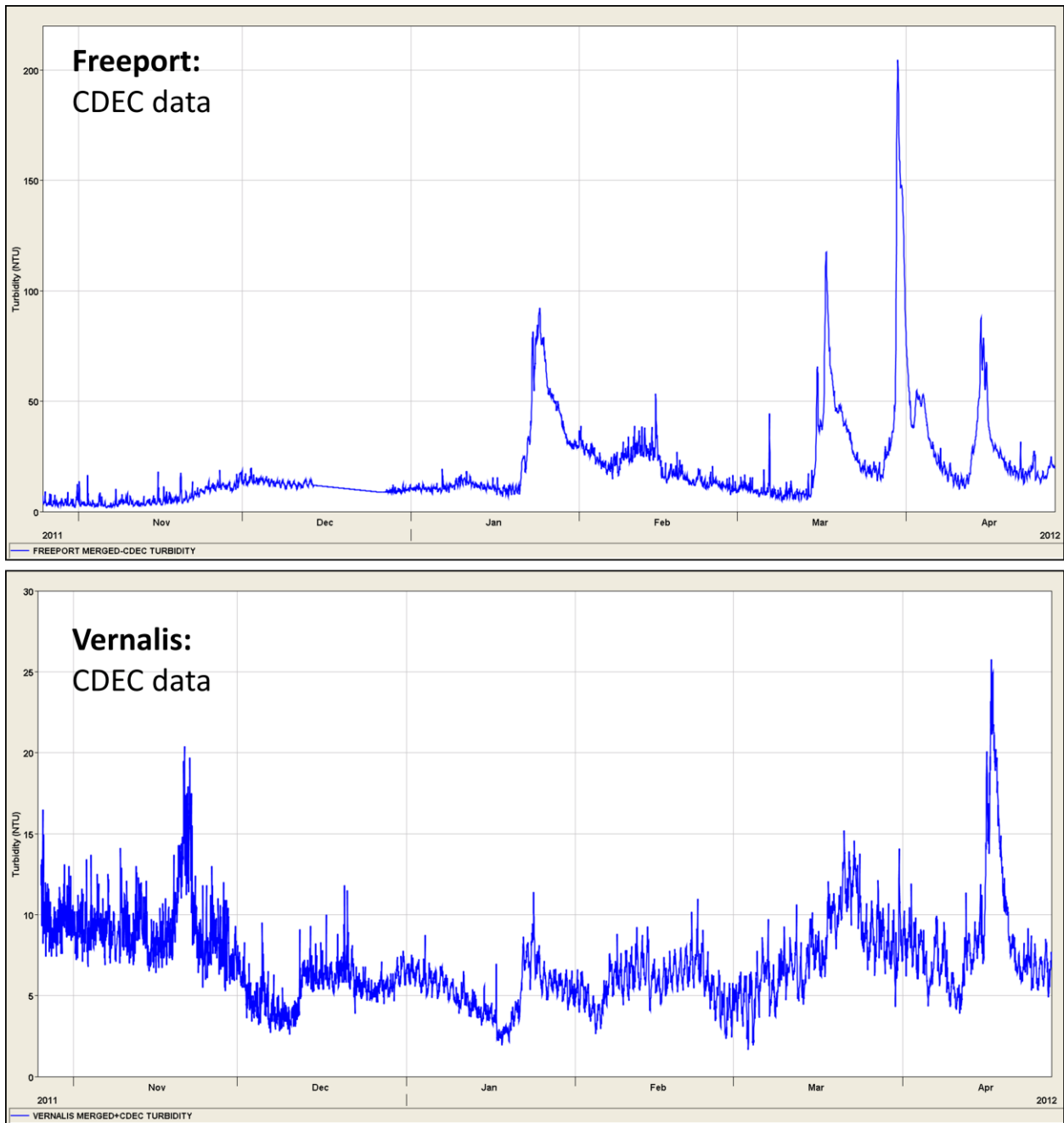


Figure 4-9 WY2012 turbidity BC at Freeport and Vernalis – only CDEC data was available for this time frame.

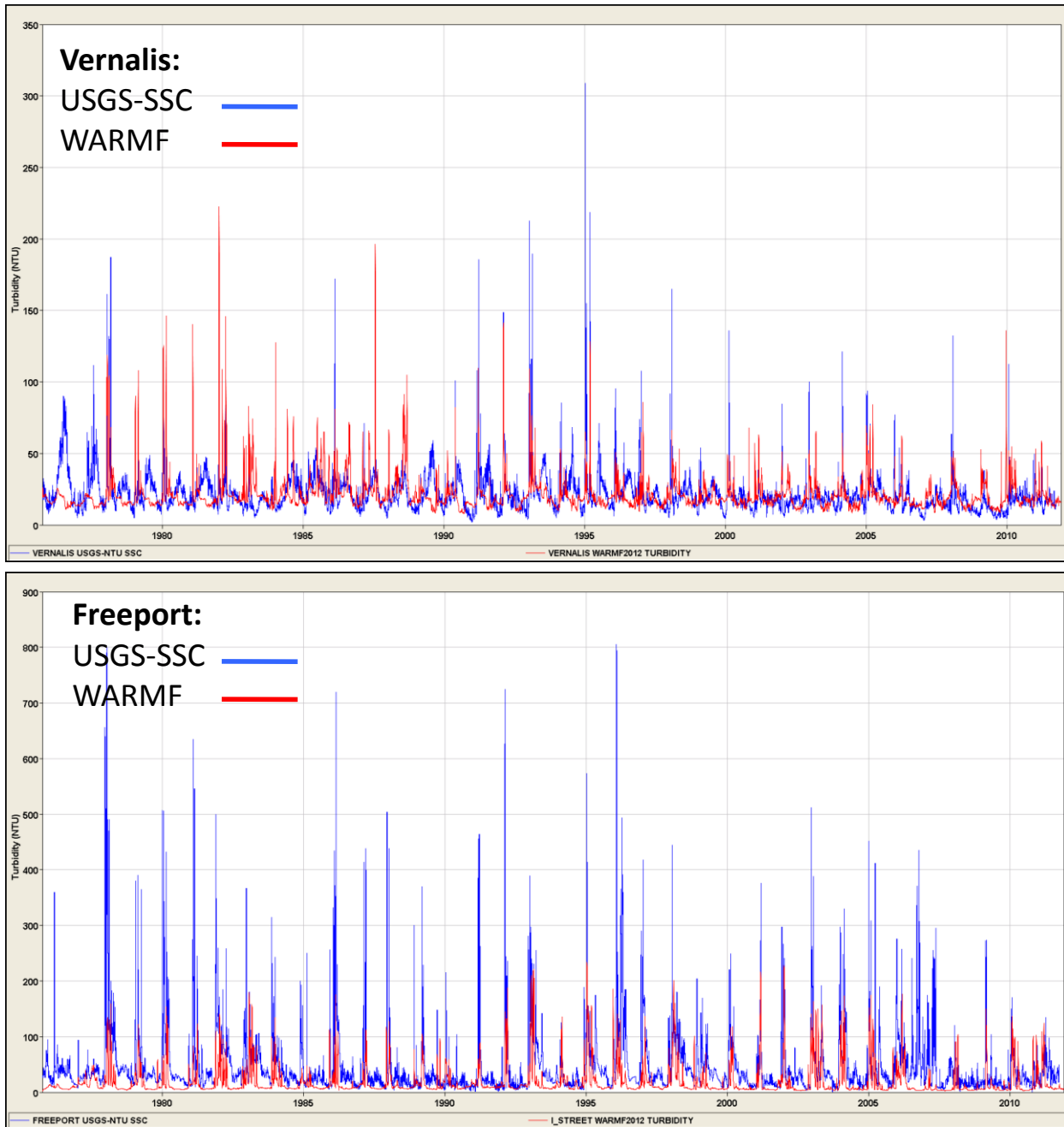


Figure 4-10 Long-term simulation options for the Freeport and Vernalis turbidity boundary conditions. USGS-SSC values were transformed to turbidity using a linear translation. Both data sets are composed of daily data.

5 Calibration Results

5.1 Calibration priorities

There were five major steps (versions) in setting calibration parameters in the calibration process – at the end of each step, calibration statistics were computed and compared with statistics calculated for the original DMS model calibration for WY2010 and WY2011. Daily-averaged data and model results were used to assess the quality of the calibration. The final set of settling parameters (K_3) used in the calibration can be found in the file “rate_coefficient_delta_ncc_turbidity_V5.inp”. A visual representation of these values and their placement in the model grid is seen in Figure 3-3 through Figure 3-5.

During the calibration process, a priority was placed on improving the calibration statistics at the three compliance locations. A particular emphasis was placed on the PBIAS statistic, and considerable effort was undertaken to decrease the absolute value of this statistic without sacrificing the quality of the other statistics at the compliance location, as well as at other locations used in the calibration process. The reasoning behind this objective was that if forecast modeling of turbidity was used to assist the Delta Smelt Working Group, getting the magnitude of the turbidity as close as possible to reality would best benefit the working group’s ability to correctly influence Delta operations. Additional reasons for minimizing the value of the PBIAS statistic are related to the ability to apply corrections to long-term averaged results – for example, if a given location is generally modeled as higher than data (negative PBIAS), then the interpretation of that model value can be assessed with the additional knowledge given by an average PBIAS value.

5.2 Calibration metrics

5.2.1 Location-specific calibration metric

A location-specific calibration metric was calculated using four statistics in the high flow seasons of WY2010 and WY2011: R^2 , NSE, RMSE and PBIAS. A weighted average approach was used in order to give priority to improvements in the PBIAS statistic, using weights of 0.15, 0.15, 0.2 and 0.5 for R^2 , NSE, RMSE and PBIAS, respectively. Both R^2 and NSE have optimal values at 1.0, with smaller (or negative for NSE) values indicating a poorer fit between model and data. On the other hand, RMSE and PBIAS have optimal values at zero and increases in the magnitude of the statistic indicate a poorer calibration fit. In order to calculate a location-specific statistic that could also be used for the calibration as a whole (i.e., over the entire model domain), the following formula was used at each location:

Location Metric=

$$0.15 * R^2 + 0.15 * NSE + 0.2 * (RMSE / \text{Min}(RMSE, DMS_RMSE))^{-1} + 0.5 * (\text{MIN}(\text{ABS}(PBIAS), \text{ABS}(PBIAS_DMS)))^{-1}$$

where DMS_RMSE refers to the value of the RMSE statistic calculated by the DMS calibration of the QUAL turbidity model, RMSE refers to the newly revised calibration statistic (by RMA), and ABS(PBIAS) refers to the absolute value of the PBIAS statistic in this formula. A similar nomenclature applies to the PBIAS_DMS statistic. Calculated in this way, the magnitude of the Location Metric is higher when the overall calibration is better in one of the simulations, *i.e.*, in comparing the new calibration with the

DMS calibration. Because the PBIAS and RMSE statistics are calculated as inverses, smaller (absolute) values give a higher magnitude for the Location Metric.

A similar set of Location Metrics were calculated to compare the simulation results of the two sets of boundary conditions used to develop simulations for the ANN application – i.e., comparing the Mixed-SSC-WARMF and WARMF-Only simulation results. Note that the calculations for the Location Metric in the calibration comparison (original-DMS vs. Recalibration) preclude direct comparison of the Location Metrics from the calibration simulation with the Location Metrics from the Mixed-SSC-WARMF and WARMF-Only simulation results.

5.2.2 Model Skill: Three Delta-wide calibration metrics

Background information on the use of “Model Skill” metrics is supplied in Section 11.1, Appendix I. In this section, we supply metrics specific to this project that quantify model skill.

Three overall, Delta-wide calibration metrics were calculated for each water year:

1. The sum of the calibration Location Metrics at the three compliance locations
2. The sum of the calibration Location Metrics at all available data locations
3. The weighted sum: $0.8 * (\text{sum of the Location Metrics at the three compliance locations}) + 0.2 * (\text{sum of all other Location Metrics})$.

The Location Metrics are shown with two decimal places, while the overall metrics are shown to one decimal place. Tabular results are presented for WY2010 and WY2011 in Section 5.3 for both the Location Metrics and the three Model Skill metrics.

A similar set of overall metrics for comparing Model Skill were calculated to compare the two sets of boundary conditions used to develop simulations for the ANN application. In this case, the comparison was between the Mixed-SSC-WARMF and the WARMF-Only simulations. These results are shown in Section 6.2.

5.3 Calibration results for WY2010 and WY2011, comparing revised and original DMS calibration simulations

The following set of five tables – Table 5-1 through Table 5-5 – illustrate the location-specific and overall (Model Skill, Table 5-5) calibration metrics and statistics used to assess the revised calibration and the original DMS calibration of the QUAL turbidity model. The first four tables illustrate the individual statistics used, plus the calculated location metric in the final column. The color scheme is used solely to highlight difference between the revised calibration and the initial DMS calibration, *i.e.*, whether a statistic was better (blue) in the comparison. Occasions where the compared statistics were equal are not color-highlighted.

The revised calibration made improvements in the overall calibration for WY2010 (compare Table 5-1 and Table 5-2), although the compliance site Location Metric only improved at Victoria Canal-Byron. The only Location Metric where the DMS calibration was better than the recalibration was at Decker Island,

and in that case the difference was insignificant. Note that the DMS calibrated their turbidity model to WY2010.

In WY2011 (compare Table 5-3 and Table 5-4), the recalibration produced significant improvements not only in the Location Metrics in general, but also in the individual statistical measures at each of the compliance locations (with no sacrifice at these locations).

Table 5-5 documents the Model Skill assessment statistics. The statistics clearly indicate that the overall model skill was improved by the recalibration effort. Note that each of these statistics reflects the subjective decision to bias a specific statistic that was intentionally introduced in the recalibration effort:

1. A bias during the calibration process toward improving the PBIAS statistics over other individual statistics at each location - this is reflected in the Location Metric statistics.
2. A bias in the calibration and in the analysis for improving the compliance Location Metric statistics over the other locations for which statistics were calculated - this is reflected in the “Compliance Only” and “Weighted Sum of Location Metric” statistics.

Table 5-1 WY2010 revised calibration of QUAL turbidity – final calibration run. Bold font in the name indicates compliance locations; blue font in the statistics denotes an improved result in comparison with Table 5-2.

	R ²	NSE	RMSE	PBIAS	Location Metric
Antioch	0.8	-0.1	12	-6	0.78
Cache-Ryer	0.9	0.8	15	-17	0.96
Decker	0.9	0.9	12	-9	0.96
False River	0.7	0.6	8	11	0.90
Georgiana-Below	1.0	1.0	7	5	1.00
Georgiana -Sac	0.9	0.9	14	-1	0.98
Grant line	0.9	0.7	7	9	0.93
Holland Cut	0.6	0.4	5	26	0.84
Hood	1.0	1.0	9	-7	0.99
Little-Potato-SI-Term	0.7	0.7	7	19	0.92
Mallard	0.9	0.8	12	2	0.95
Middle-R-Holt	0.9	0.8	5	53	0.94
Miner-SI	1.0	1.0	10	-15	0.99
Moke-at-SJR	1.0	0.9	10	-21	0.98
Mossdale	0.9	0.9	16	12	0.96
Prisoner-Pt	0.9	0.9	4	26	0.98
Prisoner-Pt-Term	0.7	0.6	10	55	0.90
Rio Vista	0.9	0.9	13	-14	0.98
Rough-n-Ready	0.6	0.2	12	6	0.81
SJR-Garwood	0.6	0.2	16	-3	0.80
3Mile-SJR	1.0	0.9	6	-4	0.98
Turner Cut-Holt	0.5	-0.1	7	7	0.73
Victoria Canal-Byron	0.4	0.2	3	40	0.79

Table 5-2 WY2010 DMS calibration of QUAL turbidity. Bold font in the name indicates compliance locations; blue font in the statistics denotes an improved result in comparison with Table 5-1.

	R ²	NSE	RMSE	PBIAS	Location Metric
Antioch	0.8	0.1	11	10	0.60
Cache-Ryer	0.9	0.8	15	-17	0.96
Decker	0.9	0.9	12	-8	0.97
False River	0.7	0.6	8	12	0.85
Georgiana-Below	1.0	1.0	7	5	1.00
Georgiana -Sac	0.9	0.9	14	-1	0.98
Grant line	0.9	0.8	7	23	0.65
Holland Cut	0.6	0.4	5	26	0.84
Hood	1.0	1.0	9	-7	0.99
Little-Potato-SI-Term	0.7	0.7	7	19	0.92
Mallard	0.9	0.9	13	20	0.49
Middle-R-Holt	0.9	0.7	5	56	0.90
Miner-SI	1.0	1.0	10	-15	0.99
Moke-at-SJR	1.0	0.9	10	-21	0.98
Mossdale	0.9	0.9	16	12	0.96
Prisoner-Pt	0.9	0.9	4	26	0.98
Prisoner-Pt-Term	0.7	0.6	10	57	0.88
Rio Vista	0.9	0.9	13	-14	0.98
Rough-n-Ready	0.6	0.5	11	38	0.45
SJR-Garwood	0.6	0.5	14	28	0.41
3Mile-SJR	0.9	0.9	7	-5	0.81
Turner Cut-Holt	0.5	0.4	6	33	0.44
Victoria Canal-Byron	0.5	0.4	4	47	0.74

Table 5-3 WY2011 revised calibration of QUAL turbidity – final calibration run. Bold font in the name indicates compliance locations; blue font in the statistics denotes an improved result in comparison with Table 5-4.

	R²	NSE	RMSE	PBIAS	Location Metric
Antioch	0.4	-0.3	5	8	0.71
Cache-Ryer	0.8	0.8	11	12	0.93
Decker	0.7	0.7	9	11	0.92
False River	0.4	0.2	5	17	0.79
Georgiana-Below	0.8	0.7	13	23	0.92
Georgiana -Sac	1.0	1.0	3	9	0.99
Grant Line	0.7	0.7	7	18	0.90
Grant Line - Tracy	0.7	0.7	7	18	0.92
Holland Cut	0.0	0.0	9	34	0.70
Hood	0.7	0.5	7	0	0.88
Little-Potato-SI-Term	0.9	0.7	5	-19	0.93
Mallard	0.5	-1.0	8	10	0.63
Middle-R-Howard	0.6	0.6	8	-5	0.51
Middle-R-Holt	0.7	0.6	2	-2	0.90
Miner-SI	0.8	0.8	6	-6	0.94
Moke-at-SJR	0.9	0.9	4	-11	0.98
Mossdale	0.7	0.7	7	16	0.92
N Mokelumne	0.6	0.6	9	-35	0.89
Prisoner-Pt	0.9	0.8	2	17	0.95
Prisoner-Pt-Term	0.7	0.0	5	-1	0.81
Rio Vista	0.7	0.7	12	-3	0.90
Rough-n-Ready	0.8	0.8	6	24	0.95
SJR-Garwood	0.8	0.7	10	28	0.92
S Mokelumne	0.8	0.7	6	-11	0.87
3Mile-SJR	0.9	0.7	4	-2	0.93
Turner Cut-Holt	0.8	0.8	3	8	0.81
Victoria Canal-Byron	0.8	0.8	2	2	0.93

Table 5-4 WY2011 DMS calibration of QUAL turbidity. Bold font in the name indicates compliance locations; blue font in the statistics denotes an improved result in comparison with Table 5-3.

	R²	NSE	RMSE	PBIAS	Location Metric
Antioch	0.4	-0.3	5	16	0.44
Cache-Ryer	0.8	0.8	11	12	0.93
Decker	0.7	0.7	10	11	0.91
False River	0.4	0.2	5	19	0.73
Georgiana-Below	0.8	0.7	13	23	0.92
Georgiana -Sac	1.0	1.0	3	9	0.99
Grant Line	0.7	0.7	8	26	0.74
Grant Line - Tracy	0.8	0.7	7	23	0.80
Holland Cut	0.0	0.0	9	36	0.67
Hood	0.7	0.5	7	0	0.88
Little-Potato-SI-Term	0.9	0.7	5	-19	0.93
Mallard	0.5	-1.0	9	21	0.34
Middle-R-Howard	0.6	0.6	8	-1	0.88
Middle-R-Holt	0.7	0.6	2	6	0.58
Miner-SI	0.8	0.8	6	-6	0.94
Moke-at-SJR	0.9	0.9	4	-11	0.98
Mossdale	0.8	0.8	7	18	0.86
N Mokelumne	0.6	0.6	9	-36	0.87
Prisoner-Pt	0.8	0.8	3	22	0.82
Prisoner-Pt-Term	0.7	0.0	5	3	0.43
Rio Vista	0.7	0.7	12	-3	0.90
Rough-n-Ready	0.9	0.8	7	37	0.73
SJR-Garwood	0.8	0.7	12	39	0.75
S Mokelumne	0.8	0.7	6	-10	0.92
3Mile-SJR	0.9	0.6	4	-2	0.79
Turner Cut-Holt	0.8	0.8	3	6	0.95
Victoria Canal-Byron	0.8	0.8	2	9	0.56

Table 5-5 Overall calibration metrics for the revised final calibration run and the initial DMS section calibration run. Blue font indicates a superior calibration result.

RMA revised calibration of QUAL turbidity	WY2010	WY2011
Compliance Only	2.6	2.6
Sum of Location Metrics	21.1	23.4
Weighted Sum of Location Metrics	5.8	6.2
DMS calibration of QUAL turbidity	WY2010	WY2011
Compliance Only	2.6	2.0
Sum of Location Metrics	18.8	21.3
Weighted Sum of Location Metrics	5.3	5.5

6 Evaluation of USGS-SSC data and WARMF Model Output as Boundary Conditions at Freeport and Vernalis

6.1 Background

The objective of this portion of the project (*i.e.*, Objective 2 in Section 1) was to develop a long-term Historical QUAL turbidity model to use in training a Turbidity ANN. In this section, the results evaluate the use of USGS-SSC data or WARMF model output as boundary conditions at Freeport and Vernalis in WY2010 and WY2011. The hydrodynamic boundary conditions are identical to those used in the recalibration effort. The SSC data used in the simulations as a proxy for turbidity input was downloaded directly from the USGS website, and the WARMF model output was supplied to RMA by Systech. Model residuals are used to calibrate model statistics in comparison with CDEC data for WY2010 and WY2011, as discussed in Section 3.3.

In Section 7, this documentation considers the use of these alternative boundary conditions in the long term model (1975 – 2011) in comparison with EMP data. The hydrodynamic conditions for the long-term model, *i.e.* HYDRO input, were supplied to RMA by the DMS.

6.2 WY2010 and WY2011 Model Results

Two sets of simulations were prepared for the WY2010 and WY2011 periods described in previous sections. The “Mixed-SSC-WARMF” simulations used a combination of USGS-SSC data and WARMF model calculations for turbidity boundary conditions, while the “WARMF-Only” simulations used WARMF model calculations for all inflow boundary conditions.

A set of five tables – Table 6-1 through Table 6-5 – document the individual residual statistics, the Location Metrics and the Model Skill assessment (Table 6-5) for the two sets of simulations. In general, the Location Metrics for the WARMF-Only simulations for WY2010 and WY2011 show a larger number of locations where the Location Metrics were superior to the Mixed-SSC-WARMF simulations, EXCEPT at the compliance locations. This observation is reflected in the Model Skill assessments – Table 6-5 – where the Mixed-SSC-WARMF simulations were superior to the WARMF-Only simulations for the “Compliance Only” model skill metric. On the other hand, the WARMF-Only simulations were superior in each of the other two Model Skill metrics in WY2010.

Two additional tables – Table 6-6 and Table 6-7 – are included for purposes of discussion only, as the results in Column 1 are NOT directly comparable to those in Columns 2 and 3 in these tables. However, it is safe to say that using turbidity data as boundary conditions (*vs.* WARMF or USGS-SSC data) produces a more consistent set of positive results for the Location Metrics than either of the other two options.

Figure 6-1 through Figure 6-8 illustrate contour plots of (interpolated) DSM2 15-minute output – in Figure 6-4 and Figure 6-8, the model output was daily-averaged before the contour plots were produced.

Figure 6-1 through Figure 6-4 illustrate WY2010 model comparisons using the Mixed-SSC-WARMF and the WARMF-Only sets of boundary conditions. A peak flow period began in late January and was accompanied by relatively high turbidity values. Figure 6-1 illustrates that the San Joaquin inflow turbidity was higher in the Mixed-SSC-WARMF simulation. Daily-averaged CDEC data values on January 24, 2010 are: Holland Cut = 5.7 NTU; Prisoner Point = 20.1 NTU; and, Victoria Canal = 7.2 NTU. The Mixed-SSC-WARMF simulation had slightly better performance overall in matching this data, but the results in terms of compliance exceedance was the same – only the Prisoner Point value was exceeded in the data and in both of the simulations.

Figure 6-5 through Figure 6-8 illustrate WY2010 model comparisons using the Mixed-SSC-WARMF and the WARMF-Only sets of boundary conditions. A peak flow period began in late January and was accompanied by high turbidity values. Figure 6-5 illustrates that the San Joaquin inflow turbidity was higher and the Sacramento inflow turbidity was lower in the Mixed-SSC-WARMF simulation than the WARMF-Only simulation. Daily-averaged CDEC data values on March 28, 2011 are: Holland Cut = 11.2 NTU; Prisoner Point = 22.2 NTU; and, Victoria Canal = 27.8 NTU. Although results in both simulations were high in comparison with the data, the Mixed-SSC-WARMF simulation clearly had better performance overall in matching the data, but the results in terms of compliance exceedance was the same, as both models overestimated the Holland Cut compliance value. However, the daily-averaged data at Holland Cut was exceeded the next day (12.7 NTU) and in subsequent days, so overall both of the simulations were successful at predicting the potential for exceeding the compliance values at all three locations, only the timing was off by one day.

Table 6-1 WY2010 Mixed-SSC-WARMF residual results. Bold font in the name indicates compliance locations; blue font in the statistics denotes an improved result in comparison with Table 6-2.

	R²	NSE	RMSE	PBIAS	Location Metric
Antioch	0.6	-0.2	13	-15	0.44
Cache-Ryer	0.7	0.7	20	-26	0.43
Decker	0.6	0.6	25	-16	0.49
False River	0.8	0.7	6	3	0.93
Georgiana-Below	0.4	0.4	43	-9	0.69
Georgiana-Sac	0.4	0.4	44	-16	0.33
Grant Line	0.9	0.0	19	-69	0.44
Holland Cut	0.8	0.7	3	17	0.93
Hood	0.4	0.4	42	-24	0.39
Little-Potato-SI-Term	0.6	0.6	9	13	0.88
Mallard	0.6	0.6	18	-2	0.88
Middle-R-Holt	0.7	0.7	5	42	0.91
Miner-SI	0.4	0.4	40	-32	0.46
Moke-at-SJR	0.5	0.5	26	-35	0.66
Mossdale	0.8	0.7	36	-70	0.60
Prisoner-Pt	0.7	0.7	6	13	0.90
Prisoner-Pt-Term	0.6	0.5	10	48	0.87
Rio Vista	0.6	0.6	27	-25	0.45
Rough-n-Ready	0.6	-1.0	22	-70	0.28
SJR-Garwood	0.7	-1.0	32	-93	0.14
3mile-SJR	0.7	0.7	12	-13	0.43
Turner Cut-Holt	0.4	-1.6	11	-58	0.23
Victoria Canal-Byron	0.3	0.4	3	15	0.80

Table 6-2 WY2010 WARMF-Only residual results. Bold font in the name indicates compliance locations; blue font in the statistics denotes an improved result in comparison with Table 6-1.

	R²	NSE	RMSE	PBIAS	Location Metric
Antioch	0.5	-0.2	13	-5	0.75
Cache-Ryer	0.7	0.7	18	-2	0.91
Decker	0.6	0.6	23	-5	0.87
False River	0.6	0.5	9	13	0.42
Georgiana-Below	0.5	0.5	39	7	0.84
Georgiana-Sac	0.5	0.5	40	1	0.84
Grant Line	0.3	0.3	12	25	0.79
Holland Cut	0.7	0.6	4	22	0.75
Hood	0.5	0.5	36	-5	0.86
Little-Potato-SI-Term	0.5	0.4	10	14	0.77
Mallard	0.5	0.5	20	5	0.55
Middle-R-Holt	0.7	0.6	5	52	0.76
Miner-SI	0.5	0.5	33	-12	0.86
Moke-at-SJR	0.5	0.5	25	-23	0.84
Mosssdale	0.2	0.2	38	25	0.75
Prisoner-Pt	0.7	0.7	7	19	0.73
Prisoner-Pt-Term	0.5	0.5	10	52	0.81
Rio Vista	0.6	0.6	24	-5	0.88
Rough-n-Ready	0.1	0.1	14	31	0.74
SJR-Garwood	0.3	0.3	15	18	0.79
3mile-SJR	0.7	0.7	13	0	0.89
Turner Cut-Holt	0.1	0.1	7	33	0.73
Victoria Canal-Byron	0.5	0.5	4	48	0.47

Table 6-3 WY2011 Mixed-SSC-WARMF residual results. Bold font in the name indicates compliance locations; blue font in the statistics denotes an improved result in comparison with Table 6-4.

	R²	NSE	RMSE	PBIAS	Location Metric
Antioch	0.2	-2.5	9	-38	0.35
Cache-Ryer	0.6	0.6	16	-37	0.74
Decker	0.6	0.3	16	-39	0.76
False River	0.2	-0.8	8	-25	0.61
Georgiana-Below	0.0	-0.7	29	-42	0.38
Georgiana-Sac	0.1	-2.1	27	-67	0.21
Grant Line	0.6	0.6	8	19	0.32
Grant Line - Tracy	0.6	0.6	8	19	0.40
Holland Cut	0.0	-0.1	9	19	0.30
Hood	0.1	-3.4	27	-84	0.06
Little-Potato-SI-Term	0.7	0.6	13	-95	0.86
Mallard	0.3	-5.7	15	-33	-0.18
Middle-R-Howard	0.4	0.4	9	-5	0.78
Middle-R-Holt	0.8	0.8	2	-16	0.94
Miner-SI	0.1	-1.8	29	-96	0.29
Moke-at-SJR	0.2	-1.4	23	-100	0.43
Mossdale	0.7	0.7	7	18	0.41
N Mokelumne	0.1	-2.1	27	-1300	0.35
Prisoner-Pt	0.5	0.5	3	-7	0.85
Prisoner-Pt-Term	0.5	-2.4	9	-43	0.42
Rio Vista	0.5	0.3	20	-67	0.75
Rough-n-Ready	0.6	0.6	7	24	0.46
SJR-Garwood	0.7	0.6	11	28	0.58
S Mokelumne	0.7	-0.1	16	-73	0.77
3mile-SJR	0.6	-1.2	13	-60	0.59
Turner Cut-Holt	0.7	0.7	4	-10	0.92
Victoria Canal-Byron	0.8	0.8	2	1	0.94

Table 6-4 WY2011 WARMF-Only residual results. Bold font in the name indicates compliance locations; blue font in the statistics denotes an improved result in comparison with Table 6-3.

	R²	NSE	RMSE	PBIAS	Location Metric
Antioch	0.4	-4.3	11	-41	0.04
Cache-Ryer	0.6	0.3	19	-28	0.80
Decker	0.6	0.0	18	-34	0.77
False River	0.4	-1.2	9	-32	0.46
Georgiana-Below	0.2	-0.6	27	-24	0.64
Georgiana-Sac	0.4	-1.9	24	-46	0.48
Grant Line	0.7	0.7	6	0	0.91
Grant Line - Tracy	0.6	0.6	7	1	0.87
Holland Cut	0.0	-0.2	10	-4	0.65
Hood	0.3	-5.0	27	-60	-0.01
Little-Potato-SI-Term	0.8	-1.0	13	-87	0.67
Mallard	0.4	-7.7	17	-28	-0.42
Middle-R-Howard	0.7	0.8	7	-27	0.51
Middle-R-Holt	0.5	-0.1	4	-41	0.34
Miner-SI	0.3	-2.0	27	-71	0.44
Moke-at-SJR	0.5	-1.7	22	-83	0.52
Mossdale	0.5	0.5	8	0	0.84
N Mokelumne	0.7	-1.8	25	-1200	0.53
Prisoner-Pt	0.6	0.3	5	-24	0.42
Prisoner-Pt-Term	0.6	-2.7	10	-54	0.27
Rio Vista	0.5	0.0	22	-57	0.75
Rough-n-Ready	0.8	0.7	5	6	0.92
SJR-Garwood	0.7	0.6	9	12	0.89
S Mokelumne	0.7	-0.7	17	-70	0.69
3mile-SJR	0.6	-2.6	15	-59	0.38
Turner Cut-Holt	0.7	0.7	5	-30	0.53
Victoria Canal-Byron	0.8	0.3	5	-33	0.28

Table 6-5 Overall metrics for the two sets of boundary conditions – Mixed SSC-WARMF and WARMF-Only.

Mixed USGS-SSC and WARMF BC	WY2010	WY2011
Compliance Only	2.6	2.1
Sum of Location Metrics	13.5	14.3
Weighted Sum of Location Metrics	4.3	4.1
WARMF-Only BC	WY2010	WY2011
Compliance Only	2.0	1.4
Sum of Location Metrics	17.6	14.2
Weighted Sum of Location Metrics	4.7	3.6

Table 6-6 Cross-comparison WY2010 results for Location Metrics. Note that the Recalibration results in this Table are NOT directly comparable to the other two columns, as the Location Metrics were calculated in comparison to the DMS model.

WY2010	Location Metric Recalibration	Location Metric Mixed	Location Metric All WARMF
Antioch	0.78	0.44	0.75
Cache-Ryer	0.96	0.43	0.91
Decker	0.96	0.49	0.87
False River	0.90	0.93	0.42
Georgiana-Below	1.00	0.69	0.84
Georgiana-Sac	0.98	0.33	0.84
Grant Line	0.93	0.44	0.79
Holland Cut	0.84	0.93	0.75
Hood	0.99	0.39	0.86
Little-Potato-SI-Term	0.92	0.88	0.77
Mallard	0.95	0.88	0.55
Middle-R-Holt	0.94	0.91	0.76
Miner-SI	0.99	0.46	0.86
Moke-at-SJR	0.98	0.66	0.84
Mossdale	0.96	0.60	0.75
Prisoner-Pt	0.98	0.90	0.73
Prisoner-Pt-Term	0.90	0.87	0.81
Rio Vista	0.98	0.45	0.88
Rough-n-Ready	0.81	0.28	0.74
SJR-Garwood	0.80	0.14	0.79
3mile-SJR	0.98	0.43	0.89
Turner Cut-Holt	0.73	0.23	0.73
Victoria Canal-Byron	0.79	0.80	0.47

Table 6-7 Cross-comparison WY2011 results for Location Metrics Note that the Recalibration results in this Table are NOT directly comparable to the other two columns, as the Location Metrics were calculated in comparison to the DMS model.

WY2011	Location Metric Recalibration	Location Metric Mixed	Location Metric All WARMF
Antioch	0.71	0.35	0.04
Cache-Ryer	0.93	0.74	0.80
Decker	0.92	0.76	0.77
False River	0.79	0.61	0.46
Georgiana-Below	0.92	0.38	0.64
Georgiana-Sac	0.99	0.21	0.48
Grant Line	0.90	0.32	0.91
Grant Line - Tracy	0.92	0.40	0.87
Holland Cut	0.70	0.30	0.65
Hood	0.88	0.06	-0.01
Little-Potato-SI-Term	0.93	0.86	0.67
Mallard	0.63	-0.18	-0.42
Middle-R-Howard	0.51	0.78	0.51
Middle-R-Holt	0.90	0.94	0.34
Miner-SI	0.94	0.29	0.44
Moke-at-SJR	0.98	0.43	0.52
Mossdale	0.92	0.41	0.84
N Mokelumne	0.89	0.35	0.53
Prisoner-Pt	0.95	0.85	0.42
Prisoner-Pt-Term	0.81	0.42	0.27
Rio Vista	0.90	0.75	0.75
Rough-n-Ready	0.95	0.46	0.92
SJR-Garwood	0.92	0.58	0.89
S Mokelumne	0.87	0.77	0.69
3mile-SJR	0.93	0.59	0.38
Turner Cut-Holt	0.81	0.92	0.53
Victoria Canal-Byron	0.93	0.94	0.28

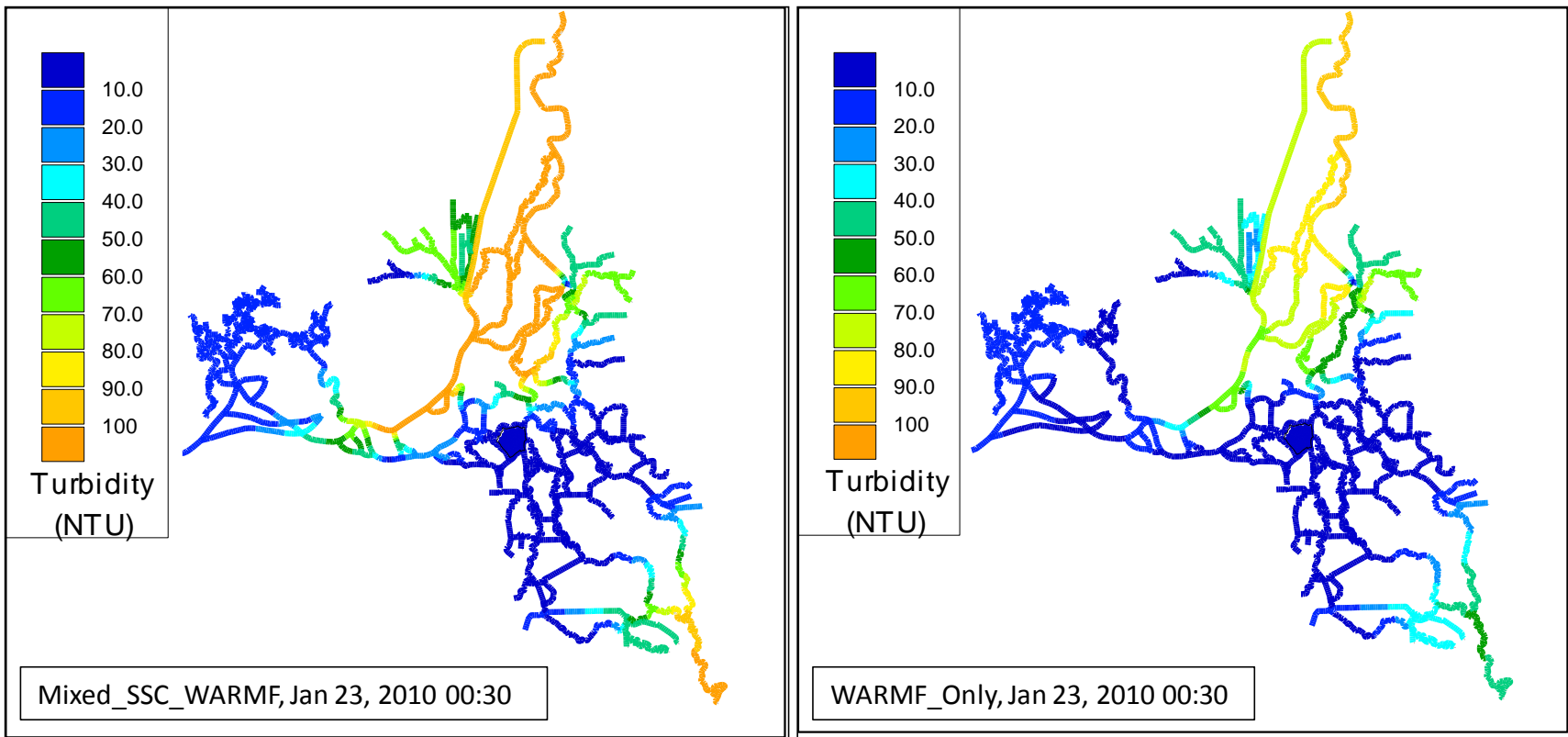


Figure 6-1 WY2010 contour plot comparison of the Mixed-SSC-WARMF and WARMF-Only simulations during a peak inflow period before turbidity reached the central Delta.

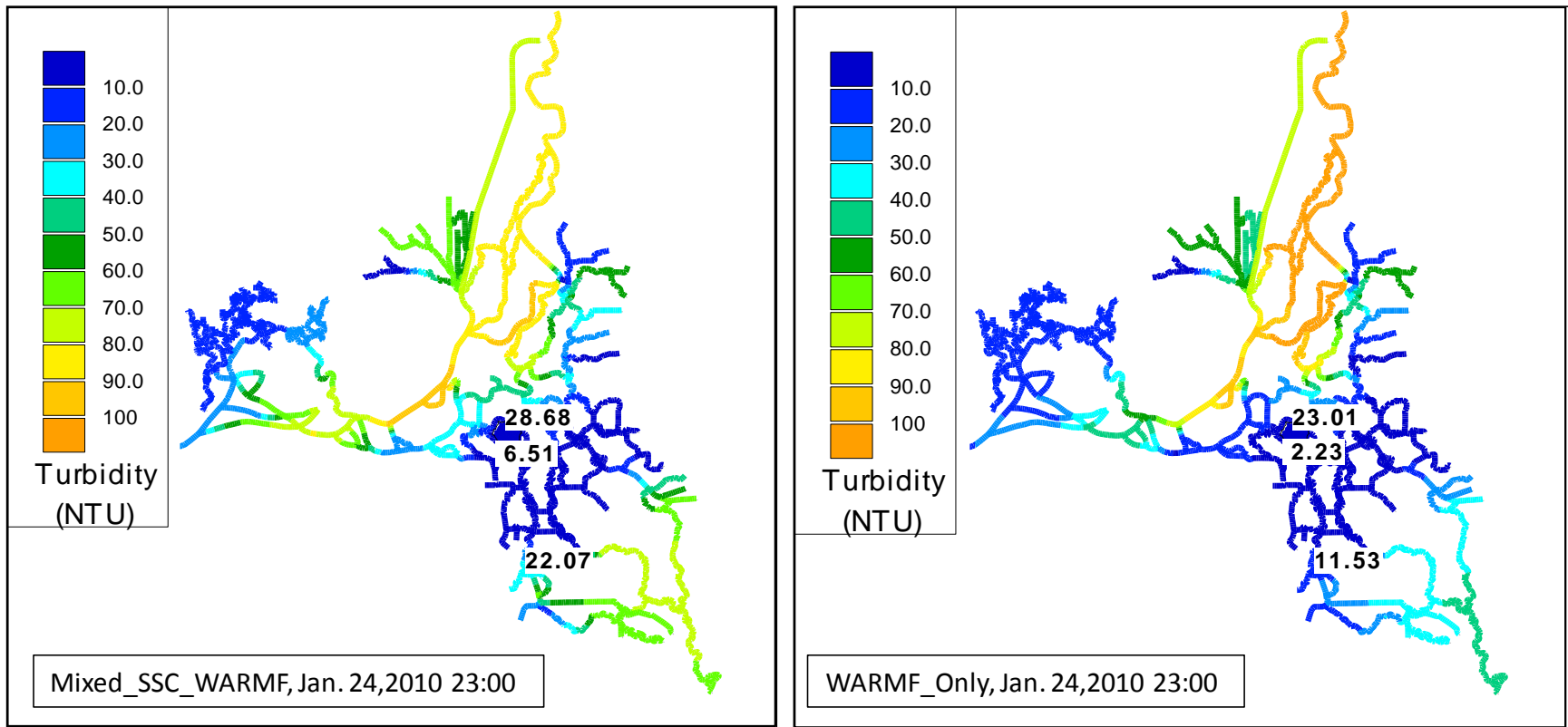


Figure 6-2 WY2010 contour plot comparison of the Mixed-SSC-WARMF and WARMF-Only simulations, with values shown for modeled 15-min compliance location turbidity on Jan. 24, 2010.

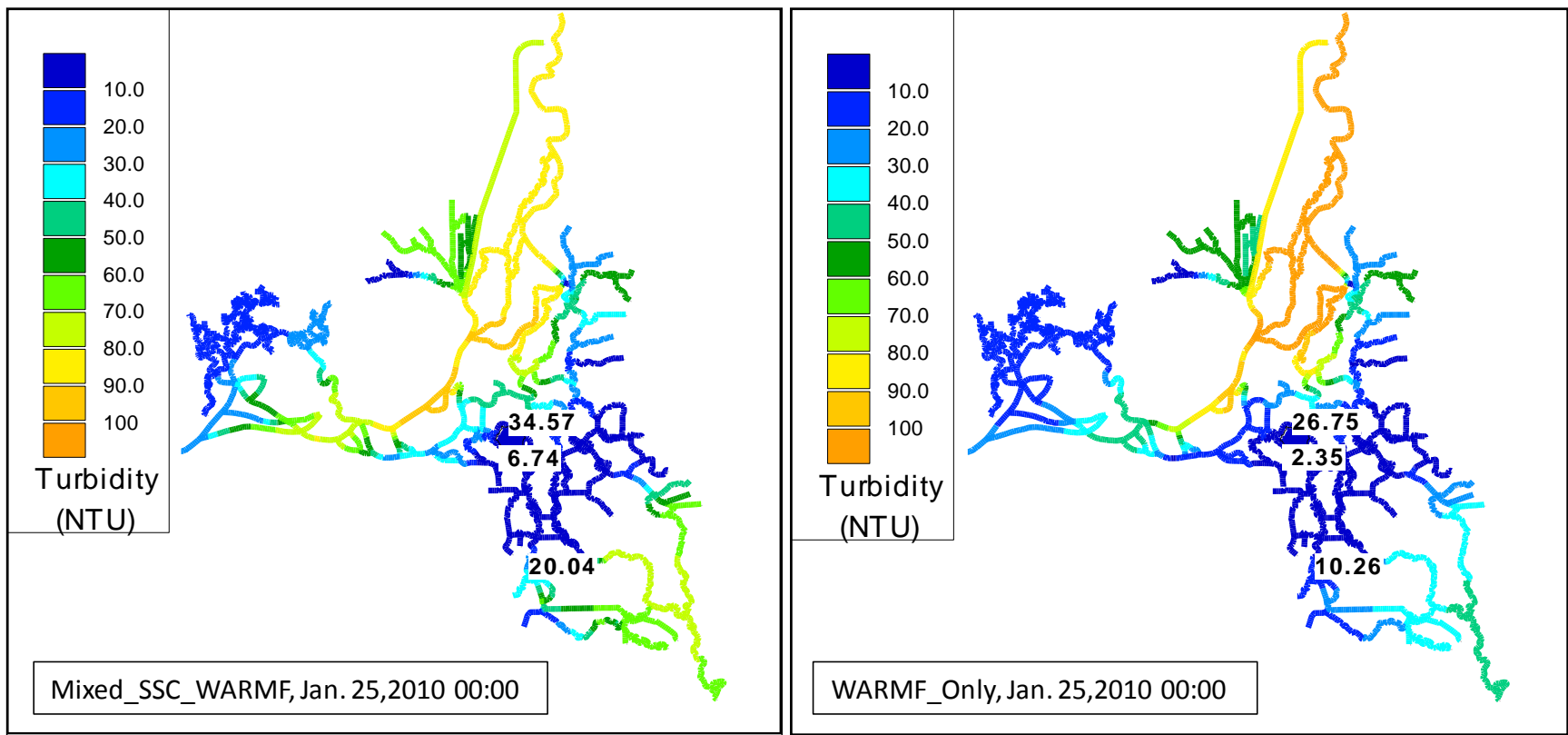


Figure 6-3 WY2010 contour plot comparison of the Mixed-SSC-WARMF and WARMF-Only simulations, with values shown for modeled 15-min compliance location turbidity on Jan. 25, 2010.

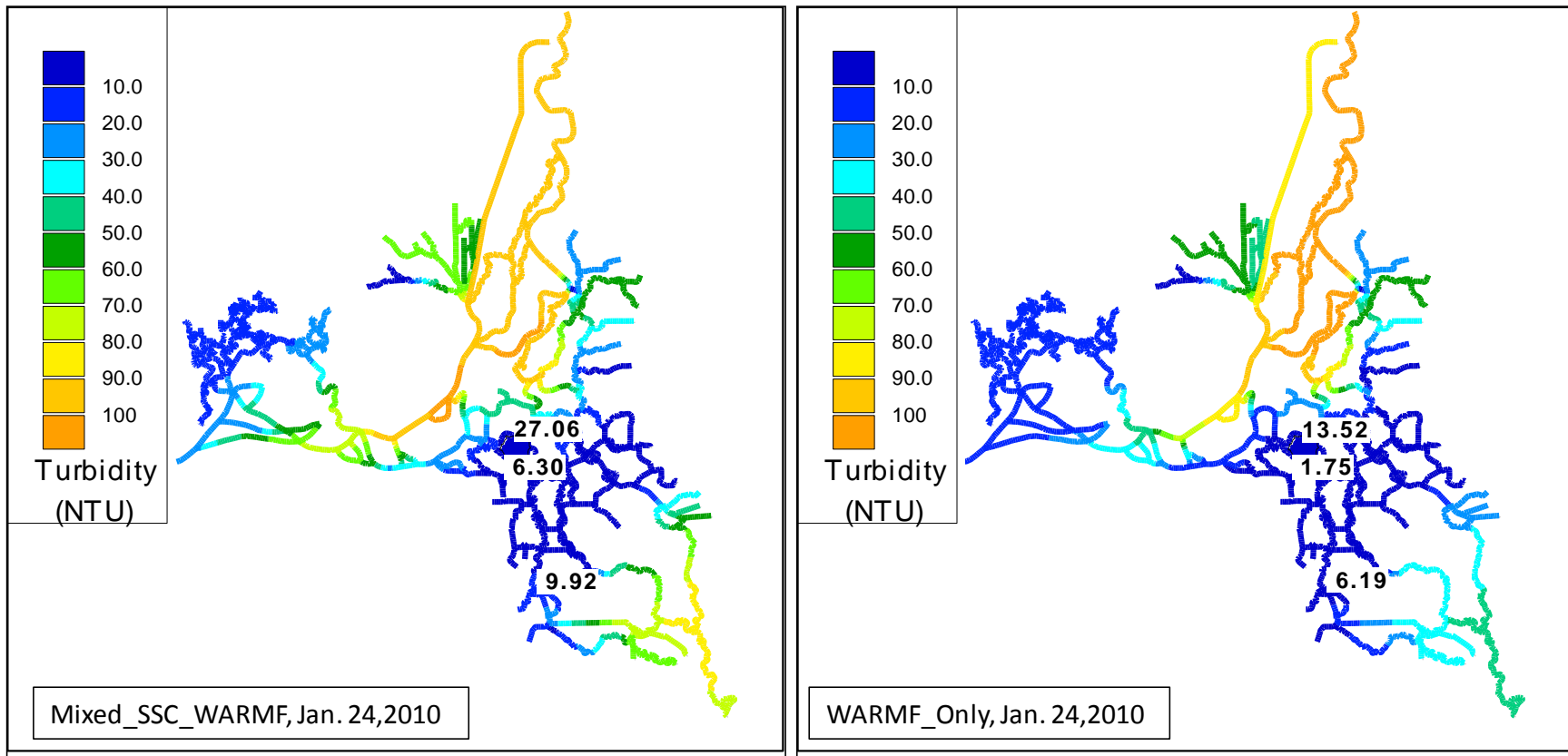


Figure 6-4 WY2010 contour plot comparison of the Mixed-SSC-WARMF and WARMF-Only simulations – date chosen for modeled daily peak Victoria Canal compliance location turbidity on Jan. 24, 2010. In comparison with Figure 6-2, these daily average values are much lower than 15-minute results, particularly in Victoria Canal. Neither model exceeded the compliance value at all three locations.

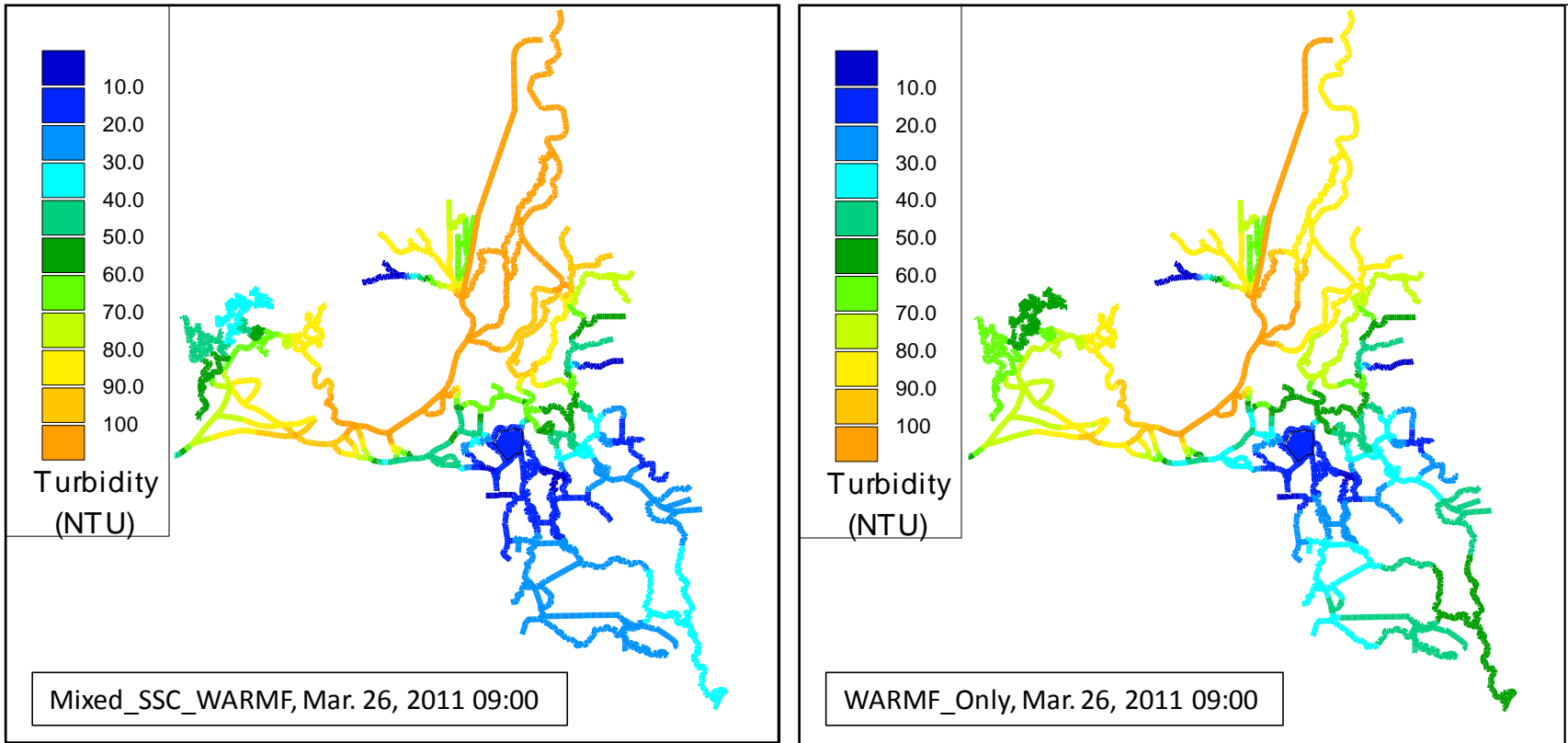


Figure 6-5 WY2011 contour plot comparison of the Mixed-SSC-WARMF and WARMF-Only simulations during a peak inflow period. Turbidity has intruded into the Central Delta.

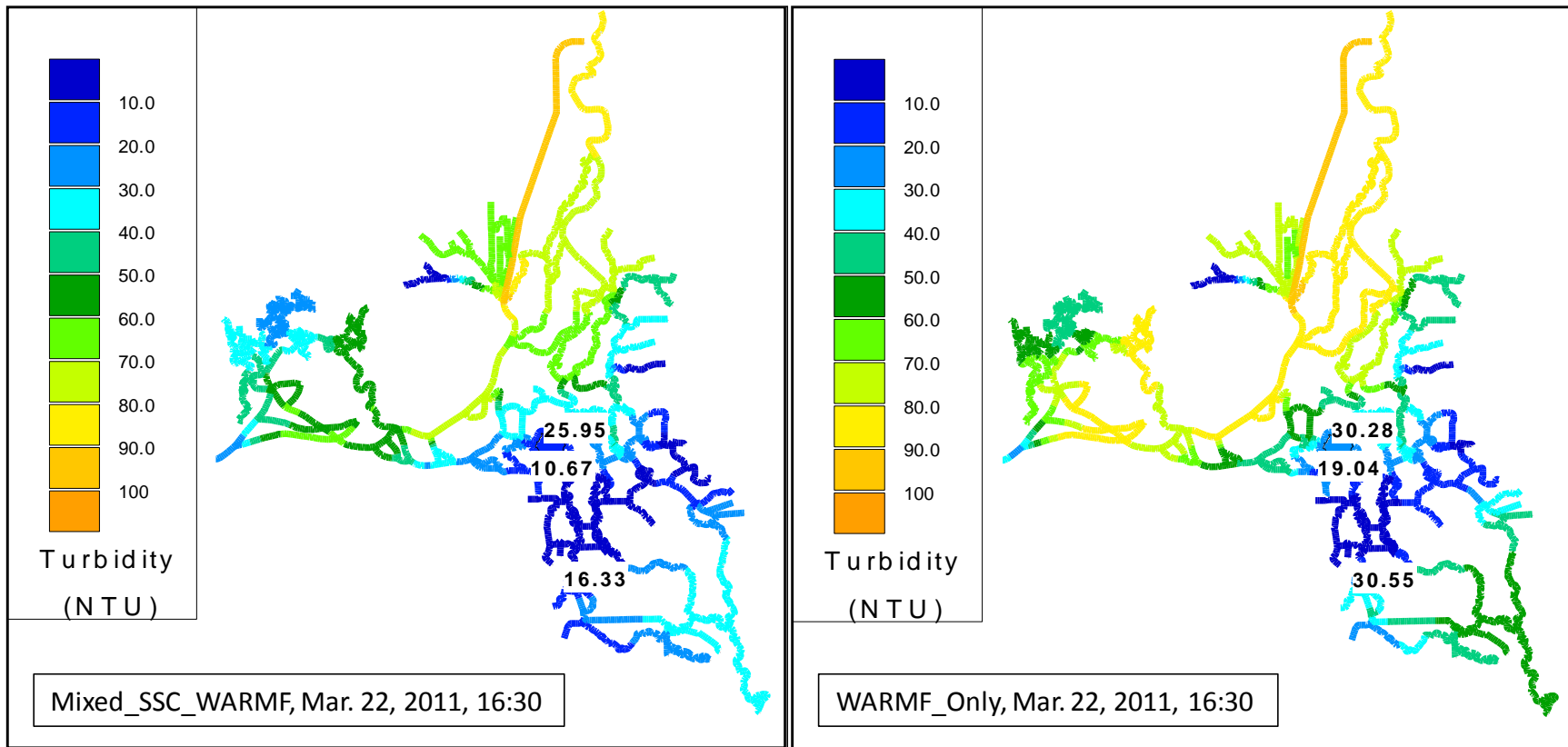


Figure 6-6 WY2011 contour plot comparison of the Mixed-SSC-WARMF and WARMF-Only simulations, with values shown for modeled 15-min compliance location turbidity on Mar. 22, 2011. This is the peak time for compliance location values for the WARMF-Only simulation.

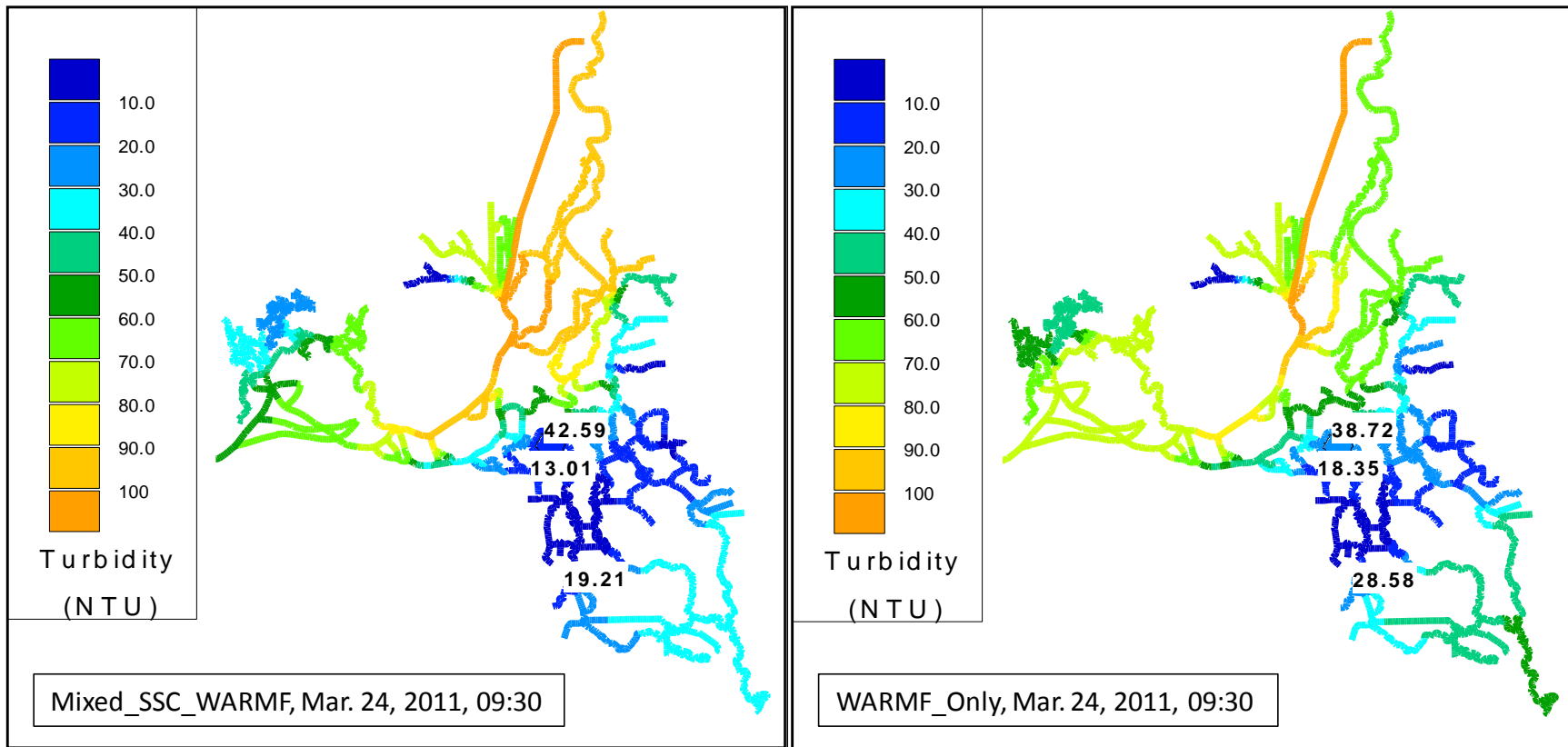


Figure 6-7 WY2011 contour plot comparison of the Mixed-SSC-WARMF and WARMF-Only simulations, with values shown for modeled 15-min compliance location turbidity on Mar. 22, 2011. This is the peak time for compliance location values for the Mixed-SSC-WARMF simulation.

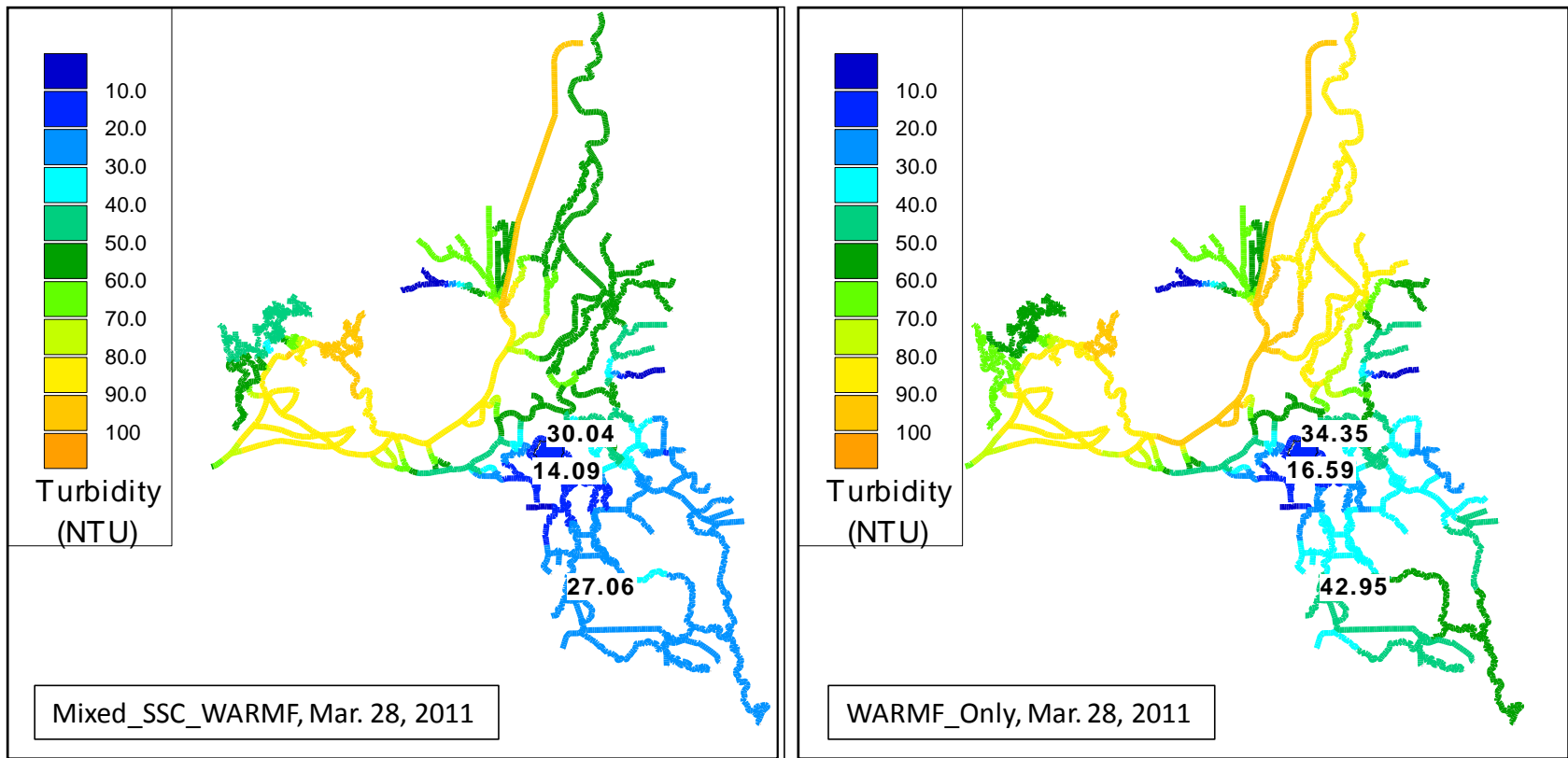


Figure 6-8 WY2011 contour plot comparison of the Mixed-SSC-WARMF and WARMF-Only simulations, The time was chosen for modeled daily peak Victoria Canal compliance location turbidity on Mar. 28, 2011. Both simulations exceeded the compliance maximum of 12 NTU at all three locations.

7 Results of the Long Term QUAL Historical Turbidity Simulation – Water Years 1975 - 2011

In this section of the documentation, the focus is on the final step in satisfying Objective Two of the project - supporting the development of a Turbidity ANN interfacing with the DSM2 QUAL turbidity model output from the recalibrated model. This third and final step used “early years”, 1975 – 1990, and “recent years”, 1991 – 2011, model set-ups with both the Mixed-SSC-WARMF and WARMF-Only boundary conditions to calculate model residual statistics in comparison with Environmental Monitoring Program (EMP) grab sample data.

The objective of this step was to further assess these two sets of boundary conditions. Statistics were computed at each available data location in each time frame (recent years and early years) by comparing EMP with daily averaged model results – note that EMP data did not include the three compliance locations. In these statistics, the entire time frame was used, not just the high flow portion of the water years.

7.1 EMP data

EMP measurements occur approximately monthly at numerous locations in the Delta. The locations for these measurements within the DSM2 model domain – shown in Figure 7-1 through Figure 7-4 – have changed over the years, with some locations being phased out and some locations being phased in. Samples are collected from shore-based collection locations and by boat (*i.e.*, from DWR or USBR research vessels). Details on sample collection and field methods are available at the following website:

<http://www.water.ca.gov/bdma/meta/discrete.cfm>

For comparison with EMP data, QUAL long-term turbidity model results were daily averaged. Although the EMP measurements are essentially instantaneous, the collection time was not included in the metadata, only the collection date.

7.2 Simulation results – Model residuals and regressions comparing long-term simulations with EMP data

QUAL model output was specified at all EMP data locations, and the 15-minute model output was daily averaged. The residual (data – model) and regression calculations used the EMP data and daily-averaged model output on the same date. Plots comparing model output and EMP along with regression plots and residual histograms with detailed statistics were created for each available EMP location. Figure 7-5 and Figure 7-6 illustrate these plots for the EMP location D26, which is also known as SJR at Potato Point, for both the WARMF-Only (Figure 7-5) and the Mixed-SSC-WARMF (Figure 7-6) simulations.

Residual statistics, regressions and the associated statistics were calculated as discussed in Section 3.3 using the reduced set of QUAL turbidity output (*i.e.*, only at EMP data dates). As previously mentioned, the long-term model was run in two time frames – the early years from 10/1975 – 12/1990 and the recent years from 01/1991 – 12/2012. EMP data comparisons shortened these frames somewhat, and in

some cases in the recent years the data acquisition only occurred for a few of the modeled years. Plots for each EMP location and each time frame are found in Appendices V1 and VII Sections 15 and 16 for each of the simulations.

The statistical results are collated in Table 7-1 through Table 7-4. The final column in each table lists the sign (+ or -) of the PBIAS statistic to allow easy reference as to whether the simulation tends to overestimate the data (negative bias) or underestimate the data (positive bias). Table 7-1 (WARMF-Only) and Table 7-2 (Mixed-SSC-WARMF) document the results for the early years (1975 – 1990) simulations, and Table 7-3 (WARMF-Only) and Table 7-4 (Mixed-SSC-WARMF) document and compare the simulation results for the recent years (1991 – 2011). Blue font indicates that the statistic in at that location was superior to the statistic in the comparison table. Occasions where the compared statistics were equal are not color-highlighted.

The final row of each table lists the sum of the statistics in each column – each sum gives an indication of the full-period, Delta-wide skill of the simulation for comparisons. The R^2 statistics is maximized at 1.0, so a higher sum indicates a superior result in the comparison tables. The NSE statistics is also maximized at 1.0, with negative values indicating that the data mean is a better estimate of the data than the model – so a more positive or less negative result is superior. The RMSE and PBIAS statistics are both maximized at zero, so in these cases a smaller value indicates a superior result in the comparison tables. The absolute value of the PBIAS statistic was summed.

7.3 Summary of results

In examining the final column in the four tables, “Sign Bias”, these statistics show that the WARMF-Only simulation has a regular bias resulting in an under-prediction of the EMP data at the great majority of locations in both time frames, while the Mixed-SSC-WARMF simulations has a mixed set of under- and over-predictions.

In the both the early years and recent years time frames, the Mixed-SSC-WARMF simulations have a superior result in the sum of the R^2 and $AbsoluteValue(PBIAS)$ statistics, while the WARMF-Only simulations have a superior result in the other two summed statistics, NSE and RMSE.

Given the initial decision to minimize the error in the PBIAS statistic, the statistical results give a slight edge to the use of the Mixed-SSC-WARMF simulations in the long-term simulations. However, when viewed as whole, neither model performed very well in reproducing the EMP turbidity data, so the result can be viewed as neutral in assessing which of the models has better performance – *i.e.*, neither set of boundary conditions is clearly better.

Figure 7-7 through Figure 7-9 illustrate contour plots of (interpolated) DSM2 15-minute output – in Figure 7-9 the model output was daily-averaged before the contour plots were produced. Late December 1983 is used as an example of a high flow period to compare the results of the two simulation models – using Mixed-SSC-WARMF and WARMF-Only boundary conditions. Although data at the three compliance locations was not available to use in comparison for the model results, in Figure 7-9, it is useful to compare the modeled result in terms of the potential for exceeding the 12 NTU compliance maximum. Figure 7-9 gives the date, December 28th, at which the Victoria Canal location reaches its

maximum value. Although the magnitude of the predictions are different at the three compliance locations, both simulations predict that only two of the three locations will exceed the 12 NTU maximum during this high flow, high turbidity event.

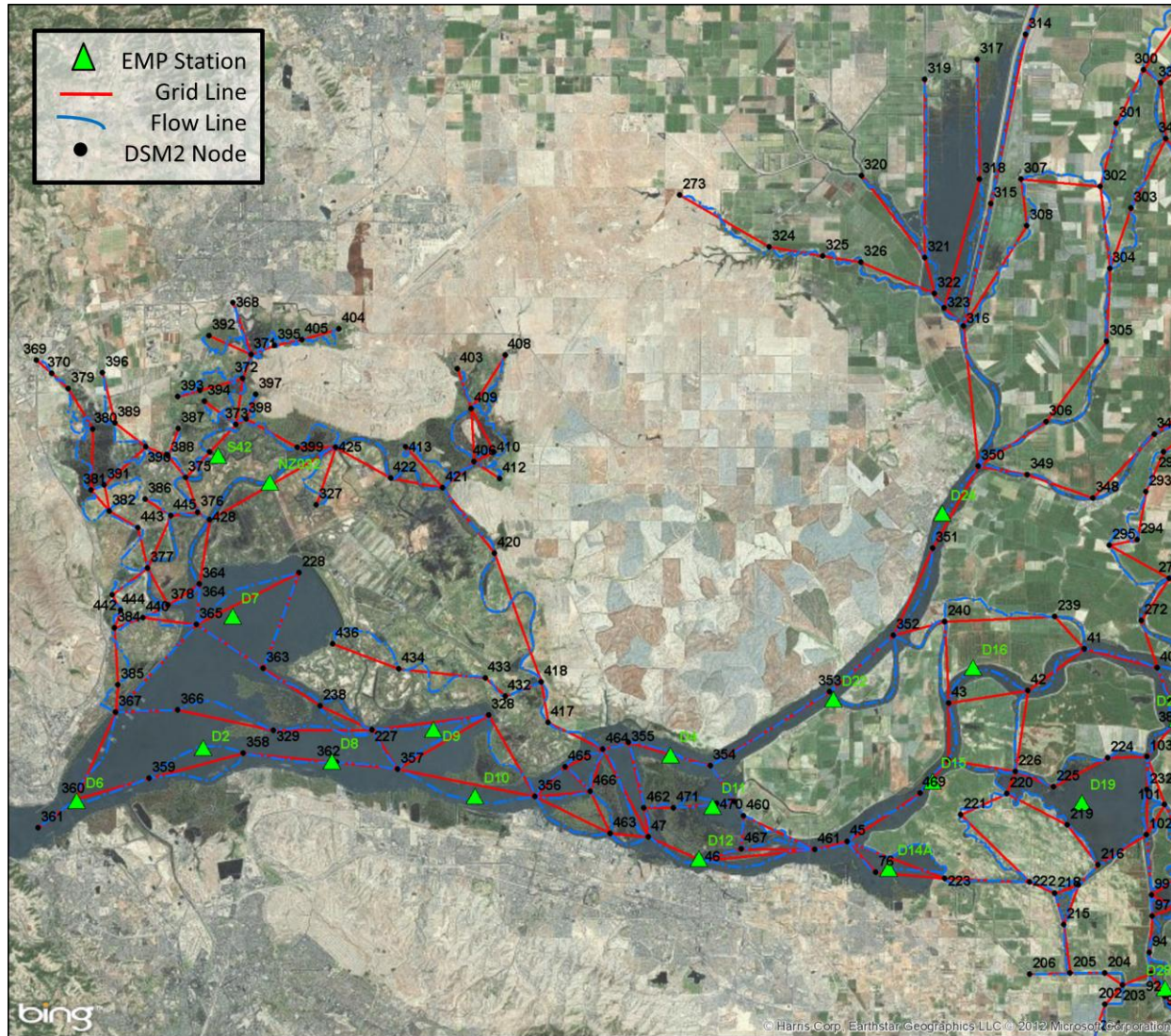


Figure 7-1 The figure shows the location of EMP stations (green triangles), DSM2 channels (red) and nodes (black) in the western Delta.

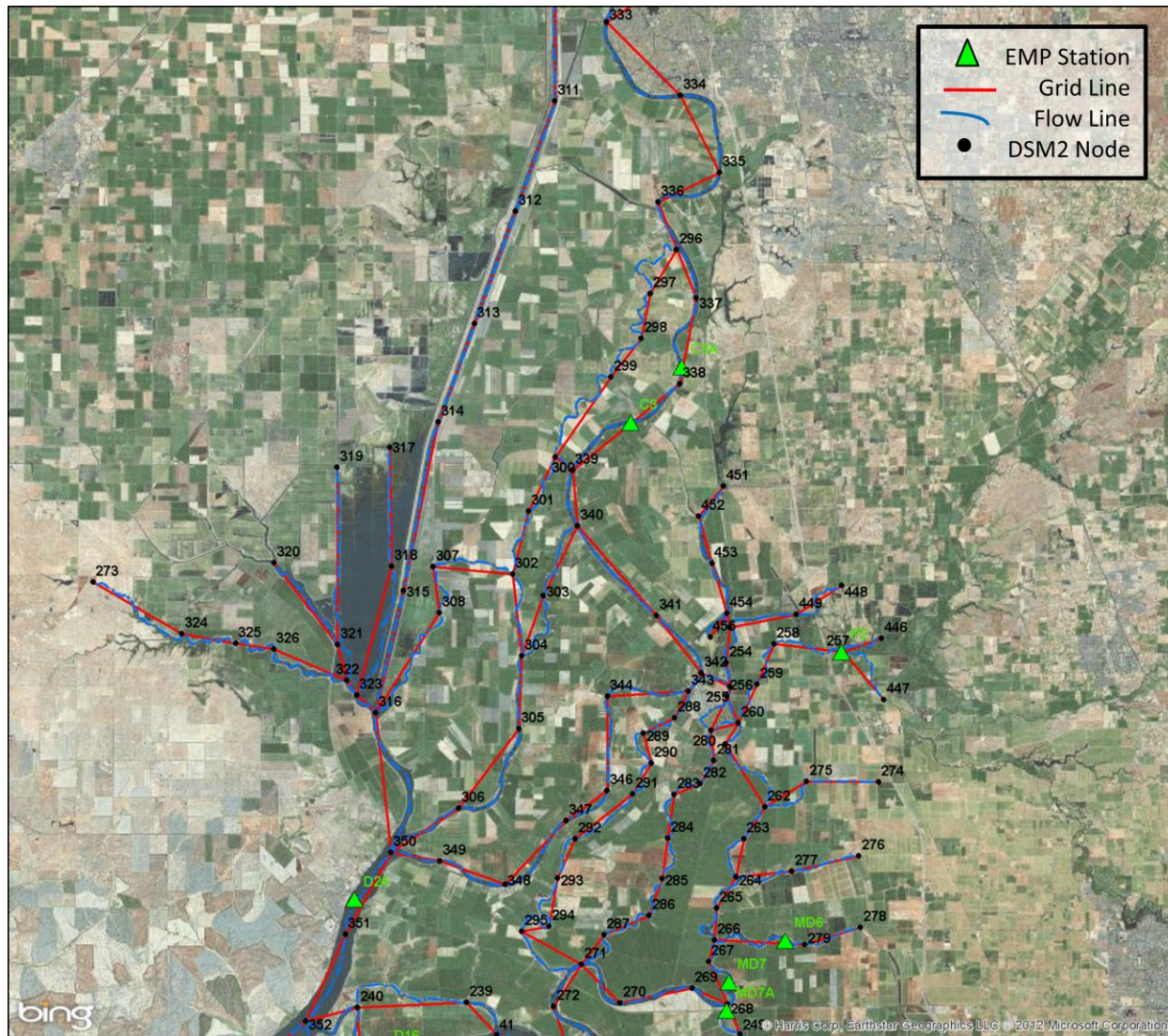


Figure 7-2 The figure shows the location of EMP stations (green triangles), DSM2 channels (red), and nodes (black) in the northern Delta.

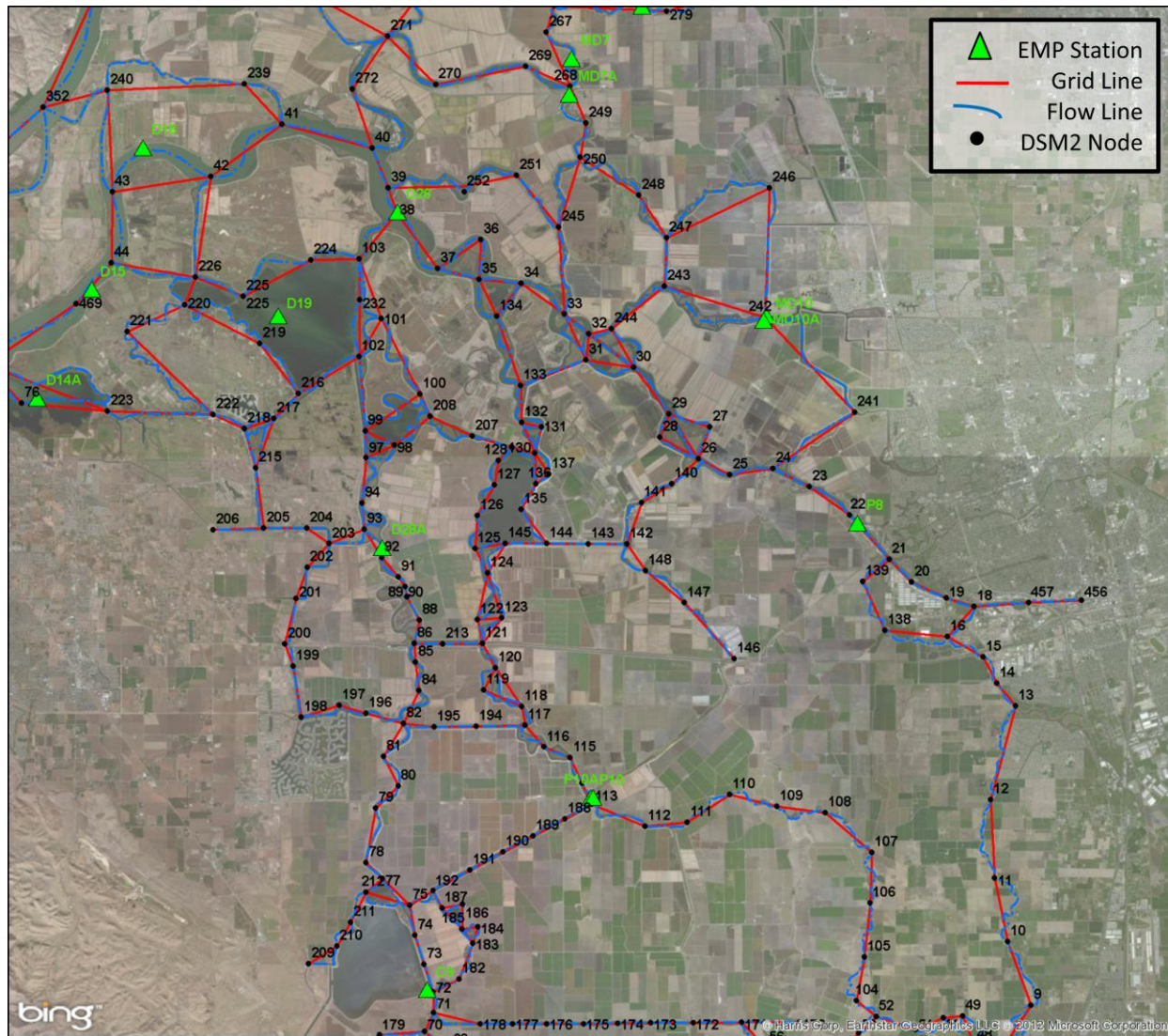


Figure 7-3 The figure shows the location of EMP stations (green triangles), DSM2 channels (red) and nodes (black) in the eastern Delta.

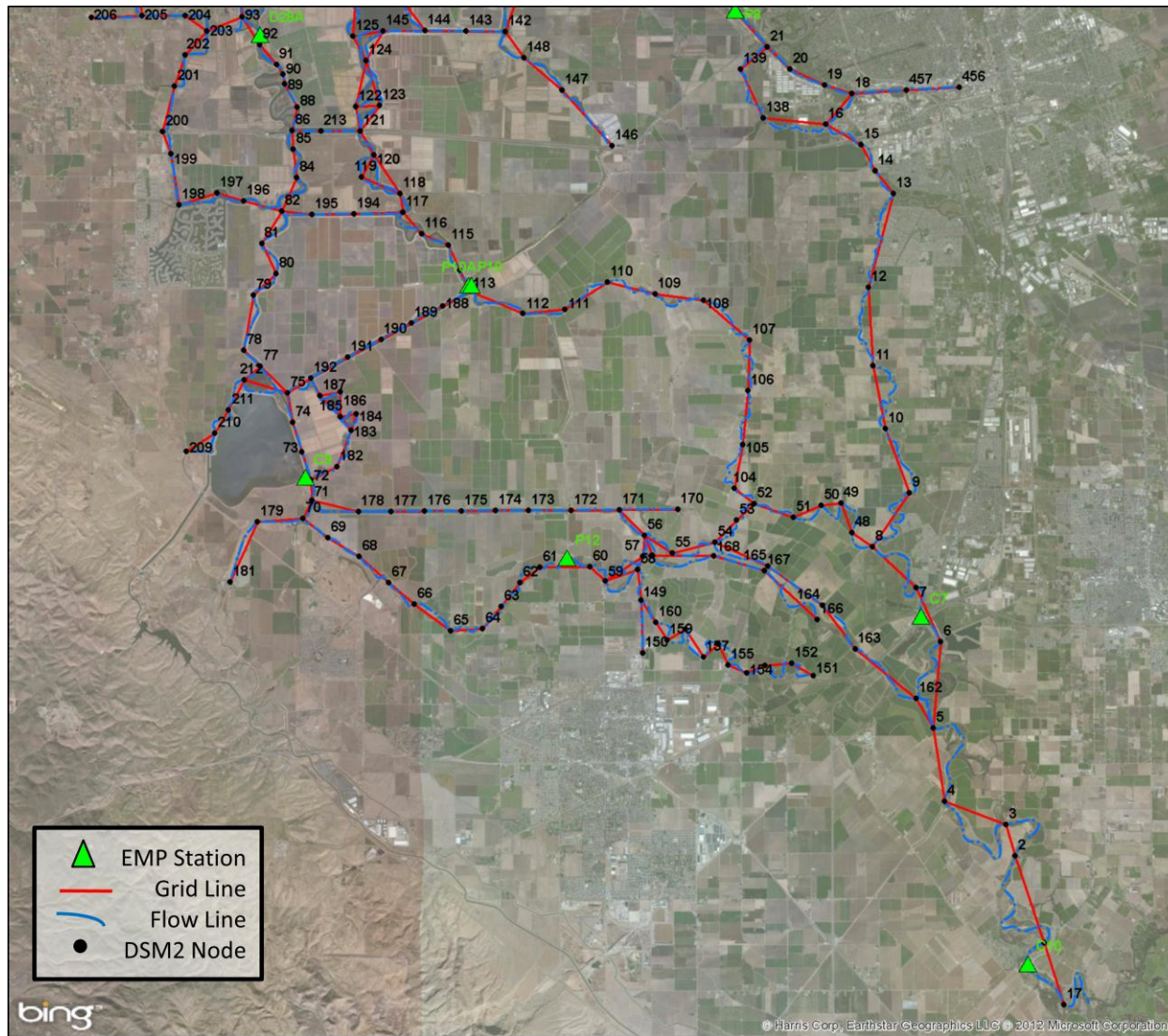


Figure 7-4 The figure shows the location of EMP stations (green triangles), DSM2 channels (red) and nodes (black) in the southern Delta.

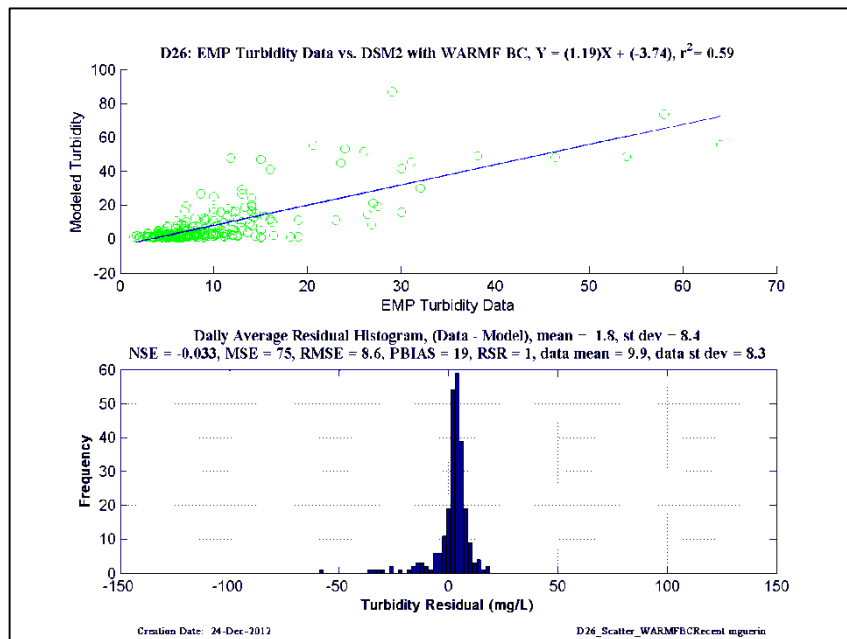
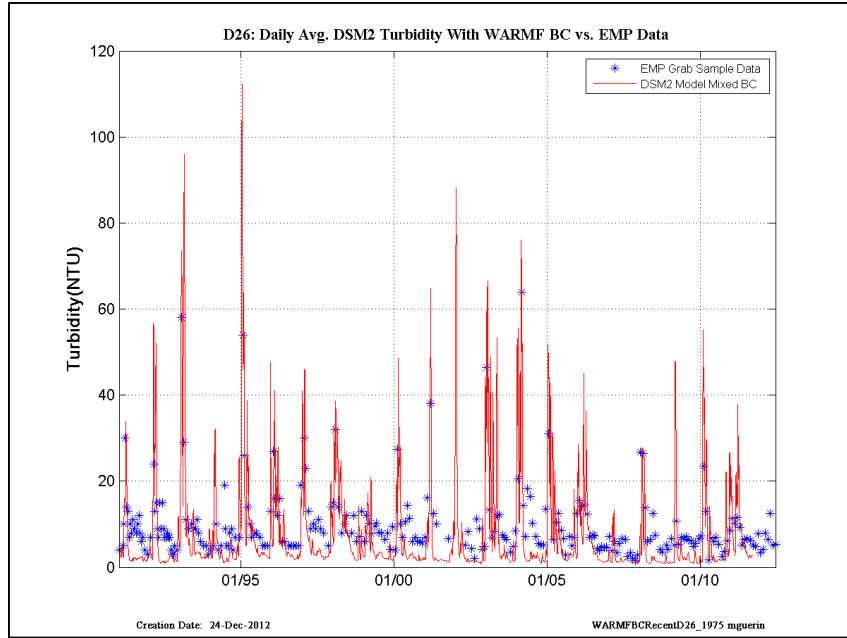


Figure 7-5 WARMF-Only results at D26 in the recent years time frame.

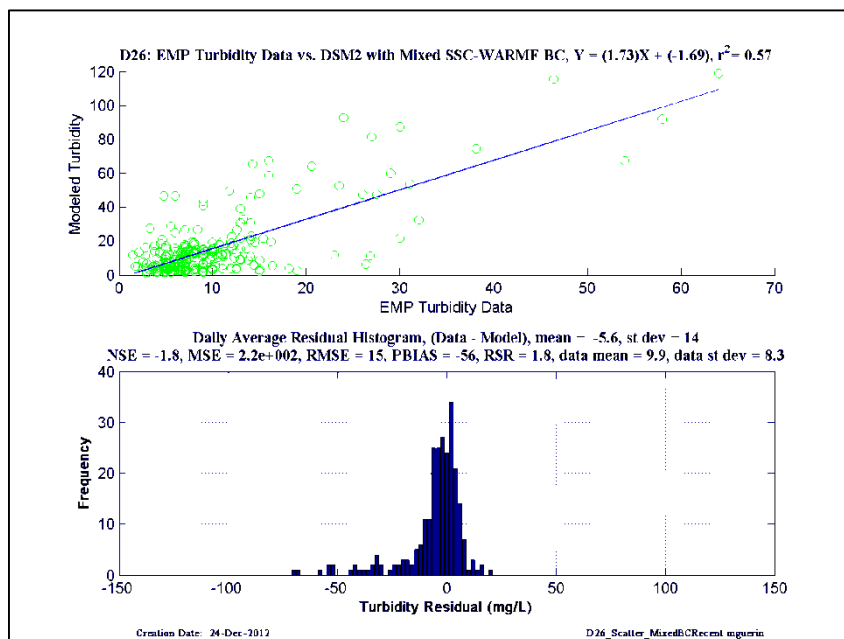
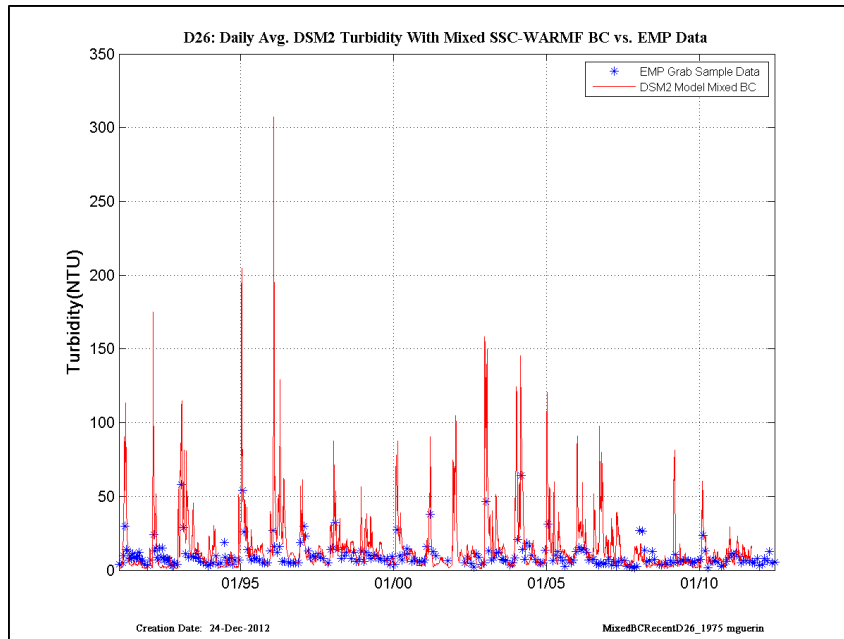


Figure 7-6 Mixed-SSC-WARMF results at D26 in the recent years time frame.

Table 7-1 WARMF-Only boundary conditions simulation for early years (1975 – 1990). Blue font in the statistics denotes an improved result in comparison with Table 7-2.

WARMF-Only	EMP Location	R ²	NSE	RMSE	PBIAS	Sign Bias
GREENES/HOOD	C3	0.52	-0.047	12	-21	-
Mossdale	C7	0.10	-0.81	13	-19	-
CCFB entrance	C9	0.17	-0.52	11	56	+
SJR-McCune	C10	0.06	-0.29	16	4	+
SAC R Above Point SAC	D4	0.21	-0.11	22	52	+
SUISUN BAY NR MTZ	D6	0.29	0.25	11	-57	-
GRIZZLY BAY	D7	0.02	-0.08	25	43	+
SLM001, SUISUN NR NICHOLS	D8	0.07	-0.46	17	27	+
HONKER BAY	D9	0.02	-0.2	26	55	+
Mallard-Sl., RSAC075	D10	0.13	-0.29	20	44	+
SHERMAN ISLAND	D11	0.31	0.11	18	60	+
RSAN007	D12	0.08	-0.43	14	56	+
BIG BREAK NR OAKLEY	D14A	0.02	-0.12	16	71	+
SJR-JP, RSAN018	D15	0.21	-0.13	11	61	+
RSAN024 TWITCHELL	D16	0.22	-0.59	11	53	+
Franks Tract	D19	0.00	-0.13	13	77	+
Sac at Decker	D22	0.36	-0.48	17	37	+
Rio Vista	D24	0.53	0.4	15	12	+
SJR AT POTATO PT	D26	0.25	0.13	8.8	42	+
OLD-R-BACON, ROLD024	D28A	0.07	-0.27	11	73	+
RSMKL008,LIT-POT-SL-TERM	MD7A	0.29	0.21	7.9	45	+
DISAPPOINTMENT SL	MD10	0.24	0.18	13	80	+
SJR BUCKLEY COVE	P8	0.39	-0.42	8.2	45	+
RMID023	P10A	0.30	-0.19	9.2	63	+
ROLD059	P12	0.10	-0.96	12	40	+
SLSUS012, SUSIUN SL S OF VOLANTI	S42	0.06	-0.27	36	63	+
		Sum	Sum	Sum	Sum(ABS)	
Sum of Statistics		5.0	-5.5	394	1235	

Table 7-2 Mixed-SSC-WARMF boundary conditions simulation for early years (1975 – 1990). Blue font in the statistics denotes an improved result in comparison with Table 7-1.

Mixed-SSC-WARMF	EMP Location	R ²	NSE	RMSE	PBIAS	Sign Bias
GREENES/HOOD	C3	0.69	-4.5	39	-240	-
Mossdale	C7	0.53	0.44	8.2	-20	-
CCFB entrance	C9	0.20	0.17	10	59	+
SJR-McCune	C10	0.71	0.7	7.9	-0.94	-
SAC R Above Point SAC	D4	0.14	-2.6	33	-3.6	-
SUISUN BAY NR MTZ	D6	0.42	0.25	13	-75	-
GRIZZLY BAY	D7	0.01	-0.58	26	21	+
SLM001, SUISUN NR NICHOLS	D8	0.09	-2.4	24	-9.3	-
HONKER BAY	D9	0.03	-1.3	28	23	+
Mallard-Sl., RSAC075	D10	0.12	-2.8	27	2.2	+
SHERMAN ISLAND	D11	0.26	-1.5	21	21	+
RSAN007	D12	0.20	-3.4	17	14	+
BIG BREAK NR OAKLEY	D14A	0.01	-0.92	16	40	+
SJR-JP, RSAN018	D15	0.15	-2.4	13	15	+
RSAN024, TWITCHELL	D16	0.26	-4.5	15	-5.3	-
Franks Tract	D19	0.03	-0.32	11	53	+
Sac at Decker	D22	0.22	-6.2	36	-49	-
Rio Vista	D24	0.42	-2.1	40	-120	-
SJR AT POTATO PT	D26	0.19	-1.4	13	-21	-
OLD-R-BACON, ROLD024	D28A	0.04	-0.21	10	61	+
RSMKL008,LIT-POT-SL-TERM	MD7A	0.24	-0.95	10	-18	-
DISAPPOINTMENT SL	MD10	0.31	0.29	13	84	+
SJR BUCKLEY COVE	P8	0.37	0.19	7.9	54	+
RMID023	P10A	0.19	-0.12	8.5	61	+
ROLD059	P12	0.20	0.11	10	44	+
SLSUS012, SUSIUN SL S OF VOLANTI	S42	0.03	-0.54	28	29	+
		Sum	Sum	Sum	Sum(ABS)	
Sum of Statistics		6.1	-36.6	486	903	

Table 7-3 WARMF-Only boundary conditions simulation for recent- years (1991 – 2011). Blue font in the statistics denotes an improved result in comparison with Table 7-4.

WARMF-Only	EMP Location	R ²	NSE	RMSE	PBIAS	Sign Bias
GREENES/HOOD	C3	0.34	-0.17	26	-21	(Not used)
Mossdale	C7	0.22	0.19	17	8.9	+
CCFB entrance	C9	0.46	0.46	9.5	69	+
SJR-McCune	C10	0.21	0.21	18	18	+
SAC R Above Point SAC	D4	0.48	-0.43	19	24	+
SUISUN BAY NR MTZ	D6	0.5	0.45	9.5	-29	-
GRIZZLY BAY	D7	0.22	0.13	26	33	+
SLM001, SUISUN NR NICHOLS	D8	0.25	-0.65	17	7.2	+
HONKER BAY	D9	0.38	0.29	24	32	+
Mallard-Sl., RSAC075	D10	0.26	-0.75	18	23	+
SHERMAN ISLAND	D11	0.43	0.11	17	34	+
RSAN007	D12	0.33	-0.34	14	35	+
BIG BREAK NR OAKLEY	D14A	0.37	0.33	12	49	+
SJR-JP, RSAN018	D15	0.48	-0.97	12	41	+
RSAN024 TWITCHELL	D16	0.48	-0.45	11	34	+
Sac at Decker	D22	0.37	-1.9	20	28	+
Rio Vista	D24	0.63	0.014	20	3.2	+
SJR AT POTATO PT	D26	0.59	-0.033	8.6	19	+
OLD-R-BACON, ROLD024	D28A	0.46	0.21	6.7	56	+
RSMKL008,LIT-POT-SL-TERM	MD7A	0.56	0.0054	9	13	+
DISAPPOINTMENT SL	MD10	0.11	0.057	9.3	71	+
SJR BUCKLEY COVE	P8	0.24	0.033	8.5	42	+
RMID023	P10A	0.47	0.46	7.2	69	+
ROLD059	P12	0.032	-0.17	18	73	+
		Sum	Sum	Sum	Sum(ABS)	
Sum of Statistics		8.9	-2.9	357	811	

Table 7-4 Mixed-SSC-WARMF boundary conditions simulation for recent years (1991 – 2011). Blue font in the statistics denotes an improved result in comparison with Table 7-3.

Mixed-SSC-WARMF	EMP Location	R ²	NSE	RMSE	PBIAS	Sign Bias
GREENES/HOOD	C3	0.34	-1.5	46	(Missing)	N/A
Mossdale	C7	0.89	0.82	9.4	-21	-
CCFB entrance	C9	0.41	0.17	8.8	55	+
SJR-McCune	C10	0.65	0.65	12	11	+
SAC R Above Point SAC	D4	0.17	-6.7	45	-50	-
SUISUN BAY NR MTZ	D6	0.57	0.44	11	-45	-
GRIZZLY BAY	D7	0.18	-0.39	30	6.2	+
SLM001, SUISUN NR NICHOLS	D8	0.19	-3	28	-36	-
HONKER BAY	D9	0.34	-0.92	27	6.9	+
Mallard-Sl., RSAC075	D10	0.23	-2	22	-15	-
SHERMAN ISLAND	D11	0.3	-0.98	23	0.71	+
RSAN007	D12	0.23	-1.6	18	-7.1	-
BIG BREAK NR OAKLEY	D14A	0.36	-0.29	14	18	+
SJR-JP, RSAN018	D15	0.46	-1.1	15	5.2	+
RSAN024 TWITCHELL	D16	0.48	-1	15	-22	-
Sac at Decker	D22	0.28	-4.4	27	-41	-
Rio Vista	D24	0.55	-1.4	33	-70	-
SJR AT POTATO PT	D26	0.57	-1.8	15	-56	-
OLD-R-BACON, ROLD024	D28A	0.23	-0.92	7.7	27	+
RSMKL008,LIT-POT-SL-TERM	MD7A	0.45	-0.86	13	-34	-
DISAPPOINTMENT SL	MD10	0.1	0.086	9.2	-71	-
SJR BUCKLEY COVE	P8	0.29	0.064	8.3	41	+
RMID023	P10A	0.57	0.41	6	53	+
ROLD059	P12	0.23	0.034	16	66	+
		Sum	Sum	Sum	Sum(ABS)	
Sum of Statistics		9.1	-26.2	459	758	

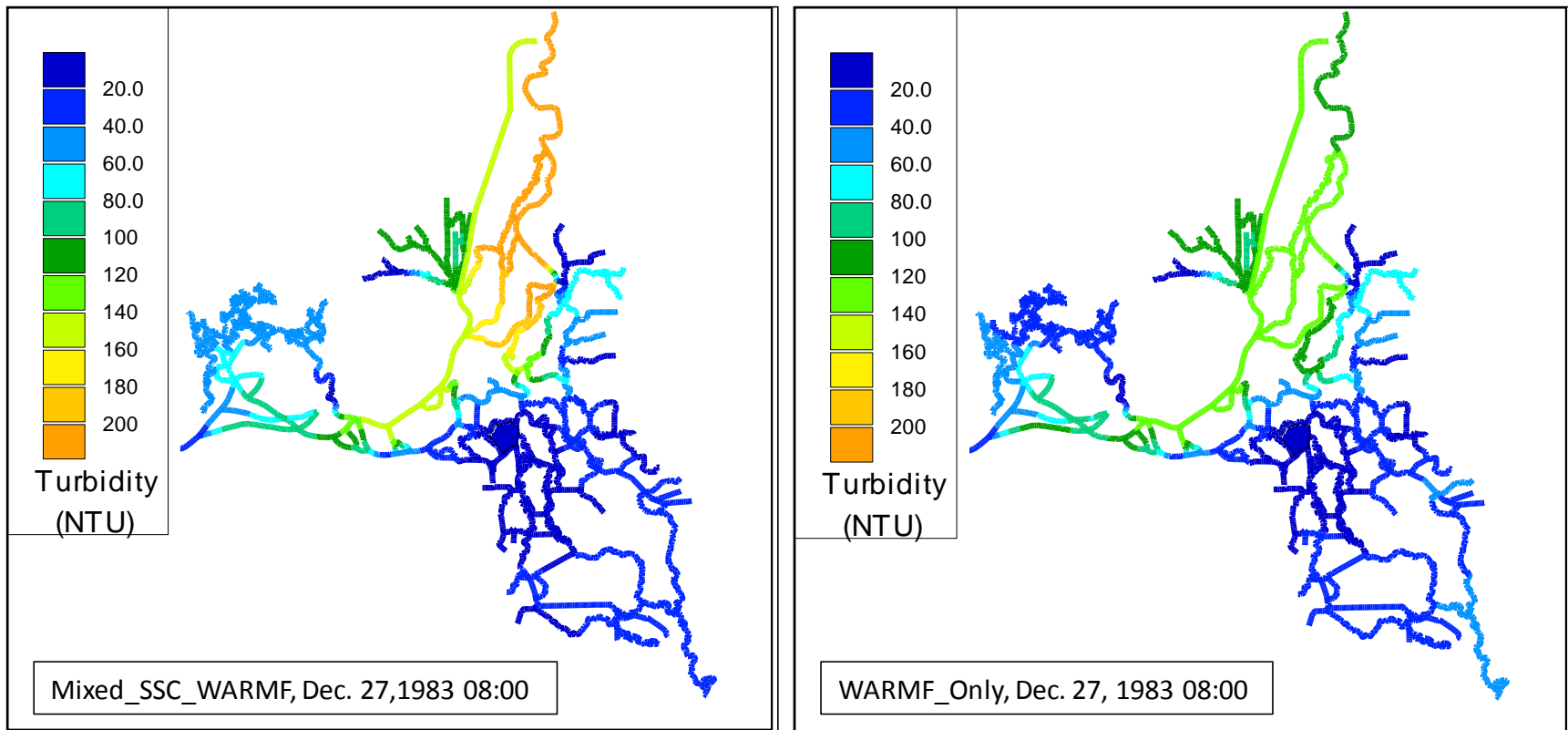


Figure 7-7 Comparison of 15-minute model results on Dec. 27, 1983 at 08:00 with the Mixed-SSC-WARMF and WARMF-Only boundary conditions during a high inflow period.

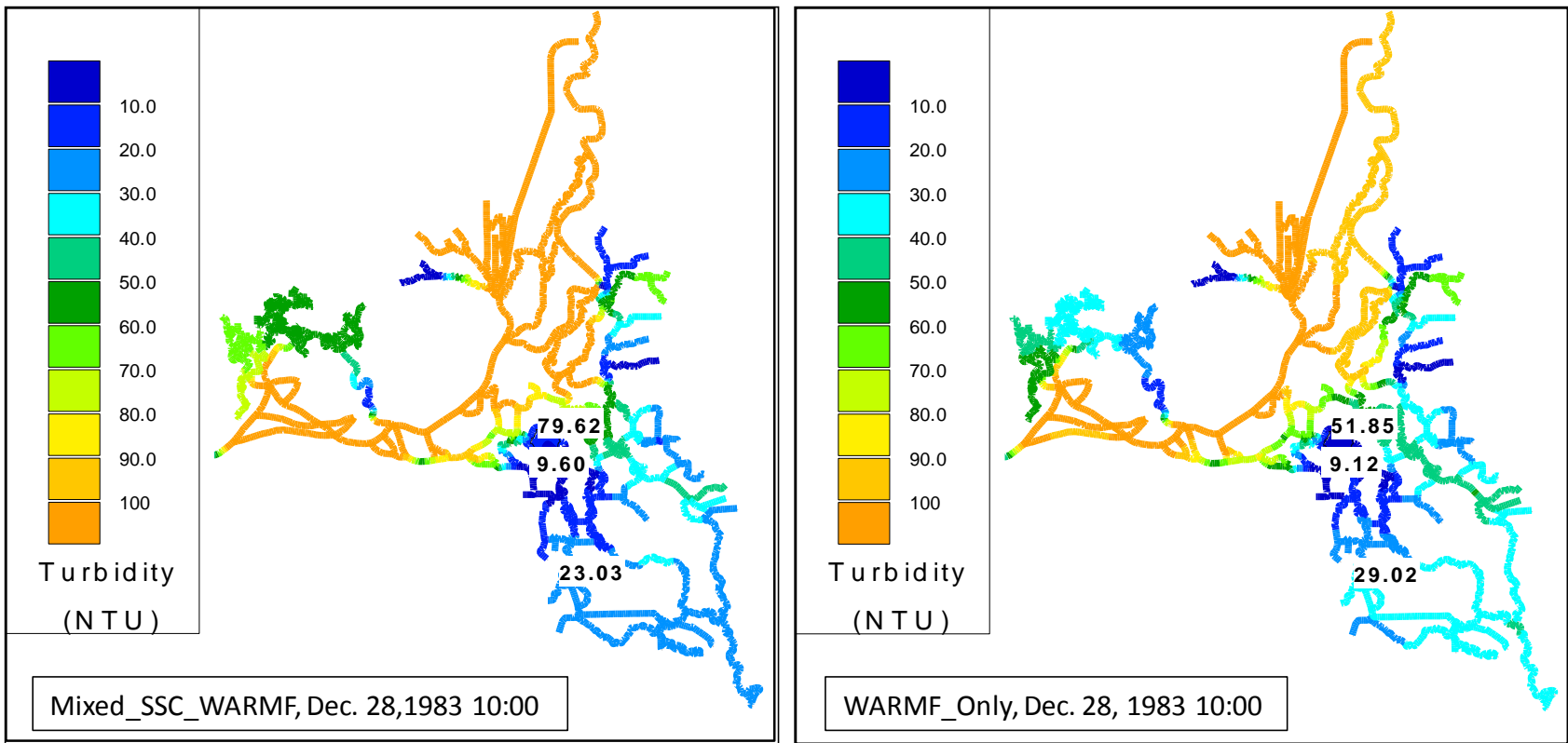


Figure 7-8 Comparison of 15-minute model results on Dec. 28, 1983 at 10:00 at the time of maximum turbidity values at the three compliance locations with the Mixed-SSC-WARMF and WARMF-Only boundary conditions. Note change in scale from previous contour plot.

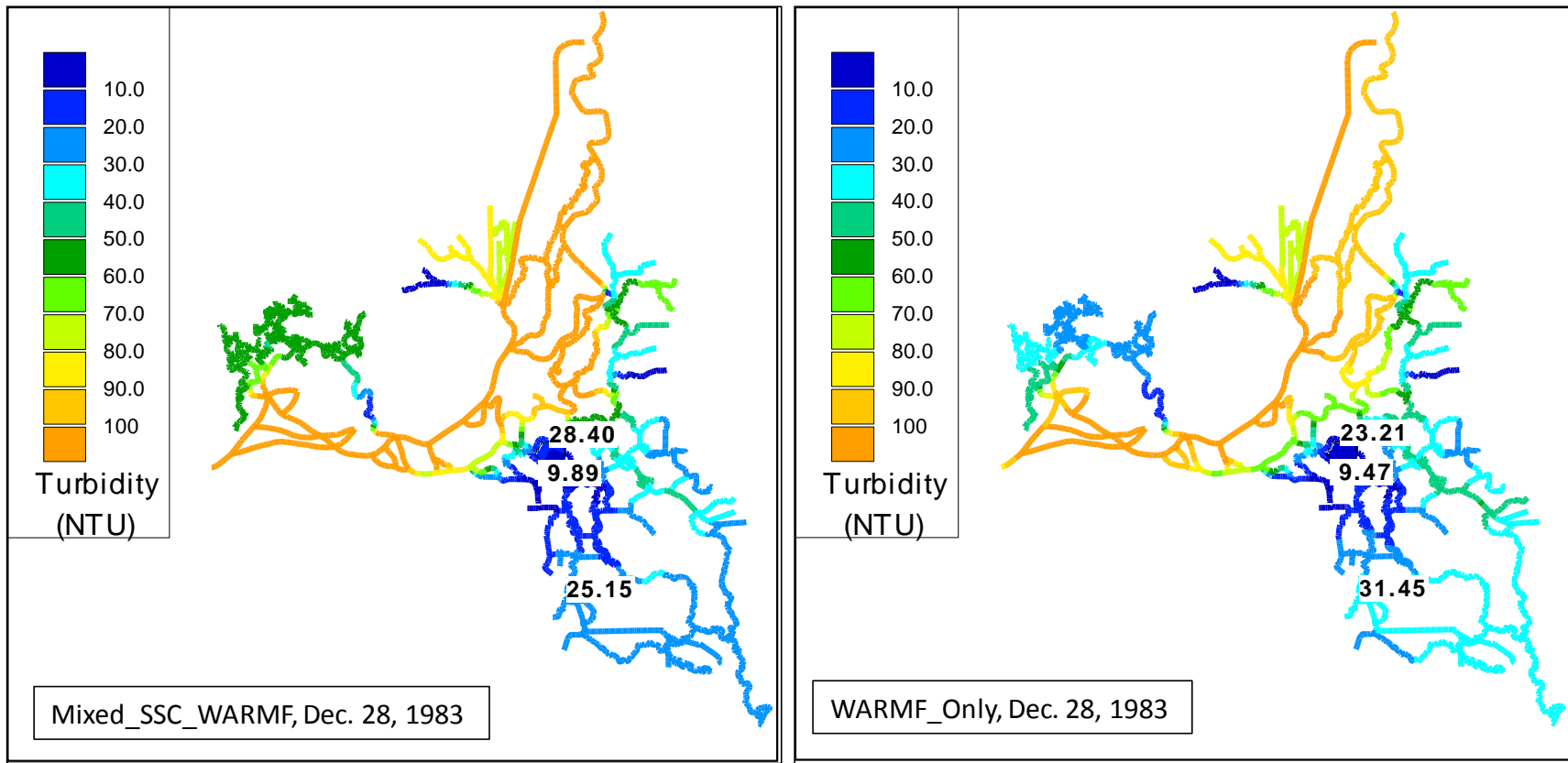


Figure 7-9 Comparison of daily-averaged model results on Dec. 28, 1983 at 10:00 at the time of maximum turbidity values at the three compliance locations with the Mixed-SSC-WARMF and WARMF-Only boundary conditions. Only two of three compliance stations had turbidity values over the maximum of 12 NTU. This day gives the daily maximum at the Victoria Canal location.

8 Formation of South Delta Turbidity Bridge

In this section, model results from the Mixed-SSC-WARMF simulation are used to investigate conditions under which a “turbidity bridge” is formed in the South Delta. Since the condition defining the establishment of a turbidity bridge has not yet been precisely defined, in this report the compliance value of 12 NTU in daily-averaged model output is used as an indicator of bridge formation at selected south Delta locations. The modeled years 1991 – 2000 are used as a basis to investigate bridge formation conditions, in part because in these years model output generally had believable matches for EMP data, particularly for San Joaquin River turbidity (see Figure 4-10). Although many more years were modeled in these long-term historical simulations, since sediment supply in the Delta has been decreasing since 1957, as documented by Wright and Schoellhamer (2004), these modeled years were selected as representing a broad variation in inflow boundary conditions that are more likely representative of current conditions than earlier years.

8.1 Analysis methodology

Modeled boundary conditions for inflows, exports, and turbidity concentration along with modeled OMR (Old+Middle River) flow were surveyed to establish general trends relating modeled turbidity values in the central and south Delta with the boundary conditions in water years 1991 – 2000. Only the high flow/high turbidity periods during the months November to May were included for analysis. Although the period for delta smelt movement generally ends sooner than May, the analysis only considering modeled conditions, not the relationship between turbidity and delta smelt.

During the analysis period, the eastside inflow and turbidity boundary conditions – Calaveras, Mokelumne and Cosumnes Rivers – were deemed to be a minor influence in modeled turbidity, so were not considered further in the analysis.

A turbidity animation using daily-averaged model output was developed for the analysis period and used to identify the establishment of a 12 NTU bridge between the central and south Delta in contour plots. Six locations were chosen to monitor during this period, both in contour plots and as daily-averaged time series – the locations are identified in Figure 8-1 and are shown as numerical turbidity concentrations (NTU) in each of the contour plots and in time series graphs of modeled turbidity. For the purposes of this report, a turbidity bridge was deemed to have formed when a 12 NTU route was established either through Middle River or through Old River linking the turbidity output locations in the central and south Delta. During the high flow/high turbidity period, approximate values or a ranges of values were documented in a table for the most important parameters used in the analysis.

8.2 Results

Table 8-1 and Figure 8-2 through Figure 8-21 summarize the results of the analysis. A turbidity bridge formed in each water year except 1994 and 1999 – these years are highlighted in grey in Table 8-1 along with WY1992 in which their multiple high flow/turbidity events. Several general features linking the years when turbidity bridges formed were identified:

- Very high San Joaquin River inflow (WYs 1995, 1997, 1998 and 2000)
- High Sacramento+Yolo inflow and Sacramento turbidity (WYs 1993, 1995 – 1998)
- Moderate Sacramento+Yolo inflow and moderate to high Sacramento turbidity and negative OMR flow magnitude high (WYs 1991 and 02/1992).

In WYs 04/1992, 1994 and 1999 when turbidity bridges did NOT form, San Joaquin inflow and turbidity were low, and exports and negative OMR flow were low at least periodically during the highest flow and turbidity periods investigated. Sacramento+Yolo inflow was also low during at least part of the period.

During several of the years, high turbidity originating on the Sacramento side first intruded down Old River, forming the bridge initially along that route. As the simulation progressed, the bridge eventually formed on Middle River (see, for example February in WY1992, Figure 8-4). When San Joaquin river inflow and turbidity was dominant source for forming the bridge, turbidity tended to travel into the central Delta through Middle River to form the bridge along that route, although a bridge eventually also formed in Old River (see WY1995 in March, Figure 8-11).

8.3 Summary of turbidity bridge analysis

It should be noted that this analysis is based on a turbidity model developed with synthetic or externally calculated (*i.e.*, from WARMF results) boundary conditions, so some skepticism is warranted when interpreting results. However, results suggest further data analyses could be beneficial to see if the modeled results showing preferred routes through Old River or Middle River depending on the dominant source of turbidity hold true for similar conditions in modeled scenarios. In general, the analysis shows that there are several modes under which a turbidity bridge is likely to form, which depend on the relative magnitudes of the Sacramento and San Joaquin River inflows and on the magnitude of the negative OMR flow.

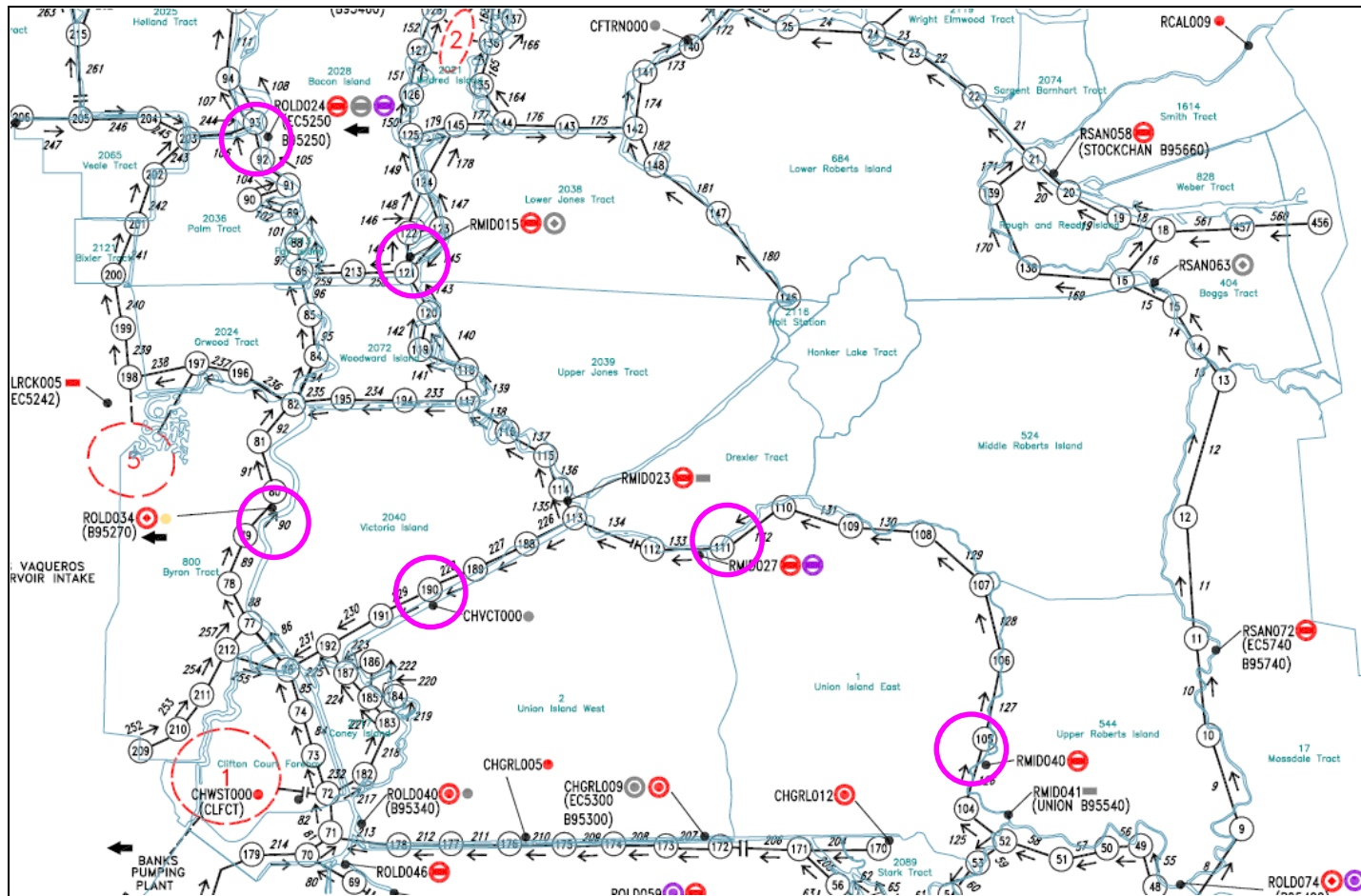


Figure 8-1 Locations used to investigate the formation of a turbidity bridge in the south Delta illustrated in the DSM2 grid.

Table 8-1 Approximate values for important flow and turbidity locations in the DSM2 model during the high flow/high turbidity periods WY1991 to WY2000. Shaded lines indicate high flow period when a turbidity bridge did not form.

	Peak Sac+Yolo Flow (CFS)	Peak Sac (NTU)	Peak SJR Flow (CFS)	Peak SJR (NTU)	OMR (CFS)	SWP+CVP (CFS)
March 1991	> 46,000	> 400	> 3800	> 90	< -8000	> 10,000
February 1992	~ 50,000	> 670	~ 5000	> 140	~ -6000	> 10,000
March/April 1992	~ 33,000	> 200	< 2000	> 90	< -8000	> 10,000
January 1993	~ 80,000	> 380	> 9300	> 200	~ -6000 to -8000	8000 to > 14000
January 1994	< 30,000	< 125	< 2600	~ 80	~ -3000 to -6000	3400 to 10,000
January 1995	> 95,000	> 570	> 11,000	> 300	~ -7000	10000 to 12000
March 1995	~ 100,000	>100	> 25,000	> 210	~ 4500 to 9000	0 to 5000
January/Feb. 1996	~ 88,000	> 800	~ 2300 to 16,000	> 80	~ -7800 to 3400	~ 4700 to 11,000
Dec./January 1997	> 110,200	> 410	> 53,000	> 100	~ 20,000	~ 3700 to 10,400
January/Feb. 1998	> 94,000	> 440	> 35,000	> 160	0 - 13,000	800 to 4000
Dec./January 1999	~ 67,000	~ 200	~ 2700 to 4700	< 50	~ -4000 to 0	2000 to 7100
Jan./February 2000	> 87,000	~ 250	> 14,000	> 130	< -8500	7000 to 13,000

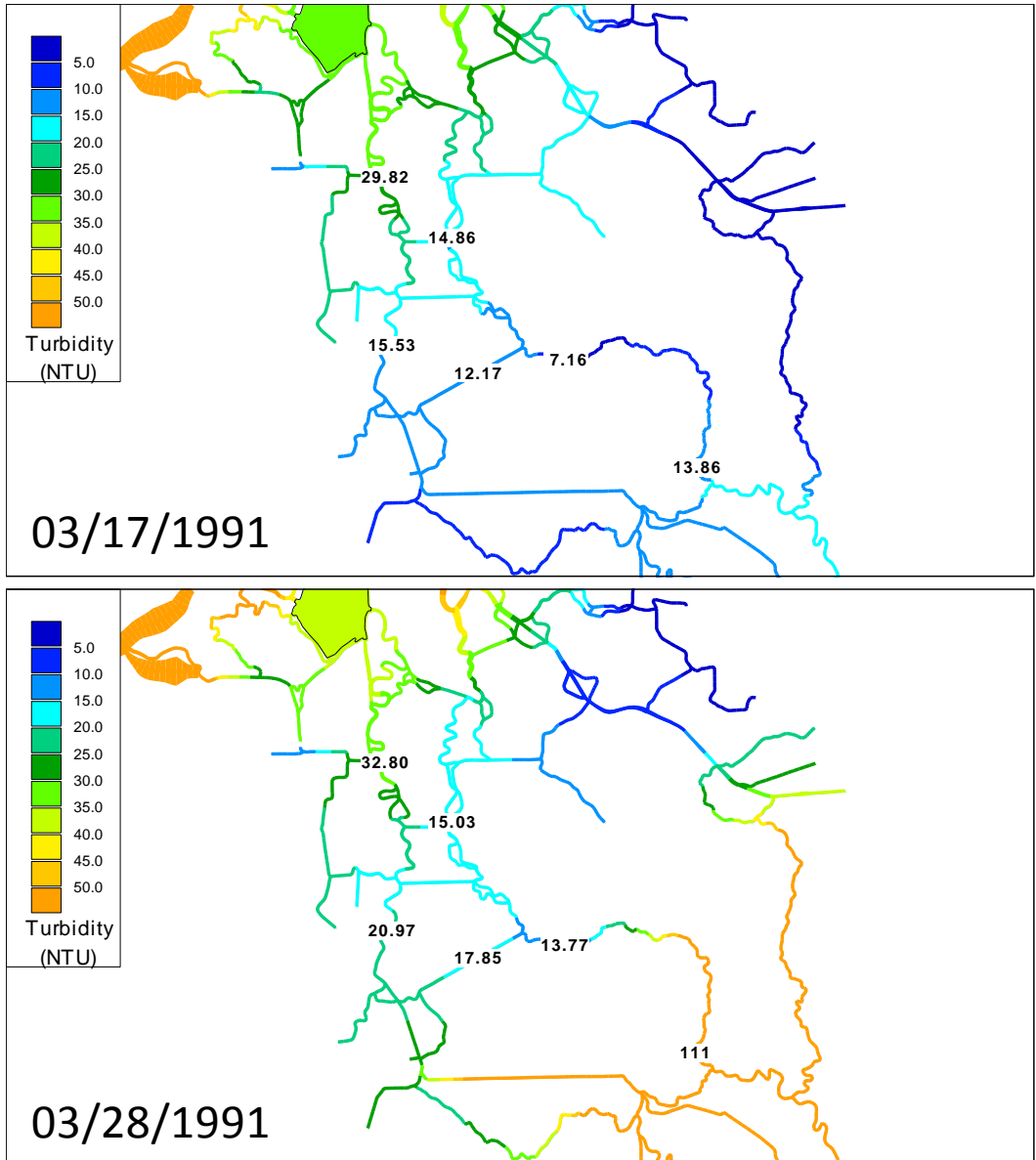


Figure 8-2 Turbidity initially intrudes from Sacramento inflow down Old and Middle Rivers - San Joaquin turbidity later influences the south Delta in WY1991.

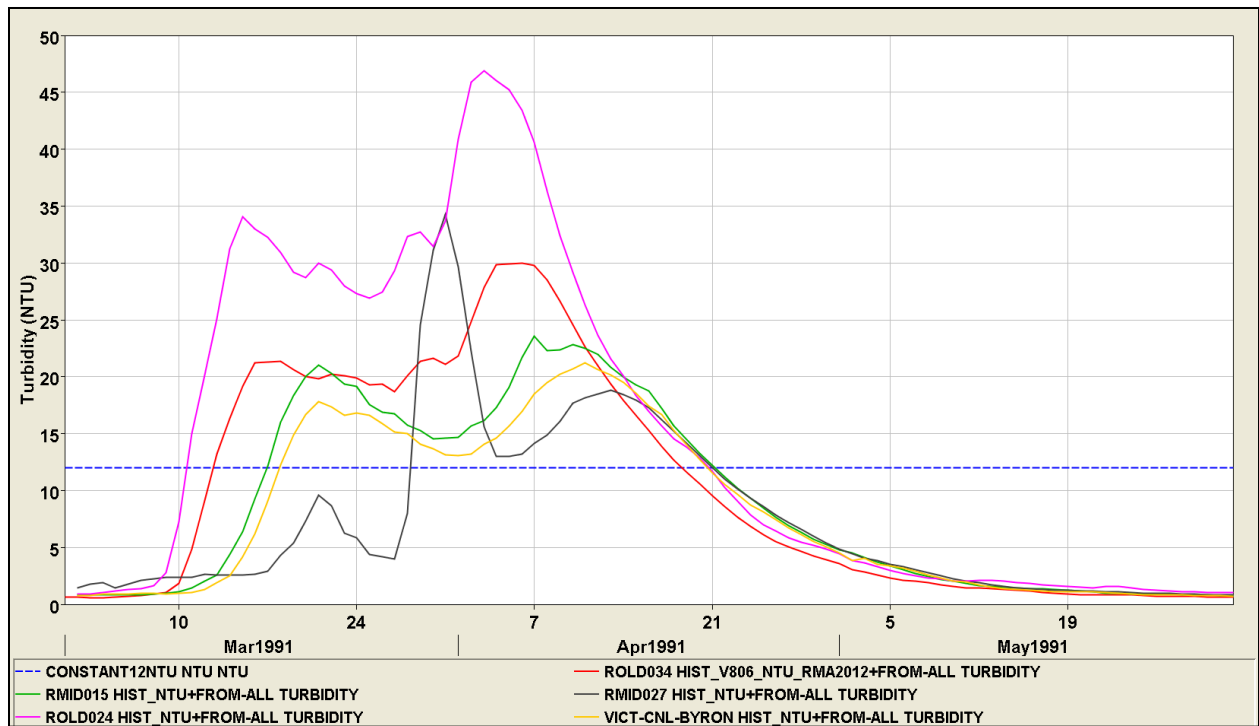


Figure 8-3 Daily-averaged turbidity time series during the formation of the turbidity bridge in WY1991. The blue dashed line is the 12 NTU compliance value.

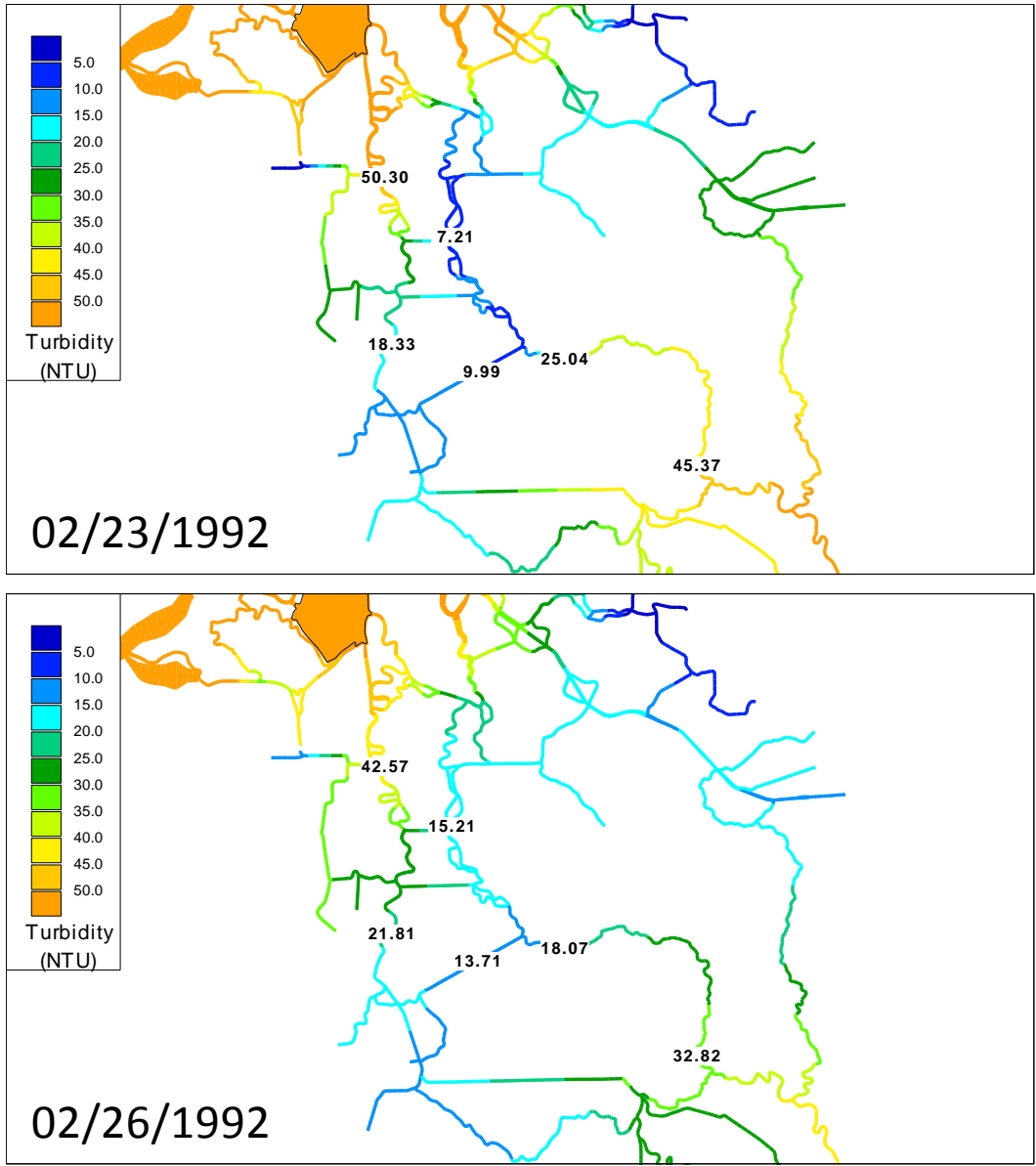


Figure 8-4 Turbidity initially intrudes from Sacramento inflow down Old River along intrusion in the south from San Joaquin turbidity – Middle River turbidity later increases above 12 NTU in February of WY1992.

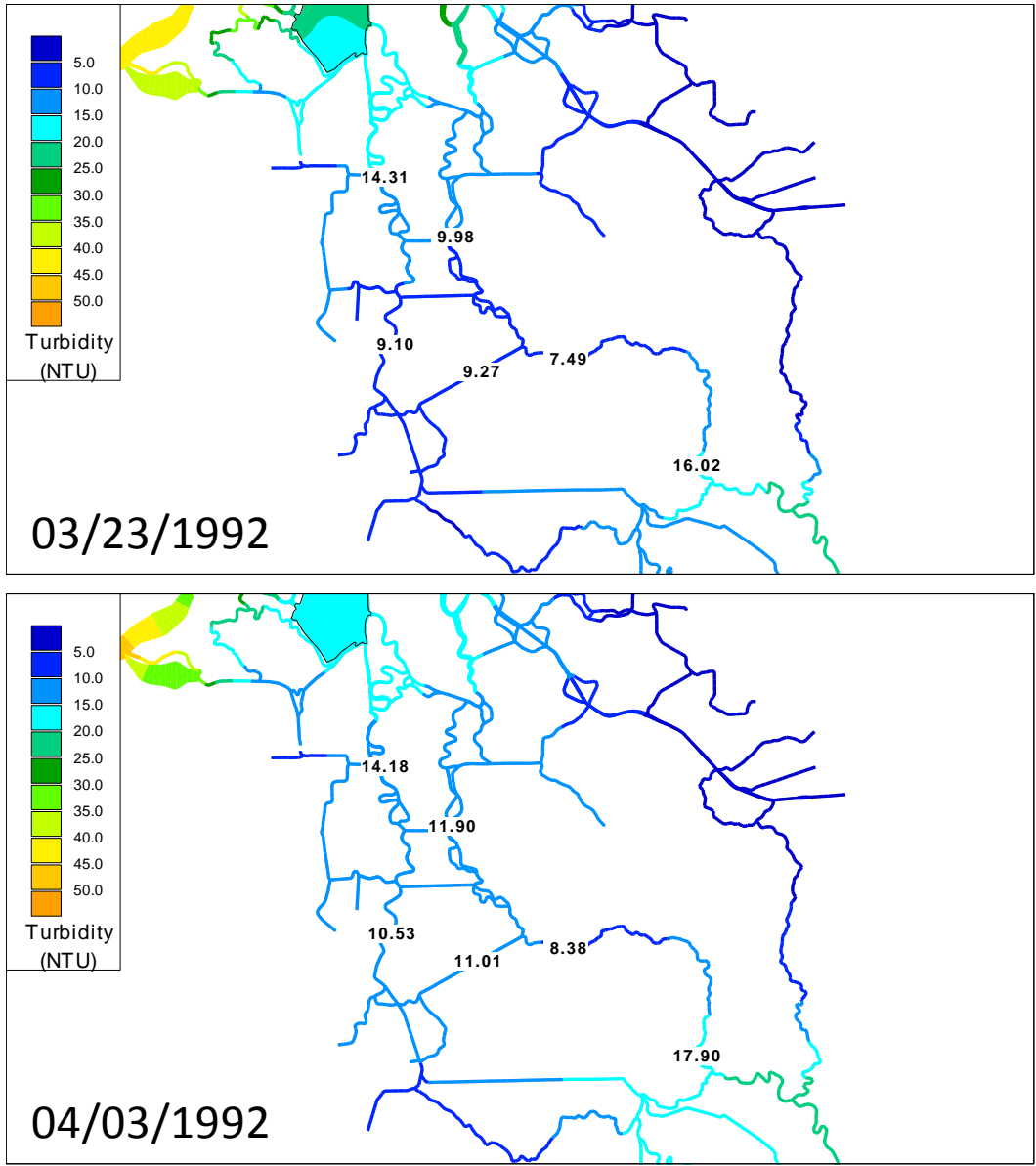


Figure 8-5 Turbidity intrudes from Sacramento inflow down Old and Middle Rivers along with some San Joaquin turbidity in the south, but a turbidity bridge never forms in March/April of WY1992.

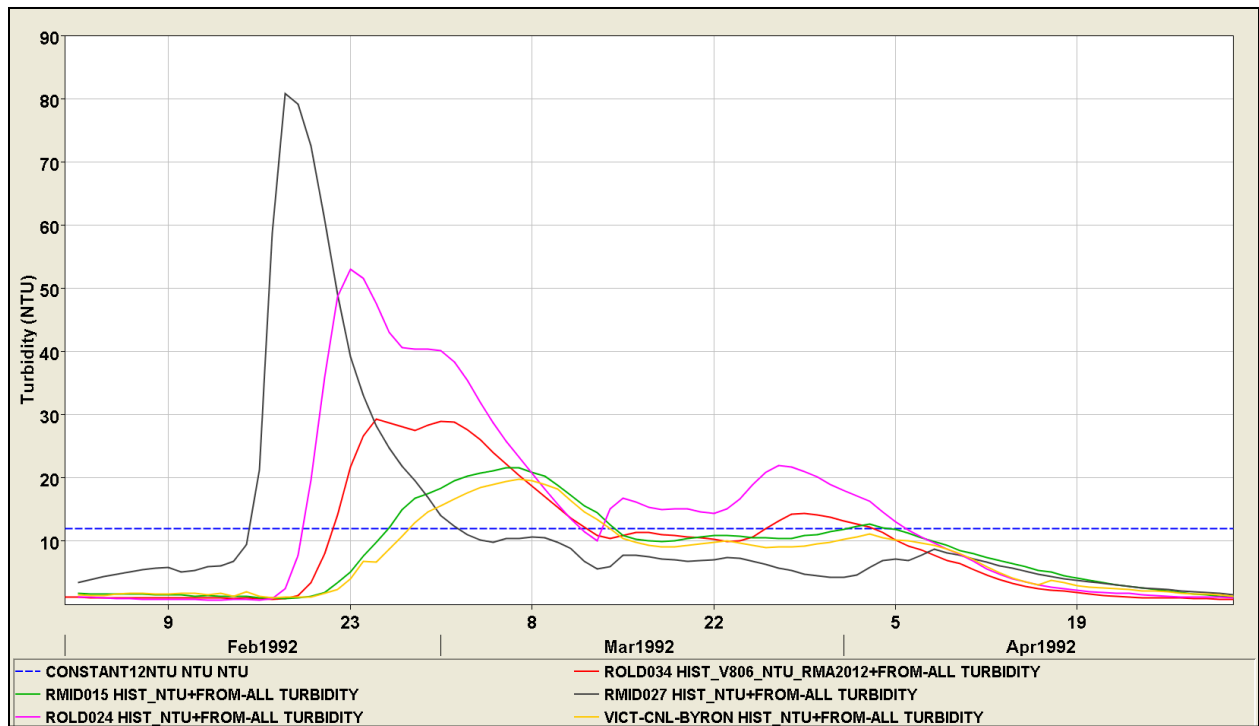


Figure 8-6 Daily-averaged turbidity time series during the formation of the turbidity bridge in WY1992. The blue dashed line is the 12 NTU compliance value.

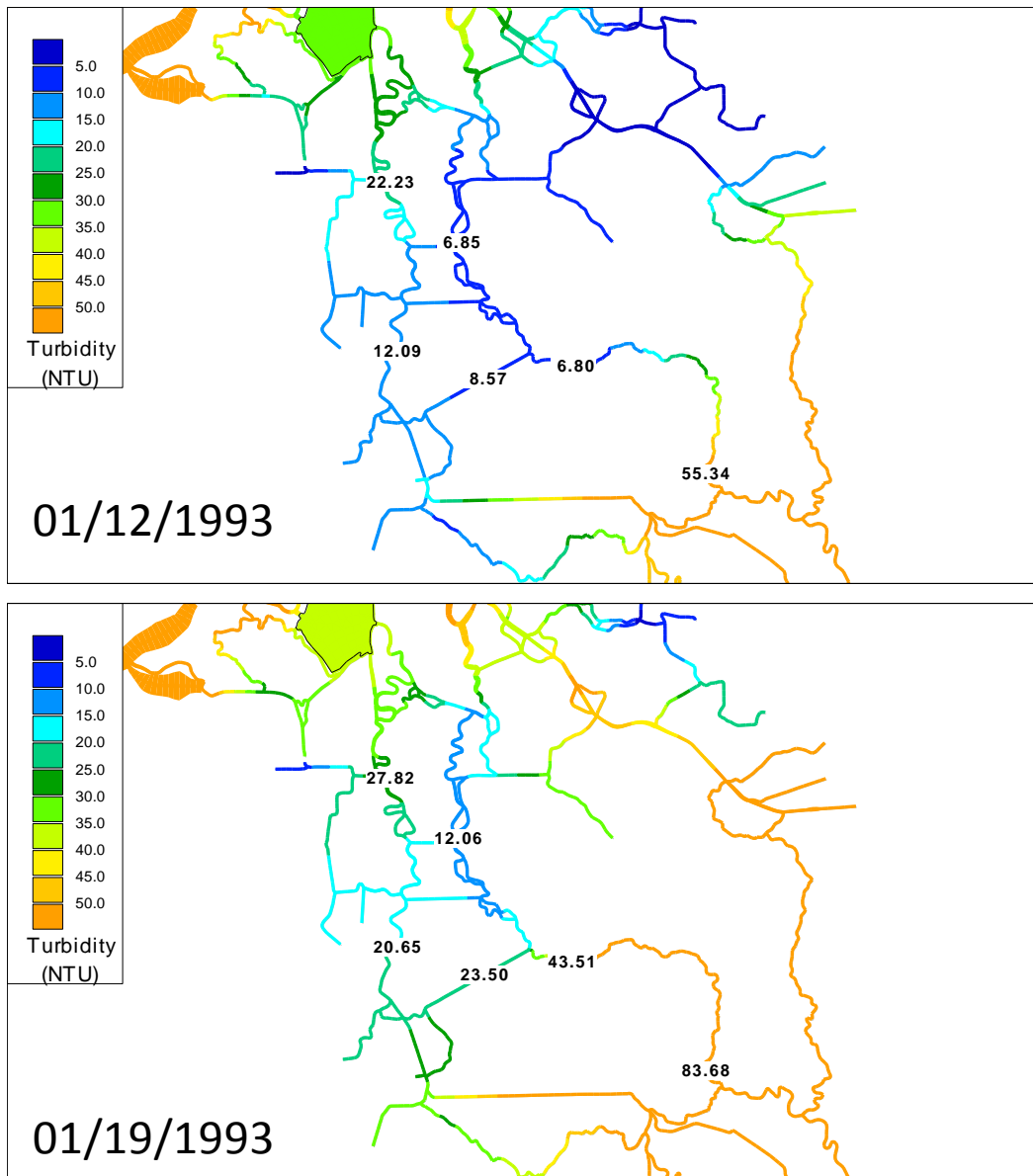


Figure 8-7 Turbidity initially intrudes from Sacramento inflow down Old River along intrusion in the south from San Joaquin turbidity – Middle River turbidity later increases above 12 NTU in January of WY1993.

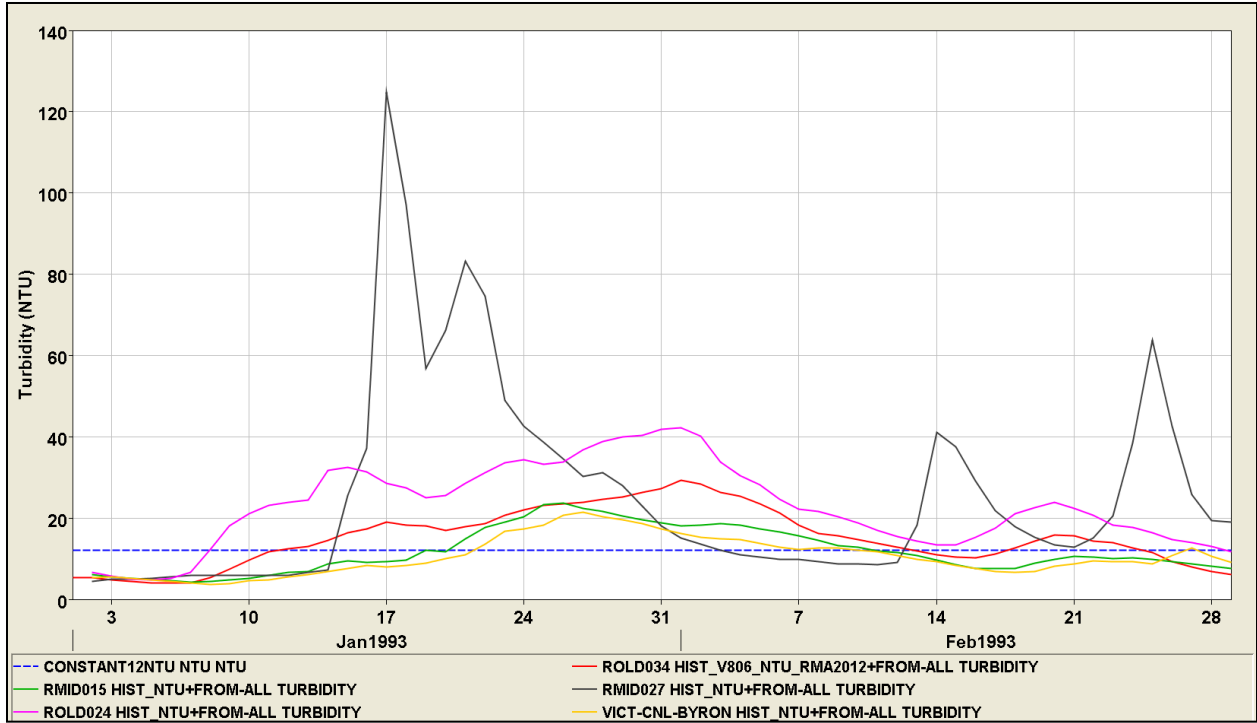


Figure 8-8 Daily-averaged turbidity time series during the formation of the turbidity bridge in WY1993. The blue dashed line is the 12 NTU compliance value.

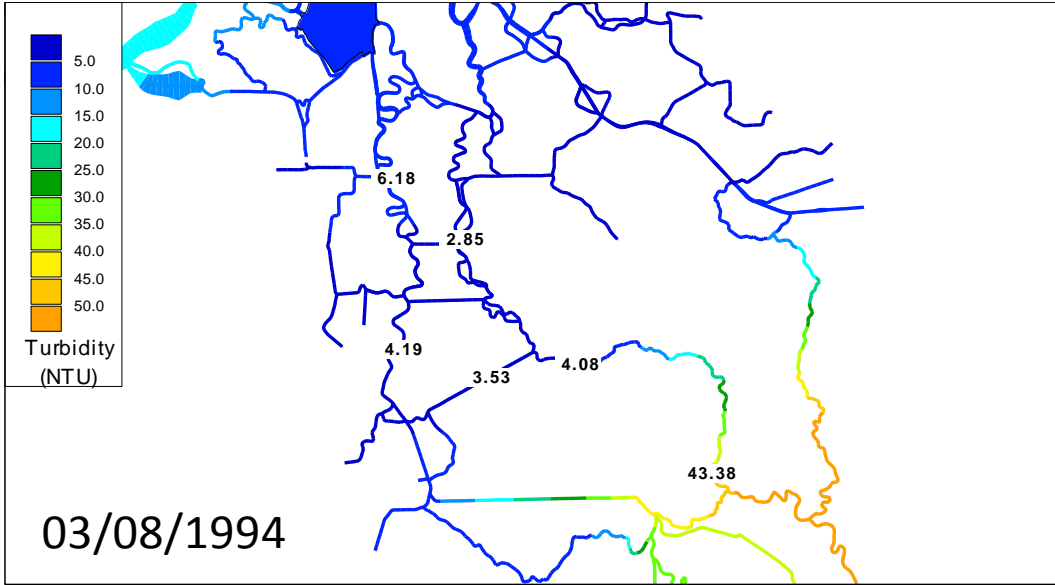


Figure 8-9 A turbidity bridge never forms in WY1994.

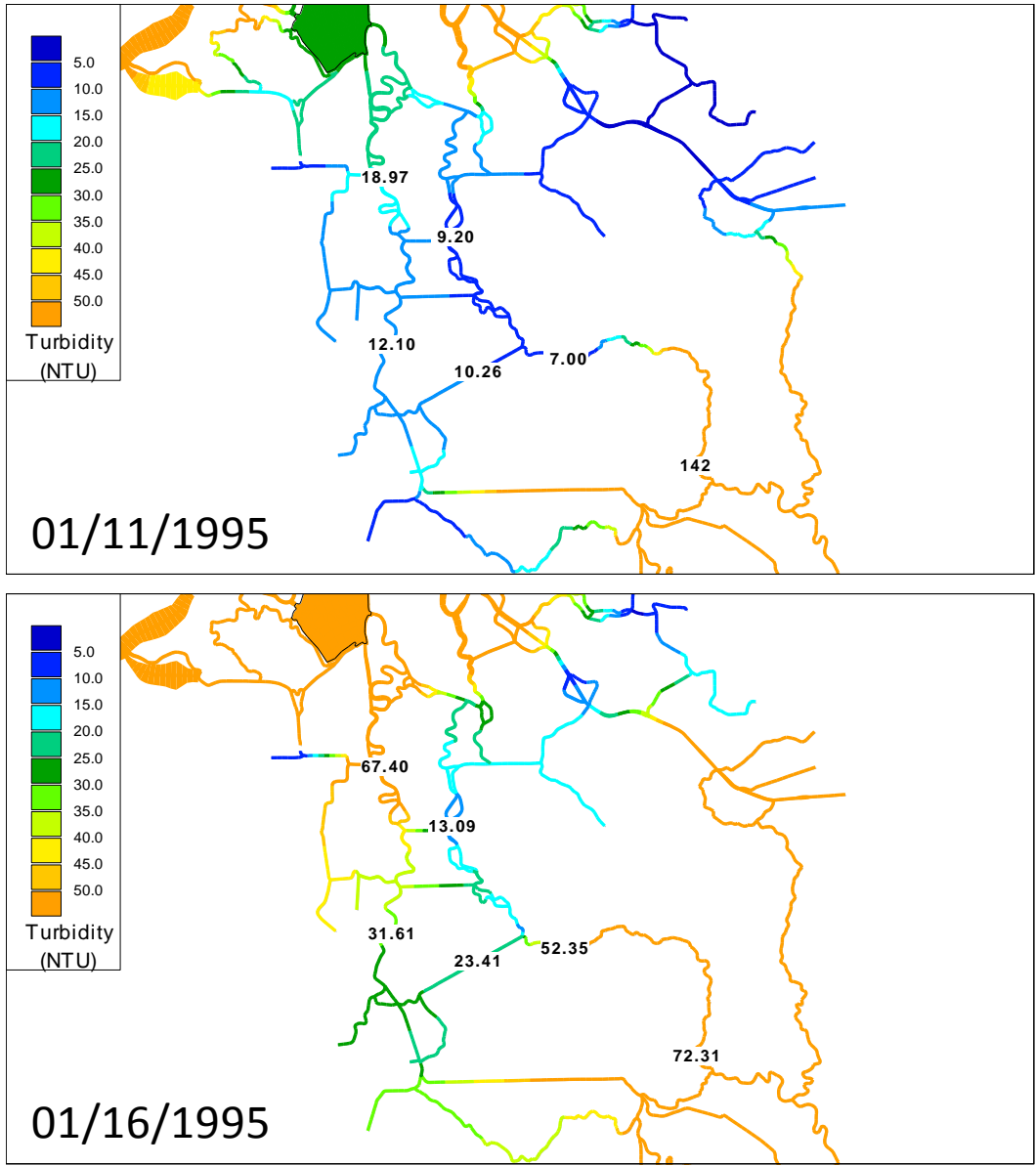


Figure 8-10 Turbidity initially intrudes from Sacramento inflow down Old River along intrusion in the south from San Joaquin turbidity – Middle River turbidity later increases above 12 NTU in January of WY1995.

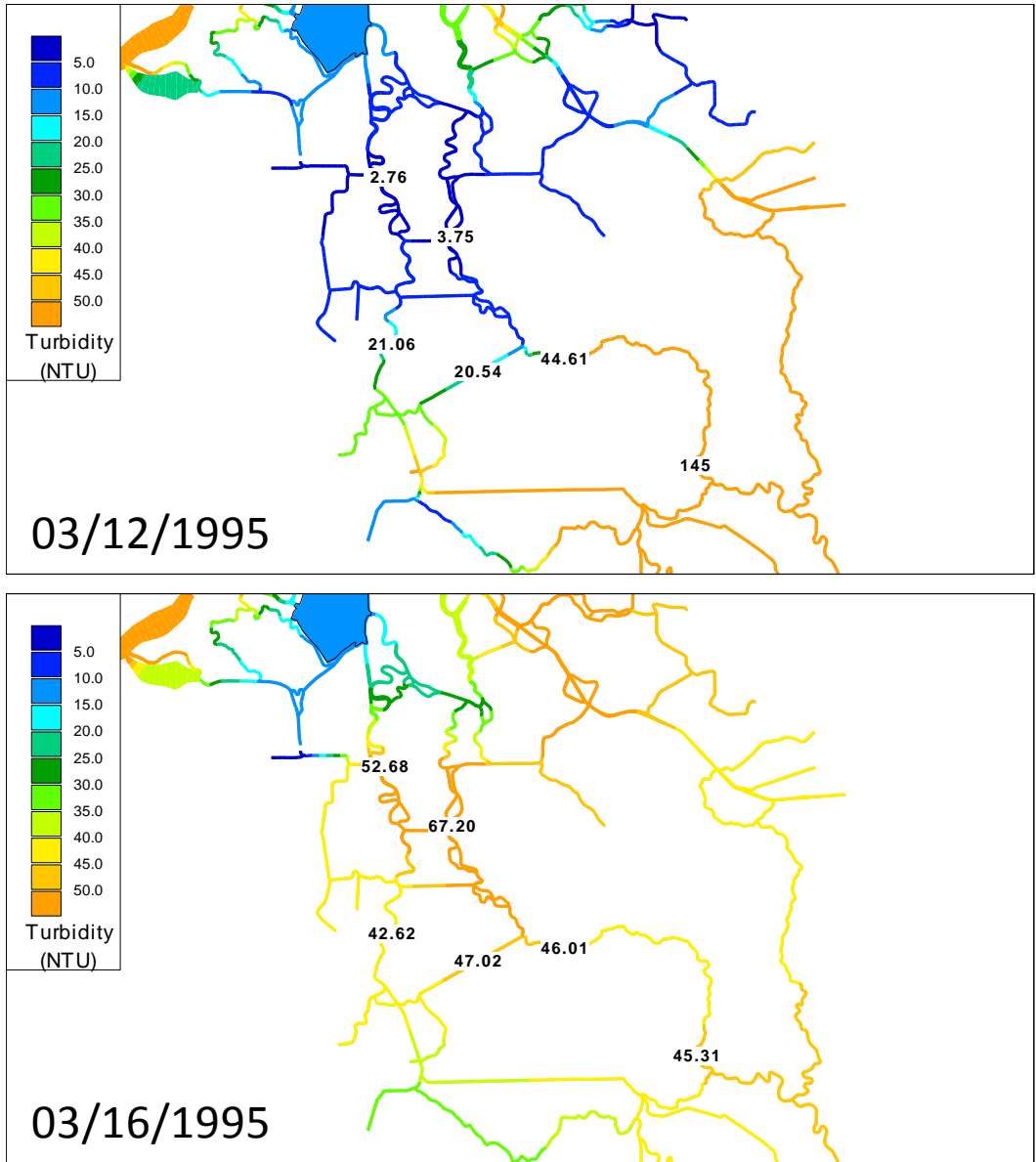


Figure 8-11 A second turbidity bridge forms in March of WY1995 primarily due to intrusion in the south from San Joaquin turbidity – turbidity increased primarily along Middle River as it flows out of the Delta.

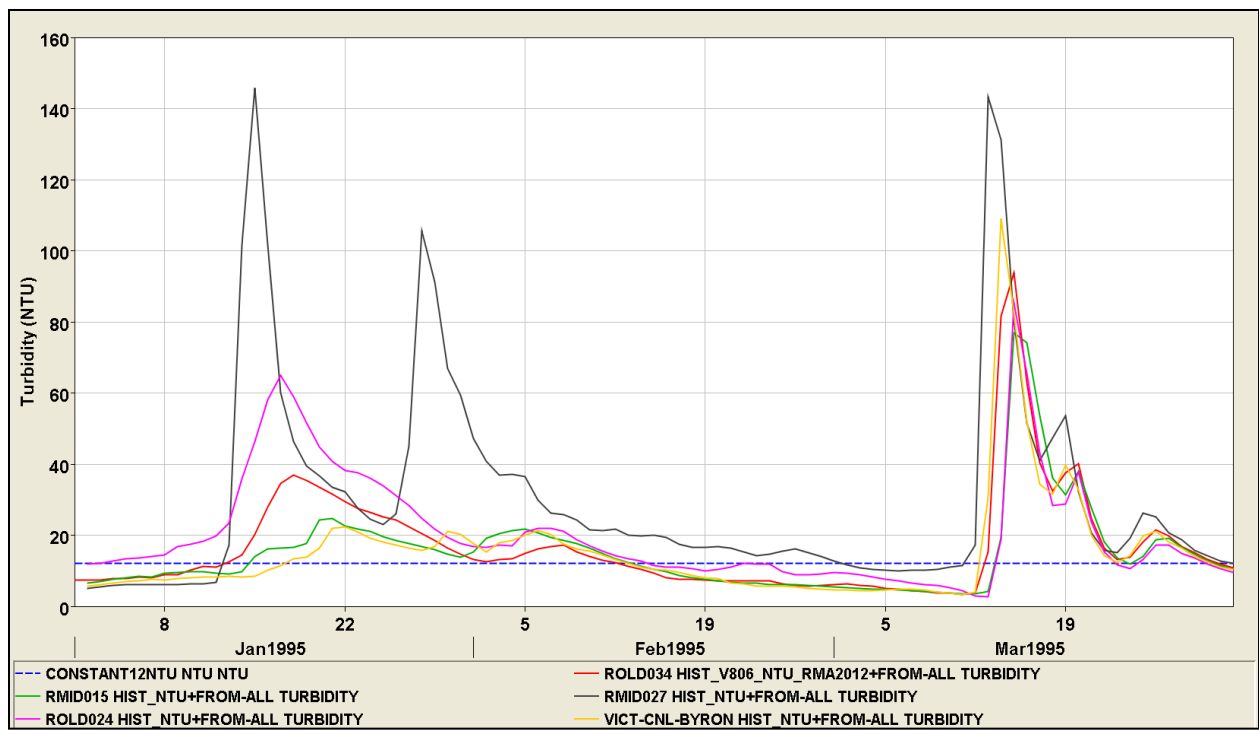


Figure 8-12 Daily-averaged turbidity time series during the formation of the turbidity bridge in WY1995. The blue dashed line is the 12 NTU compliance value.

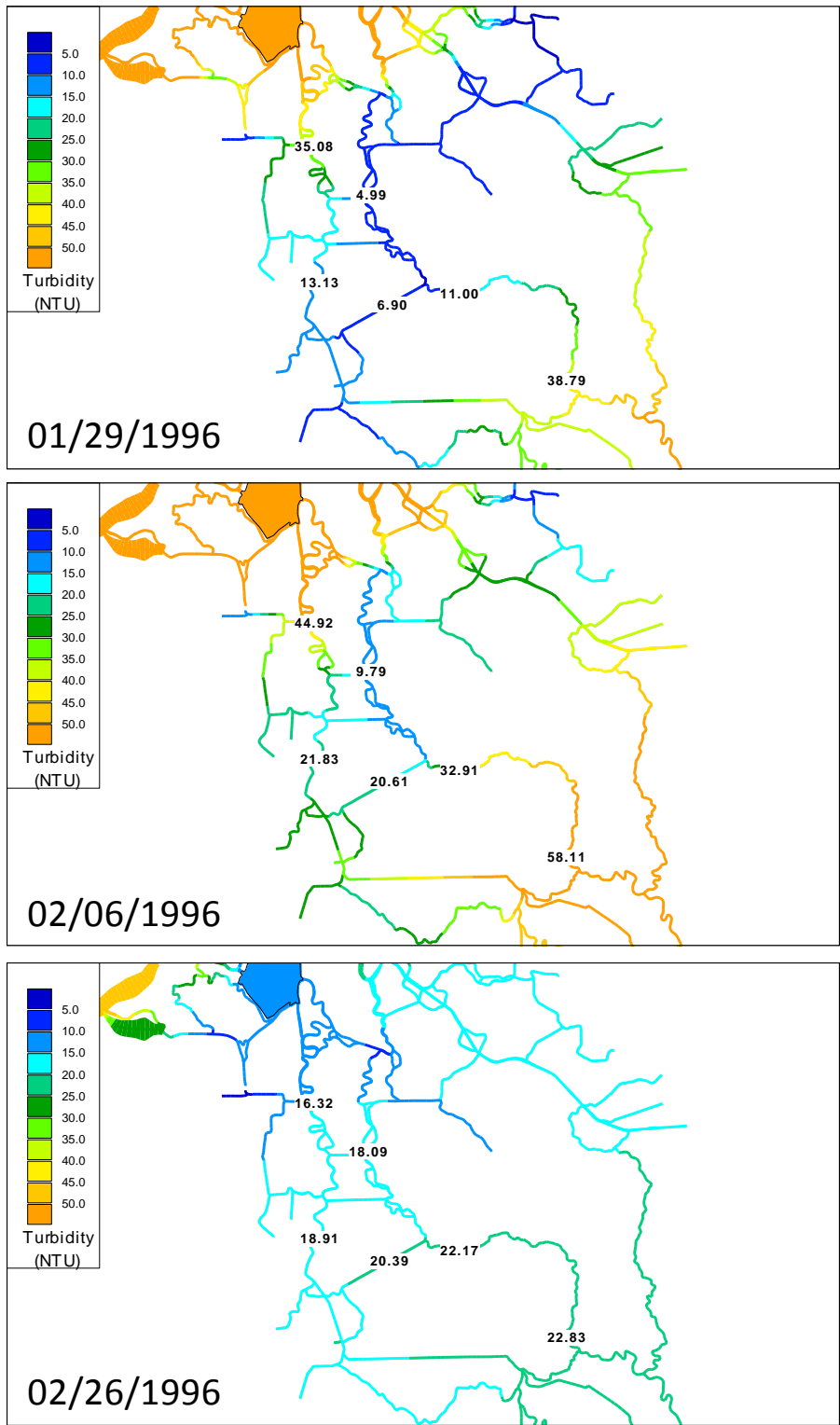


Figure 8-13 Turbidity initially intrudes from Sacramento inflow down Old River along intrusion in the south from San Joaquin turbidity – Middle River turbidity much later increases above 12 NTU in February of WY1996.

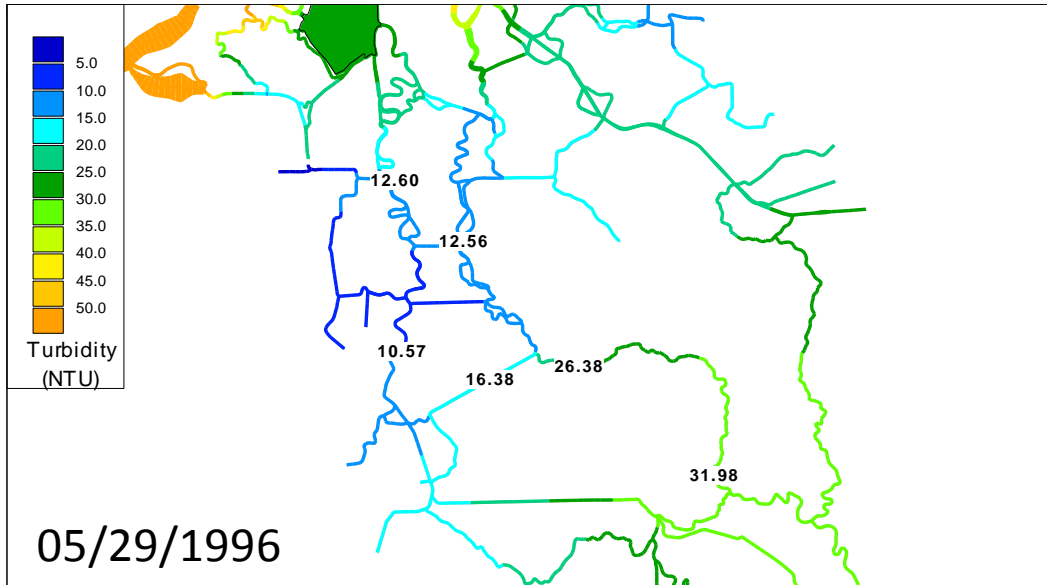


Figure 8-14 Turbidity increases above the 12 NTU level in the south Delta and along Middle River in May of WY1996.

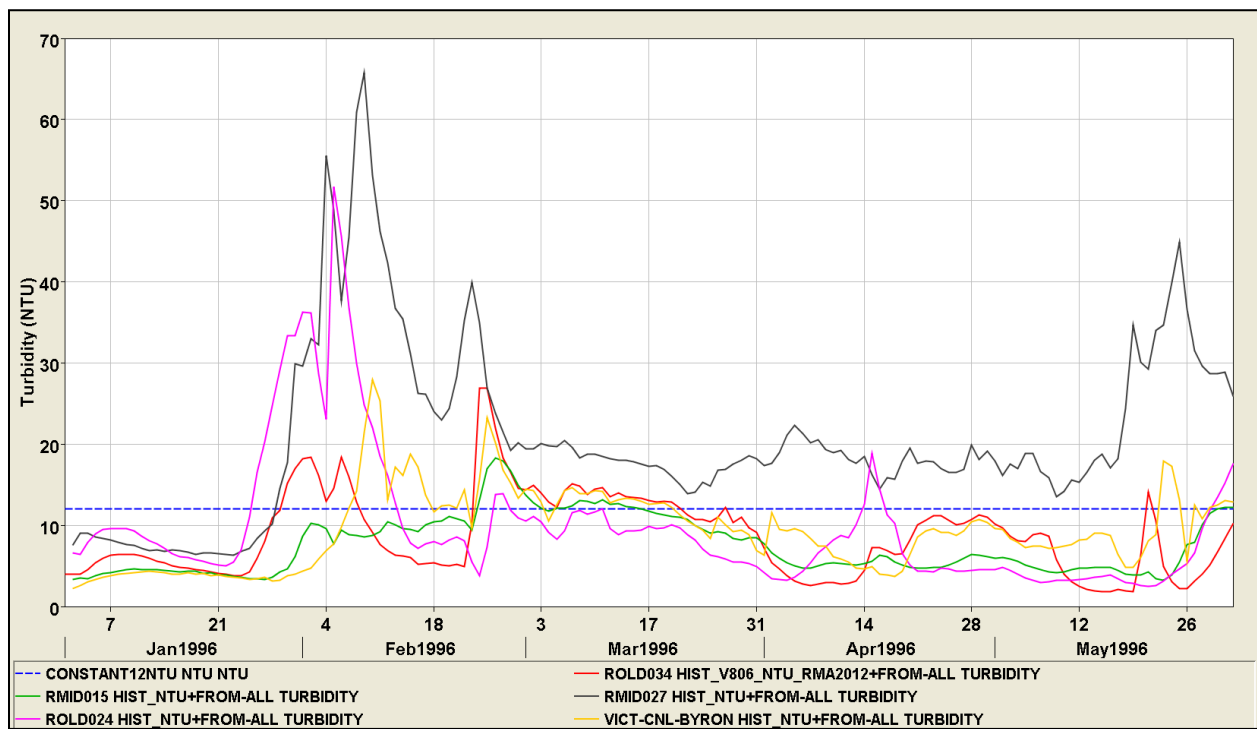


Figure 8-15 Daily-averaged turbidity time series during the formation of the turbidity bridge in WY1996. The blue dashed line is the 12 NTU compliance value.

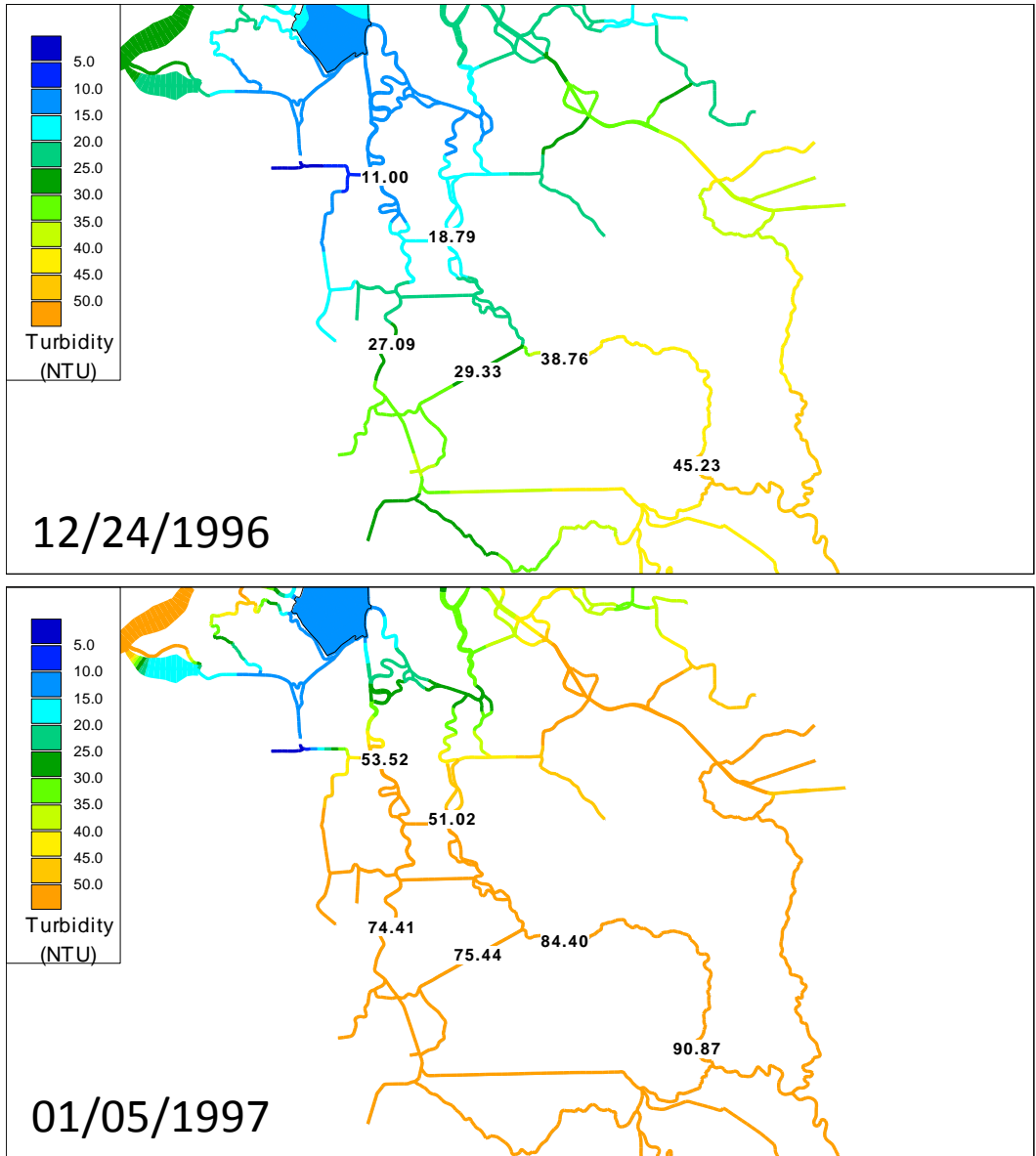


Figure 8-16 Turbidity initially intrudes from the south Delta northward due to high turbidity from San Joaquin inflow - in this case the bridge forms up Middle river in the lower San Joaquin in January of WY1997.

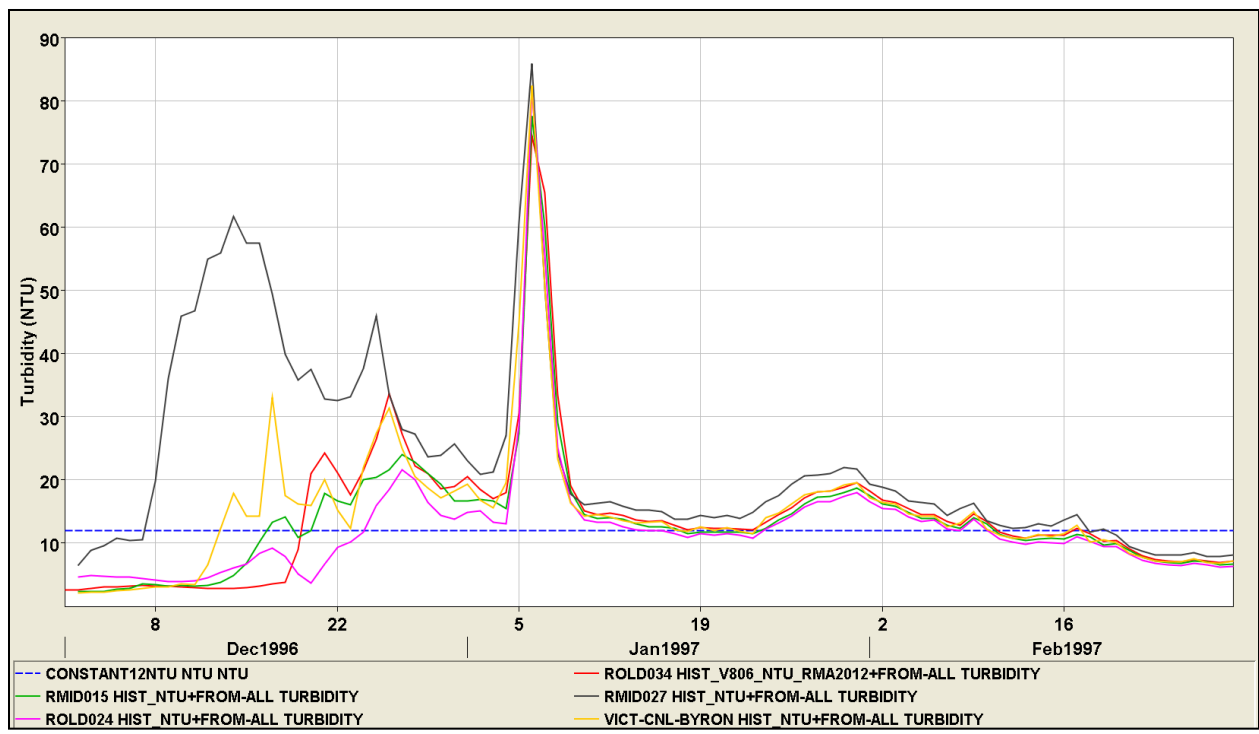


Figure 8-17 Daily-averaged turbidity time series during the formation of the turbidity bridge in WY1997. The blue dashed line is the 12 NTU compliance value.

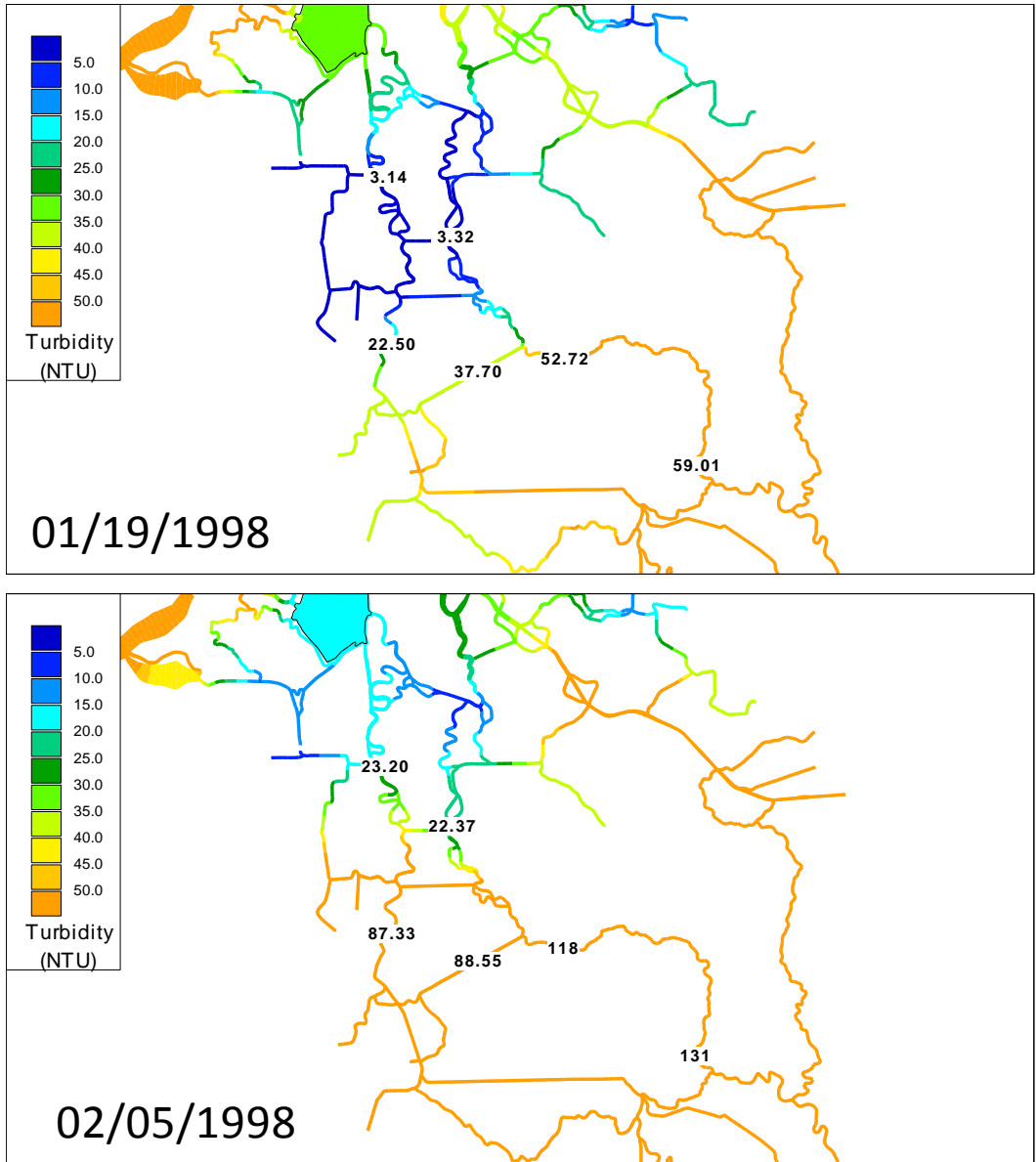


Figure 8-18 Turbidity initially intrudes from San Joaquin inflow northward in January, with the turbidity bridge forming as Sacramento turbidity flows into the central Delta in February of WY1998.

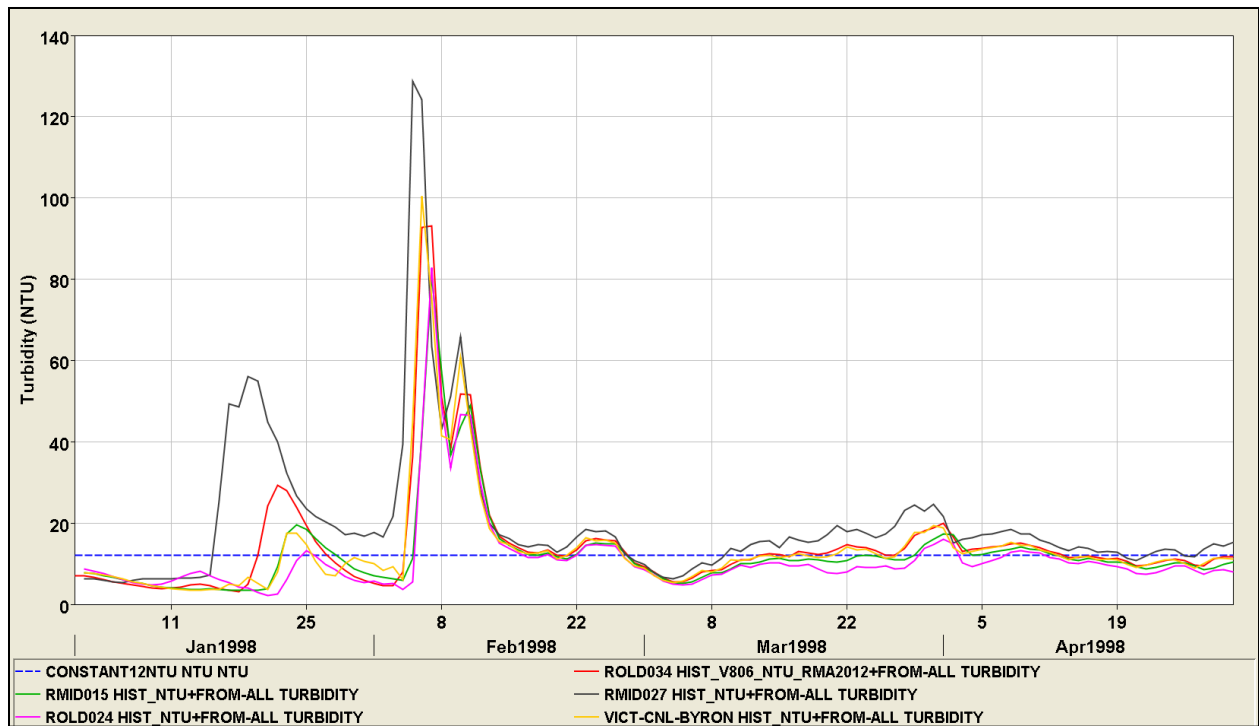


Figure 8-19 Daily-averaged turbidity time series during the formation of the turbidity bridge in WY1998. The blue dashed line is the 12 NTU compliance value.

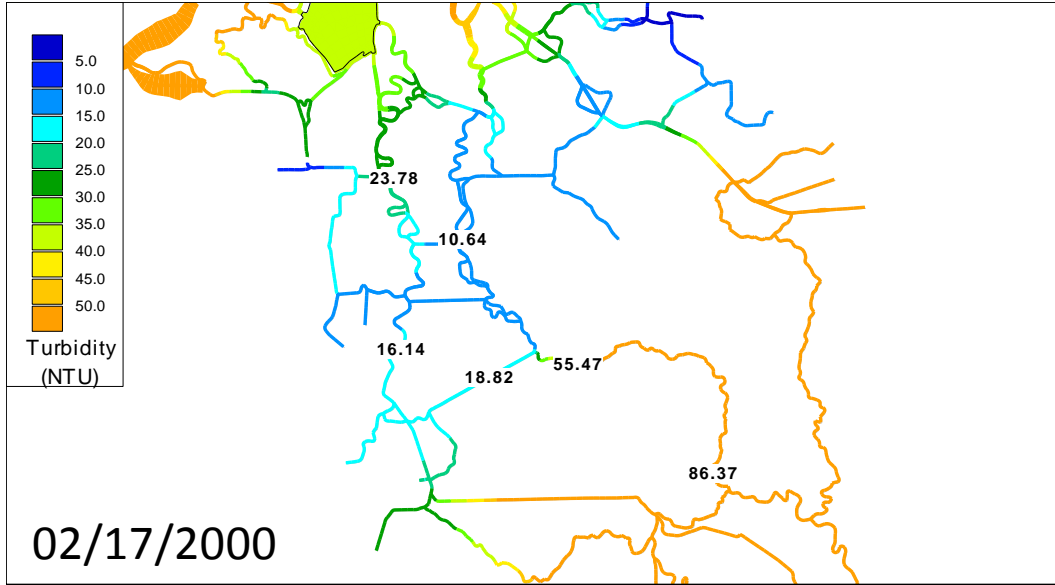


Figure 8-20 Turbidity initially intrudes from both Sacramento and San Joaquin River inflows forming a turbidity bridge initially along Old River in February of WY2000.

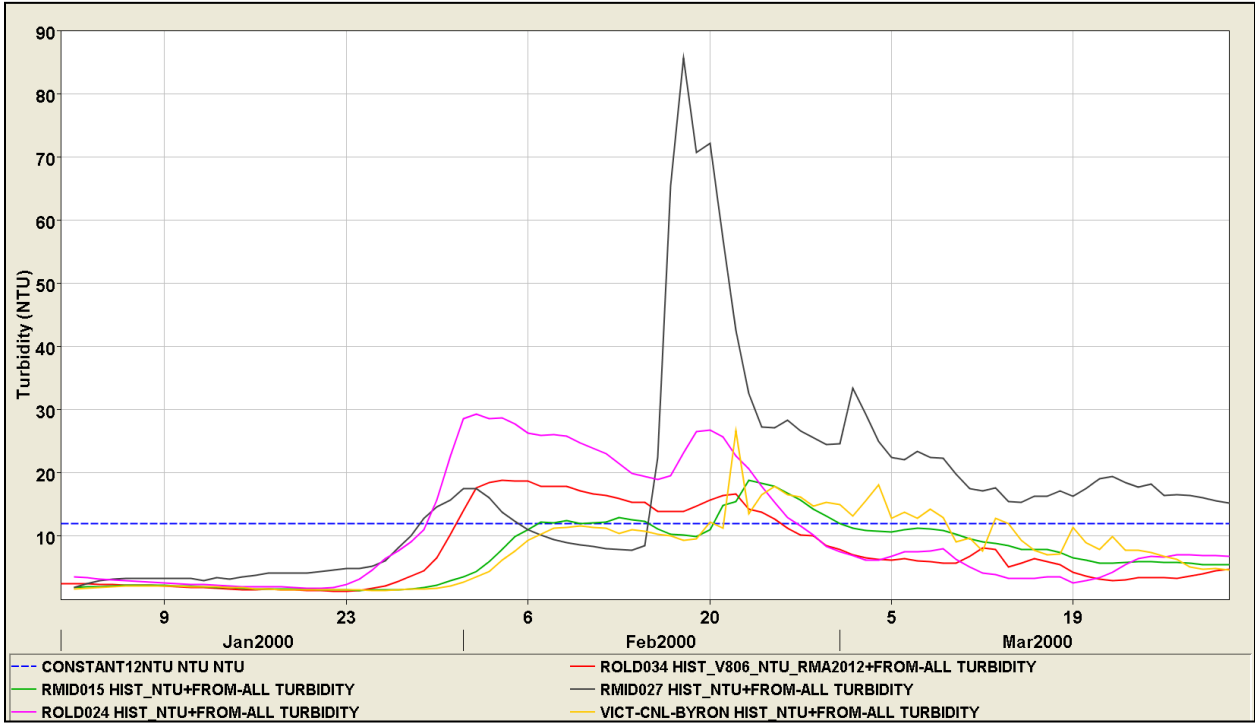


Figure 8-21 Daily-averaged turbidity time series during the formation of the turbidity bridge in WY2000. The blue dashed line is the 12 NTU compliance value.

9 Summary and Conclusions

As described in previous sections of this report, the model results described herein support two main objectives: updating and refining the QUAL turbidity transport model application; and, developing a long-term (1975 – 2011) turbidity simulation by defining a set of synthetic (*i.e.*, not based on turbidity data) turbidity boundary conditions to support training of a Turbidity ANN. To document the accomplishment of these two objectives, statistical measures were employed to quantify the success of the modeling efforts. Metrics were defined to quantify “model skill”, *i.e.*, information to aid in appropriate model application with a focus on decision support. In this application, the decision support objective was realized with a focus on maximizing model skill (*i.e.*, minimizing model error) at the three in-Delta turbidity compliance locations - at Holland Cut, Prisoner Point and Victoria Canal at Byron – as turbidity levels at these locations have the potential to influence decisions changing Delta operations.

The QUAL turbidity model calibration was refined using data available during the wet seasons of WY2010 and WY2011. After iterative calibration simulation tests, it was found that further fine-tuning of the decay constants or refinement of the original DMS parameter regions did not produce better overall statistics, so the final set of rate constants and regions represent a condition in which data location-specific model statistics for any year did not improve significantly at the data locations with an emphasis on the three compliance locations in comparison with previous simulations or in comparison with the earlier DMS calibration. As can be seen in Table 5-1 through Table 5-5 the residual statistics and the calibration metrics for the turbidity model calibration for these two wet seasons are quite different.

Minimizing the magnitude of the model bias, whether positive or negative, was given a priority over improving other statistics, as mentioned in Section 5.1 without sacrificing the quality of the other statistics. Particular attention was paid to the three compliance locations and the model bias at these locations due to their importance to the Delta Smelt Working Group and their ability to influence Delta operations. Reducing model bias has the general effect of minimizing the magnitude of the difference between the model and reality (*i.e.*, the measured turbidity). An additional reason for minimizing the value of the PBIAS statistics is related to the ability to apply corrections to long-term averaged results – for example, if a given location is generally modeled as higher than data (negative PBIAS), then the interpretation of that model value can be assessed with the additional knowledge given by the PBIAS value.

Specifically, the PBIAS statistic, *i.e.*, the percent bias, represents a means to assist interpretation of modeled results that could be applied to a modeled turbidity value at a given location. For example, the PBIAS values of 11% and 17% in the WY2010 and WY2011 recalibrated model statistics, respectively, at the False River location means that the revised calibrated Historical model underestimates the data by 11% and 17%, respectively, when using the refined set of rate coefficients and the best available boundary conditions. In a turbidity forecast model simulation, for example, this means that during the wet season of a modeled year with sufficient flow, modeled turbidity in False River could be viewed as an underestimate on what might happen in reality on the order of 14% (the average). Of course, using the statistic in this way comes with the proviso that this is an “order of” underestimate – *i.e.*, it is unlikely that a modeled value will be an overestimate, and that an underestimate will not be on the

order of 100%, for example. Note that this location was chosen as the bias was positive in both water years – this was not true at all locations.

The values in Table 5-5, the Model Skill assessment statistics, represent the overall assessment for the wet seasons of WY2010 and WY2011 (separately) for both the RMA and DMS calibration attempts. For each overall calibration metric, the RMA calibration improved the results with one exception for WY2010, in which there was no change. The WY2011 results illustrate a significant improvement over the DMS calibration, and over the WY2010 results. This latter result illustrates the point that the turbidity model calibration may not be optimal for a given water year or for a given location as the turbidity model is a simplified representation of the physical process of sediment transport.

In the development of the long-term boundary conditions to use in training the Turbidity ANN, the Mixed-SSC-WARMF set of turbidity boundary conditions was chosen over the WARMF-Only ones. This was based on the assessment that the Location Metrics at three compliance locations were generally improved in comparison with the WARMF-Only simulations in the WY2010 and WY2011 time frames. In addition, the results at the compliance locations were comparable in magnitude to the simulations using CDEC turbidity data. However, this comparison comes with the proviso that the calibration statistics are NOT directly comparable to the synthetic boundary conditions (see Section 5.2 for details).

However, in the additional long term simulations (1975 – 2011) run with the two sets of synthetic boundary conditions, the conclusion is less clear-cut. The results for the “early years” and the “recent years” simulations do not give a compelling advantage to either the Mixed-SSC-WARMF or the WARMF-only boundary conditions for use in the long term historical simulation, as comparison of the residual statistics shows that each of these models had significant difficulties in reproducing available EMP turbidity data.

Figures developed to visualize the DSM2 output (see Section 11.2 for technical details) illustrate that there are substantial differences in the resulting turbidity fields using the Mixed-SSC-WARMF or the WARMF-only boundary conditions. Although the Mixed-SSC-WARMF matched the real daily-averaged turbidity values better in the both the WY2010 (late January 2010) and WY2011 (late March 2011) examples, the result in terms of exceeding the compliance value (12 NTU) at the three locations was the same. In other words, any decision reached on the sole basis of exceeding the compliance values (e.g., on whether to change the pumping regime) would have been the same. Although data at the three compliance locations was not available to use in comparison for the model results in the example illustrating the “early period” simulation results with the two sets of boundary conditions, the magnitude of the predictions similarly predict that only two of the three locations will exceed the 12 NTU maximum during this high flow, high turbidity event.

Given these results, in some cases the WARMF model should be considered to supply both inflow and turbidity boundary conditions particularly if some improvements can be made in WARMF calculations for turbidity at Freeport and Vernalis. The reasons are two-fold: first, in these model applications, the WARMF turbidity calculation is conceptually consistent with WARMF model flow calculations while this will not necessarily be true if the flow is taken from a different source (such as measurement data or a

scenario test); and, second, with some additional effort (and funding), it is quite likely that the WARMF turbidity calculations at Vernalis and Freeport can be improved to more closely match available turbidity data. Results from WY2012 improvements in the WARMF model calculations (RMA 2012a) of turbidity conditions at Yolo Bypass, Cosumnes, Mokelumne and Calaveras Rivers were significant. This supplies confidence that improvements can be made in the more complicated turbidity boundary sources at Vernalis and Freeport.

As suggested in previous RMA documentation (RMA 2010b, 2011a, 2011b, 2012b) and in Section 2.3, development of a true suspended sediment model should be considered. The capability of a suspended sediment model to include wind-driven re-suspension of sediments, tidally-influenced suspension of sediments, variations in the character of suspended sediment composition at model boundaries, and other factors that are not considered in these turbidity model calculations, has the potential to improve the quality of model results.

The Mixed-SSC-WARMF simulation was used (for the third minor objective) to analyze the modeled conditions under which a turbidity bridge linking the central and south Delta was likely to form. The high flow/high turbidity periods of water years 1991 – 2000 were selected as they represent a wide range of conditions. The results suggest further analyses could be made to see if the modeled results showing preferred routes through Old River or Middle River depending on the dominant source of turbidity hold true for similar conditions in modeled scenarios. In general the analysis shows that there is more than one mode under which a turbidity bridge is likely to form. It should be noted that this analysis is based on a turbidity model developed with synthetic or externally calculated (i.e., from WARMF results) boundary conditions, so results should be interpreted with caution.

10 References

Department of Water Resources (DWR), 2011. Methodology for Flow and salinity Estimates in the Sacramento-San Joaquin Delta and Suisun Marsh - 32nd Annual Progress report to the State water Resources Control Board. Chapter 7, pp. 7-1 to 7-28.

Fitzpatrick, J.J. Assessing skill of eutrophication models for water quality managers. Water Environment Federation, 2009.

Hetland, R.D. Event-driven model skill assessment. *Ocean Modelling*. 11(2006): 214-223.

King, I.P., 1995. RMA11 – A two-dimensional finite element quality model, Resource Management Associates.

Joliff, J.K., J.C. Kindle, I. Shulman, B. Penta, M. A.M. Fredrichs, R. Helber, R.A. Arnone. Summary diagrams for coupled hydrodynamic-ecosystem skill assessment. *J of Marine Systems*. 76(2009): 64-82.

Keenlyside, N.S., M. Latif, J. Jungclaus, L. Kornlueh, E. Roeckner. Advancing decadal-scale climate prediction in the North-Atlantic sector. *Nature*, Vol. 453, May 2008. 84-88.

Moriasi, D.N., J.G. Arnold, M.W. Van Liew, R.L. Bingner, R.D. Harmel, and T.L. Vieth. 2007 Model evaluation guidelines for systematic quantification of accuracy in watershed simulations. *Transactions of the ASABE*. Vol. 50(3).

Resource Management Associates, Inc. (RMA), 2008. "San Francisco Bay-Delta Turbidity Modeling", prepared for Metropolitan Water District of Southern California.

Resource Management Associates, Inc. (RMA), 2009a "Particle Tracking and Analysis of Adult and Larval/Juvenile Delta Smelt for 2-Gates Demonstration Project", prepared for Metropolitan Water District of Southern California.

Resource Management Associates, Inc. (RMA), 2009b. "Numerical Modeling in Support of Suisun Marsh PEIR/EIS: Technical Appendix", prepared for Jones and Stokes Associates.

Resource Management Associates, Inc. (RMA), 2010a. Spatial Animation of Observed Turbidity Time Series for the Sacramento-San Joaquin Delta.

Resource Management Associates, Inc. (RMA), 2010b. Turbidity and Adult Delta Smelt Forecasting with RMA 2-D Models: December 2009 – May 2010.

Resource Management Associates, Inc. (RMA), 2011a. Turbidity and Adult Delta Smelt Forecasting with RMA 2-D Models: December 2010 – February 2011.

Resource Management Associates, Inc. (RMA), 2011b. Simulations for water years 2001, 2004, 2008 and 2009.

Resource Management Associates, Inc. (RMA), 2012a. RMA/Systech Collaboration to Improve WARMF Model Turbidity Estimates.

Resource Management Associates, Inc. (RMA), 2012b. Turbidity and Adult Delta Smelt Modeling with RMA 2-D Models: December 2011 – February 2012.

Stow, C.A., J. Joliff, D.J. McGillicuddy Jr, S.C. Doney, J.I. Allen, M. A.M. Fredrichs, K.A. Rose, P. Wallhead. Skill assessment for coupled biological/physical models of marine systems. *J of Marine Systems*. 76(2009): 4-15.

Taylor, K.E. Summarizing multiple aspects of model performance in a single diagram. PCMDI Report No 55 (Revised), Sept. 2000.

Trucano, T.G., L.P. Swiler, T. Igusa, W.L. Oberkampf, M. Pilch. 2006. Calibration, validation, and sensitivity analysis: What's what. *Reliability Engr. & System Safety*. Vol. 91: 10-11. pp 1331 – 1357.

Wright, S.A. and D.H. Schoelhamer, 2004. Trends in the sediment yield of the Sacramento River, California, 1957-2001. *San Francisco estuary and Watershed Science*, 2(2), 1-14.

11 Appendix I

11.1 Model Skill

11.1.1 Background

In this section, information is presented on model skill. A number of publically-available articles were identified as pertinent background information for the project. This information constitutes a brief overview of the topic of model skill, and is not considered or intended to be comprehensive. Instead, this assessment is intended to supply some basic definitions and to note recent applications of model skill metrics, with a focus on water quality applications

Although the two objectives of the project were clear at the outset, criteria were not specified for determining the sufficiency of the QUAL turbidity calibration or the “best” set of synthetic boundary conditions for the long term turbidity model. Given the nature of the turbidity model as a proxy for suspended sediment transport, it was clear that a model calibration step might improve the quality of the calibration in some locations in one year, but deteriorate the quality in those locations in a different year. Thus, it was necessary to define at least one metric for the model domain that could be used to quantify calibration progress and to determine a criterion for model selection. For this project, model selection amounted to choosing between competing sets of boundary conditions to use in developing a long-term Historical turbidity model (1975 – 2011).

The motivation behind the investigation of current practice in model skill assessment is the potential that the DSM2 turbidity model output might be used to as a tool to support decisions on Delta operations, potentially in forecasting situations. In general, in those cases where model output may be used in decision support, an assessment of model accuracy is important as decision-makers must weigh the importance they attach to forecasting results and the possible outcome of alternative actions (Stow *et al.* 2009, Fitzpatrick 2009).

The definition of model skill was not universal in the articles reviewed, but in this document we adopt the definition that “model skill” is a measure of the accuracy of a model (Stow *et al.* 2009) – other authors have similarly defined model skill as “fidelity to the truth” (Joliff *et al.* 2009). Since the observations used to assess model skill are imperfect, essentially the “Truth” cannot be known (Joliff *et al.* 2009) so quantification or assessment of observational error is an important component in the overall assessment of model skill. It was noted (as of 2009) that the routine application of rigorous model skill assessment was not broadly reflected in the refereed literature, and that the “community standard” of model-to-data comparisons was the basic visual time series comparison plot (Stow *et al.* 2009).

All authors proposed the use of some sort of model skill metric, either using known statistical measures or in some cases novel assessment metrics (Taylor 2000, Joliff *et al.* 2009, Hetland 2006, Fitzpatrick 2009). Model skill was used both to provide information for model selection and implementation (Stow *et al.* 2009). Given the diversity of application and selection of model metrics, it was apparent that the

choice of metrics applied and level of skill necessary for a given application were dependent on the context, goals and the spatial and temporal scales of importance (Stow *et al.* 2009, Fitzpatrick 2009).

It was apparent in the articles reviewed that some measure of subjectivity in the metrics chosen for model skill assessment was inevitable. For example, although a model should be able to simulate both the amplitude and the pattern of variability, the decision of which of these factors is more important is dependent on the application (Taylor 2000).

For univariate comparisons of model output and observations, both graphical techniques (*e.g.*, time series plots) and quantitative metrics were recommended, frequently using residuals and the associated statistics as well as direct comparisons (*e.g.*, correlation coefficient). An interesting graphical technique was developed for multivariate comparisons (Taylor 2000) that was used to monitor overall model performance as a model evolved and in assessing the merits of competing models. Some authors used somewhat more advanced statistical techniques (Hetland 2006, Keenlyside *et al.* 2008)

11.1.2 Decisions on model skill assessment for this project

Four statistics were chosen as basic to calibration accuracy at the locations where CDEC data was available - the Nash-Sutcliffe efficiency (NSE), Percent Bias (PBIAS) and root mean square error (RMSE) calculated using model residuals and the R^2 goodness of fit statistic calculated from the regression equation between model output and data. The residual statistics were chosen based on the analysis presented in (Moriasi *et al.*, 2007). Note that these statistics are among the selection of quantitative metrics noted as useful in the assessment of model skill (Stow *et al.* 2009). Other statistics were calculated, and visual representations of the data-model fit and of the histogram of residuals were presented along with additional residual statistics and the data-model regression plot.

At the outset of the calibration effort, a decision was made as a model skill criterion to optimize the accuracy of the model at the three Delta turbidity compliance locations – at Holland Cut, Prisoner Point and Victoria Canal at Byron – and to minimize the magnitude of the model bias without sacrificing the desired values of the other two residual statistics in the WY2010 and WY2011 calibration years if possible. Given that initial choice, the selection of the “Best” choice of boundary conditions for the long-term model was also made primarily on the basis of the ability of the given set of boundary conditions to minimize the model error at the three compliance locations. Subsequent to the calibration effort and the choice of boundary conditions, additional metrics were developed to quantify overall model skill in the DSM2 model domain as a comparison.

Additional detail on the model skill assessment metrics chosen for this project is presented in Section 5.2. It is noted that the quantification of observational error (of the turbidity measurements) was not considered, nor were the statistical characteristics of the data specifically considered at measurement locations. In future applications, it would be valuable to specifically consider the statistical characteristics of the observations independent of the residual calculations at the outset of the model skill evaluation process as the “true” state of the modeled system, although unknown, can be assumed to lie within the bounds of observational uncertainty (Stow *et al.* 2009).

11.2 Spatial Animation

11.2.1 Background

Resource Management Associates developed a method of generating spatial contours of point time series data based on interpolation over an RMA finite element model geometry (RMA 2010a) as a demonstration application in 2010. The first application of this capability was to display observed turbidity data in the Delta for January and February 2010 using a portion of the RMA Delta model grid as a template.

For this project, RMA wanted to visualize the one-dimensional output of the DSM2 turbidity model. It was clear that a one-dimensional grid was more appropriate to give a more accurate sense of the DSM2 modeling capability. However, the methodology is identical. Portions of the original documentation (RMA 2010a) have been revised and updated for the current project in the following section.

11.2.2 Interpolation methodology

The spatial interpolation is performed by linear super-position of point values multiplied by spatial weighting functions. Time series are collected at Delta locations where each location is defined at a specified node in a finite element model network. In the original application (RMA 2010a), the time series were located at the available turbidity stations in the Delta, so a portion of the RMA grid was deleted in regions lacking a near-by data location. In the applications used in this project, the time series are produced as output from a DSM2 model run. The definition of the grid used in this project is covered in the next section – it is a one-dimensional grid except in the region of Franks Tract where two dimensions were used to accommodate the special geometry and calculations in DSM2 as conceptualized in this region.

The methodology proceeds as follows: a sequence of weight functions $\phi_i, i=1, \dots, m$ where m is the number of time series locations is constructed such that:

1. $0 \leq \phi_i(x,y) \leq 1$ for all locations (x,y) in the grid.
2. $\phi_i(x_b, y_i) = 1$ at the time series location (x_b, y_i) , and these locations correspond to a node in the grid.
3. $\phi_i(x_b, y_i) = 0$ at time series locations (x_j, y_j) different from (x_b, y_i) , $1 \leq j \leq m$.
4. $\sum_{i=1}^m \phi_i(x, y) = 1$ at any grid location (x,y) .

The approach RMA used to produce the weight functions was to solve the Laplace equation with Neumann boundary conditions in two dimensions (x,y) :

$$\frac{d^2 \phi_i}{dx^2} + \frac{d^2 \phi_i}{dy^2} = 0$$

And at the boundaries:

$$\frac{d^2\phi_i}{dn} = 0$$

Constraints (1) and (2) from above also apply here.

For the one-dimensional channel sections, the Laplace equation reduces to:

$$W \frac{d^2\phi_i}{dx^2} = 0$$

where W is the channel width.

Once the weight functions have been computed, the value $E(x,y)$ used in the animation at any given location (x,y) in the grid is given by:

$$E(x, y) = \sum_{i=1}^m E_i(x, y) \times \phi_i(x, y)$$

where $E_i(x,y)$, $i=1, \dots, m$, is the value observed at the time series location i associated with weighting function ϕ_i , and $\phi_i(x,y)$ is the value of the weighting function at the given location (x,y) .

The spatial interpolation methodology leads to an approximately linear variation between observed stations. The accuracy of the spatial distribution when used with DSM2 model output depends on the density of the observation stations.

11.2.3 Grid development

The interpolation grid incorporates the one-dimensional channels from the existing RMA multi-dimensional Delta model. The two-dimensional areas of the RMA Delta model were replaced with new one-dimensional channel sections which generally follow the channel layout of the DSM2 Delta model. The open water area of Franks Tract was gridded using coarse two-dimensional elements. The simplification from the RMA Delta grid was performed to speed the interpolation computation and minimize the interpolation file size. Furthermore, there was the desire not to over represent the interpolated product with the projection of a one-dimensional result to a detailed two-dimensional grid.

Figure 11-1 illustrates the predominantly one-dimensional grid used in this project to visualize DSM2 model output. Figure 11-2 illustrates the geo-referenced locations from the interpolation grid where DSM2 model output was located (pink stars). Note the interpolation grid is different from the DSM2 grid, so the interpolation locations are slightly misplaced from the DSM2 channels, shown as thin black lines in Figure 11-2.

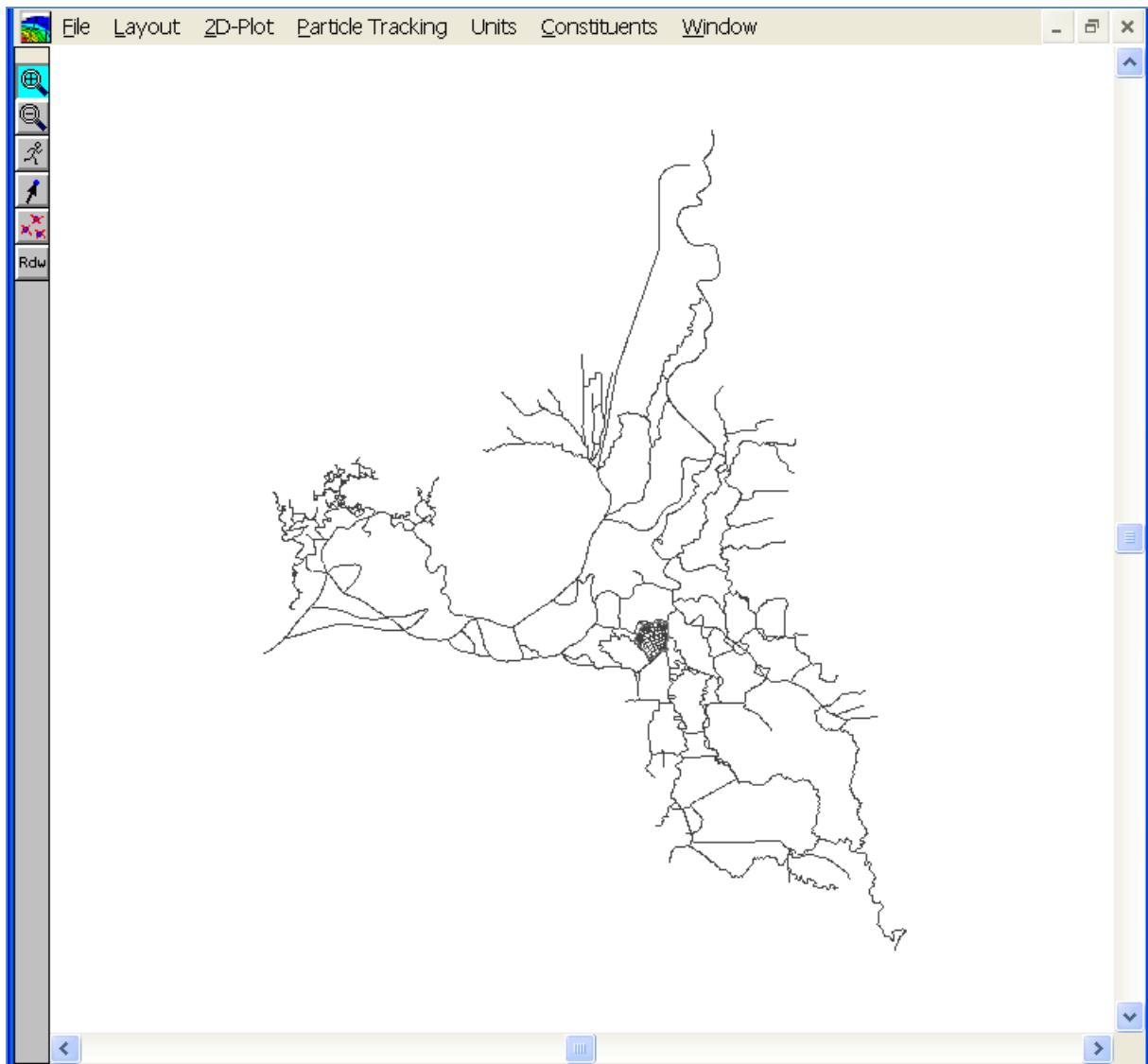


Figure 11-1 This figure illustrates the grid developed to visualize DSM2 one-dimensional model output. Note the Franks Tract area was developed in 2-D.

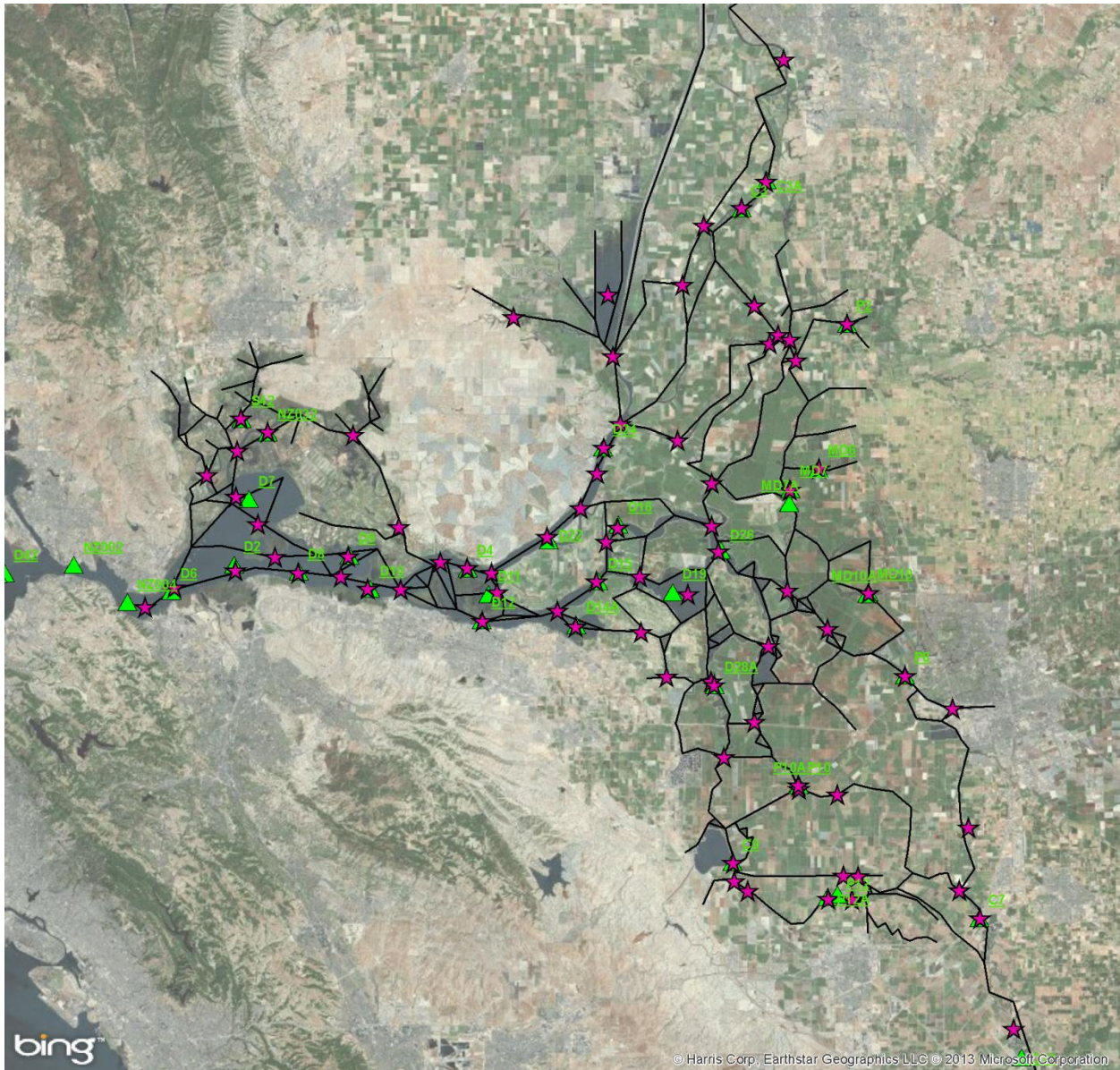


Figure 11-2 The pink stars indicate the locations where DSM2 output is used to create the interpolated contours. Green triangles are EMP data locations. Black lines denote the channels in the DSM2 model grid. Note the interpolation grid (Figure 11-1) is different from the DSM2 grid.

12 Appendix II – Updated QUAL Turbidity calibration statistics

12.1 Daily-averaged CDEC data and model output – WY2011

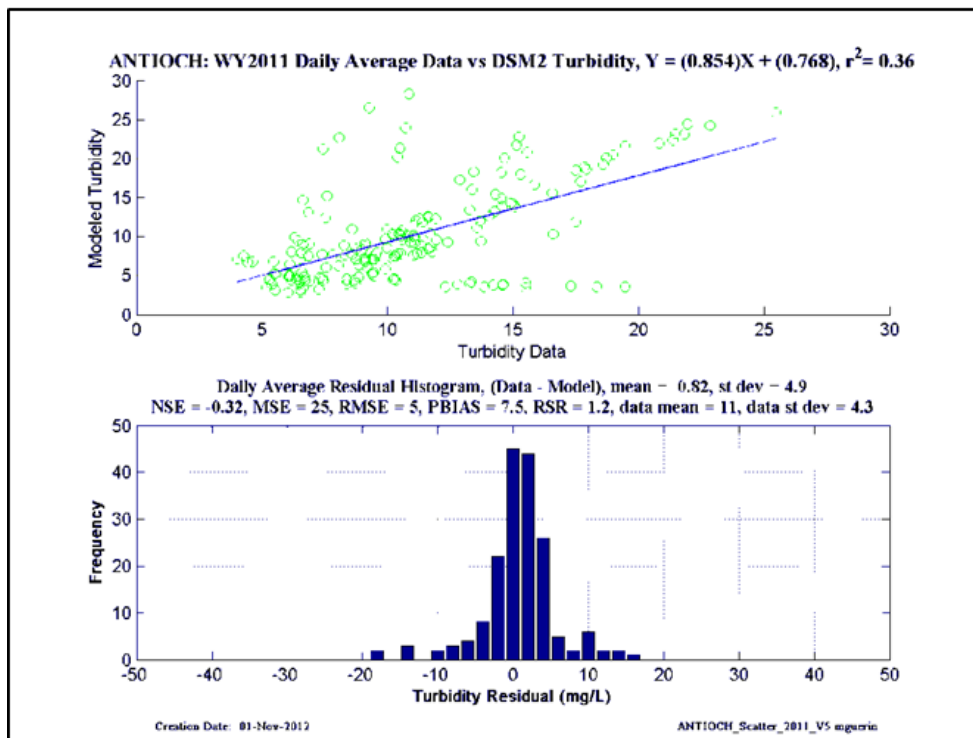
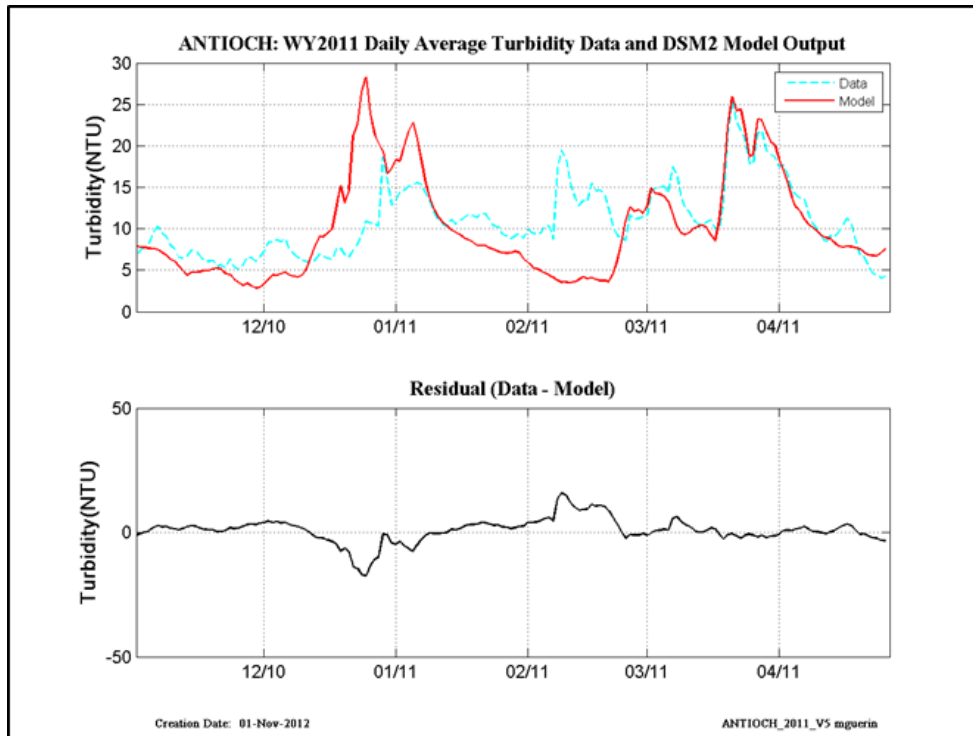


Figure 12-1 WY2011 revised calibration results at Antioch.

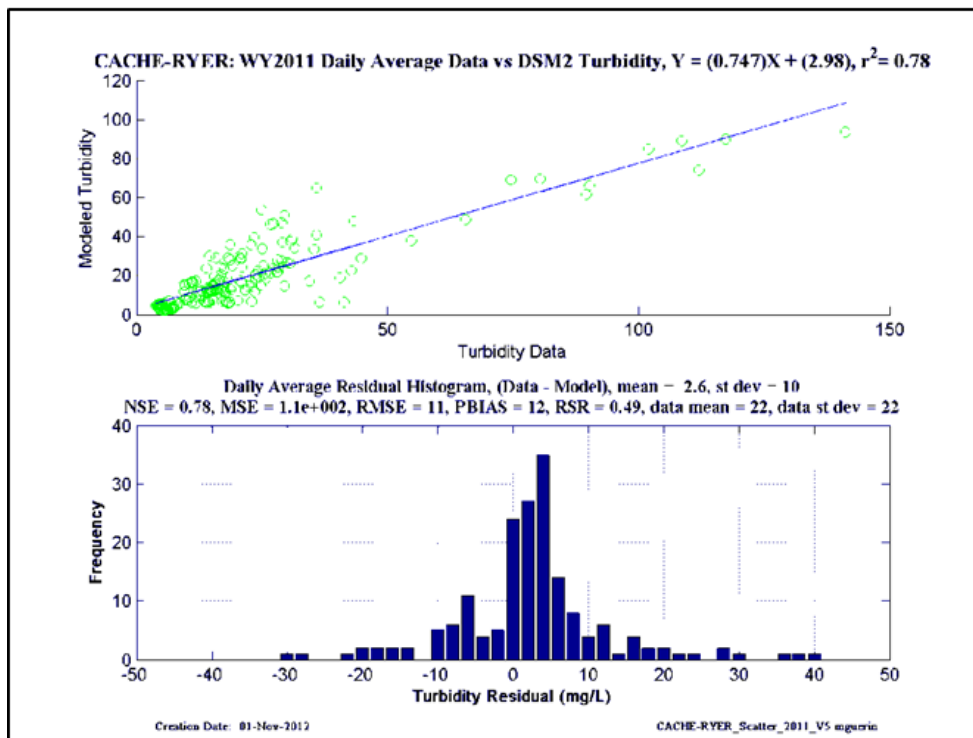
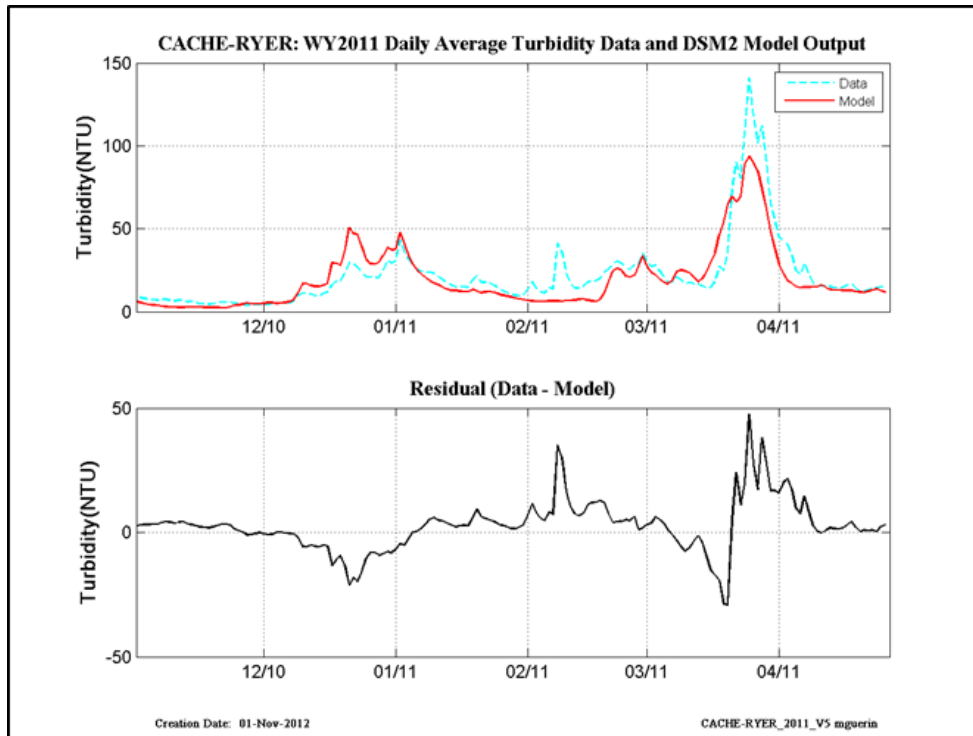


Figure 12-2 WY2011 revised calibration results at Cache-Ryer.

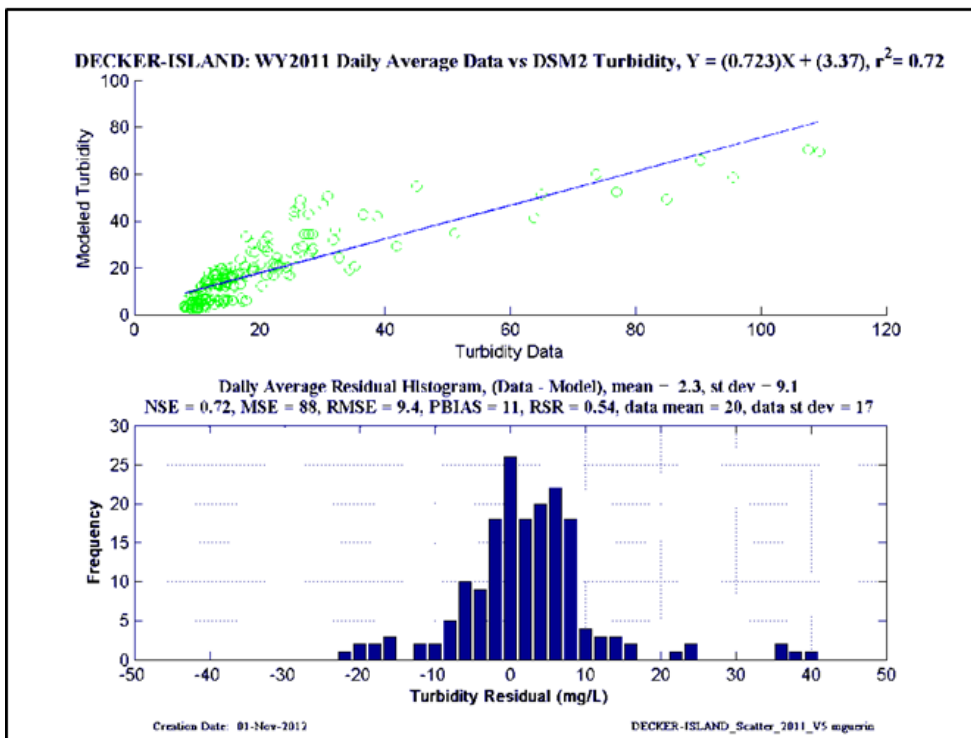
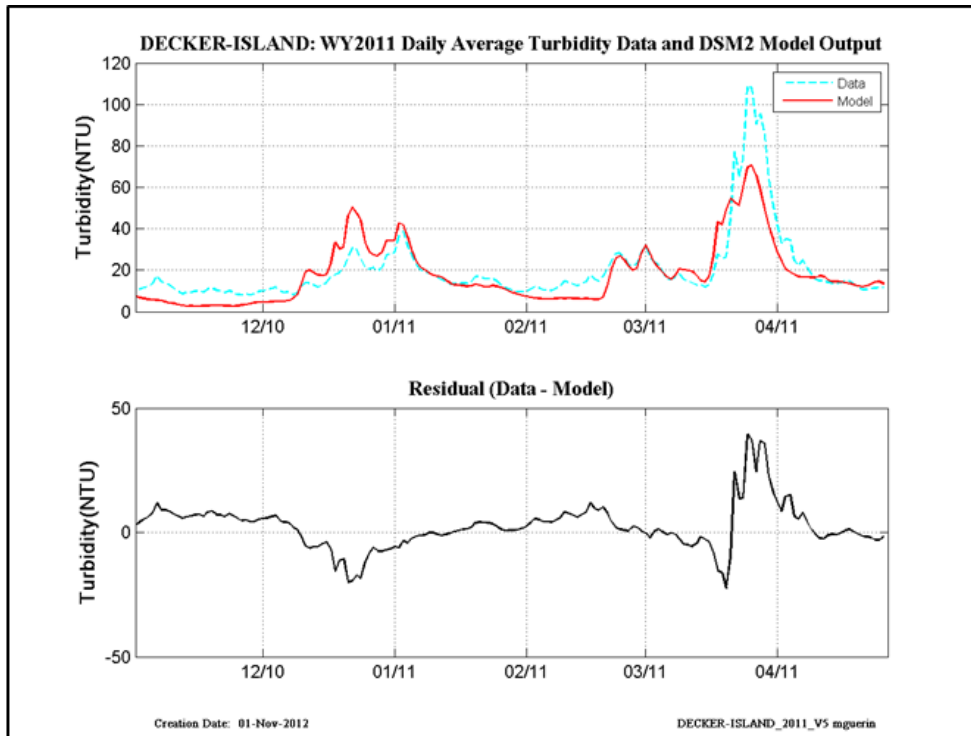


Figure 12-3 WY2011 revised calibration results at Decker Island.

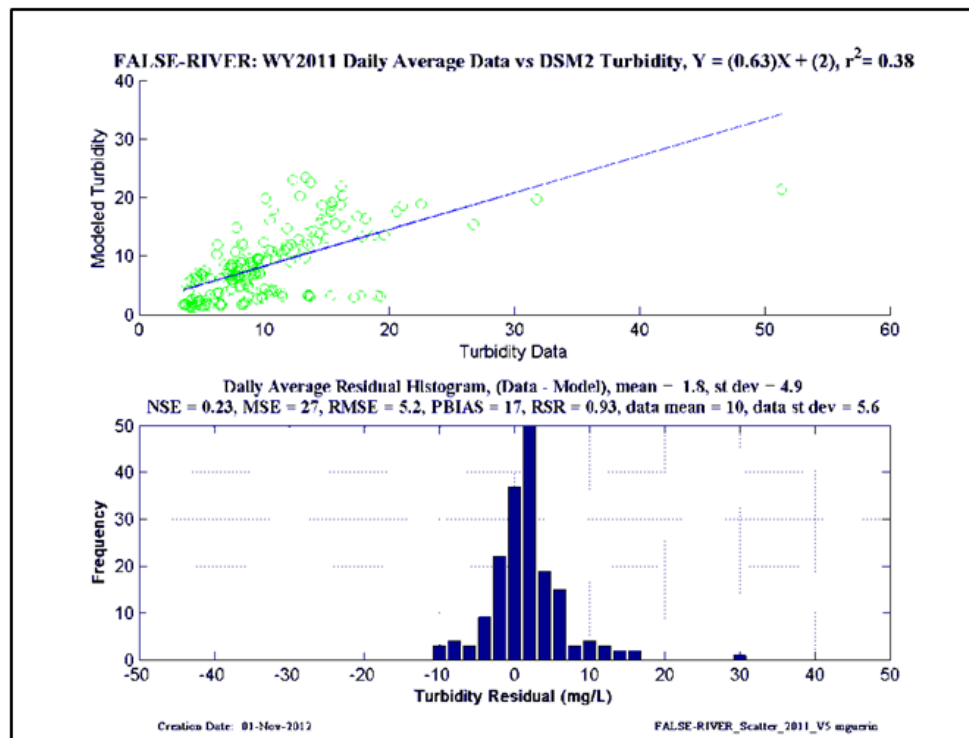
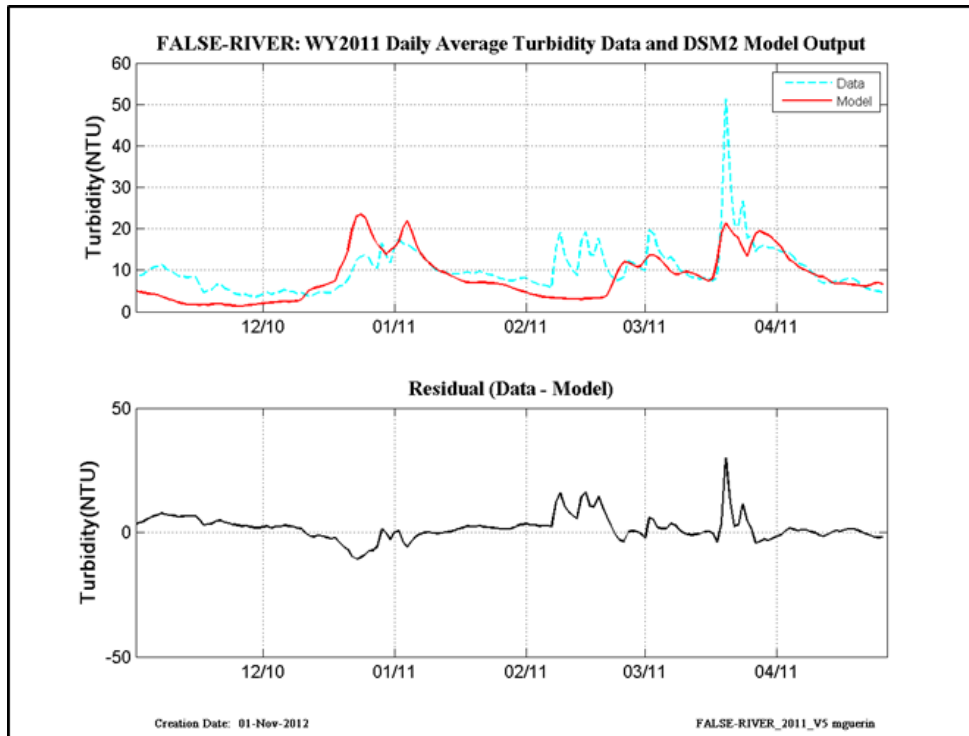


Figure 12-4 WY2011 revised calibration results at False River.

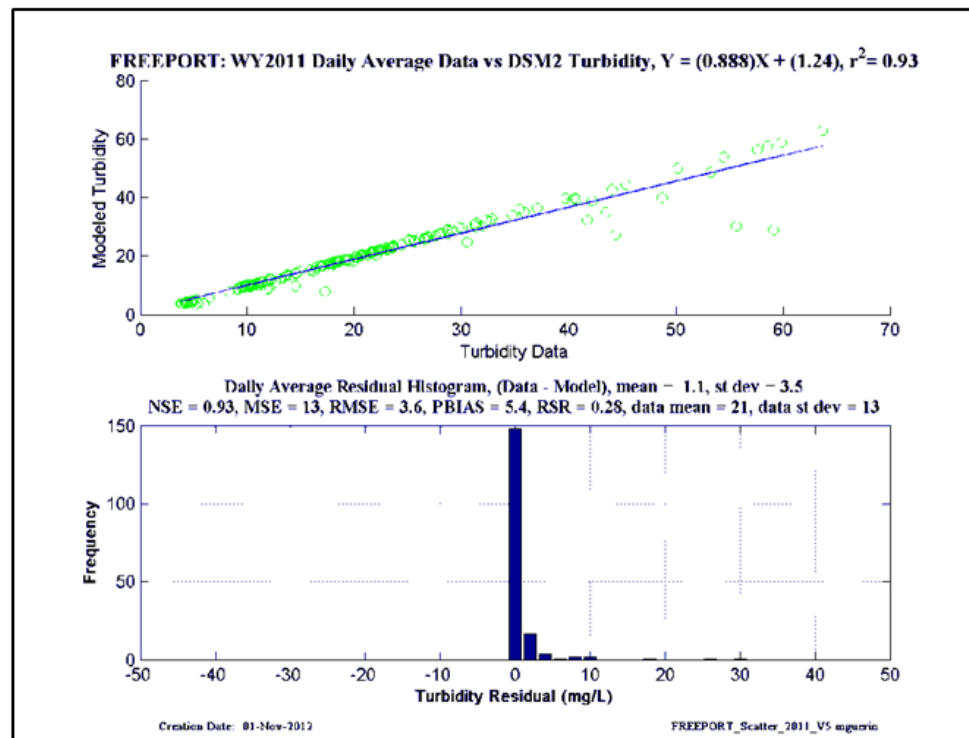
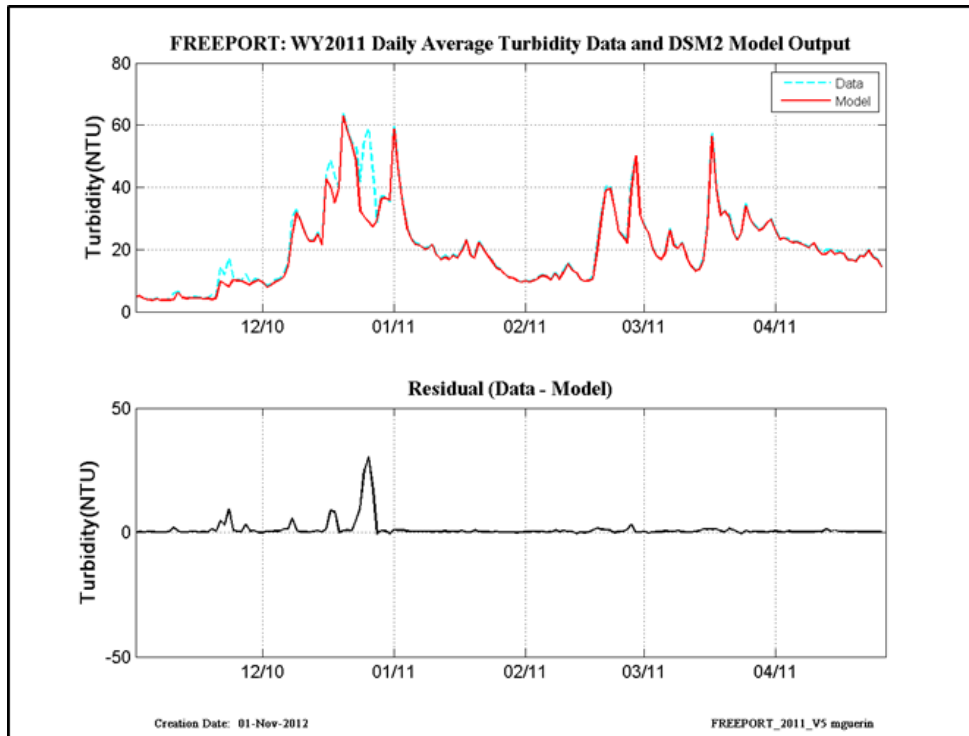


Figure 12-5 WY2011 revised calibration results at Freepport.

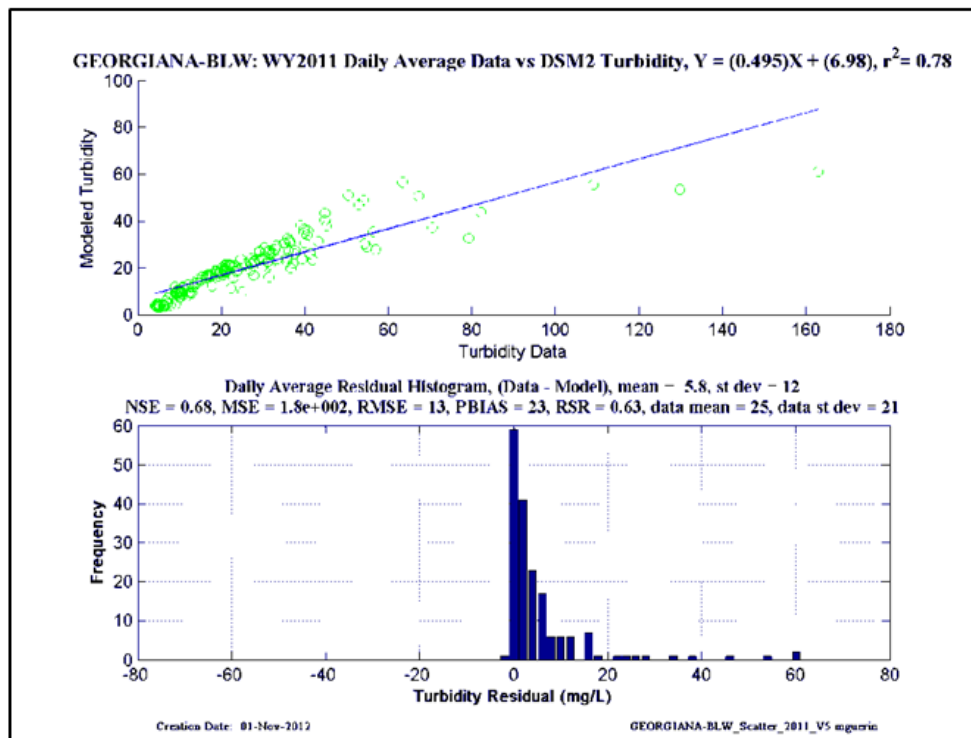
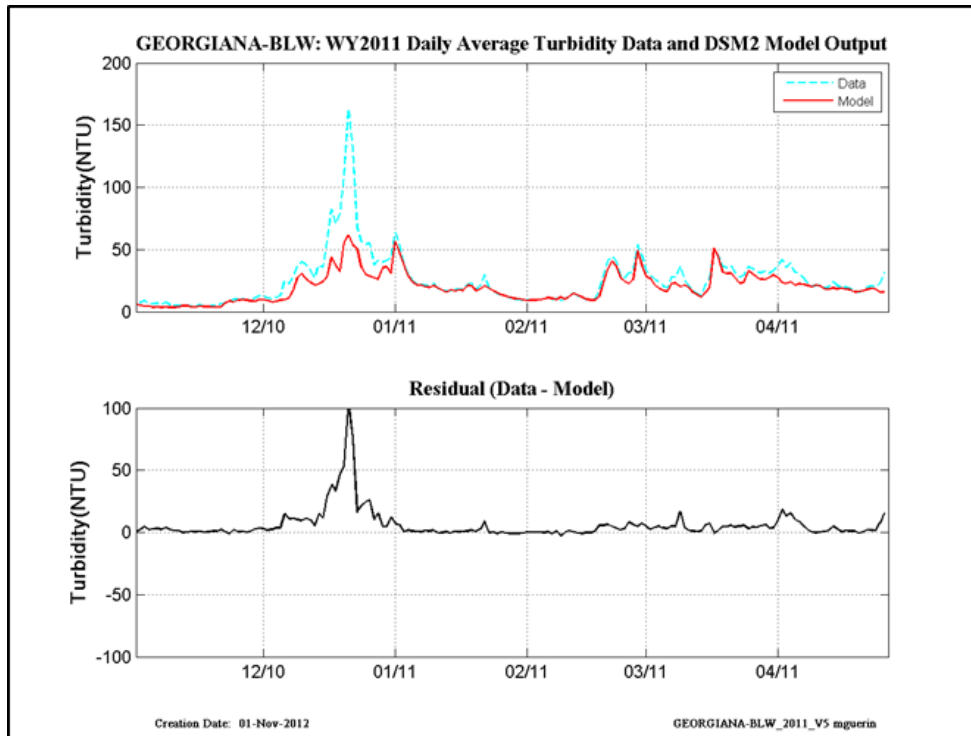


Figure 12-6 WY2011 revised calibration results at Georgiana-Below-Sac.

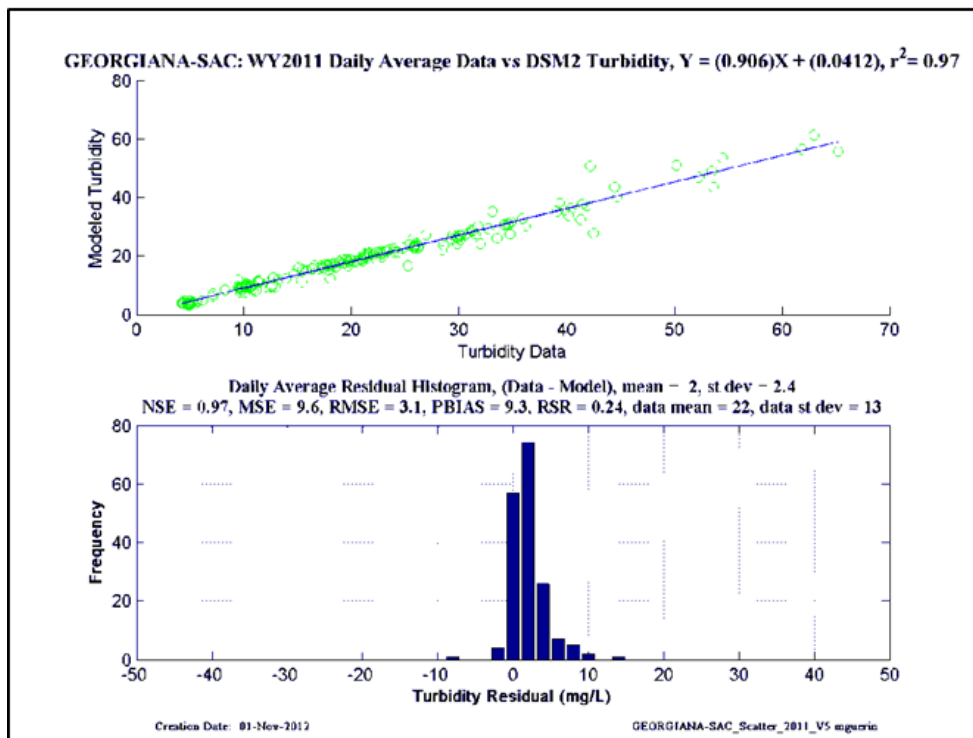
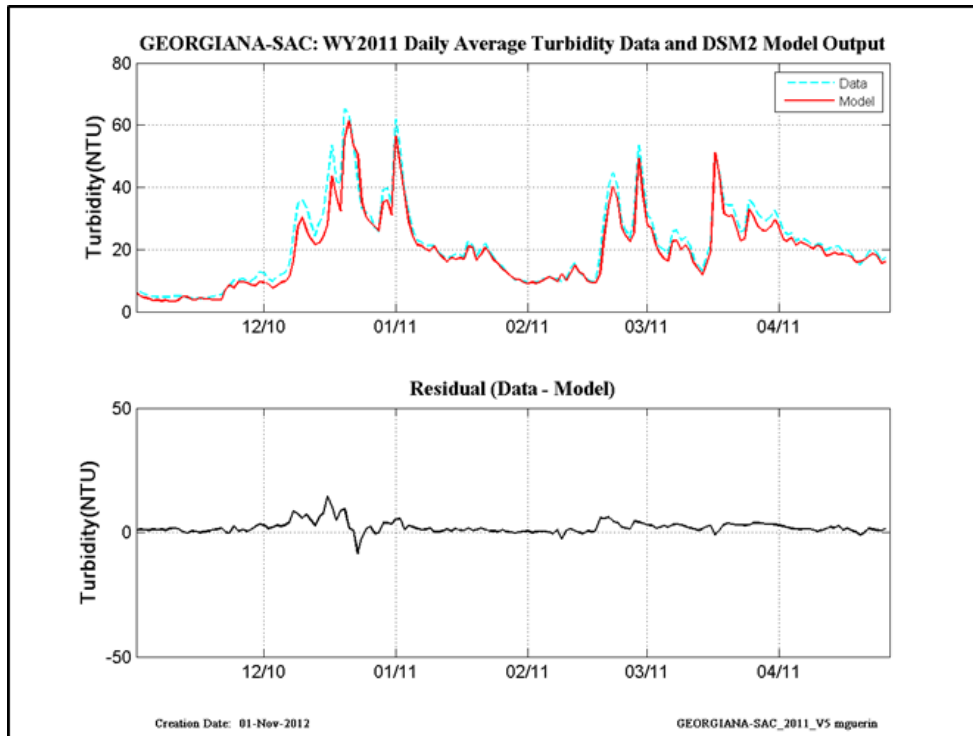


Figure 12-7 WY2011 revised calibration results at Georgiana-at-Sac.

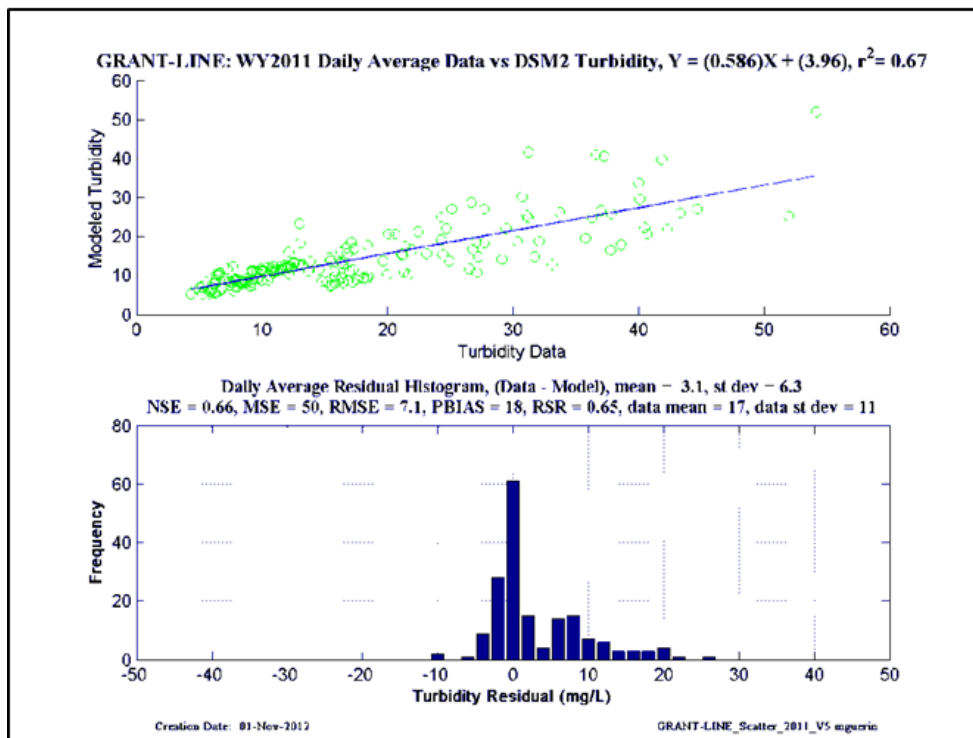
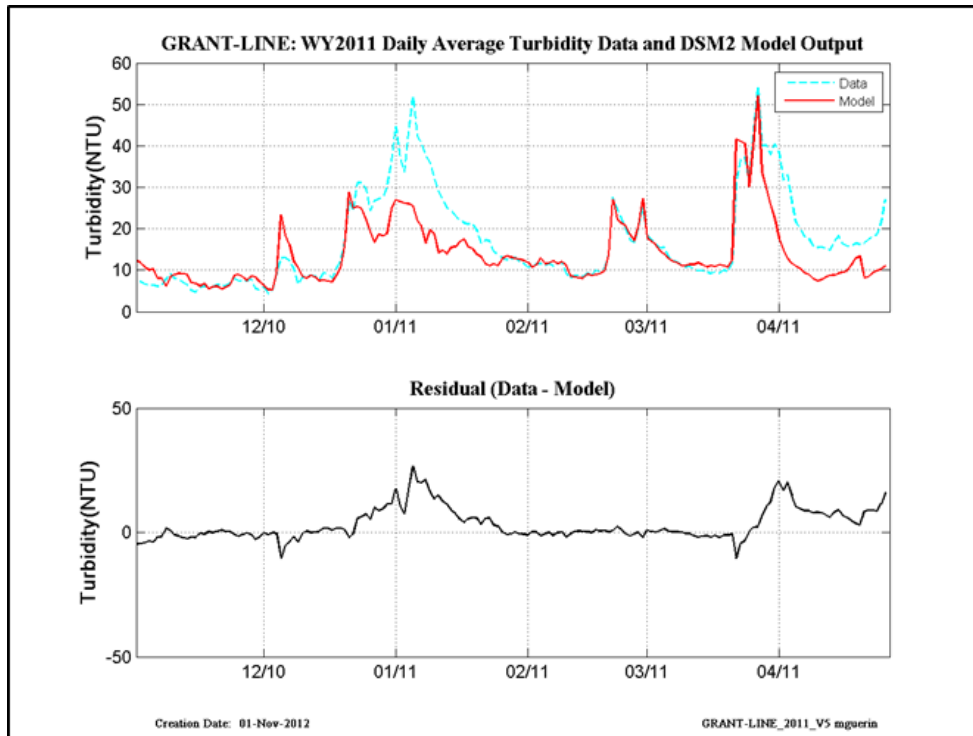


Figure 12-8 WY2011 revised calibration results at Grant Line.

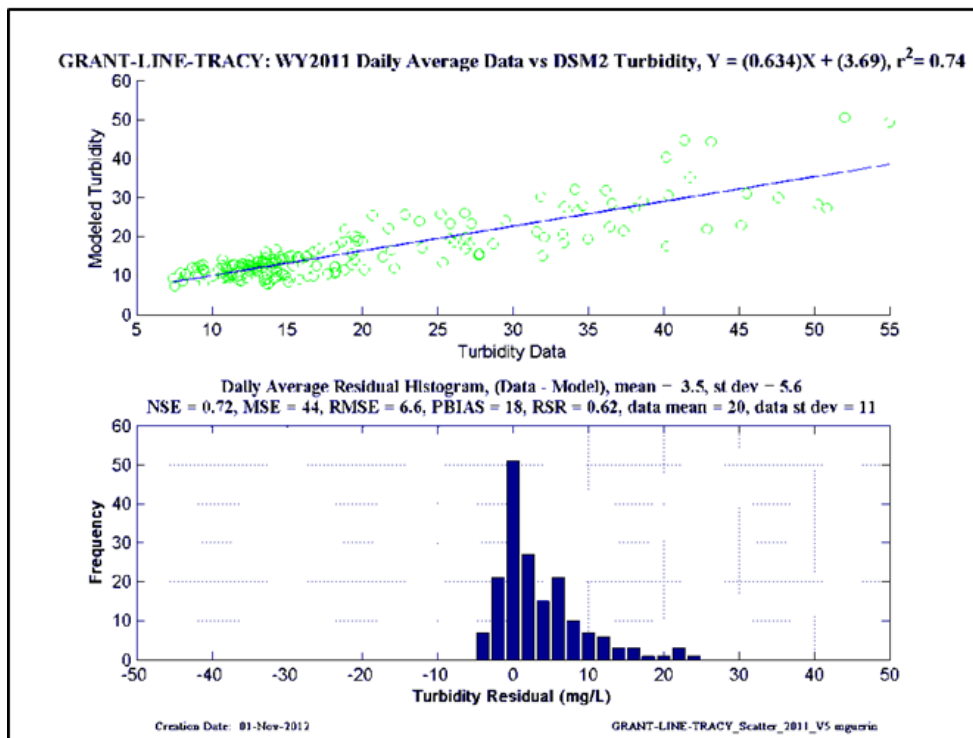
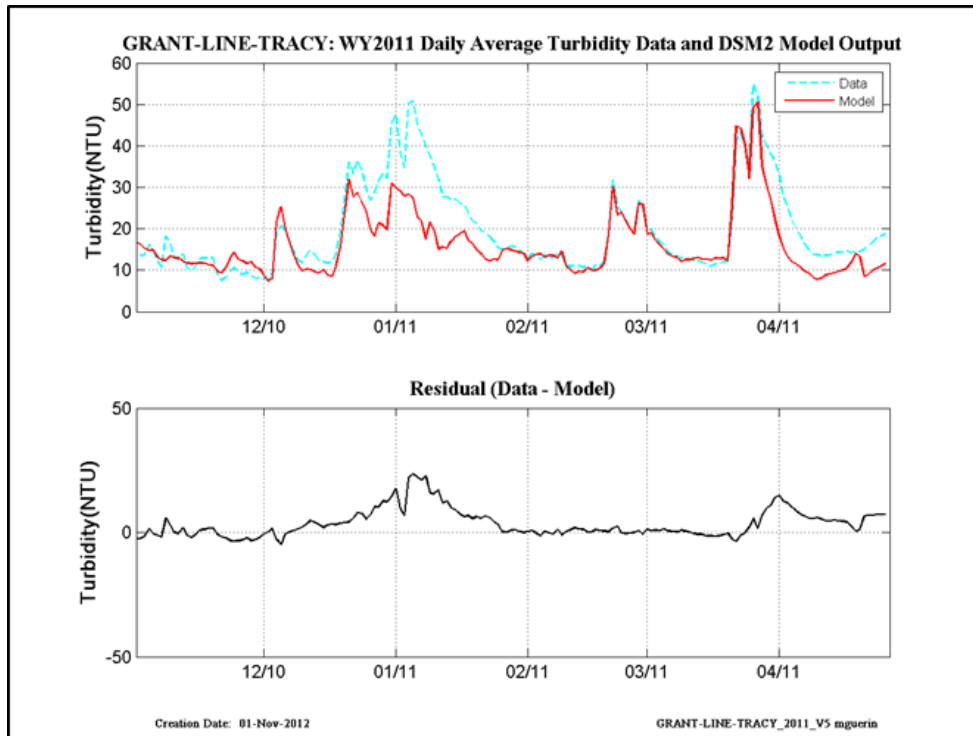


Figure 12-9 WY2011 revised calibration results at Grant-Line Tracy.

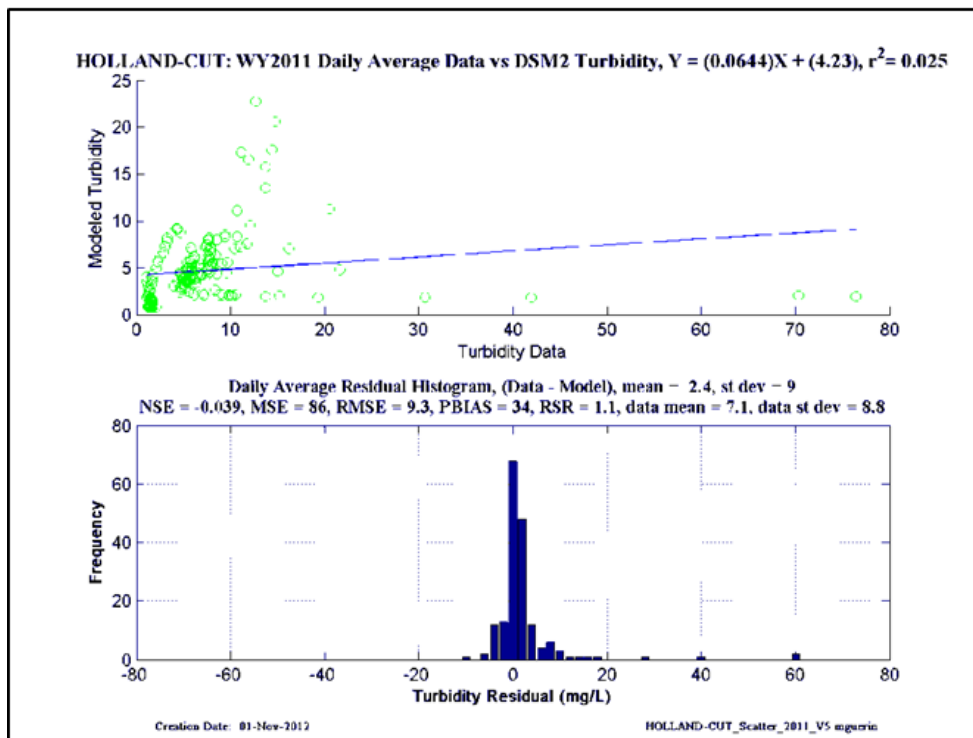
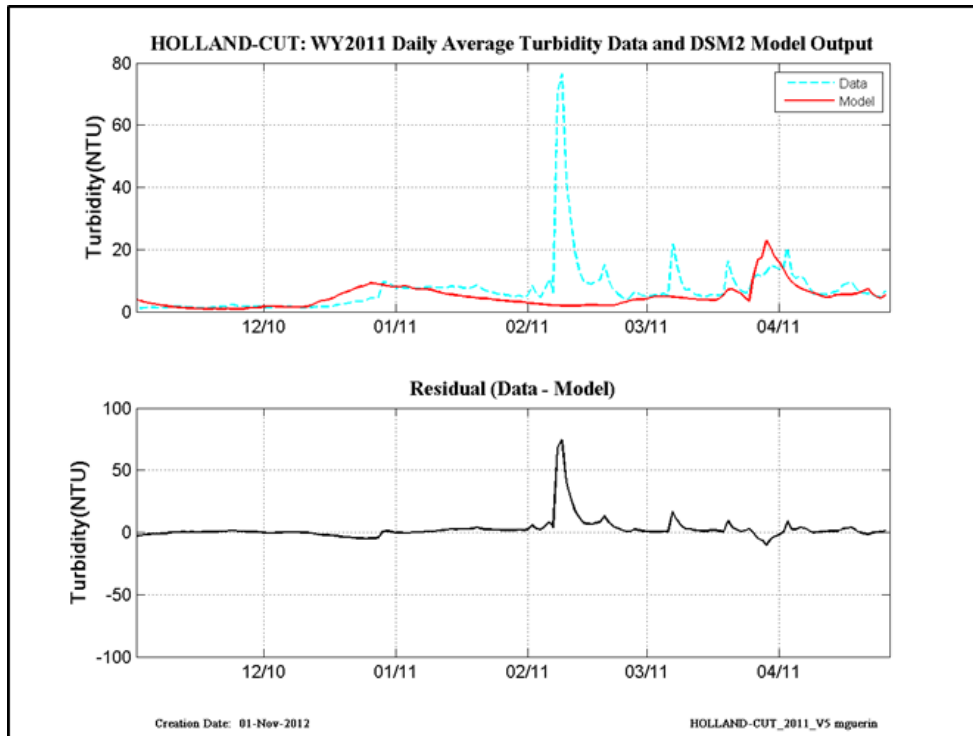


Figure 12-10 WY2011 revised calibration results at Holland Cut.

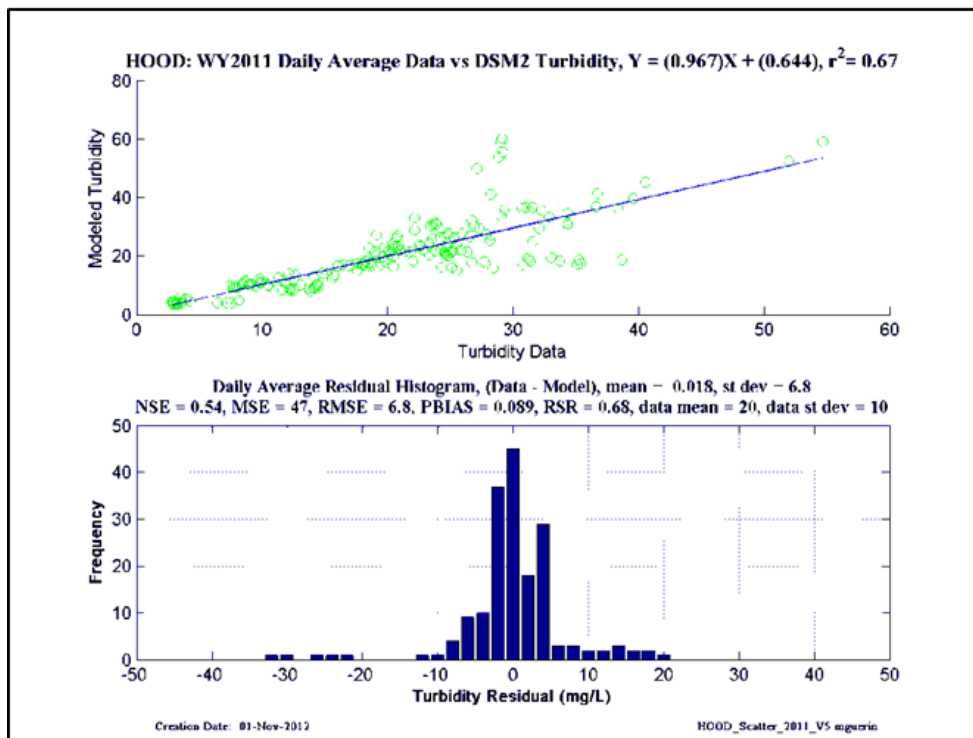
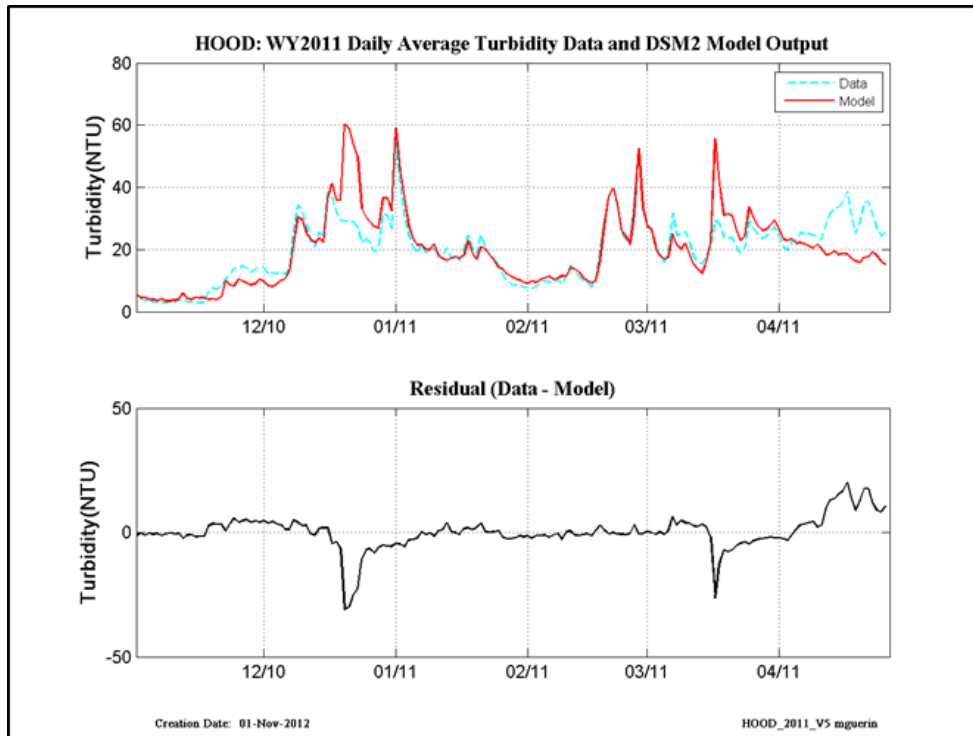


Figure 12-11 WY2011 revised calibration results at Hood.

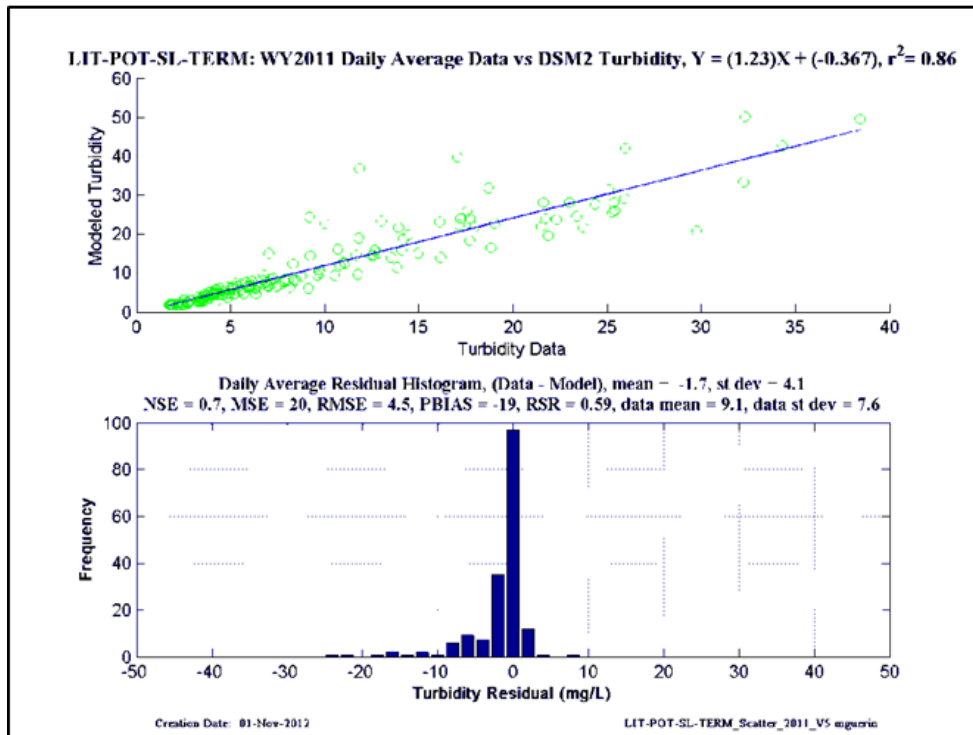
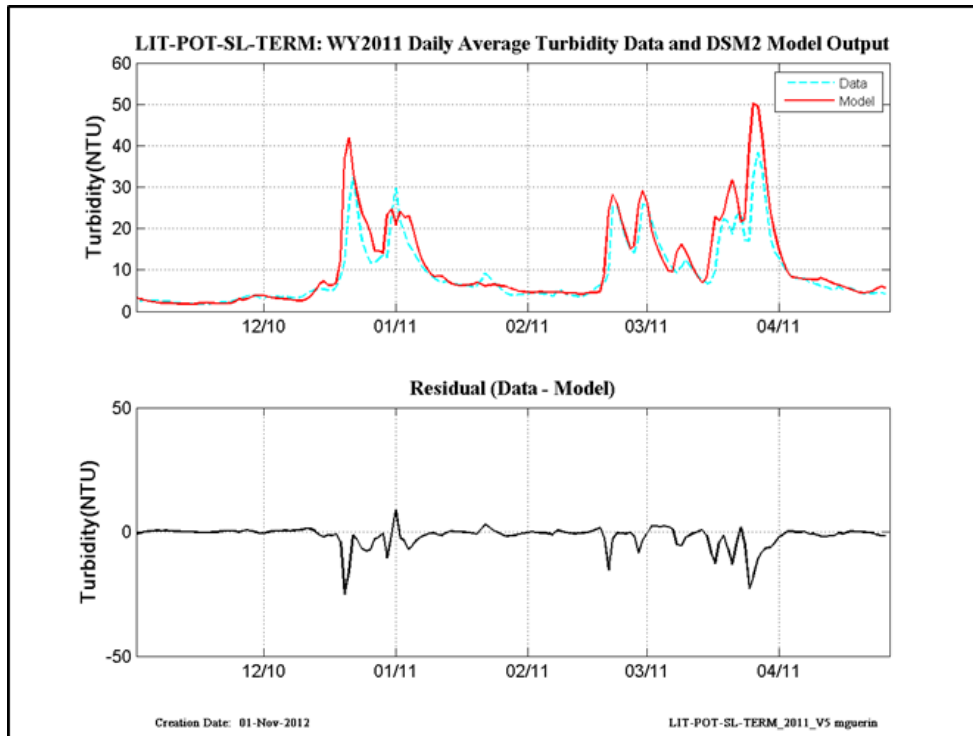


Figure 12-12 WY2011 revised calibration results at Little Potato Slough-at-Terminus.

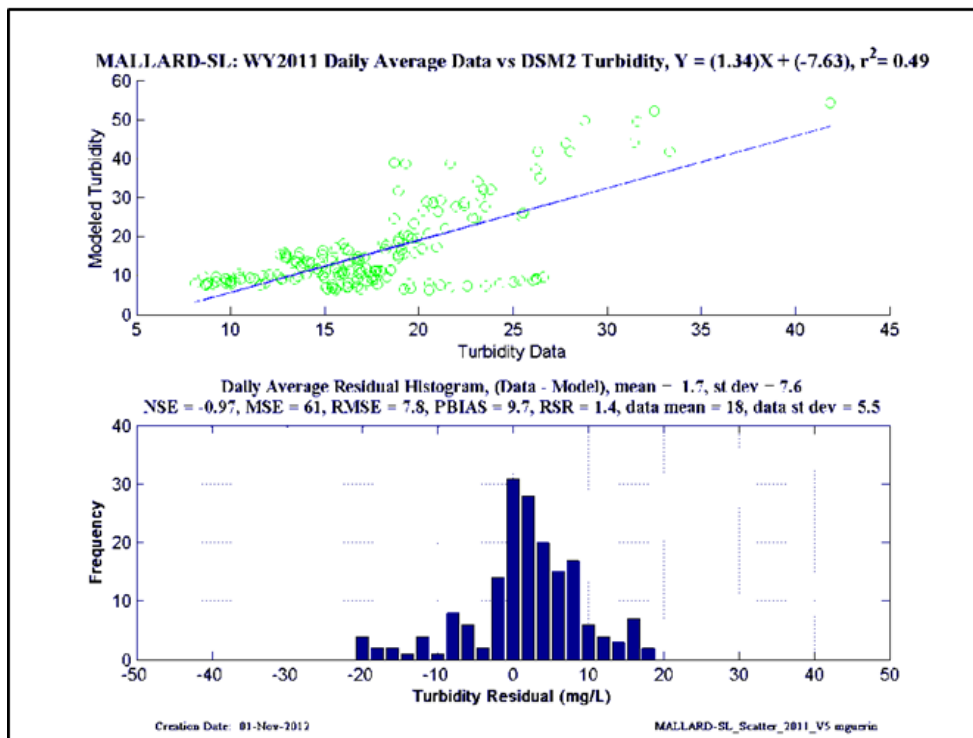
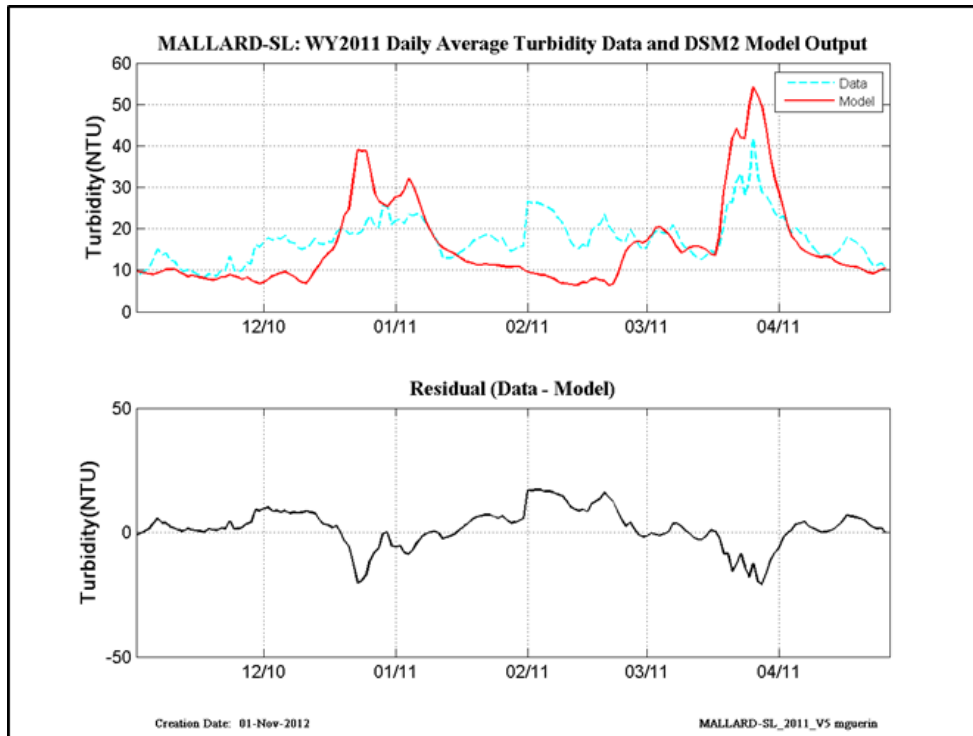


Figure 12-13 WY2011 revised calibration results at Mallard Slough.

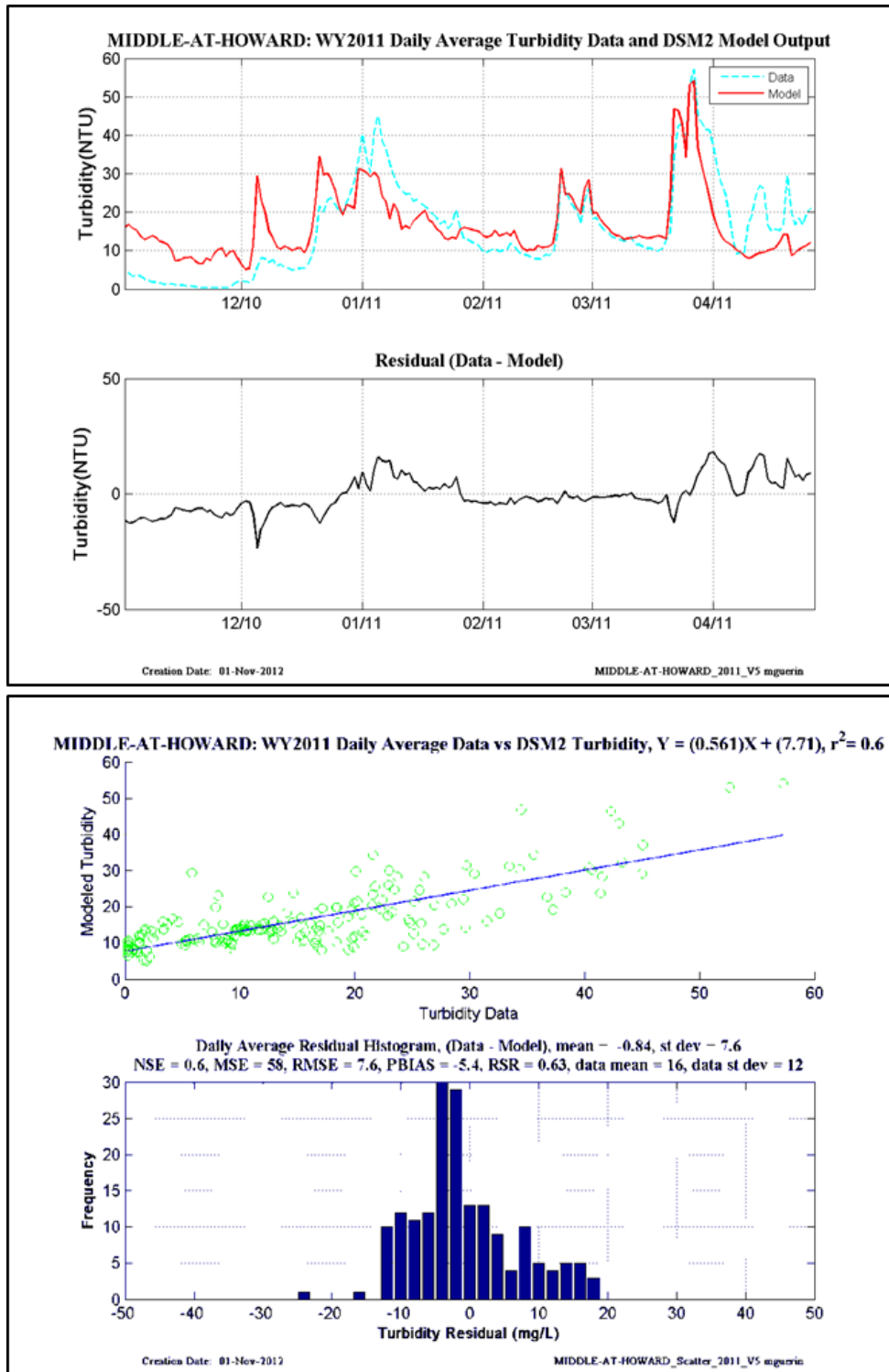


Figure 12-14 WY2011 revised calibration results at Middle River-at-Howard Rd.

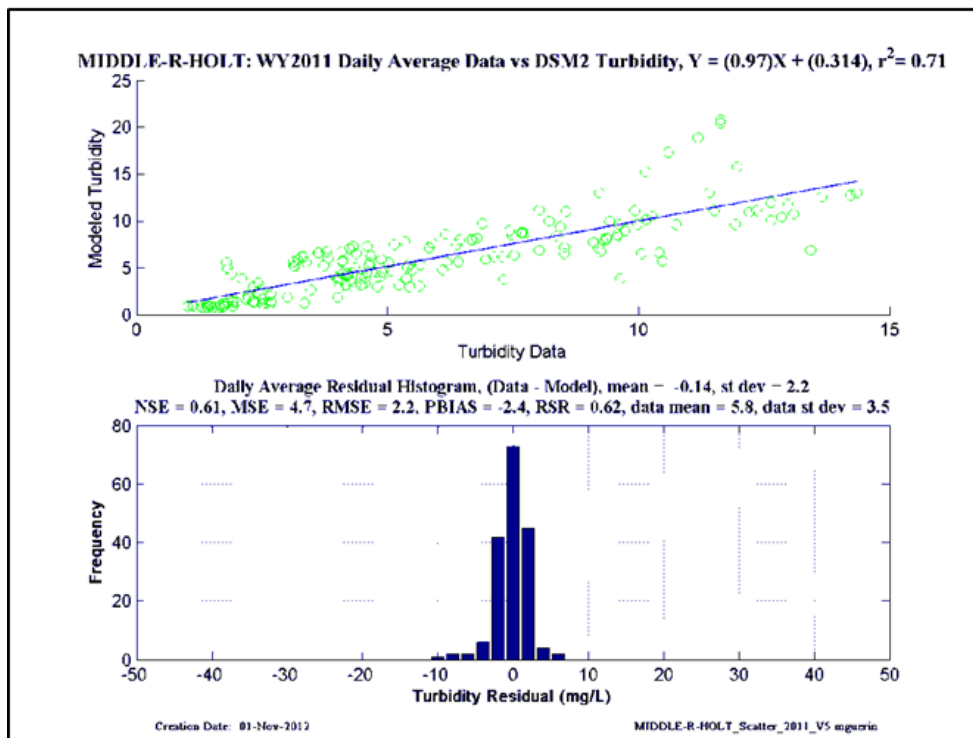
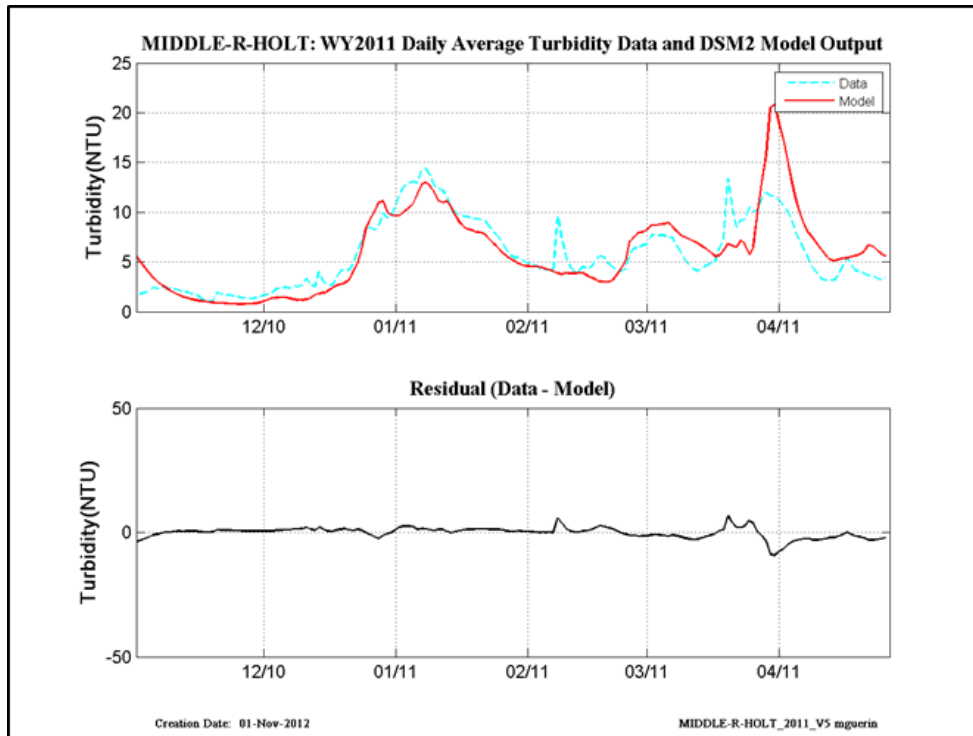


Figure 12-15 WY2011 revised calibration results at Middle River-at-Holt.

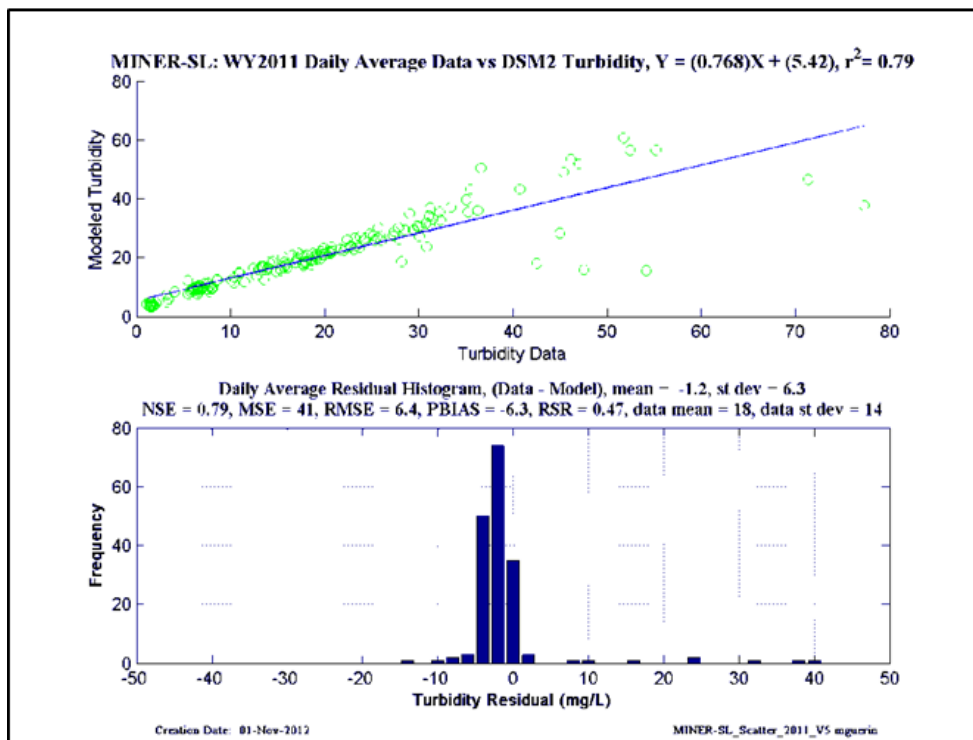
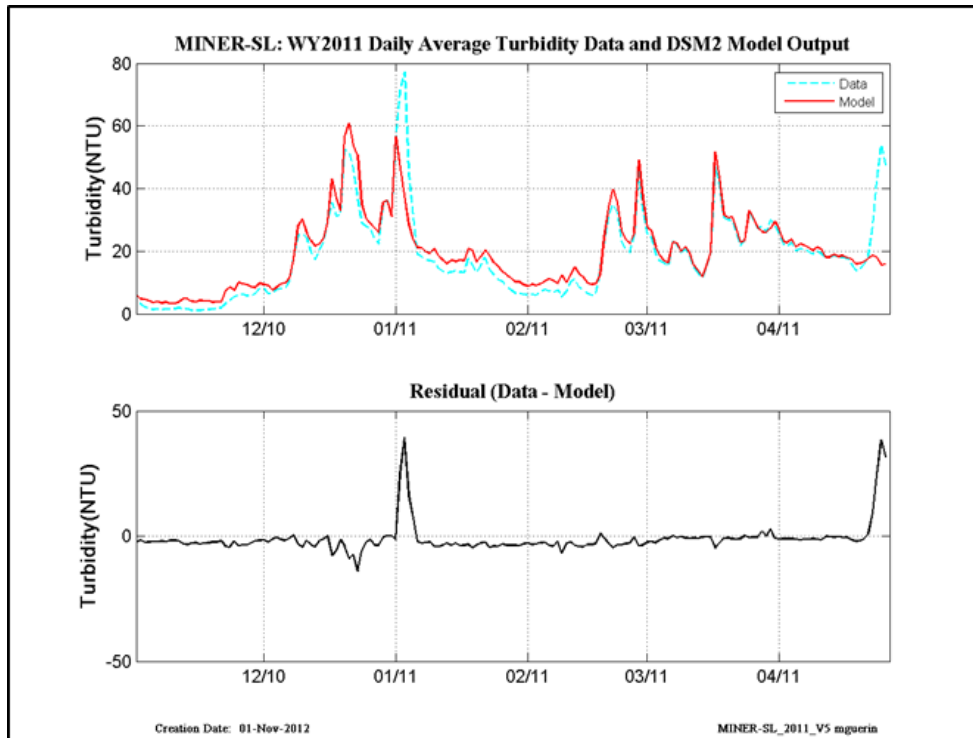


Figure 12-16 WY2011 revised calibration results at Miner Slough.

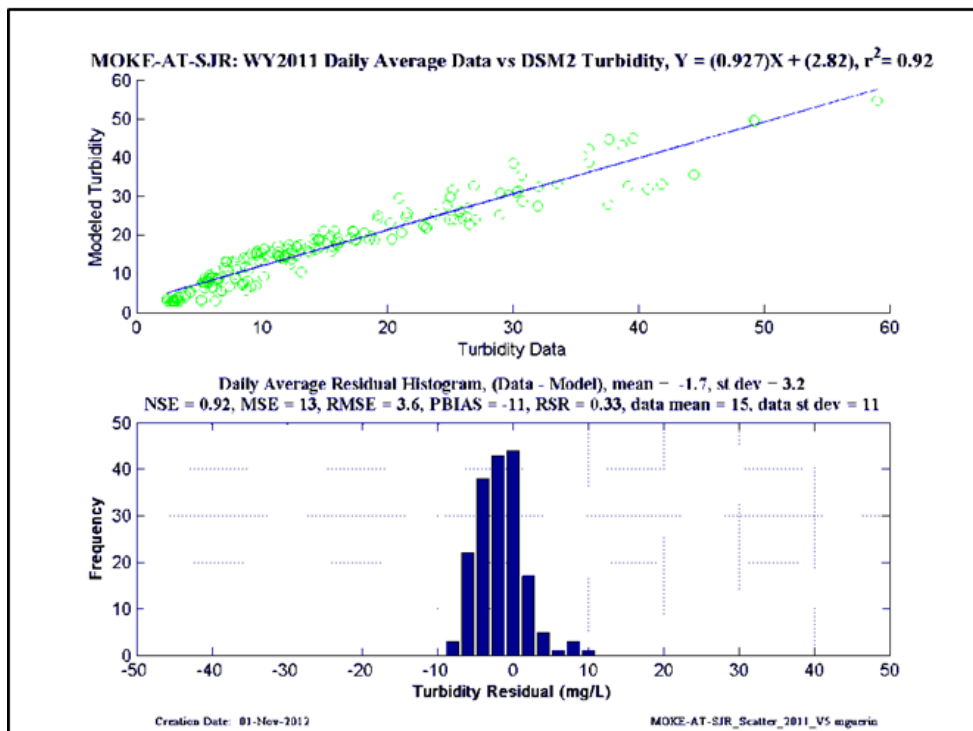
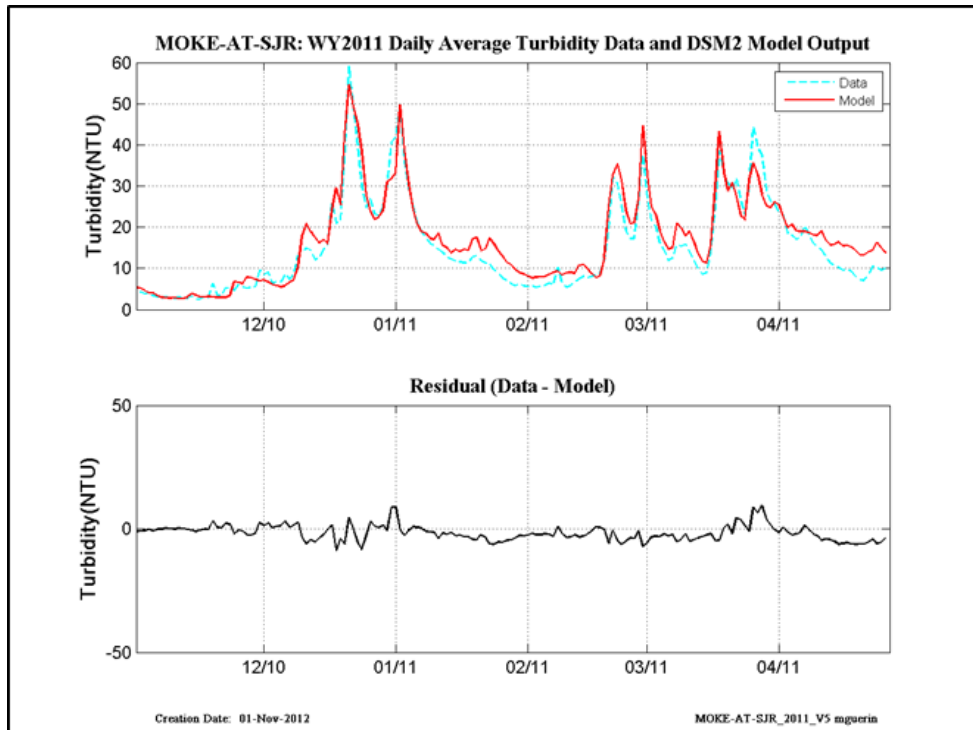


Figure 12-17 WY2011 revised calibration results at Mokelumne-at-San Joaquin.

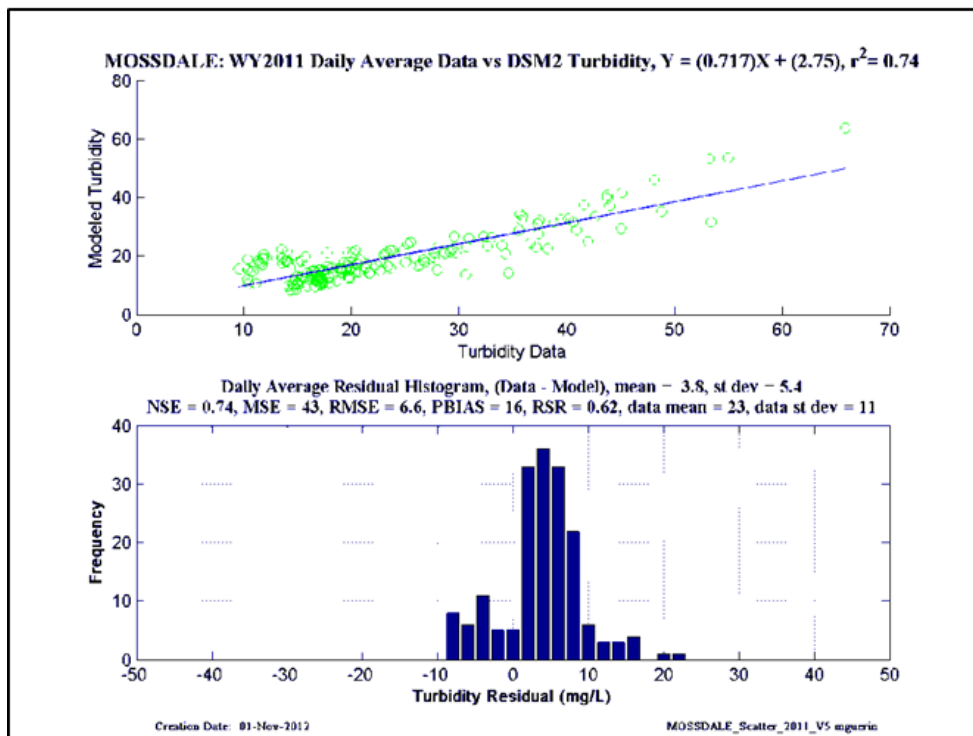
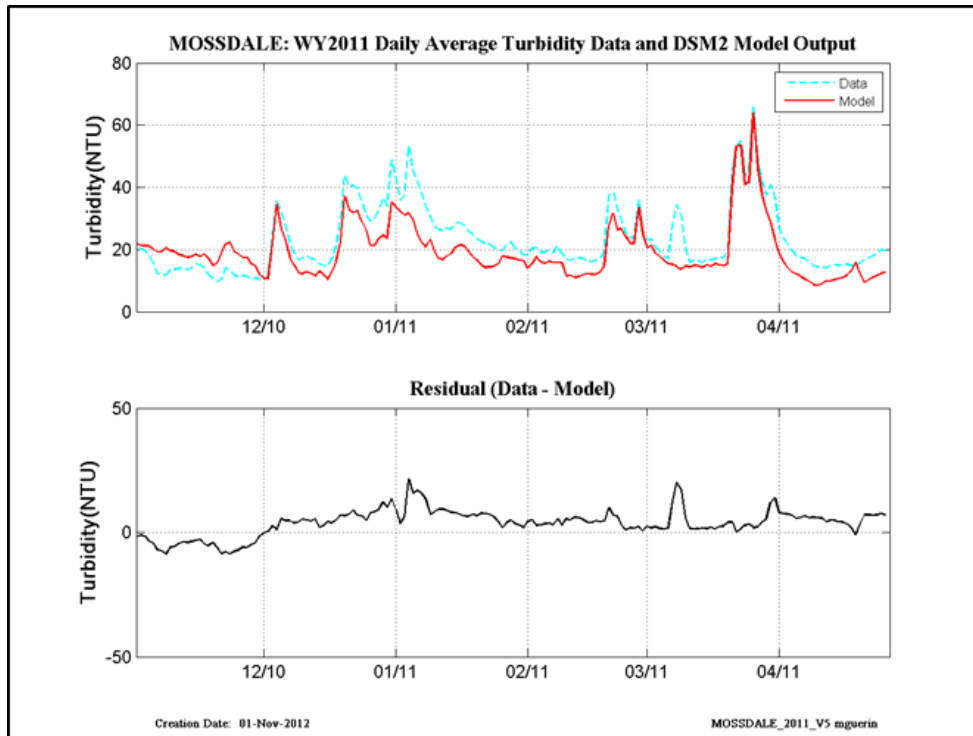


Figure 12-18 WY2011 revised calibration results at Mossdale.

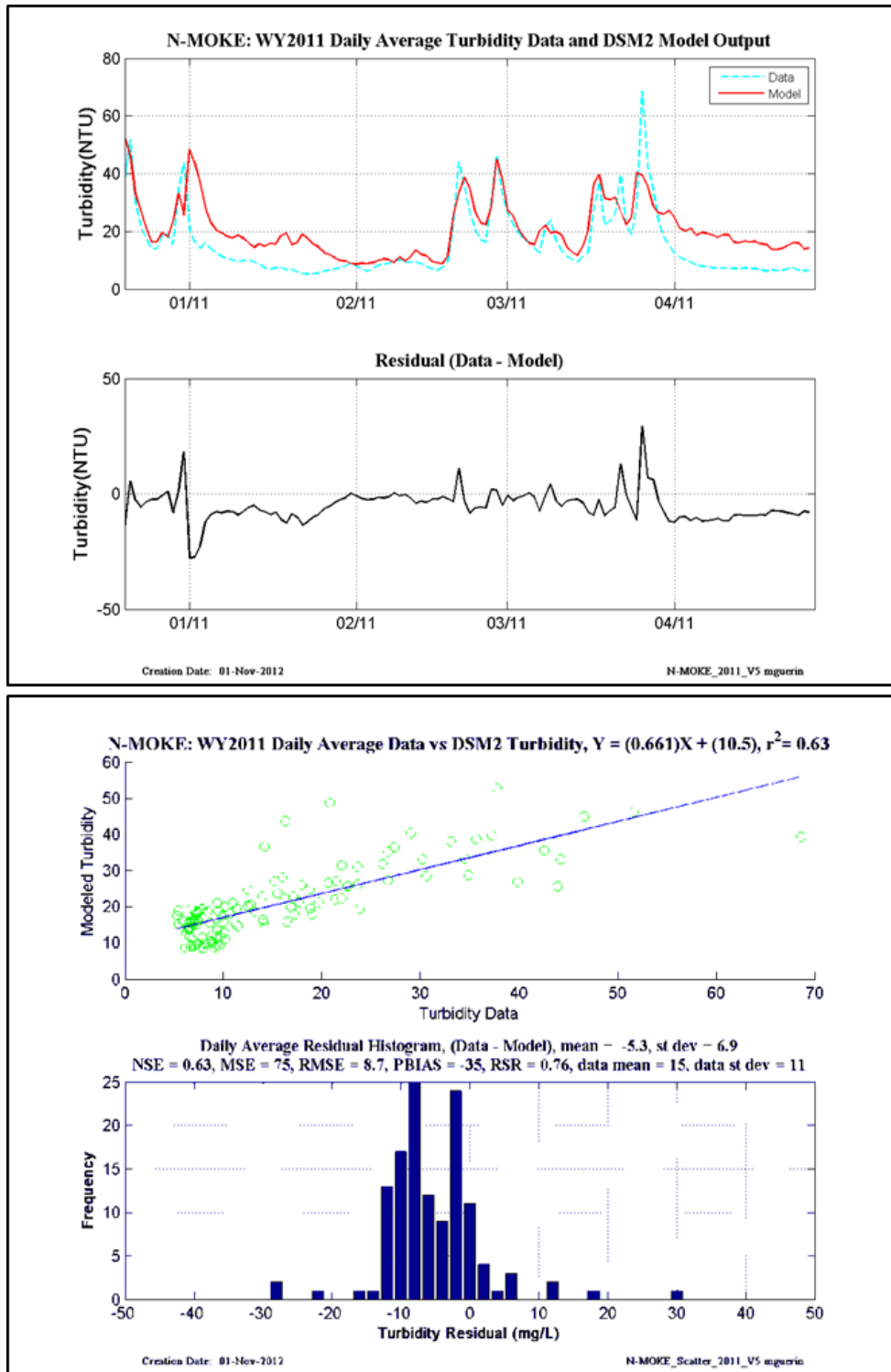


Figure 12-19 WY2011 revised calibration results at North Mokelumne.

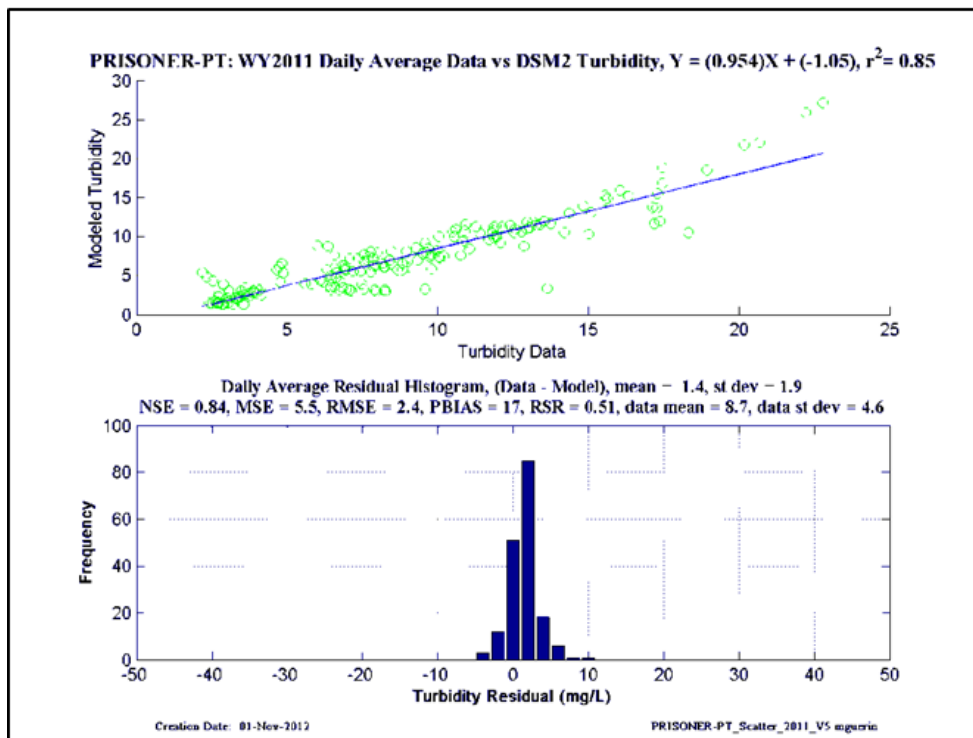
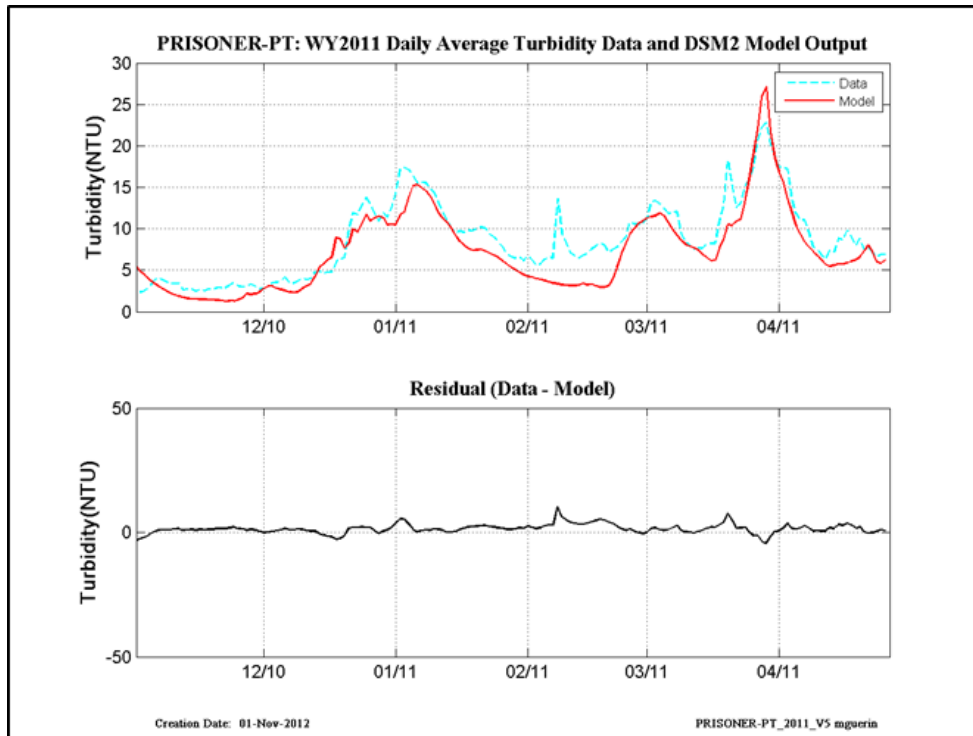


Figure 12-20 WY2011 revised calibration results at Prisoner Point.

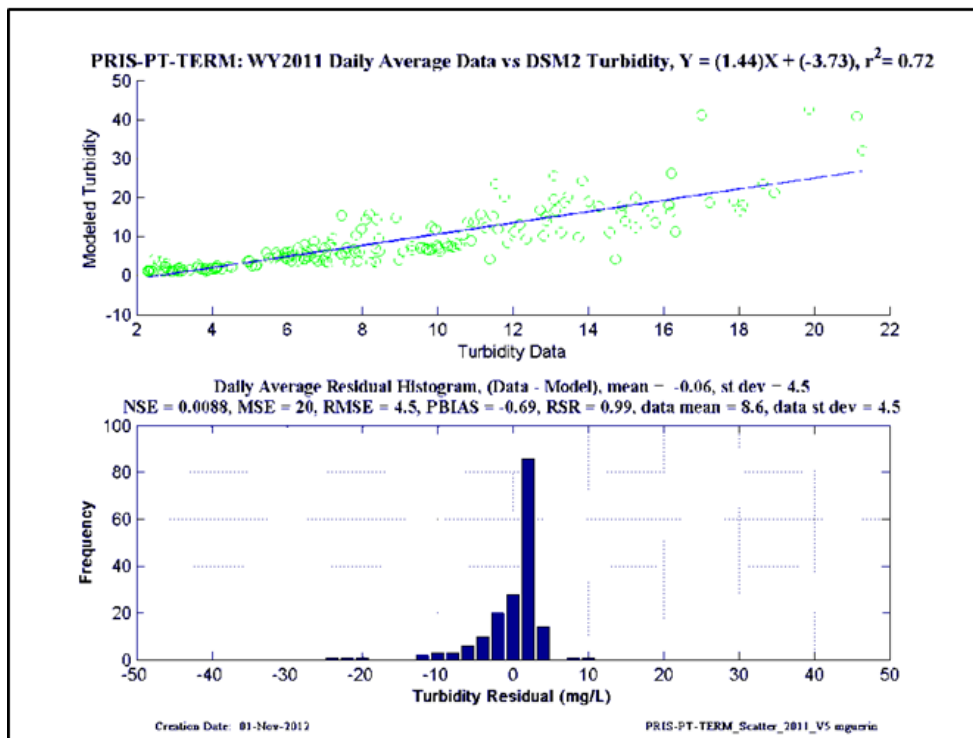
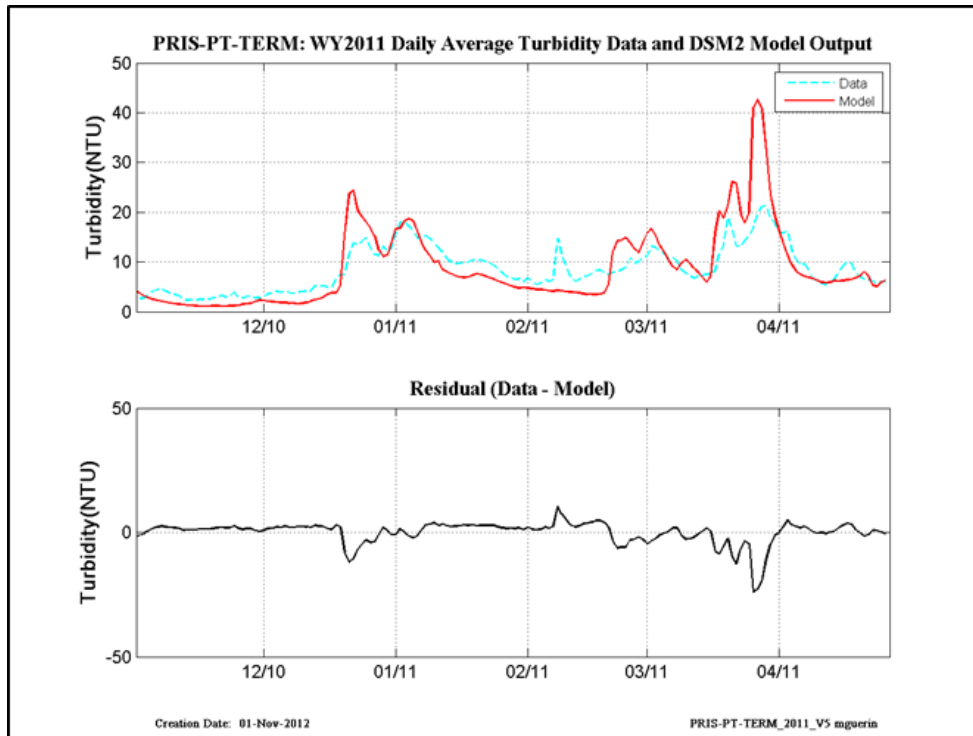


Figure 12-21 WY2011 revised calibration results at Prisoner Point-at-Terminus.

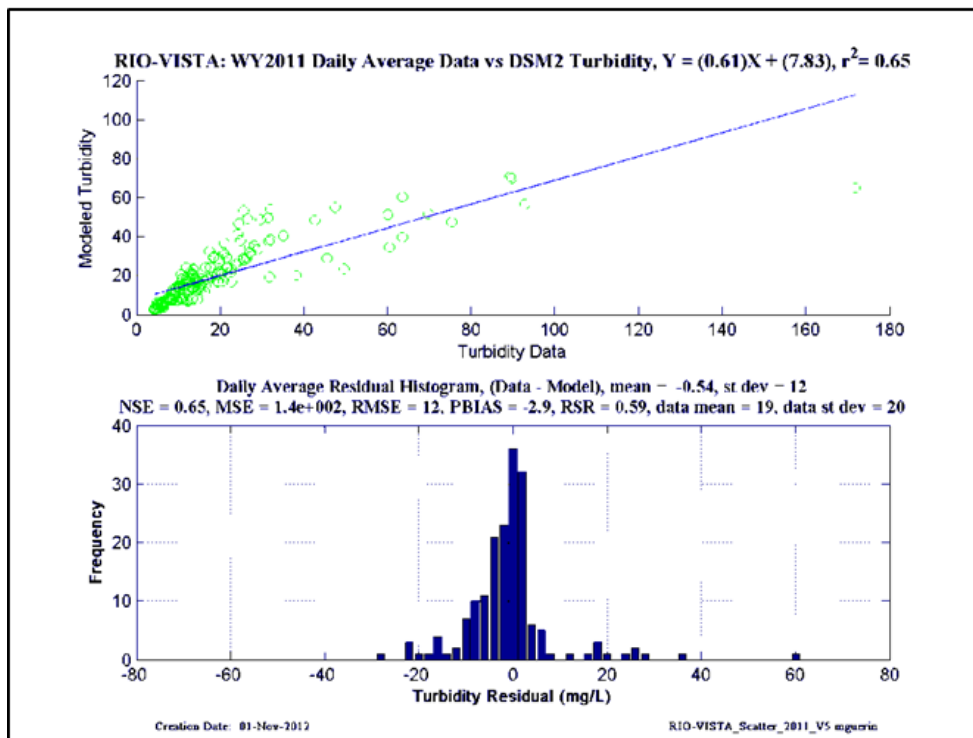
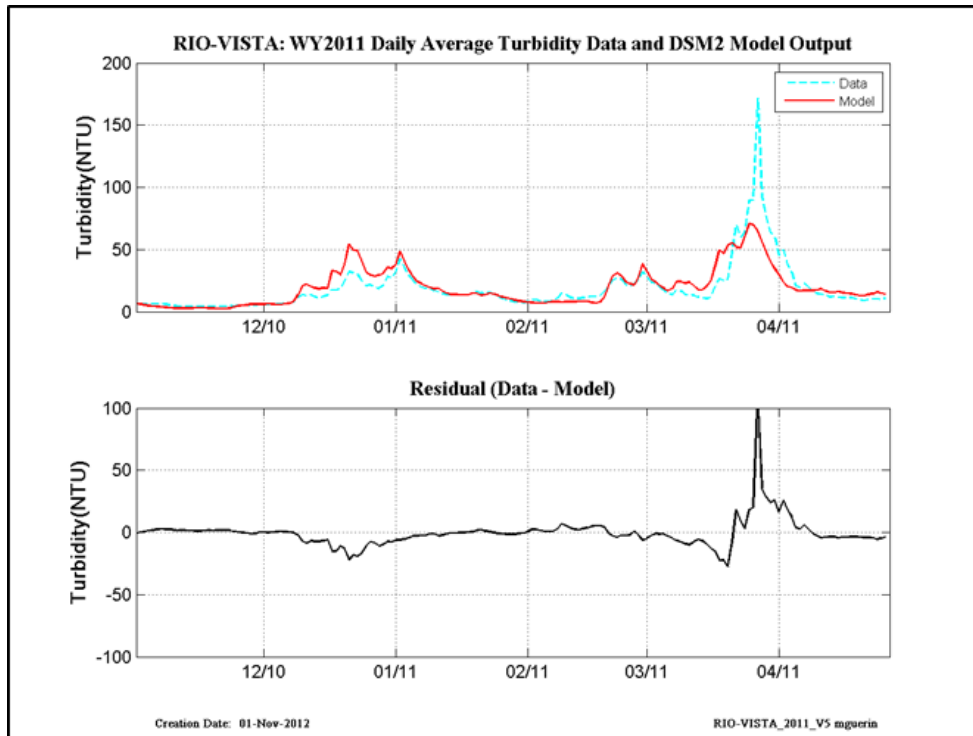


Figure 12-22 WY2011 revised calibration results at Rio Vista.

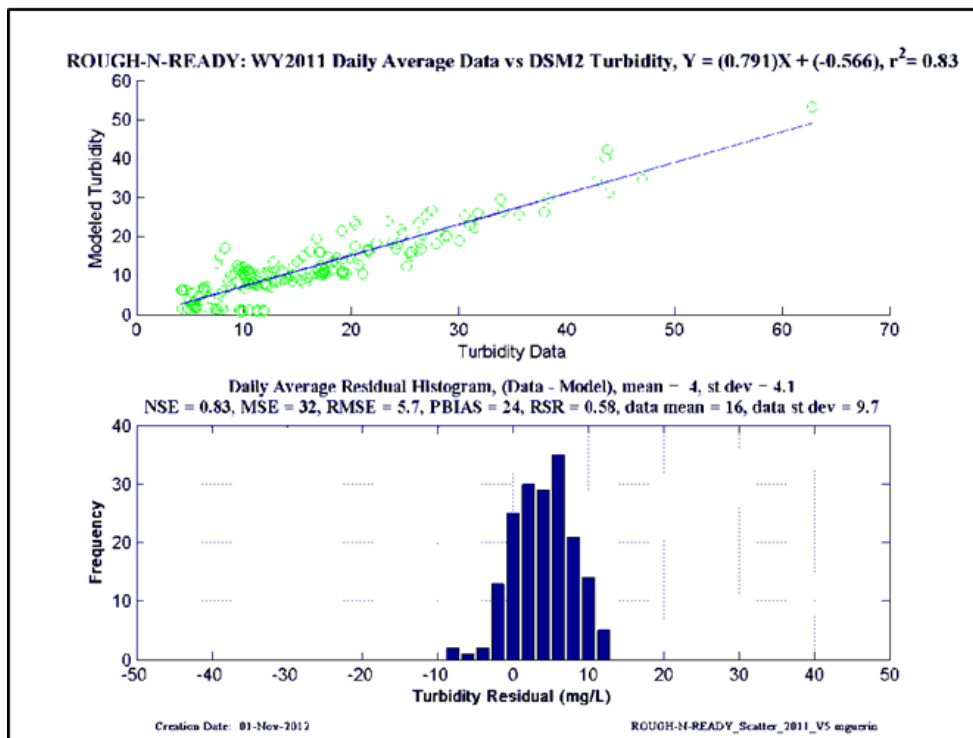
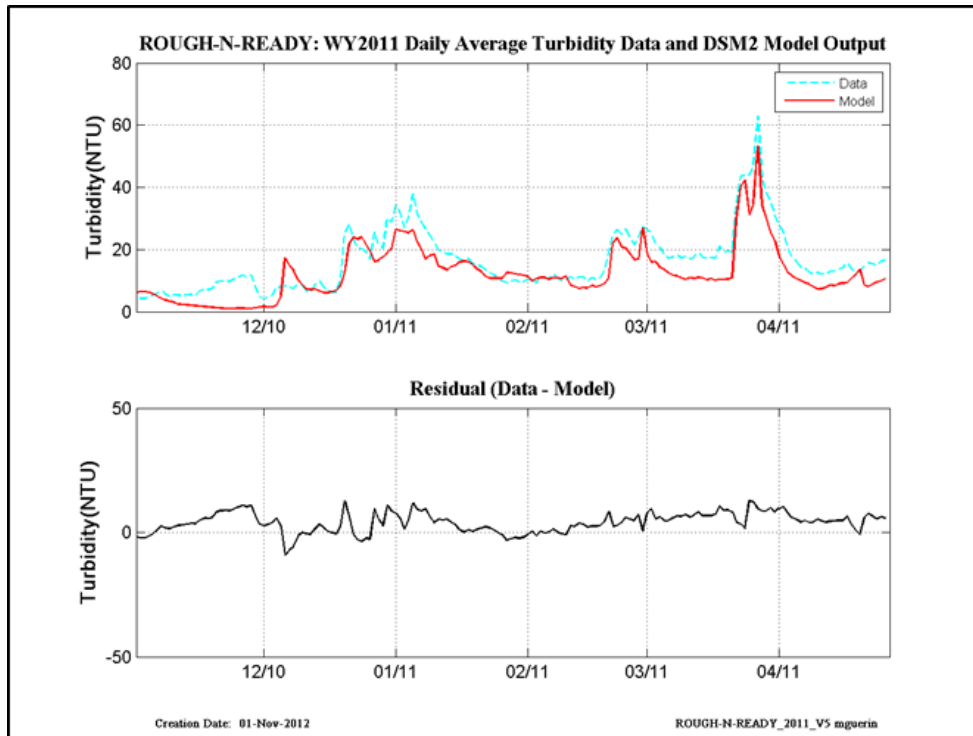


Figure 12-23 WY2011 revised calibration results at Rough-N-Ready Island.

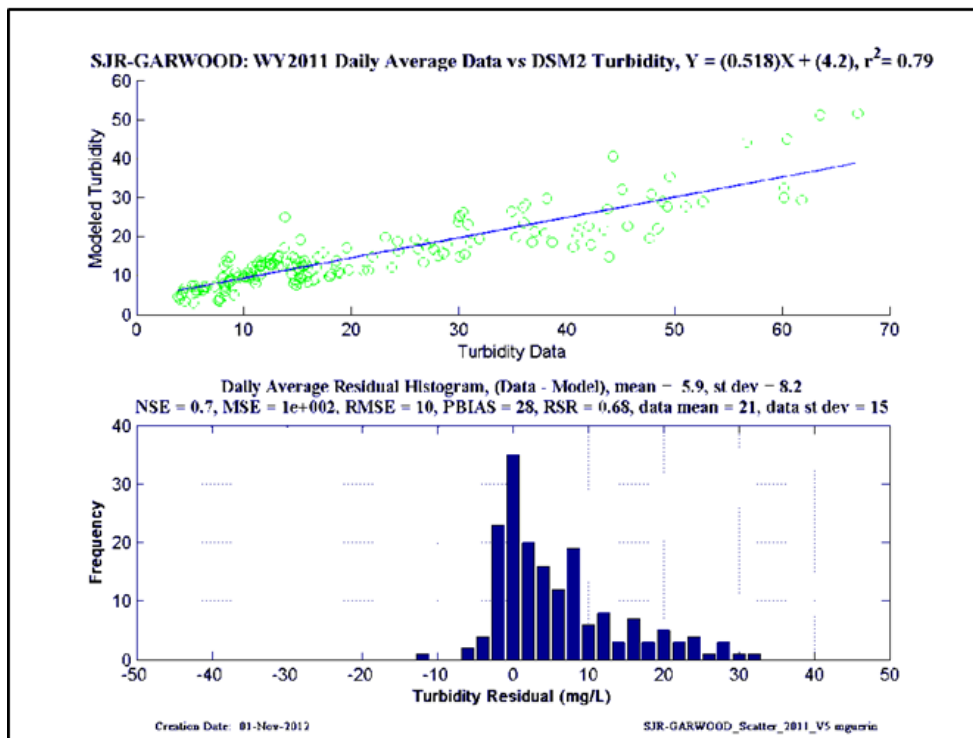
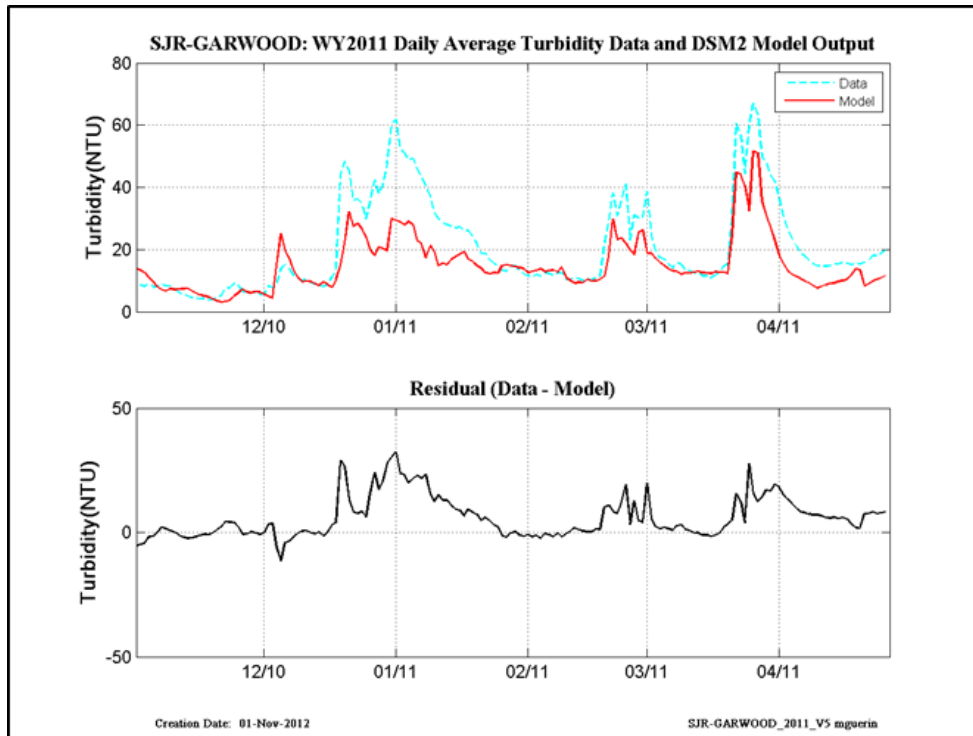


Figure 12-24 WY2011 revised calibration results at San Joaquin-at-Garwood.

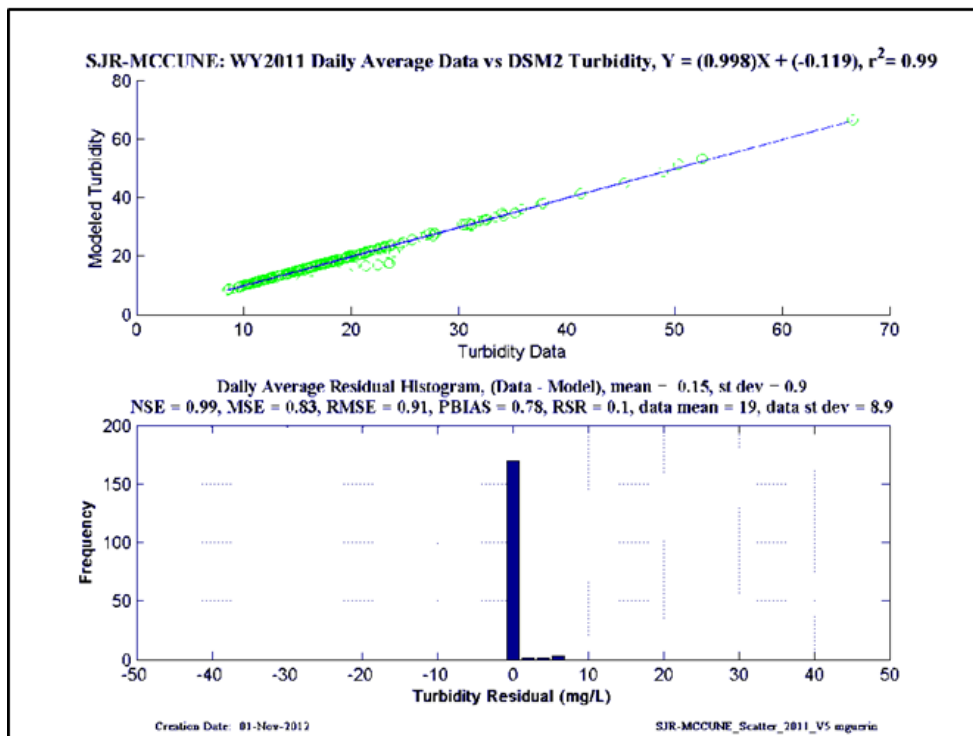
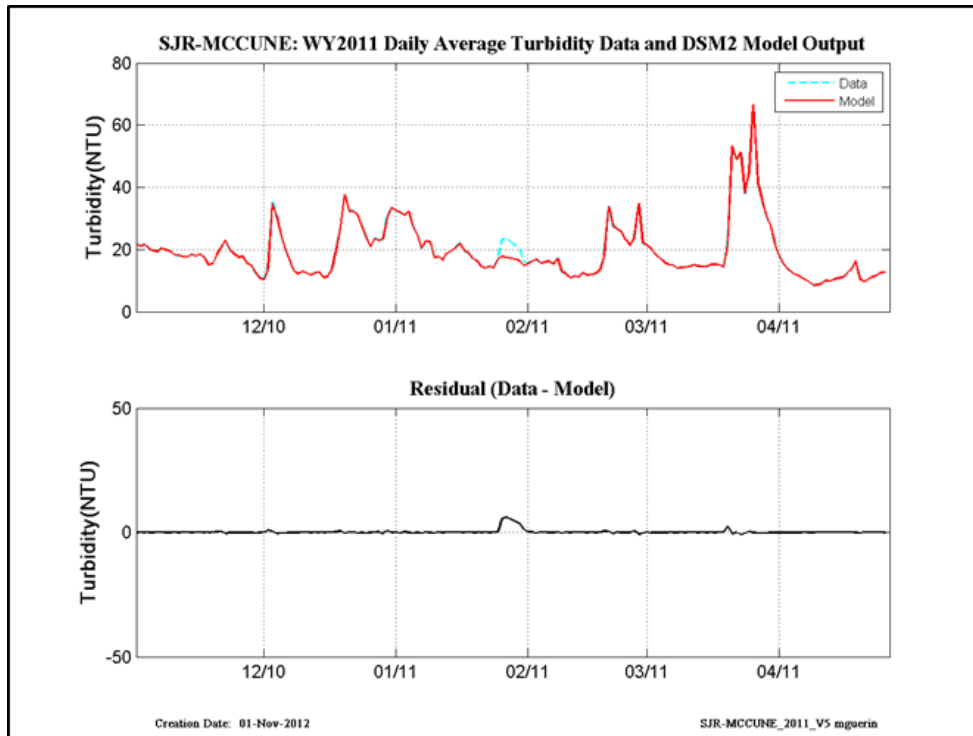


Figure 12-25 WY2011 revised calibration results at San Joaquin-at-McCune (Vernalis).

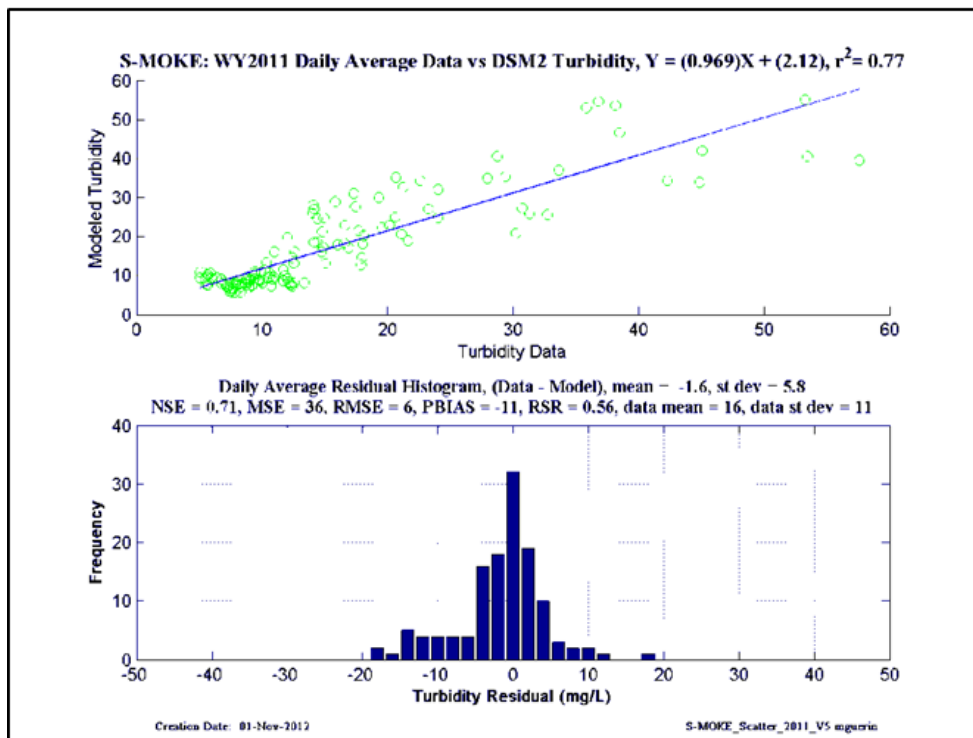
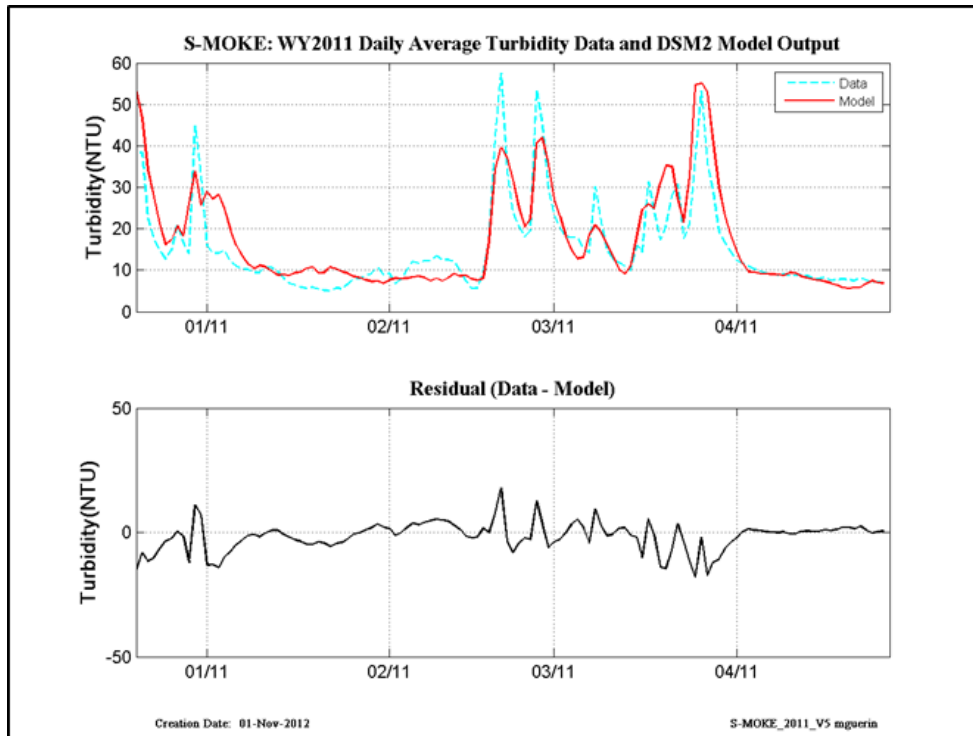


Figure 12-26 WY2011 revised calibration results at South Mokelumne.

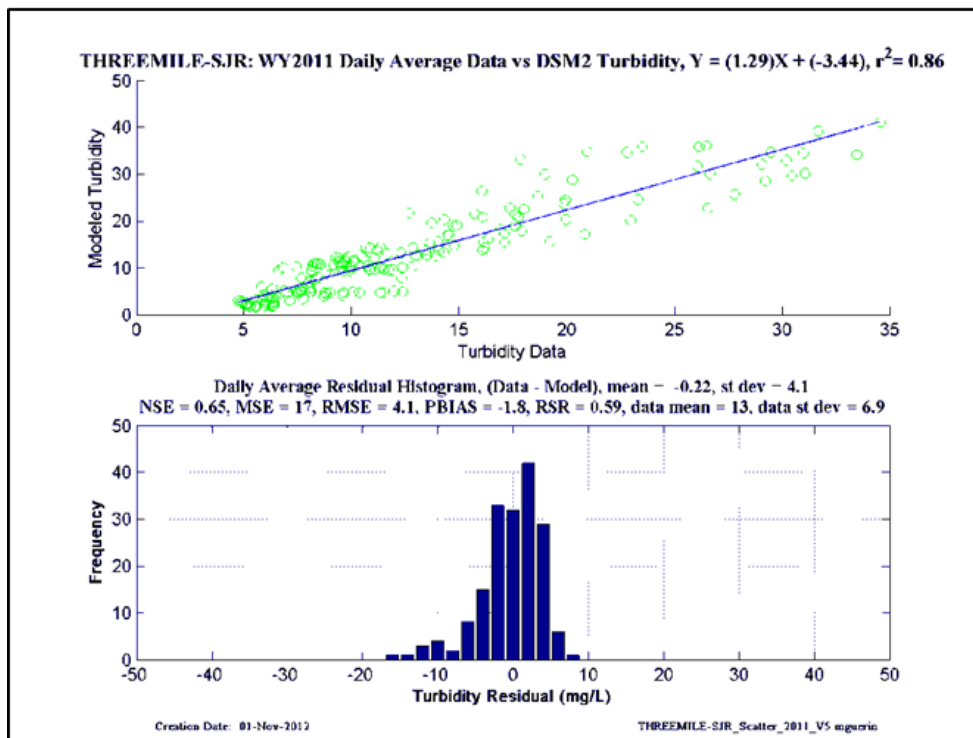
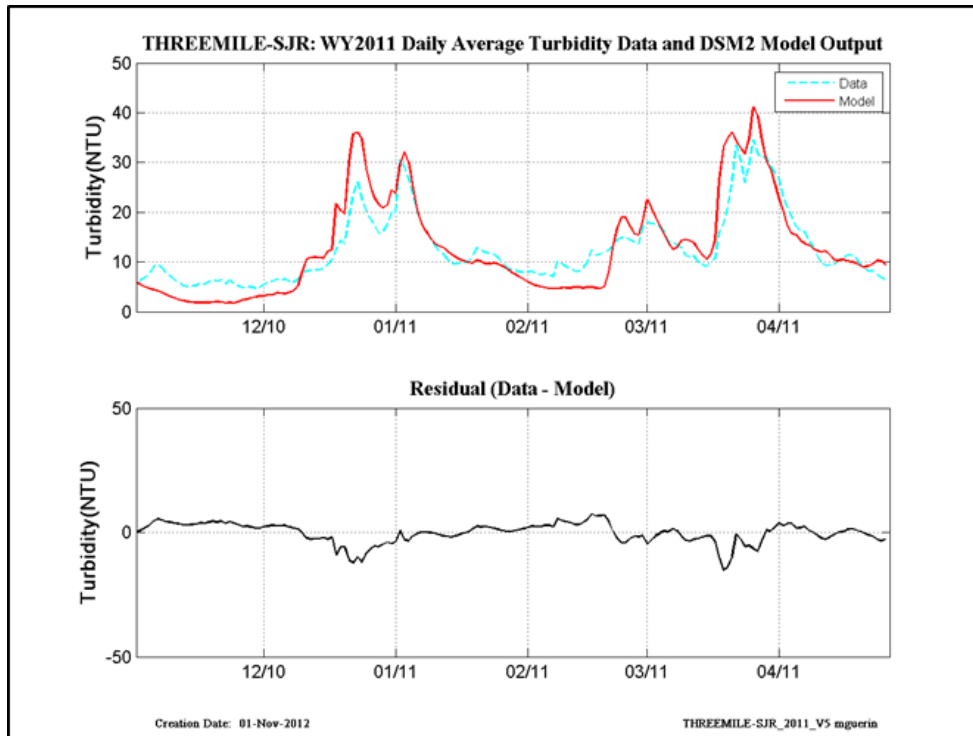


Figure 12-27 WY2011 revised calibration results at Threemile-Slough-at-San Joaquin.

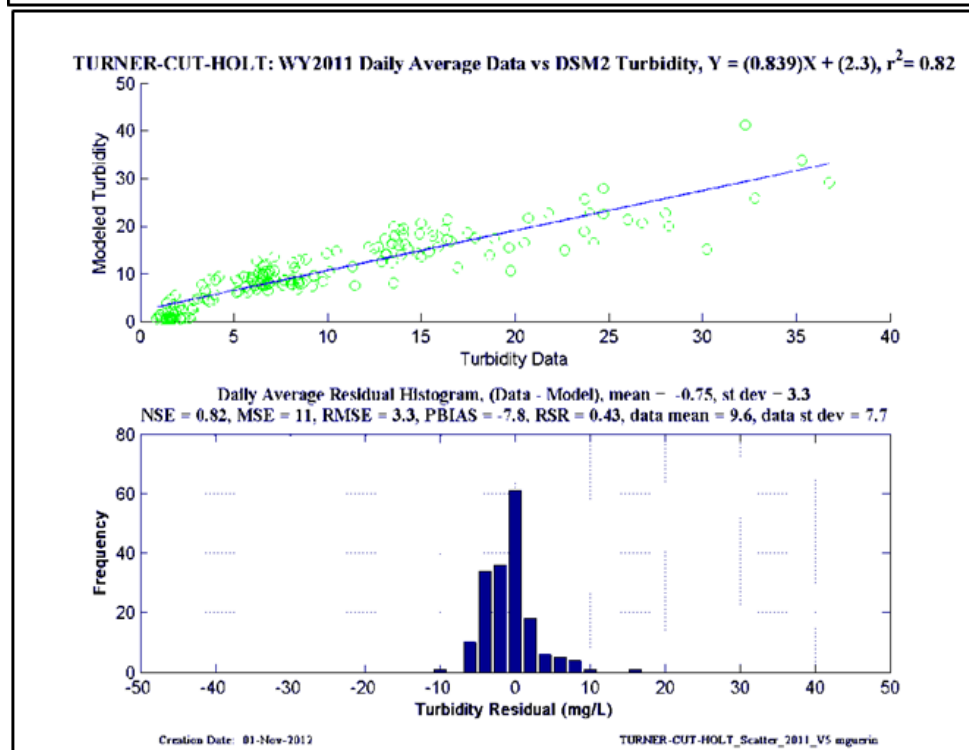
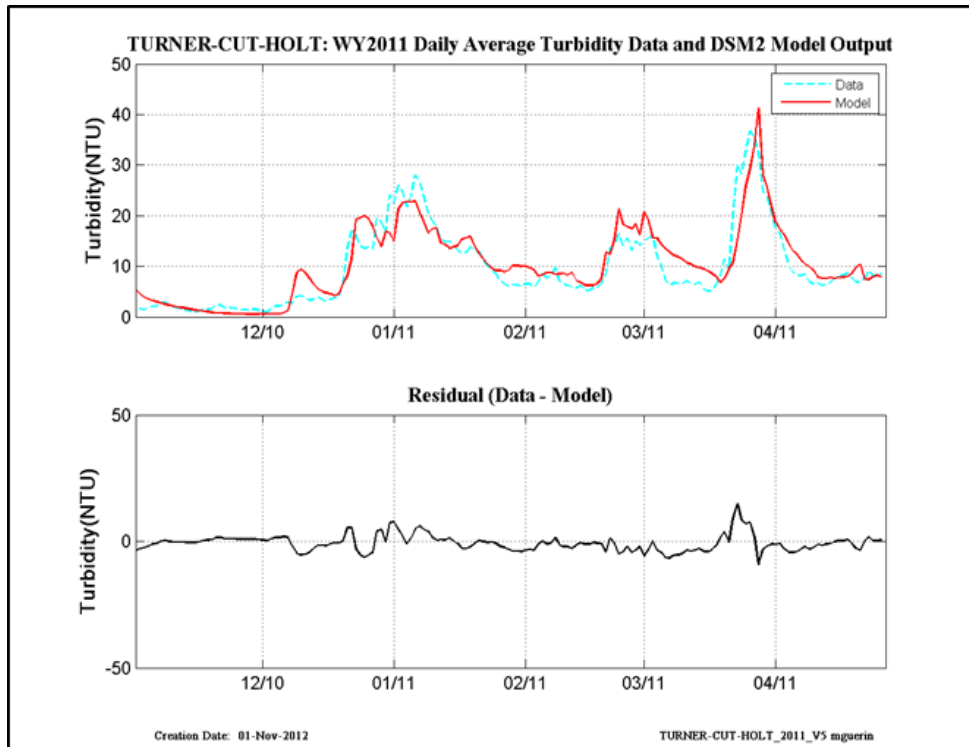


Figure 12-28 WY2011 revised calibration results at Turner Cut-at-Holt.

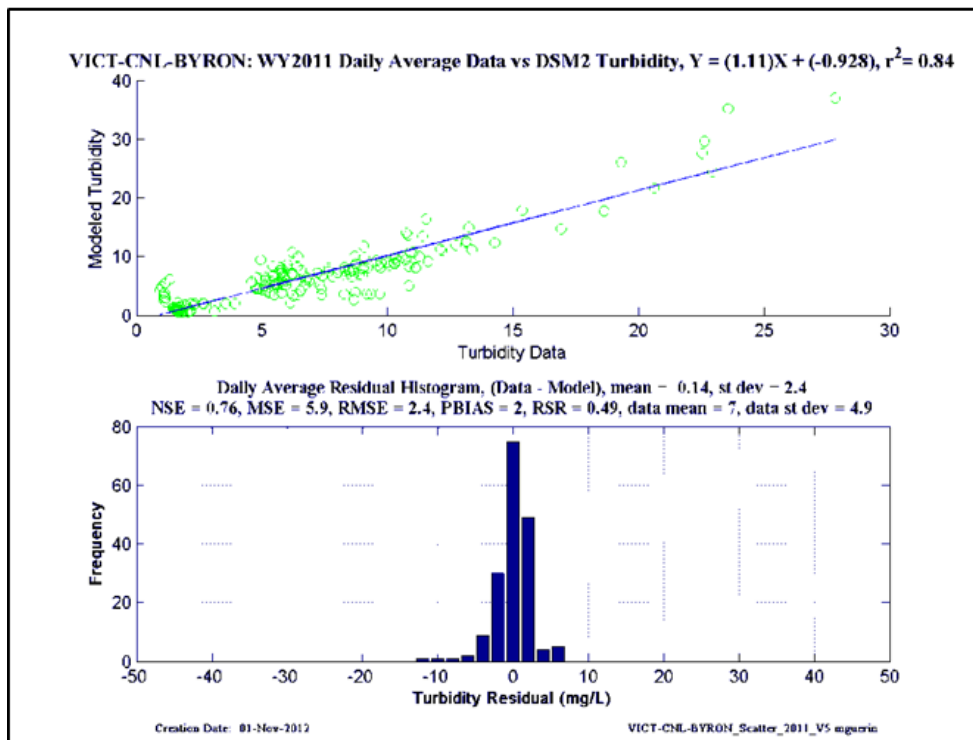
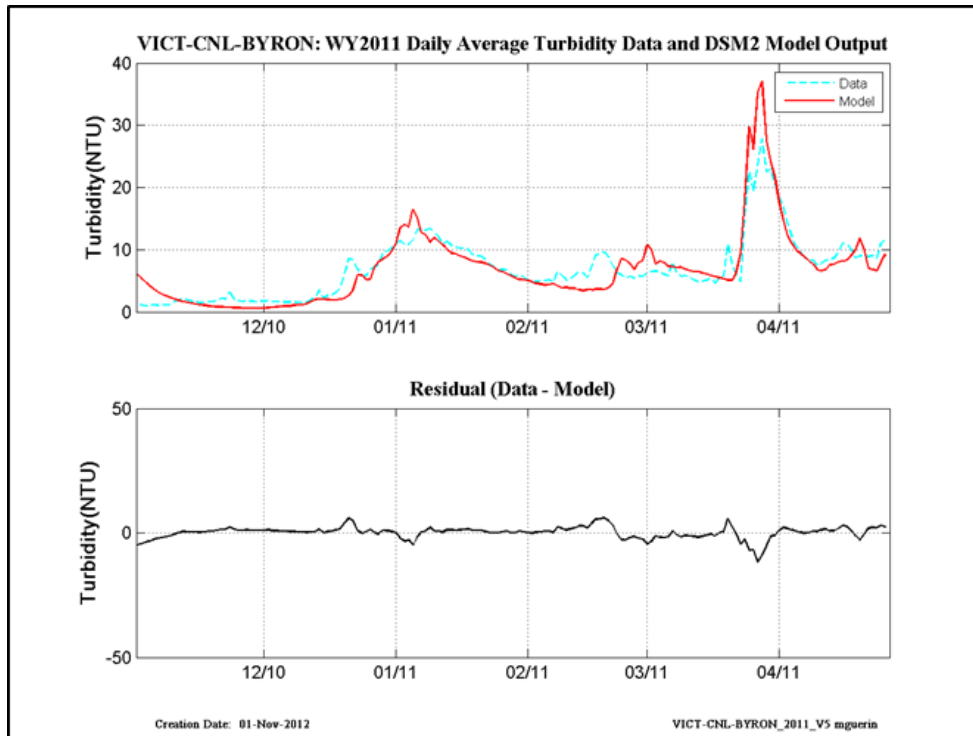


Figure 12-29 WY2011 revised calibration results at Victoria Canal-at-Byron.

12.2 Daily-averaged CDEC data and model output - WY2010

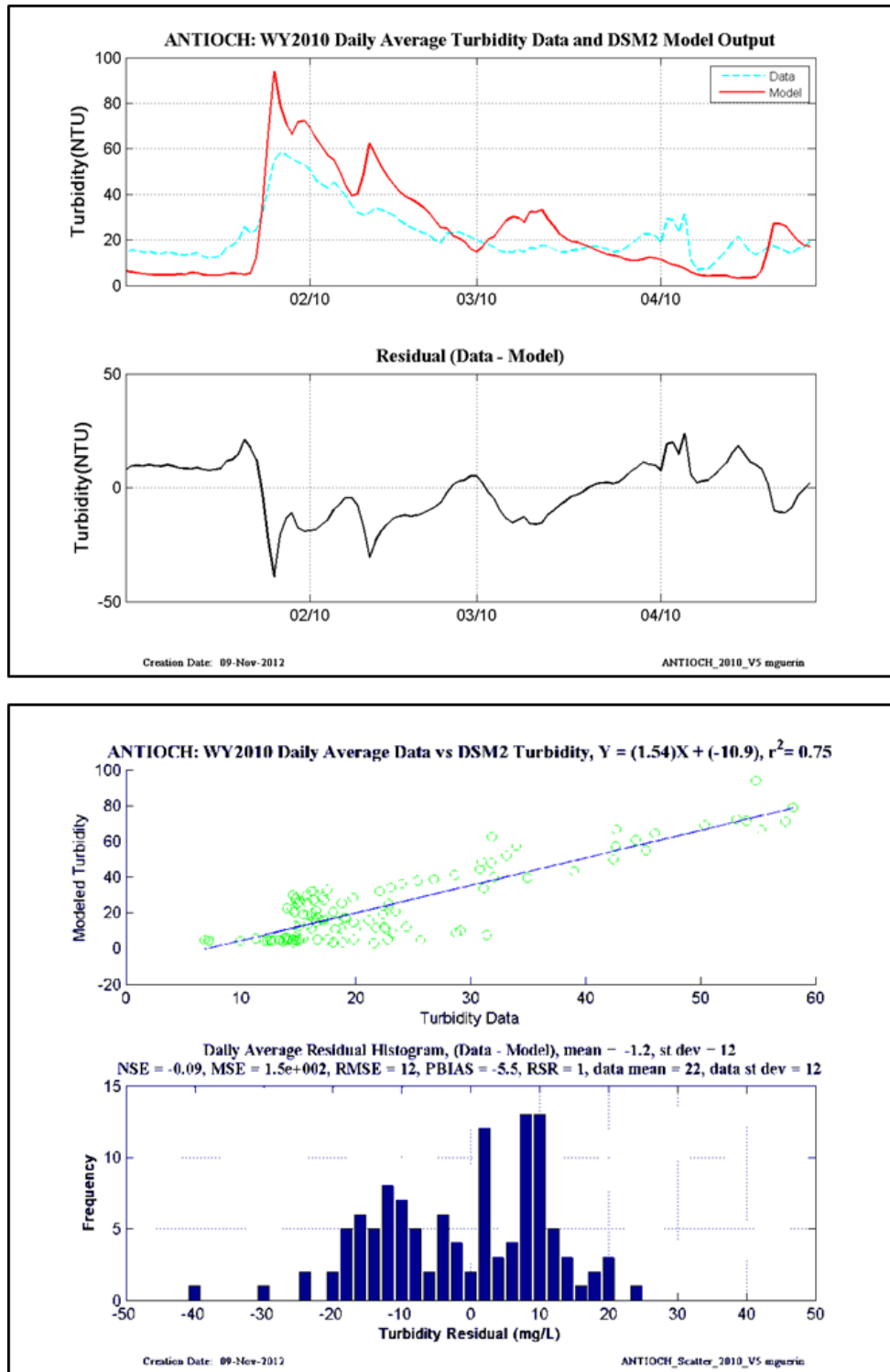


Figure 12-30 WY2010 revised calibration results at Antioch.

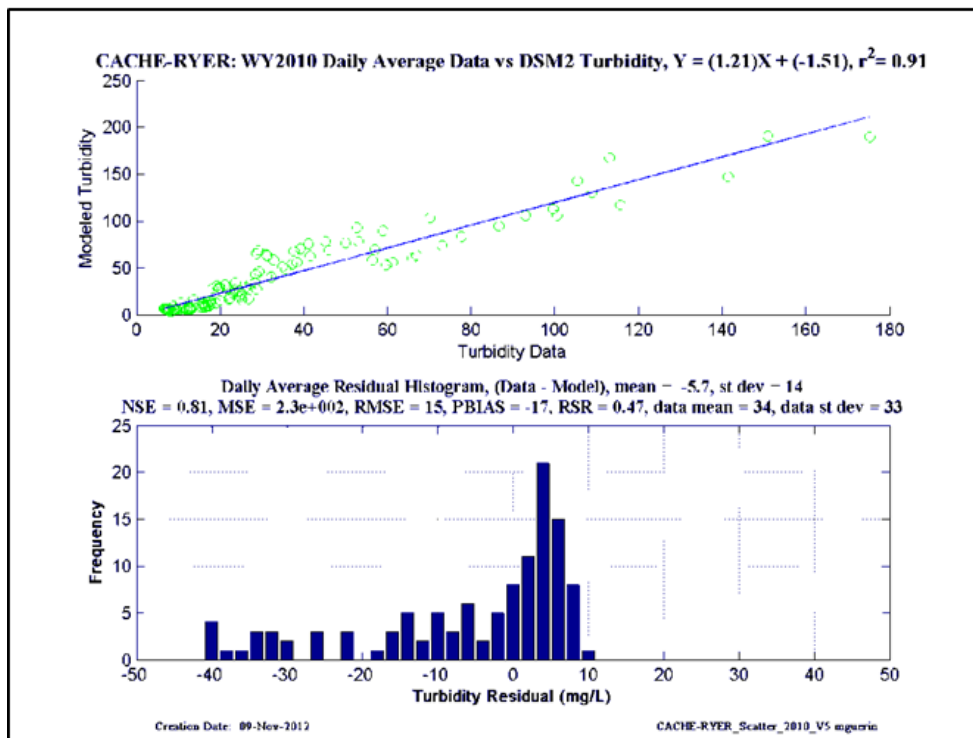
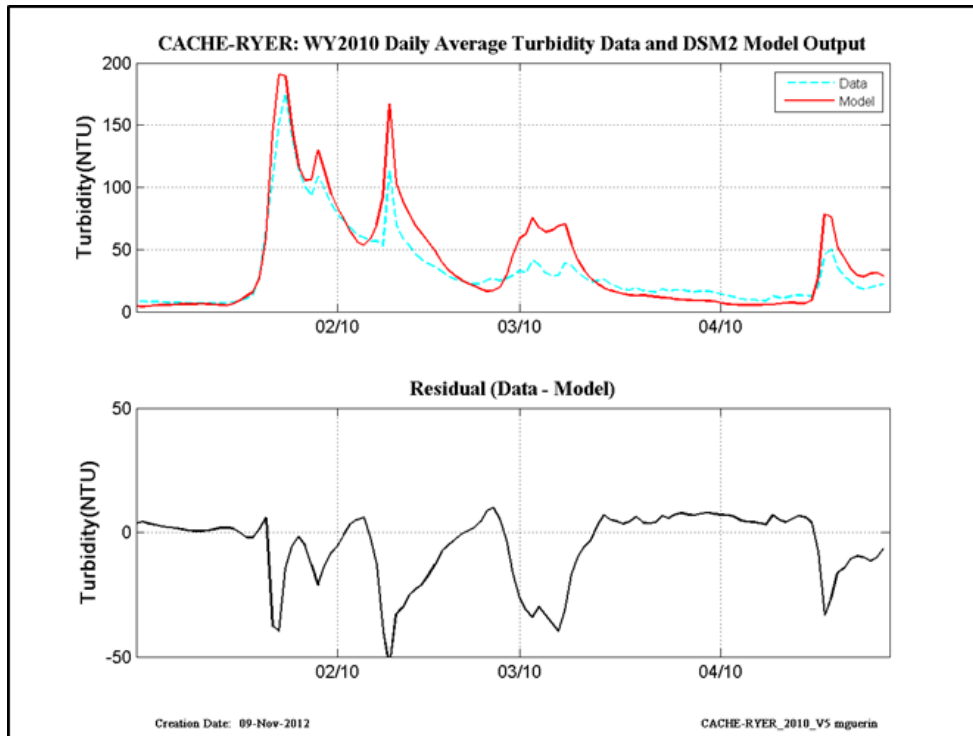


Figure 12-31 WY2010 revised calibration results at Cache-at-Ryer Island.

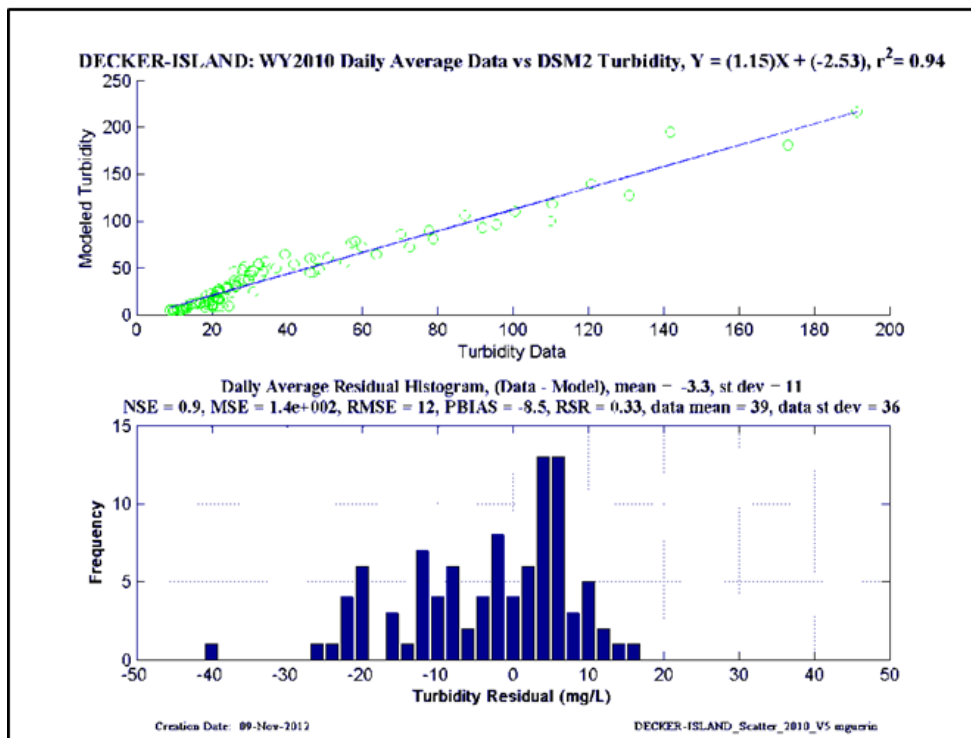
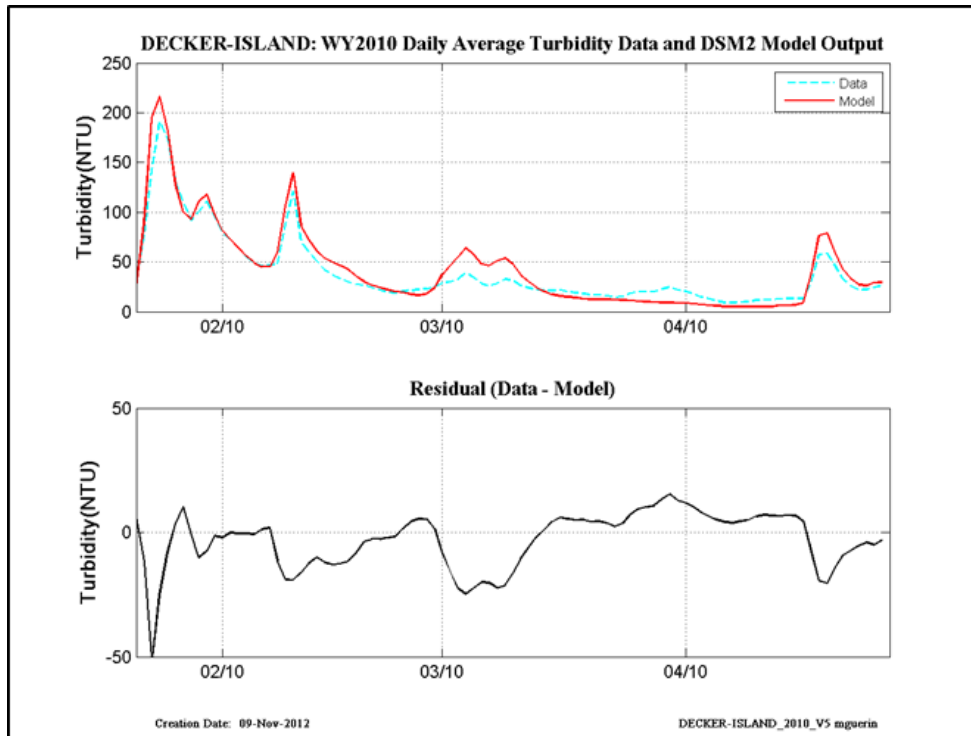


Figure 12-32 WY2010 revised calibration results at Decker Island.

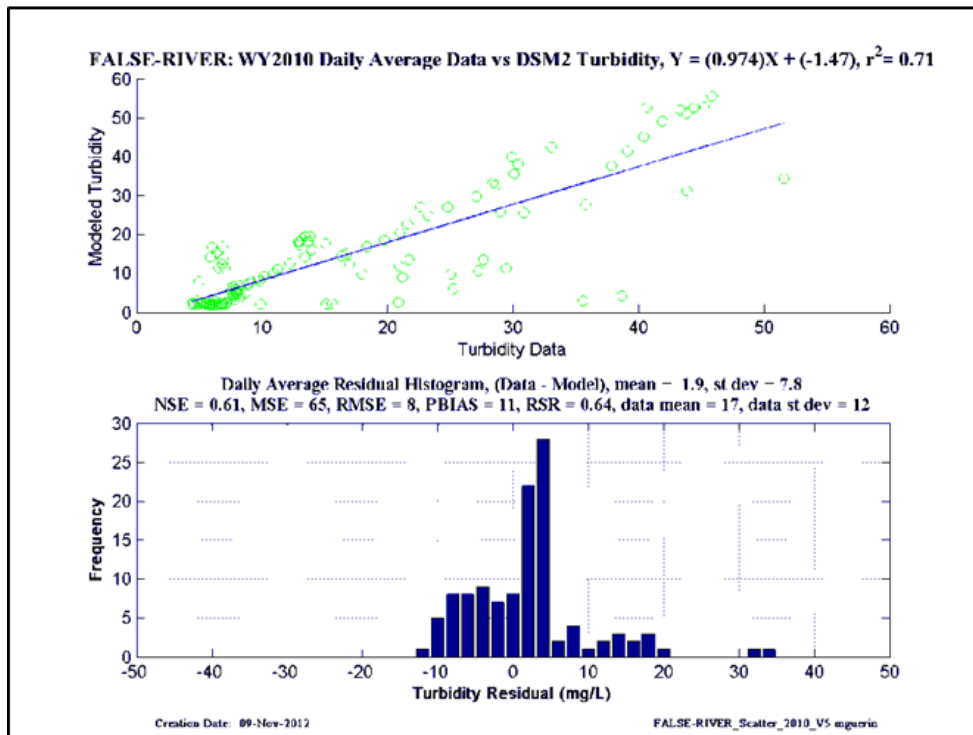
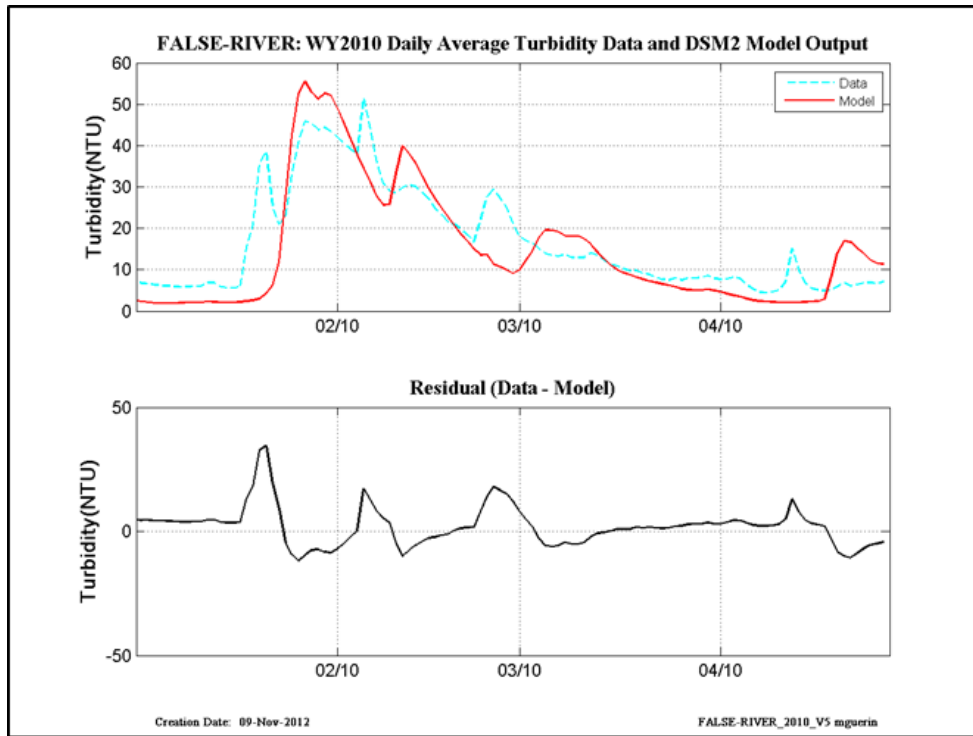


Figure 12-33 WY2010 revised calibration results at False River.

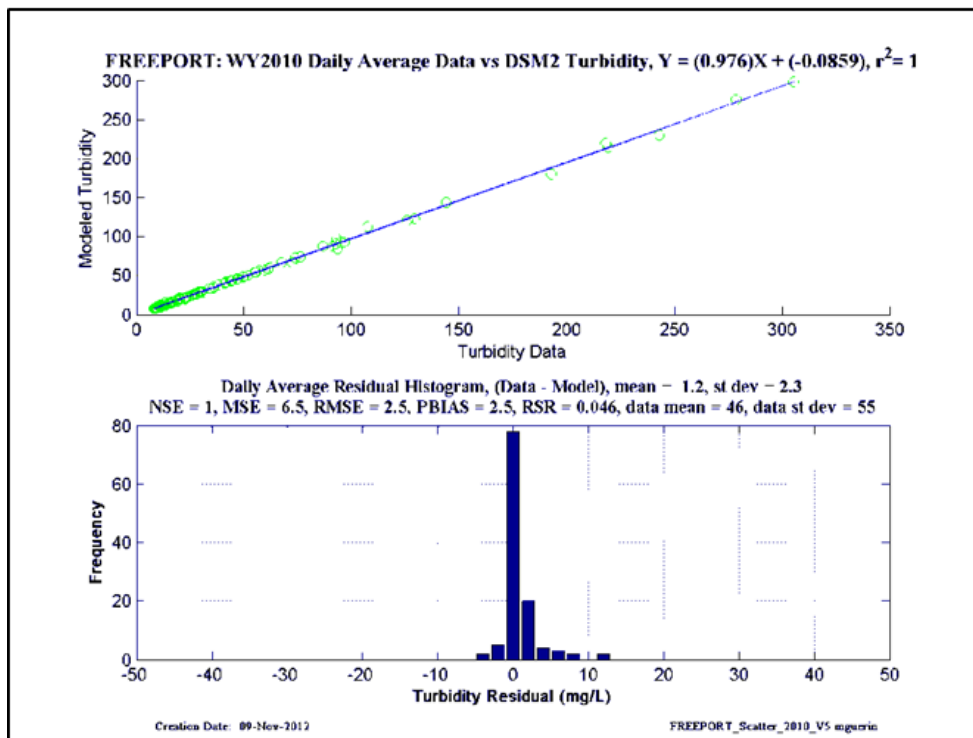
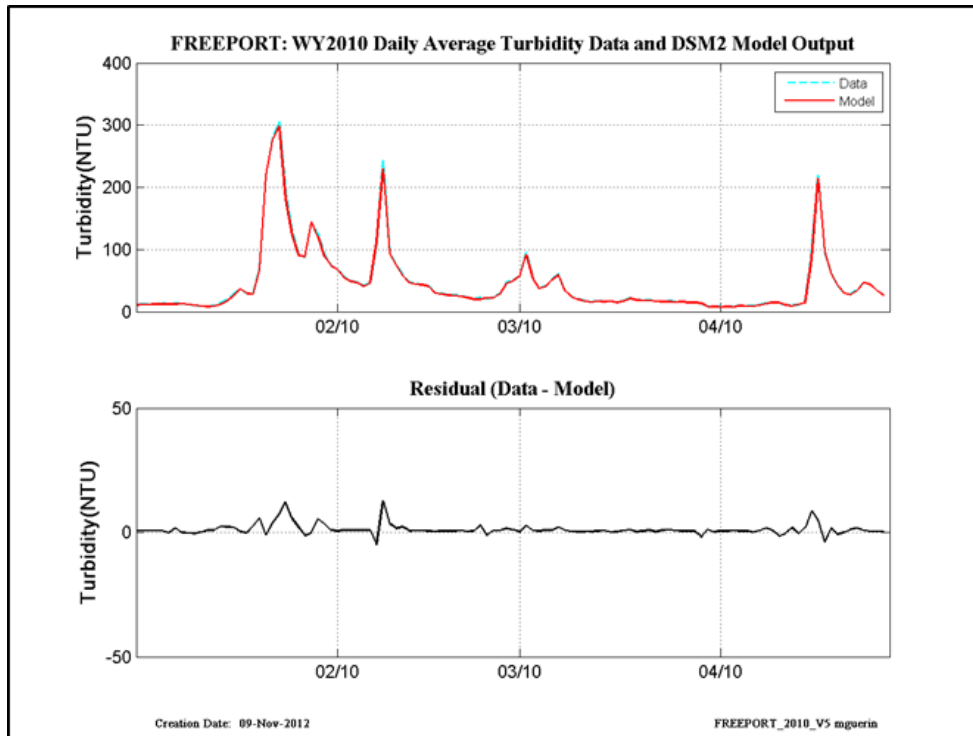


Figure 12-34 WY2010 revised calibration results at Freeport.

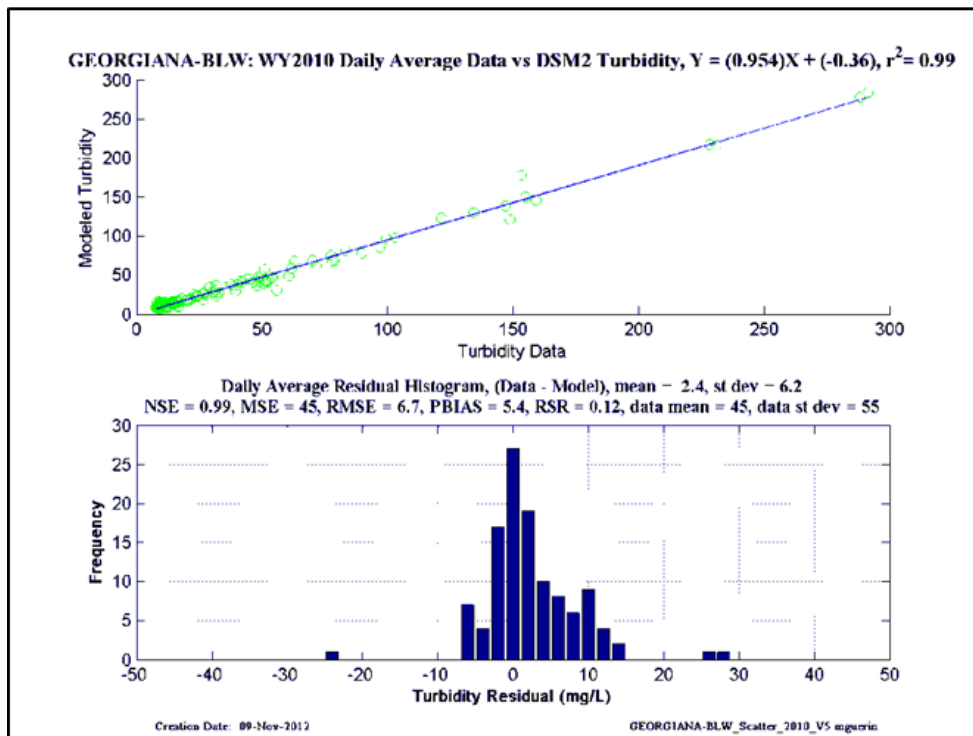
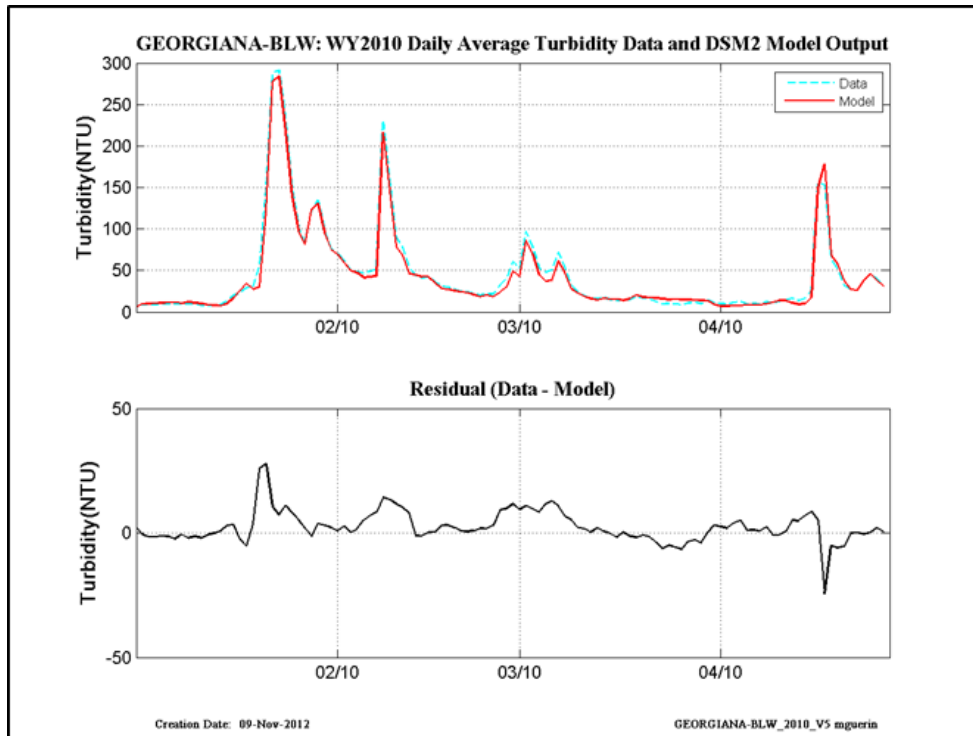


Figure 12-35 WY2010 revised calibration results at Georgiana-Below-Sac.

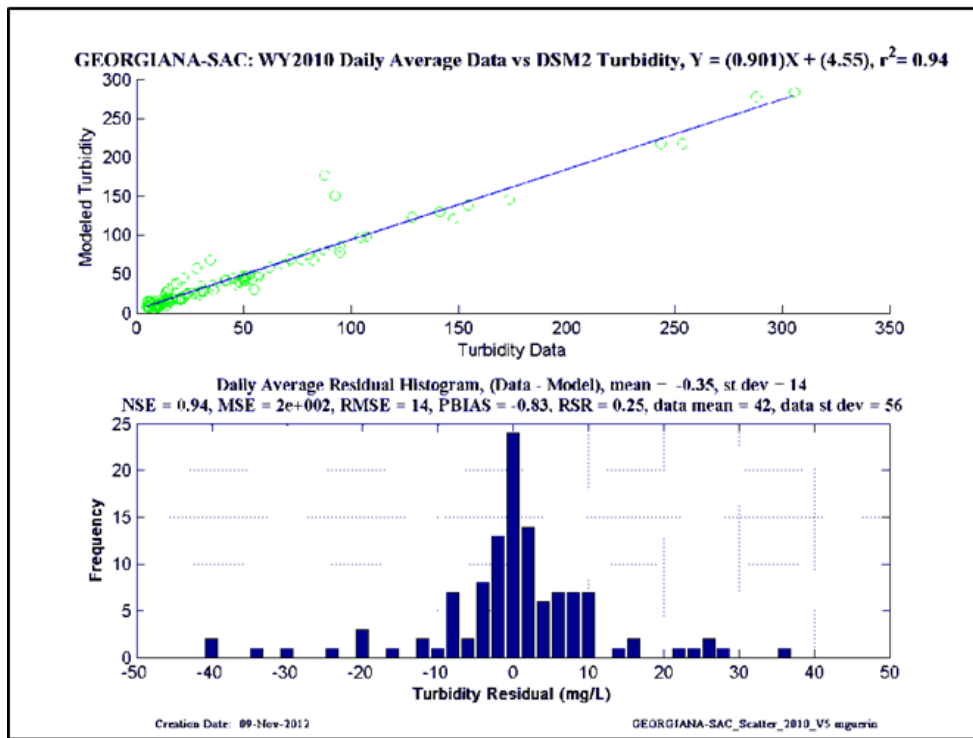
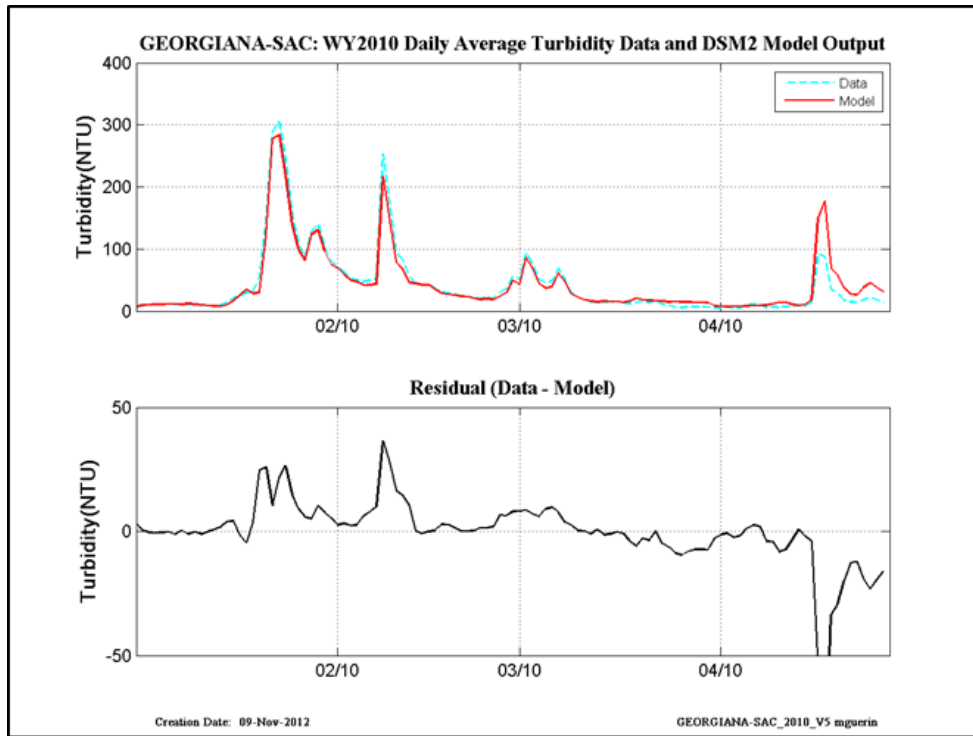


Figure 12-36 WY2010 revised calibration results at Georgiana-Sac.

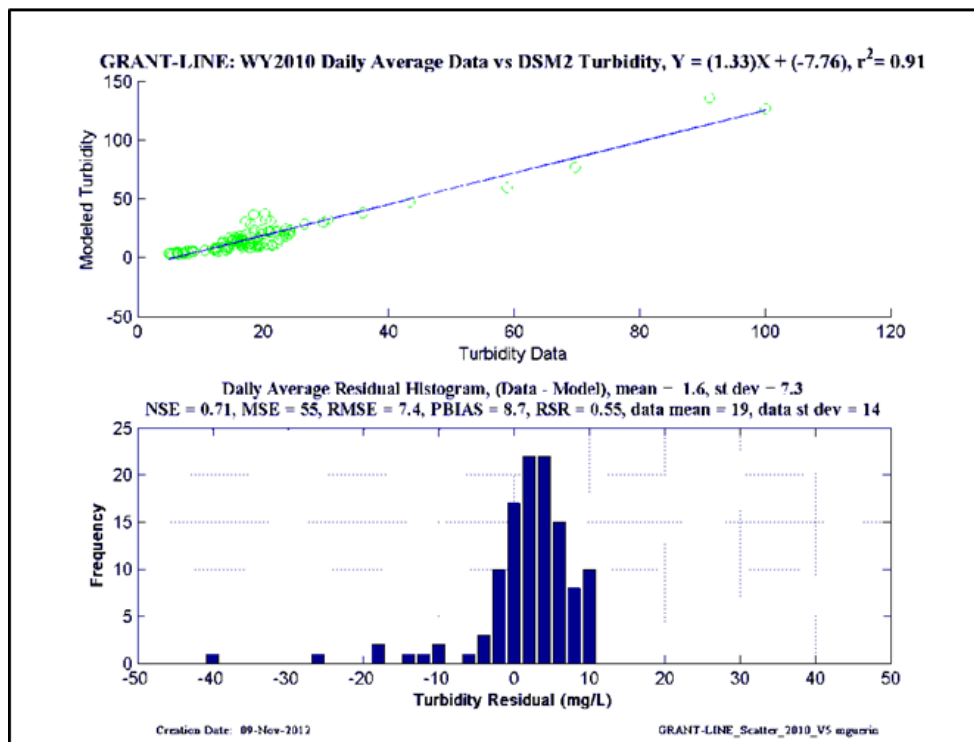
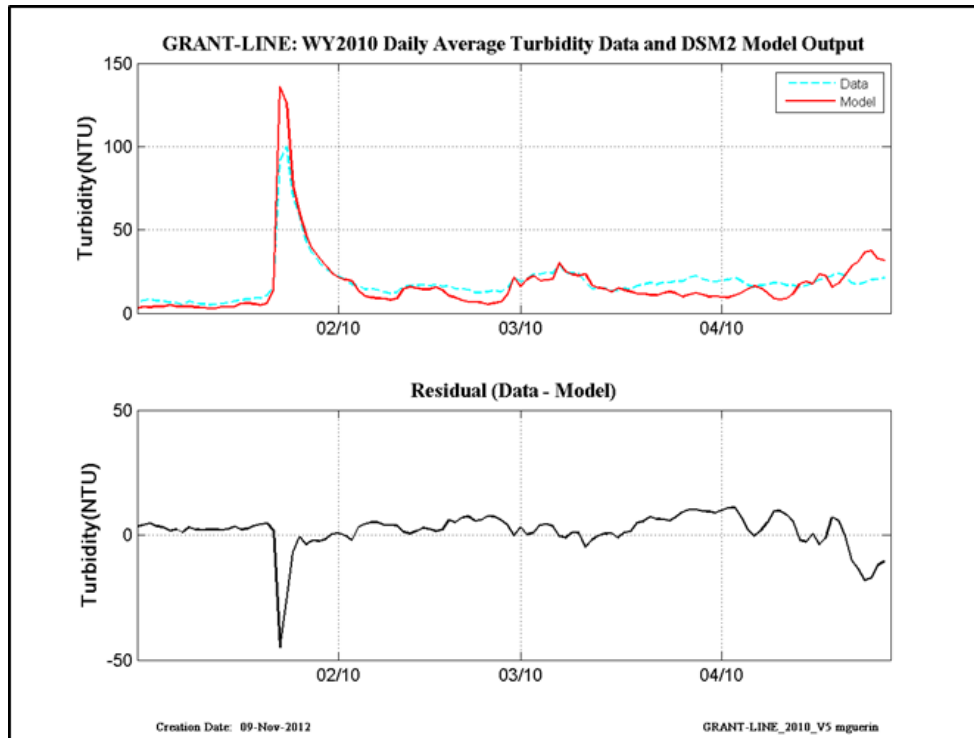


Figure 12-37 WY2010 revised calibration results at Grant Line.

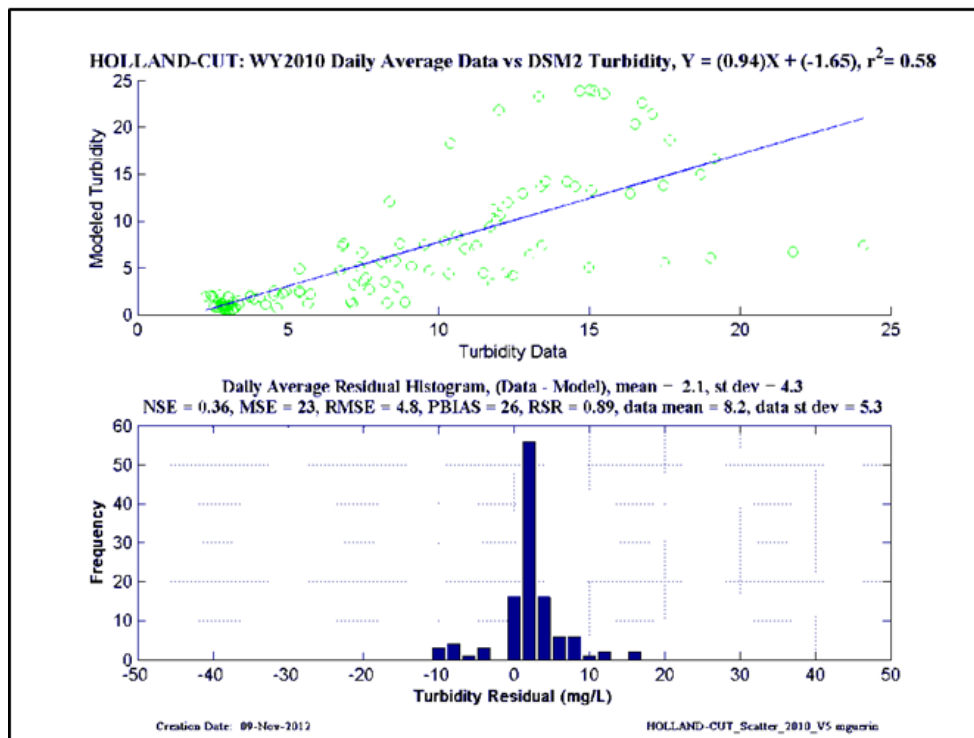
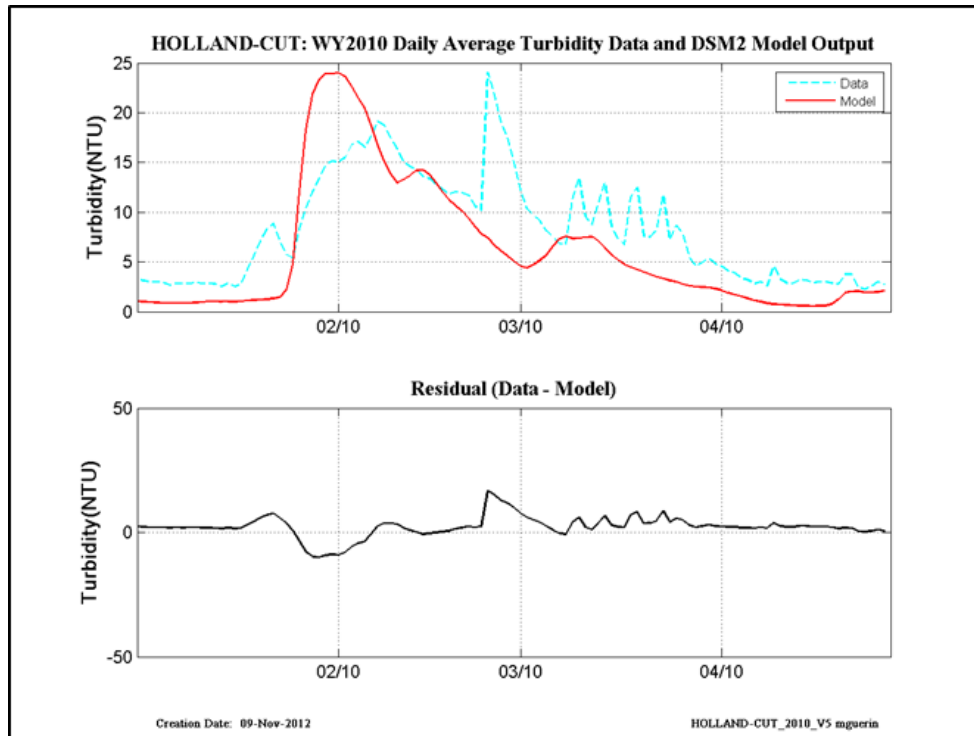


Figure 12-38 WY2010 revised calibration results at Holland Cut.

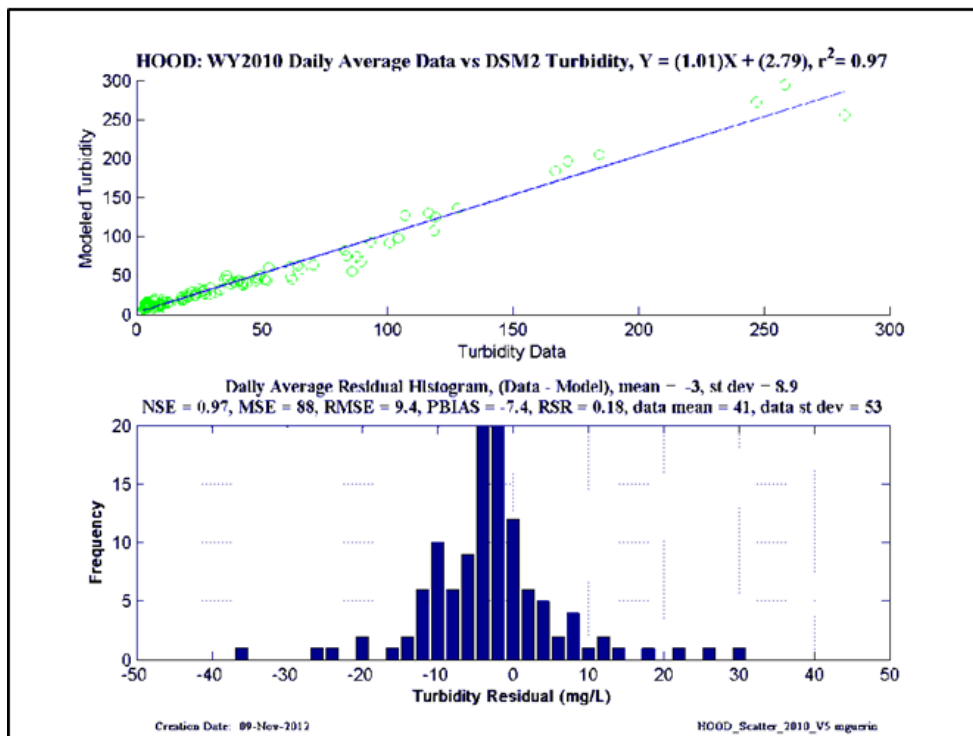
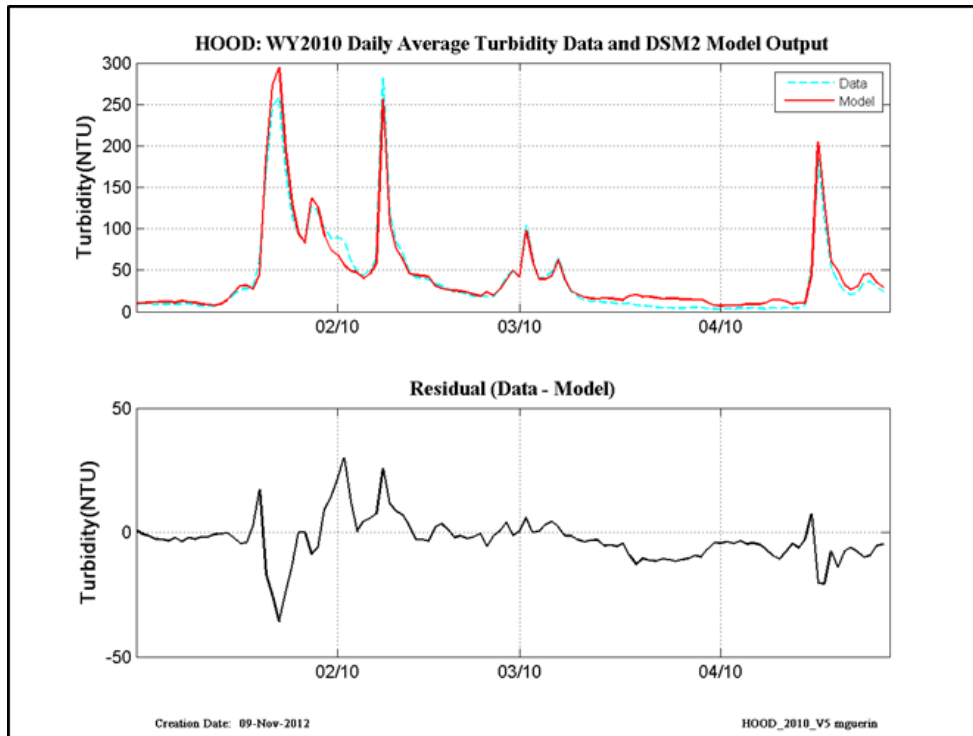


Figure 12-39 WY2010 revised calibration results at Hood.

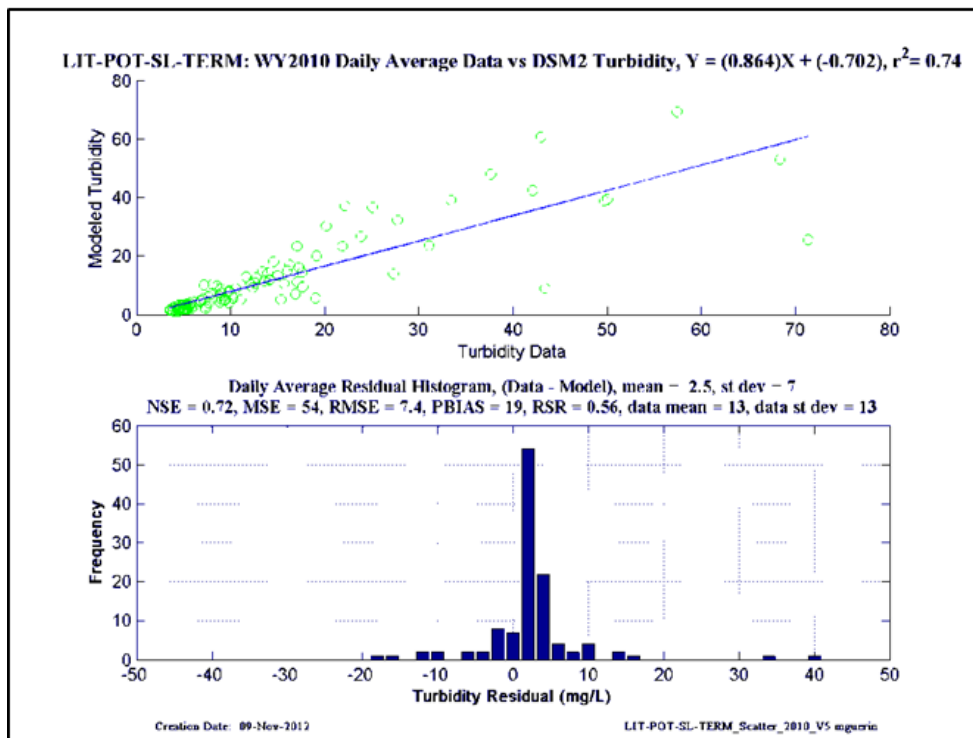
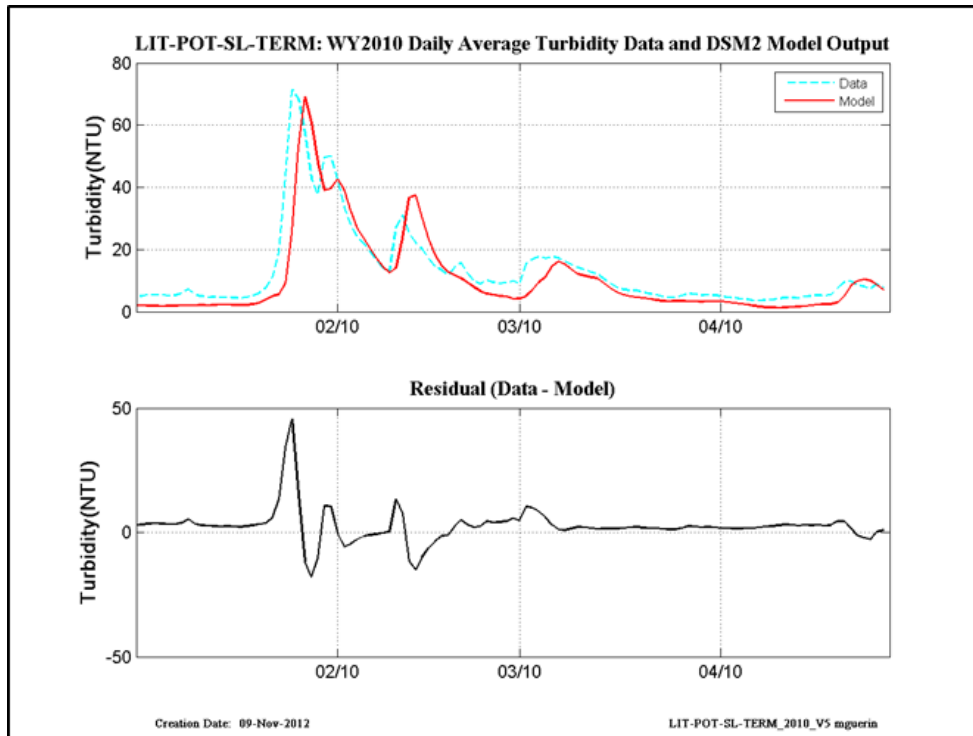


Figure 12-40 WY2010 revised calibration results at Little Potato Slough-at-Terminus.

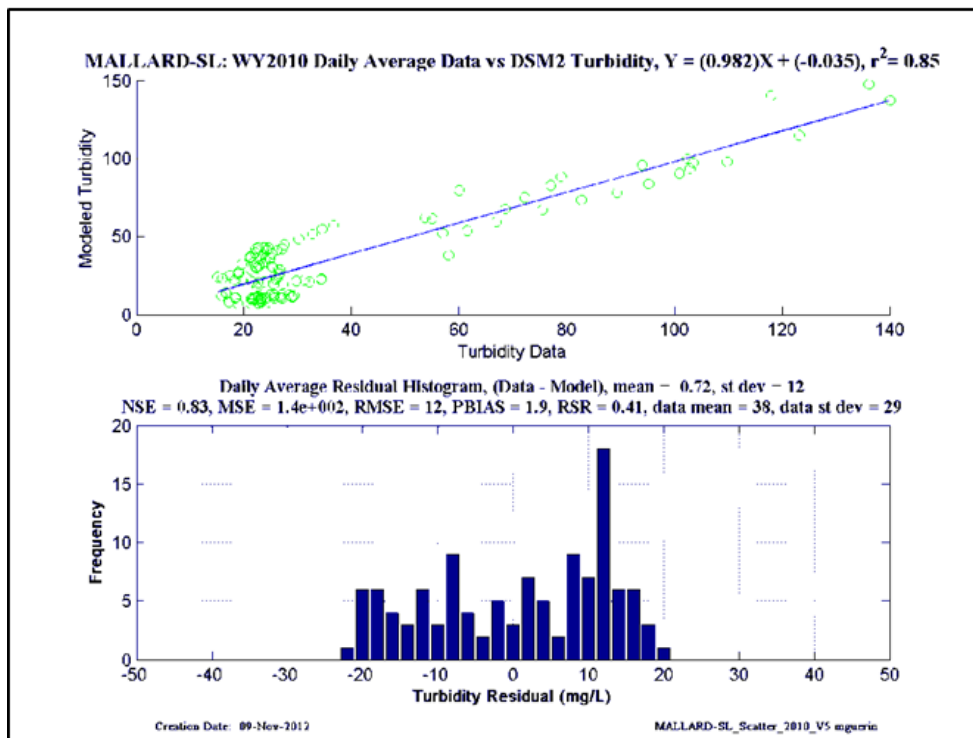
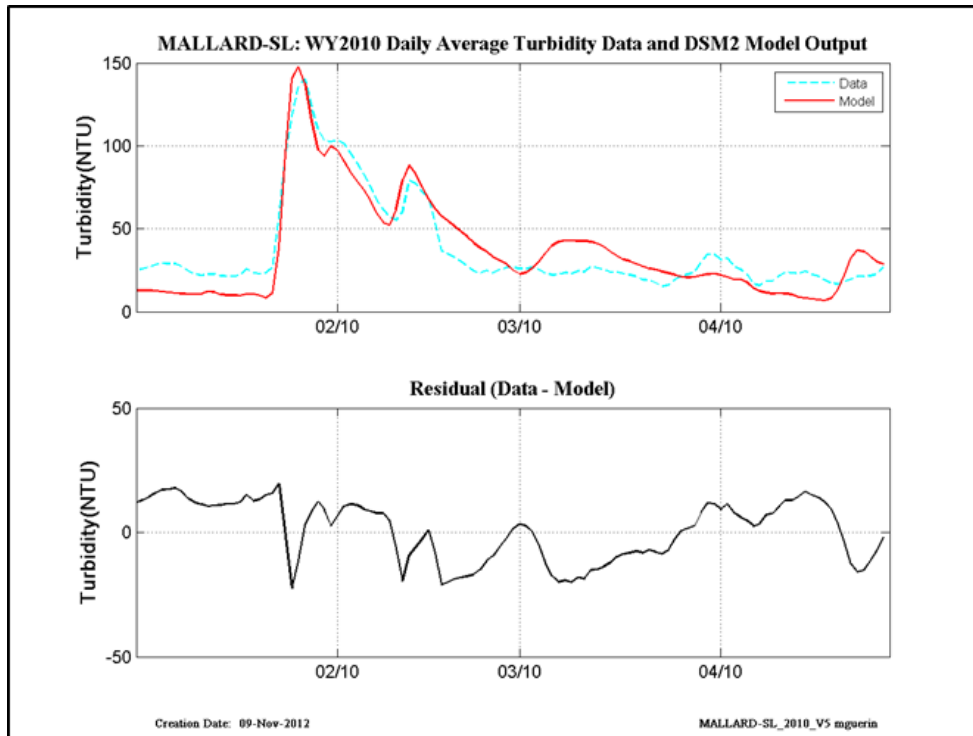


Figure 12-41 WY2010 revised calibration results at Mallard Slough.

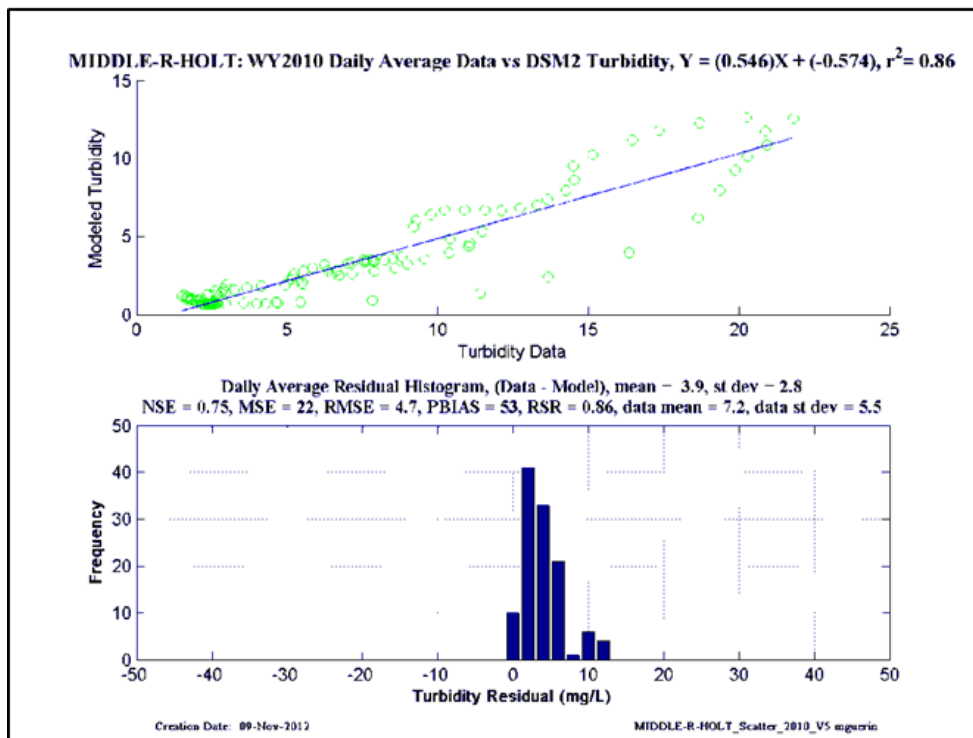
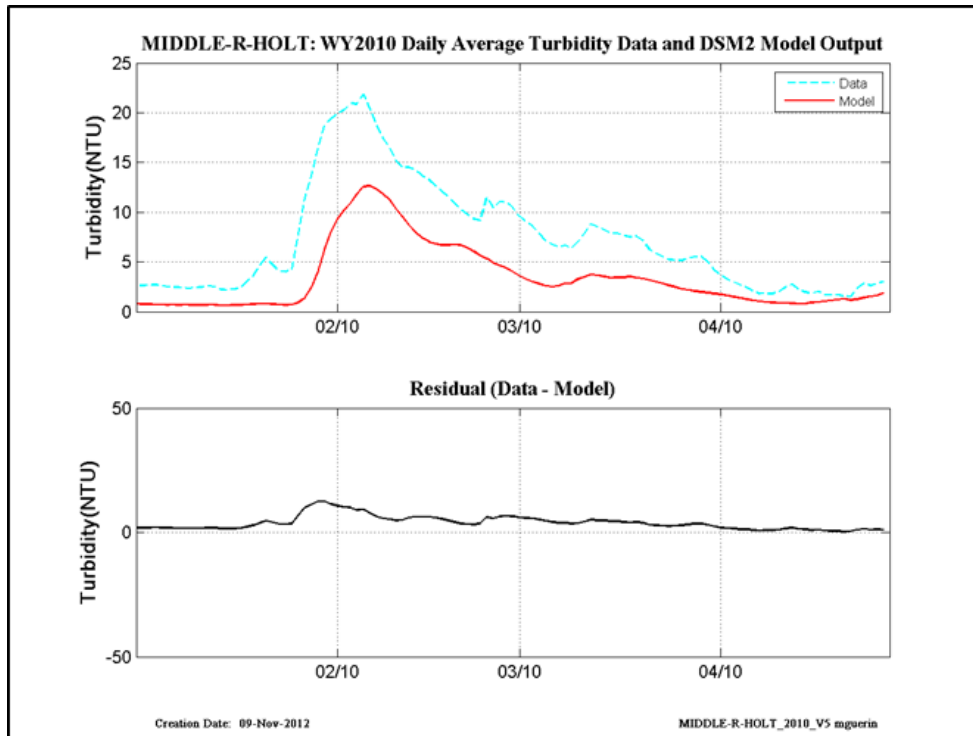


Figure 12-42 WY2010 revised calibration results at Middle River-at-Holt.

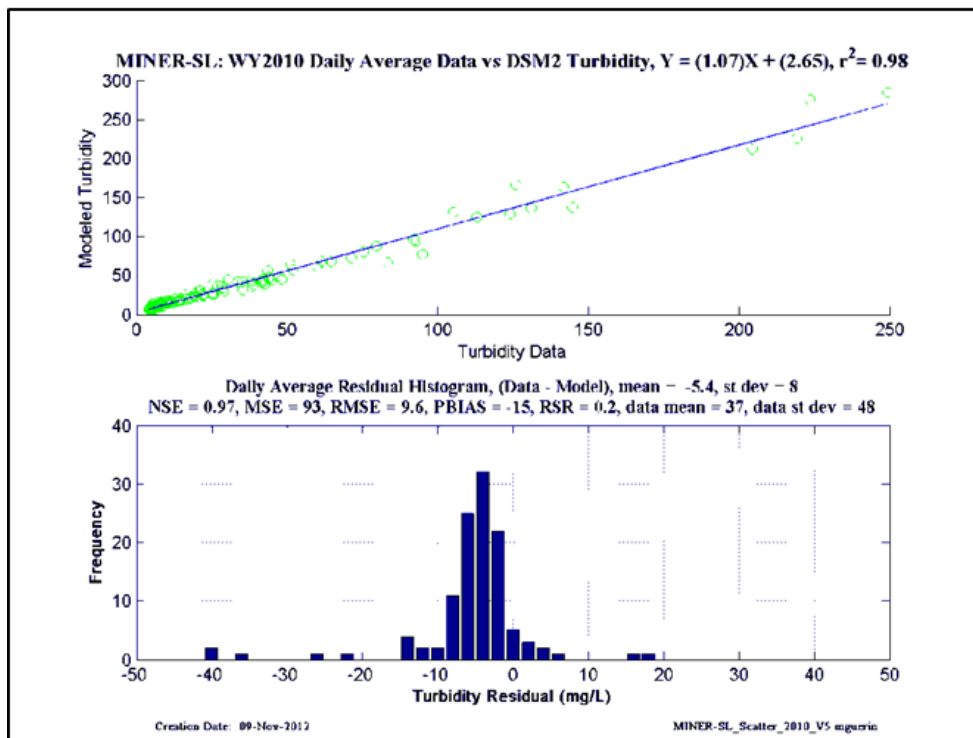
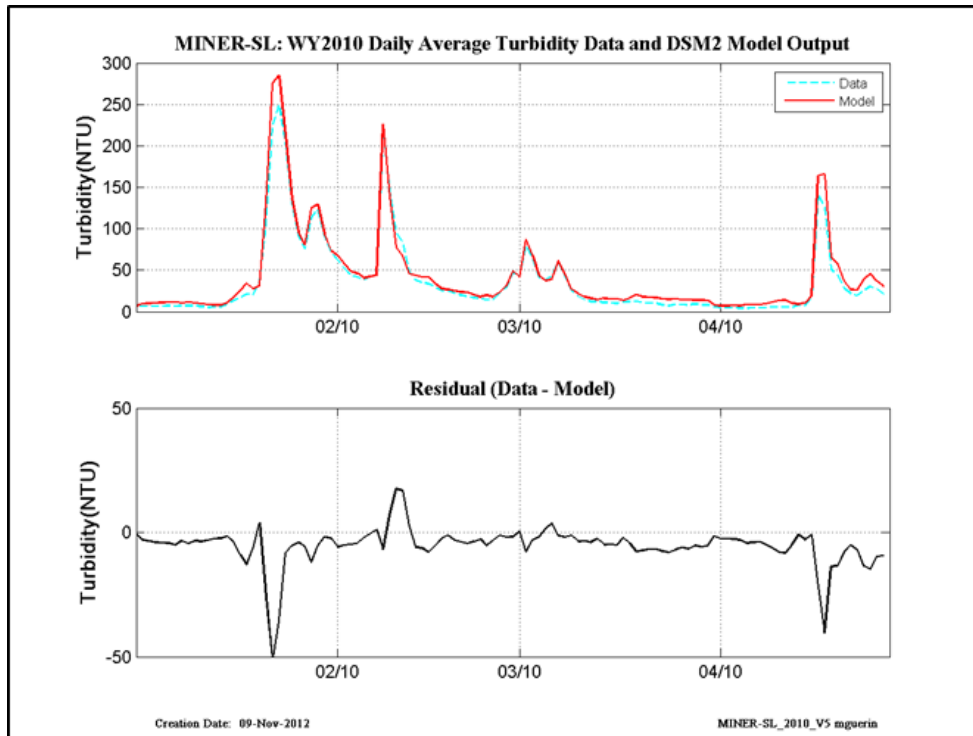


Figure 12-43 WY2010 revised calibration results at Miner Slough.

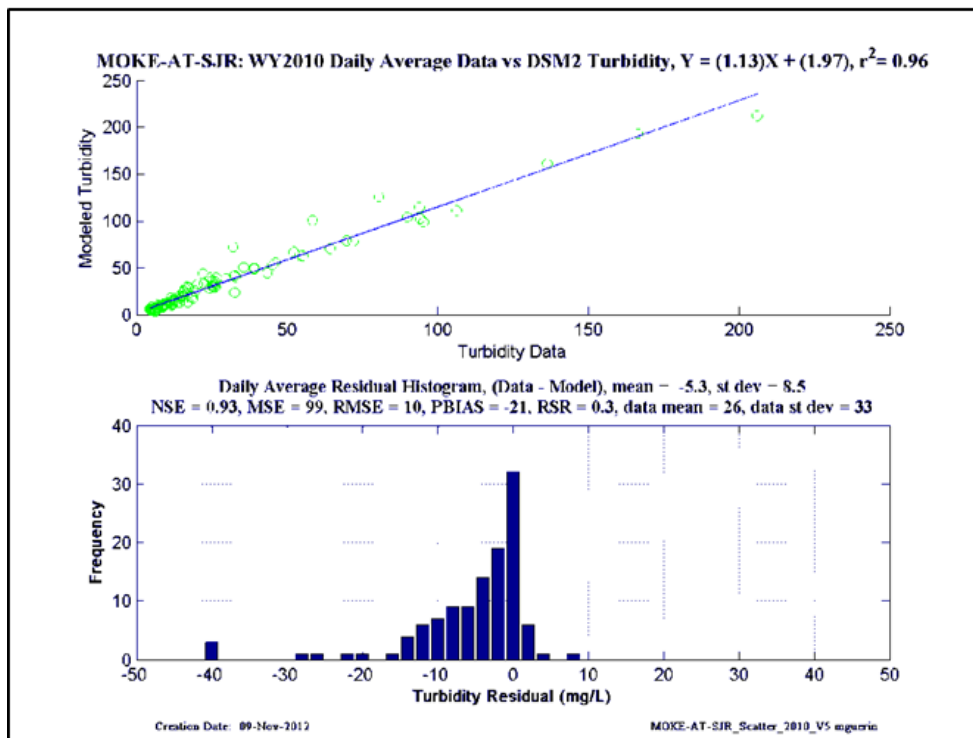
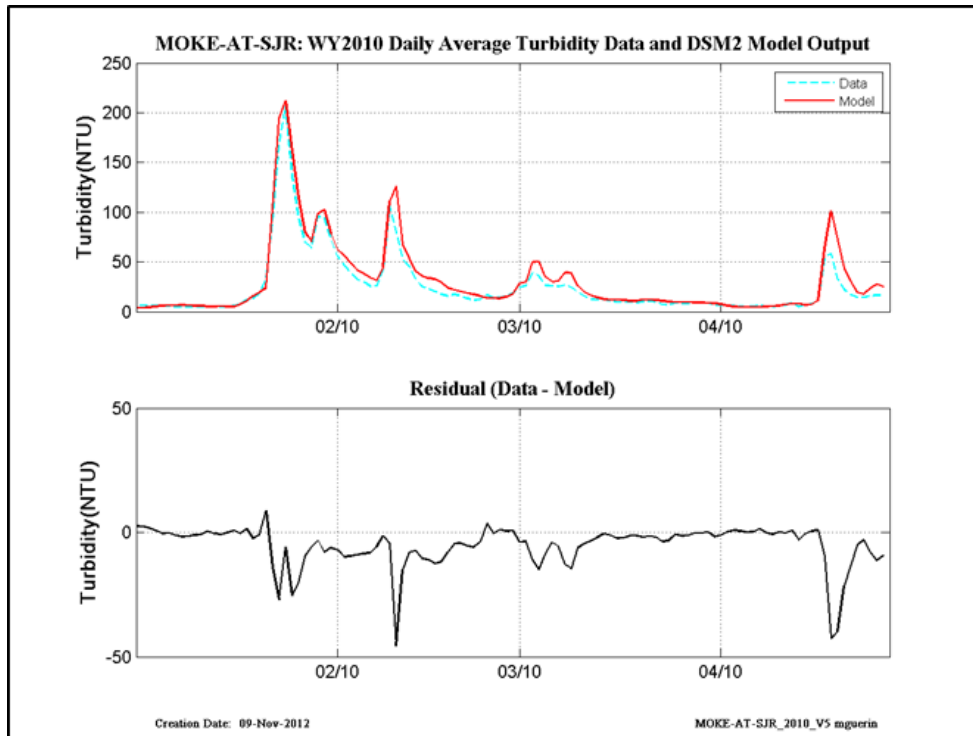


Figure 12-44 WY2010 revised calibration results at Mokelumne-at-San Joaquin.

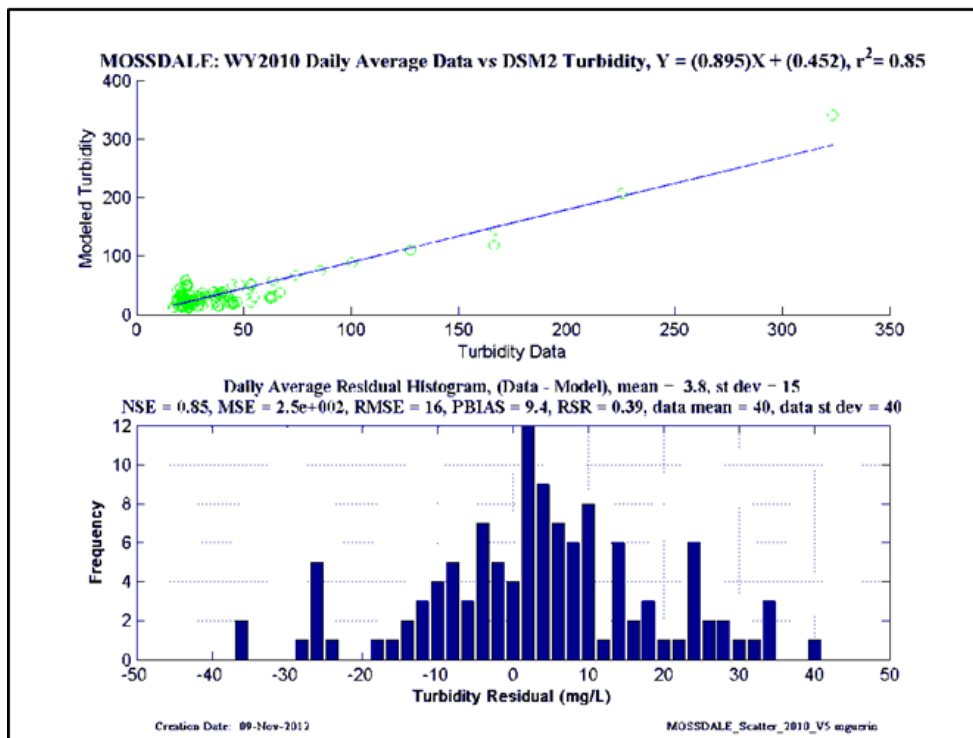
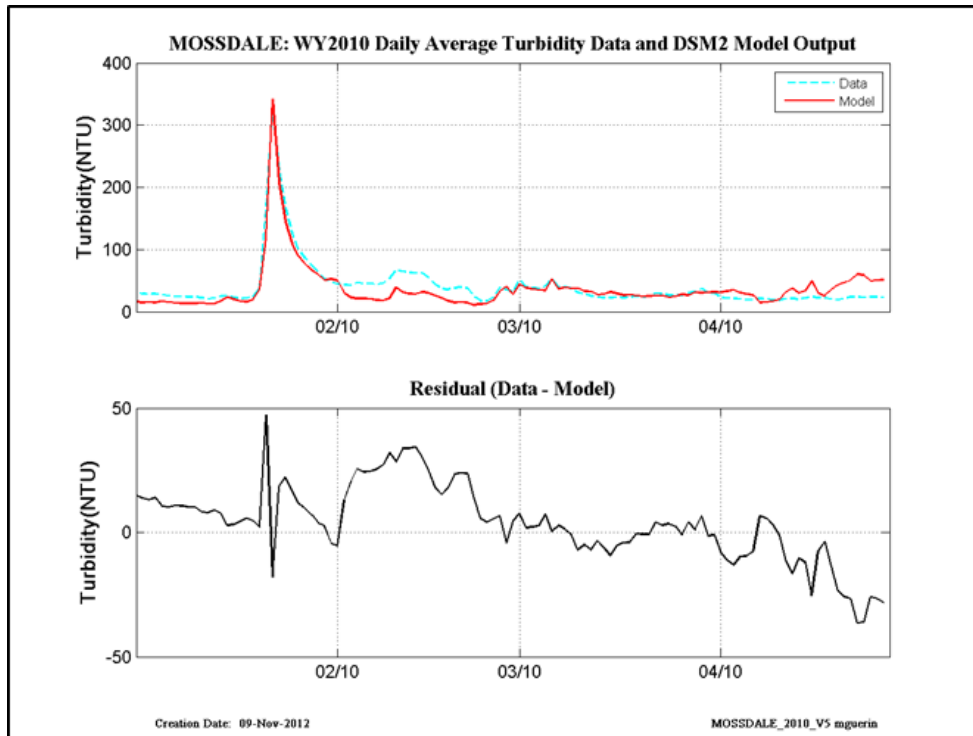


Figure 12-45 WY2010 revised calibration results at Mossdale.

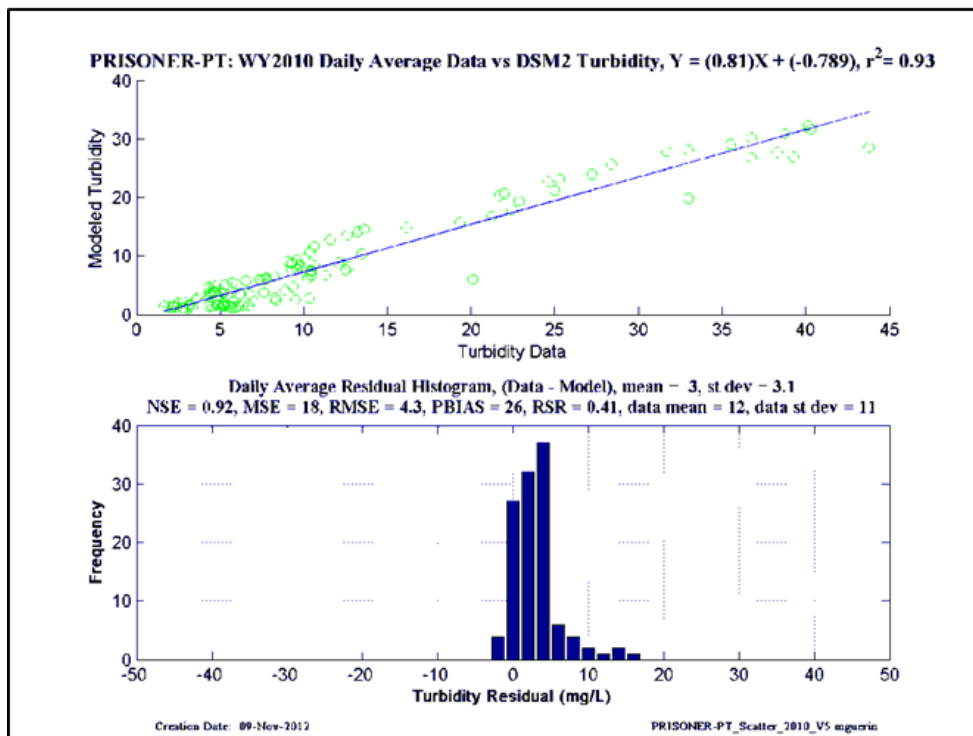
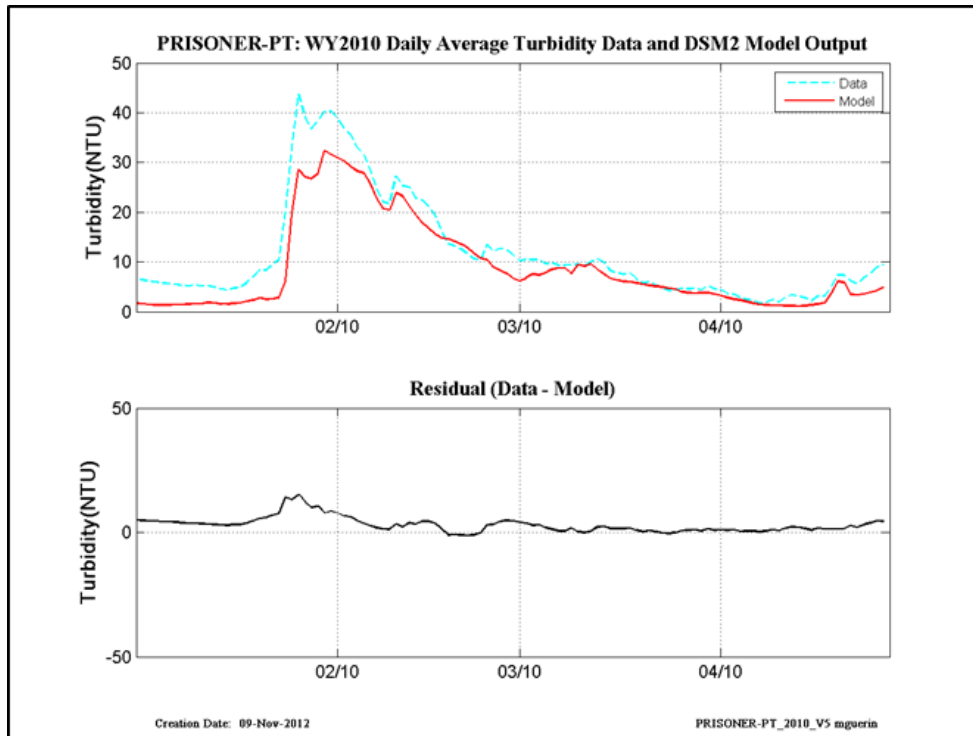


Figure 12-46 WY2010 revised calibration results at Prisoner Point.

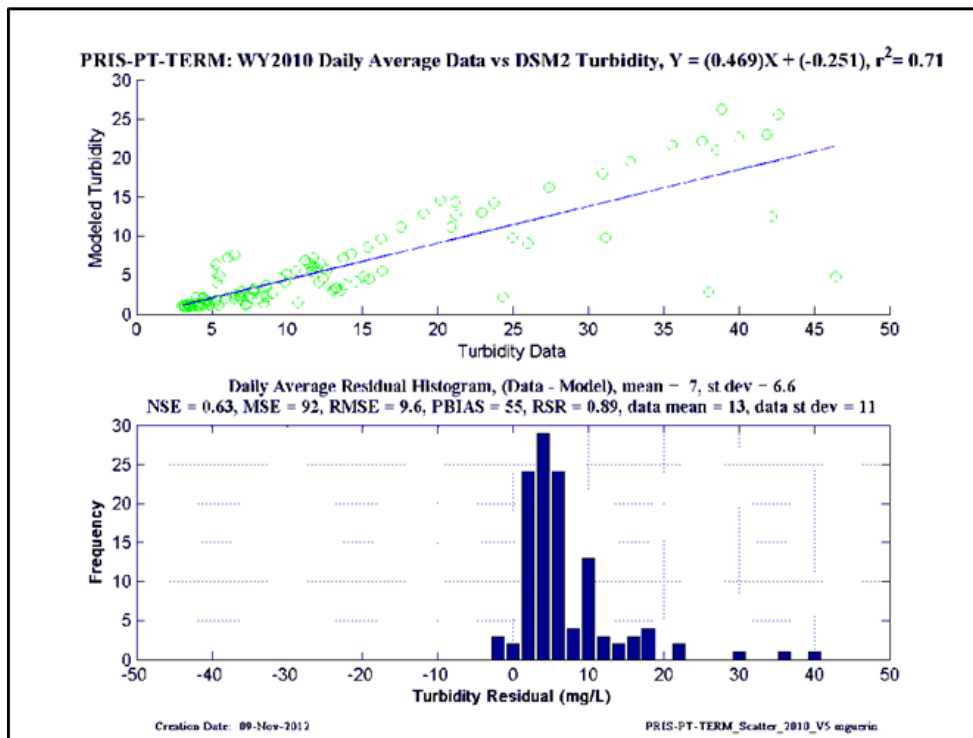
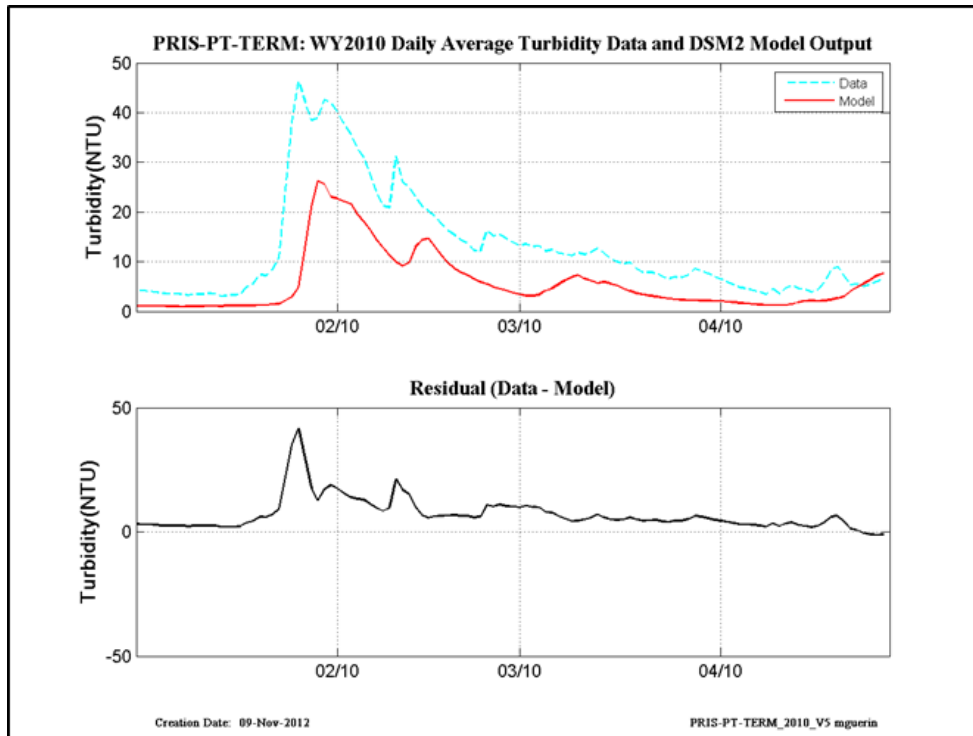


Figure 12-47 WY2010 revised calibration results at Prisoner Point-at-Terminus.

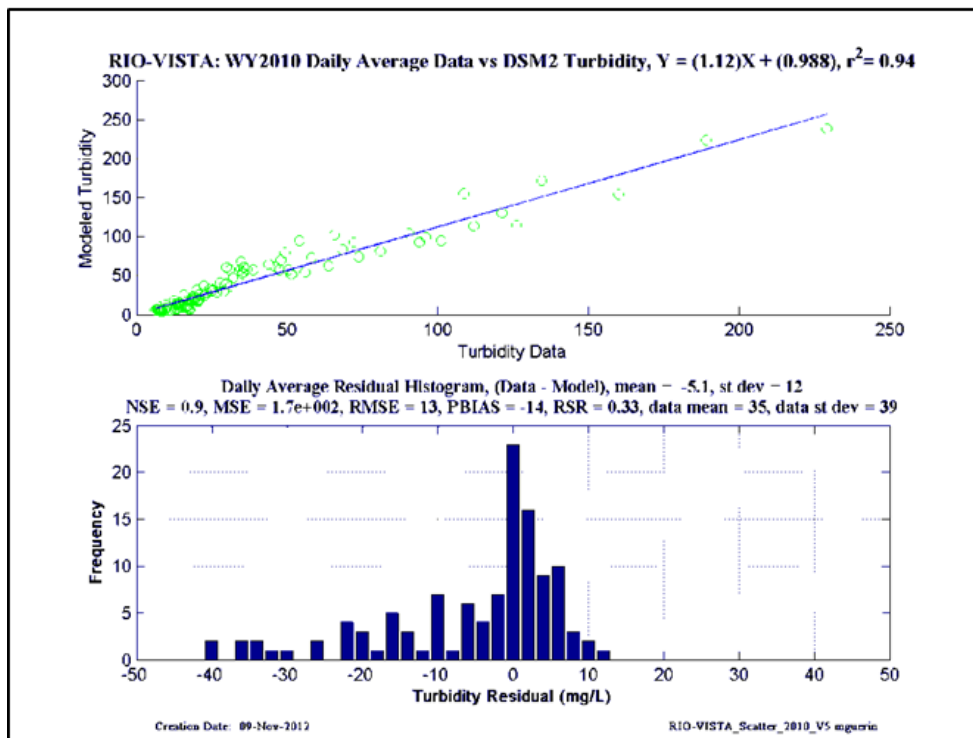
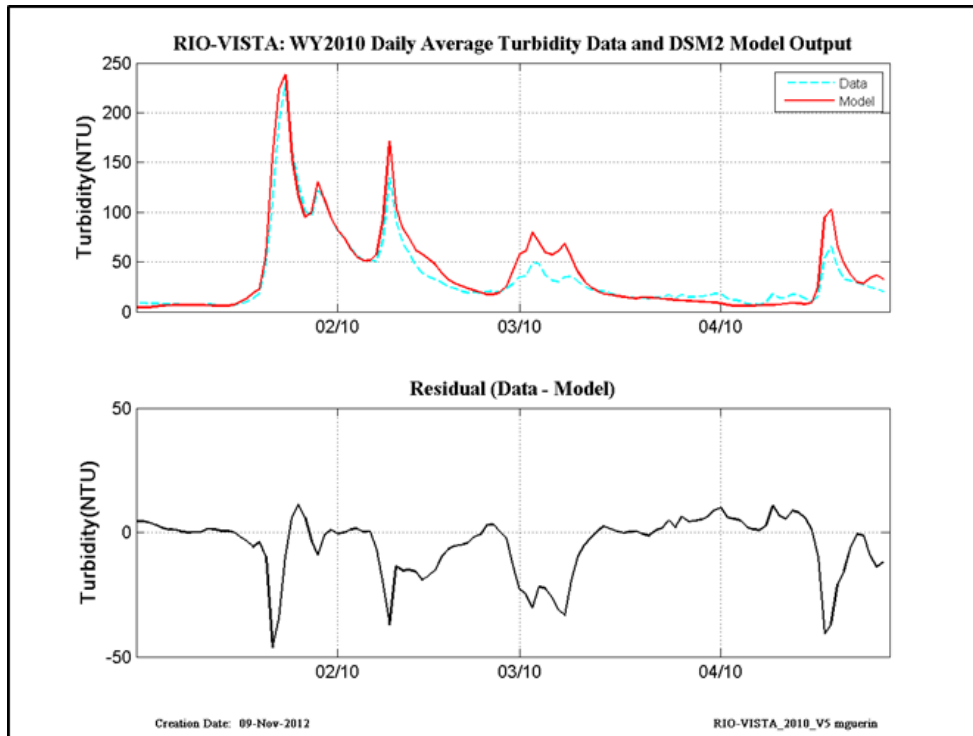


Figure 12-48 WY2010 revised calibration results at Rio Vista.

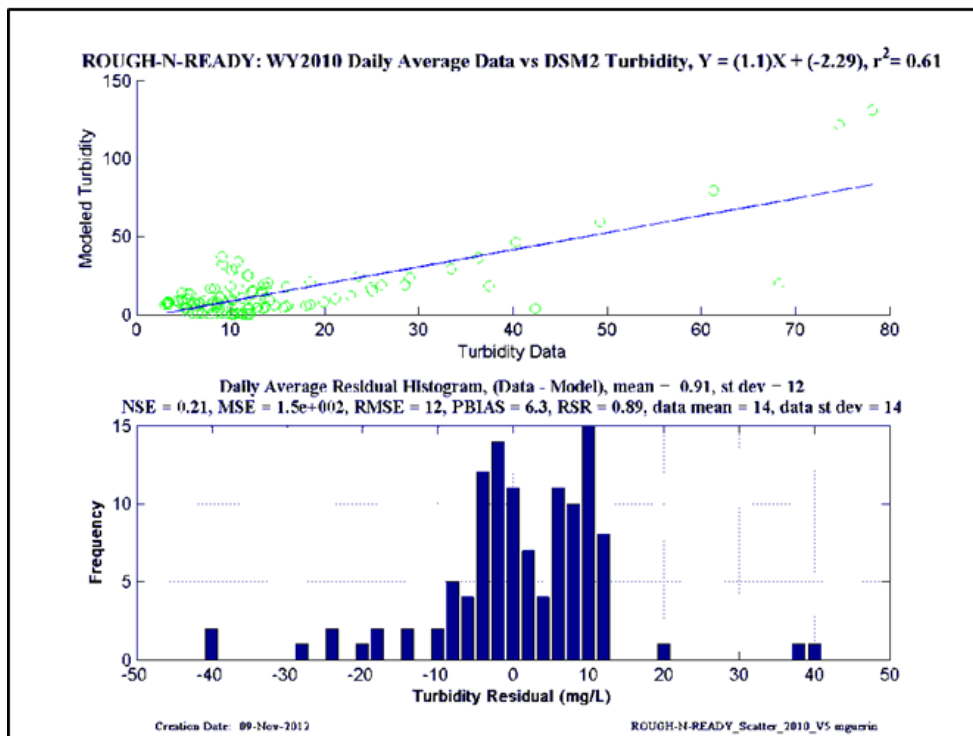
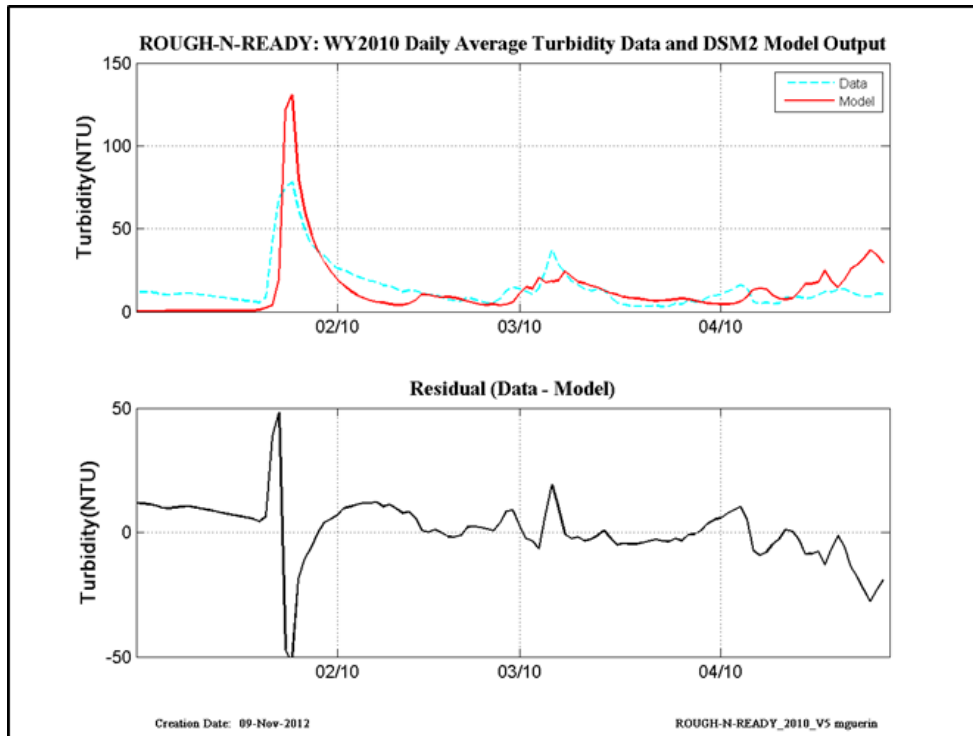


Figure 12-49 WY2010 revised calibration results at Rough-N-Ready Island.

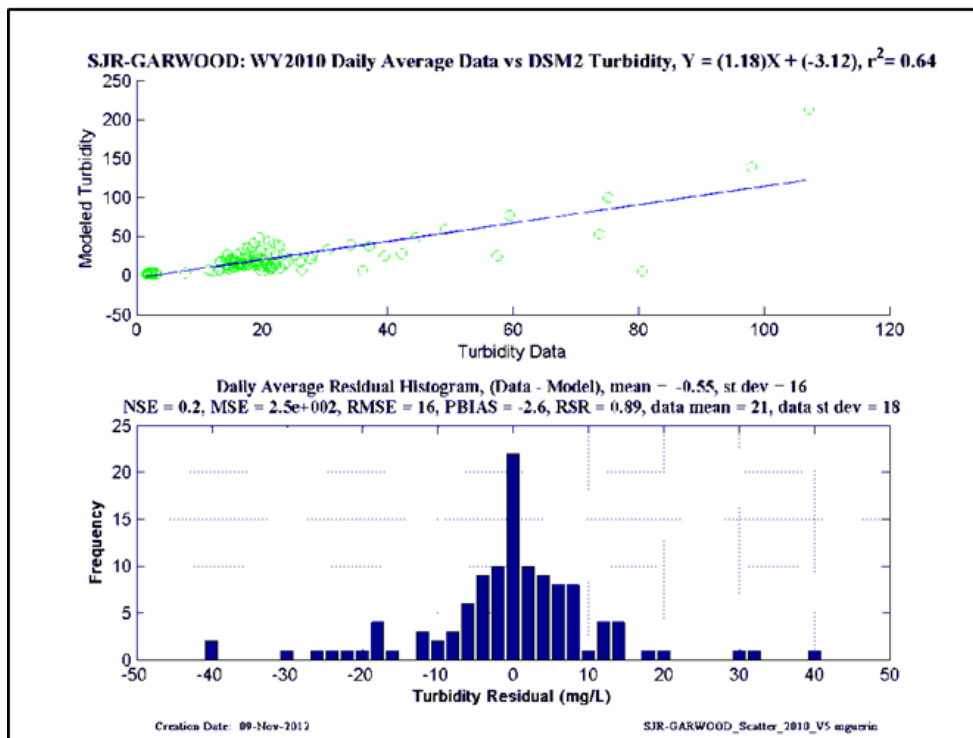
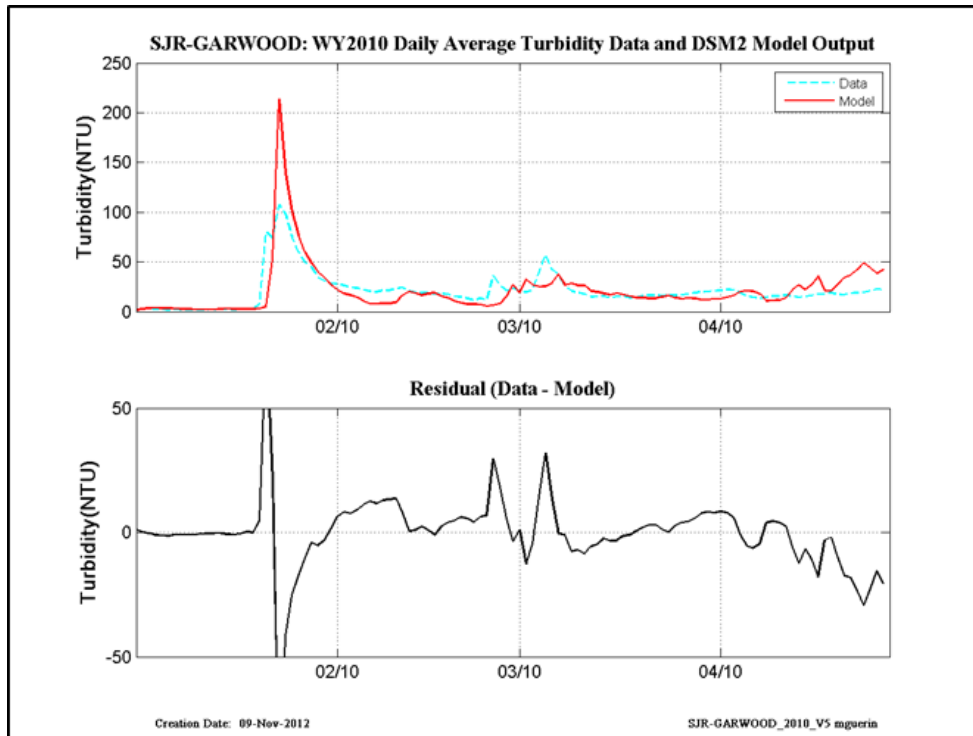


Figure 12-50 WY2010 revised calibration results at San Joaquin-at-Garwood.

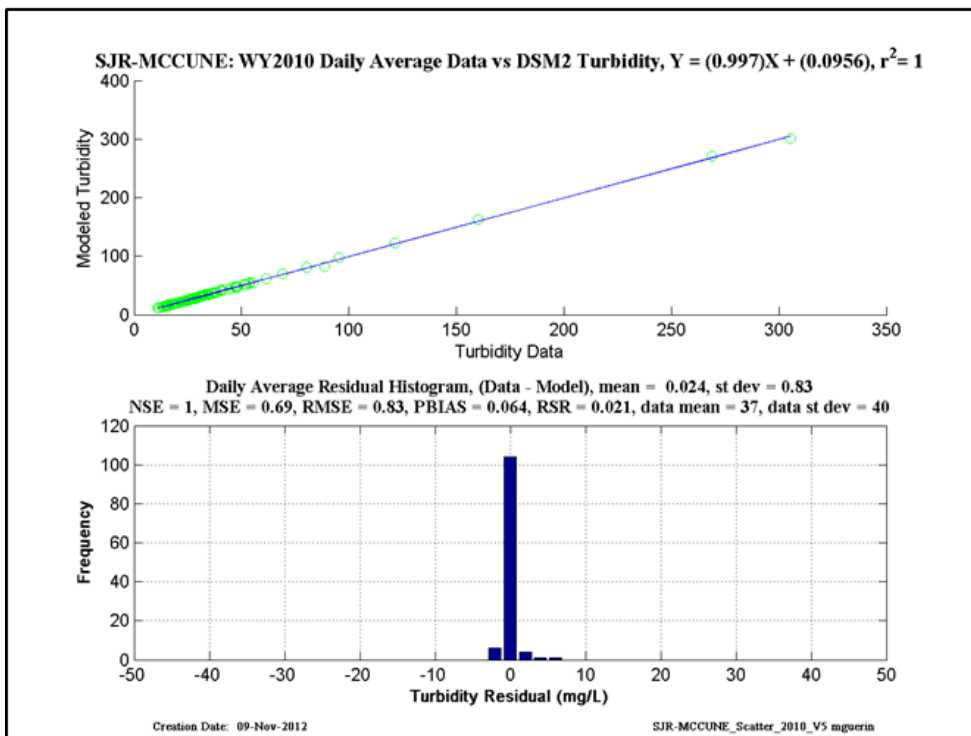
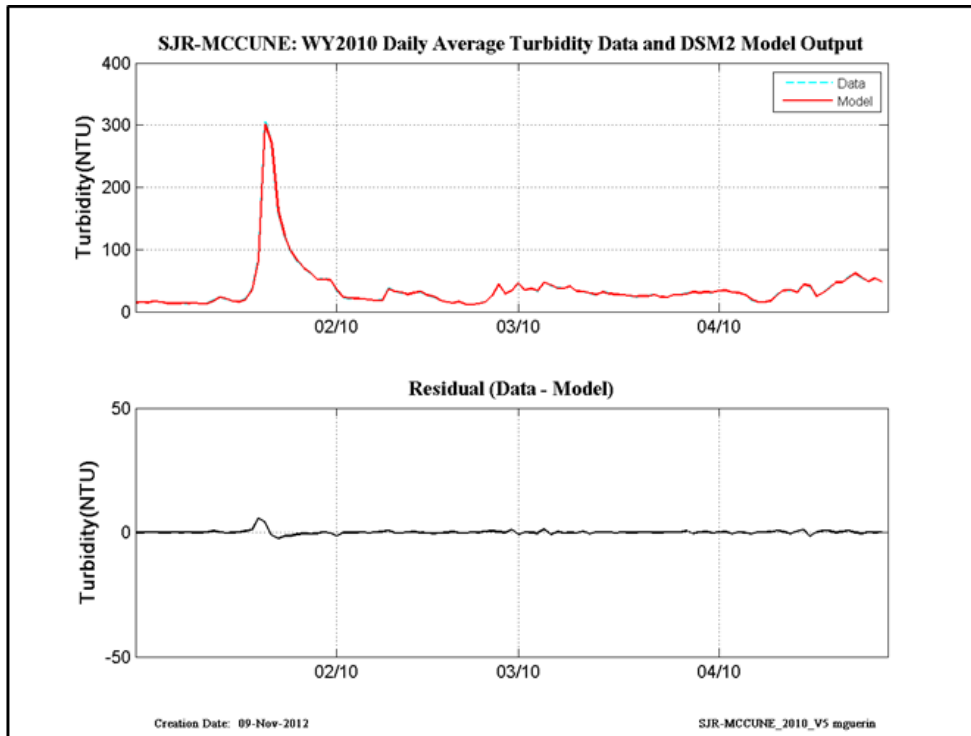


Figure 12-51 WY2010 revised calibration results at San Joaquin-at-McCune (Vernalis).

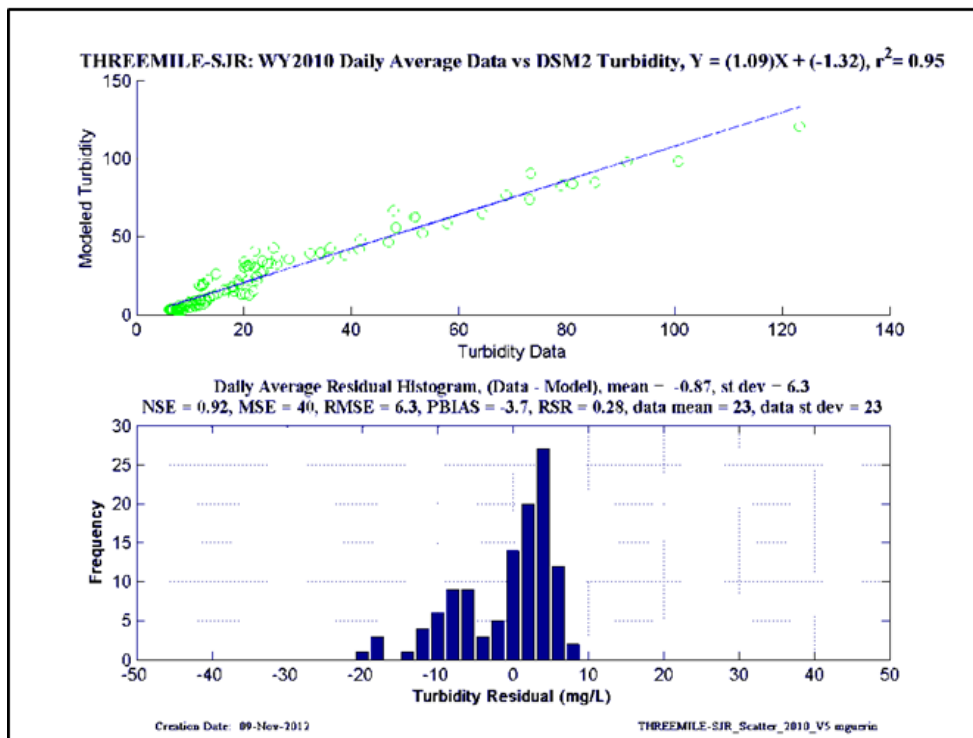
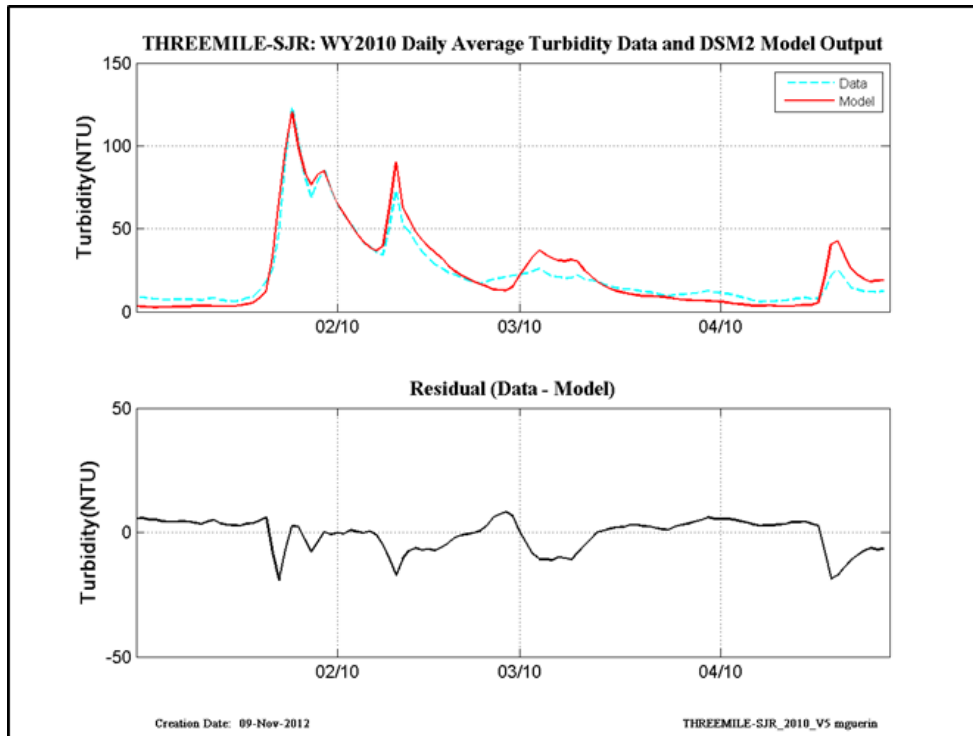


Figure 12-52 WY2010 revised calibration results at Threemile-Slough-at-San Joaquin.

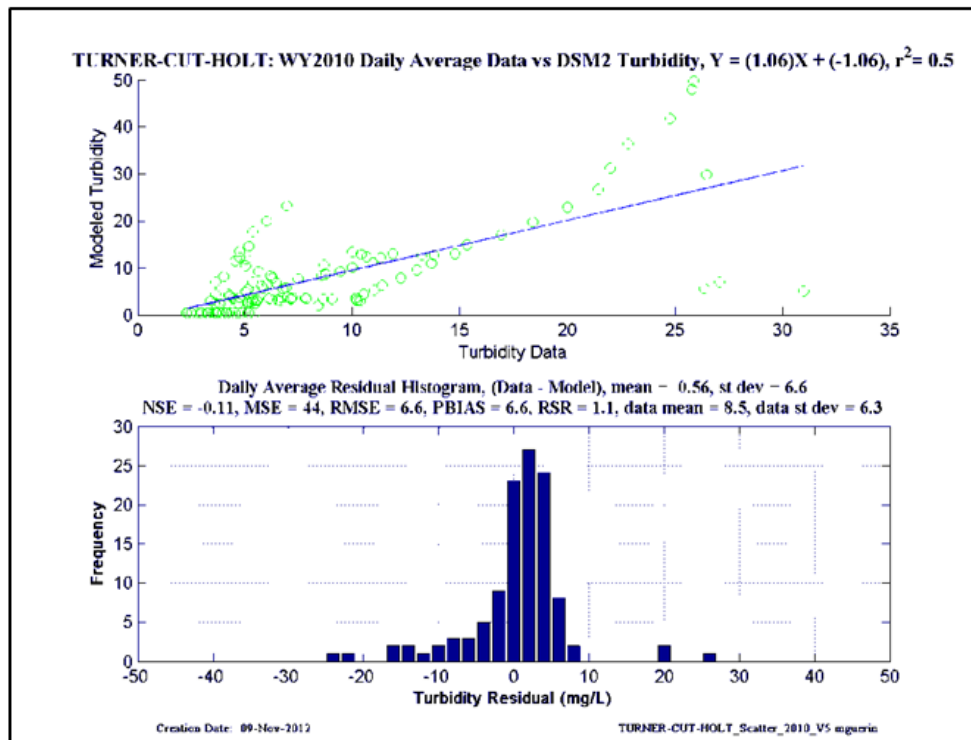
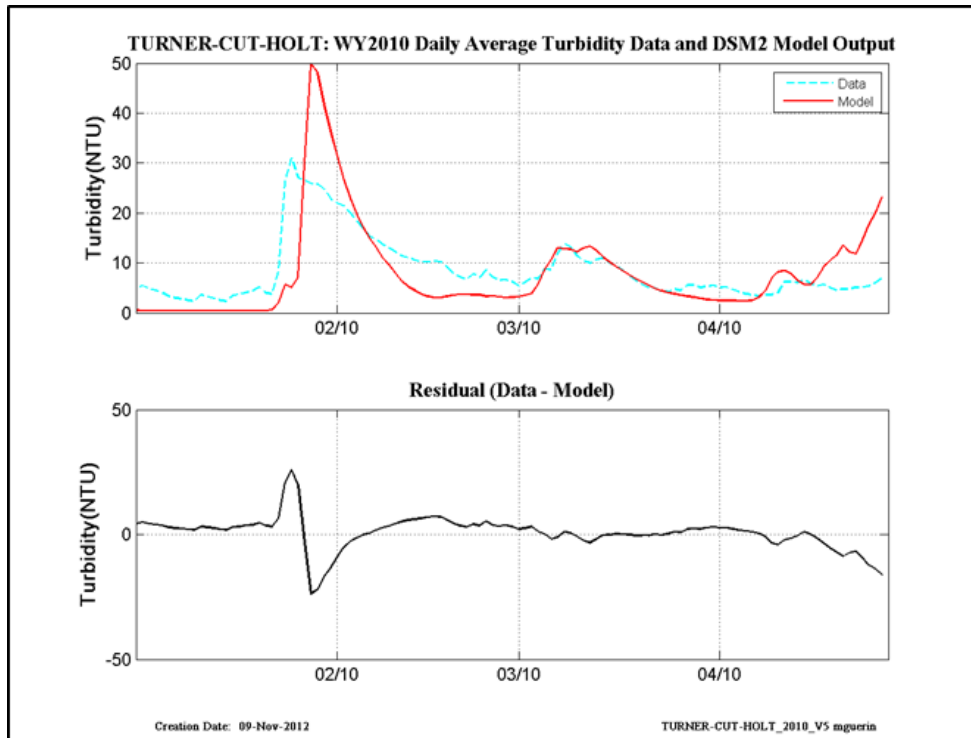


Figure 12-53 WY2010 revised calibration results at Turner Cut-at-Holt.

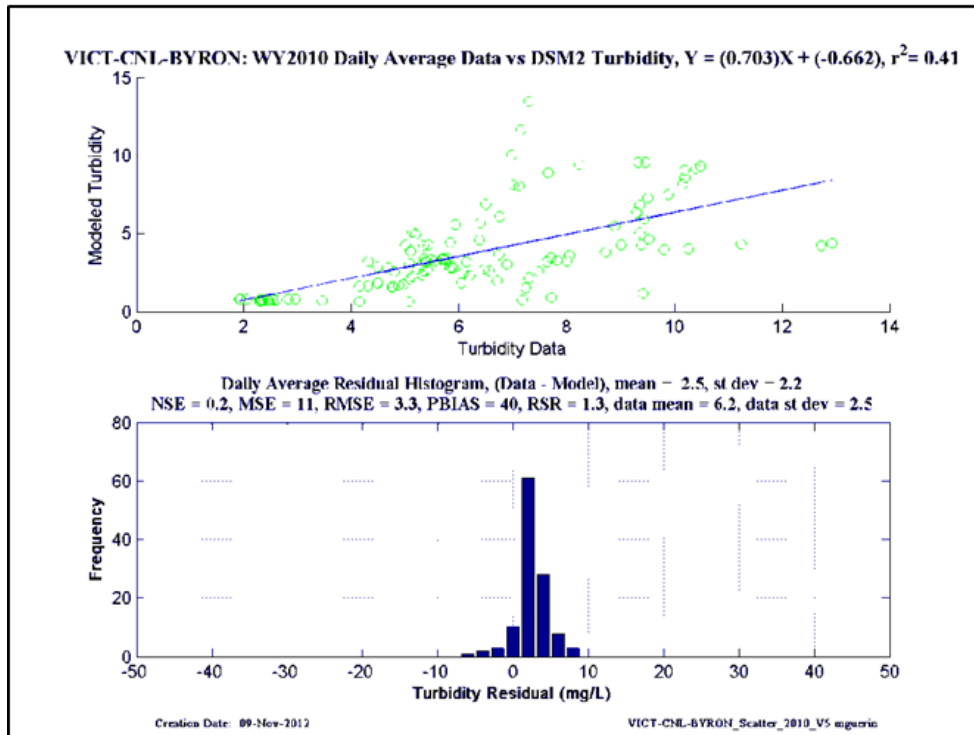
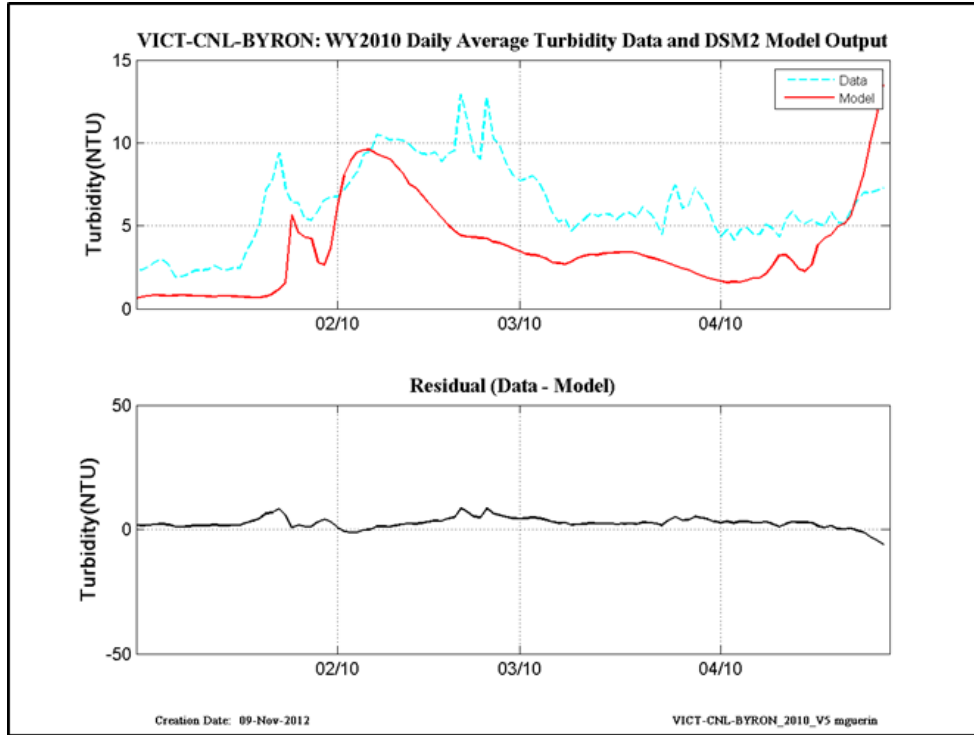


Figure 12-54 WY2010 revised calibration results at Victoria Canal-at-Byron.

13 Appendix III – Initial QUAL turbidity calibration by DMS

13.1 Daily-averaged CDEC data and model output – WY2011

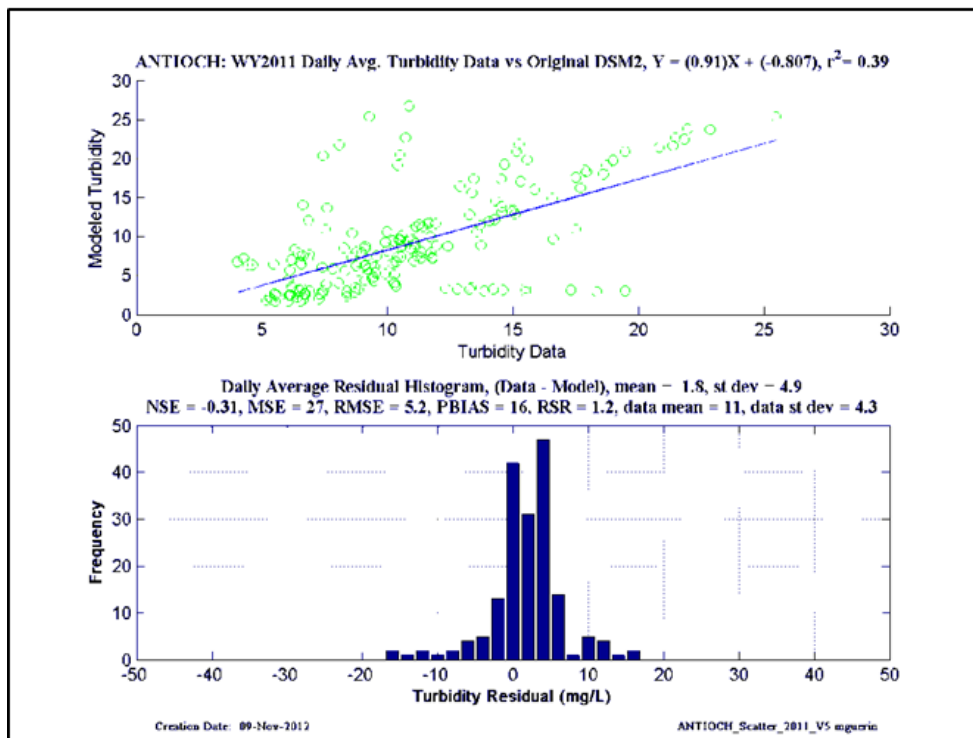
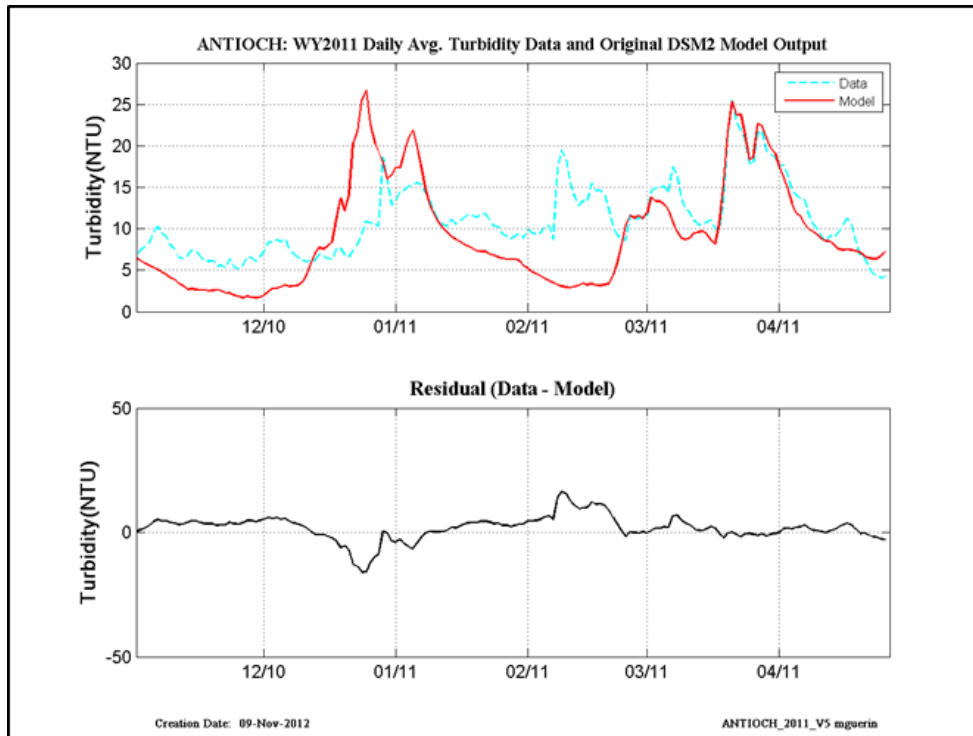


Figure 13-1 WY2011 original calibration results at Antioch.

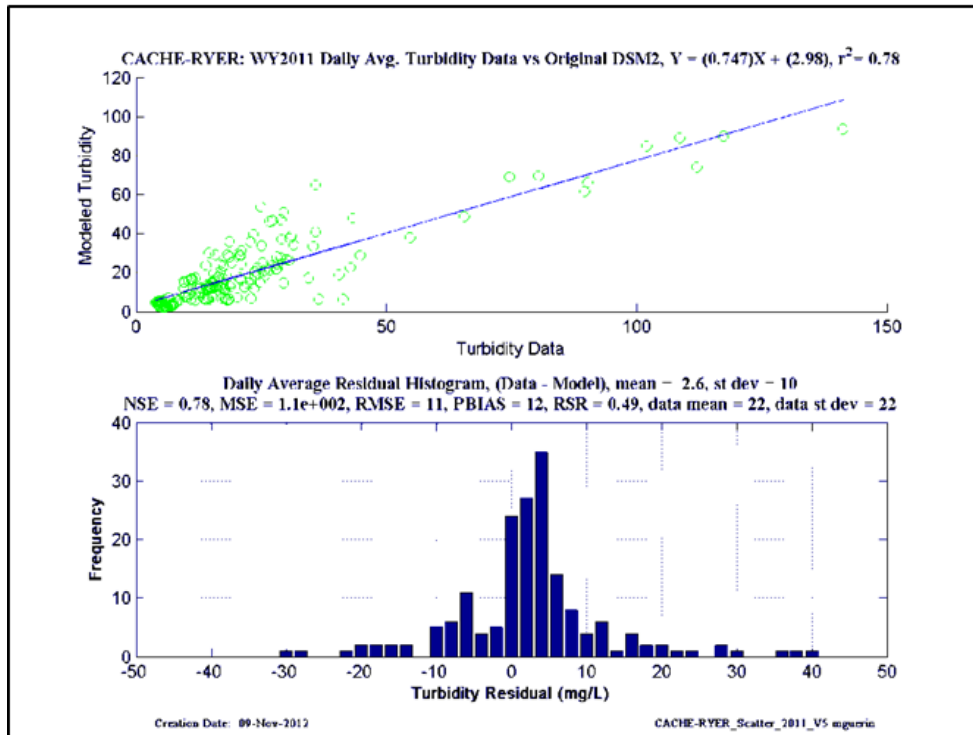
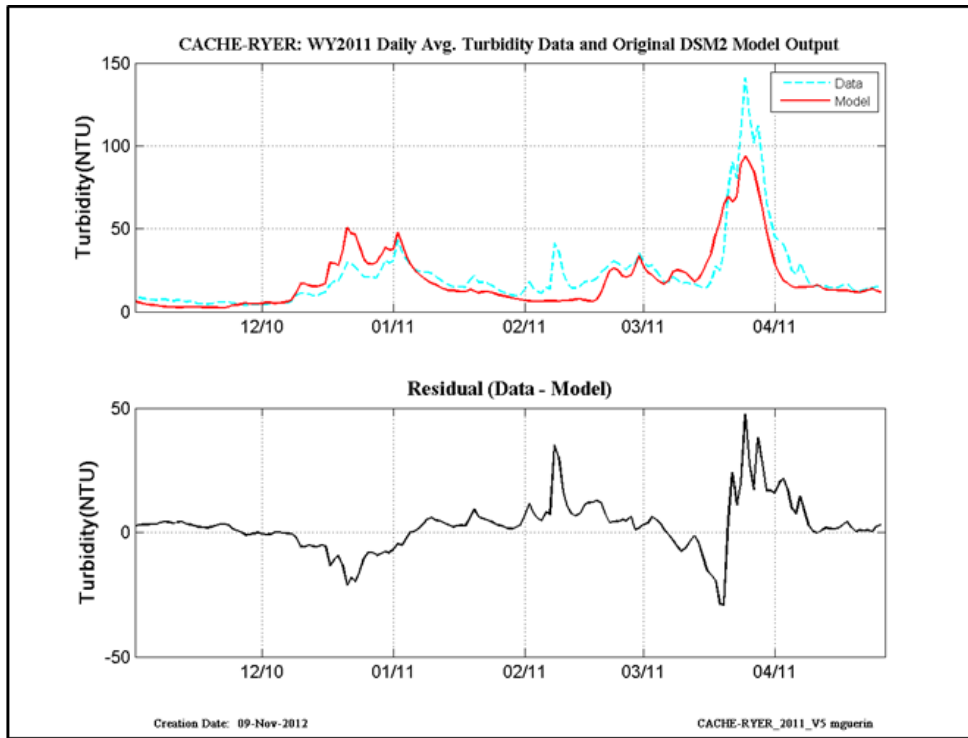


Figure 13-2 WY2011 original calibration results at Cache-at-Ryer Island.

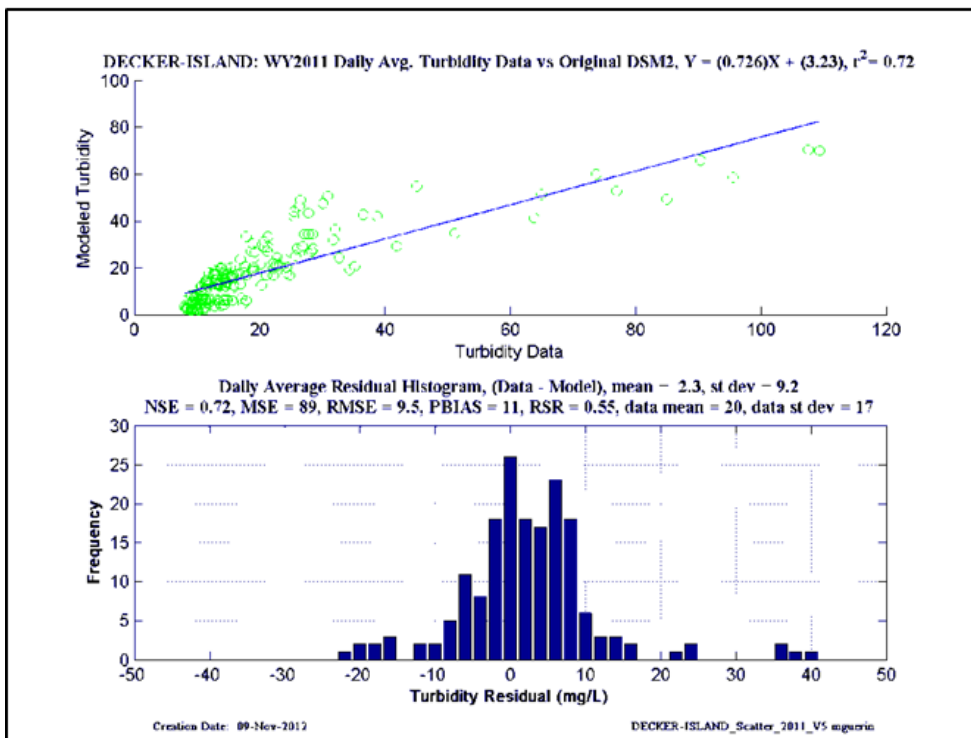
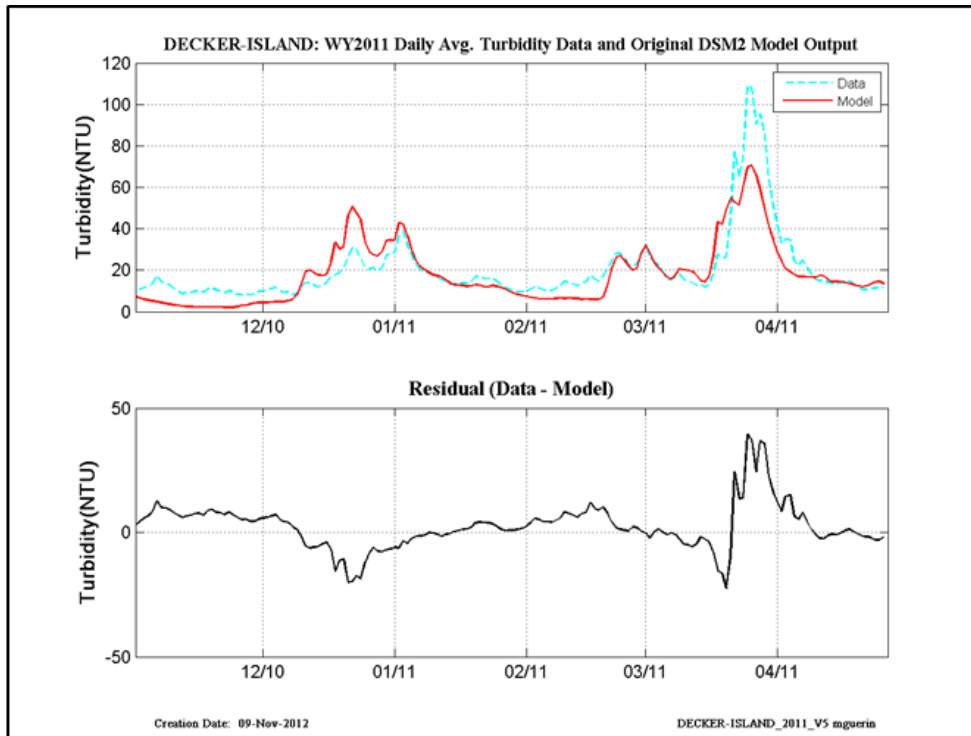


Figure 13-3 WY2011 original calibration results at Decker Island.

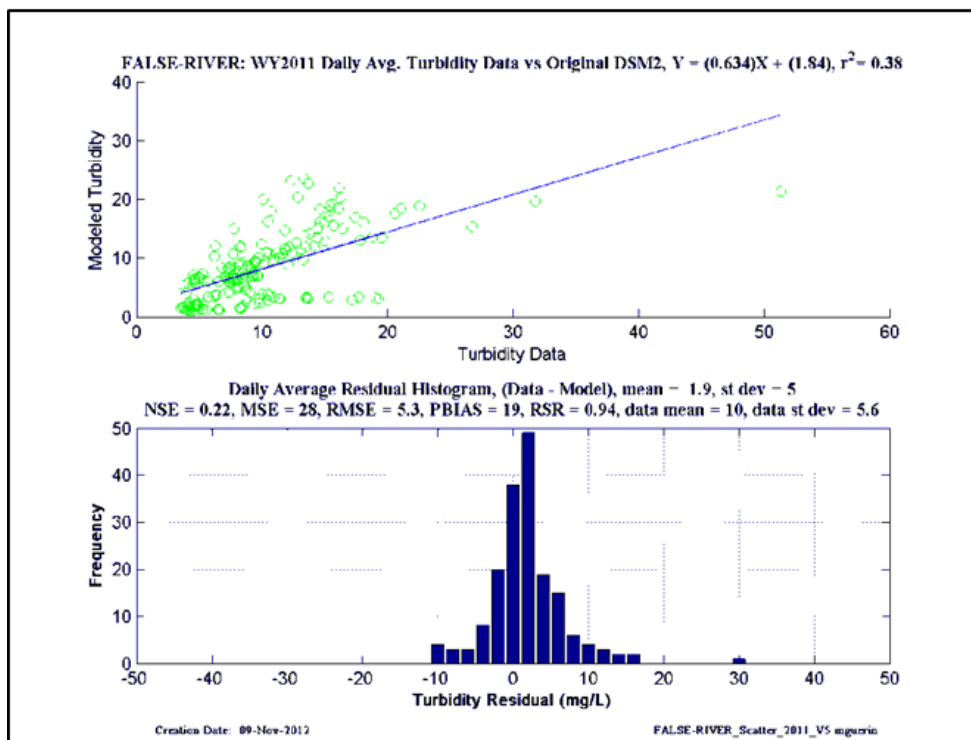
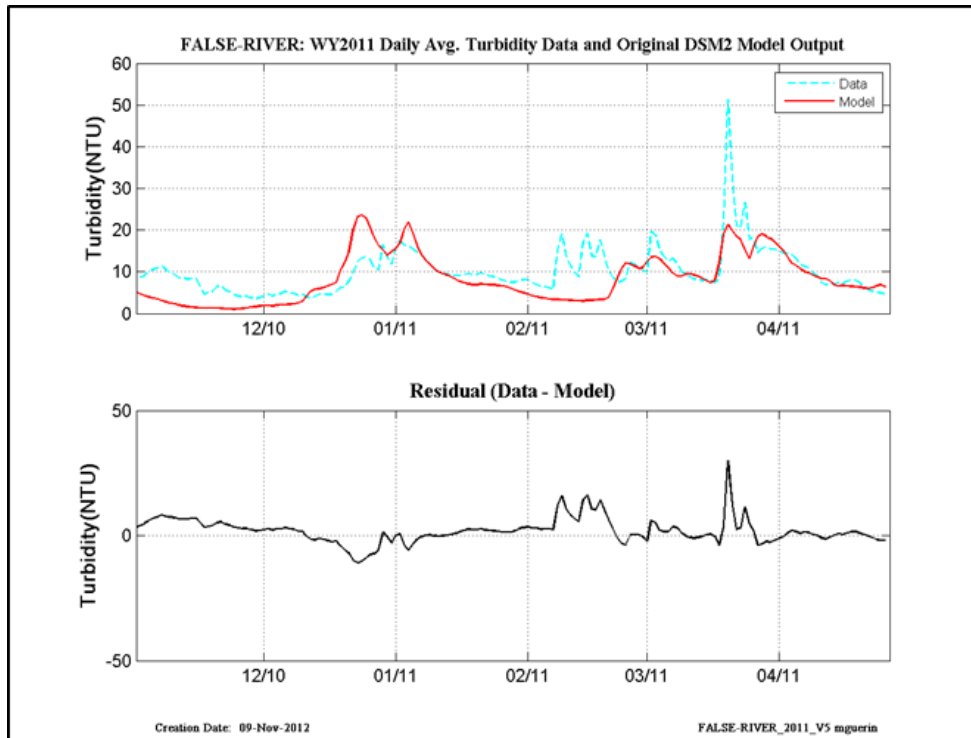


Figure 13-4 WY2011 original calibration results at False River.

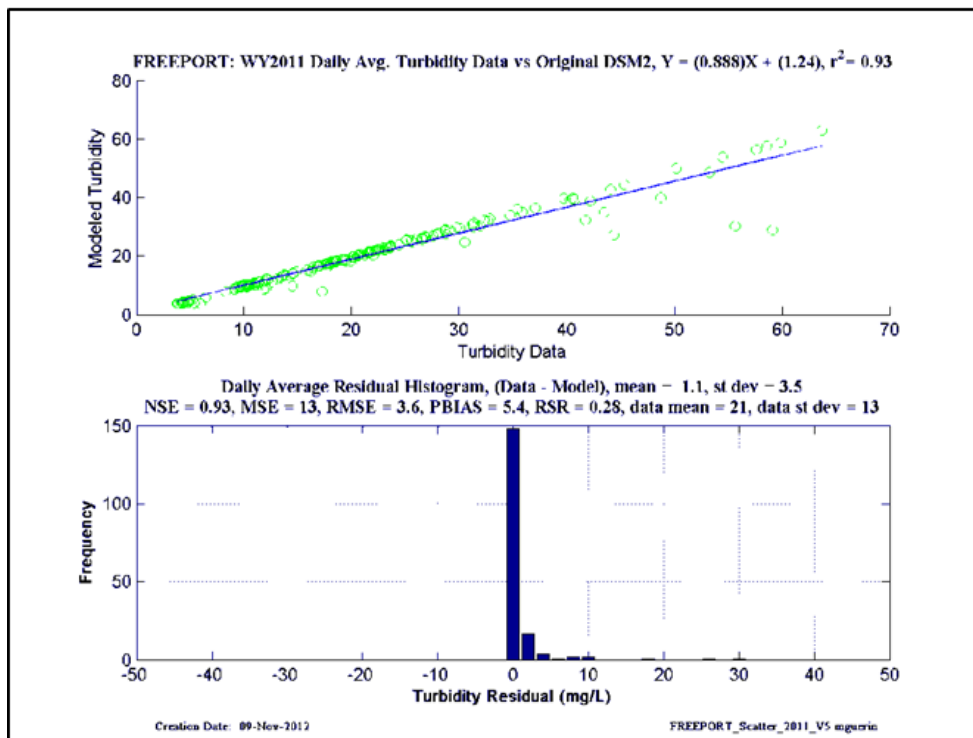
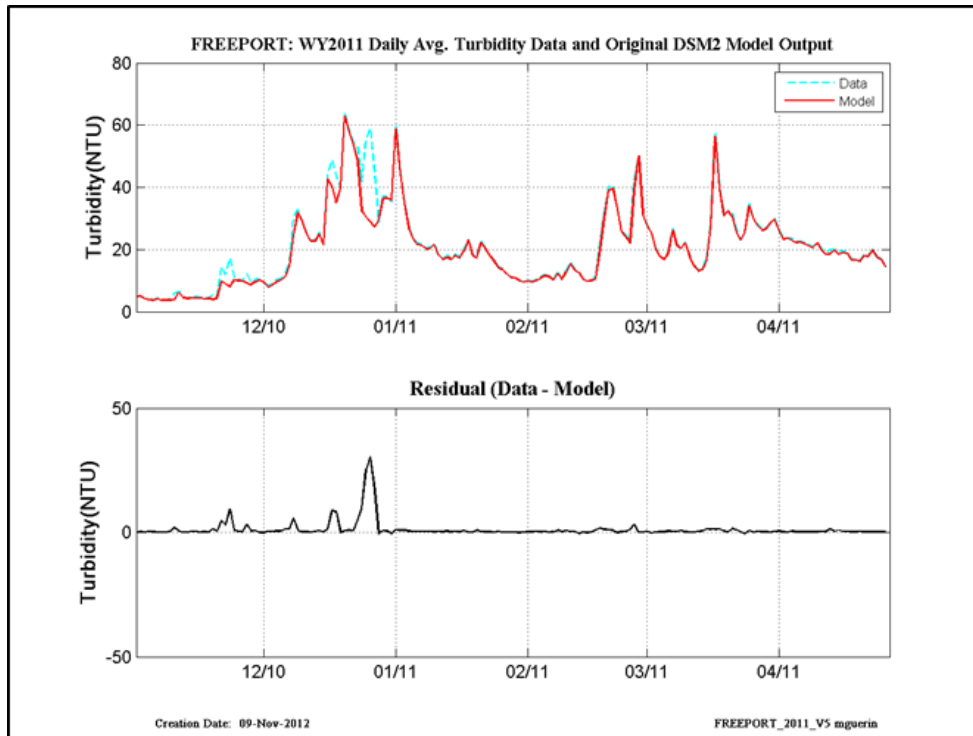


Figure 13-5 WY2011 original calibration results at Freeport.

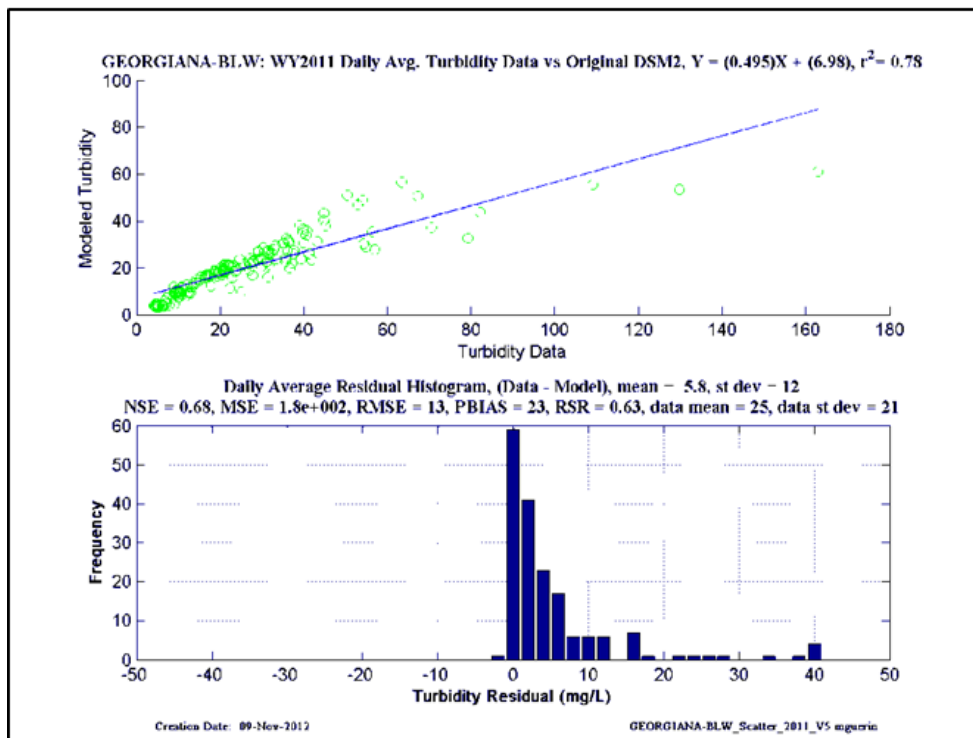
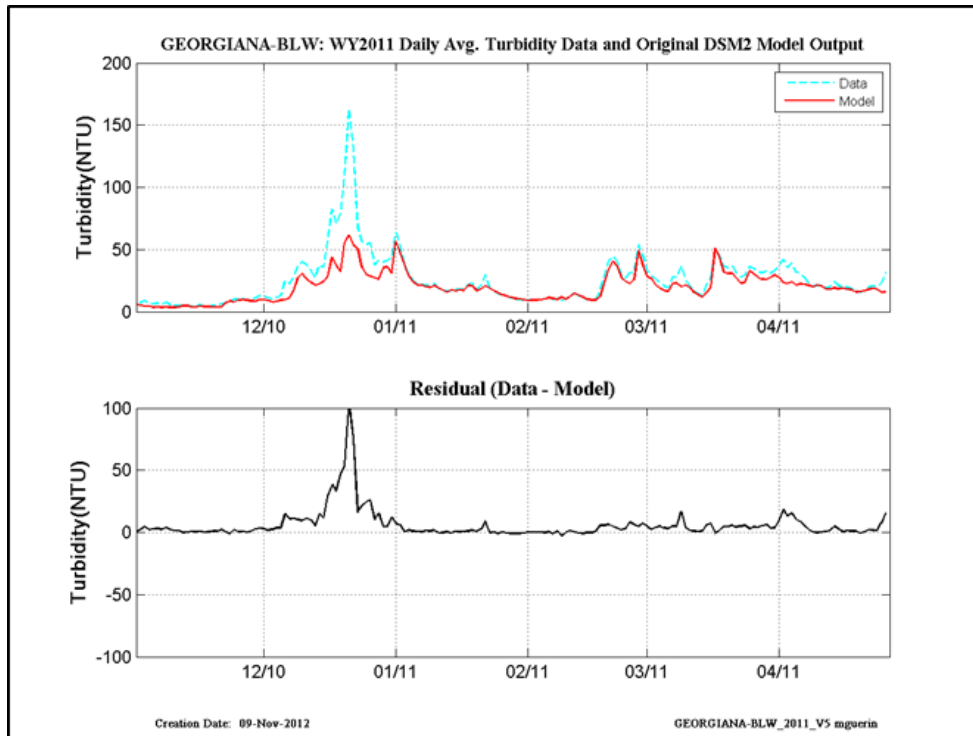


Figure 13-6 WY2011 original calibration results at Georgiana-Below-Sac.

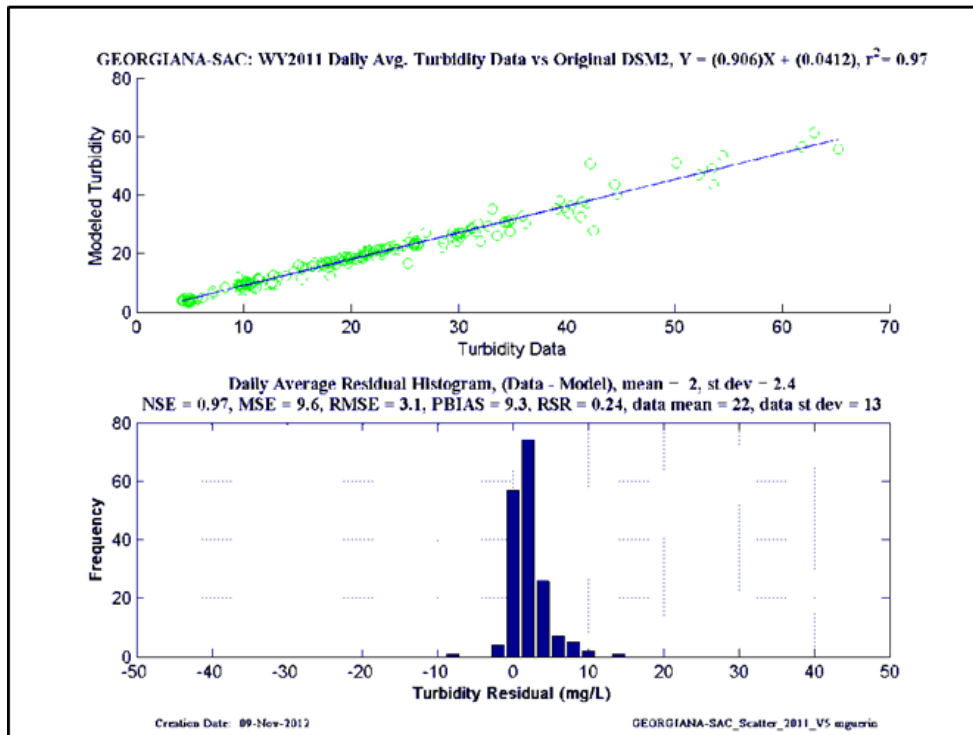
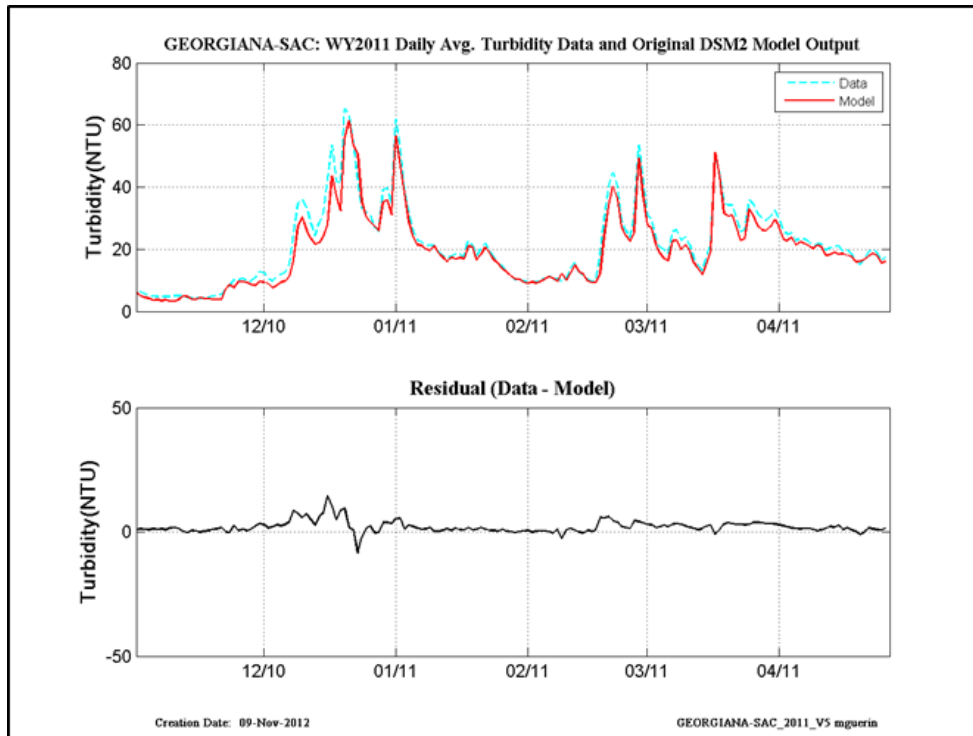


Figure 13-7 WY2011 original calibration results at Georgiana-Sac.

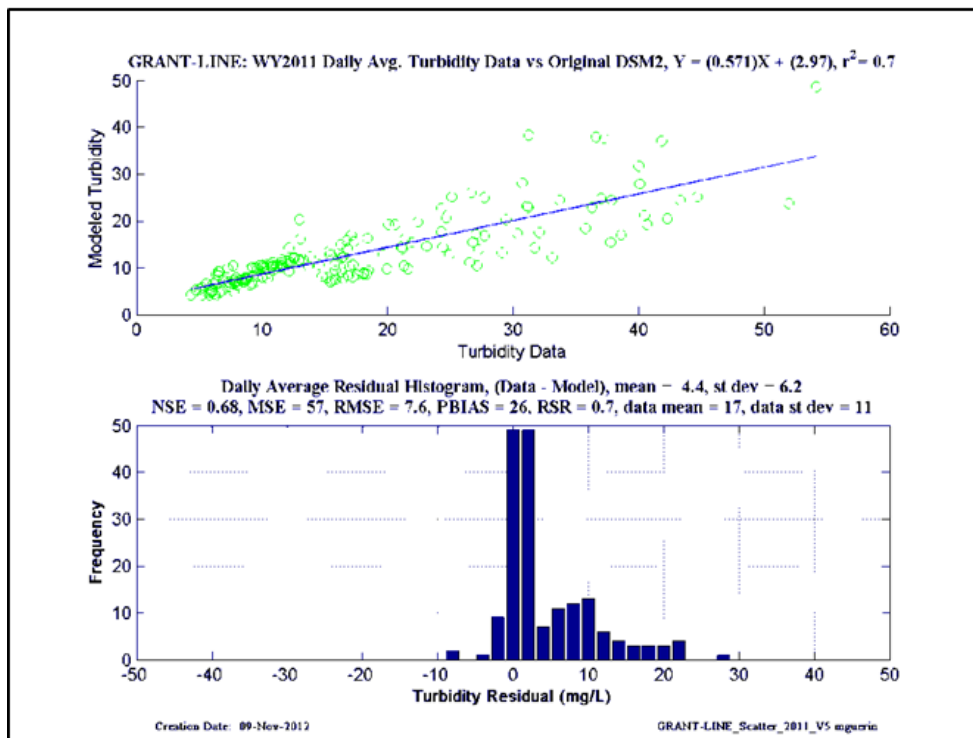
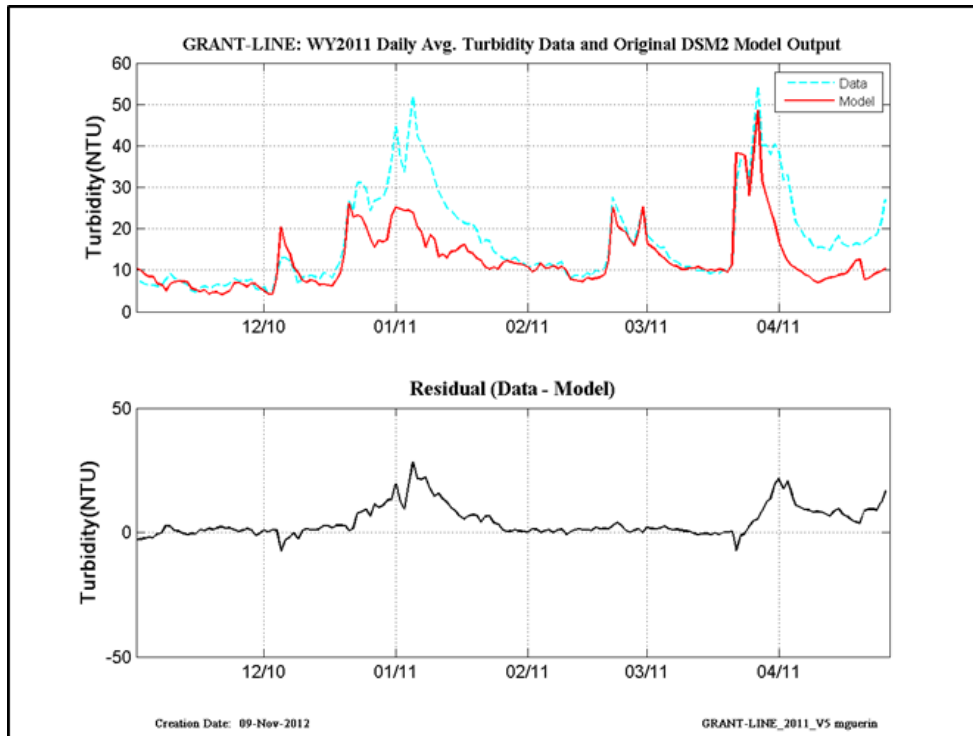


Figure 13-8 WY2011 original calibration results at Grant Line.

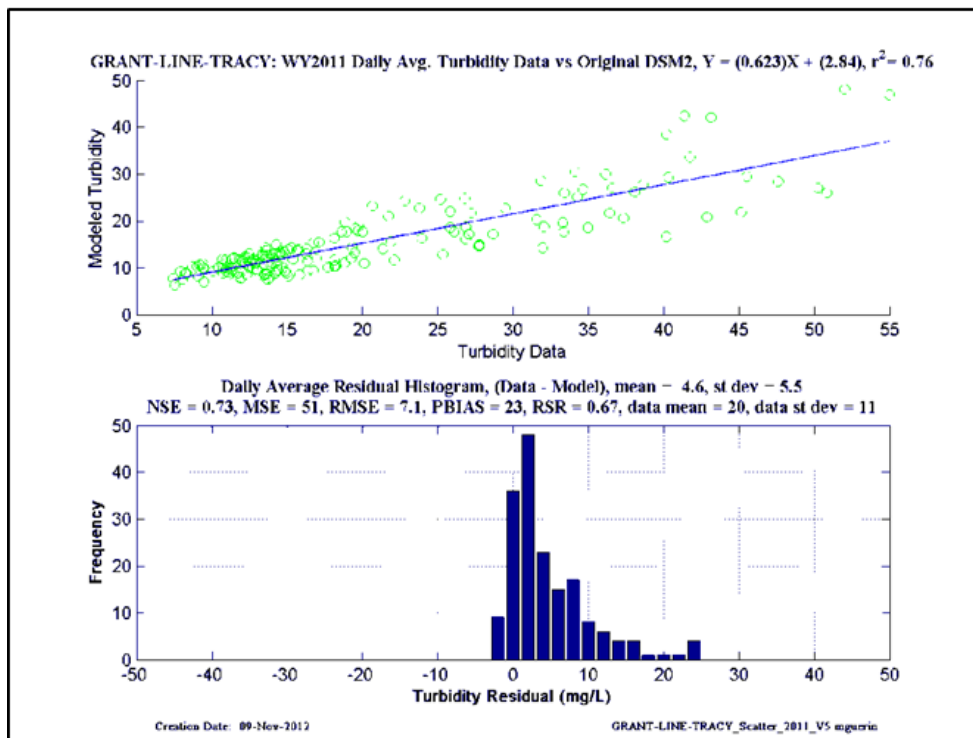
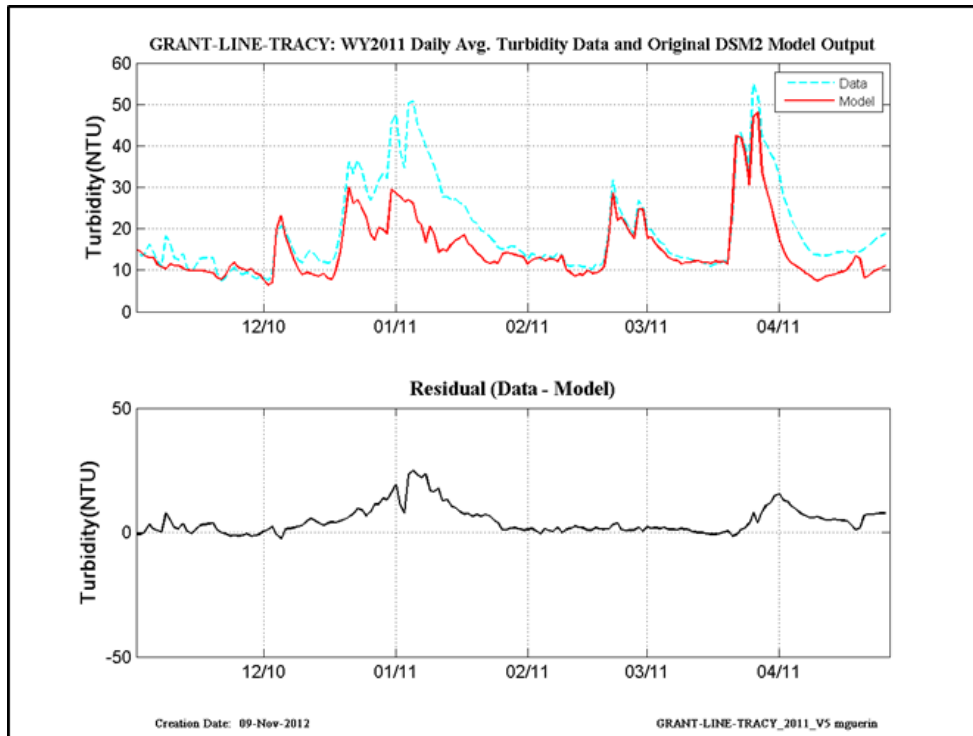


Figure 13-9 WY2011 original calibration results at Grant Line-Tracy.

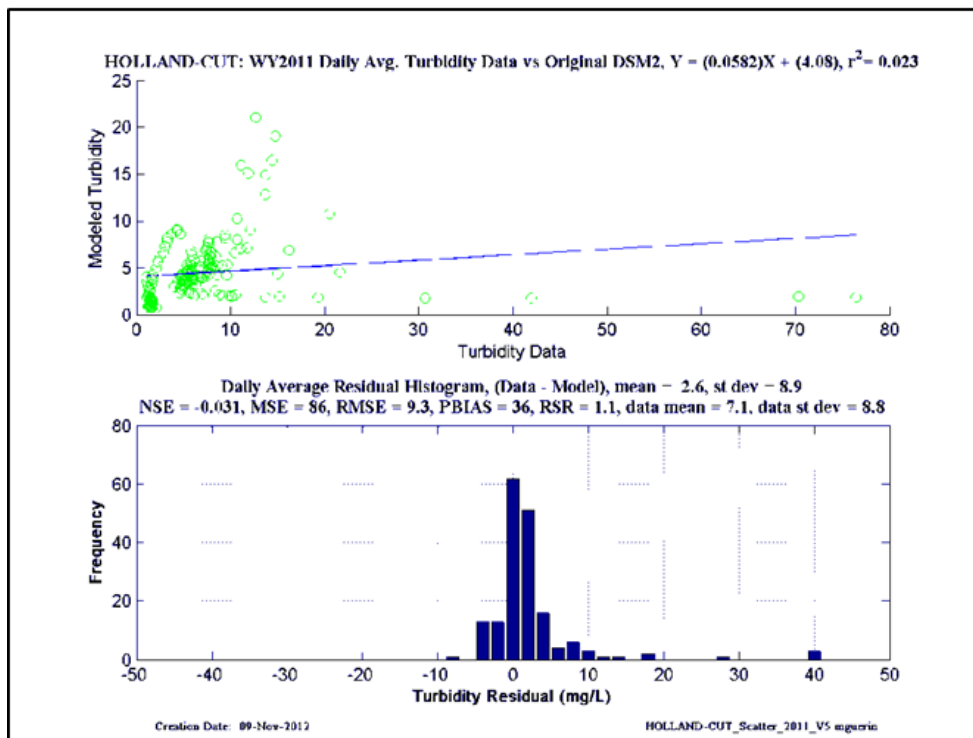
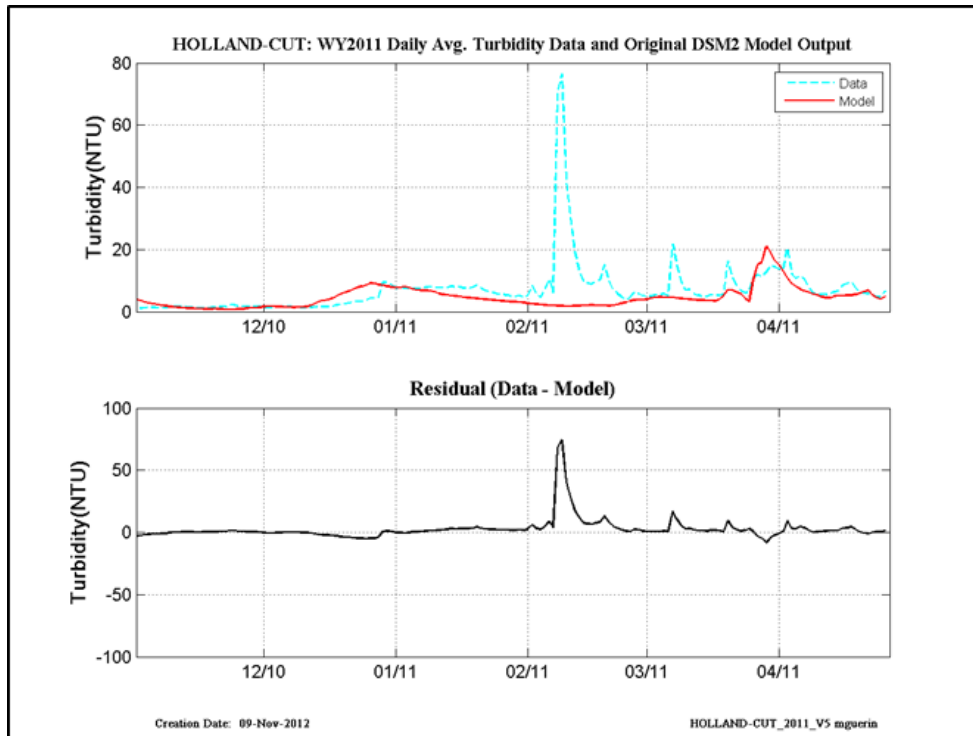


Figure 13-10 WY2011 original calibration results at Holland Cut.

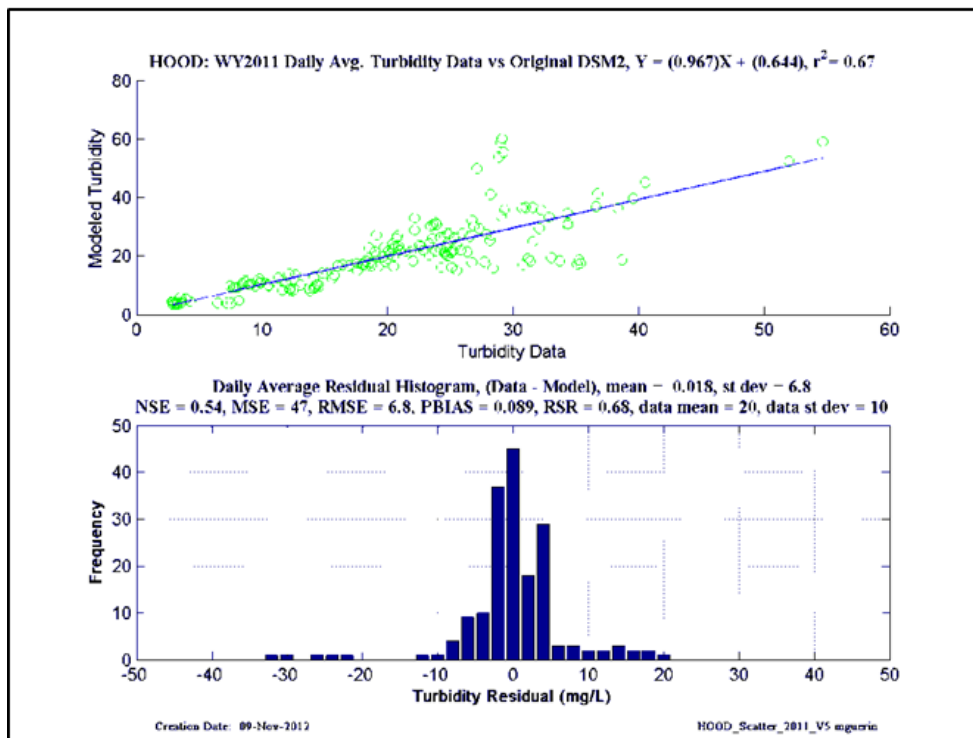
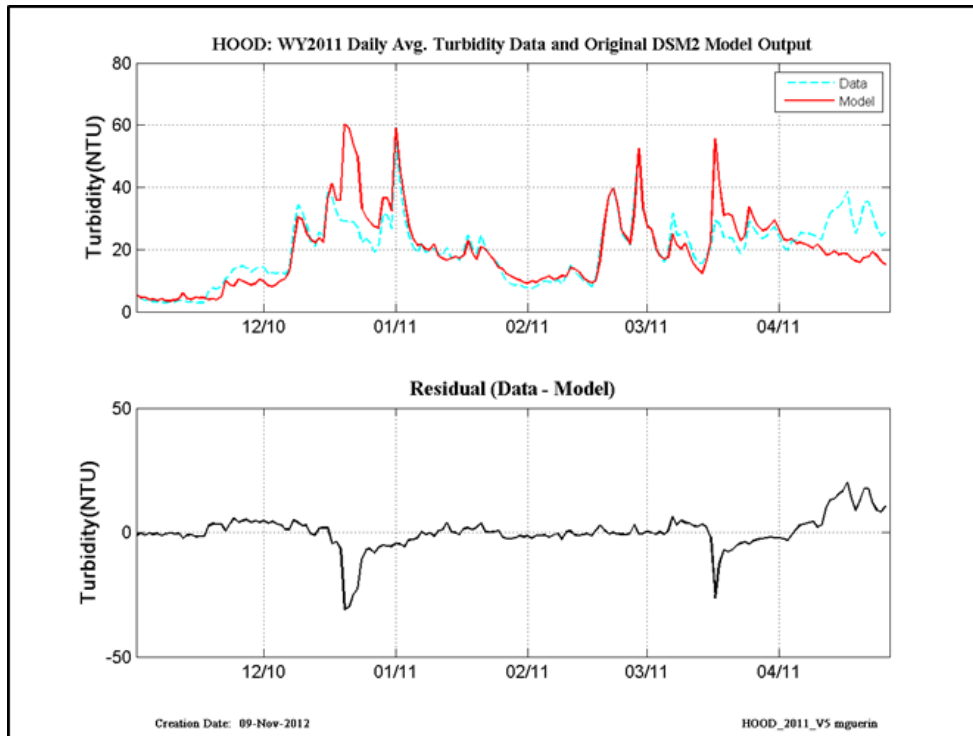


Figure 13-11 WY2011 original calibration results at Hood.

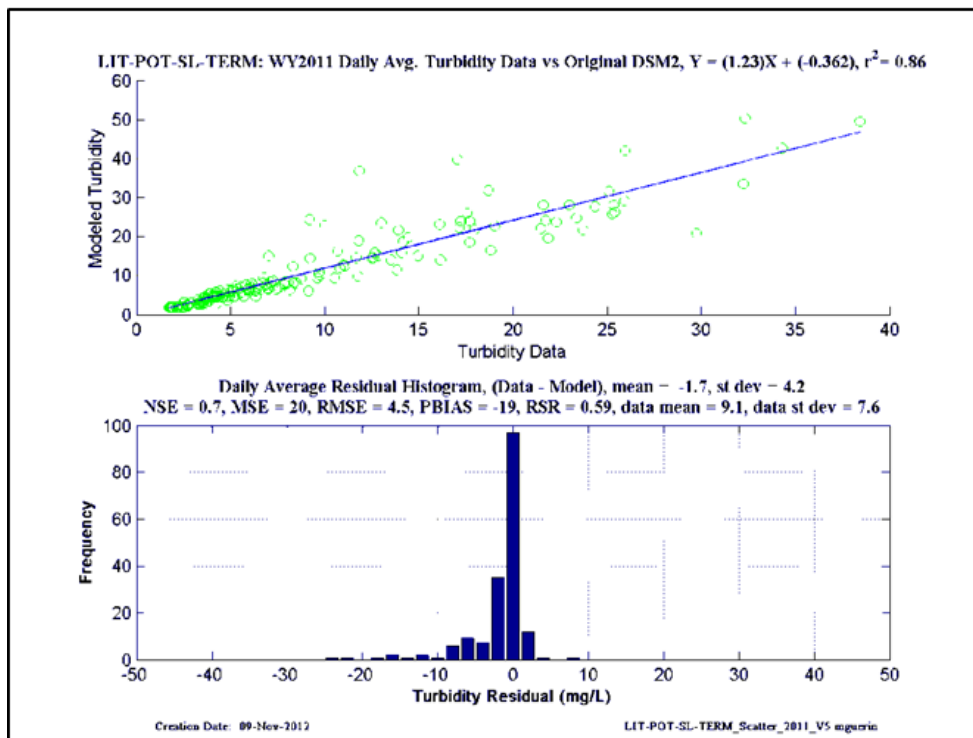
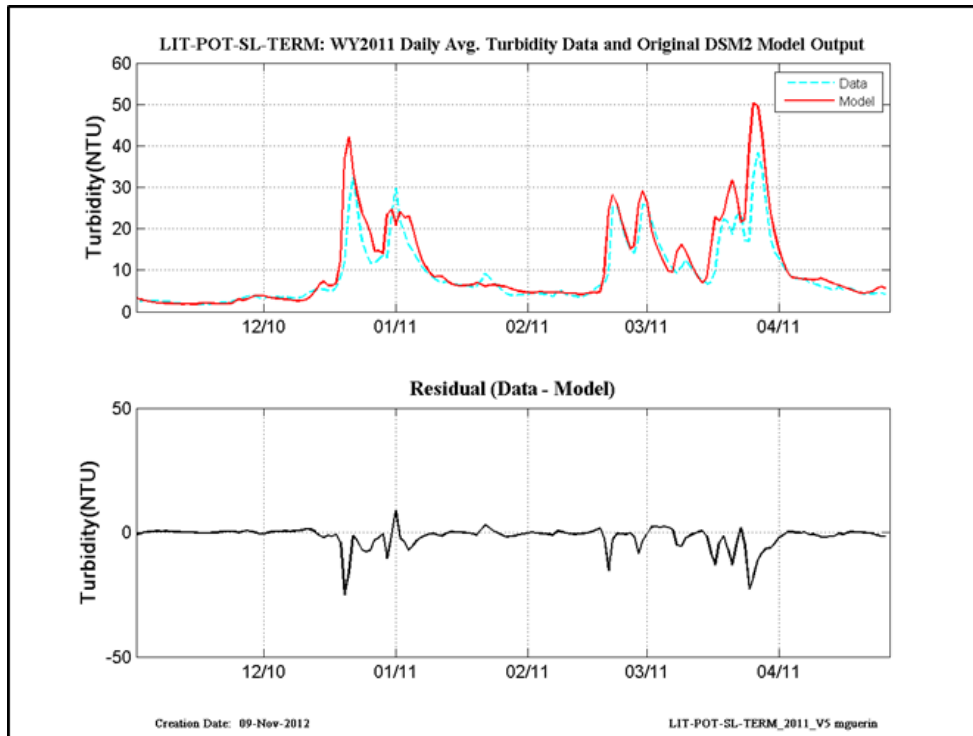


Figure 13-12 WY2011 original calibration results at Little Potato Slough-at-Terminus.

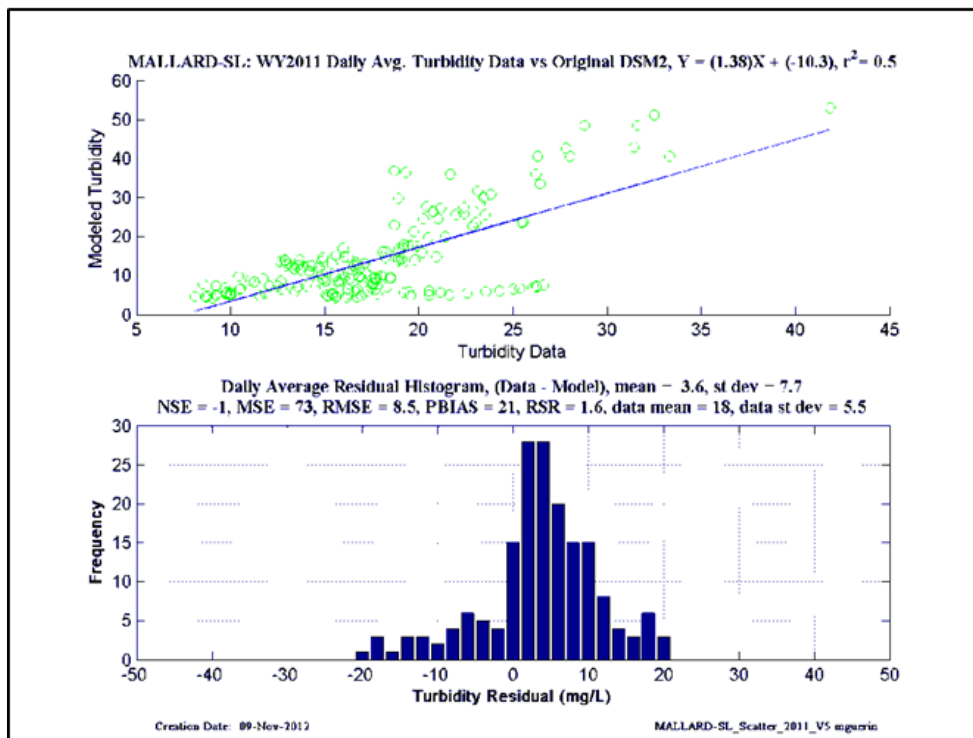
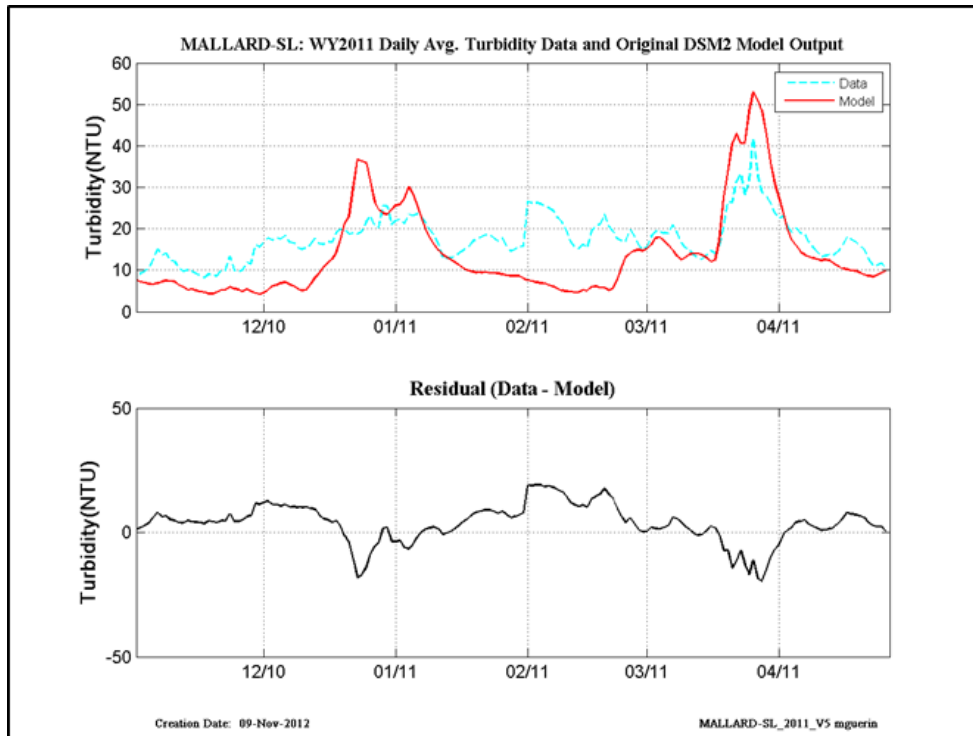


Figure 13-13 WY2011 original calibration results at Mallard Slough.

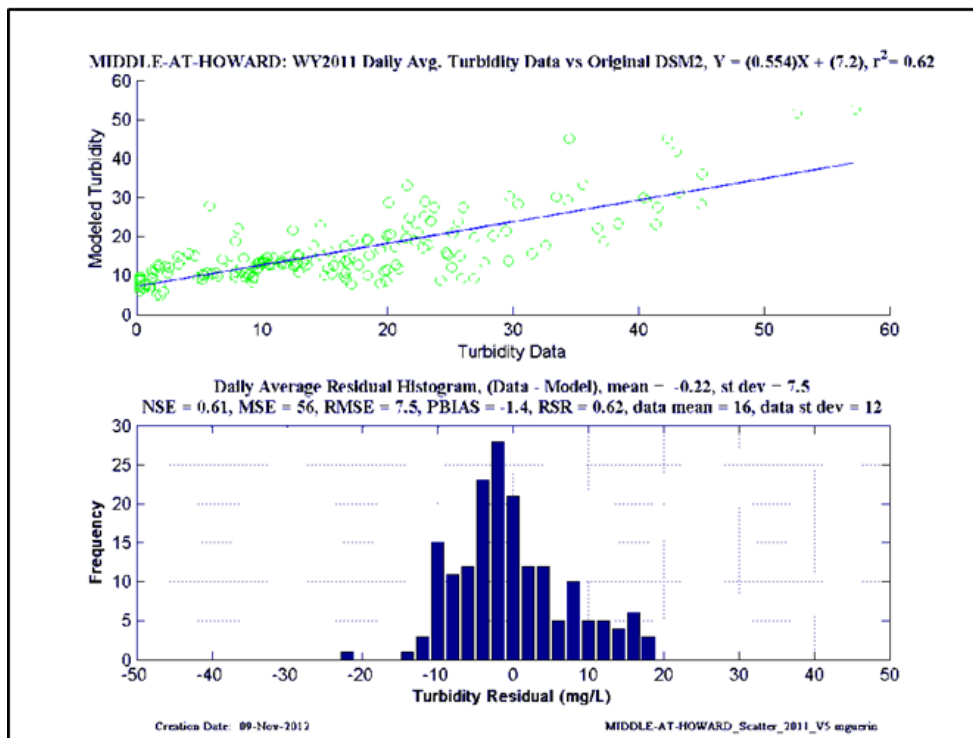
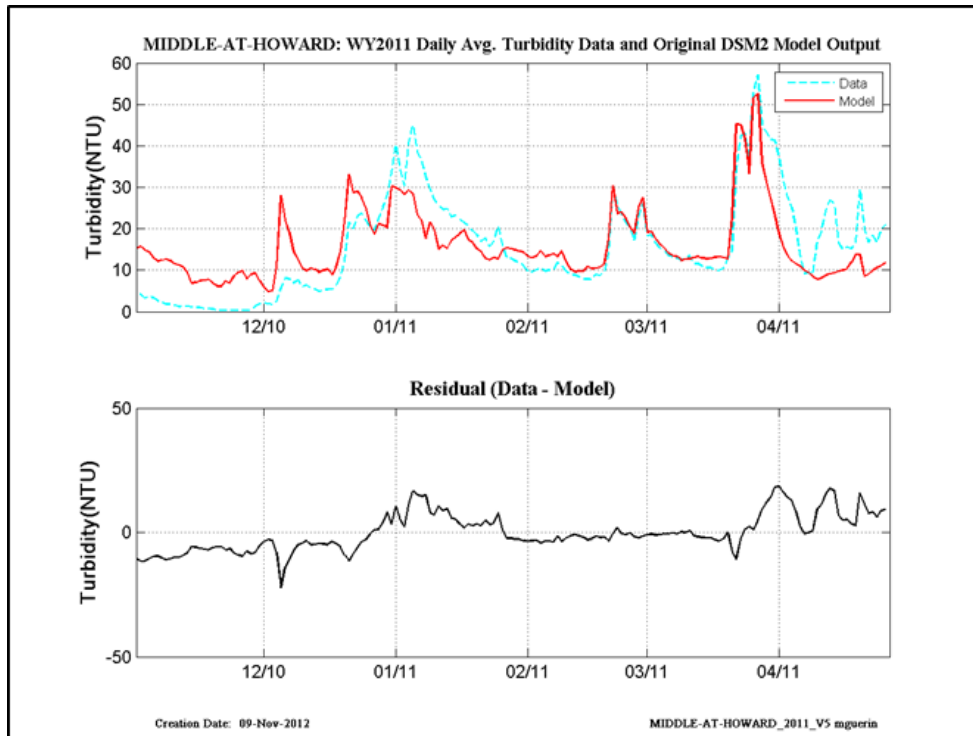


Figure 13-14 WY2011 original calibration results at Middle River-at-Howard.

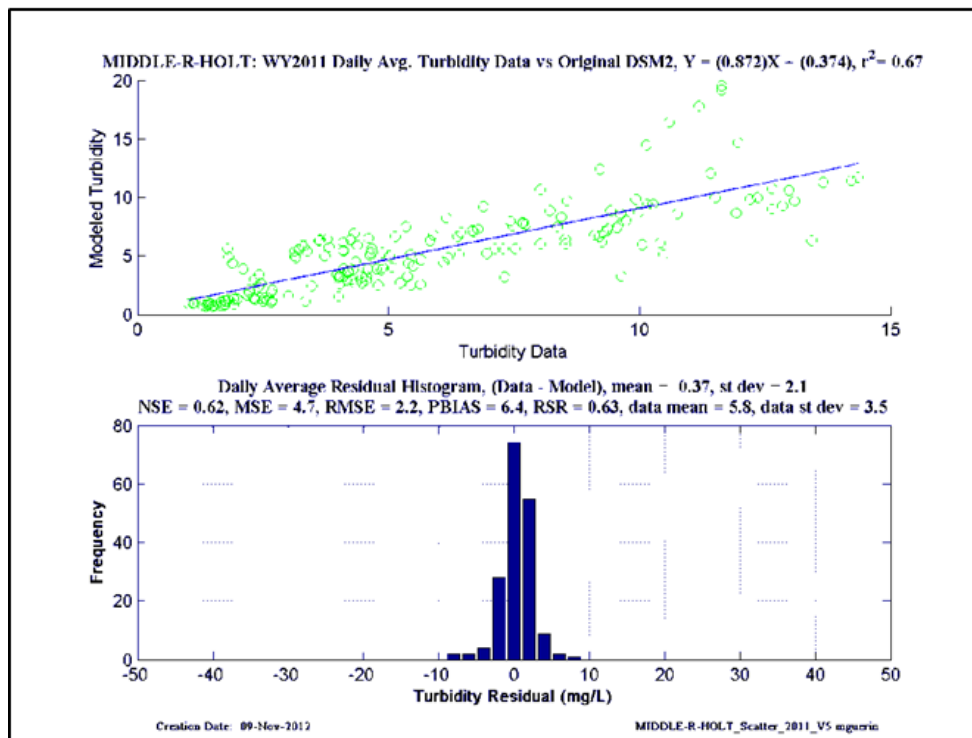
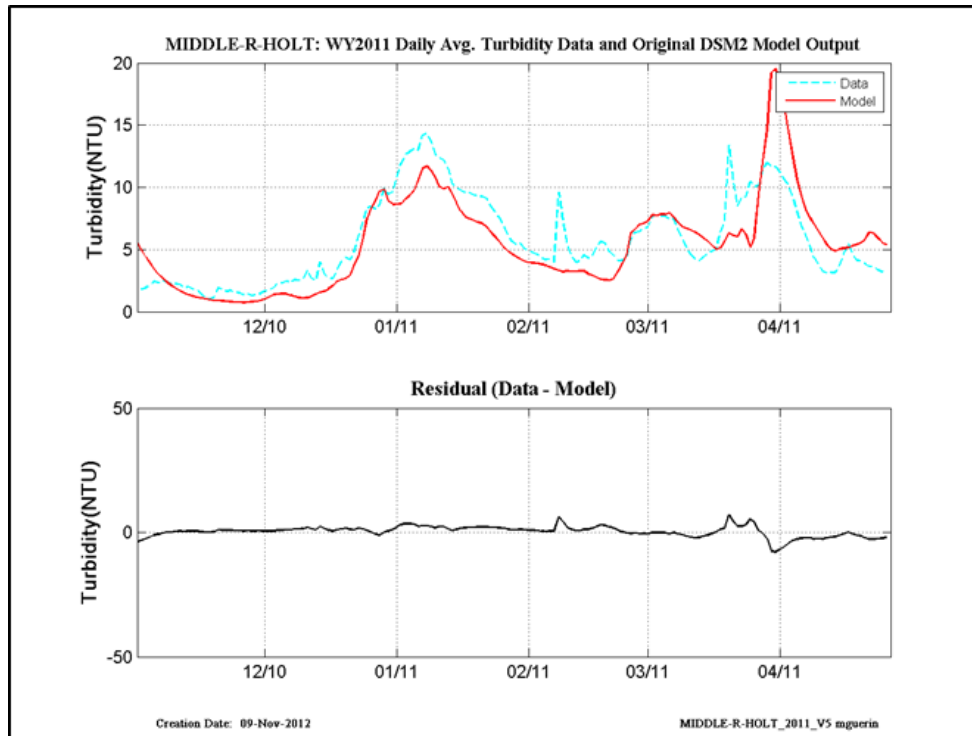


Figure 13-15 WY2011 original calibration results at Middle River-at-Holt.

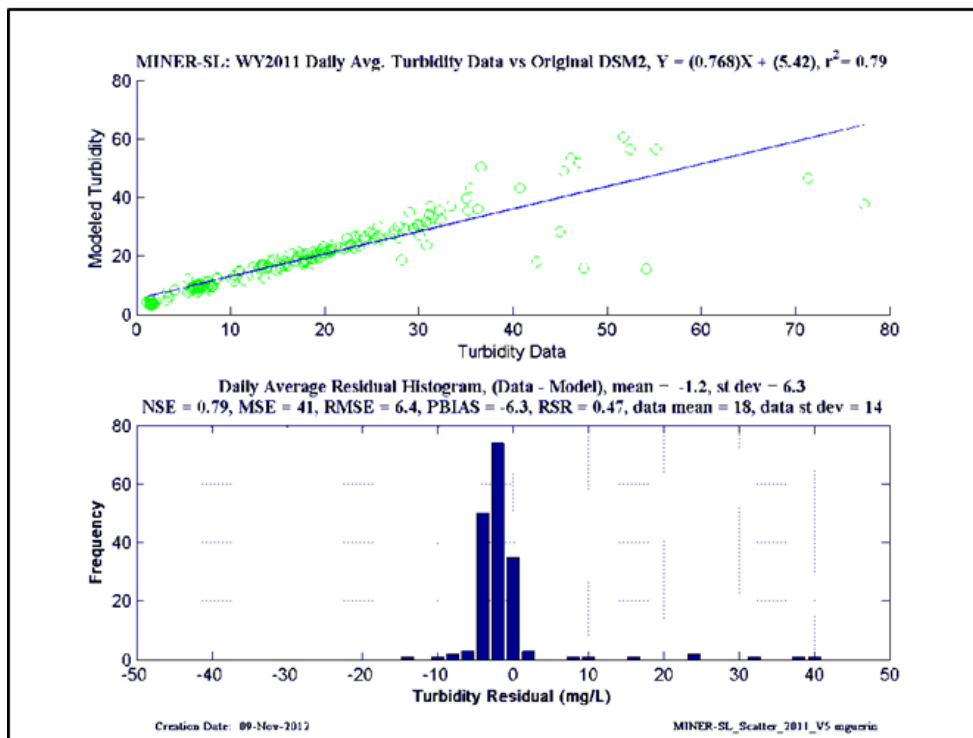
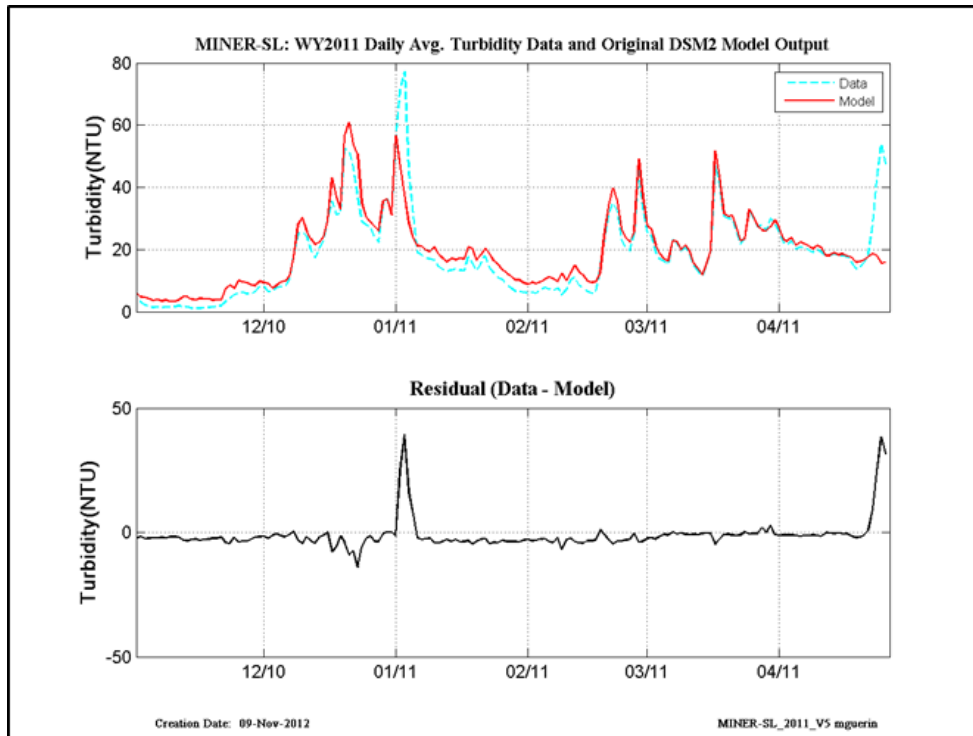


Figure 13-16 WY2011 original calibration results at Miner Slough.

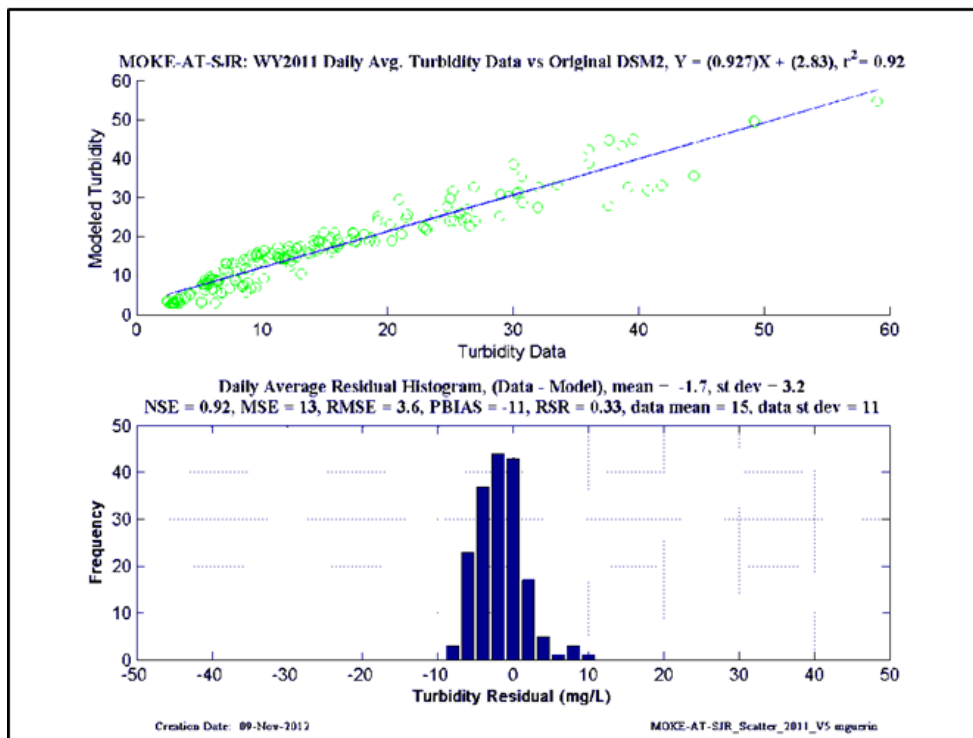
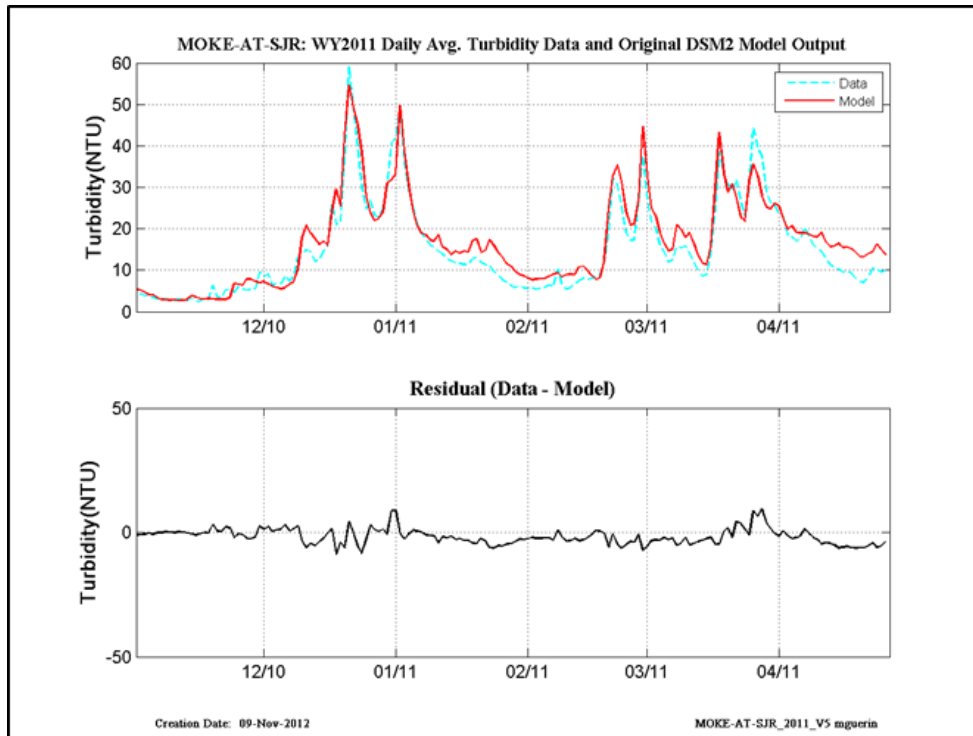


Figure 13-17 WY2011 original calibration results at Mokelumne-at-San Joaquin.

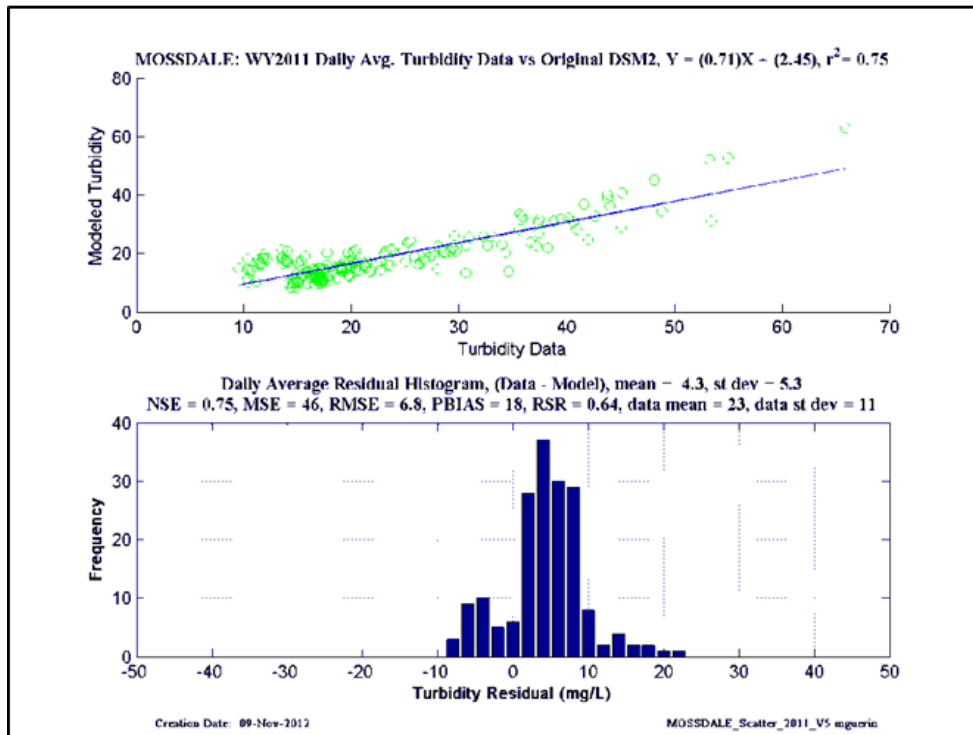
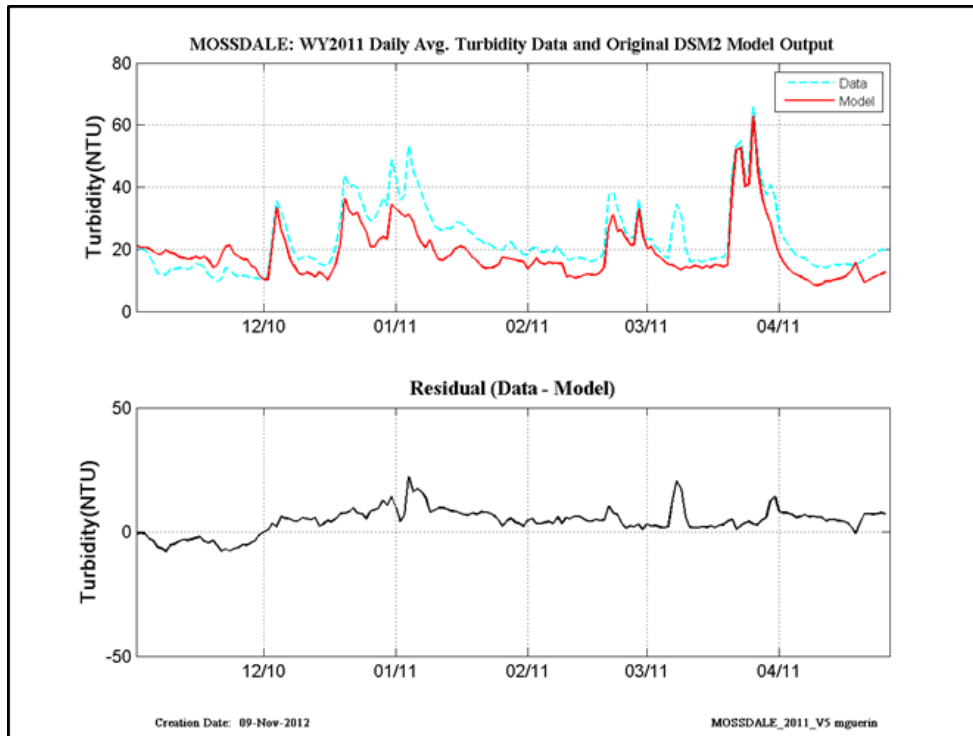


Figure 13-18 WY2011 original calibration results at Mossdale.

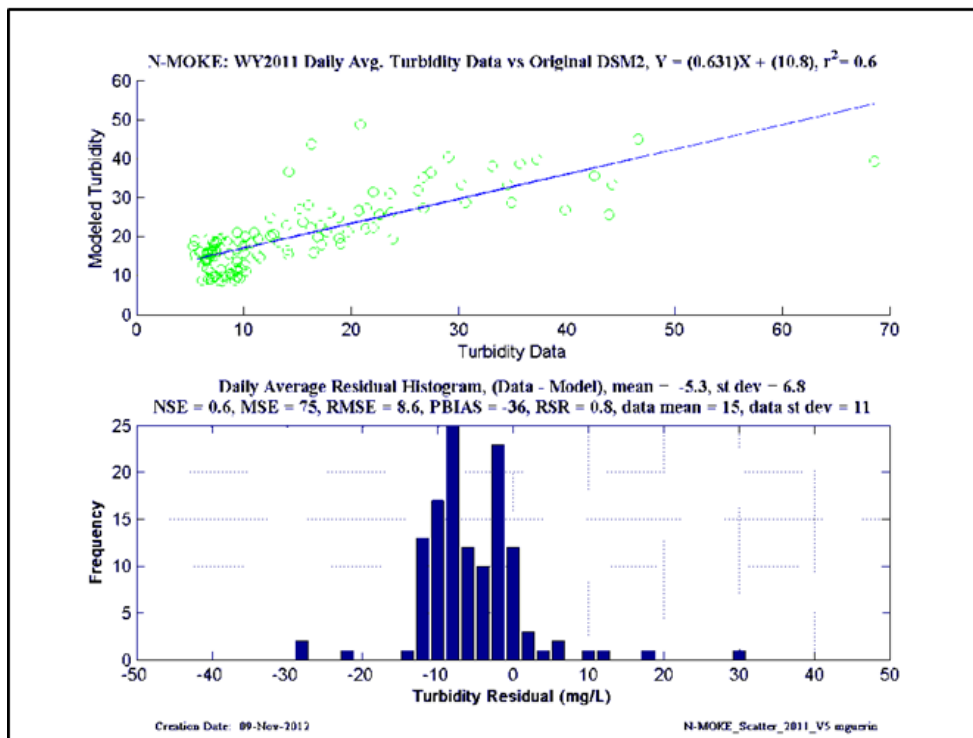
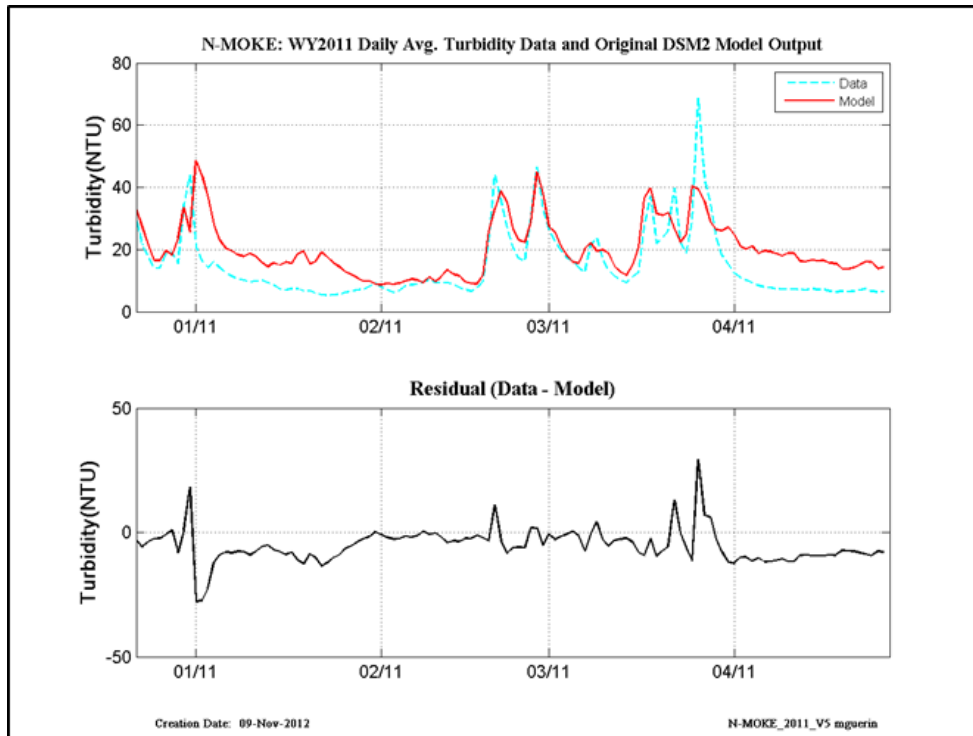


Figure 13-19 WY2011 original calibration results at North Mokelumne.

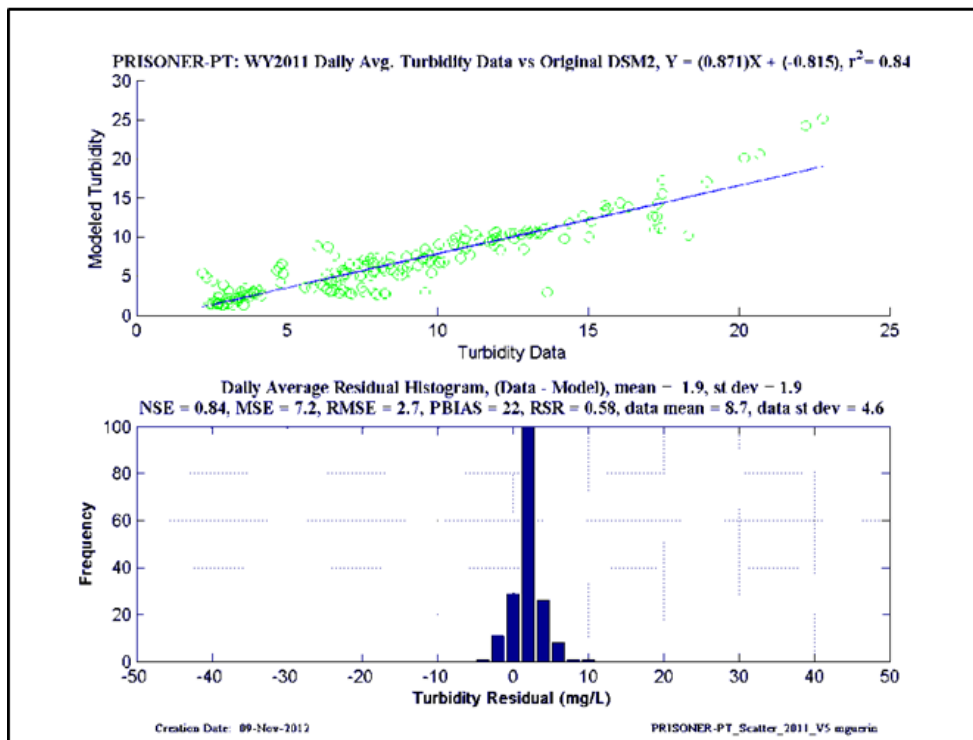
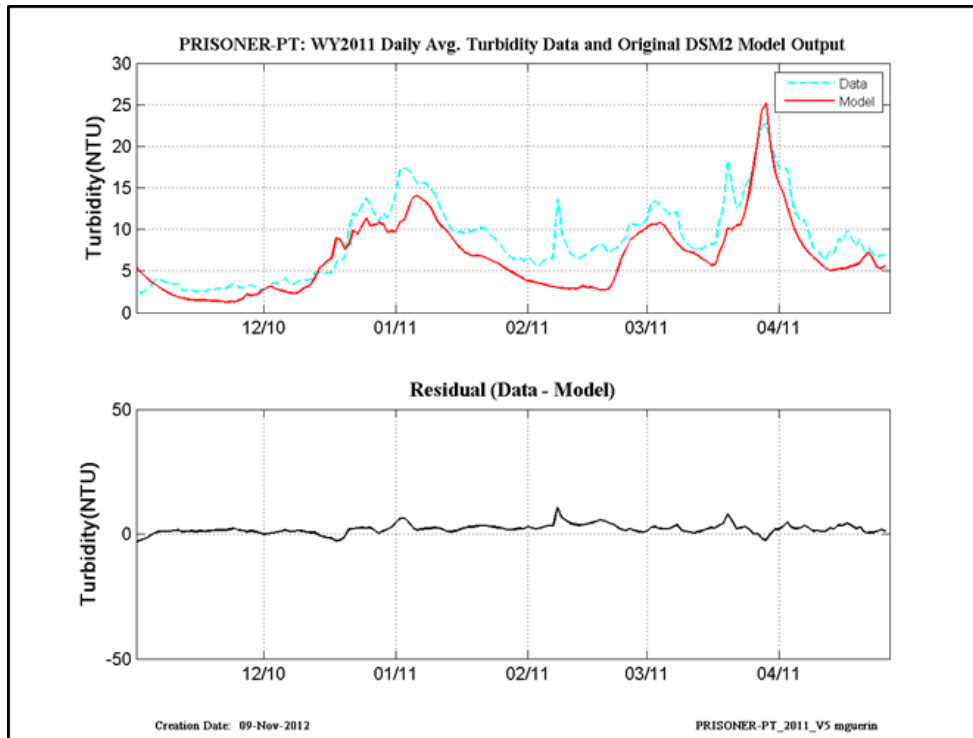


Figure 13-20 WY2011 original calibration results at Prisoner Point.

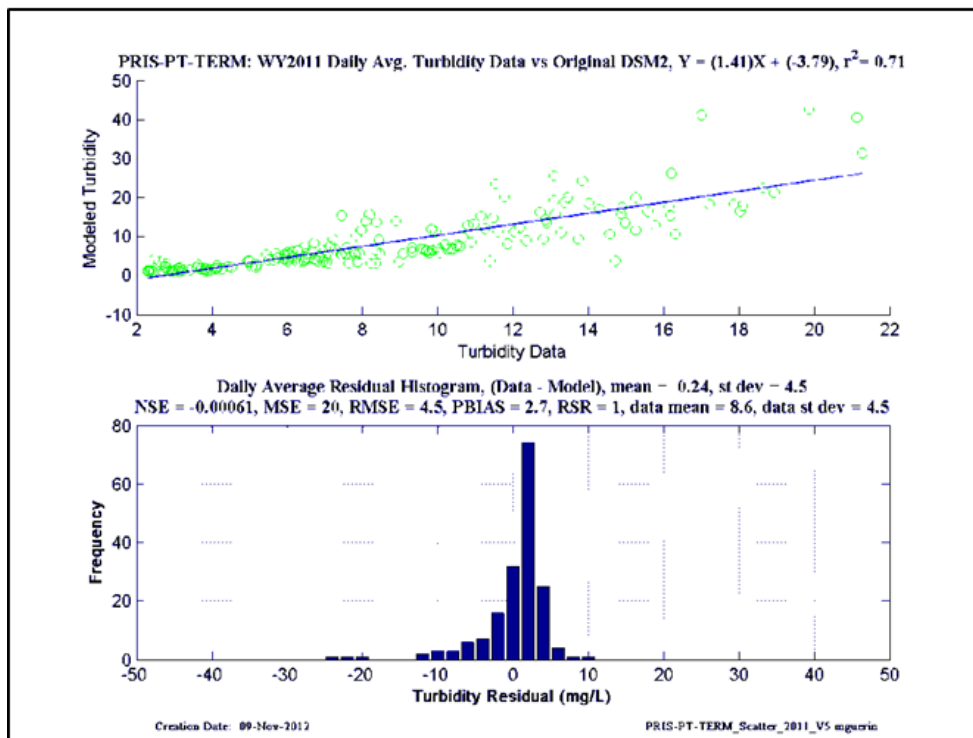
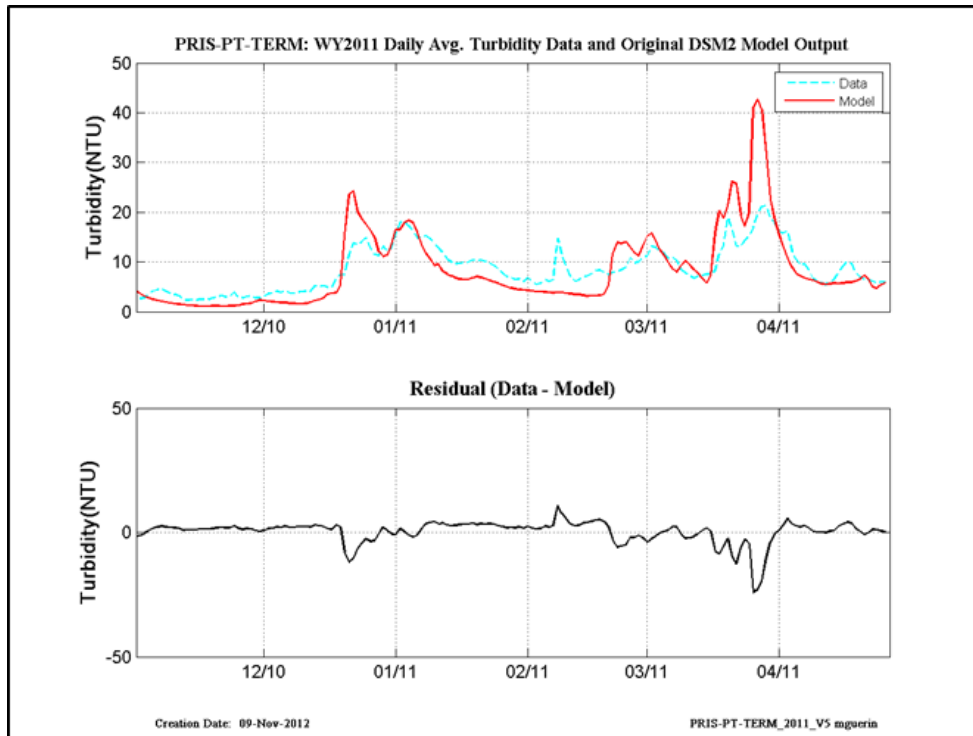


Figure 13-21 WY2011 original calibration results at Prisoner Point-at-Terminus.

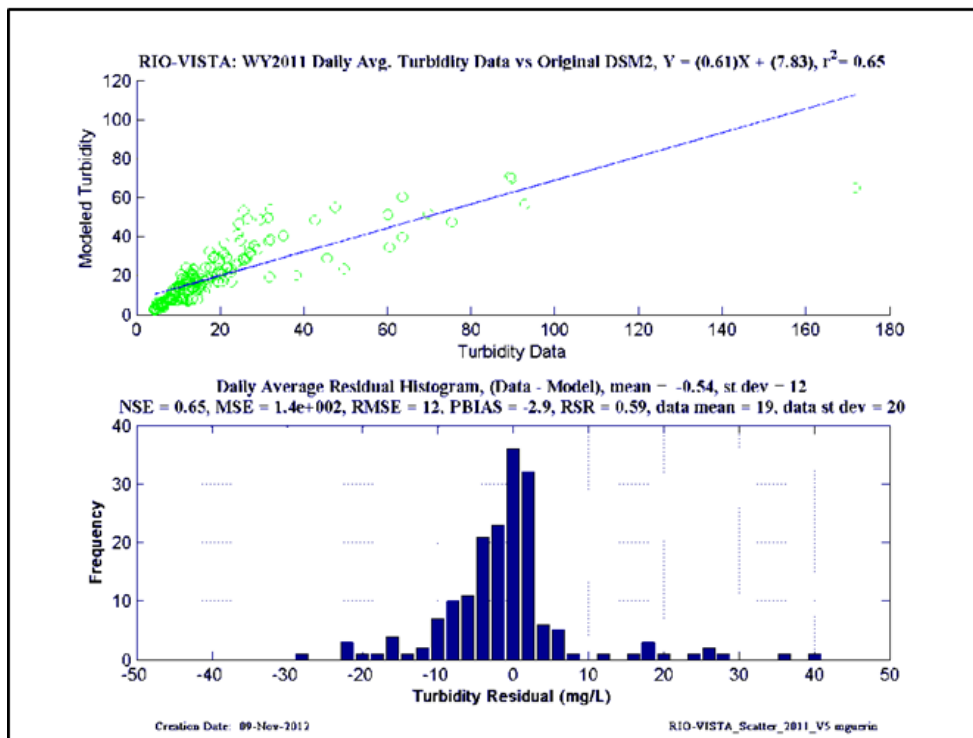
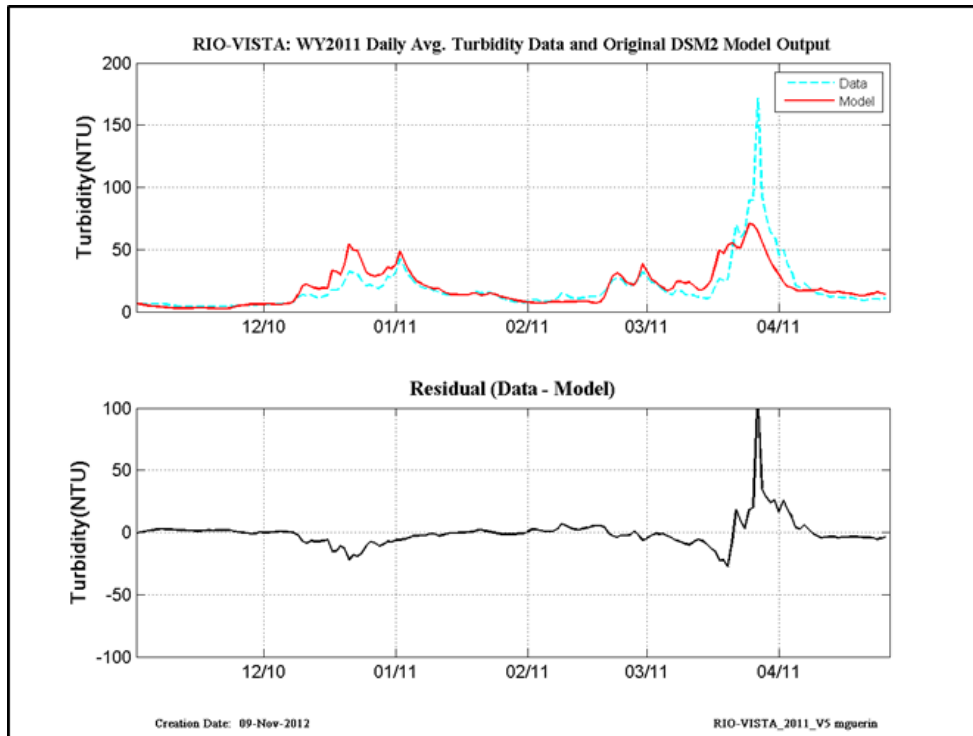


Figure 13-22 WY2011 original calibration results at Rio Vista.

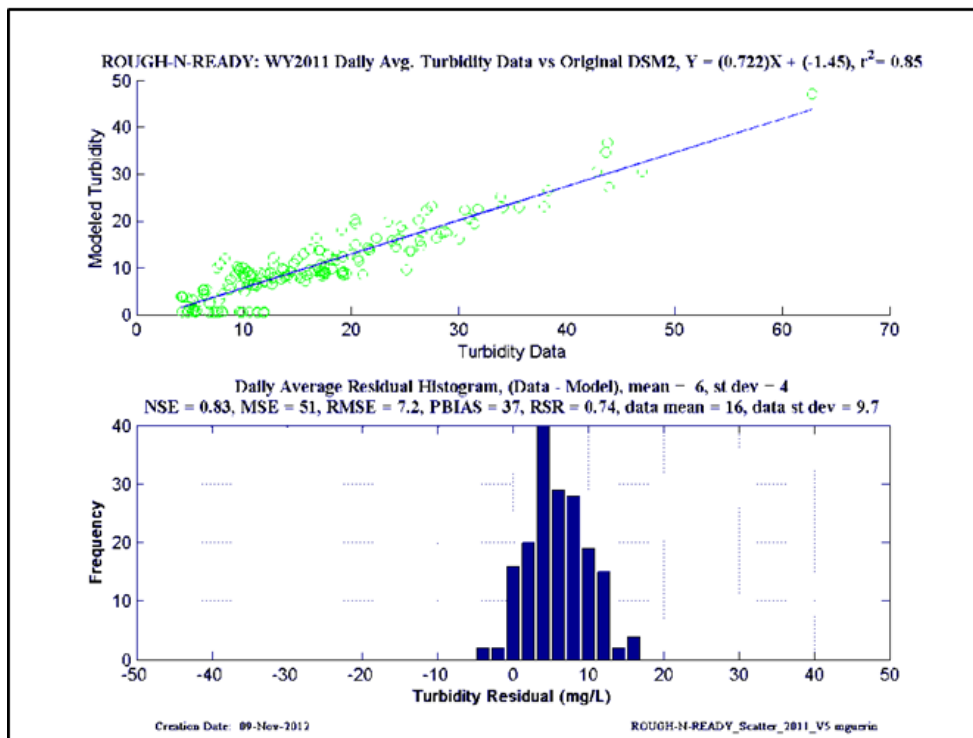
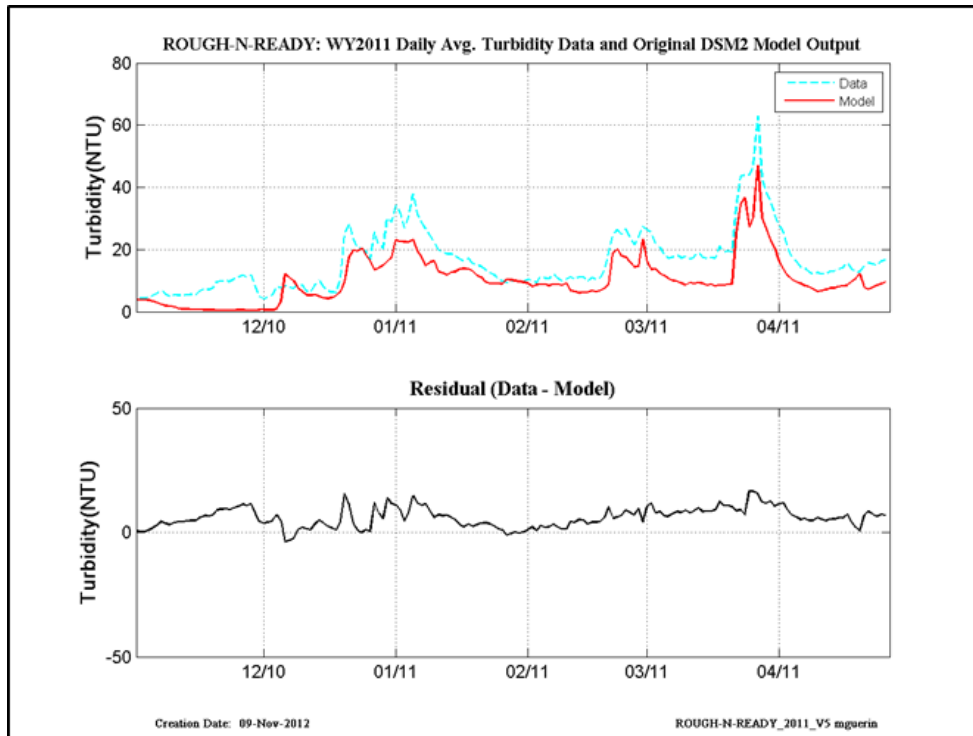


Figure 13-23 WY2011 original calibration results at Rough-N-Ready Island.

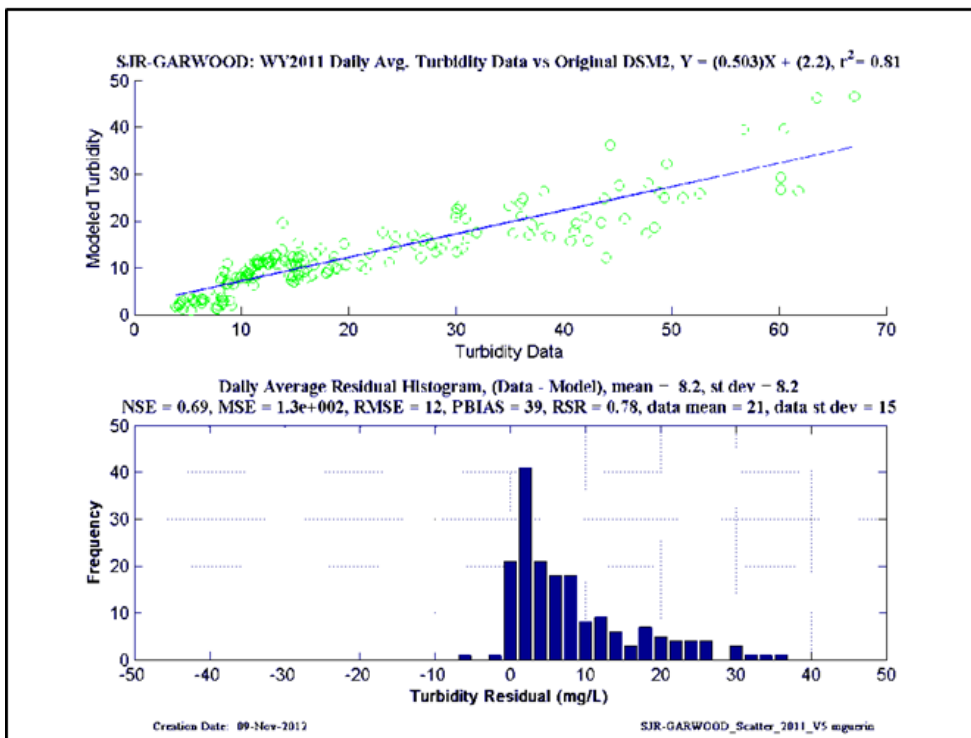
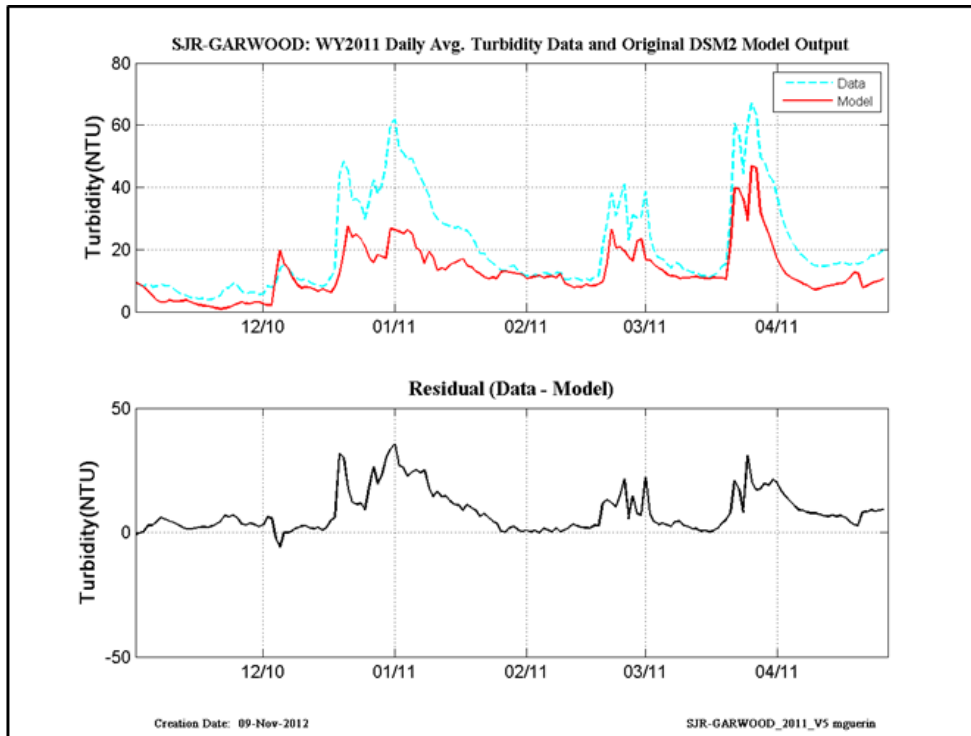


Figure 13-24 WY2011 original calibration results at San Joaquin-at-Garwood.

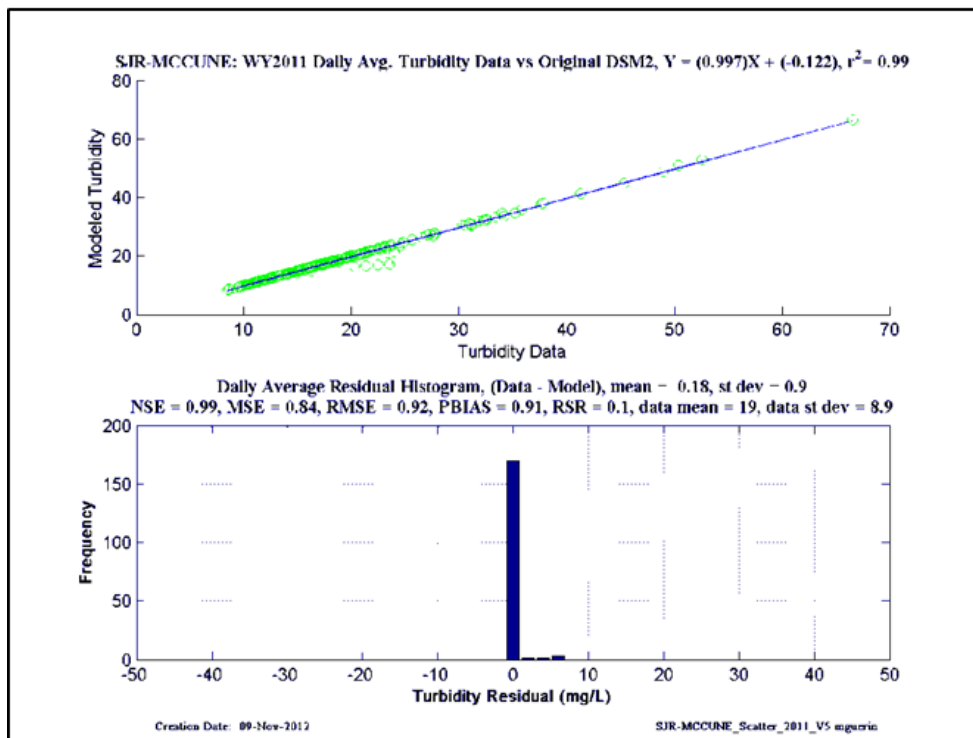
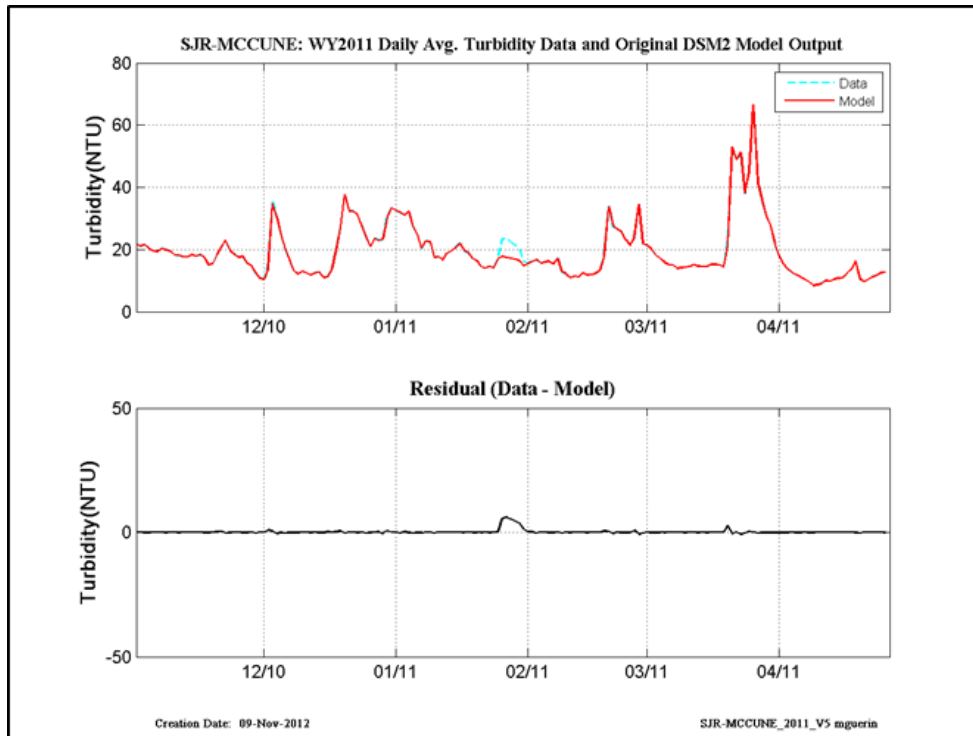


Figure 13-25 WY2011 original calibration results at San Joaquin-at-McCune (Vernalis).

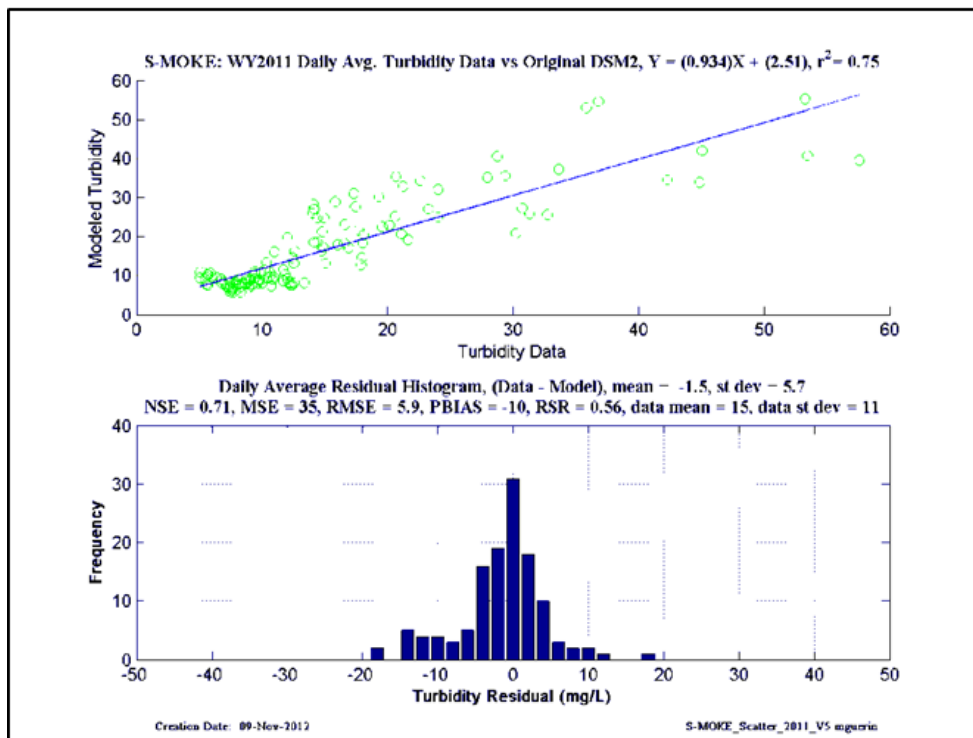
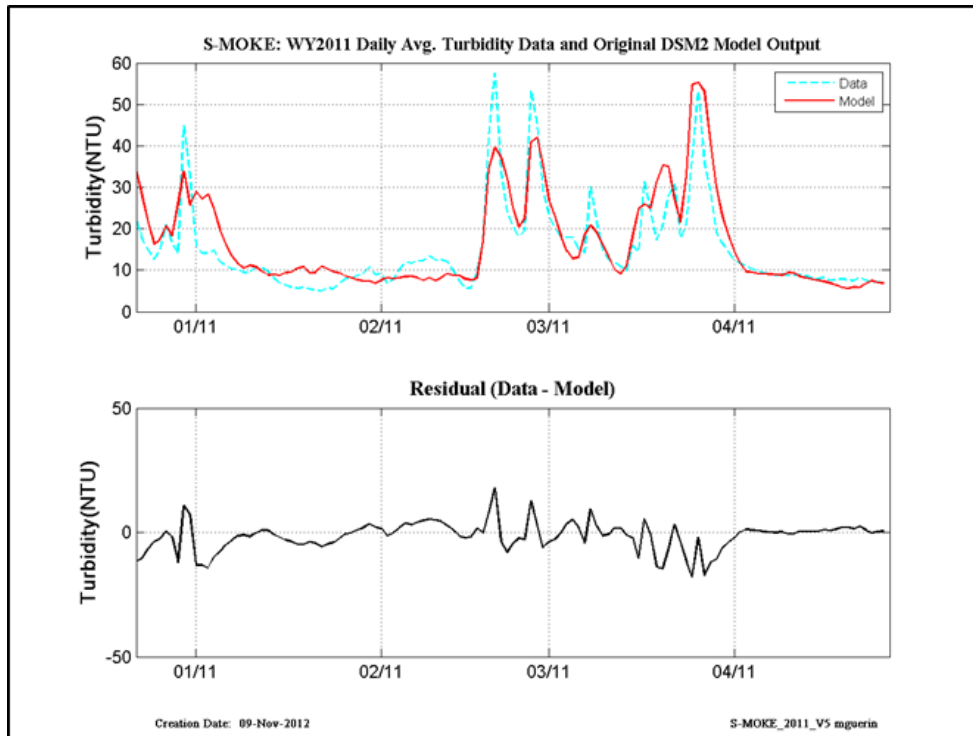


Figure 13-26 WY2011 original calibration results at South Mokelumne.

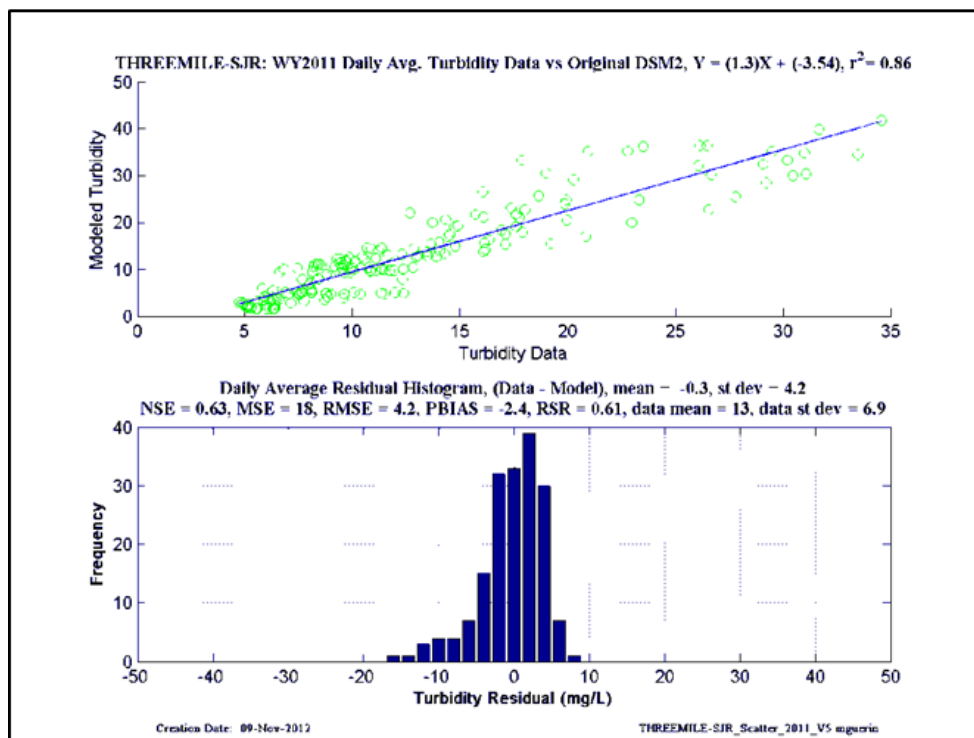
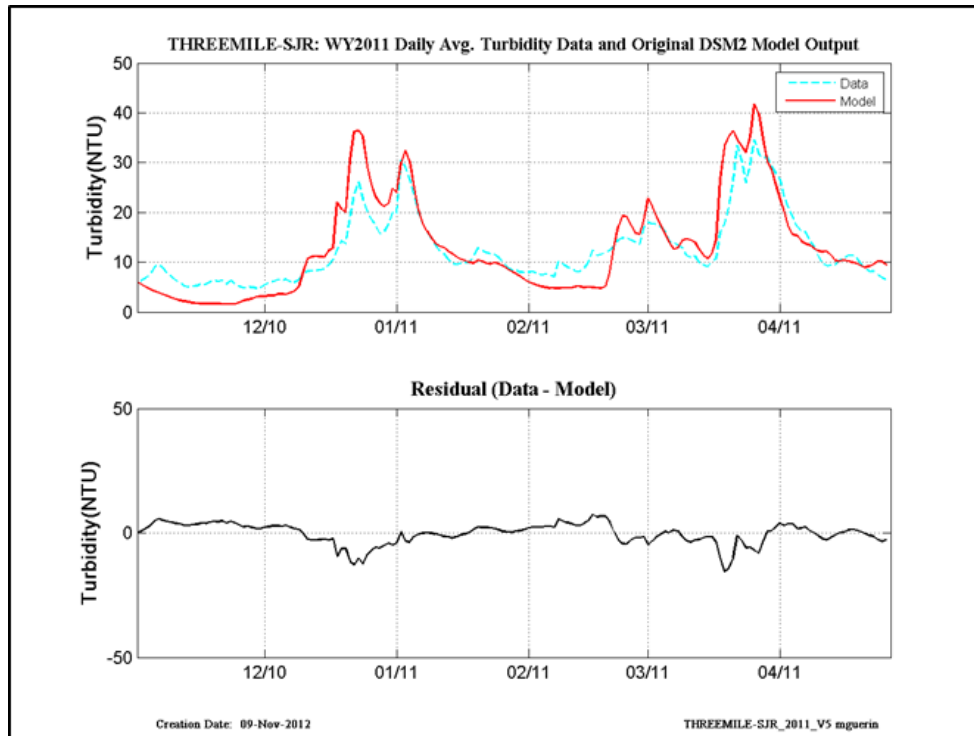


Figure 13-27 WY2011 original calibration results at Threemile-Slough-at San Joaquin.

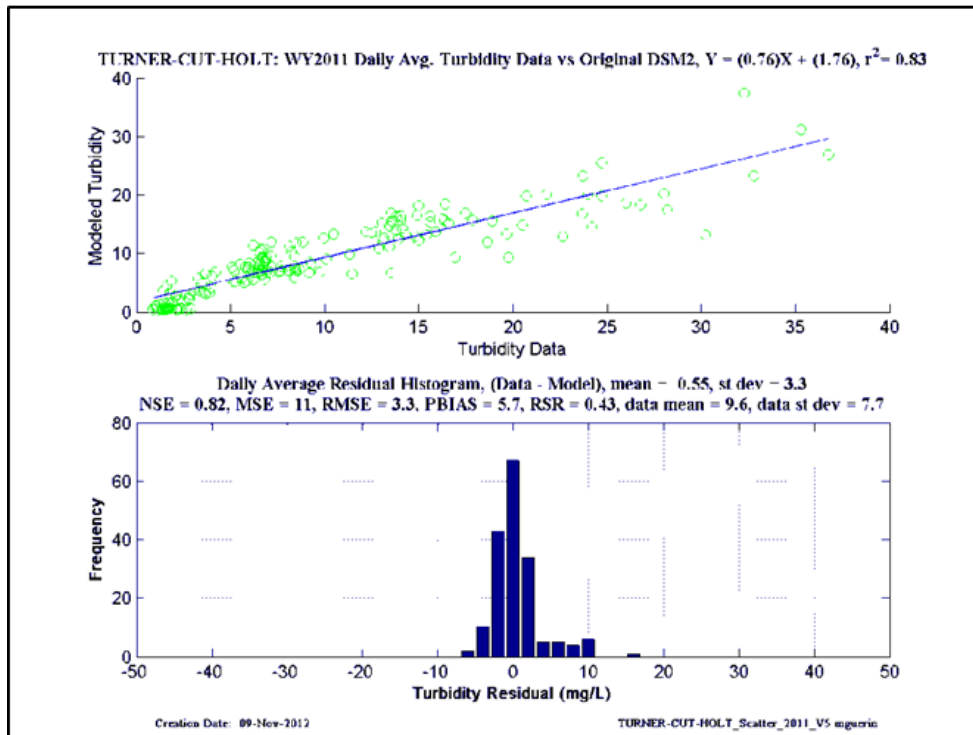
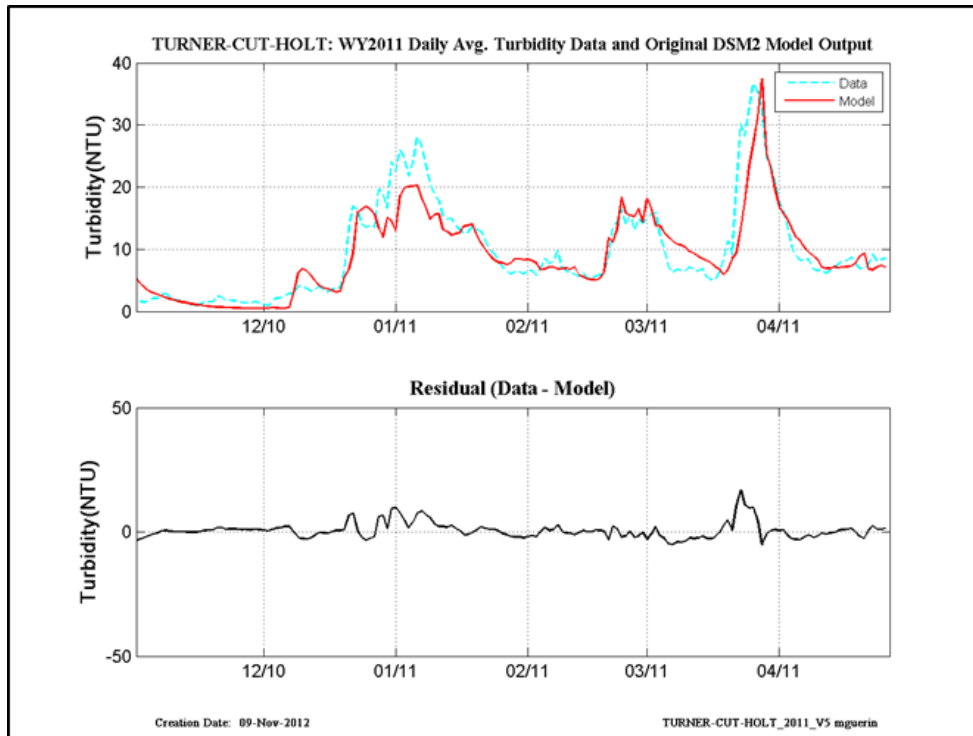


Figure 13-28 WY2011 original calibration results at Turner Cut-at-Holt.

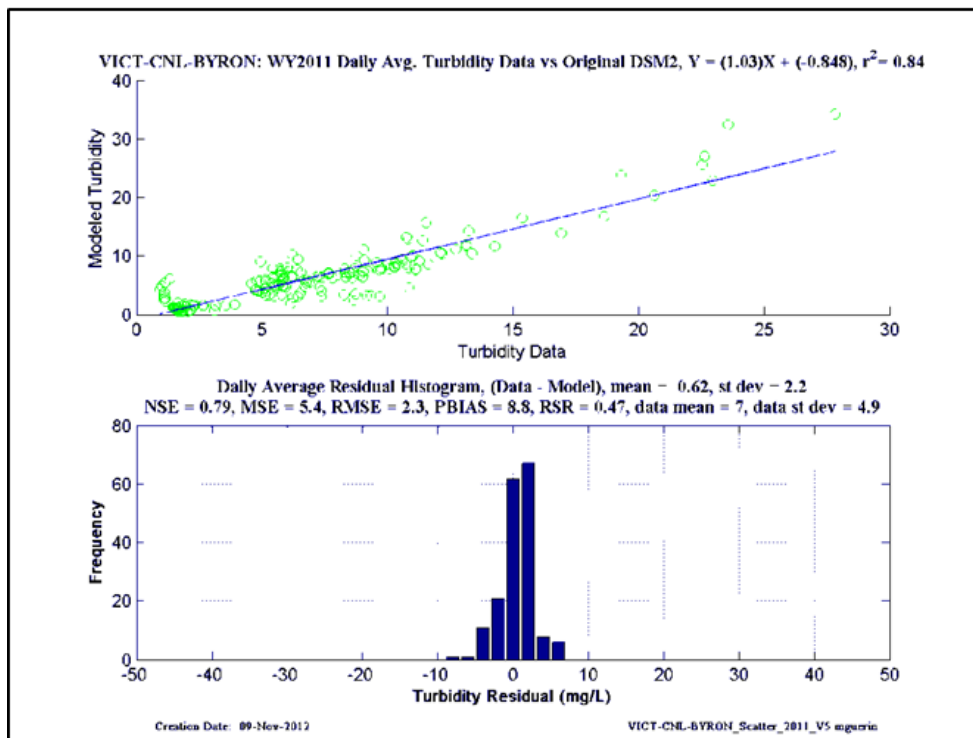
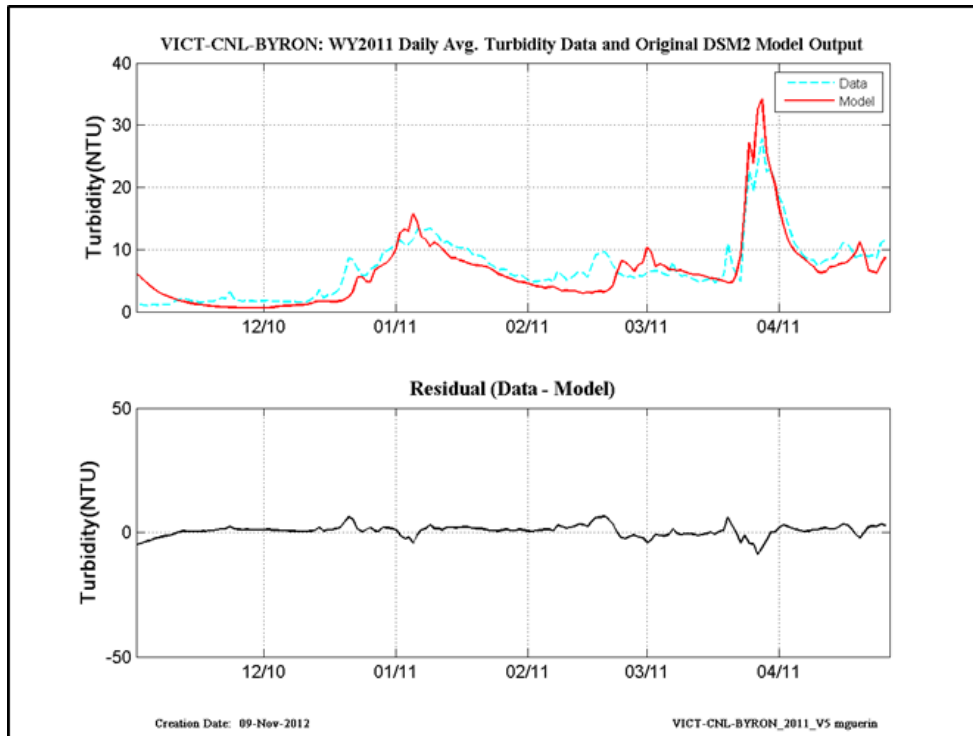


Figure 13-29 WY2011 original calibration results at Victoria Canal-at-Byron.

13.2 Daily-averaged CDEC data and model output- WY2010

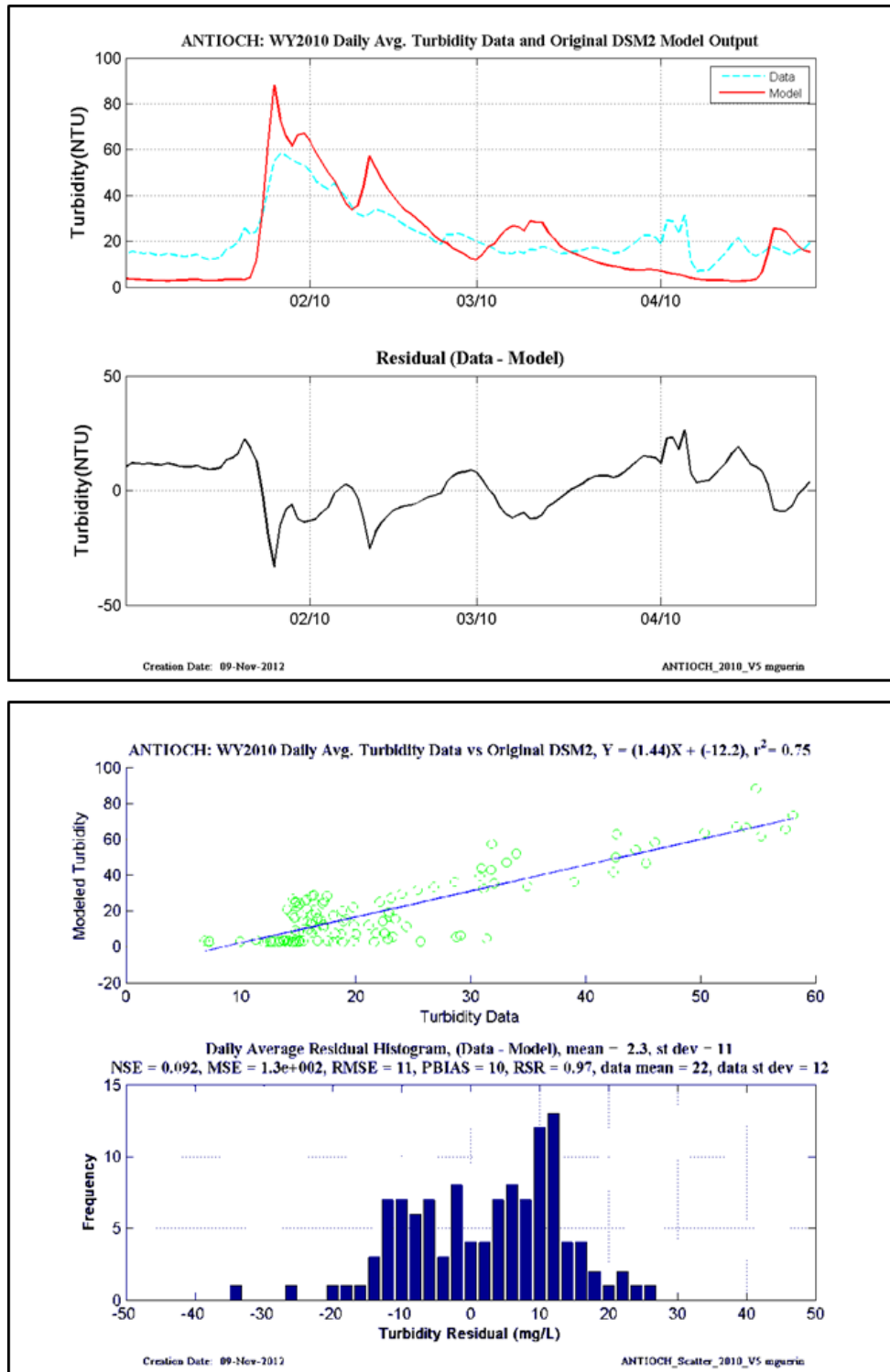


Figure 13-30 WY2010 original calibration results at Antioch.

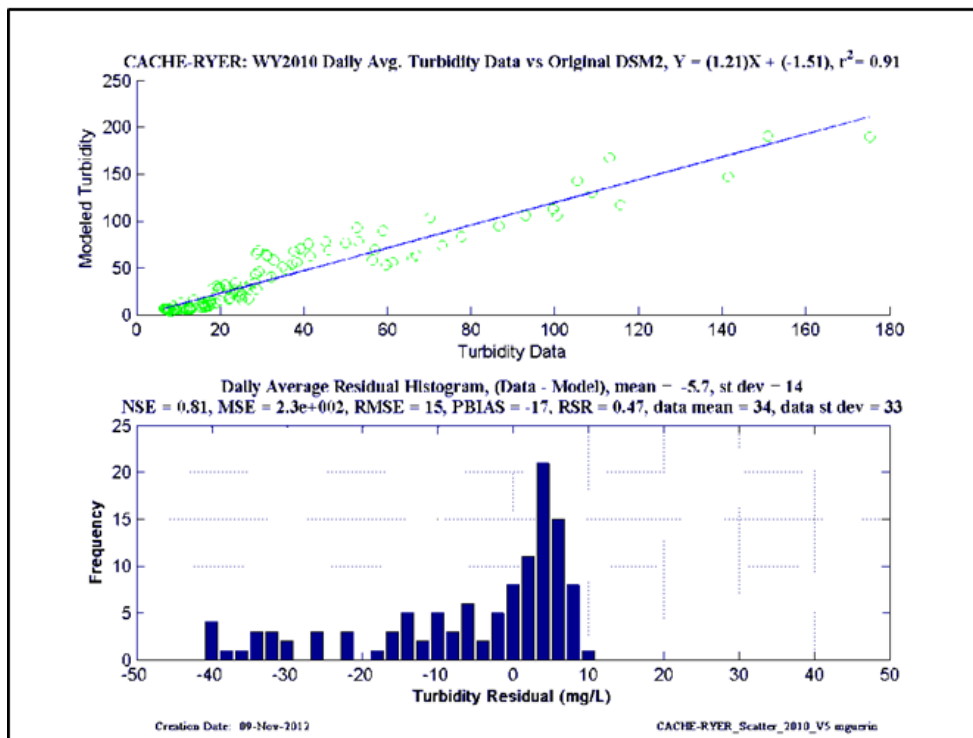
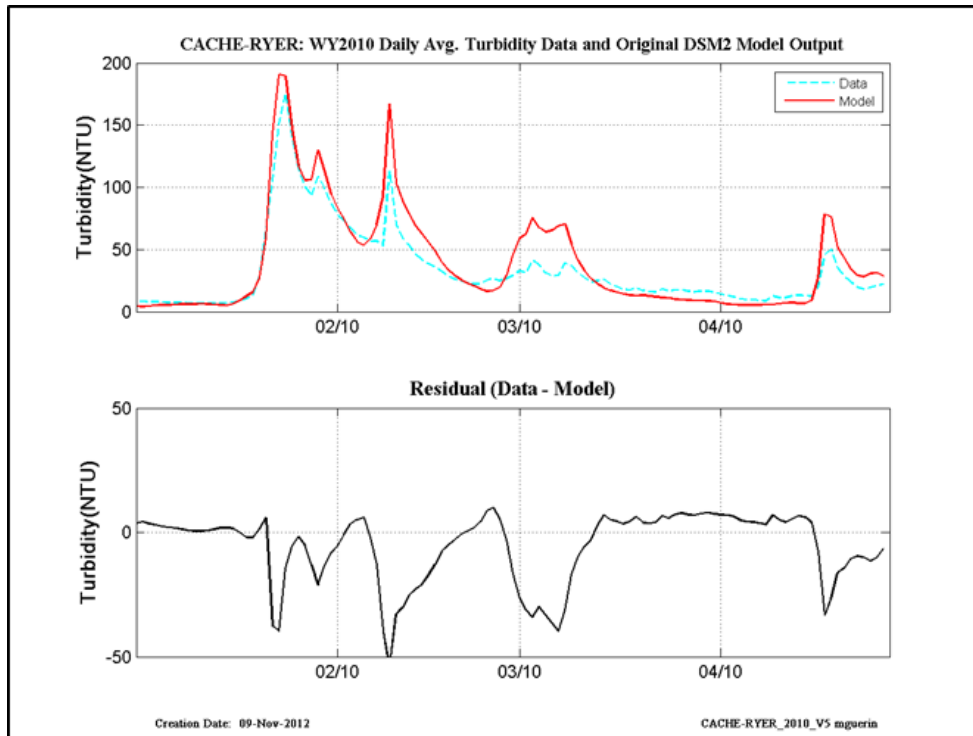


Figure 13-31 WY2010 original calibration results at Cache-at-Ryer Island.

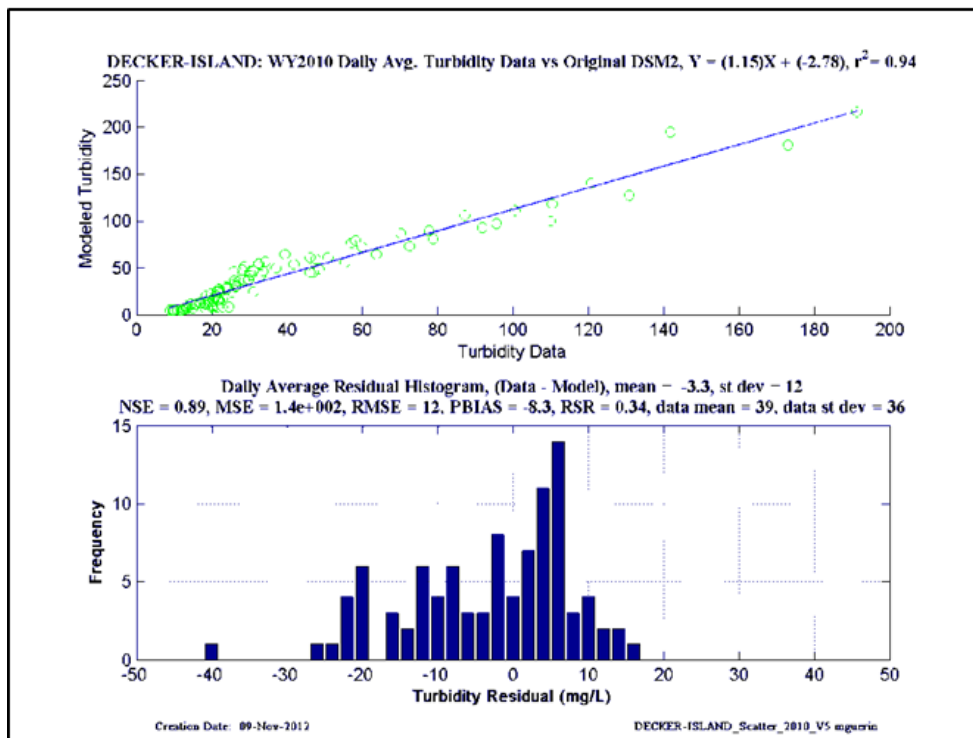
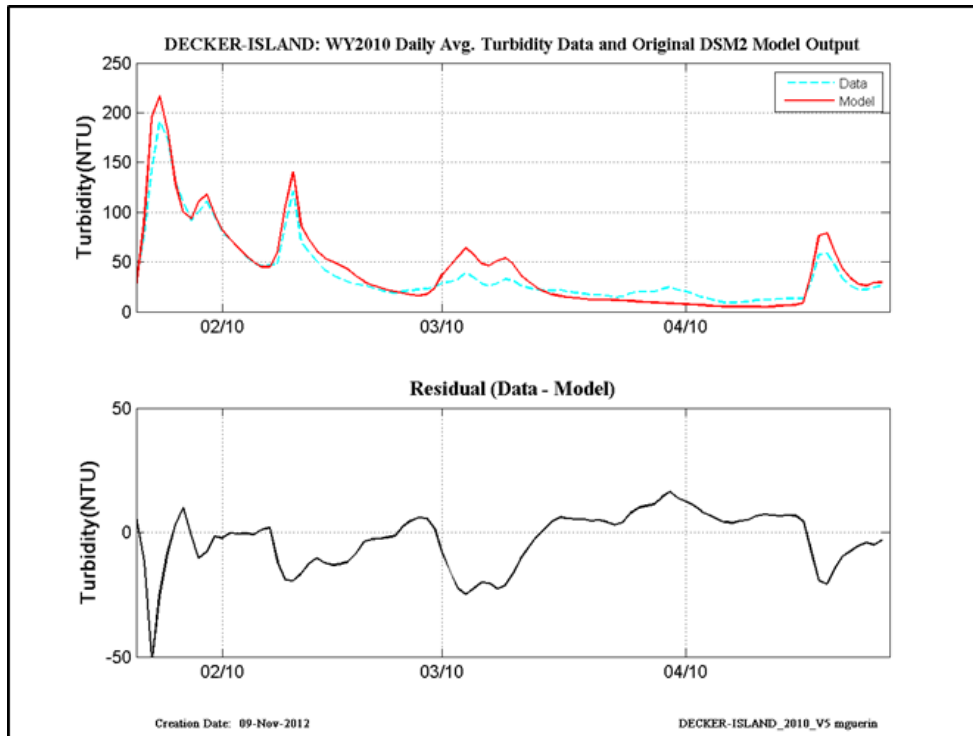


Figure 13-32 WY2010 original calibration results at Decker Island.

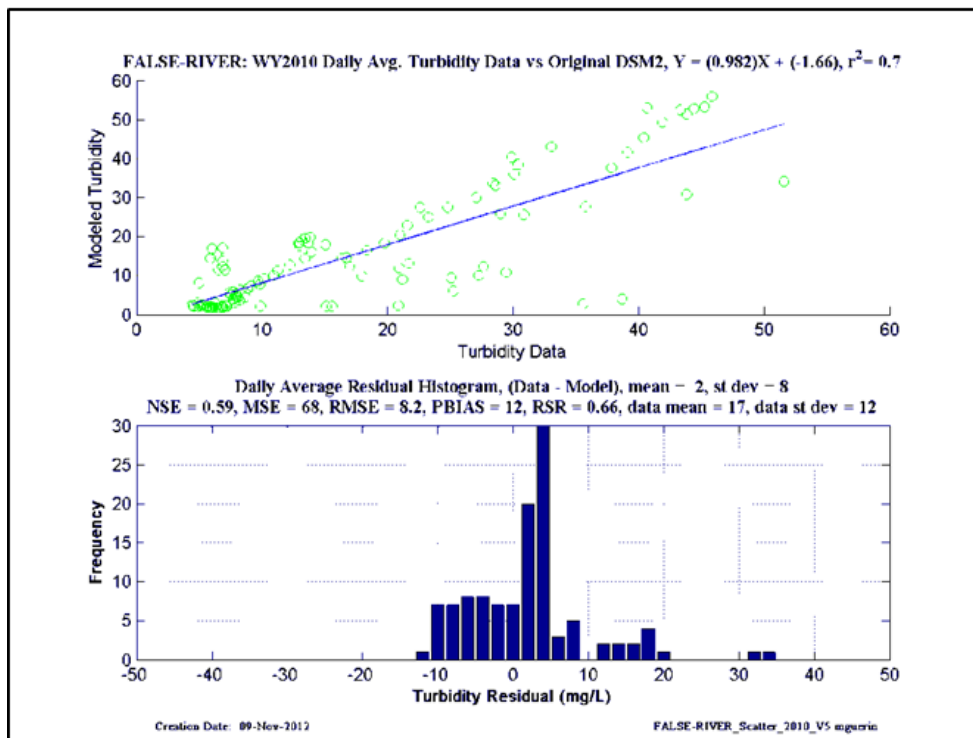
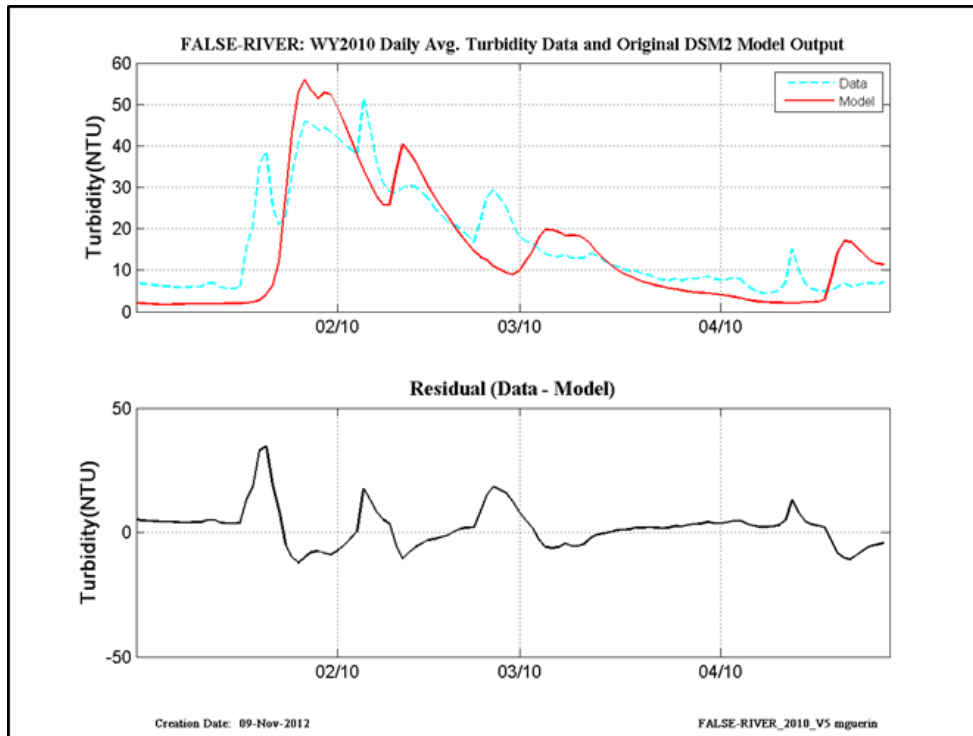


Figure 13-33 WY2010 original calibration results at False River.

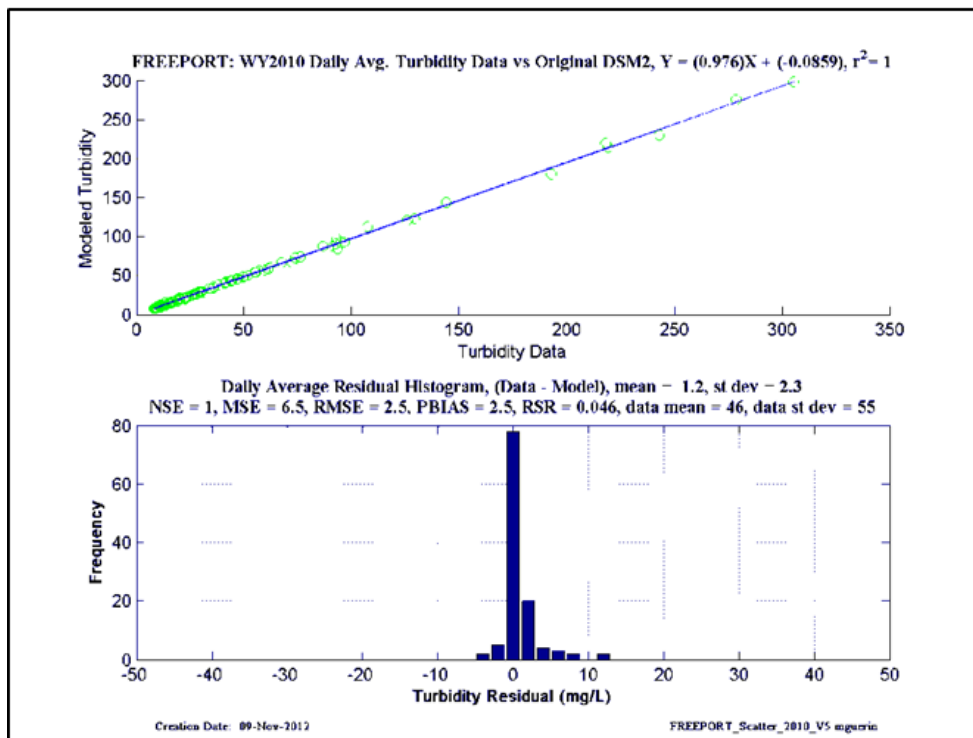
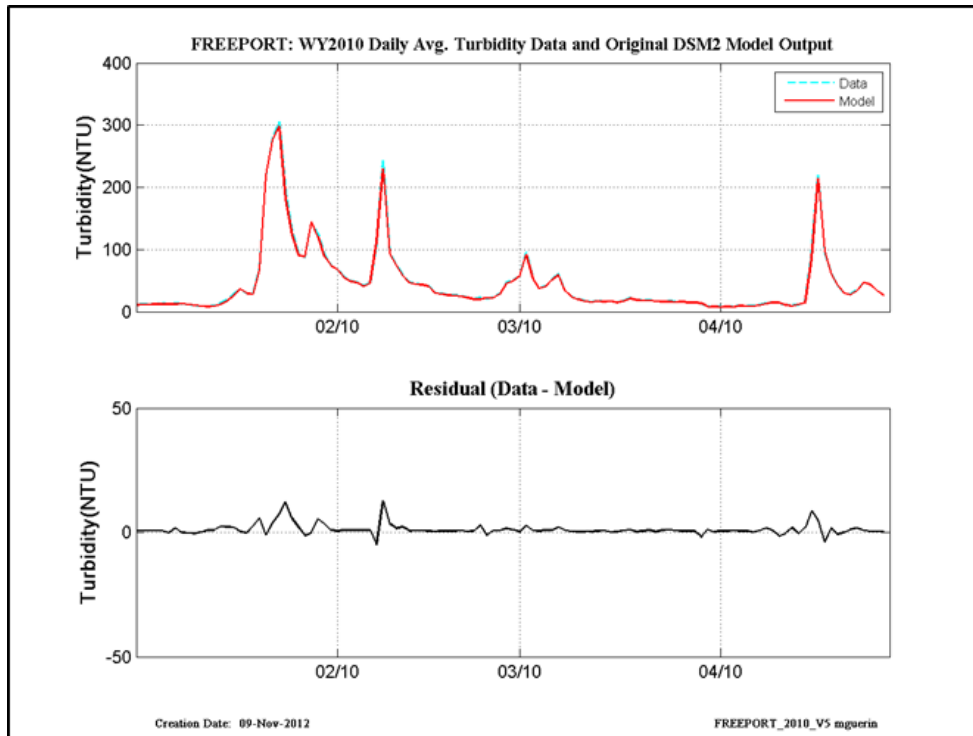


Figure 13-34 WY2010 original calibration results at Freeport.

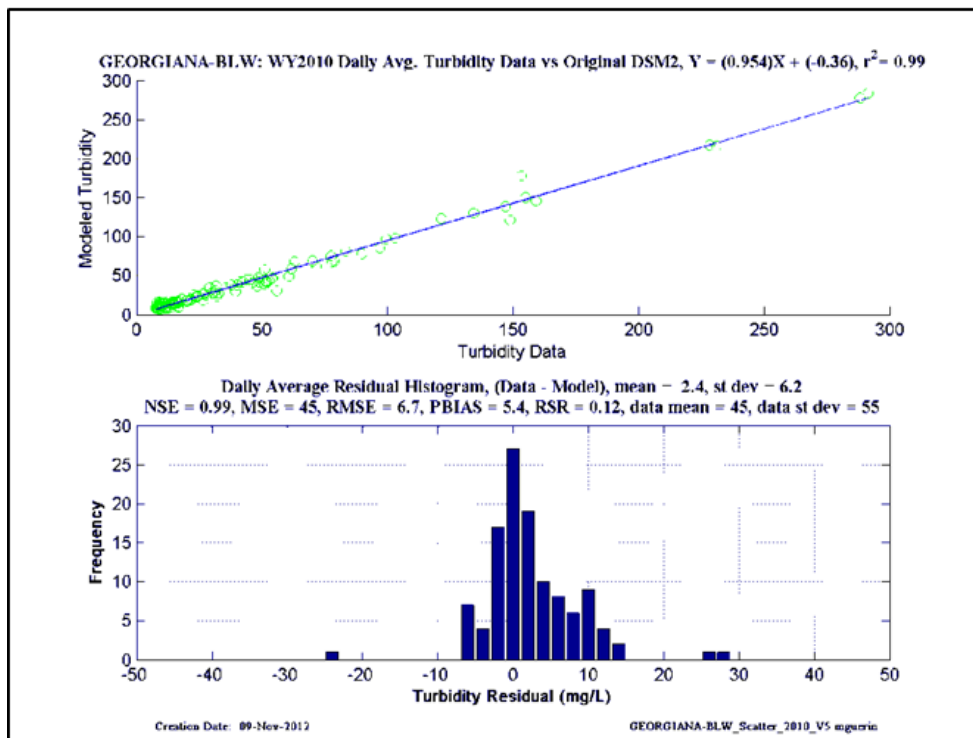
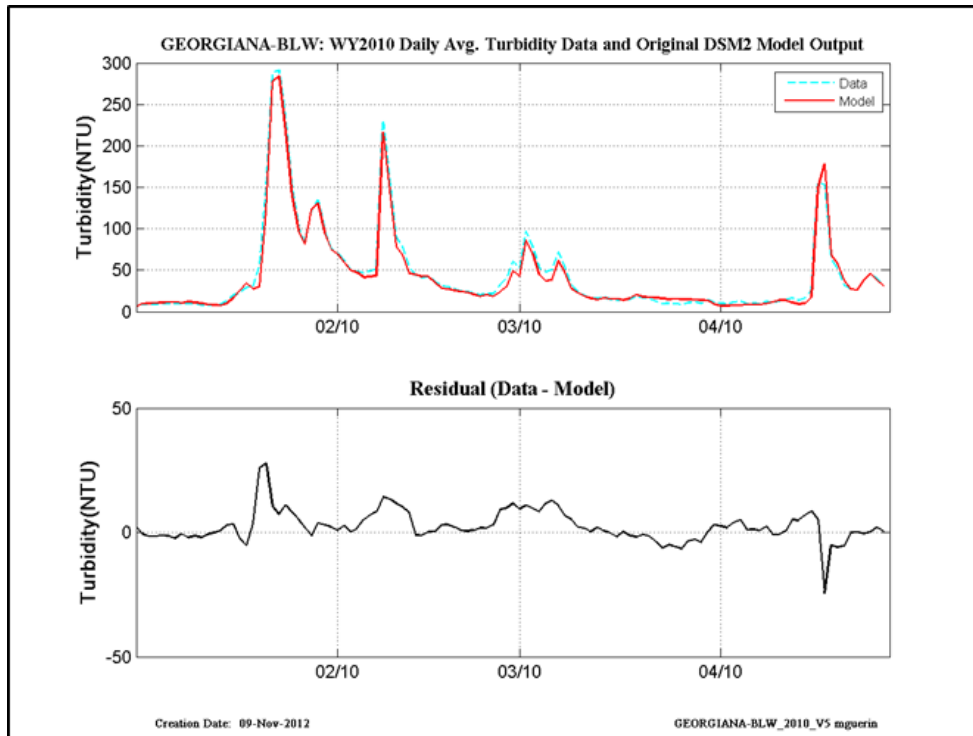


Figure 13-35 WY2010 original calibration results at Georgiana-Below-Sac.

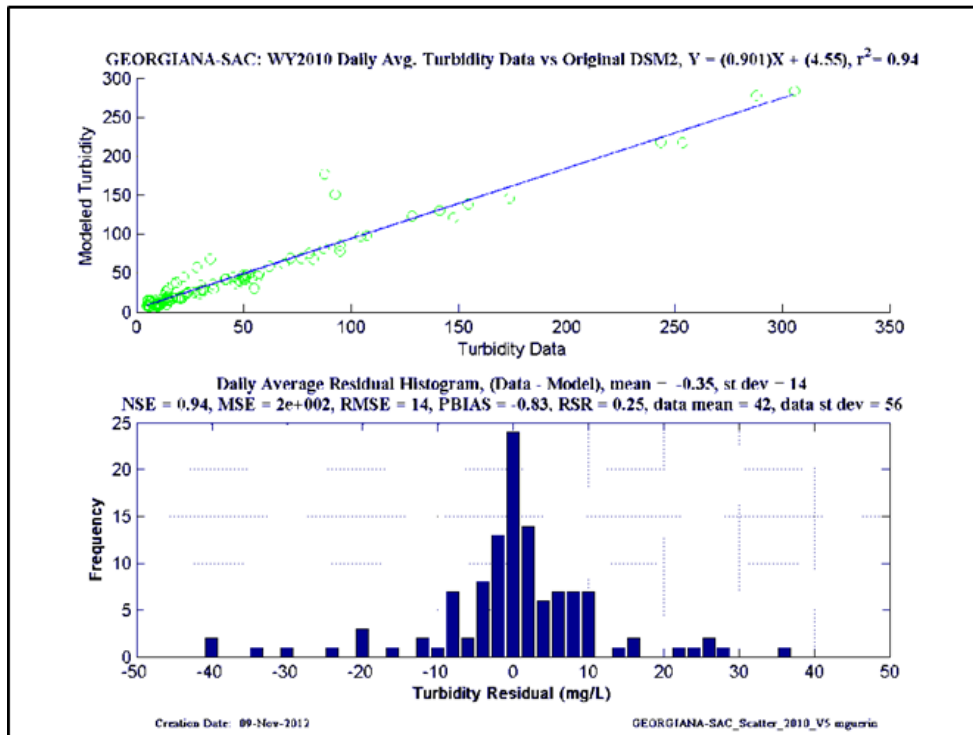
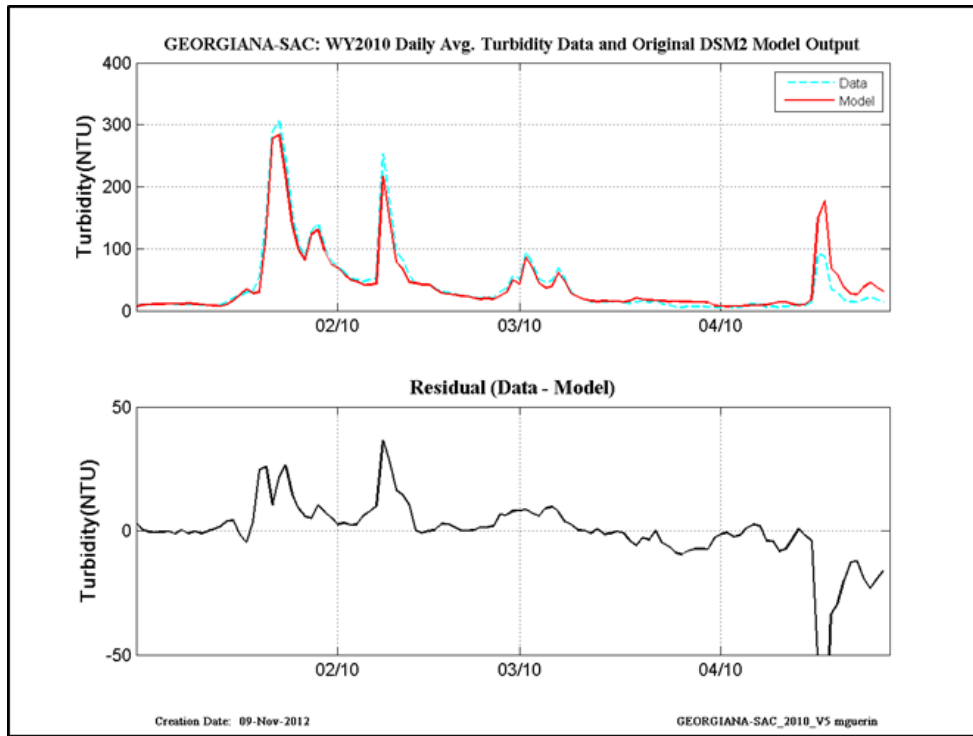


Figure 13-36 WY2010 original calibration results at Georgiana-Sac.

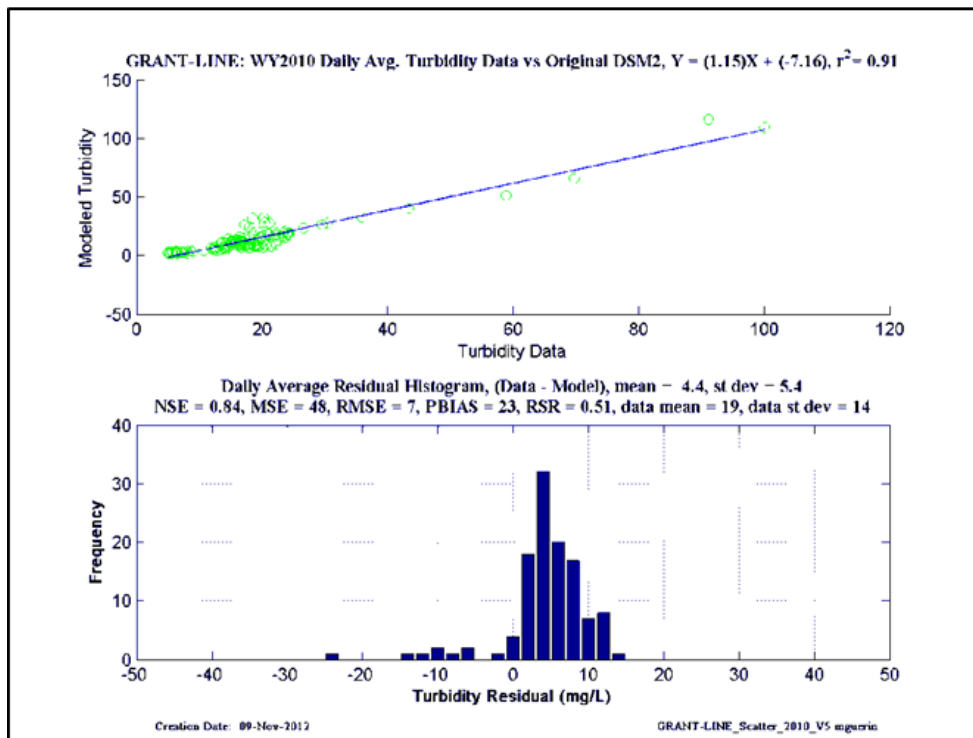
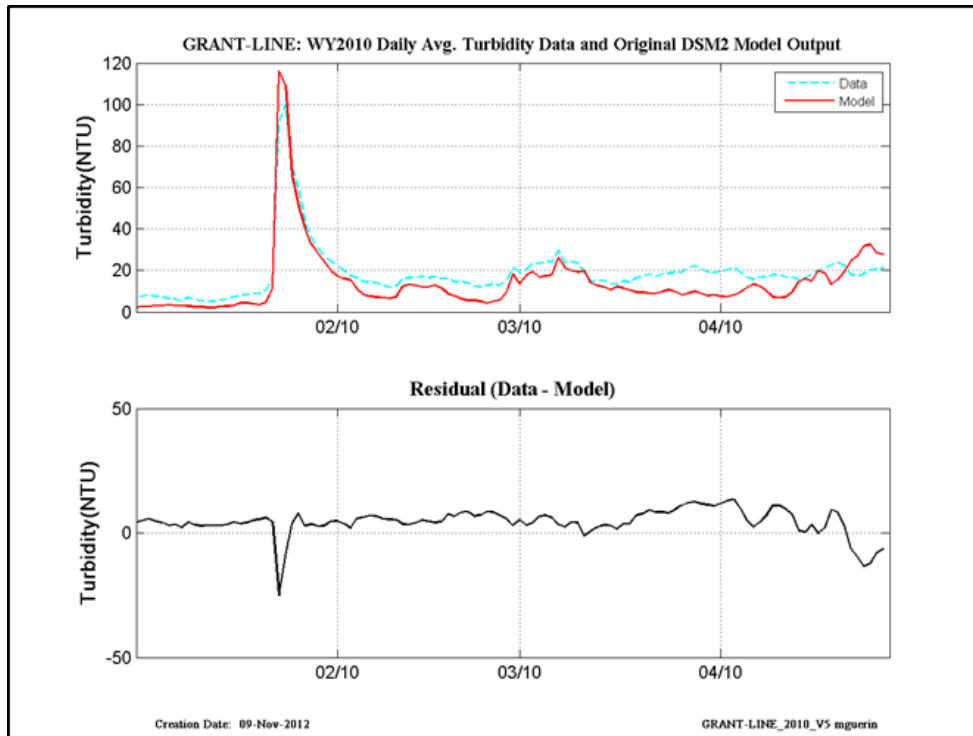


Figure 13-37 WY2010 original calibration results at Grant Line.

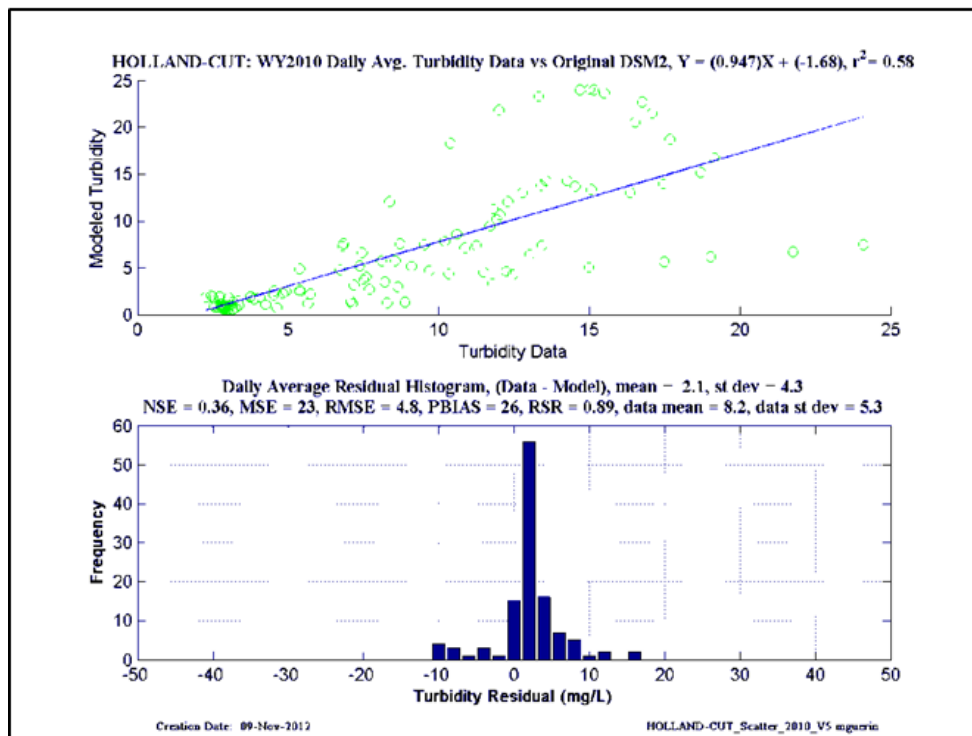
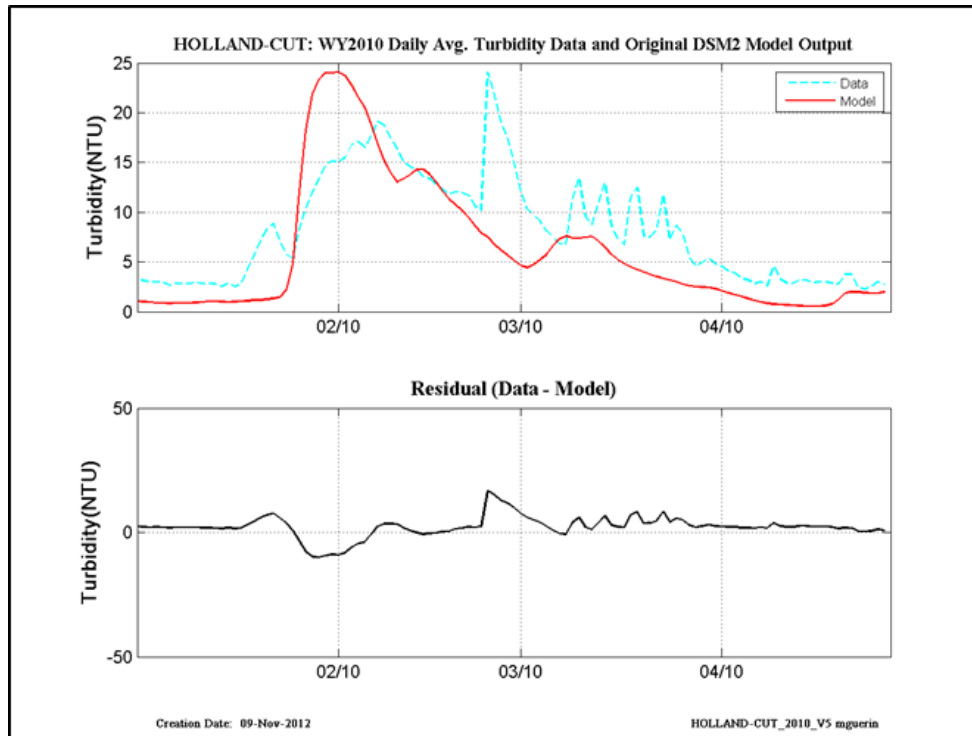


Figure 13-38 WY2010 original calibration results at Holland Cut.

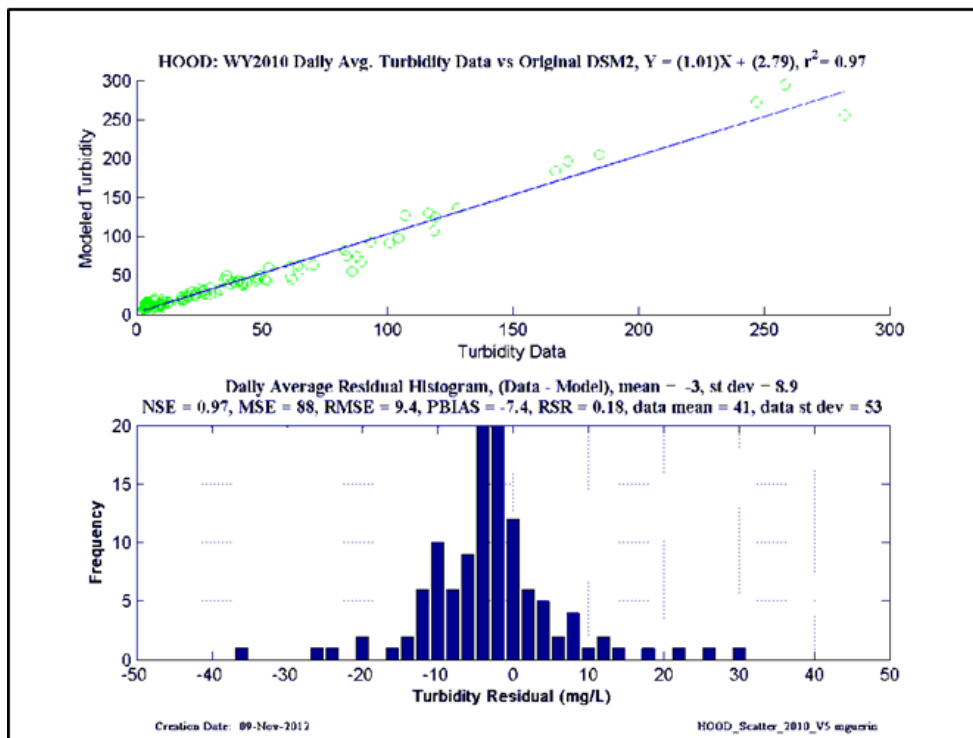
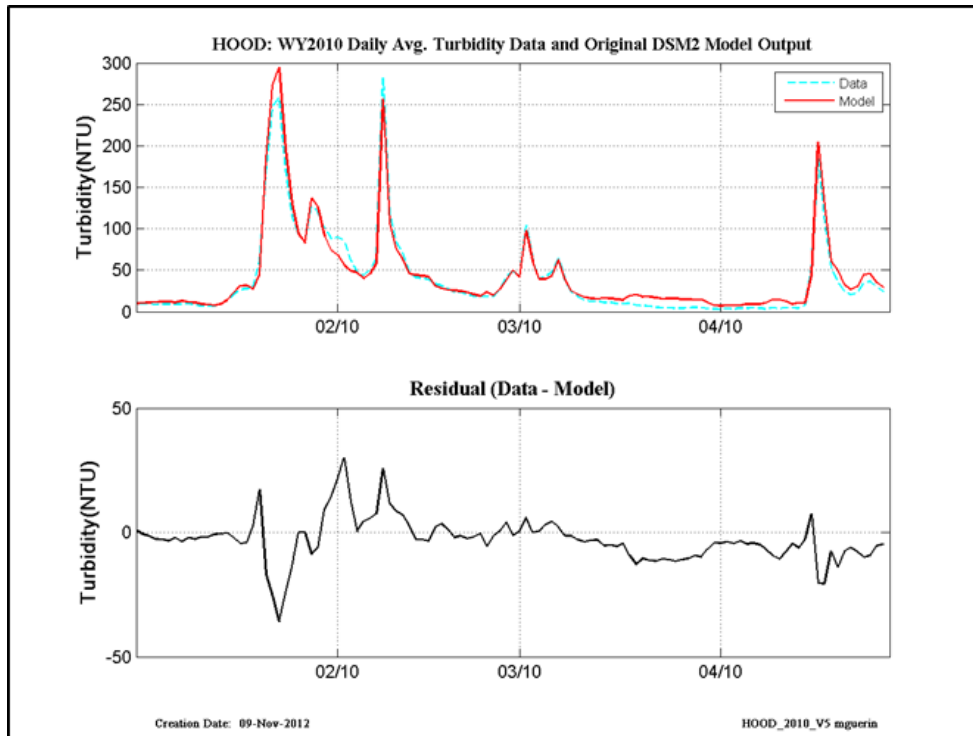


Figure 13-39 WY2010 original calibration results at Hood.

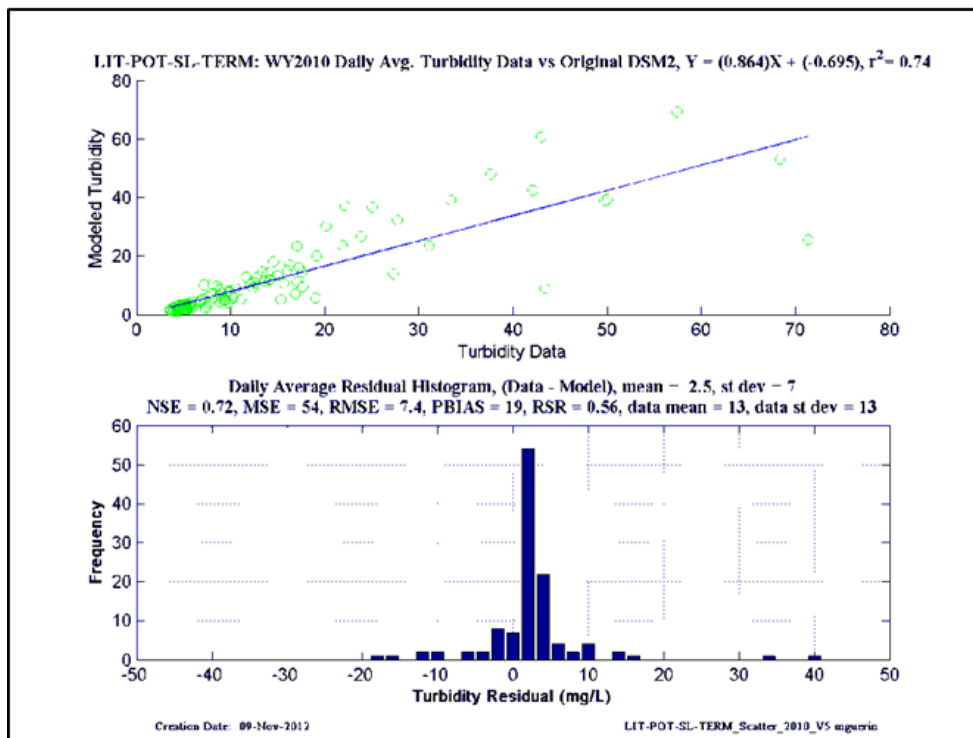
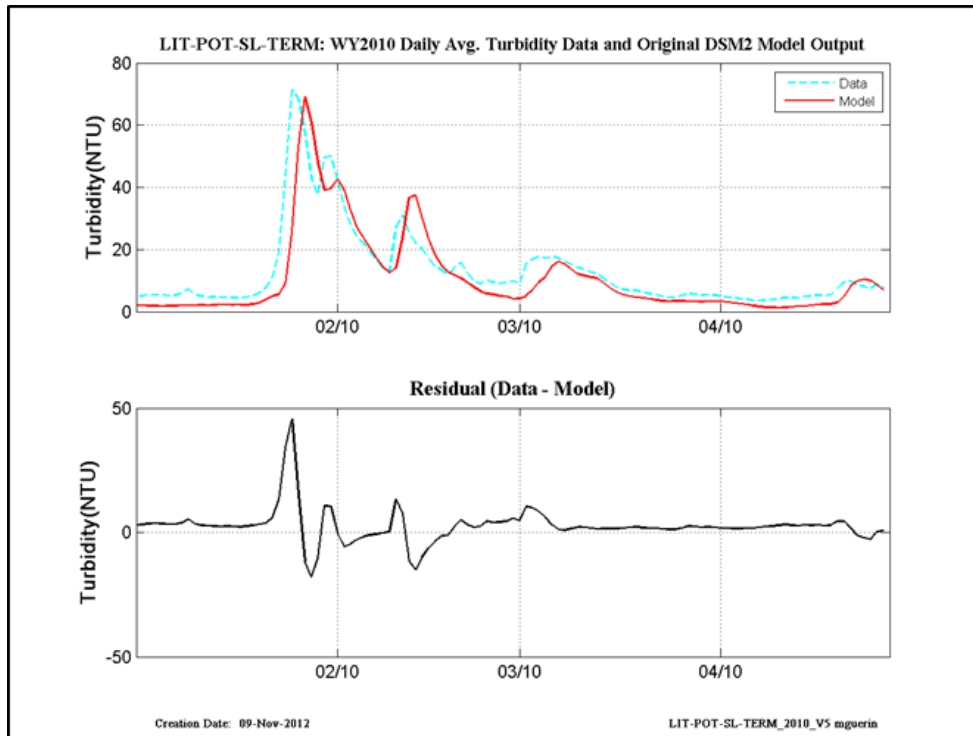


Figure 13-40 WY2010 original calibration results at Little Potato Slough-at-Terminus.

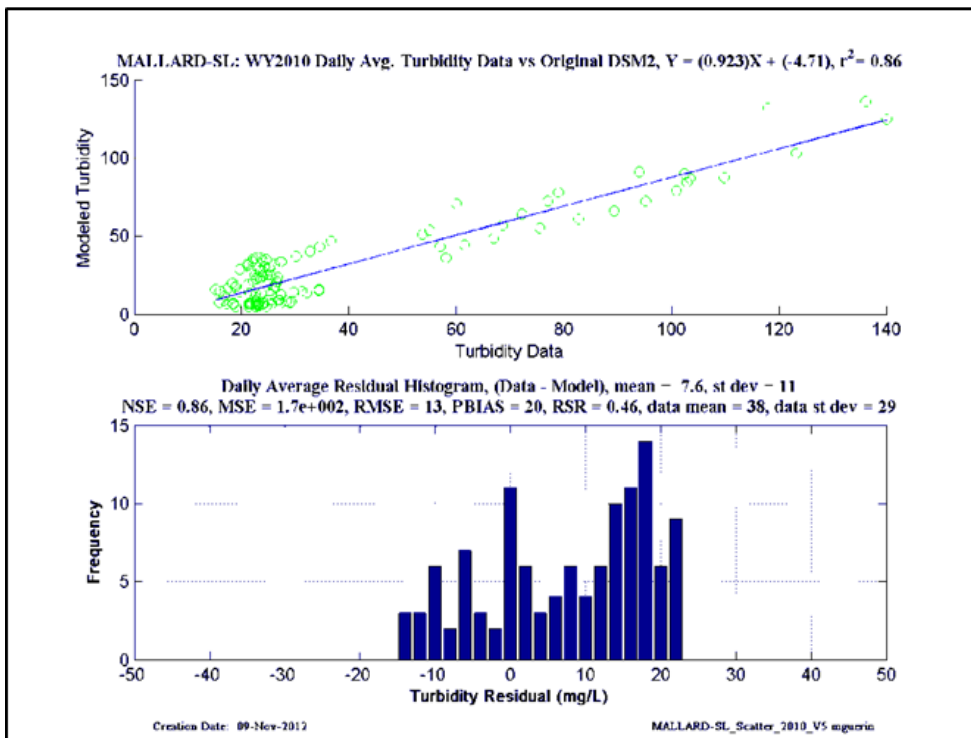
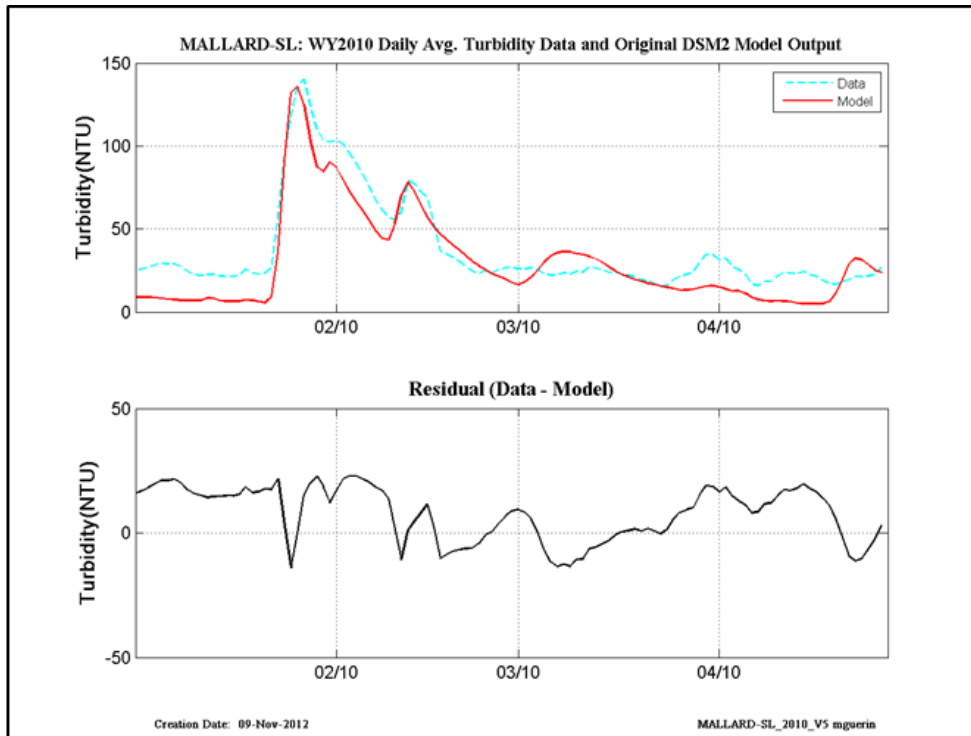


Figure 13-41 WY2010 original calibration results at Mallard Slough.

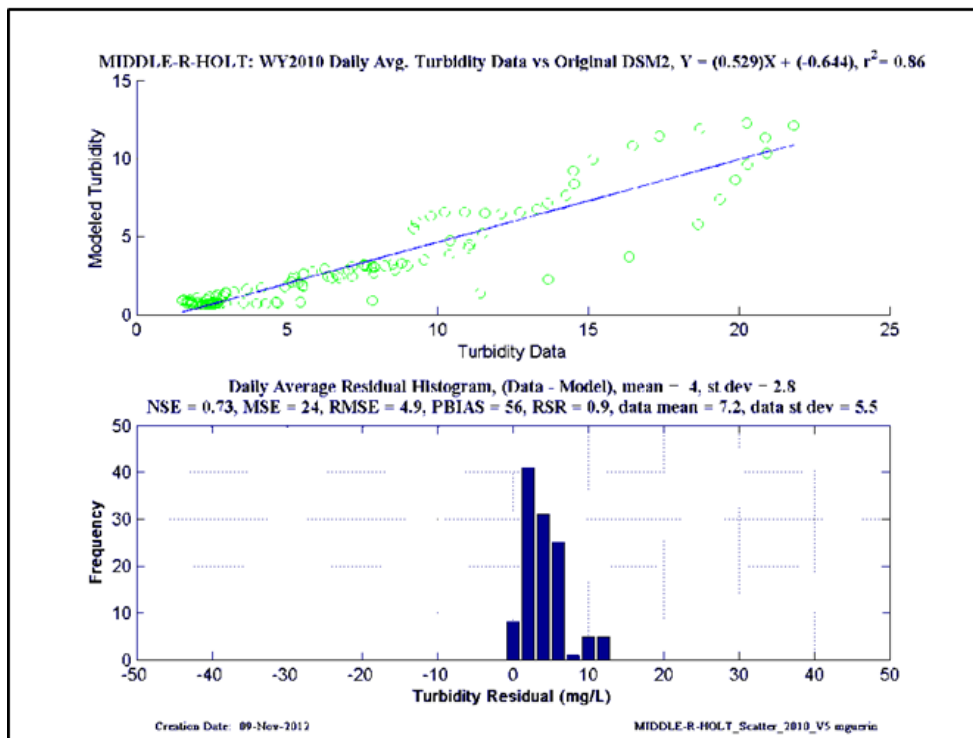
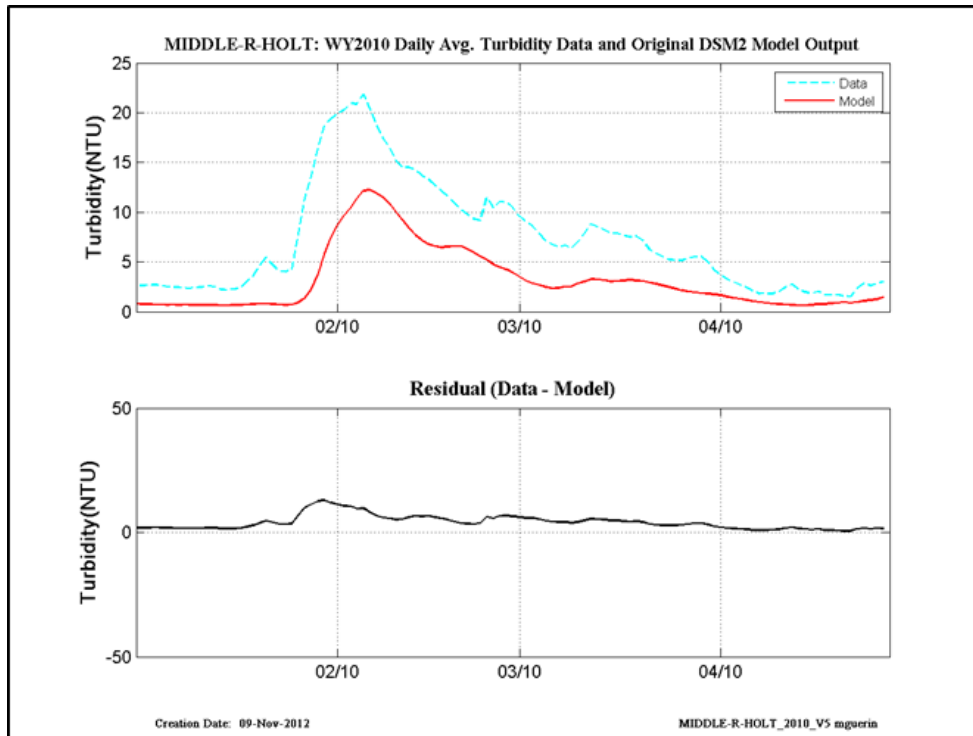


Figure 13-42 WY2010 original calibration results at Middle River-at-Holt.

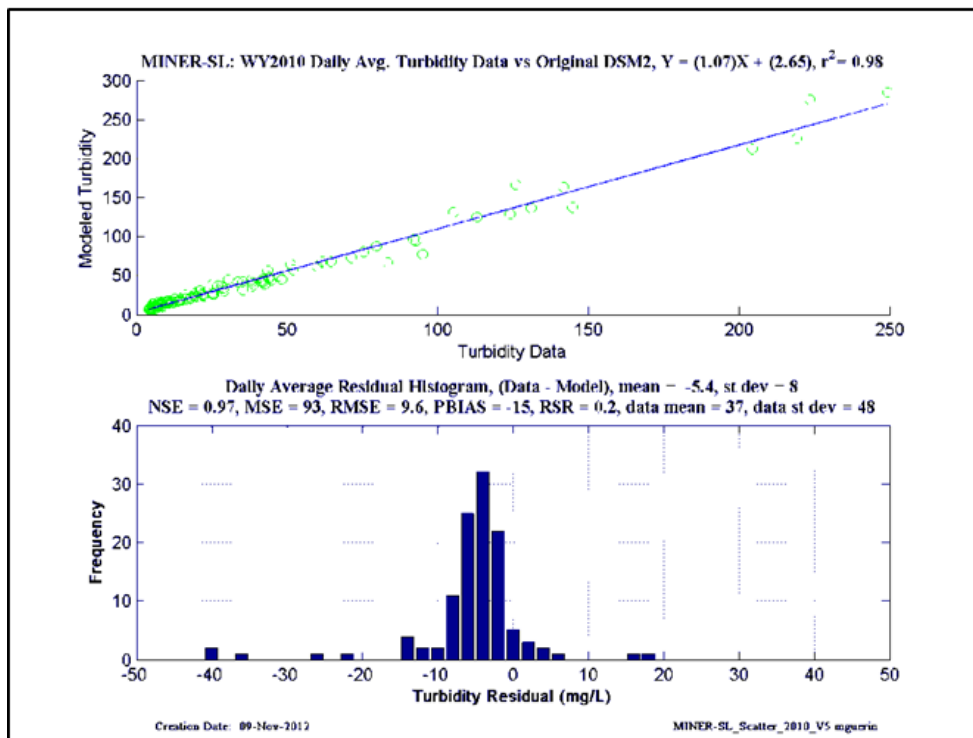
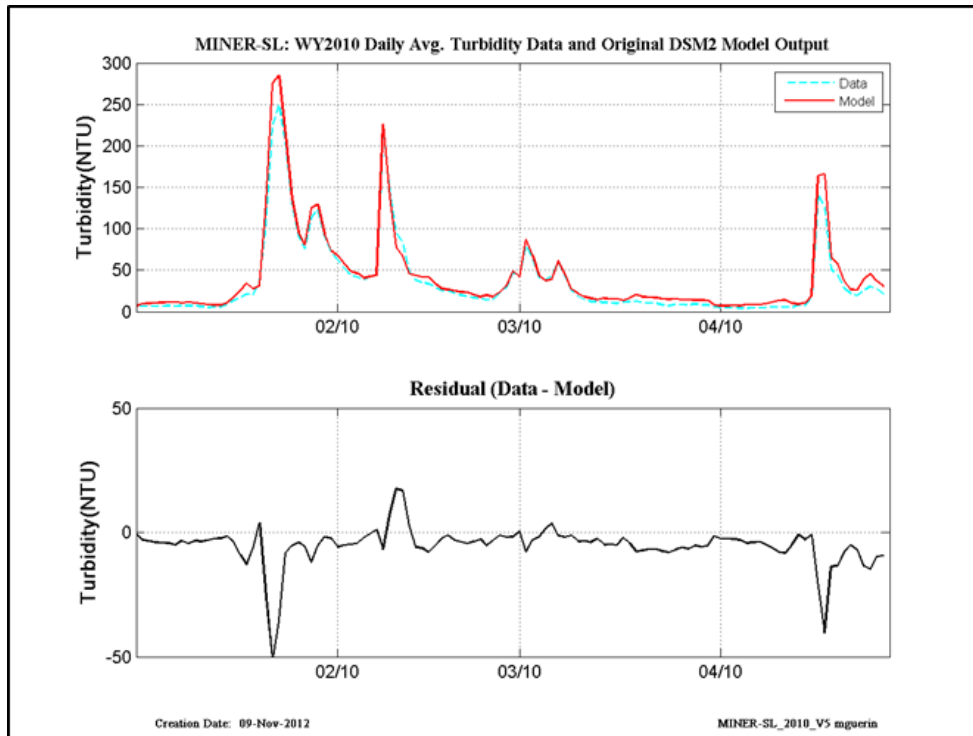


Figure 13-43 WY2010 original calibration results at Miner Slough.

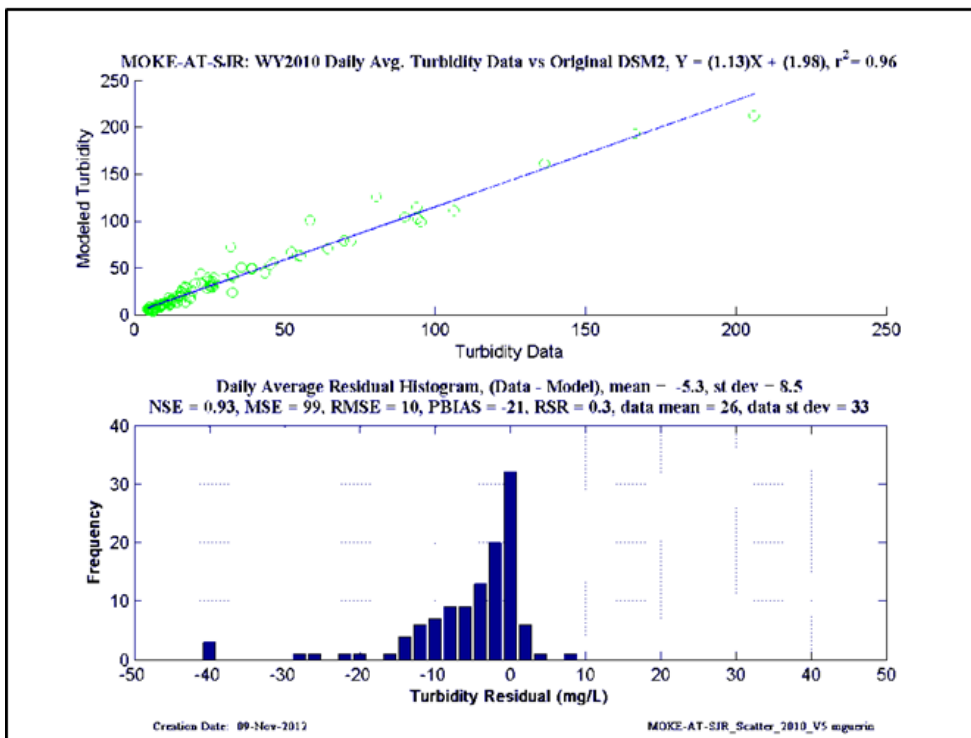
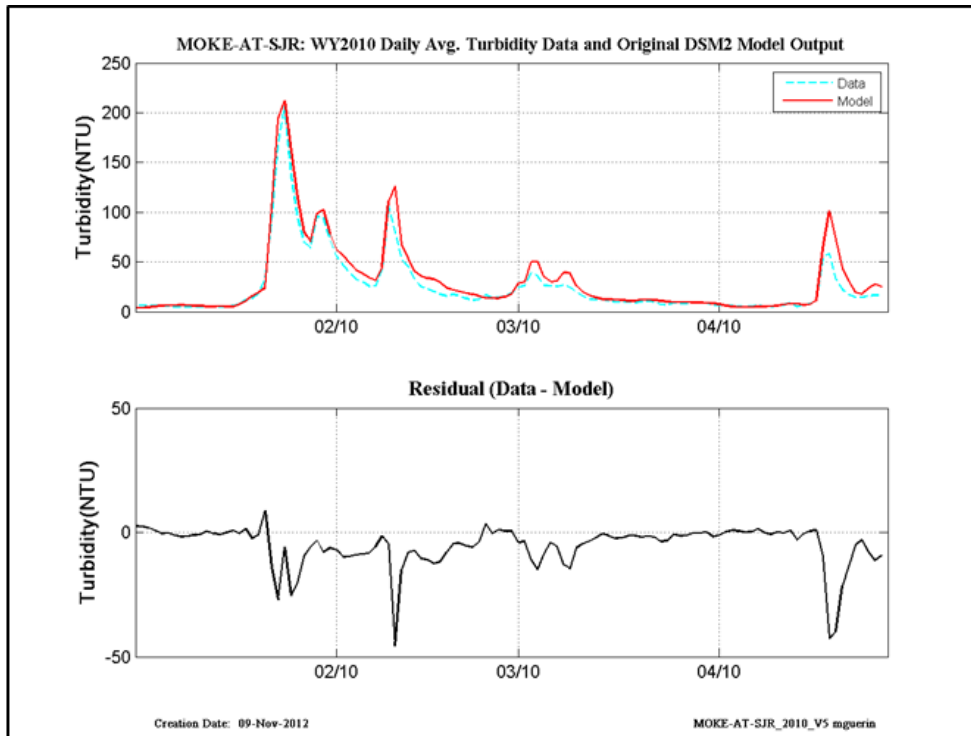


Figure 13-44 WY2010 original calibration results at Mokelumne-at-San Joaquin.

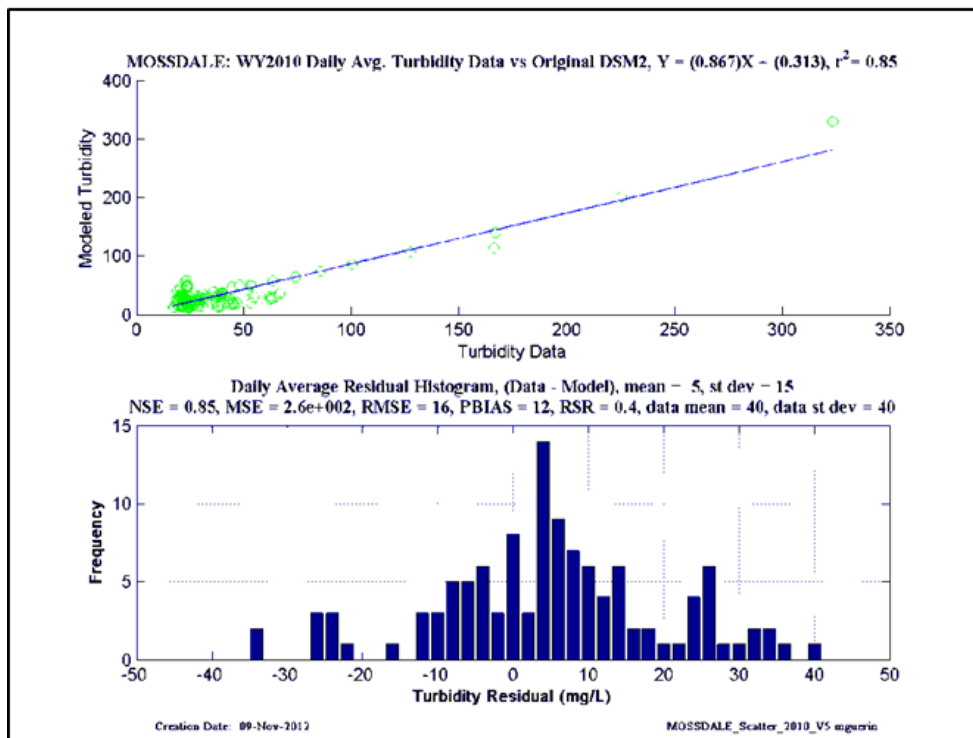
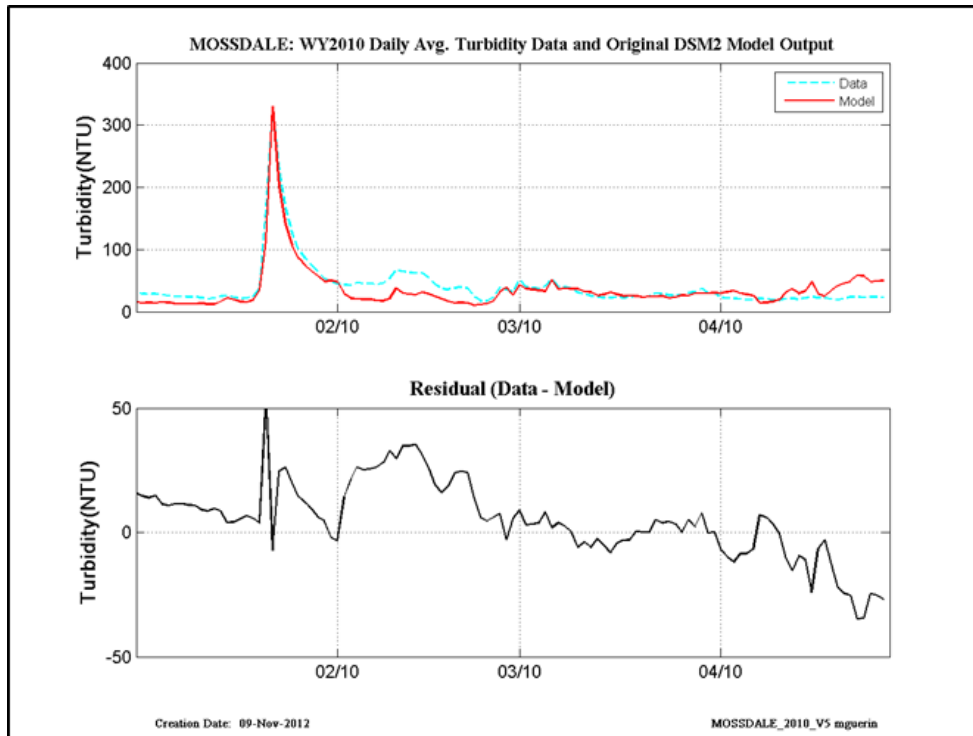


Figure 13-45 WY2010 original calibration results at Mossdale.

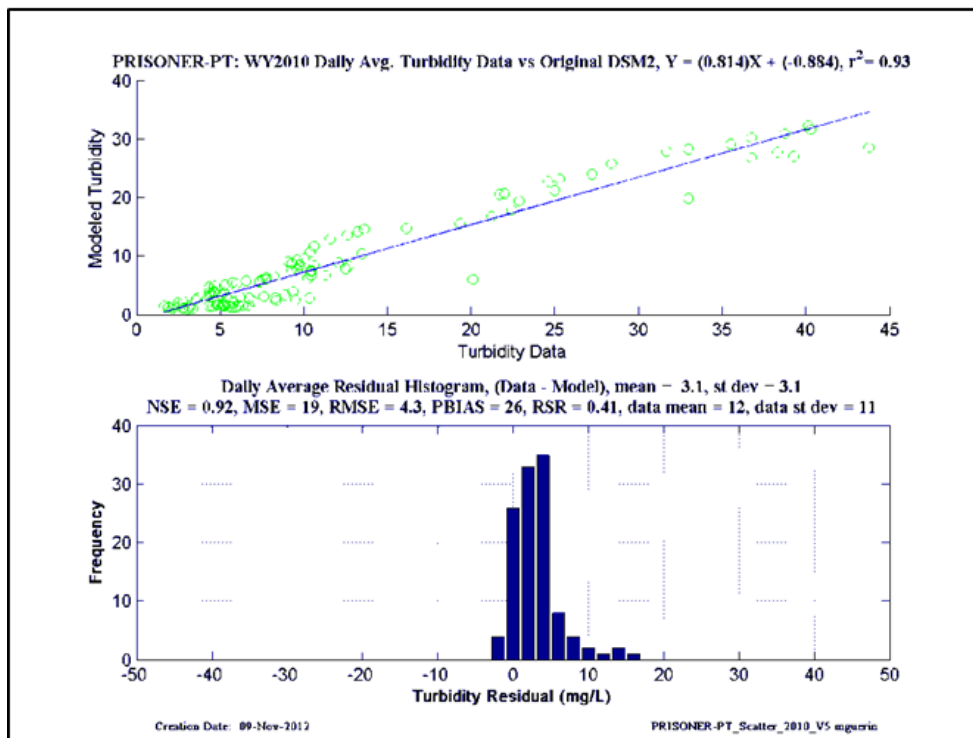
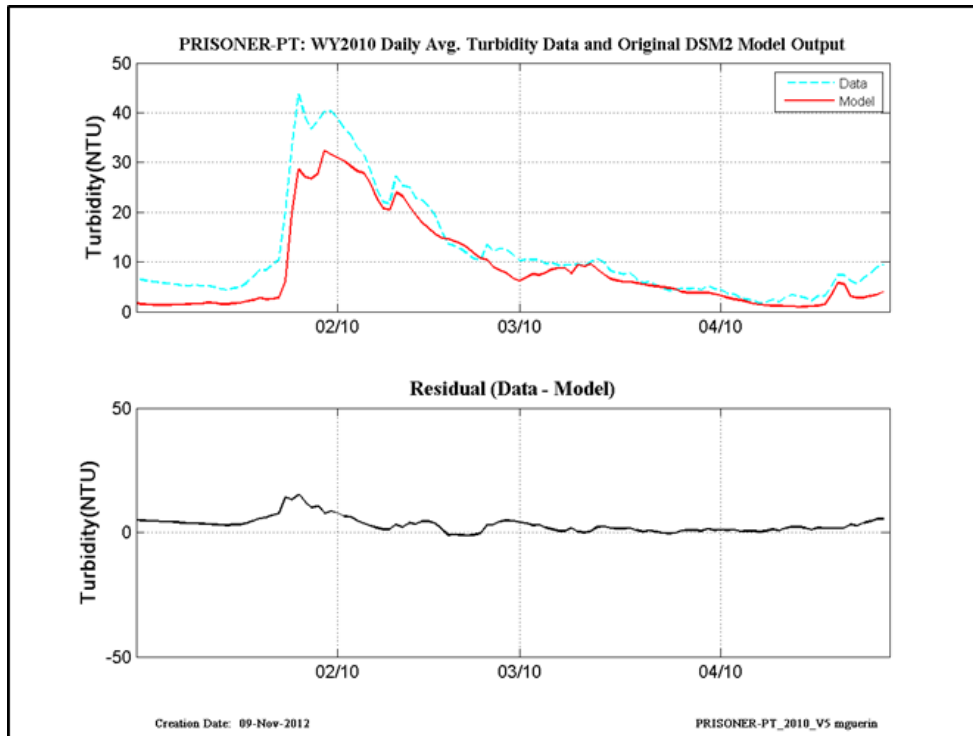


Figure 13-46 WY2010 original calibration results at Prisoner Point.

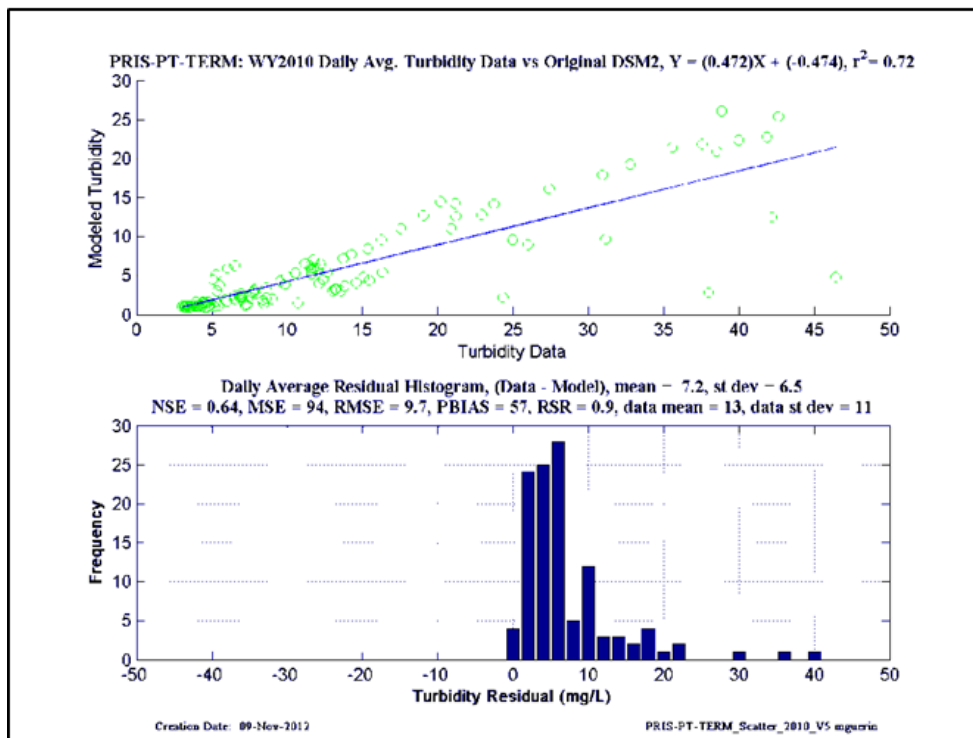
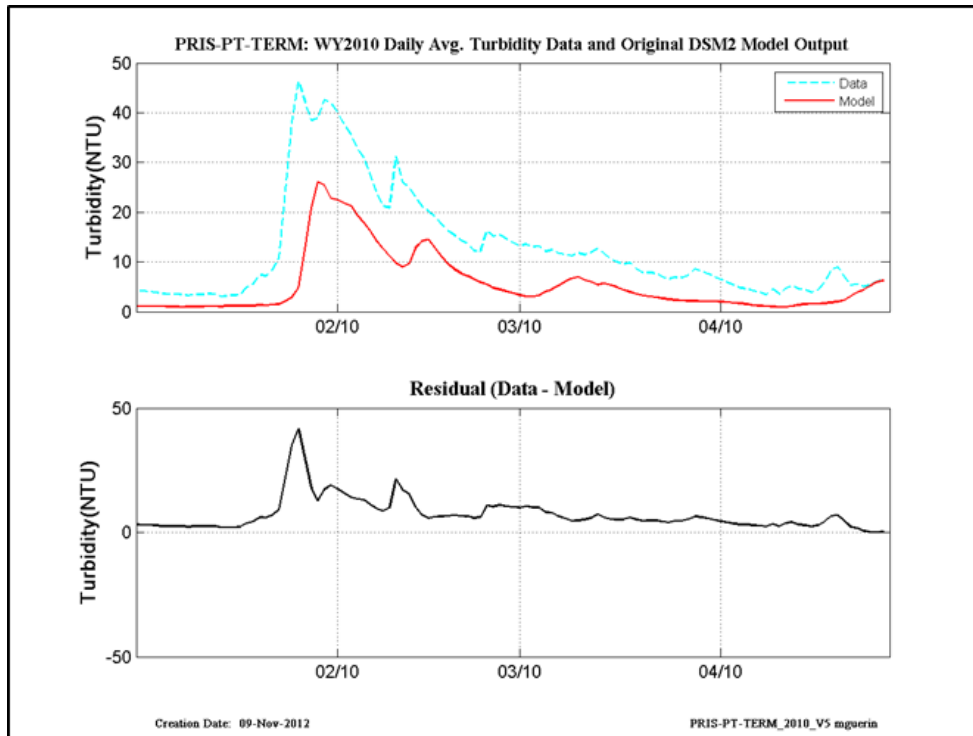


Figure 13-47 WY2010 original calibration results at Prisoner Point-at-Terminus.

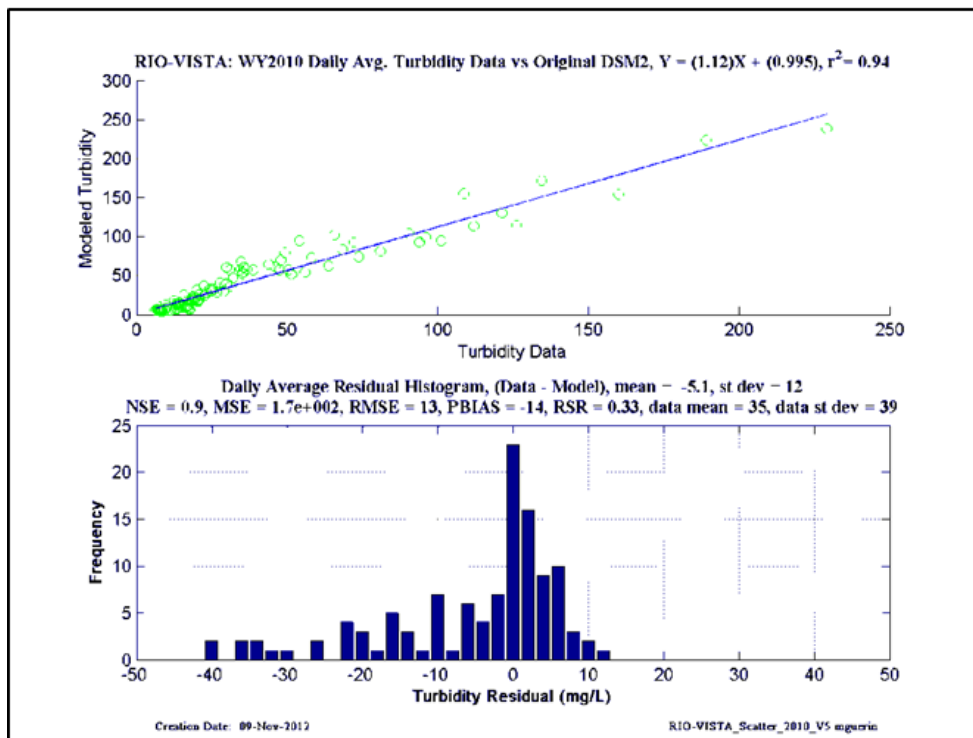
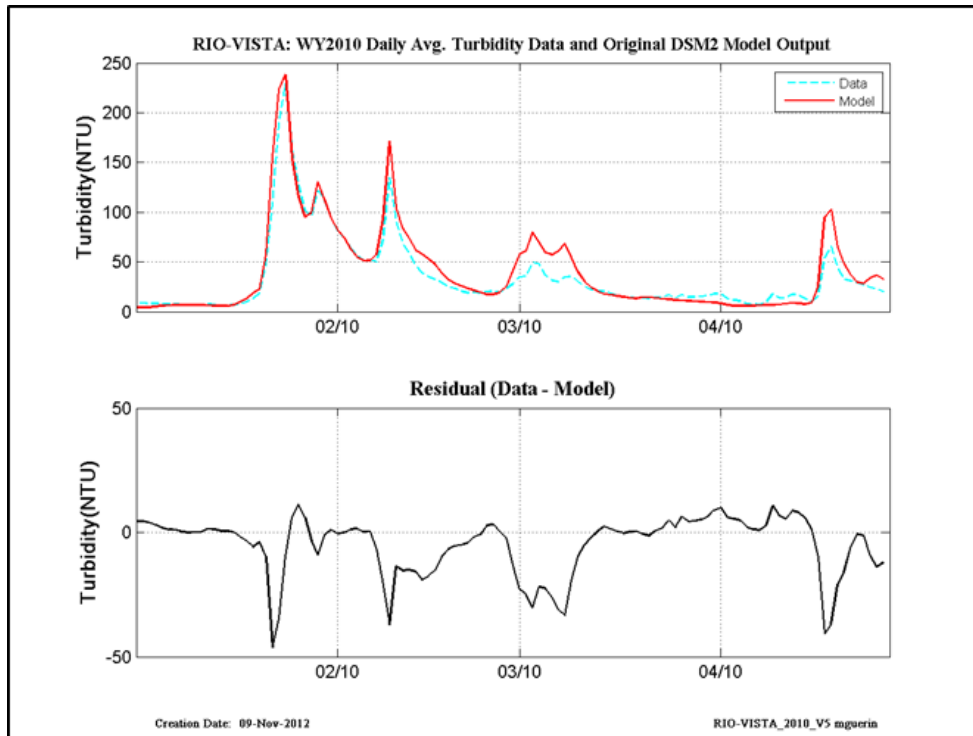


Figure 13-48 WY2010 original calibration results at Rio Vista.

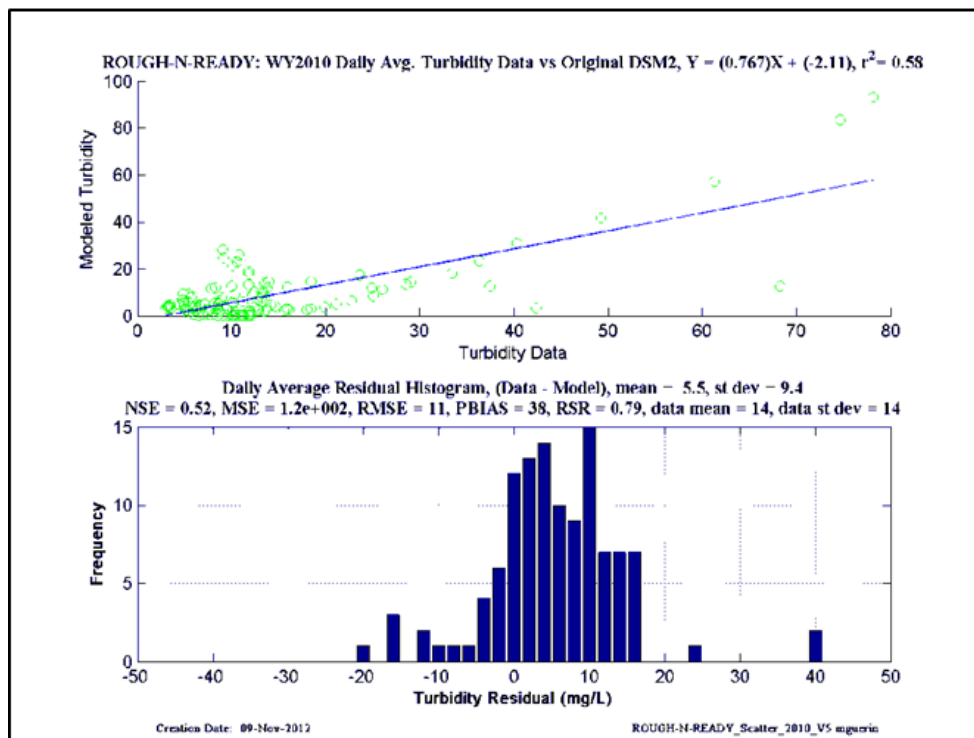
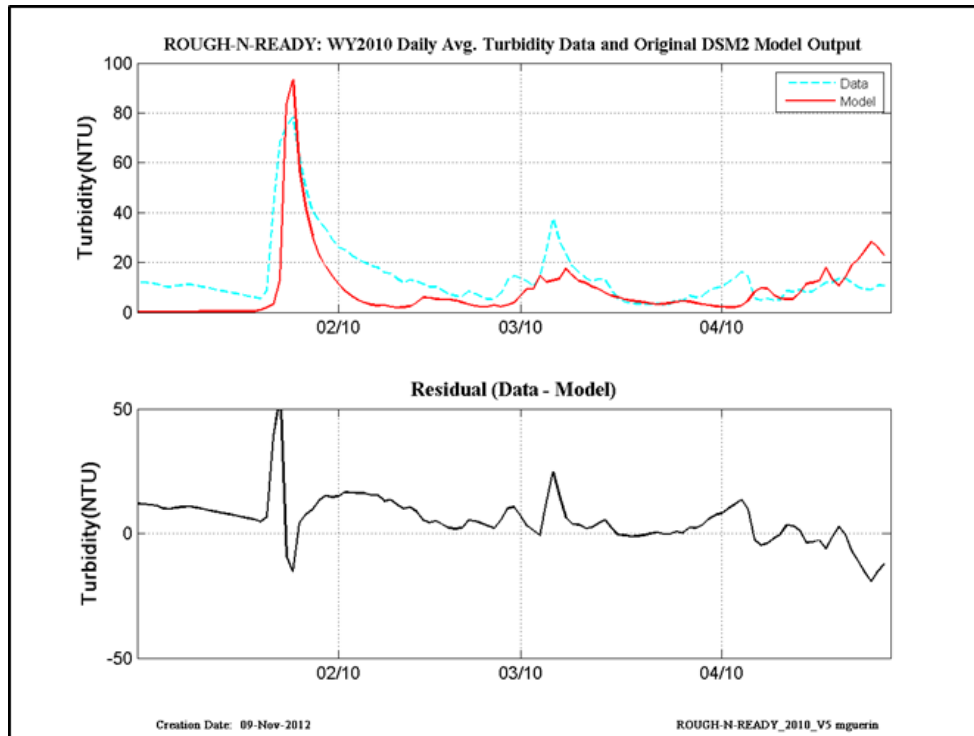


Figure 13-49 WY2010 original calibration results at Rough-N-Ready Island.

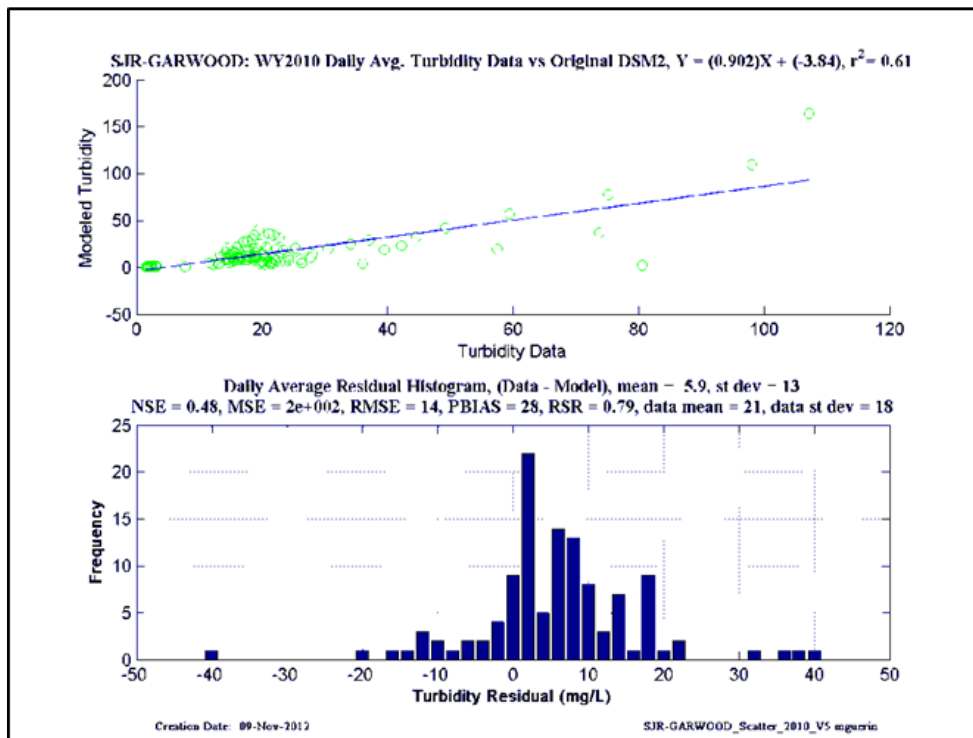
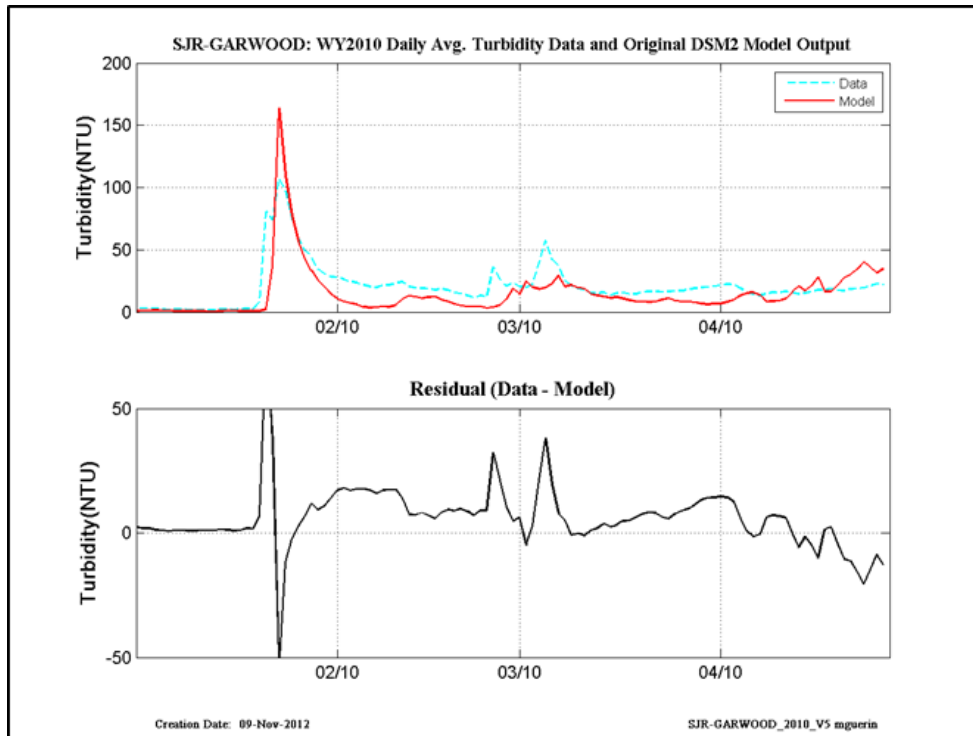


Figure 13-50 WY2010 original calibration results at San Joaquin-at-Garwood.

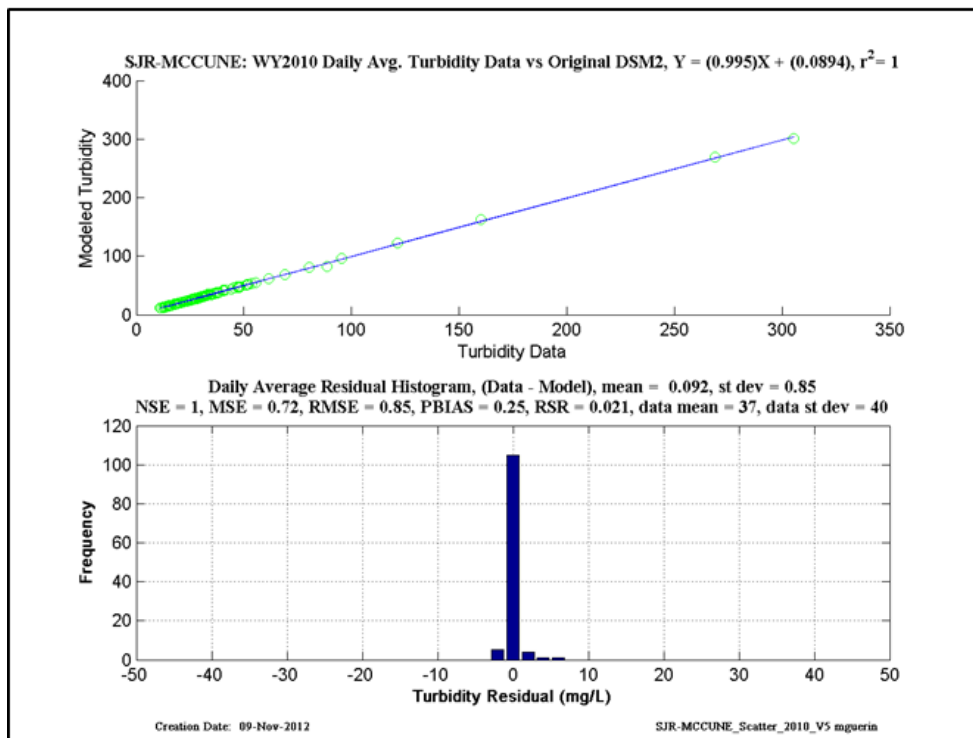
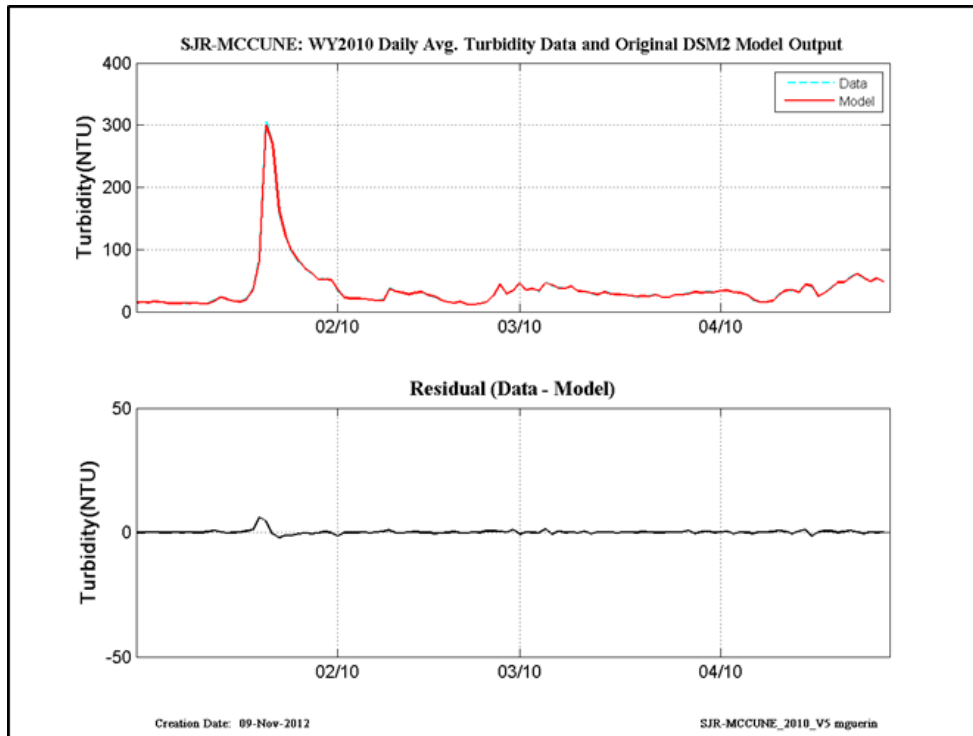


Figure 13-51 WY2010 original calibration results at San Joaquin-at-McCune (Vernalis).

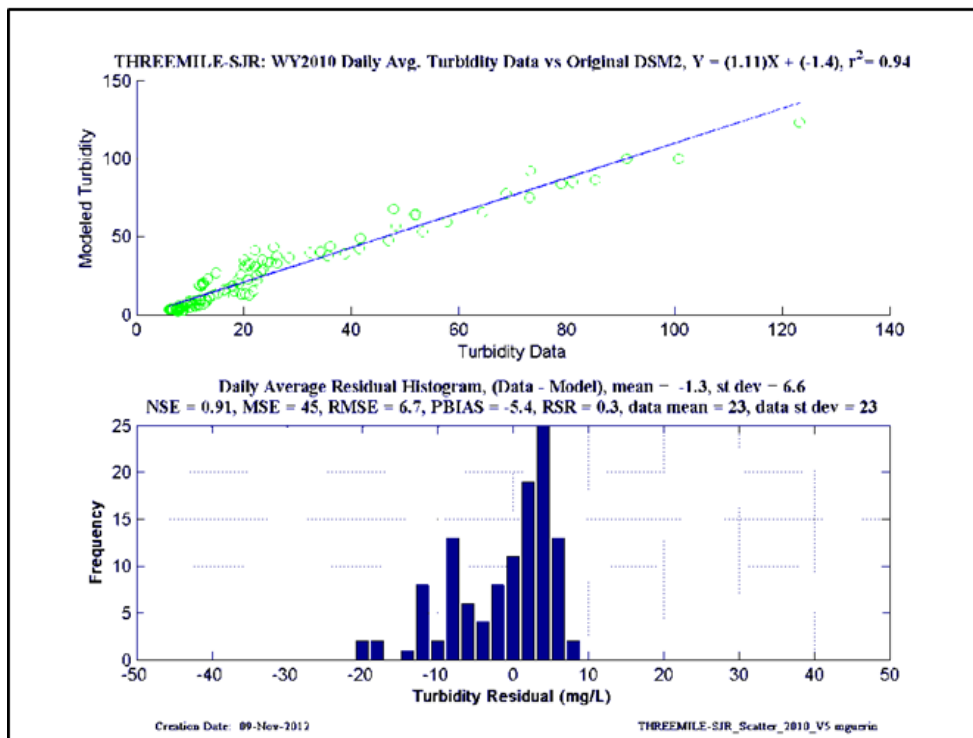
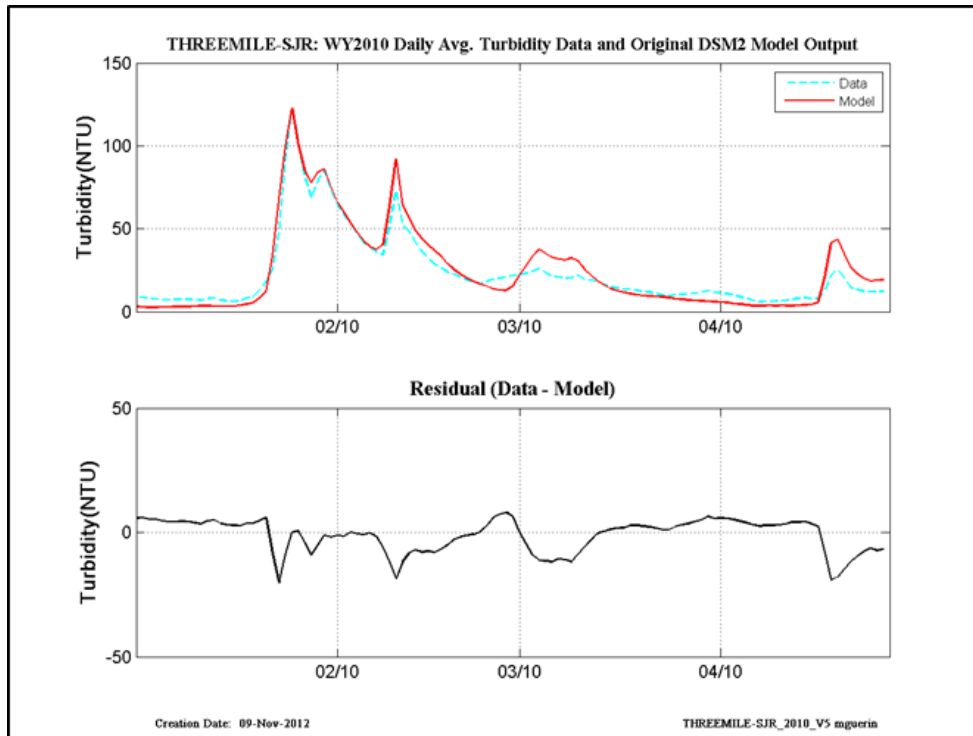


Figure 13-52 WY2010 original calibration results at Threemile-Slough-at-S\an Joaquin.

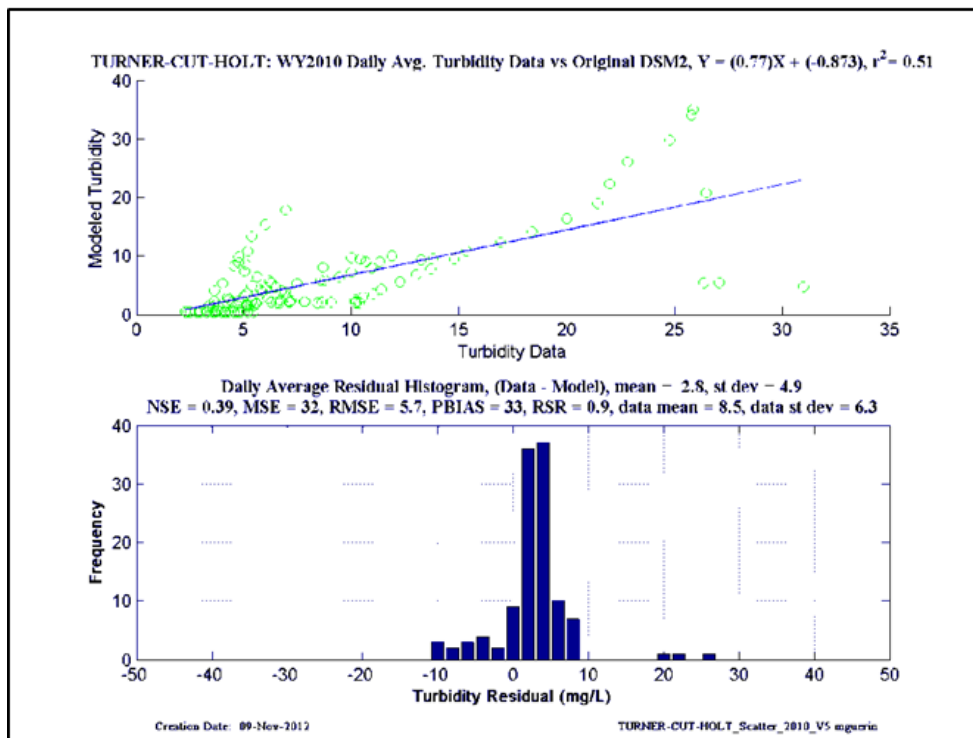
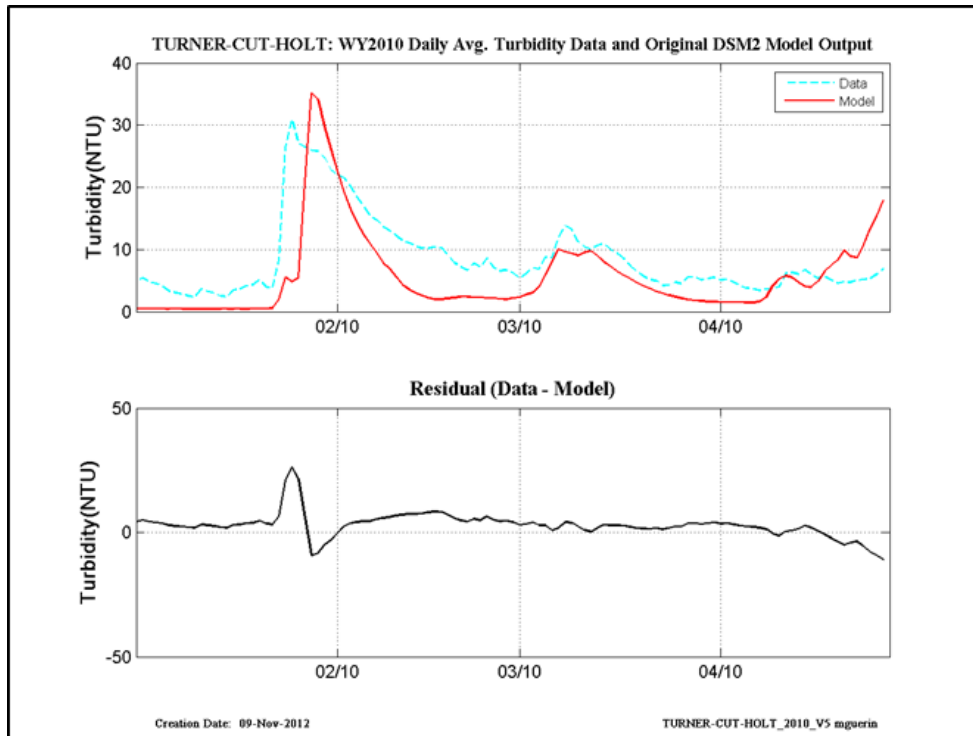


Figure 13-53 WY2010 original calibration results at Turner Cut-at-Holt.

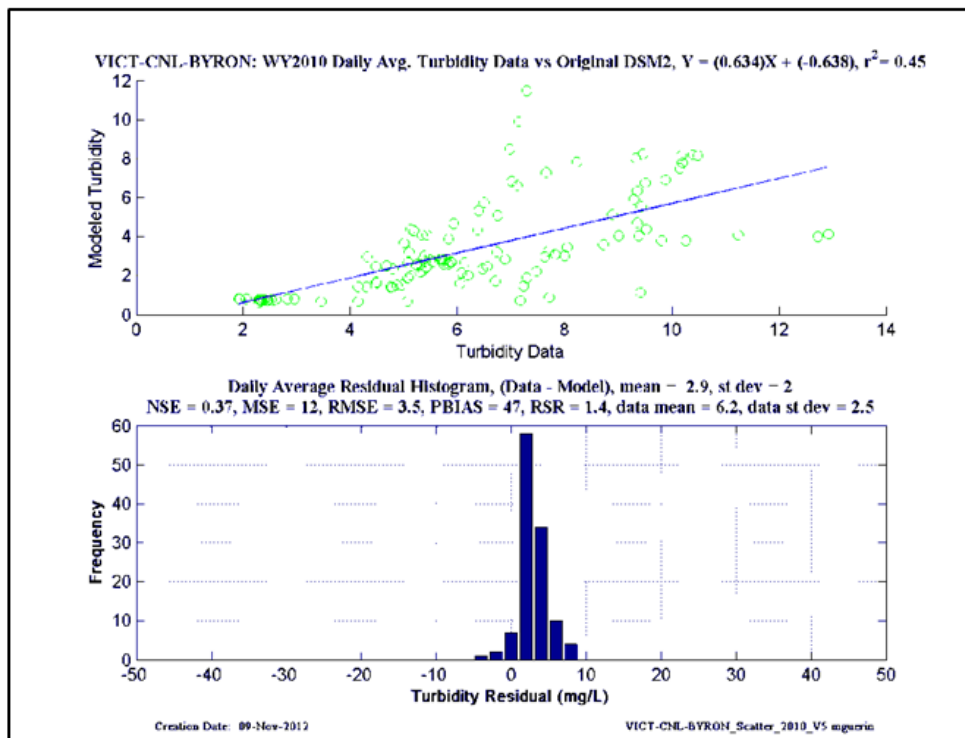
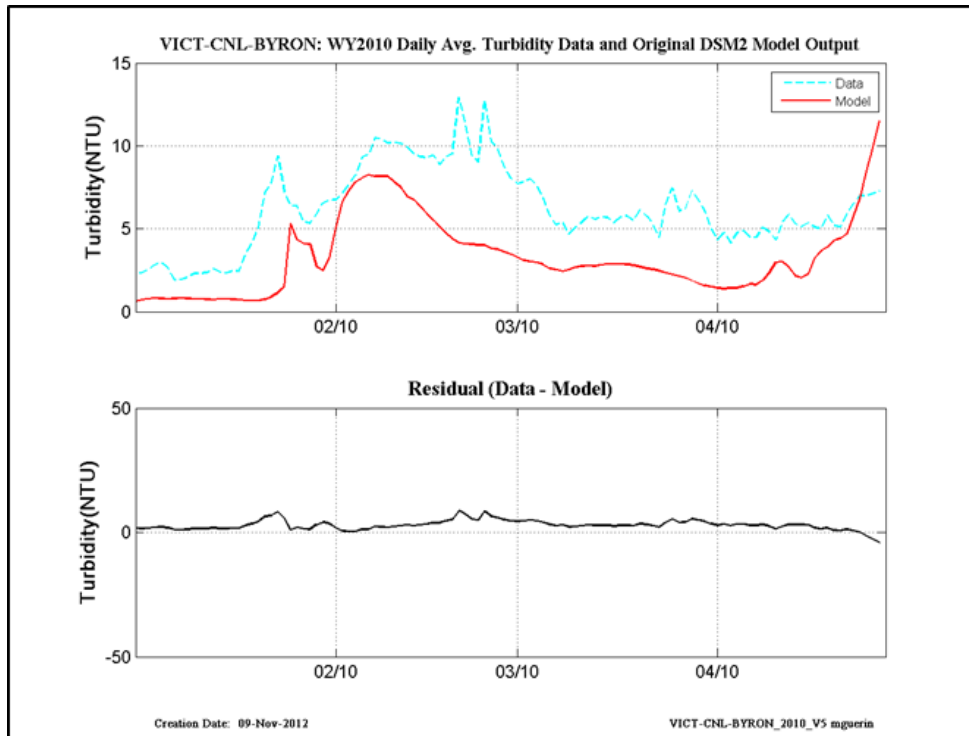


Figure 13-54 WY2010 original calibration results at Victoria Canal-at-Byron.

14 Appendix IV – Updated QUAL Turbidity calibration statistics, 15-min

14.1 Fifteen Minute CDEC data and model output – WY2011

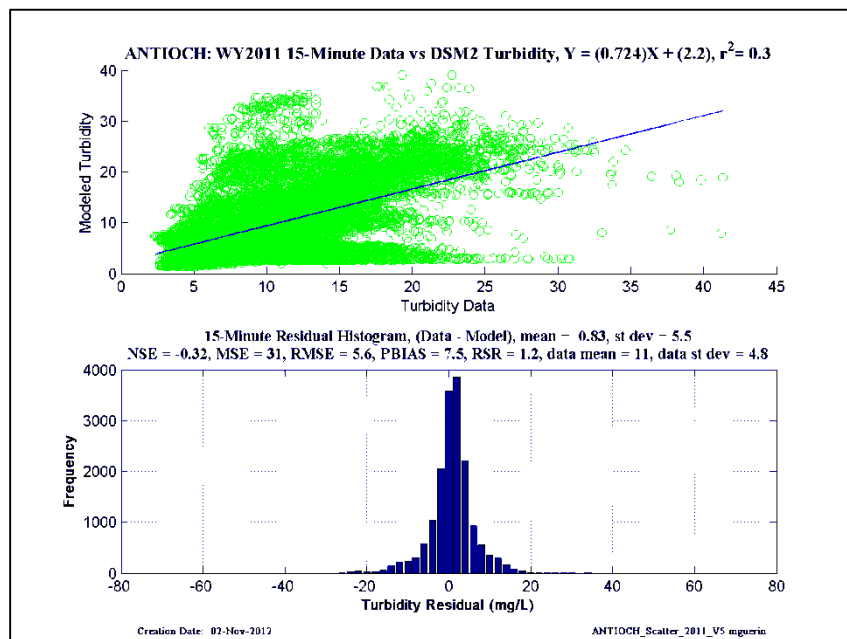
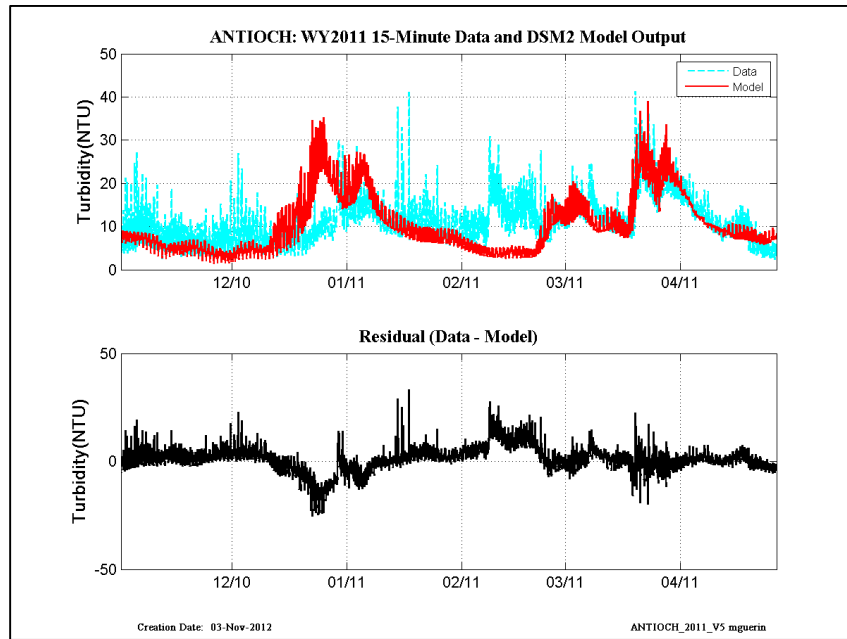


Figure 14-1 WY2011 15-min revised calibration results at Antioch.

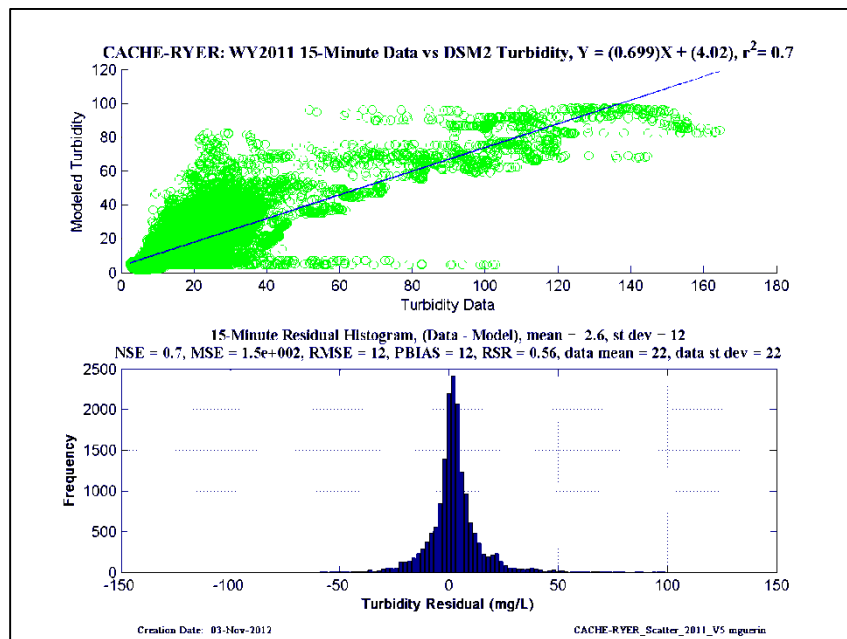
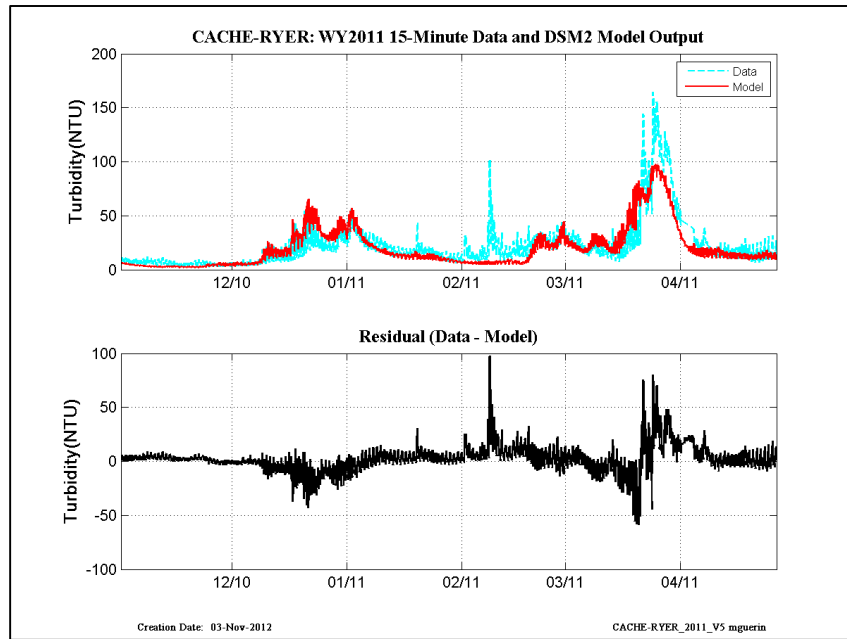


Figure 14-2 WY2011 15-min revised calibration results at Cache-Ryer.

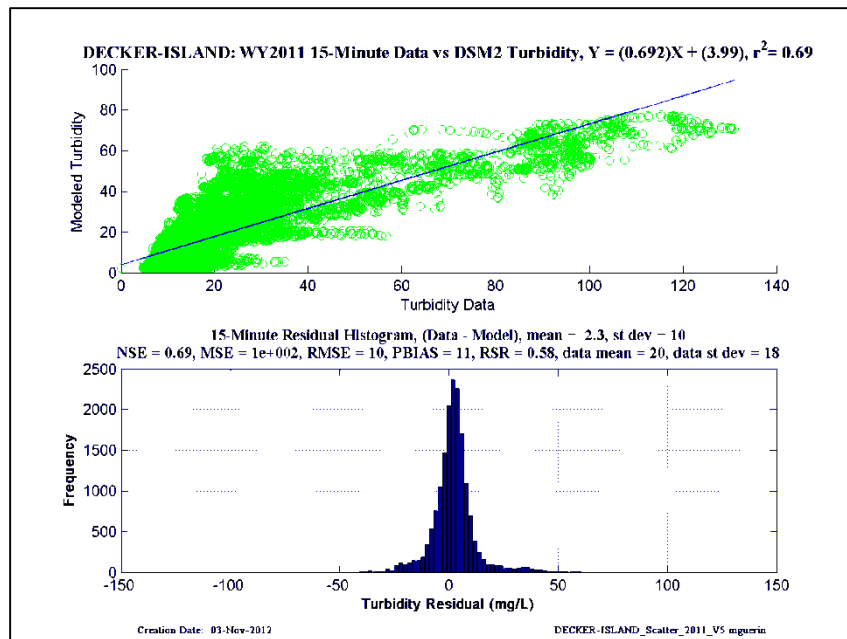
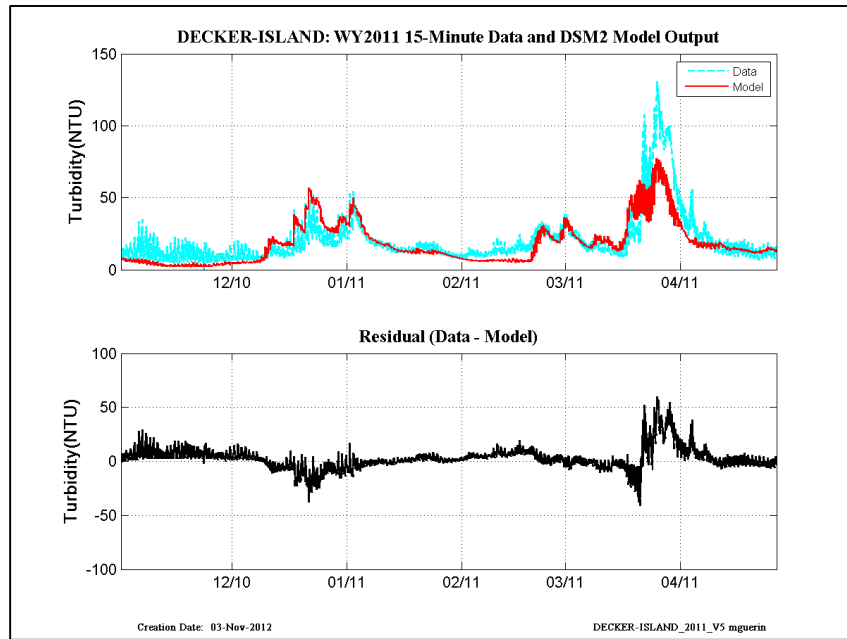


Figure 14-3 WY2011 15-min revised calibration results at Decker Island.

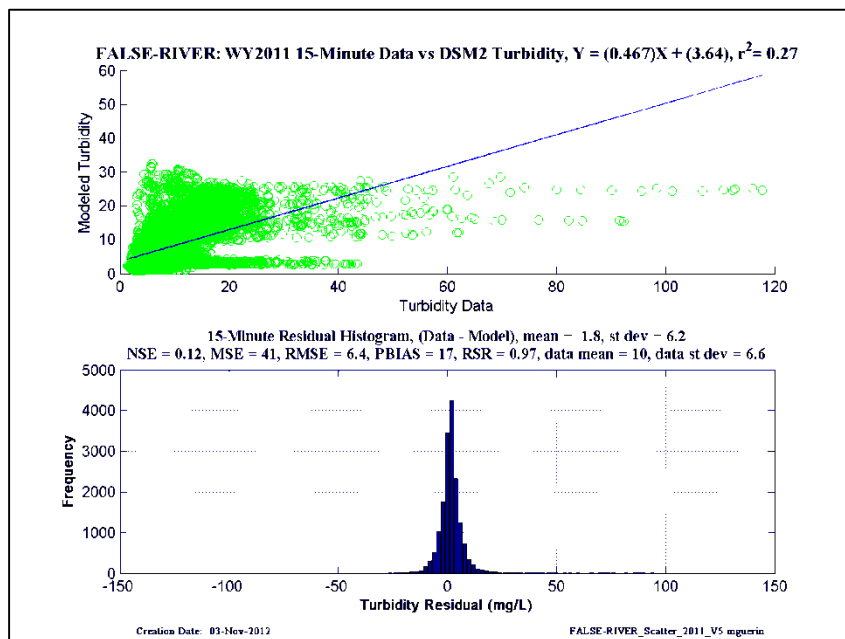
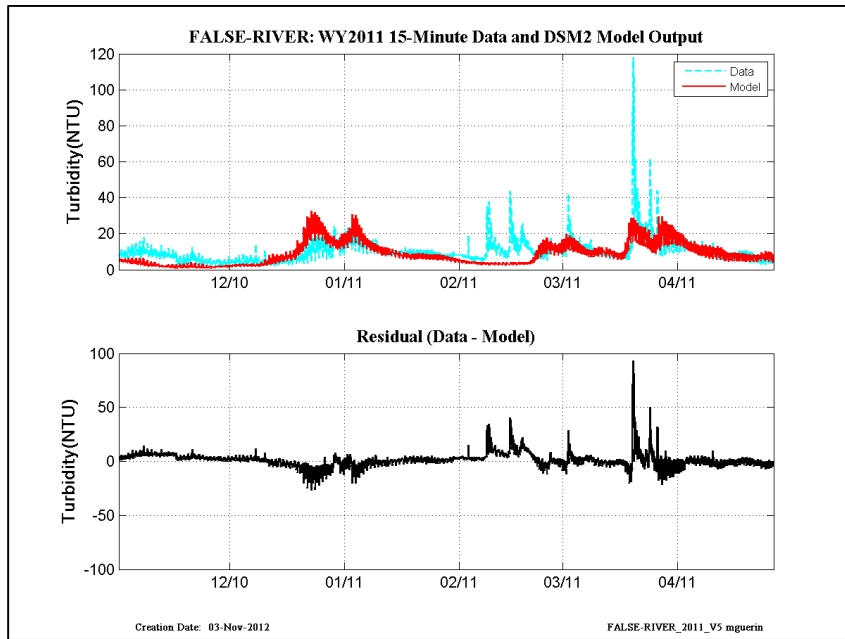


Figure 14-4 WY2011 15-min revised calibration results at False River.

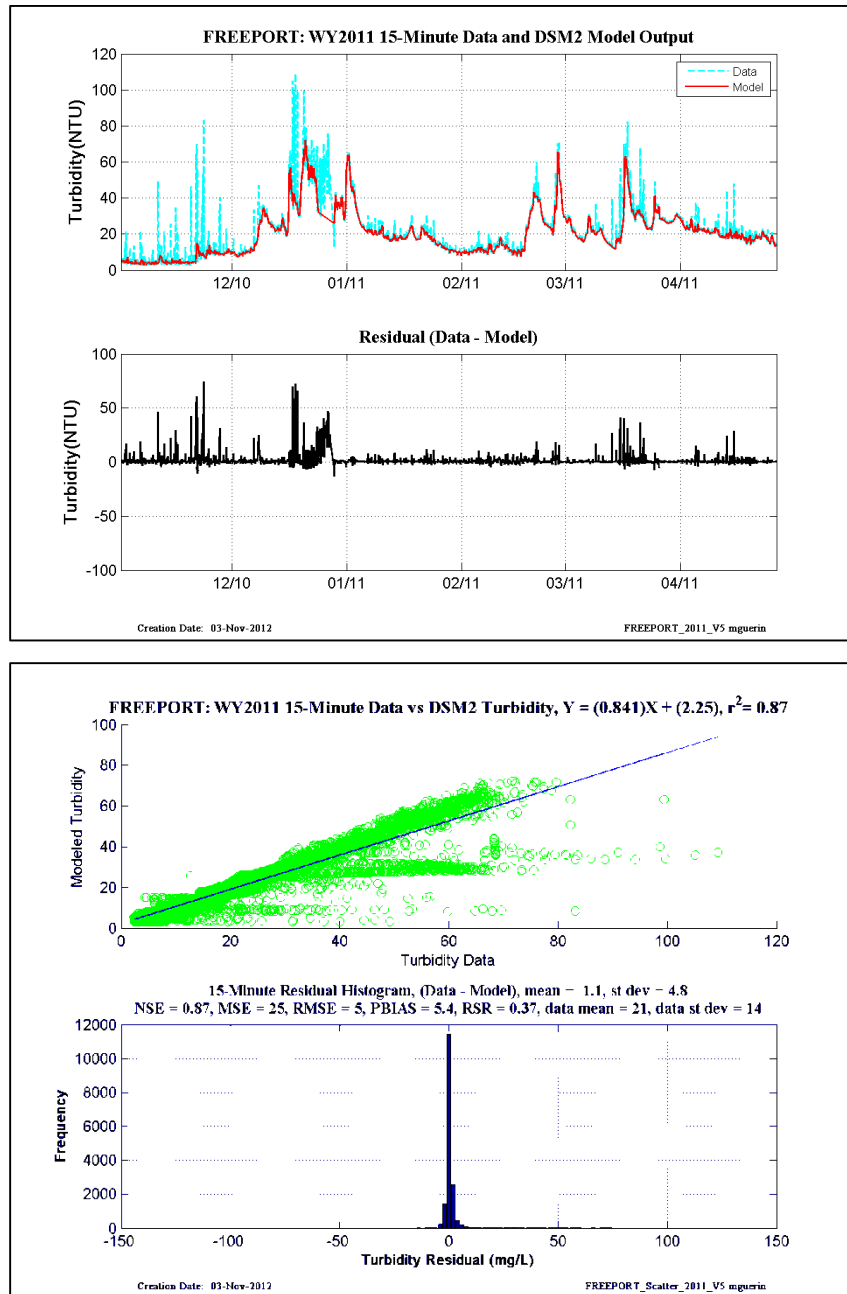


Figure 14-5 WY2011 15-min revised calibration results at Freeport.

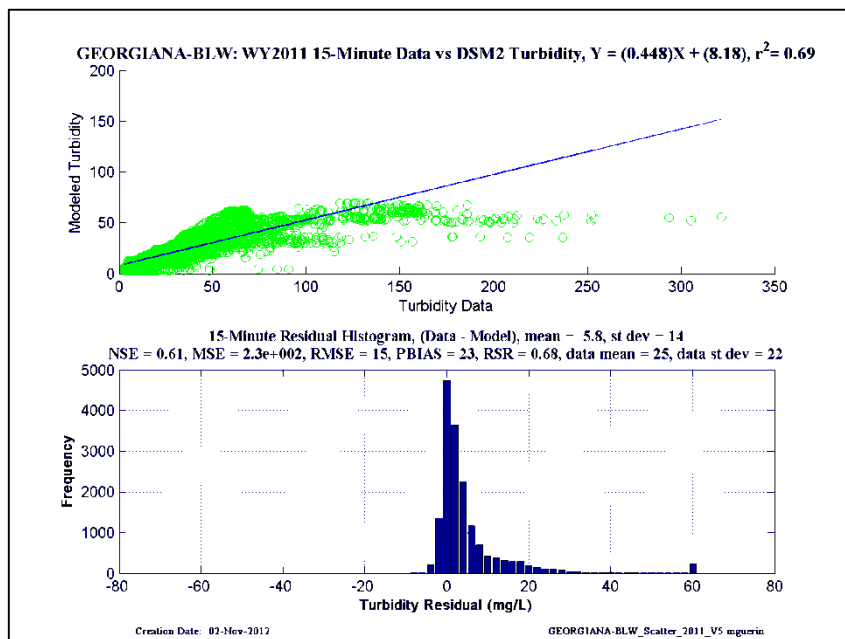
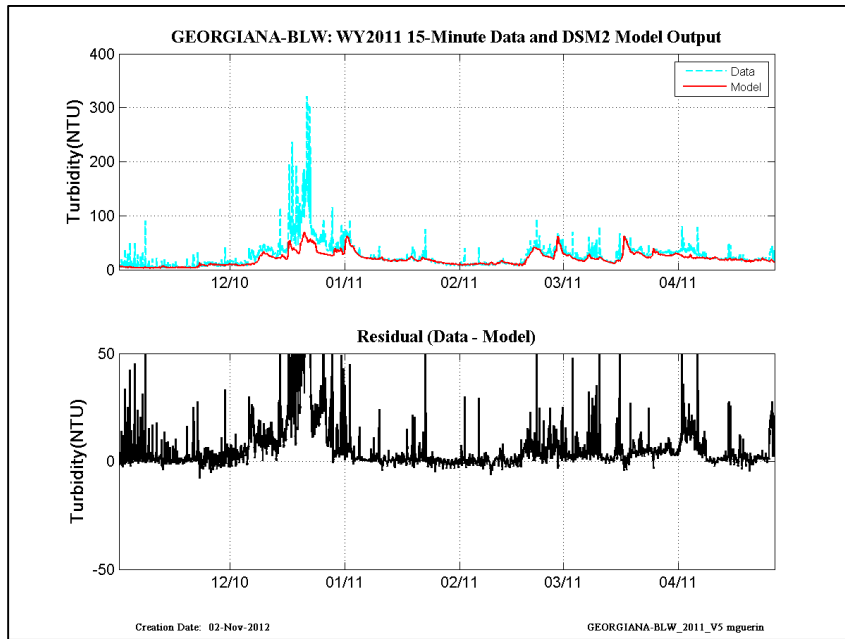


Figure 14-6 WY2011 15-min revised calibration results at Georgiana-Below-Sac.

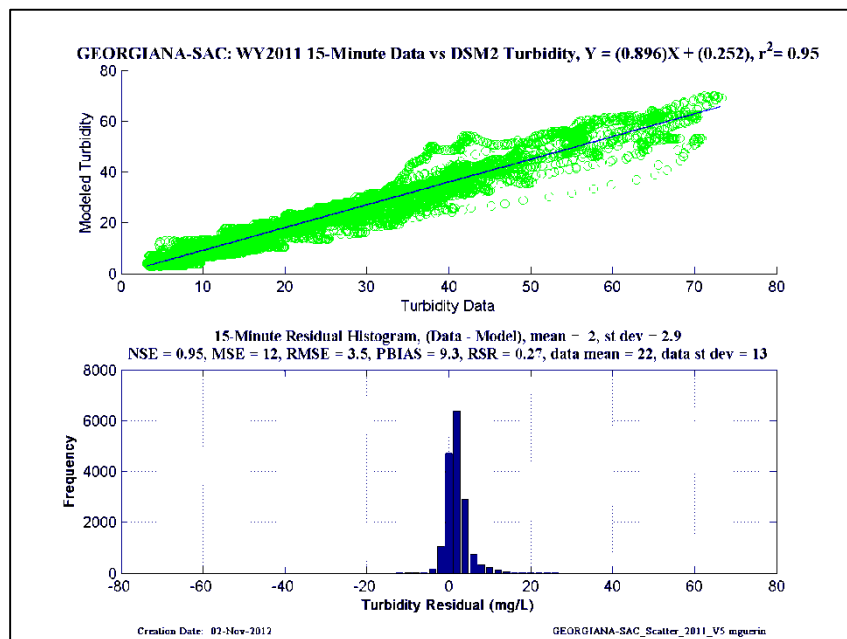
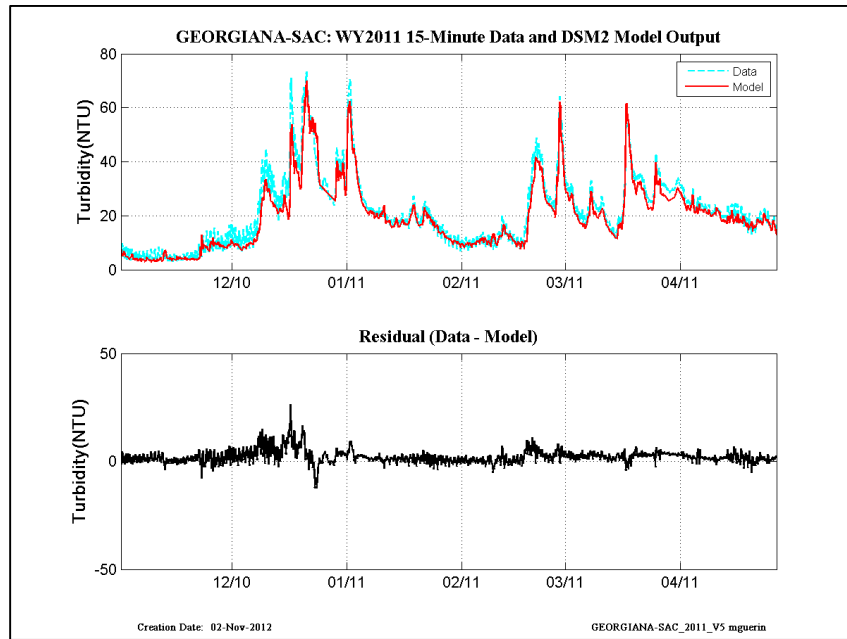


Figure 14-7 WY2011 15-min revised calibration results at Georgiana-at-Sac.

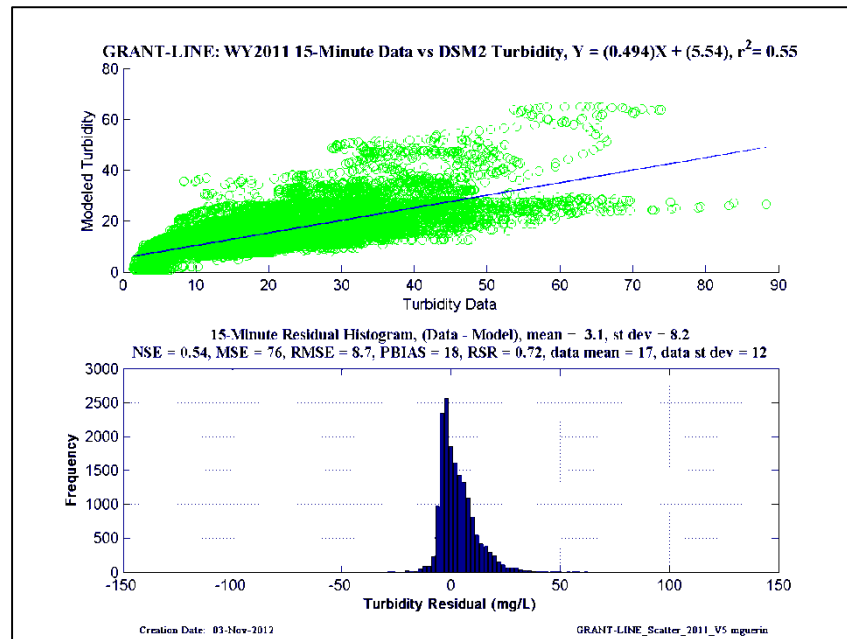
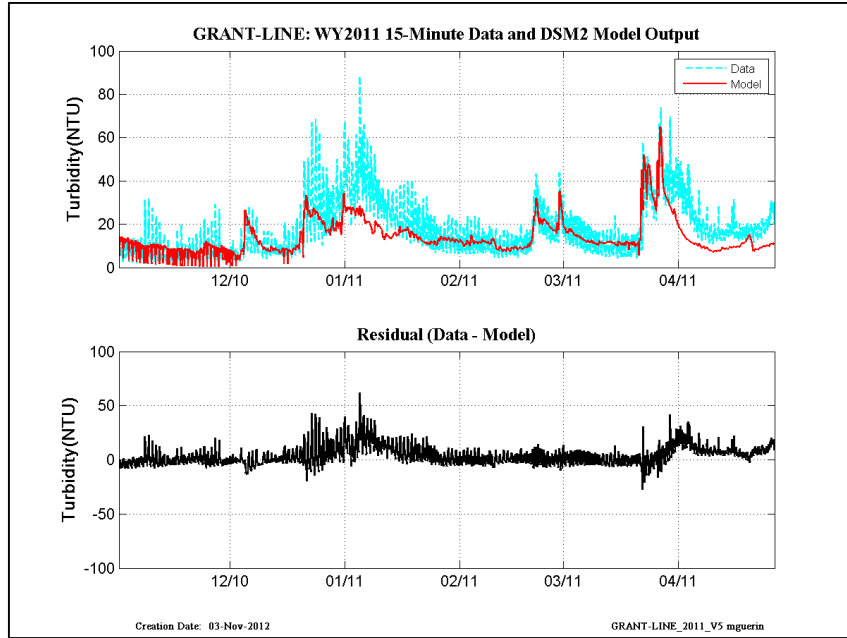


Figure 14-8 WY2011 15-min revised calibration results at Grant Line.

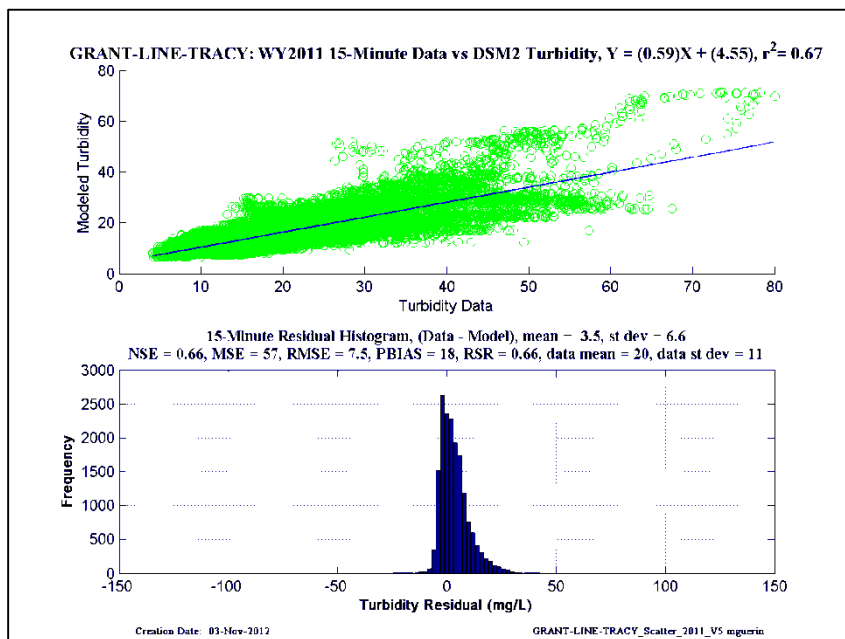
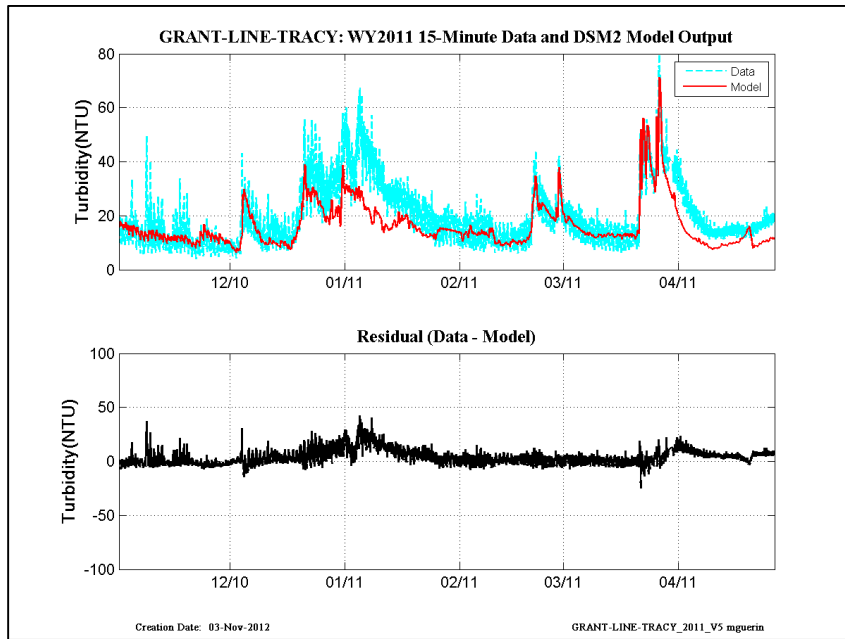


Figure 14-9 WY2011 15-min revised calibration results at Grant-Line Tracy.

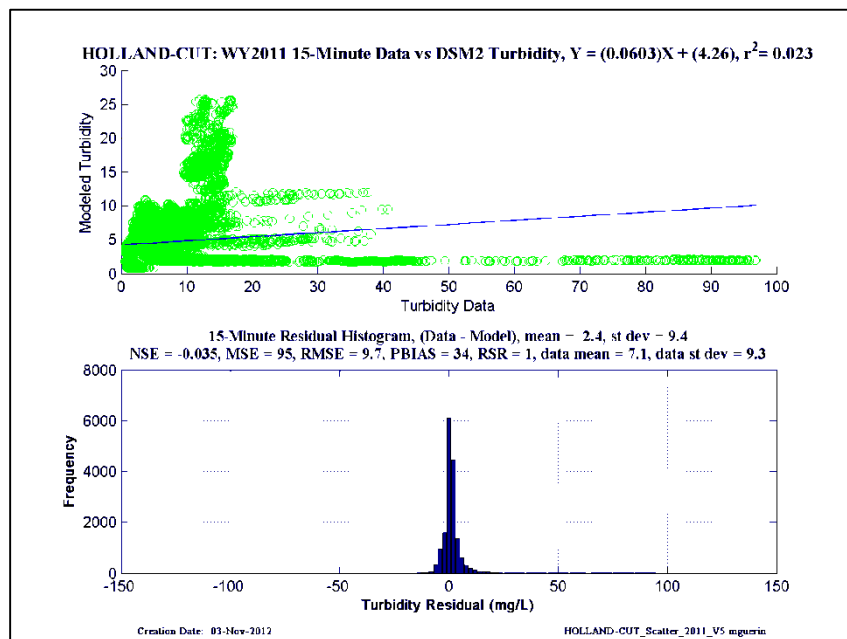
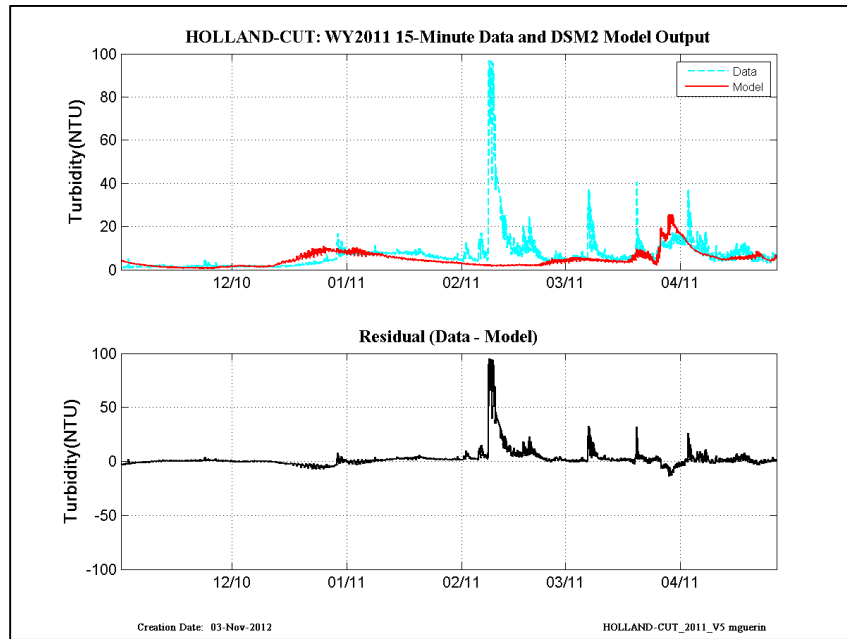


Figure 14-10 WY2011 15-min revised calibration results at Holland Cut.

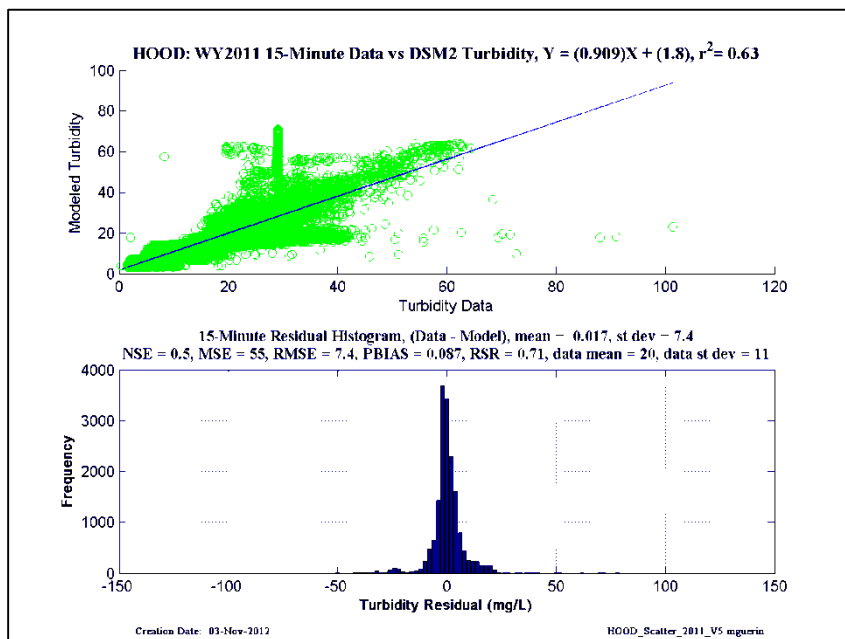
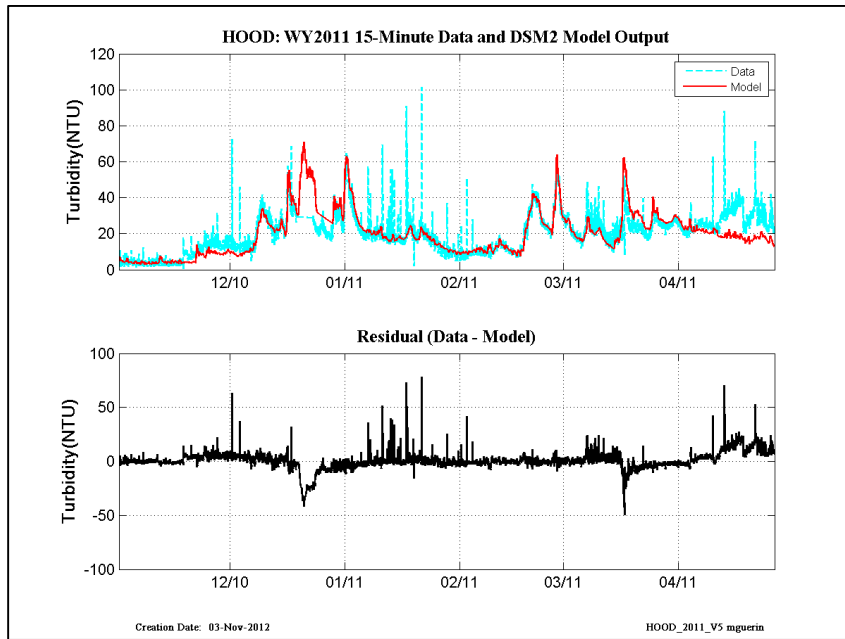


Figure 14-11 WY2011 15-min revised calibration results at Hood.

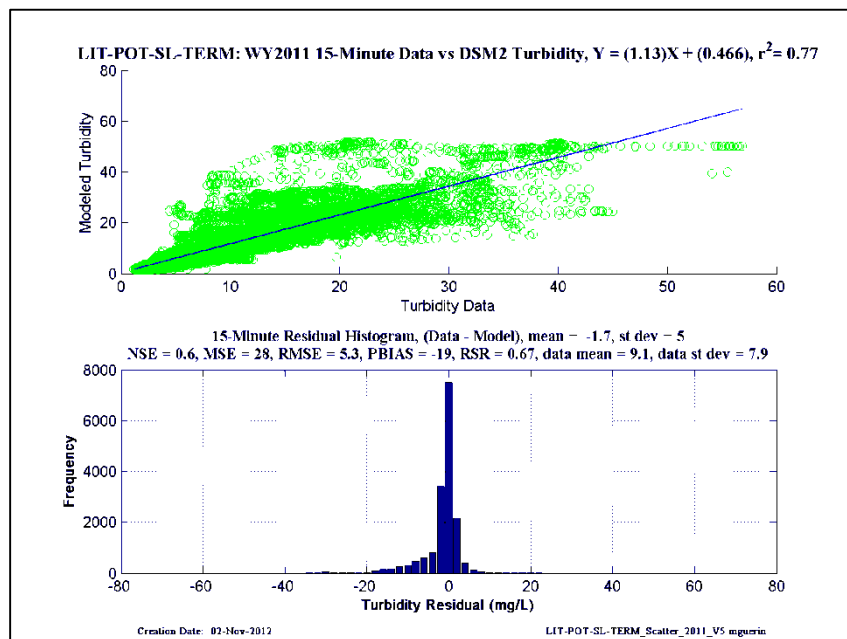
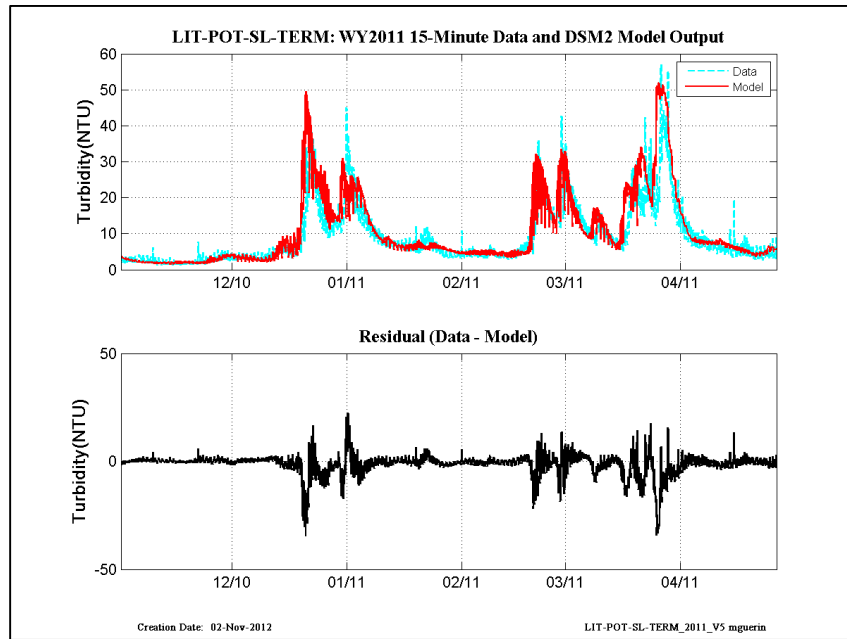


Figure 14-12 WY2011 15-min revised calibration results at Little Potato Slough-at-Terminus.

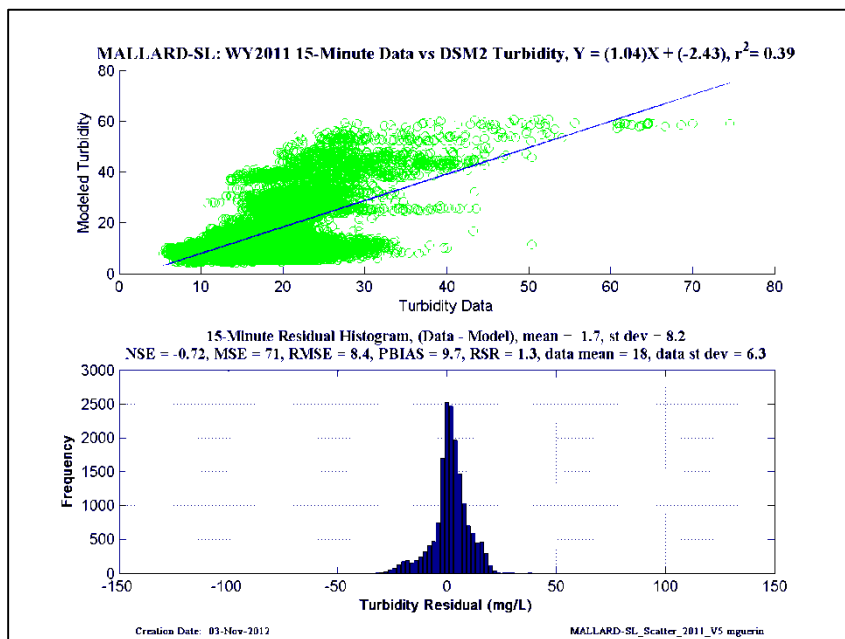
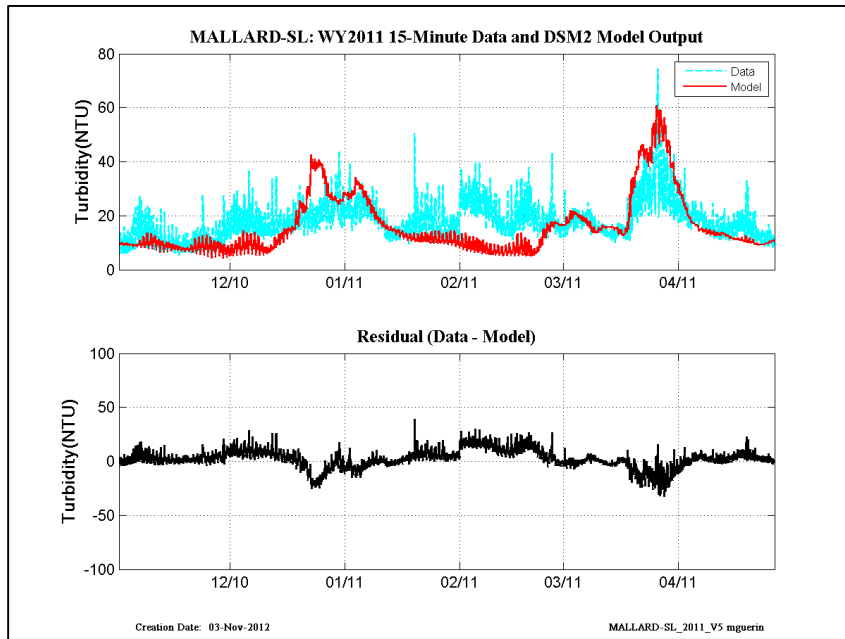


Figure 14-13 WY2011 15-min revised calibration results at Mallard Slough.

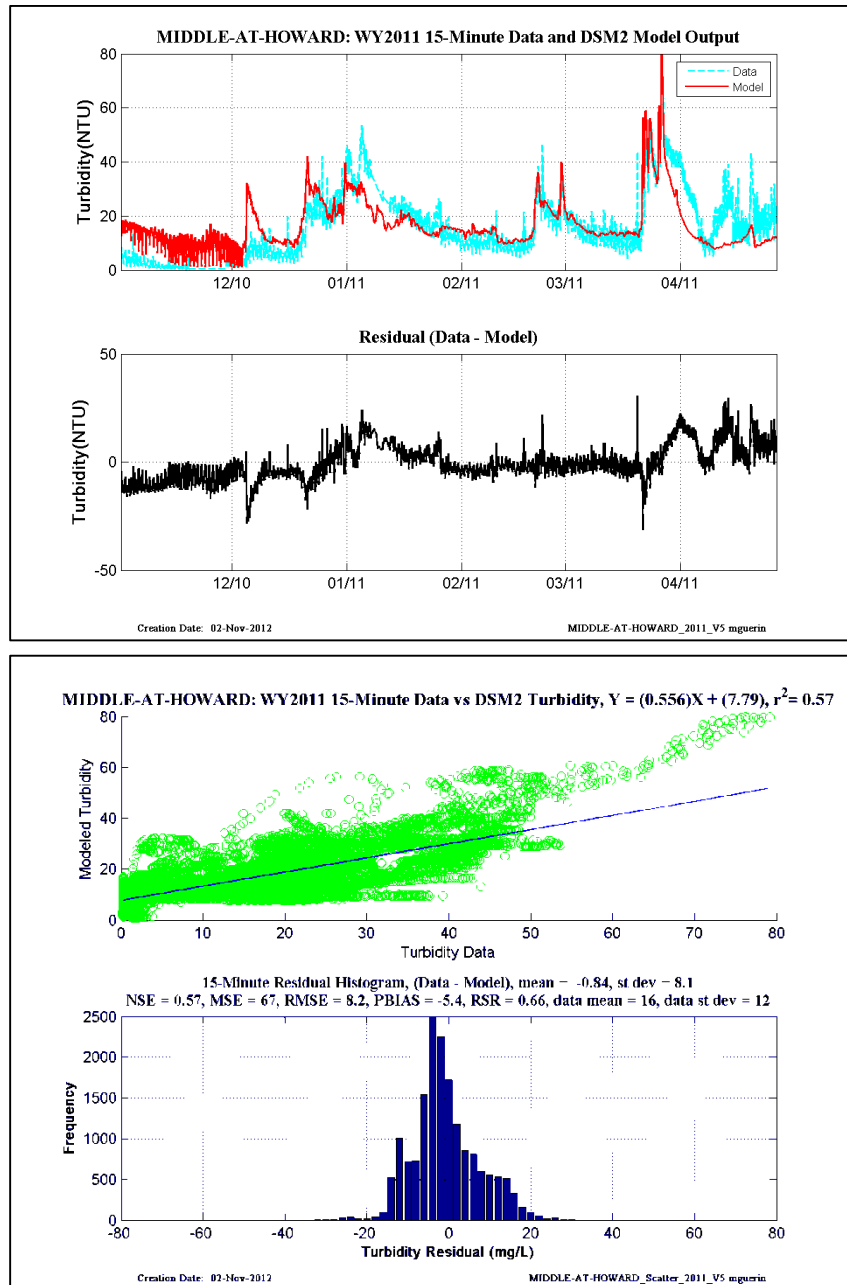


Figure 14-14 WY2011 15-min revised calibration results at Middle River-at-Howard Rd.

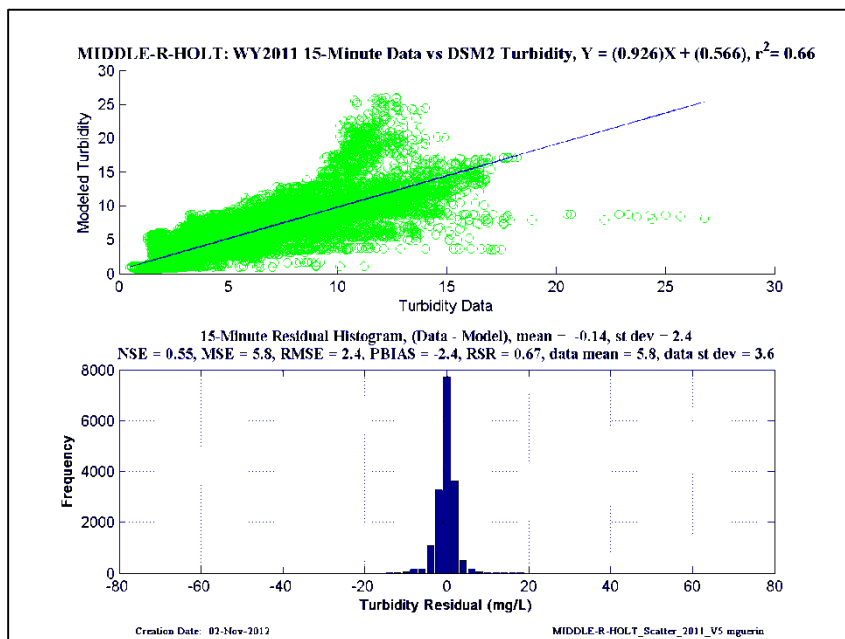
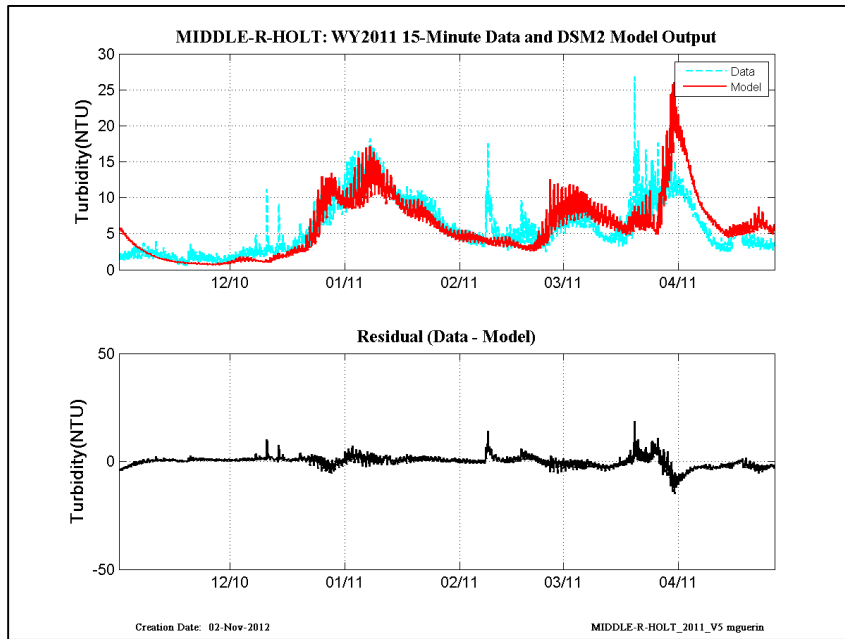


Figure 14-15 WY2011 15-min revised calibration results at Middle River-at-Holt.

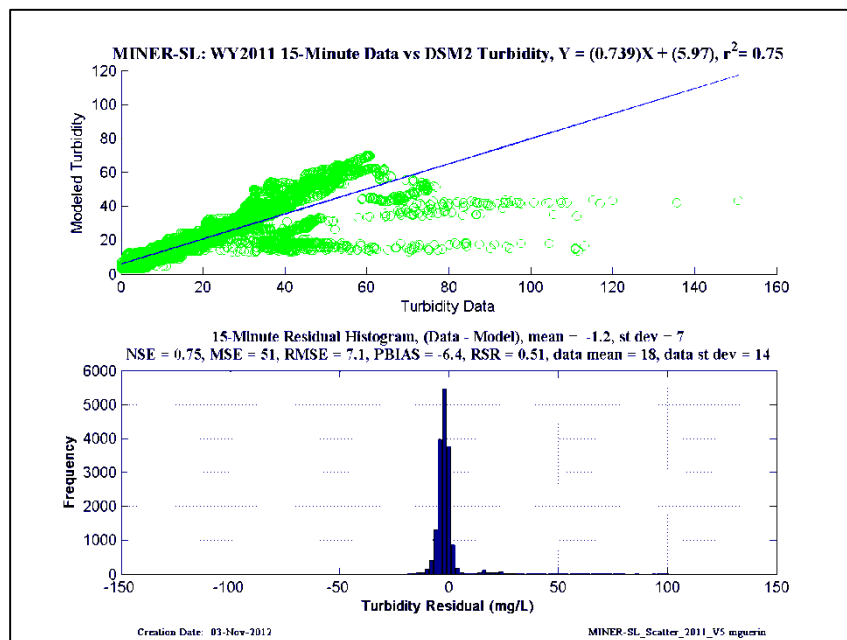
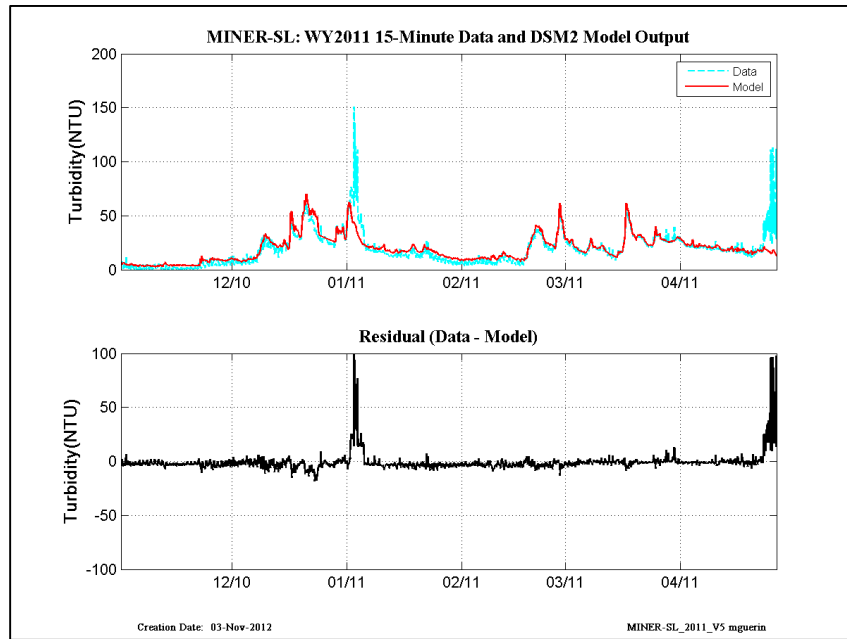


Figure 14-16 WY2011 15-min revised calibration results at Miner Slough.

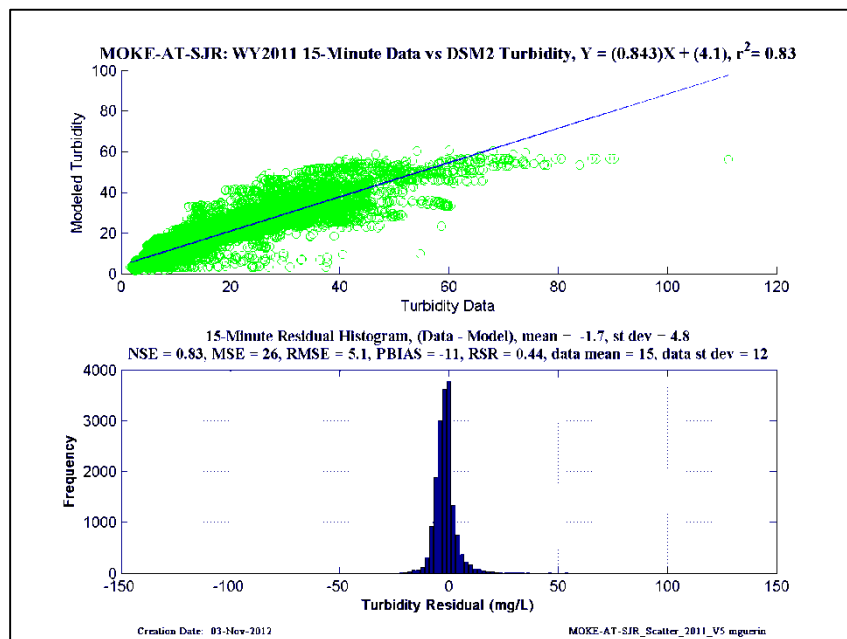
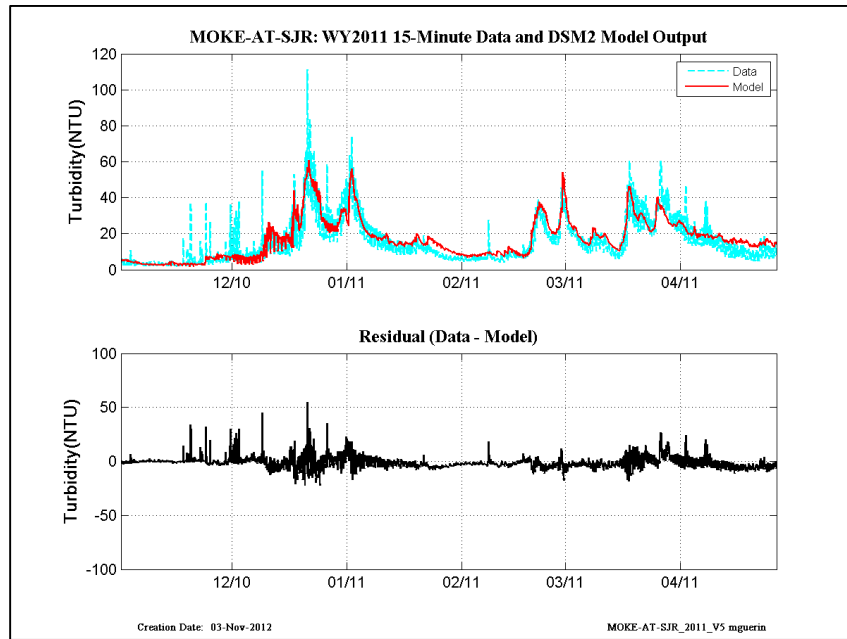


Figure 14-17 WY2011 15-min revised calibration results at Mokelumne-at-San Joaquin.

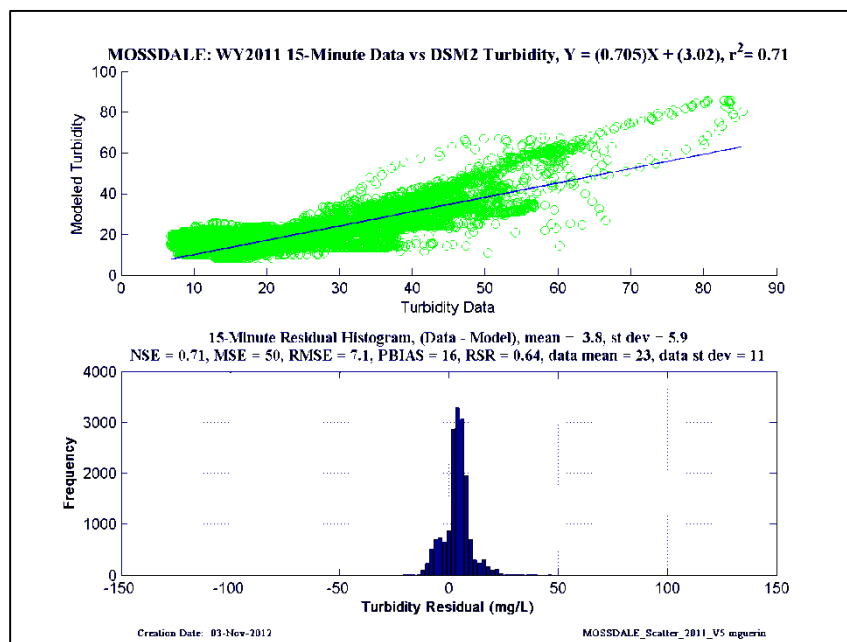
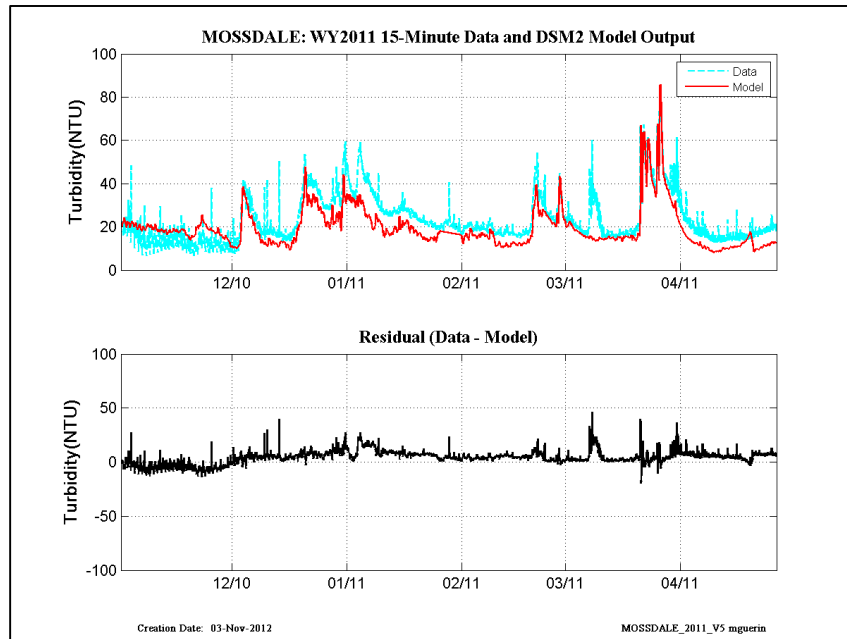


Figure 14-18 WY2011 15-min revised calibration results at Mossdale.

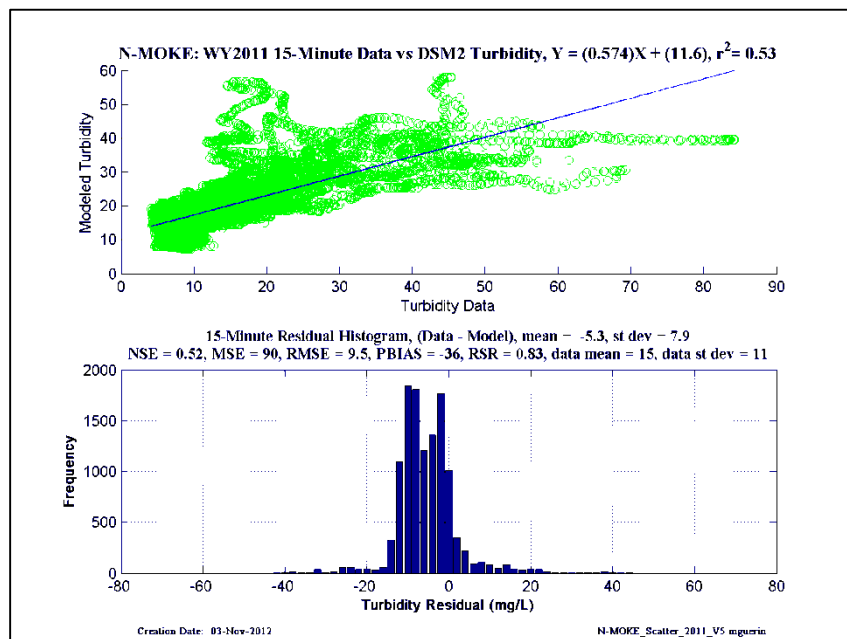
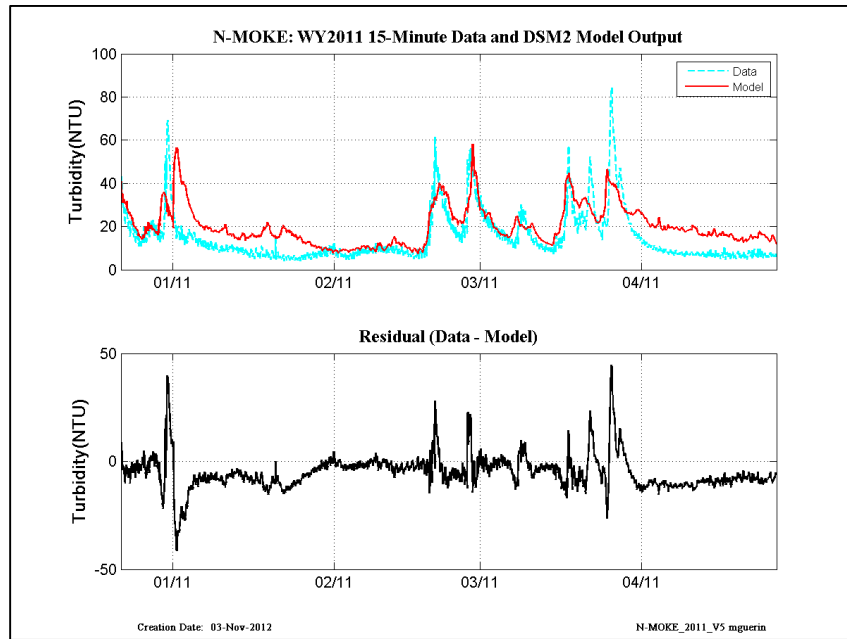


Figure 14-19 WY2011 15-min revised calibration results at North Mokelumne.

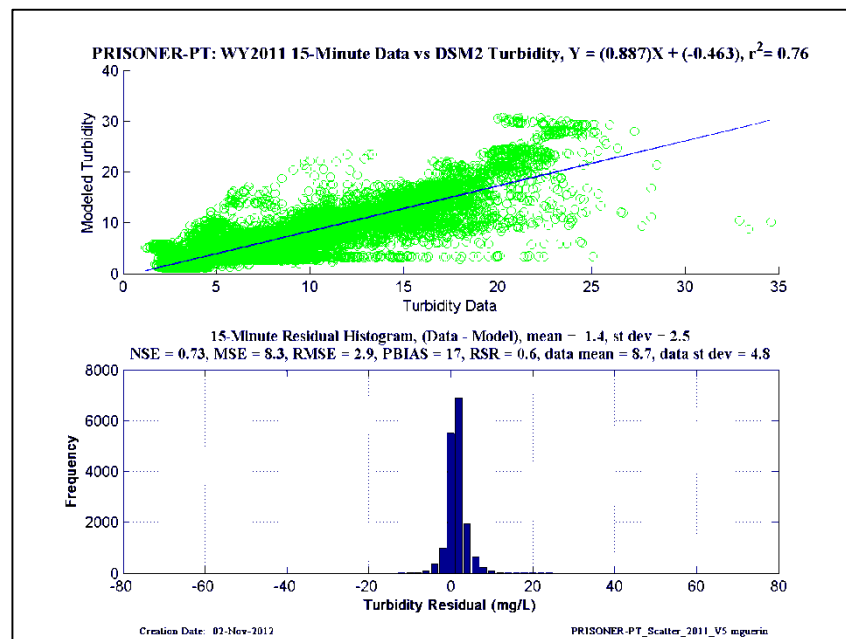
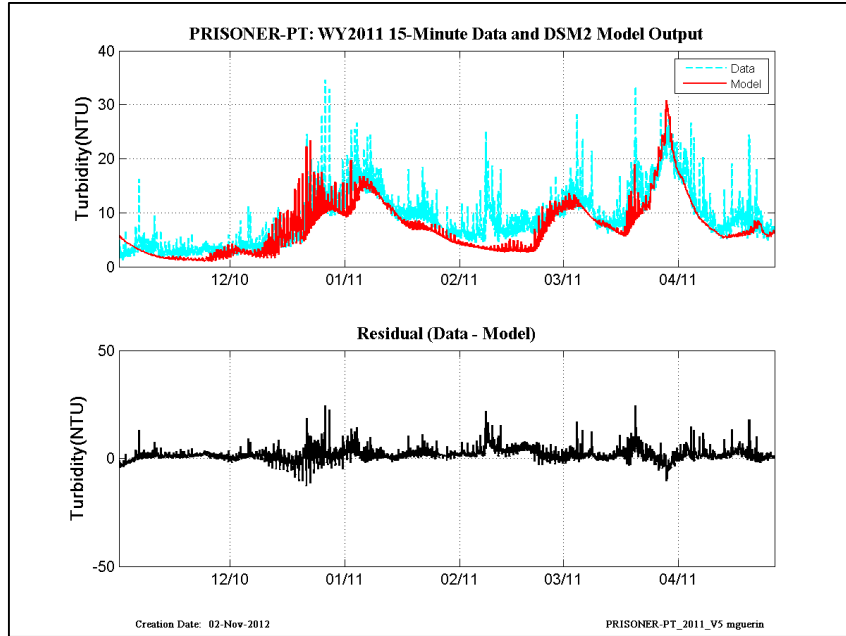


Figure 14-20 WY2011 15-min revised calibration results at Prisoner Point.

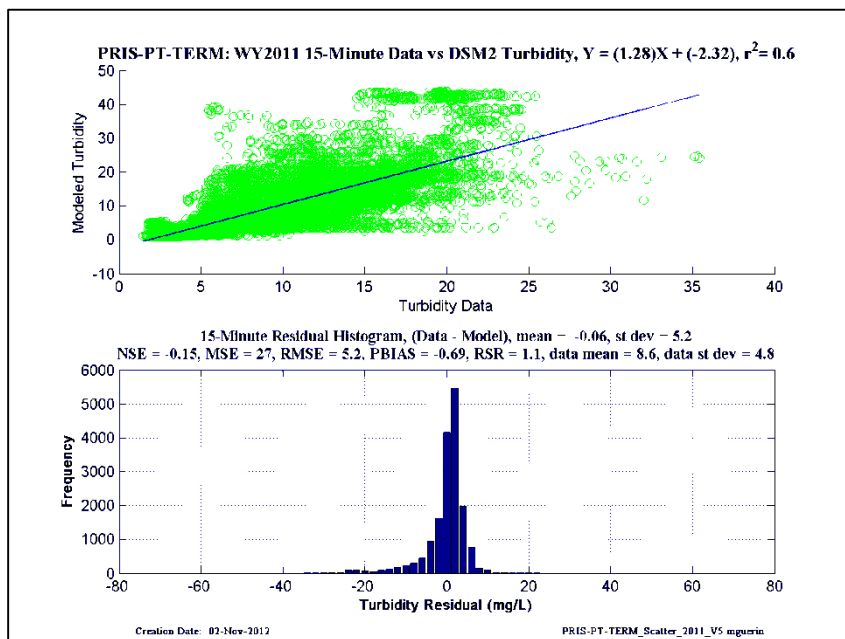
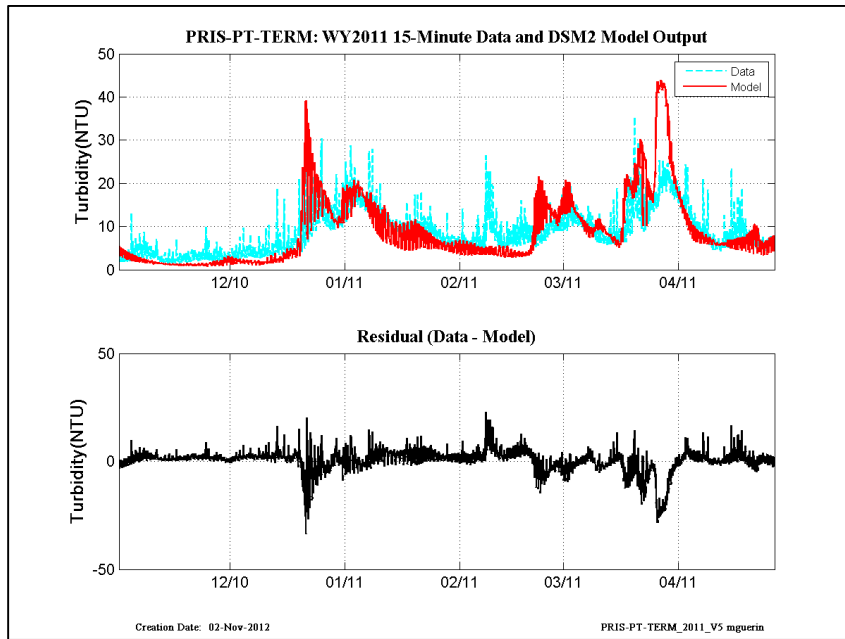


Figure 14-21 WY2011 15-min revised calibration results at Prisoner Point-at-Terminus.

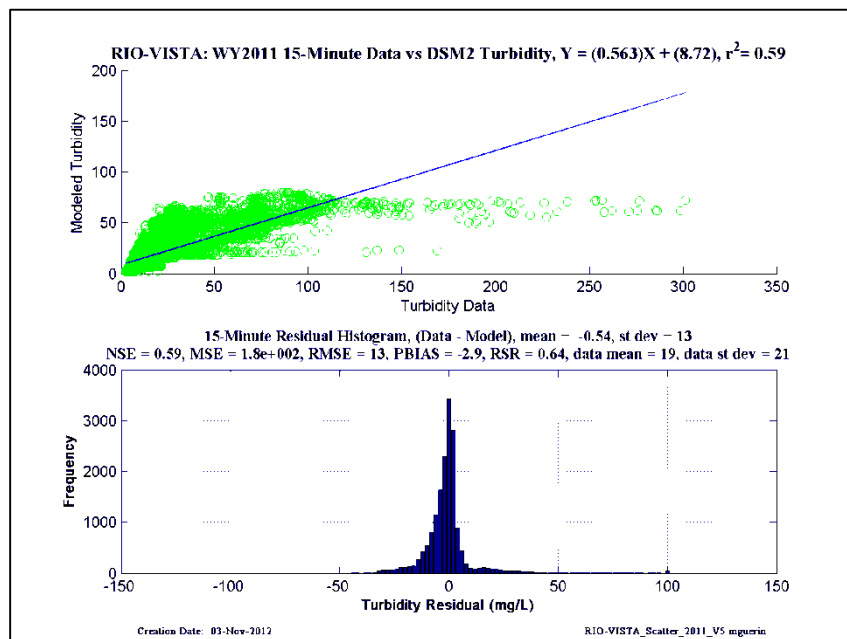
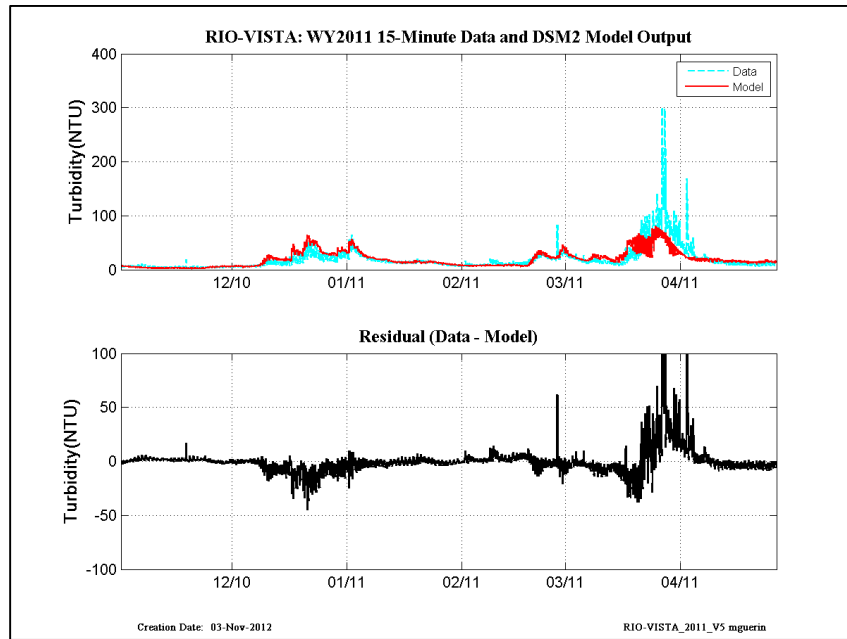


Figure 14-22 WY2011 15-min revised calibration results at Rio Vista.

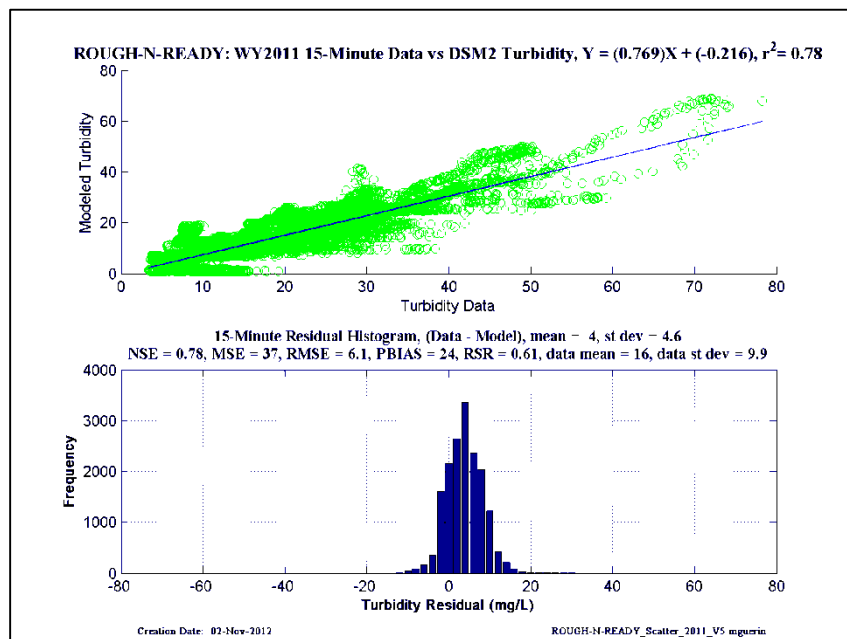
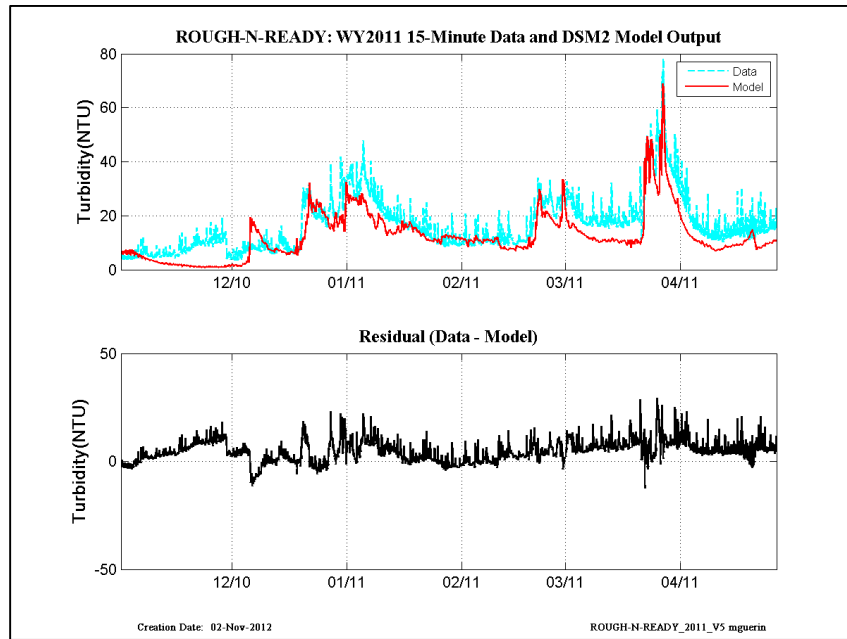


Figure 14-23 WY2011 15-min revised calibration results at Rough-N-Ready Island.

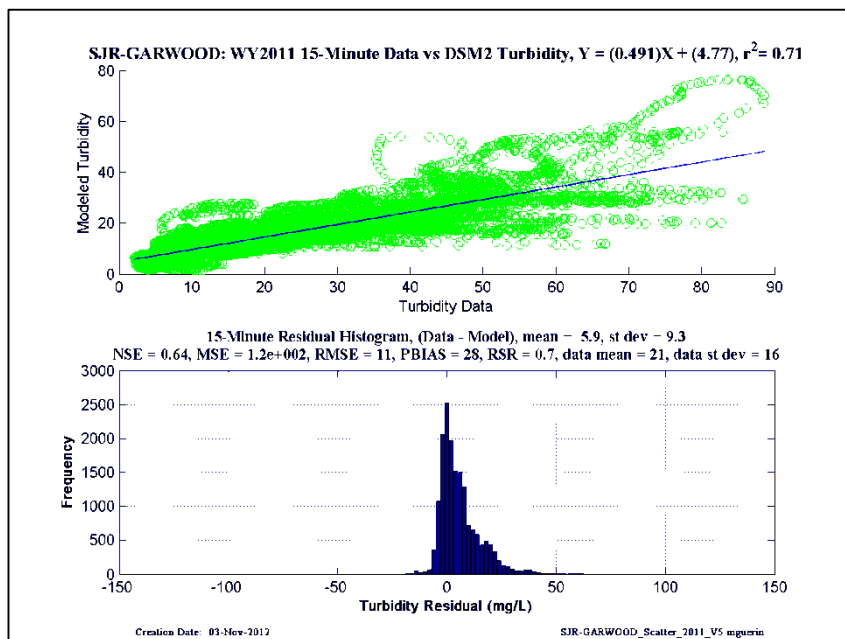
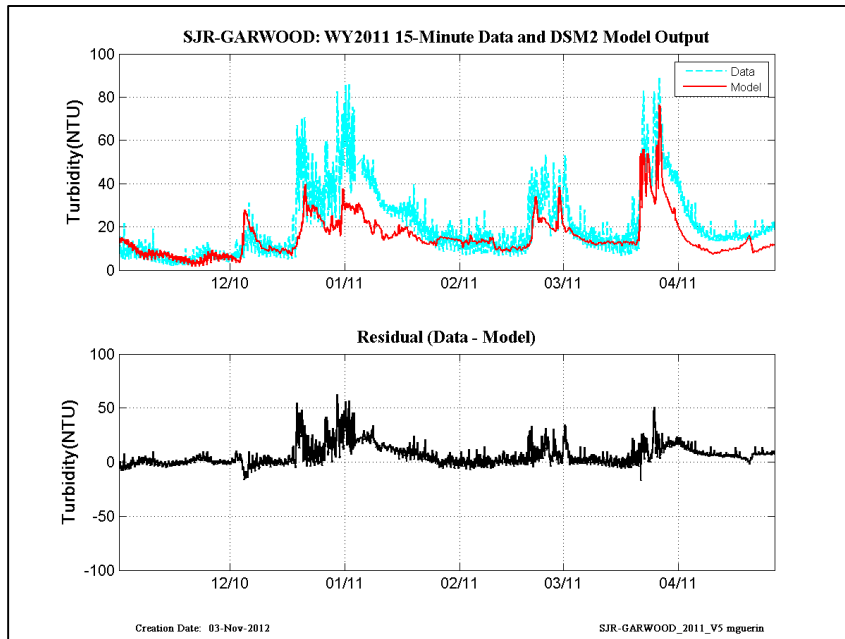


Figure 14-24 WY2011 15-min revised calibration results at San Joaquin-at-Garwood.

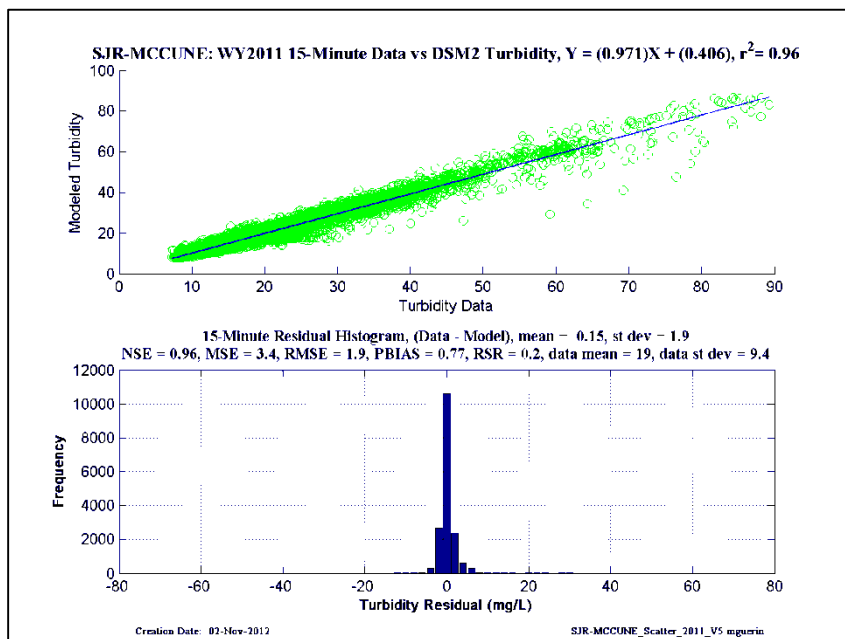
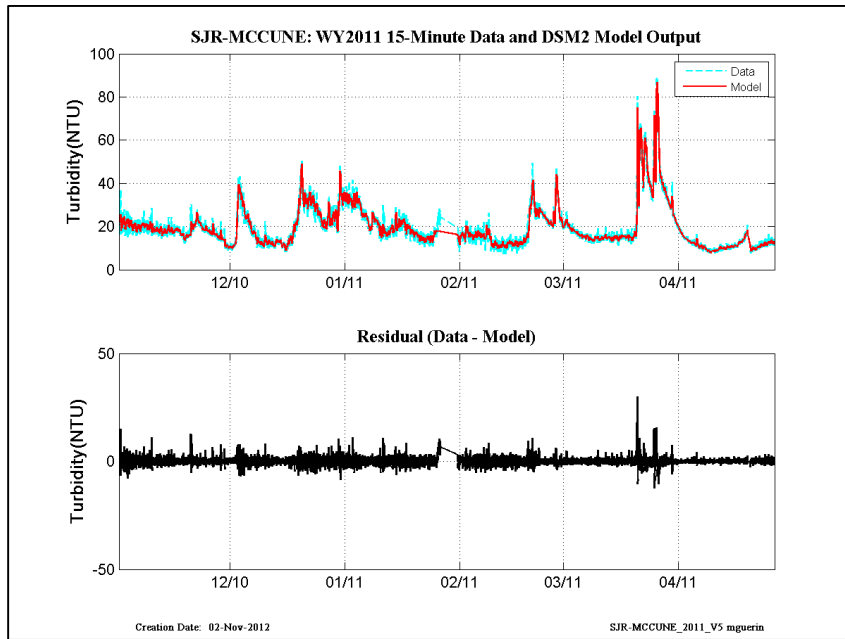


Figure 14-25 WY2011 15-min revised calibration results at San Joaquin-at-McCune (Vernalis).

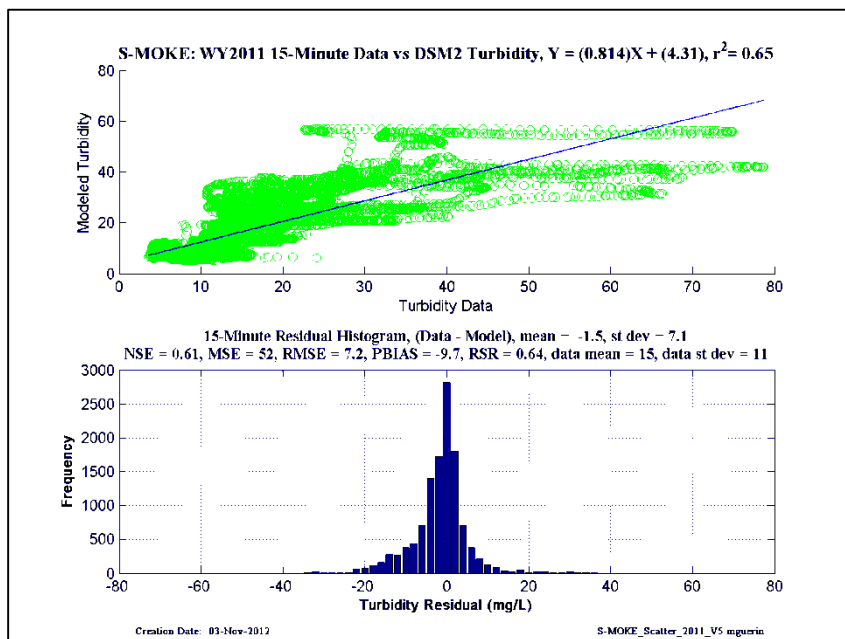
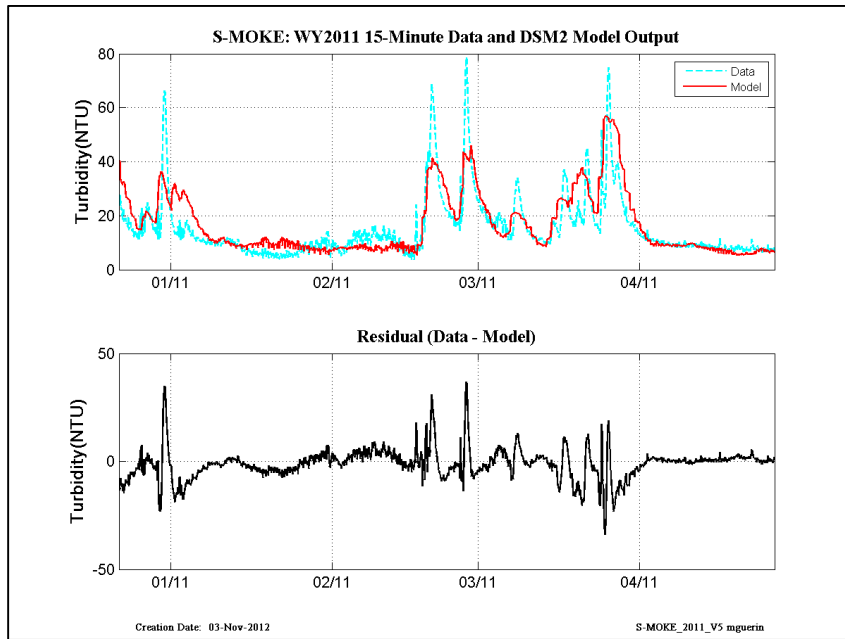


Figure 14-26 WY2011 15-min revised calibration results at South Mokelumne.

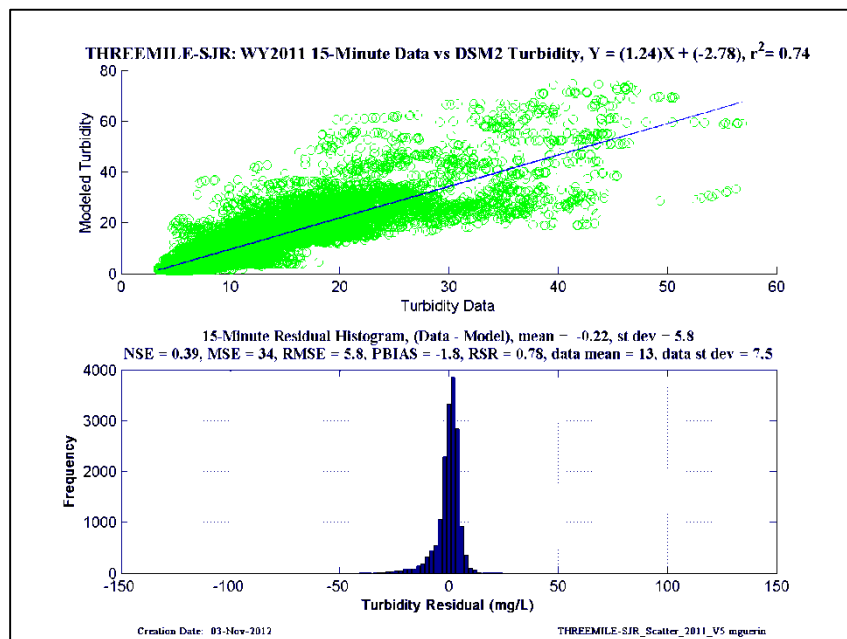
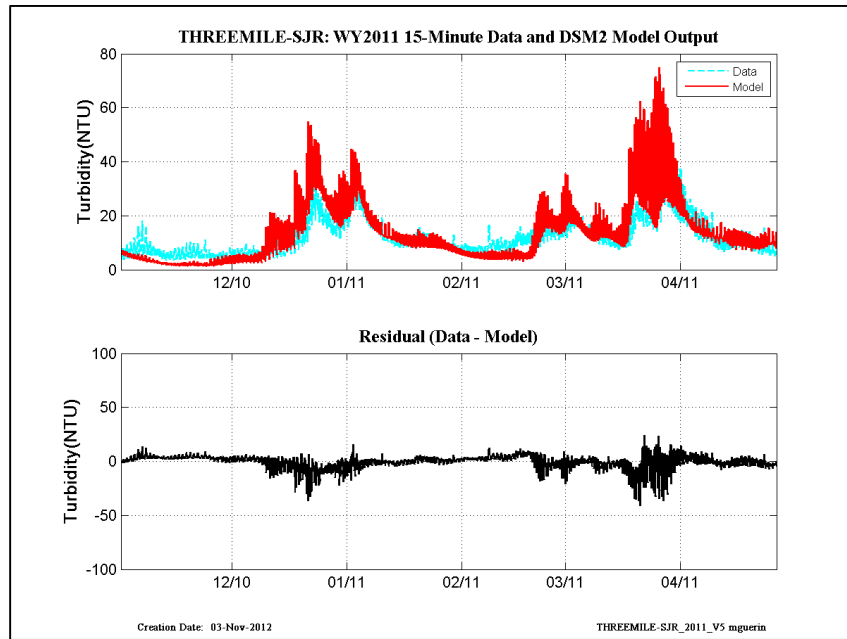


Figure 14-27 WY2011 15-min revised calibration results at Threemile-Slough-at-San Joaquin.

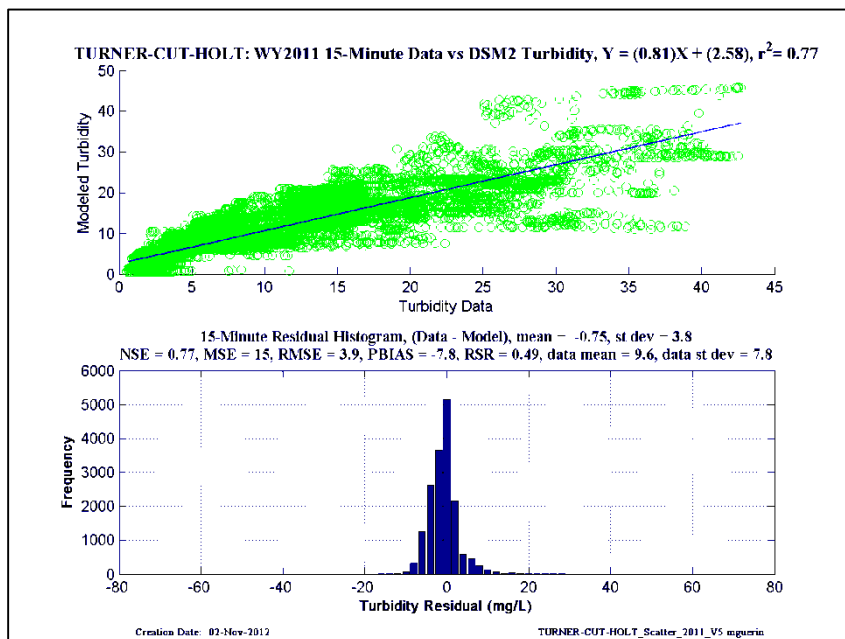
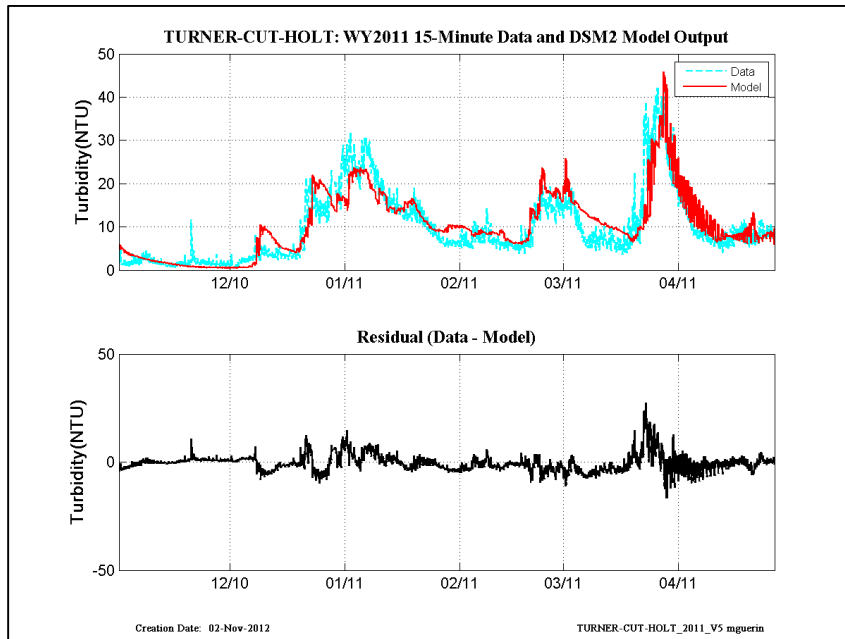


Figure 14-28 WY2011 15-min revised calibration results at Turner Cut-at-Holt.

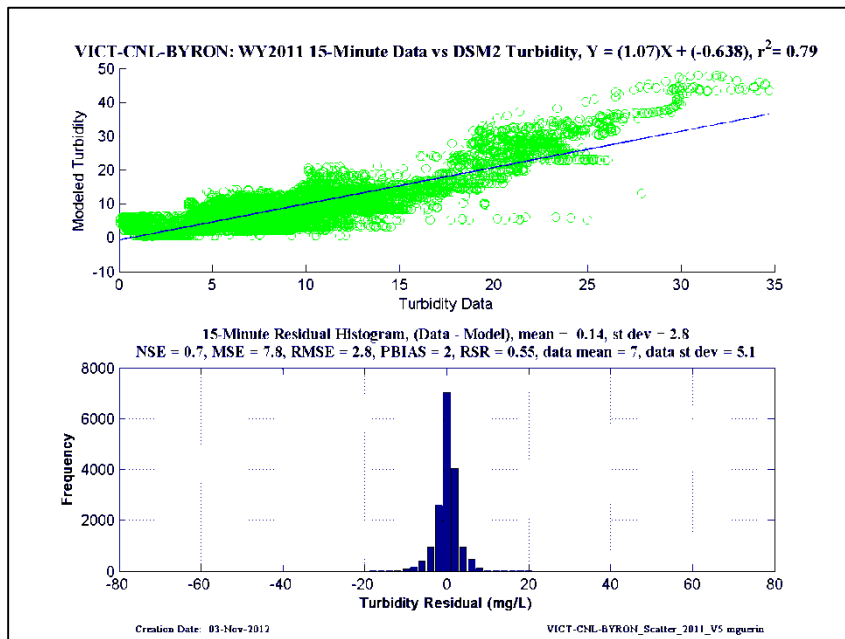
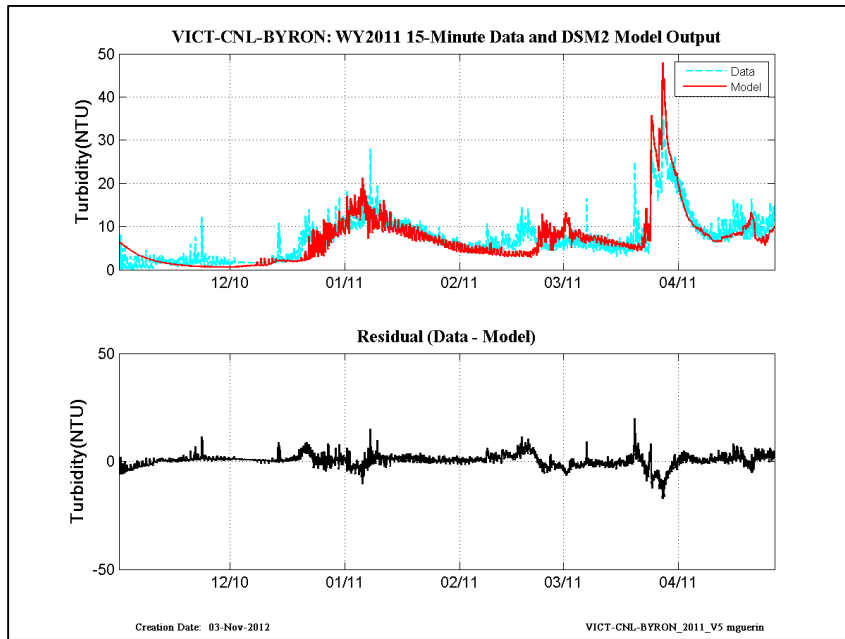


Figure 14-29 WY2011 15-min revised calibration results at Victoria Canal-at-Byron.

14.2 Fifteen minute CDEC data and model output – WY2010

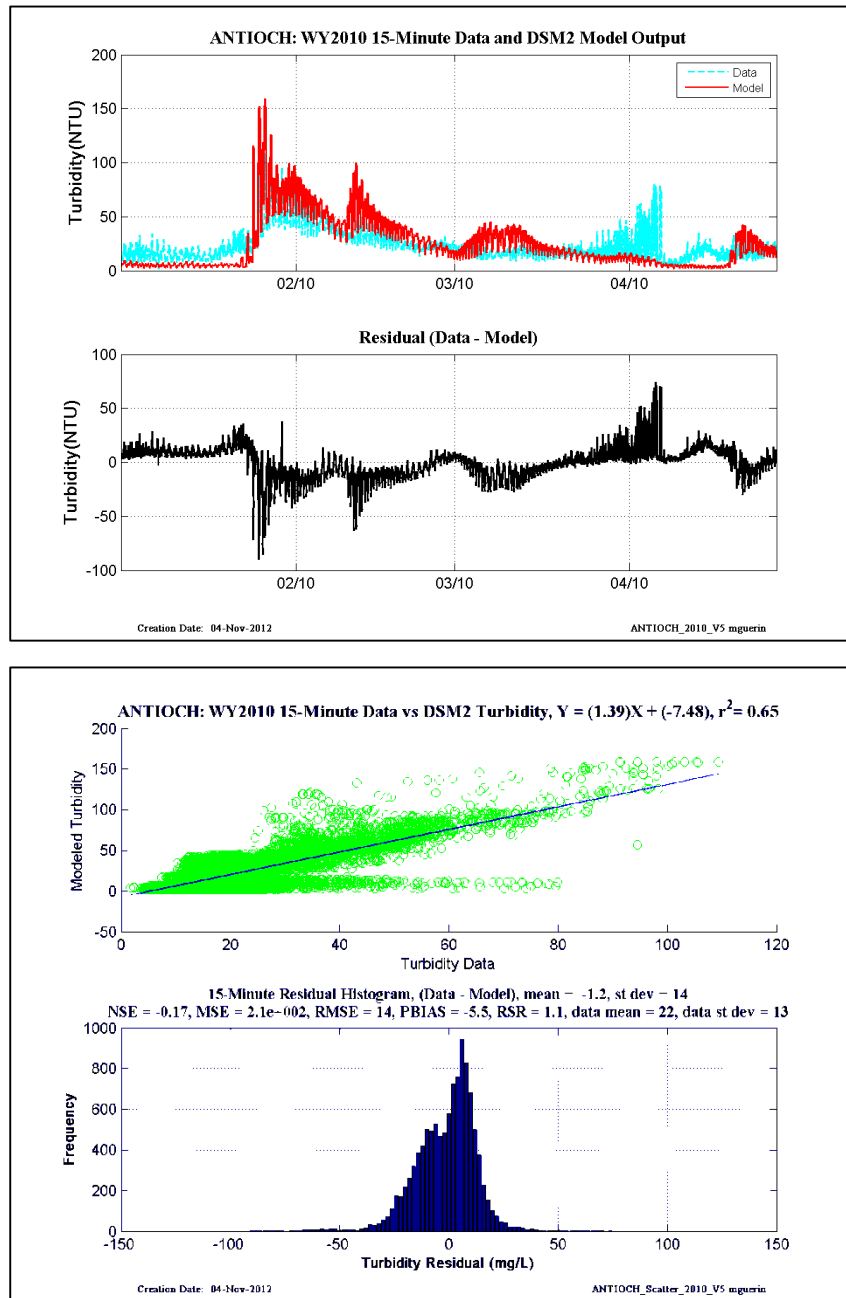


Figure 14-30 WY2010 15-min revised calibration results at Antioch.

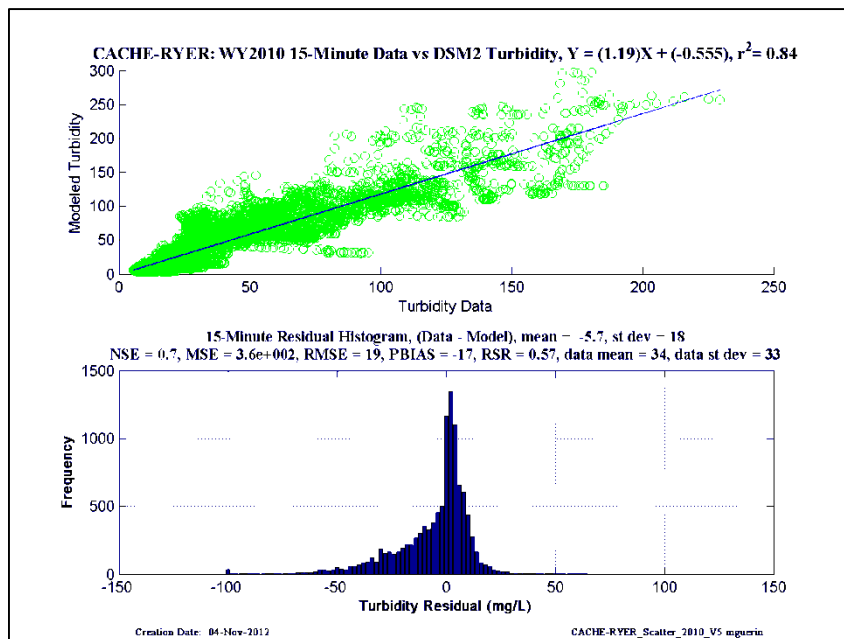
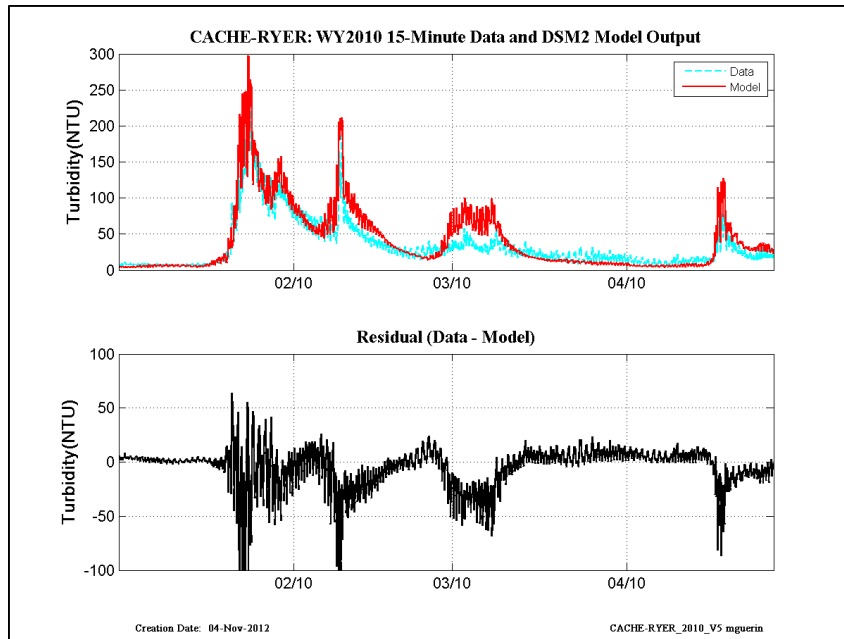


Figure 14-31 WY2010 15-min revised calibration results at Cache-at-Ryer Island.

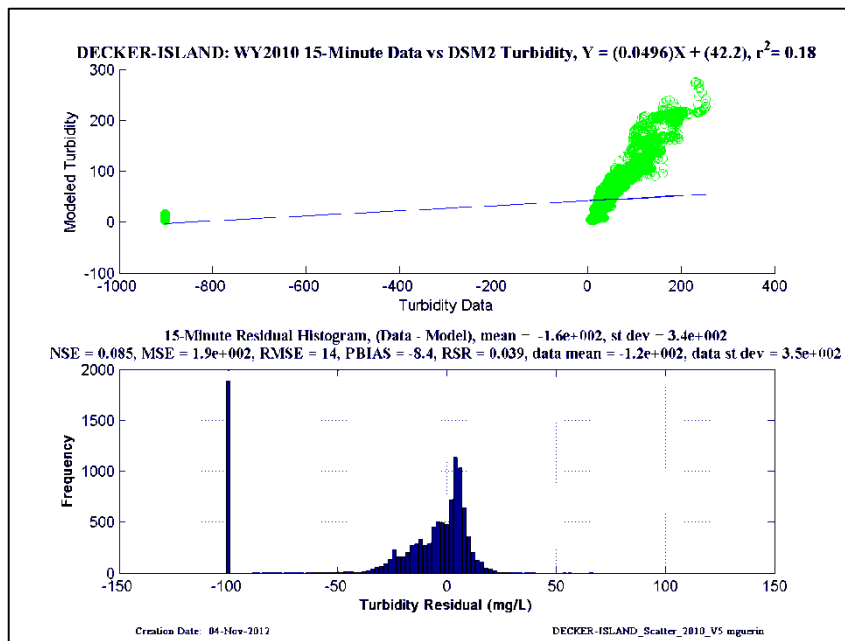
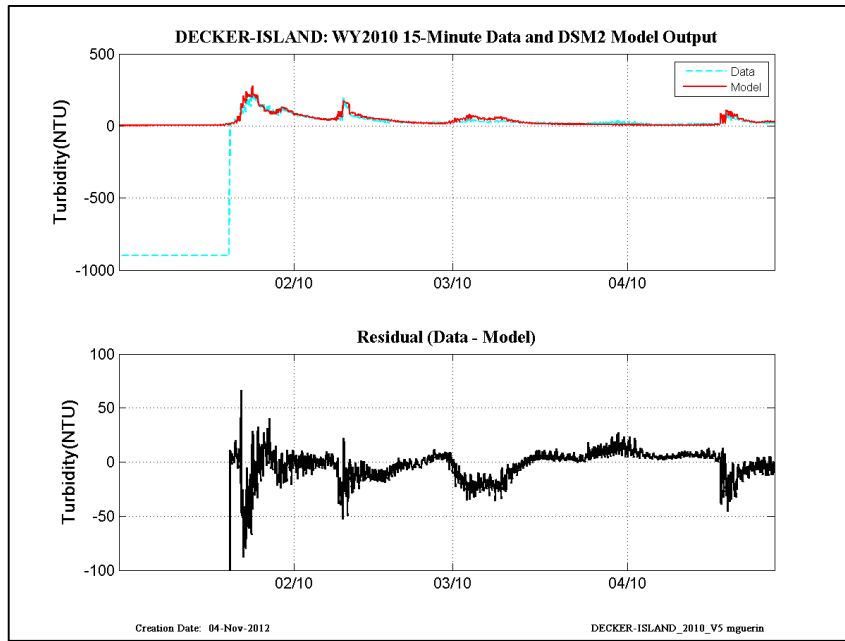


Figure 14-32 WY2010 15-min revised calibration results at Decker Island.

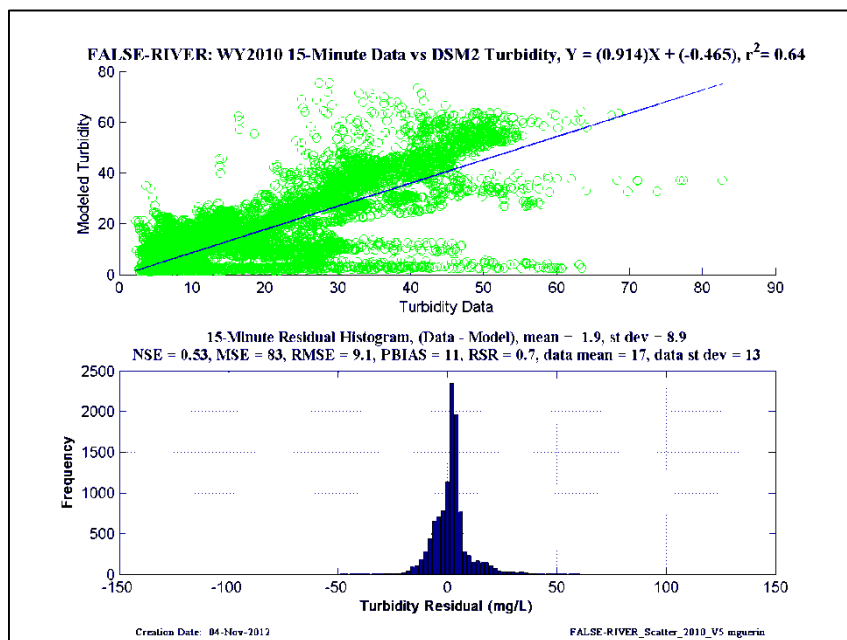
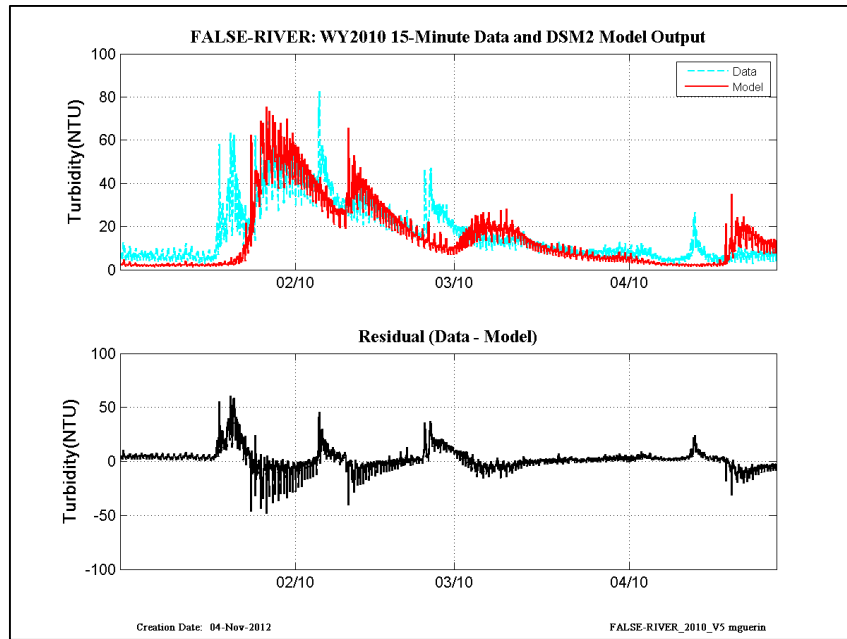


Figure 14-33 WY2010 15-min revised calibration results at False River.

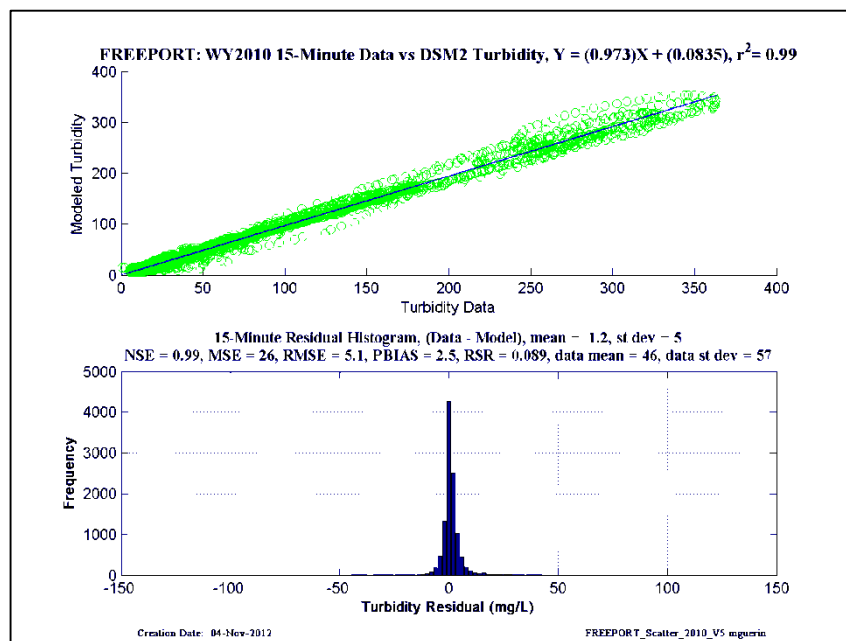
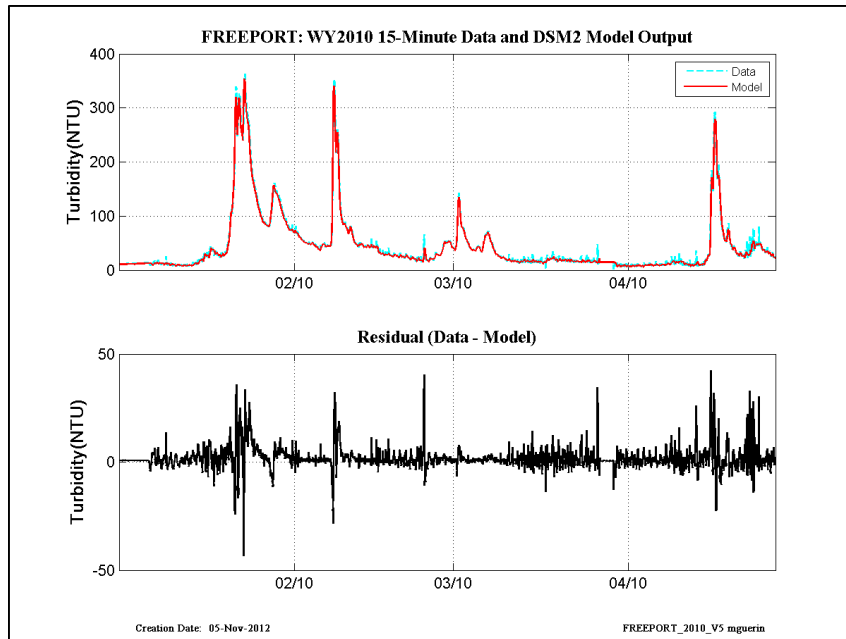


Figure 14-34 WY2010 15-min revised calibration results at Freeport.

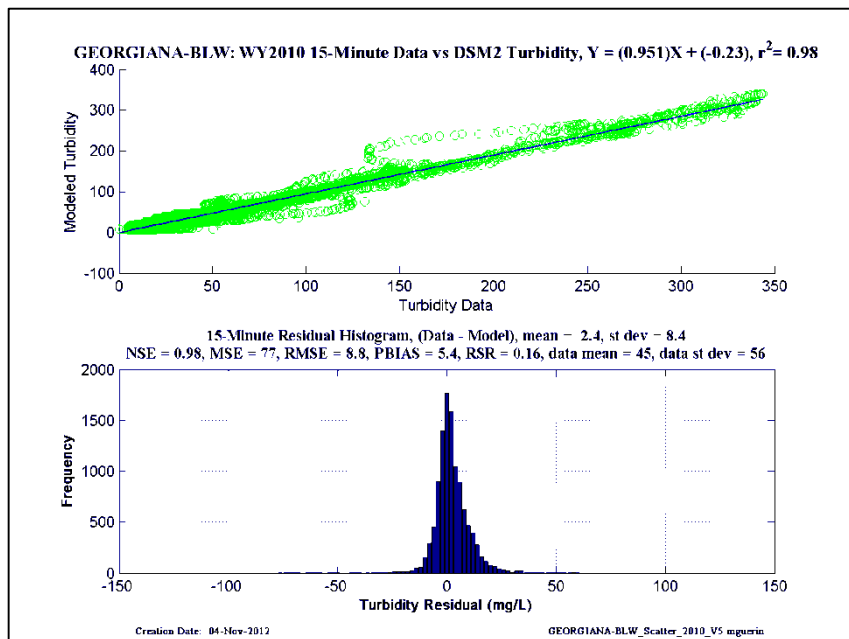
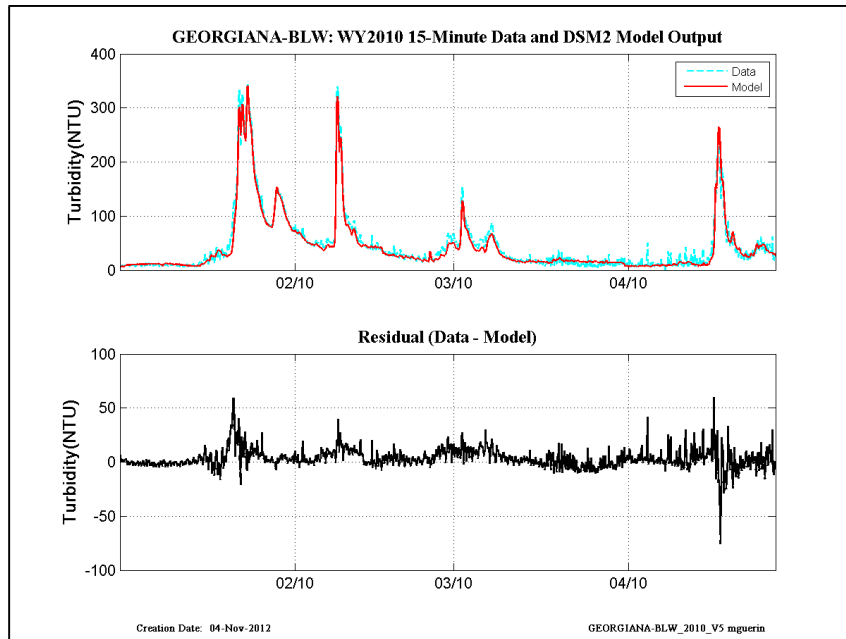


Figure 14-35 WY2010 15-min revised calibration results at Georgiana-Below-Sac.

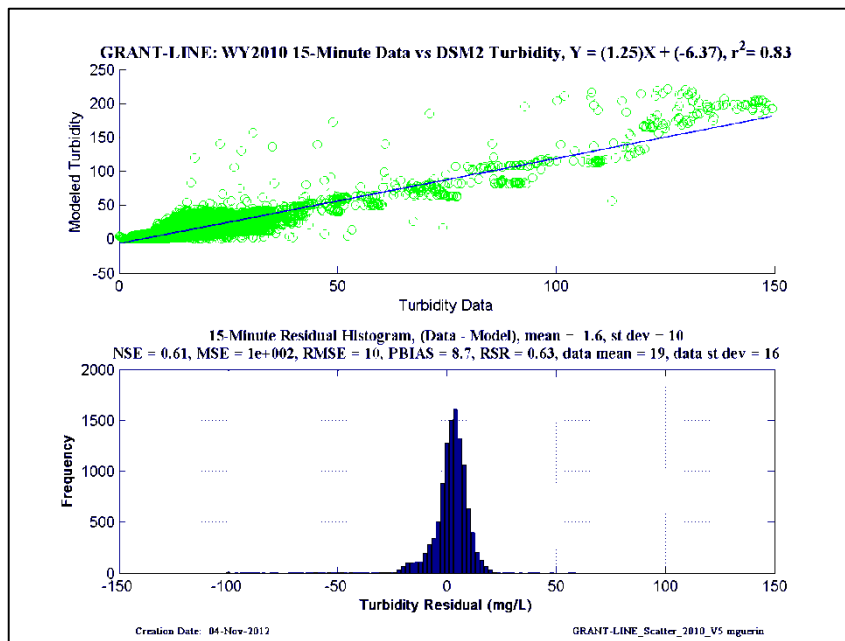
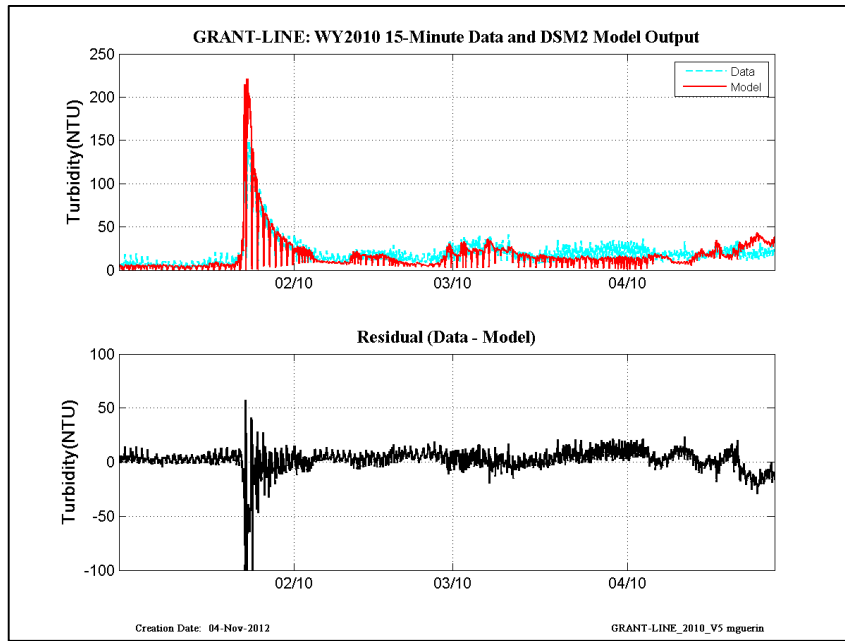


Figure 14-36 WY2010 15-min revised calibration results at Grant Line.

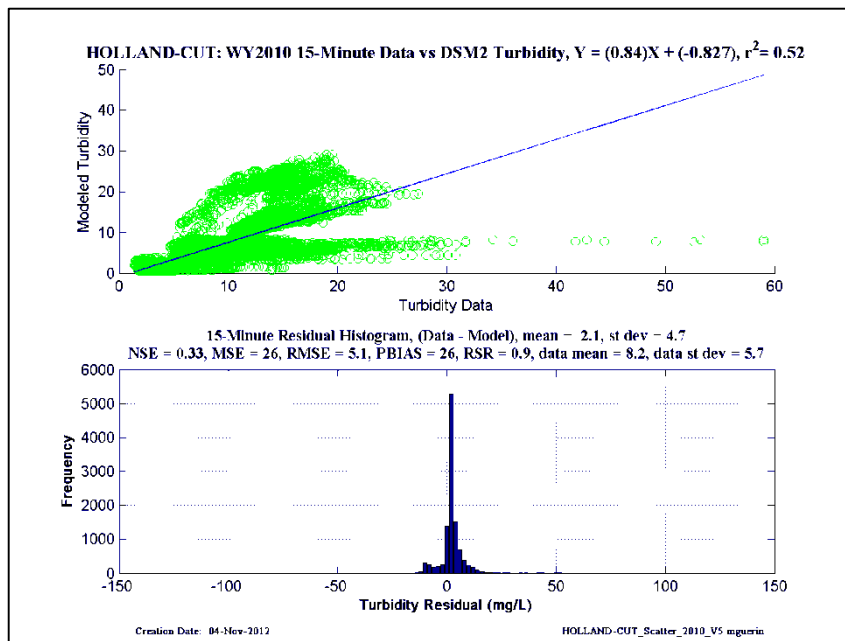
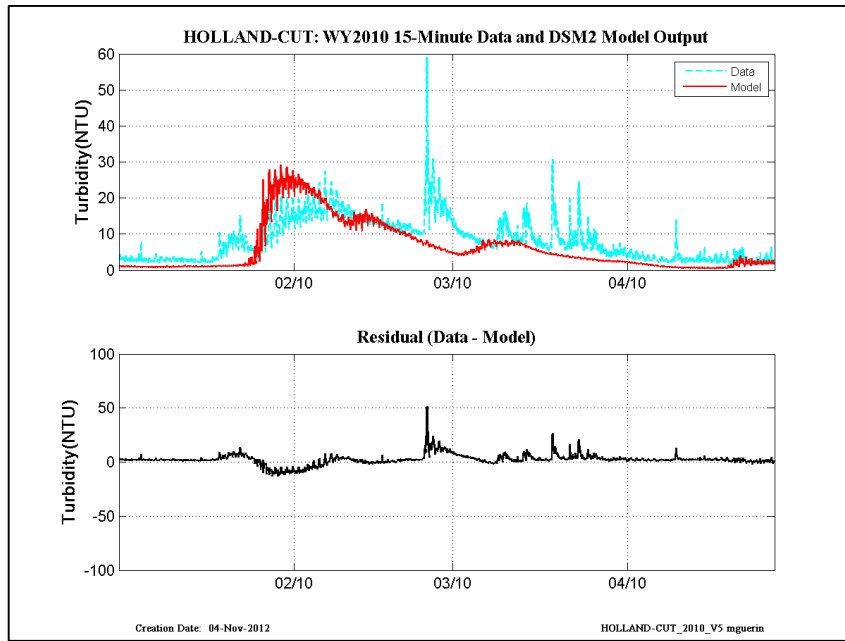


Figure 14-37 WY2010 15-min revised calibration results at Holland Cut.

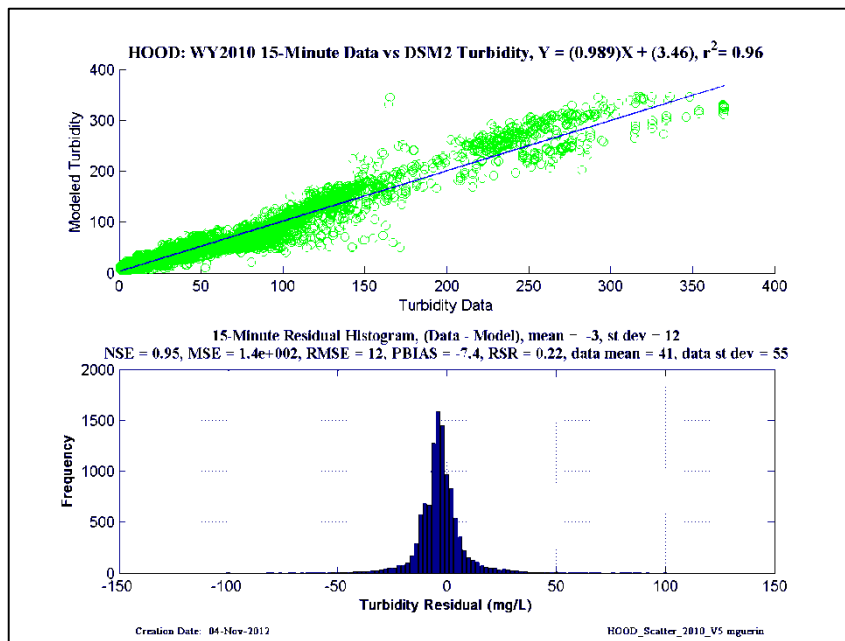
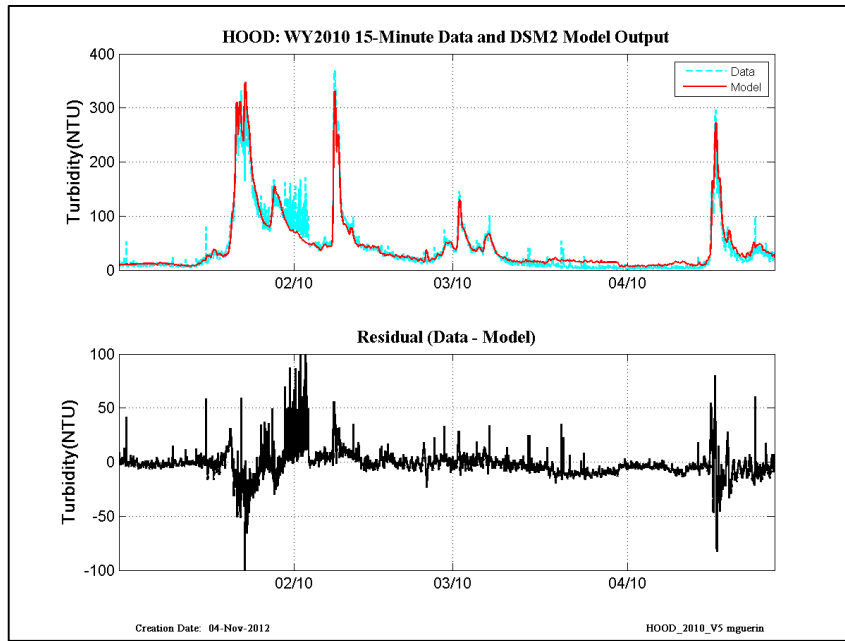


Figure 14-38 WY2010 15-min revised calibration results at Hood.

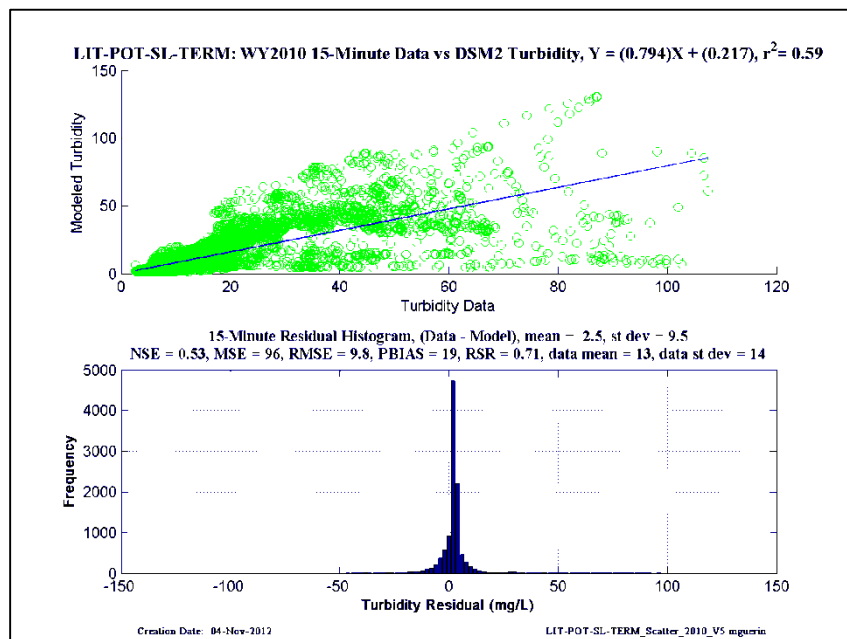
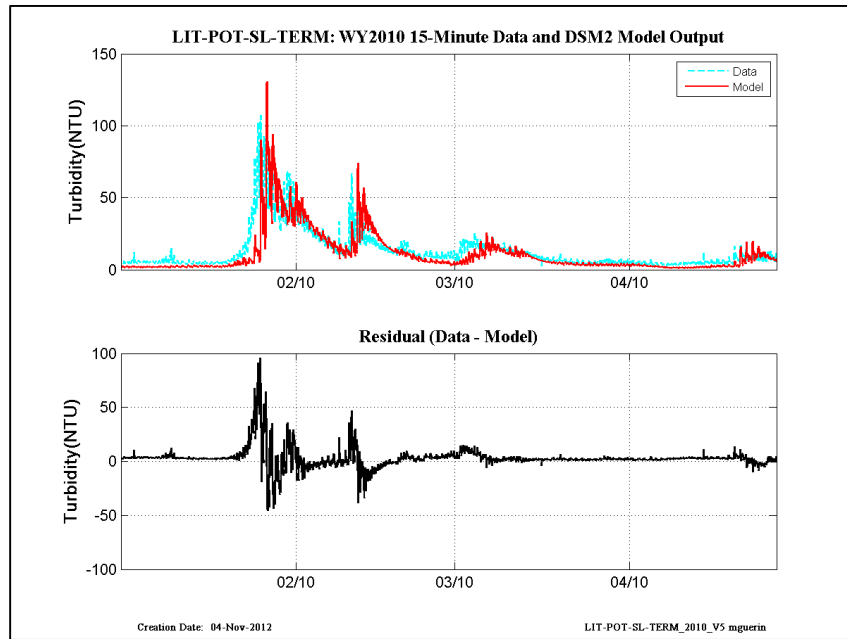


Figure 14-39 WY2010 15-min revised calibration results at Little Potato Slough-at-Terminus.

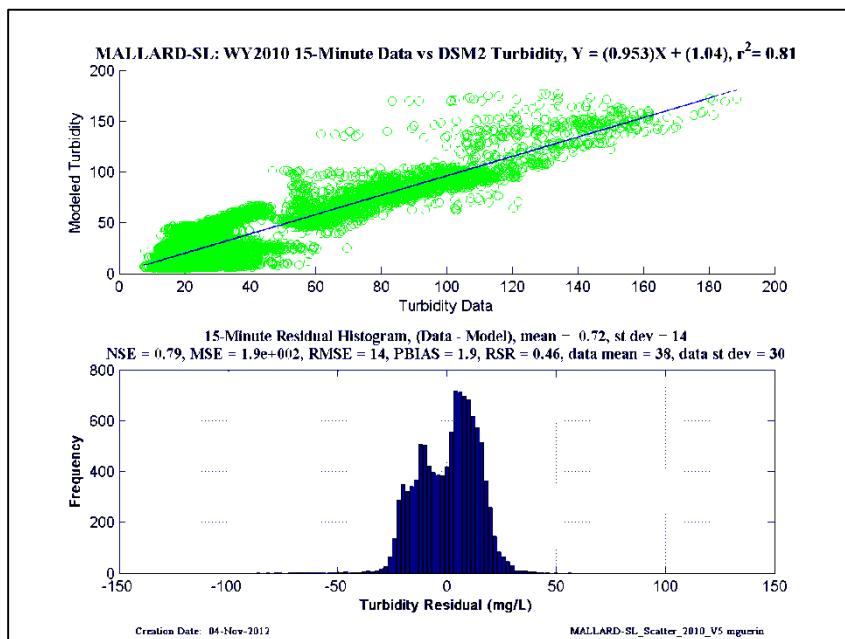
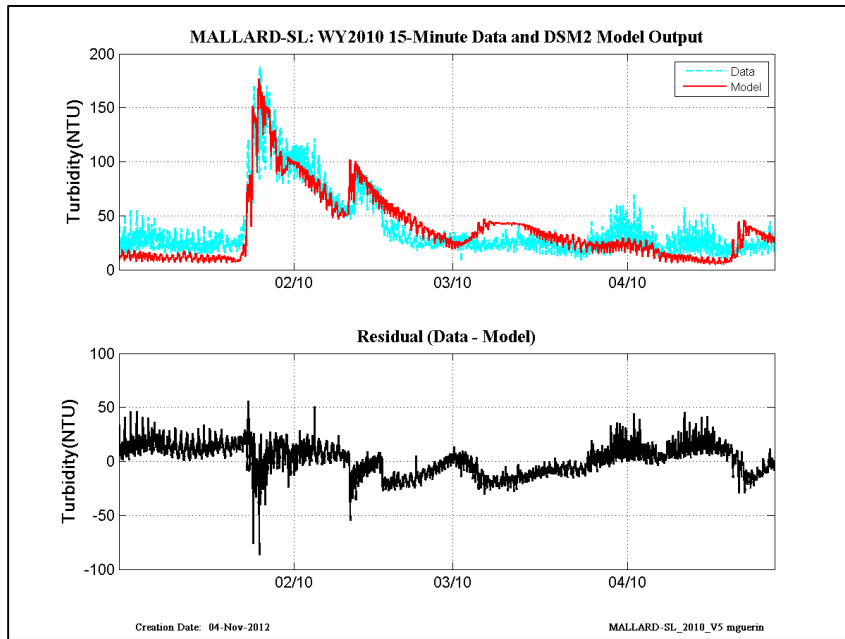


Figure 14-40 WY2010 15-min revised calibration results at Mallard Slough.

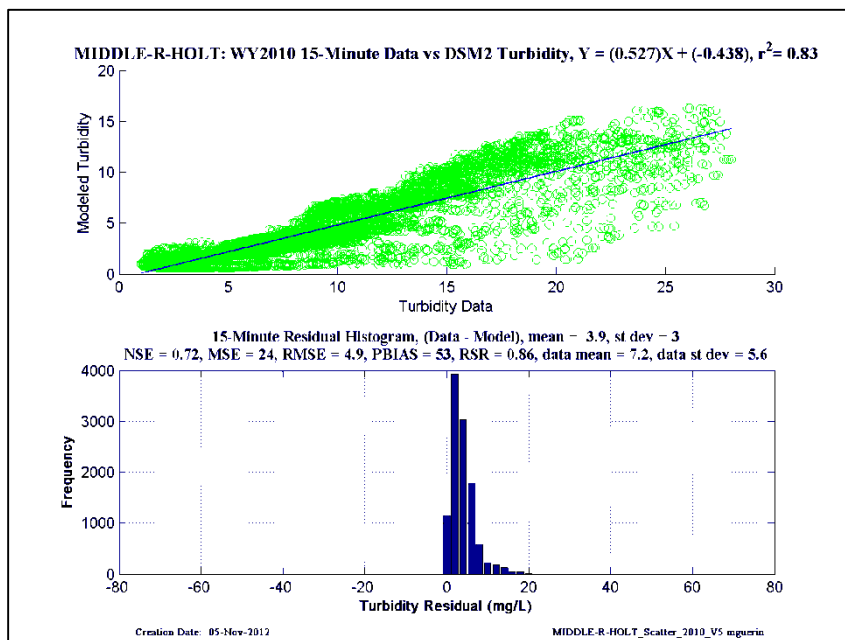
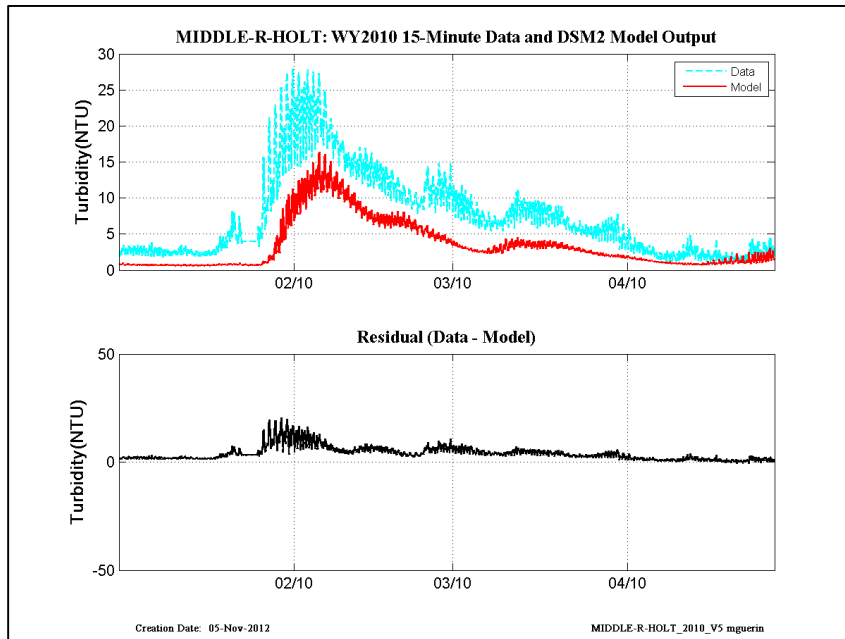


Figure 14-41 WY2010 15-min revised calibration results at Middle River-at-Holt.

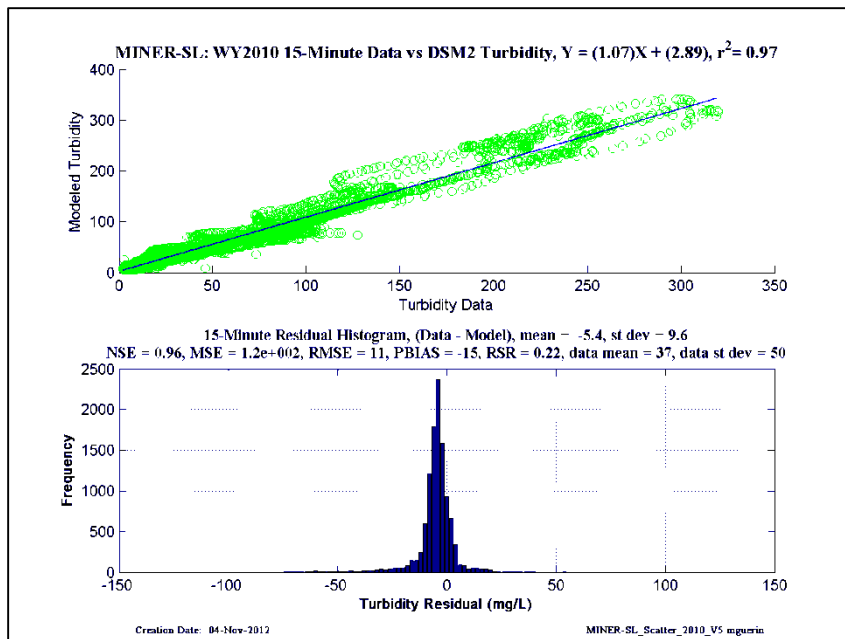
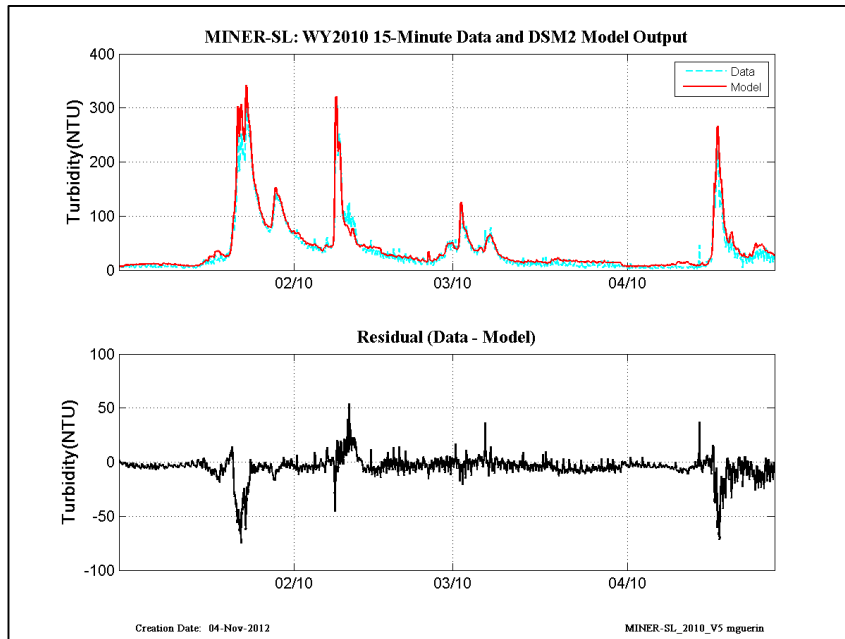


Figure 14-42 WY2010 15-min revised calibration results at Miner Slough.

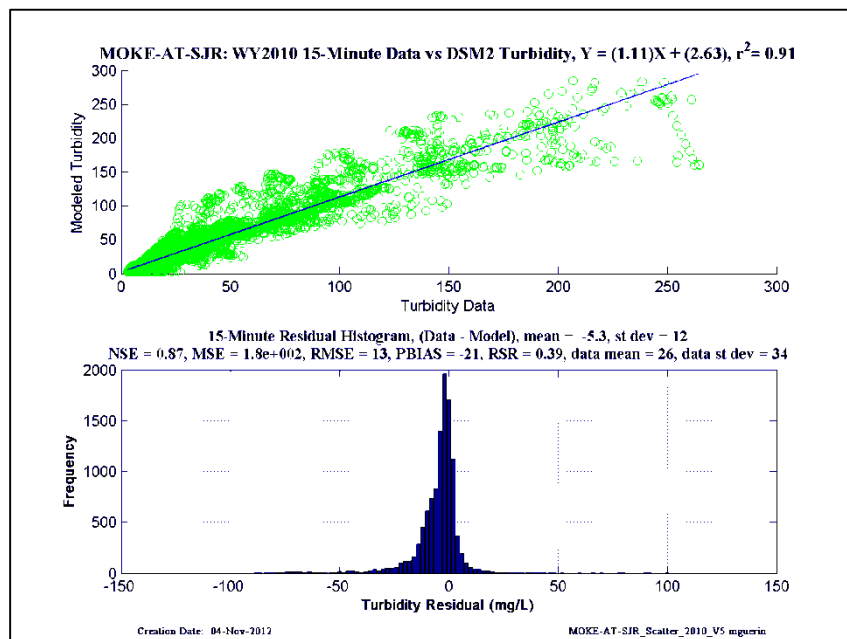
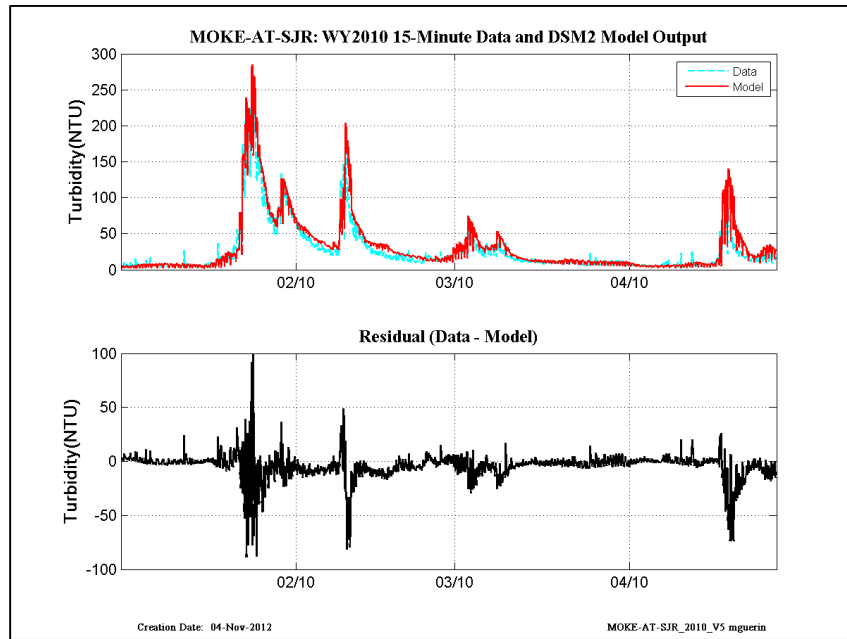


Figure 14-43 WY2010 15-min revised calibration results at Mokelumne-at-San Joaquin.

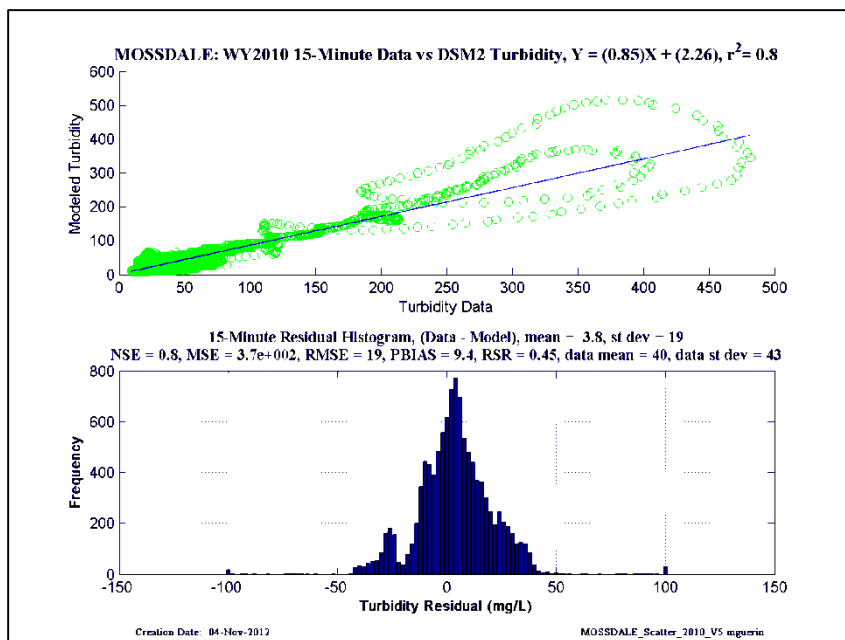
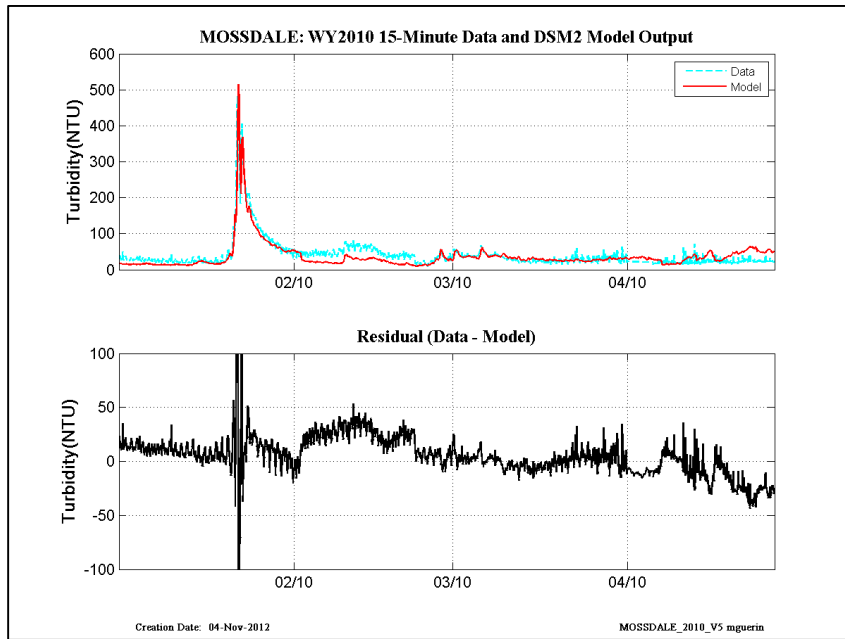


Figure 14-44 WY2010 15-min revised calibration results at Mossdale.

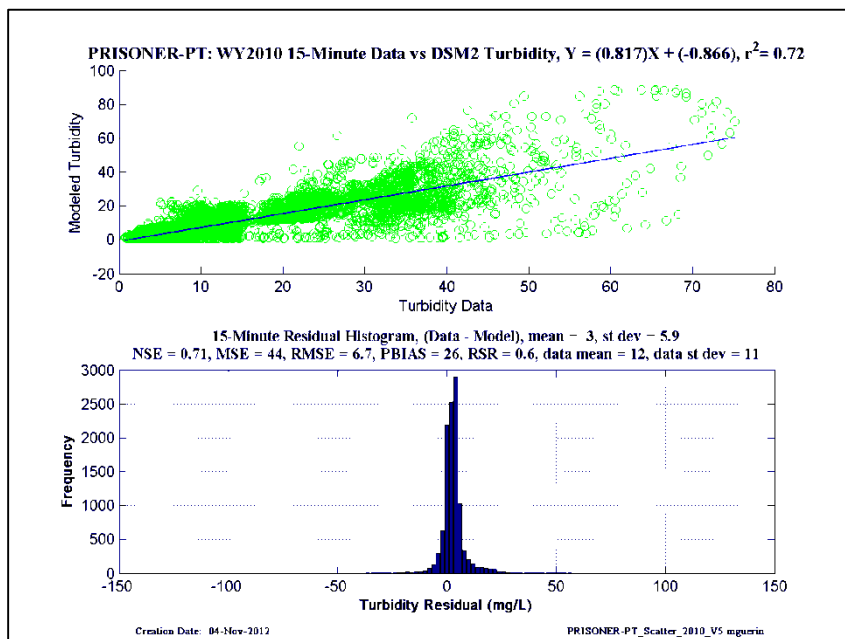
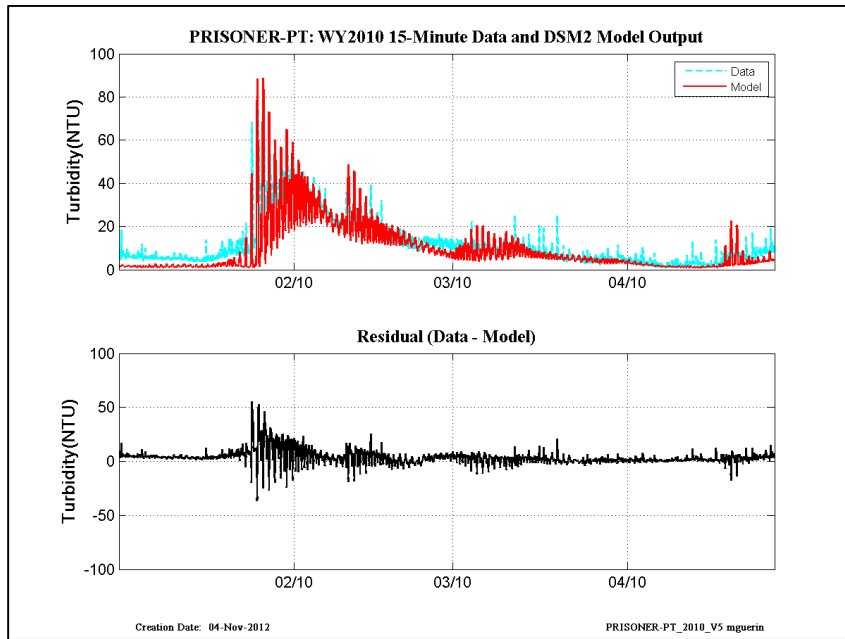


Figure 14-45 WY2010 15-min revised calibration results at Prisoner Point.

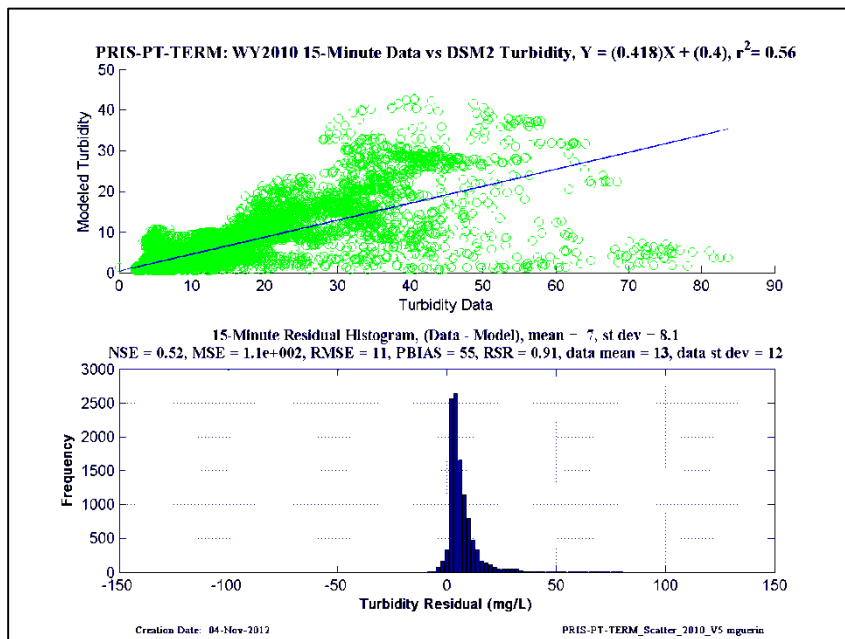
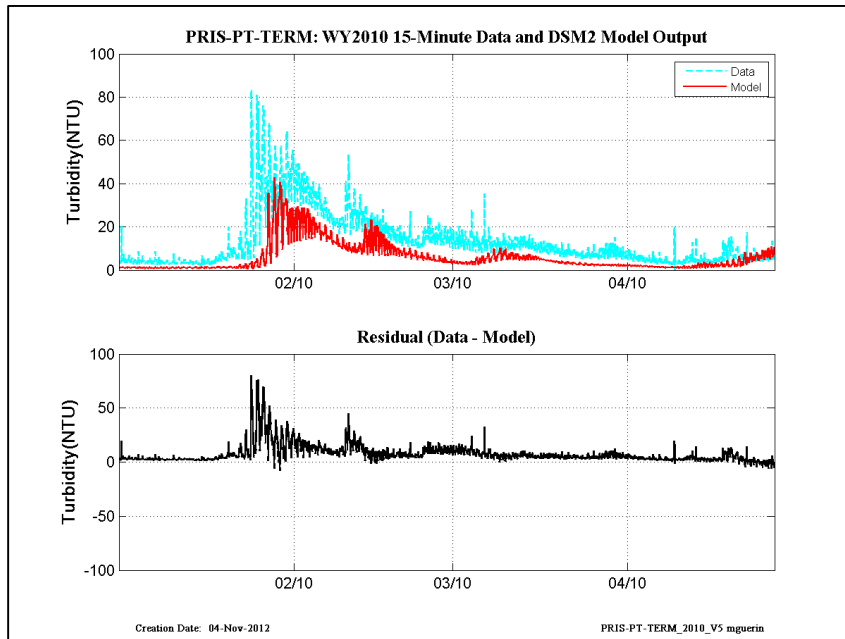


Figure 14-46 WY2010 15-min revised calibration results at Prisoner Point-at-Terminus.

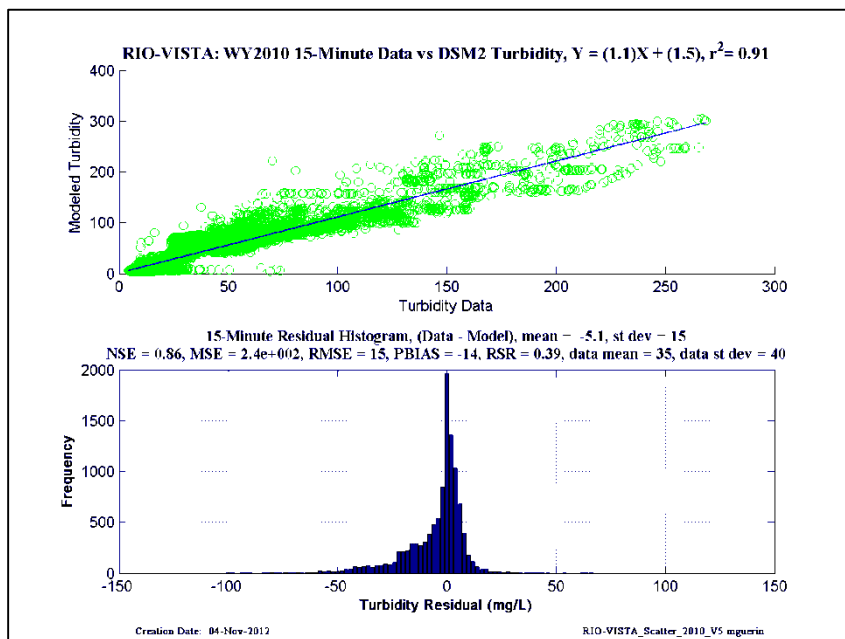
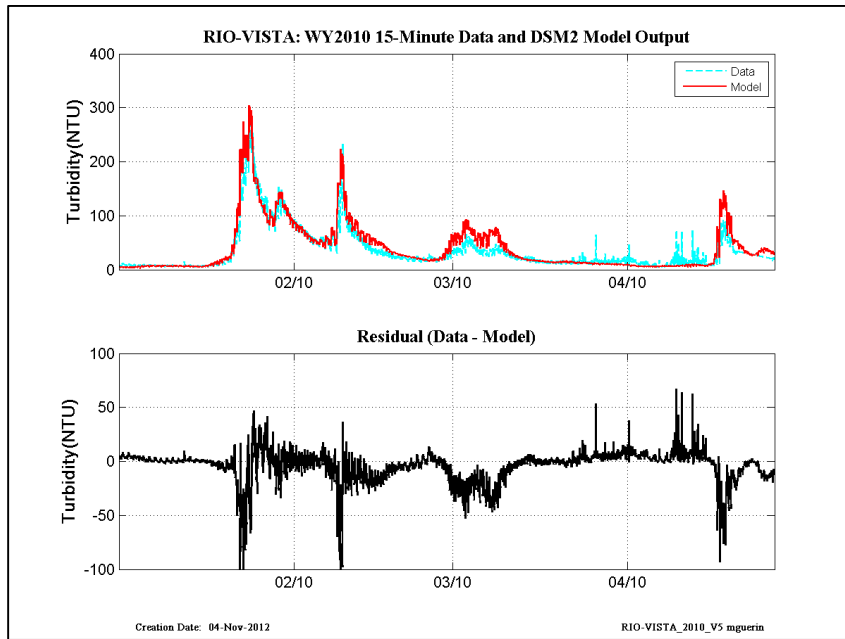


Figure 14-47 WY2010 15-min revised calibration results at Rio Vista.

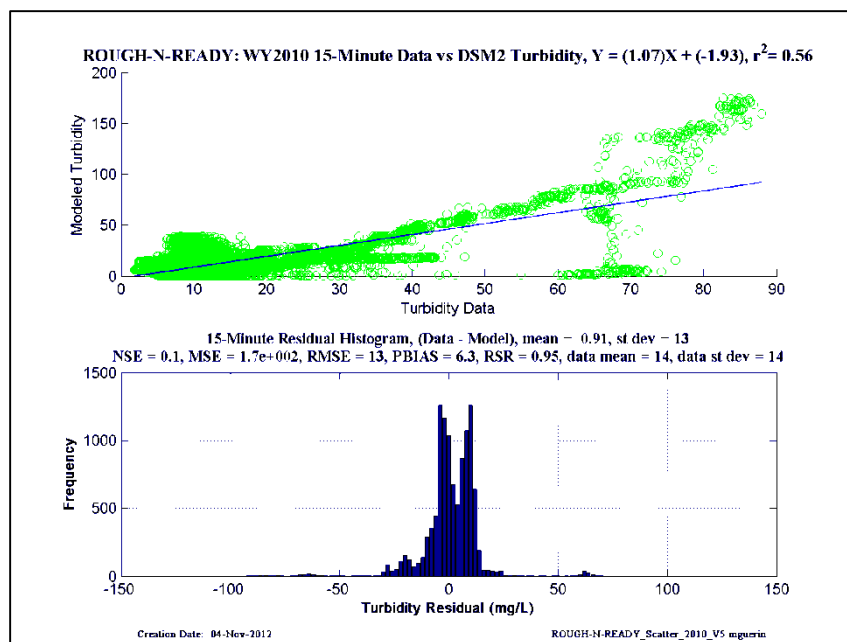
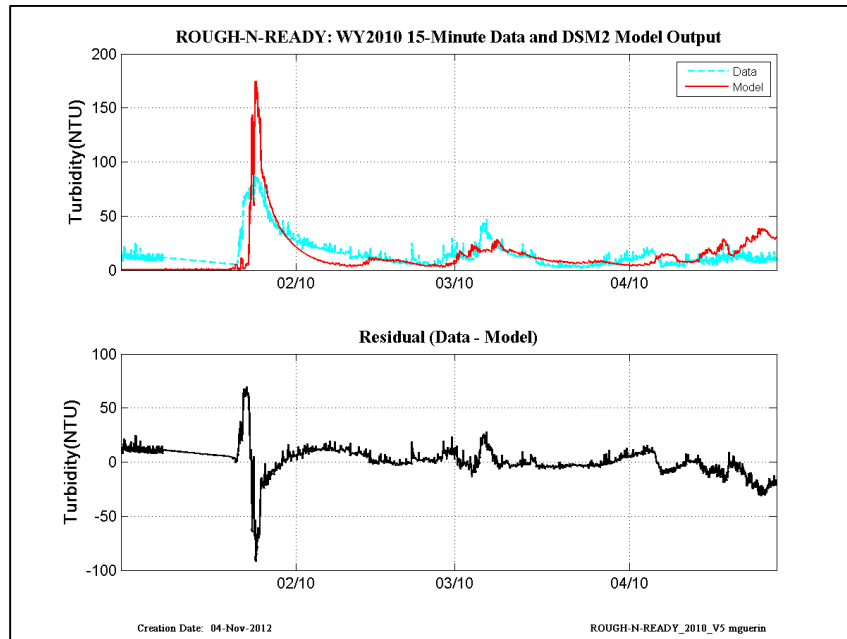


Figure 14-48 WY2010 15-min revised calibration results at Rough-N-Ready Island.

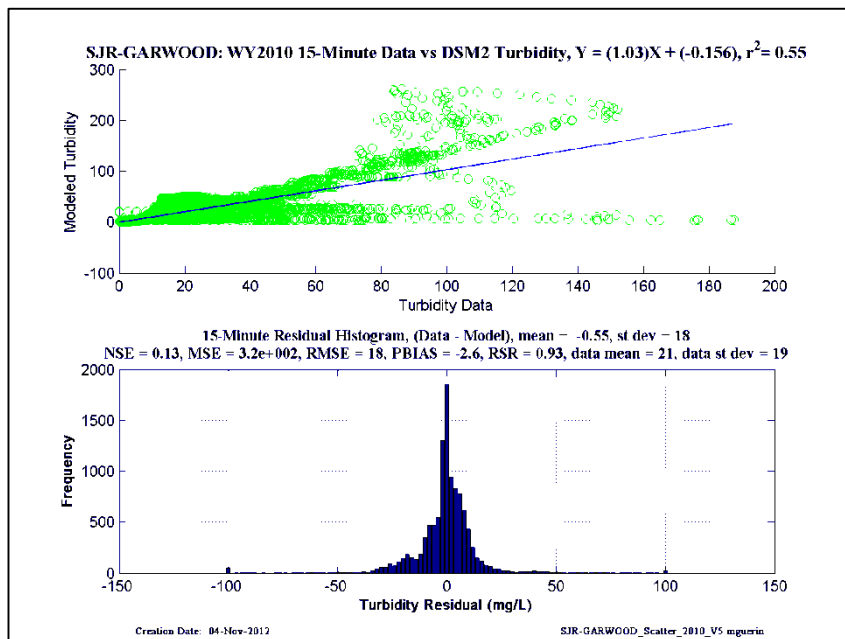
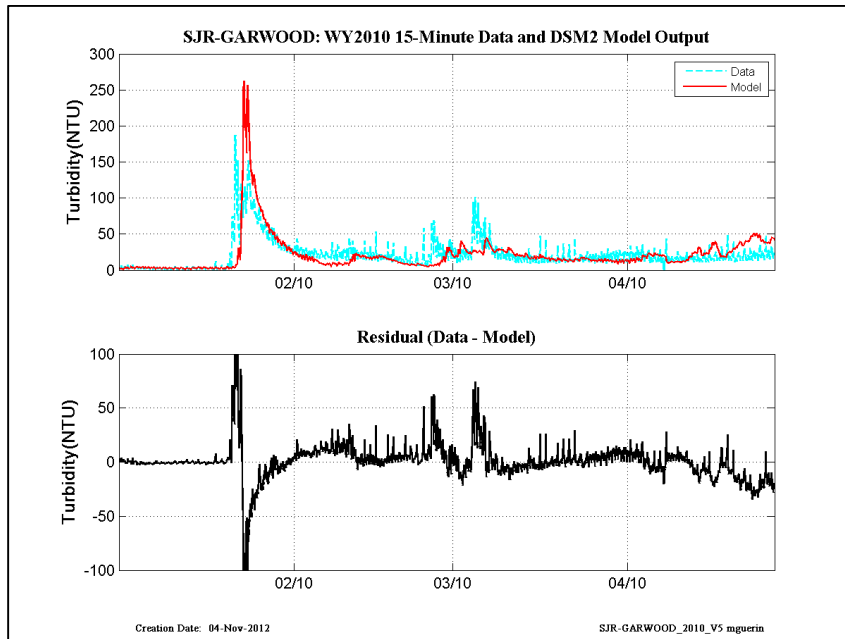


Figure 14-49 WY2010 15-min revised calibration results at San Joaquin-at-Garwood.

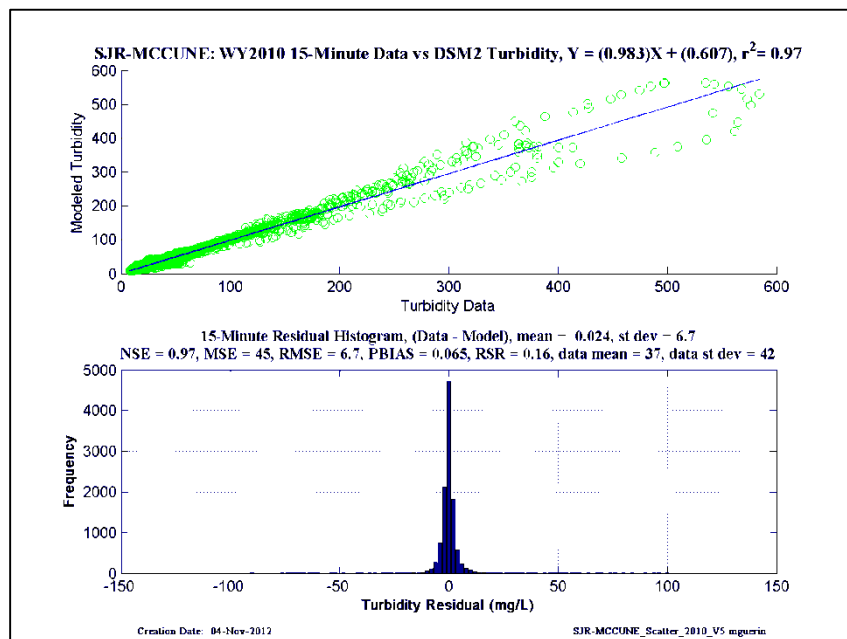
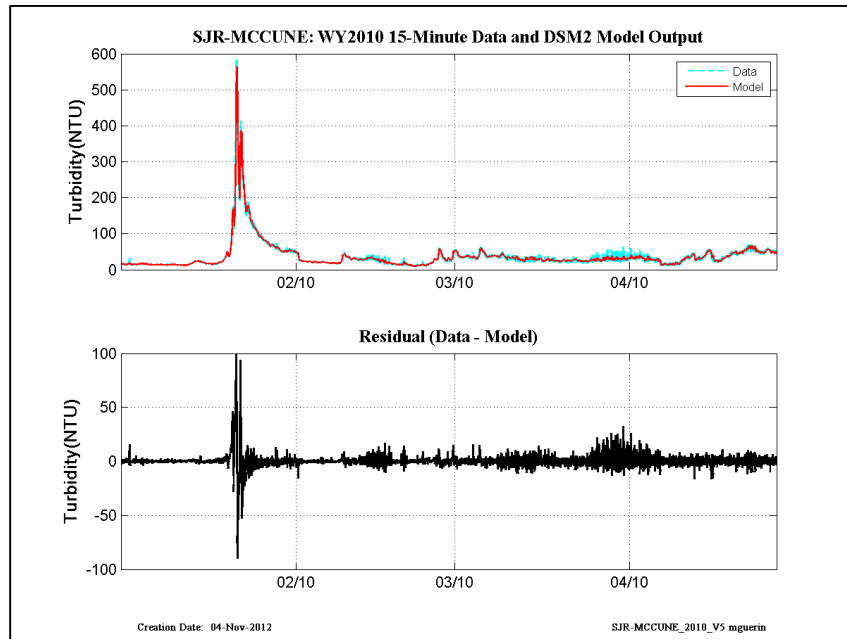


Figure 14-50 WY2010 15-min revised calibration results at San Joaquin-at-McCune (Vernalis).

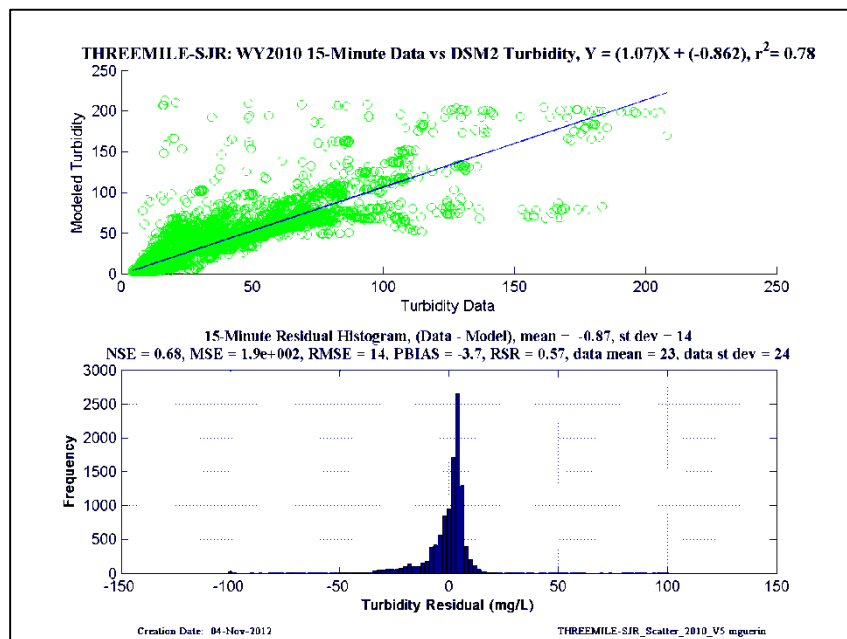
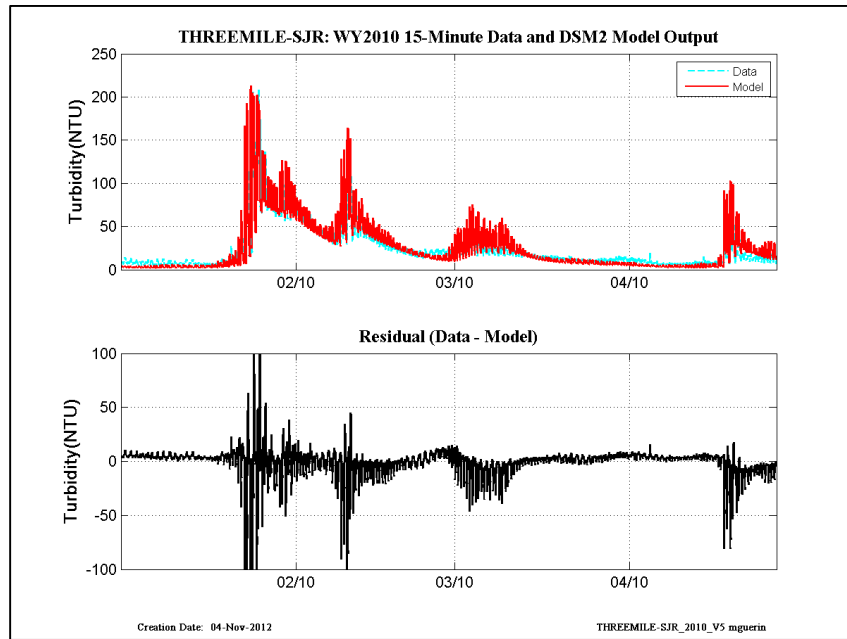


Figure 14-51 WY2010 15-min revised calibration results at Threemile-Slough-at-San Joaquin.

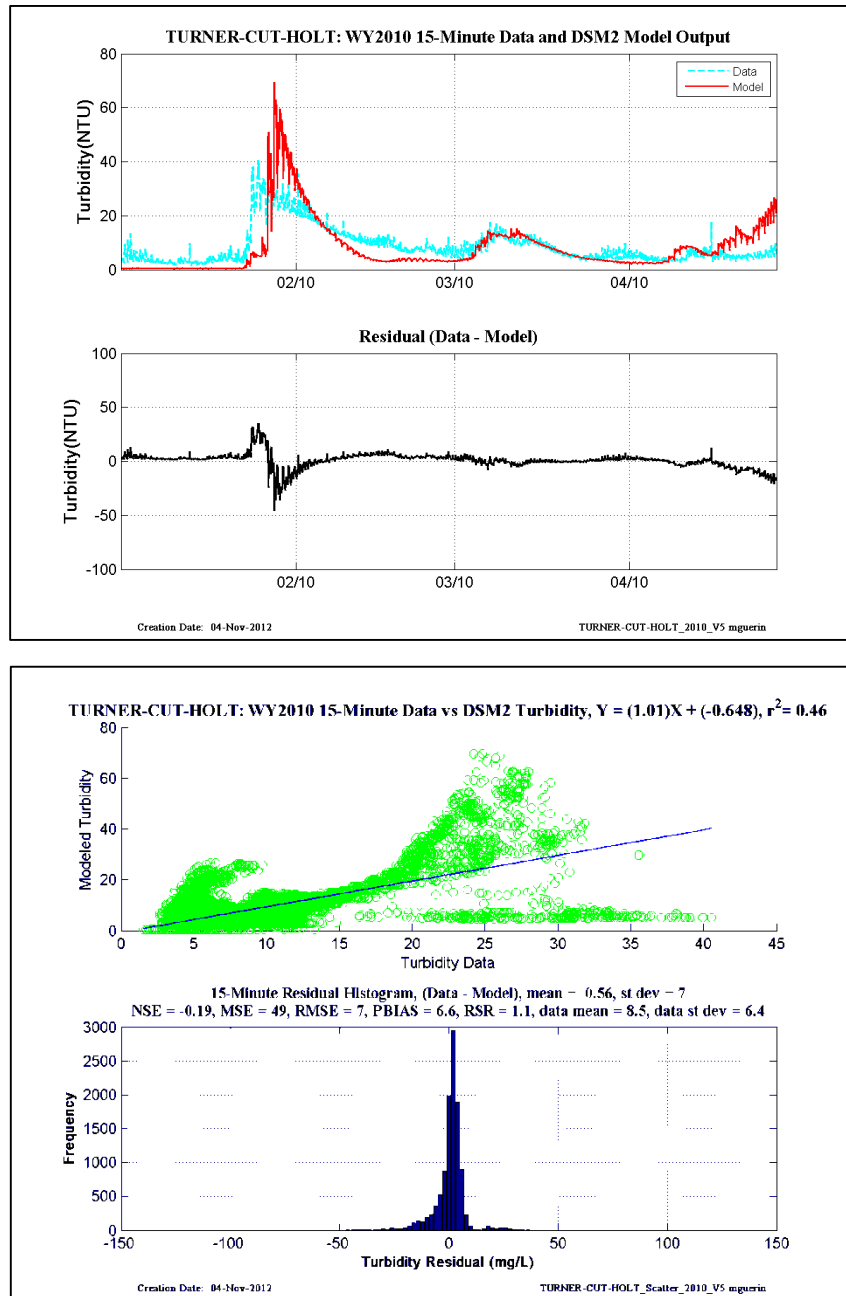


Figure 14-52 WY2010 15-min revised calibration results at Turner Cut-at-Holt.

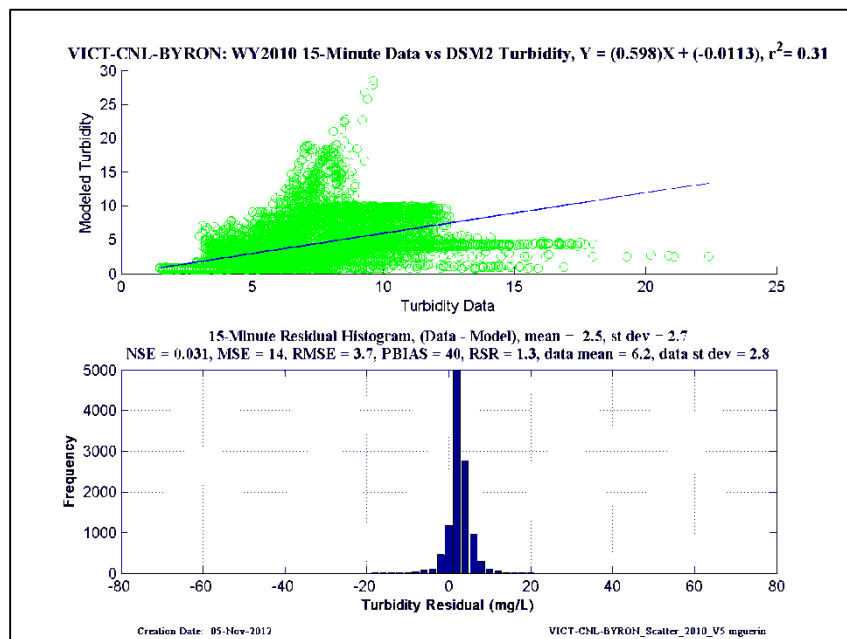
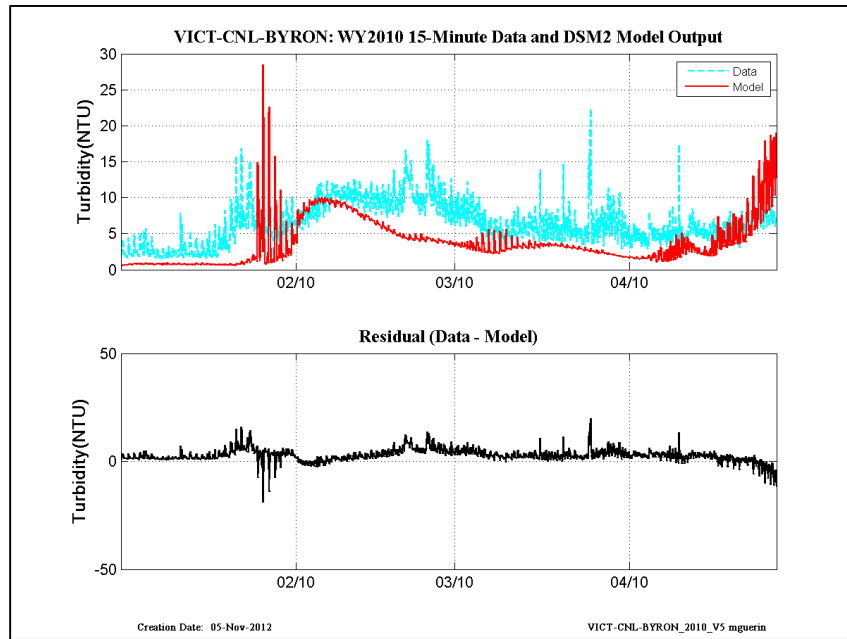


Figure 14-53 WY2010 15-min revised calibration results at Victoria Canal-at-Byron.

14 Appendix V – Figures and Statistics Documenting WY2010 and WY2011 with Mixed-SSC-WARMF and WARMF-Only Model Boundary Conditions

15.1 WY2010 Mixed-SSC-WARMF results

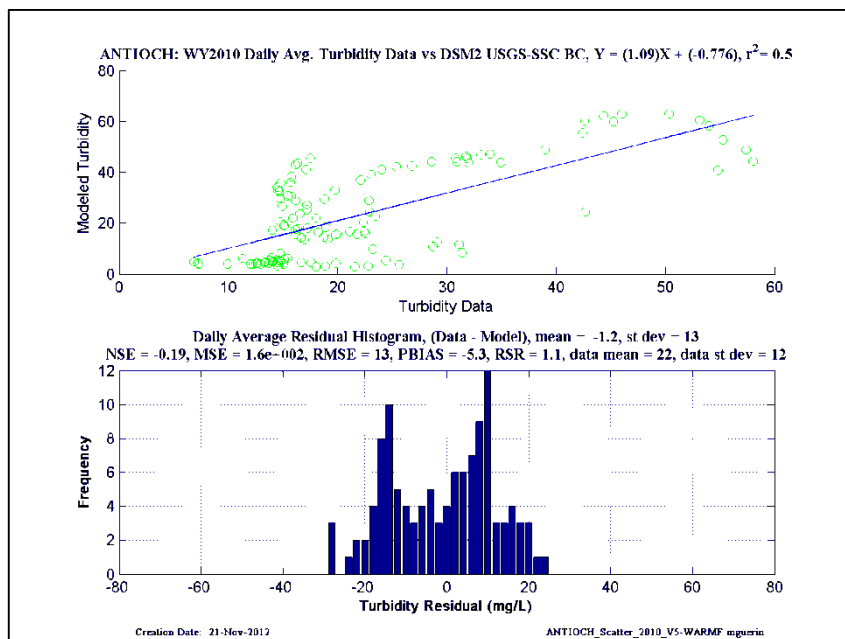
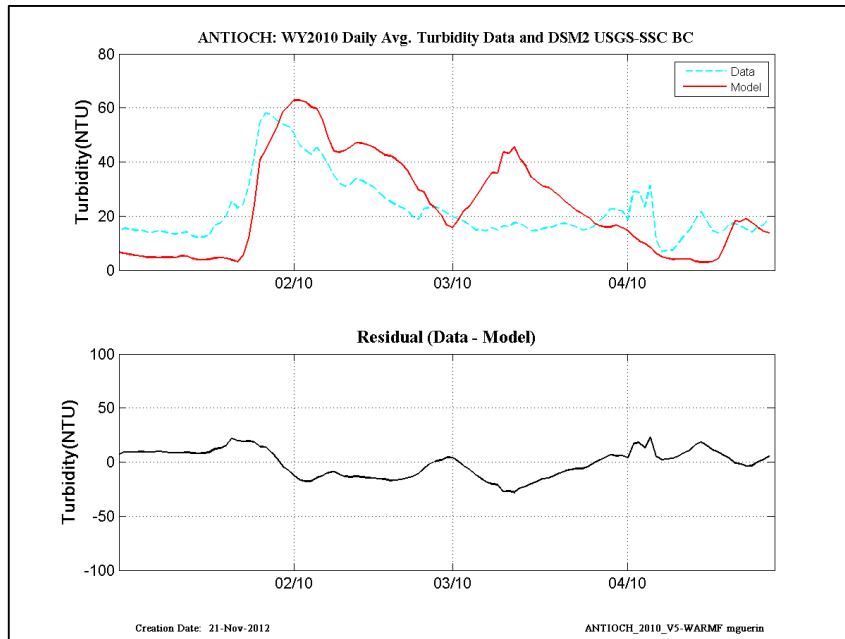


Figure 14-1 WY2010: WY2010: DSM2 daily-averaged turbidity model results using Mixed-SSC-WARMF turbidity at the inflow boundaries– location is Antioch.

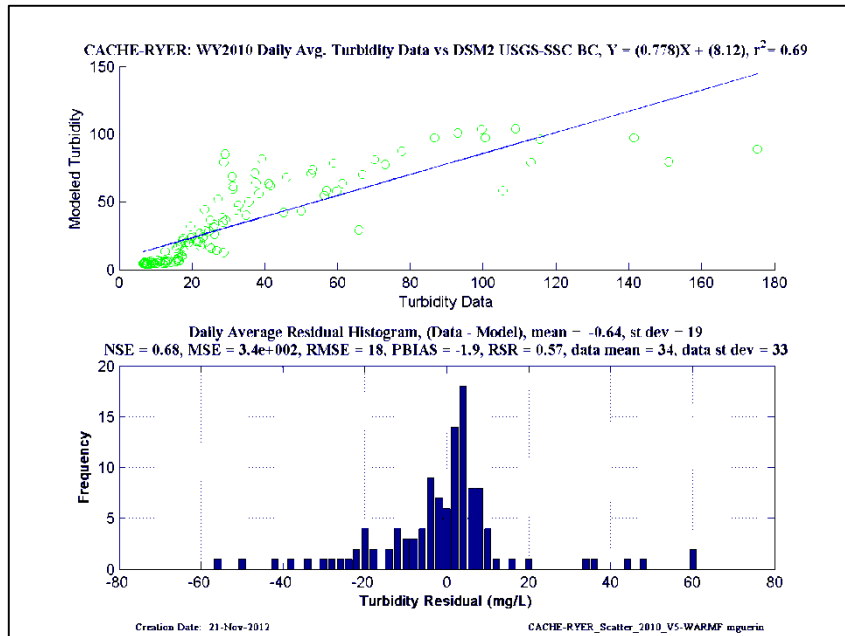
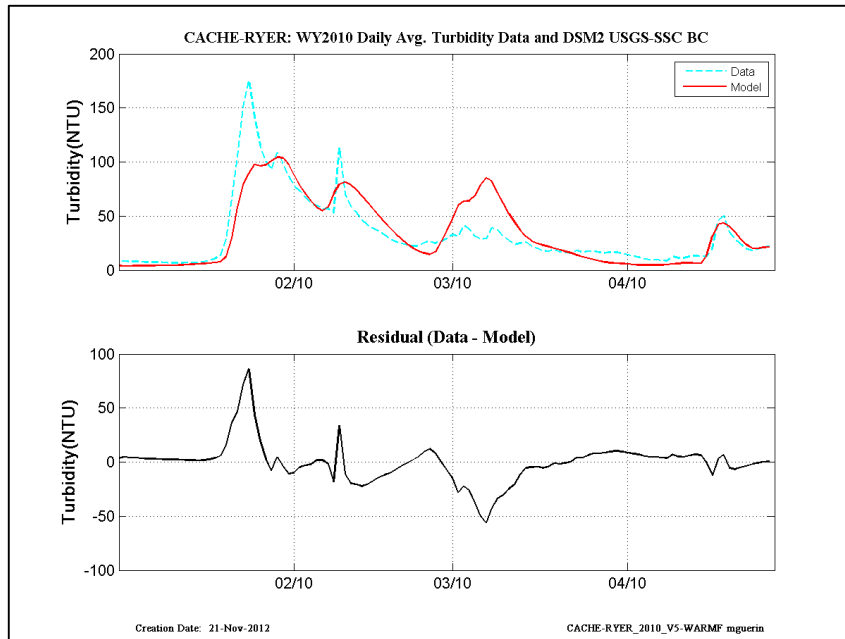


Figure 14-2 WY2010: WY2010: DSM2 daily-averaged turbidity model results using Mixed-SSC-WARMF turbidity at the inflow boundaries– location is Cache-at-Ryer.

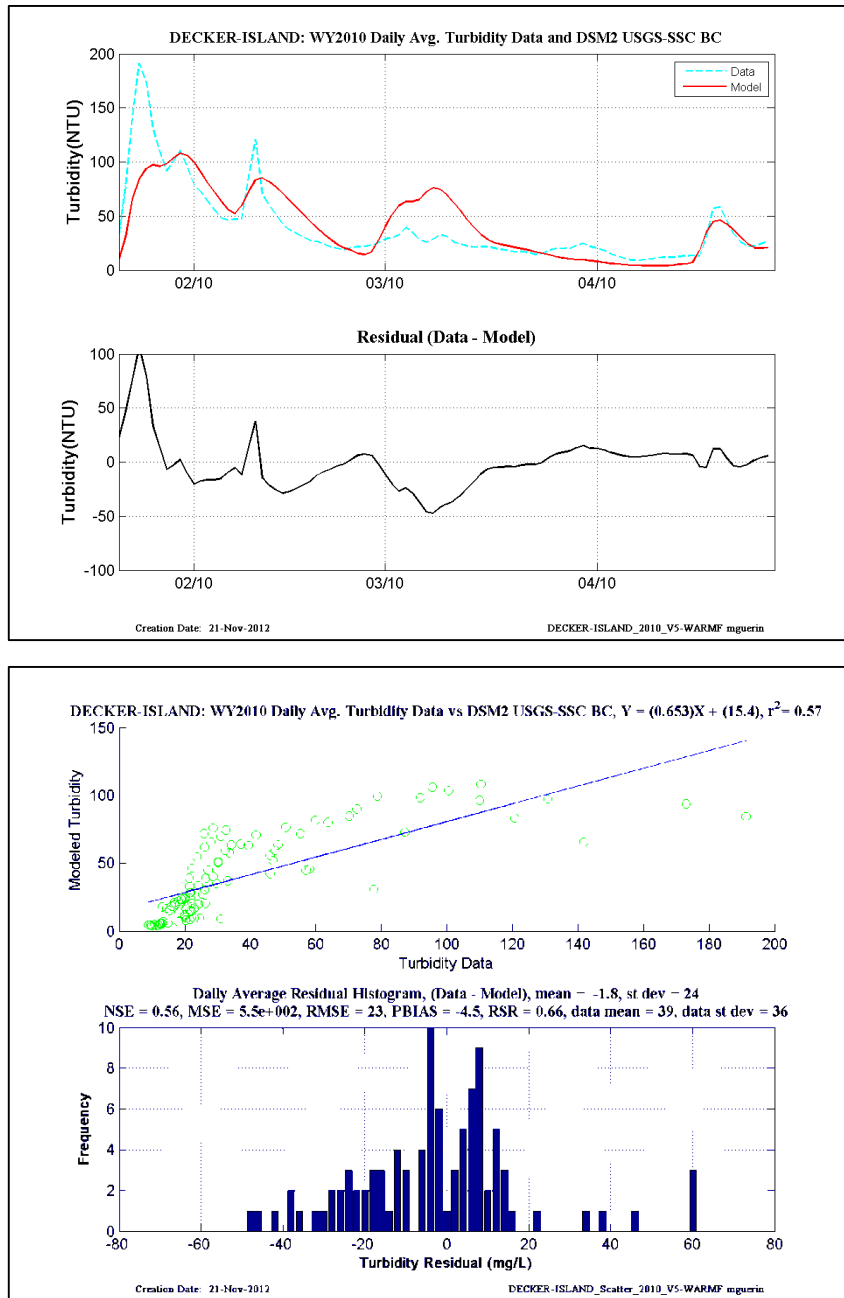


Figure 14-3 WY2010: WY2010: DSM2 daily-averaged turbidity model results using Mixed-SSC-WARMF turbidity at the inflow boundaries— location is Decker-Island.

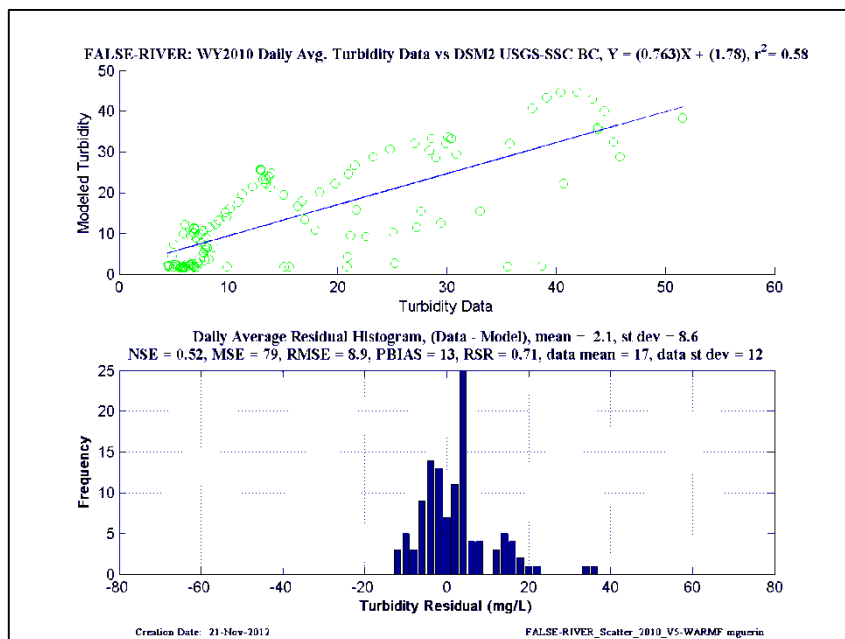
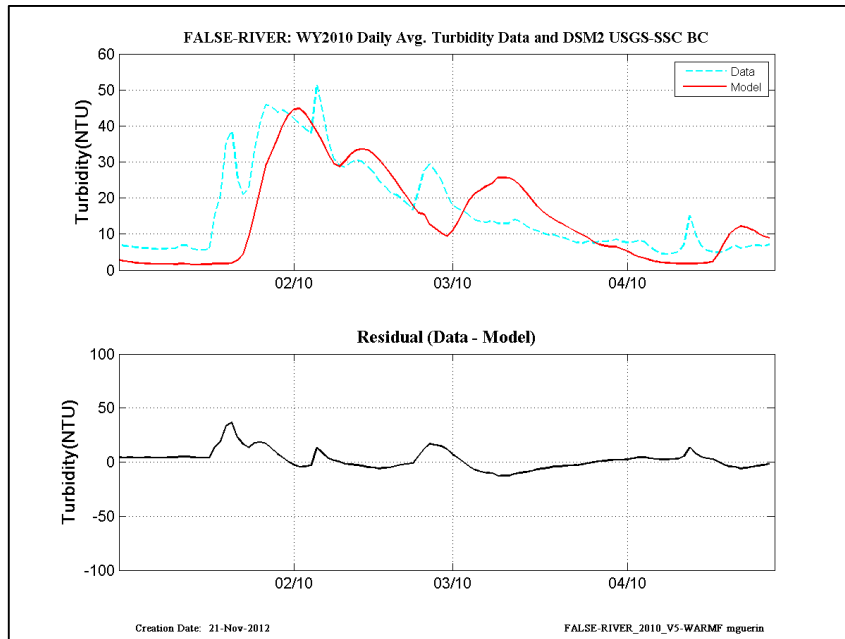


Figure 14-4WY2010: DSM2 daily-averaged turbidity model results using Mixed-SSC-WARMF turbidity at the inflow boundaries– location is False-River.

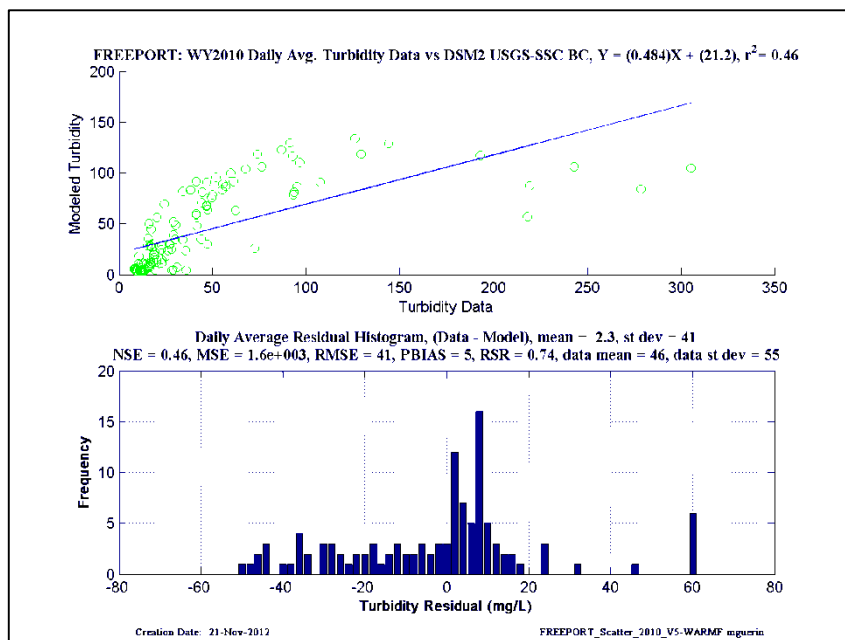
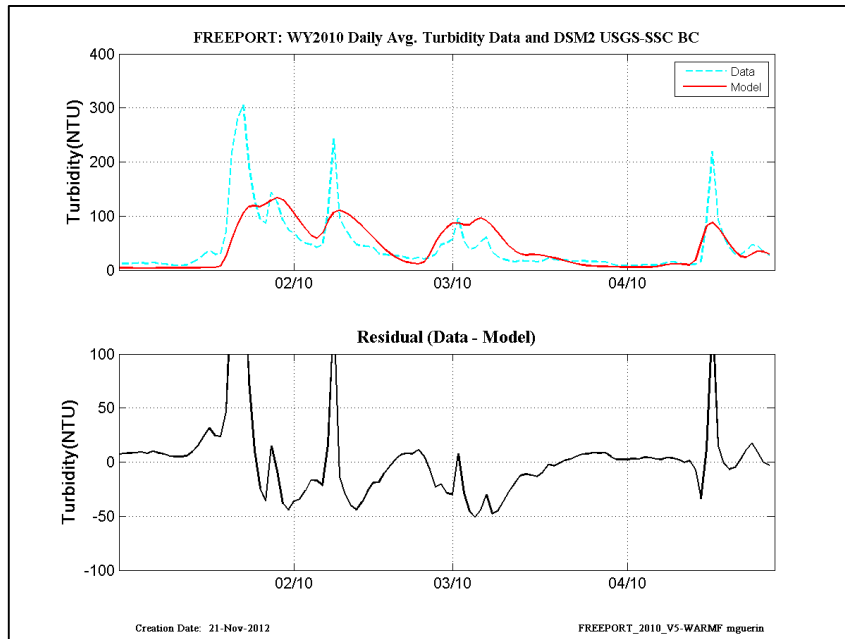


Figure 14-5WY2010: DSM2 daily-averaged turbidity model results using Mixed-SSC-WARMF turbidity at the inflow boundaries– location is Freeport.

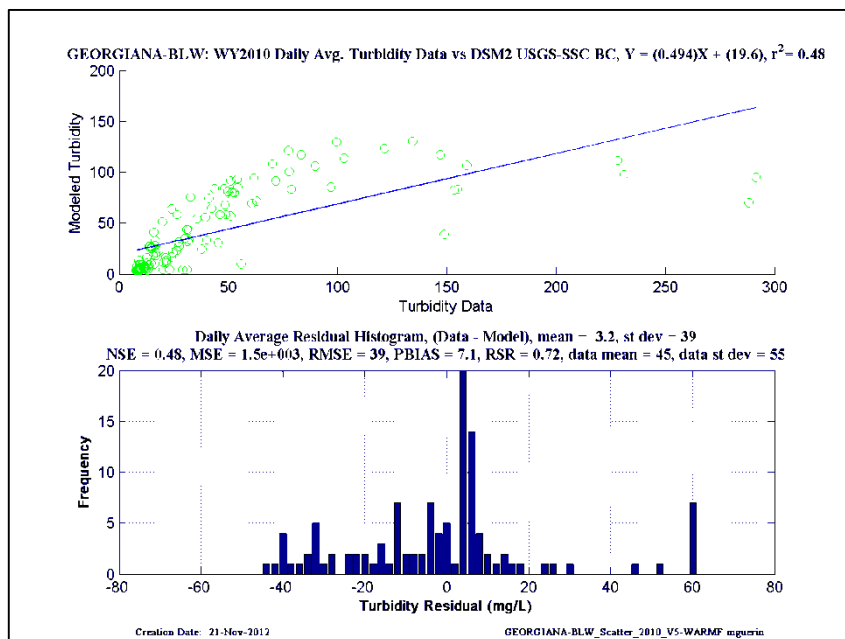
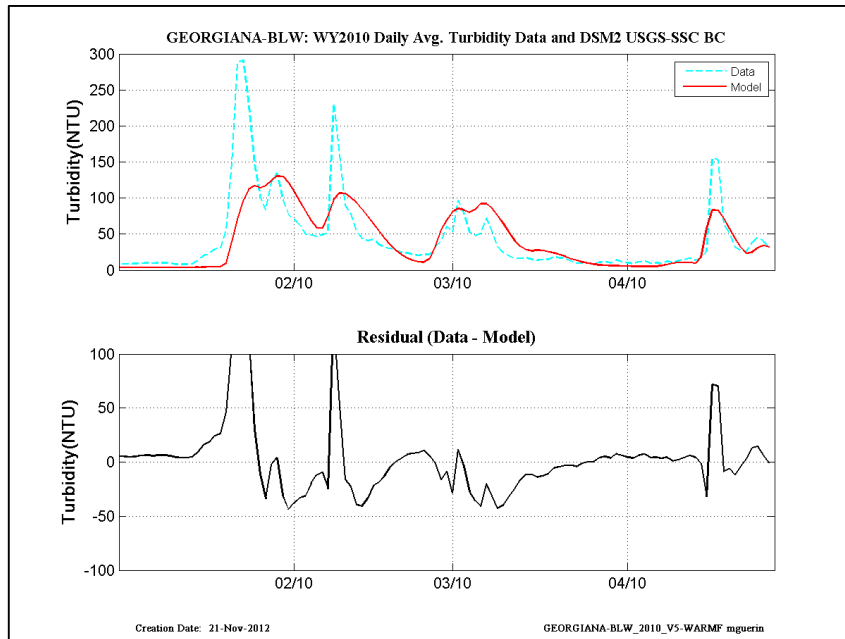


Figure 14-6 WY2010: DSM2 daily-averaged turbidity model results using Mixed-SSC-WARMF turbidity at the inflow boundaries— location is Georgiana-Below-Sac.

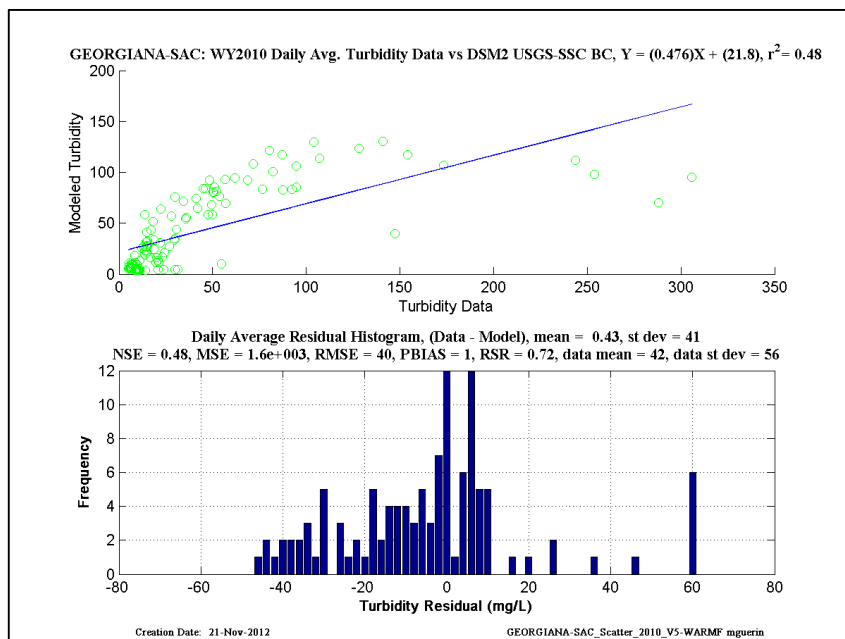
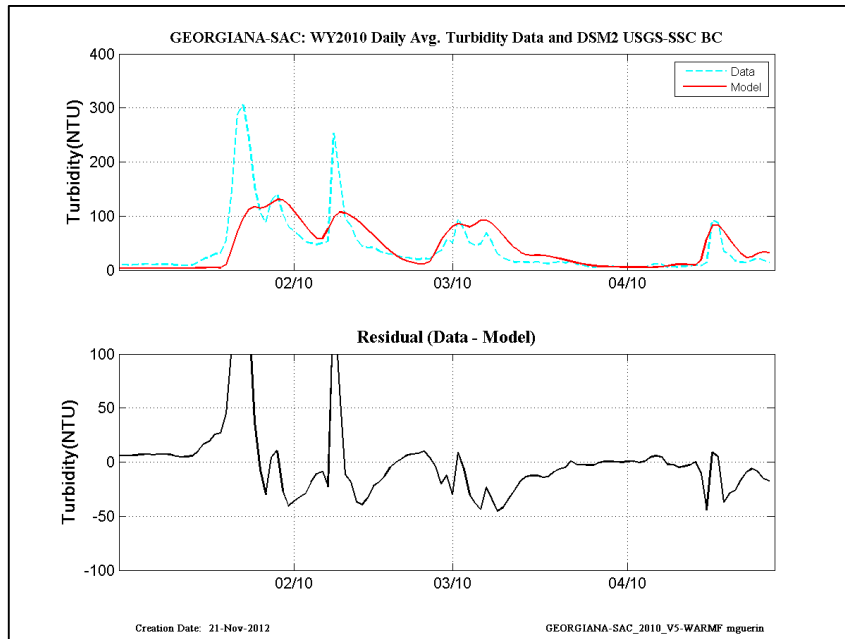


Figure 14-7 WY2010: DSM2 daily-averaged turbidity model results using Mixed-SSC-WARMF turbidity at the inflow boundaries— location is Georgiana-Sac.

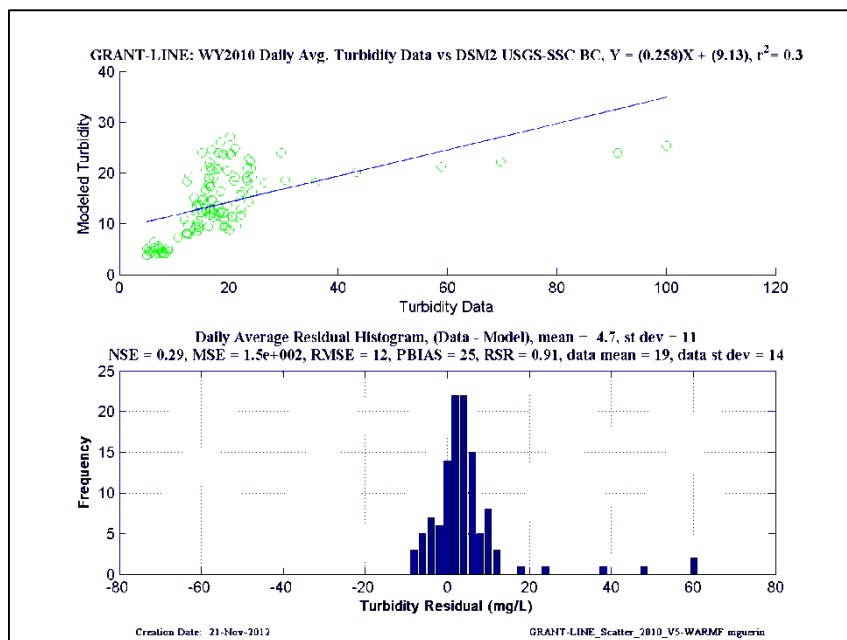
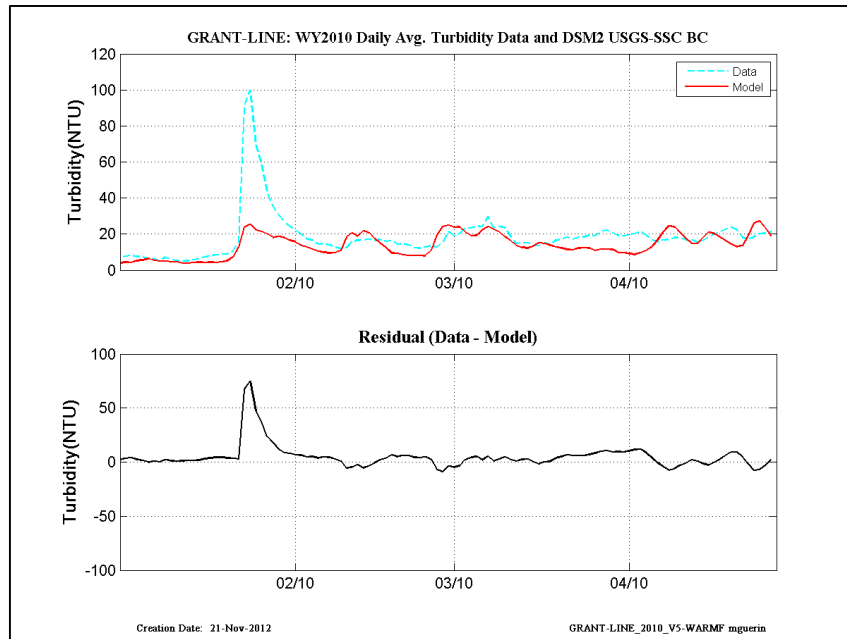


Figure 14-8WY2010: DSM2 daily-averaged turbidity model results using Mixed-SSC-WARMF turbidity at the inflow boundaries– location is Grant-Line.

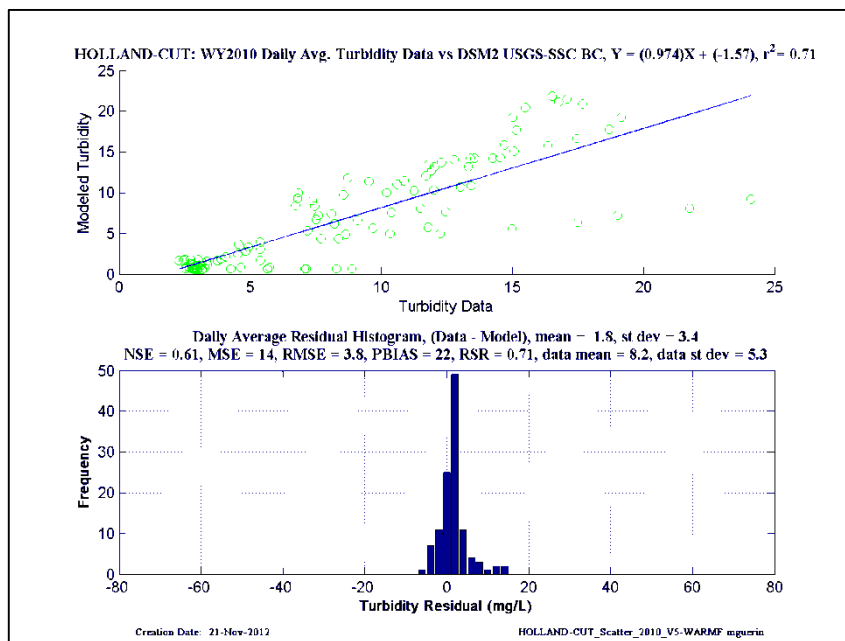
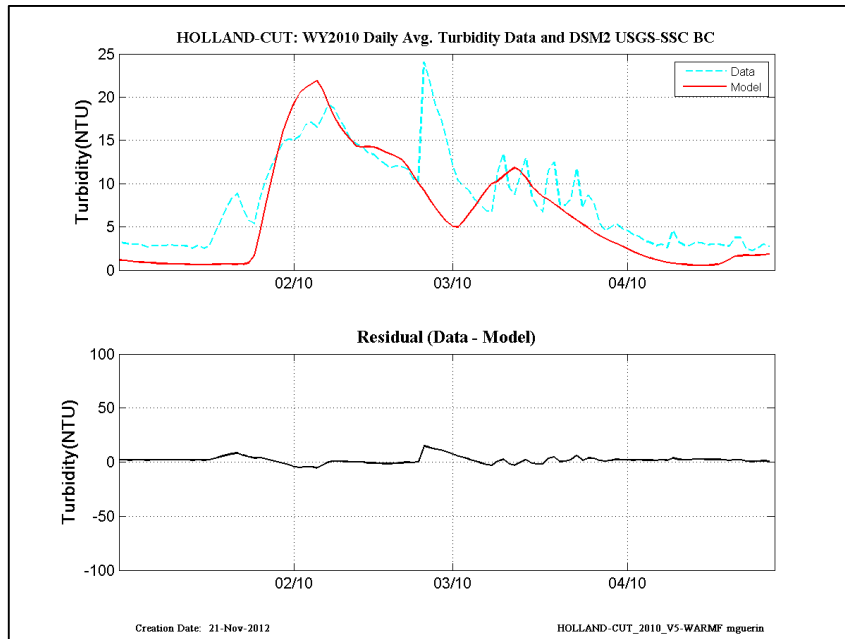


Figure 14-9WY2010: DSM2 daily-averaged turbidity model results using Mixed-SSC-WARMF turbidity at the inflow boundaries– location is Holland-Cut.

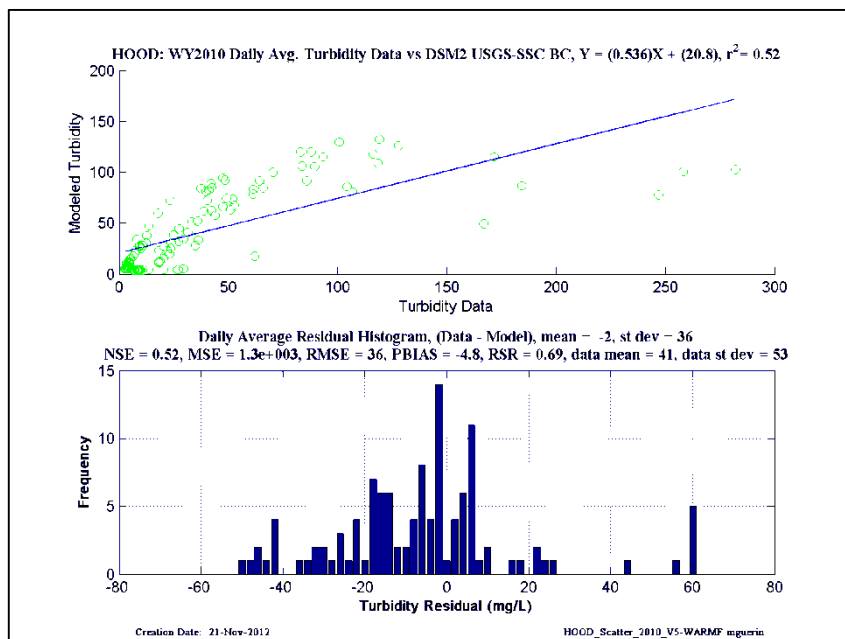
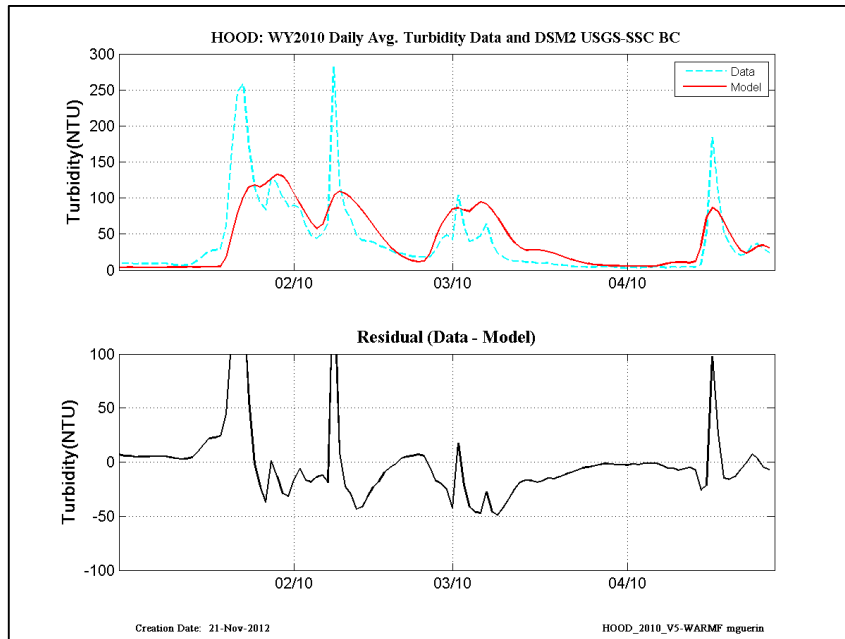


Figure 14-10 WY2010: DSM2 daily-averaged turbidity model results using Mixed-SSC-WARMF turbidity at the inflow boundaries– location is Hood.

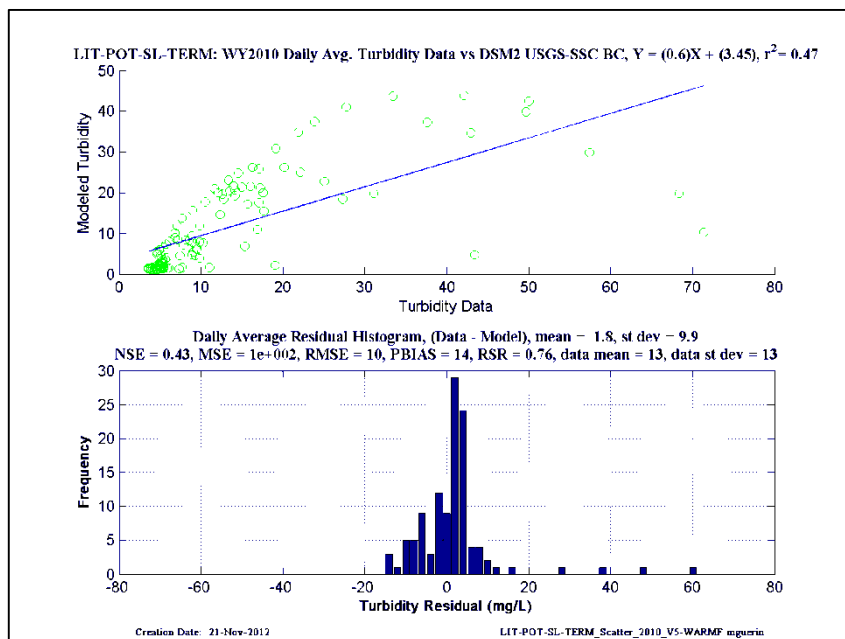
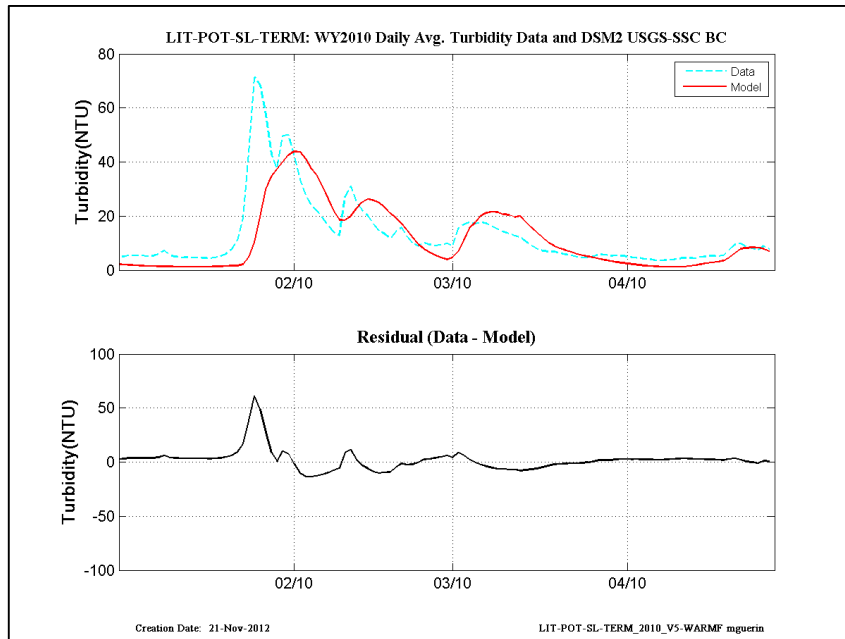


Figure 14-11WY2010: DSM2 daily-averaged turbidity model results using Mixed-SSC-WARMF turbidity at the inflow boundaries– location is Little-Potato-Slough-at-Terminous.

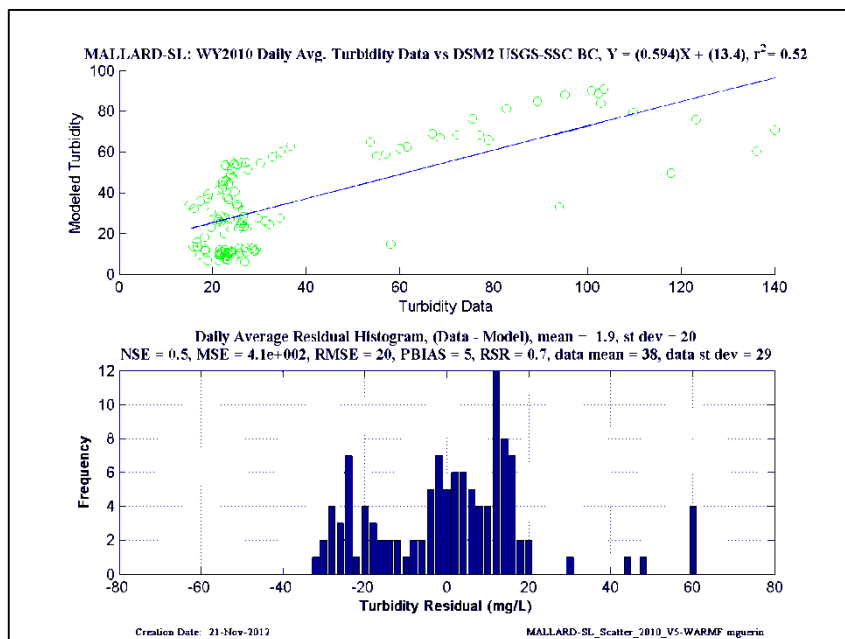
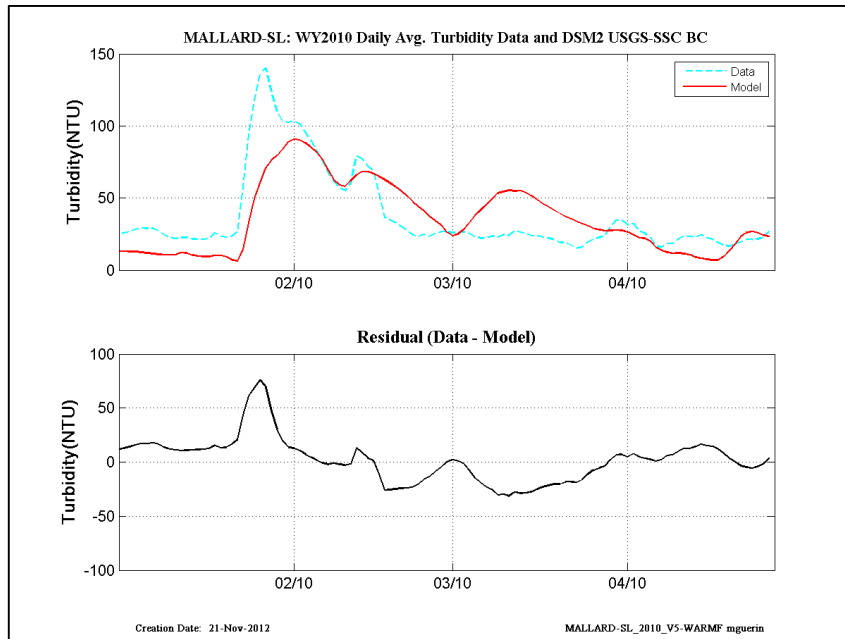


Figure 14-12WY2010: DSM2 daily-averaged turbidity model results using Mixed-SSC-WARMF turbidity at the inflow boundaries– location is Mallard Slough.

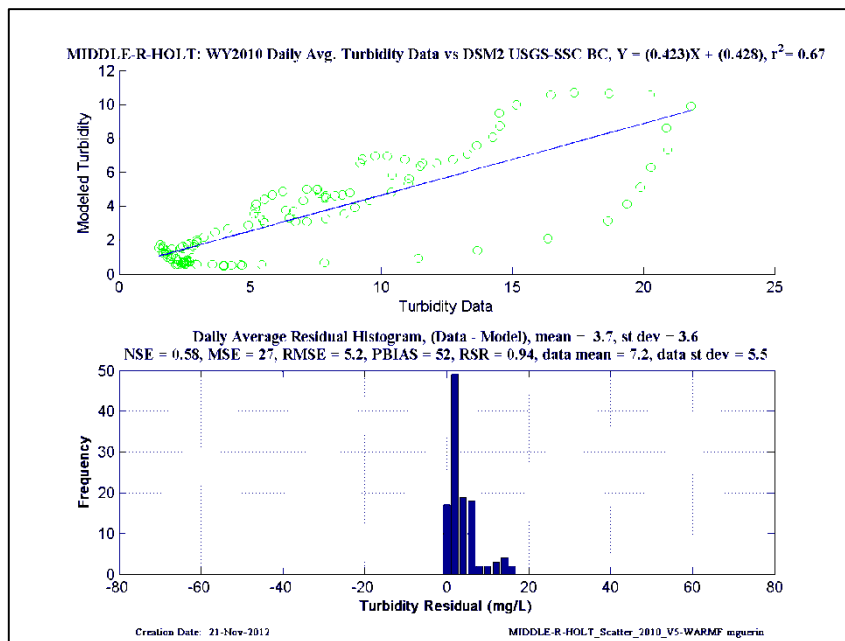
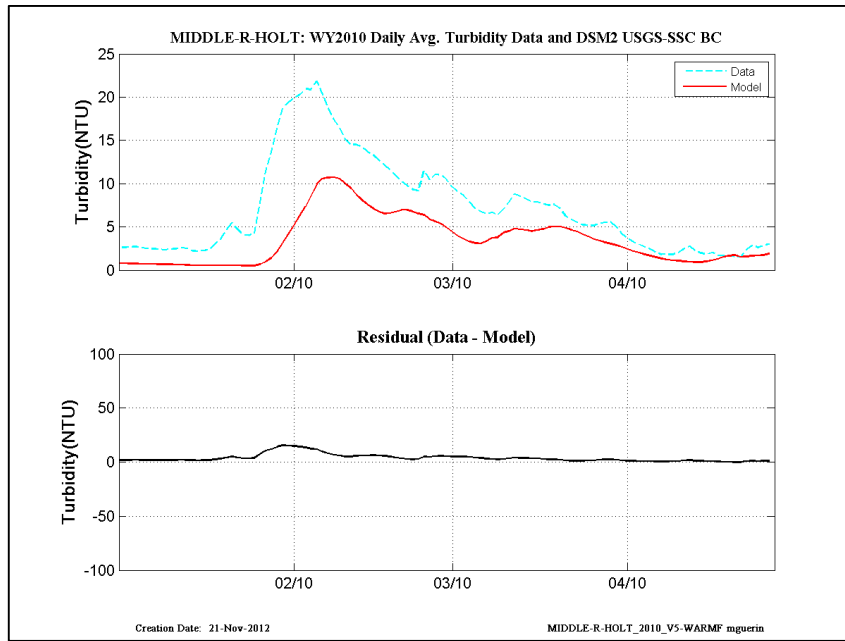


Figure 14-13 WY2010: DSM2 daily-averaged turbidity model results using Mixed-SSC-WARMF turbidity at the inflow boundaries— location is Middle-River-at-Holt.

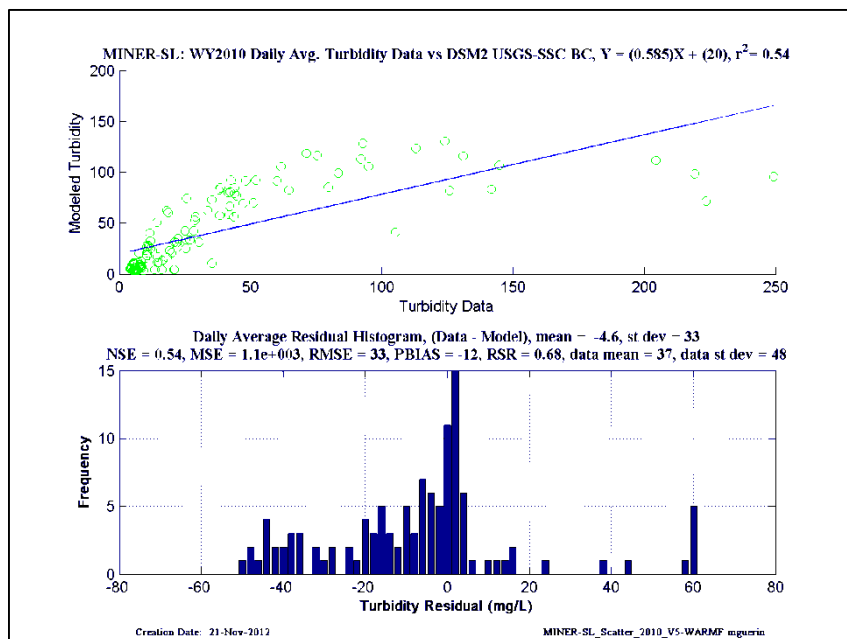
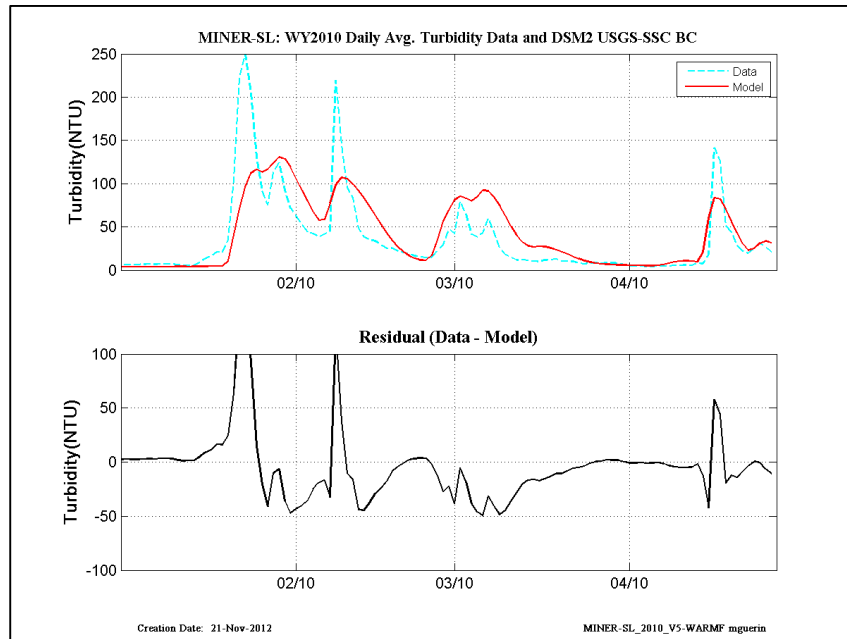


Figure 14-14WY2010: DSM2 daily-averaged turbidity model results using Mixed-SSC-WARMF turbidity at the inflow boundaries– location is Miner Slough.

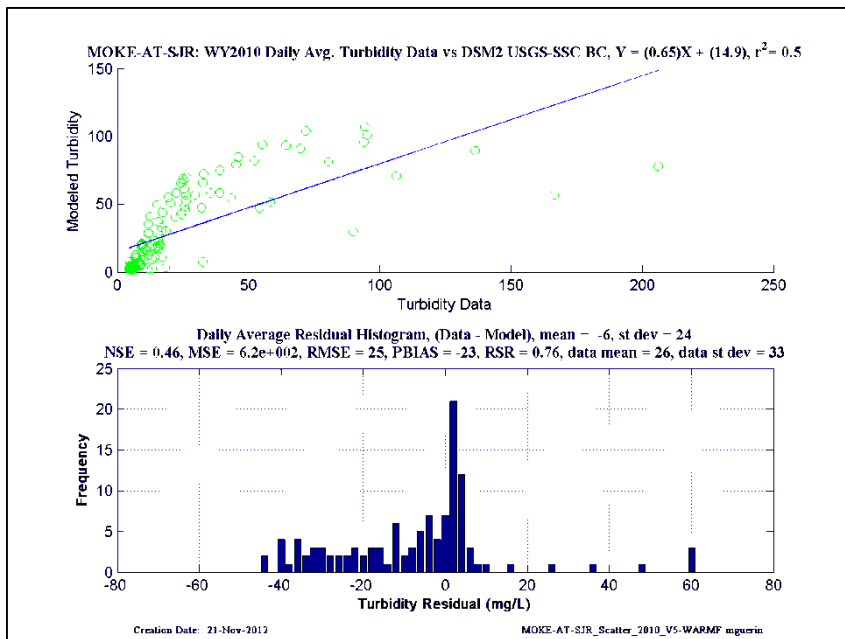
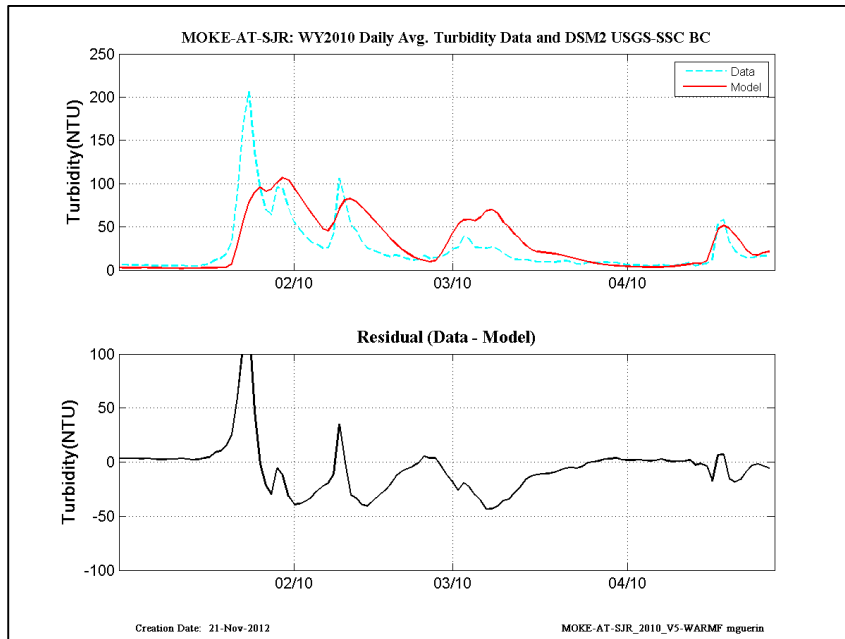


Figure 14-15WY2010: DSM2 daily-averaged turbidity model results using Mixed-SSC-WARMF turbidity at the inflow boundaries– location is Mokelumne-at-San Joaquin.

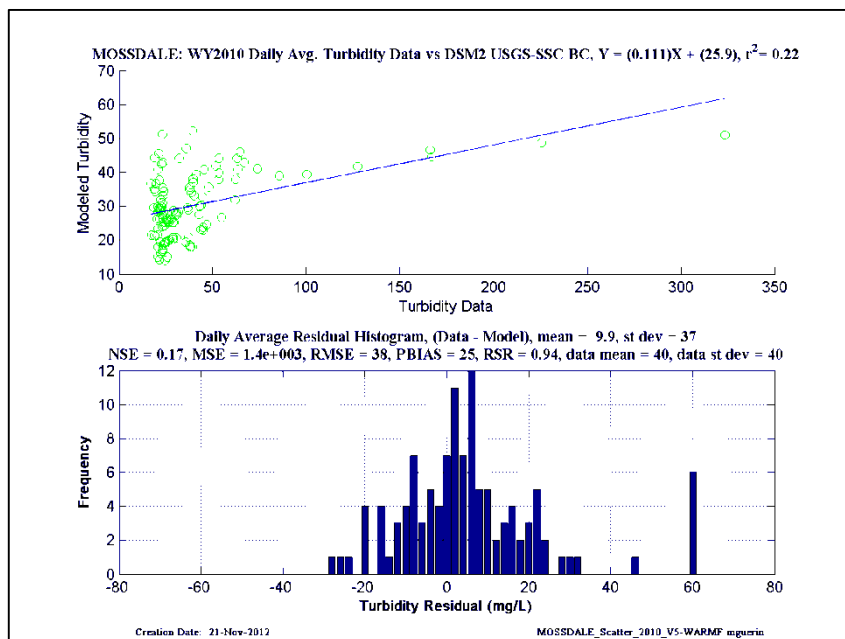
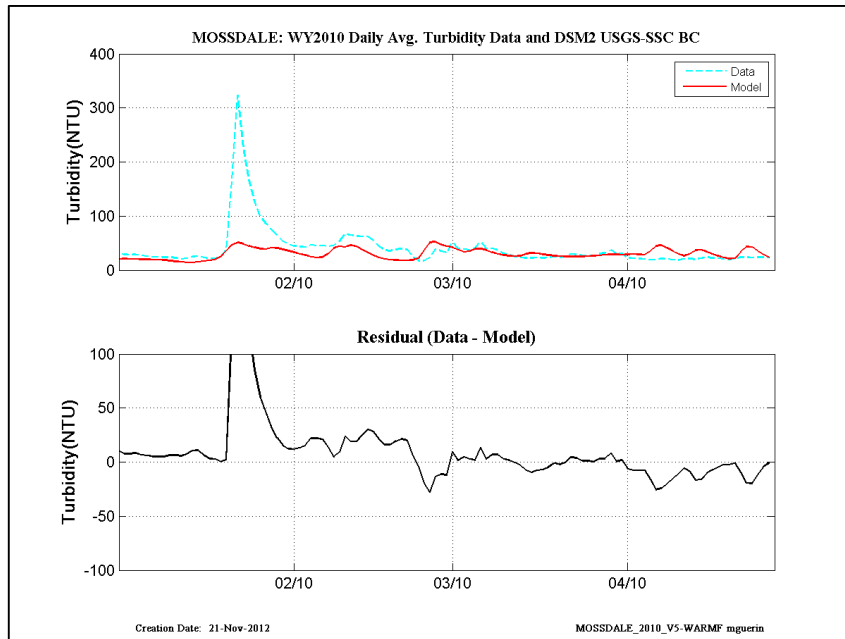


Figure 14-16 WY2010: DSM2 daily-averaged turbidity model results using Mixed-SSC-WARMF turbidity at the inflow boundaries– location is Mossdale.

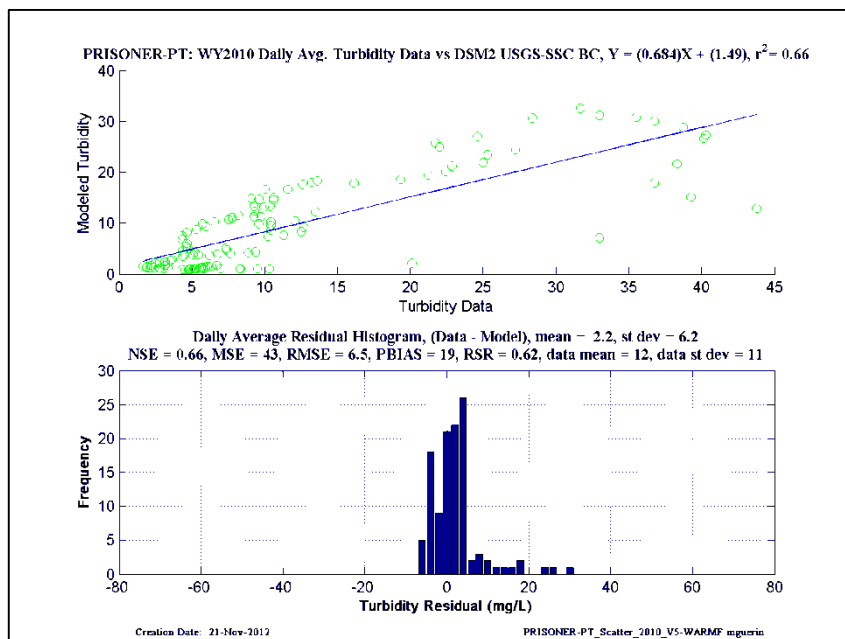
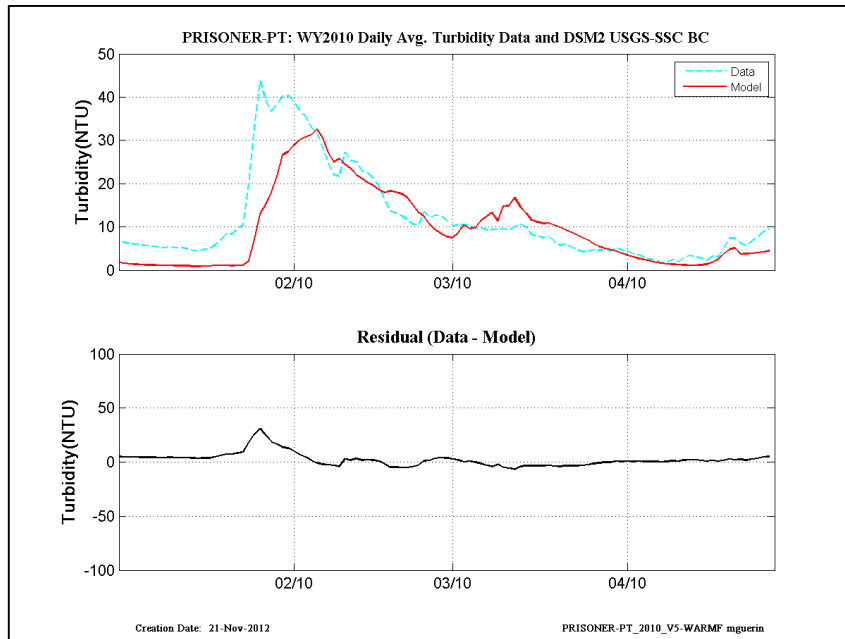


Figure 14-17WY2010: DSM2 daily-averaged turbidity model results using Mixed-SSC-WARMF turbidity at the inflow boundaries– location is Prisoner-Point.

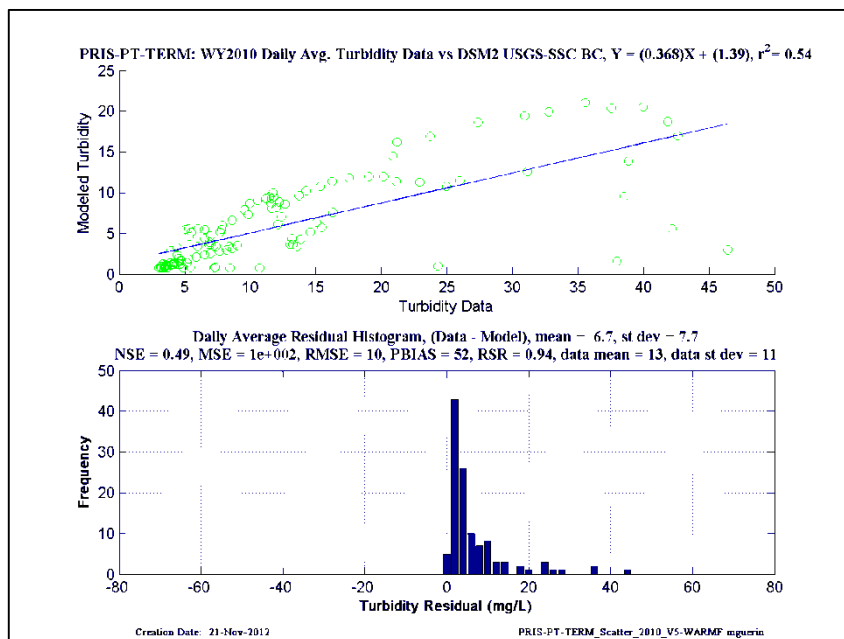
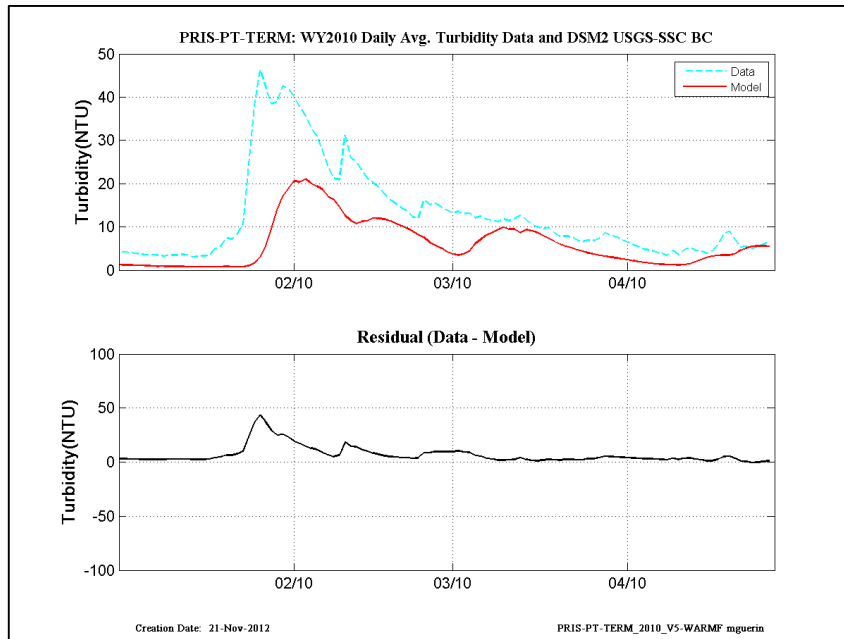


Figure 14-18WY2010: DSM2 daily-averaged turbidity model results using Mixed-SSC-WARMF turbidity at the inflow boundaries– location is Prisoner-Point-at-Terminus.

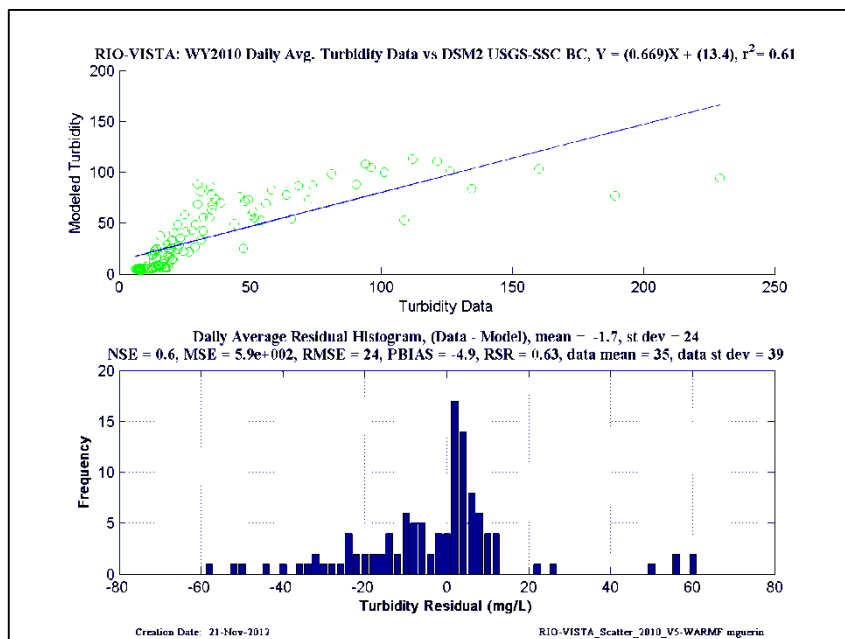
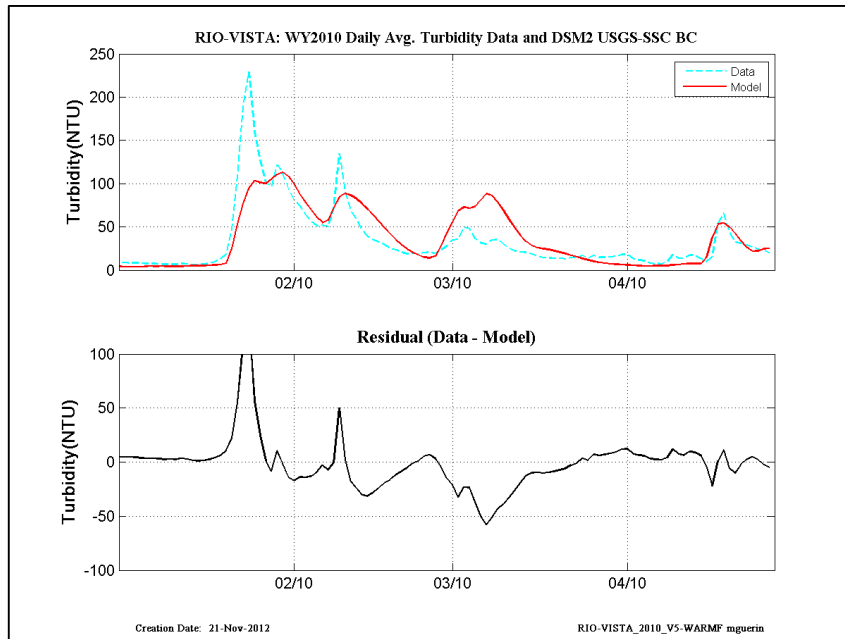


Figure 14-19 WY2010: DSM2 daily-averaged turbidity model results using Mixed-SSC-WARMF turbidity at the inflow boundaries— location is Rio Vista.

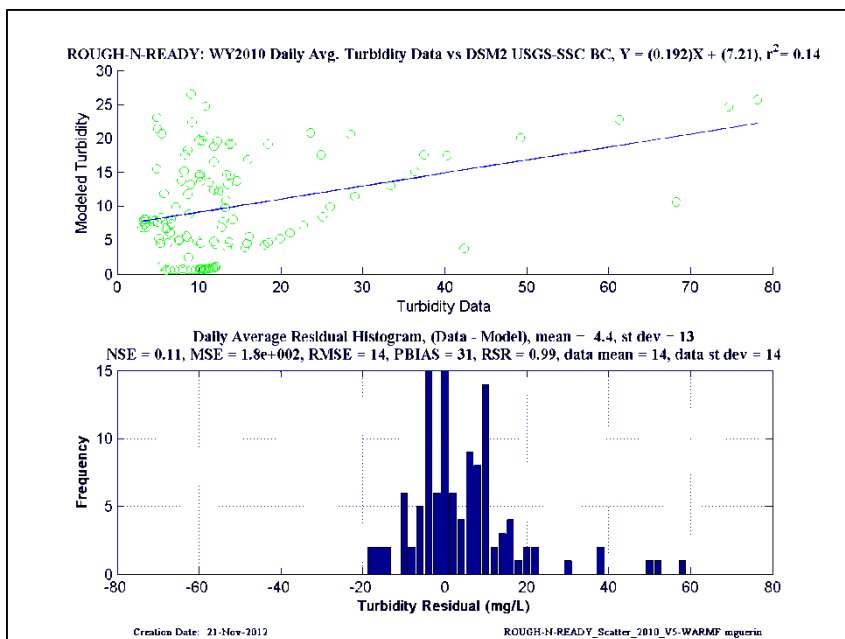
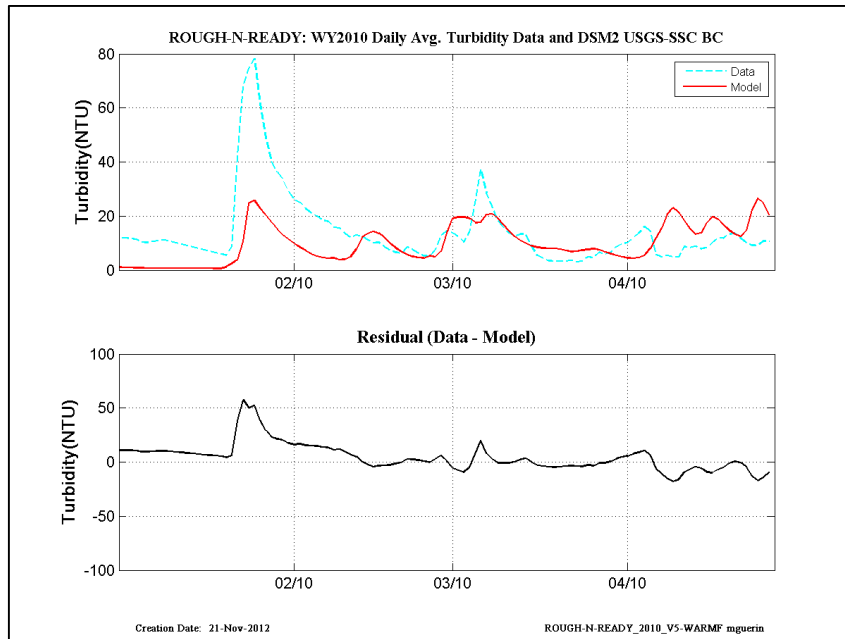


Figure 14-20 WY2010: DSM2 daily-averaged turbidity model results using Mixed-SSC-WARMF turbidity at the inflow boundaries– location is Rough-N-Ready Island.

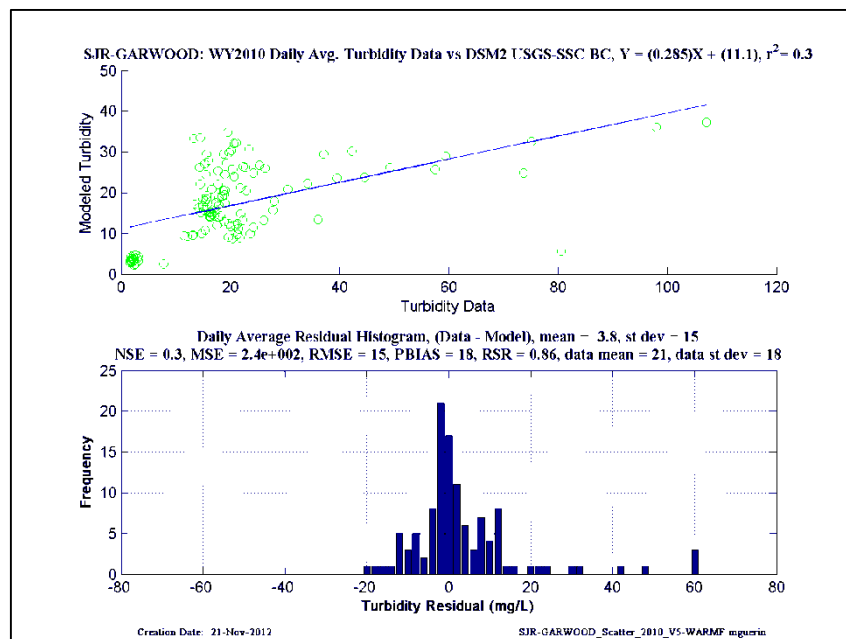
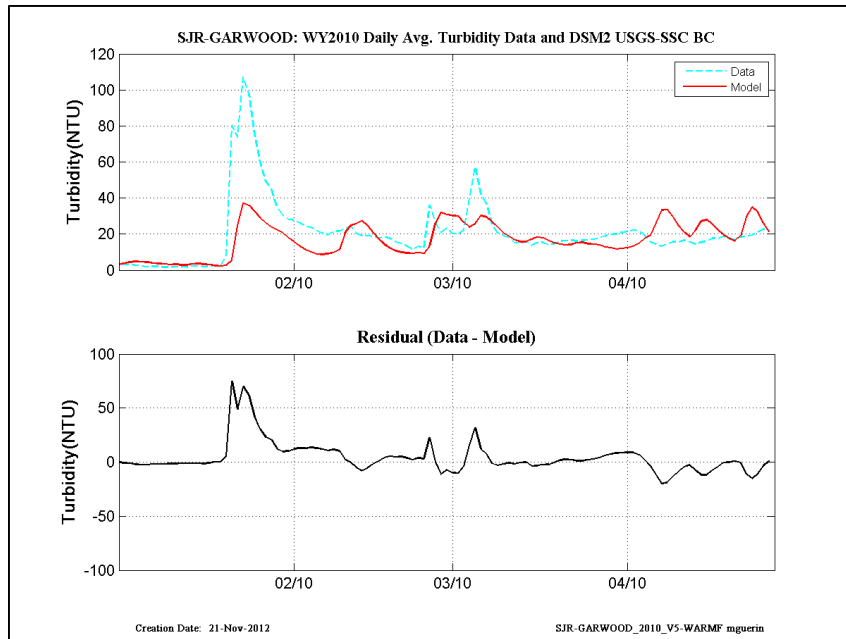


Figure 14-21 WY2010: DSM2 daily-averaged turbidity model results using Mixed-SSC-WARMF turbidity at the inflow boundaries– location is San Joaquin-at-Garwood.

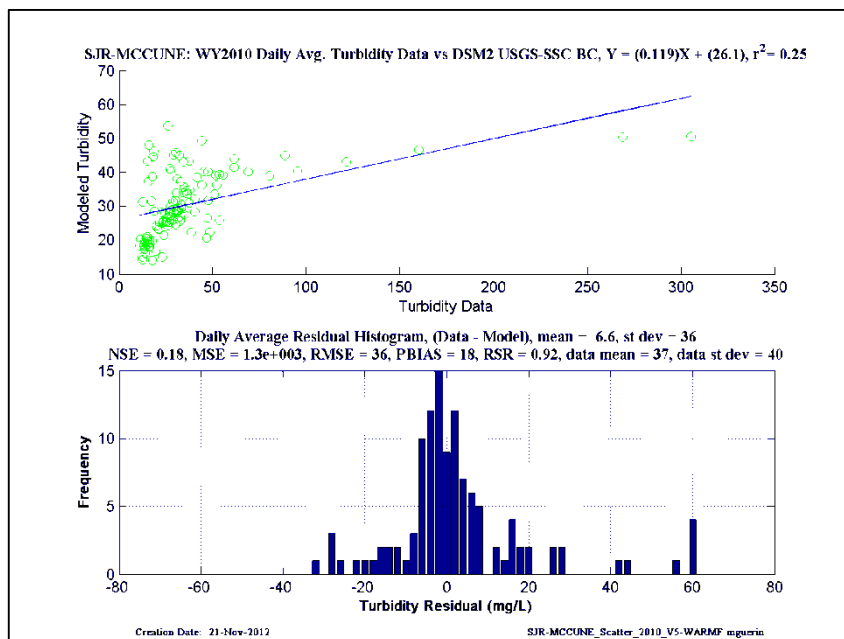
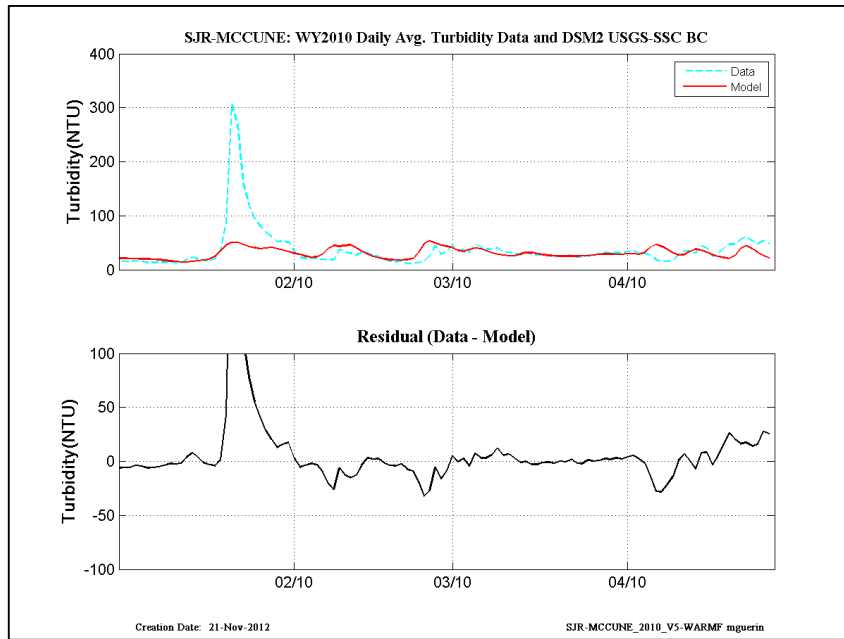


Figure 14-22 WY2010: DSM2 daily-averaged turbidity model results using Mixed-SSC-WARMF turbidity at the inflow boundaries– location is San Joaquin-at-McCune.

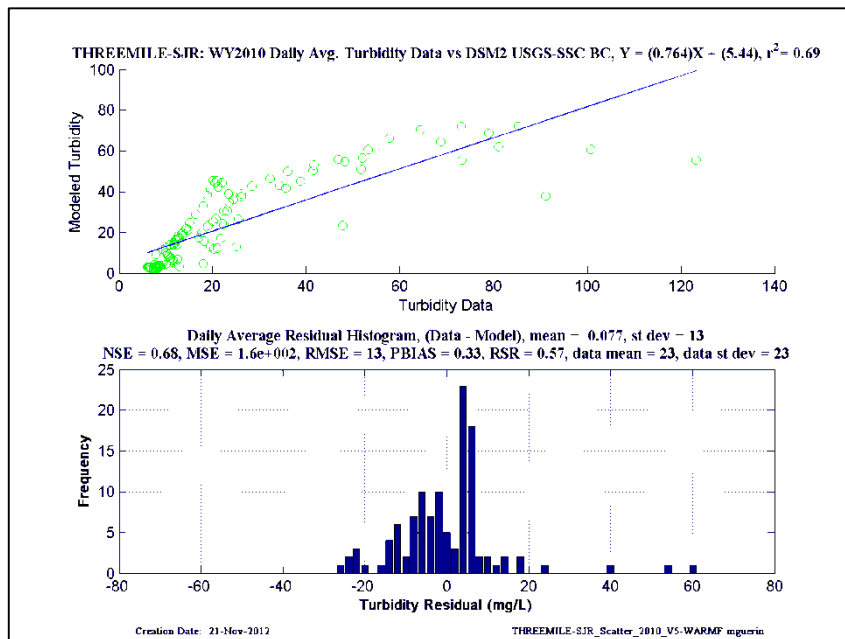
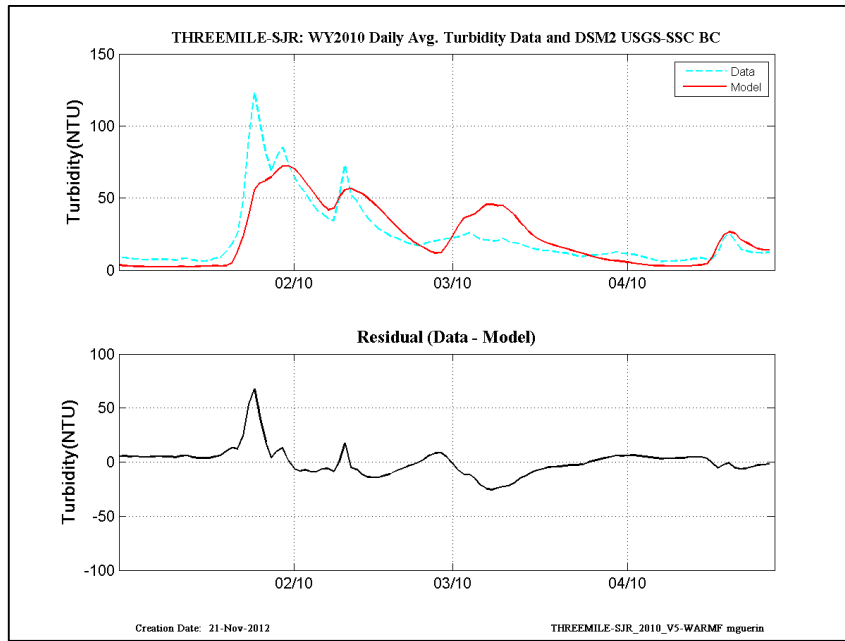


Figure 14-23 WY2010: DSM2 daily-averaged turbidity model results using Mixed-SSC-WARMF turbidity at the inflow boundaries– location is Threemile-Slough-at-San Joaquin.

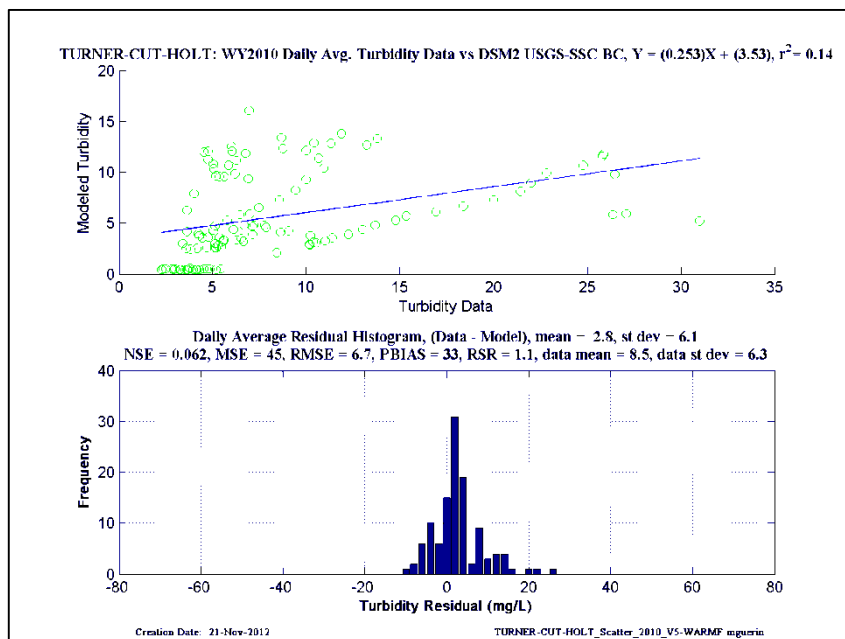
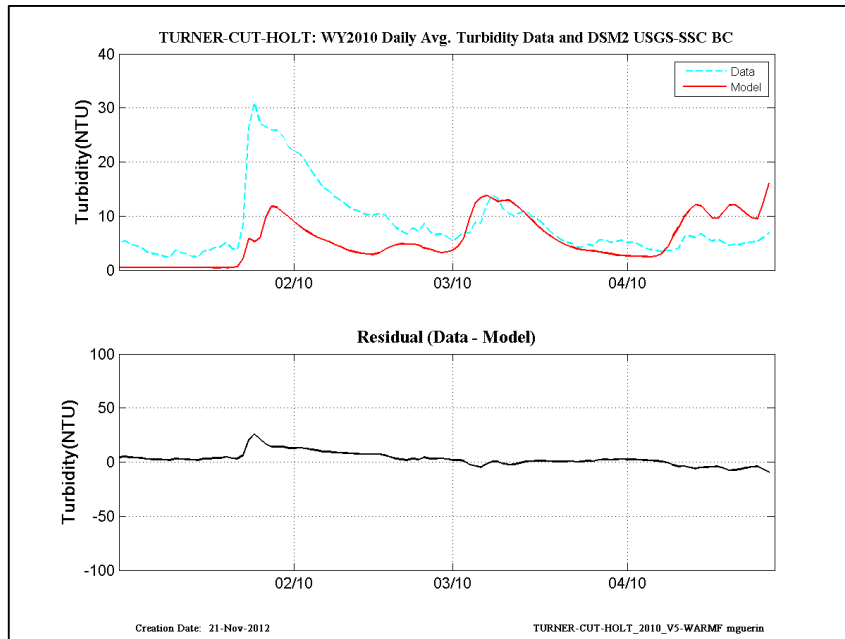


Figure 14-24 WY2010: DSM2 daily-averaged turbidity model results using Mixed-SSC-WARMF turbidity at the inflow boundaries– location is Turner-Cut-at-Holt.

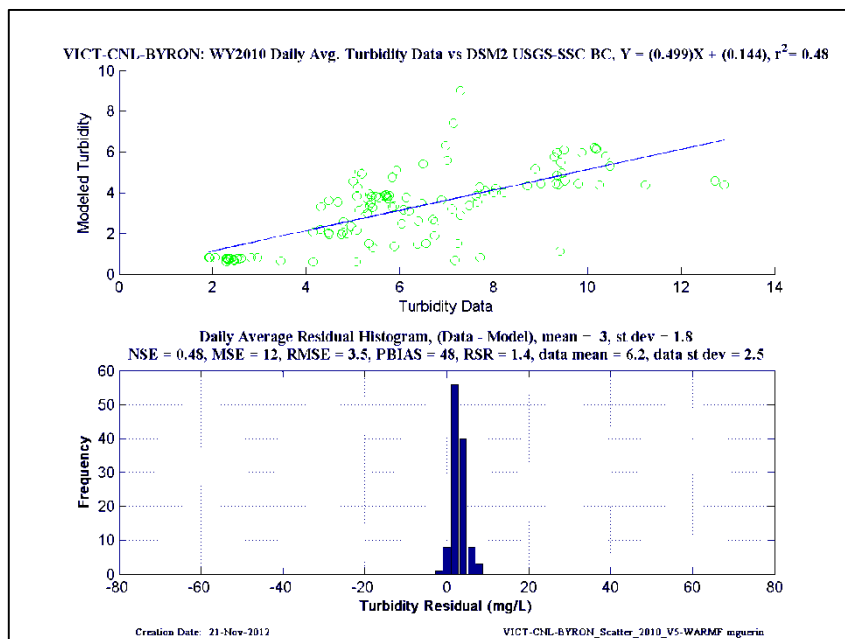
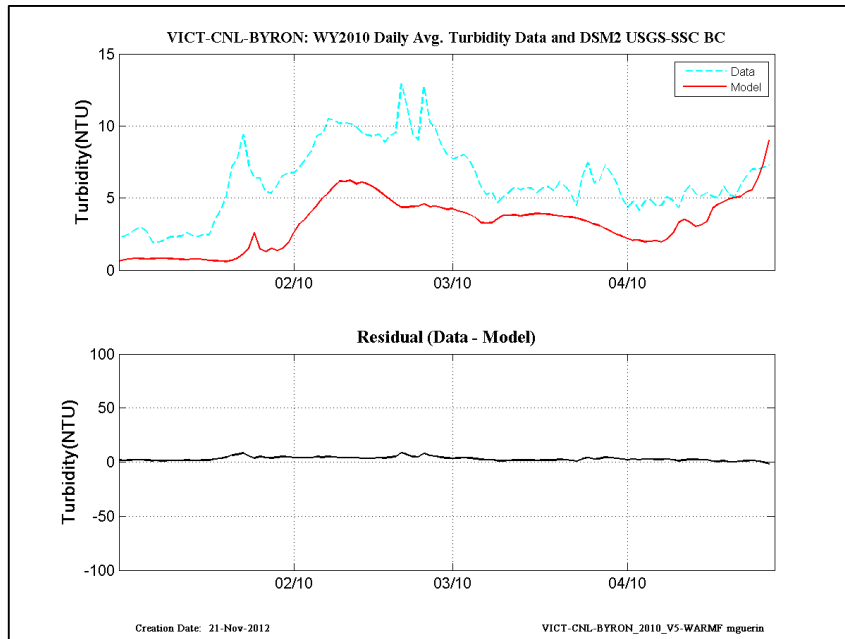


Figure 14-25 WY2010: DSM2 daily-averaged turbidity model results using Mixed-SSC-WARMF turbidity at the inflow boundaries– location is Victoria-Canal-at-Byron.

15.2 WY2011 Mixed-SSC-WARMF results

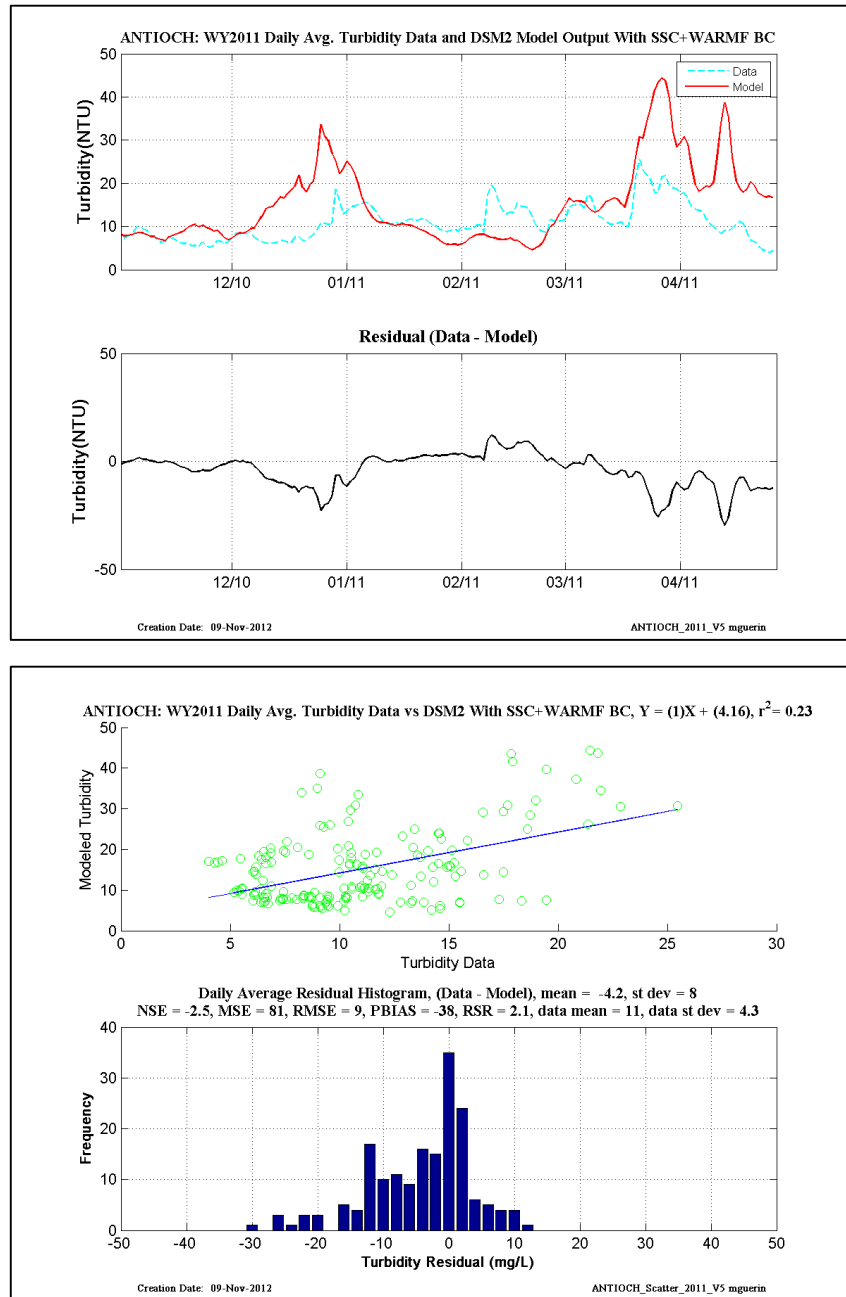


Figure 14-26 WY2011: DSM2 daily-averaged turbidity model results using Mixed-SSC-WARMF turbidity at the inflow boundaries– location is Antioch.

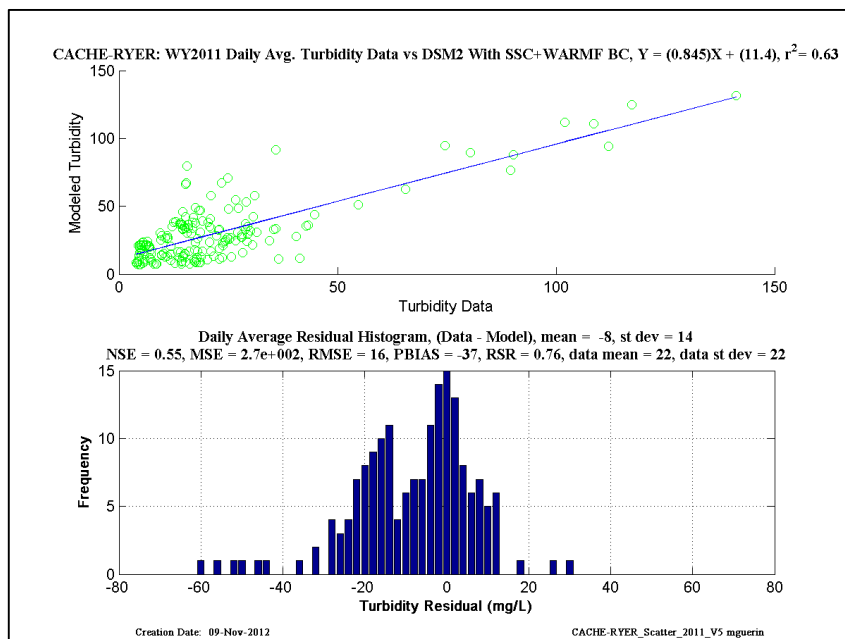
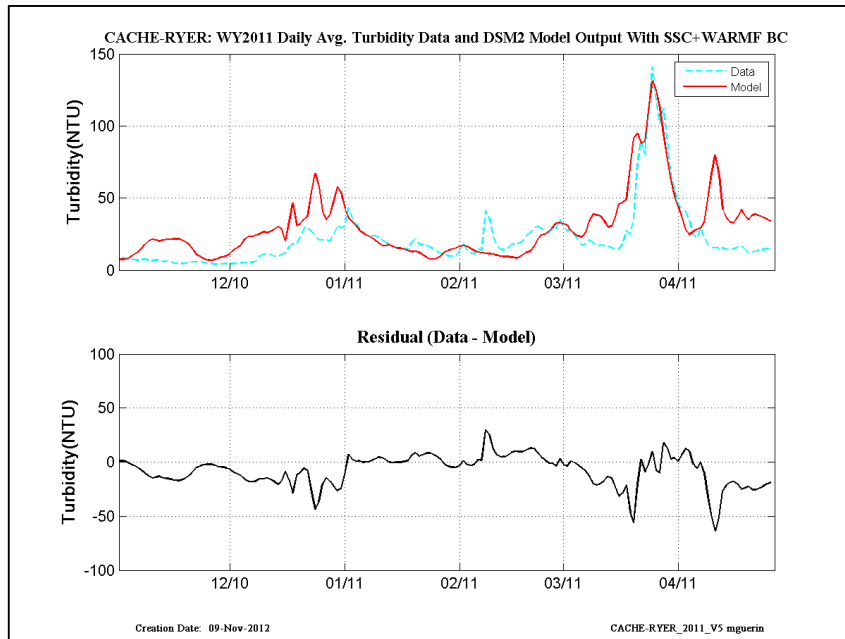


Figure 14-27 WY2011: DSM2 daily-averaged turbidity model results using Mixed-SSC-WARMF turbidity at the inflow boundaries– location is Cache-at-Ryer.

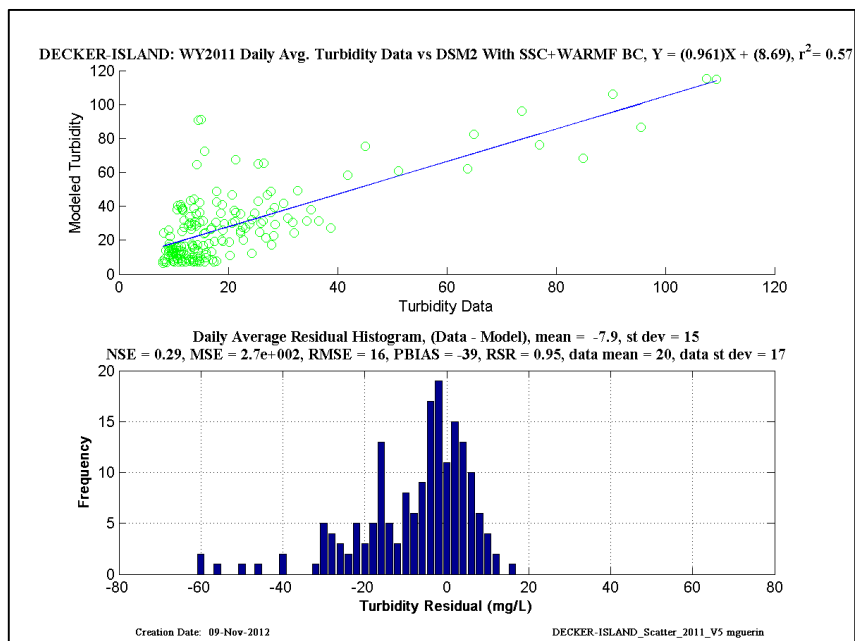
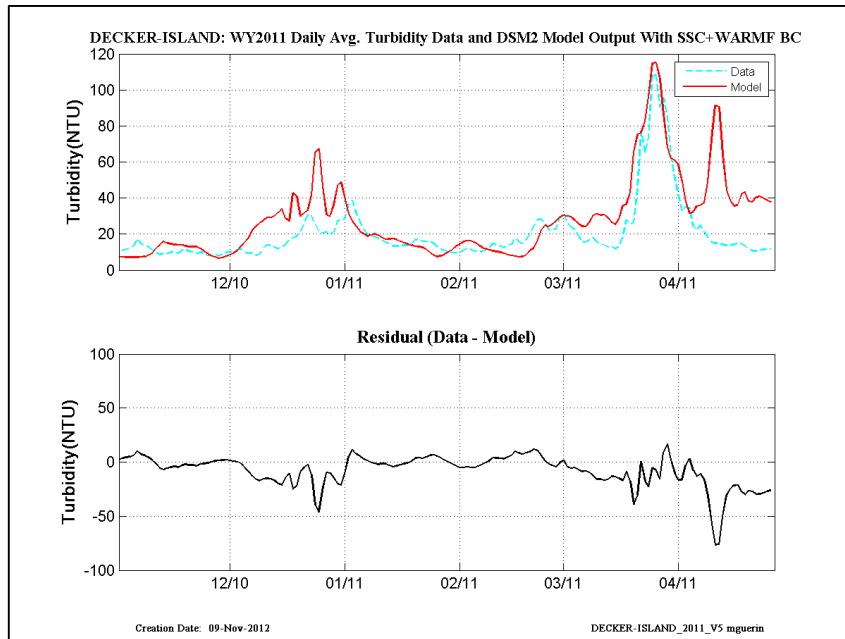


Figure 14-28 WY2011: DSM2 daily-averaged turbidity model results using Mixed-SSC-WARMF turbidity at the inflow boundaries– location is Decker-Island.

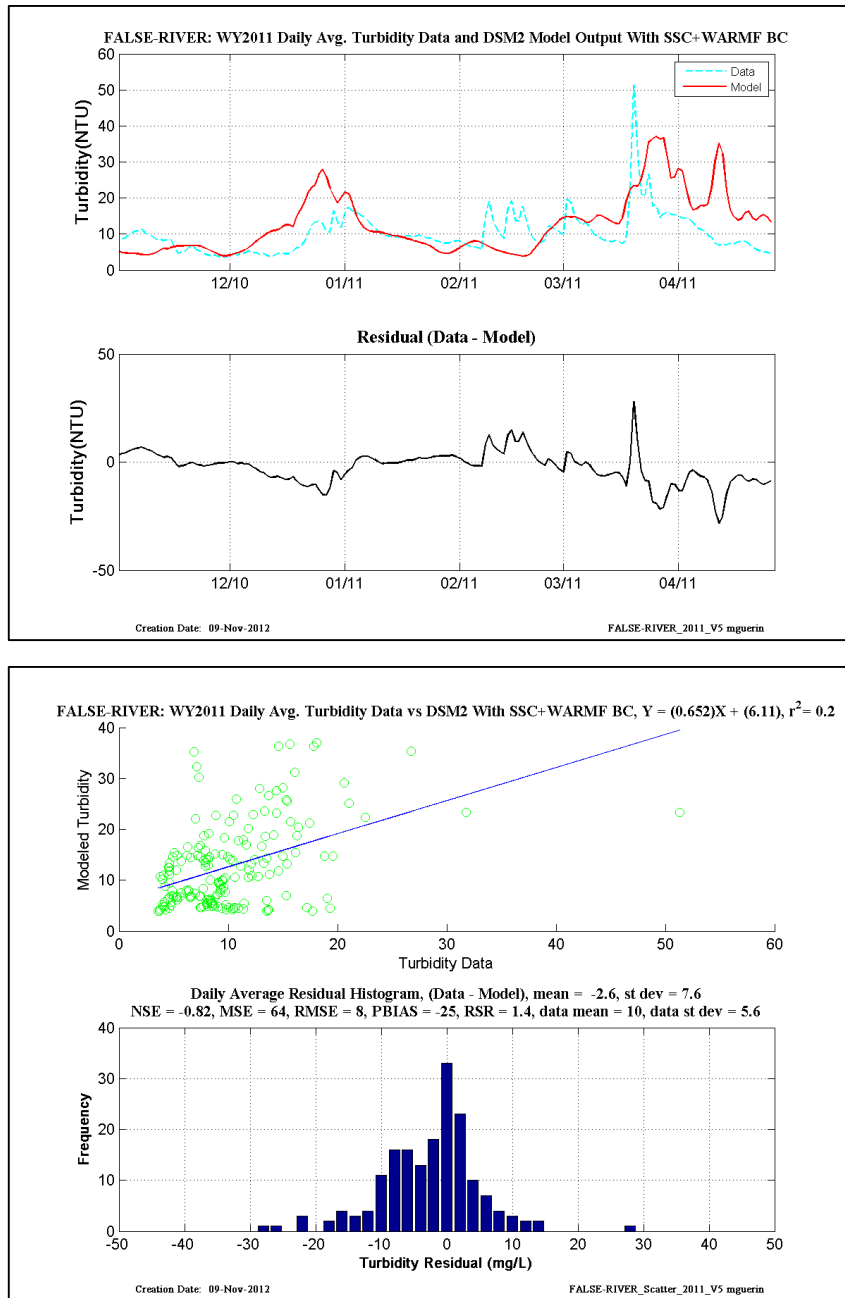


Figure 14-29 WY2011: DSM2 daily-averaged turbidity model results using Mixed-SSC-WARMF turbidity at the inflow boundaries– location is False-River.

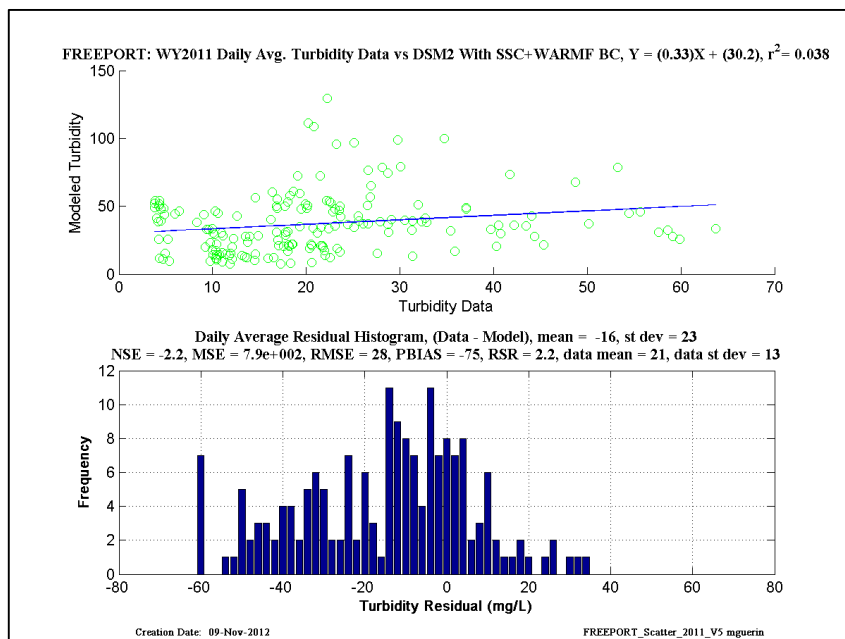
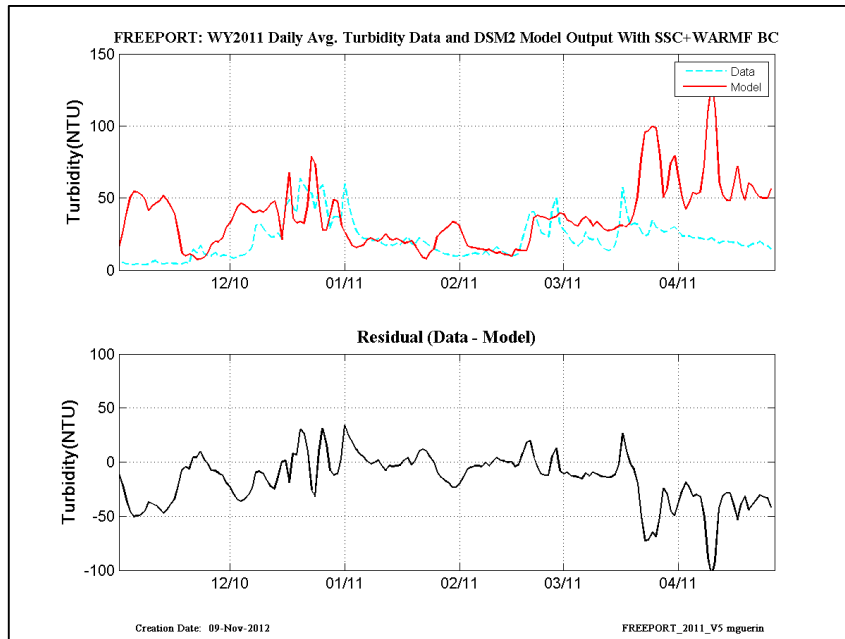


Figure 14-30 WY2011: DSM2 daily-averaged turbidity model results using Mixed-SSC-WARMF turbidity at the inflow boundaries– location is Freepoint.

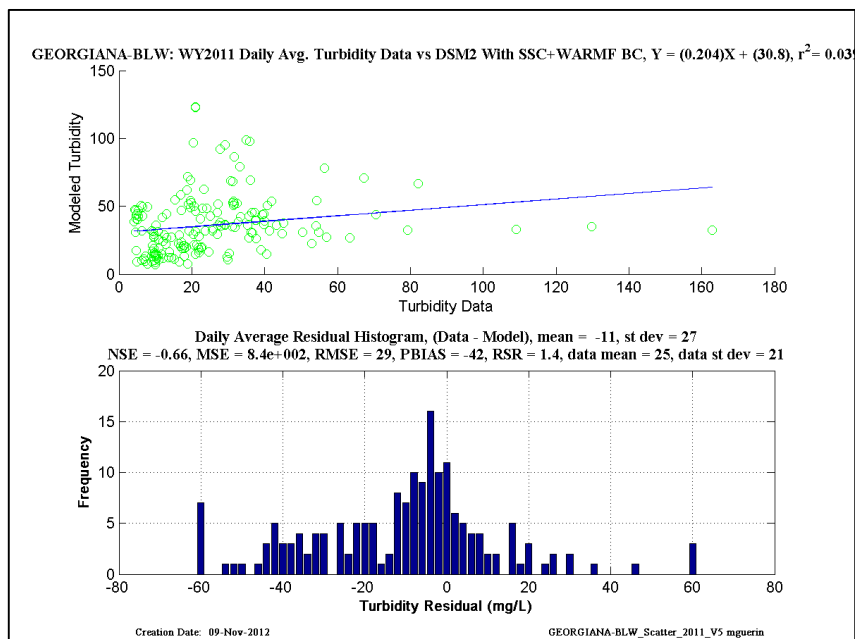
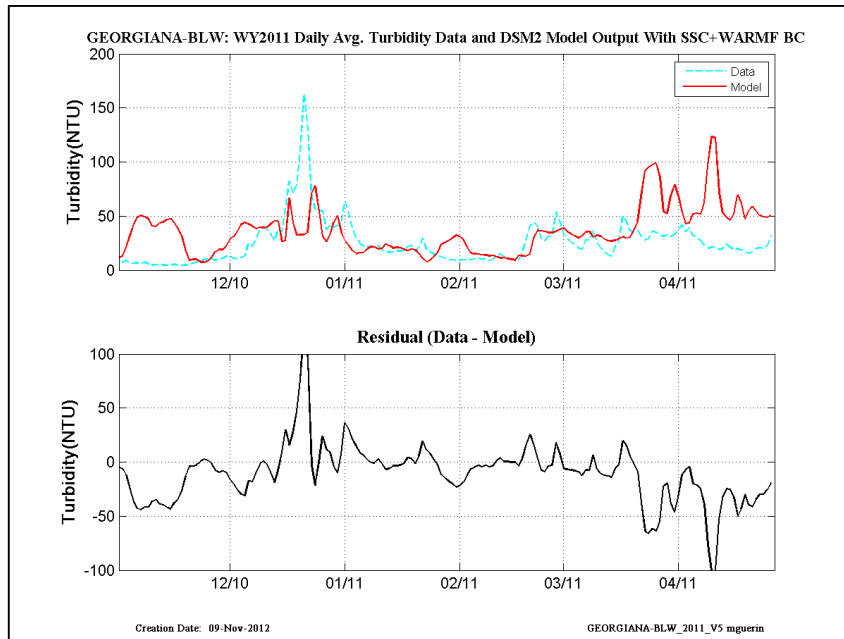


Figure 14-31 WY2011: DSM2 daily-averaged turbidity model results using Mixed-SSC-WARMF turbidity at the inflow boundaries– location is Georgiana- Below-Sac.

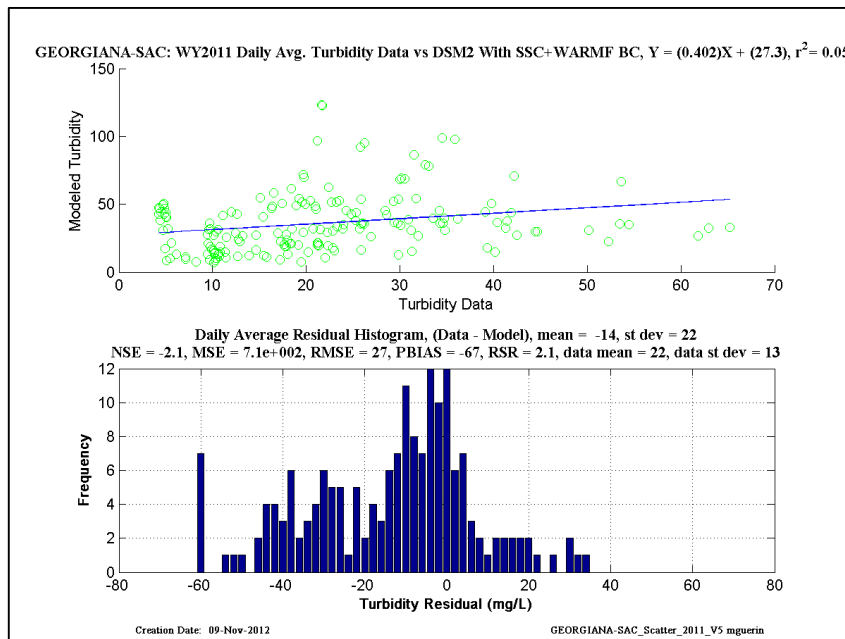
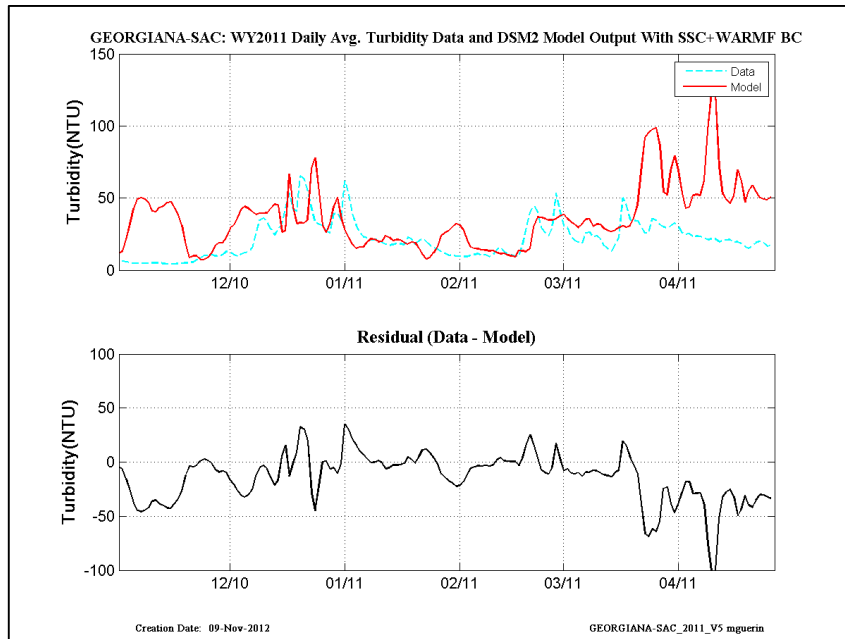


Figure 14-32 WY2011: DSM2 daily-averaged turbidity model results using Mixed-SSC-WARMF turbidity at the inflow boundaries– location is Georgiana at Sac.

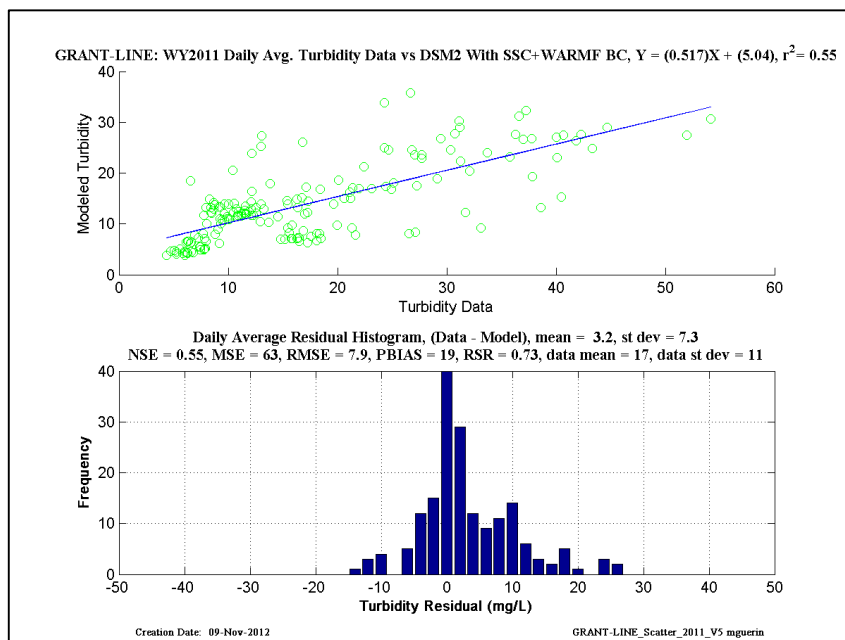
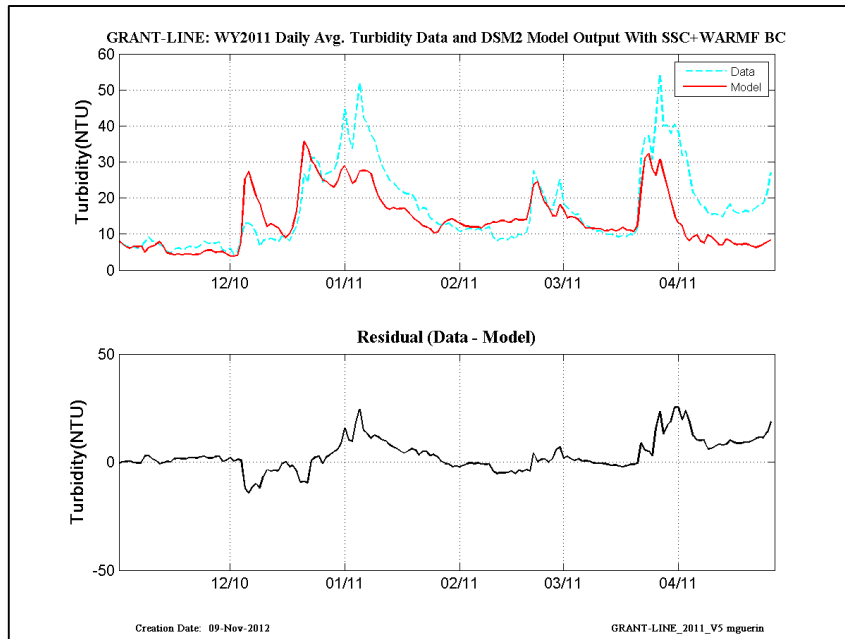


Figure 14-33 WY2011: DSM2 daily-averaged turbidity model results using Mixed-SSC-WARMF turbidity at the inflow boundaries– location is Grant Line.

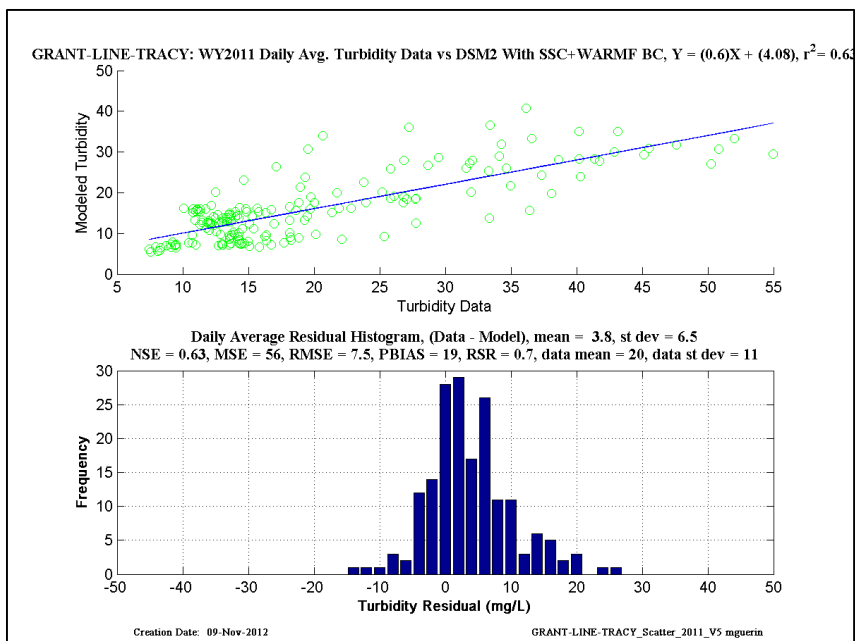
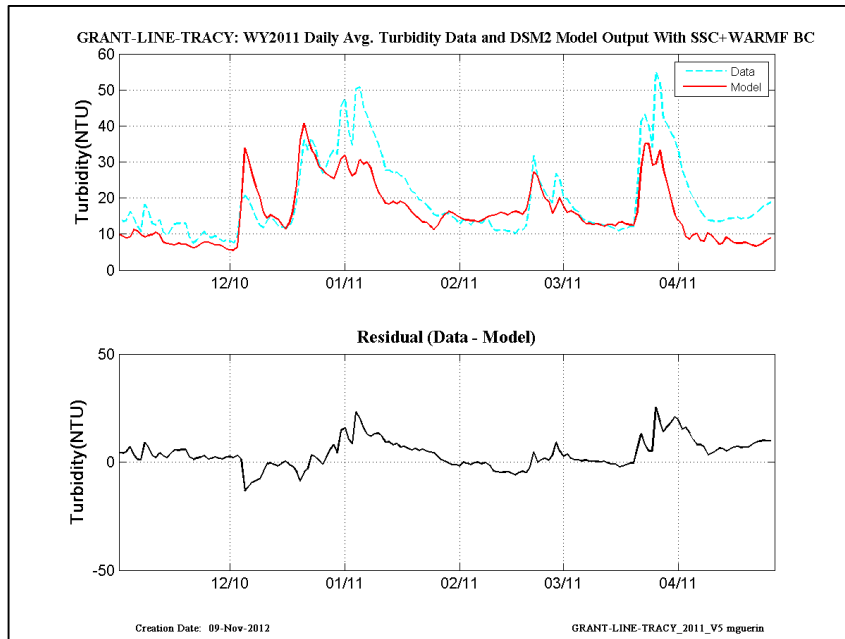


Figure 14-34 WY2011: DSM2 daily-averaged turbidity model results using Mixed-SSC-WARMF turbidity at the inflow boundaries– location is Grant-Line-at-Tracy.

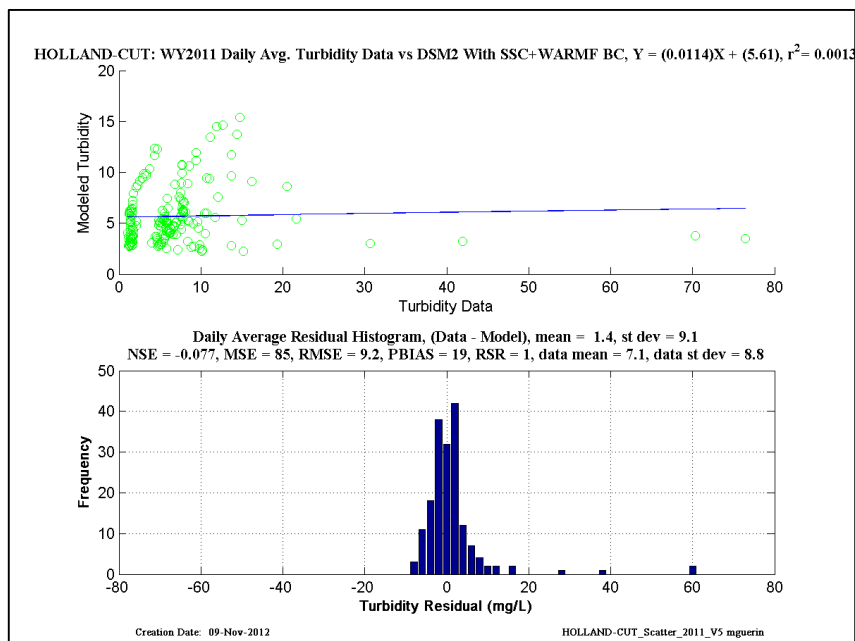
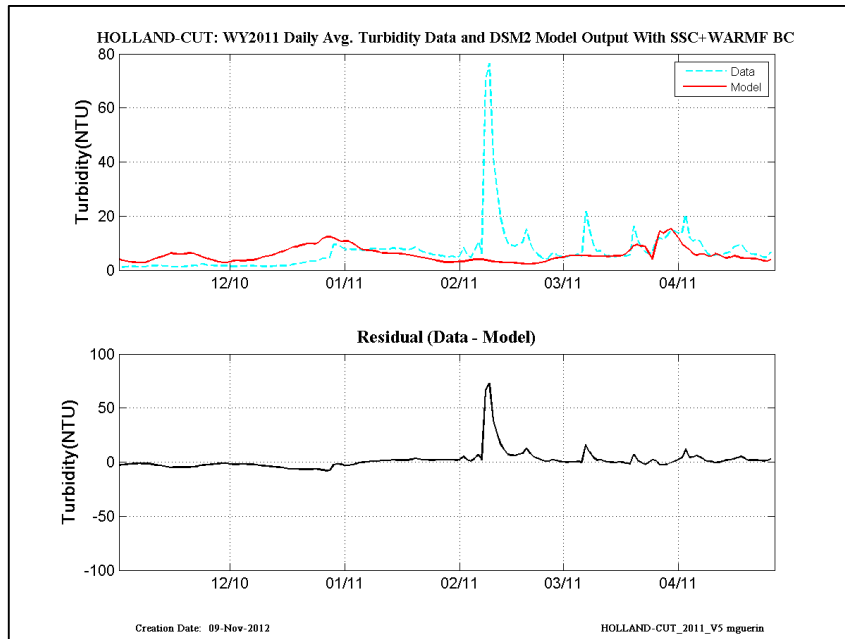


Figure 14-35 WY2011: DSM2 daily-averaged turbidity model results using Mixed-SSC-WARMF turbidity at the inflow boundaries– location is Holland Cut.

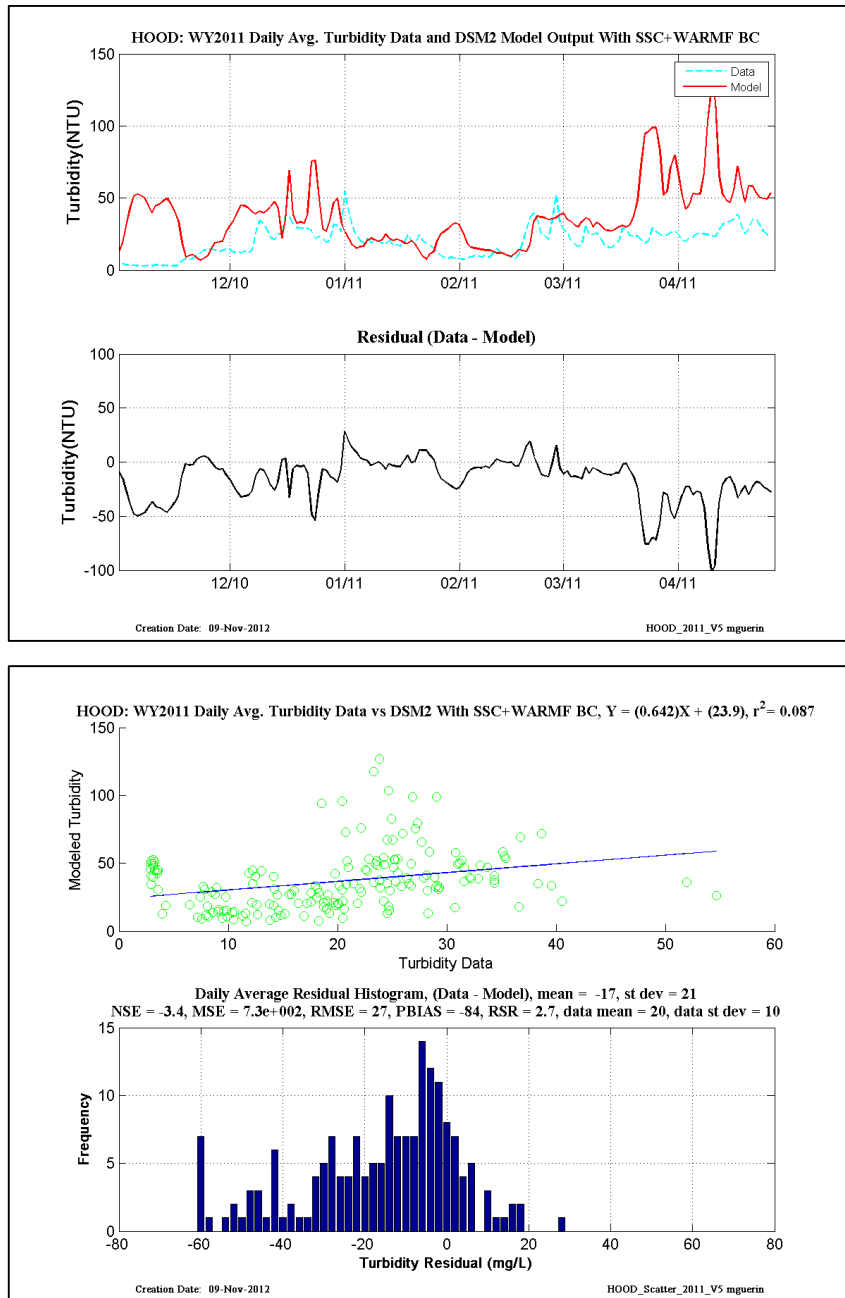


Figure 14-36 WY2011: DSM2 daily-averaged turbidity model results using Mixed-SSC-WARMF turbidity at the inflow boundaries– location is Hood.

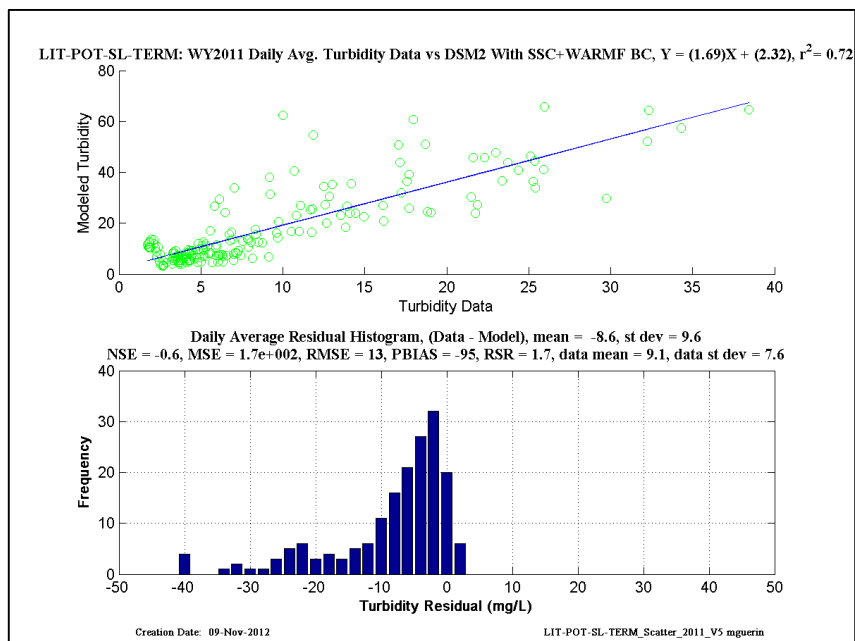
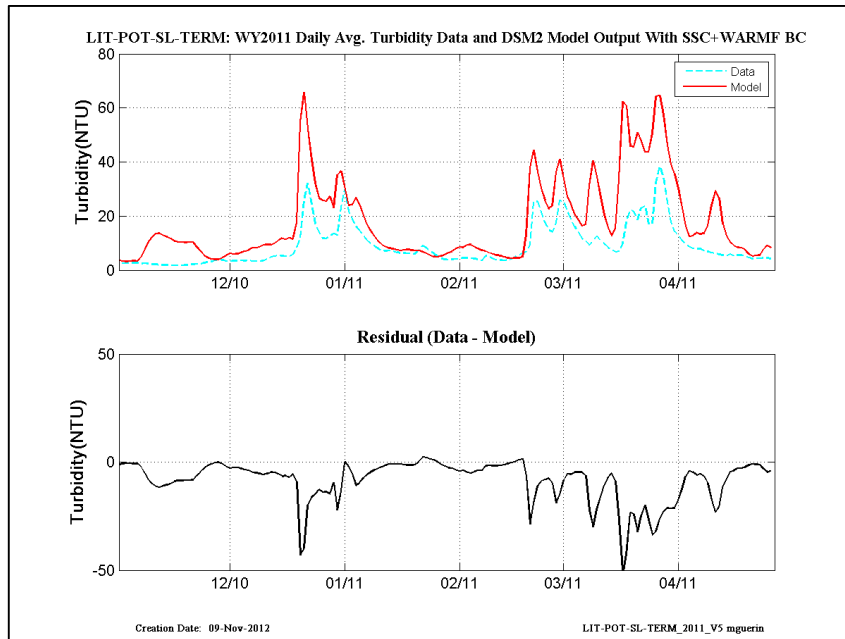


Figure 14-37 WY2011: DSM2 daily-averaged turbidity model results using Mixed-SSC-WARMF turbidity at the inflow boundaries– location is Little-Potato-Slough-at-Terminus.

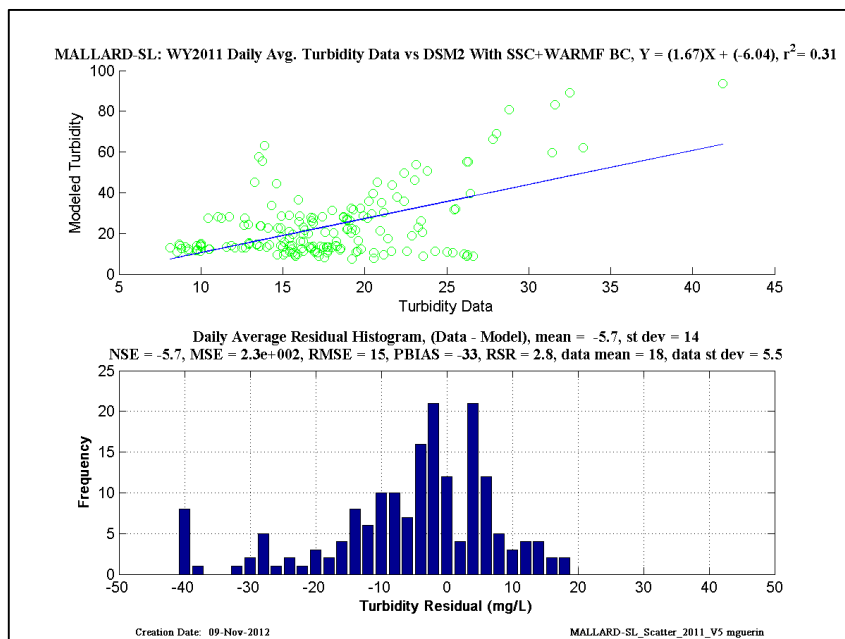
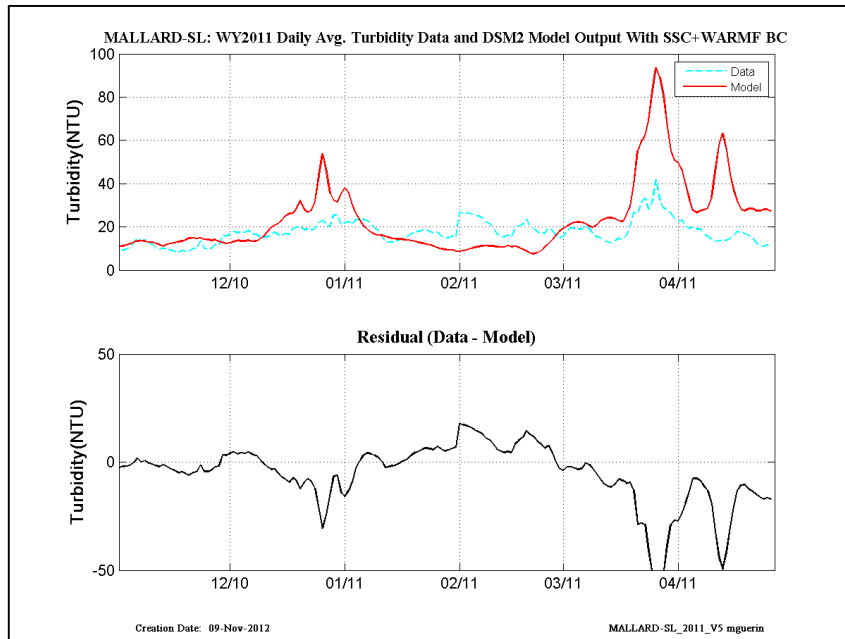


Figure 14-38 WY2011: DSM2 daily-averaged turbidity model results using Mixed-SSC-WARMF turbidity at the inflow boundaries– location is Mallard Slough.

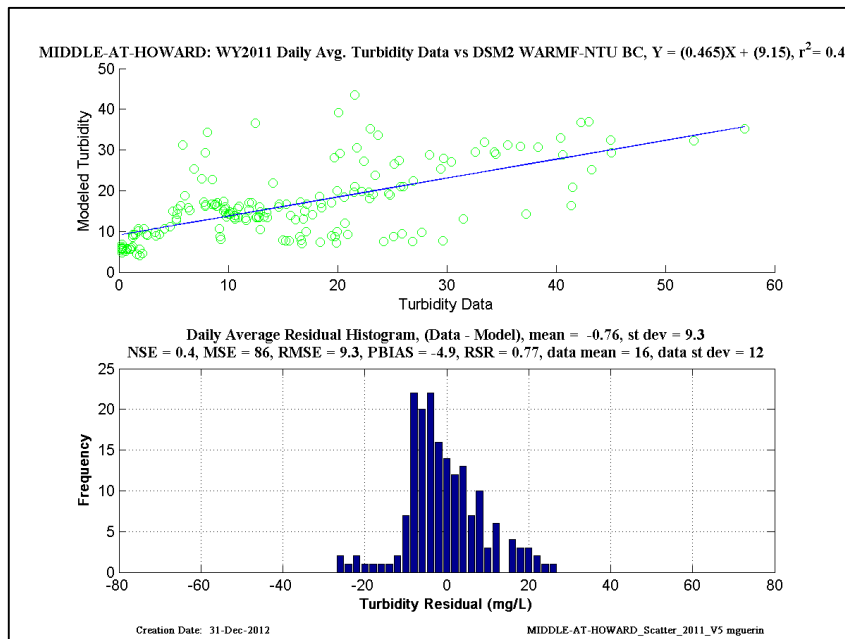
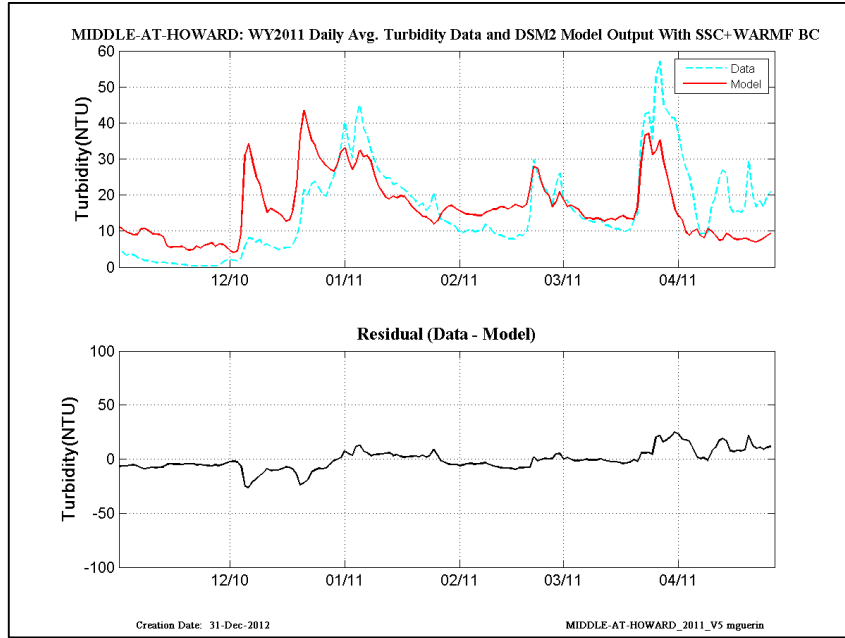


Figure 14-39 WY2011: DSM2 daily-averaged turbidity model results using Mixed-SSC-WARMF turbidity at the inflow boundaries– location is Middle River at Howard.

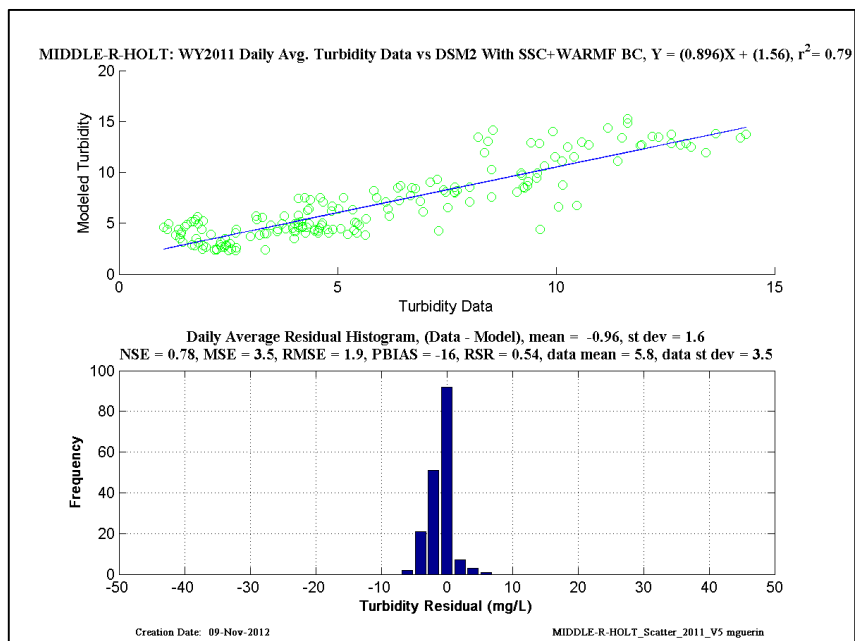
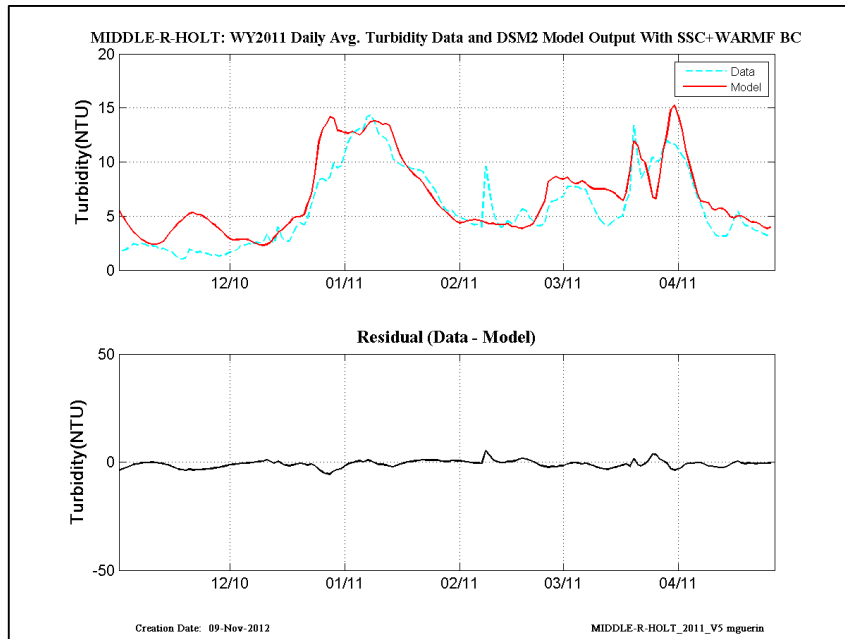


Figure 14-40 WY2011: DSM2 daily-averaged turbidity model results using Mixed-SSC-WARMF turbidity at the inflow boundaries– location is Middle River at Holt.

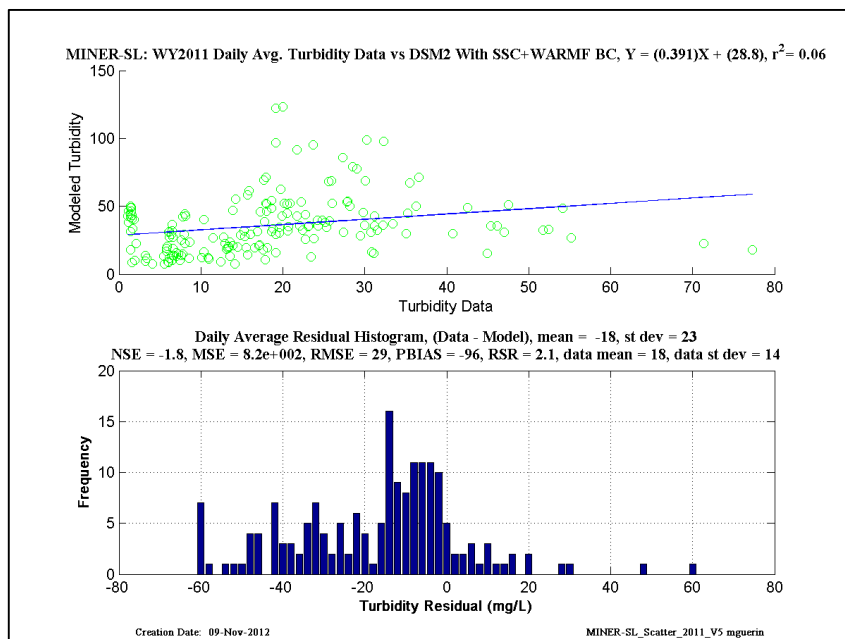
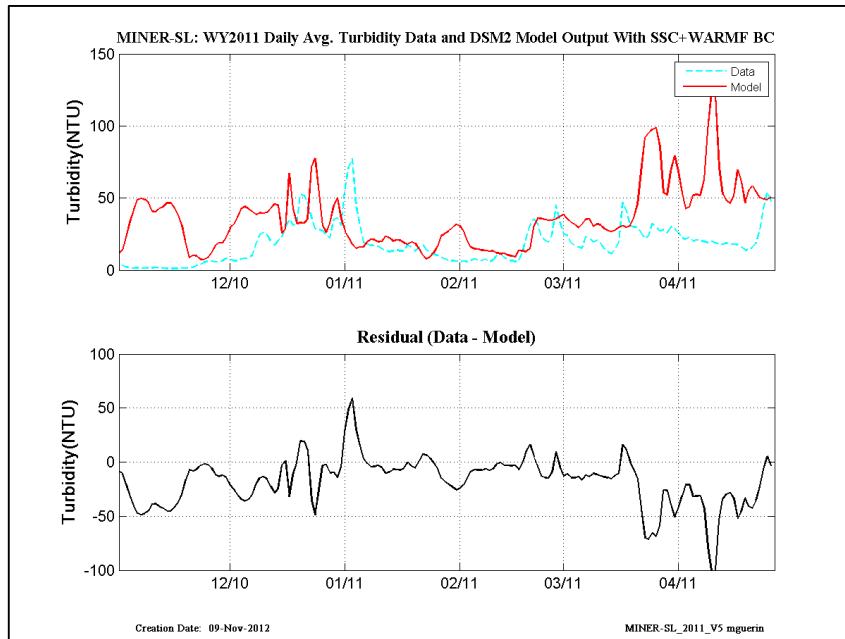


Figure 14-41 WY2011: DSM2 daily-averaged turbidity model results using Mixed-SSC-WARMF turbidity at the inflow boundaries– location is Miner Slough.

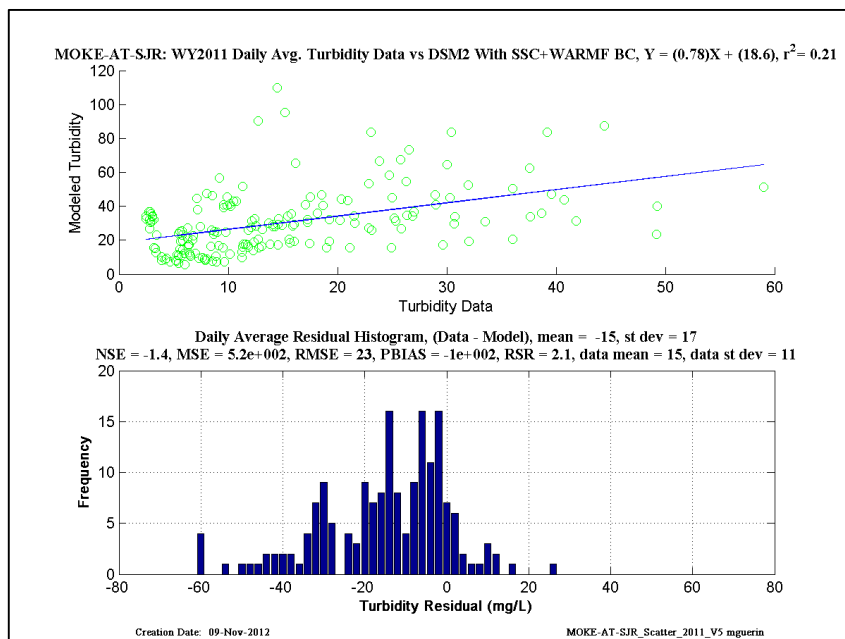
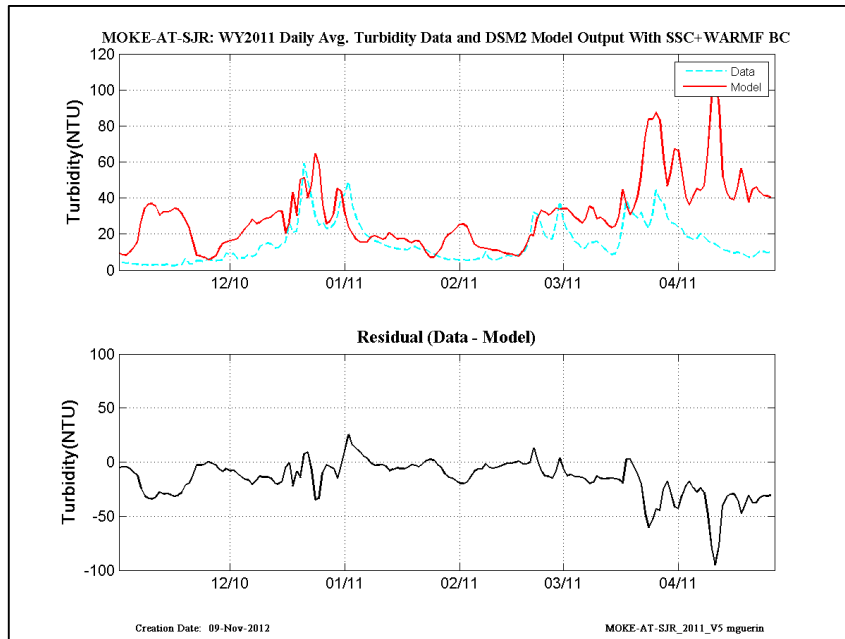


Figure 14-42 WY2011: DSM2 daily-averaged turbidity model results using Mixed-SSC-WARMF turbidity at the inflow boundaries– location is Mokelumne at San Joaquin River.

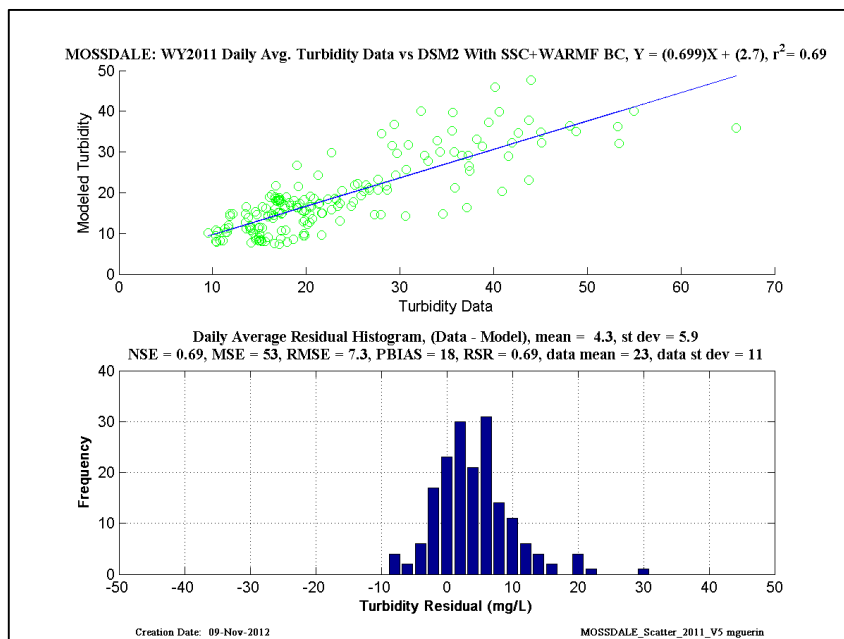
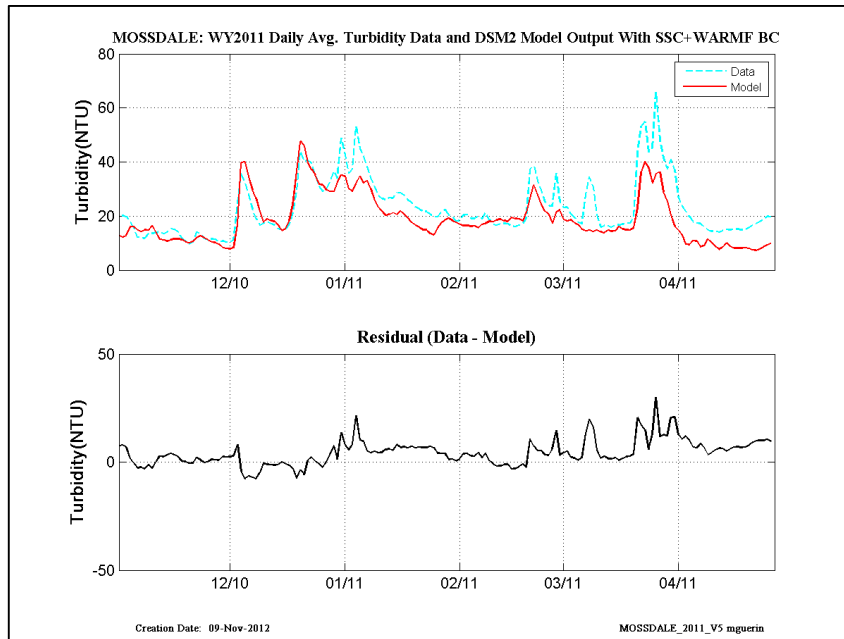


Figure 14-43 WY2011: DSM2 daily-averaged turbidity model results using Mixed-SSC-WARMF turbidity at the inflow boundaries– location is Mossdale.

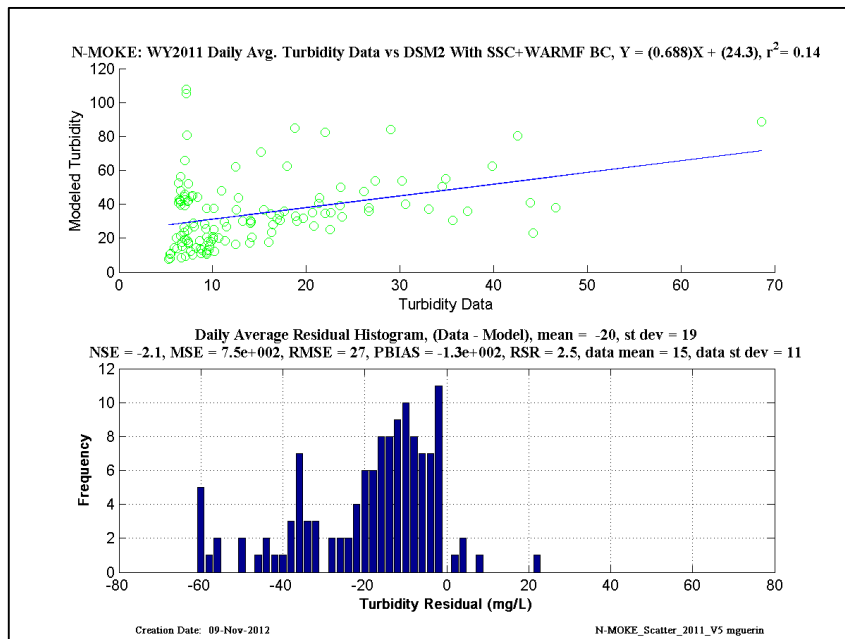
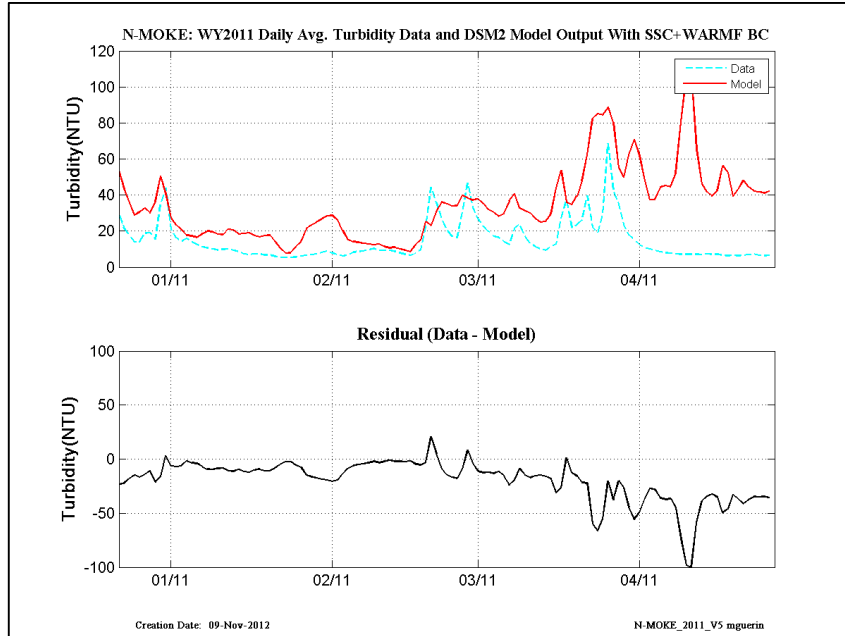


Figure 14-44 WY2011: DSM2 daily-averaged turbidity model results using Mixed-SSC-WARMF turbidity at the inflow boundaries– location is North Mokelumne.

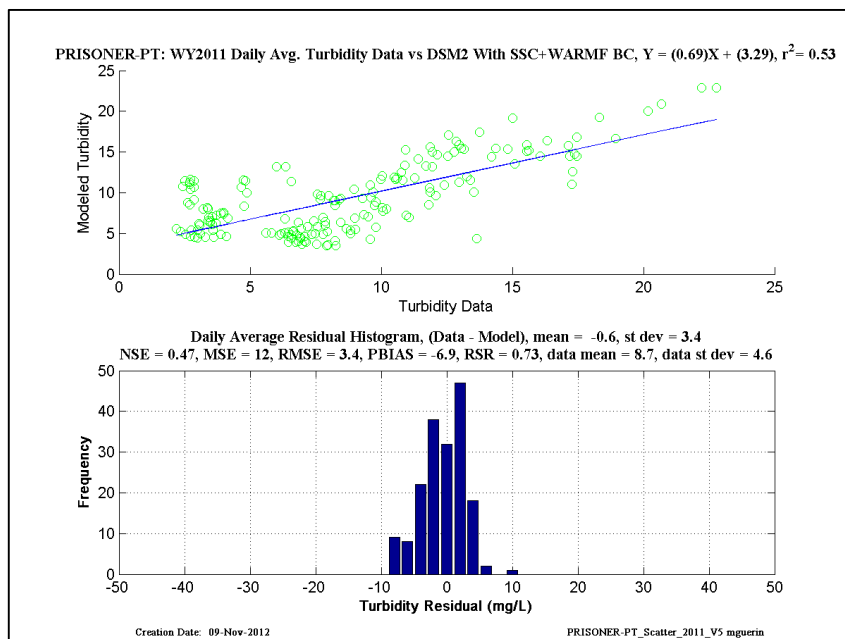
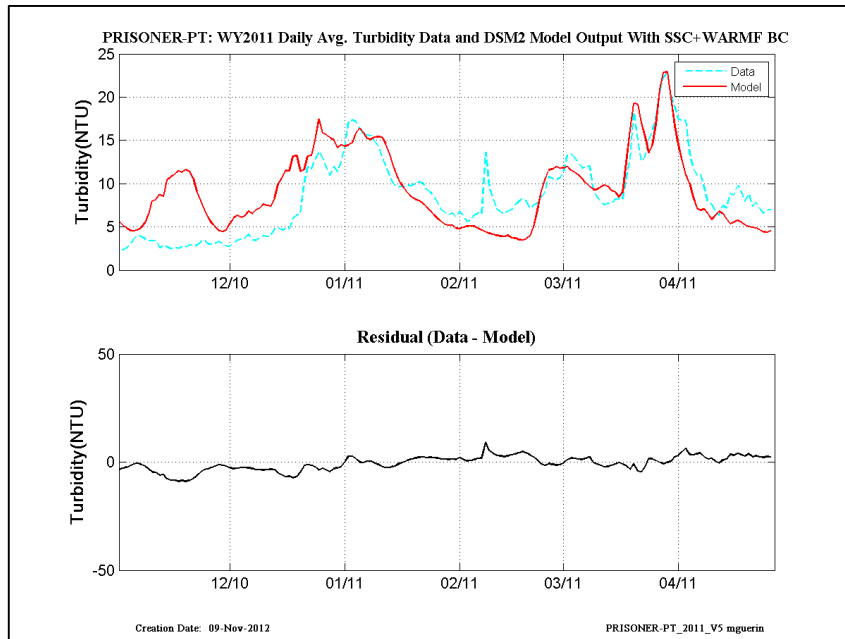


Figure 14-45 WY2011: DSM2 daily-averaged turbidity model results using Mixed-SSC-WARMF turbidity at the inflow boundaries– location is Prisoner Point.

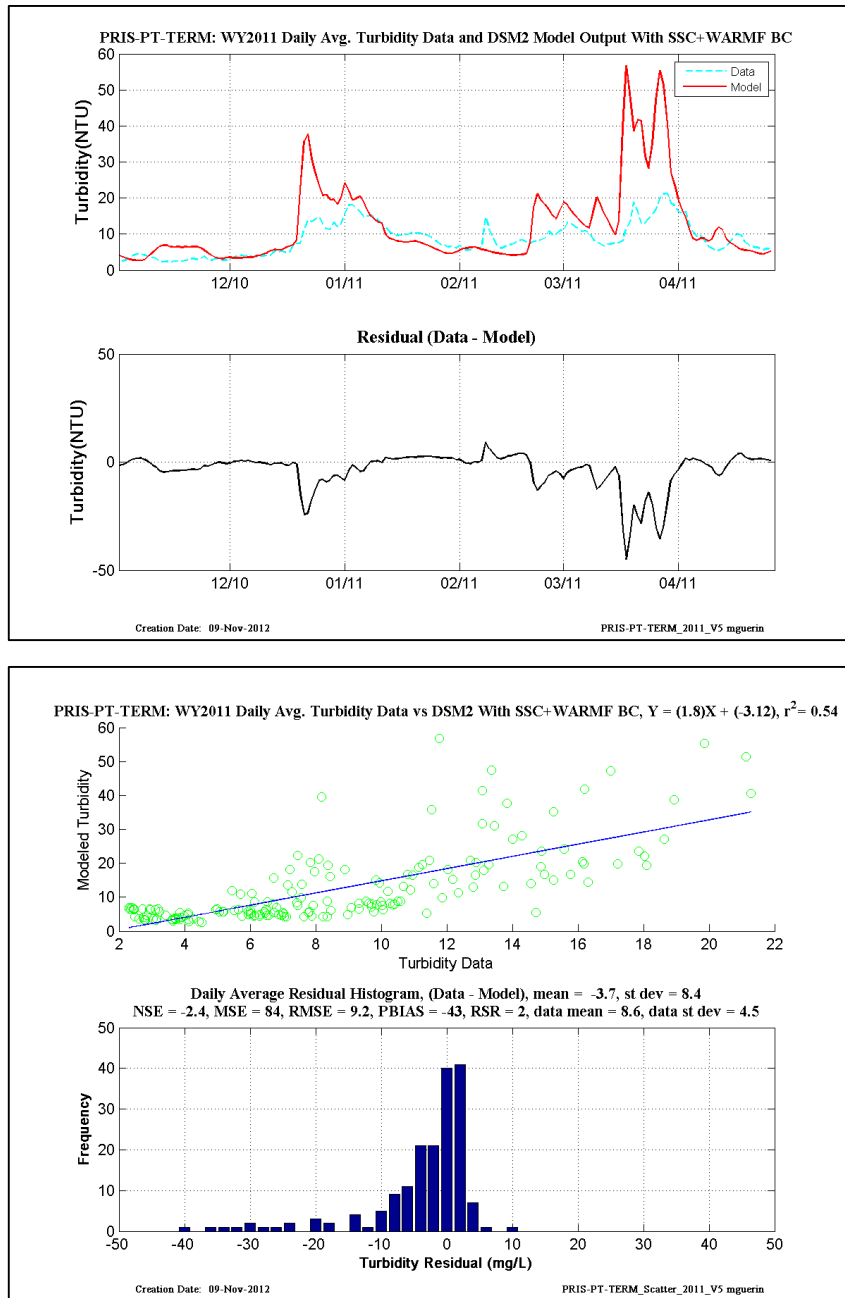


Figure 14-46 WY2011: DSM2 daily-averaged turbidity model results using Mixed-SSC-WARMF turbidity at the inflow boundaries– location is Prisoner Point at Terminous.

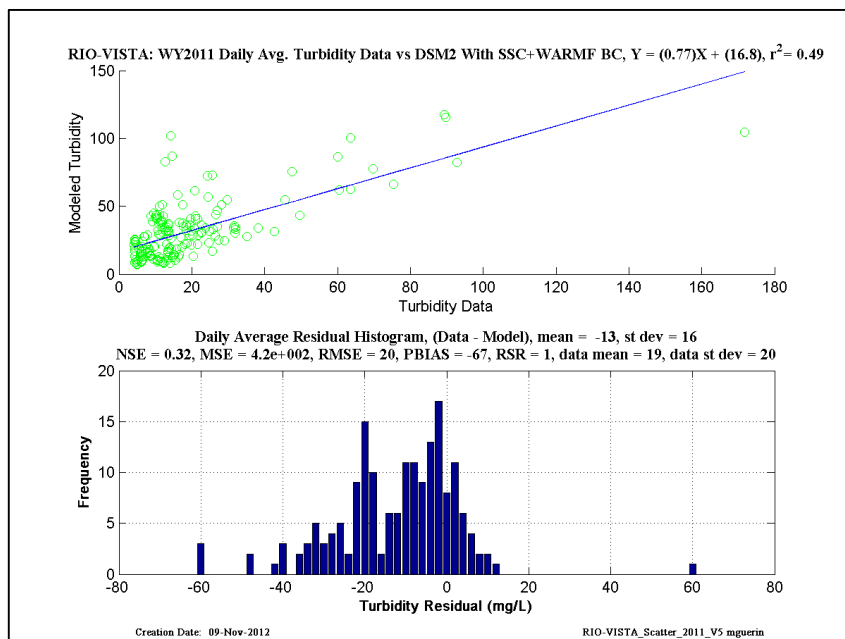
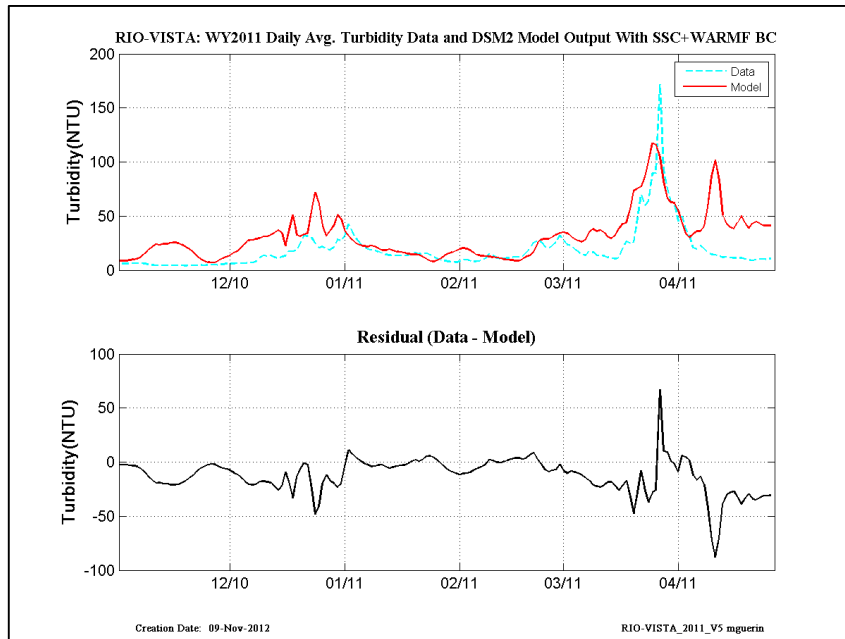


Figure 14-47 WY2011: DSM2 daily-averaged turbidity model results using Mixed-SSC-WARMF turbidity at the inflow boundaries– location is Rio Vista.

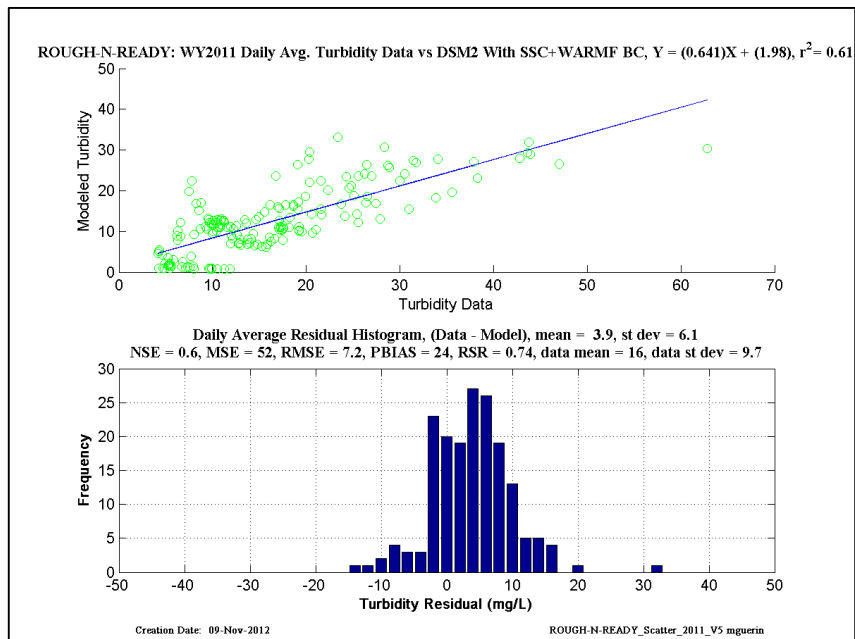
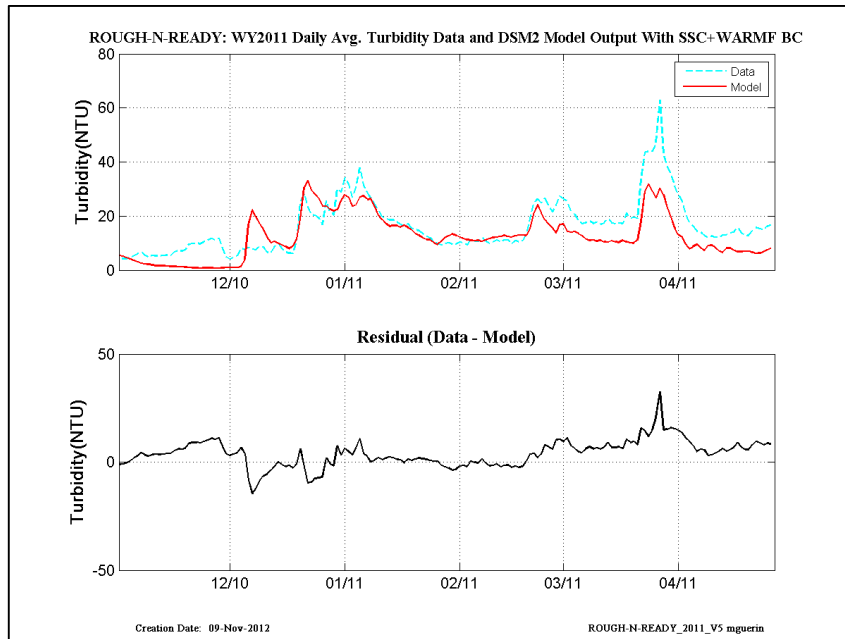


Figure 14-48 WY2011: DSM2 daily-averaged turbidity model results using Mixed-SSC-WARMF turbidity at the inflow boundaries– location is Rough-N-Ready Island.

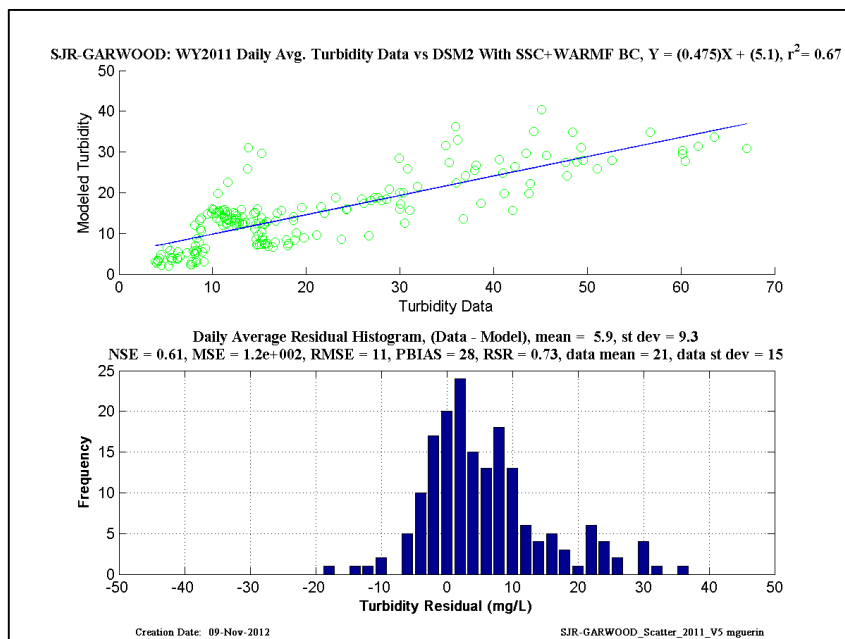
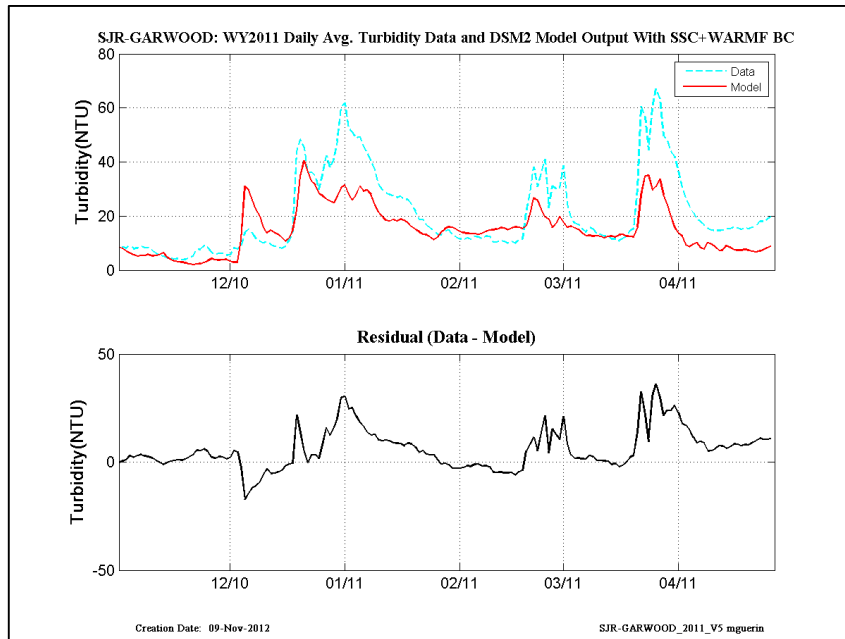


Figure 14-49 WY2011: DSM2 daily-averaged turbidity model results using Mixed-SSC-WARMF turbidity at the inflow boundaries– location is San Joaquin at Garwood.

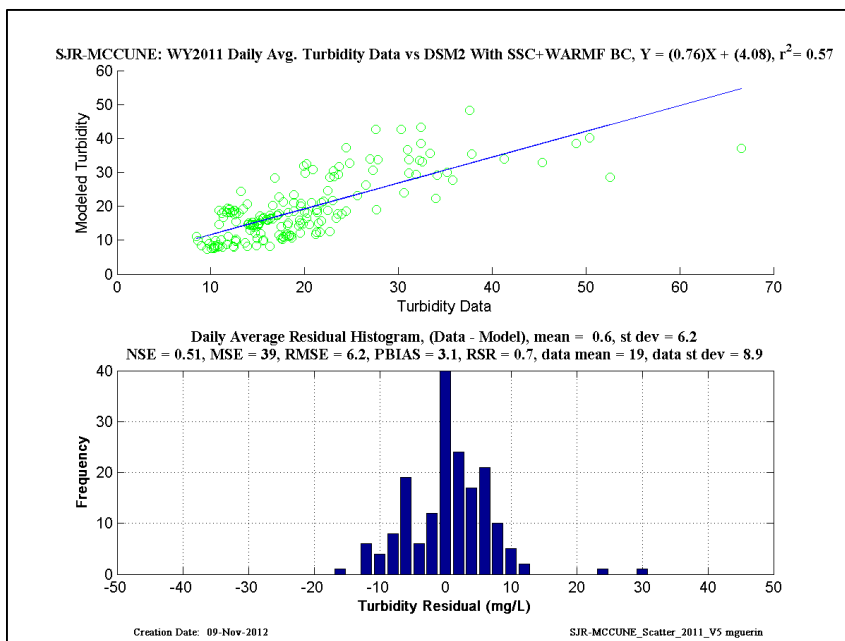
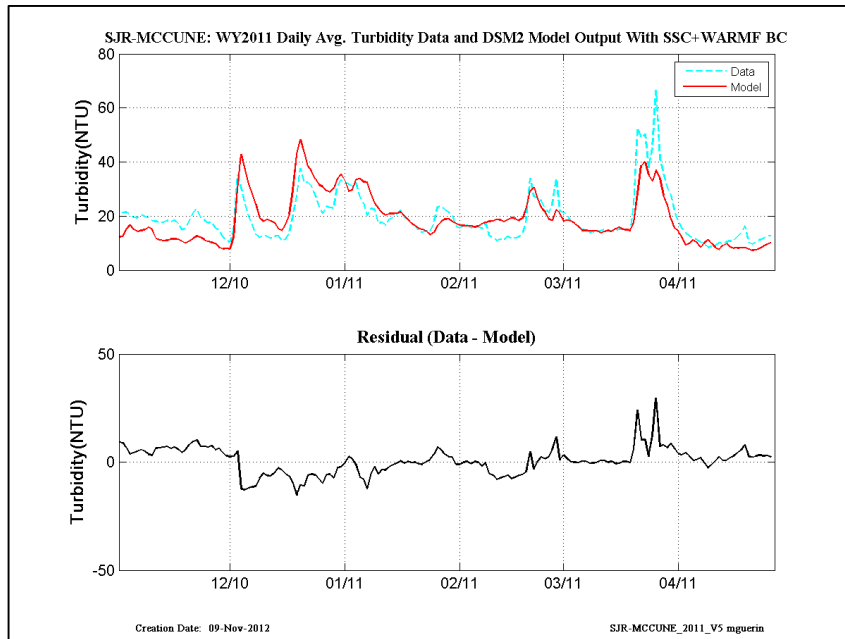


Figure 14-50 WY2011: DSM2 daily-averaged turbidity model results using Mixed-SSC-WARMF turbidity at the inflow boundaries– location is San Joaquin at McCune.

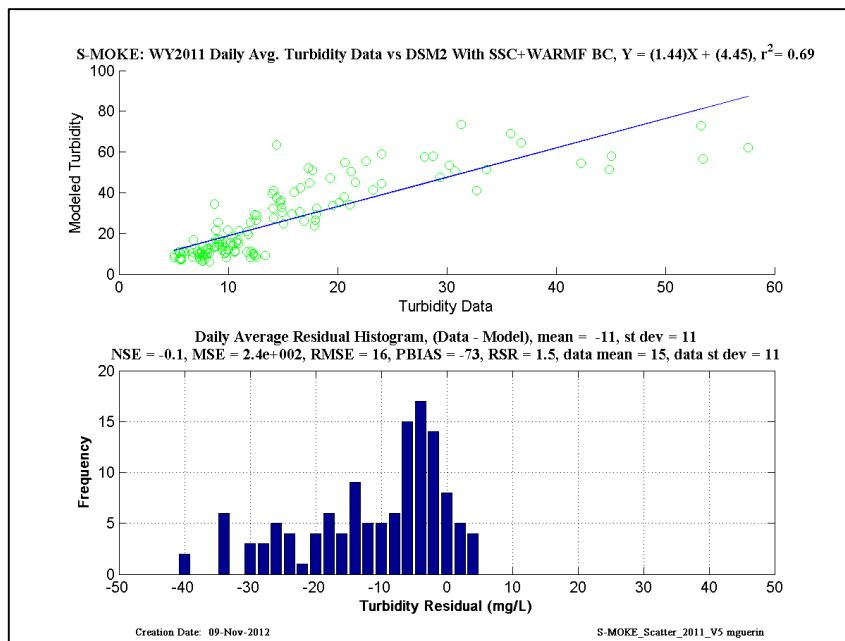
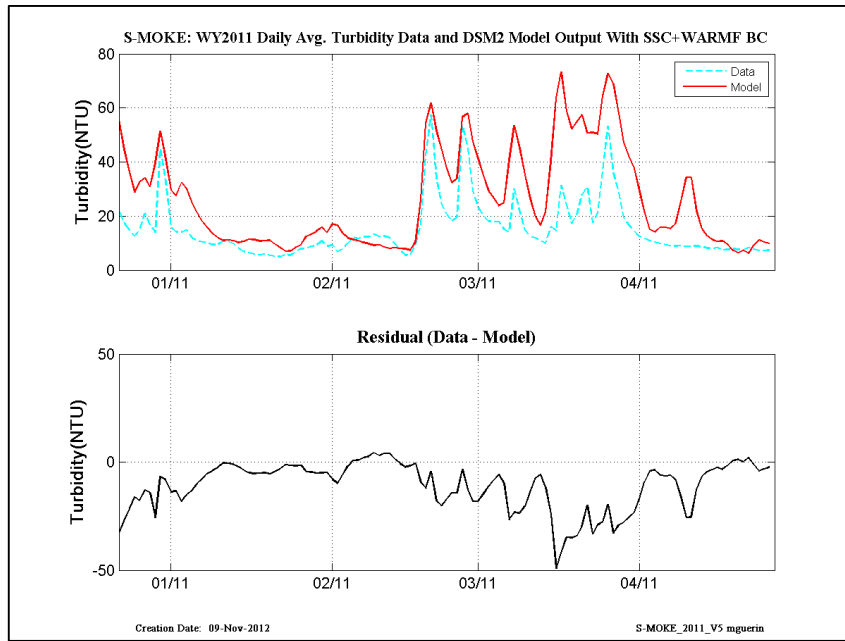


Figure 14-51 WY2011: DSM2 daily-averaged turbidity model results using Mixed-SSC-WARMF turbidity at the inflow boundaries– location is South Mokelumne.

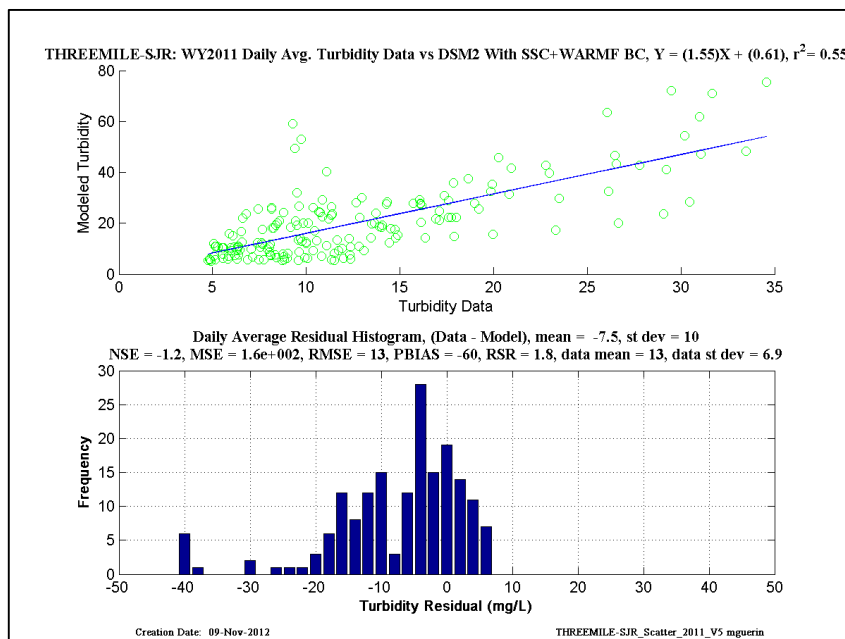
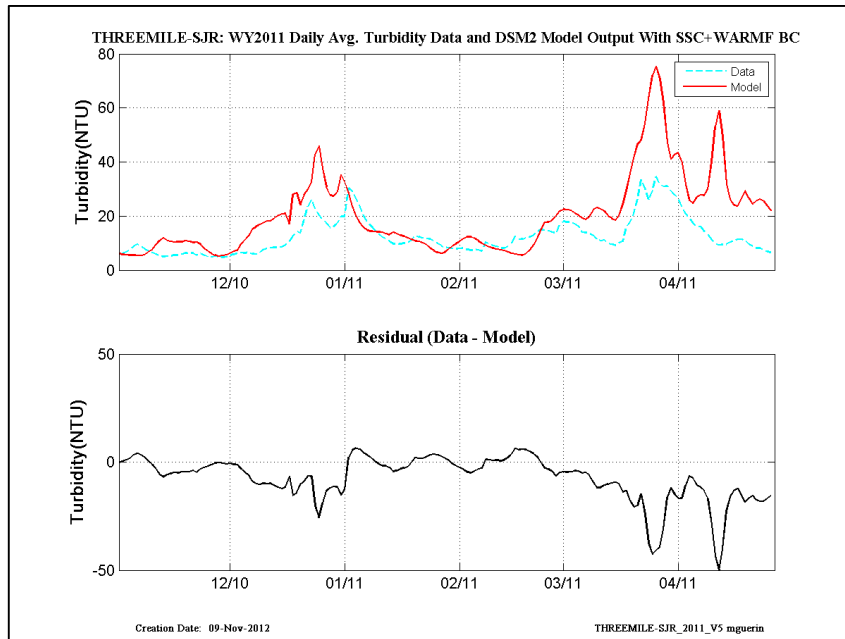


Figure 14-52 WY2011: DSM2 daily-averaged turbidity model results using Mixed-SSC-WARMF turbidity at the inflow boundaries– location is Threemile at San Joaquin.

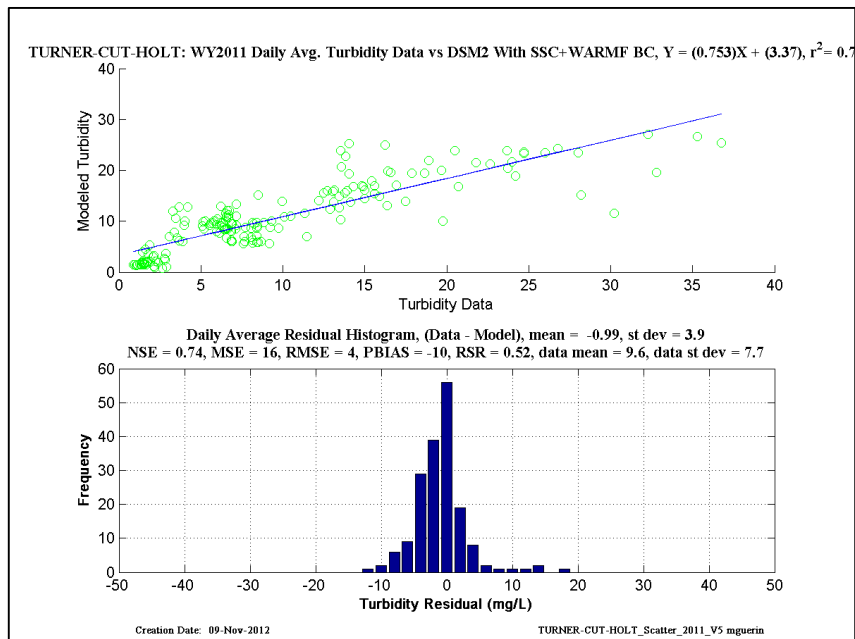
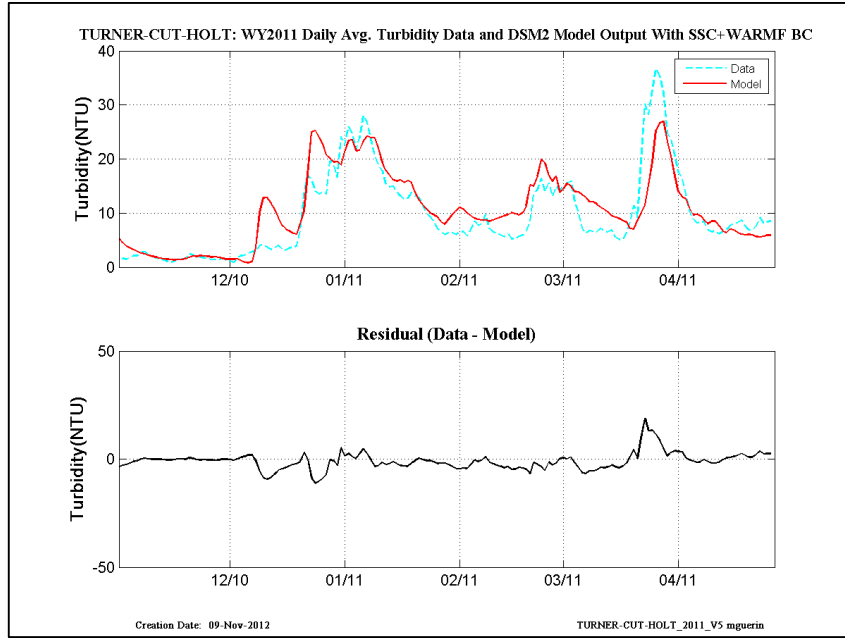


Figure 14-53 WY2011: DSM2 daily-averaged turbidity model results using Mixed-SSC-WARMF turbidity at the inflow boundaries– location is Turner Cut at Holt.

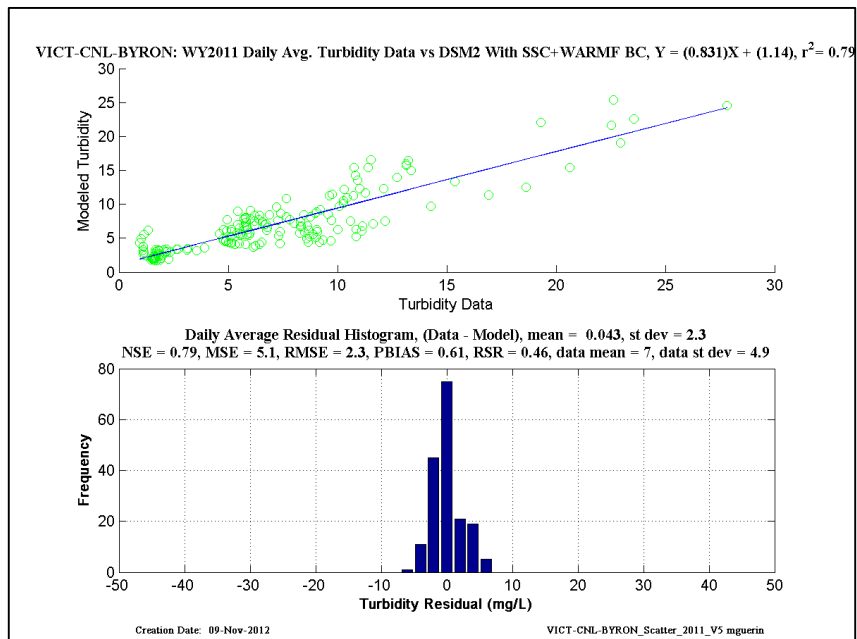
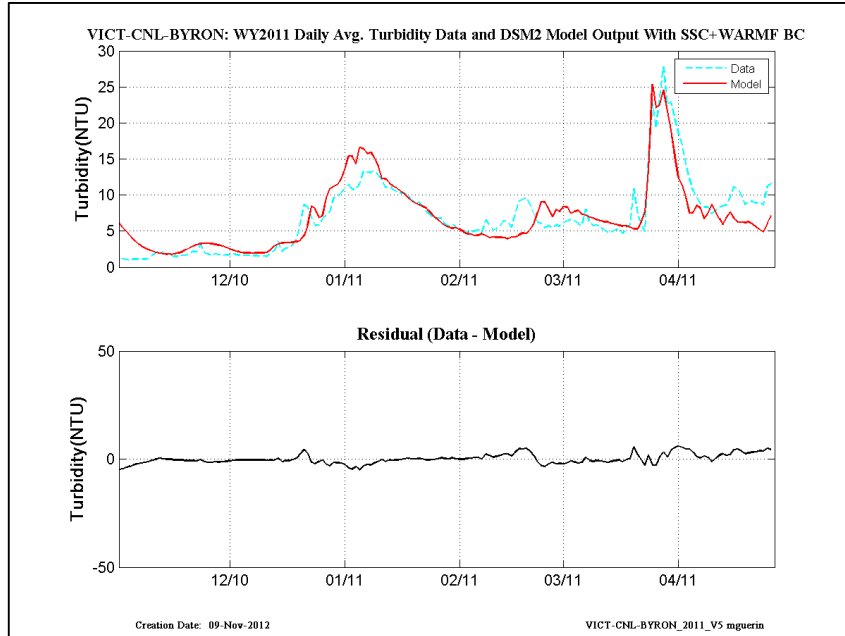


Figure 14-54 WY2011: DSM2 daily-averaged turbidity model results using Mixed-SSC-WARMF turbidity at the inflow boundaries– location is Victoria Canal at Byron.

15.3 WY2010 WARMF-Only results

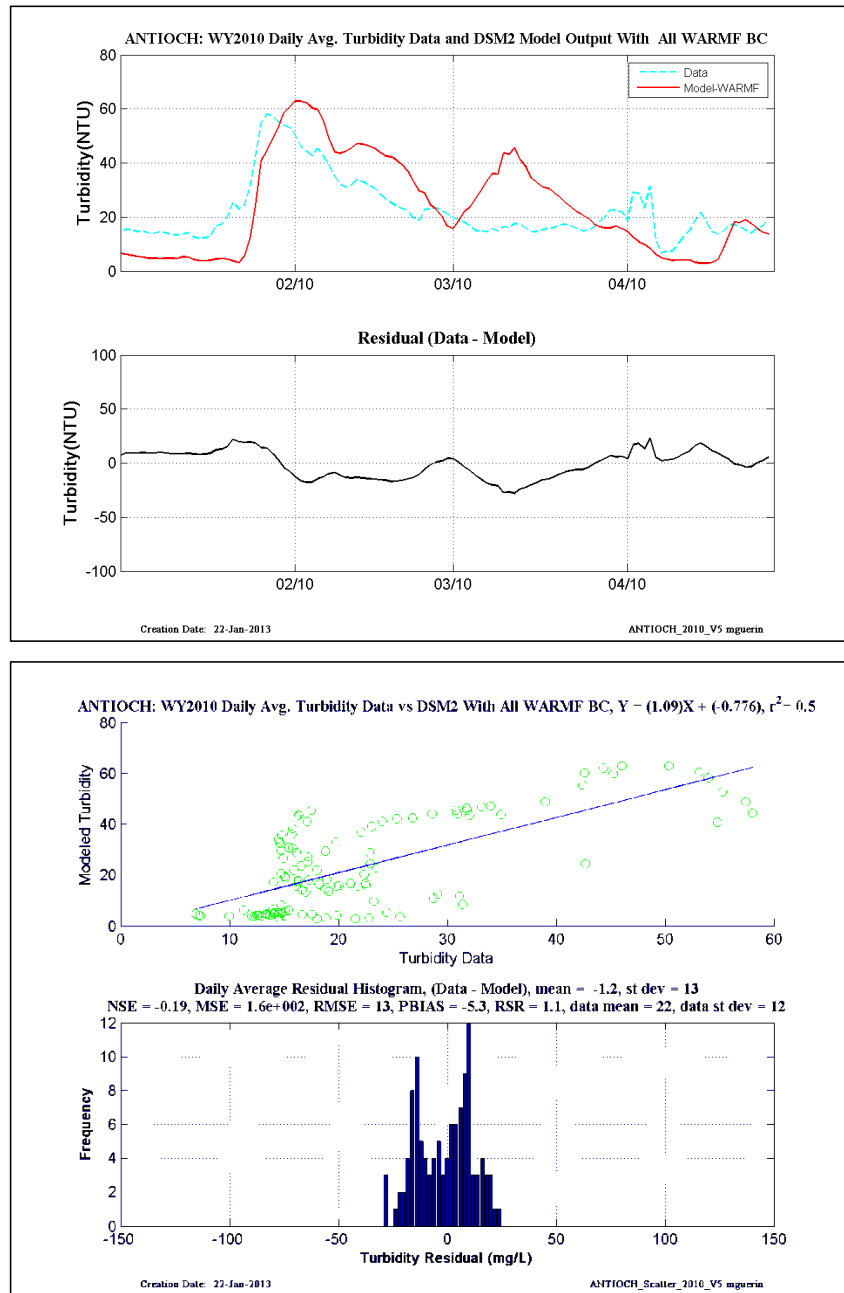


Figure 14-55 WY2010: WY2010: DSM2 daily-averaged turbidity model results using WARMF-Only turbidity at the inflow boundaries– location is Antioch.

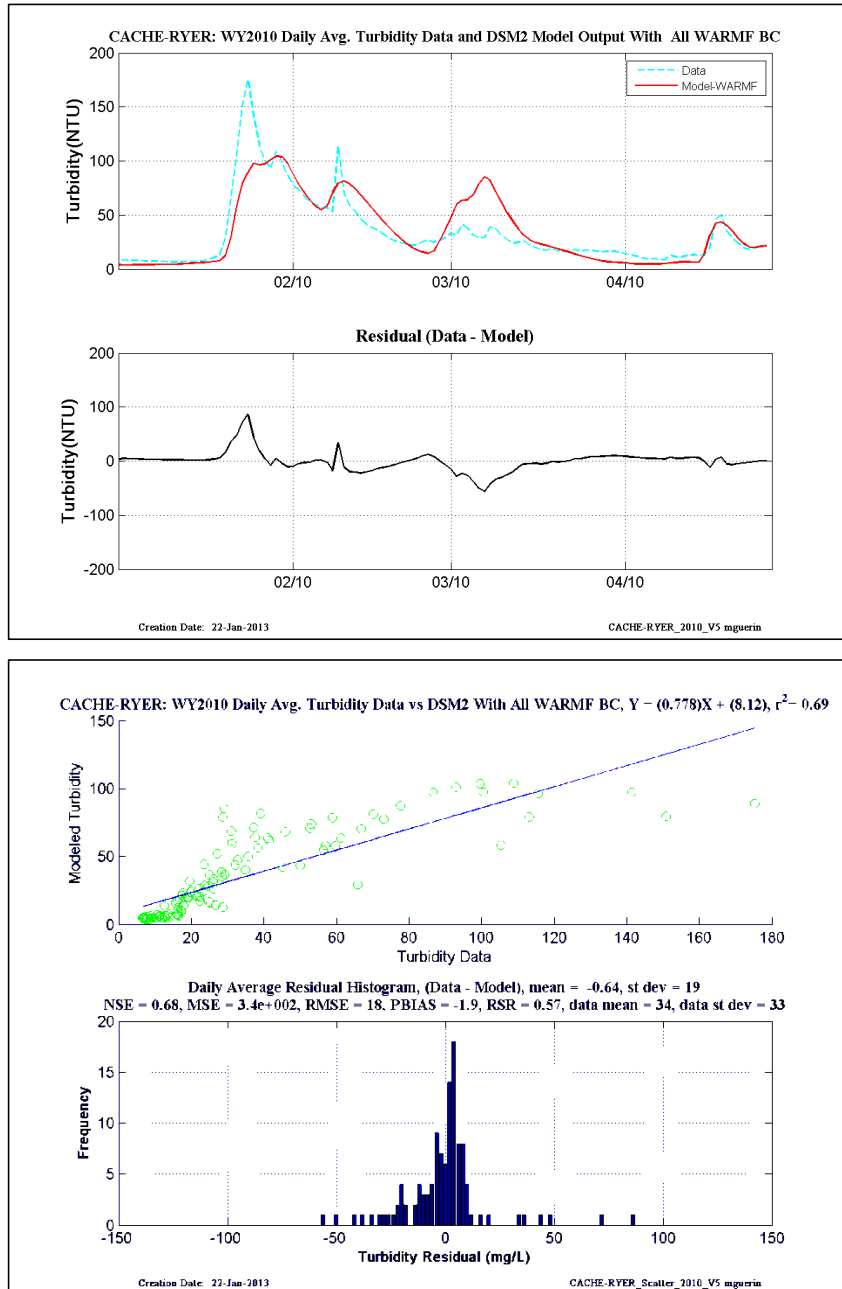


Figure 14-56 WY2010: WY2010: DSM2 daily-averaged turbidity model results using WARMF-Only turbidity at the inflow boundaries– location is Cache-at-Ryer.

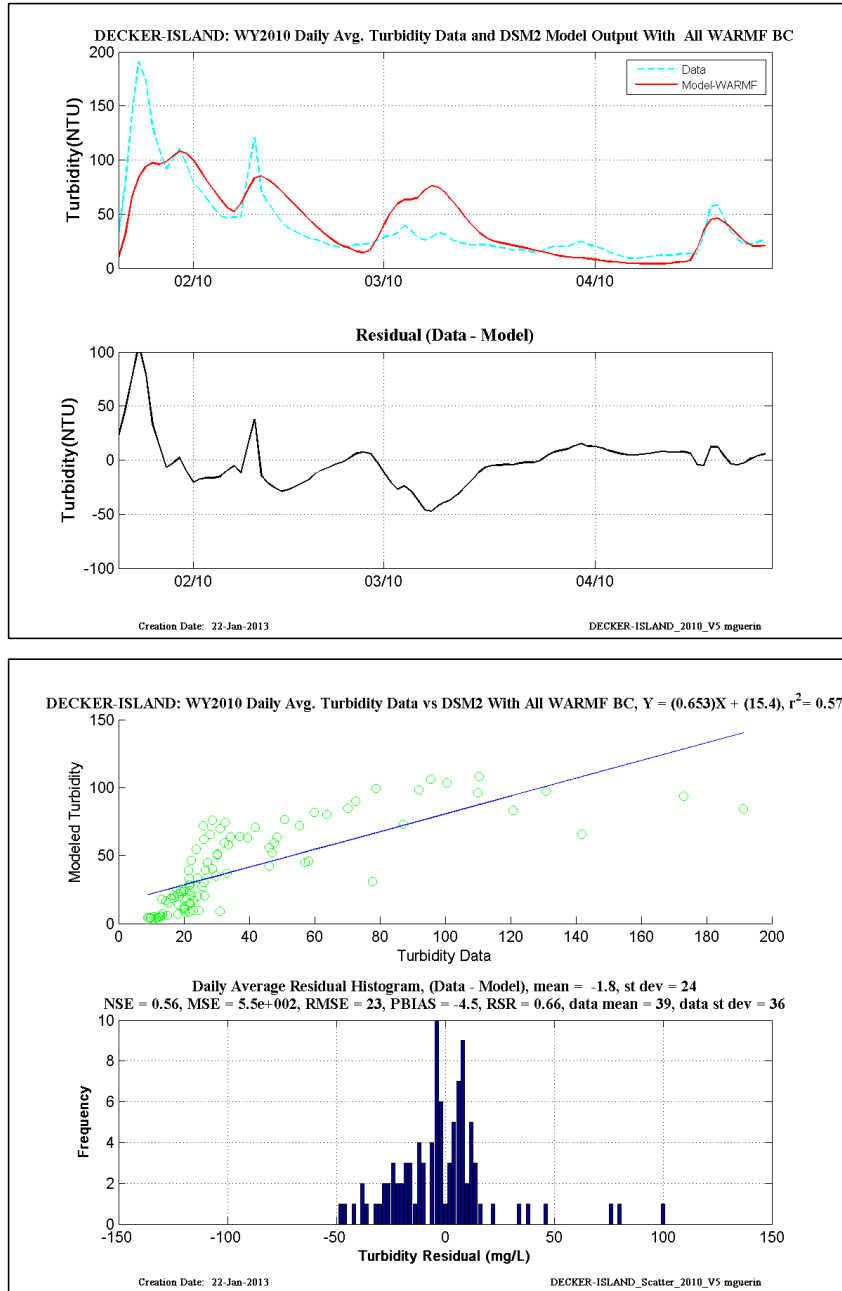


Figure 14-57 WY2010: WY2010: DSM2 daily-averaged turbidity model results using WARMF-Only turbidity at the inflow boundaries— location is Decker-Island.

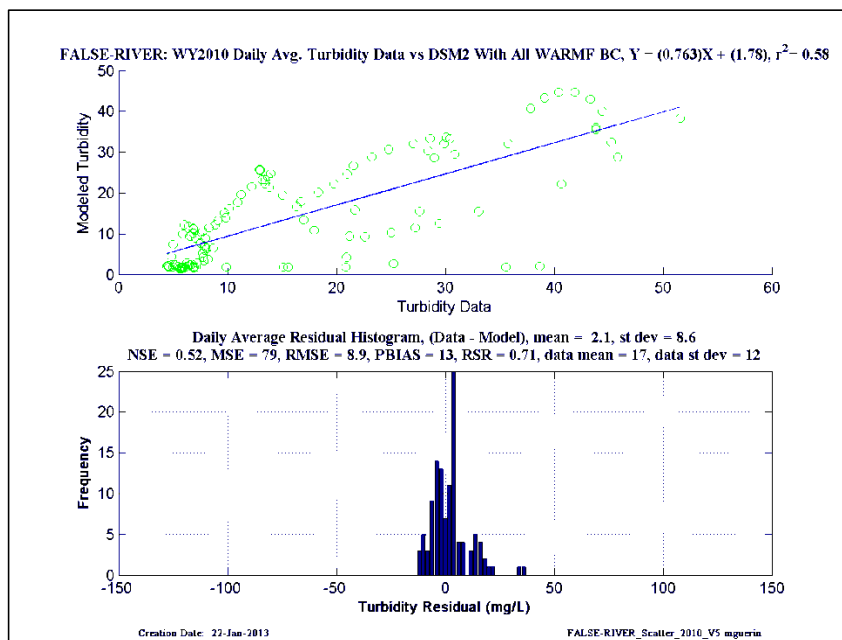
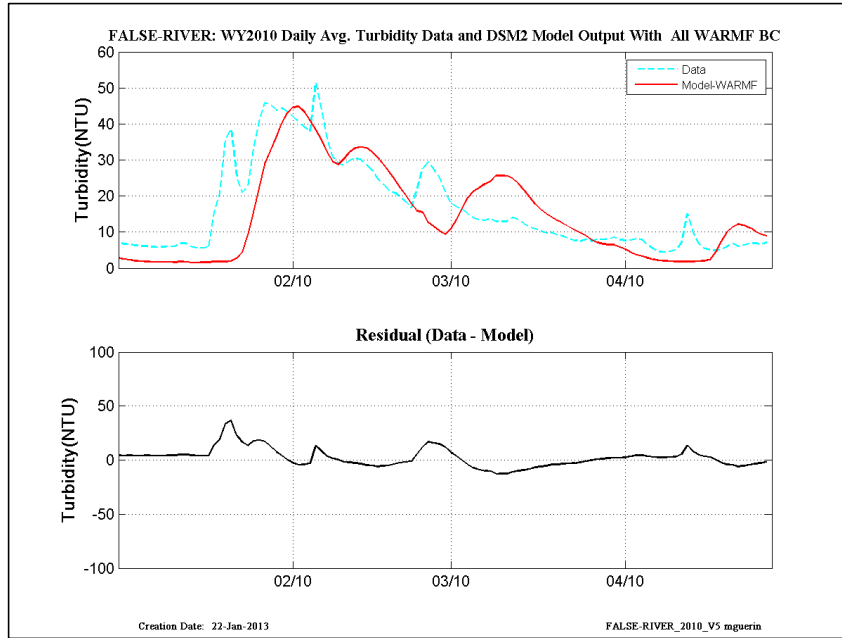


Figure 14-58 WY2010: DSM2 daily-averaged turbidity model results using WARMF-Only turbidity at the inflow boundaries— location is False-River.

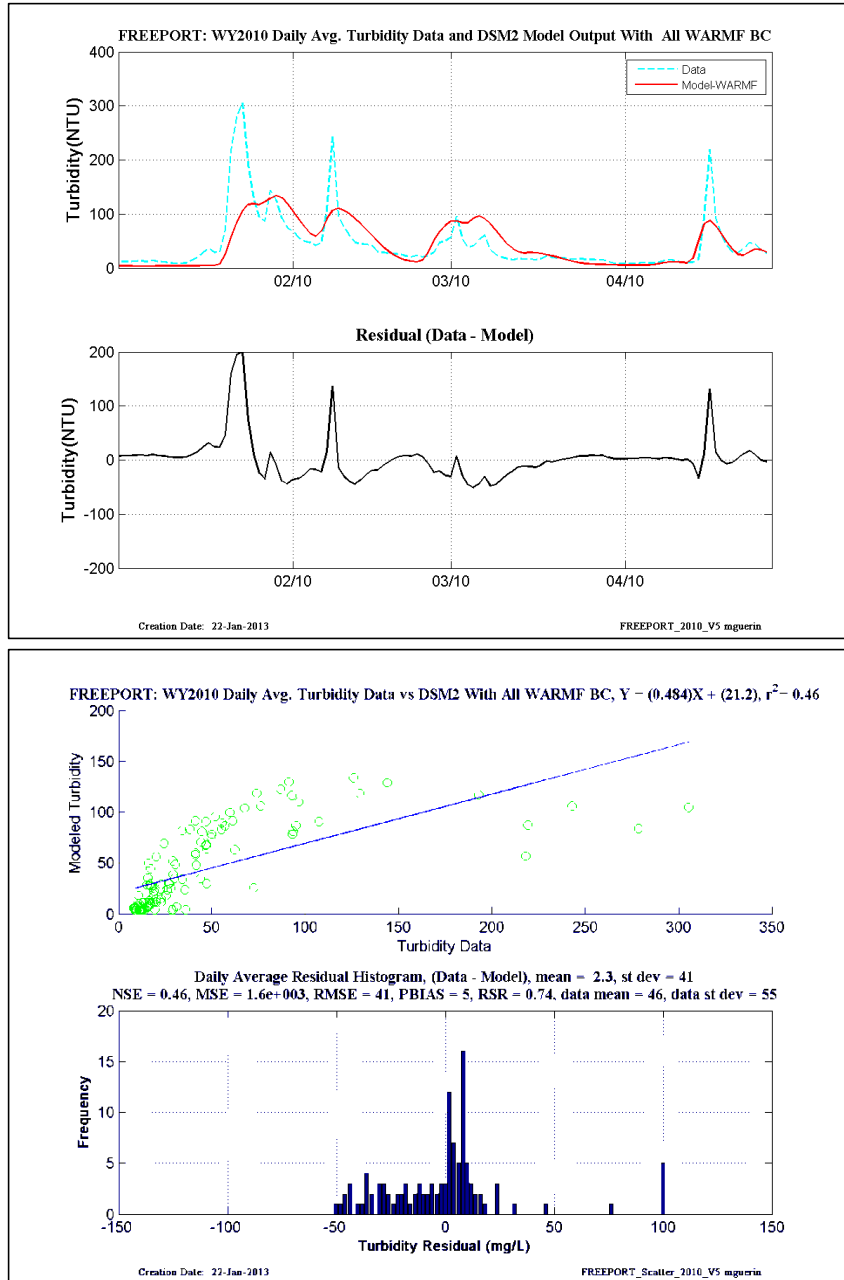


Figure 14-59 WY2010: DSM2 daily-averaged turbidity model results using WARMF-Only turbidity at the inflow boundaries– location is Freeport.

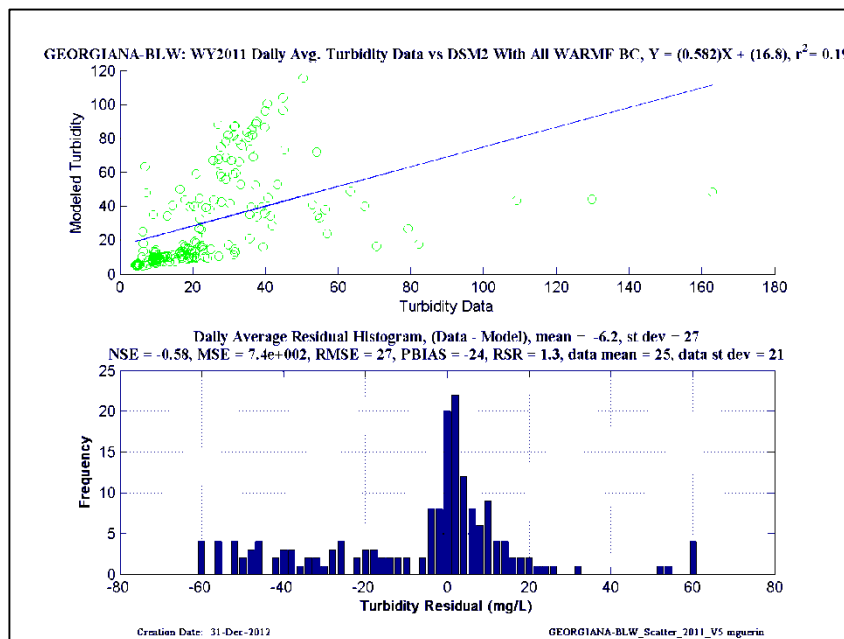
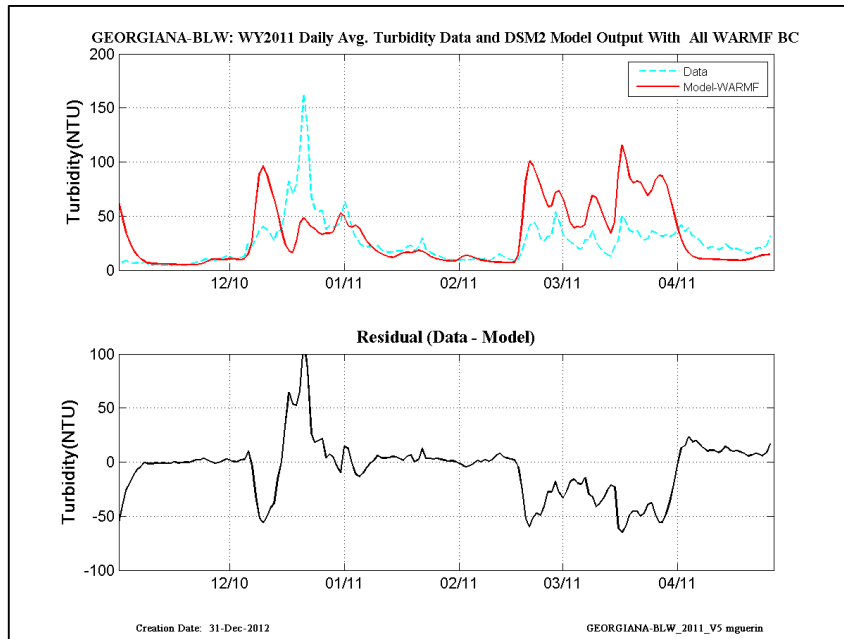


Figure 14-60WY2010: DSM2 daily-averaged turbidity model results using WARMF-Only turbidity at the inflow boundaries– location is Georgiana-Below-Sac.

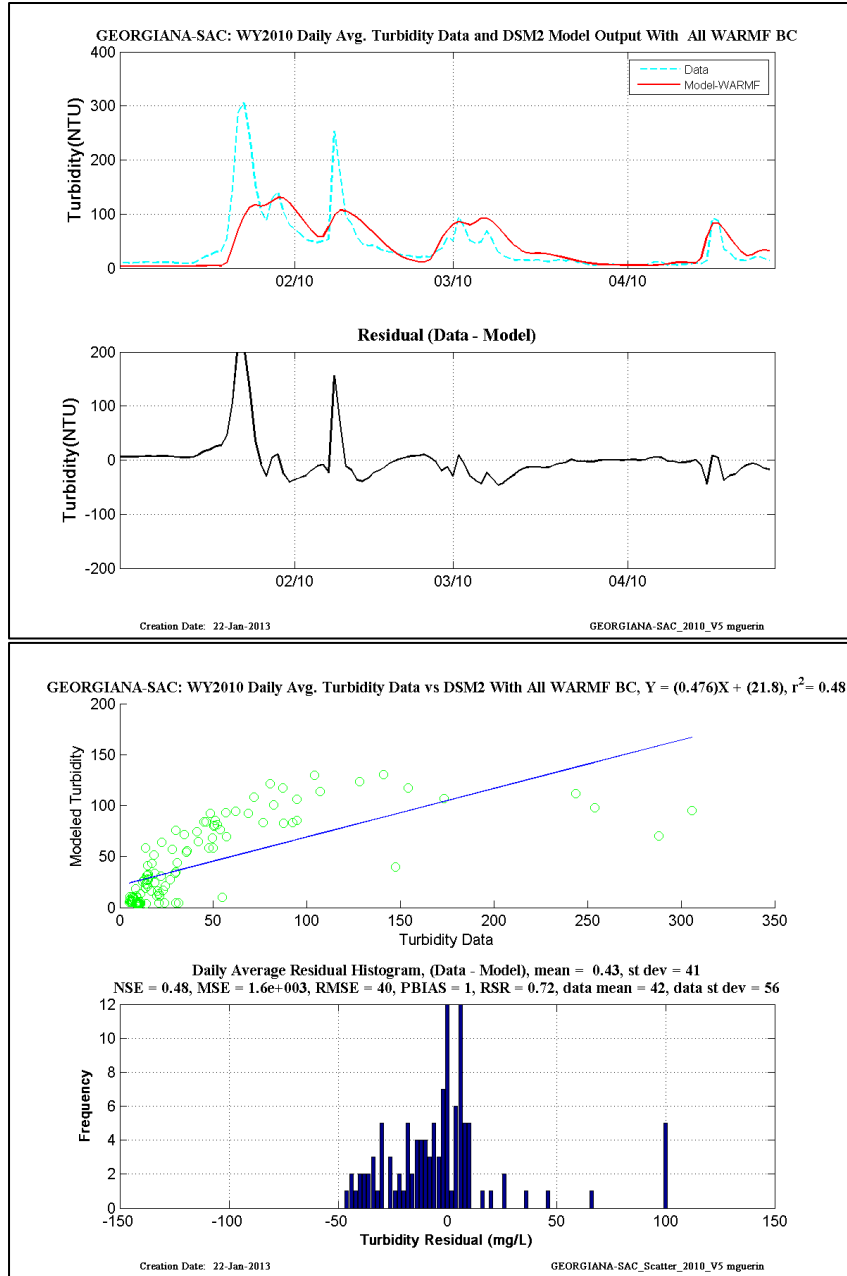


Figure 14-61WY2010: DSM2 daily-averaged turbidity model results using WARMF-Only turbidity at the inflow boundaries– location is Georgiana-Sac.

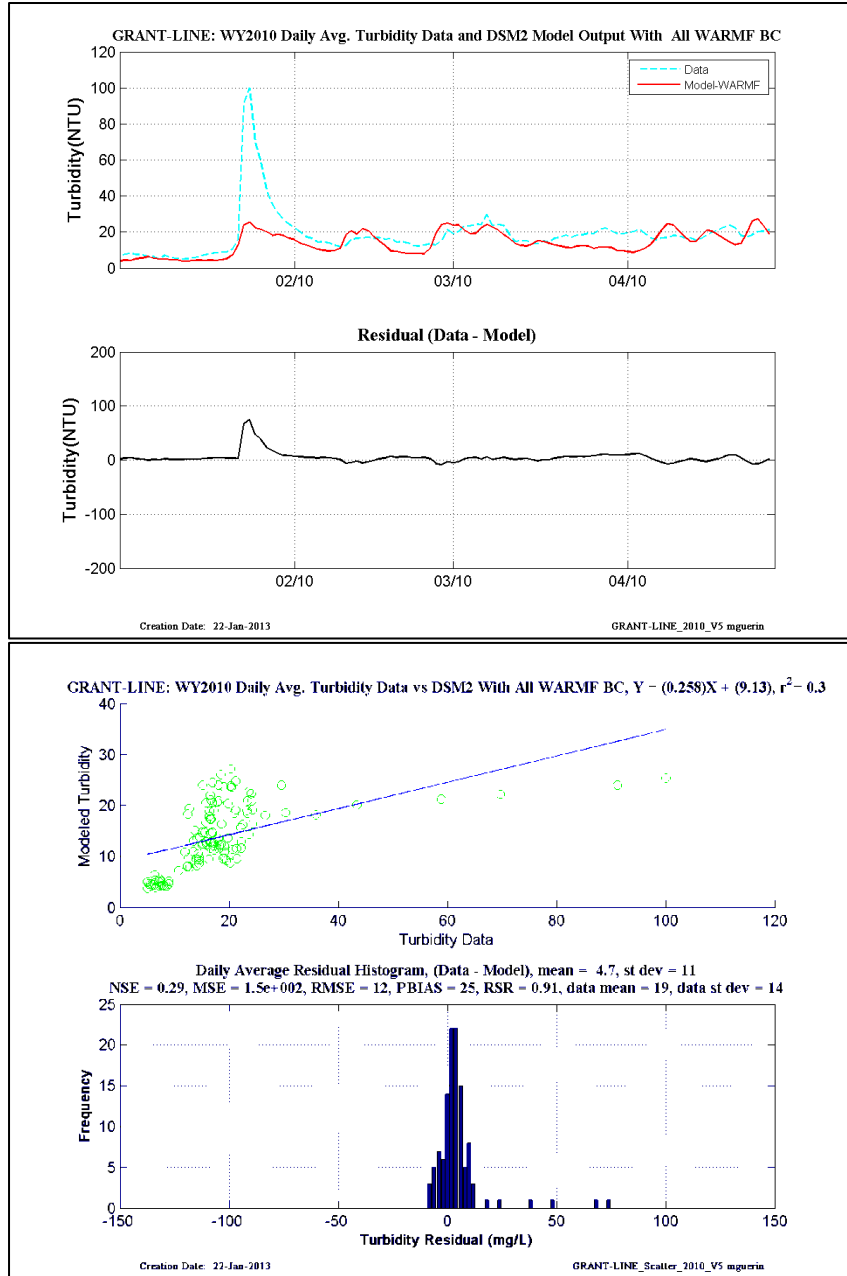


Figure 14-62WY2010: DSM2 daily-averaged turbidity model results using WARMF-Only turbidity at the inflow boundaries– location is Grant-Line.

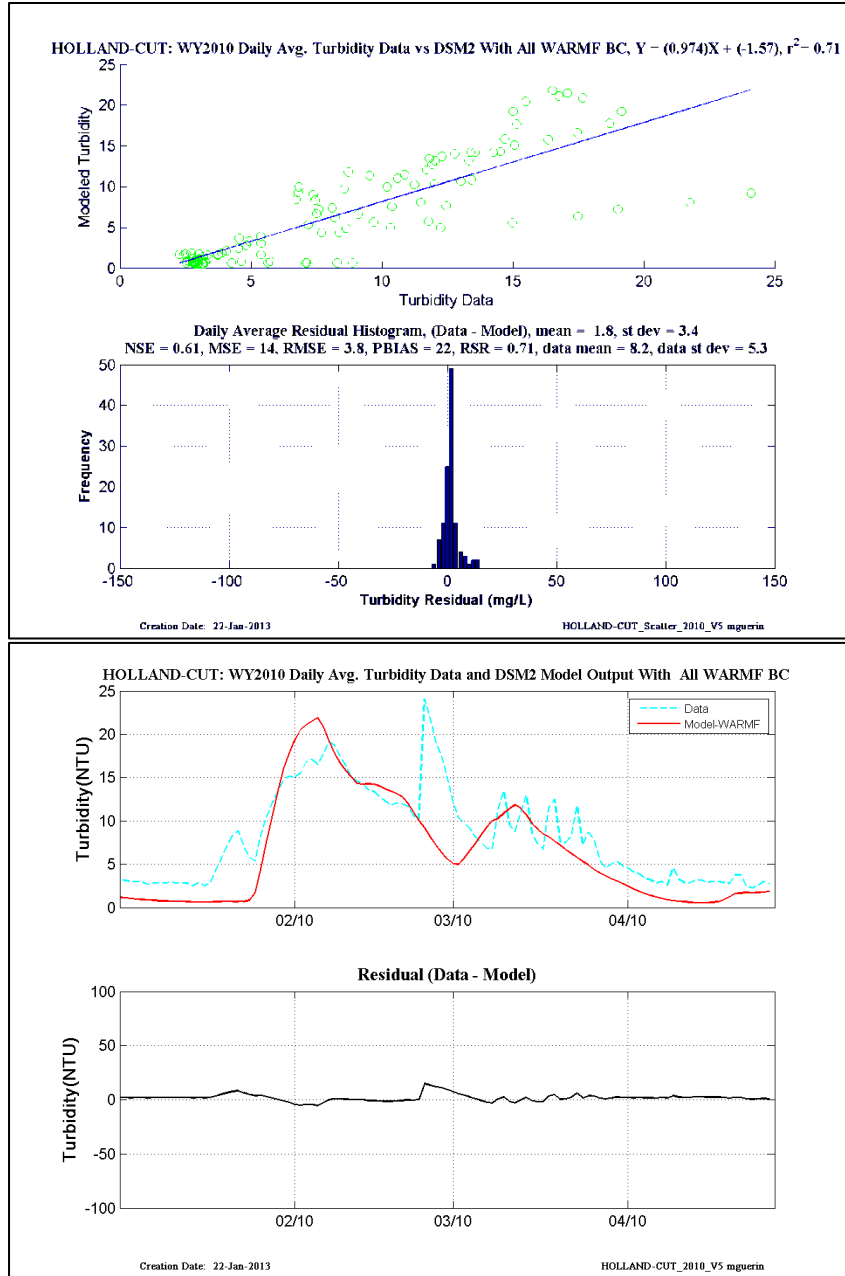


Figure 14-63WY2010: DSM2 daily-averaged turbidity model results using WARMF-Only turbidity at the inflow boundaries– location is Holland-Cut.

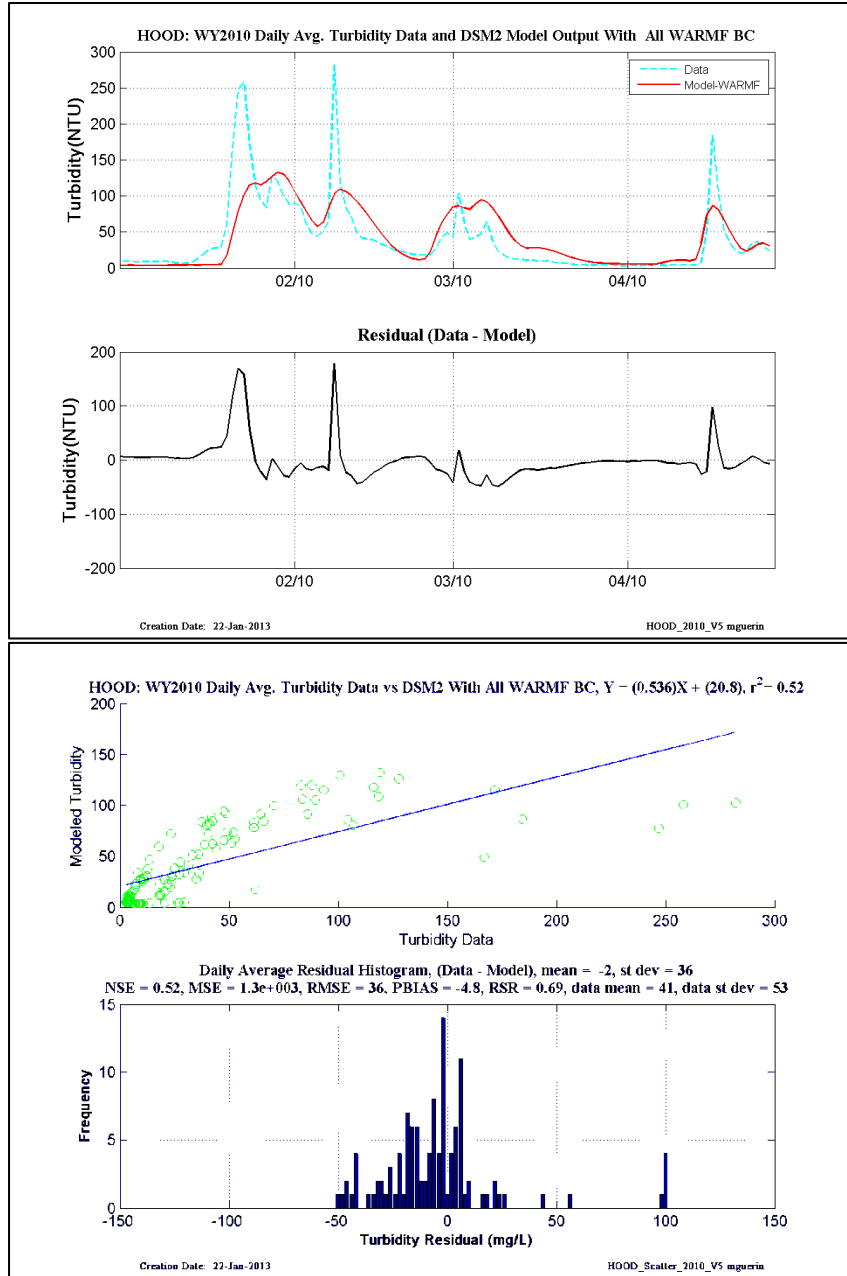


Figure 14-64WY2010: DSM2 daily-averaged turbidity model results using WARMF-Only turbidity at the inflow boundaries– location is Hood.

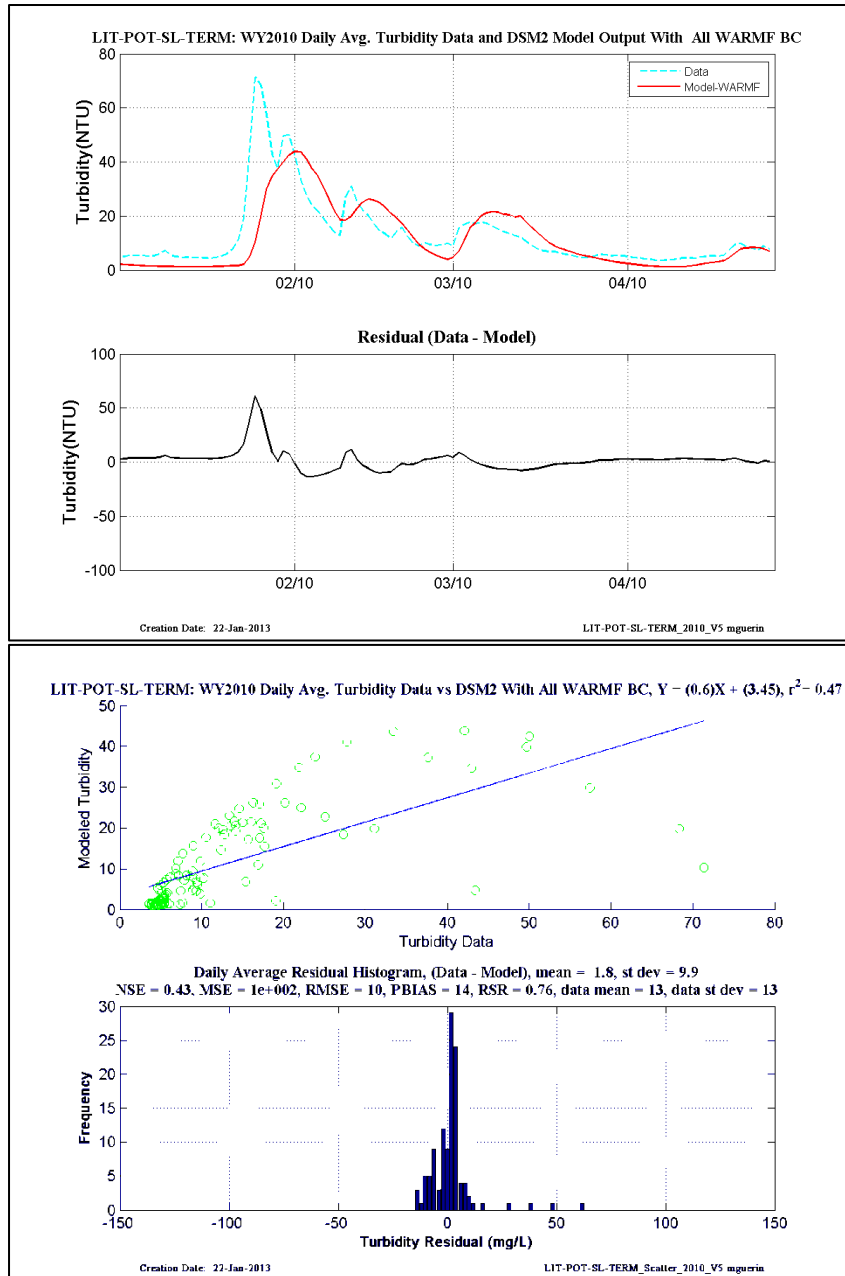


Figure 14-65WY2010: DSM2 daily-averaged turbidity model results using WARMF-Only turbidity at the inflow boundaries– location is Little-Potato-Slough-at-Terminus.

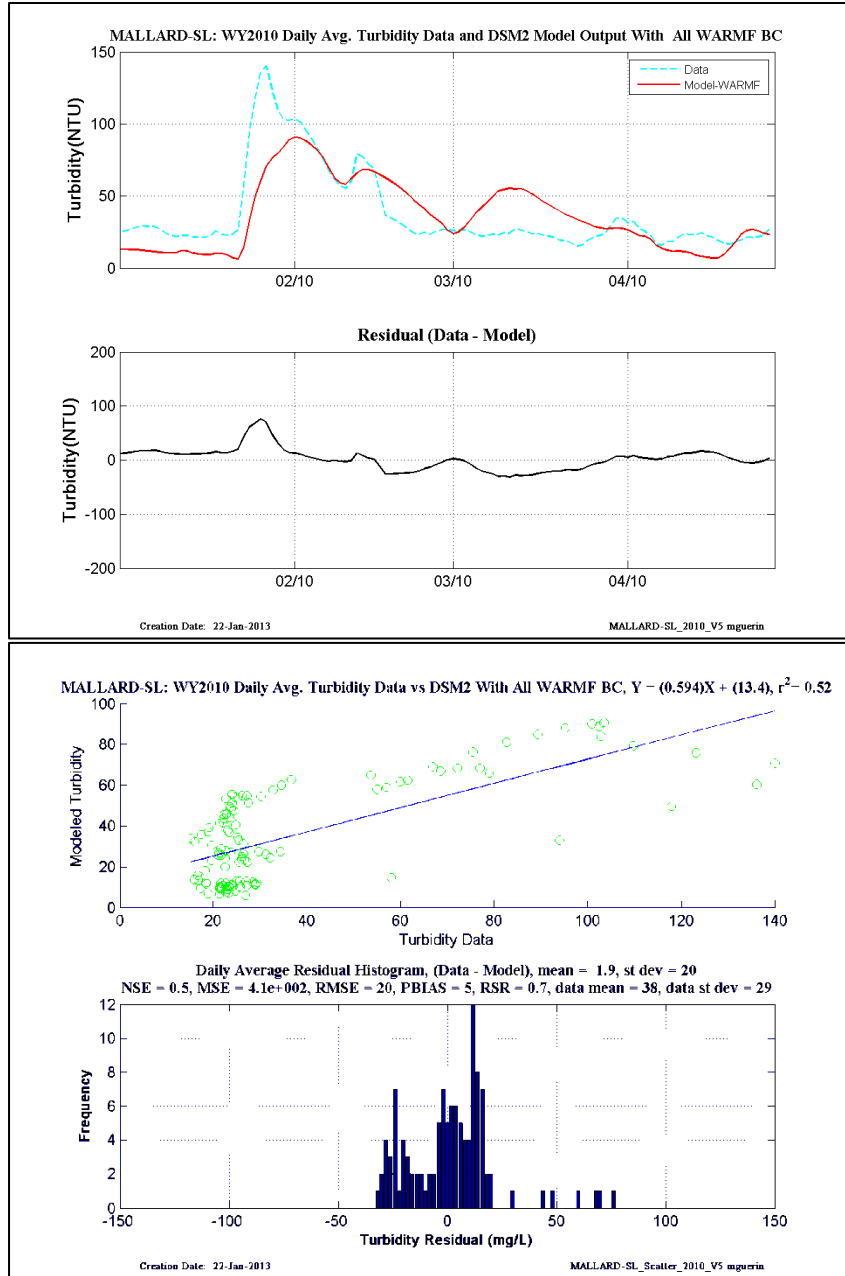


Figure 14-66WY2010: DSM2 daily-averaged turbidity model results using WARMF-Only turbidity at the inflow boundaries– location is Mallard Slough.

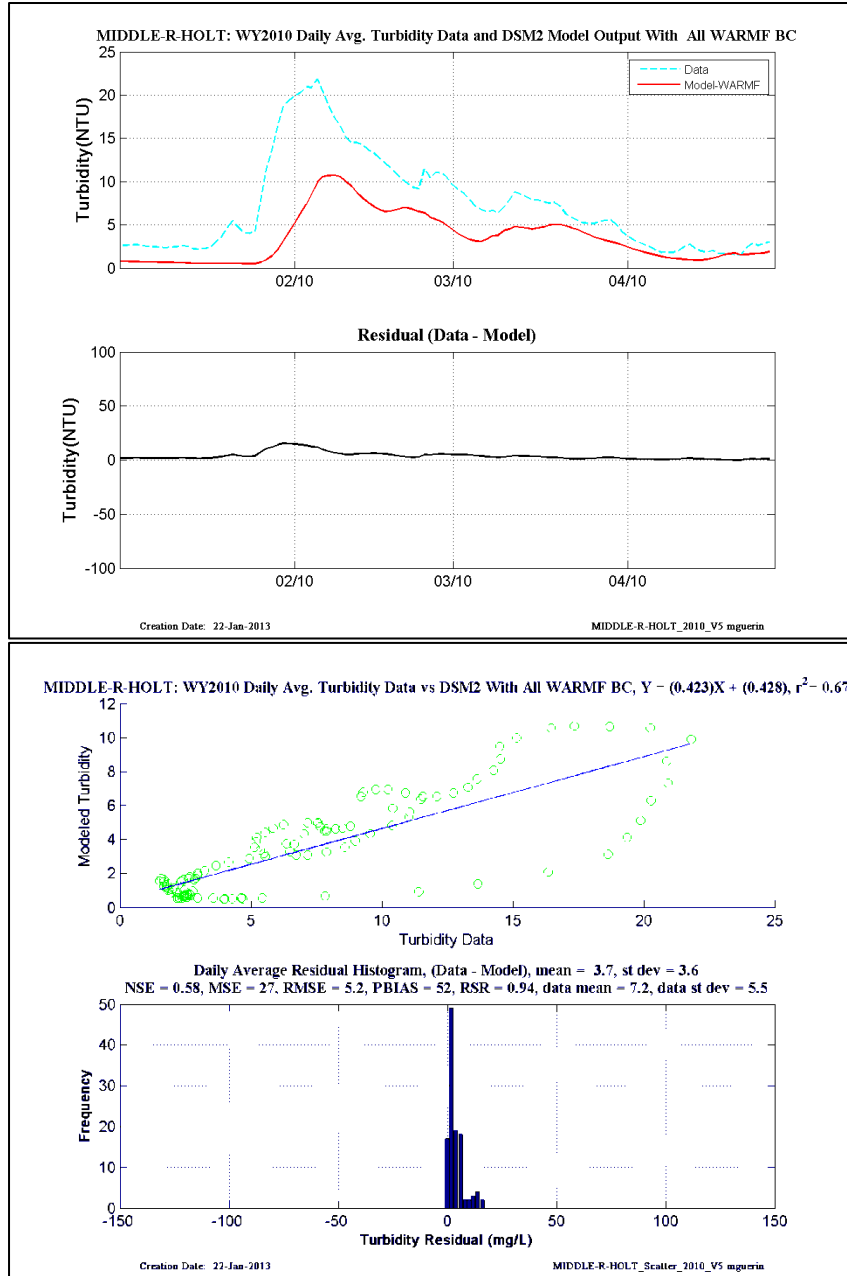


Figure 14-67WY2010: DSM2 daily-averaged turbidity model results using WARMF-Only turbidity at the inflow boundaries– location is Middle-River-at-Holt.

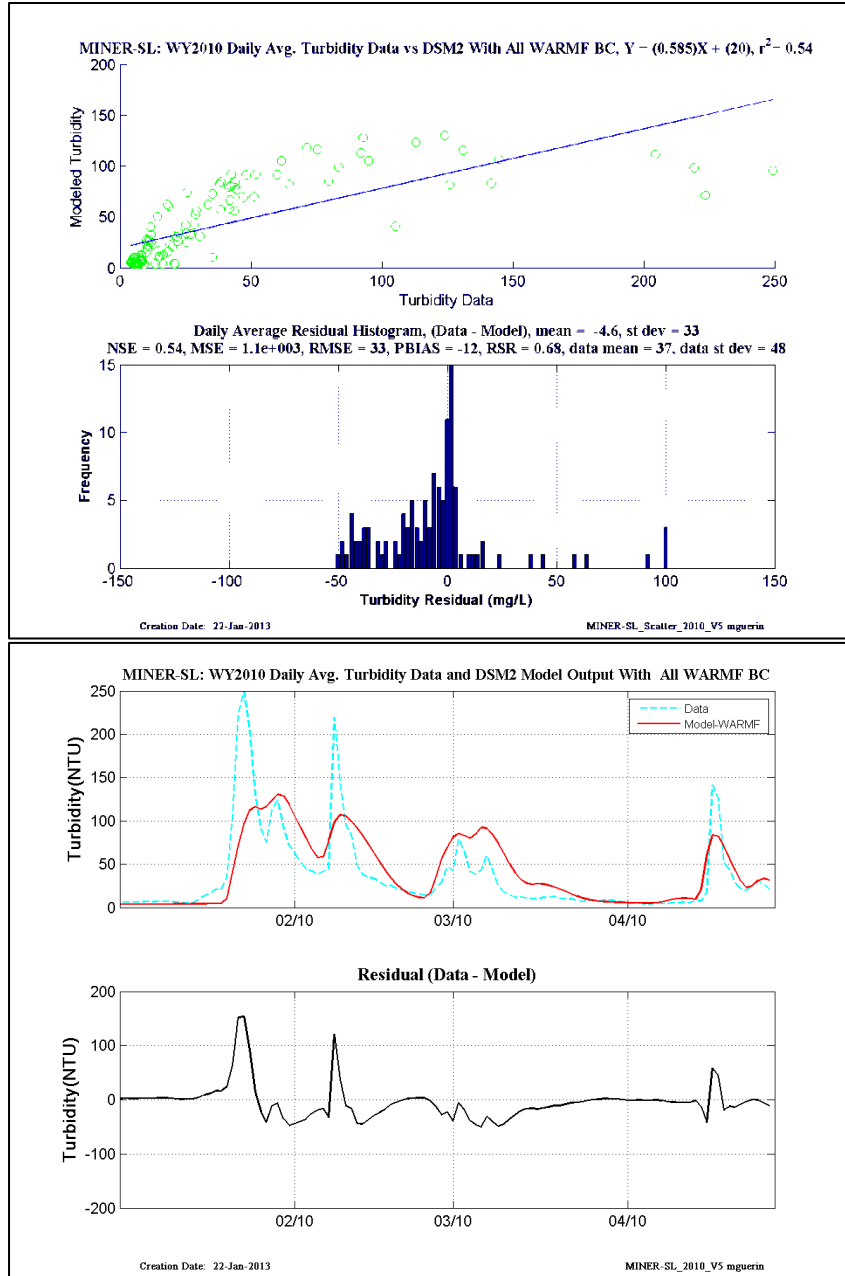


Figure 14-68WY2010: DSM2 daily-averaged turbidity model results using WARMF-Only turbidity at the inflow boundaries– location is Miner Slough.

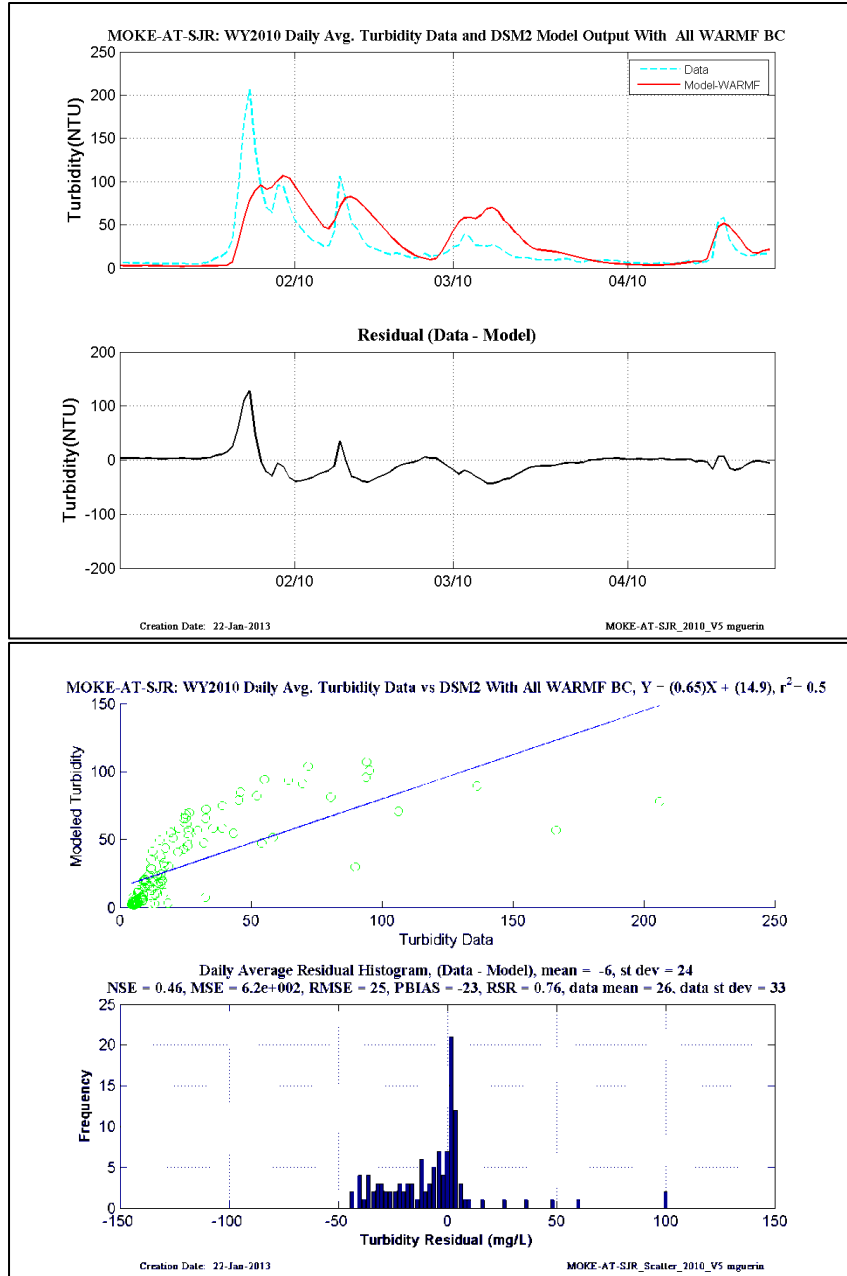


Figure 14-69WY2010: DSM2 daily-averaged turbidity model results using WARMF-Only turbidity at the inflow boundaries– location is Mokelumne-at-San Joaquin.

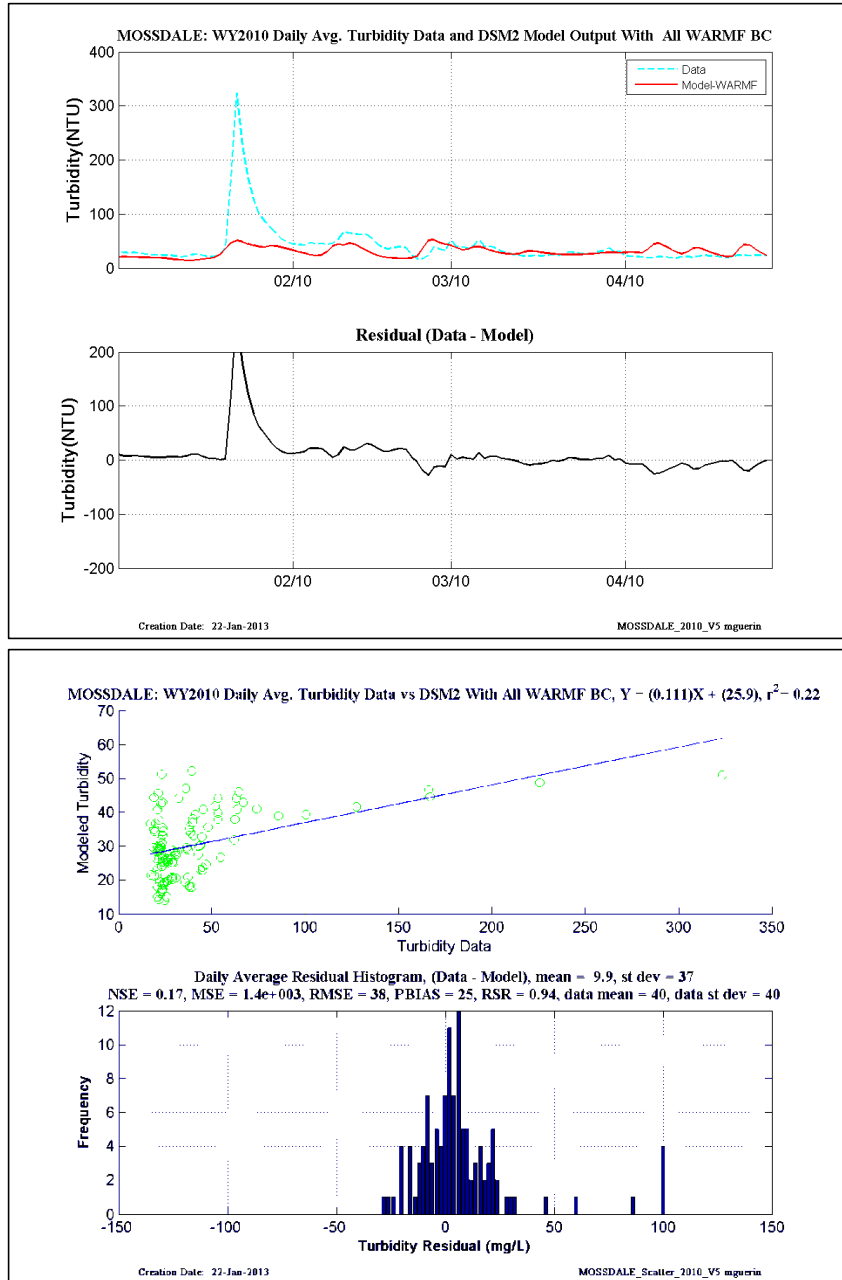


Figure 14-70WY2010: DSM2 daily-averaged turbidity model results using WARMF-Only turbidity at the inflow boundaries– location is Mossdale.

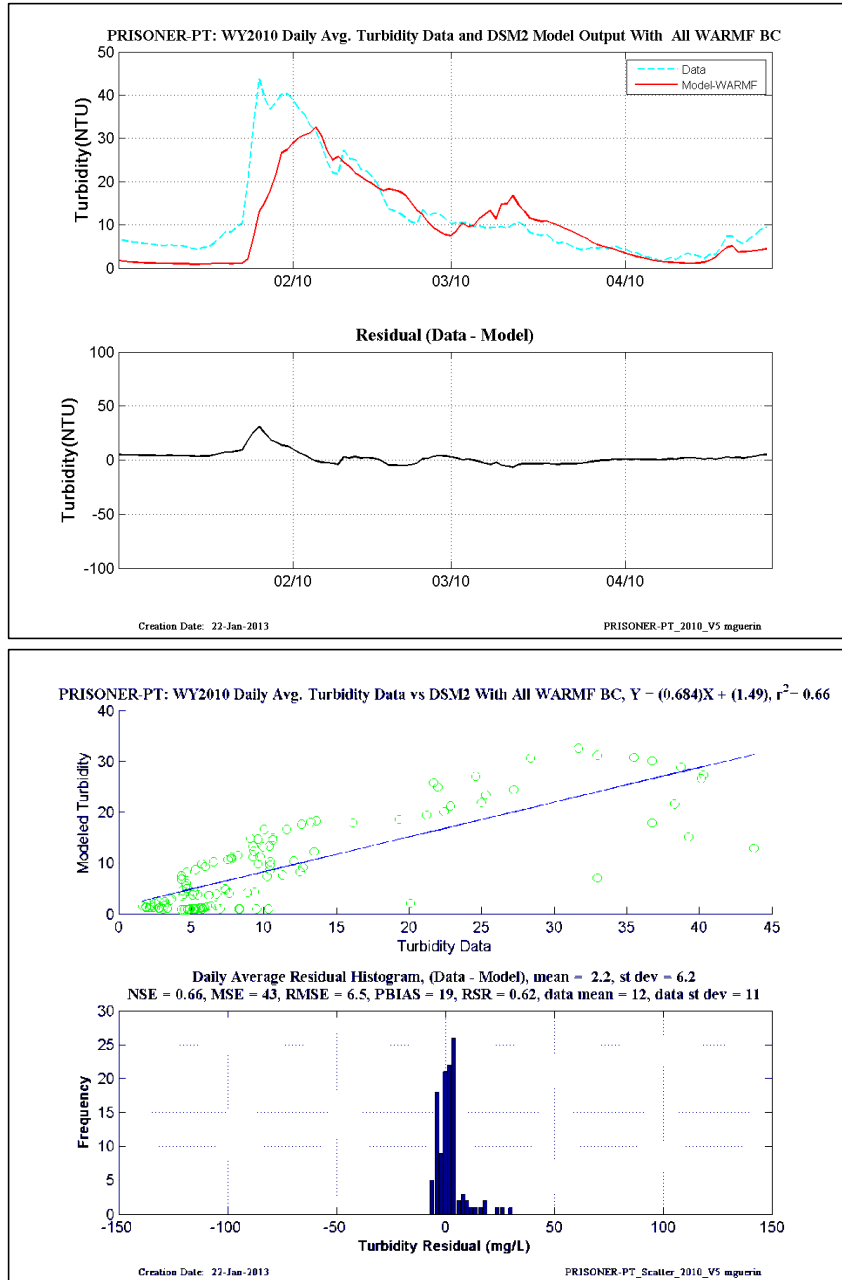


Figure 14-71WY2010: DSM2 daily-averaged turbidity model results using WARMF-Only turbidity at the inflow boundaries– location is Prisoner-Point.

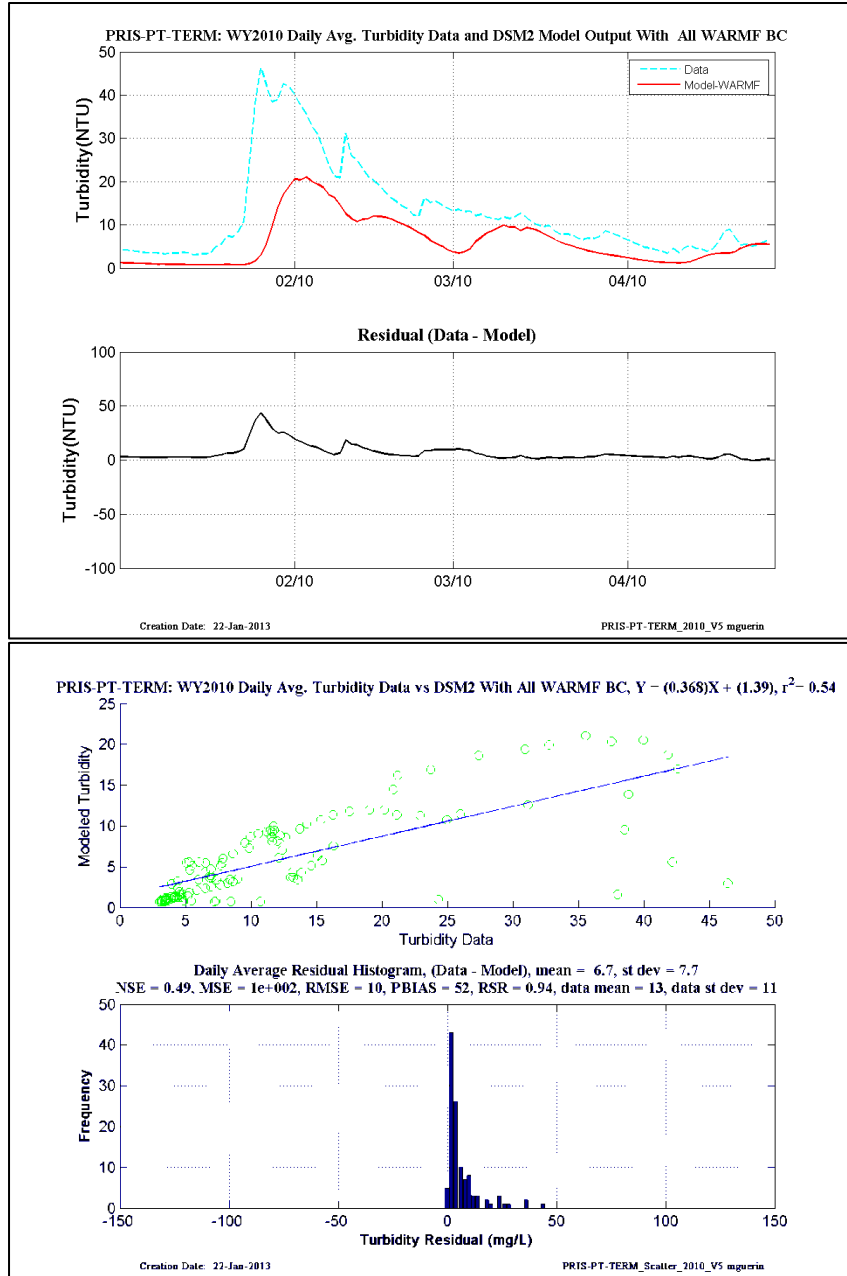


Figure 14-72 WY2010: DSM2 daily-averaged turbidity model results using WARMF-Only turbidity at the inflow boundaries– location is Prisoner-Point-at-Terminus.

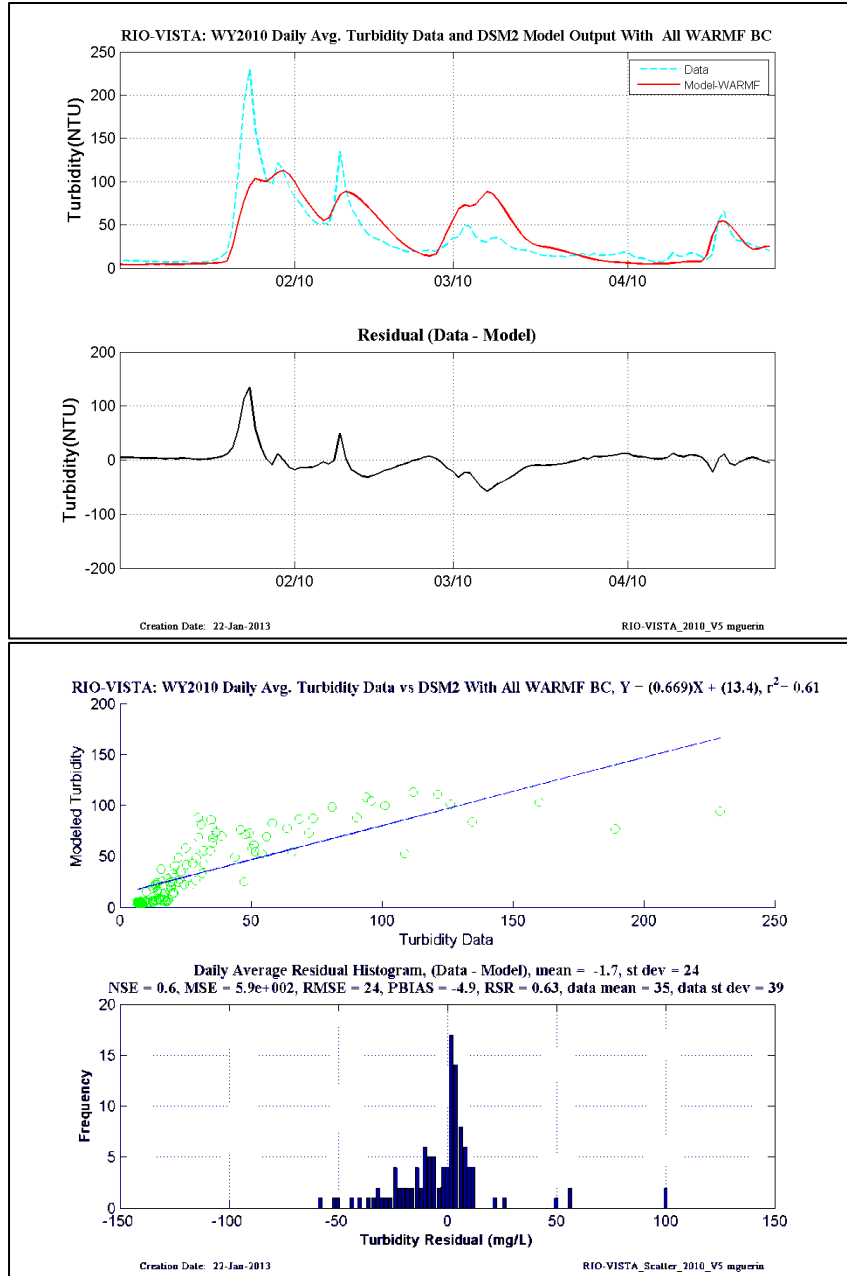


Figure 14-73WY2010: DSM2 daily-averaged turbidity model results using WARMF-Only turbidity at the inflow boundaries– location is Rio Vista.

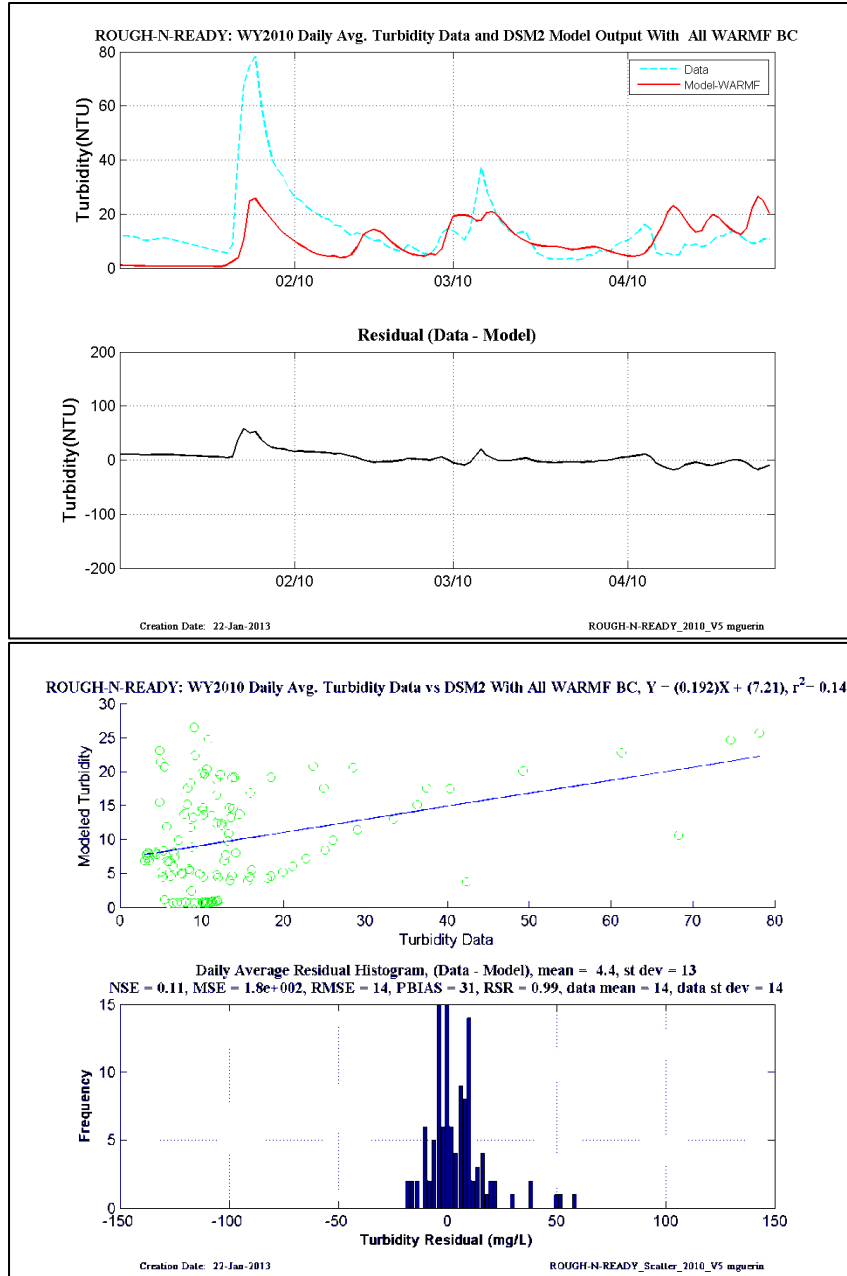


Figure 14-74 WY2010: DSM2 daily-averaged turbidity model results using WARMF-Only turbidity at the inflow boundaries– location is Rough-N-Ready Island.

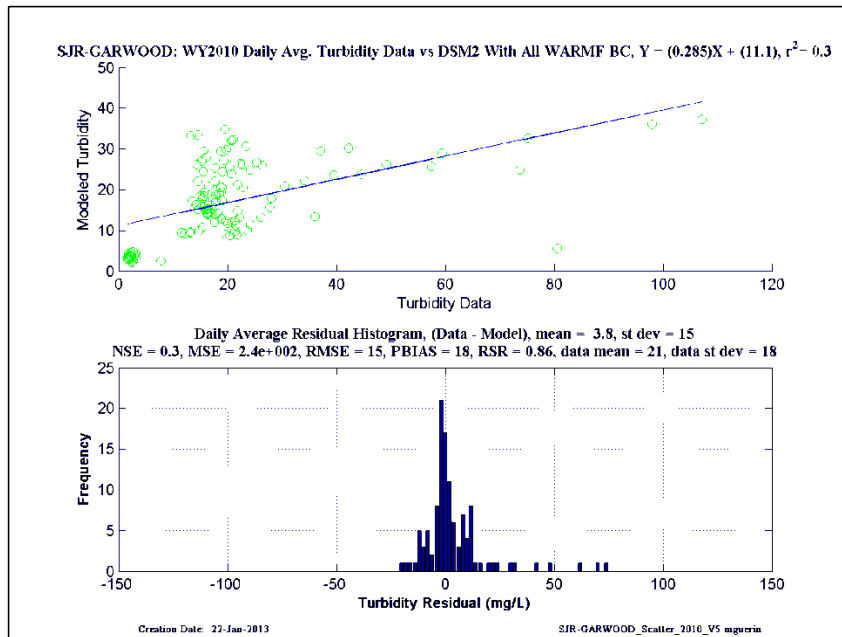
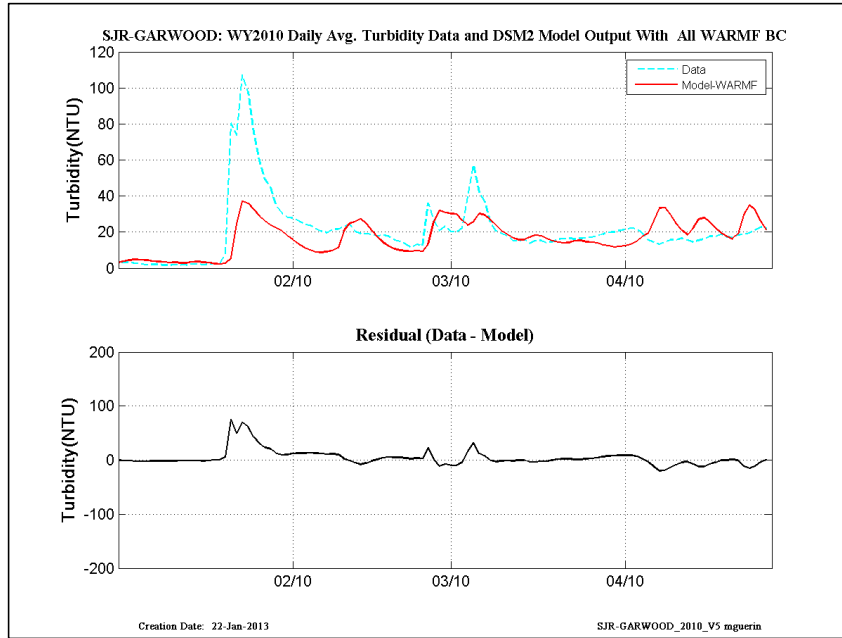


Figure 14-75 WY2010: DSM2 daily-averaged turbidity model results using WARMF-Only turbidity at the inflow boundaries– location is San Joaquin-at-Garwood.

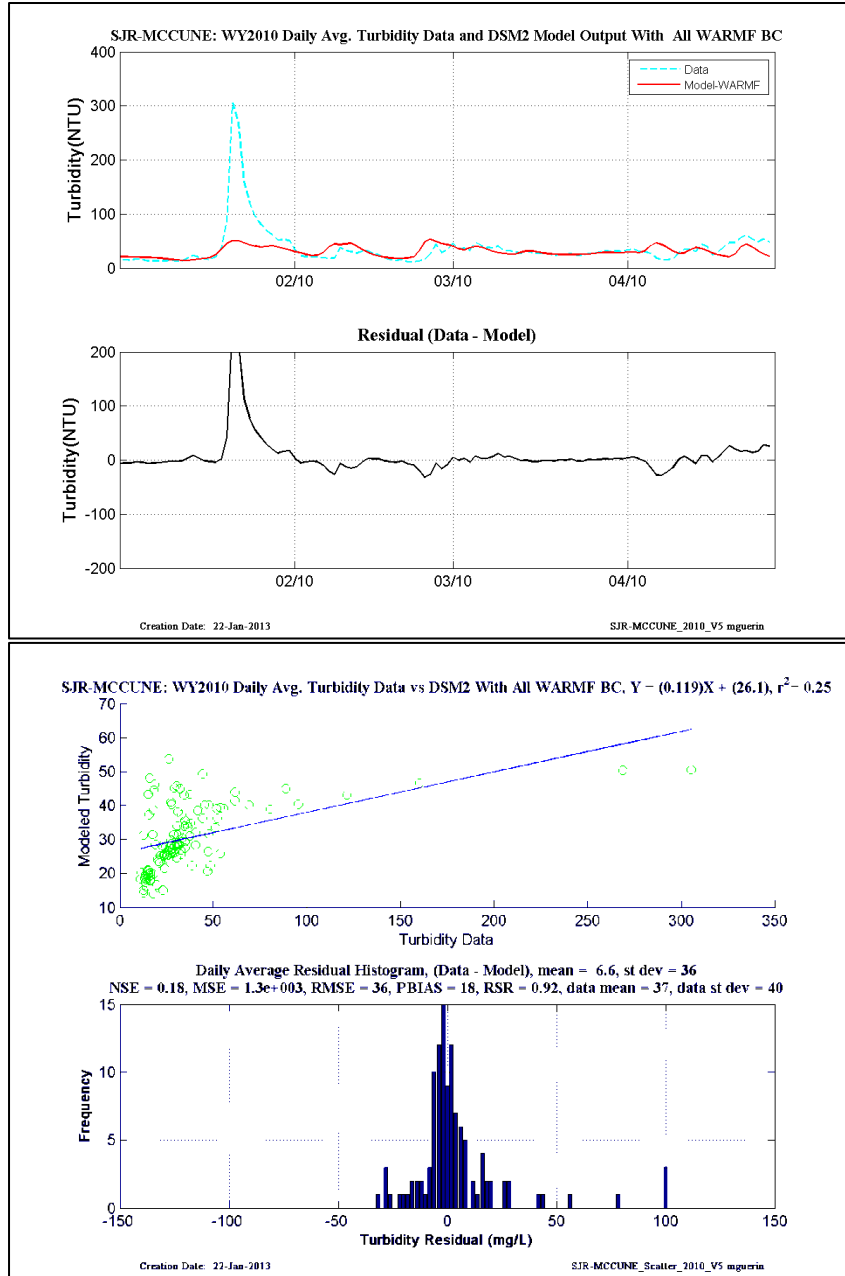


Figure 14-76 WY2010: DSM2 daily-averaged turbidity model results using WARMF-Only turbidity at the inflow boundaries– location is San Joaquin-at-McCune.

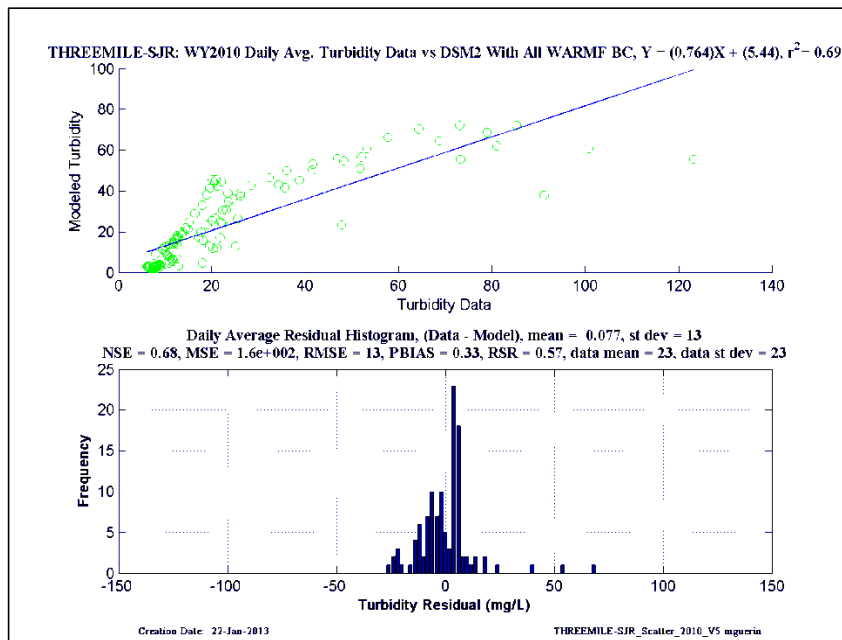
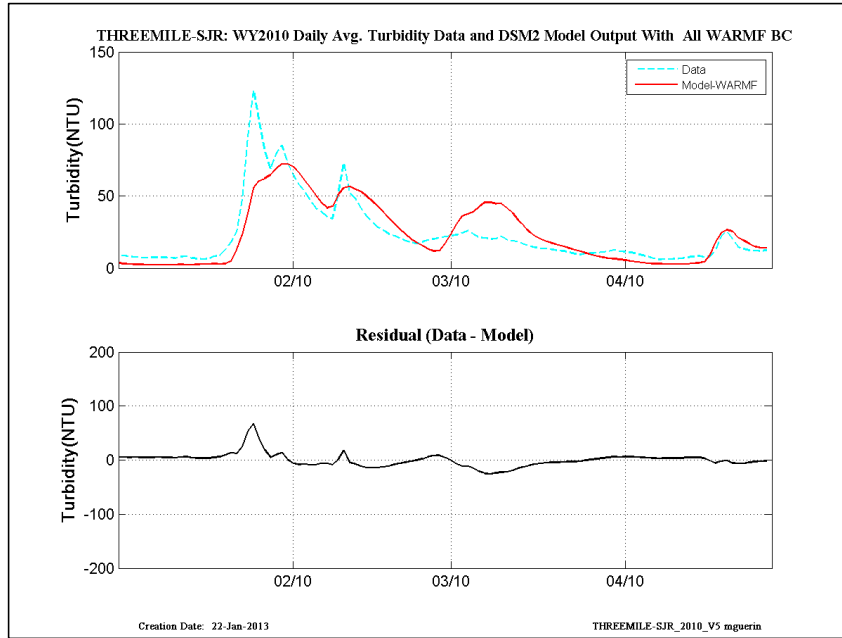


Figure 14-77 WY2010: DSM2 daily-averaged turbidity model results using WARMF-Only turbidity at the inflow boundaries– location is Threemile-Slough-at-San Joaquin.

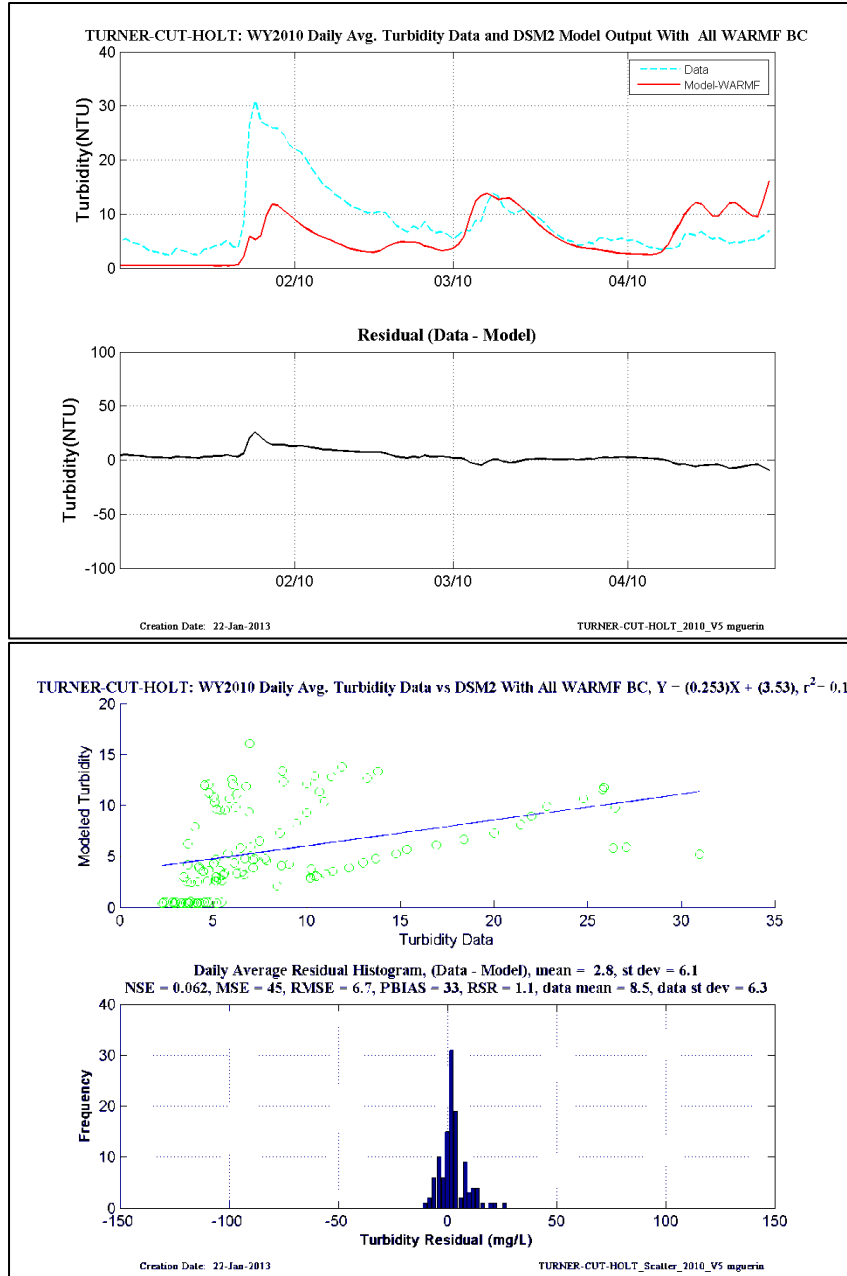


Figure 14-78 WY2010: DSM2 daily-averaged turbidity model results using WARMF-Only turbidity at the inflow boundaries– location is Turner-Cut-at-Holt.

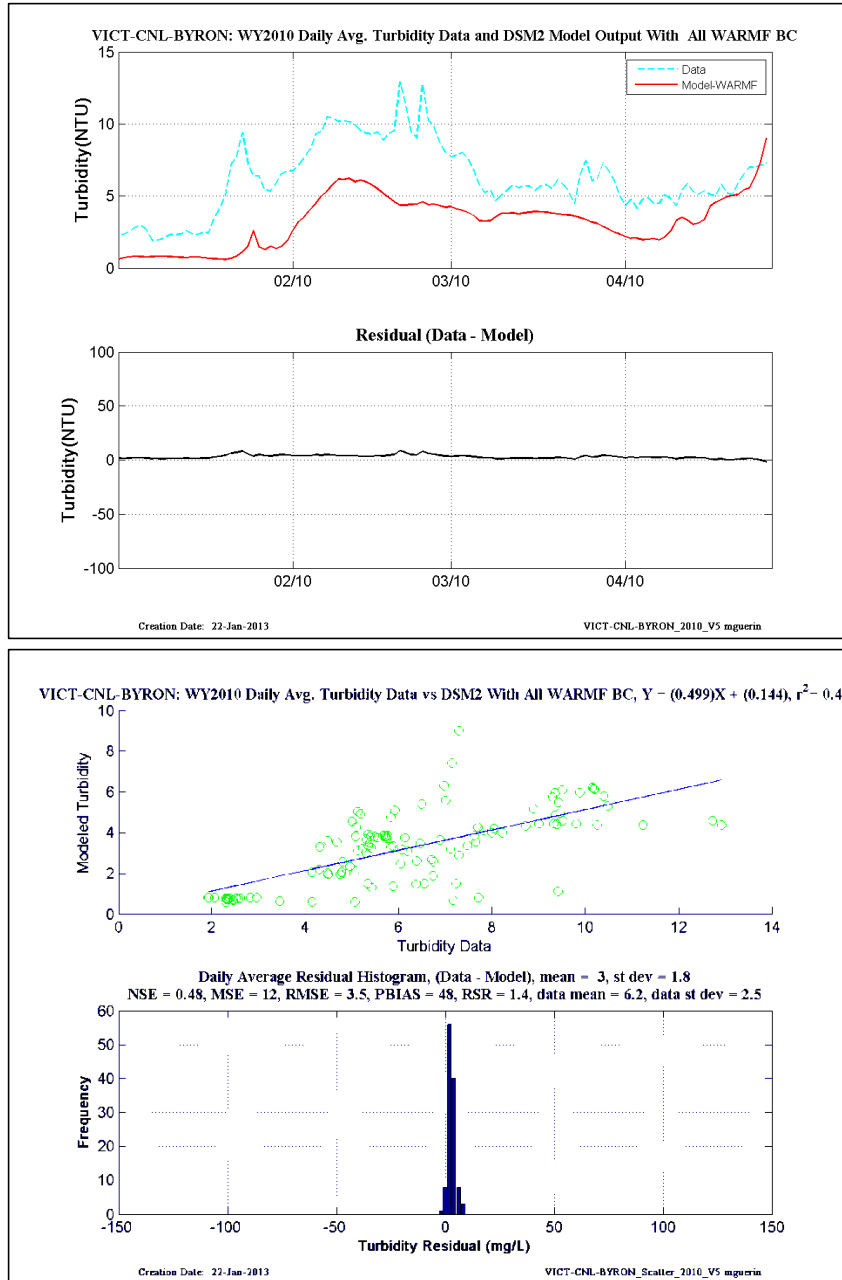


Figure 14-79 WY2010: DSM2 daily-averaged turbidity model results using WARMF-Only turbidity at the inflow boundaries– location is Victoria-Canal-at-Byron.

15.4 WY2011 WARMF-Only results

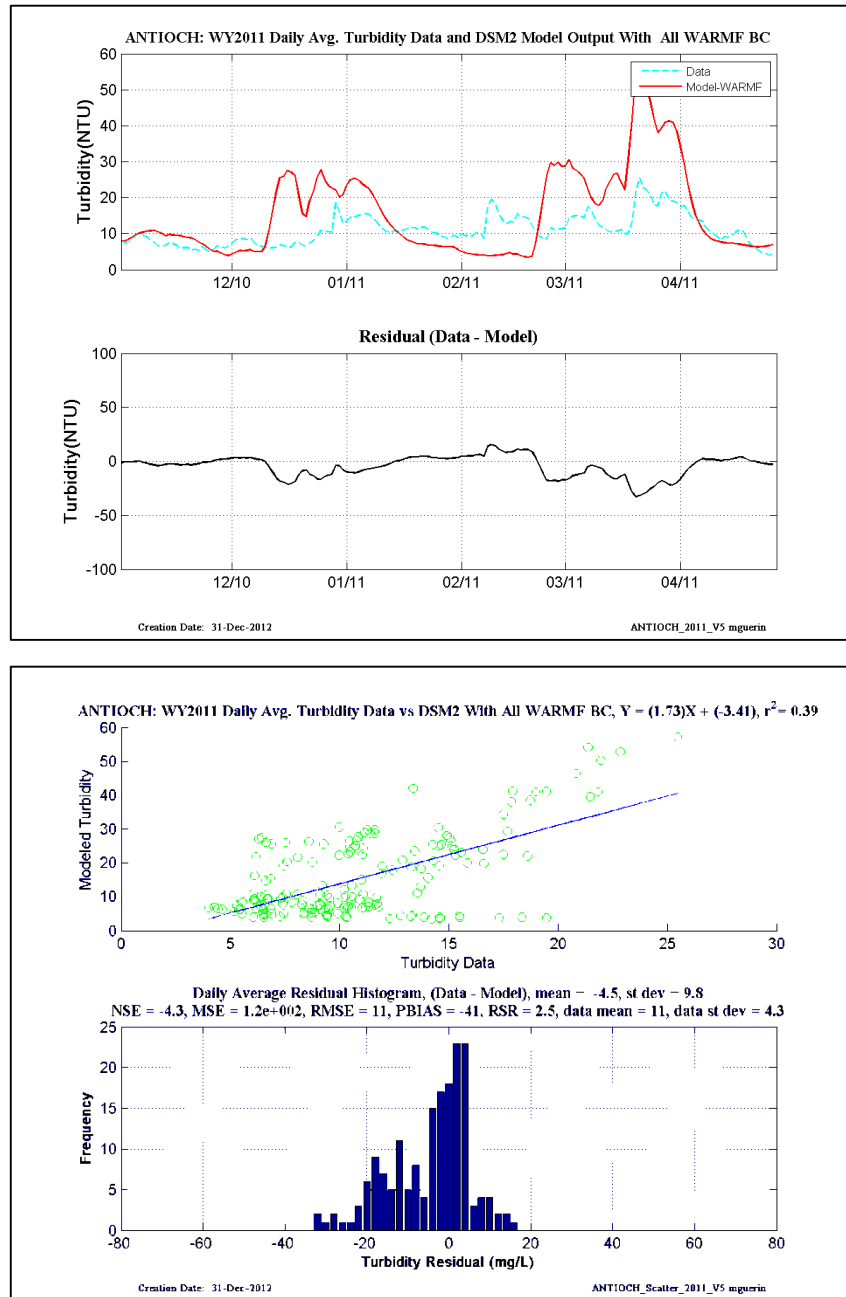


Figure 14-80 WY2011: DSM2 daily-averaged turbidity model results using WARMF-Only turbidity at the inflow boundaries– location is Antioch.

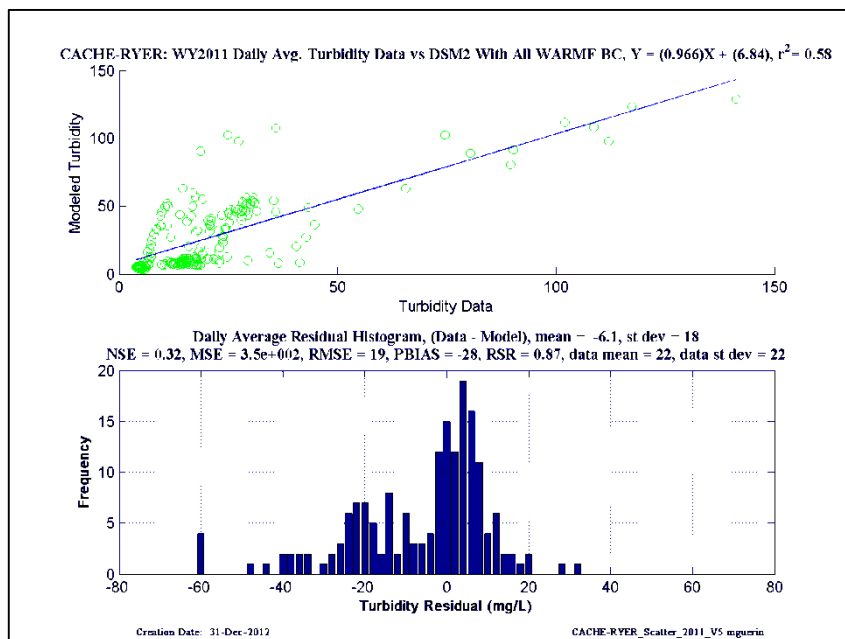
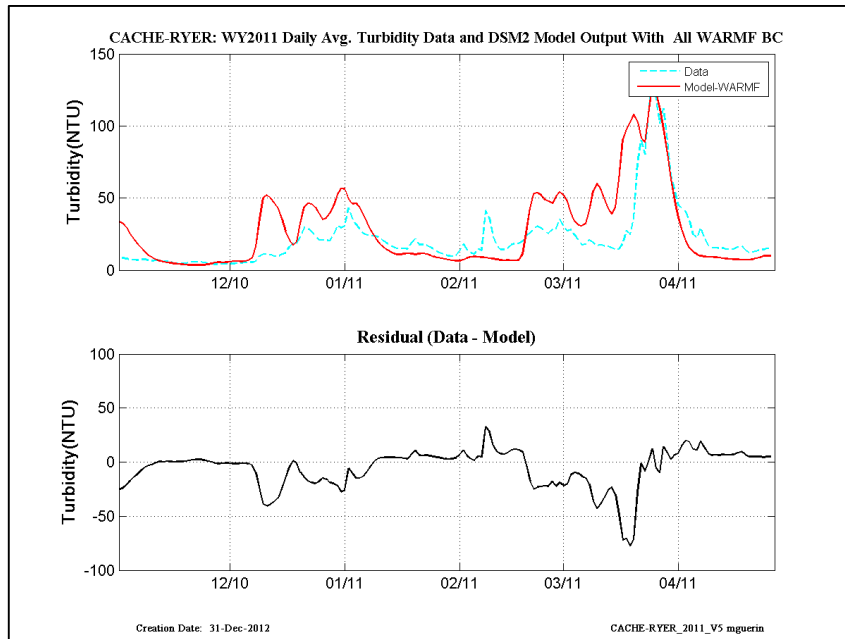


Figure 14-81 WY2011: DSM2 daily-averaged turbidity model results using WARMF-Only turbidity at the inflow boundaries– location is Cache-at-Ryer.

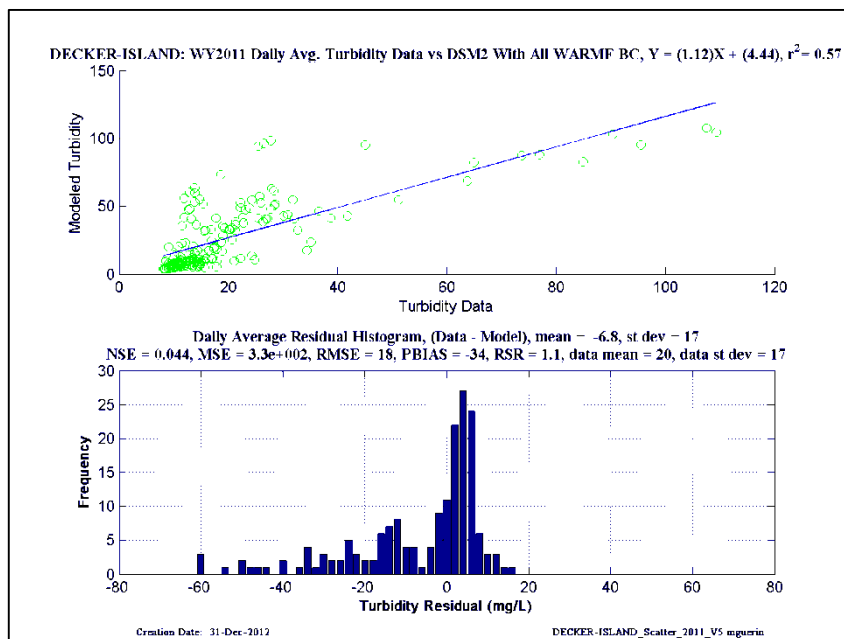
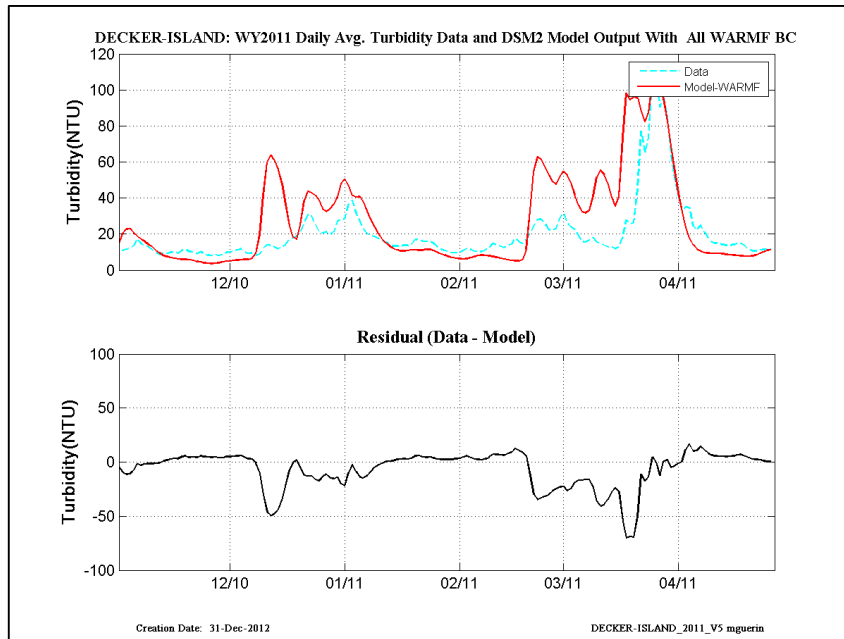


Figure 14-82 WY2011: DSM2 daily-averaged turbidity model results using WARMF-Only turbidity at the inflow boundaries– location is Decker-Island.

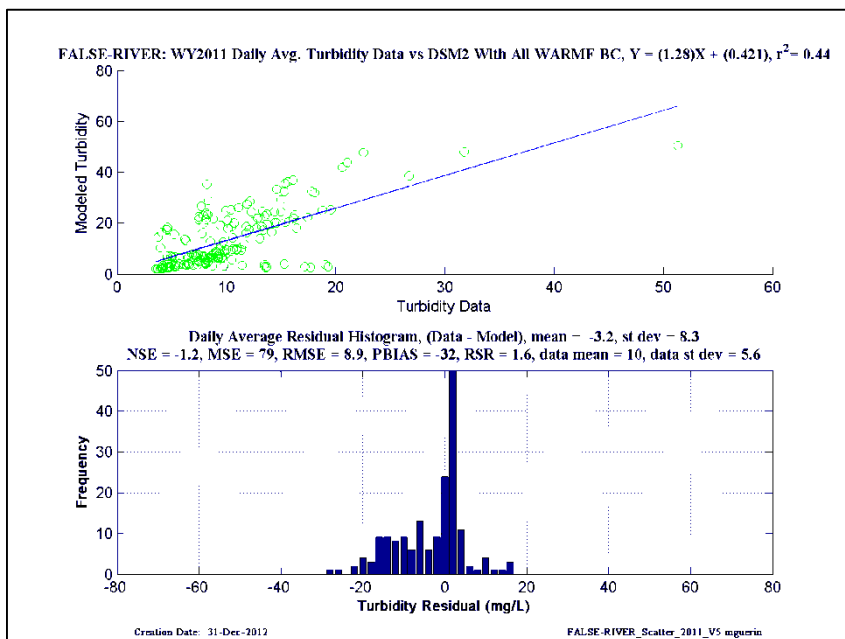
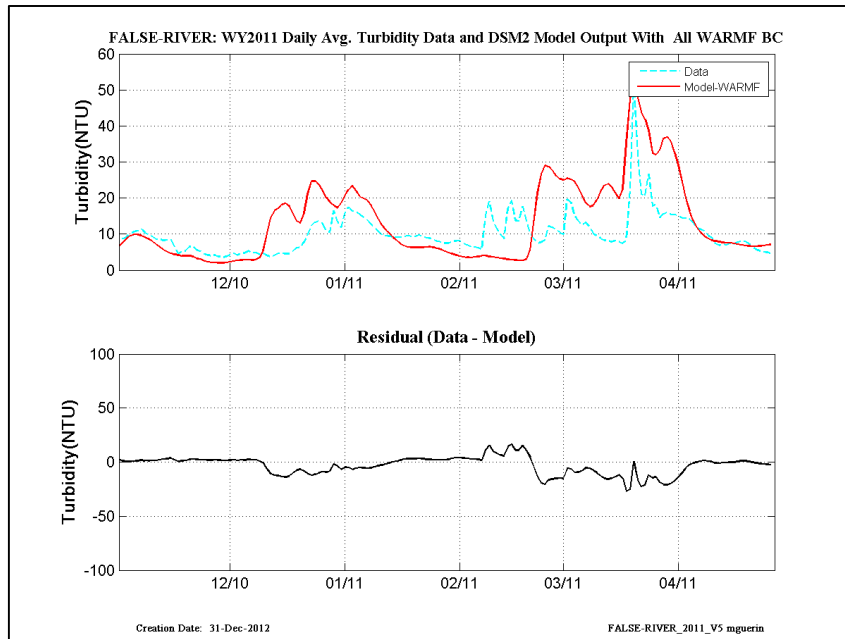


Figure 14-83 WY2011: DSM2 daily-averaged turbidity model results using WARMF-Only turbidity at the inflow boundaries– location is False-River.

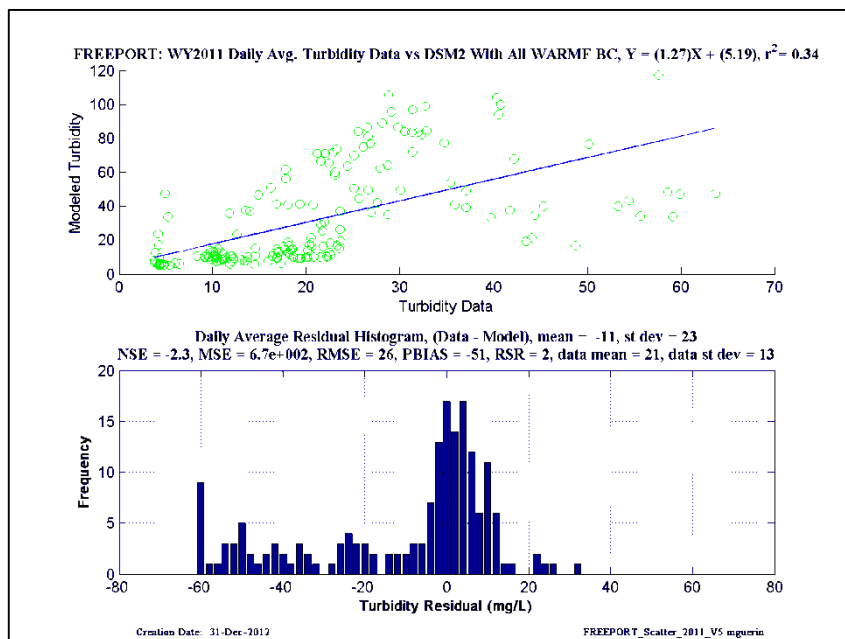
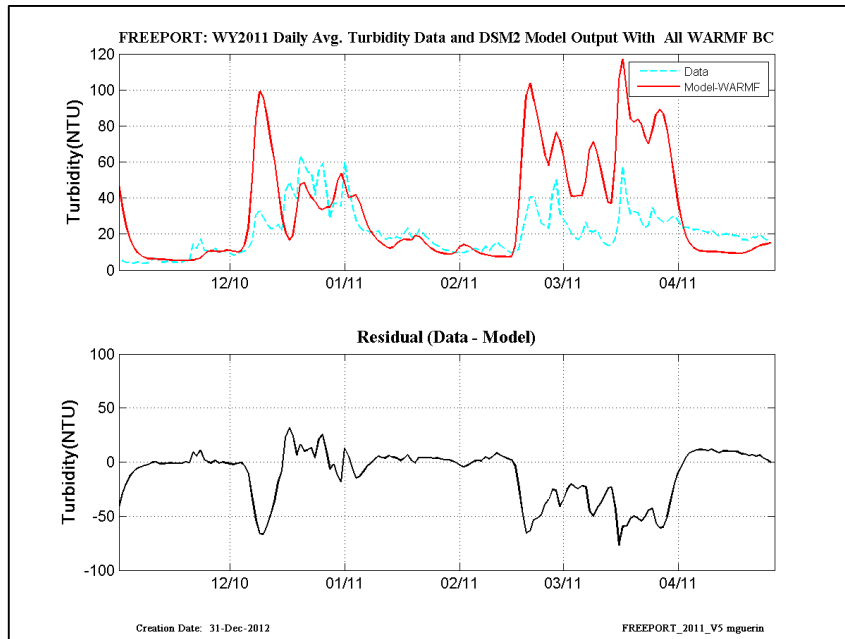


Figure 14-84 WY2011: DSM2 daily-averaged turbidity model results using WARMF-Only turbidity at the inflow boundaries– location is Freeport.

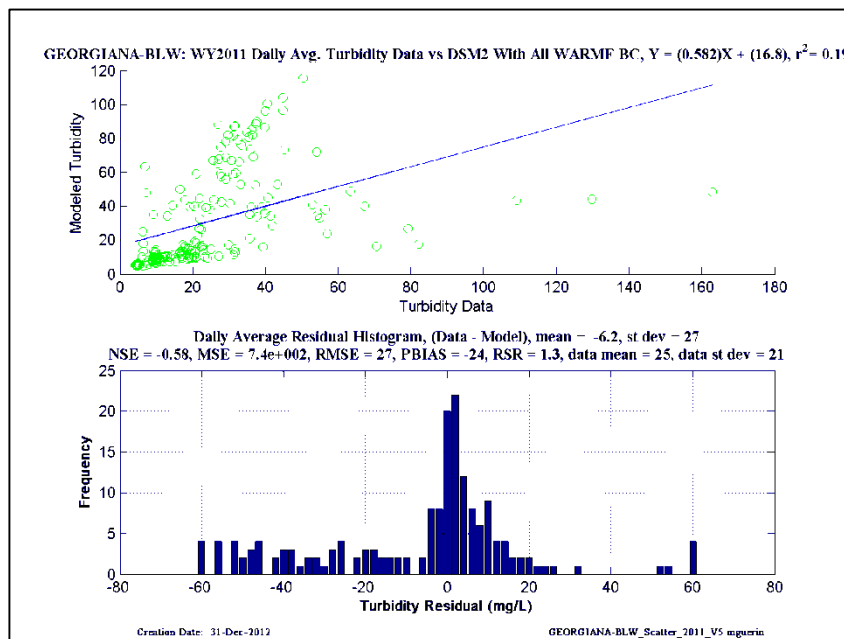
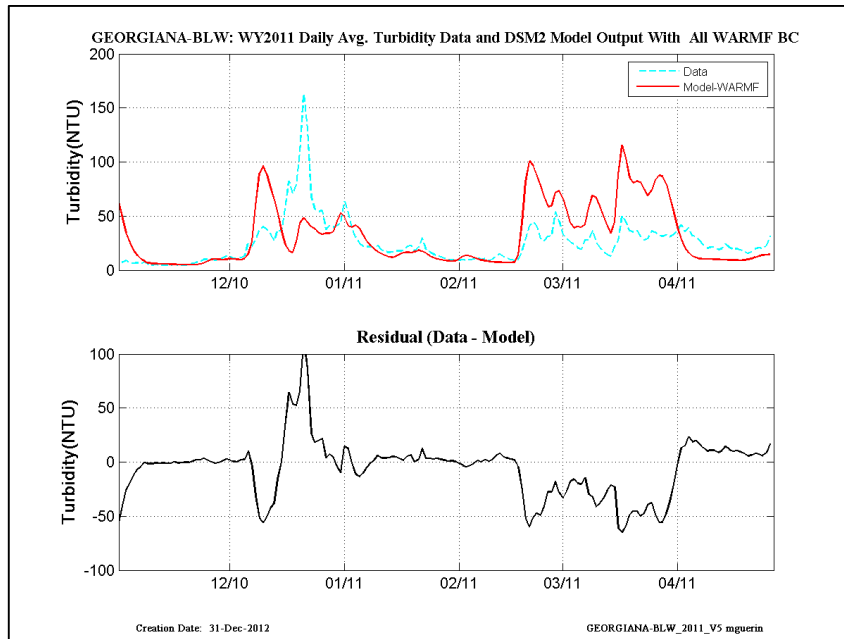


Figure 14-85 WY2011: DSM2 daily-averaged turbidity model results using WARMF-Only turbidity at the inflow boundaries– location is Georgiana- Below-Sac.

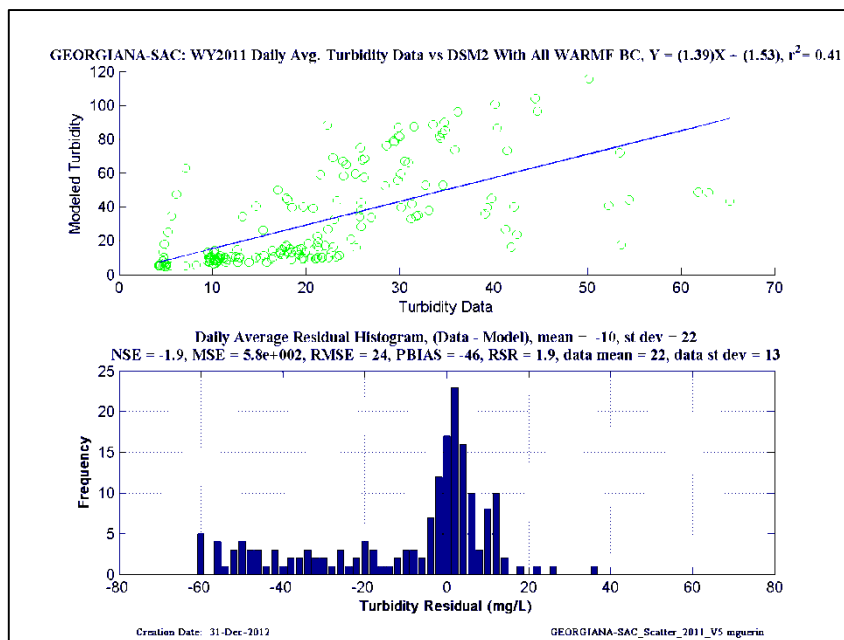
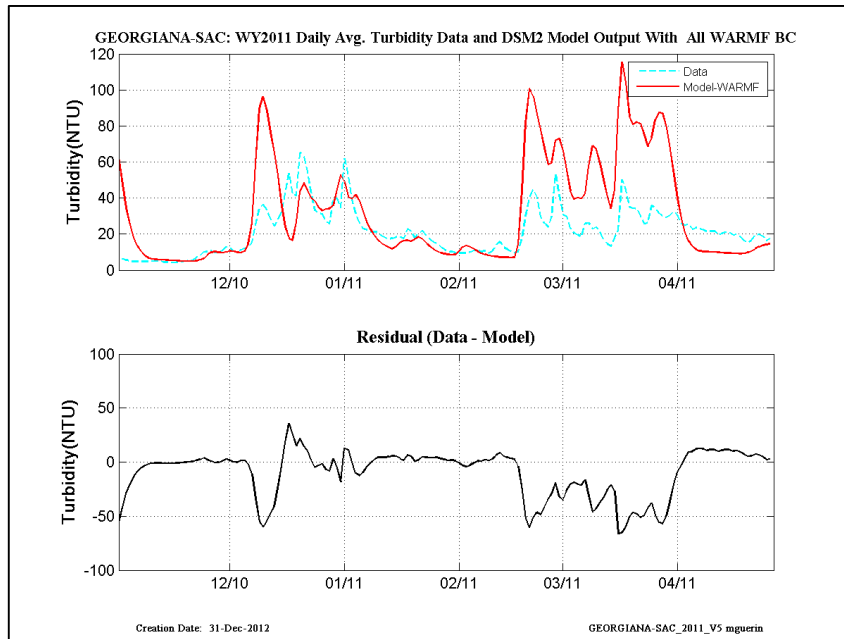


Figure 14-86 WY2011: DSM2 daily-averaged turbidity model results using WARMF-Only turbidity at the inflow boundaries— location is Georgiana at Sac.

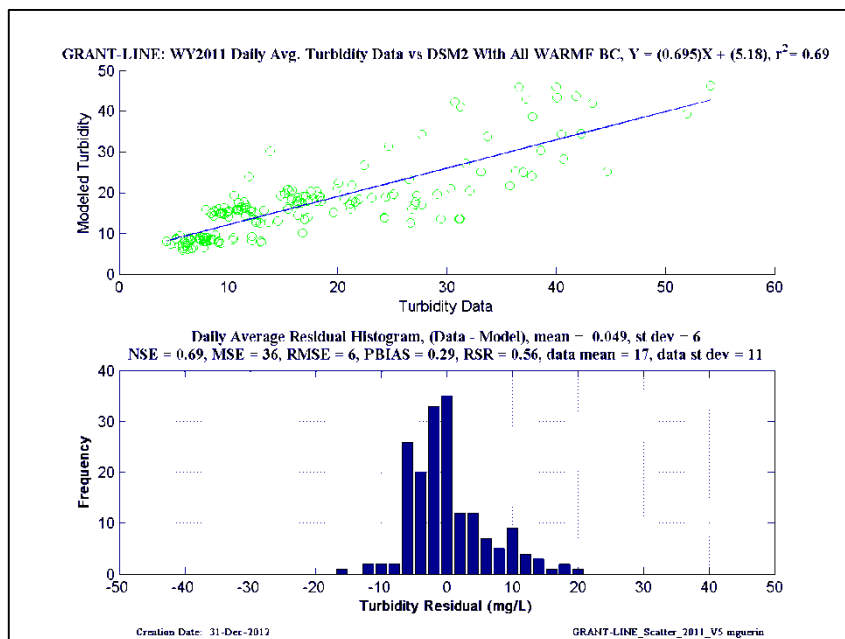
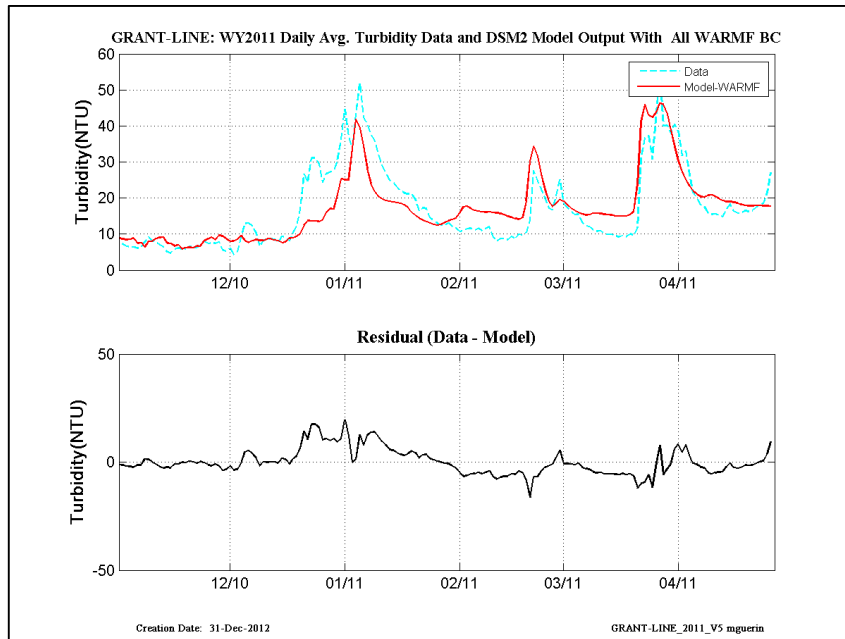


Figure 14-87 WY2011: DSM2 daily-averaged turbidity model results using WARMF-Only turbidity at the inflow boundaries– location is Grant Line.

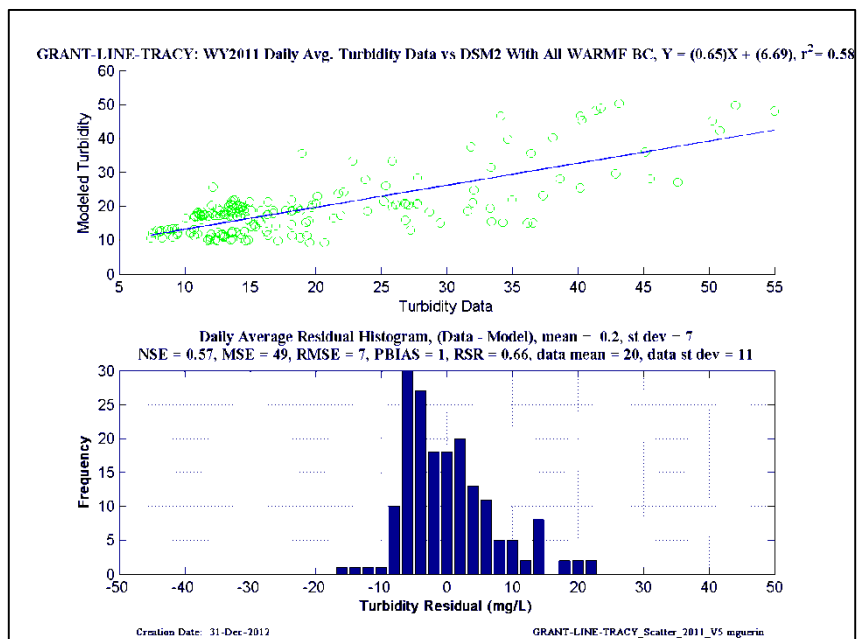
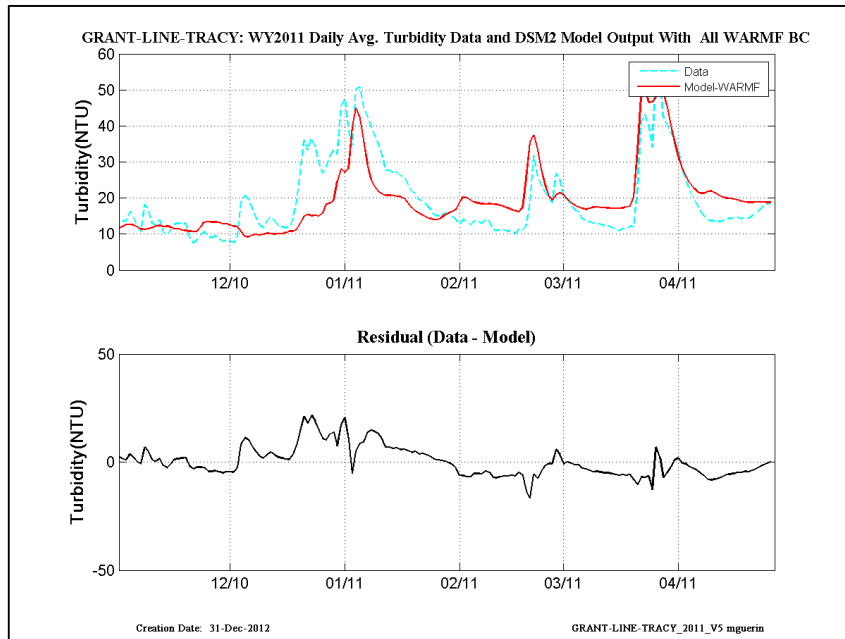


Figure 14-88 WY2011: DSM2 daily-averaged turbidity model results using WARMF-Only turbidity at the inflow boundaries– location is Grant-Line-at-Tracy.

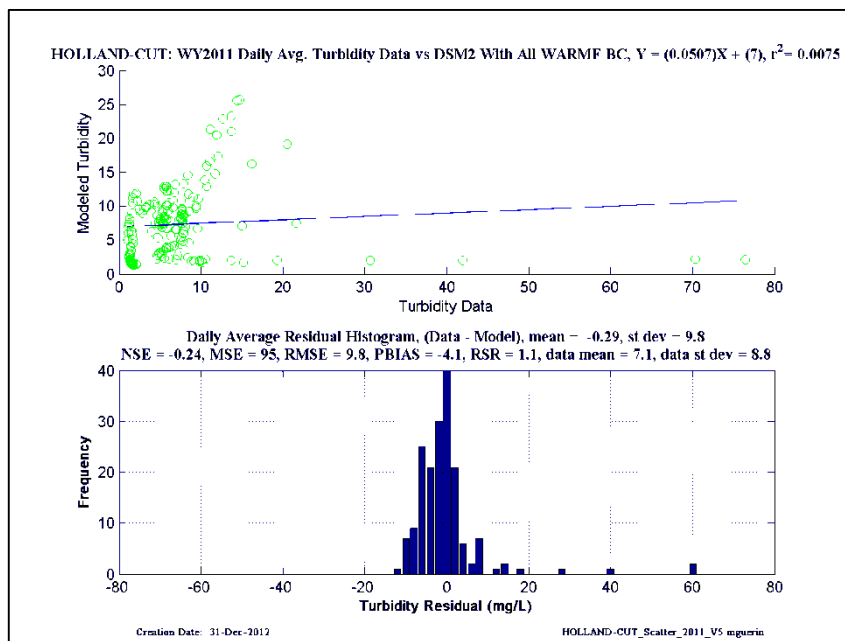
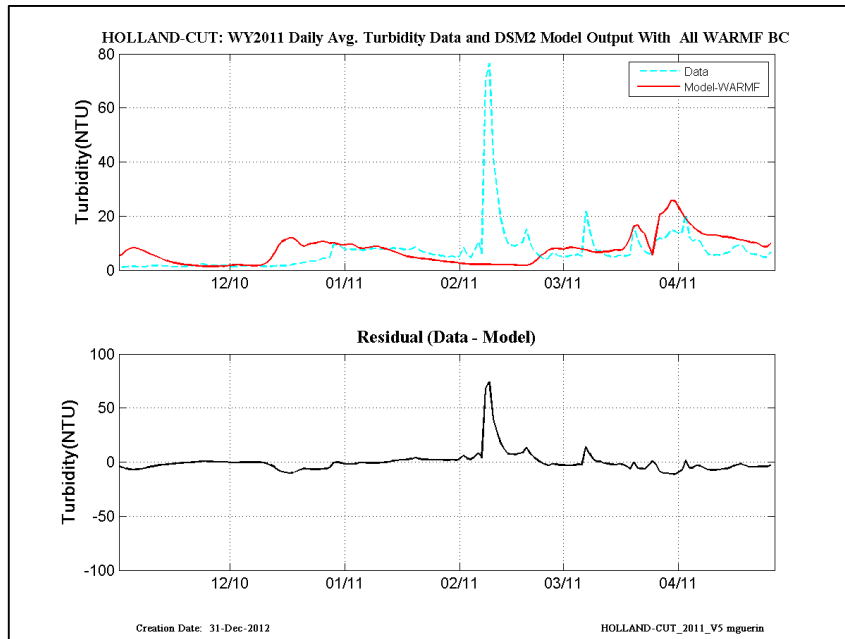


Figure 14-89 WY2011: DSM2 daily-averaged turbidity model results using WARMF-Only turbidity at the inflow boundaries– location is Holland Cut.

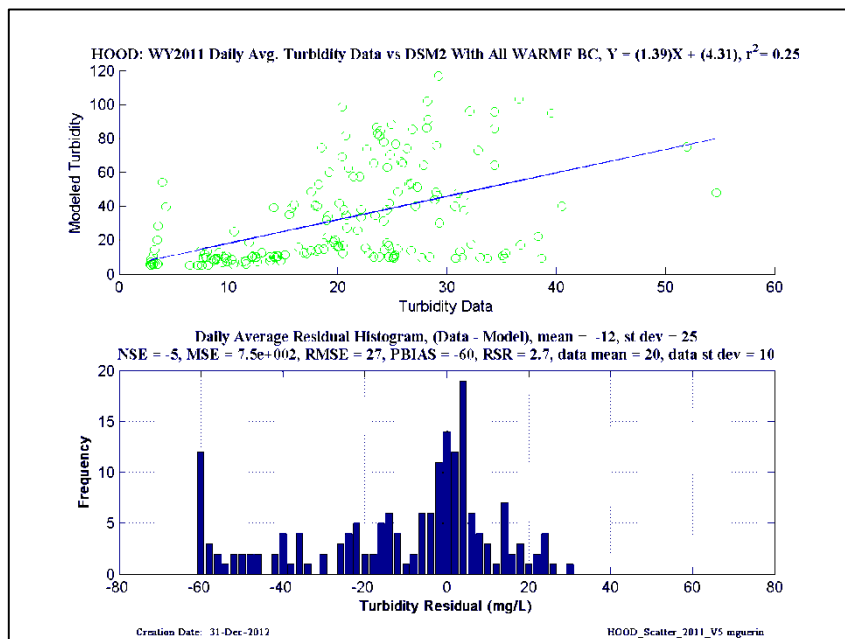
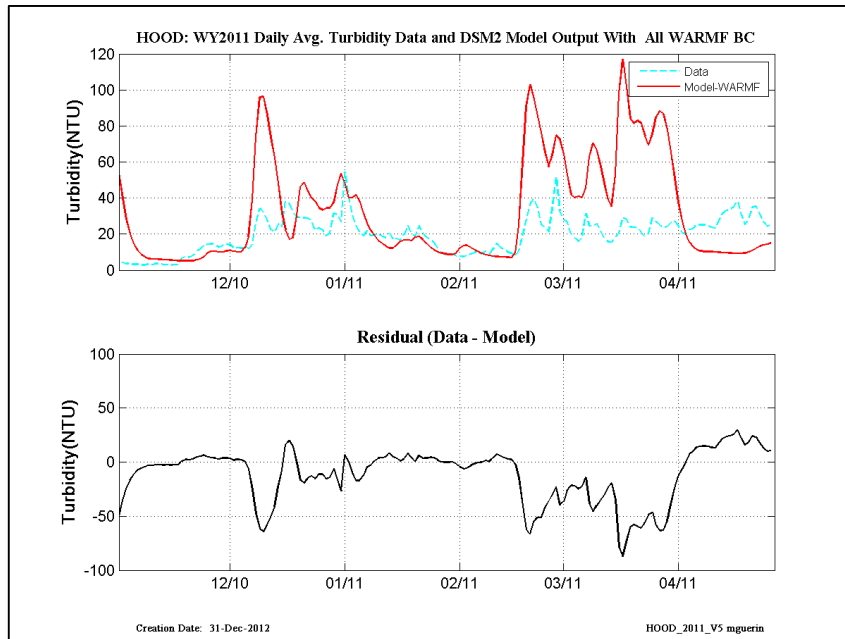


Figure 14-90 WY2011: DSM2 daily-averaged turbidity model results using WARMF-Only turbidity at the inflow boundaries– location is Hood.

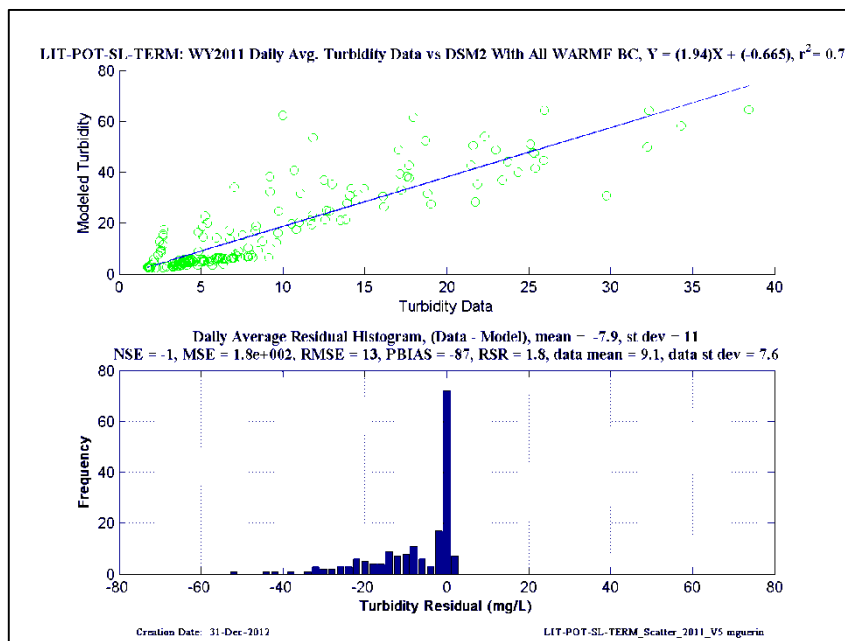
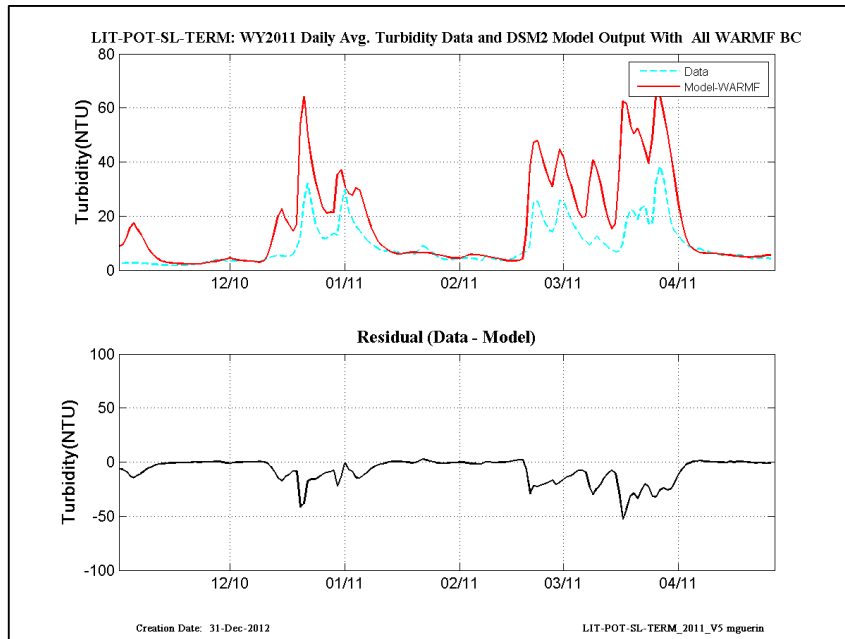


Figure 14-91 WY2011: DSM2 daily-averaged turbidity model results using WARMF-Only turbidity at the inflow boundaries– location is Little-Potato-Slough-at-Terminus.

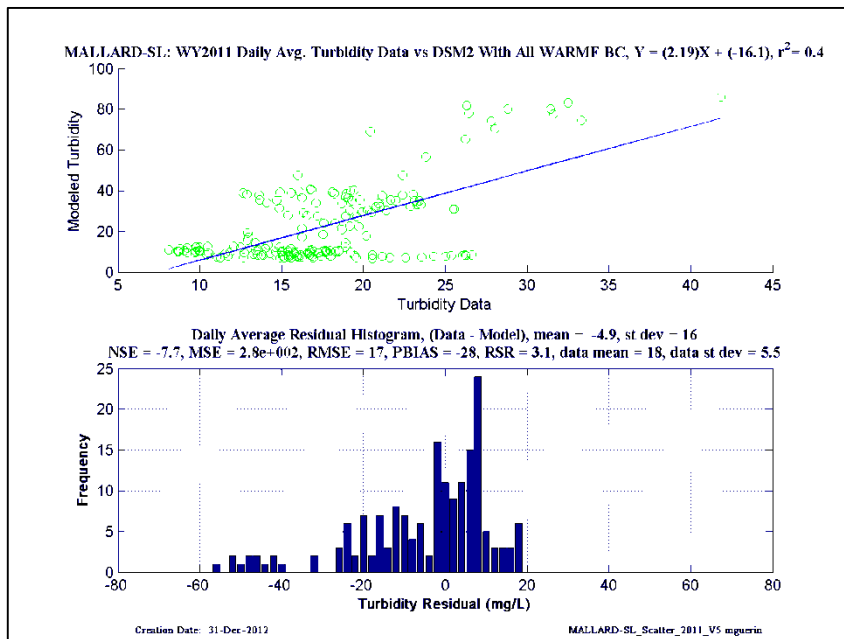
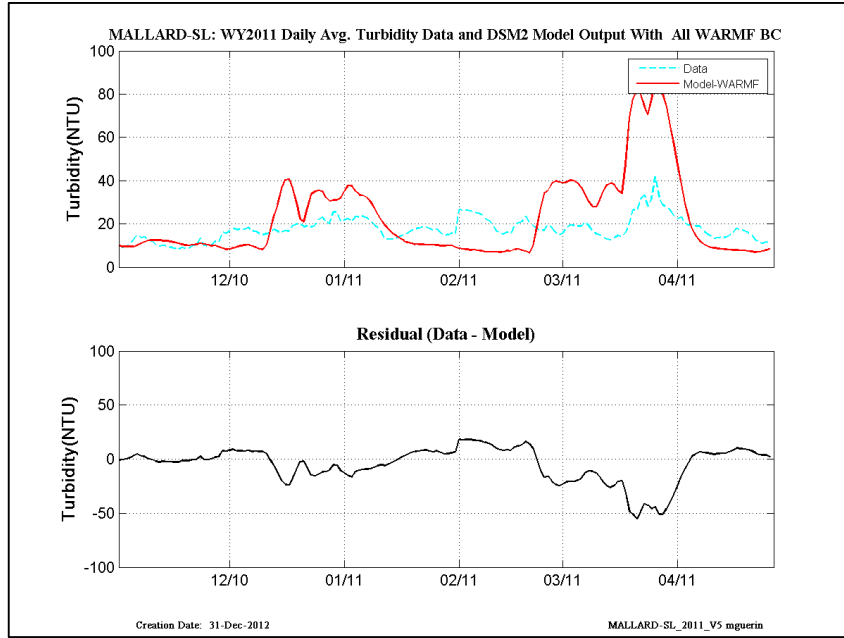


Figure 14-92 WY2011: DSM2 daily-averaged turbidity model results using WARMF-Only turbidity at the inflow boundaries– location is Mallard Slough.

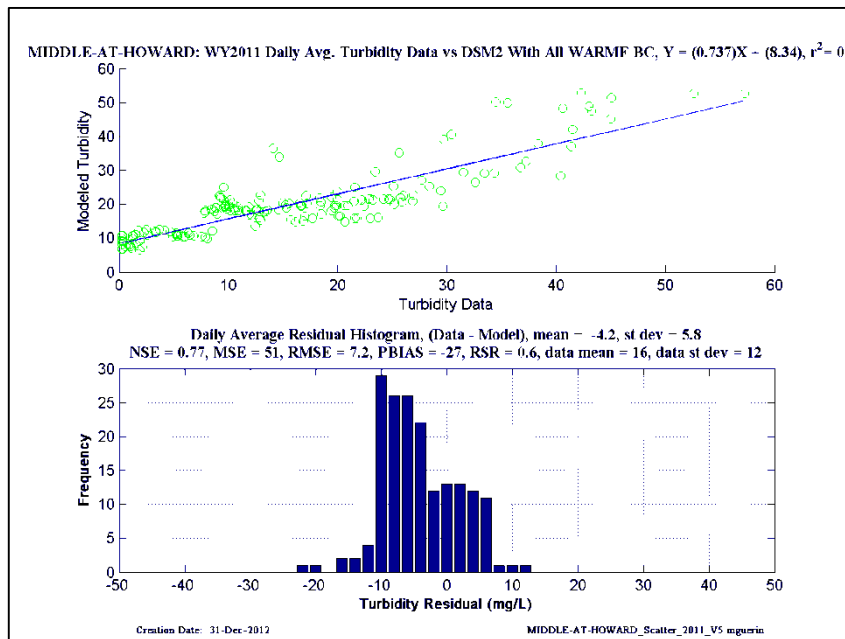
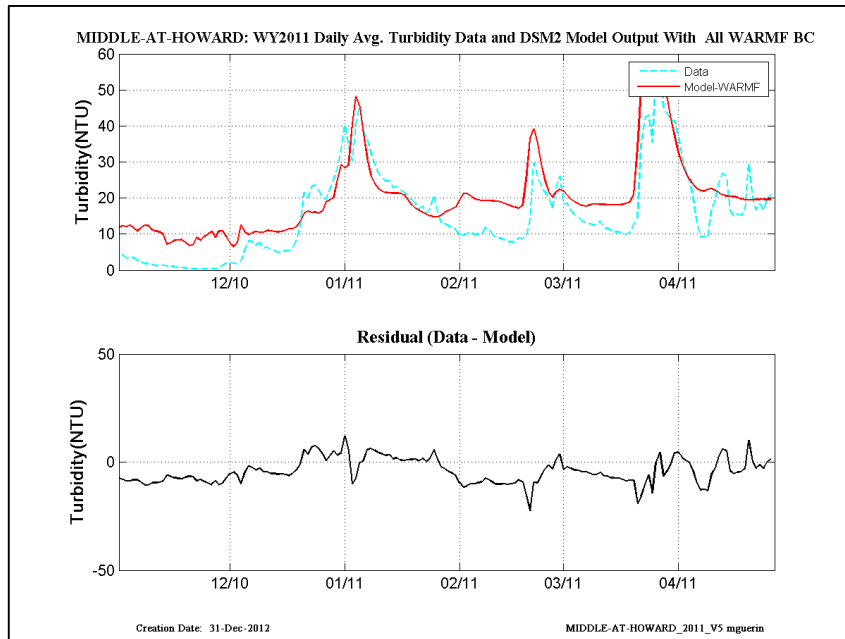


Figure 14-93 WY2011: DSM2 daily-averaged turbidity model results using WARMF-Only turbidity at the inflow boundaries– location is Middle River at Howard.

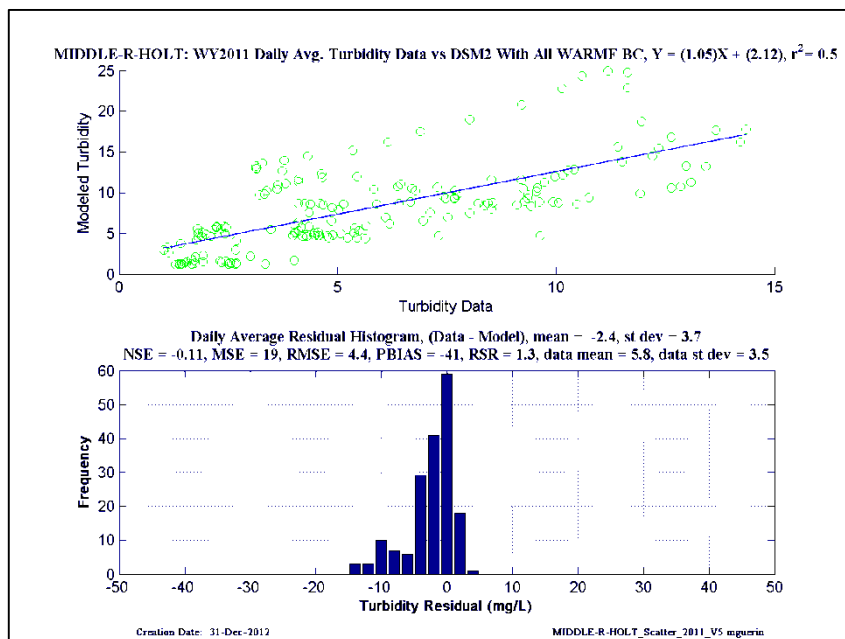
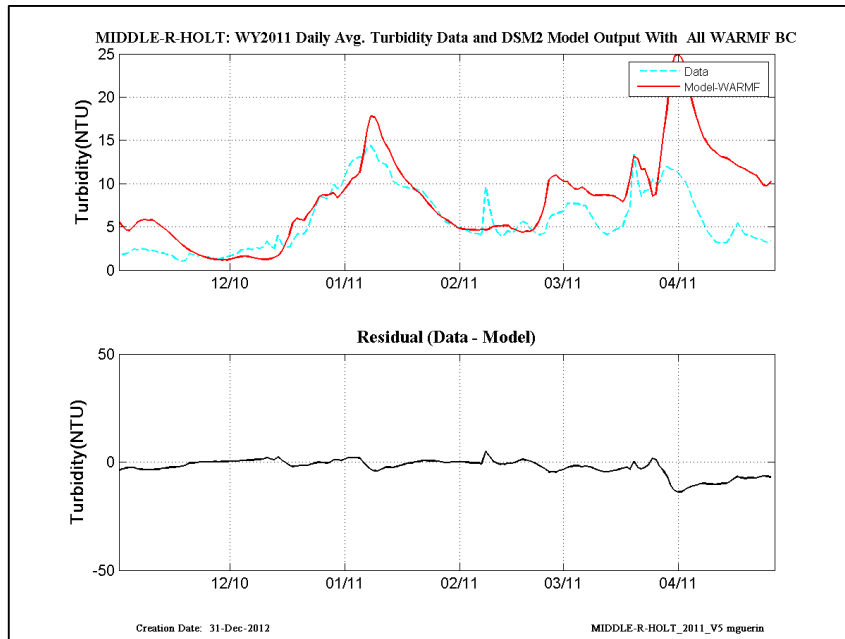


Figure 14-94 WY2011: DSM2 daily-averaged turbidity model results using WARMF-Only turbidity at the inflow boundaries– location is Middle River at Holt.

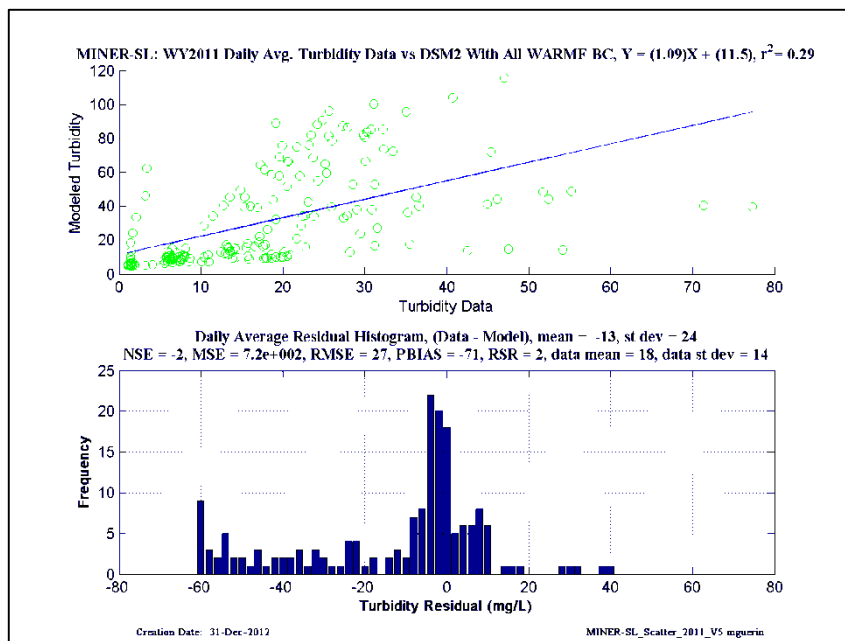
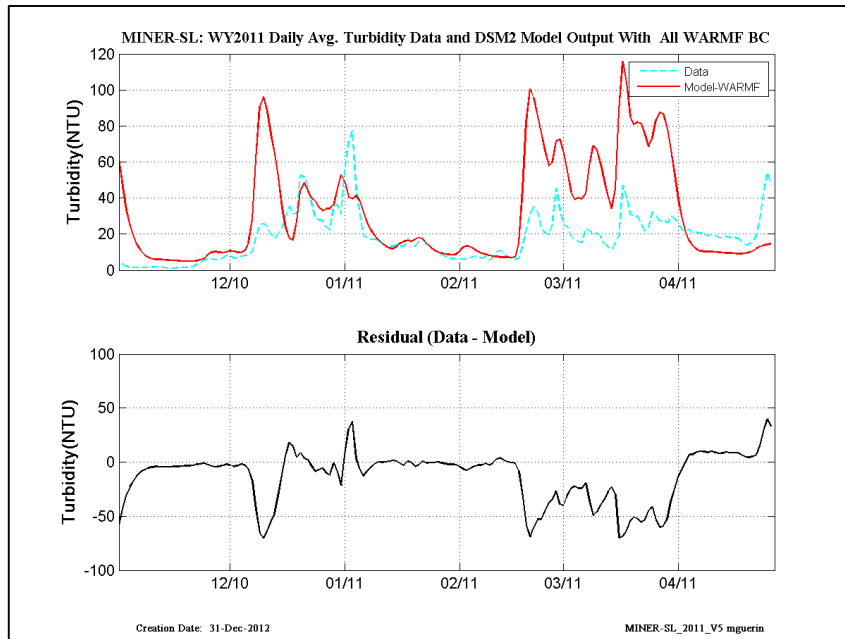


Figure 14-95 WY2011: DSM2 daily-averaged turbidity model results using WARMF-Only turbidity at the inflow boundaries– location is Miner Slough.

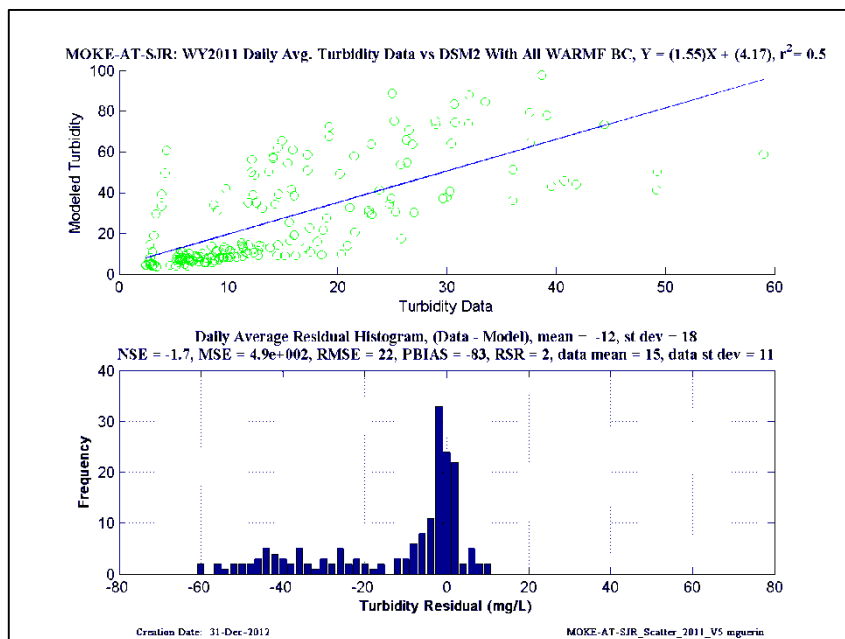
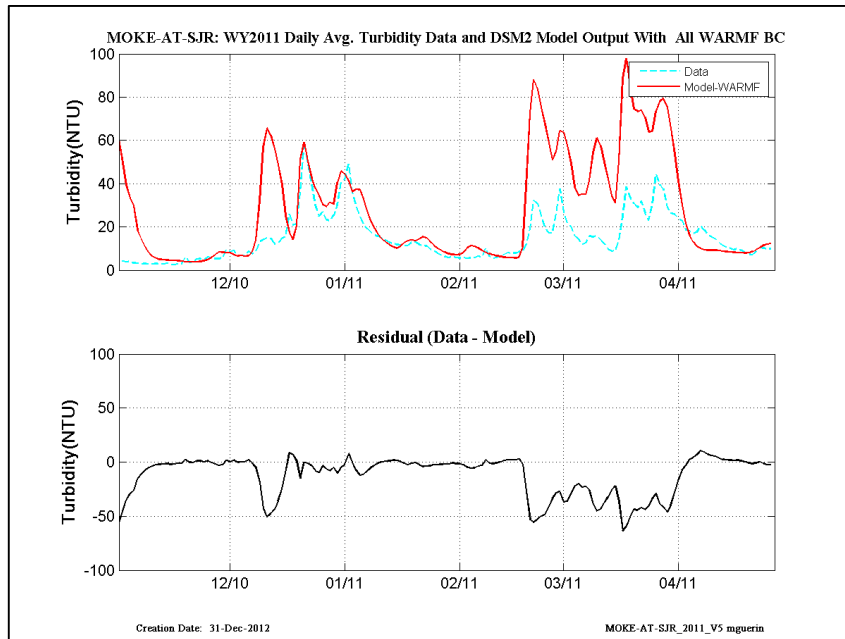


Figure 14-96 WY2011: DSM2 daily-averaged turbidity model results using WARMF-Only turbidity at the inflow boundaries– location is Mokelumne at San Joaquin River.

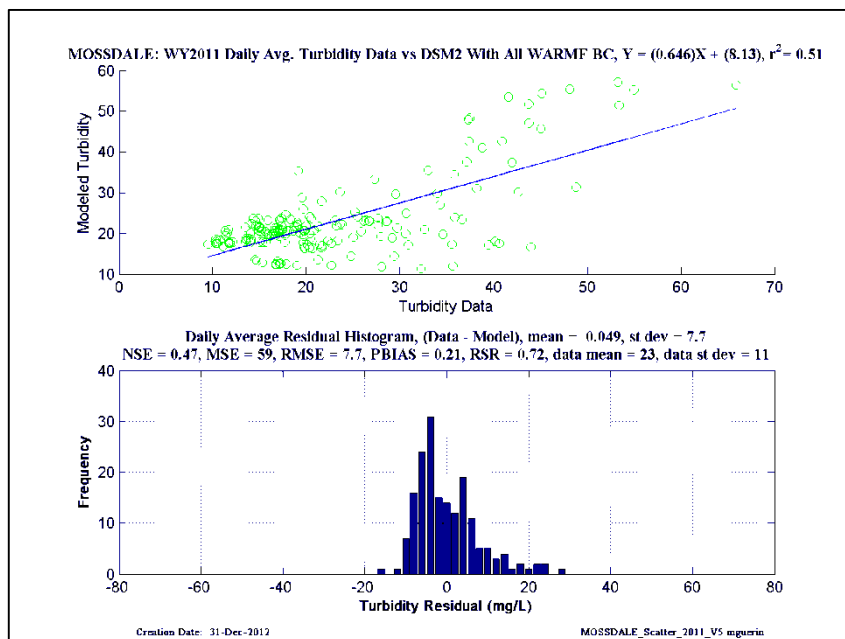
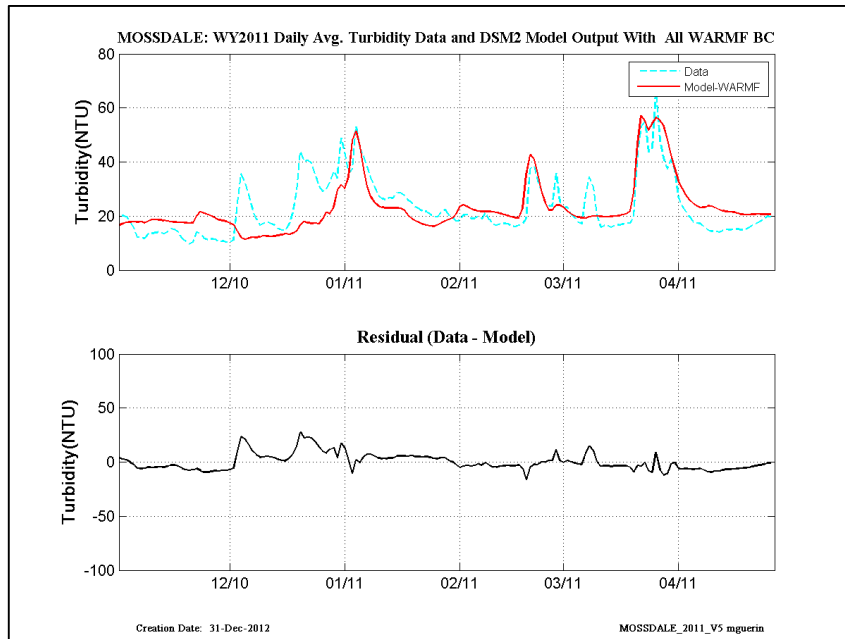


Figure 14-97 WY2011: DSM2 daily-averaged turbidity model results using WARMF-Only turbidity at the inflow boundaries– location is Mossdale.

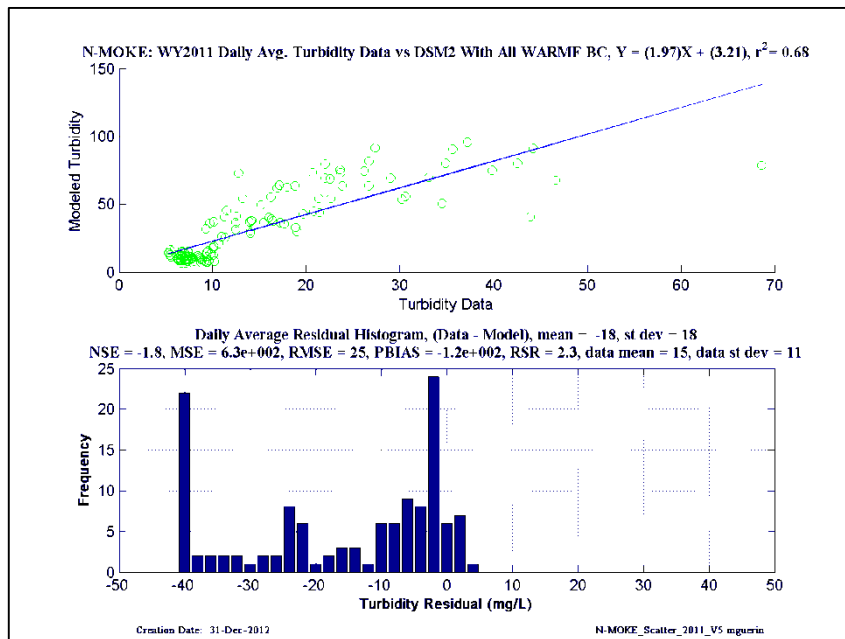
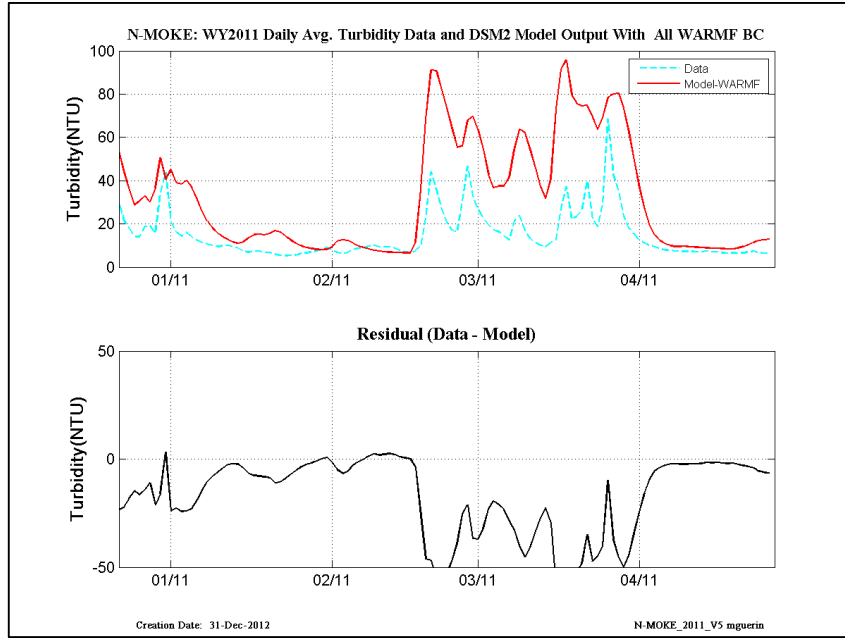


Figure 14-98 WY2011: DSM2 daily-averaged turbidity model results using WARMF-Only turbidity at the inflow boundaries– location is North Mokelumne.

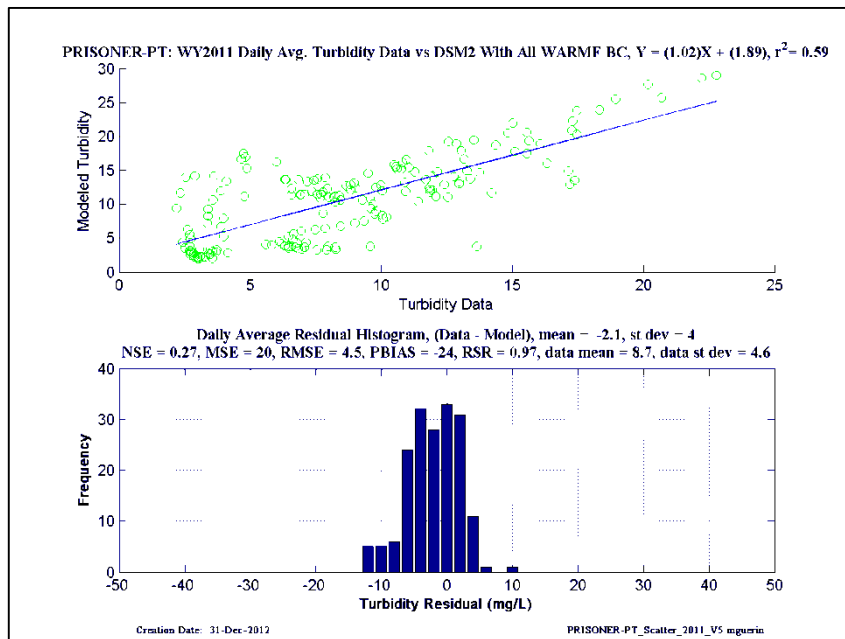
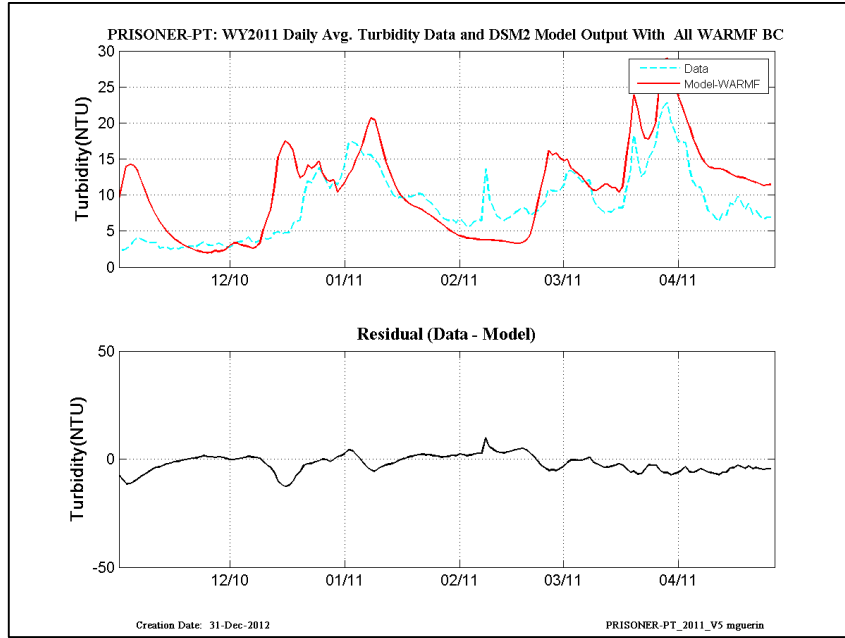


Figure 14-99 WY2011: DSM2 daily-averaged turbidity model results using WARMF-Only turbidity at the inflow boundaries– location is Prisoner Point.

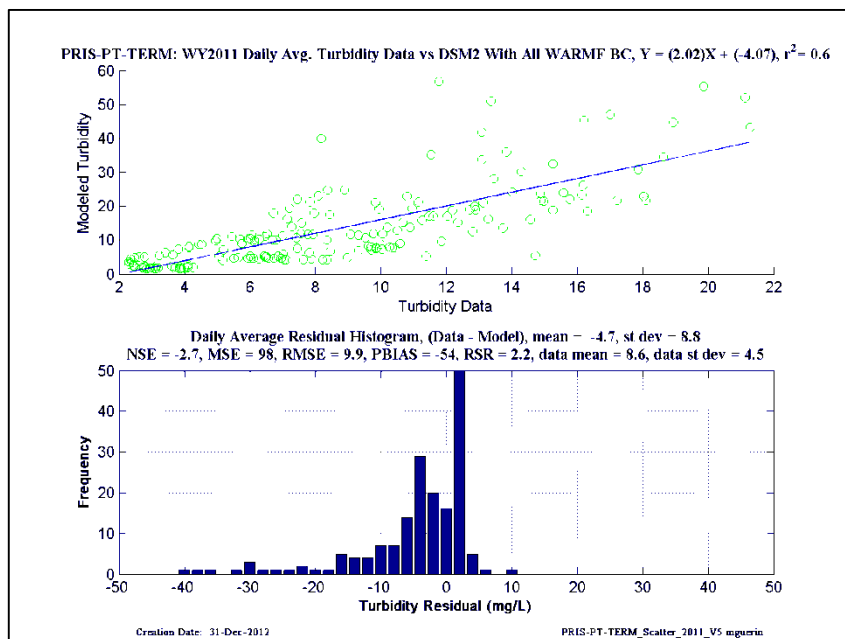
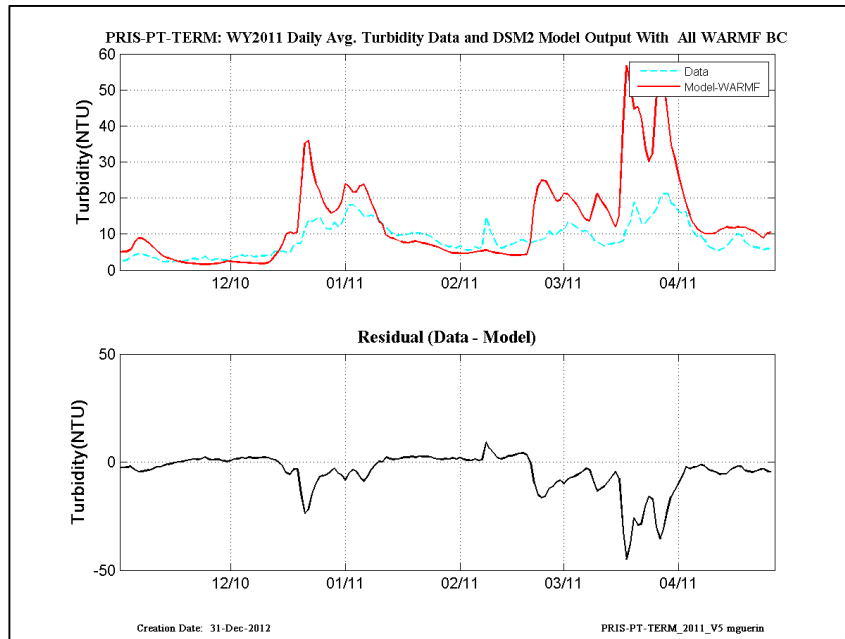


Figure 14-100 WY2011: DSM2 daily-averaged turbidity model results using WARMF-Only turbidity at the inflow boundaries– location is Prisoner Point at Terminous.

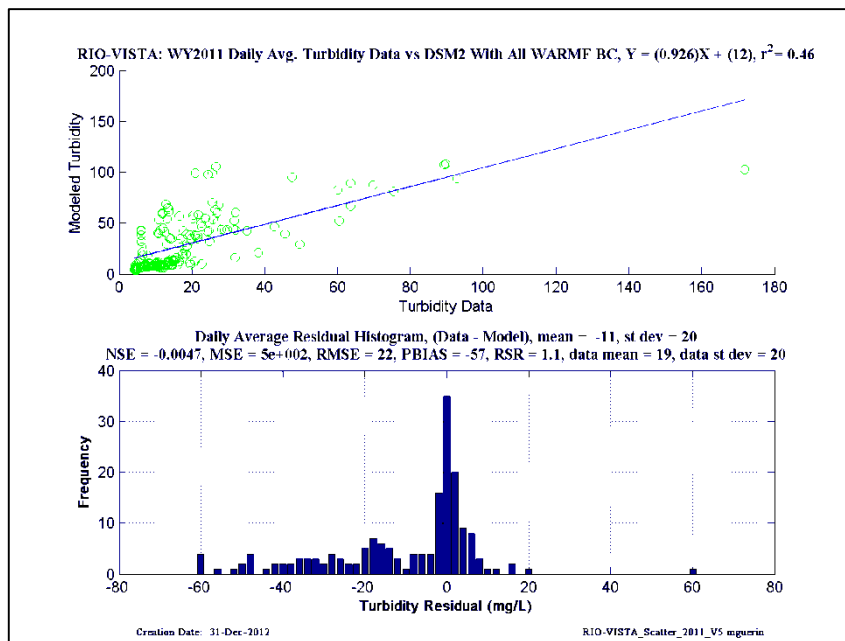
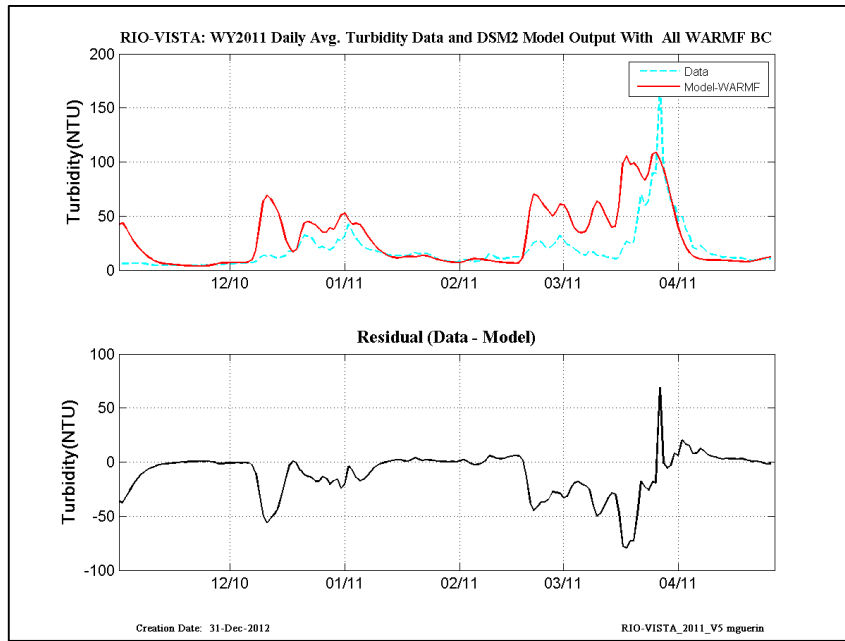


Figure 14-101 WY2011: DSM2 daily-averaged turbidity model results using WARMF-Only turbidity at the inflow boundaries– location is Rio Vista.

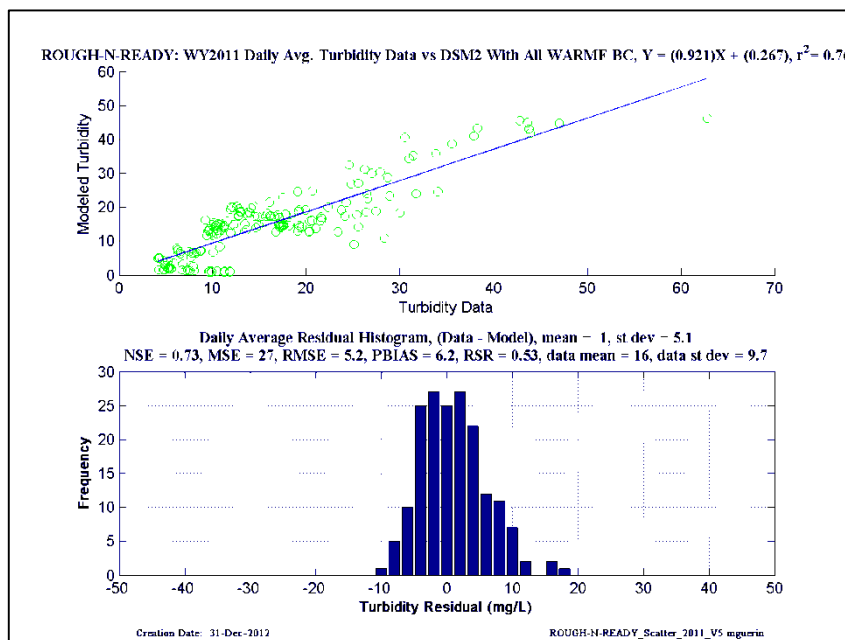
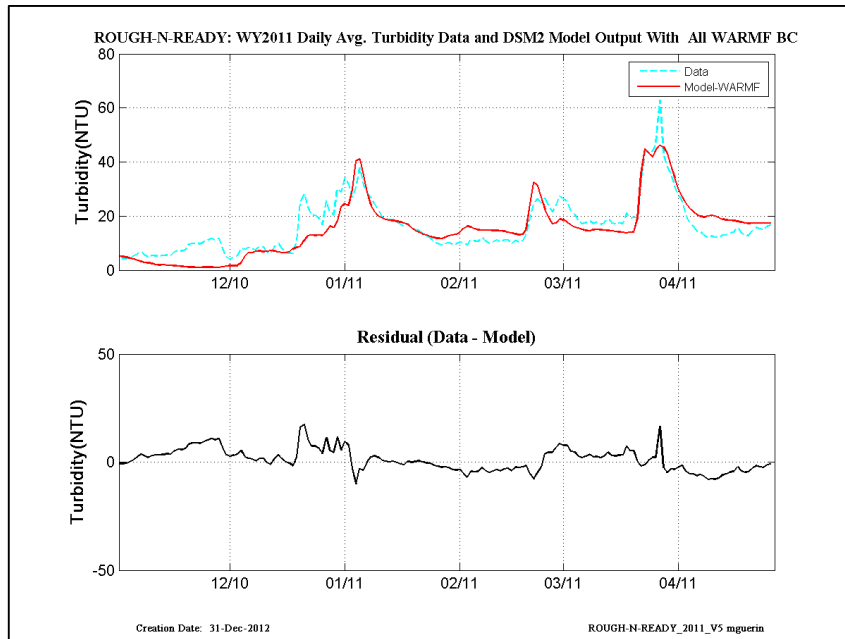


Figure 14-102 WY2011: DSM2 daily-averaged turbidity model results using WARMF-Only turbidity at the inflow boundaries– location is Rough-N-Ready Island.

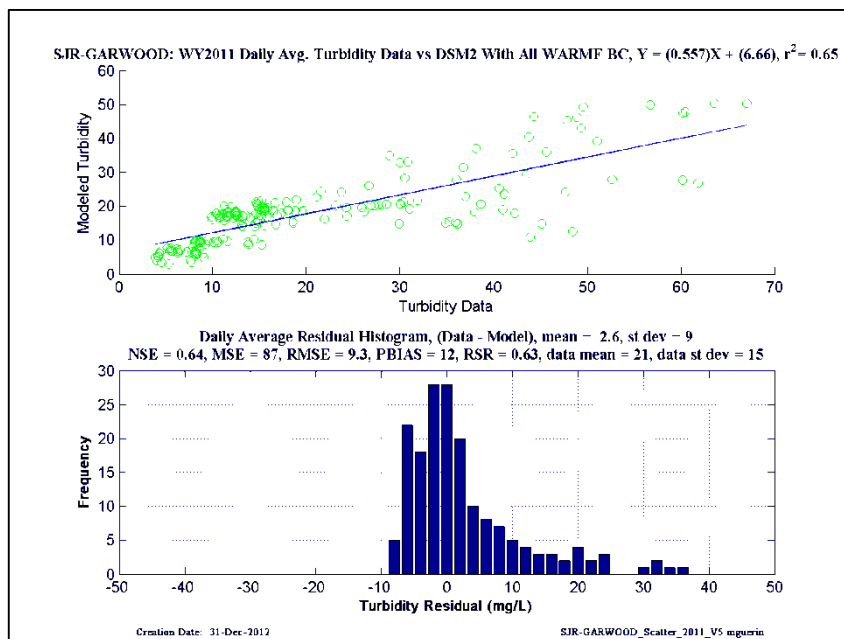
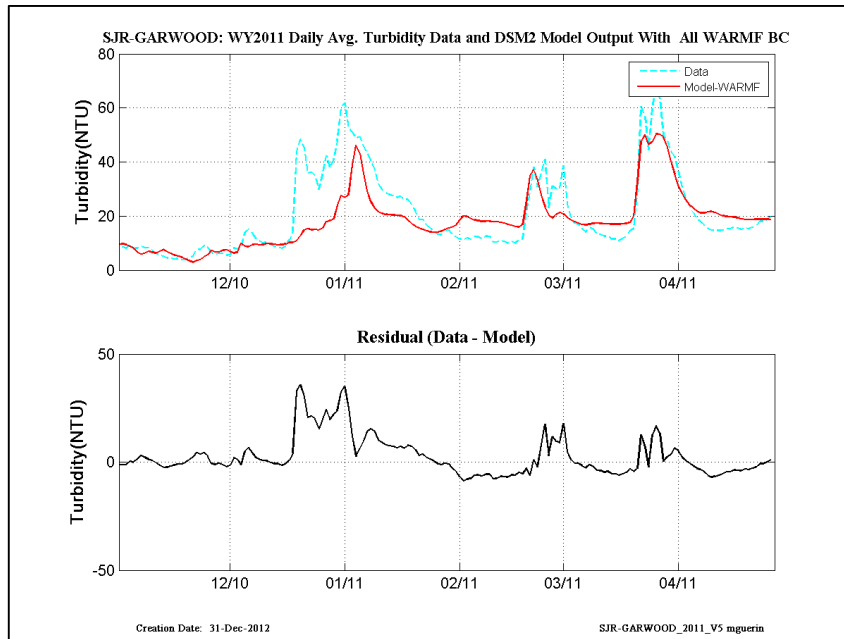


Figure 14-103 WY2011: DSM2 daily-averaged turbidity model results using WARMF-Only turbidity at the inflow boundaries– location is San Joaquin at Garwood.

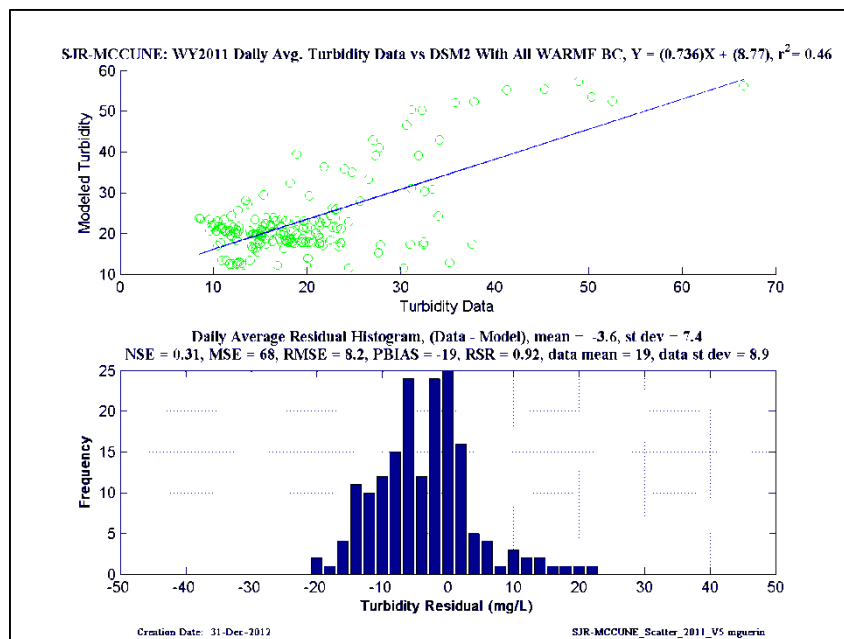
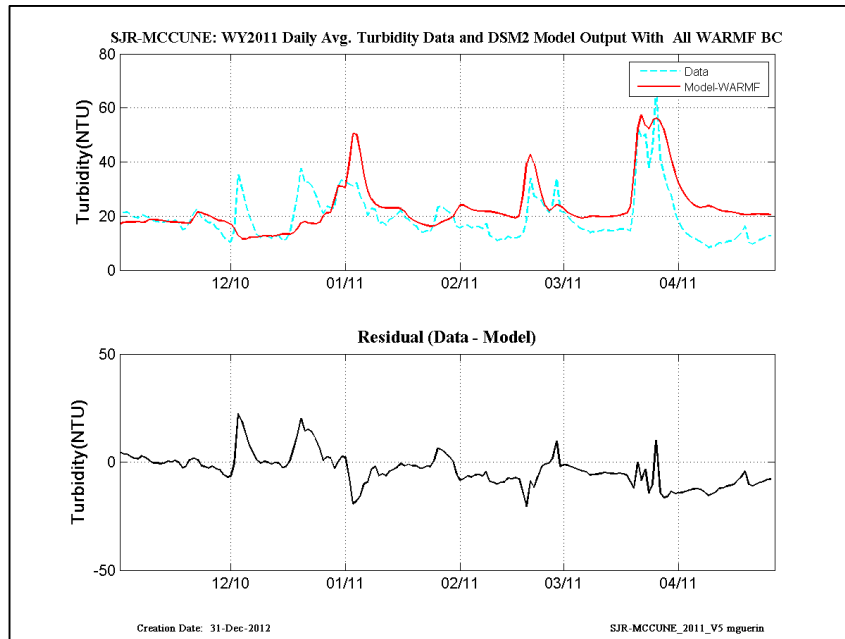


Figure 14-104 WY2011: DSM2 daily-averaged turbidity model results using WARMF-Only turbidity at the inflow boundaries– location is San Joaquin at McCune.

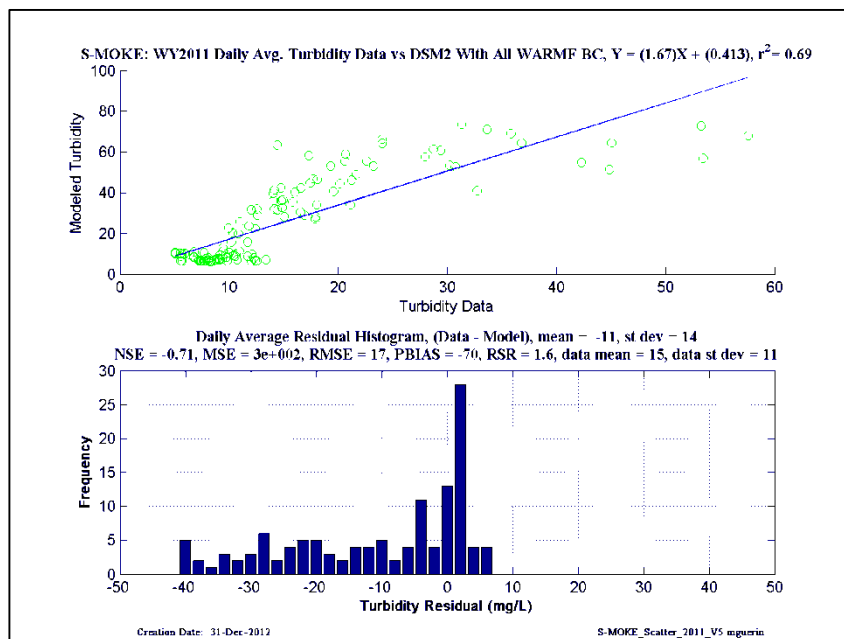
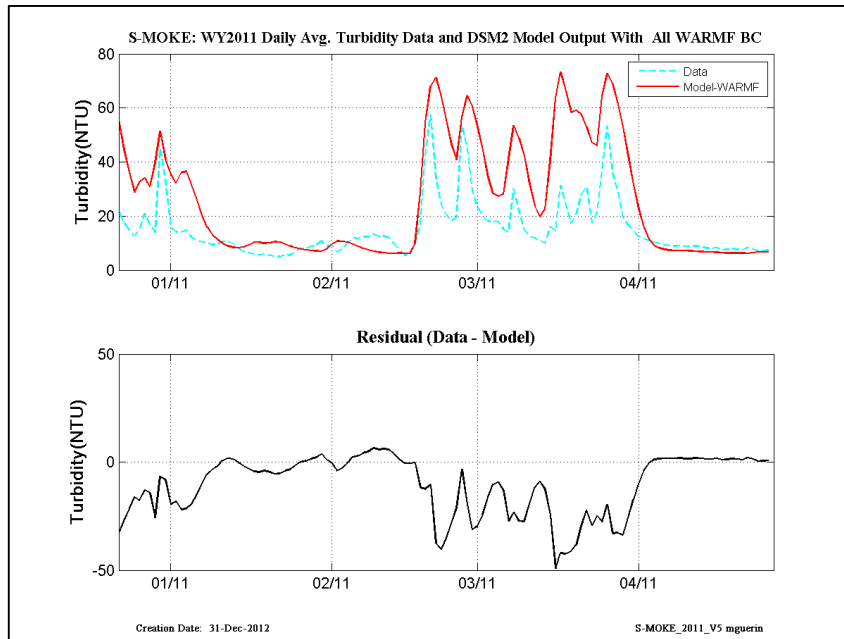


Figure 14-105 WY2011: DSM2 daily-averaged turbidity model results using WARMF-Only turbidity at the inflow boundaries– location is South Mokolumne.

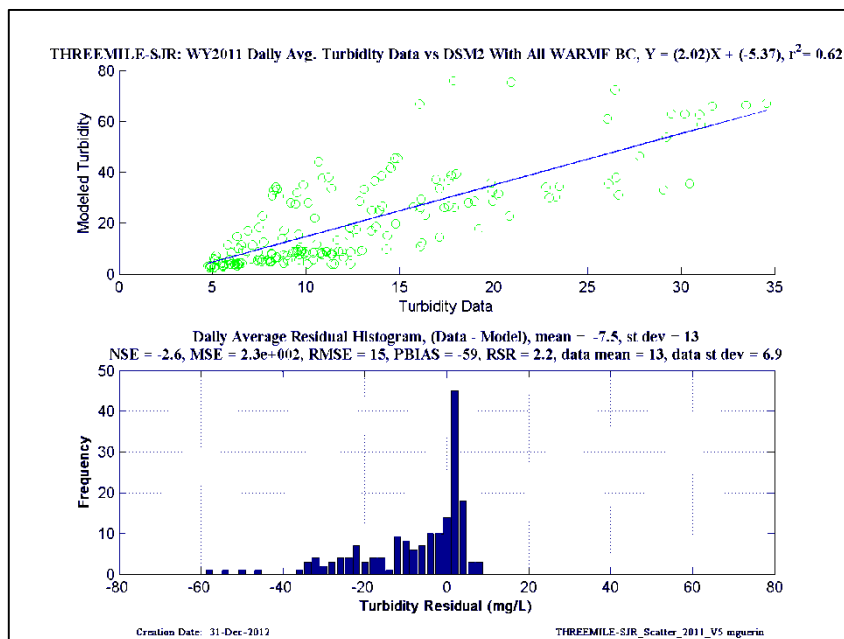
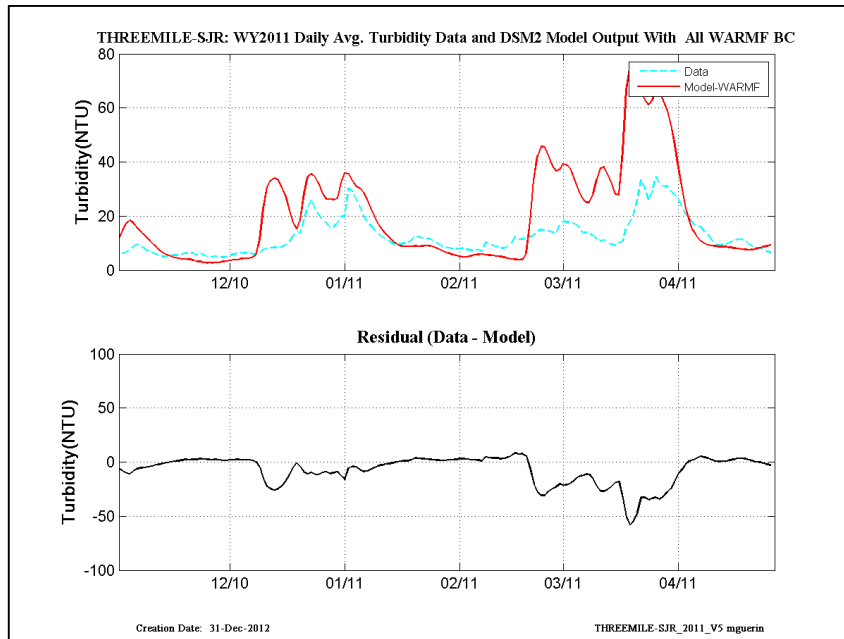


Figure 14-106 WY2011: DSM2 daily-averaged turbidity model results using WARMF-Only turbidity at the inflow boundaries– location is Threemile at San Joaquin.

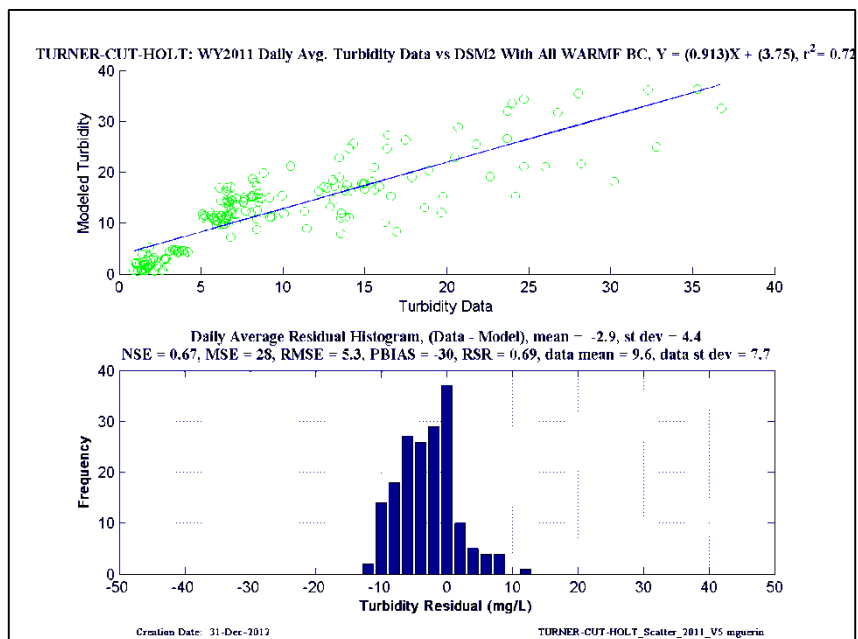
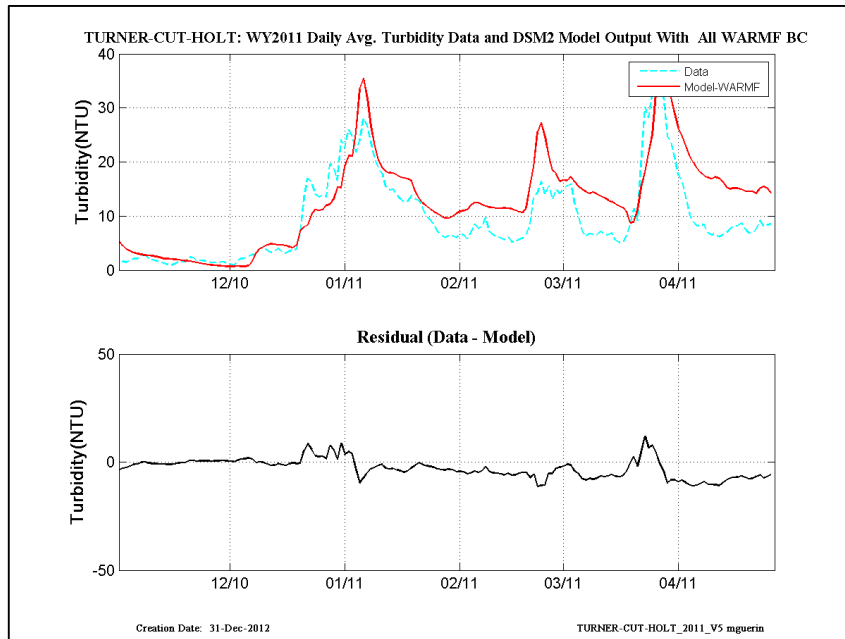


Figure 14-107 WY2011: DSM2 daily-averaged turbidity model results using WARMF-Only turbidity at the inflow boundaries– location is Turner Cut at Holt.

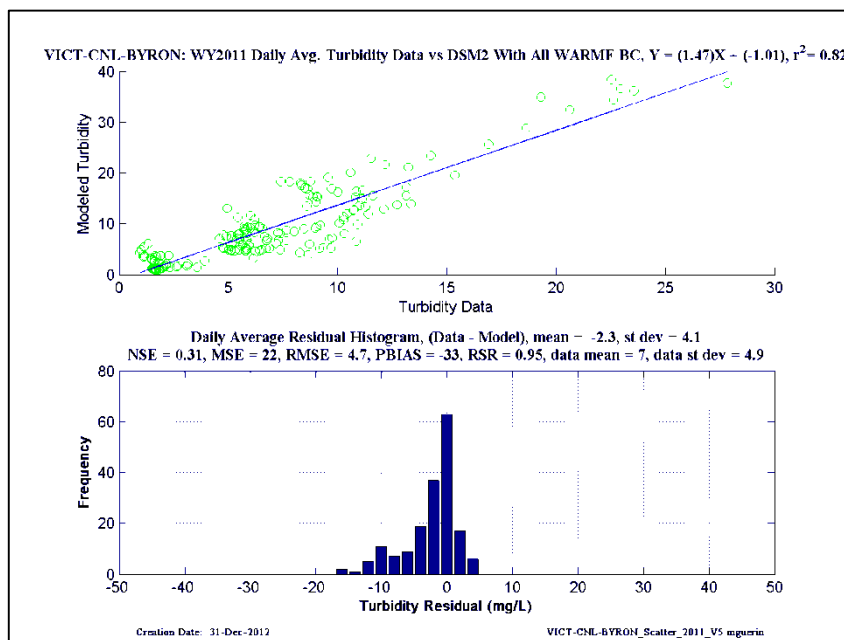
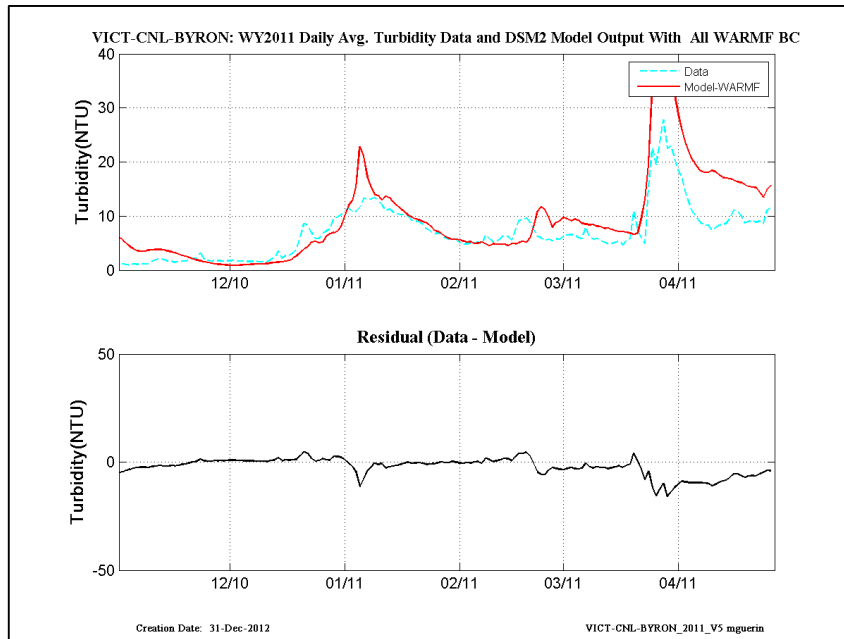


Figure 14-108 WY2011: DSM2 daily-averaged turbidity model results using WARMF-Only turbidity at the inflow boundaries– location is Victoria Canal at Byron.

**15 Appendix VI – Figures and Statistics Documenting DSM2 QUAL
Historical 1975 – 2011 Turbidity Model Application with Mixed
SSC-WARMF Boundary Conditions**

31.1 Early years: 1975 -1990

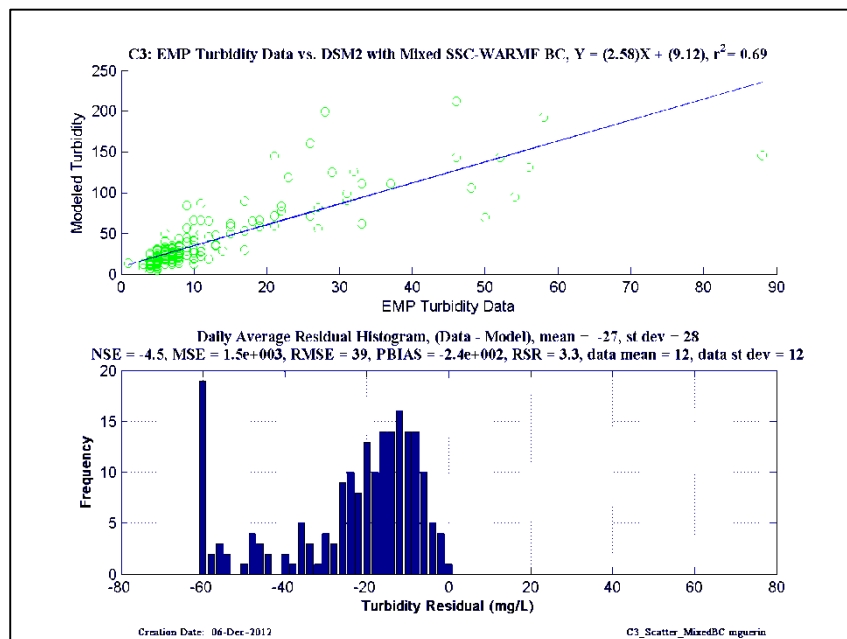
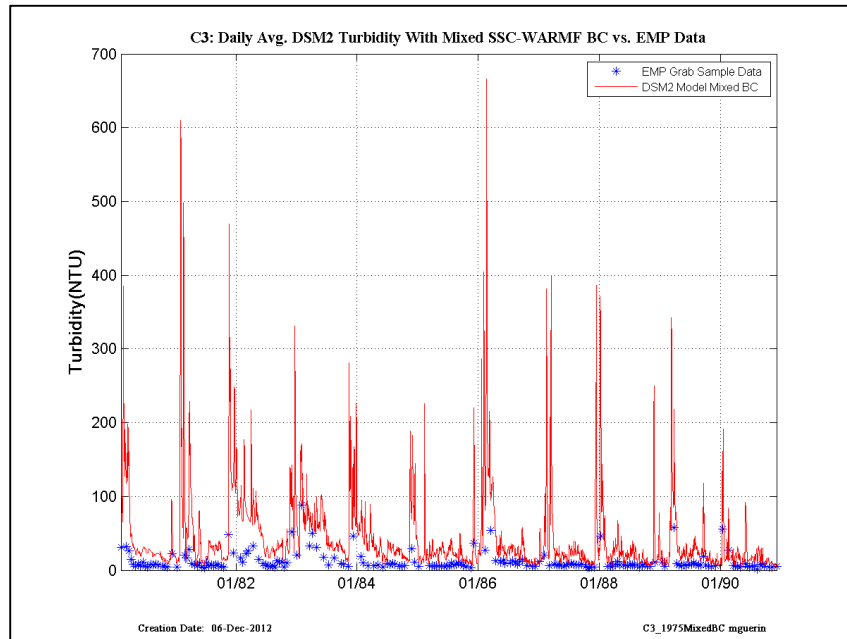


Figure 15-1 DSM2 daily-averaged turbidity model results using USGS-SSC at Freeport and Vernalis, and WARMF turbidity at other inflow boundaries compared to EMP grab-sample data, early years– location is EMP C3.

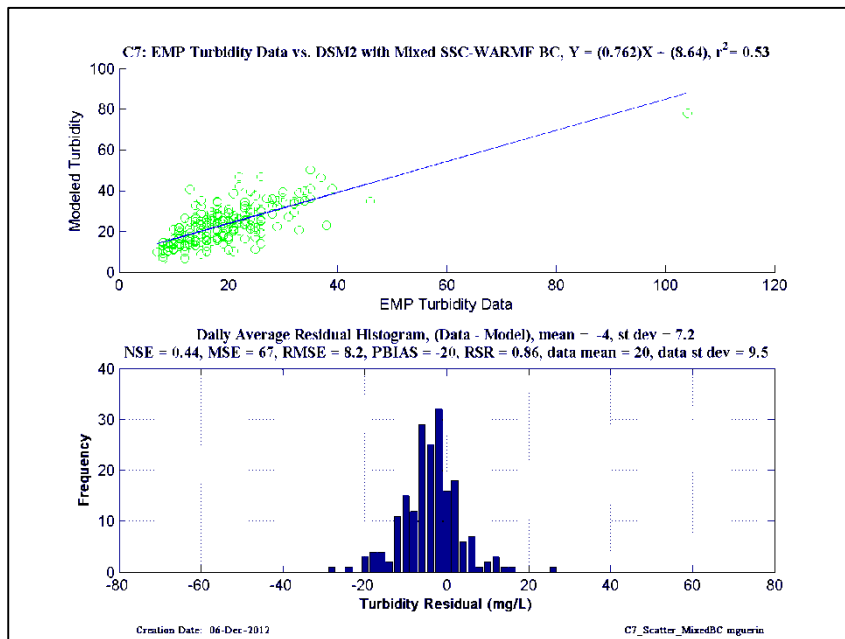
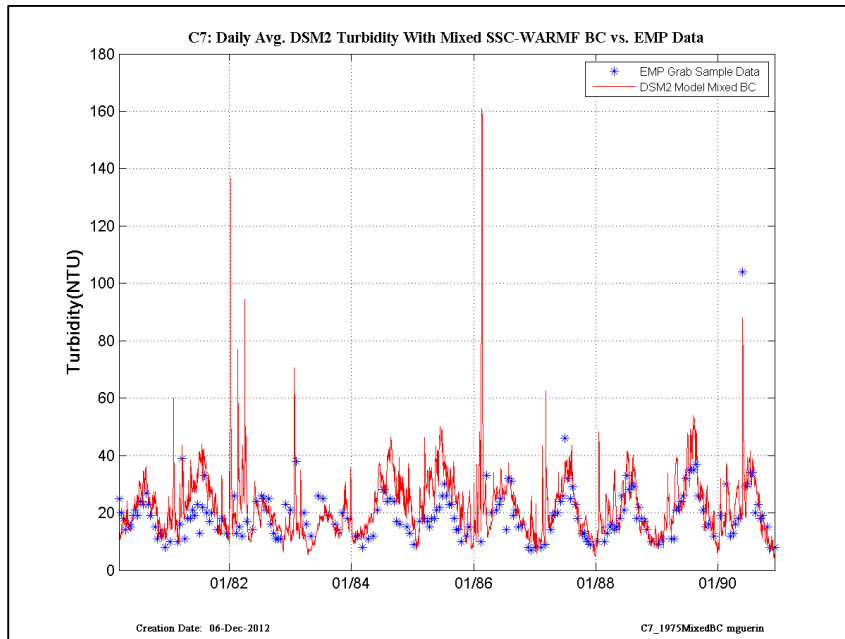


Figure 15-2 DSM2 daily-averaged turbidity model results using USGS-SSC at Freeport and Vernalis, and WARMF turbidity at other inflow boundaries compared to EMP grab-sample data, early years– location is EMP C7.

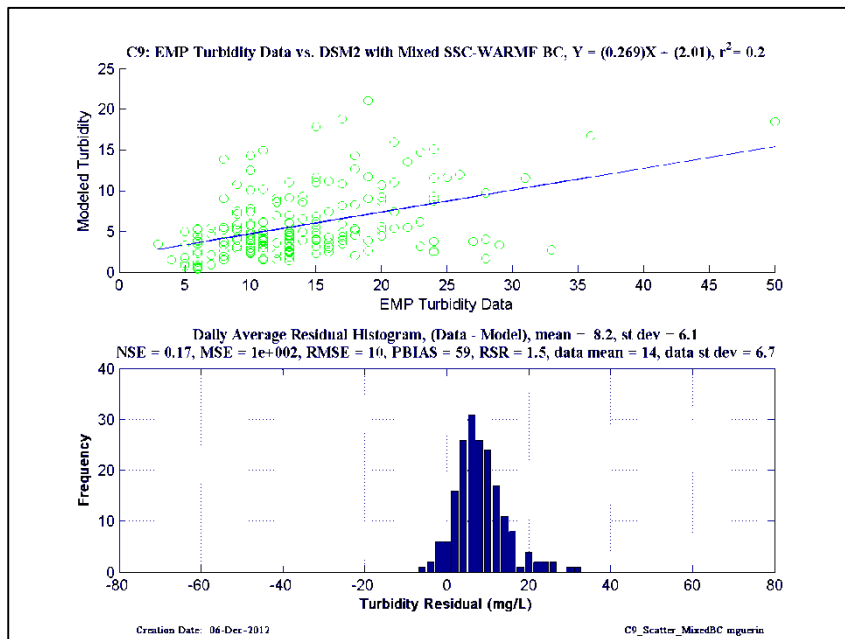
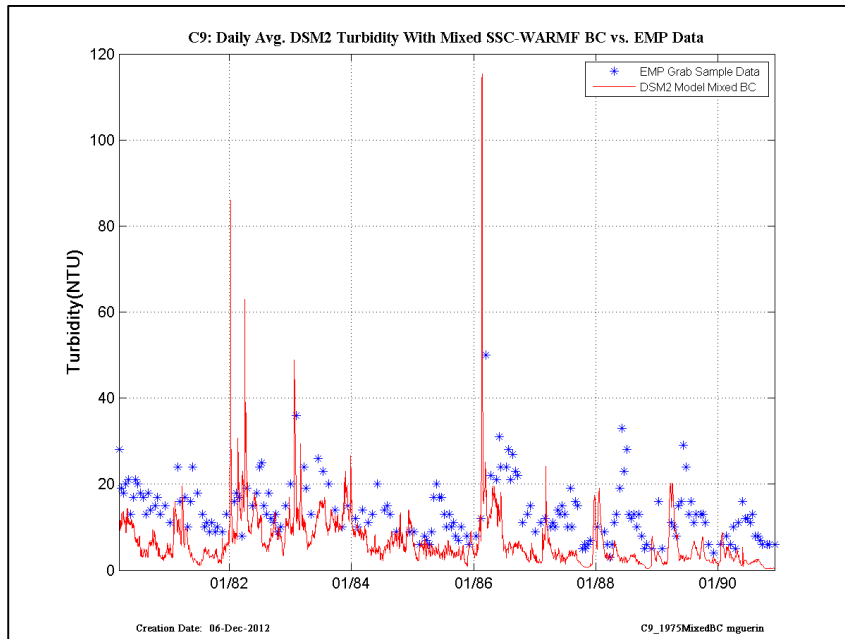


Figure 15-3 DSM2 daily-averaged turbidity model results using USGS-SSC at Freeport and Vernalis, and WARMF turbidity at other inflow boundaries compared to EMP grab-sample data, early years– location is EMP C9.

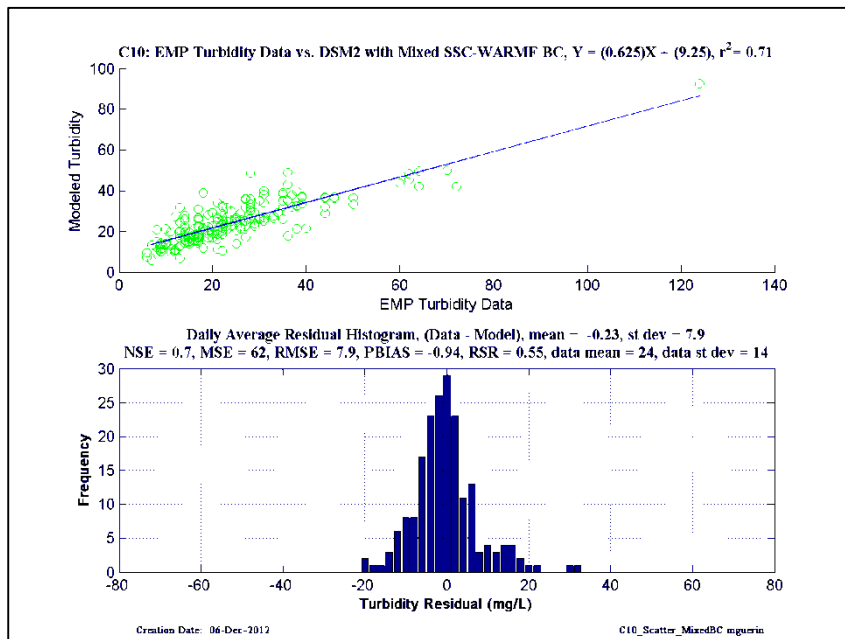
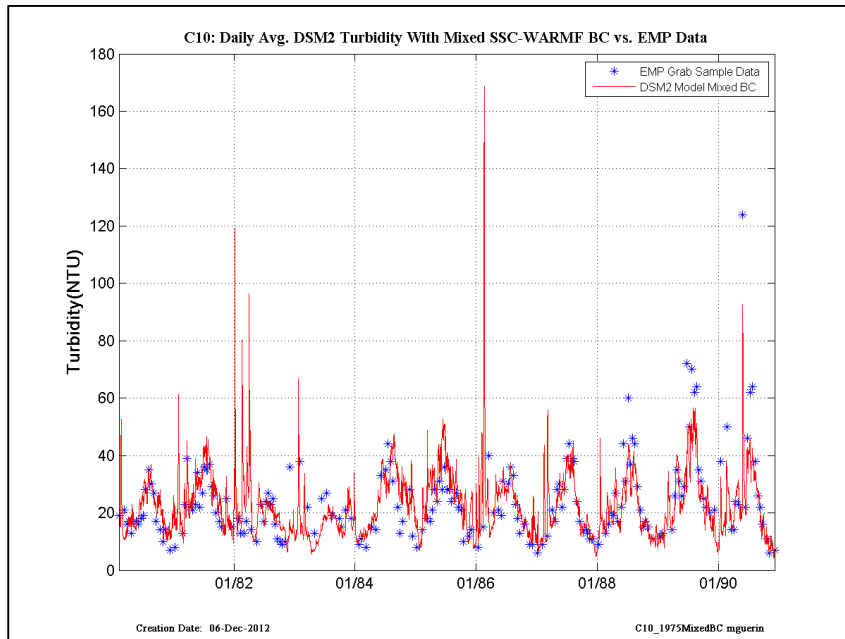


Figure 15-4 DSM2 daily-averaged turbidity model results using USGS-SSC at Freeport and Vernalis, and WARMF turbidity at other inflow boundaries compared to EMP grab-sample data, early years– location is EMP C10.

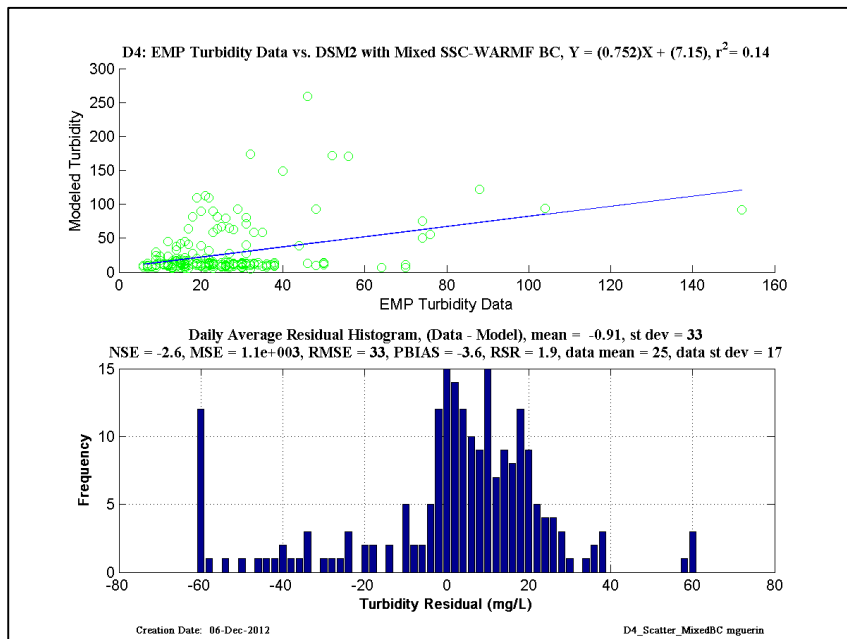
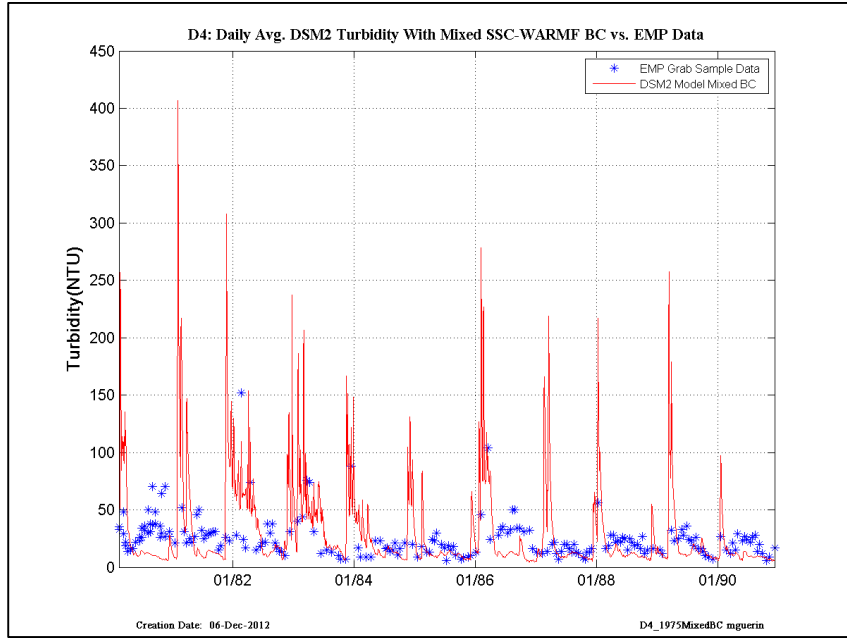


Figure 15-5 DSM2 daily-averaged turbidity model results using USGS-SSC at Freeport and Vernalis, and WARMF turbidity at other inflow boundaries compared to EMP grab-sample data, early years– location is EMP D4.

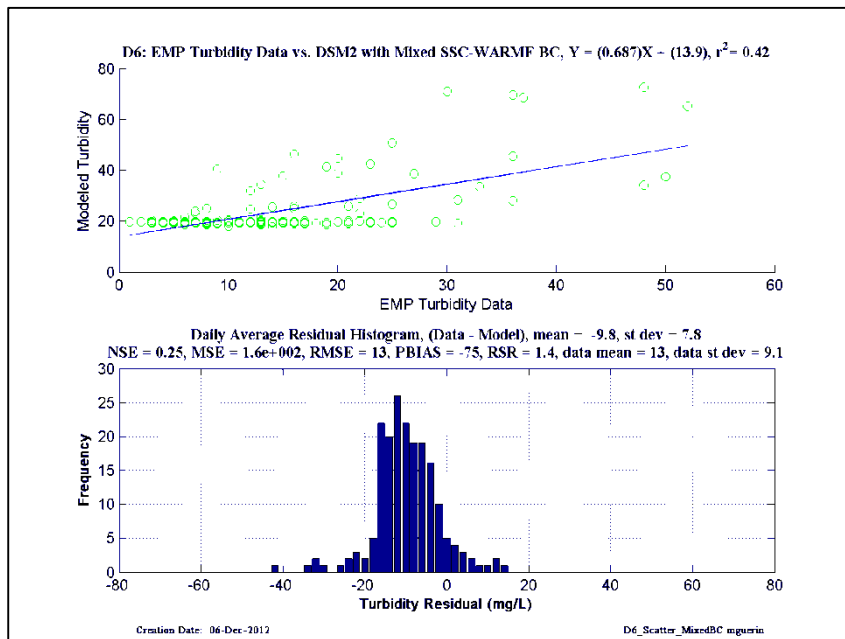
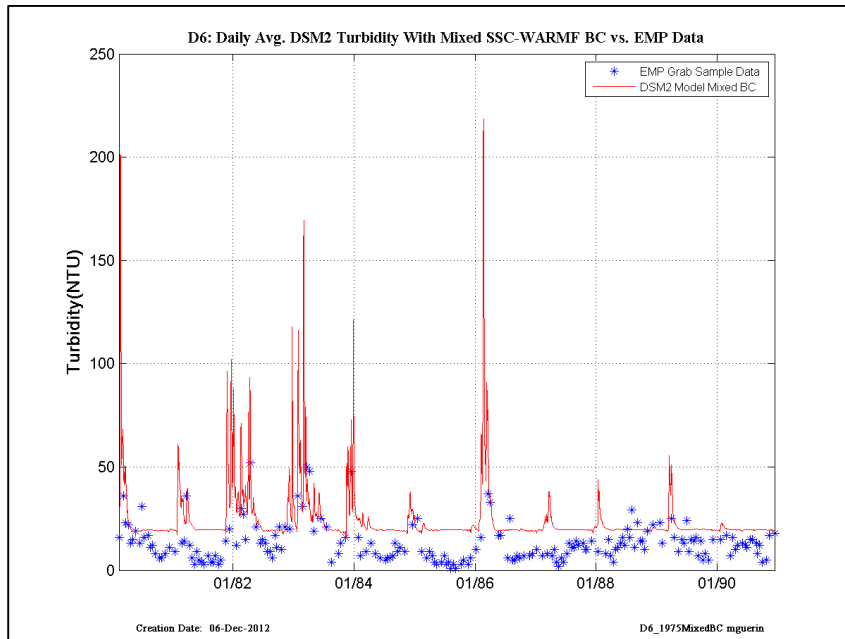


Figure 15-6 DSM2 daily-averaged turbidity model results using USGS-SSC at Freeport and Vernalis, and WARMF turbidity at other inflow boundaries compared to EMP grab-sample data, early years– location is EMP D6.

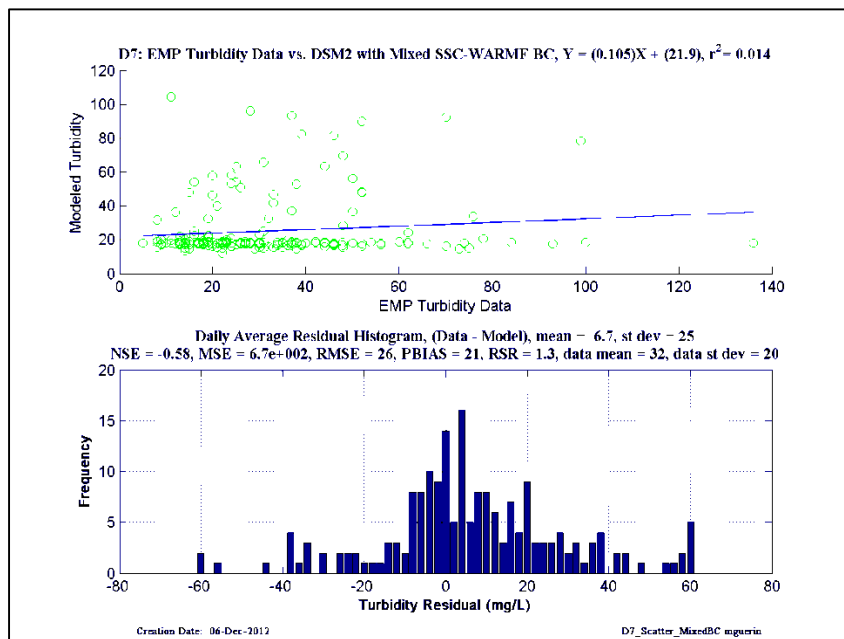
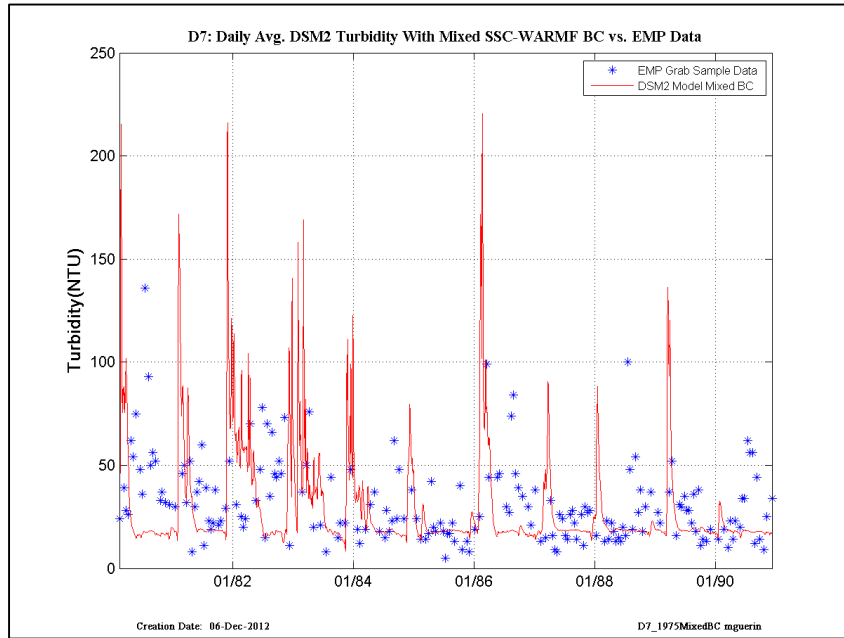


Figure 15-7 DSM2 daily-averaged turbidity model results using USGS-SSC at Freeport and Vernalis, and WARMF turbidity at other inflow boundaries compared to EMP grab-sample data, early years– location is EMP D7.

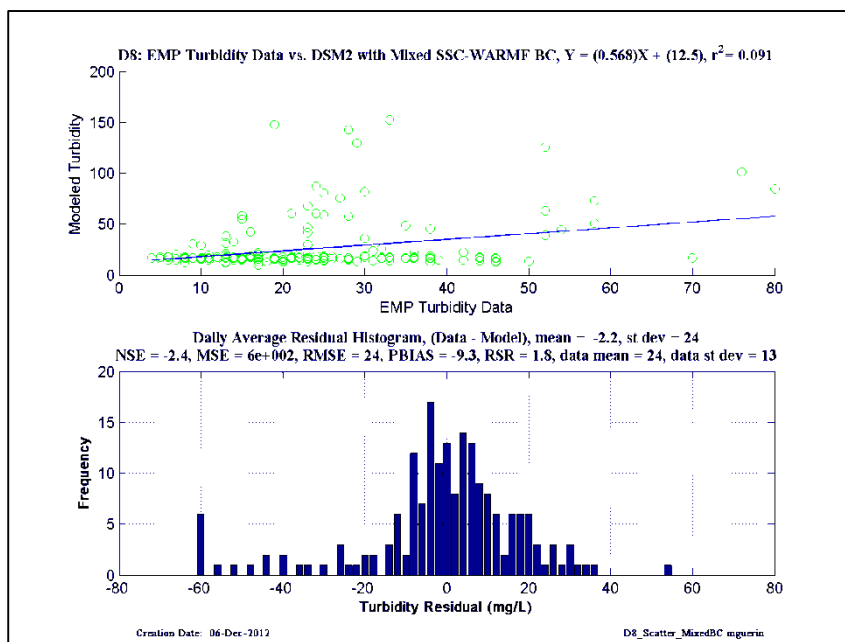
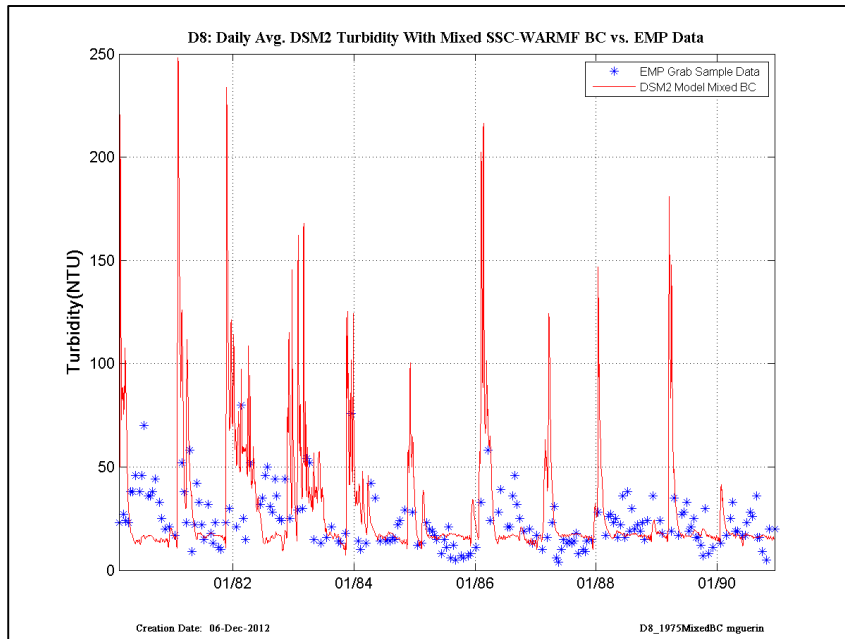


Figure 15-8 DSM2 daily-averaged turbidity model results using USGS-SSC at Freeport and Vernalis, and WARMF turbidity at other inflow boundaries compared to EMP grab-sample data, early years—location is EMP D8.

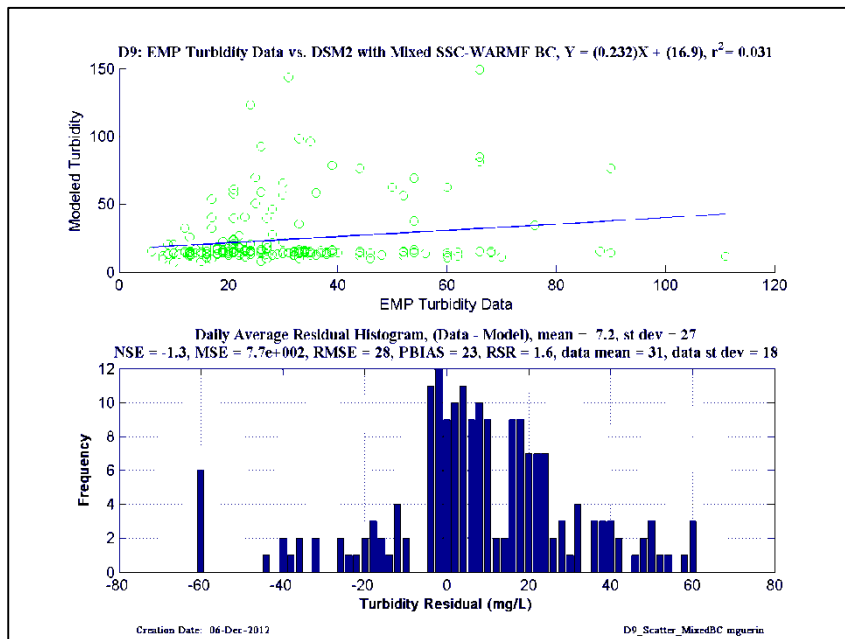
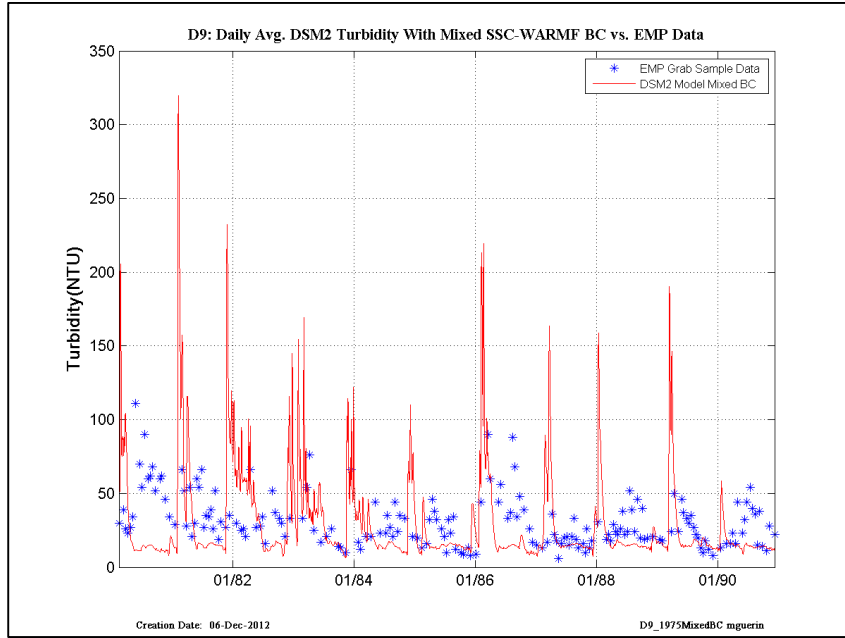


Figure 15-9 DSM2 daily-averaged turbidity model results using USGS-SSC at Freeport and Vernalis, and WARMF turbidity at other inflow boundaries compared to EMP grab-sample data, early years– location is EMP D9.

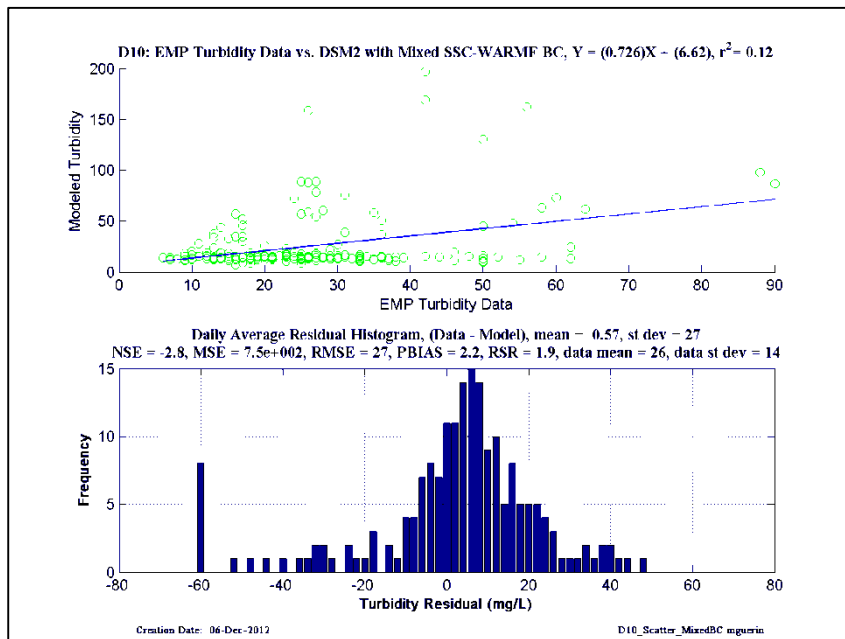
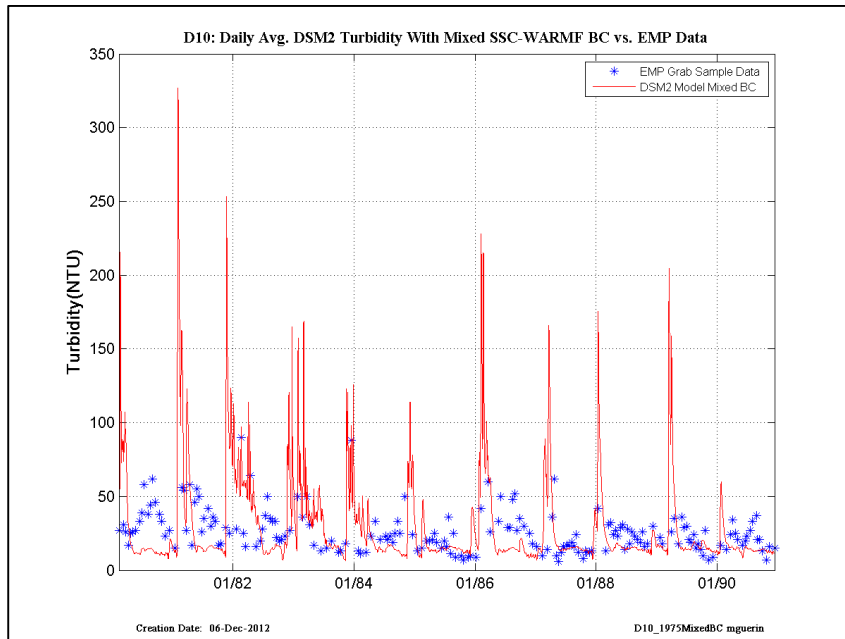


Figure 15-10 DSM2 daily-averaged turbidity model results using USGS-SSC at Freeport and Vernalis, and WARMF turbidity at other inflow boundaries compared to EMP grab-sample data, early years– location is EMP D10.

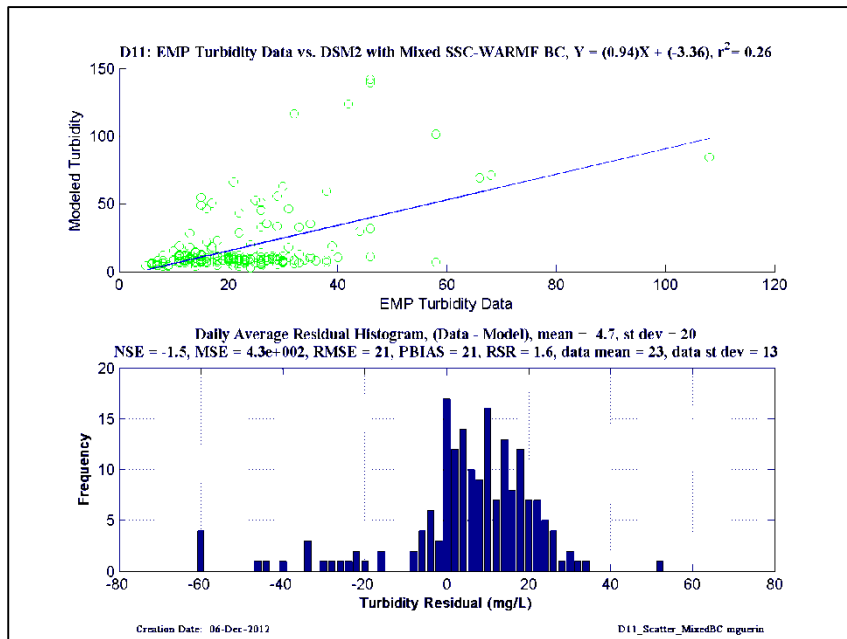
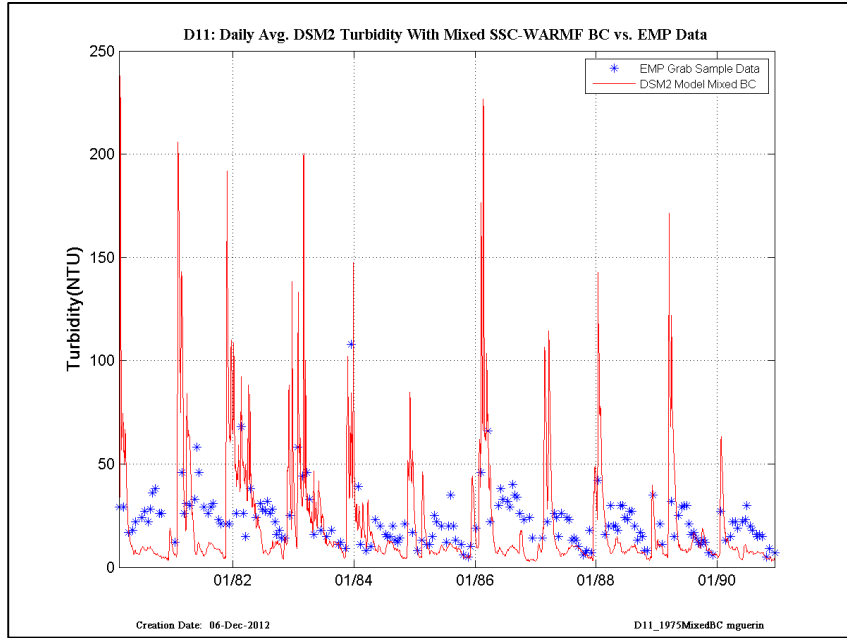


Figure 15-11 DSM2 daily-averaged turbidity model results using USGS-SSC at Freeport and Vernalis, and WARMF turbidity at other inflow boundaries compared to EMP grab-sample data, early years– location is EMP D11.

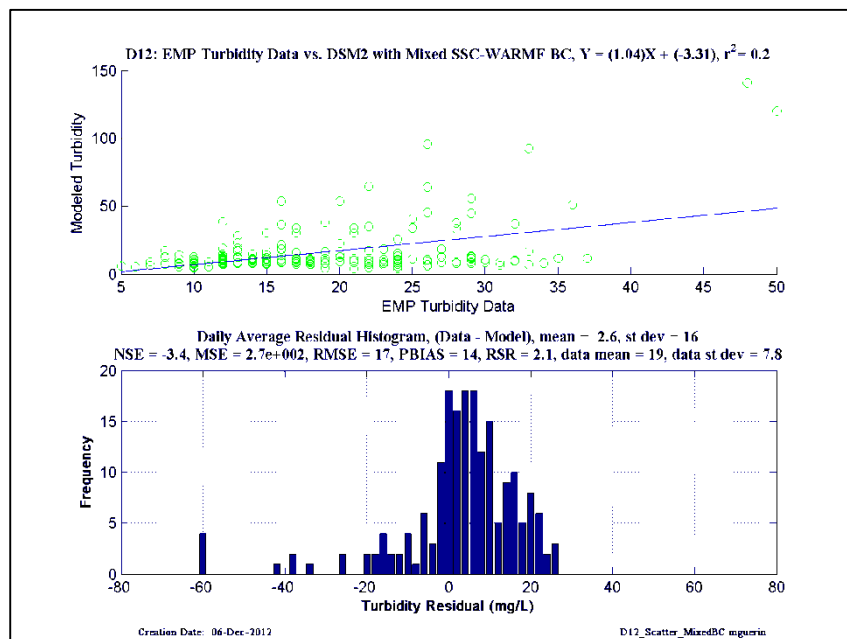
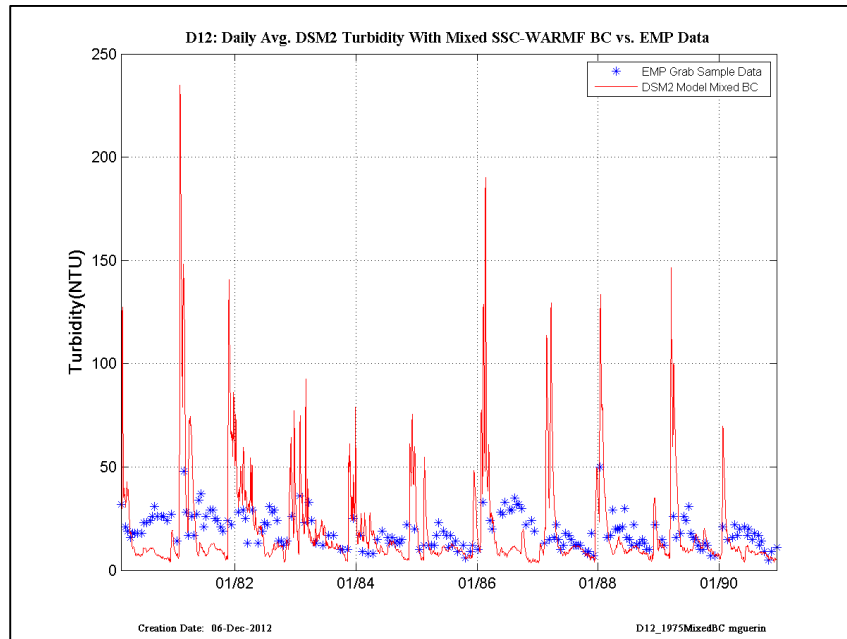


Figure 15-12 DSM2 daily-averaged turbidity model results using USGS-SSC at Freeport and Vernalis, and WARMF turbidity at other inflow boundaries compared to EMP grab-sample data, early years– location is EMP D12.

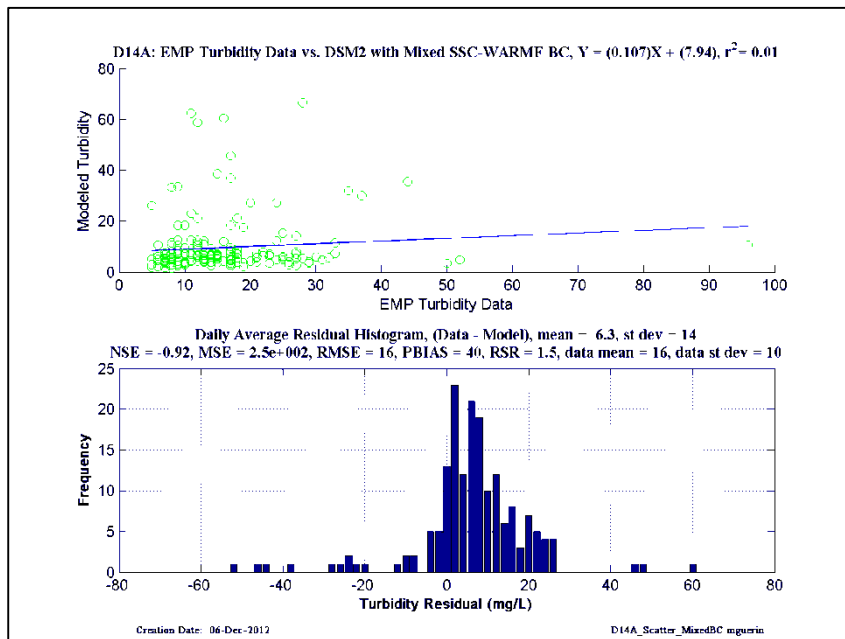
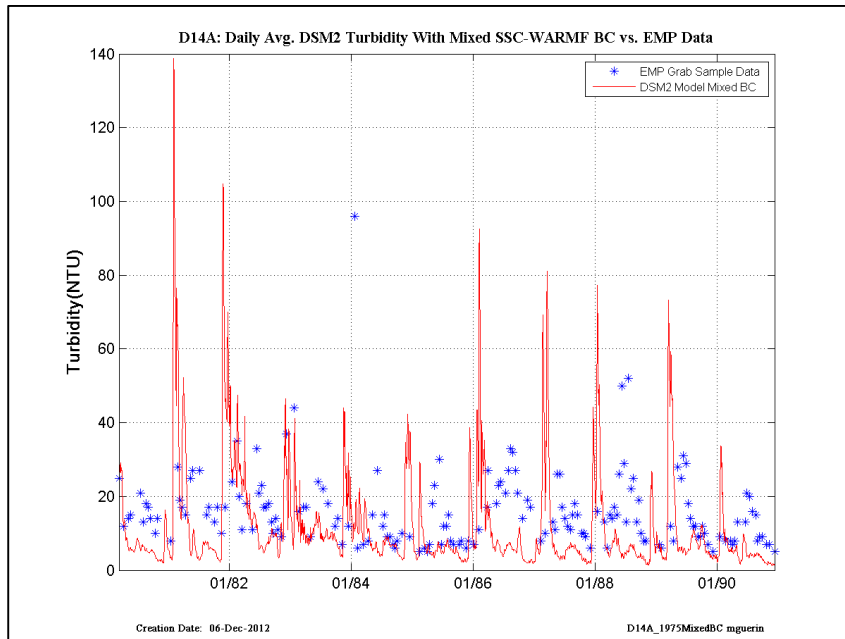


Figure 15-13 DSM2 daily-averaged turbidity model results using USGS-SSC at Freeport and Vernalis, and WARMF turbidity at other inflow boundaries compared to EMP grab-sample data, early years– location is EMP D14A.

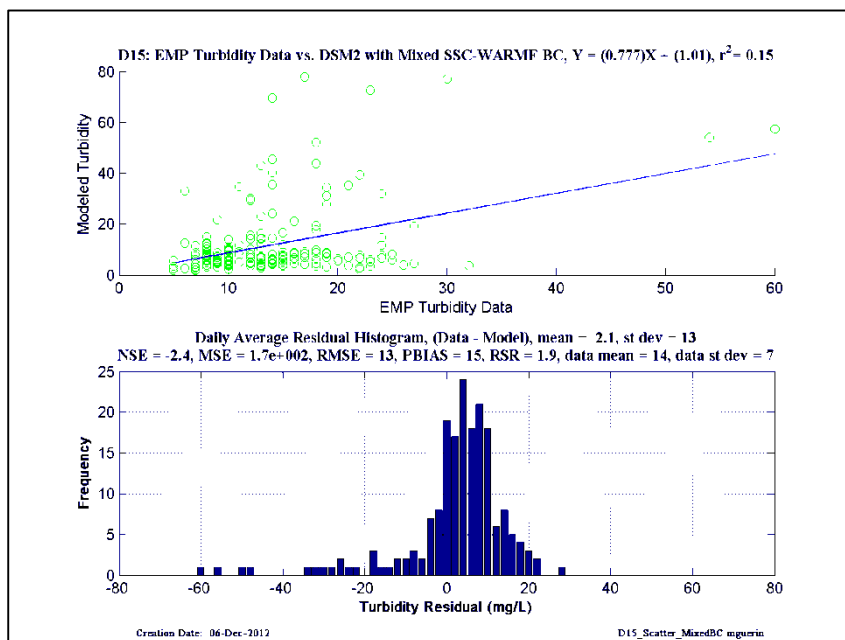
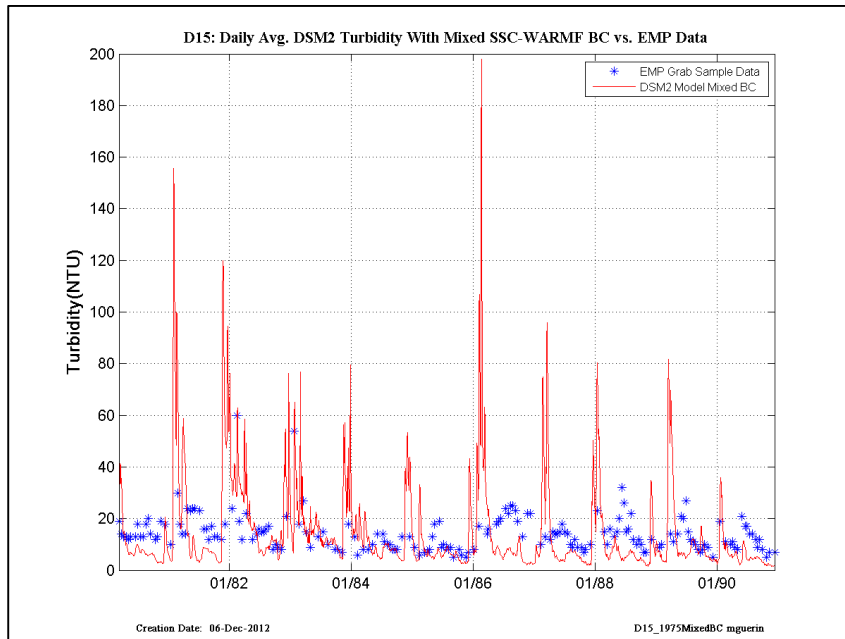


Figure 15-14 DSM2 daily-averaged turbidity model results using USGS-SSC at Freeport and Vernalis, and WARMF turbidity at other inflow boundaries compared to EMP grab-sample data, early years– location is EMP D15.

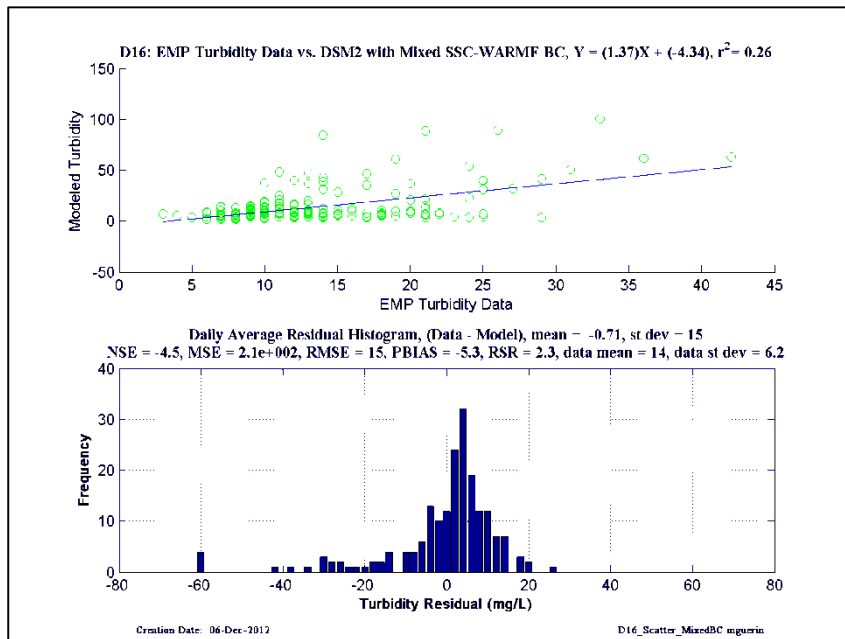
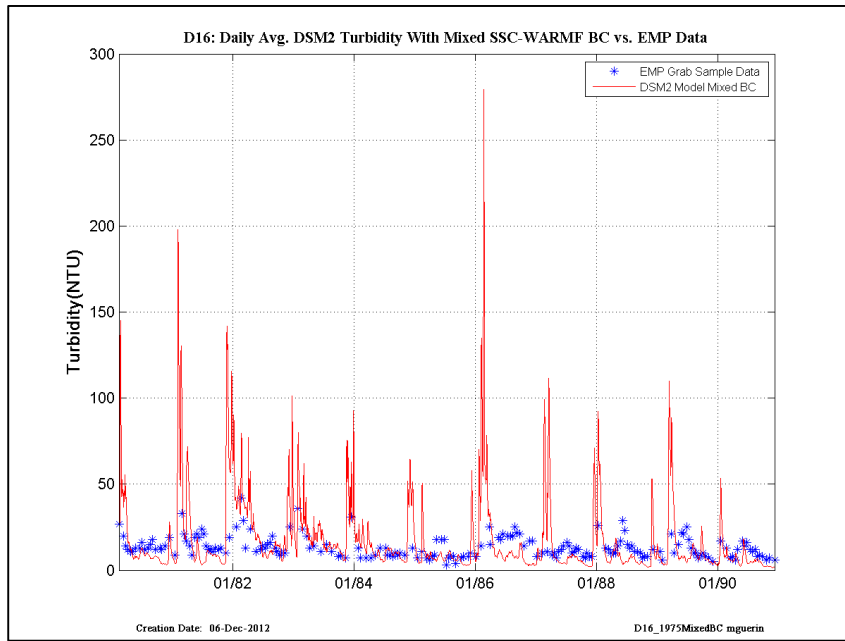


Figure 15-15 DSM2 daily-averaged turbidity model results using USGS-SSC at Freeport and Vernalis, and WARMF turbidity at other inflow boundaries compared to EMP grab-sample data, early years– location is EMP D16.

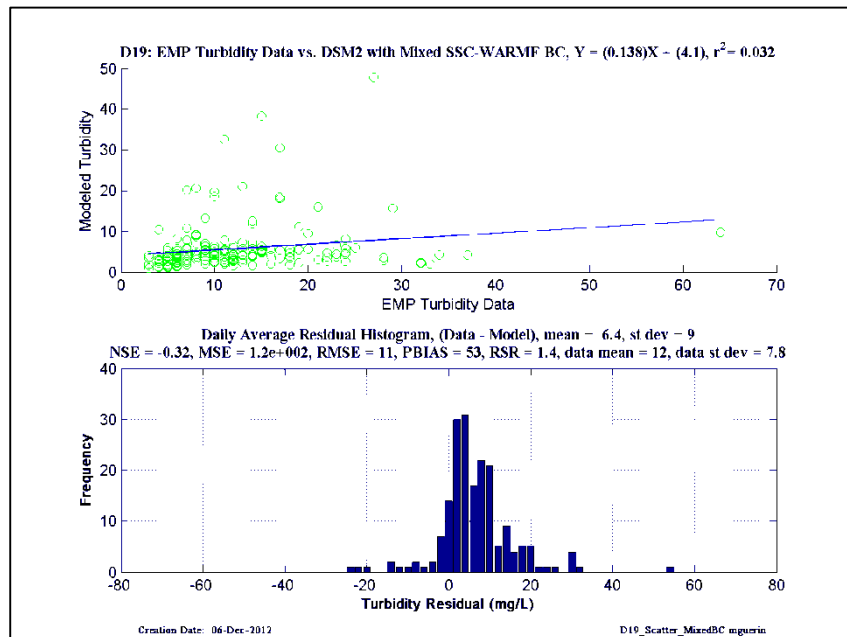
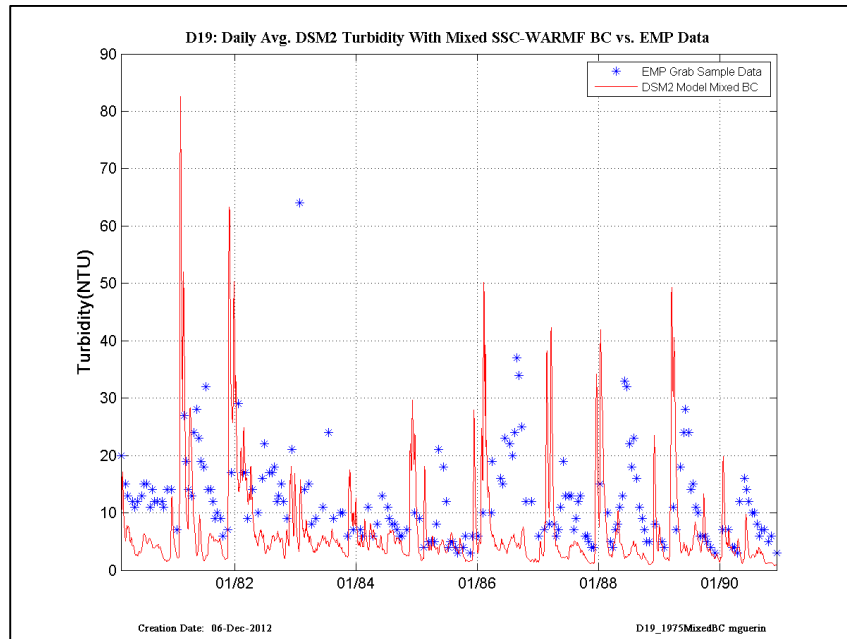


Figure 15-16 DSM2 daily-averaged turbidity model results using USGS-SSC at Freeport and Vernalis, and WARMF turbidity at other inflow boundaries compared to EMP grab-sample data, early years– location is EMP D19.

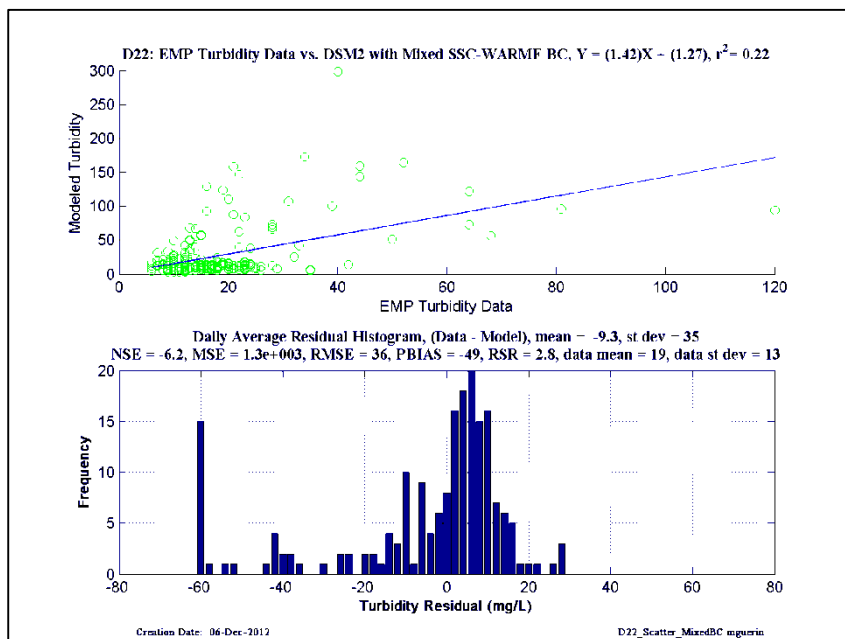
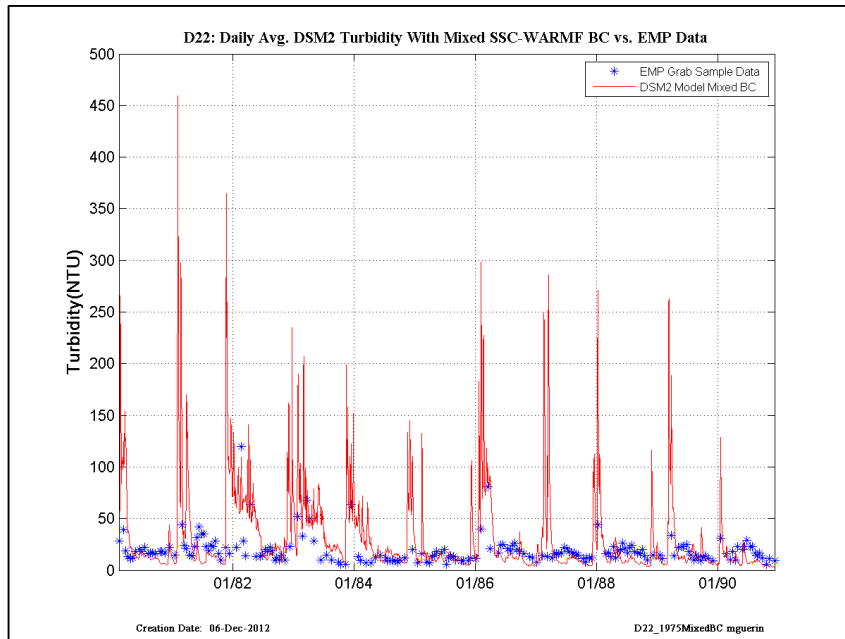


Figure 15-17 DSM2 daily-averaged turbidity model results using USGS-SSC at Freeport and Vernalis, and WARMF turbidity at other inflow boundaries compared to EMP grab-sample data, early years– location is EMP D22.

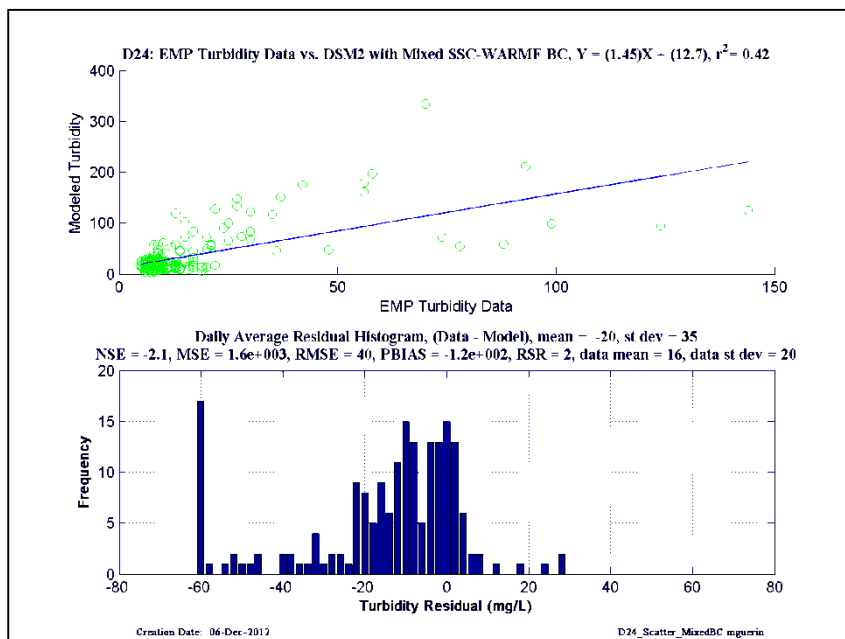
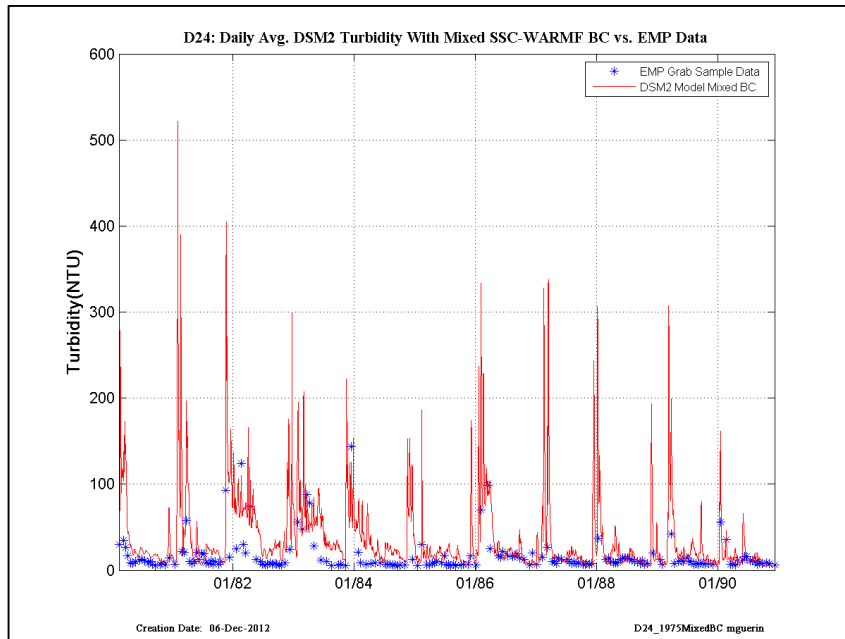


Figure 15-18 DSM2 daily-averaged turbidity model results using USGS-SSC at Freeport and Vernalis, and WARMF turbidity at other inflow boundaries compared to EMP grab-sample data, early years– location is EMP D24.

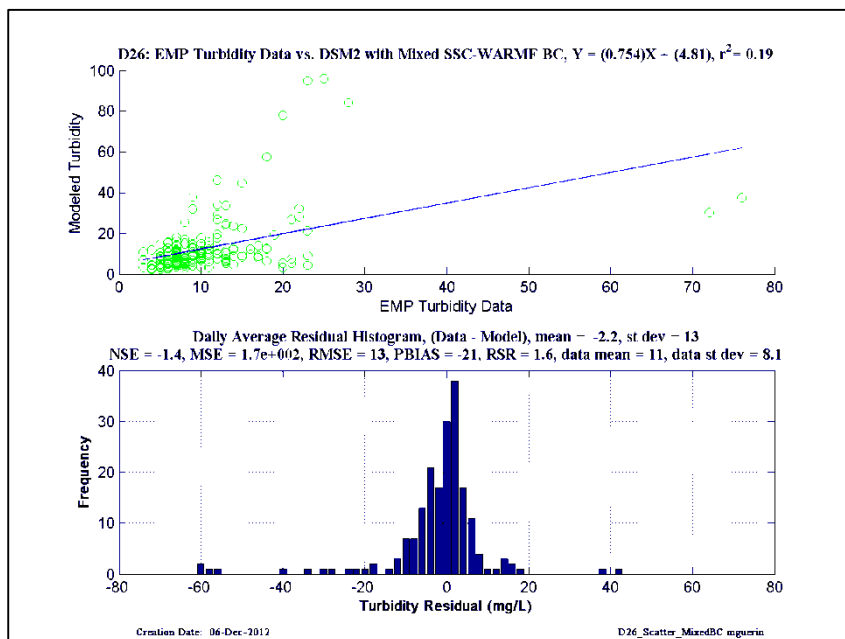
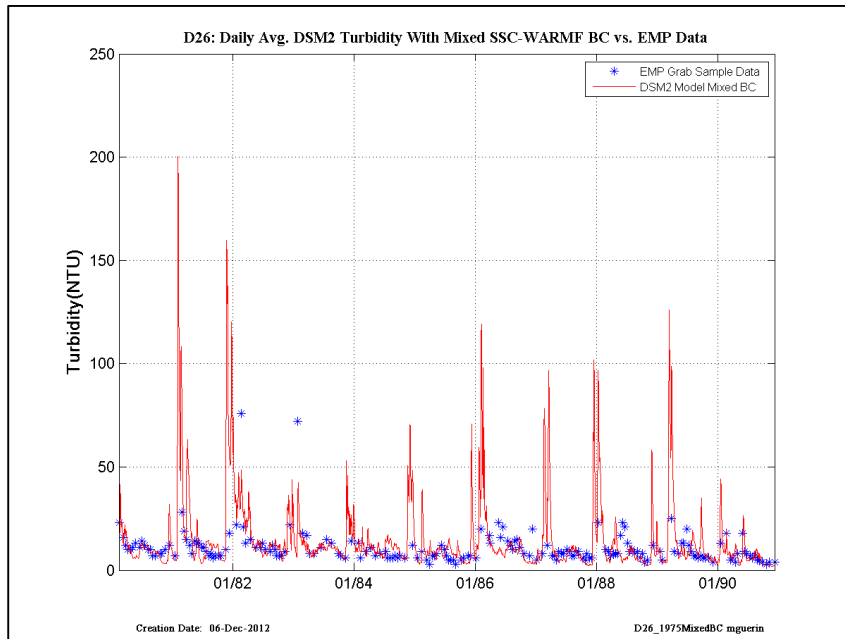


Figure 15-19 DSM2 daily-averaged turbidity model results using USGS-SSC at Freeport and Vernalis, and WARMF turbidity at other inflow boundaries compared to EMP grab-sample data, early years– location is EMP D26.

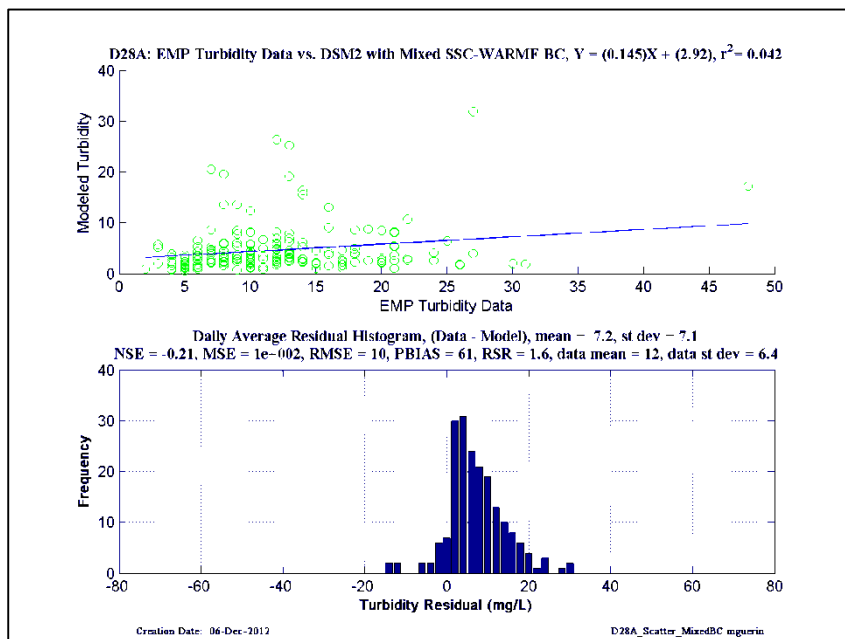
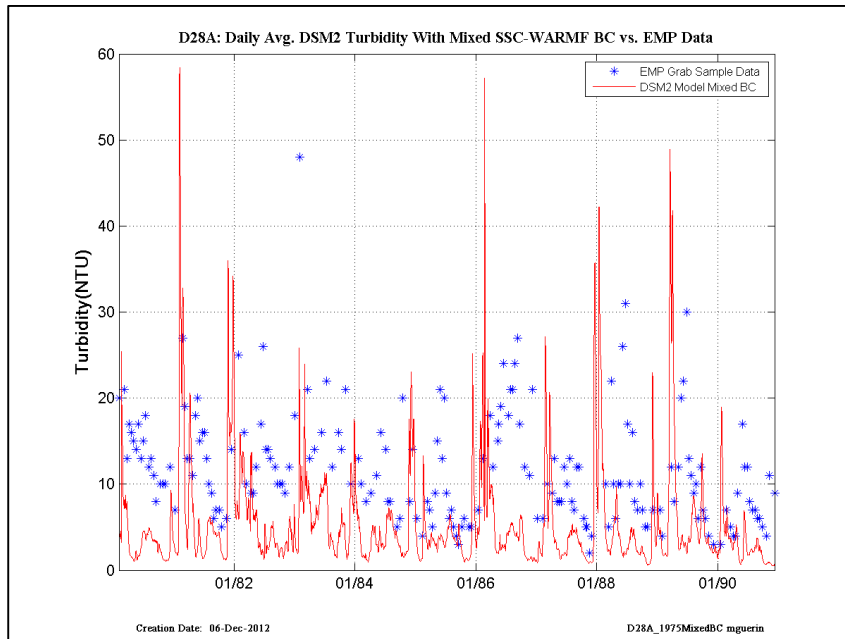


Figure 15-20 DSM2 daily-averaged turbidity model results using USGS-SSC at Freeport and Vernalis, and WARMF turbidity at other inflow boundaries compared to EMP grab-sample data, early years— location is EMP D28A.

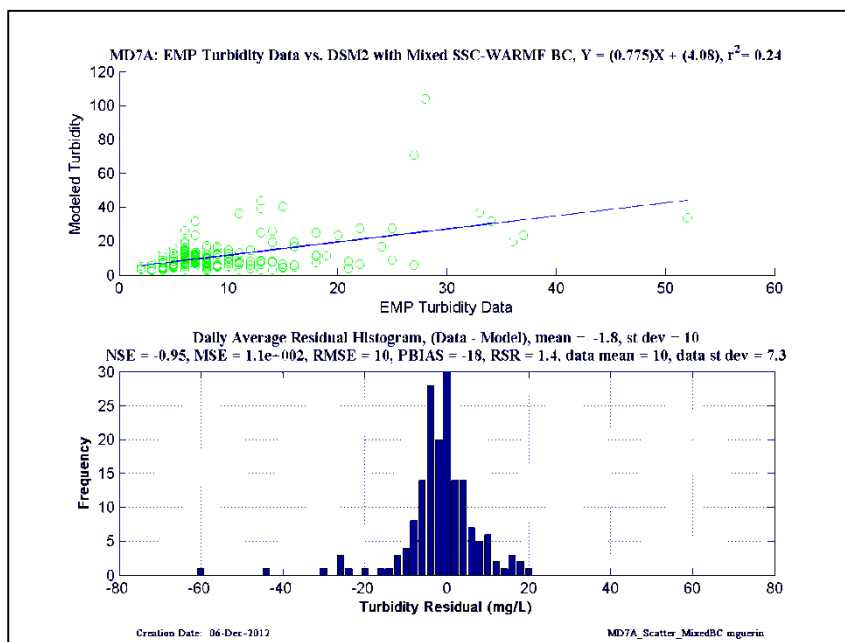
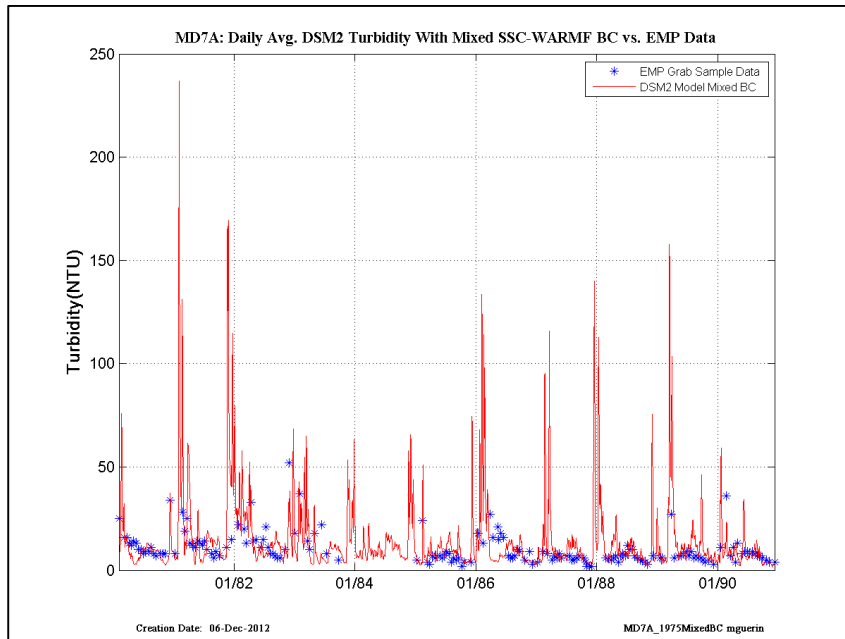


Figure 15-21 DSM2 daily-averaged turbidity model results using USGS-SSC at Freeport and Vernalis, and WARMF turbidity at other inflow boundaries compared to EMP grab-sample data, early years—location is EMP MD7A.

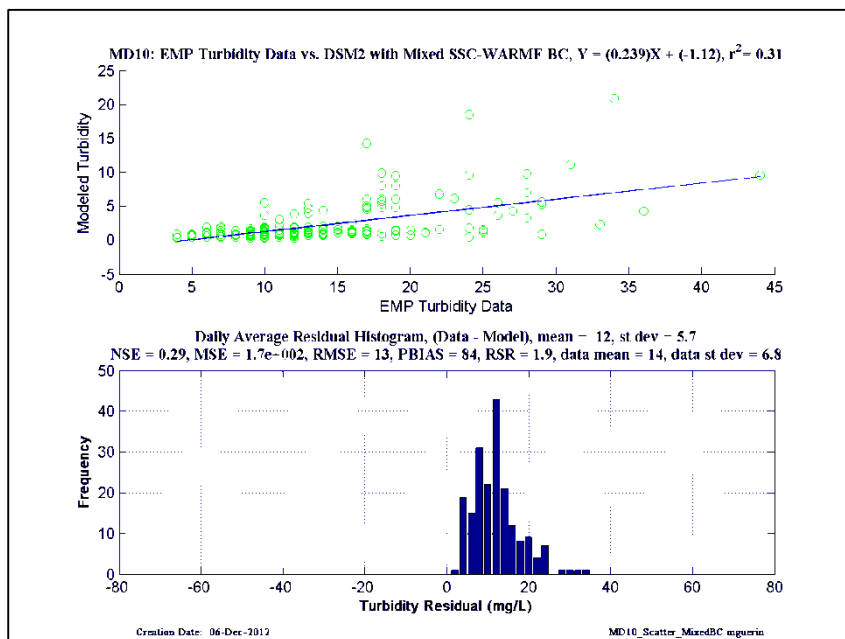
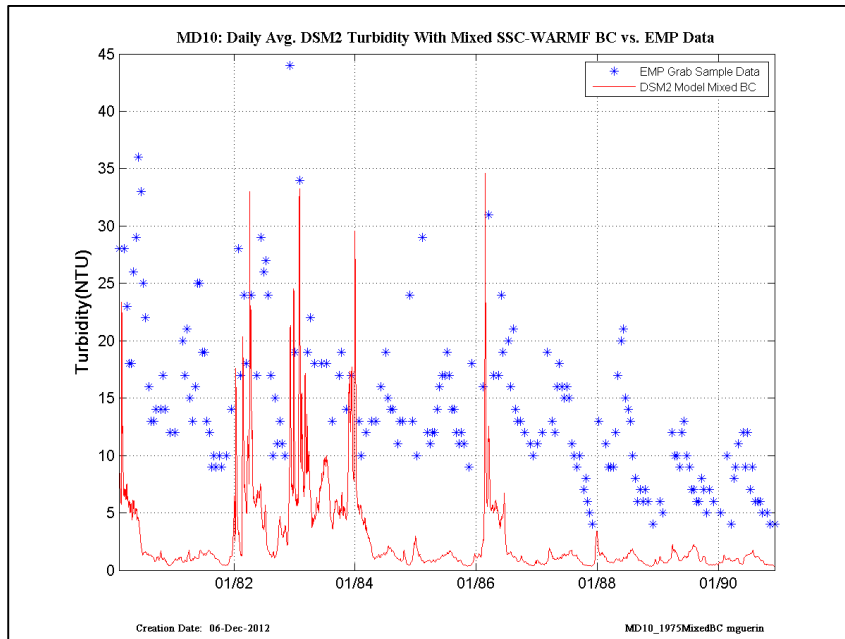


Figure 15-22 DSM2 daily-averaged turbidity model results using USGS-SSC at Freeport and Vernalis, and WARMF turbidity at other inflow boundaries compared to EMP grab-sample data, early years—location is EMP MD10.

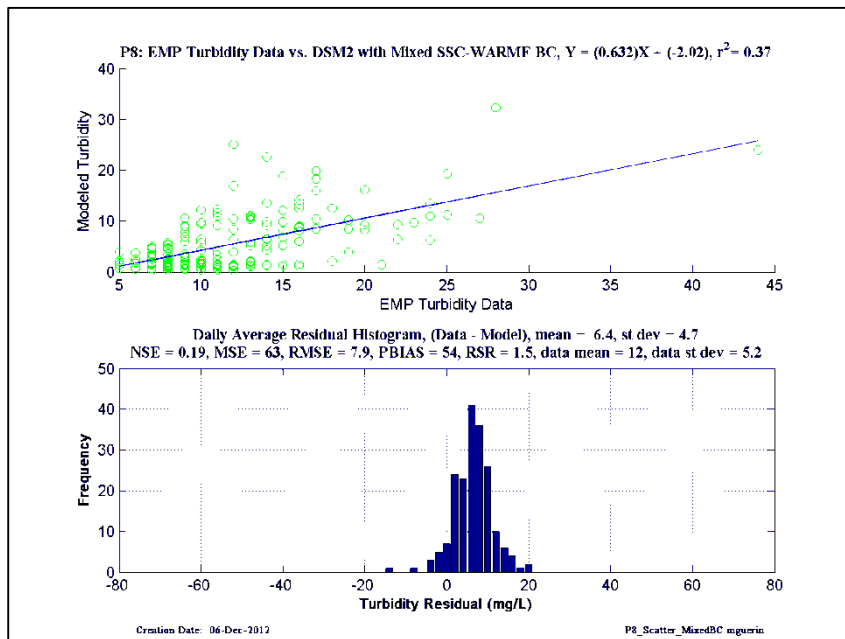
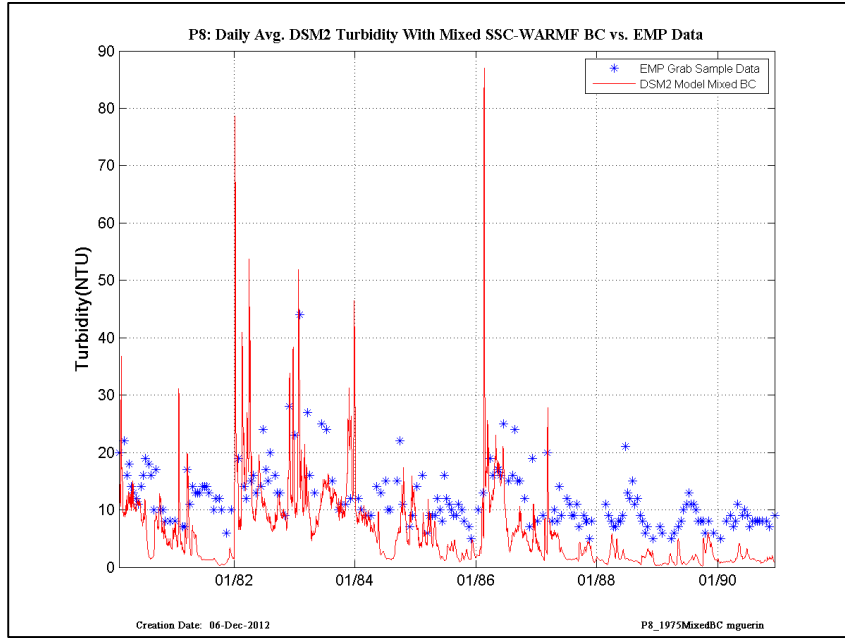


Figure 15-23 DSM2 daily-averaged turbidity model results using USGS-SSC at Freeport and Vernalis, and WARMF turbidity at other inflow boundaries compared to EMP grab-sample data, early years— location is EMP P8.

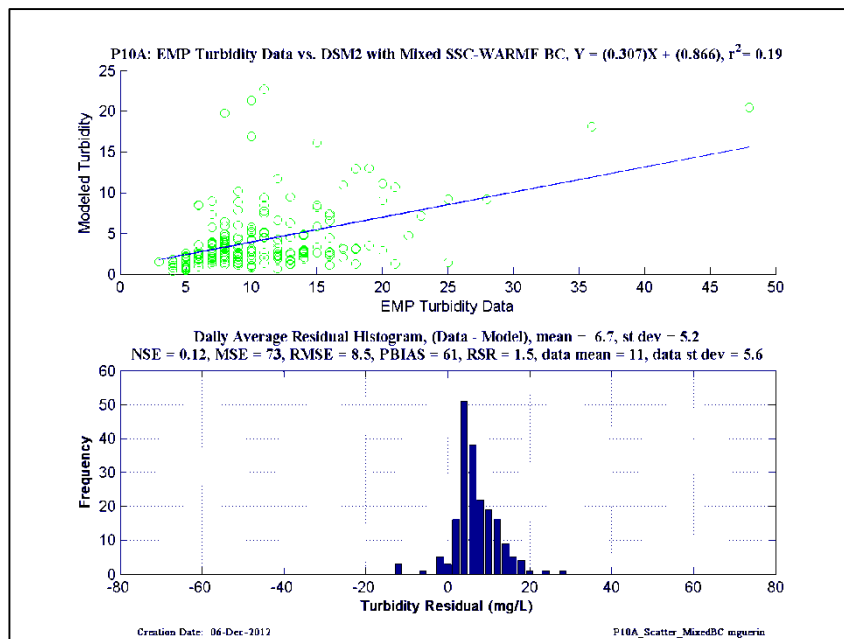
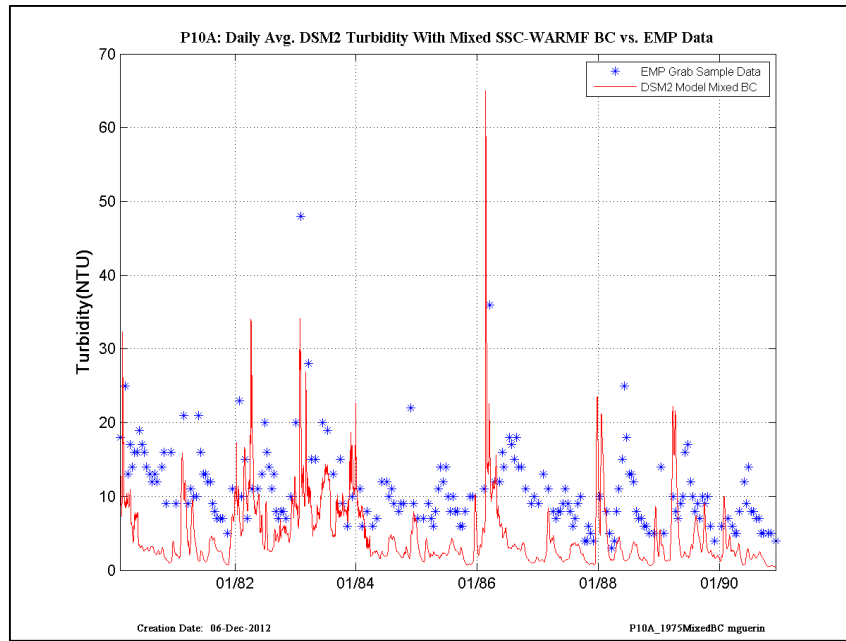


Figure 15-24 DSM2 daily-averaged turbidity model results using USGS-SSC at Freeport and Vernalis, and WARMF turbidity at other inflow boundaries compared to EMP grab-sample data, early years– location is EMP P10A.

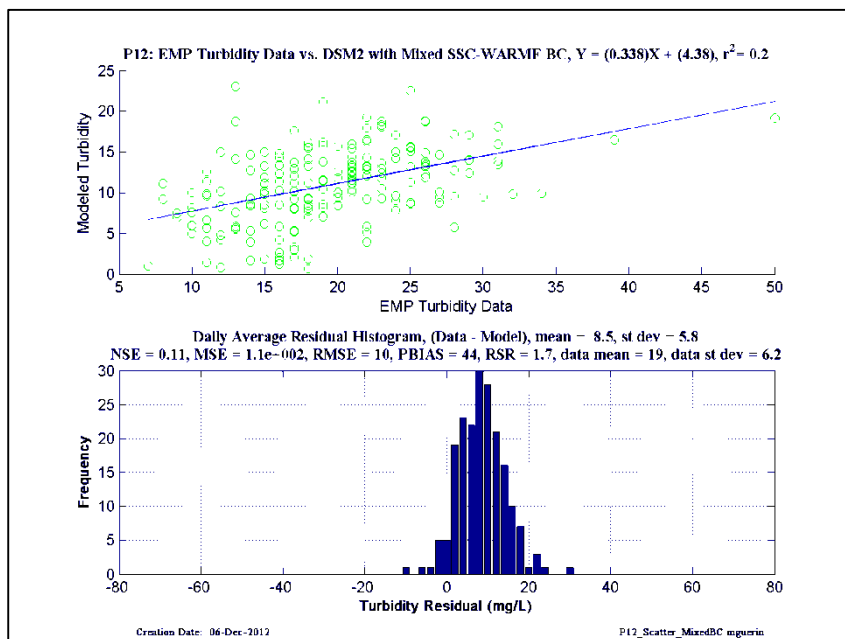
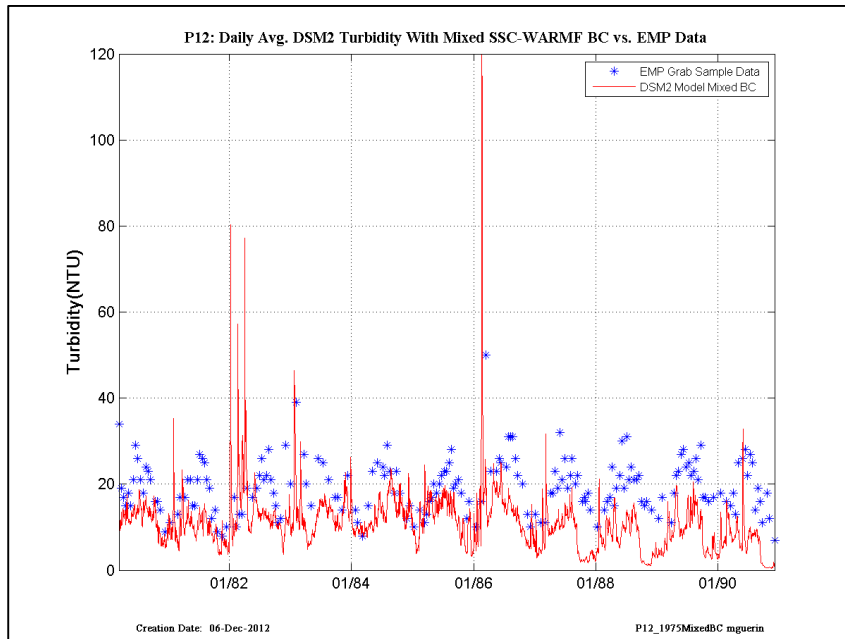


Figure 15-25 DSM2 daily-averaged turbidity model results using USGS-SSC at Freeport and Vernalis, and WARMF turbidity at other inflow boundaries compared to EMP grab-sample data, early years– location is EMP P12.

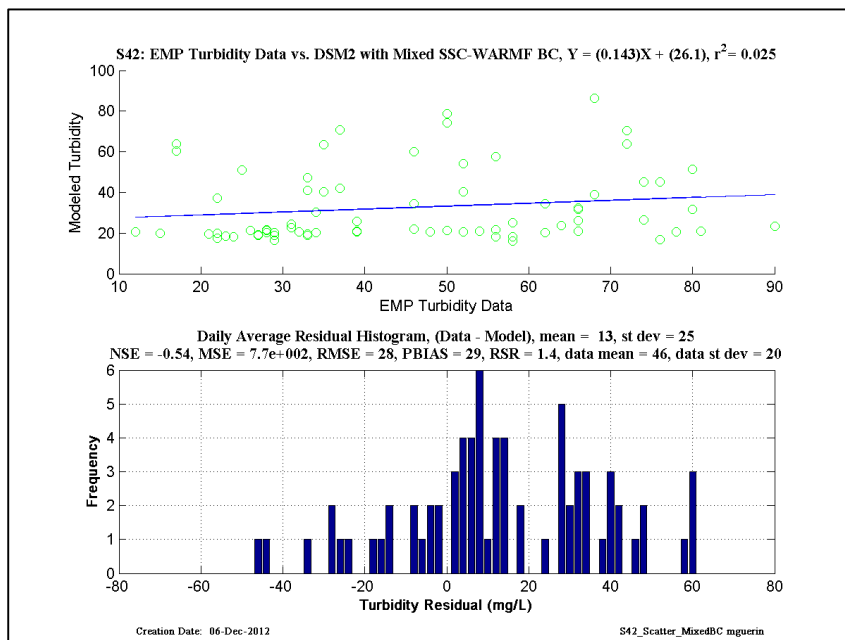
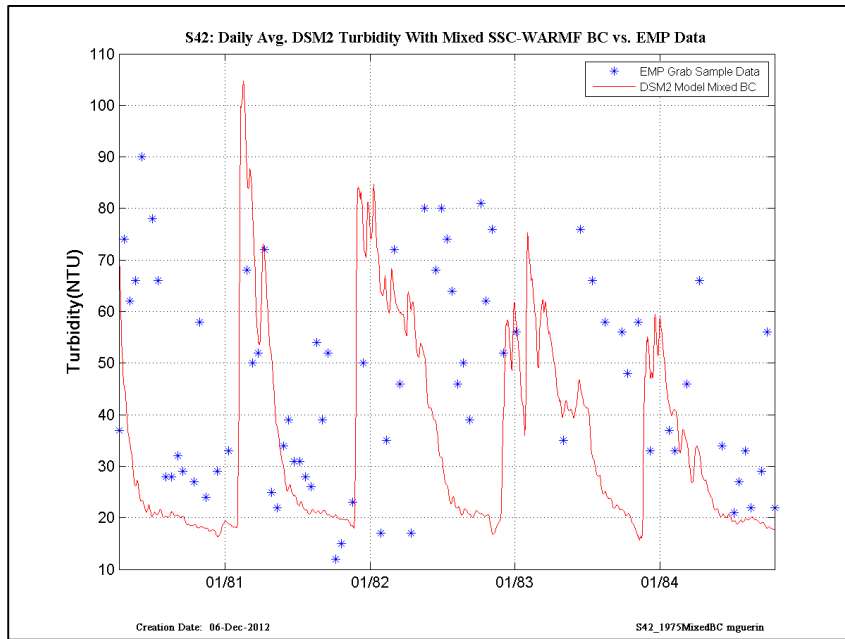


Figure 15-26 DSM2 daily-averaged turbidity model results using USGS-SSC at Freeport and Vernalis, and WARMF turbidity at other inflow boundaries compared to EMP grab-sample data, early years—location is EMP S42.

31.2 Recent years: 1991 - 2011

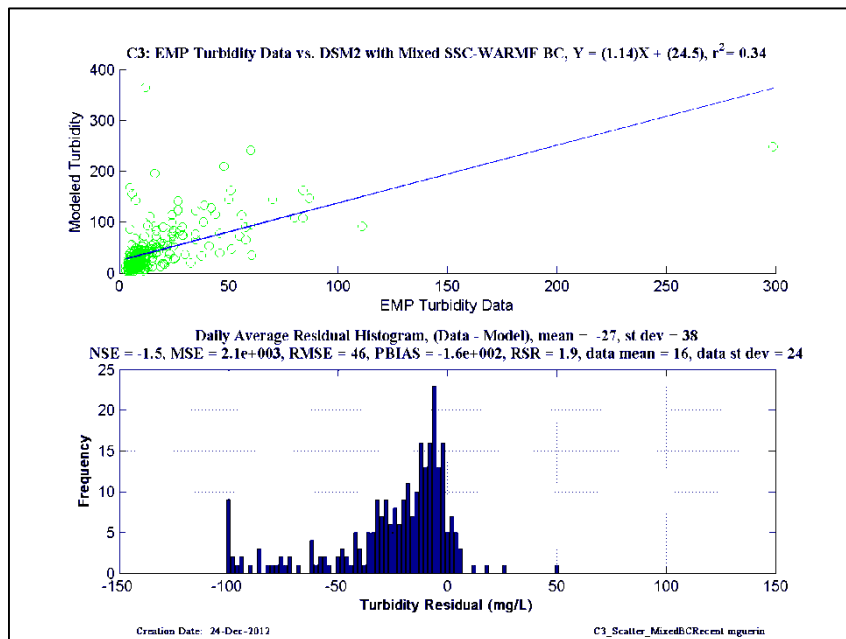
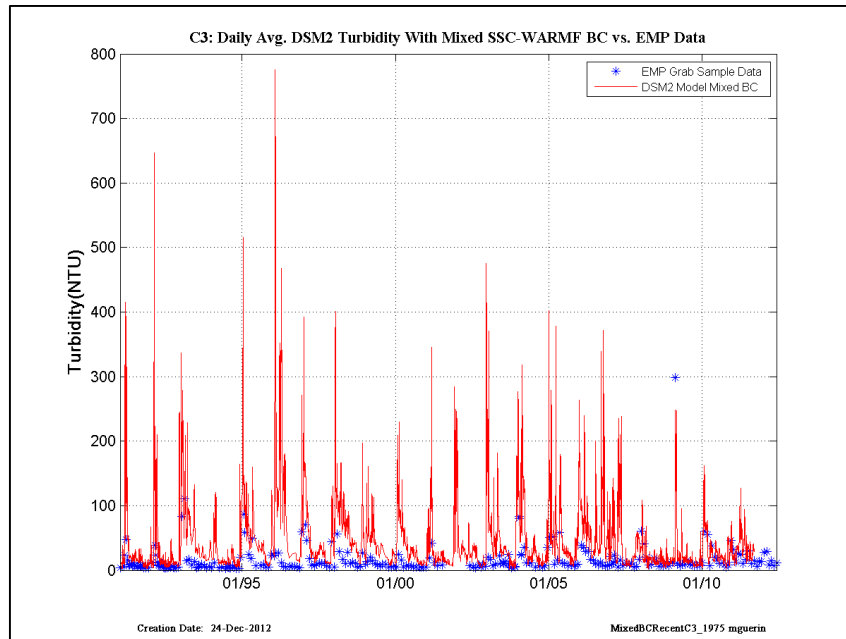


Figure 15-27 DSM2 daily-averaged turbidity model results using USGS-SSC at Freeport and Vernalis, and WARMF turbidity at other inflow boundaries compared to EMP grab-sample data, recent years– location is EMP C3.

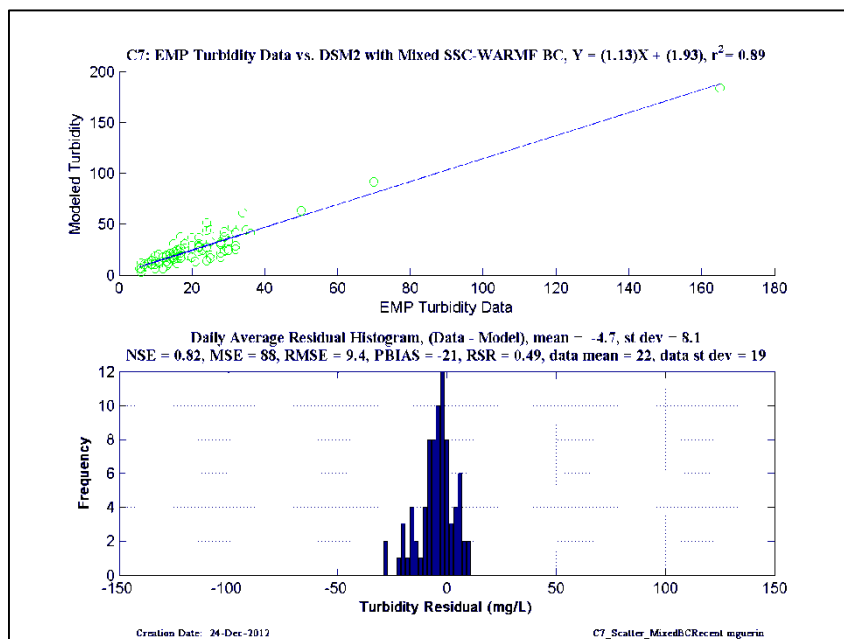
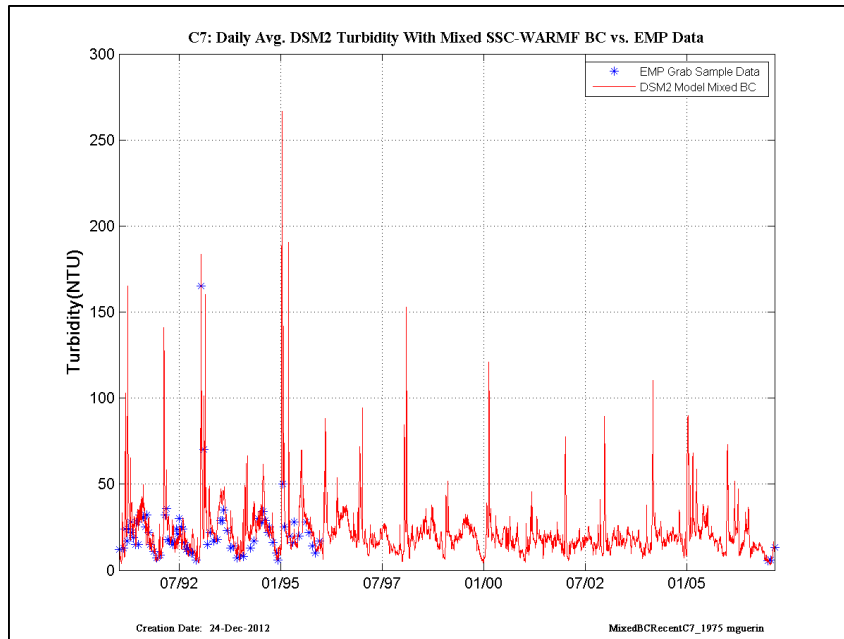


Figure 15-28 DSM2 daily-averaged turbidity model results using USGS-SSC at Freeport and Vernalis, and WARMF turbidity at other inflow boundaries compared to EMP grab-sample data, recent years— location is EMP C7.

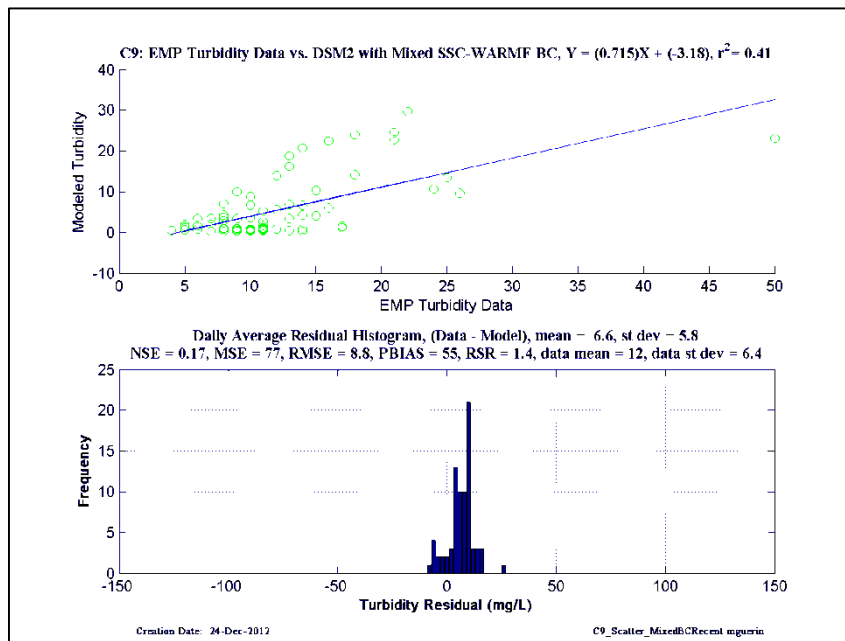
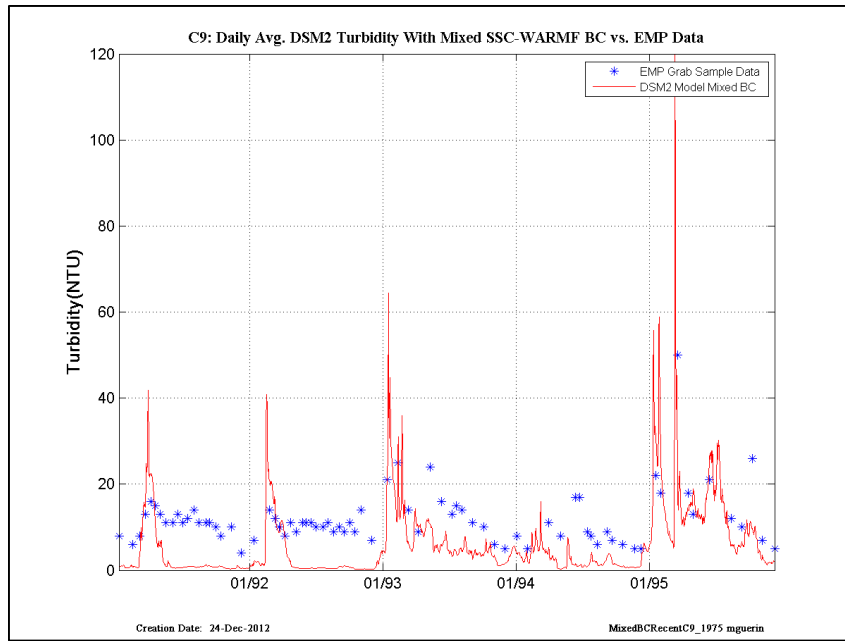


Figure 15-29 DSM2 daily-averaged turbidity model results using USGS-SSC at Freeport and Vernalis, and WARMF turbidity at other inflow boundaries compared to EMP grab-sample data, recent years– location is EMP C9.

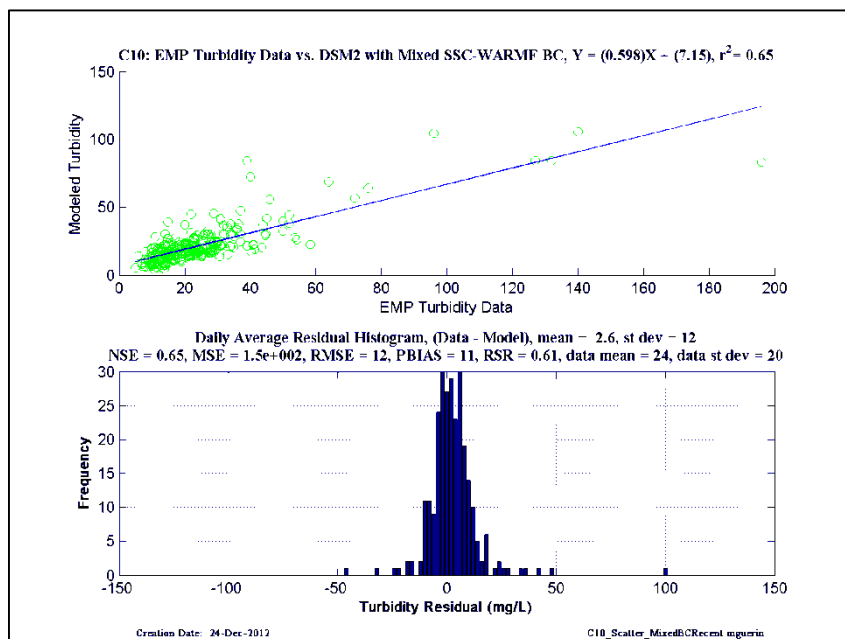
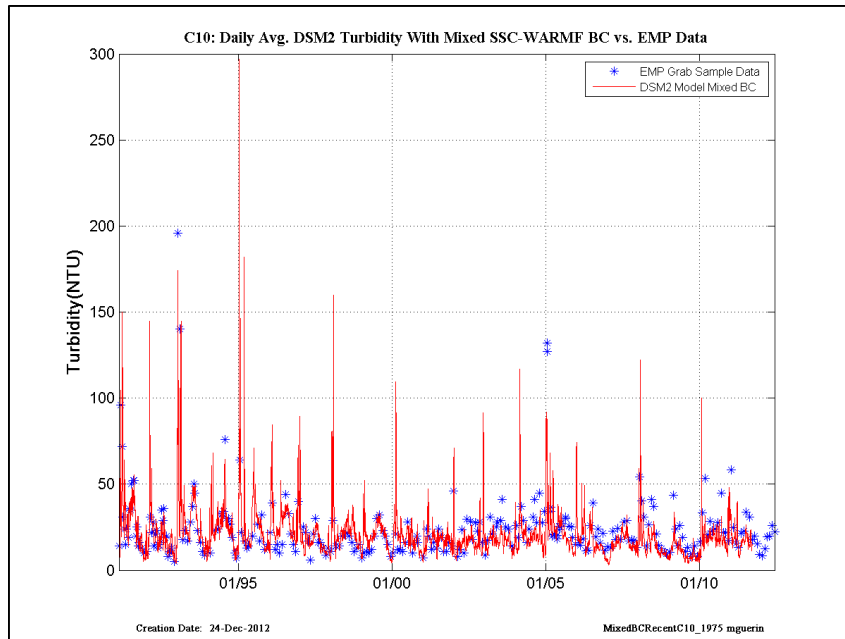


Figure 15-30 DSM2 daily-averaged turbidity model results using USGS-SSC at Freeport and Vernalis, and WARMF turbidity at other inflow boundaries compared to EMP grab-sample data, recent years– location is EMP C10.

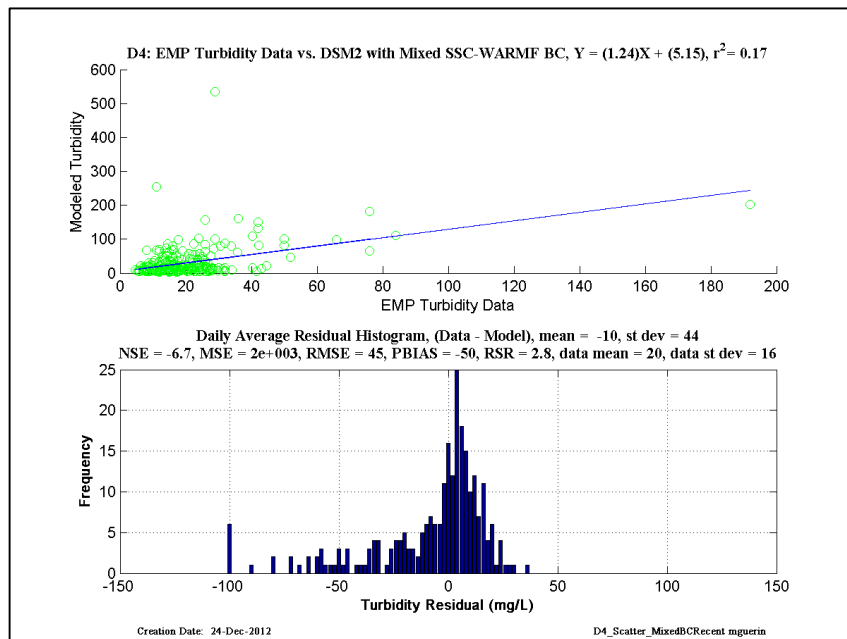
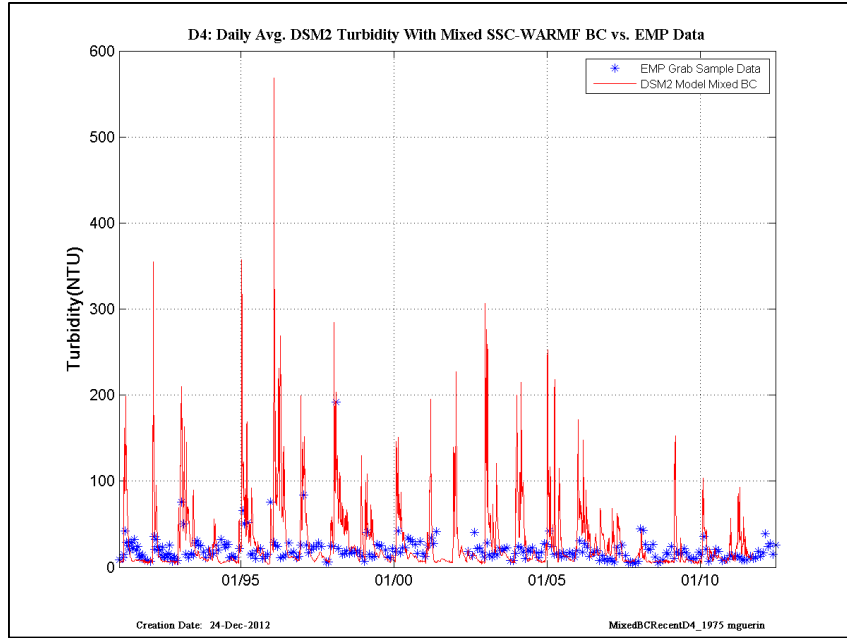


Figure 15-31 DSM2 daily-averaged turbidity model results using USGS-SSC at Freeport and Vernalis, and WARMF turbidity at other inflow boundaries compared to EMP grab-sample data, recent years– location is EMP D4.

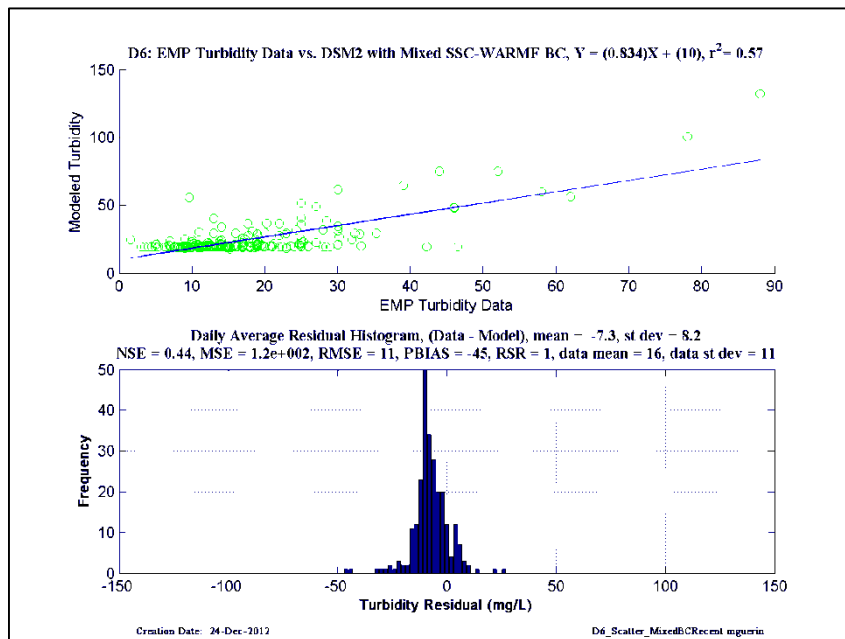
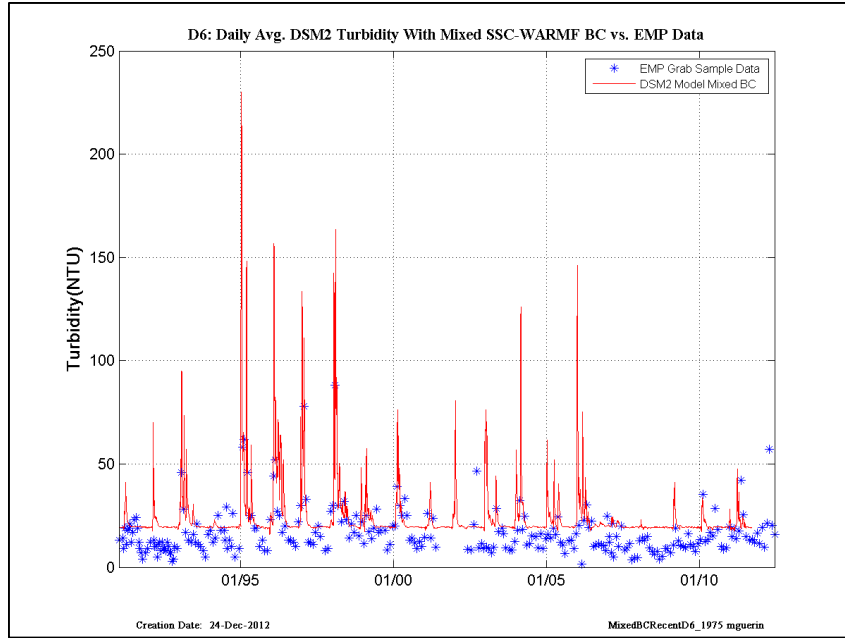


Figure 15-32 DSM2 daily-averaged turbidity model results using USGS-SSC at Freeport and Vernalis, and WARMF turbidity at other inflow boundaries compared to EMP grab-sample data, recent years— location is EMP D6.

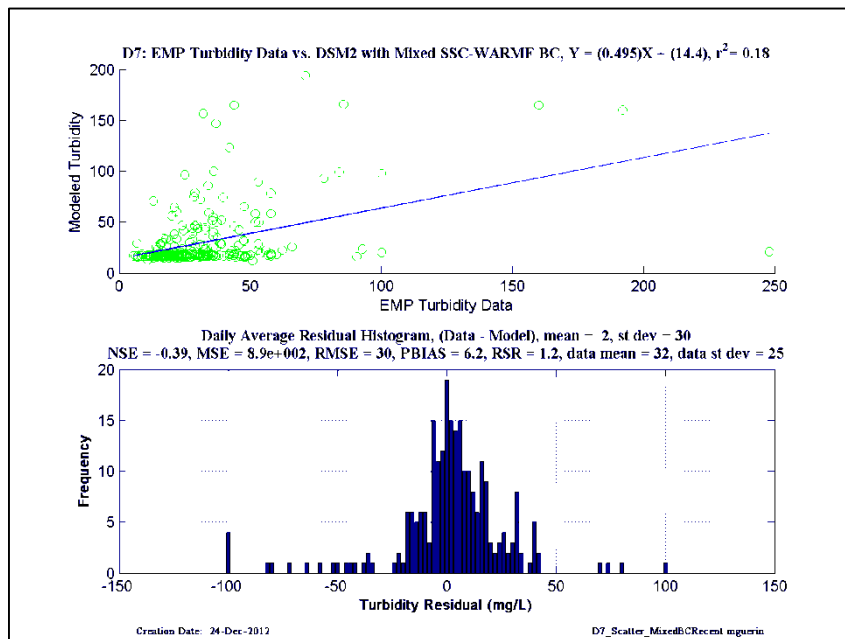
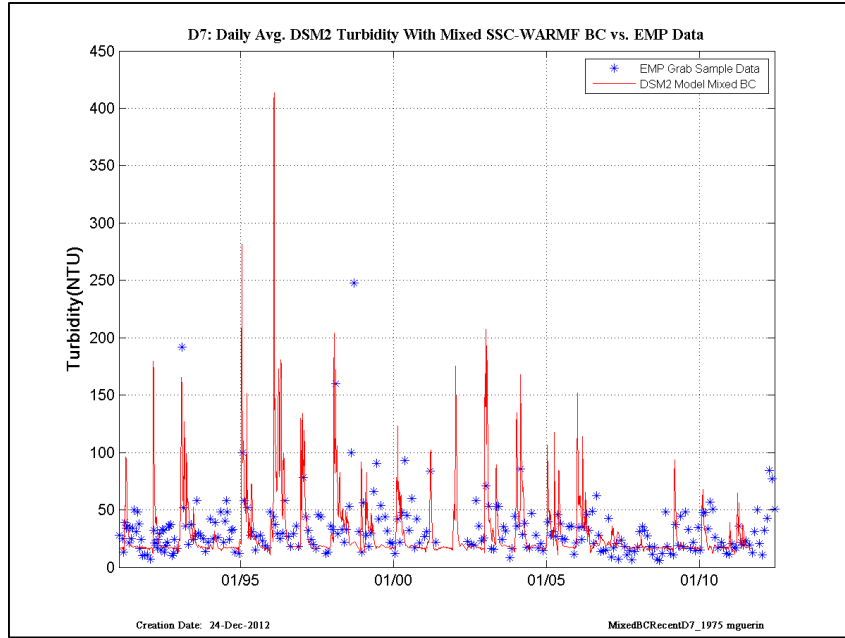


Figure 15-33 DSM2 daily-averaged turbidity model results using USGS-SSC at Freeport and Vernalis, and WARMF turbidity at other inflow boundaries compared to EMP grab-sample data, recent years– location is EMP D7.

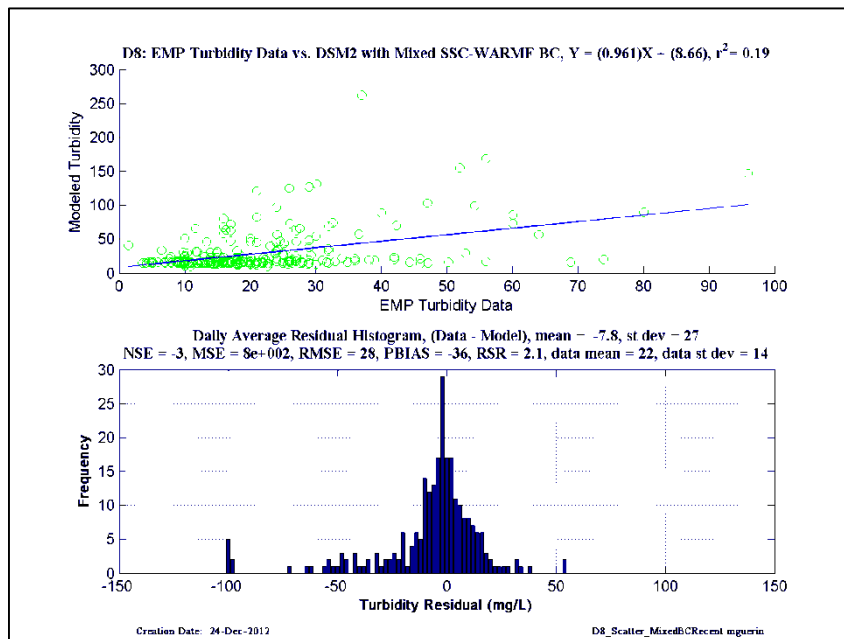
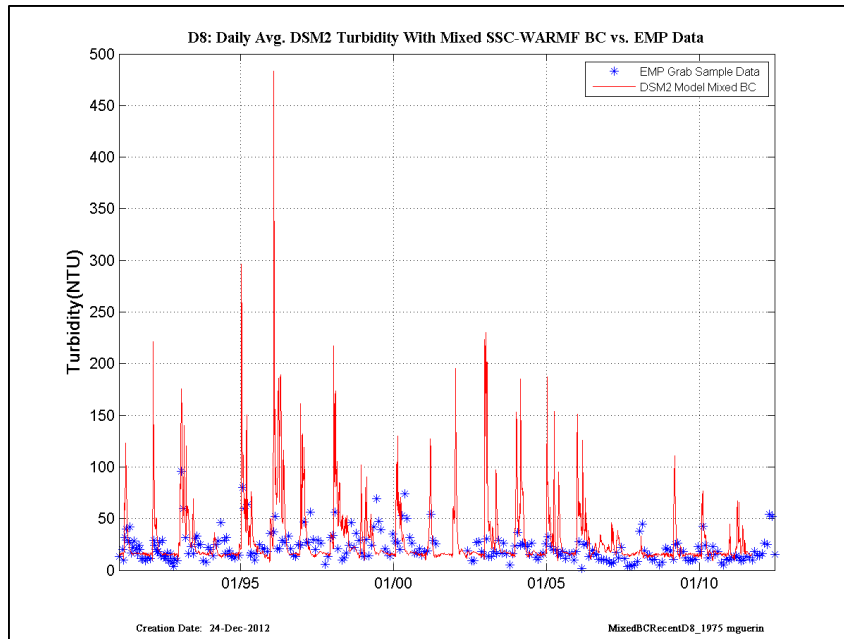


Figure 15-34 DSM2 daily-averaged turbidity model results using USGS-SSC at Freeport and Vernalis, and WARMF turbidity at other inflow boundaries compared to EMP grab-sample data, recent years– location is EMP D8.

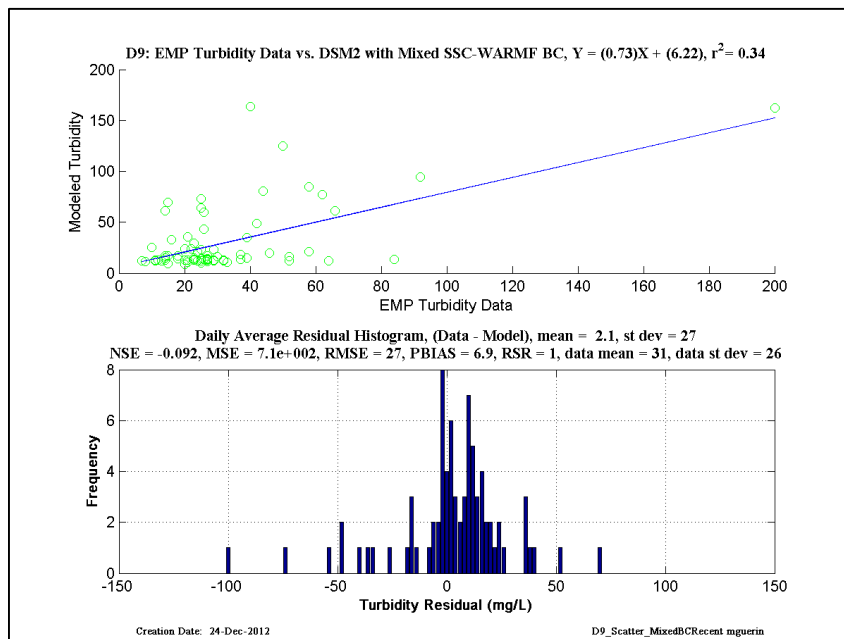
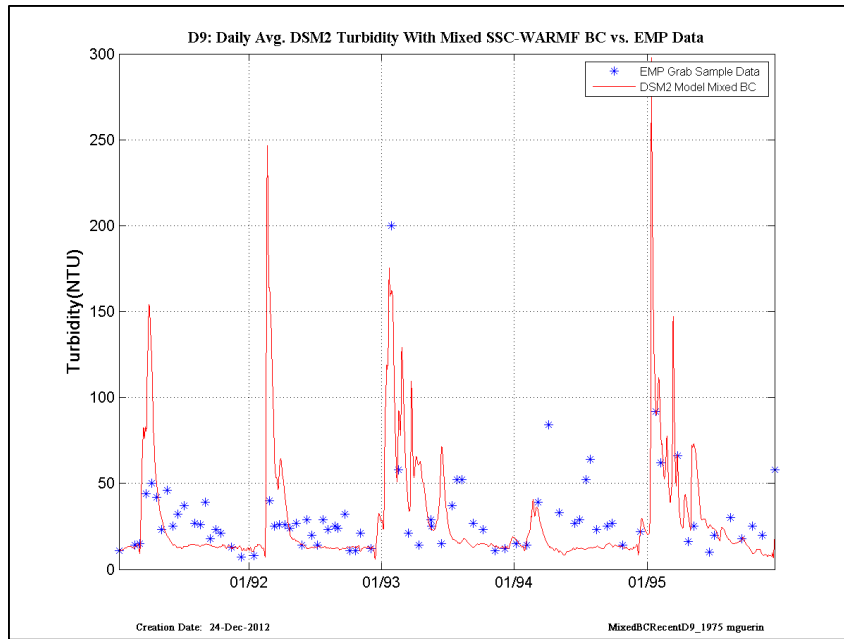


Figure 15-35 DSM2 daily-averaged turbidity model results using USGS-SSC at Freeport and Vernalis, and WARMF turbidity at other inflow boundaries compared to EMP grab-sample data, recent years– location is EMP D9.

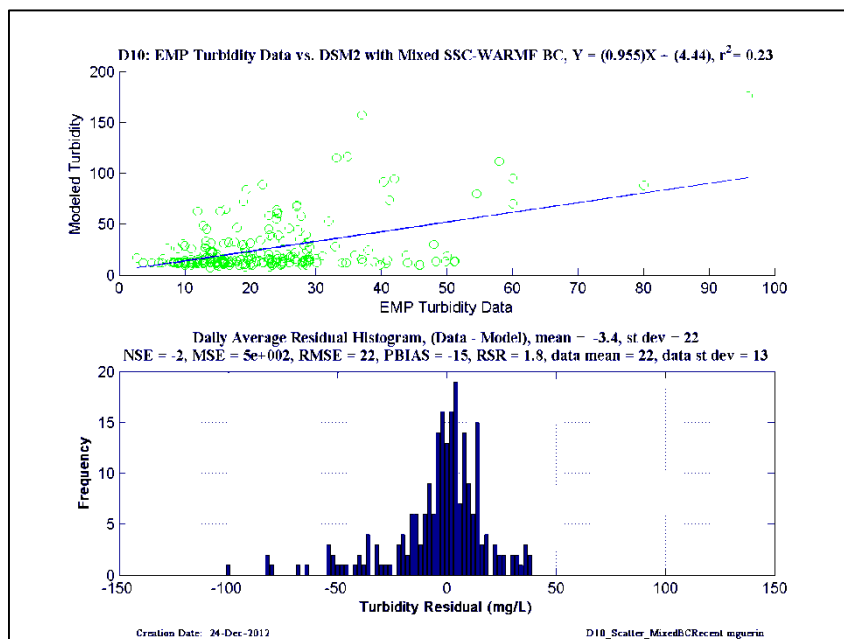
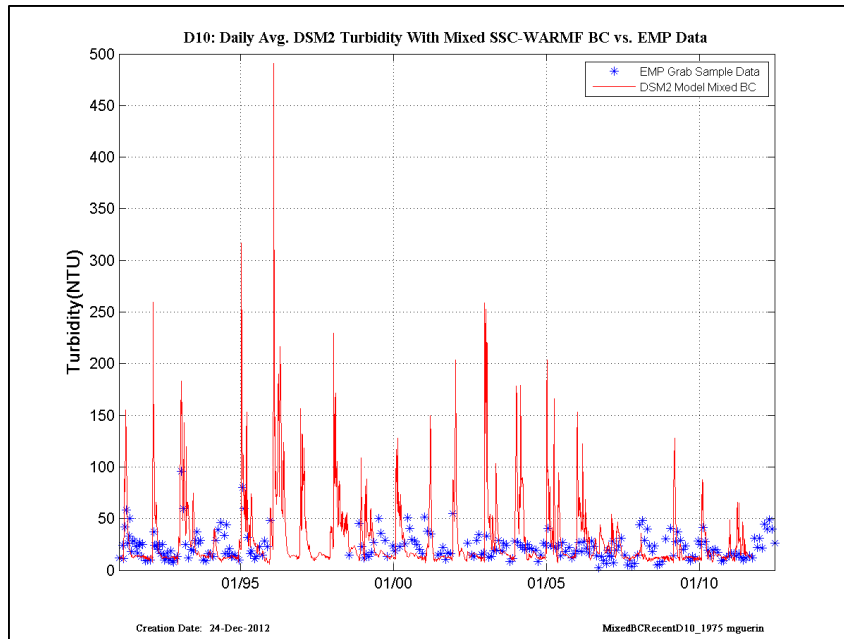


Figure 15-36 DSM2 daily-averaged turbidity model results using USGS-SSC at Freeport and Vernalis, and WARMF turbidity at other inflow boundaries compared to EMP grab-sample data, recent years— location is EMP D10.

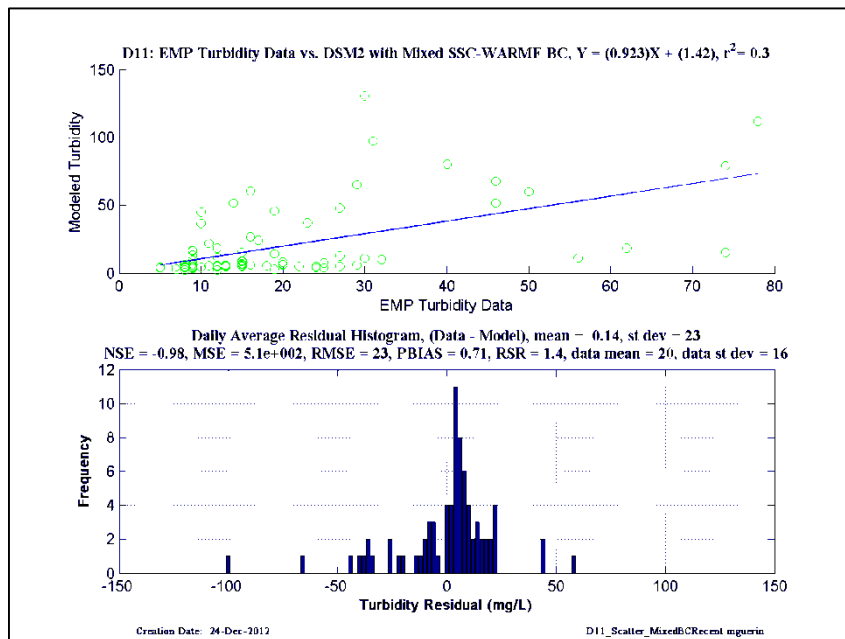
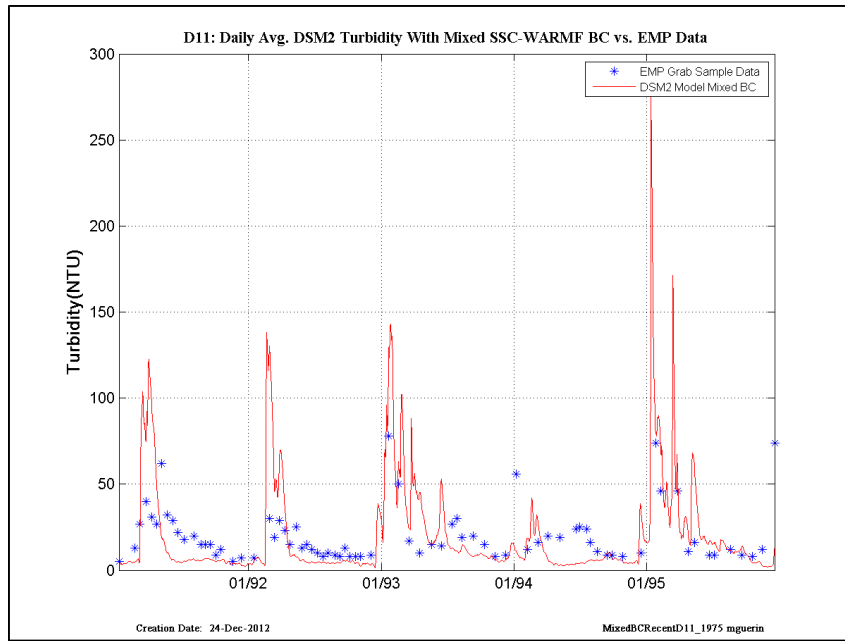


Figure 15-37 DSM2 daily-averaged turbidity model results using USGS-SSC at Freeport and Vernalis, and WARMF turbidity at other inflow boundaries compared to EMP grab-sample data, recent years– location is EMP D11.

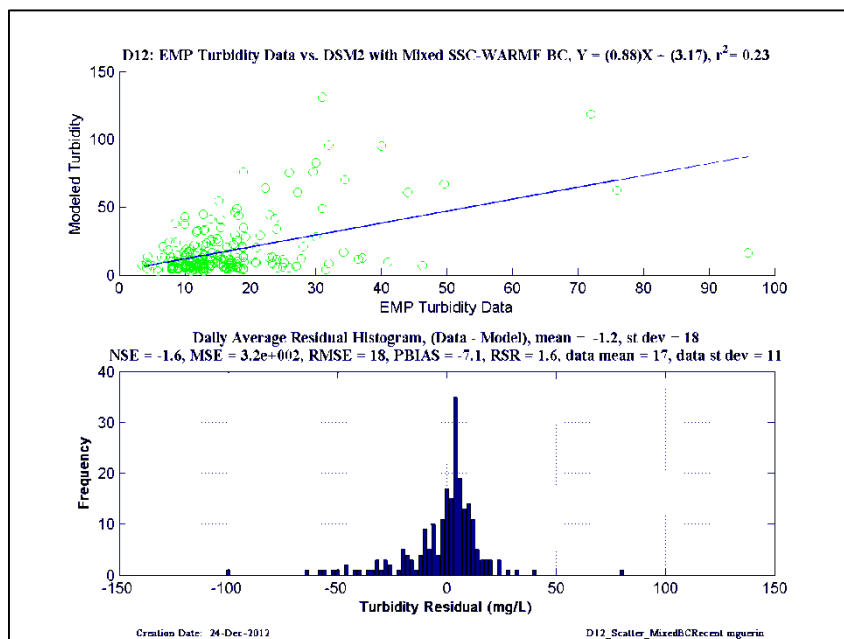
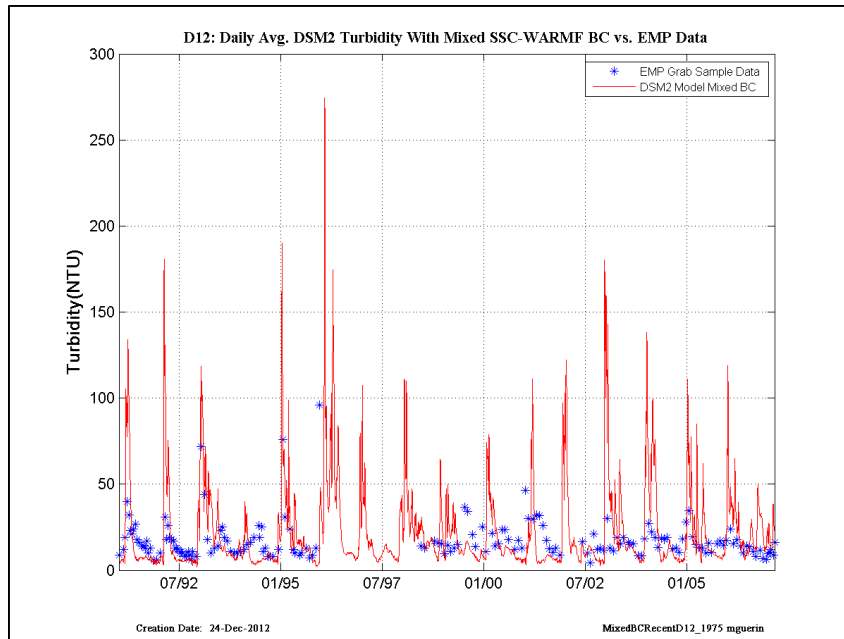


Figure 15-38 DSM2 daily-averaged turbidity model results using USGS-SSC at Freeport and Vernalis, and WARMF turbidity at other inflow boundaries compared to EMP grab-sample data, recent years– location is EMP D12.

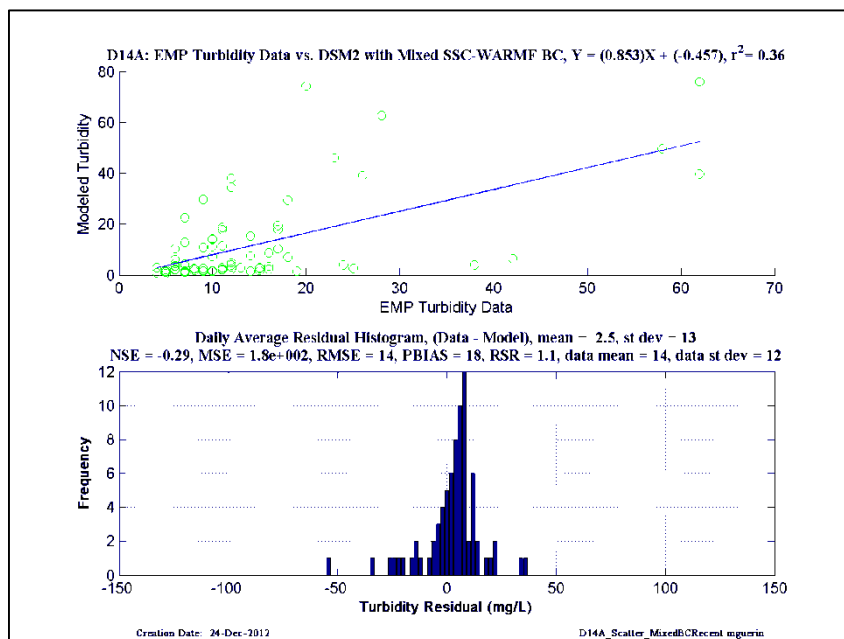
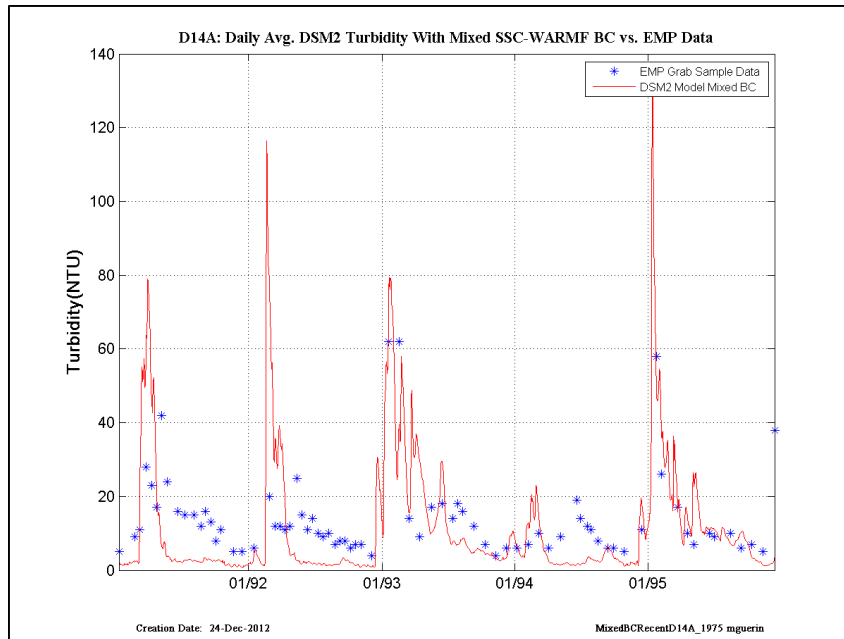


Figure 15-39 DSM2 daily-averaged turbidity model results using USGS-SSC at Freeport and Vernalis, and WARMF turbidity at other inflow boundaries compared to EMP grab-sample data, recent years– location is EMP D14A.

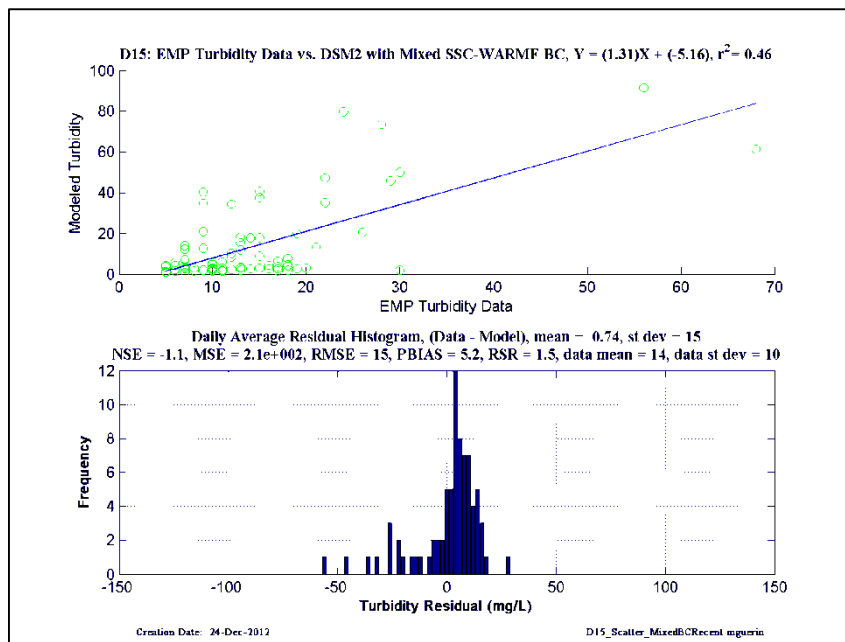
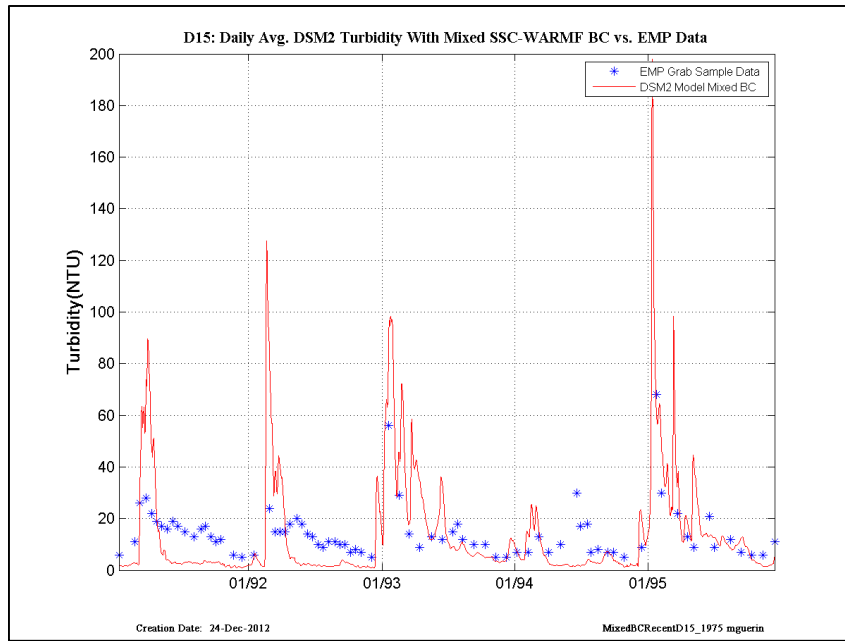


Figure 15-40 DSM2 daily-averaged turbidity model results using USGS-SSC at Freeport and Vernalis, and WARMF turbidity at other inflow boundaries compared to EMP grab-sample data, recent years– location is EMP D15.

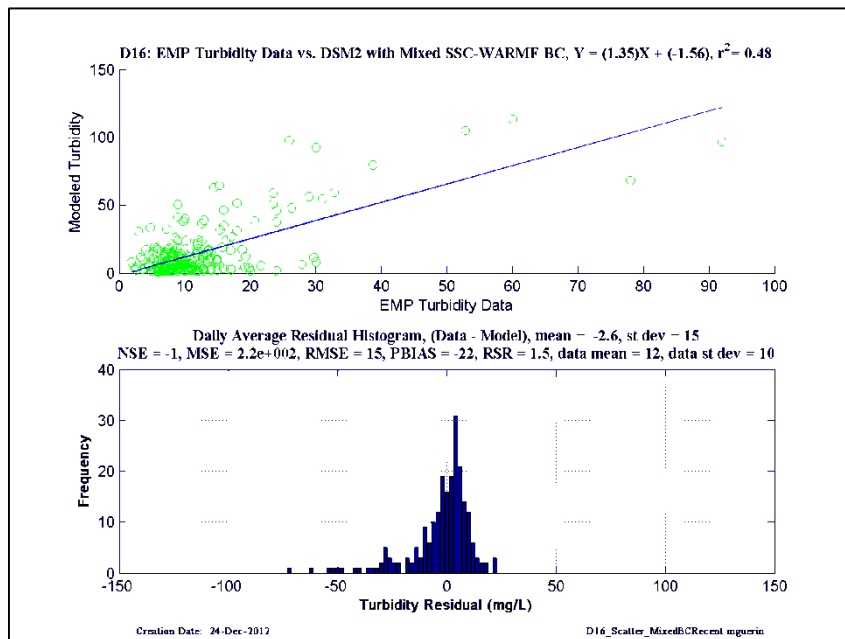
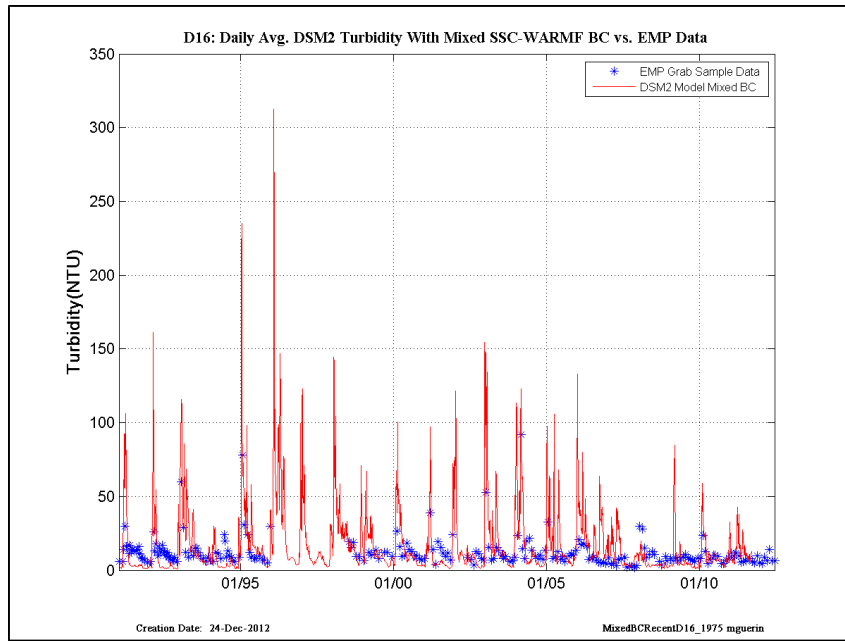


Figure 15-41 DSM2 daily-averaged turbidity model results using USGS-SSC at Freeport and Vernalis, and WARMF turbidity at other inflow boundaries compared to EMP grab-sample data, recent years– location is EMP D16.

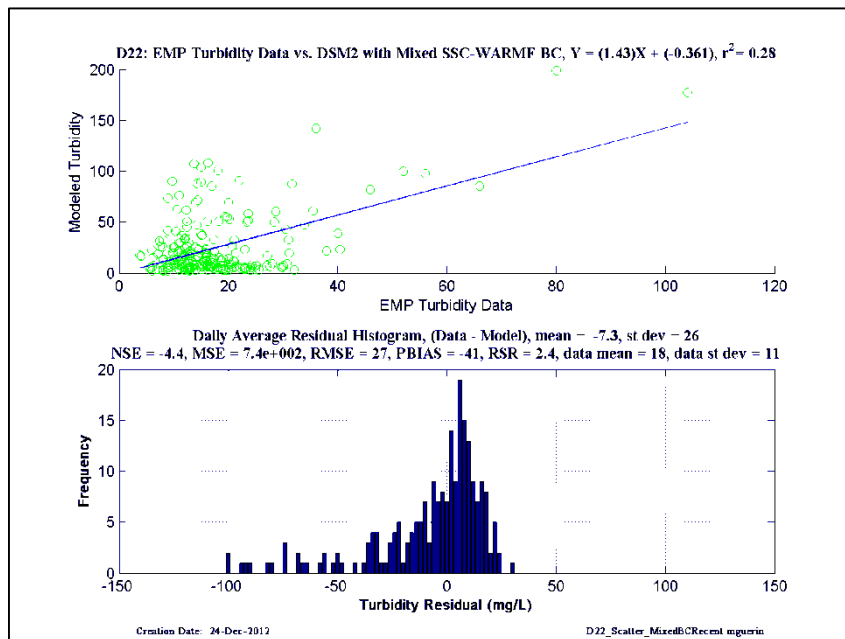
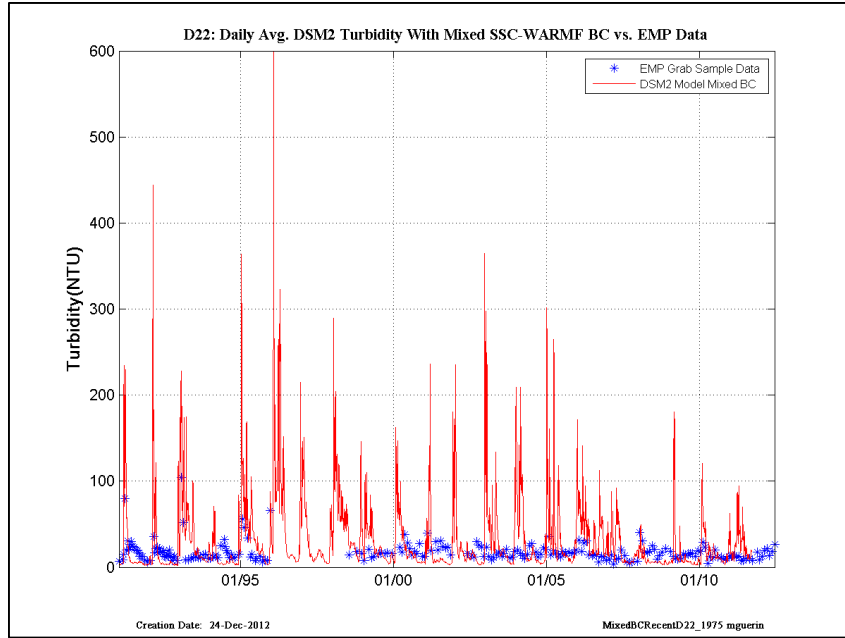


Figure 15-42 DSM2 daily-averaged turbidity model results using USGS-SSC at Freeport and Vernalis, and WARMF turbidity at other inflow boundaries compared to EMP grab-sample data, recent years– location is EMP D22.

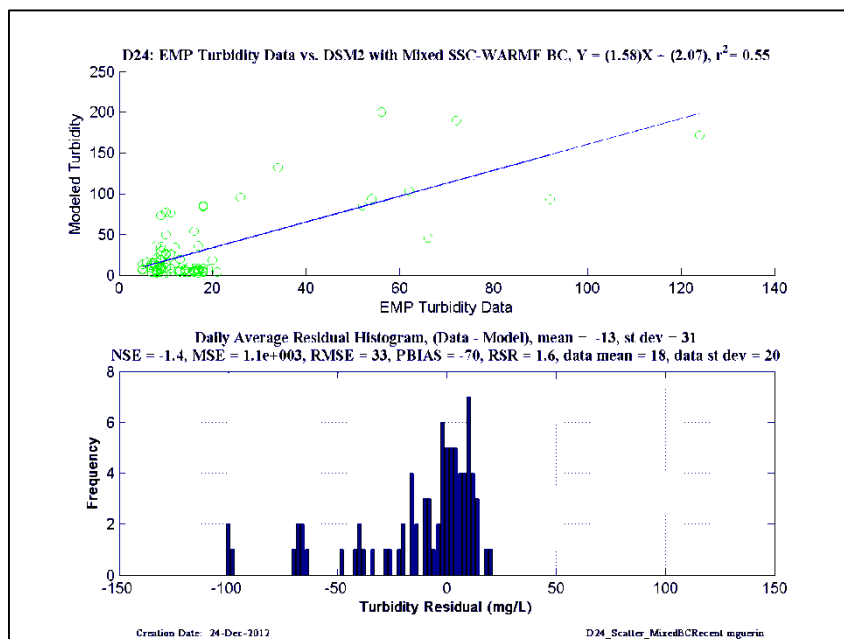
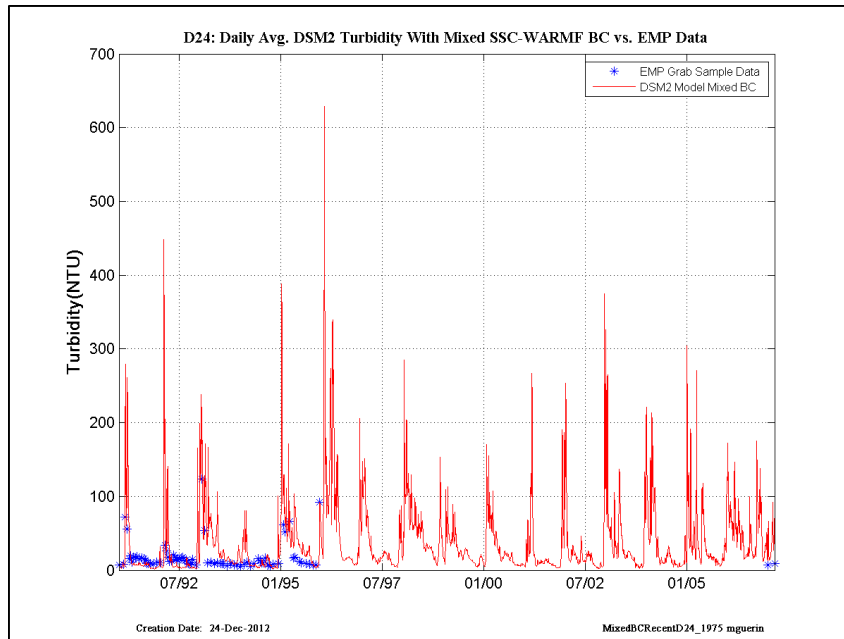


Figure 15-43 DSM2 daily-averaged turbidity model results using USGS-SSC at Freeport and Vernalis, and WARMF turbidity at other inflow boundaries compared to EMP grab-sample data, recent years– location is EMP D24.

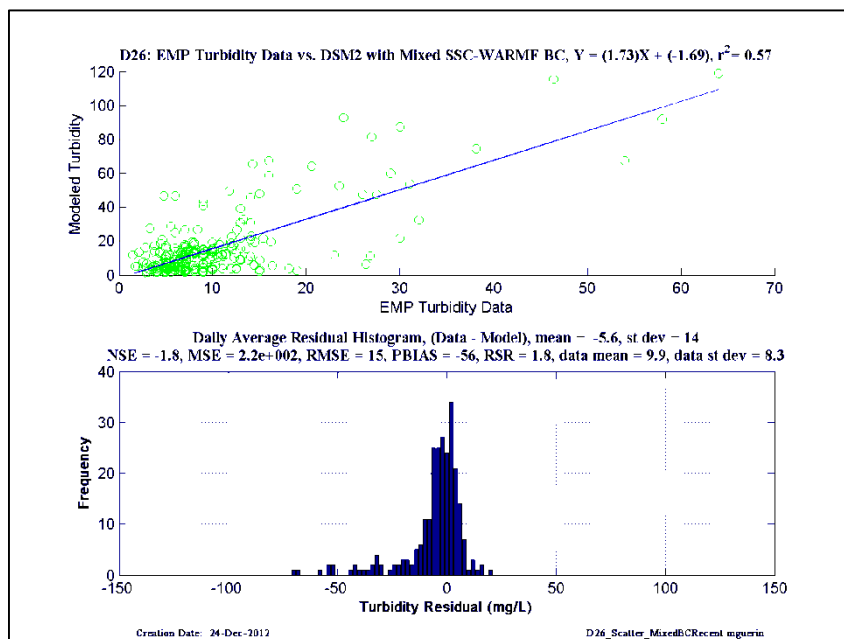
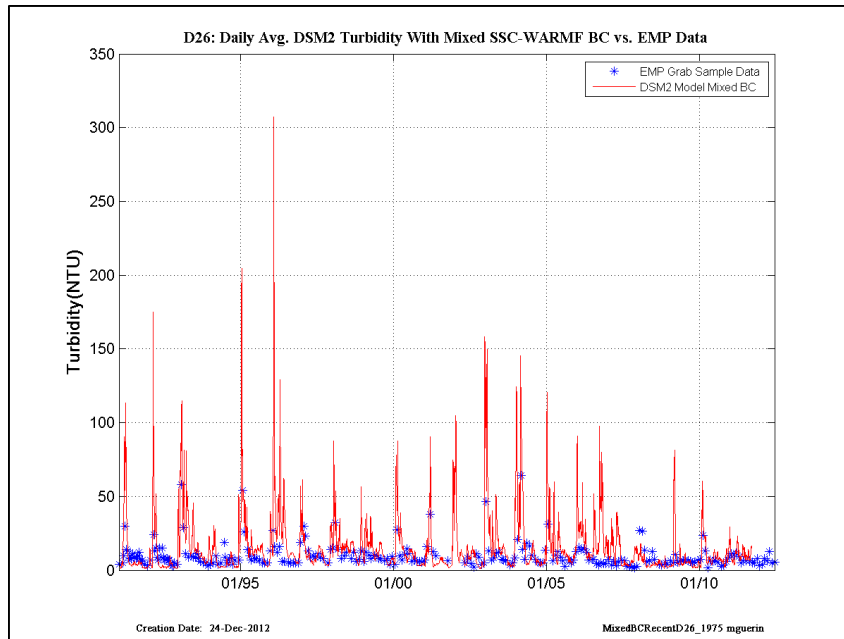


Figure 15-44 DSM2 daily-averaged turbidity model results using USGS-SSC at Freeport and Vernalis, and WARMF turbidity at other inflow boundaries compared to EMP grab-sample data, recent years– location is EMP D26.

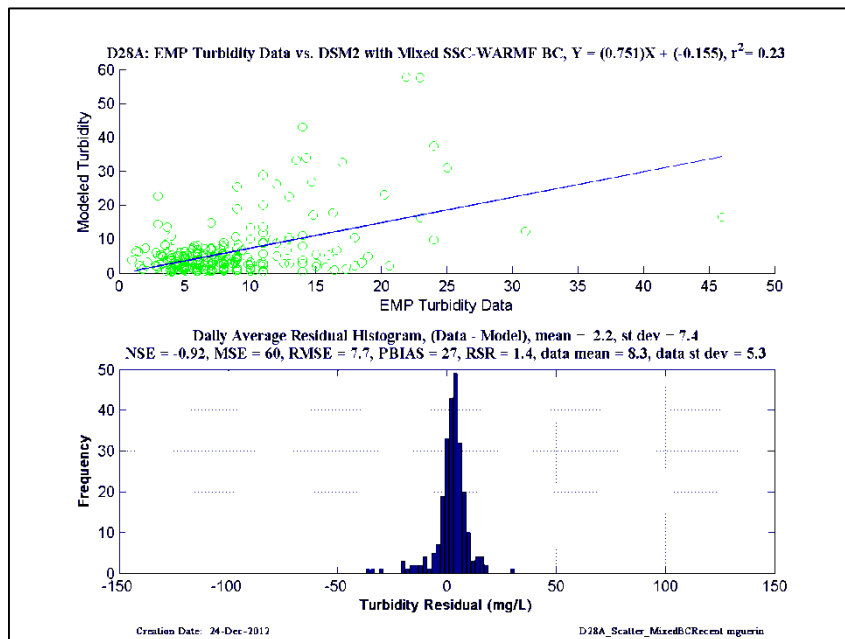
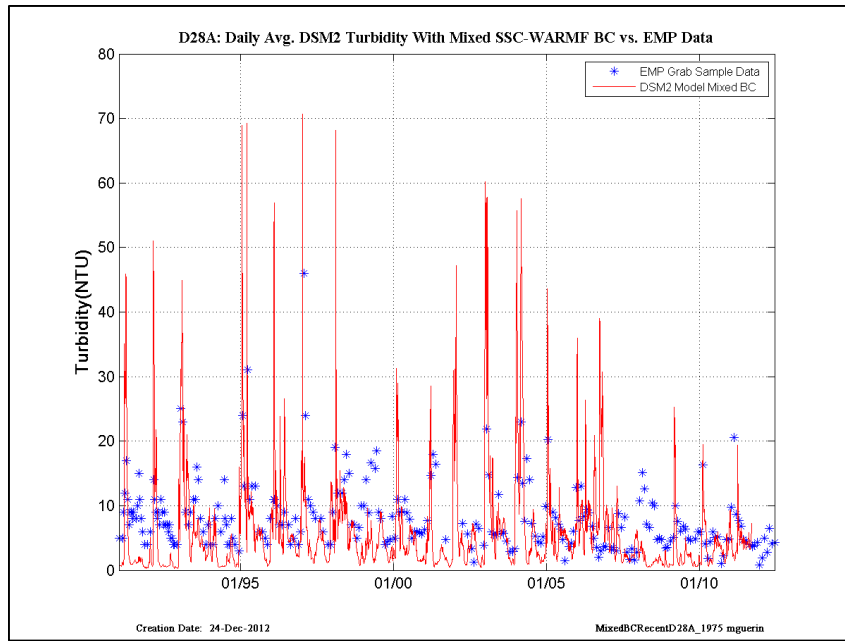


Figure 15-45 DSM2 daily-averaged turbidity model results using USGS-SSC at Freeport and Vernalis, and WARMF turbidity at other inflow boundaries compared to EMP grab-sample data, recent years— location is EMP D28A.

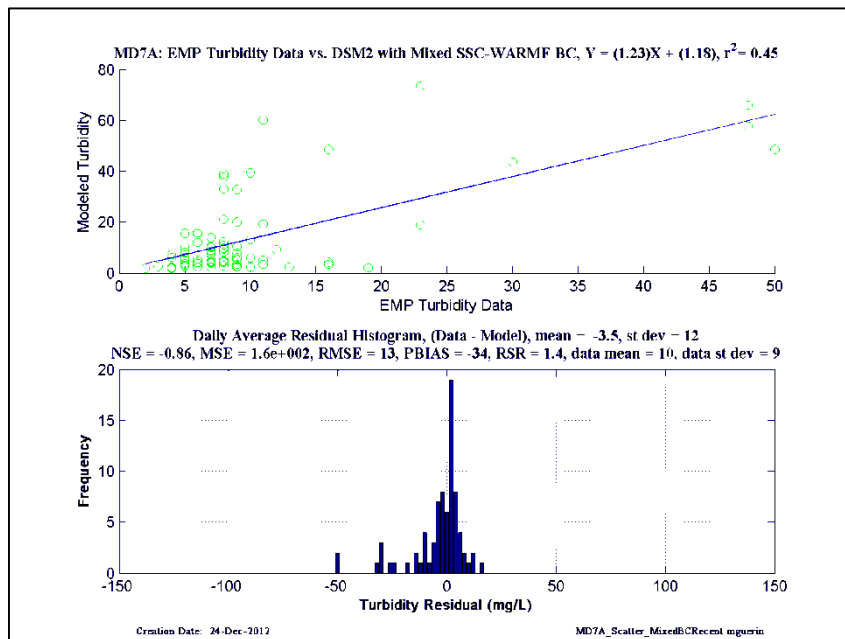
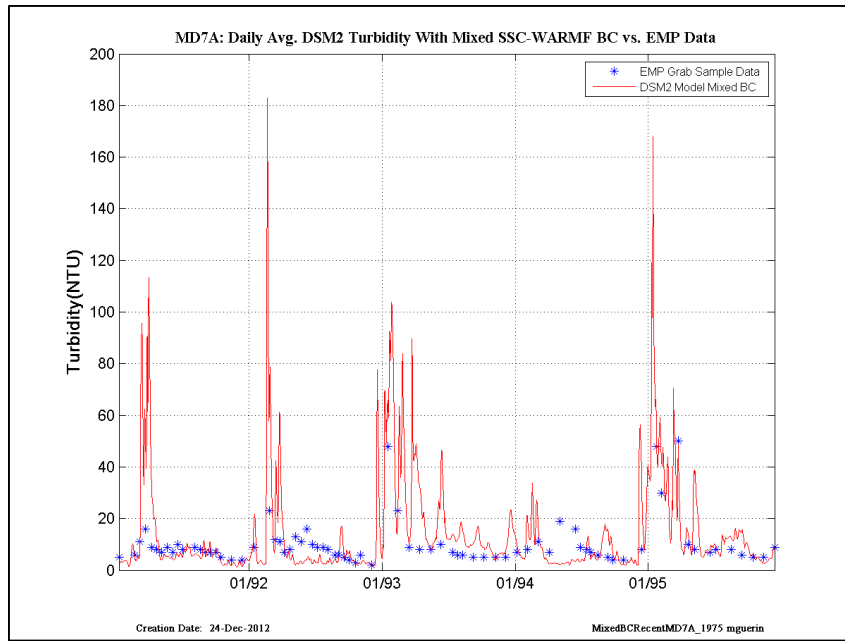


Figure 15-46 DSM2 daily-averaged turbidity model results using USGS-SSC at Freeport and Vernalis, and WARMF turbidity at other inflow boundaries compared to EMP grab-sample data, recent years— location is EMP MD7A.

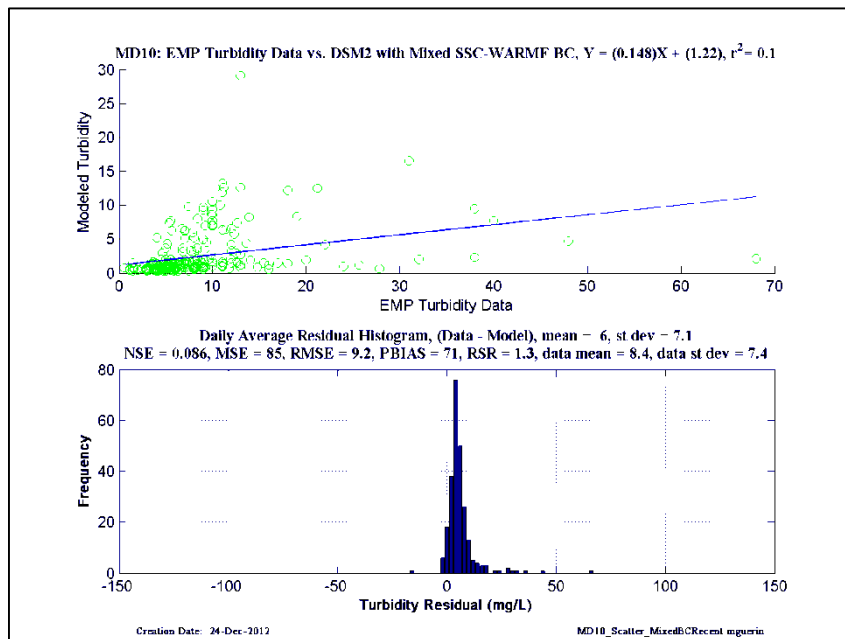
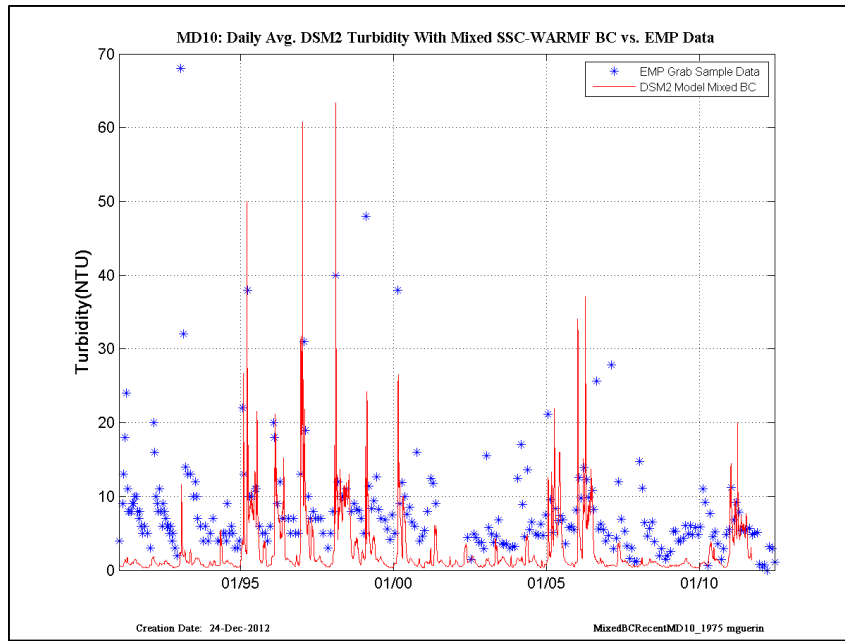


Figure 15-47 DSM2 daily-averaged turbidity model results using USGS-SSC at Freeport and Vernalis, and WARMF turbidity at other inflow boundaries compared to EMP grab-sample data, recent years— location is EMP MD10.

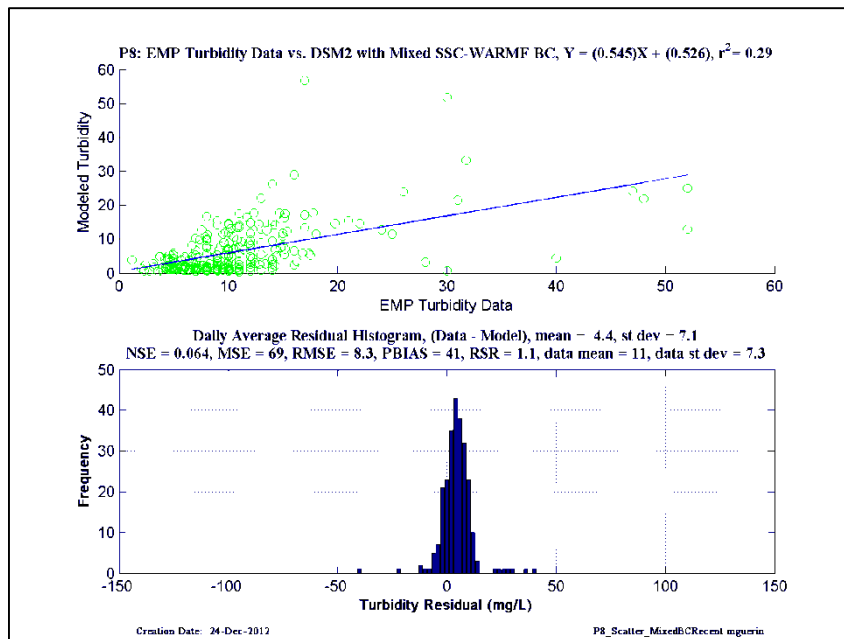
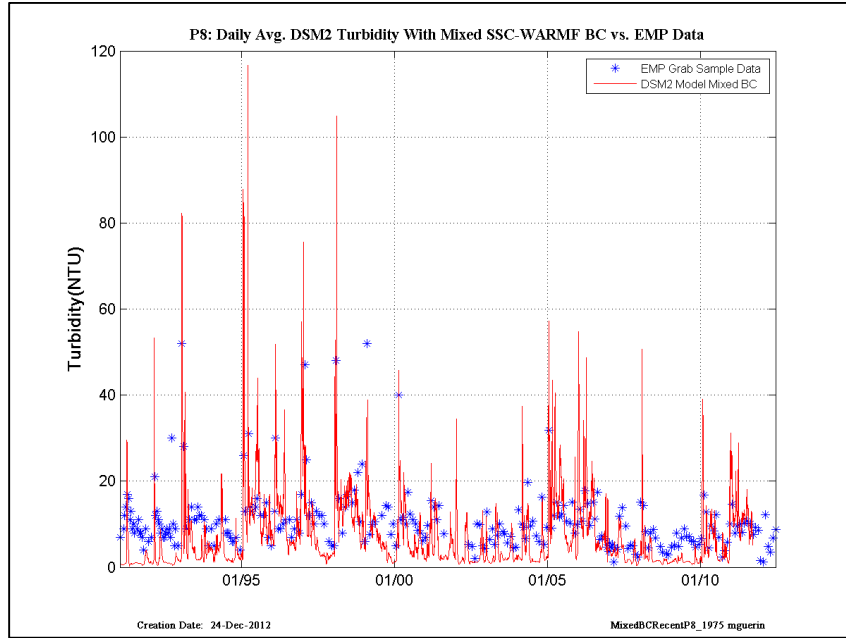


Figure 15-48 DSM2 daily-averaged turbidity model results using USGS-SSC at Freeport and Vernalis, and WARMF turbidity at other inflow boundaries compared to EMP grab-sample data, recent years— location is EMP P8.

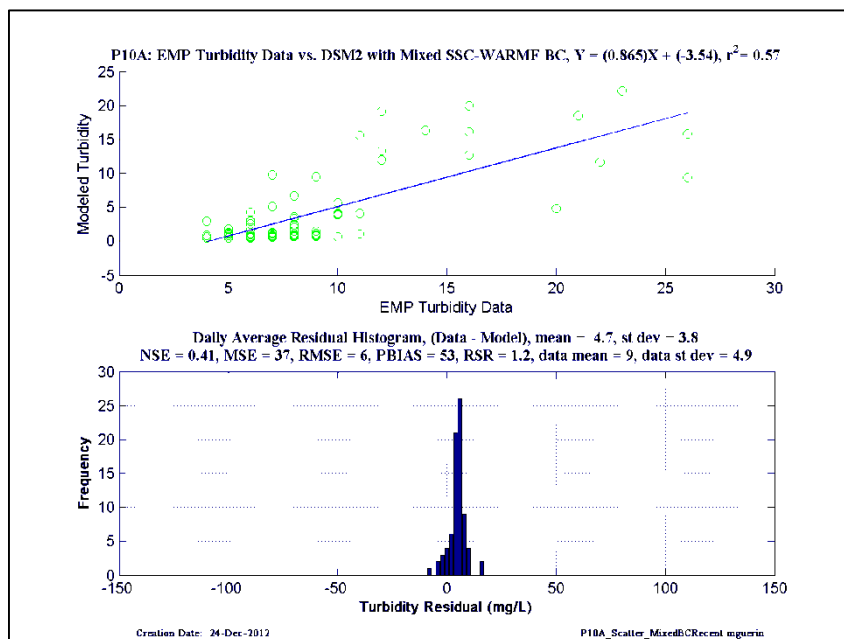
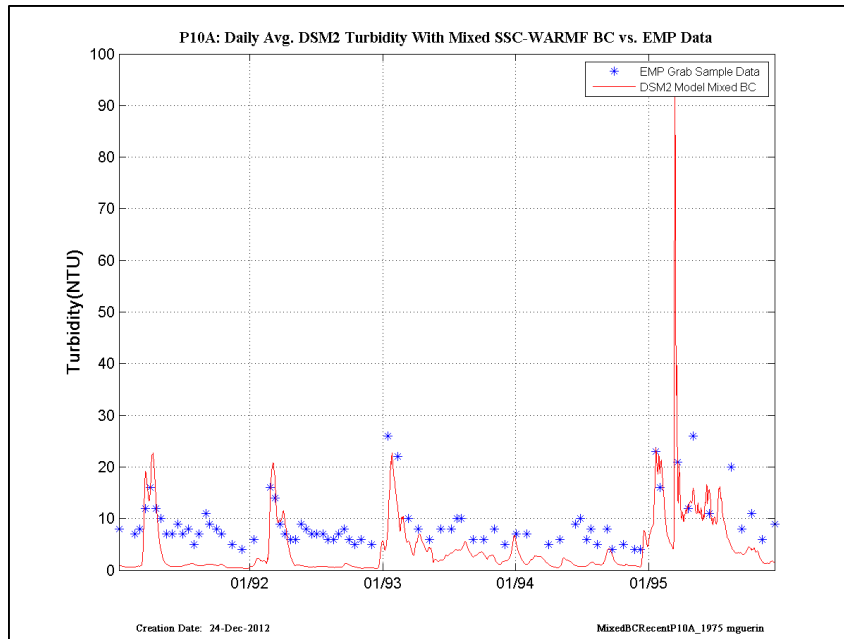


Figure 15-49 DSM2 daily-averaged turbidity model results using USGS-SSC at Freeport and Vernalis, and WARMF turbidity at other inflow boundaries compared to EMP grab-sample data, recent years– location is EMP P10A.

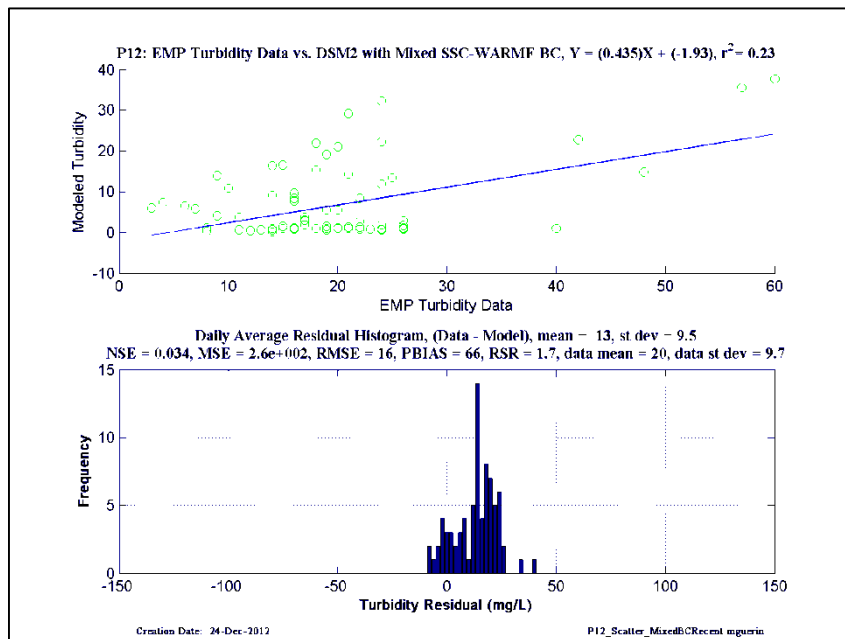
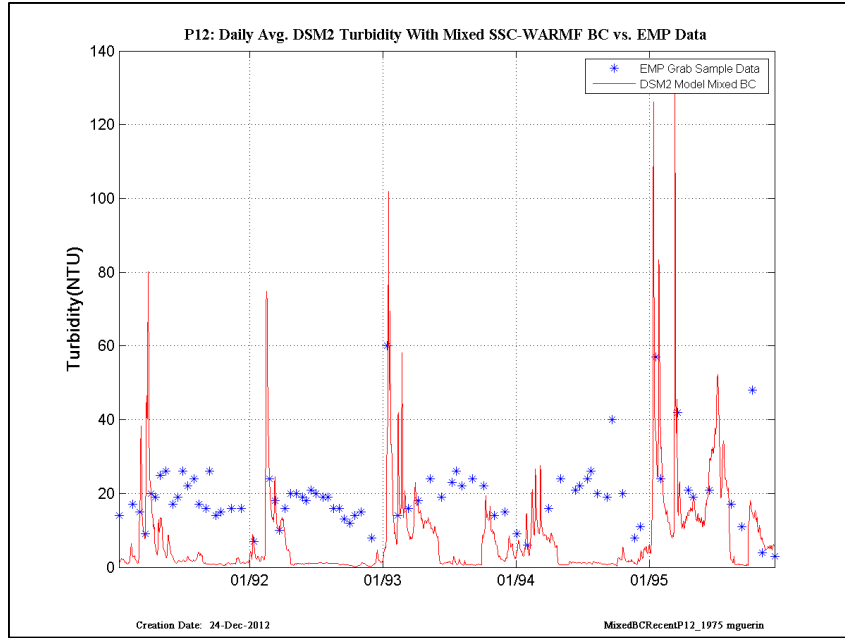


Figure 15-50 DSM2 daily-averaged turbidity model results using USGS-SSC at Freeport and Vernalis, and WARMF turbidity at other inflow boundaries compared to EMP grab-sample data, recent years– location is EMP P12.

16 Appendix VII – Figures and Statistics Documenting DSM2 QUAL Historical 1975 – Turbidity Model Application with WARMF Model Boundary Conditions

48.1 Early years: 1975 -1990

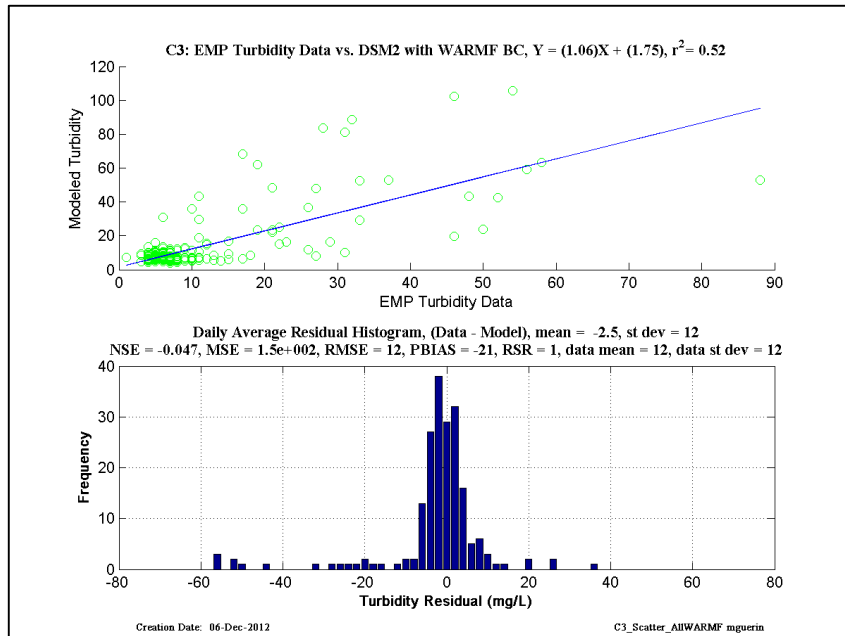
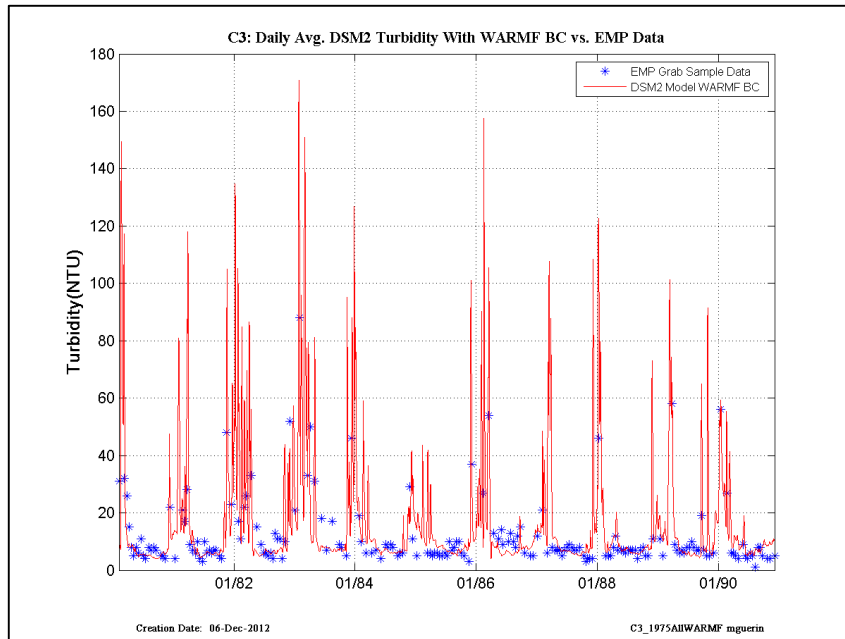


Figure 16-1 DSM2 daily-averaged turbidity model results using and WARMF model turbidity at all inflow boundaries compared to EMP grab-sample data, early years– location is EMP C3.

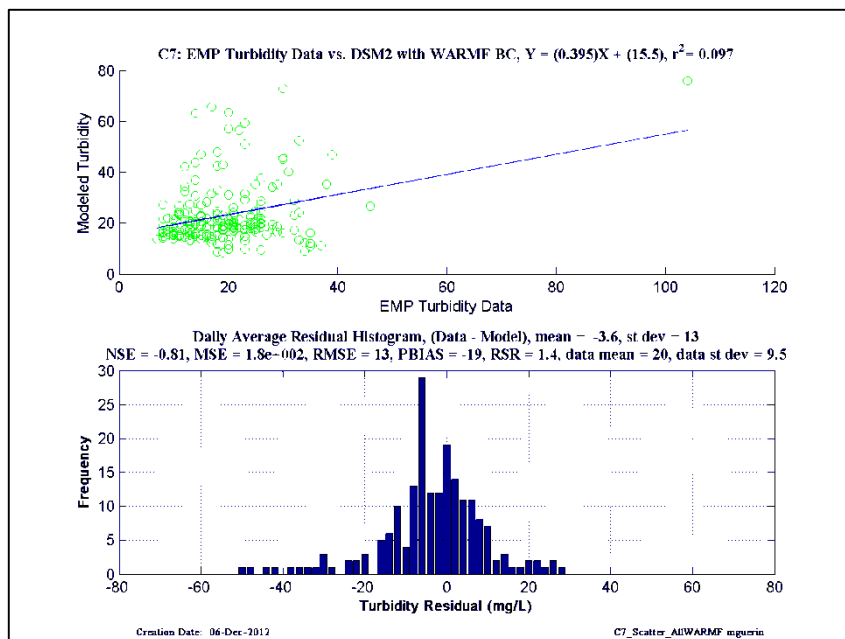
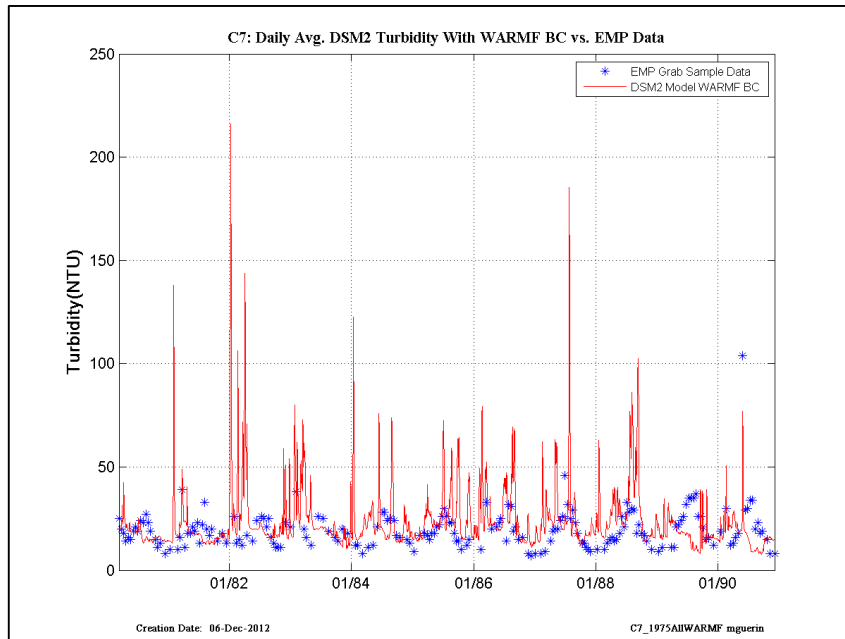


Figure 16-2 DSM2 daily-averaged turbidity model results using and WARMF model turbidity at all inflow boundaries compared to EMP grab-sample data, early years– location is EMP C7.

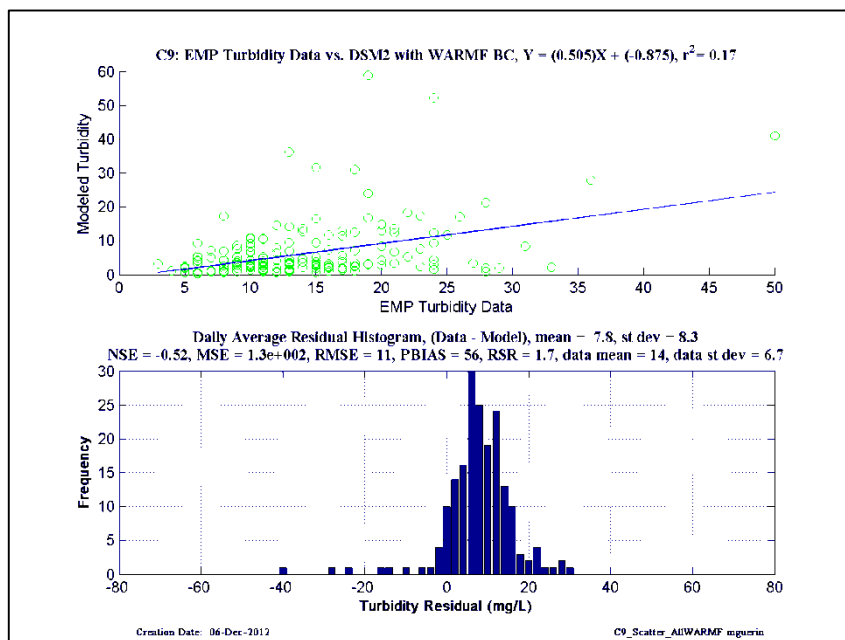
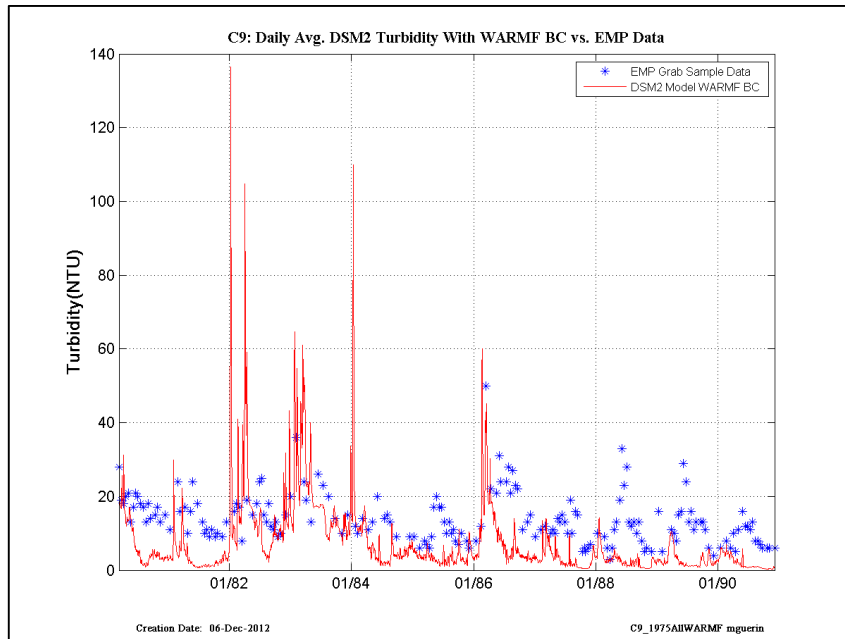


Figure 16-3 DSM2 daily-averaged turbidity model results using and WARMF model turbidity at all inflow boundaries compared to EMP grab-sample data, early years— location is EMP C9.

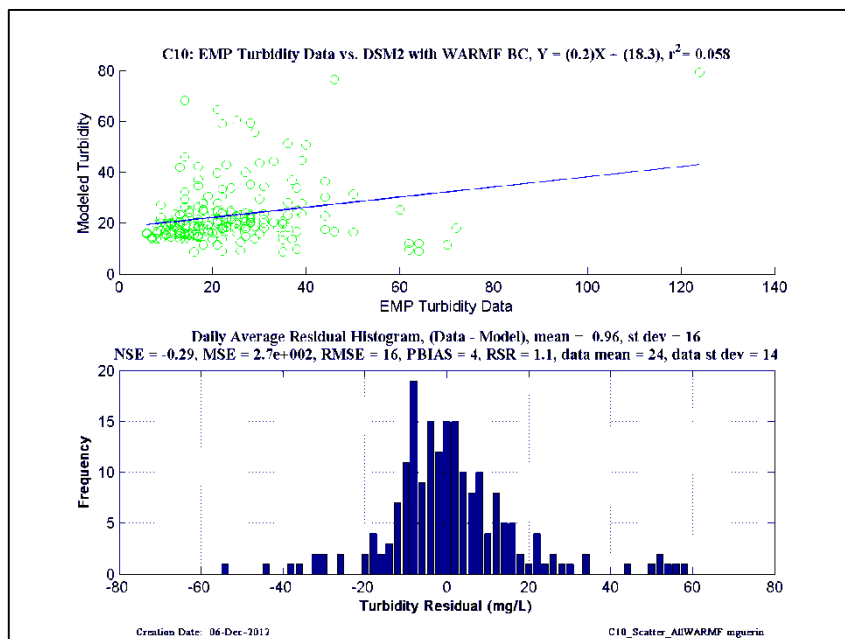
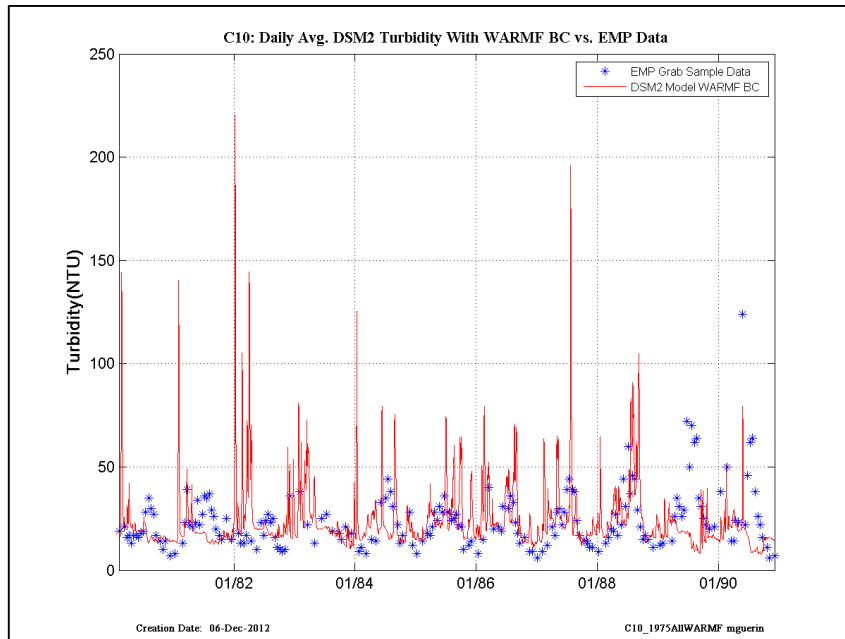


Figure 16-4 DSM2 daily-averaged turbidity model results using and WARMF model turbidity at all inflow boundaries compared to EMP grab-sample data, early years– location is EMP C10.

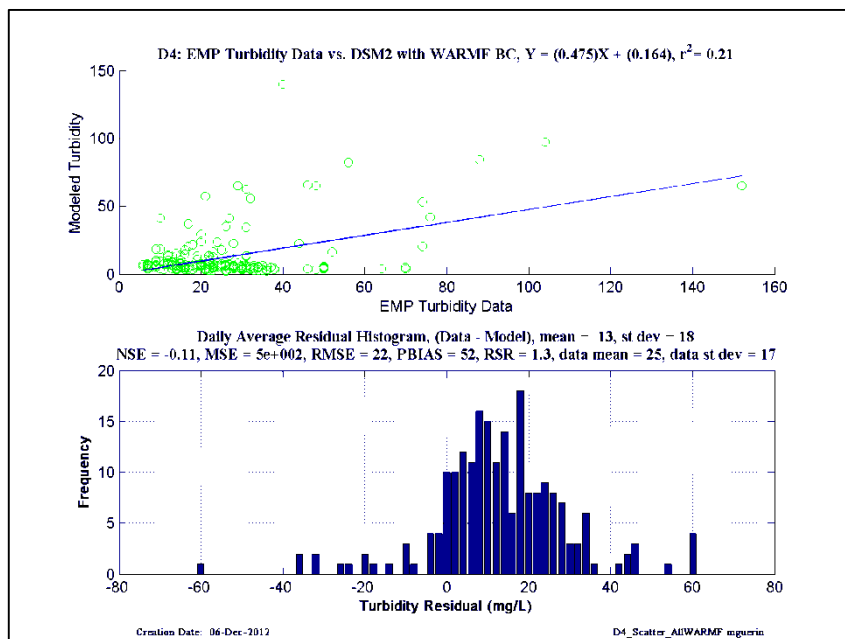
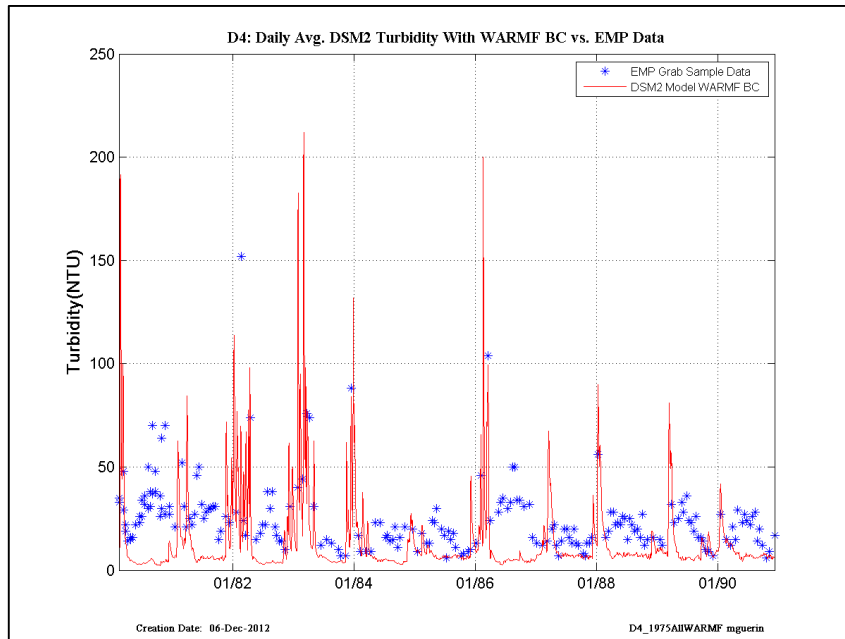


Figure 16-5 DSM2 daily-averaged turbidity model results using and WARMF model turbidity at all inflow boundaries compared to EMP grab-sample data, early years– location is EMP D4.

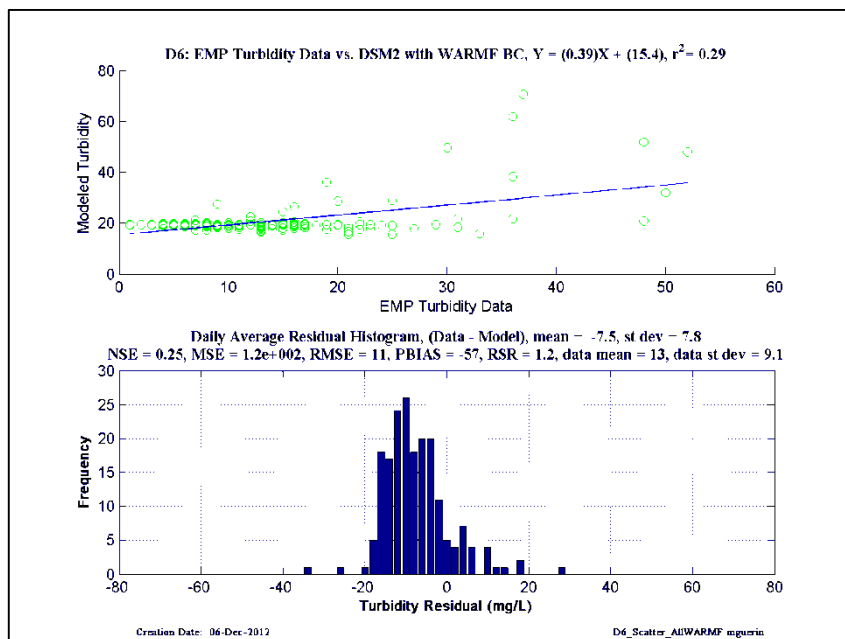
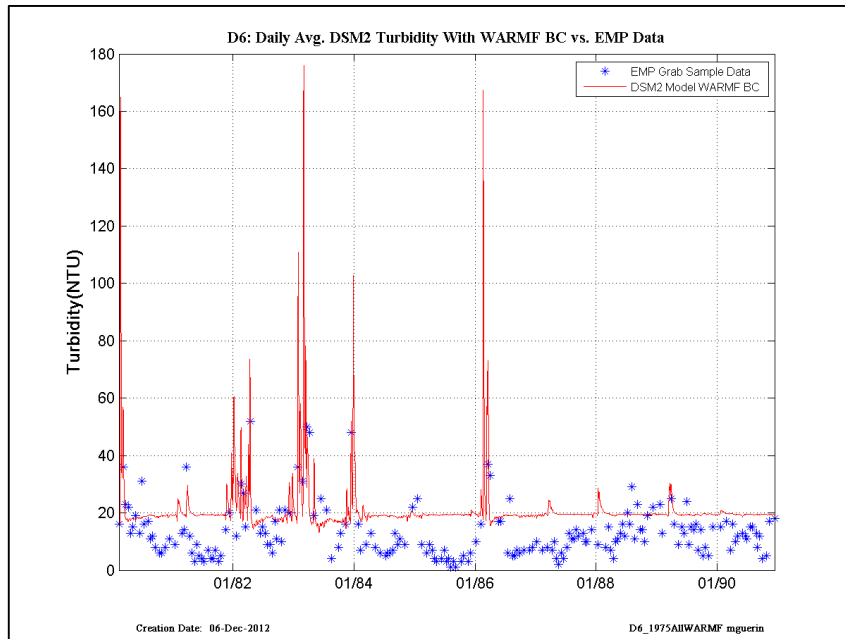


Figure 16-6 DSM2 daily-averaged turbidity model results using and WARMF model turbidity at all inflow boundaries compared to EMP grab-sample data, early years– location is EMP D6.

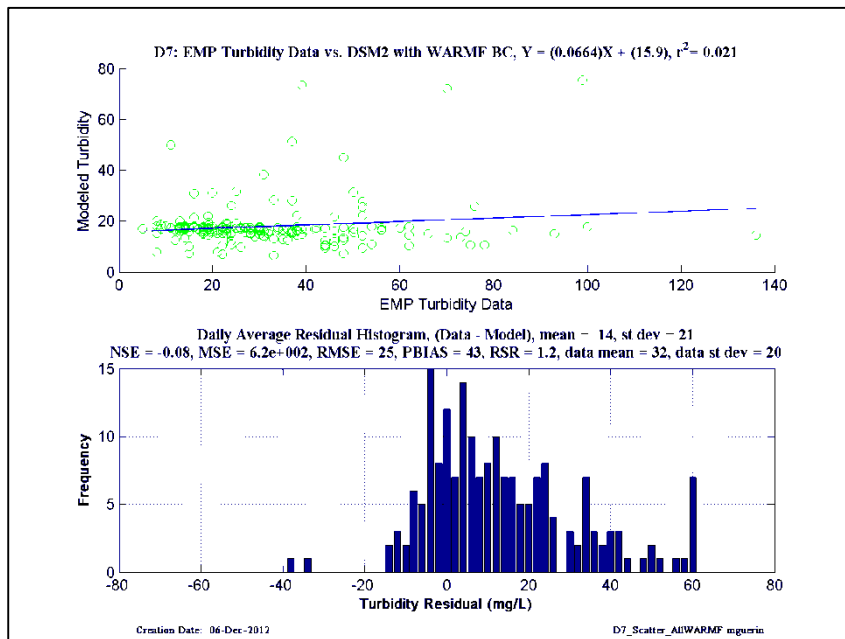
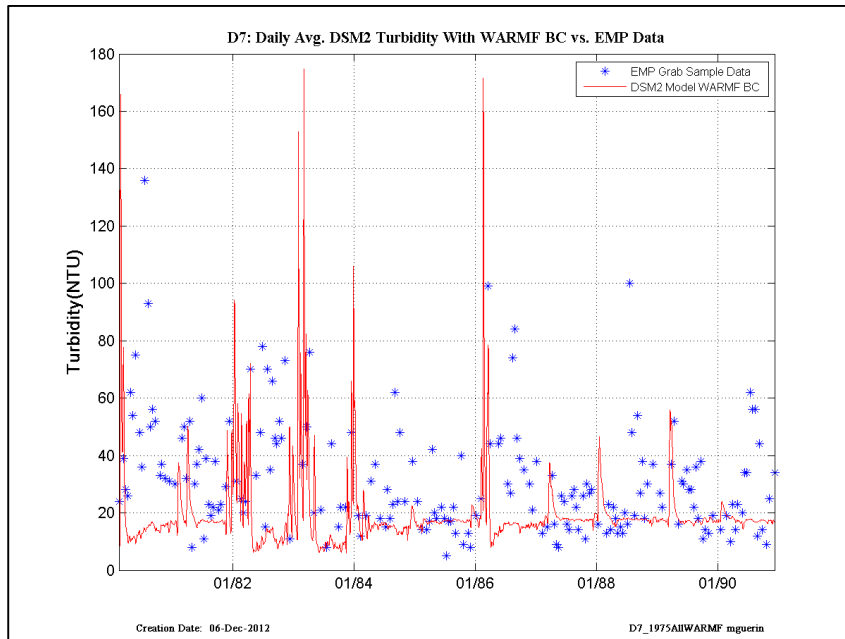


Figure 16-7 DSM2 daily-averaged turbidity model results using and WARMF model turbidity at all inflow boundaries compared to EMP grab-sample data, early years– location is EMP D7.

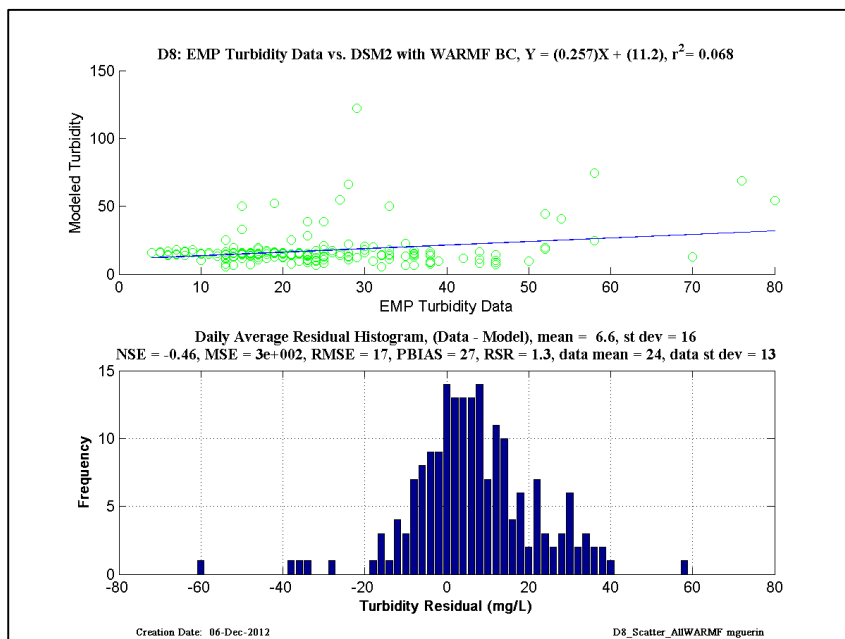
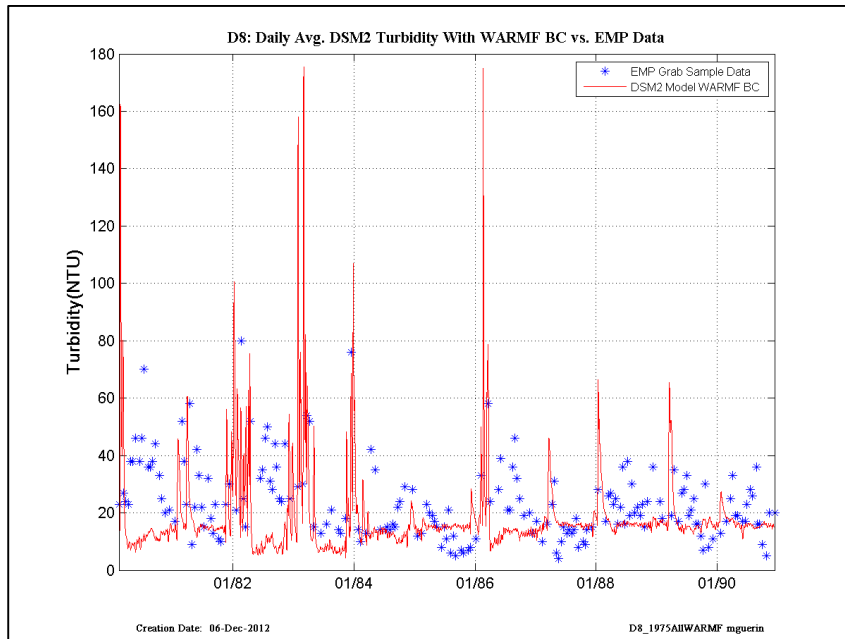


Figure 16-8 DSM2 daily-averaged turbidity model results using and WARMF model turbidity at all inflow boundaries compared to EMP grab-sample data, early years– location is EMP D8.

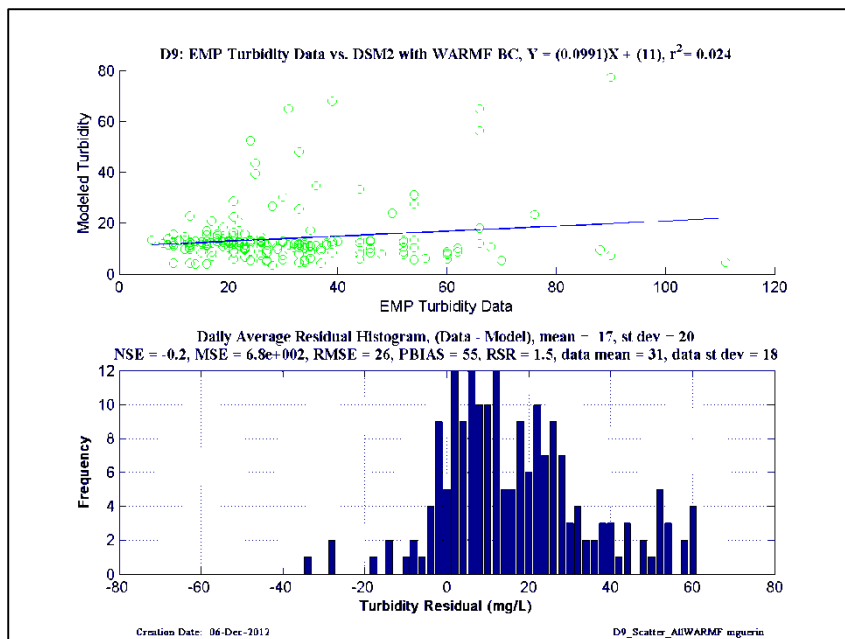
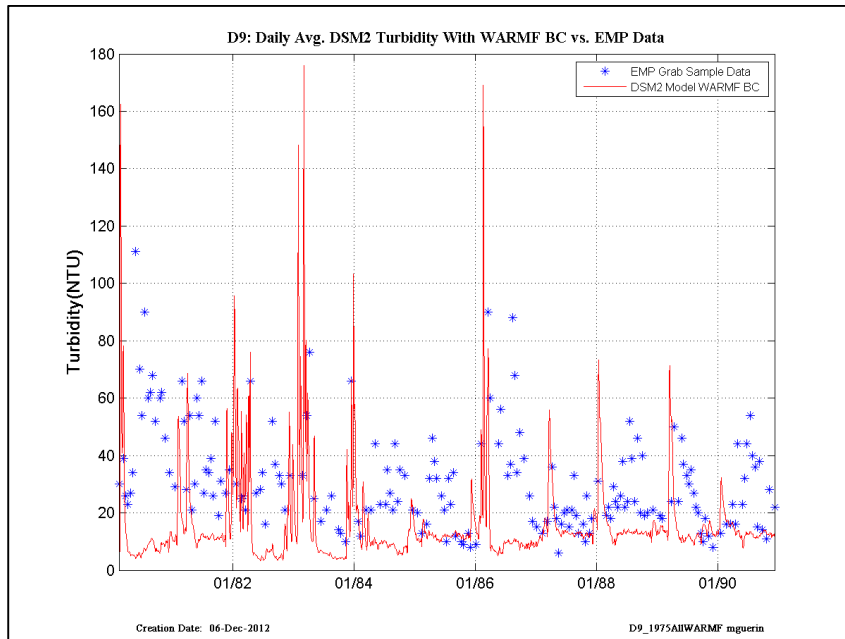


Figure 16-9 DSM2 daily-averaged turbidity model results using and WARMF model turbidity at all inflow boundaries compared to EMP grab-sample data, early years– location is EMP D9.

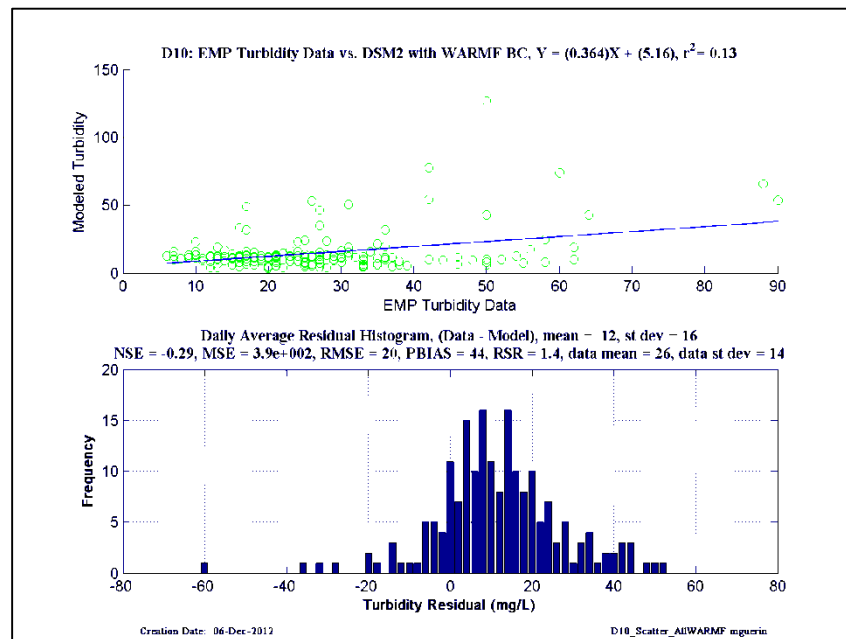
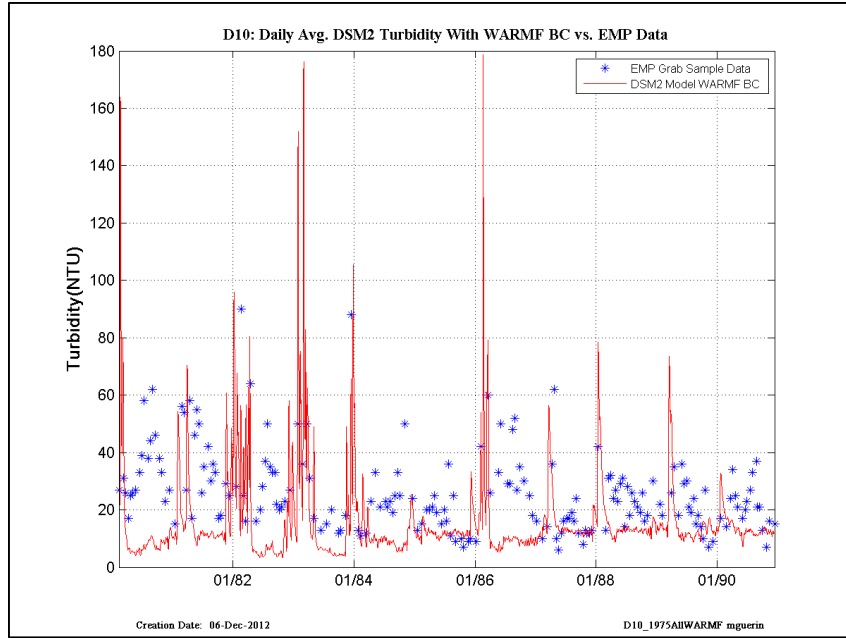


Figure 16-10 DSM2 daily-averaged turbidity model results using and WARMF model turbidity at all inflow boundaries compared to EMP grab-sample data, early years— location is EMP D10.

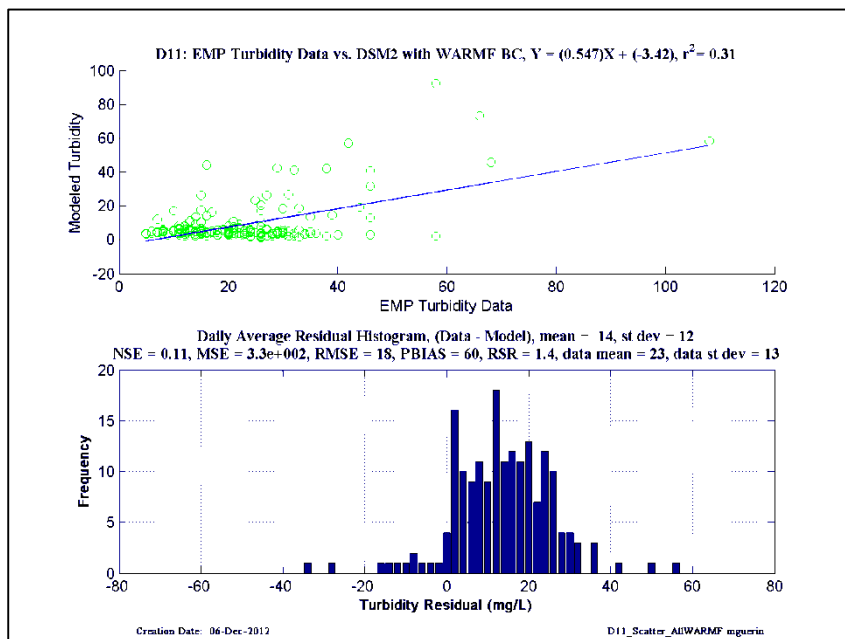
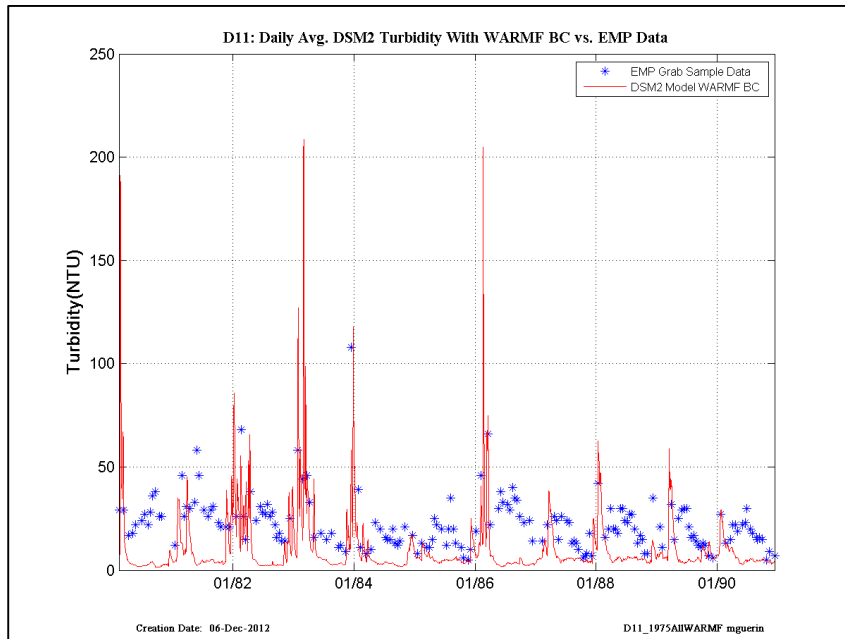


Figure 16-11 DSM2 daily-averaged turbidity model results using and WARMF model turbidity at all inflow boundaries compared to EMP grab-sample data, early years— location is EMP D11.

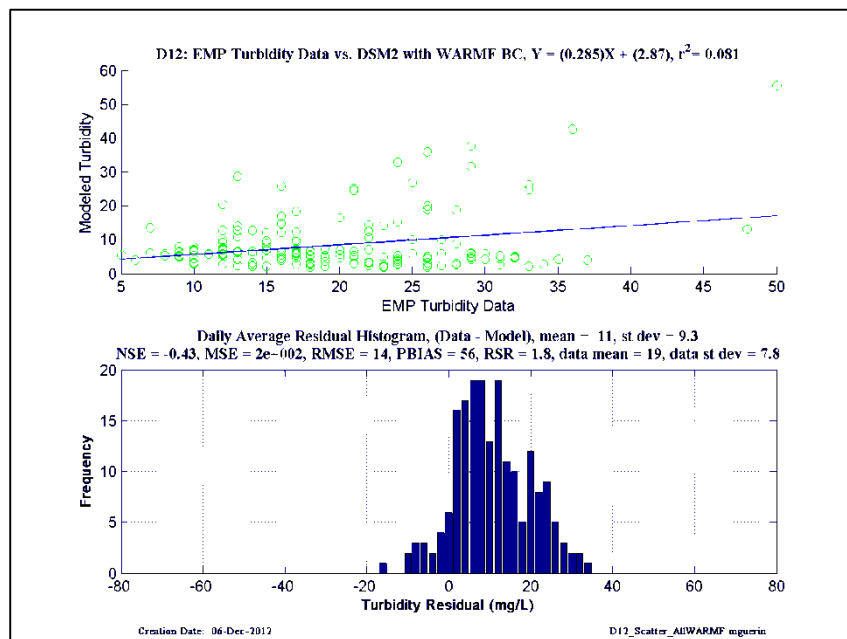
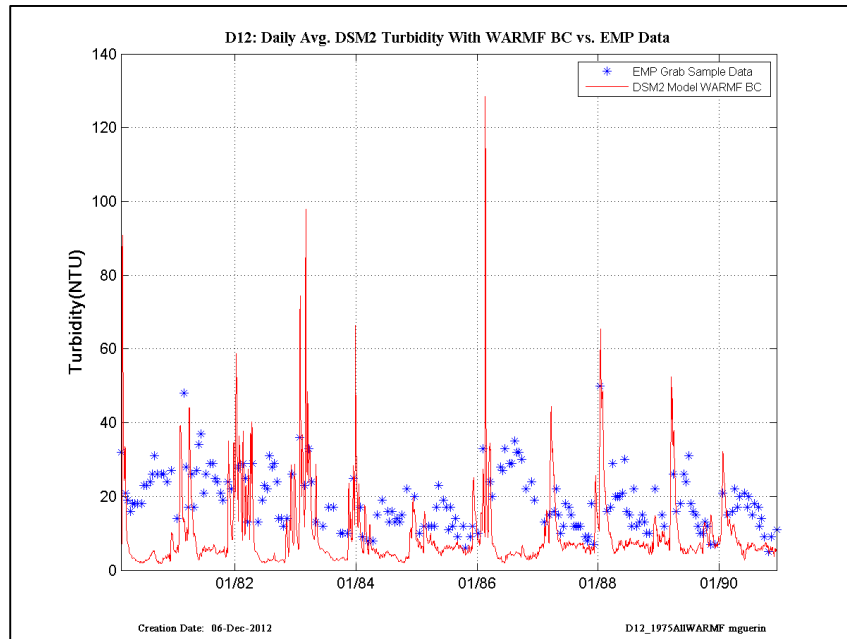


Figure 16-12 DSM2 daily-averaged turbidity model results using and WARMF model turbidity at all inflow boundaries compared to EMP grab-sample data, early years– location is EMP D12.

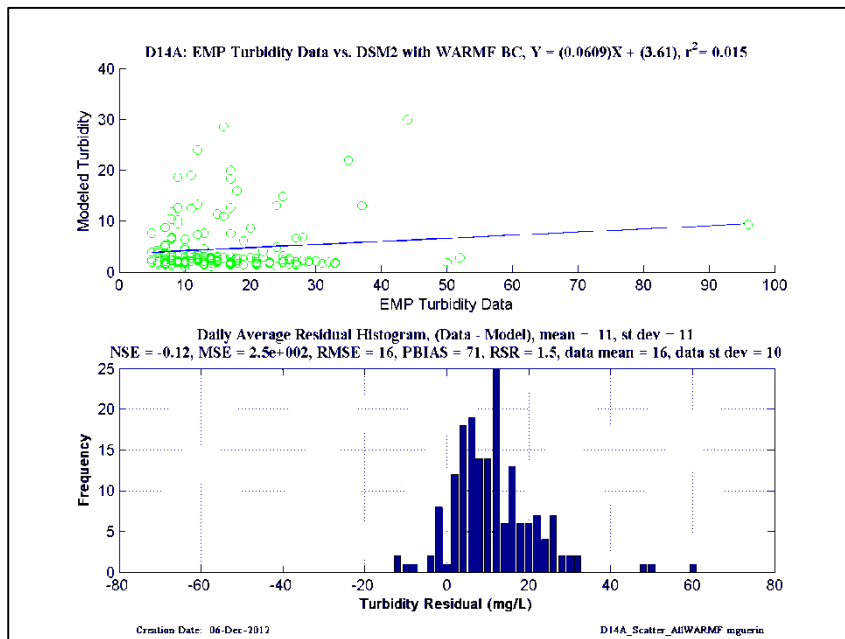
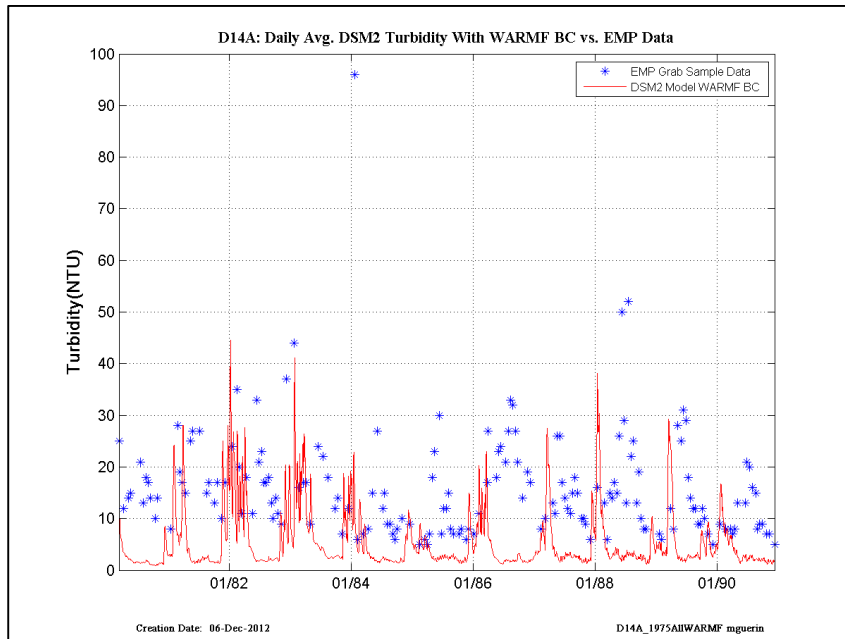


Figure 16-13 DSM2 daily-averaged turbidity model results using and WARMF model turbidity at all inflow boundaries compared to EMP grab-sample data, early years– location is EMP D14A.

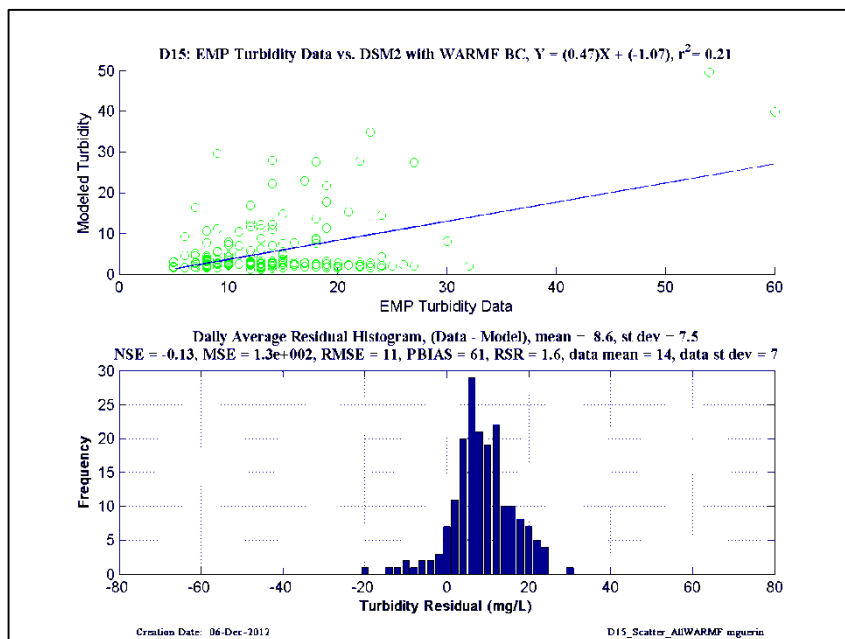
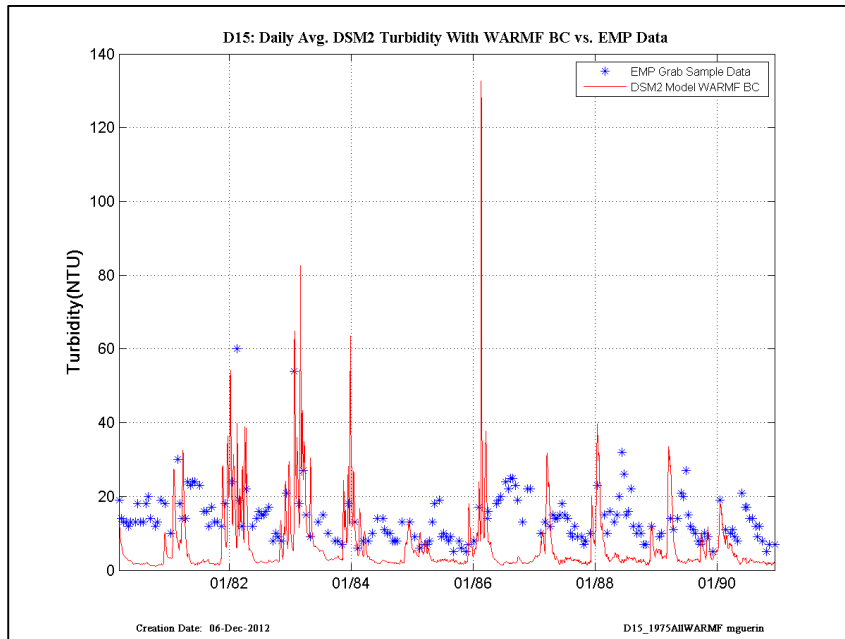


Figure 16-14 DSM2 daily-averaged turbidity model results using and WARMF model turbidity at all inflow boundaries compared to EMP grab-sample data, early years– location is EMP D15.

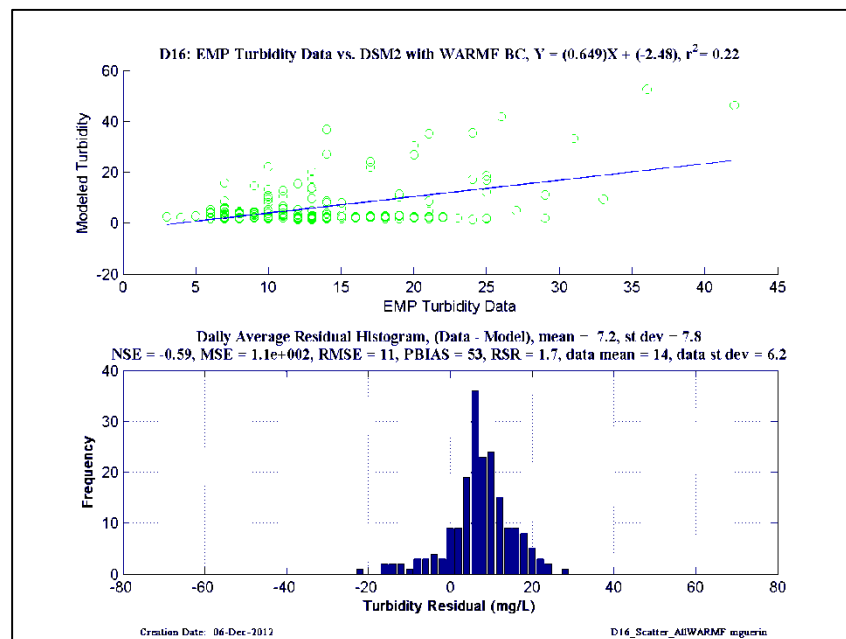
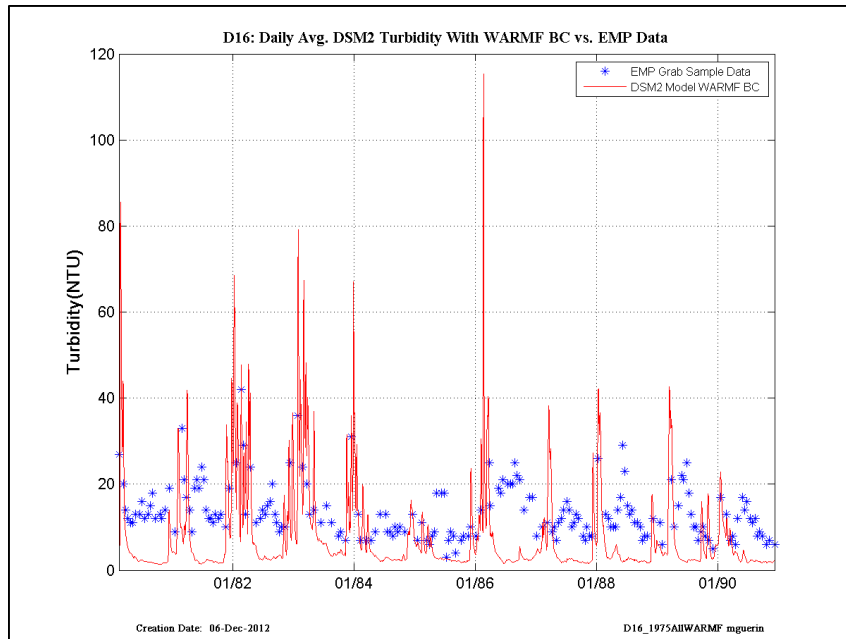


Figure 16-15 DSM2 daily-averaged turbidity model results using and WARMF model turbidity at all inflow boundaries compared to EMP grab-sample data, early years– location is EMP D16.

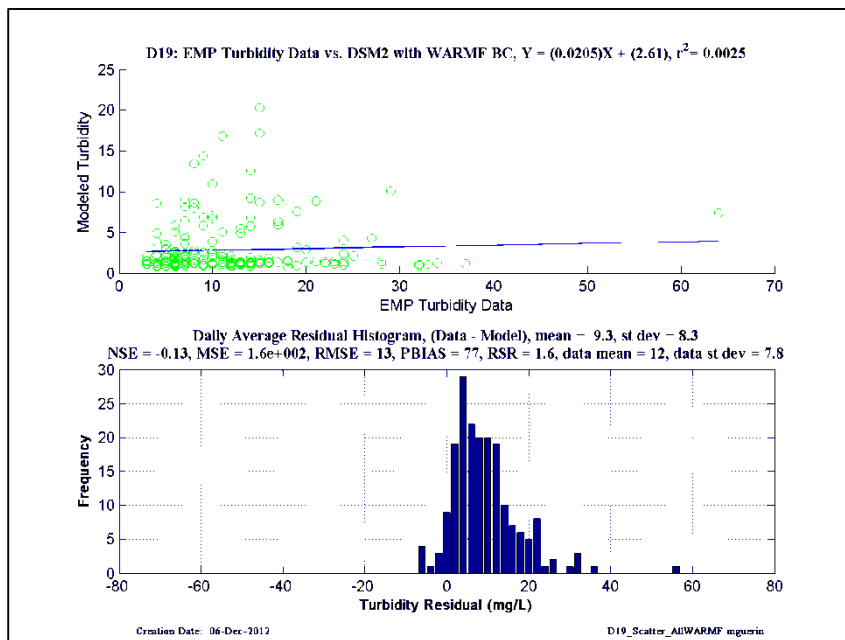
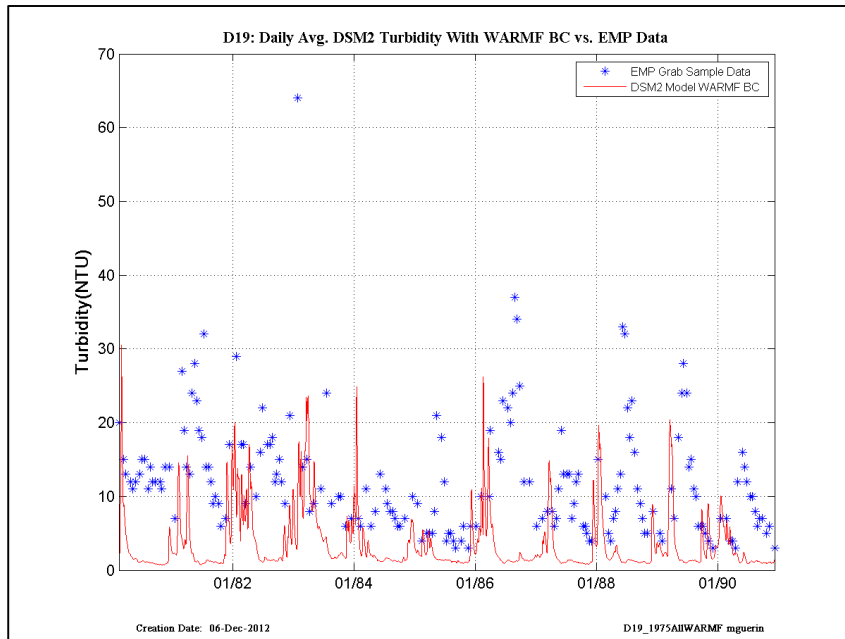


Figure 16-16 DSM2 daily-averaged turbidity model results using and WARMF model turbidity at all inflow boundaries compared to EMP grab-sample data, early years– location is EMP D19.

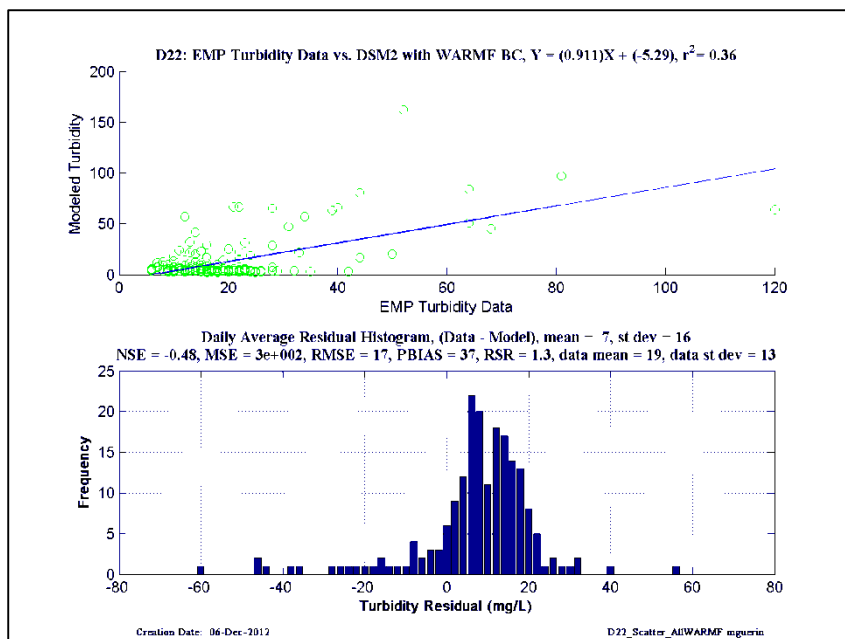
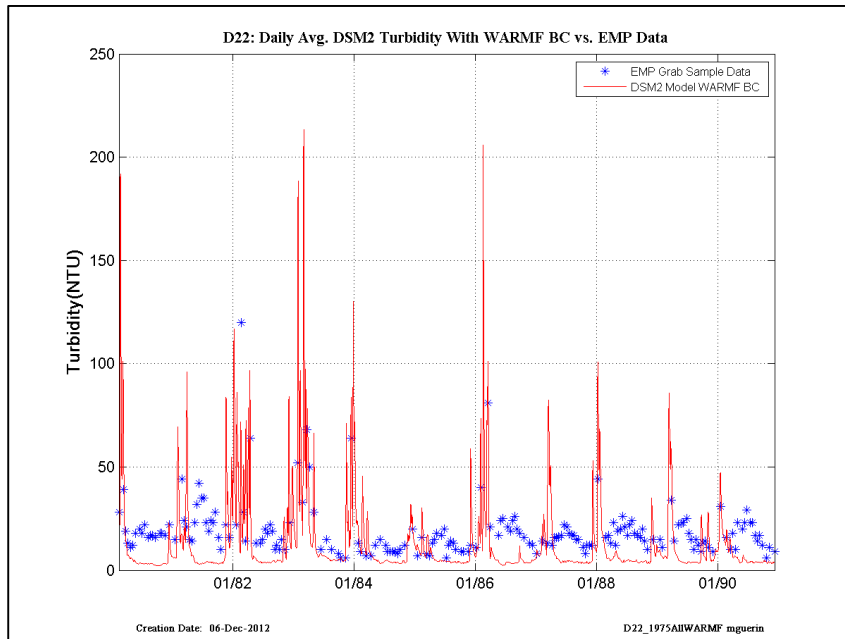


Figure 16-17 DSM2 daily-averaged turbidity model results using and WARMF model turbidity at all inflow boundaries compared to EMP grab-sample data, early years— location is EMP D22.

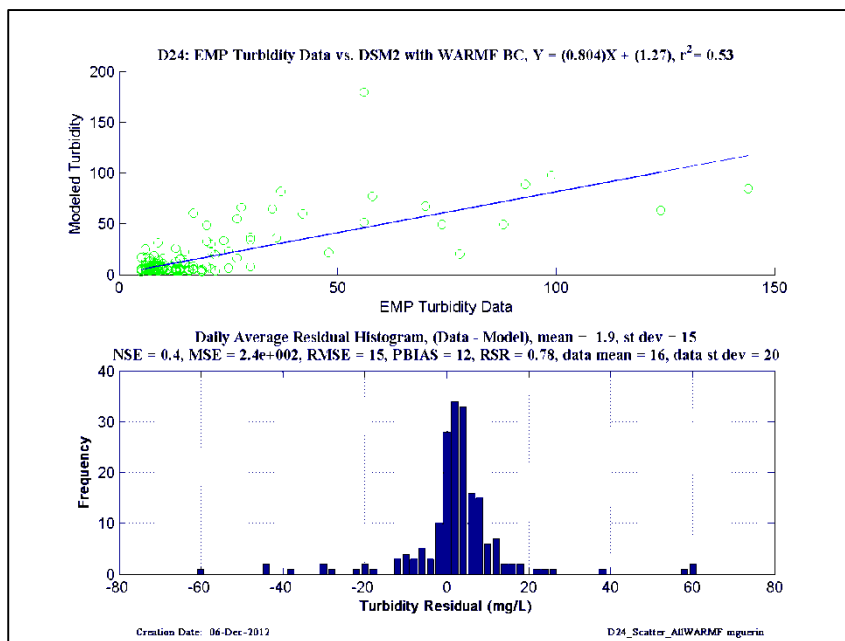
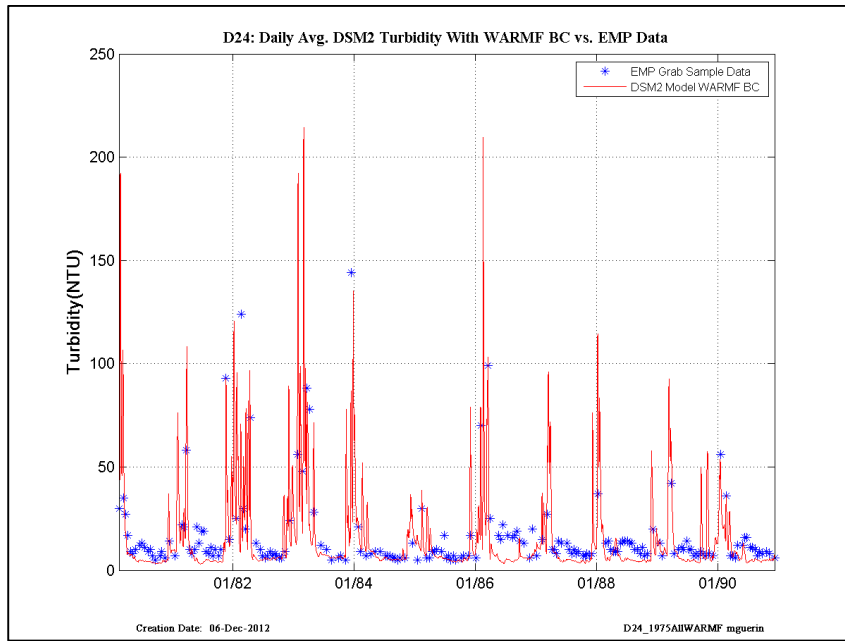


Figure 16-18 DSM2 daily-averaged turbidity model results using and WARMF model turbidity at all inflow boundaries compared to EMP grab-sample data, early years– location is EMP D24.

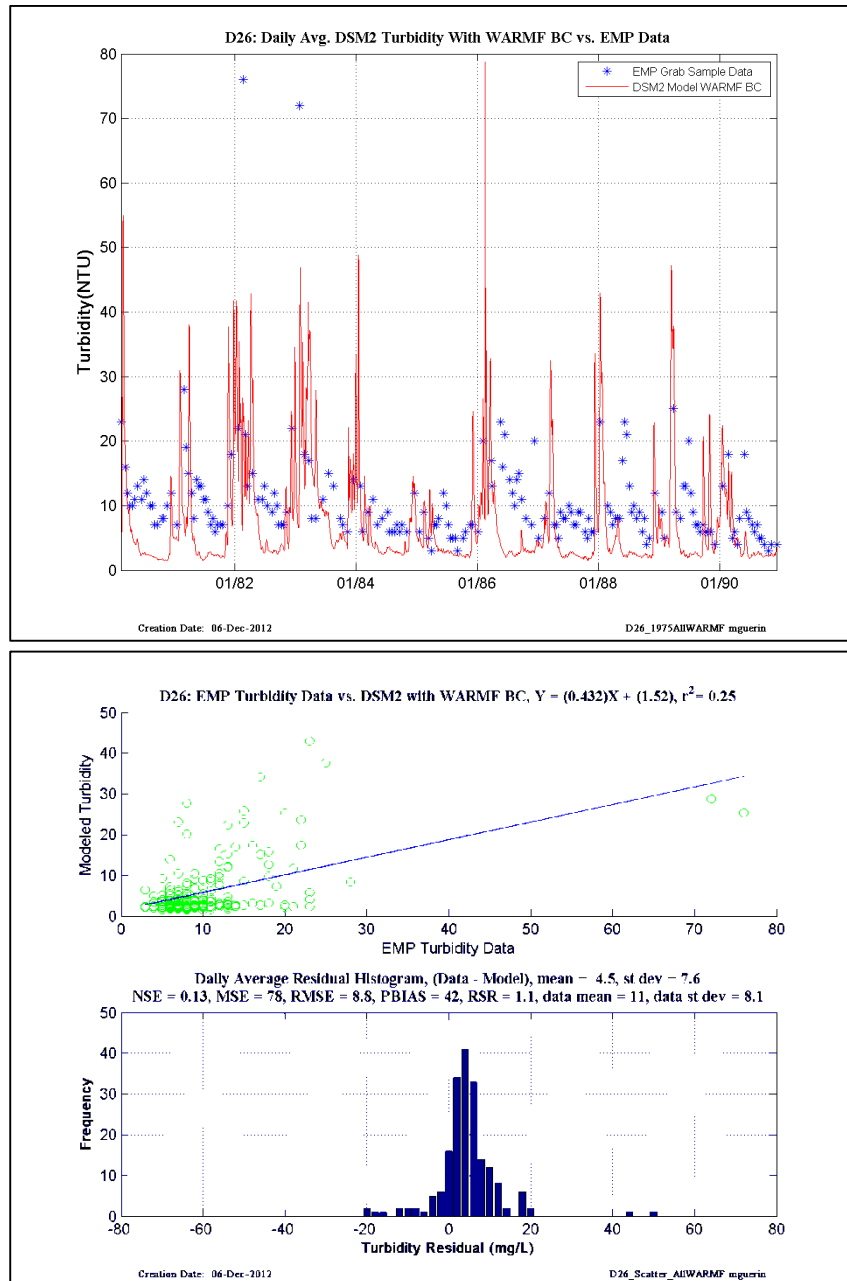


Figure 16-19 DSM2 daily-averaged turbidity model results using and WARMF model turbidity at all inflow boundaries compared to EMP grab-sample data, early years– location is EMP D26.

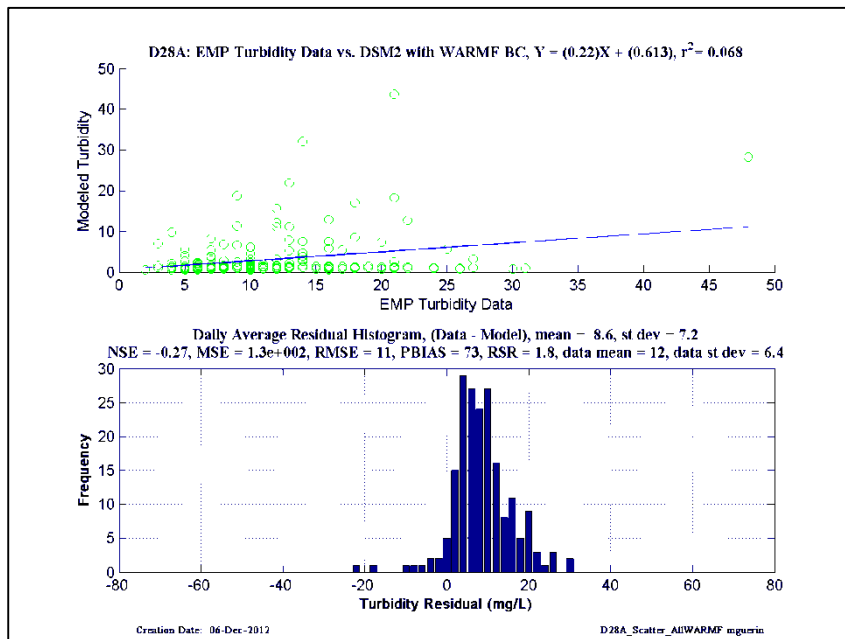
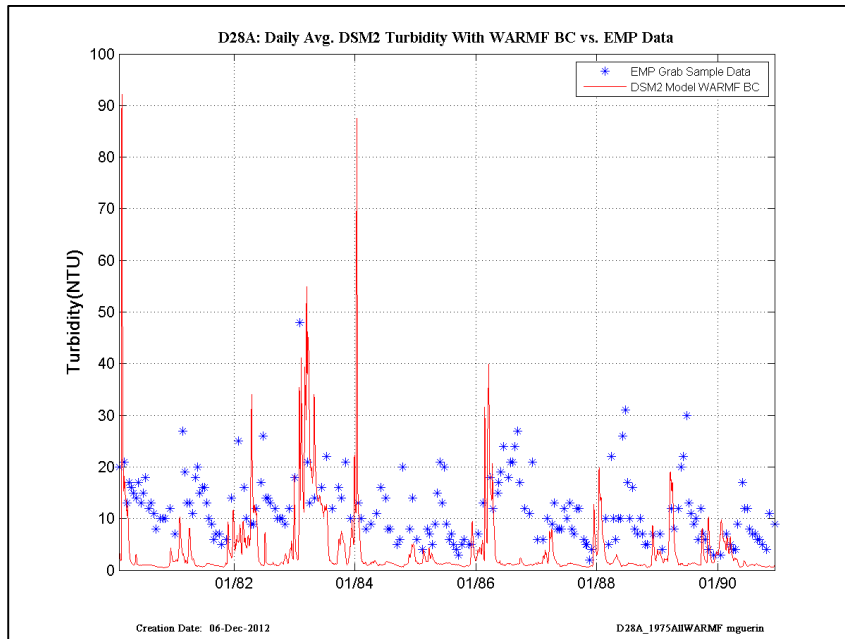


Figure 16-20 DSM2 daily-averaged turbidity model results using and WARMF model turbidity at all inflow boundaries compared to EMP grab-sample data, early years– location is EMP D28A.

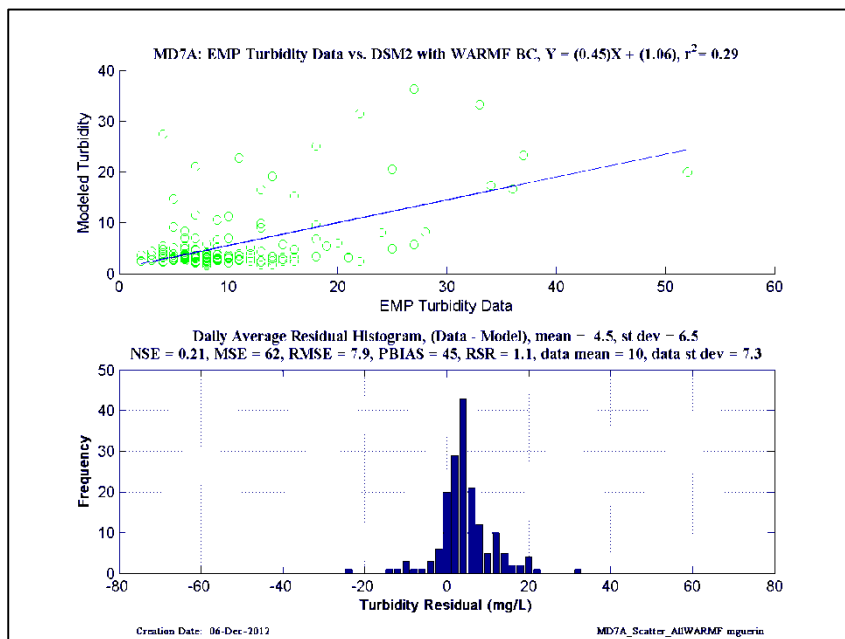
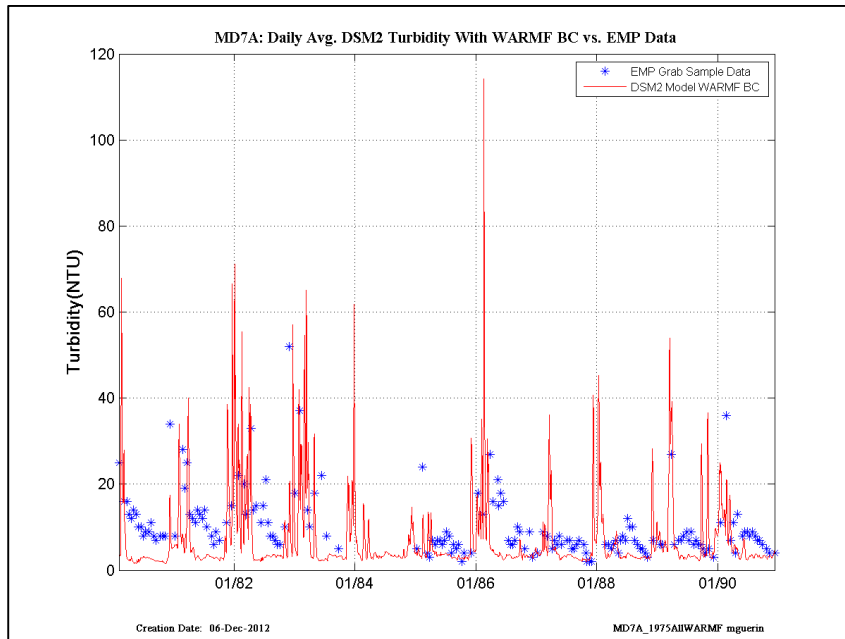


Figure 16-21 DSM2 daily-averaged turbidity model results using and WARMF model turbidity at all inflow boundaries compared to EMP grab-sample data, early years– location is EMP MD7A.

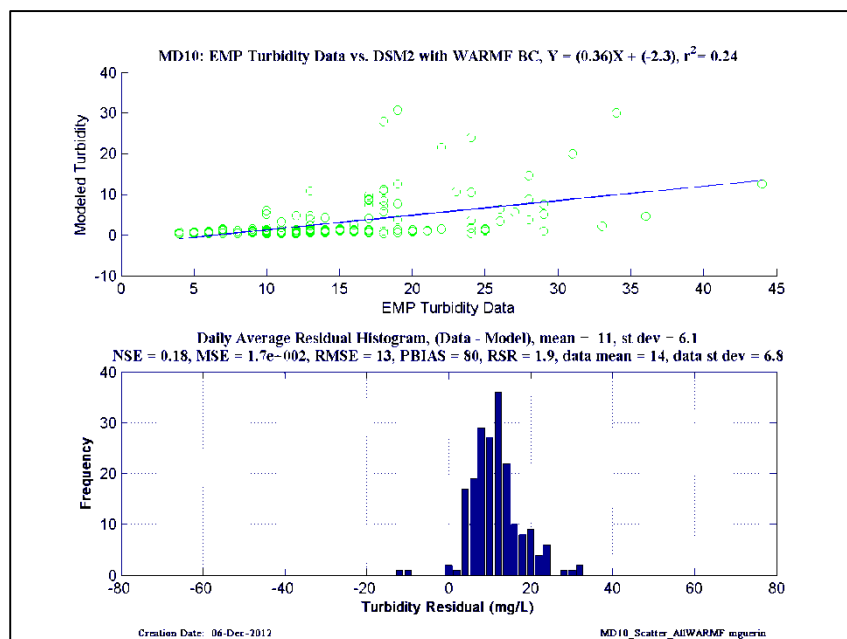
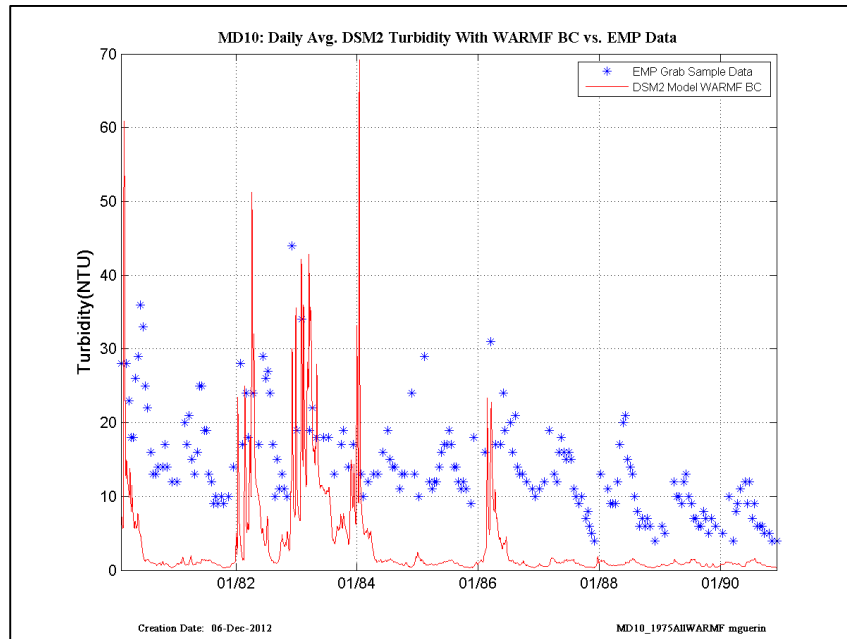


Figure 16-22 DSM2 daily-averaged turbidity model results using and WARMF model turbidity at all inflow boundaries compared to EMP grab-sample data, early years—location is MD10.

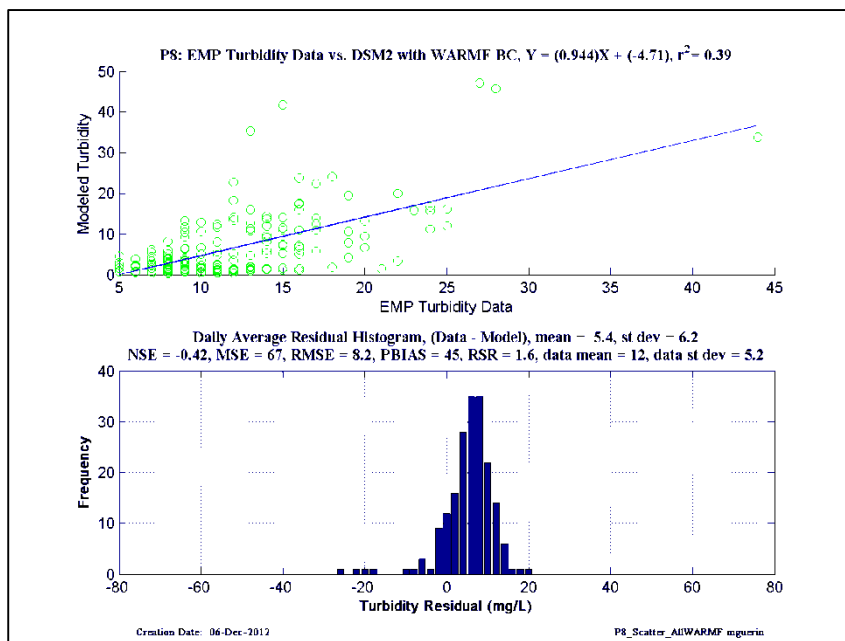
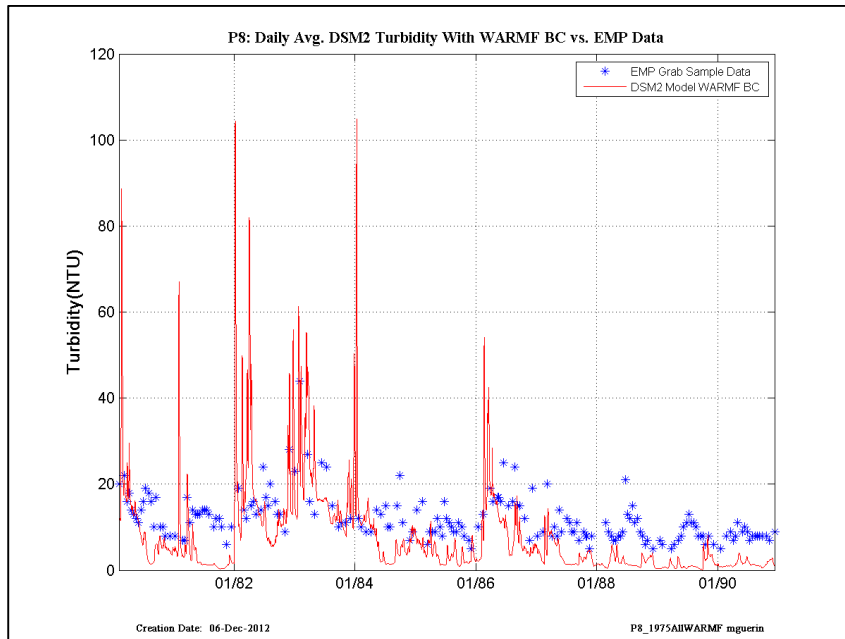


Figure 16-23 DSM2 daily-averaged turbidity model results using and WARMF model turbidity at all inflow boundaries compared to EMP grab-sample data, early years– location is P8.

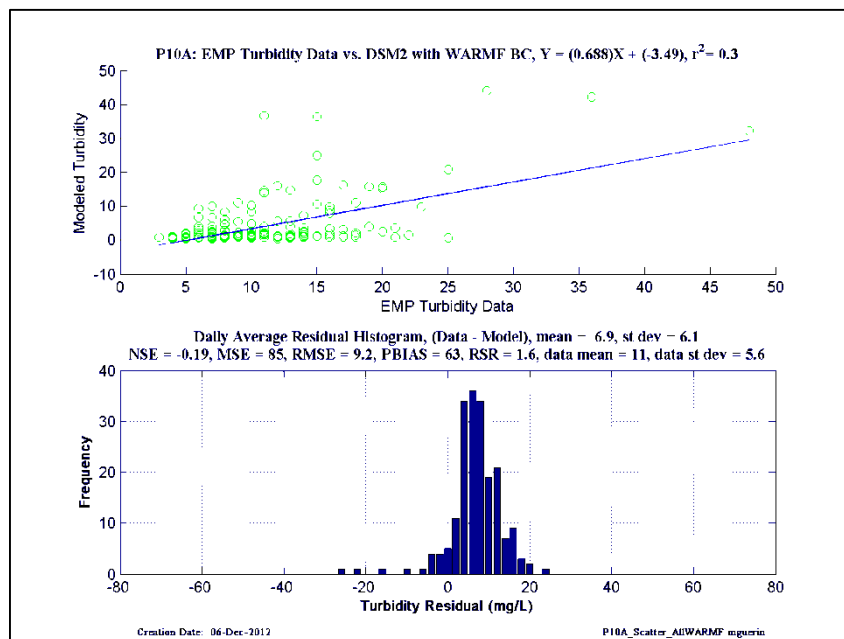
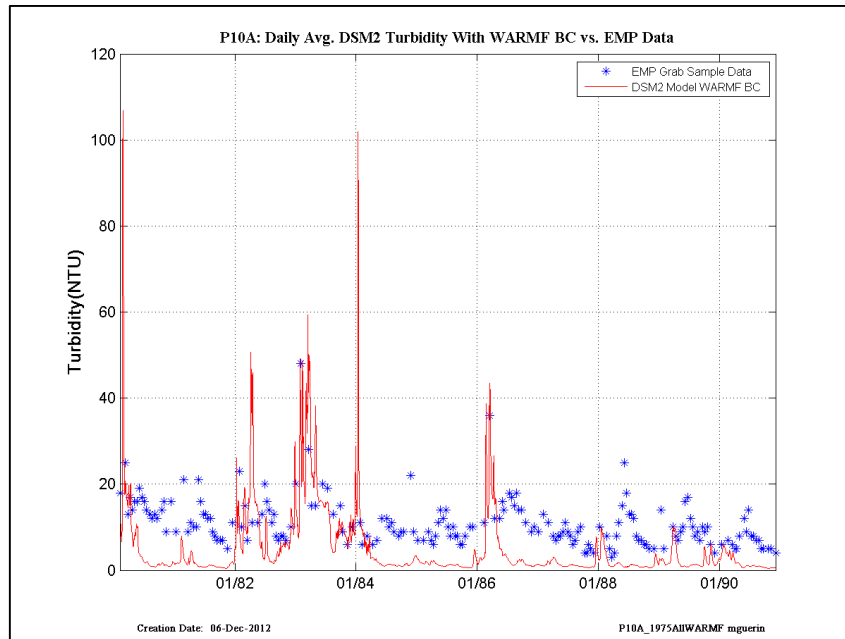


Figure 16-24 DSM2 daily-averaged turbidity model results using and WARMF model turbidity at all inflow boundaries compared to EMP grab-sample data, early years– location is P10A.

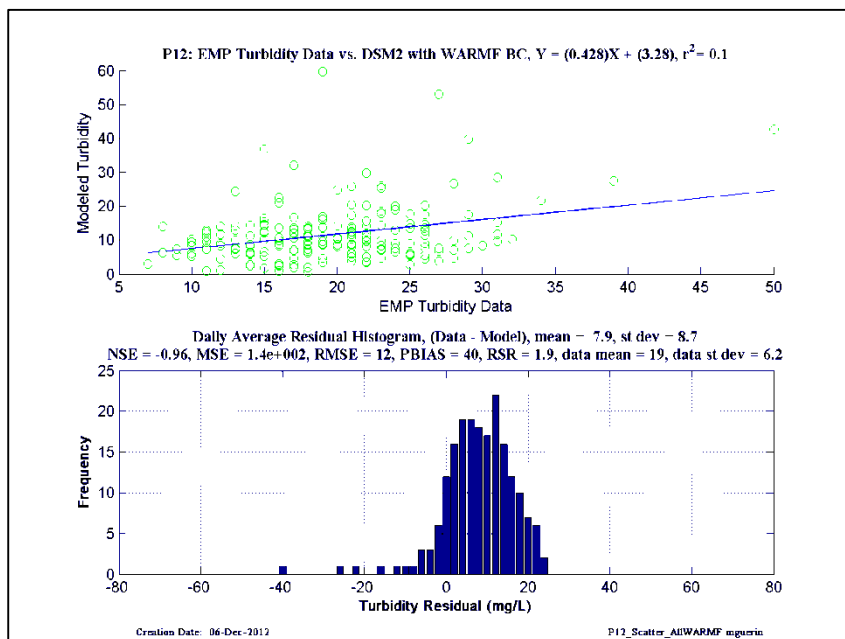
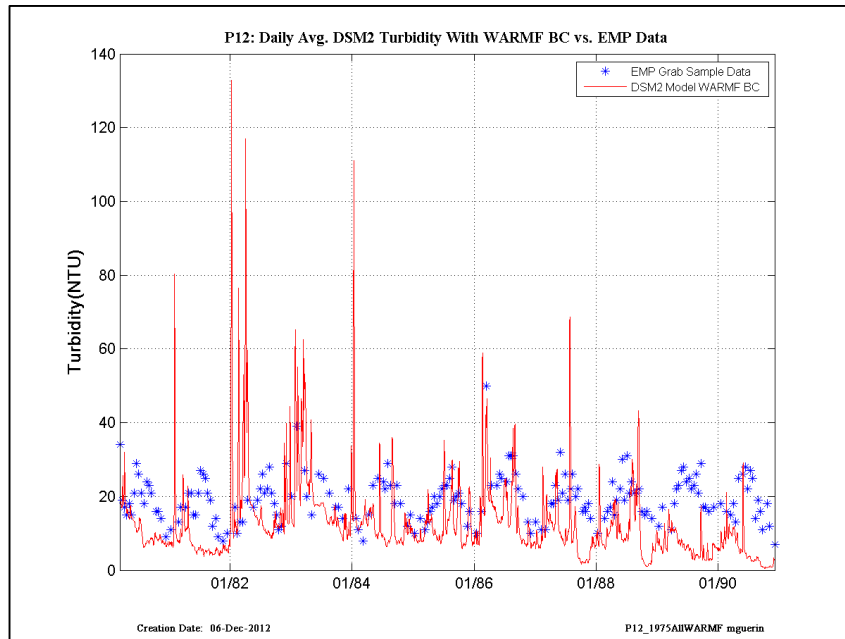


Figure 16-25 DSM2 daily-averaged turbidity model results using and WARMF model turbidity at all inflow boundaries compared to EMP grab-sample data, early years– location is P12.

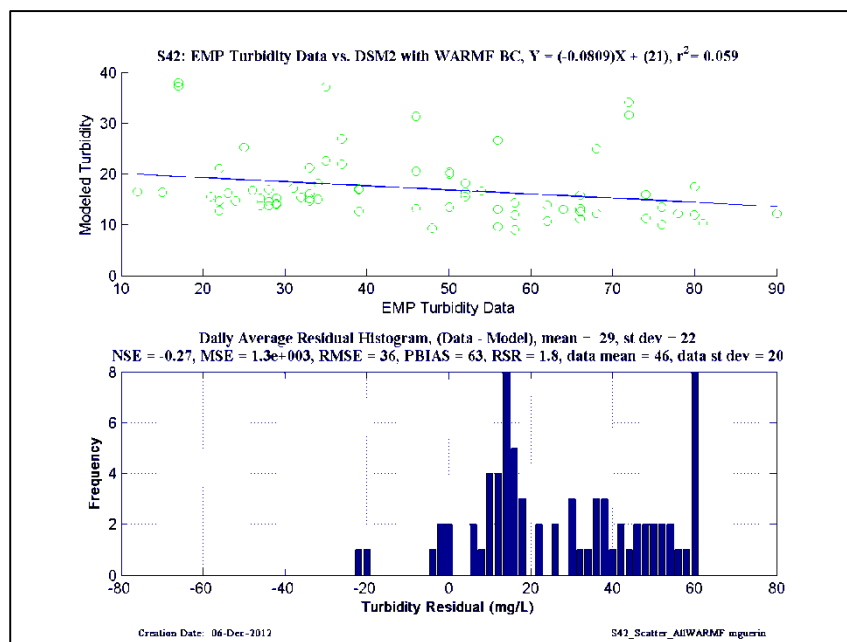
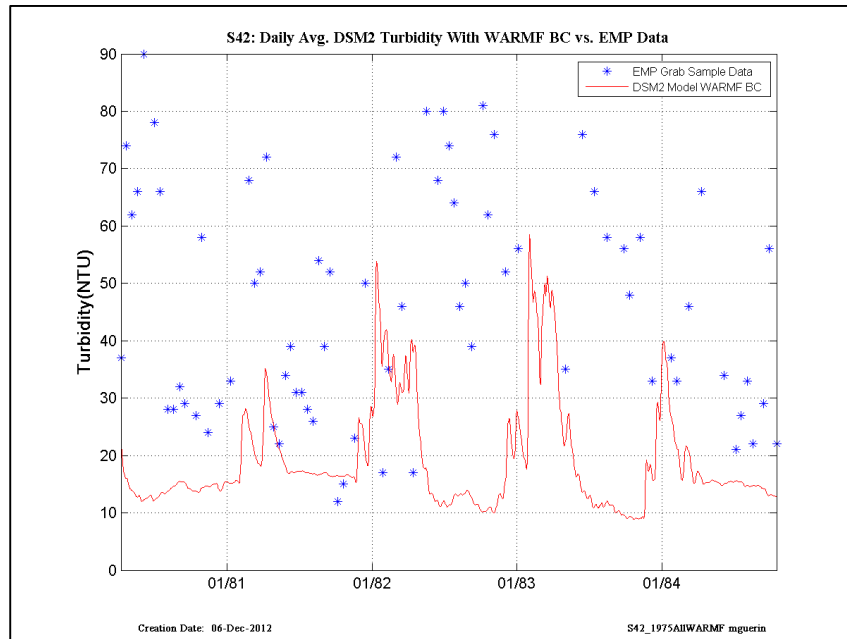


Figure 16-26 DSM2 daily-averaged turbidity model results using and WARMF model turbidity at all inflow boundaries compared to EMP grab-sample data, early years– location is S42.

48.2 Recent years: 1991 - 2011

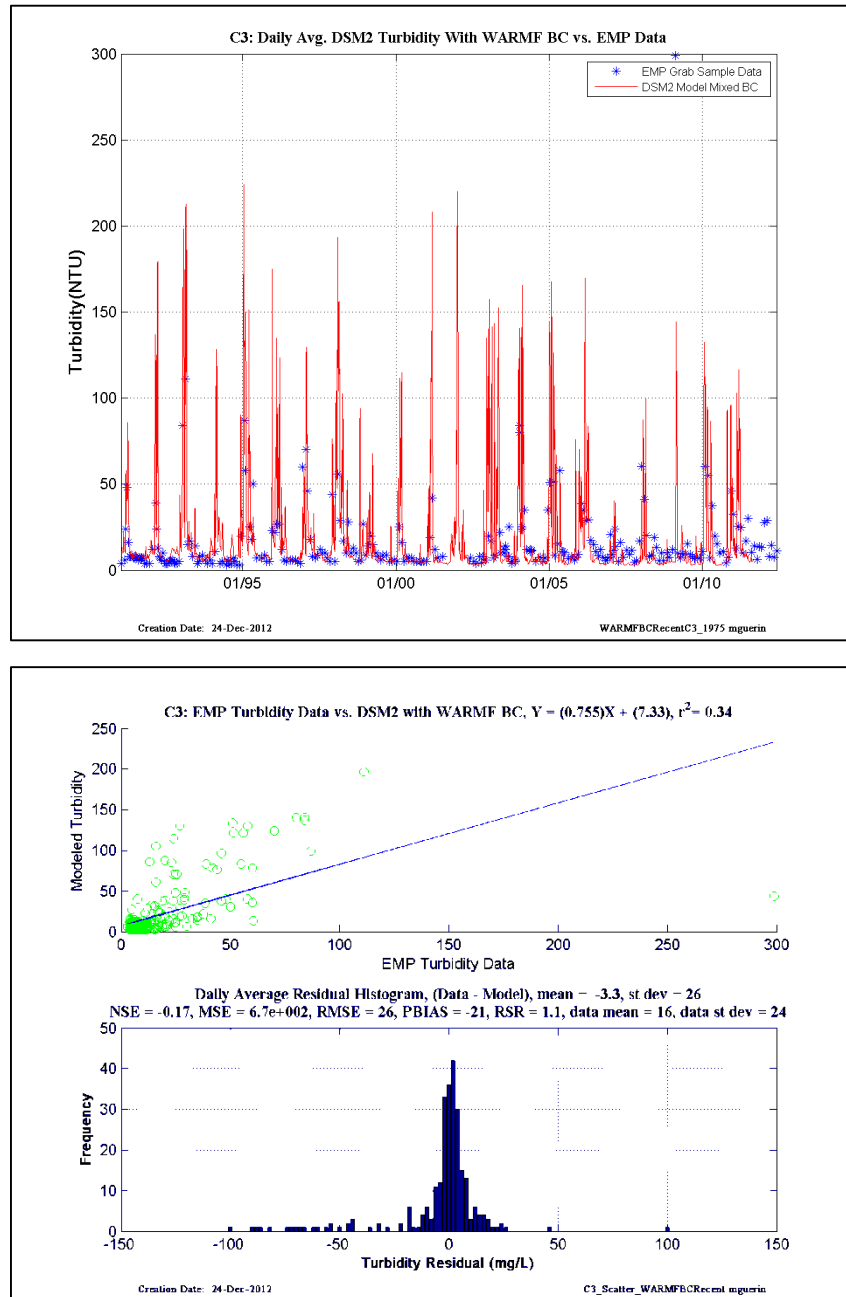


Figure 16-27 DSM2 daily-averaged turbidity model results using and WARMF model turbidity at all inflow boundaries compared to EMP grab-sample data, recent years– location is EMP C3.

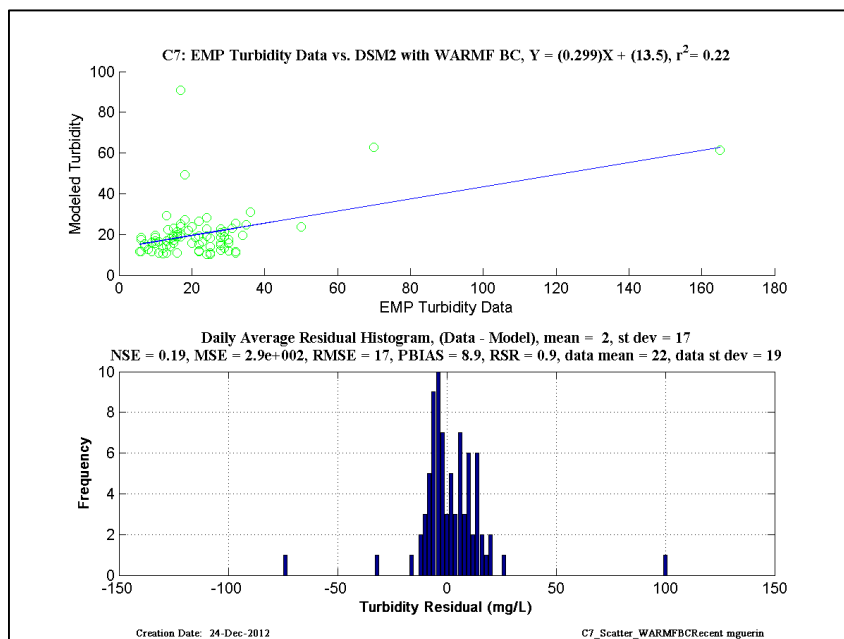
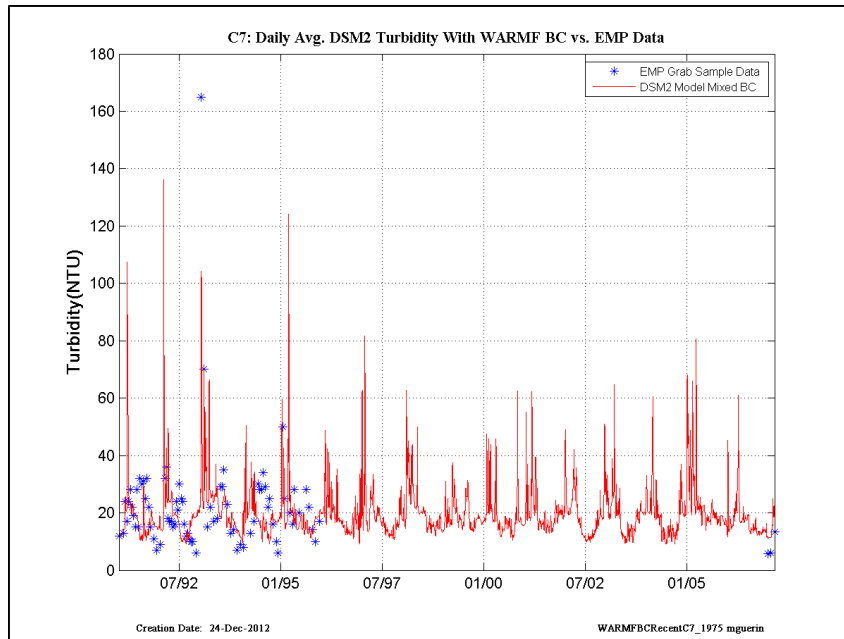


Figure 16-28 DSM2 daily-averaged turbidity model results using and WARMF model turbidity at all inflow boundaries compared to EMP grab-sample data, recent years– location is EMP C7.

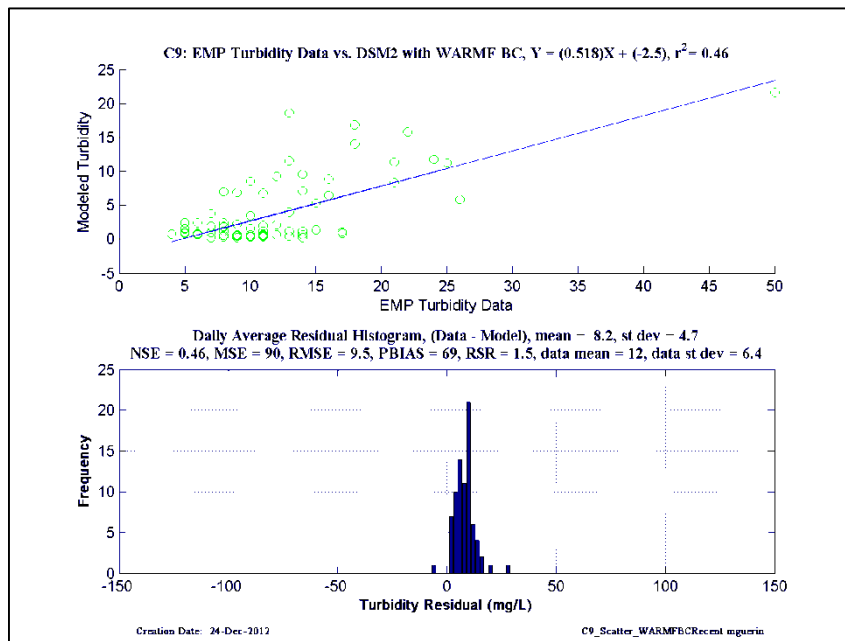
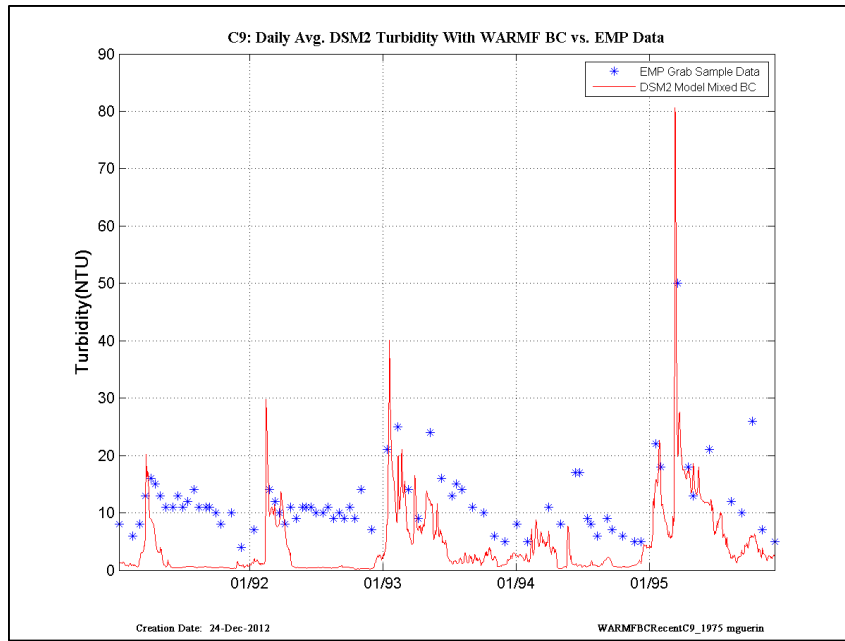


Figure 16-29 DSM2 daily-averaged turbidity model results using and WARMF model turbidity at all inflow boundaries compared to EMP grab-sample data, recent years– location is EMP C9.

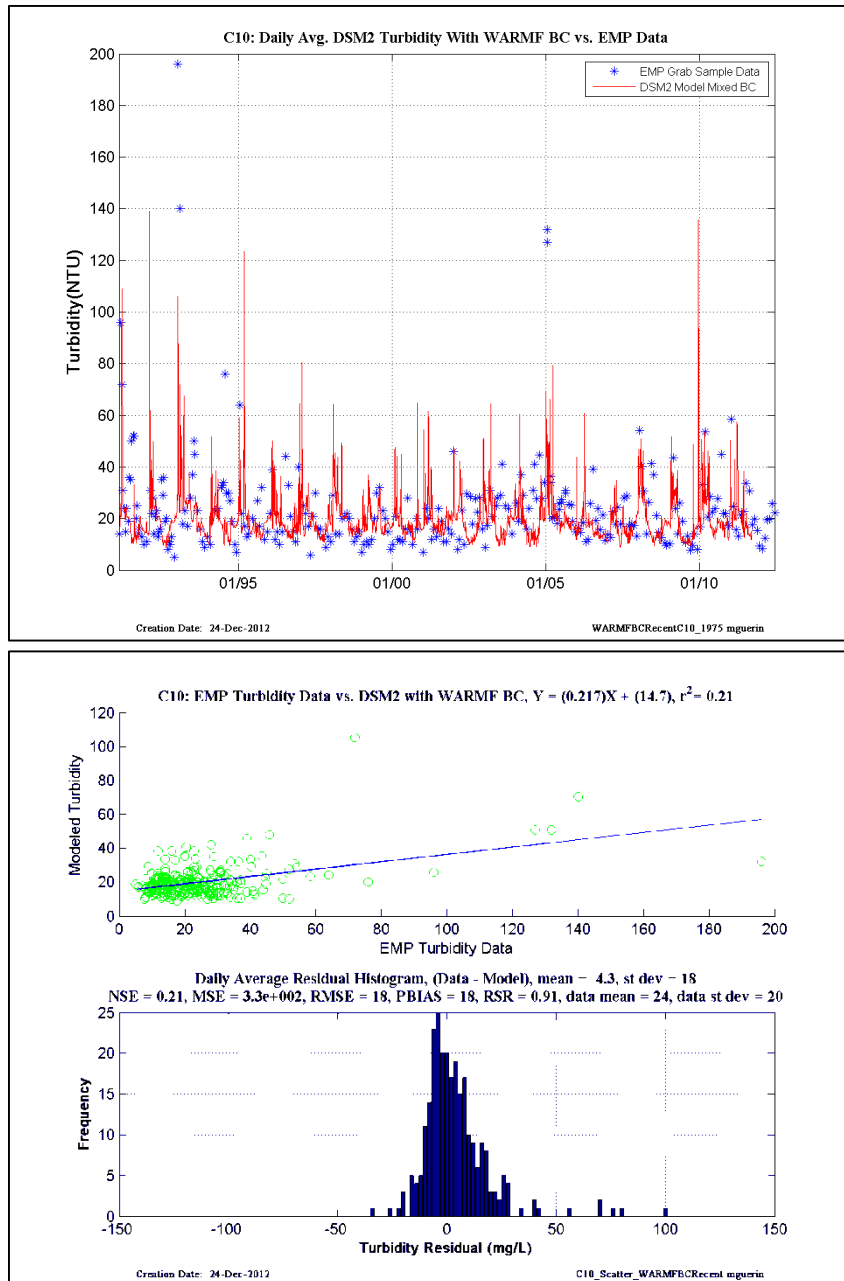


Figure 16-30 DSM2 daily-averaged turbidity model results using and WARMF model turbidity at all inflow boundaries compared to EMP grab-sample data, recent years– location is EMP C10.

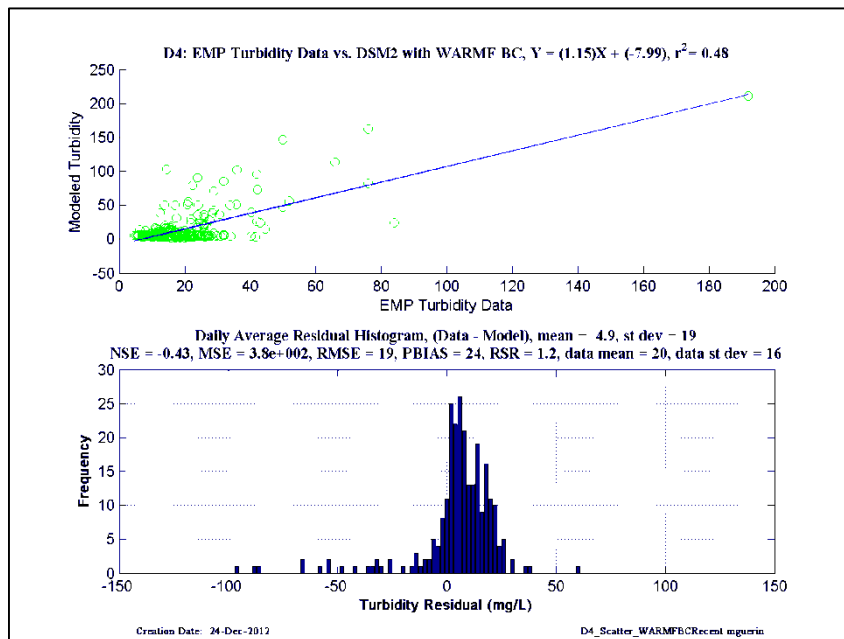
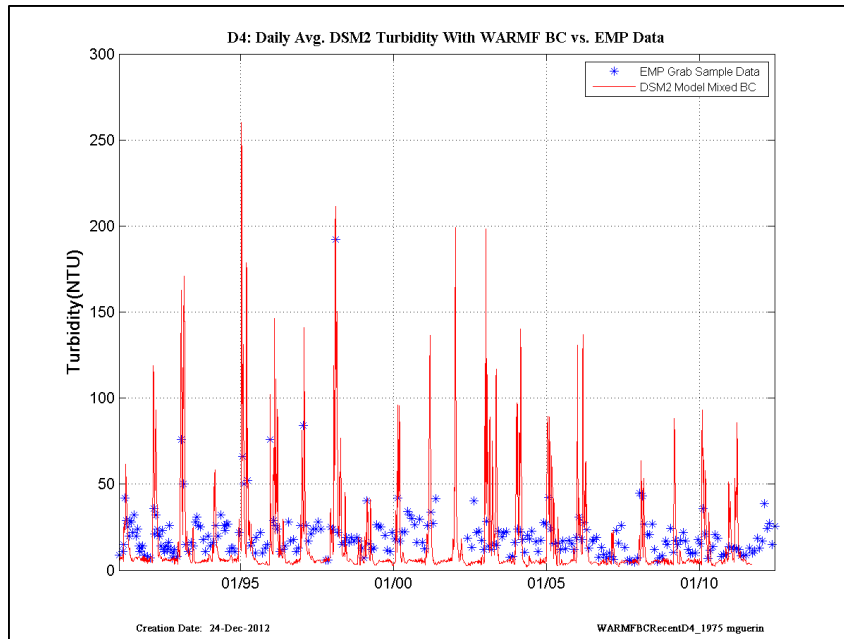


Figure 16-31 DSM2 daily-averaged turbidity model results using and WARMF model turbidity at all inflow boundaries compared to EMP grab-sample data, recent years– location is EMP D4.

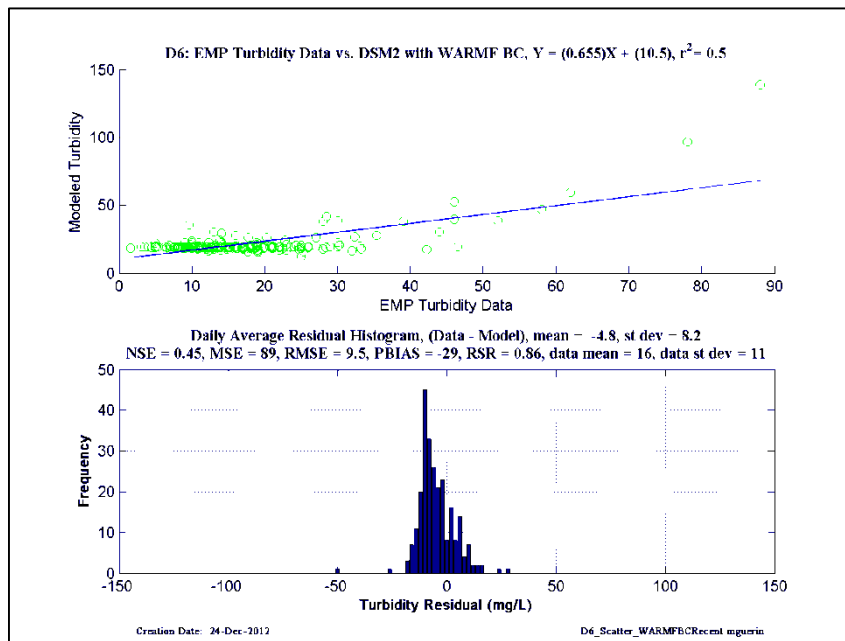
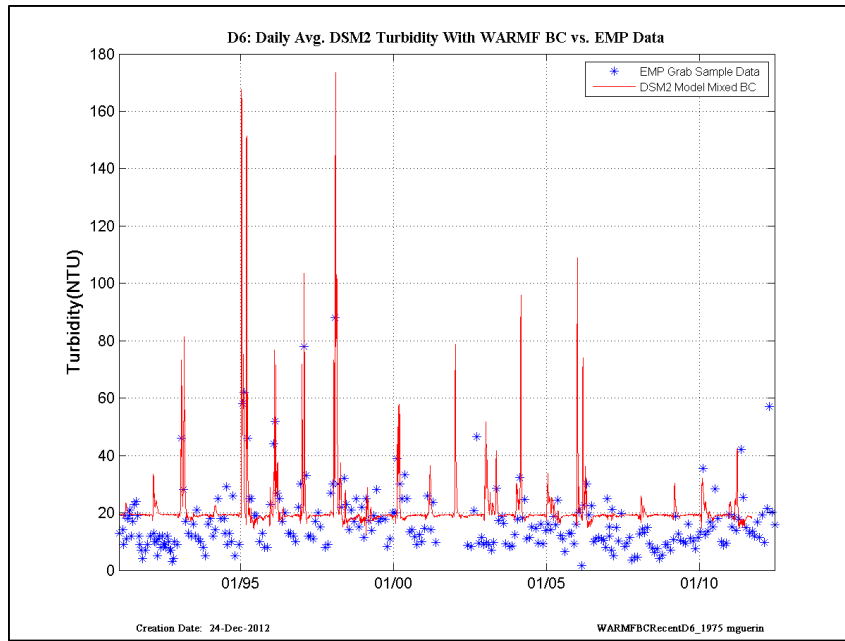


Figure 16-32 DSM2 daily-averaged turbidity model results using and WARMF model turbidity at all inflow boundaries compared to EMP grab-sample data, recent years– location is EMP D6.

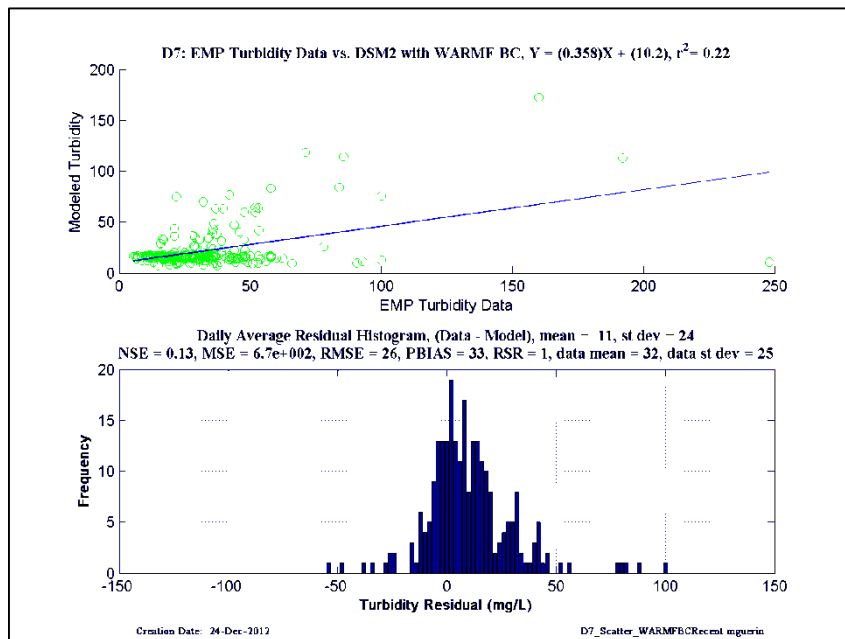
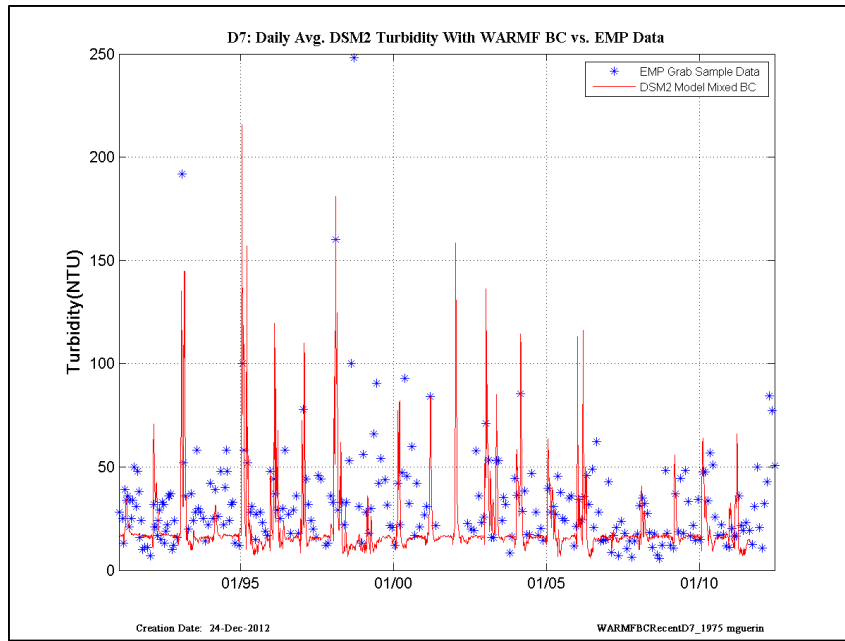


Figure 16-33 DSM2 daily-averaged turbidity model results using and WARMF model turbidity at all inflow boundaries compared to EMP grab-sample data, recent years– location is EMP D7.

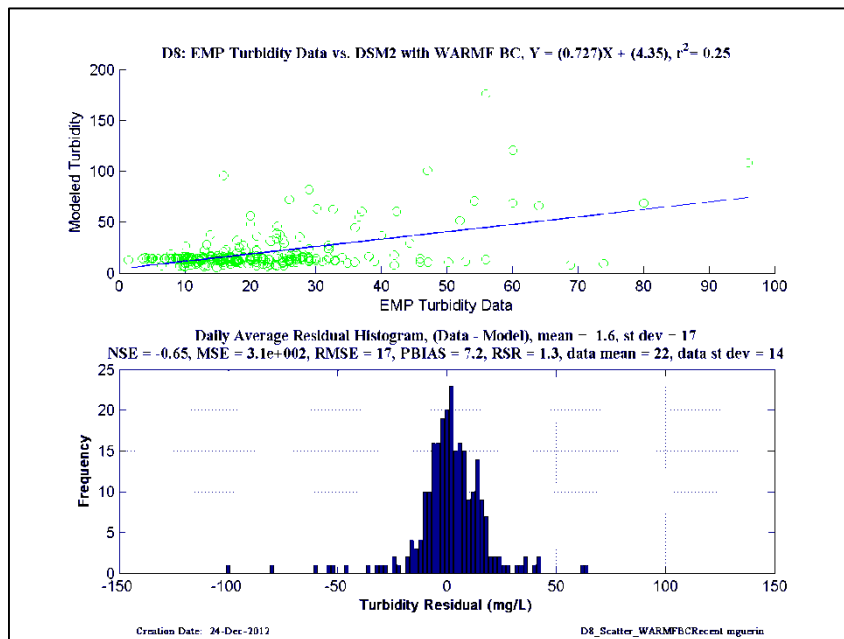
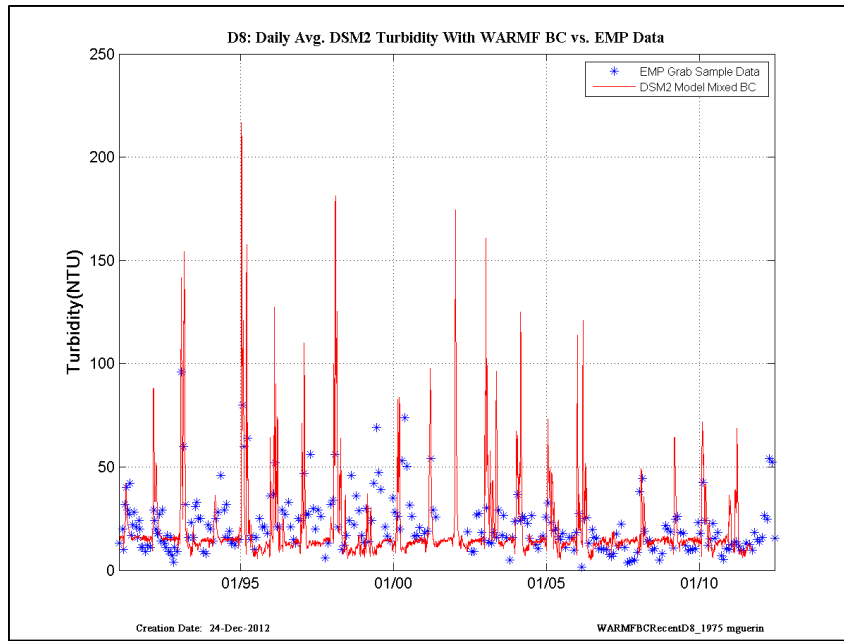


Figure 16-34 DSM2 daily-averaged turbidity model results using and WARMF model turbidity at all inflow boundaries compared to EMP grab-sample data, recent years– location is EMP D8.

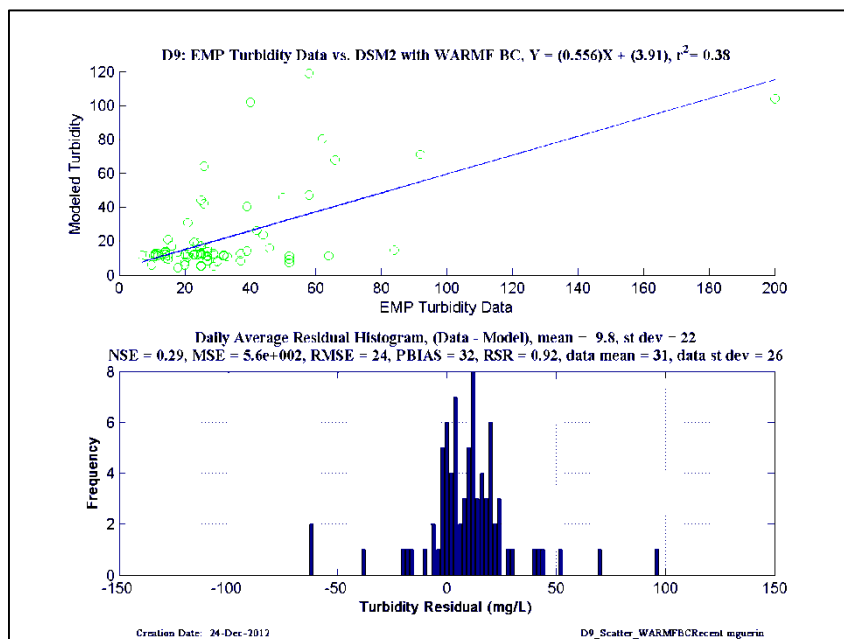
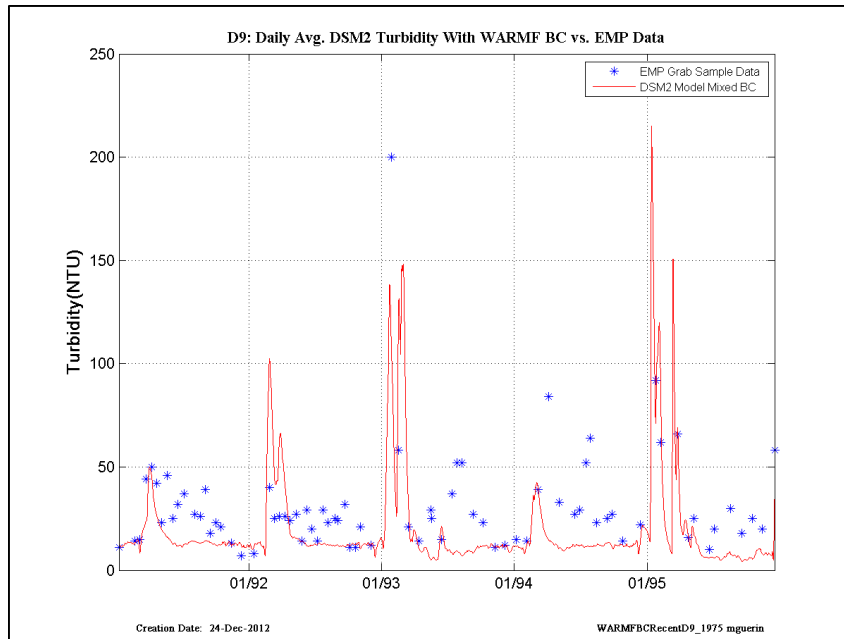


Figure 16-35 DSM2 daily-averaged turbidity model results using and WARMF model turbidity at all inflow boundaries compared to EMP grab-sample data, recent years– location is EMP D9.

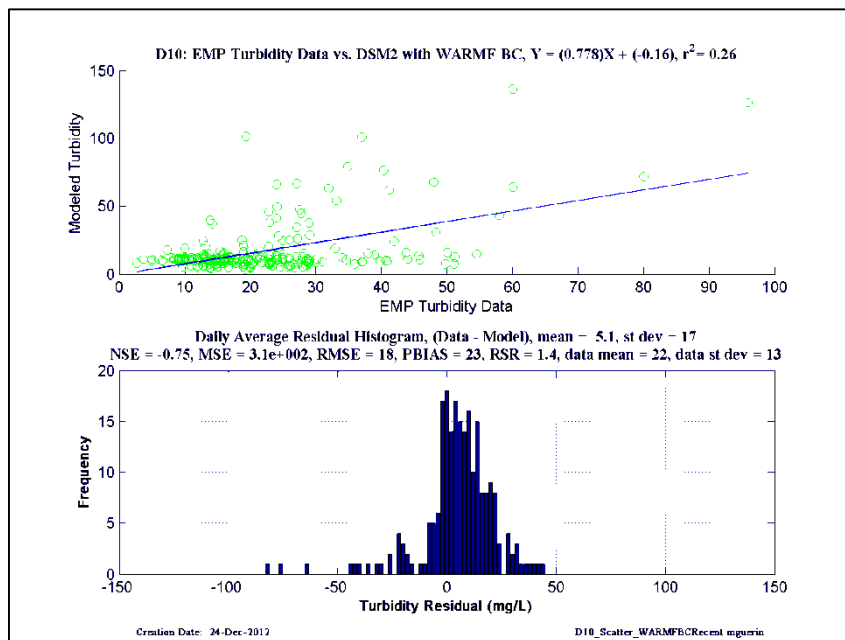
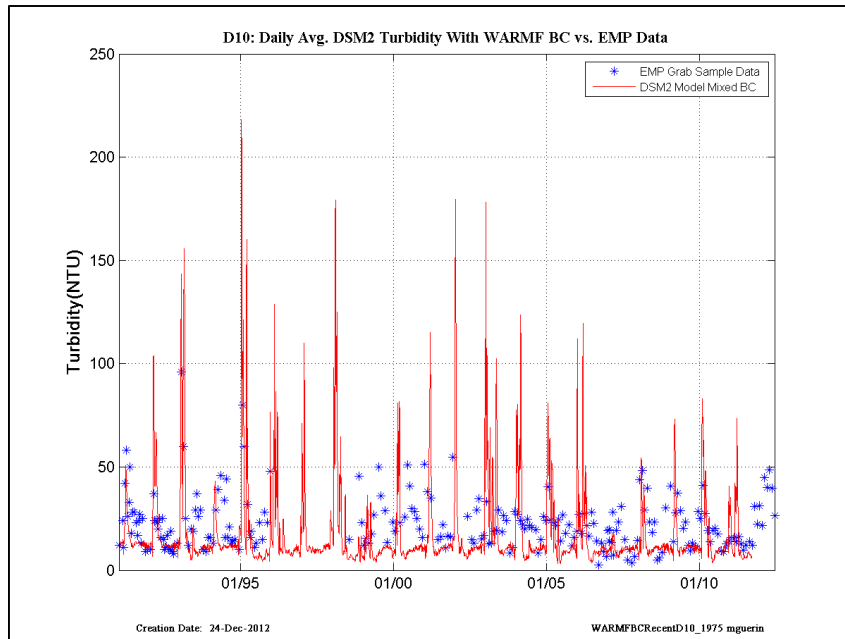


Figure 16-36 DSM2 daily-averaged turbidity model results using and WARMF model turbidity at all inflow boundaries compared to EMP grab-sample data, recent years– location is EMP D10.

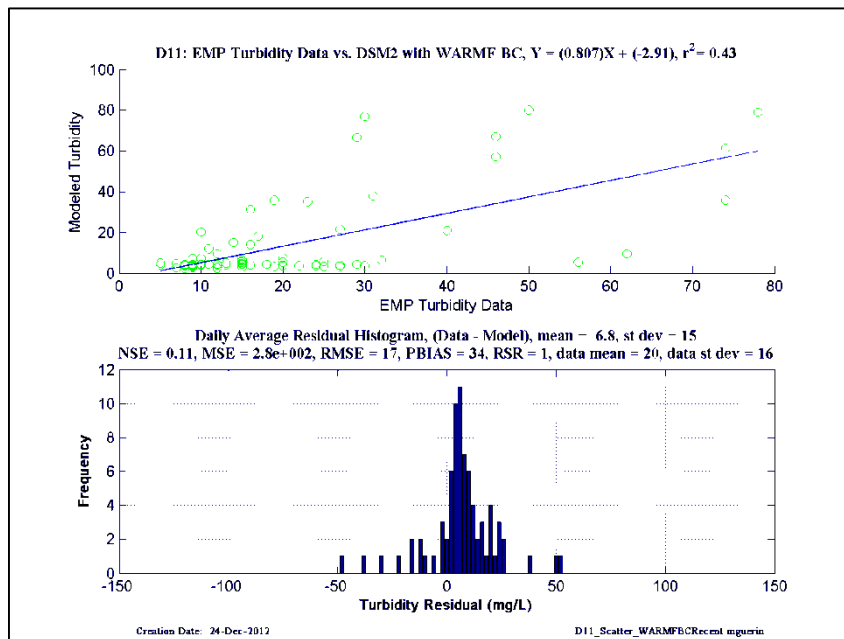
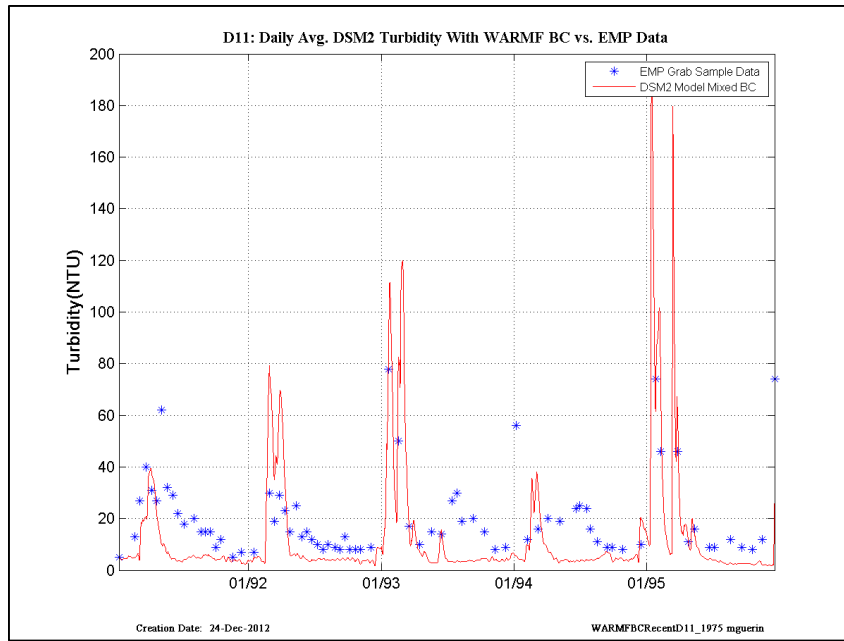


Figure 16-37 DSM2 daily-averaged turbidity model results using and WARMF model turbidity at all inflow boundaries compared to EMP grab-sample data, recent years– location is EMP D11.

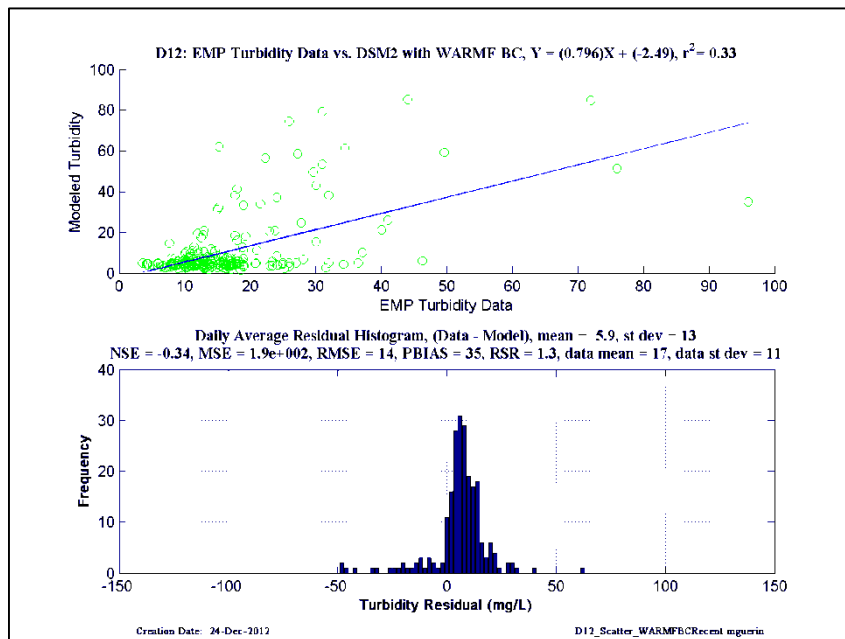
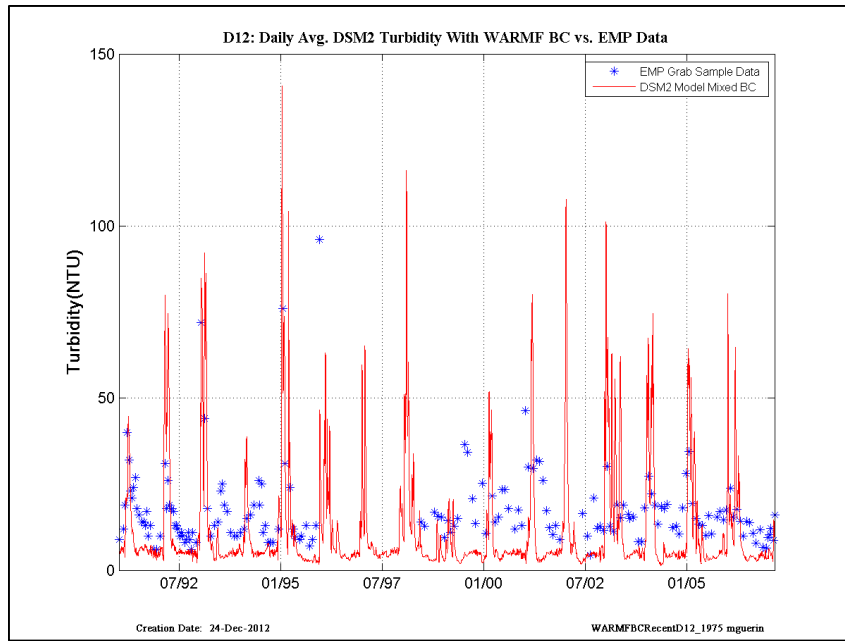


Figure 16-38 DSM2 daily-averaged turbidity model results using and WARMF model turbidity at all inflow boundaries compared to EMP grab-sample data, recent years– location is EMP D12.

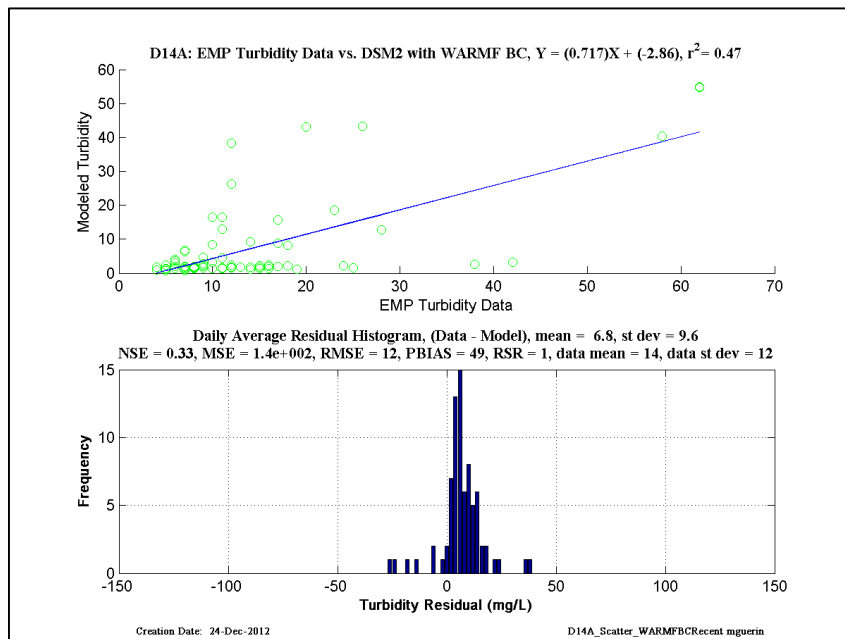
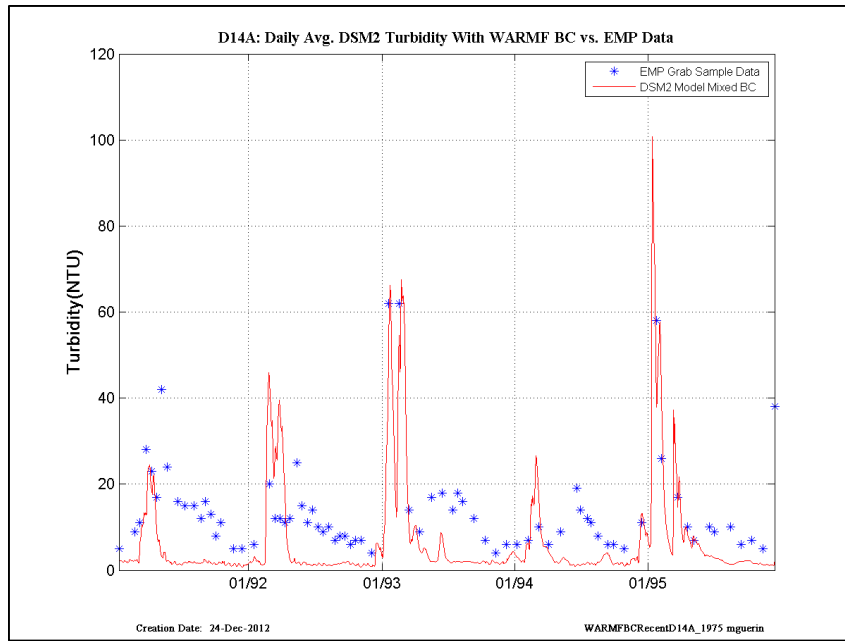


Figure 16-39 DSM2 daily-averaged turbidity model results using and WARMF model turbidity at all inflow boundaries compared to EMP grab-sample data, recent years– location is EMP D14A.

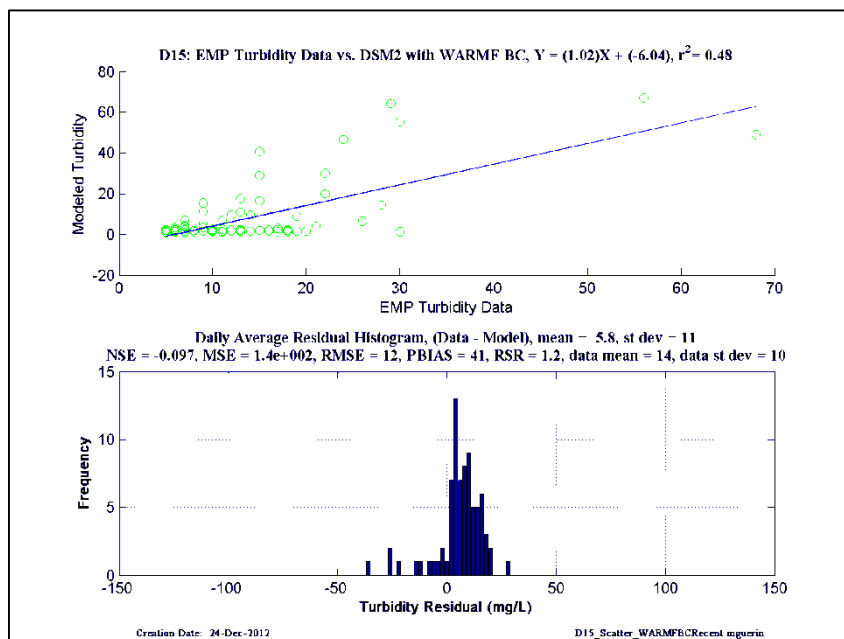
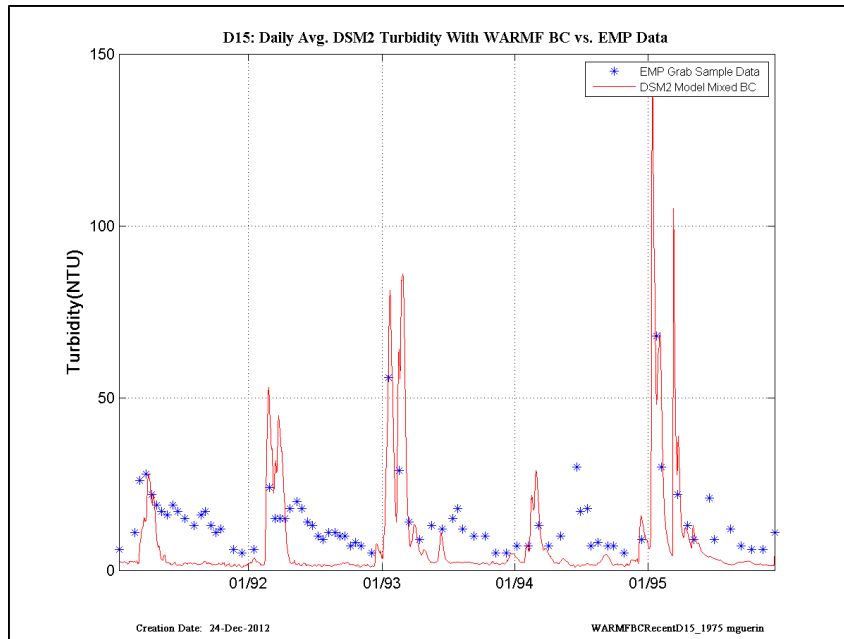


Figure 16-40 DSM2 daily-averaged turbidity model results using and WARMF model turbidity at all inflow boundaries compared to EMP grab-sample data, recent years– location is EMP D15.

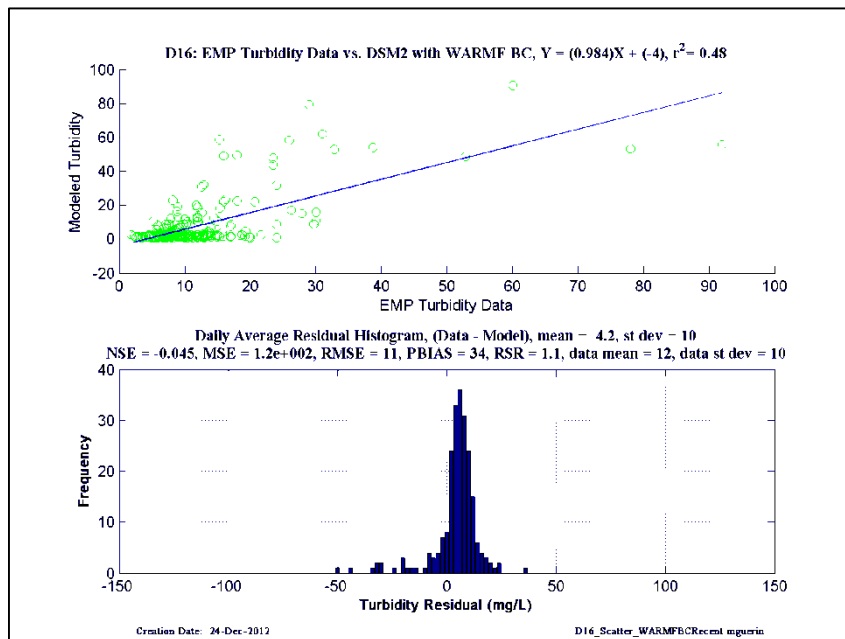
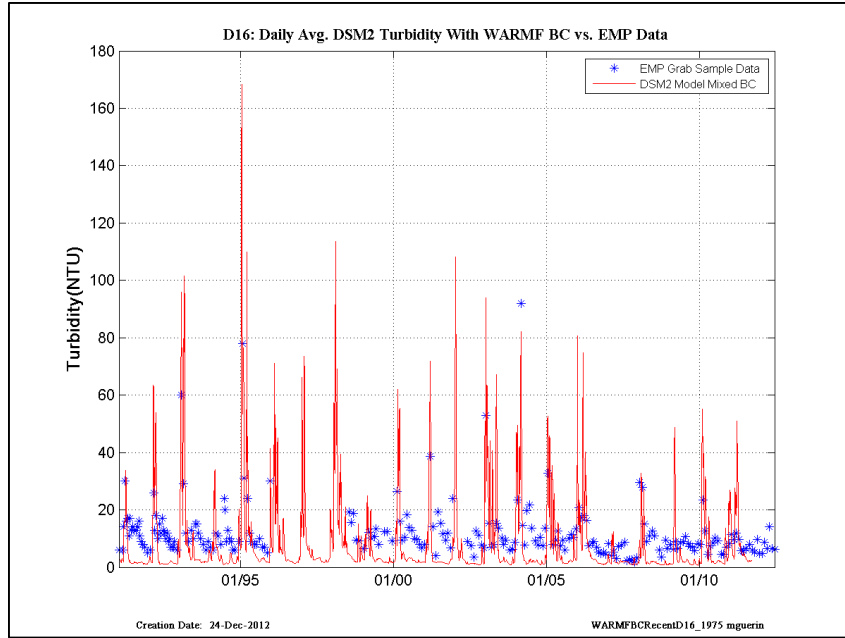


Figure 16-41 DSM2 daily-averaged turbidity model results using and WARMF model turbidity at all inflow boundaries compared to EMP grab-sample data, recent years– location is EMP D16.

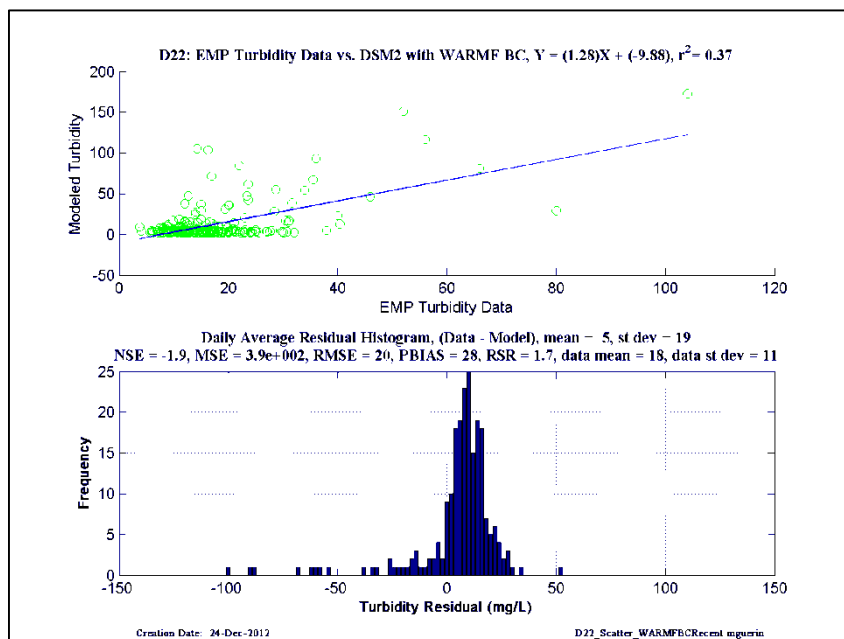
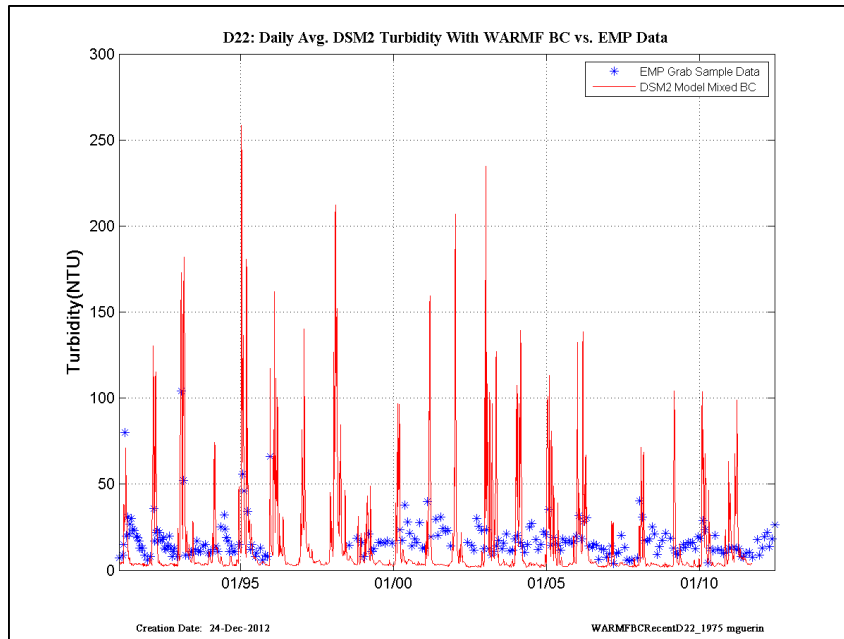


Figure 16-42 DSM2 daily-averaged turbidity model results using and WARMF model turbidity at all inflow boundaries compared to EMP grab-sample data, recent years– location is EMP D22.

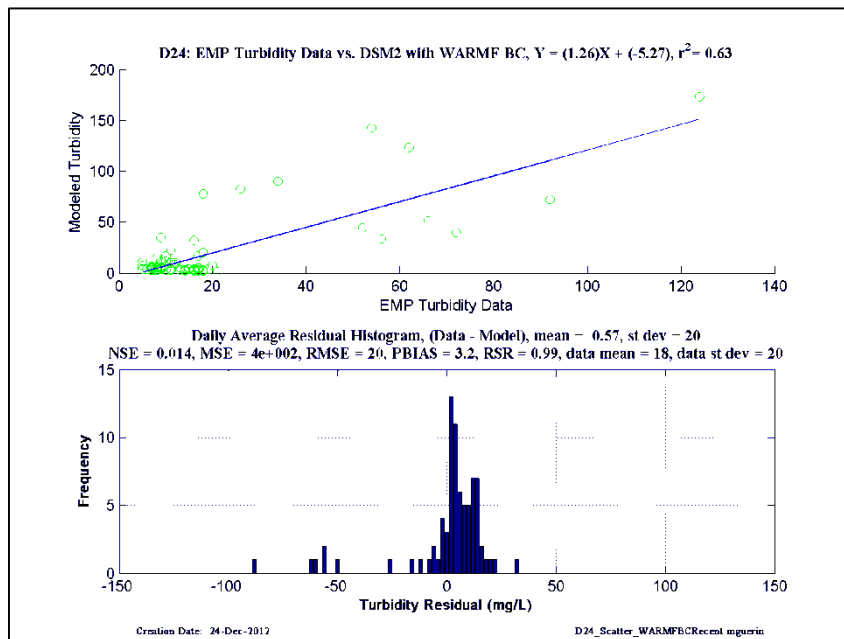
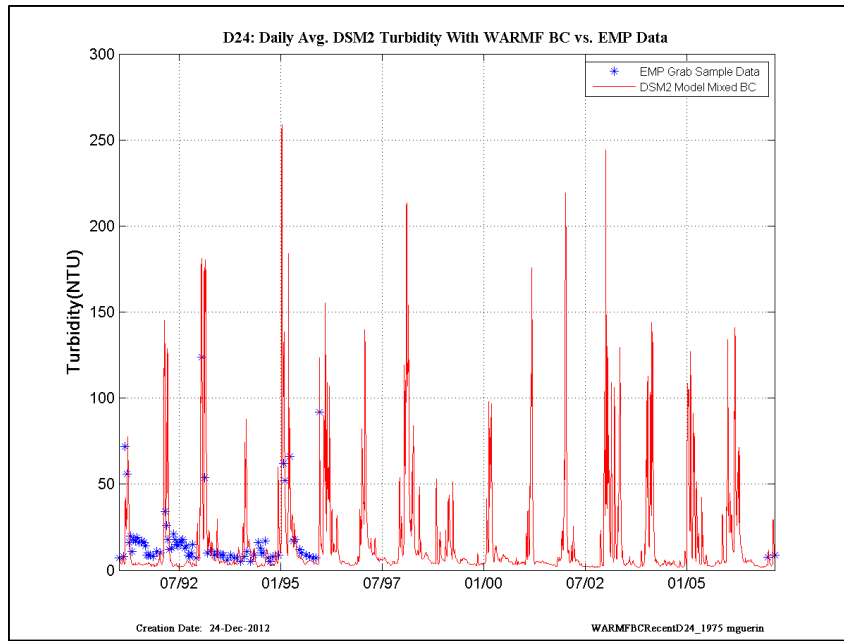


Figure 16-43 DSM2 daily-averaged turbidity model results using and WARMF model turbidity at all inflow boundaries compared to EMP grab-sample data, recent years– location is EMP D24.

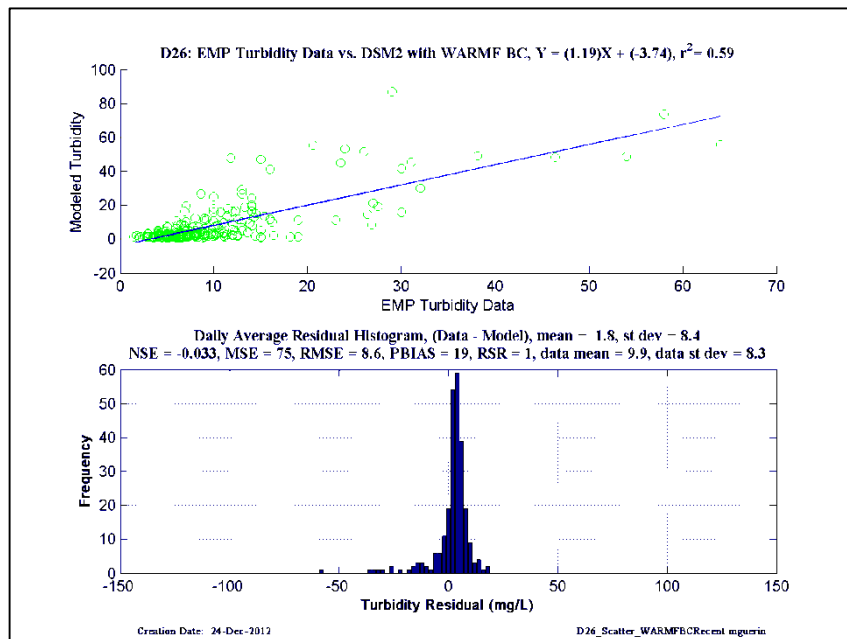
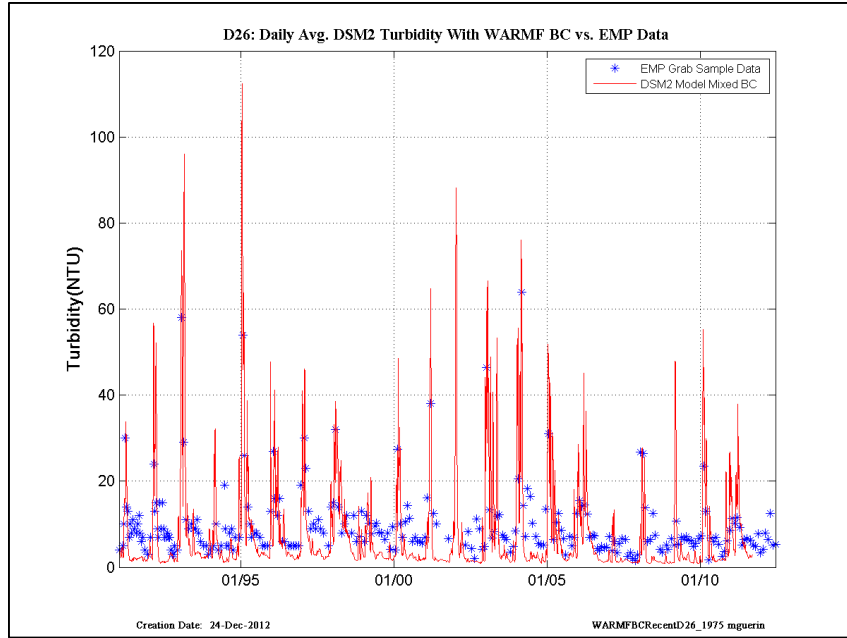


Figure 16-44 DSM2 daily-averaged turbidity model results using and WARMF model turbidity at all inflow boundaries compared to EMP grab-sample data, recent years– location is EMP D26.

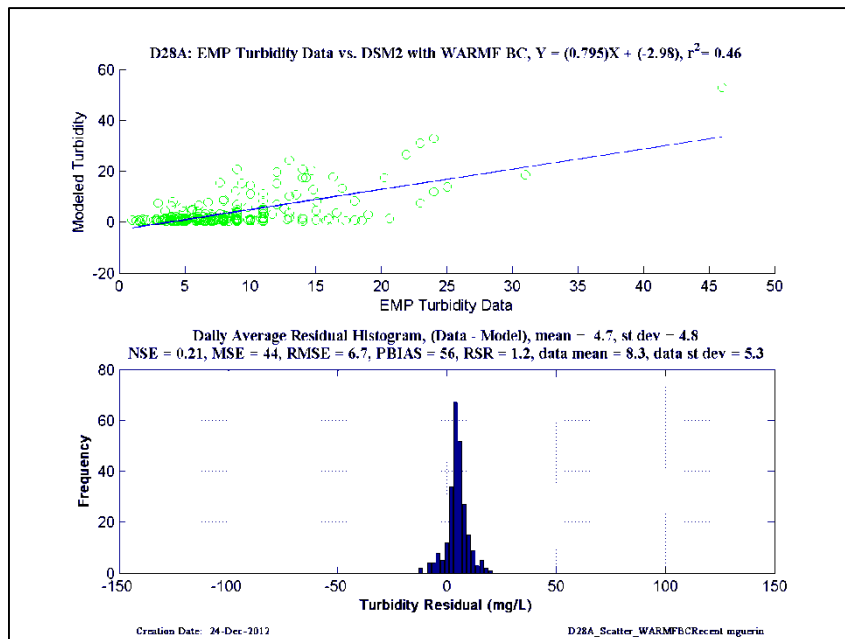
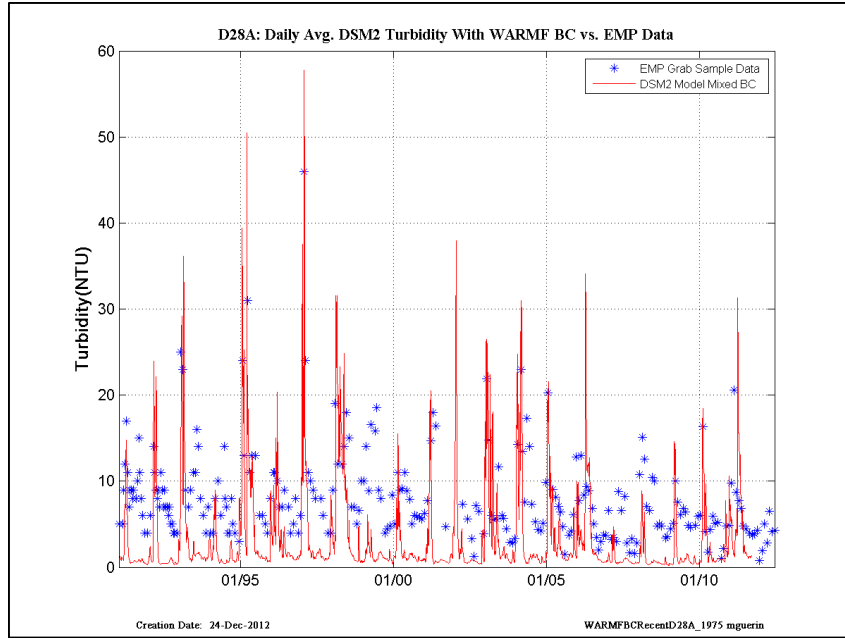


Figure 16-45 DSM2 daily-averaged turbidity model results using and WARMF model turbidity at all inflow boundaries compared to EMP grab-sample data, recent years– location is EMP D28A.

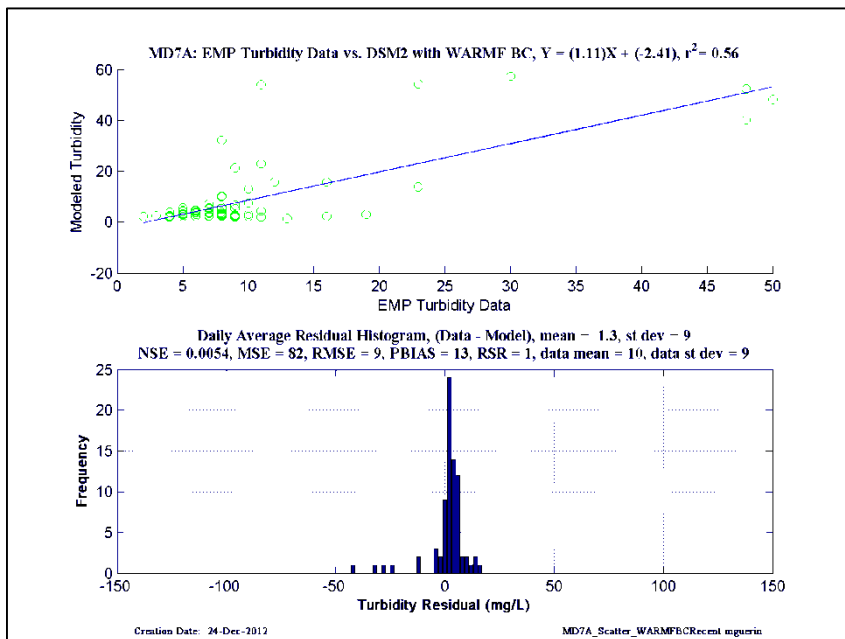
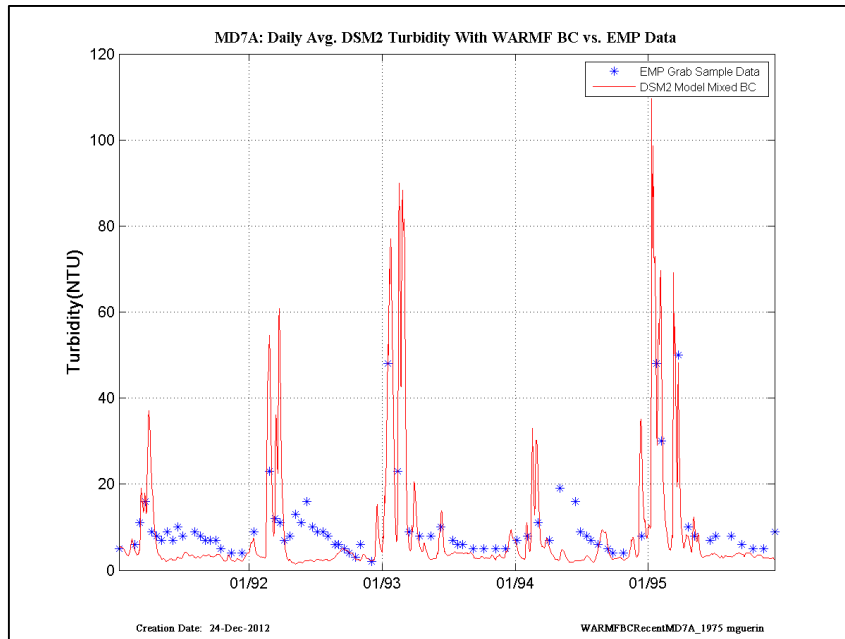


Figure 16-46 DSM2 daily-averaged turbidity model results using and WARMF model turbidity at all inflow boundaries compared to EMP grab-sample data, recent years– location is EMP MD7A.

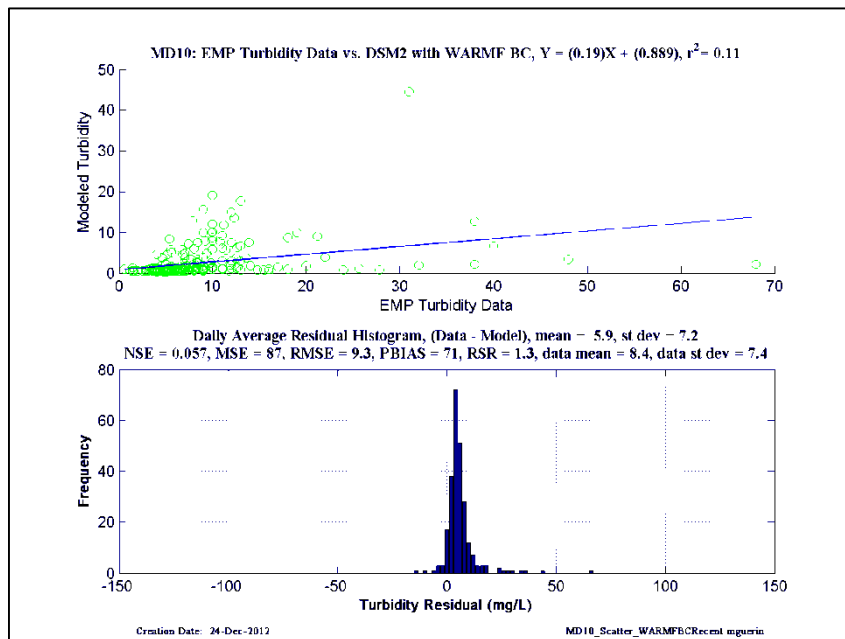
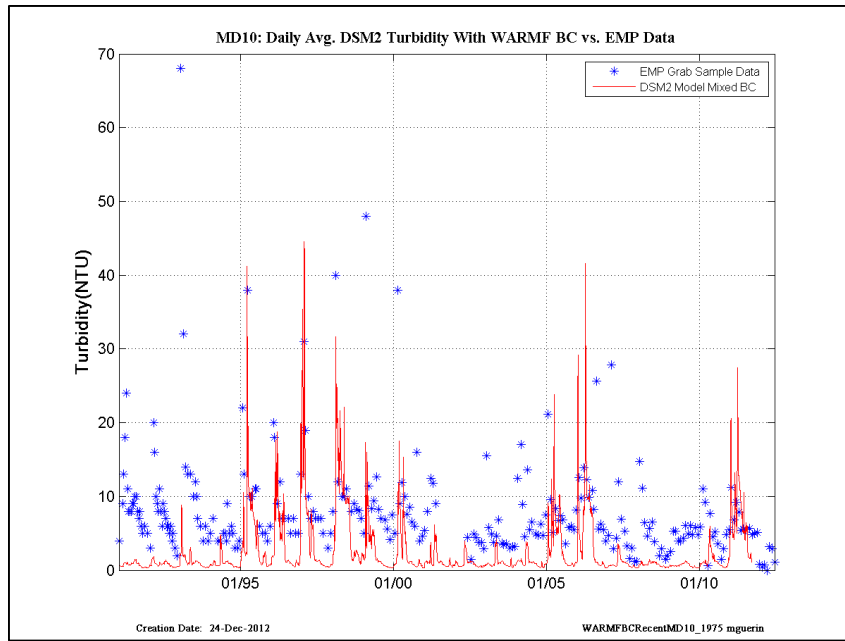


Figure 16-47 DSM2 daily-averaged turbidity model results using and WARMF model turbidity at all inflow boundaries compared to EMP grab-sample data, recent years– location is EMP MD10.

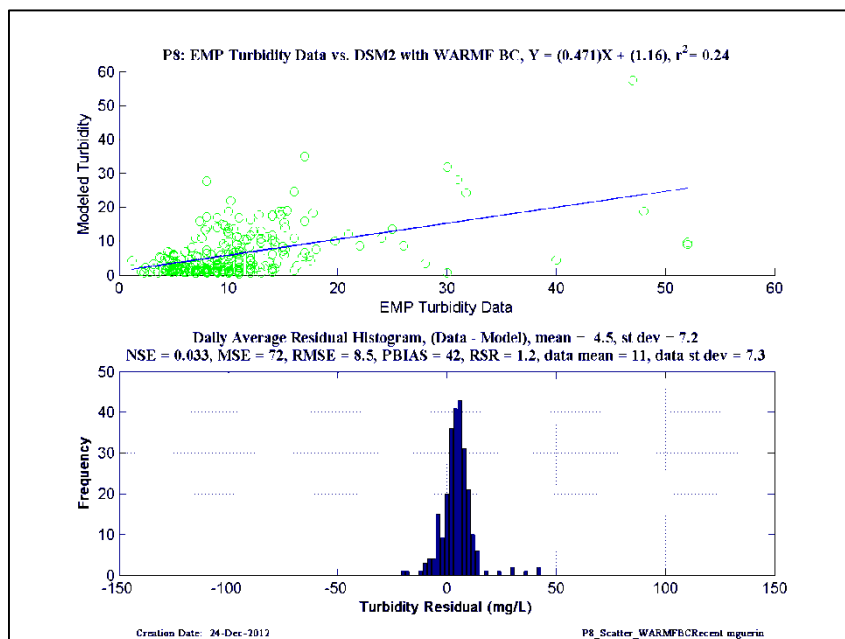
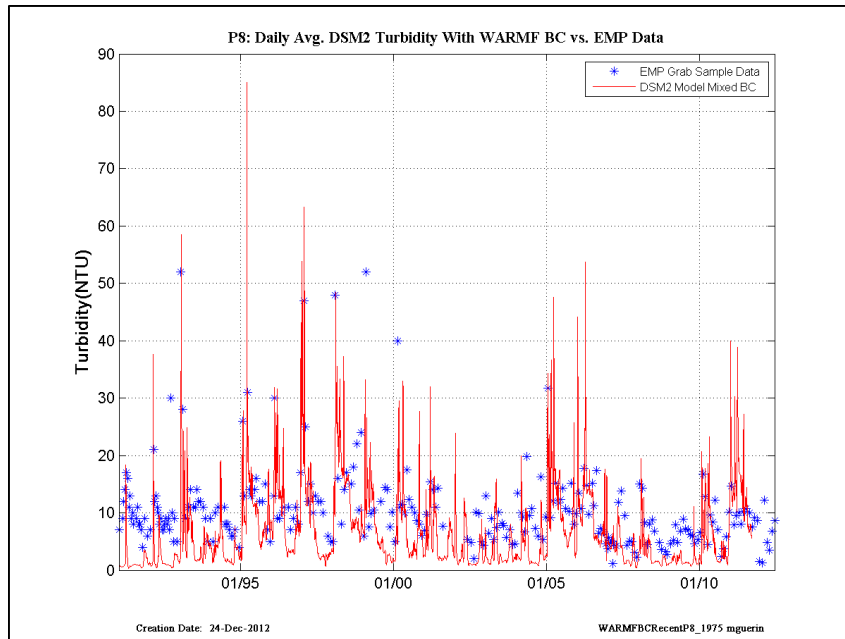


Figure 16-48 DSM2 daily-averaged turbidity model results using and WARMF model turbidity at all inflow boundaries compared to EMP grab-sample data, recent years– location is EMP P8.

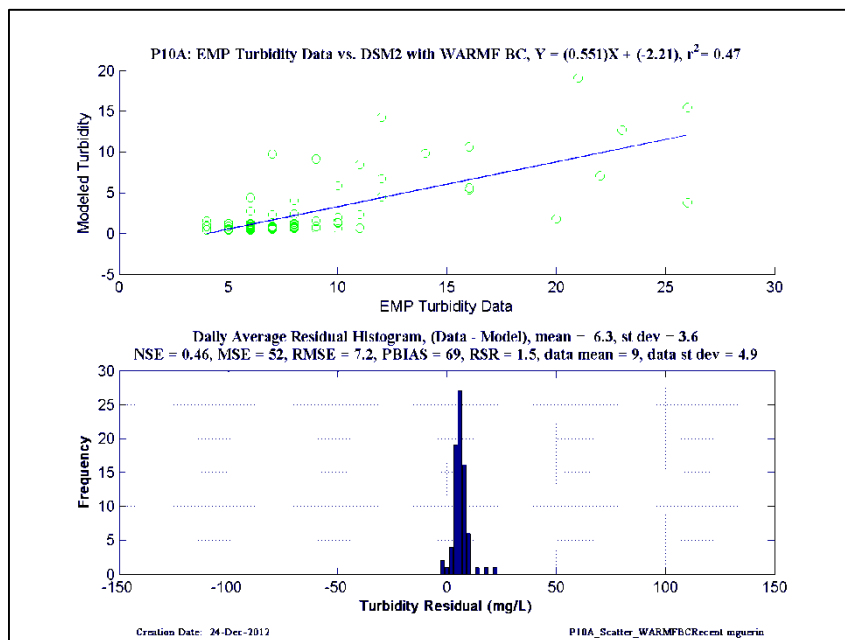
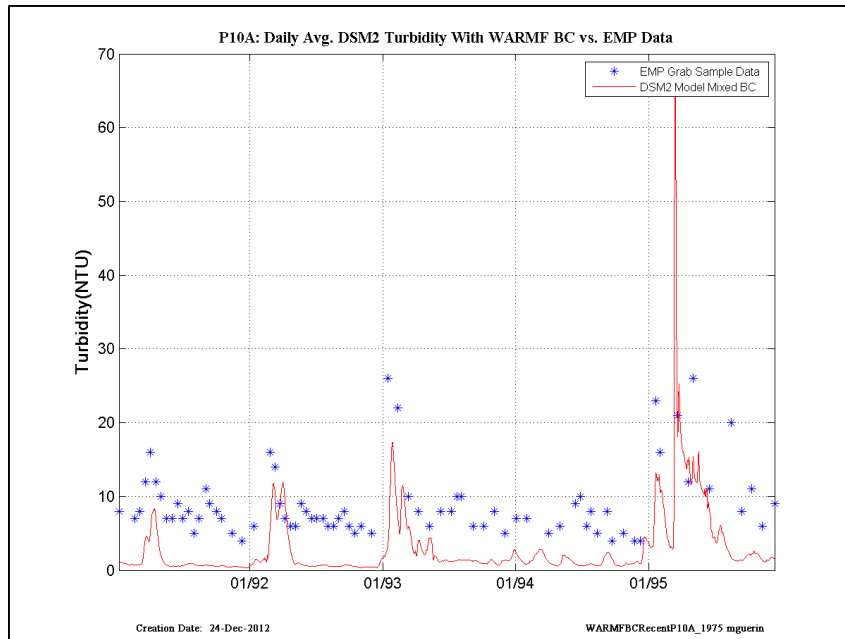


Figure 16-49 DSM2 daily-averaged turbidity model results using and WARMF model turbidity at all inflow boundaries compared to EMP grab-sample data, recent years– location is EMP P10A.

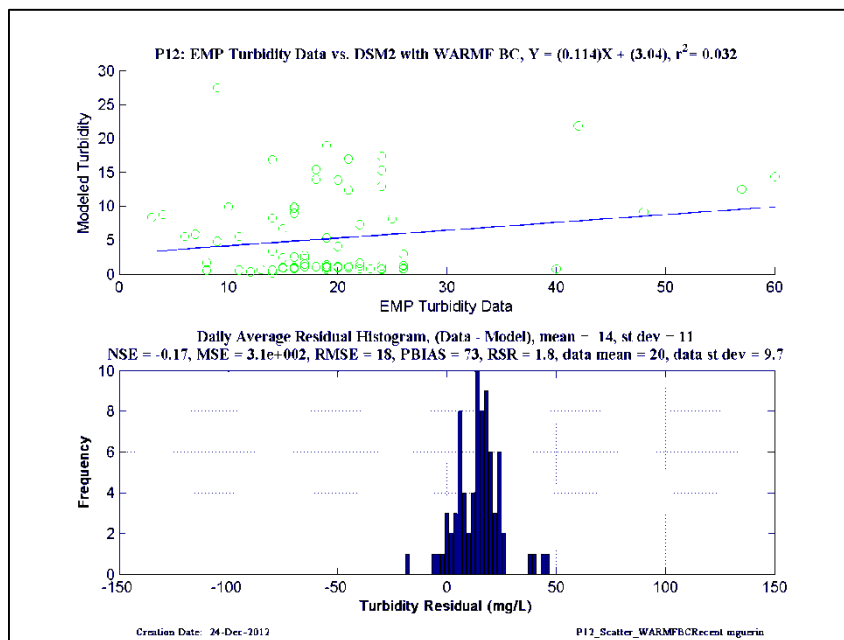
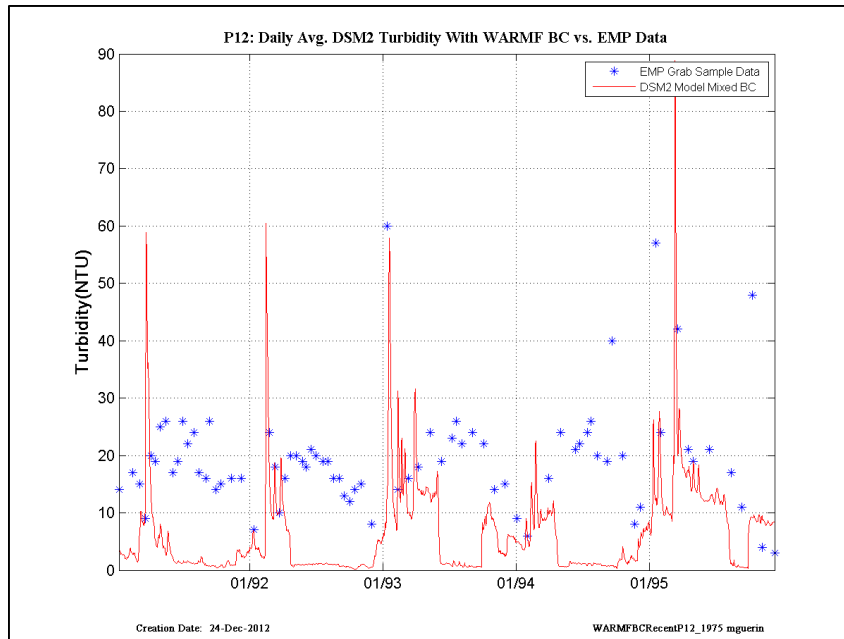


Figure 16-50 DSM2 daily-averaged turbidity model results using and WARMF model turbidity at all inflow boundaries compared to EMP grab-sample data, recent years— location is EMP P12.